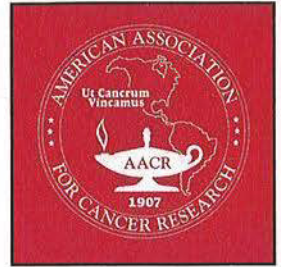


Supplement to  
**Clinical  
Cancer  
Research**

DEC 06 1999

HEALTH SCIENCES LIBRARIES

An Official Journal  
of the  
American Association  
for  
Cancer Research

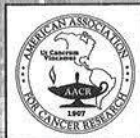


**AACR-NCI-EORTC International Conference**

# Molecular Targets and Cancer Therapeutics

**Discovery, Development,  
and Clinical Validation**

**November 16-19, 1999 • Washington Hilton and Towers • Washington, DC**



American  
Association  
for Cancer  
Research

NATIONAL  
CANCER  
INSTITUTE



**EORTC**  
European Organization for Research  
and Treatment of Cancer

November 1999 • Volume 5 • Supplement  
PP. 3729s-3897s • ISSN 1078-0432

1

OSI 2025  
APOTEX V. OSI  
IPR2016-01284



# Honoring

*...our Underwriting Sponsors for leadership support of this important international conference.*

AstraZeneca 



BRISTOL-MYERS SQUIBB  
ONCOLOGY

JANSSEN  
RESEARCH  
FOUNDATION



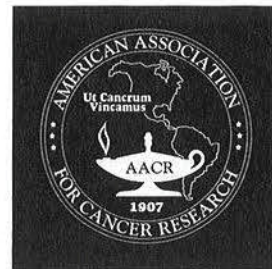
ORTHO BIOTECH

RPR  Oncology™  
rproncology.com



Clinical  
Cancer  
Research  
Supplement

An Official Journal  
of the  
American Association  
for  
Cancer Research



AACR-NCI-EORTC International Conference

# Molecular Targets and Cancer Therapeutics

## Discovery, Development, and Clinical Validation

November 16-19, 1999 • Washington Hilton and Towers • Washington, DC



American  
Association  
for Cancer  
Research

NATIONAL  
CANCER  
INSTITUTE



**EORTC**  
European Organization for Research  
and Treatment of Cancer



# RPR Oncology™



## Where Breakthroughs Are Born.™

At RPR Oncology, our commitment to innovation is not new; it began more than 40 years ago with the discovery of one of the first anthracyclines. Through our dedication, many oncology breakthroughs have been delivered to patients in need, including therapy for women with breast cancer, for patients with brain cancer, and for children and adults with leukemia. Our most recent research discoveries are designed to help patients reap the benefits of gene therapy and other new technologies. At RPR Oncology, breakthroughs are born because we're always thinking in fresh new ways.



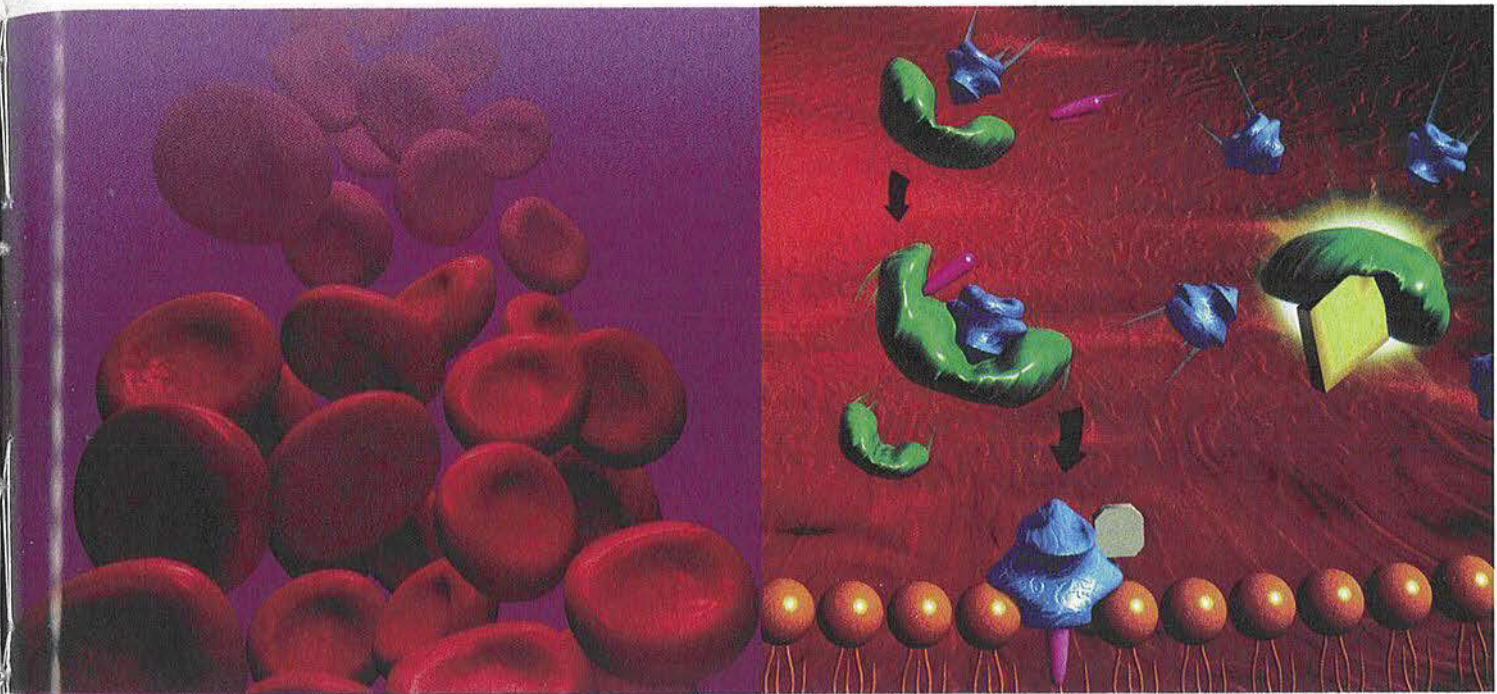
Where  
Breakthroughs  
Are Born.™





ORTHO BIOTECH

JANSSEN  
RESEARCH  
FOUNDATION



Partners in  
**Oncology**



# They All Fit Together



**Surgery • Chemotherapy • Radiotherapy**

Working Together  
For Optimal Cancer Therapy



Bristol-Myers Squibb Company  
Princeton, NJ 08543  
U.S.A.



# first for innovation and value

AstraZeneca is one of the world's major international research-based pharmaceutical companies

Since AstraZeneca introduced its first anti-cancer drug, 'Nolvadex' (tamoxifen), more than 25 years ago, investment in research has led to the discovery of new hormonal and cytotoxic anti-cancer agents, plus other innovative therapeutic strategies (such as targeting cell signalling, angiogenesis and apoptosis). As a result, AstraZeneca has an impressive portfolio of developmental agents to complement its extensive range of established oncology products.

**AstraZeneca** 

**ONCOLOGY**

'Nolvadex' is a trade mark, the property of Zeneca Limited.  
Further information is available from:

**AstraZeneca**  
A Business Unit of Zeneca Inc.  
PO Box 15437, Wilmington  
DE 19850 5437, USA

**AstraZeneca**  
Alderley House, Alderley Park  
Macclesfield, Cheshire, UK

5055/Oct '99



# Molecular Targets and Cancer Therapeutics

**Discovery, Development, and Clinical Validation**

Washington Hilton and Towers Washington, DC November 16-19, 1999

Are all of your colleagues attending  
this meeting?

Would having access to talks given  
this week be valuable to you or  
your colleagues?

AACR, in conjunction with virtualFactory, inc. is preparing a CD-ROM of selected sessions from this important meeting. This two CD-ROM set will contain audio and slide reproductions of the content presented in each session. Full search capabilities will be included along with a full transcript of each presentation.

Visit the virtualFactory booth for a demonstration, a complete list of the content included, and to order your copy. Discounts available on bulk orders.

For more information, call virtualFactory at 617.578.9127 ext. 13, email [sales@virtualfactory.com](mailto:sales@virtualfactory.com), or visit the AACR website at [www.aacr.org](http://www.aacr.org).



American  
Association  
for Cancer  
Research





1999 AACR-NCI-EORTC International Conference on

# Molecular Targets and Cancer Therapeutics

Discovery, Development, and Clinical Validation

November 16-19, 1999 • Washington, DC

Abstracts are numbered from 1 through 695; however, several numbers may be omitted in the sequence. Abstracts were either typeset or reproduced electronically from submitted material. Every effort has been made to reproduce the content of the abstracts according to the paper copy submitted, except in certain instances where changes were made to comply with AACR style. AACR does not assume any responsibility for proofreading or correcting any scientific, grammatical, or typographical errors, nor does AACR assume responsibility for errors in the conversion of customized software, newly released software, or special characters. No responsibility is assumed by the AACR, publisher and copyright owner of the *Proceedings* or by the meeting organizers for any injury and/or damage to persons or property as a matter of products liability, negligence or otherwise, or for any use or operation of any methods, products, instructions, or ideas contained in the material herein. Independent verification of diagnoses and drug dosages should be made by readers or users of this information.

*The Proceedings of the AACR-NCI-EORTC International Conference on Molecular Targets and Cancer Therapeutics* is printed for the AACR by Cadmus Journal Services, Linthicum, MD 21090-2908 and is distributed to registrants and other attendees of the 1999 AACR-NCI-EORTC International Conference. In addition, the *Proceedings* is simultaneously published as a Supplement to Volume 5 of the AACR journal *Clinical Cancer Research* (November 1999; ISSN: 1078-0432). The *Proceedings* may be obtained at a price of \$25.00 by writing to: AACR Subscription Office, P.O. Box 11806, Birmingham, AL 35202 [Telephone: (800) 633-4931 or (205) 995-1567; FAX (205) 995-1588]. Add \$6.00 for shipping for orders from outside the U.S.; expedited delivery rates are available upon request.

*The Proceedings of the AACR-NCI-EORTC International Conference on Molecular Targets and Cancer Therapeutics* is copyrighted ©1999 by the AACR. All rights reserved. Redistribution or resale of the *Proceedings* or of any materials in the *Proceedings*, whether in machine-readable, other electronic or any form, is prohibited. Reproduction for advertising or promotional purposes, by reproduction in any form, may be permitted only under license from the AACR. Any reproduction, whether electronic or otherwise of abstracts beyond that permitted by copyright law must be authorized in writing in advance by the AACR. Requests to reproduce abstracts will be considered on an individual basis and permission may be granted contingent upon payment of an appropriate fee. Reproduction requests must include a brief description of intended use. Third parties should also obtain the approval of the authors before corresponding with the AACR. Failure to comply with the foregoing restrictions and unauthorized duplication of any portion of these materials are a violation of applicable laws and may be subject to criminal prosecution and civil penalties.

No responsibility is accepted by the Editors, by the American Association for Cancer Research, Inc., or by Cadmus Journal Services for the opinions expressed by the contributors or for the contents of the advertisements herein.

Address inquiries to the Office of the American Association for Cancer Research, Inc. (AACR), Public Ledger Building, Suite 826, 150 S. Independence Mall West, Philadelphia, PA 19106-3483 [Telephone: (215) 440-9300; FAX: (215) 440-9313].

## FUTURE ANNUAL MEETINGS OF THE AACR

April 1-5, 2000 • San Francisco, CA  
March 24-28, 2001 • New Orleans, LA  
April 6-10, 2002 • San Francisco, CA



Program Committee and Special Committee for Review of Abstracts .....	vi
<b>Regular Abstracts: Poster Sessions</b>	
<b>Poster Session 1</b> .....	3729s
Section 1: Phase I Clinical Trials: New Agents, Antiangiogenesis, and Molecular Endpoints .....	3729s
Section 2: Growth Factors and Their Responses (Including Antihormonal) .....	3734s
Section 3: Metastasis and Invasion Targets .....	3739s
Section 4: Fas Pathways/Growth Factors: Biology and Therapeutics .....	3744s
Section 5: Kinase Inhibitors .....	3749s
<b>Poster Session 2</b> .....	3754s
Section 1: Cell Cycle Targets: p53, Cyclins, Cyclin-dependent Kinases .....	3754s
Section 2: Cellular Therapy, Vaccines, and Immunologic Targets .....	3758s
Section 3: New Intracellular Targets .....	3763s
Section 4: Tumor Physiology: Hypoxia, Radiosensitization, and New Extracellular Targets .....	3768s
Section 5: Phase II Studies with Molecular Endpoints .....	3772s
<b>Poster Session 3</b> .....	3776s
Section 1: Genomics and High Throughput Screens For Target Discovery (Arrays and Chips)/Signal Transduction (Related to Gene Expression) .....	3776s
Section 2: Structure-based Drug Design/Agents with Unknown or Uncertain Targets .....	3780s
Section 3: New Agents .....	3784s
Section 4: Marine Compounds and Other Natural Products, Synthetic Approaches .....	3789s
Section 5: Phase I Clinical Trials: Derivatives, New Formulations, and Combinations .....	3794s
<b>Poster Session 4</b> .....	3800s
Section 1: Signal Transduction/Signaling Targets .....	3800s
Section 2: Cytokines .....	3804s
Section 3: Antiangiogenesis/Antivascular Targets .....	3808s
Section 4: Cell Biology-based Strategies: Apoptosis and Differentiation .....	3813s
Section 5: Drug Delivery, Prodrugs, and Toxicology .....	3818s



<b>Poster Session 5</b> .....	3824s
Section 1: Molecular Markers and Tumor Imaging: Diagnosis, Progression, and Drug Responses .....	3824s
Section 2: Telomerase and Gene Therapy-based Technology .....	3828s
Section 3: Drug Resistance/Modifiers .....	3832s
Section 4: Preclinical Pharmacokinetics/Pharmacodynamics.....	3837s
Section 5: Drug Design, Metabolism, and Pharmacogenetics .....	3841s
 <b>Poster Session 6</b> .....	 3846s
Section 1: DNA-targeted Strategies: Oligodeoxynucleotides and Modulation of Repair Pathways.....	3846s
Section 2: DNA-interactive Agents .....	3851s
Section 3: Tubulin-interactive Agents .....	3855s
Section 4: Antifolates and Topoisomerase Inhibitors .....	3860s
Section 5: Chemoprevention: Targets, Models, Biomarkers, and Trials .....	3864s
 <b>Invited Abstracts: Plenary Sessions</b> .....	 3869s
Plenary Session 3: Chemistry: Generation of Diversity .....	3869s
Plenary Session 4: Biology and Target Selection II .....	3869s
Plenary Session 5: Preclinical Development .....	3869s
Plenary Session 6: Imaging Molecular Targets .....	3870s
Plenary Session 7: New Opportunities for DNA and Microtubules .....	3872s
Plenary Session 9: Changing a Concept into a Drug: The Art of Patience .....	3873s
 <b>Invited Abstracts: Workshops</b> .....	 3875s
Workshop 1: Relevance of <i>In Vivo</i> Models for Target-directed Anticancer Drug Development .....	3875s
Workshop 3: Cytostatic Agents: Methodology of Phase I/II Trials.....	3876s
Workshop 6: New Cytokines and Cell-based Therapy of Cancer.....	3876s
Workshop 7: Prevention Targets .....	3877s
Workshop 8: The Tumor Microenvironment .....	3877s
Workshop 12: Signal Transduction Targets in Cancer Drug Discovery .....	3879s
 <b>Author Index</b> .....	 3880s
 <b>Subject Index</b> .....	 3893s

Note Regarding Abstract Notation: Abstract numbers in italics denote abstracts that are published but not presented at the meeting.



# SAVE THE DATE

This collaborative series will continue  
next year in Europe.

Mark your calendar now for the

# 11<sup>th</sup>

## NCI-EORTC-AACR Symposium on New Drugs in Cancer Therapy

NOVEMBER 7-10, 2000 • AMSTERDAM



EORTC



American  
Association  
of Cancer  
Research

*Local organizer: NDDO Oncology*

*For information, contact:*

2000 Symposium Secretariat

NDDO Oncology, Free University Hospital

P.O. Box 705

PL 1007 MB, Amsterdam

The Netherlands



**April 1-5, 2000**  
**91<sup>ST</sup> ANNUAL MEETING**

Moscone Center, San Francisco, CA

Chairperson: Peter A. Jones, Los Angeles, CA  
Co-Chairpersons: Carlos A. Arteaga, Nashville, TN; Franco M. Muggia, New York, NY;  
Geoffrey M. Wahl, San Diego, CA; and Alice S. Whittemore, Stanford, CA

**JANUARY 14-18, 2000**  
**DNA Repair Defects**

Chairperson: Richard D. Kolodner, La Jolla, CA  
San Diego Hilton Beach and Tennis Resort  
San Diego, CA

**MAY 3-7, 2000**  
**Melanoma: Basic Biology and  
Immunological Approaches to Therapy**

Chairpersons: Meenhard Herlyn, Philadelphia, PA, and  
Giorgio Parmiani, Milan, Italy  
The Woodlands Resort,  
The Woodlands (near Houston), TX

**JANUARY 26-30, 2000**  
**Transcription Factor Pathogenesis of  
Cancer at the Millennium**

Chairpersons: Peter K. Vogt, La Jolla, CA, and  
Frank J. Rauscher, III, Philadelphia, PA  
Marriott Laguna Cliffs Resort, Dana Point, CA

**SEPTEMBER 20-24, 2000**  
**Cytokines and Cancer: Regulation,  
Angiogenesis, and Clinical Applications**

Chairpersons: Janice P. Dutcher, Bronx, NY; Michael Lotze,  
Pittsburgh, PA; and Giorgio Trinchieri, Philadelphia, PA  
Vail Cascade Hotel & Club, Vail, CO

**FEBRUARY 27- MARCH 2, 2000**  
**Programmed Cell Death: Regulation,  
Basic Mechanisms, and Therapeutic  
Opportunities**

Chairpersons: John C. Reed, La Jolla, CA, and  
Junying Yuan, Cambridge, MA  
Hyatt Regency Lake Tahoe, Incline Village, NV

**NOVEMBER 12-16, 2000**  
**New Targets for Cancer Intervention**  
*Joint Conference with the Israeli Cancer Society*

Chairpersons: Webster K. Cavenee, La Jolla, CA, and  
Prina Fishman, Petah Tikva, Israel  
Royal Beach Hotel, Eliat, Israel

CONTACT INFORMATION



AACR members will receive brochures on the above conferences as soon as they are available. Nonmembers should call or write:

American Association for Cancer Research  
Public Ledger Building, Suite 826  
150 S. Independence Mall West  
Philadelphia, PA 19106-3483  
215-440-9300 • 215-351-9165 (FAX)  
E-Mail: [meetings@aacr.org](mailto:meetings@aacr.org)

For regular updates to this list visit the AACR's Website, <http://www.aacr.org>



## PROGRAM COMMITTEE

Daniel D. Von Hoff, *Co-Chairperson*Robert E. Wittes, *Co-Chairperson*Jean-Claude Horiot, *Co-Chairperson*Shiro Akinaga ..... *Kyowa Hakko Kogyo Co., Shizuoka, Japan*Carmen J. Allegra ..... *NCI, Bethesda, MD*Karen S. H. Antman ..... *Columbia Presbyterian Medical Center,  
New York, NY*Susan G. Arbuck ..... *NCI, Bethesda, MD*Jean-Pierre Armand ..... *Institut Gustave Roussy, Villejuif, France*Joseph R. Bertino ..... *Memorial Sloan-Kettering Cancer Center,  
New York, NY*George R. P. Blackledge ..... *AstraZeneca Pharmaceuticals,  
Macclesfield, UK*Bruce A. Chabner ..... *Massachusetts General Hospital, Boston, MA*Micheale C. Christian ..... *NCI, Bethesda, MD*Neil J. Clendeninn ..... *Agouron Pharmaceuticals, San Diego, CA*Susan P. C. Cole ..... *Queen's University, Kingston, Ontario, Canada*O. Michael Colvin ..... *Duke Comprehensive Cancer Center,  
Durham, NC*Esteban Cvitkovic ..... *Cvitkovic Assoc. Consultants, Paris, France*Pieter H. M. DeMulder ..... *University Hospital,  
Nijmegen, The Netherlands*Maurizio D'Incalci ..... *Mario Negri Institute, Milan, Italy*Robert T. Dorr ..... *Arizona Cancer Center, Tucson, AZ*John A. Double ..... *University of Bradford, UK*Janice P. Dutcher ..... *Our Lady of Mercy Cancer Center, New York, NY*Alexander M. M. Eggermont ..... *University Hospital, Rotterdam,  
The Netherlands*Gerhard Eisenbrand ..... *University of Kaiserslautern, Germany*Elizabeth A. Eisenhauer ..... *Queen's University, Kingston,  
Ontario, Canada*Margaret Foti ..... *AACR, Philadelphia, PA*Giuseppe Giaccone ..... *Free University Hospital, Amsterdam,  
The Netherlands*Raffaella Giavazzi ..... *Mario Negri Institute, Bergamo, Italy*Tona M. Gilmer ..... *Glaxo Wellcome, Research Triangle Park, NC*Gary B. Gordon ..... *Searle & Company, Skokie, IL*Louise Barnett Grochow ..... *NCI, Rockville, MD*Axel-R. Hanauske ..... *Center for Hematology/Oncology,  
Munich, Germany*Michael John Hawkins ..... *Washington Cancer Institute,  
Washington, DC*Susan D. Hellmann ..... *Genentech, South San Francisco, CA*Wau Ki Hong ..... *UT M. D. Anderson Cancer Center, Houston, TX*Susan B. Horwitz ..... *Albert Einstein College of Medicine, New York, NY*Stephen B. Howell ..... *University of California, San Diego, CA*Loretta Itri ..... *R. W. Johnson Pharmaceutical Research Institute,  
Raritan, NJ*Corey H. Levenson ..... *ILEX Oncology, San Antonio, TX*Kim Allyson Margolin ..... *City of Hope National Medical Center,  
Duarte, CA*Silvia Marsoni ..... *Southern Europe New Drug Organization, Milan, Italy*Alex Matter ..... *Novartis Pharma AG, Basel, Switzerland*Frank McCormick ..... *University of California, San Francisco, CA*J. Patrick McGovern ..... *Pharmacia & Upjohn, Inc., Kalamazoo, MI*John Mendelsohn ..... *UT M. D. Anderson Cancer Center,  
Houston, TX*Christopher J. Michejda ..... *NCI-FCRDC, Frederick, MD*David R. Newell ..... *University of Newcastle-upon-Tyne, UK*Makoto Ogawa ..... *Aichi Cancer Center, Nagoya, Japan*Allen I. Oiliff ..... *DuPont Pharmaceuticals Company, Wilmington, DE*Homer L. Pearce ..... *Lilly Research Laboratories, Indianapolis, IN*Martine J. Piccart ..... *Institut Jules Bordet, Brussels, Belgium*Herbert M. Pinedo ..... *Free University Hospital, Amsterdam,  
The Netherlands*Pat Price ..... *Hammersmith Hospital, London, UK*Frank J. Rauscher, III ..... *Wistar Institute, Philadelphia, PA*John C. Reed ..... *Burnham Institute, La Jolla, CA*Marcel Rozenzweig ..... *Bristol-Myers Squibb Co., Princeton, NJ*Nagahiro Saijo ..... *National Cancer Center Research Institute,  
Tokyo, Japan*Edward A. Sausville ..... *NCI, Bethesda, MD*Jan H. Schornägel ..... *Netherlands Cancer Institute,  
Amsterdam, The Netherlands*Makoto Taketo ..... *University of Tokyo, Tokyo, Japan*Chris H. Takimoto ..... *NCI, Bethesda, MD*Masaaki Terada ..... *National Cancer Center, Tokyo, Japan*Jaap Verweij ..... *Rotterdam Cancer Centre, Rotterdam, The Netherlands*Paul Workman ..... *Institute of Cancer Research, Sutton, Surrey, UK*Ken Yamaguchi ..... *National Cancer Center Research Institute,  
Tokyo, Japan*Heinz H. Zwierzina ..... *Medizinische Klinik, Innsbruck, Austria*SPECIAL COMMITTEE  
FOR REVIEW OF ABSTRACTS

Joseph R. Bertino

Bruce A. Chabner

Micheale C. Christian

Neil J. Clendeninn

Susan P. C. Cole

Janice P. Dutcher

Alexander M. M. Eggermont

Susan D. Hellmann

Wau Ki Hong

Loretta Itri

W. Gillies McKenna

Martine J. Piccart

Herbert M. Pinedo

Frank J. Rauscher, III

John C. Reed

Edward A. Sausville

Jaap Verweij



**POSTER SESSION 1**  
**SECTION 1: PHASE I CLINICAL TRIALS: NEW**  
**AGENTS, ANTIANGIOGENESIS, AND MOLECULAR**  
**ENDPOINTS**

**#1 Troxacitabine (BCH-4556), a nucleoside analog with distinct stereochemical, pharmacologic and pharmacokinetic characteristics is tolerable and active in phase I studies: the NCI-C CTG experience.** Moore M, Belanger K, Dionne J, McLean M, Jolvet J, Proulx L, Baker S, Wahnman N, Seymour L. *IND Program, NCIC CTG, Kingston, BioChem Pharma Inc, Canada.*

Troxacitabine (TROX) is a dioxolane L-nucleoside analog with broad cytotoxic activity in *in-vitro* and *in-vivo* models. Other than its unique stereochemistry, TROX has distinct pharmacology: it undergoes intracellular phosphorylation (predominant intracellular form is the diphosphate) but is resistant to deamination and is a complete DNA chain terminator. These interesting characteristics led to the initiation of dose-seeking phase I studies in North America. The phase I study conducted in Canada sought to define the safety and PK profile of troxacitabine when administered as a single 30-minute infusion every 3 weeks.

45 patients (pts) with acceptable organ and marrow function who had received no more than 2 prior chemotherapy (CT) regimens were entered to 13 dose levels (DL's) and received 150 cycles of troxacitabine. The maximum tolerated dose (MTD) was reached at 12.5 mg/m<sup>2</sup>, and the dose recommended (RD) for phase II studies was 10 mg/m<sup>2</sup>. Dose limiting toxicities in the first cycle were confined to self-limited grade 4 granulocytopenia; some patients experienced a generalized maculopapular rash preventable by corticosteroids. At 10 and 12.5 mg/m<sup>2</sup>, hand-foot syndrome occurred in 6 of 13 patients (grade 3 in 2 and grade 2 in 4 patients), 2 patients had treatment discontinued. Two patients at the RD had confirmed partial responses (renal cell carcinoma and carcinoma of unknown origin); overall 18 patients had stable disease with median duration of 6 months (range 1.4–18.7 mths). PK's were linear and at 10 mg/m<sup>2</sup> AUC was 1886 ng · h/ml; C<sub>max</sub> 882 ng/ml; clearance 159 mL/min, and T<sub>1/2</sub> 12 hrs. Clearance was predominantly renal, and drug and creatinine clearance were strongly correlated. Other schedules that have been examined include a daily × 5<sup>1</sup> (RD 1.5 mg/m<sup>2</sup> iv × 5) and a weekly<sup>2</sup> (RD 3.2 mg/m<sup>2</sup>). In view of the PK profile of the compound, the convenience of the 3 weekly schedule and the demonstrable activity at the RD using this schedule, a 30 minute infusion every 3 weeks of TROX 10 mg/m<sup>2</sup> has been taken forward into phase II studies. The NCIC CTG has initiated phase II studies in renal cell and nonsmall cell lung cancer; interim safety and efficacy data will be presented.

<sup>1</sup> Stephenson J, Baker SD, Johnson T et al. Proc Am Soc Clin Oncol 1999

<sup>2</sup> Canova A, Yee L, Baker S et al. Proc Am Soc Clin Oncol 1999

**#2 Phase I and pharmacokinetic (PK) study of a novel cytotoxic agent, PNU-159548, in patients (pts) with solid tumors.** De Jonge Maja J.A., Wortelboer Monica, van der Gaast Ate, Colajori Elena, Valota Olga, Fiorentini Francesco, Verweij Jaap, Sessa Cristiana. *IOSI, Bellinzona, Switzerland; Rotterdam Cancer Institute, Rotterdam, The Netherlands; Pharmacia & Upjohn, Milano, Italy.*

PNU-159548 is the lead compound from a novel cytotoxic class (alkylcycloamines), with a unique mechanism of action combining alkylation and intercalation, and lacking cross resistance with MDR-related drugs, alkylating agents and topo-I inhibitors. In preclinical studies side-effects mainly consisted of hematologic and gastrointestinal toxicity. Two phase I and pharmacologic trials investigate the I.V. administration of PNU-159548 once every 3 weeks in patients with solid tumors. Starting dose, 1 mg/m<sup>2</sup>, was escalated with an initial accelerated phase (1 pt/dose level) followed by conventional dose escalation in 3–6 pt cohorts. The PKs of PNU-159548 and its active 13-dihydro derivative (PNU-169884) were assessed after the first administration by LC/MS-MS.

Overall, 40 pts are entered, 39 pts (median age 55 years; median ECOG PS 1) and 66 cycles are evaluable for toxicity. Dose levels studied were 1, 2, 4, 6, 9, 12 and 14 (ongoing) mg/m<sup>2</sup>. Non-hematological toxicities consisted of nausea and vomiting and were mainly mild. At several dose levels (2, 6, 9 and 12 mg/m<sup>2</sup> [1 pt each] and 14 mg/m<sup>2</sup> [2 pts]) a histamine release syndrome (fever, chills, erythema, facial edema and dyspnoea) was observed during drug administration, which recovered either spontaneously or with anti-histamine therapy. Standard prophylaxis is so far not required. Thrombocytopenia was the main hematologic toxicity and occurred in 18/40 pts during the first cycle, starting from 6 mg/m<sup>2</sup> and was DLT (PLT 50 – 25 × 10<sup>9</sup>/L for 5 days or <25.0 × 10<sup>9</sup>/L) at 6 (1/6 pts), 9 (1/10), 12 (1/9) and 14 mg/m<sup>2</sup> (3/8). Two pts with NSCLC had stable disease for 18 and 19 weeks, respectively (one pt still on treatment). PK data on PNU-159548 show a polyexponential decline, with a t<sub>1/2</sub> of 3–7 h and no significant deviation from linearity. C<sub>max</sub> of PNU-169884 is reached 0.7–1.2 h after treatment and plasma concentrations decline similarly to the parent drug. The systemic exposure to the metabolite is slightly higher than that to PNU-159548. The MTD of PNU-159548 for pretreated pts is 14 mg/m<sup>2</sup> in one study; it has not been reached yet for untreated pts and the studies remain in progress.

**#3 PNU-159548: predicting human MTD from preclinical data.** Sessa Cristiana, De Jonge Maja J.A., Ghielmini Michele, Colajori Elena, Grossi Pietro, Moneta Donatella, Zurlo Maria Grazia, Verweij Jaap. *IOSI, Bellinzona, Switzerland; Rotterdam Cancer Institute, Rotterdam, The Netherlands; Pharmacia & Upjohn, Milano, Italy.*

A model for predicting MTD in humans and possibly guiding dose escalation in phase I studies with cytotoxic agents was suggested by Parchment (1998) for compounds having myelotoxicity as DLT in the preclinical models. The model is based on the use of *in vitro* hematotoxicological data associated with *in vivo* systemic exposure in the same species. PNU-159548 is the lead compound of a novel class of cytotoxic agents (alkylcycloamines) with a promising spectrum of antitumor activity. The compound was judged to be a good candidate for a prospective validation of this model, based on its safety profile (DLT primarily leukopenia and granulocytopenia) and dose-proportionality for both parent drug and active metabolite up to MTD in animals. The relative *in vitro* myelotoxicity was tested in mouse, dog and human bone marrow precursors, thus identifying inter-species differences in drug tolerance (mouse > human > dog) and the IC90 ratios for CFU-GM were used to adjust the target AUC and predict MTD in humans. PNU-159548 is currently tested in two phase I studies with an initial accelerated titration design followed by conventional dose escalation. PKs of PNU-159548 and its major active metabolite (13-dihydro derivative) are assessed during the first cycle in all patients (pts). *In vitro* myelotoxicity of pts plasma is tested in one study to evaluate the cytotoxicity of the compound and of known/unknown metabolites in experimental conditions similar to those in the clinical setting. Overall 40 pts have been treated so far at doses ranging from 1 to 14 mg/m<sup>2</sup> (ongoing). To date, the MTD has been reached (14 mg/m<sup>2</sup>) in pretreated pts in one study. Bone marrow is confirmed to be a primary target in humans, with thrombocytopenia and neutropenia observed starting from 6 mg/m<sup>2</sup>. However, at variance with the observation in animals and based on current results, thrombocytopenia seems to be dose-limiting. PK of both parent drug and metabolite appear to be linear at the tested doses. Preliminary conclusions on the validity of the predictive model, and identification of critical factors, such as protein binding, metabolite contribution, drug-clearance rate, will be presented and discussed.

**#4 The activity and pharmacokinetics of rebeccamycin analog (NSC 655649) in cancer of the biliary tract during a phase I trial.** Dowlati A, Majka S, Hoppel C, Ingalls S, Spiro T, Gerson S, Ivy P, Willson JKV, Sedransk N, Remick SC. *Developmental Therapeutics Program, Ireland Cancer Center, Case Western Reserve University, Cleveland, OH and NCI, Bethesda, MD.*

NSC 655649 is a water soluble analog of the antitumor antibiotic rebeccamycin, which intercalates into DNA and inhibits the catalytic activity of topoisomerase II. We performed a phase I trial to determine the feasibility of administering rebeccamycin analog (RA) as a daily × 5 schedule q21 days and to study the pharmacokinetic (PK) profile. We have previously reported the preliminary data from this trial (Proc. ASCO 1999, a694). In this trial we have observed significant activity in cancer of the biliary tract. Four pts with gallbladder (GB) cancer and one patient with cholangiocarcinoma (5/27 pts) have been enrolled on this trial across all dose levels. Minor response and prolonged stable disease (SD) has been seen in each of these pts. Furthermore, all pts experienced improvement in their performance status. One pt with GB cancer treated at dose level one had a 47% response and is continuing therapy for >2 years. One pt with GB cancer had SD × 9 mos but died of sepsis and liver abscesses. One pt with GB cancer had SD × 10 mos and then progressed. One pt with GB cancer had SD × 5 months and was then taken off study because of increase in bilirubin that needed a stent placement. This pt had a CA19.9 that decreased from 2200 prior to treatment to 700 after cycle 5. The only pt with cholangiocarcinoma has SD × 4 months and is continuing therapy. RA exhibits linear PK's and compartment modeling reveals that the PK best fits a 3-compartment model with a t<sub>1/2α</sub> = 0.2 hr, t<sub>1/2β</sub> = 3.3 hr and t<sub>1/2γ</sub> = 100 hr. Preliminary data suggested enterohepatic circulation. Bile obtained from one pt on day 10 showed levels 10-fold greater than the simultaneous plasma level suggesting significant and prolonged exposure of the biliary tract to RA. Except for one pt, there was no difference in the infusion phase data for pts with cancer of the biliary tract vs other cancer types. This patient had substantially more RA in the day 2 through day 5 pre-infusion plasma. She was admitted on day 8 with biliary stent closure and therefore this deviation may have been due to progressive stent closure during the days of treatment. End of infusion peak plasma concentrations of RA did not increase in proportion to dose escalation in pts with or without biliary tract cancer. This finding is consistent with saturation of plasma protein RA binding capacity in conjunction with rapid distribution of unbound drug to some other components. PK modeling showed similar results between pts with and without cancer of the biliary tract. In conclusion, RA demonstrates activity in cancer of the biliary tract, most likely by virtue of prolonged exposure of the biliary tract to this drug. (Supported by NIH grant nos. 2 UO1 CA62502-06).



**#5 Phase I clinical and pharmacokinetic (PK) trial of E7070, a novel sulphonamide, administered daily x 5 every 3 weeks in patients with solid tumors.** Fumoleau, P., Punt, C.J.A., Priou, F., de Mulder, P.H.M., Bourcier, C., Van de Walle, B., Wanders, J., Faber, M.N., Hanauske, A.R., Ravic, M., Finnegan, V., from EORTC/ECSCG, NDDO Oncology and EISA Ltd-London, UK.

**Introduction:** E7070 is a new chloroindolyl sulfonamide inhibiting the activation of cdk2 and cyclin E in cancer cells at concentrations ranging from 1.4–131.4  $\mu\text{g/ml}$  *in vitro* and inducing cell cycle arrest in G1 and apoptosis. E7070 showed an original cytotoxicity profile suggesting a unique mechanism of action using the NCI-COMPARE program. **Study design:** E7070 was given as a 1 h. i.v. infusion (IV) on 5 consecutive days (d), repeated every 3 weeks. The total E7070 dose was escalated from 50 to 1000  $\text{mg/m}^2/\text{course}$  through 7 dose levels using a standard Phase I design (3–6 pts cohort). PK study was performed during the 1st course (cr). Patient characteristics: to date, 25 patients with miscellaneous solid tumors: 17 females/8 males, median age (yrs): 53 (27–69), median PS: 1 (0–2). **Study results:** data is summarized for 25 pts and 69 crs (1–6).

Dose-Level	No. of pts	No. of crs	DLT's
10 $\text{mg/m}^2 \times 5$	6	17	1/6 -atrial fibrillation at 2nd course
13 $\text{mg/m}^2 \times 5$	3	6	0/3
26 $\text{mg/m}^2 \times 5$	3	6	0/3
52 $\text{mg/m}^2 \times 5$	3	14	0/3
104 $\text{mg/m}^2 \times 5$	3	7	0/3
200 $\text{mg/m}^2 \times 5$ (MTD)	3	9	2/3 -febrile neutropenia, -gd 4 neutropenia & thrombocytopenia
160 $\text{mg/m}^2 \times 5$ (currently explored)	4	10	1/4 -gd 4 neutropenia & thrombocytopenia & gd 4 mucositis

Preliminary PK results indicate that E7070 displays a long half-life  $T_{1/2}$  and a large volume of distribution. At dose-levels above 52 x 5  $\text{mg/m}^2$   $C_{\text{max}}$  increases proportionally while AUC increases more than dose-proportional and the clearance &  $V_{\text{diss}}$  tend to decrease suggesting a non linearity in the PK's. So far, no response is reported.

**#6 Phase I study of PS-341, a novel proteasome inhibitor, in patients with advanced malignancies.** Papandreou Christos N, Pagliaro Lance, Millikan Randall, Dallan Danai, Herrmann John, Hong Yang, Smith Mathew, Adams Julian, Elliott Peter, Lightcap Eric, McCormack Teresa, Pien Chris, Newman Robert, Logothetis Christopher J. Department of Genitourinary Medical Oncology, The University of Texas M.D. Anderson Cancer Center, Houston, TX, 77030 and Leukosite, Inc., Boston, MA 02139

The ubiquitin-proteasome pathway plays an important role in neoplastic growth and metastasis through regulation of cell-cycle regulatory proteins (p53, p21<sup>waf1</sup>, and p27<sup>Kip1</sup>). In addition, it regulates the activation of the nuclear factor NF- $\kappa$ B, a key transcriptional regulator of cell adhesion molecules (E-Selectin, intercellular adhesion molecule-1 (ICAM-1) and vascular cell adhesion molecule-1 (VCAM-1)), which are involved in tumor metastasis and angiogenesis *in vivo*. We are currently conducting a Phase I trial with PS-341, a proteasome inhibitor, in patients with advanced malignancies. **Objectives:** 1) Define maximum tolerated dose and dose limiting toxicity of PS-341 as an intravenous (i.v.) push administration over a range of doses (0.13–0.75  $\text{mg/m}^2$ ) in patients with advanced malignancies. 2) Correlate toxicity with proteasome inhibition in peripheral blood. **Methods:** To date, 12 patients (9: androgen-independent prostate cancer, 2: metastatic renal cell carcinoma, 1: metastatic colon cancer) have been treated (4 at: 0.13  $\text{mg/m}^2$  and 2 each at: 0.25, 0.4, 0.6, 0.75  $\text{mg/m}^2$ ) with i.v. PS-341 weekly for 4 weeks in a 6-week cycle. Dose escalation is defined by the continuous reassessment method. Proteasome activity in patients' peripheral blood is measured ex-vivo using fluorogenic peptide substrates. **Results:** All patients completed at least one cycle of treatment. Four of 12 patients received 2 or more cycles of PS-341. No toxicity has been observed so far. One patient achieved partial response (major radiographic response of retroperitoneal lymph nodes (RPLN) without PSA change) and a second patient had radiographic stabilization of RPLN with unchanged PSA. A 55–60% proteasome inhibition in peripheral blood has been achieved at the current dose level (0.75  $\text{mg/m}^2$ ). **Conclusion:** 1) Up to the current dose of PS-341, no toxicity was observed. 2) At 24 hrs after drug infusion, proteasome inhibition was achieved as predicted. 3) Responses were seen even at low levels of proteasome inhibition. Further dose escalation (with pharmacokinetics and proteasome inhibition studies) is in progress. This early evidence of clinical activity without toxicity justifies further development of this agent with a novel mechanism of action. This work was supported by awards from the Association for the Cure of Cancer of the Prostate (CaPCURE) to C.N.P. and C.J.L.

**#7 CCI-779, A new Rapamycin analog, Has Antitumor Activity at Doses Inducing Only Mild Cutaneous Effects and Mucositis: Early Results of an Ongoing Phase I Study.** J. Alexandre\*, E. Raymond\*, H. Depenbrock\*, S. Mekhaldi\*, E. Angevin\*, C. Palliet\*, A. Hanauske\*, J. Frisch, A. Feussner, J.P. Armand\*. Department of Medicine, Institut Gustave-Roussy, 94805 Villejuif cedex, France, Onkologische Tagesklinik\*, München, Germany, Genetics Institute, München, Germany.

Like rapamycin, CCI-779 interacts with the protein kinase mTOR thus preventing the phosphorylation of eIF4E-BP1 and p70S6K thereby inhibiting the initiation of the translation of messenger RNAs. We report the early results of a phase I study of CCI-779 given as a weekly 30 min. i.v. infusion in patients (pts) with advanced solid tumors. So far, 12 patients (pts) have been treated at the doses of 7.5, 15.0, 22.5, 34.0, 45.0, and 60.0  $\text{mg/m}^2/\text{w}$  using a modify continuous reassessment method for dose escalation. CCI-779 does not appear so far to have any significant immunosuppressive effect. No opportunistic infection was observed. The immunophenotype of peripheral lymphocytes (CD3, CD4, CD6, CD45, CD14, and CD56) and the mitogen proliferation assays (phytohemagglutinin, concanavaline A, PWM) did not reveal any significant modifications. However, a reactivation of peri-oral herpes lesions was observed in 5 pts within the first month of treatment and rapidly resolved under oral acyclovir. Interestingly, significant tumor regressions were rapidly observed in 2 pts with lung metastasis of renal cell carcinomas both treated with 15  $\text{mg/m}^2/\text{w}$  and in one patient with a neuroendocrine tumor of the lung treated with 22.5  $\text{mg/m}^2/\text{w}$ . Responses occurred after 8 weekly doses. Additionally, 2 patients experienced tumor stabilization. Neither grade III-IV nor dose-limiting toxicity have been reported so far. Only mild grade I-II skin reactions and mucositis were observed at each dose level but did not increase in intensity while the dose-escalation was performed. Dryness of the skin with mild itching, fine scaling, and mild facial erythema occurred in 6 pts after the 1st infusion and lasted during the overall period of treatment. Mild hypersensitivity reactions were observed in all the pts including: (1) sub-acute urticaria in 1 pt immediately after the 1st infusion which did not reoccur during subsequent cycles, (2) <<Eczema-like>> lesions on the anterior side of arms in 2 pts, and (3) aseptic follicles were associated with self-limited erythematous papules with central vesiculations occurring in bold areas in 7 pts. In the latest 7 pts, concomitantly to the skin reactions, grades I or II mucositis were observed associated with genital mucous membrane erosion in 1 pt. Skin biopsies were performed in all the pts experiencing skin reactions and consistently showed an aspect of folliculitis with infiltrate of neutrophils associated with non-specific superficial peri-capillary dermatitis. With repeated dosing transient regressions were usual, accelerated in some patients by topical steroid therapy and antiseptics. No alopecia was reported. Nails changes consisting of thickness and dystrophy progressively increased in pts receiving more than 8 doses. The study is ongoing to determine the dose limiting toxicity and the dose to be recommended for phase II studies.

**#8 Phase I clinical and pharmacokinetic (PK) study of the Cryptophycin analog LY 355703 administered on an every 3 weeks (wke) schedule.** Paganl, O., Greim, G., Welgand, K., Westphal, K., Van den Bosch, S., DePas, T., Burgess, M., Weimer, I. and Sessa, C. IOSI, Balinzona, CH; Klinikum Nürnberg, Nürnberg, D; EIO, Milano, I; Lilly Research Centre, Windlesham, UK.

Cryptophycins are antimitotic antitumor agents from blue-green algae which inhibit microtubule dynamics with characteristics partially like vinblastine and partially like paclitaxel. The synthetic Cryptophycin LY355703 is highly potent (*in vitro* activity at picomolar concentrations) has antitumor activity in murine and human tumor xenografts, and high activity in tumors expressing the MDR phenotype, including models resistant to paclitaxel. In toxicology studies dose-limiting toxicities (DLT) were neutropenia in rats and diarrhea in dogs, the latter being the most sensitive species. The starting dose for this study on a single q 3wks schedule was 0.1  $\text{mg/m}^2$ , corresponding to 1/10 of the Maximum Tolerated Dose in dogs; doses were escalated according to a modified Continual Reassessment Method. LY355703 was administered as 2 h i.v. infusion. Premedication with i.v. Dexamethasone, H<sub>2</sub> and H<sub>2</sub> antagonists 30 min before LY dose was given starting from the 0.88  $\text{mg/m}^2$  dose because of moderate hypersensitivity reactions to Cremophor EL observed at the previous dose (0.88  $\text{mg/m}^2$ ). The plasma concentration of LY355703 was investigated by LC-MS-MS method with a detection limit of 0.25  $\text{ng/mL}$ . Twenty-nine patients (pts) with a variety of solid tumors (soft tissue sarcoma 8, renal 5, colon 4) and 10 dose levels have been evaluated so far. At the highest dose level of 1.92  $\text{mg/m}^2$ , 2 of 5 pts presented self-limiting DLTs (G3 neuropathic pain in 1 pt, G3 myalgia and constipation in the other) which appeared within 3 days of the infusion and required opioids. The dose of 1.7  $\text{mg/m}^2$  was then tested in 2 pts with occurrence of self-limiting G3 myalgia within 48 hours in both, in spite of prophylactic analgesia. Overall, peripheral neuropathy was mainly sensory and of moderate degree and not necessarily dose related nor cumulative; neutropenia was sporadic and only moderate; total alopecia was observed only in pts who presented DLTs. PK was linear from 0.1  $\text{mg/m}^2$  to 1.92  $\text{mg/m}^2$  with mean ( $\pm$ SD)  $t_{1/2}$  of 2.6 hr ( $\pm$ 1.02),  $Cl_p$  of 90.4 L/hr ( $\pm$ 50.3) and no apparent correlation to



DLT in patients was demonstrated. Objective responses have not as yet been observed. Additional pts are being accrued at 1.48 mg/m<sup>2</sup> to define the most appropriate Ph II dose.

**#9 BAY 12-9566, a selective, non-peptidic biphenyl inhibitor of matrix metalloproteinases (MMPs): summary of phase I clinical and pharmacokinetic (PK) results.** Lathia C., Seymour L., Grochow L., Eckhardt G., Erlichman C., Hirte R., Goel R., Ellis I., Humphrey R. *NCI-Canada Clinical Trials Group; Johns Hopkins; CRTG; Mayo Clinic; Bayer Inc.; Bayer Corp.*

**Introduction:** MMPs are involved in invasion, metastasis and angiogenesis. MMPs 2 & 9 are overexpressed in the tumor/stroma of multiple cancers, and are thus attractive targets for inhibition. BAY 12-9566 (BAY) has nM inhibitory activity against MMPs 2, 3 & 9 with anti-invasive, anti-metastatic and anti-angiogenic activity in preclinical models.

**Methods:** Four dose ranging trials of oral BAY were conducted in North America to define PK/safety. Dose limiting toxicity (DLT) was toxicity  $\geq$  grade 3; symptomatic, dose limiting or  $\geq$  7 days grade 2. Maximum tolerated dose (MTD) was declared if  $\geq$  2 pts experienced DLT. Eligible pts had PS 0-2 and acceptable organ function.

**Results:** 69 eligible pts (median age 67 yrs) with CRC (31), breast (10), RCC (10), ovary (7), sarcoma (7), melanoma (6) and other (18) were enrolled to 9 dose levels. Dose related effects were limited to mild anemia and reversible, mild to moderate reduction in platelet counts (plts) (nadir d 15-27); in 4 heavily pretreated pts, plts fell to 50-100,000 leading to prophylactic dose reduction. Mild reversible GI effects (nausea, flatulence) and transaminase elevations were observed in some pts; musculoskeletal effects were not reported. MTD was not reached although DLT (plts) was seen in 1 pt at each of 3 dose levels. Due to the low aqueous solubility of BAY, there were less than proportional increases in C<sub>max</sub> and AUC with doses > 100 mg/day. BAY exhibited a biexponential plasma concentration-time profile and was rapidly absorbed (mean t<sub>max</sub> 1-4 hrs). The half-life of BAY is 100 hrs.

**Efficacy:** 2/7 pts with ovarian cancer had 28% and 37% decrease in CA-125 levels. 32 (36%) pts remained on BAY for 100 days or more, 11 (12%) for 200 days or more, and 5 (6%) for greater than one year (metastatic CRC (2), metastatic RCC (1), taxol-resistant ovarian (1), mesothelioma (1)).

**Conclusions:** Oral BAY (800 mg bid) is well tolerated with transient and usually clinically insignificant decreases in platelet counts and mild anemia the only dose related toxicities.

**#10 A phase I dose escalation study of docetaxel with G-CSF support given three weekly in patients with solid tumors.** Mitchell PLR, Bassar R, Ng S, Harris M, Chipman M, Grigg A, Mansfield R, Gargano JA, Jeffrey AL, Soulas F, Appia F, Green M. *CDCT (Austin & Repatriation, Royal Melbourne, and Western Hospitals), Melbourne, Australia, and Rhone-Poulenc Rorer, Melbourne and Paris.*

In previous studies of docetaxel (TXT) given q21d over 1 hr, dose limiting toxicity (DLT) was neutropenia and its complications. To explore dose intensification of this schedule, G-CSF was used in a phase I dose escalation study. Eligible patients (pts) were performance status 0-2 and had received  $\leq$  one prior chemotherapy regimen for advanced disease. The maximum tolerated dose (MTD) was defined as the dose where  $\geq$  3 out of 6 pts developed a DLT during cycle 1 (NCICTC neurotoxicity  $\geq$  grade III at any time or  $\geq$  grade II on day 21, prolonged febrile neutropenia, or other toxicities  $\geq$  grade III). A 3 day steroid prophylaxis was given, and pts received G-CSF (lenograstim) 5  $\mu$ g/kg/day sc from day 2 until neutrophils  $\geq$  1  $\times$  10<sup>9</sup>/l. 35 pts with various solid tumors were entered. Median age was 57 yrs (29-76) and 16 pts had previously received chemotherapy. TXT dosing commenced at 110 mg/m<sup>2</sup> as a one hour infusion q21d and was escalated by 10 mg/m<sup>2</sup> for cohorts of 3-6 pts. At TXT 170 mg/m<sup>2</sup>, 2 of 3 pts experienced DLTs: grade III neuropathy and grade III skin toxicity respectively and this was considered to be the MTD. The same DLTs were observed in 2 other pts, both treated at TXT 130 mg/m<sup>2</sup> (2 of 6 pts at this dose level). Of the first 29 pts, grade IV neutropenia was observed in 10 pts (35%). The median neutrophil nadir occurred prior to day 8, with day 8 being the median day of G-CSF cessation. Only 3 pts developed febrile neutropenia, which was not prolonged. Mobilisation of progenitor cells was examined during cycle one for all pts. Median CD34<sup>+</sup> cell levels rose from 0.1  $\times$  10<sup>6</sup>/l at baseline to a peak of 2.2  $\times$  10<sup>6</sup>/l on day 8, and 60% of pts had peak levels  $\geq$  1  $\times$  10<sup>6</sup>/l. 25 breast cancer pts with no prior chemotherapy for advanced disease are currently being recruited at the recommended dose of TXT 160 mg/m<sup>2</sup>. Presently 12 pts have been treated at TXT 160 mg/m<sup>2</sup> without DLTs. In conclusion, TXT 160 mg/m<sup>2</sup> given q21d with G-CSF support may be administered safely to this patient population. The neutrophil nadir occurred early. Only 35% of pts experienced grade IV neutropenia and the incidence of febrile neutropenia was low. Mobilisation of haemopoietic progenitor cells by this regimen of TXT with lenograstim was demonstrated.

**#11 Phase I clinical and pharmacokinetic study of Intravenous estramustine phosphate (IV-EMP).** Hudes, G.R., Haas, N.B., Yeslow, G., Gillon, T., Bruns, M., Gunnarsson, P.O., Ellman, M., Nordie, O., Kopreski, M., Hartley-Aap, B. *Fox Chase Cancer Center, Philadelphia PA and Pharmacia and Upjohn, Kalamazoo, MI*

Oral estramustine phosphate (EMP) is used extensively for treatment of hormone refractory prostate cancer (HRPC). Nausea and fluid retention are common dose-limiting toxicities (DLT). By avoiding first-pass hepatic metabolism, intravenous administration may reduce toxicity and achieve higher plasma concentrations of EMP active metabolites. We administered IV-EMP by 30-90 min i.v. infusion weekly  $\times$  4, cycles repeated every 4 weeks. IV-EMP dose was escalated from 500 to 3000 mg/m<sup>2</sup>. All 31 patients enrolled had metastatic HRPC and 13/31 (42%) had prior chemotherapy, including prior oral EMP in 10 (32%).

**Results:** Of 4 patients treated at 3000 mg/m<sup>2</sup>, 3 had DLT: grade 3 fatigue in two patients, and grade 3 hepatotoxicity and cardiotoxicity (reversible LBBB with hypotension) in a third patient. Nausea/vomiting (grade 1-2) were usually limited to the day of treatment. Transient rectal burning at the start of infusion was common and relieved by increasing infusion duration. IV-EMP pharmacokinetics were dose-independent from 500-2000 mg/m<sup>2</sup>, and C<sub>max</sub> and AUC values for active metabolites estramustine (EAM) and estromustine (EOM) increased dose-proportionally. At 2000 mg/m<sup>2</sup>, mean  $\pm$  SD values for EMP total clearance, V<sub>d</sub> and T<sub>1/2</sub> were 48.6  $\pm$  18.6 ml/hr/kg, 171  $\pm$  57 ml/kg, and 2.5  $\pm$  0.4 hr. C<sub>max</sub> values for EAM and EOM were 10.4  $\pm$  2.9  $\mu$ M and 15.6  $\pm$  5.1  $\mu$ M. T<sub>1/2</sub> for the metabolites ranged from 80 to >100 hrs, resulting in day 7 (C<sub>min</sub>) concentrations exceeding .1  $\mu$ M for EAM and 1  $\mu$ M for EOM, comparable to steady-state concentrations achieved with standard dose oral EMP. Of 19 patients with elevated pretreatment PSA who received  $\geq$  4 weeks of IV-EMP, 9 (47.4%) had  $\geq$  50% declines.

**Conclusions:** IV-EMP is active in HRPC and appears to be better tolerated than oral EMP. The MTD on a weekly  $\times$  4 schedule is 2500 mg/m<sup>2</sup> and the recommended dose for phase II evaluation in HRPC is 2000 mg/m<sup>2</sup>. High EOM and EAM C<sub>max</sub> values following IV-EMP may be particularly advantageous for antimicrotubule drug combinations.

**#12 A multicenter, dose escalating study in patients with AIDS-related Kaposi's sarcoma.** Arastéh, K; Miles, S; Gill, P; Jacobs, M; Friedman-Kien, A; Gracey, S; Barkhimer, D; Hannah, A; Scigalla, P; and Langecker, P. *Auguste-Viktoria-Krankenhaus; UCLA CARE Center; USC Norris Cancer Center; St. Francis Memorial Hospital; NYU Medical Center; SUGEN, Inc.*

Angiogenesis is one of the most important features of AIDS-associated Kaposi's sarcoma (AIDS-KS). The strong expression of both Flk-1/KDR and flt-1 in small stromal vessels in and around tumors suggests that Vascular Endothelial Growth factor (VEGF) may be an important regulator of the edema and angiogenesis seen in Kaposi's sarcoma. SU5416 is a specific Flk-1 antagonist, decreasing VEGF-stimulated Flk-1 phosphorylation and VEGF-mediated signaling.

Up to 30 patients with cutaneous AIDS-KS who are stable or have progressed under current therapy are being treated with escalating doses of SU5416 administered twice weekly I.V. Starting dose was 65 mg/m<sup>2</sup>, escalated to 85, 110 and 145 mg/m<sup>2</sup>. Plasma levels of SU5416 and its metabolites, protease inhibitor levels, HIV viral load, and T-cell subset counts are measured. Lesion size, extent of edema, as well as investigator and patient global assessments are performed at four-week intervals. Response categorization is based on standard ACTG criteria. Patients must maintain a stable anti-retroviral therapy regimen to be evaluable.

To date, twenty HIV+ male patients with AIDS-related Kaposi's sarcoma, ages from 30-52 (m = 37), with KPS of 70-100 have received doses of SU5416 ranging from 65-145 mg/m<sup>2</sup> for up to four cycles of therapy (29 days per cycle). Among the first eighteen patients in whom outcome could be assessed, eleven have evidence of biological activity (flattening, shrinkage or dissolution of lesions; reduction or dissolution of edema), four patients had stable disease, and three patients had progressive disease. Individual patients showing response reported pain reduction and increased mobility, such as the ability to walk without assistance, wear and tie shoes, eat and swallow normally, etc.

At the current dose, no dose-limiting toxicity has been observed to date. Individual patients treated at the higher doses reported mild headaches, which decreased with continued therapy. Several patients observed transient nausea. Two of the twenty patients discontinued treatment due to local toxicity at the site of SU5416 administration (which may be ameliorated by peripheral access device).

SU5416 appears to have biological activity in AIDS-KS patients, even those that have failed multiple prior therapies. Side effects reported to date are mild to moderate and responsive to supportive care.

**#13 A Phase II/III study of SU5416 in combination with 5-FU/leucovorin in patients with metastatic colorectal cancer.** L ROSEN<sup>1</sup>, P ROSEN<sup>1</sup>, R AMADO<sup>1</sup>, D CHANG<sup>1</sup>, M MULAY<sup>1</sup>, M PARSONS<sup>1</sup>, B LAXA<sup>1</sup>, P LANGECKER<sup>2</sup>, S GRACEY<sup>2</sup>, A SIEK<sup>2</sup>, AND A HANNAH<sup>2</sup> <sup>1</sup>UCLA Medical Center, Los Angeles, CA; <sup>2</sup>SUGEN, Inc., S. San Francisco, CA.

Adenocarcinoma of the large bowel affects more than 155,000 patients per year in the U.S.; 20-25% present with metastases or will develop local



recurrence or metastatic disease. Serum levels of vascular endothelial growth factor (VEGF) in colorectal cancer patients correlate positively with stage of disease, formation of liver metastases and rate of disease progression. SU5416, a receptor tyrosine kinase, decreases VEGF-stimulated Flk-1 phosphorylation. Inhibiting VEGF-driven neovascularization *in vivo* by SU5416 reduces or prevents tumor regrowth or metastasis proliferation. In preclinical studies using a human colon cancer cell line, daily administration of SU5416 in combination with 5-FU produced 55% tumor growth inhibition, an additive effect over either agent used alone.

Up to 30 patients with untreated metastatic colorectal cancer are treated with increasing doses of SU5416 administered twice weekly i.v., in combination with standard doses of 5-FU/LV therapy administered under either the Mayo Clinic or Roswell Park regimens. Starting dose of SU5416 was 85 mg/m<sup>2</sup>, escalated to 145 mg/m<sup>2</sup>. The primary objective of the study is to determine if these three agents can be safely combined for future Phase II/III trials. Data regarding response rate, time to progression, survival and pharmacokinetic interactions are being collected.

To date, 16 patients (ages from 33-76, KPS 70-100) have been treated. On the Mayo Clinic regimen, 3 patients have been treated at 85 mg/m<sup>2</sup> of SU5416; 7 at 145 mg/m<sup>2</sup>. On the Roswell Park regimen, 3 patients have been treated at 85 mg/m<sup>2</sup>; 3 at 145 mg/m<sup>2</sup>.

As expected, 5-FU/LV-related toxicity predominates. To date, no dose-limiting toxicity attributable to SU5416 has been observed. Both regimens appear to be tolerable combined with full-dose SU5416. Individual patients treated at the higher doses reported mild headaches, which decreased with continued therapy. Several patients observed transient nausea. One patient with a central venous catheter experienced a pulmonary embolism and DVT; the relationship to SU5416 is not known. Other side effects reported are generally mild to moderate and responsive to minimal supportive care. To date, no patient has experienced progressive disease. Longest length of time on study is 5+ cycles (more than 130 days on study).

**#14 Combretastatin A4 phosphate (CA4P) selectively targets vasculature in animal and human tumors.** Justin GJS, Galbraith SM, Taylor NJ, Maxwell R, Tozer G, Baddelay H, Wilson I, Prise V. Mount Vernon Hospital, Northwood, Middlesex, UK.

CA4P dramatically reduces blood flow in animal tumours at non toxic doses, causing haemorrhagic necrosis.

**Aim:** To determine the dose response and reversibility of CA4P on tumour blood flow in rats and humans.

**Methods:** The blood flow of tumours and normal tissues in BD9 rats bearing P22 carcinosarcomas was measured using radiolabelled iodoantipyrine (IAP). Serial dynamic Gd-DTPA contrast MRI scans were performed on the same tumour model and on patients in the CRC phase 1 trial of CA4P. The maximum gradient on the signal intensity time curve from the dynamic series of T1 weighted MR images was used as a measure of perfusion. Patients were treated once weekly for 3 doses with intra-patient dose escalation allowed until grade 2 toxicity was seen.

**Results:** Tumour blood flow measured by IAP in rats was reduced to <20% of pre treatment levels at 10 mg/kg by 6 hrs post CA4P, with recovery to 80% of pre treatment levels by 24 hrs. At 100 mg/kg blood flow reduced to <5% at 6 hrs and the reduction was maintained at 24 hrs. The only organ with substantial blood flow reduction at any dose was the spleen (80% at 100 mg/kg). Dynamic MRI measurements in the same tumour model demonstrated a reduction in gradient to 76% of pre treatment levels at 6 hrs at 10 mg/kg, with complete recovery at 24 hrs and reduction to 71% of pre treatment levels at 100 mg/kg, maintained at 24 hrs. 7 of 14 patients treated with 5 to 88 mg/m<sup>2</sup> CA4P had serial MRI scans. The main toxicity has been grade 2 tumour pain occurring within 2 hours at the highest dose. Reductions in gradient up to 65% measured by MRI have been seen at dose levels above 10 mg/m<sup>2</sup>, and where multiple scans have been performed on an individual patient at 88 mg/m<sup>2</sup>, a similar time course to that seen in rats has been demonstrated, with maximal reduction to 71% of pre treatment levels at 6 hrs and recovery to 86% of pre treatment levels by 24 hrs.

**Conclusions:** CA4P selectively reduces tumour blood flow in human as well as animal tumours. The time course of action is similar in rat and human tumours.

**#15 A phase I and pharmacokinetic (PK) study of the unique angiogenesis inhibitor squalamine lactate (MSI-1256F).** Patnaik Amita, Rowinsky Eric, Hammond Lisa, Thurman Allison, Hidalgo Manuel, Slu Lillian, Williams Jon, Holroyd Ken, Nelson Kim, Von Hoff Daniel D, Eckhardt S. Gail. Cancer Therapy and Research Center and South Texas Veterans Health Care System, Audie Murphy Division, San Antonio, TX, and Magainin Pharmaceuticals Inc., Plymouth Meeting, PA.

Squalamine (MSI-1256F), originally derived from the liver of the dogfish shark *Squalus acanthias*, is a novel noncytotoxic aminosterol with potent antiangiogenesis effects *in vitro* and *in vivo*. The agent, which is chemically synthesized as a 7-24-dihydroxylated-24-sulfated cholestane steroid conjugated to a spermicide at C3, prevents neovascularization of tumors by inhibition of mitogen-induced proliferation, as well as the migration of endothelial cells. Chick chorioallantoic membranes, which bear striking similarity to tumor capillaries, show significant reduction in caliber after the

application of as little as 0.1 µg/mL of squalamine following a one hour exposure. This phase I study was performed to evaluate the feasibility and pharmacokinetic behaviour of squalamine when administered as a 5-day continuous infusion every 3 weeks, utilizing the continual reassessment method (CRM) of dose escalation and the accrual of a single patient at dose levels associated with minimal toxicity. Thus far, 21 patients have received 39 courses at the following dose levels: 6, 12, 24, 34, 47.6, 66.64, 93, 130, 182, 255, 357 mg/m<sup>2</sup>/day. Patient characteristics include: median age of 62 years (range 20-76), median performance status 1, prior treatment: chemotherapy, 11; radiation + chemotherapy, 10. Brief grade 3-4 transaminase elevations have occurred in 2/4 and 2/6 patients at the 357 mg/m<sup>2</sup>/day and 255 mg/m<sup>2</sup>/day levels, respectively. Transaminase elevations have occurred between days 3 and 5, with resolution within 24-48 hours of stopping the infusion. Toxicities that are not dose-limiting include grade 1-2 nausea/vomiting (11), grade 1-2 fatigue (14), and grade 1-2 anorexia (9). Preliminary noncompartmental PK analysis in 13 patients treated at doses between 6 mg/m<sup>2</sup> and 357 mg/m<sup>2</sup> has revealed steady-state concentrations ranging from 0.21 µg/mL to 10.42 µg/mL. Clearance (3.73 ± 0.9 L/hr) does not vary significantly with dose. Over the range of dosages explored in this trial, the steady state plasma concentrations of squalamine appeared to increase linearly. Squalamine is well tolerated up to dosages of 255 mg/m<sup>2</sup> and at dose levels evaluated thus far, demonstrates biologically relevant plasma concentrations approaching those required for antiangiogenic effects *in vitro*. Further patient enrollment is continuing at the 357 mg/m<sup>2</sup> dose level, to obtain more experience and better define the toxicity profile of this agent.

**#16 Phase I pharmacokinetic study of single dose intravenous (IV) combretastatin A4 prodrug (CA4P) in patients (pts) with advanced cancer.** Remick SC, Dowlati A, Robertson K, Spiro T, Connell C, Levitan N, and Stratford M. Developmental Therapeutics Program, Ireland Cancer Center, Case Western Reserve University, Cleveland, OH and Gray Laboratory, Mt. Vernon Hospital, London, UK.

CA4P disodium phosphate is a novel anti-tumor vascular targeting agent, which is the first of a series of combretastatin analogues to enter the clinic. CA4P is a prodrug and is rapidly dephosphorylated to the active compound combretastatin, which has a broad range of cytotoxicity in preclinical models. The drug binds the colchicine-binding site on tubulin, and inhibits microtubule assembly. Animal studies have confirmed immediate shutdown of tumor vasculature that appears selective and does not affect normal vessels. Based on these observations, we have embarked on a phase I trial single IV dose of CA4P (10-min infusion) at 3-wk intervals in pts with advanced malignancy. To date a total of 12 pts (5M/7F) have been treated. All pts have received prior therapy. A total of 46 cycles of therapy have been given over 4 dose levels to pts each [18, 36, 60 and 90 mg/m<sup>2</sup>-14, 8, 12, 12\* (8\* cycles reduced dose to 60 mg/m<sup>2</sup> after DLT)] respectively. A variable symptom complex has been identified across all dose levels several hours following infusion. Faint flush, abdominal pain, and other pain in sites of known tumor have been observed. Dose-limiting toxicity (DLT) has been encountered at 90 mg/m<sup>2</sup>, including an episode of grade 3 pulmonary toxicity (shortness of breath) and a reversible episode (during cycle 2) of acute coronary ischemia (without sequelae and with preservation of normal myocardial function) thought secondary to coronary vasospasm. Preliminary pharmacokinetic analysis in a single pt at 60 mg/m<sup>2</sup> yielded for CA4 t<sub>1/2α</sub> of 7.3 min, t<sub>1/2β</sub> 40.1 min, and AUC<sub>0-24h</sub> 13.3 µmol.h/L; for CA4 t<sub>1/2α</sub> of 4.0 min, t<sub>1/2β</sub> 1.11 h, t<sub>1/2γ</sub> 6.74 h, and AUC<sub>0-24h</sub> 2.12 µmol.h/L; and for C<sub>4gluc</sub> t<sub>1/2α</sub> of 4.01 h and AUC<sub>0-24h</sub> 95.4 µmol.h/L. The drug is primarily metabolized by glucuronidation. A pt with anaplastic thyroid carcinoma has had a complete response. (This trial is supported by a clinical research grant from OXIGENE, Inc., Boston, MA.)

**#17 A phase I trial of BCL2 antisense drug G3139 (Genta, Inc.) delivered by continuous intravenous infusion alone and in combination with weekly paclitaxel.** Morris, Michael J., Tong, William, P., Cordon-Cordo, Carlos, Drobnjak, Marija, Kelly, William K., Slovins, Susan F., Terry, Kathryn L., DiPaola, Robert, S., Rosen, Neal, and Scher, Howard I. Memorial Sloan-Kettering Cancer Center, NY, NY.

G3139 is an 18 mer oligonucleotide that targets the messenger RNA of BCL2, a gene associated with tumor growth and resistance to therapy. We have previously reported on 15 patients who were treated with G3139 at doses up to 2.3 mg/kg/day as a single agent by continuous intravenous infusion. No dose limiting toxicities were encountered. In preclinical studies, G3139 acts synergistically with the taxanes. In an extension of our clinical trial, dose escalations continued and patients who received doses of 4.1 mg/kg/d or higher were treated with the combination of G3139 and weekly paclitaxel at 100 mg/m<sup>2</sup> during cycles 2 and 3. In addition to pharmacokinetic assessments, peripheral blood lymphocytes were stained by immunohistochemistry for BCL2 expression throughout each treatment cycle.

A total of 32 patients have been treated to date, up to 5.3 mg/kg/day of G3139. These include 21 patients with prostate cancer, 7 renal cell, 1 esophageal, 1 colon, 1 sarcoma, and 1 unknown primary. The dose levels were 0.6, 1.3, 1.7, 2.3, 3.1, 4.1, and 5.3 mg/kg/day, with each cohort composed of 3-6 patients. Three patients have been treated with the combination of G3139 and weekly paclitaxel. Median number of paclitaxel doses per patient is 3 (range 1-5). Grade III toxicities possibly attributable to drug with G3139 monotherapy



are leukopenia (1 pt), arthralgias (1 pt), fatigue (1 pt), and rash (1 pt); there have been no grade IV drug-related toxicities. Toxicities possibly conferred by the addition of paclitaxel to the regimen are restricted to grade II mucositis (1 pt). The percentage of lymphocytes staining for BCL2 can decline within 1-2 cycles of treatment with G3139 as a single agent and returns to baseline off treatment. We conclude that at the doses tested to date G3139 is well tolerated in combination with paclitaxel, and that little additive toxicity is seen with the two agents. Staining of peripheral lymphocytes for BCL2 confirms targeting of the protein product. The results of Western blotting to determine the optimal biologic dose are ongoing. Supported by Genta Corporation, CaPCURE, CA 05826 and CA09207.

**#18 Bryostatins C and cisplatin: phase I study with pharmacodynamic guidance.** Muggia Franco, Liebes Leonard, Oratz Ruth, Fry David, Wadler Scott, Hochster Howard, Rosenthal Mark, Hamilton Anne, NYU Medical Center/Montefiore Medical Center (U-01 CA#76642-01)

Bryostatins C (Bryo) is a potent inhibitor of certain protein kinase C (PKC) isoforms. In HeLa cells Basu and Lazo (Cancer Res 1992;52:3119-24) demonstrated enhancement of cisplatin cytotoxicity following a 24 h exposure of Bryo. This enhancement occurred at concentrations of 0.1-10  $\mu$ M of Bryo, and was absent at higher concentrations. In a dose-escalation design we treated 28 melanoma patients in cohorts of 3 with Bryo 10, 15, 20, 25 and 30  $\mu$ g/m<sup>2</sup> for 24 h preceding cisplatin 50 mg/m<sup>2</sup>, and one cohort with Bryo 30  $\mu$ g/m<sup>2</sup> and cisplatin 75 mg/m<sup>2</sup>. No dose limiting toxicities (DLT) were observed; the only toxicities were attributable to cisplatin, and myalgia was not observed. One partial response was noted.

Once Bryo detection was achieved, the protocol was modified to 1 h Bryo at 40  $\mu$ g/m<sup>2</sup> prior to cisplatin 50 mg/m<sup>2</sup> and opened to accrual of patients with various malignancies. An organic plasma extraction procedure is used to simultaneously extract Bryo while precipitating plasma proteins, and a plasma assay based on the detection of Bryo by HPLC using UV detection at 266 nm along with parallel detection by mass spectroscopy has been developed. The assay in its current state has a sensitivity of 1 ng/ml, but is being extended to at least 0.20 ng/ml through developments in the extraction procedure. Preliminary data show that the analysis of the Bryo plasma extracts by mass spectroscopy yields at a 10-fold increase in sensitivity over the HPLC analysis. In 3 patients receiving 40  $\mu$ g/m<sup>2</sup>, Bryo measured immediately after the infusion and prior to cisplatin was detected in 2 patients (16 and 4 nM respectively), and was undetectable in a third. Inhibition of PKC $\delta$  has been demonstrated by Western blotting in mononuclear cells.

Since Bryo levels appear to be close to *in vitro* modulatory concentrations and no DLTs are yet apparent, we plan to now expand accrual in the Bryo 40-60  $\mu$ g/m<sup>2</sup> dose range. The current aim is to document the range of concentrations of Bryo achieved by the 1 h infusion, and the effects of Bryo-modified cisplatin on PKC isoforms in mononuclear cells, as compared to cisplatin alone.

**#19 A phase I pilot clinical trial to study the effects of mifepristone in patients with operable prostate cancer.** El Etreby, M. Fathy, Lewis, Jill E., Ogle, Thomas F., Allsbrook, William C. and Lewis, Ronald W. Medical College of Georgia, Augusta, GA.

**Introduction and Objectives:** The antitumor activity of the antiprogesterin, mifepristone in experimental prostate cancer models, as well as extensive experience with antiprogesterins as potent mammary tumor inhibitors via induction of progesterone receptor (PR)-mediated apoptosis, suggest that antiprogesterins might also represent an effective new approach for the management of human prostate cancer.

**Methods:** Eight patients with clinically localized and previously untreated prostate cancer were randomly assigned to one of two groups. Five patients were treated orally with mifepristone tablets (200 mg/day) and three patients received matching placebo from the day of informed consent until the day of radical prostatectomy for up to five weeks.

**Results:** In 80% of the mifepristone-treated patients a significant time-dependent decrease in the serum total (up to 80% inhibition) and free (up to 88% inhibition) PSA was observed as compared with the corresponding pretreatment values. This effect was clearly evident as early as one week after the start of treatment. The PR was measurable in prostate tissue of all patients (ranging from 200 to 345 f mol/mg protein). The "neoadjuvant" dramatic response of serum PSA was associated with morphological evidences of apoptosis and induction of DNA fragmentation in the radical prostatectomy specimens as well as with an increase in serum TGF $\beta$  protein concentration. These findings reflect most probably a mifepristone-induced inhibition of prostate cancer cell growth or prostate cancer regression (induction of apoptosis). TGF $\beta$  seems to be involved in this receptor-mediated interaction of mifepristone with the cell surface mechanism. The safety profile of mifepristone was excellent in all treated patients. However, an increase in the serum ACTH and androstenedione levels was evident as a manifestation of the antigluccorticoid activity of this antiprogesterin.

**Conclusions:** Our results indicate that antiprogesterins represent a potentially relevant new development for the management of prostate cancer.

**#20 A clinical, pharmacodynamic and pharmacokinetic phase I study of SCH 66336 (SCH) an oral inhibitor of the enzyme farnesyl transferase given once daily in patients with solid tumors.** Awada A, Eskens F, Ploccart MJ, Van der Gaast A, Bleiberg H, Cutler DL, Fumoleau P, Wanders J, Faber MN, Verweij J for the EORTC-Early Clinical Studies Group, NDDO Oncology and Schering-Plough Research Institute.

**Introduction:** SCH66336 (tricyclic nucleus) is a non peptidic farnesyl transferase inhibitor. In pre-clinical studies, SCH induced not only tumor growth inhibition but also tumor regression. In a previous study, SCH was given twice daily continuously. The recommended dose was 200 mg BID and the plasma half life ranged from 3.6-12.3 hours (ASCO 1999, abs. 600). Thus, in this study continuous once daily oral administration of SCH was studied. Pharmacokinetic and pharmacodynamic studies were performed on days 1 and 15. **Patients characteristics:** Twelve patients with miscellaneous solid tumors; 8 males/4 females; median age: 61 yrs range (41-77); med. PS: 1 (1-2). **Study results:** Patients were treated at two dose levels: 300 mg (6 pts) and 400 mg (6 pts). The median duration of treatment was 1.5 months (range 1-3). At 300 mg, no dose-limiting toxicity (DLT) was observed. The toxicities seen were grade 1/2 and consisted of diarrhea, vomiting, anorexia, fatigue, and weight loss (approximately 6 kg). At 400 mg, the same toxicities reported at 300 mg were observed and 2 patients developed grade 2 serum creatinine increase (reversible following hydration). The diarrhea was more pronounced at 400 mg (2 pts grade 1, 3 pts grade 2, 1 pt grade 3) but controlled by loperamide. At 400 mg, 3 patients interrupted treatment due to toxicities (only one patient had a DLT (diarrhea grade 3)). No grade 3/4 hematological toxicity nor retinal changes were observed. At the dose levels studied, the pattern of toxicities observed using once daily schedule is comparable to the BID schedule. The pharmacokinetics at 300 and 400 mg once daily are being analysed and will be compared to patients treated at 200 mg BID. The pharmacodynamic analysis (buccal smears for oral mucosal pre-lamin A determination) is ongoing.

**#21 Phase I study of 5-FU, leucovorin, and vitamin E and correlation with urinary F<sub>2</sub> isoprostane production in patients with advanced malignancies.** Stipanov M, Morrow JD, Shyr Y, Hande KR, Blanke CD, Boelng A, Dorminy C, Browning R, McKinney J, Coffey RJ Jr, Beauchamp RD, Rothenberg ML. Vanderbilt University Medical Center and the Vanderbilt-Ingram Cancer Center, Nashville, TN.

We previously demonstrated that antioxidants, such as Vitamin E, induced growth arrest in colon cancer cells *in vitro* and could enhance chemotherapy-induced apoptosis through the induction of p21<sup>WAF1/CIP1</sup>. Vitamin E also improved tumor control *in vivo* in 5-FU-treated athymic nude mice bearing human colorectal cancer xenografts (Nat Med 1997;11:1233-1241). These observations led us to perform a Phase I trial of 5-FU 425 mg/m<sup>2</sup> + leucovorin 20 mg/m<sup>2</sup> IV qd x 5, q 4-5 weeks (Mayo Clinic/NCCTG schedule) with Vitamin E 3200 IU qd given continuously, beginning 2 weeks prior to chemotherapy. The trial was initiated using full doses of chemotherapy and was designed to de-escalate Vitamin E if the Grade 3-4 toxicity rate of this 3-drug regimen exceeded the 35-40% rate that would be expected with this schedule of 5-FU + LV alone. Thirteen pts were enrolled and 12 received at least 1 cycle of 5-FU + LV and were evaluable for toxicity (1 pt had PD during Vit. E run-in phase). Median age: 50 (25-74). Performance status: 0: 3; 1: 7; 2: 3. Two patients each had malignant mesothelioma and small bowel adenocarcinoma, and 1 pt each had, ovarian, head and neck, pancreatic, renal cell, non-small cell lung, and cervical cancer, melanoma, and osteosarcoma. Only a single dose level was tested. Fifty-eight per cent of patients experienced Grade 3 toxicities during Cycle 1 with the most common being neutropenia (33%) and abdominal cramping (25%). No Grade 4 toxicities were observed. 24-hour urine samples were collected prior to the initiation of Vit. E and prior to each cycle of chemotherapy and assayed for F<sub>2</sub> isoprostanes, prostaglandin-like compounds derived from free-radical-catalyzed peroxidation of arachidonic acid, as a potential surrogate marker for antioxidant effect of Vitamin E. Analysis of urinary F<sub>2</sub> isoprostanes and correlation with clinical outcome and toxicity is underway. At the present time, we conclude that Vitamin E can be administered in conjunction with full-dose 5-FU + LV without enhancement of clinical toxicity. This trial was supported by NCI Cancer Center Support Grant #P30 CA68485.

**#22 Phase I, pharmacokinetic and correlative tumor kinetic studies of SR-45023A, a novel, oral anticancer drug.** Alberts David, Sibley Leslie, Hallum Alton, Stratton-Custis Mary, Garcia Dava, Gleason-Guzman Mary, Salmon Sydney, Santabarbara Pedro, Niesor Eric, Floret Simon and Bentzen Craig. Arizona Cancer Center, Tucson, AZ, ILEX Oncology, San Antonio, TX and Sympher, Geneva, Switzerland.

SR-45023A is an orally active, non-myelosuppressive agent which selectively inhibits cell proliferation and induces tumor cell apoptosis through the intracellular receptor FXR. We are performing a phase I study at the Arizona Cancer Center, using a daily x 14 oral dosing schedule with courses repeated every 3 weeks. Dose-limiting, non-myelosuppressive toxicity was observed at the dose level of 250 mg/m<sup>2</sup>/day with 4 of 5 patients experiencing > grade 2 abdominal pain and/or elevation in liver function tests. No  $\geq$  grade 2 drug-related toxicities were observed in the 3 patients treated at the dose level of 125 mg/m<sup>2</sup>/day. Plasma concentra-



tions of SR-45023A were assayed using a Hewlett Packard gas chromatograph with a HP-5 15 m x 0.32 mm column. At 125 mg/m<sup>2</sup>/day in one uncomplicated study patient, the plasma C<sub>max</sub> was 7.25 µg/ml and plasma AUC (0-12 hr) was 71.2 µg · hr/ml with a t<sub>1/2</sub> (terminal) = 103 hrs. In 3 patients treated at 250 mg/m<sup>2</sup>/day, the mean plasma C<sub>max</sub> was 13.67 µg/ml and the mean plasma AUC (0-12 hr) = 133.1 µg · hr/ml. We performed *in vitro* clonogenic <sup>3</sup>H-thymidine endpoint assays on 17 fresh ovarian cancers, simultaneously comparing the single agent cytotoxicities of SR-45023A, cisplatin and paclitaxel. At 10 µM and 20 µM (~5 and 10 µg/ml, respectively), 65% and 100% of the ovarian cancers were sensitive (i.e. >50% inhibition of tumor cell growth) to SR-45023A in comparison to sensitivity rates of 92% for cisplatin (10 µg/ml) and 62% for paclitaxel (5 µg/ml). These *in vitro* assay results, taken together with our preliminary plasma pharmacokinetic data suggest that SR-45023A should be clinically active at the 125 mg/m<sup>2</sup>/day dose level. In fact, one study patient with recurrent, stage III ovarian cancer experienced a reduction in serum CA-125 concentration from 3,013 U/ml to 554 U/ml while receiving 8+ courses of SR-45023A at dose levels of 125 and 250 mg/m<sup>2</sup>/day. An additional patient with metastatic melanoma experienced stable disease during 9+ courses of therapy. This continuing phase I trial likely will define a phase II trial dose of 125 mg/m<sup>2</sup>/day x 14 days every 3 weeks; however we are extending our phase I study to evaluate a continuous daily dosing schedule, starting at 125 mg/m<sup>2</sup>/day.

**#23** A phase I study of intensive-dose melphalan, topotecan and VP-16 phosphate (MTV) followed by autologous stem cell rescue in patients with multiple myeloma. Sullivan DM, Partyka JS, Fields KK, Goldstein SC, Field TL, Djulbegovic B, Perkins JB, Mofsaac CE, Lush RM, Daiton WS. *Clinical Investigations & BMT Programs, Moffitt Cancer Center & Research Institute, University South Florida, Tampa, Florida.*

The dose-escalation of topotecan (TPT) in combination with melphalan and VP-16 phosphate, followed by stem cell rescue, was investigated in the treatment of multiple myeloma. *In vitro* data suggest that tumor cell kill is optimal when the drugs are given as alkylator → topoisomerase (topo) I inhibitor → topo II inhibitor. Thus, the drugs were sequenced as a 30 min infusion of melphalan (150 mg/m<sup>2</sup>, total) followed immediately by a 30 min infusion of TPT each d times 3, followed by a 4 h infusion of VP-16 phosphate for 2 d (2400 mg/m<sup>2</sup>, total etoposide equivalents). TPT was not administered to the first cohort of patients. Twenty-seven patients with a median age of 54 yo (38-66) have been treated with 3 dose levels of TPT (10-20 mg/m<sup>2</sup>, total). The maximum tolerated dose of TPT has not been reached, although for patients receiving TPT (dose levels 2-4) grade 3 and 4 mucositis was observed in 100% of patients. Other grade 3 or 4 regimen-related toxicities for all patients include enteritis (59%), and nausea/vomiting (19%). The median number of days of TPN and length of hospital stay were 8 (0-18) and 23 (19-30), respectively. There have been no regimen-related deaths. The median day post stem cell infusion to engraftment is 10 for ANC > 500/µl and 17.5 for platelets > 50,000/µl, untransfused. Complete (6) and partial (5) responses have occurred in 11 of 19 evaluable patients (58%). The overall survival and event free survival for all patients at 6 months were 95 ± 4.9% and 78 ± 10%, respectively. These data suggest that MTV is well tolerated in this patient population and has antineoplastic activity in the treatment of multiple myeloma. In addition to measuring the expression and activities of topo I and II in myeloma cells, the pharmacokinetic predictability of a melphalan test dose is being evaluated. TPT and VP-16 phosphate were provided to patients by SmithKline Beecham and Bristol-Myers Squibb, respectively. Supported in part by NIH grant CA82050.

**#24** Combination chemotherapy and donor lymphocyte infusion for treatment of aggressive hematologic malignancies in relapse after allogeneic bone marrow transplantation. Mookerjee Bijoyee<sup>1,2</sup>, Couzi Rima<sup>1</sup>, Seber Adrianna<sup>1</sup>, Miller Carole<sup>1</sup>, Noga Steven<sup>1</sup>, Douglas Tracy<sup>1</sup>, Altomonte Viki<sup>1</sup>, Gore Steven<sup>1</sup>, Jones Richard<sup>1</sup>, Vogelsang Georgla<sup>1</sup>, Fuchs Ephraim<sup>1</sup>. 1) Johns Hopkins Oncology Center, 2) University of Maryland Greenebaum Cancer Center, Baltimore, MD.

Relapse following allogeneic bone marrow transplantation (BMT) remains an important cause of treatment failure. Short-term remissions can be achieved with chemotherapy in 30-50% of patients and a second BMT is associated with high mortality and morbidity. Donor lymphocyte infusion (DLI) is successful in treating most relapsed chronic myeloid leukemia (CML) in chronic phase. Unfortunately, DLI is less successful in other hematologic malignancies. To improve the efficacy of DLI, immunostimulatory cytokines or administration of pre-DLI chemotherapy has been tried without success. In patients given pre-DLI chemotherapy, DLI was deferred till complete hematological recovery. Chemotherapy timed appropriately can augment anti-tumor efficacy of donor lymphocytes by elimination of tumor-induced host suppressor T-cells. We conducted a study to ascertain the maximum chemotherapy that could be administered in a fixed time sequence with DLI. Patients with relapsed aggressive hematologic malignancies with good performance status (ECOG 0-2), without graft-versus-host disease (GVHD) and off immunosuppressive medications were eligible. At the first level, four patients were treated with etoposide (400 mg/m<sup>2</sup>/day) for three days (D1-D3), cyclophosphamide (50 mg/kg ideal body weight [IBW]) on D8 and DLI (10<sup>8</sup> CD3<sup>+</sup> cells/kg IBW) on

D10. One patient died of progressive disease and considered inevaluable. Their course was complicated by mucositis, neutropenic fevers and acute GVHD, none of which were dose limiting. At the next level, liposomal doxorubicin at 20 mg/m<sup>2</sup> was added. All three patients developed dose limiting toxicity. Two patients developed grade IV acute GVHD, and one patient died from its complications. Another succumbed to heart failure. Of the remaining patients, two had poor-risk AML with complex cytogenetic changes, one had CML in lymphoid blast crisis and one had diffuse large cell lymphoma. All patients remain in complete remission (CR) at 16, 12, 13 & 6 months follow-up, respectively. At D30 evaluation, all patients evaluated had 100% donor bone marrow and had achieved a CR. Three patients are being enrolled at a modified level-1 regimen with etoposide at 200 mg/m<sup>2</sup>/day. Combination chemotherapy and DLI is a reasonable approach for treating patients with relapsed hematologic malignancies after allogeneic BMT. These preliminary results although exciting require a phase II study to evaluate efficacy.

## SECTION 2: GROWTH FACTORS AND THEIR RESPONSES (INCLUDING ANTIHORMONAL)

**#25** The Hsp90 chaperone system as a potential therapeutic target: identification of a geldanamycin dimer that induces the selective degradation of HER-family tyrosine kinases. Zheng, Fuzhong F.; Münster, Pamela N.; Kuduk, Scott; Danilshesky, Samuel; Sepp-Lorenzino, Laura; Rosen, Neal. *Memorial Sloan-Kettering Cancer Center, 1275 York Ave., New York, NY 10021.*

Geldanamycin (GM) is a natural product that binds to Hsp90 and induces the degradation of a subset of signaling proteins. GM is a potent inducer of cell growth arrest and apoptosis. The members of the HER family of receptor tyrosine kinases are the most sensitive targets of GM we have identified so far. Cancer cells which overexpress HER2 are especially sensitive to GM-induced growth inhibition. These observations support the clinical development of GM or its derivatives as agents for the treatment of tumors that express high levels of this protein such as breast cancers. A geldanamycin derivative, 17-allylaminogeldanamycin, is currently being studied in phase I clinical trials. However, its lack of cellular target specificity suggests that its clinical use may be limited by significant toxicity. Activation of HER-kinases involves homo- and hetero-dimerization among family members. We synthesized a family of GM dimers in order to create a drug that would interact with the Hsp90 associated with each of the elements of the HER-dimer. We identified a selective GM dimer, GMD-4c in which two GM molecules are attached at their 17-carbon position by a four-carbon linker. It has selective activity against HER-kinases as compared to IGF-1 receptor, Raf-1, and estrogen receptor. Selectivity requires both intact GM moieties, and is a function of linker length. GMD-4c and GM are both potent inducers of the Rb-dependent G1 block and apoptosis of breast cancer cell lines, but only GM, not GMD-4c, significantly inhibits the growth of the murine myeloid cell line 32D that lacks HER-kinases. Thus, the GMD-4c dimer induces the selective degradation of HER-family kinases and specifically inhibits the growth of HER-dependent tumor cell lines. This work supports the idea that selective ansamycins with a different, more restricted spectrum of action than the parent molecules can be synthesized, and are likely to be less toxic since their effects on other key signaling proteins are attenuated. This work represents a new strategy for inhibiting growth receptor functions in human tumors.

**#26** Anti-HER2 immunoliposomes provide a vehicle for targeted intracellular drug delivery and provide enhanced therapeutic efficacy with doxorubicin. Park, J.W., Kirpotin, D., Shalaby, R., Hong, K., Shao, Y., Nielsen, U., Marks, J.D., Papahadjopoulos, D., and Benz, C.C. *UCSF & Liposome Research Laboratory/CPMCRI, S.F., CA 94115.*

Anti-HER2 immunoliposomes (ILs) combine the tumor-targeting properties of certain anti-HER2 monoclonal antibodies (MAB) with the pharmacokinetic and drug delivery advantages of sterically stabilized liposomes (Ls). Anti-HER2 ILs bind efficiently to and internalize in HER2-overexpressing cells *in vitro*, resulting in intracellular drug delivery. *In vivo*, ILs display long circulation after single or multiple doses in normal adult rats that is identical to that of sterically stabilized liposomes. However, in HER2-overexpressing tumor xenograft models, *in vivo* treatment with gold-labeled ILs results in a markedly different pattern of intratumoral distribution and mechanism of delivery than non-targeted Ls. While Ls accumulate extracellularly or within macrophages, ILs penetrate extensively throughout tumor tissue and internalize to tumor cell cytoplasm. Thus ILs, unlike Ls, achieve tumor-targeted intracellular drug delivery. This novel mechanism may account for the significantly enhanced efficacy of ILs against HER2-overexpressing tumors. Doxorubicin (dox)-loaded anti-HER2 ILs display potent and selective anticancer activity. In four different HER2-overexpressing tumor xenograft models, anti-HER2 ILs-dox produce growth inhibition, regressions, and cures. Anti-HER2 ILs-dox is significantly superior to all other relevant treatment conditions, including free dox, liposomal dox, anti-HER2 MAB (rhMAB HER2, Herceptin™). Anti-HER2 ILs-dox is



also significantly superior to combination therapies including free dox + free rhuMAB HER2 and commercial liposomal dox (Doxil™) + free rhuMAB HER2. In addition to ILs containing rhuMAB HER2-Fab', we have generated and evaluated new anti-HER2 MAb fragments for use with immunoliposomes, including anti-HER2 scFv's and diabodies. All anti-HER2 ILs tested yield equivalent efficacy in therapy studies, and are again superior to control liposomal dox. In preparation for clinical studies of anti-HER2 ILs-dox, immunoliposome production is undergoing scale up, including development of a conjugation procedure using preformed liposomal dox as starting material. We conclude that anti-HER2 ILs represent a novel and promising technology for tumor-targeted intracellular drug delivery.

**#27 ZD1839 (Iressa™) an epidermal growth factor receptor (EGFR) tyrosine kinase inhibitor, inhibits proliferation in normal and preinvasive breast epithelia.** Chan KC, Knox WF, Woodburn JR, Potten CS, Bundred NJ. *University Hospital of South Manchester, and Zeneca Pharmaceuticals, UK.*

Estrogen receptor (ER) negative comedo Ductal Carcinoma in Situ (DCIS) expresses the  $erbB_2$  oncogene and epidermal growth factor receptor. We sought to determine if blocking of EGFR with an EGFR tyrosine kinase inhibitor (ZD1839) prevents heterodimerization of EGFR with the  $erbB_2$  receptor and signal transduction of both receptors leading to decreased epithelial proliferation in normal and DCIS human breast tissue.

Normal and DCIS tissue from 8 women undergoing therapeutic surgery were xenografted into female nude mice. Daily gavage with either ZD1839 at 100–200 mg/kg or vehicle for 14 days commenced 2 weeks post implant. Xenografts were removed on days 14, 21, and 28. Epithelial proliferation was assessed by counting 1000 cells after Ki67 immunostaining. ZD1839 increased apoptosis ( $p < 0.05$ ) after 7 days of treatment and inhibited proliferation compared to controls after 14 days (see table).

Ki67 Labelling Index	Day 0	Day 21		Day 28	
		Control	ZD1839	Control	ZD1839
DCIS Median	19.9	10.6	7.2	23	3.2*
Interquartile range	5.7 – 30.9	2.2 – 39.2	0.5 – 21.2	2.2 – 39.2	0–8.3
Normal breast Median	7.6	3.3	0.7*	6.1	1.8*
Interquartile range	4.4 – 12.9	0.8 – 4.8	0 – 1.3	3.4 – 7.8	0.7 – 3.9

\* $p < 0.05$

The growth of MDA MB 231 breast cancer cells was also inhibited *in-vitro* at 1  $\mu$ M of ZD1839 and *in-vivo* at 200 mg/kg ( $p < 0.05$ ). ZD1839, an EGFR tyrosine kinase inhibitor, has potential as a chemopreventative agent and as adjuvant therapy in ER negative DCIS.

**#28 Antitumor effects and potentiation of cytotoxic drugs activity in human cancer cell lines by ZD-1839 (Iressa™), an EGFR-specific tyrosine kinase inhibitor.** Ciardello F., Caputo R., Bianco R., Pomato G., Damiano V., De Placido S., Bianco A.R., Tortora G. *Cattedra di Oncologia Medica, Università di Napoli Federico II, Naples, Italy.*

TGF $\alpha$  controls cancer cell growth through autocrine pathways. Overexpression of TGF $\alpha$  and its receptor (EGFR) is associated with aggressive disease and poor prognosis in human epithelial cancers. The EGFR has been proposed as target for anticancer therapy. Several compounds blocking ligand-induced EGFR activation have been developed. ZD-1839 is a quinazoline-derivative that selectively inhibits the EGFR tyrosine kinase and is under clinical development in cancer patients. The antiproliferative activity of ZD 1839 in human ovarian (OVCA-3), breast (ZR-75-1, MCF-10A ras) and colon cancer (GEO) cells, that coexpress EGFR and TGF $\alpha$ , was evaluated. ZD-1839 treatment inhibited colony formation in soft agar in a dose-dependent manner in all cancer cell lines. The antiproliferative effect was mainly cytostatic. However, treatment with higher doses determined a 2- to 4-fold increase in apoptosis. Previous studies have suggested the potentiation of the antitumor activity of various cytotoxic drugs by anti-EGFR monoclonal antibodies. Therefore, ZD-1839 was tested in combination with cytotoxic drugs differing for the mechanism(s) of action, such as cisplatin, carboplatin, oxaliplatin, taxol, taxotere, doxorubicin, etoposide, topotecan, and tomudex. A dose-dependent supra-additive increase in growth inhibition *in vitro* was observed when cancer cells were treated with each cytotoxic drug and ZD-1839. The combined treatment markedly enhanced apoptotic cell death induced by single agent treatment. ZD-1839 was also evaluated *in vivo* in nude mice bearing established human GEO colon cancer xenografts alone and in combination with taxol, topotecan or tomudex. ZD-1839 determined a reversible dose-dependent inhibition of tumor growth since GEO tumors resumed the growth rate of controls at the end of the treatment period. In contrast, an almost complete GEO tumor regression was observed in all mice treated with ZD-1839 in combination with taxol, topotecan or tomudex. This determined a prolonged mice survival significantly different as compared to controls or to single agent-treated mice. These results provide a rationale for the evaluation of the anticancer activity of the combination of the

EGFR-specific tyrosine kinase inhibitor ZD-1839 and cytotoxic drugs in clinical trials and indicate the likely efficacy of the agent in a wide range of solid tumors. ZD-1839 was kindly provided by AstraZeneca, Macclesfield, UK.

**#29 A pharmacokinetic/pharmacodynamic trial of ZD1839 (Iressa™), a novel oral epidermal growth factor receptor tyrosine kinase (EGFR-TK) inhibitor, in patients with 5 selected tumor types (a phase I/II trial of continuous once-daily treatment).** Baselga, J., LoRusso, P., Herbst, R., Rischin, D., Ranson, M., Maddox, A.-M., Averbuch, S. *Vall d'Hebron, Spain; Harper Hospital, MI, US; MD Anderson Cancer Center, TX, US; Peter McCallum Institute, Australia; Christie Hospital, UK; University of Arkansas, US; AstraZeneca.*

ZD1839 (Iressa™) is a selective inhibitor of EGFR-TK. Between March and June 1999, 58 patients (pts) [performance status 0–1] with 5 selected advanced tumors (NSCLC (29), head and neck (10), ovarian (7), colorectal (6) and prostate (6)), have been enrolled in this phase I/II trial. Dose escalation (150 mg/day to 1000 mg/day, 14 pts per cohort) was followed by randomized selected dose-level expansion (20 per cohort). ZD1839 was given twice on day 1 and once-daily for 28 consecutive days. Therapy continued in the absence of symptomatic disease progression or significant toxicity. In addition to pharmacokinetic investigations, pharmacodynamic studies were performed pre- and post-treatment in normal skin and accessible tumors in consenting patients. Interim PK and PD results will be presented. A total of 72 28-day treatment courses have been completed in 52 pts. All pts were evaluated for safety. There were no grade 3–4 drug-related adverse events, 10% of pts had diarrhea, 7% nausea, 7% anorexia, grade 1–2. Mechanism-based skin reactions (dry skin, papular/pustular rashes, grade 1–2), reported in 19% of pts, did not worsen despite continued therapy. Two deaths occurred: 1 progressive disease and 1 at 225 mg due to pulmonary thromboembolism. 43 pts were evaluable for response using revised WHO criteria (partial response  $\geq 30\%$  decrease in unidimensional sum of diameters). Among 34 NSCLC pts, there was 1 partial response (2+ month) at 150 mg, and a 20% and a 22% tumor reduction at 150 and 300 mg, respectively in pretreated patients. In 3/9 pts with head and neck tumors treated at 150 mg, a 20% reduction, a >60% visual reduction of a large lip tumor and decrease in dermal metastases occurred. In addition one prostate carcinoma patient had a 25% tumor reduction and a decrease in PSA from 66 to 20 at 2+ month. Subjective symptomatic pain relief have been reported. Enrollment is ongoing at 300 and 400 mg dose levels. Summary: This trial confirms the acceptable tolerability of ZD1839 (oral EGFR-TK inhibitor) administered as a continuous once-daily schedule. Additionally, anti-tumor activity in NSCLC and head and neck cancers was reported when ZD1839 was given as monotherapy.

**#30 Paclitaxel enhances the effects of the anti-epidermal growth factor receptor monoclonal antibody C225 in mice with metastatic human bladder transitional cell carcinoma.** Inoue, Keiji, Slaton, Joel W., Perrotte, Paul, Davis, Darren W., Bruns, Christine J., Hicklin, Daniel J., McConkey, David, Radinsky, Robert, and Dinney, Colin P. N. from *The University of Texas M.D. Anderson Cancer Center.*

Previously we reported that when cells of the human transitional cell carcinoma (TCC) 253J B-V growing orthotopically within the bladder of athymic nude mice were treated with the anti-epidermal growth factor receptor (EGFR) monoclonal antibody C225, angiogenesis was inhibited, resulting in regression of the primary tumor and inhibition of metastasis. In this study, we evaluated whether paclitaxel enhanced this therapeutic effect of C225. *In vitro* the proliferation of 253J B-V cells was inhibited more by the combination of C225 and paclitaxel compared to either agent alone. *In vivo* therapy with C225 and paclitaxel resulted in significantly greater regression of tumors compared with either agent alone. The combination was most effective when paclitaxel was administered 2 days before C225. When this schedule was used, the median bladder tumor weight was 85 mg (range: 69–133 mg) compared with 168 mg (range: 72–288 mg) after C225 alone ( $P < 0.05$ ), and 273 mg (range: 83–563 mg) after paclitaxel alone, ( $P < 0.005$ ). The incidence of spontaneous lymph node metastasis was also reduced by the combination of C225 with paclitaxel, although this result did not significantly differ from results after the use of C225 alone. Treatment with paclitaxel and C225 downregulated the expression of basic fibroblast growth factor, vascular endothelial cell growth factor, interleukin-8, and matrix metalloproteinase type 9 and inhibited tumor-induced neovascularity compared with untreated controls ( $P < 0.005$ ). Moreover, the combination of C225 and paclitaxel enhanced apoptosis in tumor and endothelial cells compared with either agent alone ( $P < 0.005$ ).

These studies indicate that therapy with paclitaxel increases the ability of C225 to inhibit tumorigenicity and metastasis. This effect is mediated by inhibition of angiogenesis and induction of apoptosis.

**#31 Regression of human pancreatic carcinoma and inhibition of metastasis by blockade of EGF-R signal transduction is enhanced in combination with gemcitabine.** Harbison, M.T., Bruns, C.J., Davis, D.W., Tsan, R., Portera, C., McConkey, D.J., and Radinsky, R. *Department of Cancer Biology, University of Texas M.D. Anderson Cancer Center, 1515 Holcombe Blvd., Houston, TX 77030.*



**INTRODUCTION:** Activation of the epidermal growth factor receptor is involved in aberrant proliferation and intracellular signaling in numerous solid malignancies. The purpose of this study was to evaluate the effect down-regulating EGF-R activity could inhibit pancreatic tumor growth and metastasis and to determine the mechanism by which this occurs. A secondary aim was to determine if combination therapy with Gemcitabine (GEM) could accentuate the anti-tumor response to EGF-R blockade.

**METHODS:** The highly metastatic human pancreatic carcinoma cells (L3.6p1, 1x10<sup>6</sup>) was implanted into the pancreas of nude mice. Beginning on day 8, the mice were treated with either EGF-R antibody (MAb C225) (i.p. 1mg, biweekly), C225+GEM (i.p., 250mg/kg, biweekly), GEM alone, or saline (n=10/group). Primary tumors were harvested for immunohistochemistry and immunofluorescence microscopy to determine expression of VEGF, IL-8, activated EGF-R, PCNA, cell death (TUNEL), microvessel density (CD31), and apoptotic endothelial cells (CD31/TUNEL double labelling). In vitro, Western and Northern Blot analyses, ELISA, and gel shift assays were used to analyze the effect of C225+/- Gemcitabine on cultured L3.6p1 cells.

**RESULTS:** *In vitro* treatment of L3.6p1 cells with C225 resulted in inhibition of EGF-R autophosphorylation, however, only 30% cytostasis. C225 led to a dose-dependent decrease in VEGF and IL-8 at both the mRNA and protein levels (p<0.001). One hour treatment of L3.6p1 cells with C225 resulted in a significant decrease in NFκB activation. *In vivo* gemcitabine demonstrated a modest decrease in tumor volume, liver metastases, microvessel density, and PCNA. In addition, Gemcitabine increased slightly the TUNEL positive tumor cells and endothelial cells. C225 alone was more effective in inducing apoptosis in both the tumor and its vasculature. In addition it decreased VEGF and IL-8 production, tumor cell proliferation, microvessel density, tumor volume and liver metastases. The combination of C225 and gemcitabine proved to be the most effective reducing tumor volume and liver metastases to zero. The angiogenic markers were severely reduced and the apoptotic events dramatically increased.

**CONCLUSION:** These experiments demonstrate that therapies targeting EGF-R signalling in combination with Gemcitabine have a significant anti-tumor effect mediated, in part, by the inhibition of cellular proliferation and angiogenesis which leads to apoptosis, tumor regression, and inhibition of metastasis.

**#32 Expression of VEGF and its receptor FLT4 (VEGFR3) in human thyroid diseases.** Shushanov S., Karamysheva A., Stavrovskaya A., Bronstein, M., Adelalde, J., Geneix, J., Jacquemier, J., Birnbaum, D., Institute of Carcinogenesis, Cancer Research Centre, Moscow, Russia, Endocrinological Research Centre, Moscow, Russia, U119 Inserm and Institute Pasteur-Calmettes, Marseille, France.

VEGF, a member of the vascular endothelial growth factors (VEGF) family, is supposed to play a role in the maintenance of lymphatic endothelial differentiation. The data concerning the expression of VEGF and of its receptor, FLT4/VEGFR3, in human pathology are scarce.

The goal of our study was to investigate the role of the VEGF/FLT4 system in human thyroid tumor development. For this purpose, the expression of VEGF and FLT4 mRNA was studied in 38 samples of different thyroid pathologies by means of RT-PCR. Because two VEGFR3 isoforms, FLT4 short (FLT4s) and FLT4 long (FLT4l) exist, three pairs of specific primers were designed revealing the total expression of both isoforms (FLT4), or the expression of each isoform.

In thyroid adenocarcinomas the gene activity of VEGF, and of FLT4 and FLT4s was decreased to 62% (VEGF) and 37% (both FLT4 and FLT4s) of samples, as compared with 90% and 100% in all other thyroid pathologies. FLT4l was the most often expressed in thyroid adenomas (69%) and autoimmune diseases (57%), while 87% of adenocarcinomas were FLT4l-negative.

At the protein level, immunohistochemical staining of the thyroid adenocarcinoma and adenoma sections with anti-FLT4 antibodies (kindly provided by K. Alltalo) confirmed these findings.

**Conclusions:** FLT4 gene expression is decreased in thyroid adenocarcinomas in comparison with other thyroid disorders. FLT4s isoform is expressed in all FLT4-positive samples, while the expression of the FLT4l isoform seems to be specific for certain thyroid disorders. VEGF gene is expressed in most thyroid tissue samples.

**#33 Retroviral transduction of a dominant negative epidermal growth factor receptor into ovarian cancer cell lines.** Gillette-Cloven Noelle, Kothari Nayantara, Datta Shoibal, Bonzon Christine, Howoruzsko Agnieszka, Van Nostrand Kristi, Fan Hung. University of California Irvine, CA USA and Karolinska Institute, Stockholm, Sweden.

Overexpression of the epidermal growth factor receptor (EGFR) occurs frequently in ovarian cancers and has been associated with a poor prognosis. The dominant negative receptor (DNR) is truncated in the cytoplasmic domain and therefore lacks a tyrosine kinase. Expression of the DNR has been shown to inhibit growth in pancreatic cancer cells.

**Aim:** To test the effects of a dominant negative EGFR introduced into ovarian cancer cells using a retroviral vector.

**Methods:** Two ovarian cancer cell lines, NuTu-19 and cisplatin resistant NuTuCPR, were each infected with a retroviral vector encoding either the

gene for a dominant negative EGFR or β-galactosidase. NIH/3T3 cells were concomitantly infected and served as a nontumorigenic standard of comparison.

**Results/Conclusions:** Ovarian cancer cell lines were infected 3-4 times more efficiently than NIH/3T3 cells. Both NuTu-19 and NuTuCPR cells infected with the dominant negative vector showed strong inhibition of colony formation (98% and 99.2%, respectively). These observations indicate that a dominant negative EGFR may be a useful therapeutic tool in the treatment of cisplatin sensitive and resistant ovarian cancers. When compared to DNR infected NuTu-19 cells, DNR infected NuTuCPR cells were observed to form larger and more cohesive colonies at earlier times, suggesting a relative resistance to the effects of the vector.

**#34 Modulation of epidermal growth factor receptor expression by chemotherapeutic agents in breast cancer cell lines.** Welch, James N., Chrysoygelos, Susan A., Ph.D. and Clarke, Robert, Ph.D. Departments of Oncology, Biochemistry & Molecular Biology, and Physiology & Biophysics, Lombardi Cancer Center, Georgetown University, Washington, DC, 20007.

The progression of breast cancer from a localized, hormone-dependent primary tumor to an aggressive, hormone-independent metastatic condition is a largely uncharacterized process at the cellular and molecular levels. Our premise is that signaling by the epidermal growth factor receptor (EGFR) promotes this progression and is increased in response to cytotoxic drugs. The goal of our research is to 1) characterize the effects of exposure of breast cancer cells to chemotherapeutic agents on the expression of EGFR, and 2) characterize how the increased EGFR aids in cell survival and drug resistance. Our initial experiments demonstrate that exposure to the anti-metabolite methotrexate (MTX), a dihydrofolate reductase inhibitor, at concentrations of 0.05 to 50 μM over 72 hours induces increased EGFR expression (at both the mRNA and protein levels) in MCF-7 breast cancer cells. Our data also demonstrate that the growth rate of MCF-7 cells after treatment with MTX at these doses becomes more responsive to EGF stimulation (compared with untreated cells). In addition, we have found that over-expression of EGFR (by way of stable transfection of an EGFR expression vector) renders MCF-7 cells tolerant to an approximately one log-fold higher dose of MTX (compared to stable transfectant controls). We have achieved similar results with a second anti-metabolite compound, trimetrexate, and are testing compounds acting through other cytotoxic mechanisms. These data suggest that concomitant treatment with compounds that block EGFR-signaling could increase therapeutic response to some cytotoxic drugs and/or inhibit the emergence of drug resistance.

**#35 Human renal cell carcinoma cells lines secrete Fibroblast Growth Factor (FGF) and stimulate vascular endothelial cell growth.** Dickson Gretchen, Tran Sothi, Kim Younghoon, Logan Theodore, Wong Michael KK. University of Pittsburgh Cancer Institute, Pittsburgh, PA 15213 and Indiana University Cancer Center.

Renal cell carcinomas are highly angiogenic tumors. These tumors can be widely metastatic and are relatively resistant to conventional chemotherapy and radiotherapy. Renal cell carcinomas can produce a variety of angiogenic factors, including Fibroblast Growth Factors (FGF). It is becoming increasingly evident that secretion of FGF may be a central event in the stepwise progression to full malignancy.

FGF-1 is a prototype of the FGF family and is a potent, tightly regulated, angiogenic factor. FGF-1 transcripts lack the leader signal sequence motif necessary to direct secretion through the conventional Golgi-ER pathway and there is mounting evidence to implicate a novel secretion pathway. Although the FGF pathway is likely to play an important role in the biology of renal cell carcinomas, the current understanding of renal cell carcinoma's ability to produce and secrete biologically active FGF remains poorly defined.

Primary human renal cell carcinoma cell lines were derived and established *in vitro*. RT-PCR using FGF-1-specific primers demonstrates the presence of FGF-1 transcripts. Ultra-sensitive Western Blot analysis of these cell lines shows immunopositive 18 kD FGF. Significantly, FGF-1 is also detected in the renal cell carcinoma conditioned media and the amount secreted can be increased by heat-shocking these cells at 42°C for 18 hours. Typan Blue viability assays show that >95% of cells are intact. These observations are in keeping with the known characteristics of the non-conventional FGF-1 secretion pathway. The biologic activity of the secreted FGF was assessed using a two-well co-cultivation system. In this system, renal cell carcinoma cells are able to significantly stimulate the growth of human umbilical vein endothelial cells as compared to both control cell lines and transfected cell lines engineered to secrete FGF-1.

Thus, human renal cell carcinoma cells not only synthesize, but also are capable of secreting bio-active FGF-1. These observations provide a molecular basis for its clinical behavior and serve as guideposts for the development of novel anti-tumor strategies.

**#36 Mutant Met-mediated transformation is ligand-dependent and can be inhibited by HGF antagonists.** Micheli Paolo, Basilico Cristina, Pennacchietti Selma, Maffà Antonella, Tamagnone Luca, Giordano Silvia, Bardelli Alberto and Comoglio Paolo M. Department of Molecular Oncology, Institute for Cancer Research and Treatment, University of Torino, I-10060 Candiolo (Torino), Italy.



Mutations in the genes encoding for Met, Ret and Kit receptor tyrosine kinases invariably result in increased kinase activity and in the acquisition of transforming potential. However, the requirement of receptor ligands for the transformation process is still unclear. We have investigated the role of hepatocyte growth factor (HGF), the high-affinity ligand for Met, in mutant Met-mediated cell transformation. We provide evidence that the transforming potential displayed by mutant forms of Met found in human cancer is not only sensitive but entirely dependent on the presence of HGF, by showing that mutant Met transforms NIH3T3 fibroblasts, which produce endogenous HGF, but is not able to transform epithelial cells, unless exogenous HGF is supplied. Accordingly, mutant Met-induced transformation of NIH3T3 cells can be inhibited by HGF antagonists and increased by HGF stimulation. We also show that an engineered Met receptor which contains an oncogenic mutation but is impaired in its ability to bind HGF completely loses its transforming activity, which can be rescued by causing receptor dimerization using a monoclonal antibody. These results indicate that point mutations resulting in Met kinase activation are necessary but not sufficient to cause cell transformation, the latter being dependent on ligand-induced receptor dimerization. They also suggest that mutant Met-driven tumor growth depends on the availability and tissue distribution of active HGF, and provide proof-of-concept for the treatment of mutant-Met related pathologies by HGF-antagonizing drugs.

**#37 Preclinical studies of vitamin D (calcitriol) and glucocorticoid effects on vitamin D receptor (VDR) and retinoid X receptor (RXR) expression: Potential for therapy.** Hershberger, Pamela A, Bernard, Ronald J, Modzelewski, Ruth A, Yu, Wei-Dong, Trump, Donald L, and Johnson, Candace S. *Departments of Pharmacology and Medicine, University of Pittsburgh Cancer Institute, Pittsburgh, PA 15213.*

Preclinical studies demonstrate that calcitriol has significant antiproliferative activity both *in vitro* and *in vivo* in a number of murine, rat and human xenograft model systems. Calcitriol induces G0/G1 arrest, modulates expression of p27 and p21 and induces PARP cleavage, an increased bax/bcl-2 ratio and phosphatidylserine exposure, all markers of apoptosis. Dexamethasone (dex) significantly enhances the anti-tumor effect of calcitriol *in vitro* and *in vivo* in a murine squamous cell carcinoma (SCC) model. Dex mediates these activities through effects on VDR expression, by significantly increasing VDR ligand binding. To determine whether these effects were specific for dex, studies were initiated to examine the effect of methylprednisolone (mp) on these activities. In SCC, by both *in vitro* and *in vivo* clonogenic assay, dex (0.5  $\mu$ M and 9  $\mu$ g/mouse, respectively) significantly increased calcitriol-mediated anti-proliferative effects whereas mp (3  $\mu$ M and 45  $\mu$ g/mouse) had no effect. By single-point saturation, dex significantly increased VDR ligand binding as compared to treatment with mp over increasing dose concentrations. When VDR protein was examined by Western blot analysis, a significant increase in VDR protein was observed with dex and calcitriol as well as with mp. By Western blot analysis of whole cell lysates from SCC, dex, mp and calcitriol increased RXR $\alpha$  (associates with VDR, forms a heterodimer and binds to the vitamin D response element, VDRE) expression as compared to control cells. When calcitriol was combined with dex, no change was observed as compared to dex alone, however, when SCC were treated with calcitriol and mp, a decrease in expression of RXR $\alpha$  was observed as compared to mp or dex alone. These results demonstrate that a differential modulation is observed with calcitriol and dex as compared to mp with respect to enhancement of anti-tumor activity, VDR ligand binding and RXR $\alpha$  expression. Supported by grants from NIH CA67267, DOD PC970576 and CaPCURE.

**#38 The ErbB2 receptor represents a potential target for novel therapies in childhood medulloblastoma.** Gilbertson R.J., Herman R., Pearson A.D.J., and Lunec J. *University of Newcastle upon Tyne, UK.*

Recently we identified an important role for the ErbB2 receptor tyrosine kinase in determining the development and progression of childhood medulloblastoma (Gilbertson *et al.*, *Cancer Res.*, 1997 & 1998). Therefore, we have explored the potential of this oncoprotein to act as a novel therapeutic target in this disease. First, we investigated the *in vitro* growth inhibitory and molecular pharmacological properties of the anti-chaperone agents geldanamycin (GA), 17-Allylaminodemethoxygeldanamycin (17AAG) and radicicol (R) in the medulloblastoma cell lines, DAOY, Med1 and Med8A, that express low, intermediate and high levels of the ErbB2 receptor respectively. DAOY (low ErbB2) demonstrated IC<sub>50</sub> values for GA, 17AAG and R of 14 nM, 9 nM and 15 nM respectively. The Med1 and Med8A lines were less sensitive with mean IC<sub>50</sub> values for the three drugs of 33 nM and 60 nM respectively. While 30 nM of each agent produce  $\geq$ 50% reduction of ErbB2 protein expression in DAOY cells within 24 hours, similar treatment reduced ErbB2 expression in Med1 cells by only 20% and did not effect the expression level in Med8A. In contrast,  $\geq$ 640 nM of each agent reduced expression of ErbB2 (and other chaperone client molecules including Raf1 and when present mutant p53) in each cell line  $\geq$ 90%. Paradoxically, low doses of each drug appeared to stimulate the growth of each cell line by 10% to 40%. This was investigated further in the Med8A high ErbB2 expressing cell line. Doses  $\leq$ 8 nM, which generated a 20% increase in growth, were also shown to generate increased expression of ErbB2, Raf1 and HSP90 to 140%, 200% and 120% respectively relative to controls. Second, we investigated the ability of the

anti-ErbB2 monoclonal antibody Herceptin™ (supplied by Genentech Inc.) to inhibit the *in vitro* growth of the three medulloblastoma cell lines. Maximal effect was seen against the high ErbB2 expressing line Med8A in which a 30% reduction in growth rate was generated with 5  $\mu$ g/ml of antibody. The Med1 cell line demonstrated a small but significant 10% reduction in growth, while DAOY growth was not effected by Herceptin™. These data support the hypothesis that the ErbB2 receptor represents a potential novel therapeutic target for medulloblastoma. The anti-chaperone agents have complex effects against medulloblastoma cells which is likely to reflect their mode of action and influence on the expression of other chaperone client proteins in addition to ErbB2.

**#39 Phase I and II trials of 1 $\alpha$ -hydroxyvitamin D<sub>2</sub> in patients with metastatic hormone-refractory prostate cancer.** Bailey HH, Ripple G, Bruskewitz R, Bishop C, Wilding G. *University of Wisconsin Comprehensive Cancer Center, Madison, WI.*

Vitamin D metabolites have been shown to have significant anticancer potential *in vitro* and *in vivo*, but clinical use is limited by hypercalcemia. Vitamin D analogues are being developed with less calcemic effects but similar growth inhibitory effects. 1 $\alpha$ -hydroxy-vitamin D<sub>2</sub> (1 $\alpha$ -OH-D<sub>2</sub>) is such an analogue. Vitamin D has been implicated as a factor in prostate cancer via epidemiologic studies as well as multiple *in vitro* studies showing excellent therapeutic potential. We have completed a phase I/II study of 1 $\alpha$ -OH-D<sub>2</sub> administered orally once a day continuously in patients with metastatic hormone-refractory prostate cancer (HRPC) and have an ongoing phase II study in the same patient population. Twenty-one patients were treated at 5 dose levels (L1-5  $\mu$ g/day, L2-7.5  $\mu$ g, L3-10  $\mu$ g, L4-12.5  $\mu$ g, L5-15  $\mu$ g). Transient hypercalcemia (grade 1 and 2) not requiring dose modifications was noted in a patient at L2 and L4. Level 5 (15  $\mu$ g/day) (9 patients) toxicity consisted of 2 patients with grade 1 hypercalcemia and 2 patients with grade 2 and 3 hypercalcemia and associated grade 2 increases in serum creatinine. Hypercalcemia without obvious sequelae was commonly associated with ingestion of 1 $\alpha$ -OH-D<sub>2</sub>. All toxicity resolved spontaneously or with stopping drug. Clinical activity was observed in 2 patients (L1 and 2) with significant regression of soft-tissue disease as well as 6 patients with stable disease for >6 months. Prostate specific antigen levels did not correlate with the above objective responses. A phase II trial of 1 $\alpha$ -OH-D<sub>2</sub> in patients with HRPC has begun based on the above trial (12.5  $\mu$ g once a day, continuously). Nine patients (3 active, 6 off study) have been entered to date with enrollment continuing. Supported by Bone Care International, Madison, WI, and DAMD17-98-1-8503.

**#40 Interaction of Tamoxifen, Genistein, and Vitamin E in the Growth Inhibition of Human Androgen-Independent Prostate Cancer Cell Lines.** Hugo, E.R., Hartman, D., Rees, P., Fritz, D., Hurst, B., and Carter, J.H. *Wood Hudson Cancer Research Laboratory, Newport, KY 41071.*

Metastatic prostate cancer is a leading cause of death in men. Initially, most forms of this cancer are repressed by the removal of these hormones and several treatment courses are based on this phenomenon. Growth inhibition by androgen removal, however, is often transient, with the carcinoma growth becoming independent of exogenous androgens. There is evidence that the emergence of androgen-independent prostate cancer (AIPC) may be in part due to exposure to estrogens. In this study, we have examined the effects of Tamoxifen ((Z)-[4-(1,2-diphenyl-1-butenyl)phenoxy]-N, N-dimethylethanamine 2-hydroxy-1,2,3-propanetricarboxylate) (Tam), and antiestrogen, Genistein (4',5,7-trihydroxyisoflavone) (Gen), a soy phytoestrogen, and vitamin E ( $\alpha$ -tocopherol succinate) (VitE) on the growth of three cell lines derived from metastatic prostate adenocarcinomas: LNCaP, DU-145, and PC-3. Tamoxifen competes with estrogen for receptor binding sites where both Gen and VitE may indirectly effect estrogen-mediated growth stimulation by decreasing the number of estrogen receptors found in the cell. Effects on cell lines were monitored by quantification of proliferation using direct cell counts and bioreduction of the tetrazolium compound MTS. We found: (1) that Tam shows a dose and time dependent inhibition of growth of androgen-independent cell lines, and (2) that nanomolar concentrations of either Gen or VitE increase the effectiveness of Tamoxifen. The synergistic inhibitory effects of Tam, VitE, and Gen on androgen-independent cell lines provide evidence for the potential use of these compounds as chemotherapeutic agents in the treatment of AIPC.

**#41 The use of the Prostate Xenograft CWR22 and Its Androgen Independent Sublines in the Preclinical Development of Herceptin.** Higgins, B., Fox, W.C., Malese, K., Fazzari, M., Scher, H.J., Agus, D.B. *Department of Medical Oncology, Memorial Sloan Kettering Cancer Center, 1275 York Avenue, New York, NY 10021.*

Preclinical xenograft studies can serve as predictors of the clinical potential of cancer therapeutics. Emphasis has recently been put on developing new and improved models of prostate cancer, which recapitulate the disease in a fashion that will allow for screening of potential therapeutics. The androgen dependent prostate xenograft CWR22 and its androgen independent sublines (CWR22R, CWRSA1, CWRSA4, CWRSA6) have many characteristics of human prostate cancer, including the production of PSA in an androgen-dependent fashion and tumor regression after



androgen withdrawal. We have studied a recombinant, humanized anti-Her-2/neu antibody (Herceptin®) in this preclinical model of human prostate cancer. When administered i.p. at a dose of 20 mg/kg twice weekly, Herceptin had no effect on tumor growth in any of the androgen independent tumors. However, significant growth inhibition was observed in the androgen-dependent CWR22 (68% growth inhibition;  $p=0.03$  for trajectories of the average tumor volume of the groups). These results were verified in another more widely used androgen-dependent xenograft model LNCaP (89% growth inhibition;  $p=0.002$ ). There was a significant increase in PSA index (ng PSA/ml serum/mm<sup>3</sup> tumor) in CWR22 xenografted mice compared with controls (CWR22, 18-fold relative to pretreatment value versus 1.0-fold,  $p=0.0001$ ), despite the tumor response. Initial data from clinical trials in patients with androgen independent disease have demonstrated a lack of significant clinical activity. Clinical trials in hormone-naïve patients are currently underway. The preclinical testing of Herceptin in CWR22 and its androgen independent sublines clearly demonstrates how this prostate cancer model can be used to guide the development of clinical trials for cancer therapeutics.

**#42 Antitumor activity of mifepristone, tamoxifen and the combination of both in human LNCaP prostate cancer models in nude mice.** El Etreby, M. Fathy, Liang, Yayun, and Lewis, Ronald W. *Medical College of Georgia, Augusta, GA.*

**Background:** Previously published results suggest a tumor inhibitory effect of antiprogesterins and antiestrogens in prostate cancer models. The objective of the present studies is to determine whether androgen-sensitive and androgen-insensitive variants of the well characterized LNCaP human prostate cancer cell line exhibit stable differences in their sensitivity to an *in vivo* antitumor activity of the antiprogesterin, mifepristone, the antiestrogen tamoxifen or the combination of both.

**Methods:** Exponentially growing LNCaP, LNCaP-C4 and LNCaP-C4-2 prostate cancer cells in culture were mixed with matrigel and injected s.c. in the flank of 6 to 8 week old male nude mice. The tumors were permitted to grow until they reached a volume of 200–300 mm. The animals were then randomly assigned to groups of 10 animals each. Treatment groups received either mifepristone (50 mg/kg/day s.c.) or 2 × 15 mg tamoxifen pellets (20 mg/kg/day) or a combination of both. Tumor volume was determined weekly. After 4 weeks of treatment, the tumors were harvested and wet weights determined.

**Results:** The inoculated tumor cells produced progressive growing tumors in male nude mice. However, the androgen-insensitive LNCaP-C4-2 cells showed the most aggressive and most rapid growth rate and shortest time to tumor progression. The tumors derived from the LNCaP-C4 cells exhibited a higher rate of tumor growth as compared with those derived from the parental androgen-sensitive LNCaP cells. In all models, mifepristone and tamoxifen treatment caused a significant retardation of tumor progression. After 28 days of treatment, significant inhibition (up to 60%) of tumor growth was observed in the mifepristone and the tamoxifen treatment groups as compared with the corresponding control groups. An additive effect was clearly evident in the combination group.

**Conclusions:** The antitumor activity of mifepristone and tamoxifen, suggest a potential clinical benefit of the use of antiprogesterins and/or tamoxifen as novel non-androgen ablation therapeutic approaches in the management of prostate cancer.

**#43 bFGF induces cell death and decreases *in vivo* tumour growth of Ewing's sarcoma cells, which may in part be mediated by expression of a variant FGFR3.** Sturla Lisa M, Selby Peter J, Lewis Ian J and Burchill Susan A. *Candlelighter's Children's Cancer Research Laboratory, ICRF Cancer Medicine Research Unit and Paediatric Oncology, St. James University Hospital, Leeds LS9 7TF, United Kingdom.*

Basic fibroblast growth factor (bFGF) is mitogenic in many tumour cell types. However, we have recently shown bFGF-decreases Ewing's sarcoma cell number *in vitro*. The aim of this study was to characterise the *in vitro* and *in vivo* effects of bFGF in Ewing's sarcoma, and determine whether the different effects of bFGF are due to distinct patterns of FGF receptor (FGFR) expression.

The *in vitro* effect of bFGF on proliferation was measured by bromodeoxyuridine incorporation (Amersham), and on cell death by electron microscopy, labelling with annexin v (Alexis) and staining with acridine orange (Sigma). FGFR's were identified by immunocytochemistry using an FGFR-1 antibody (Santa Cruz) and characterised by reverse transcriptase polymerase chain reaction. The effect of bFGF on xenograft implantation and growth, following subcutaneous injection, was examined in NuNu mice.

bFGF (5–80 ng/ml) induced a significant decrease in Ewing's sarcoma cell proliferation. This was accompanied by an increase in cell death demonstrated by induction of apoptosis and an increase in necrotic cell number. Growth of Ewing's sarcoma's *in vivo* was significantly reduced following subcutaneous injection with bFGF (10–200 ng/mouse/day). All the Ewing's sarcoma cell lines examined expressed the four high affinity FGFR's, as did the neuroblastoma cell lines in which bFGF induces proliferation. However, in the Ewing's sarcoma cells a variant FGFR-3 was identified. Direct sequence analysis demonstrated this receptor lacked 30 base pairs corresponding to a region between the second and third Ig-like loops of the extracellular domain (which includes a glycosylation site), the

second half of the third Ig-like loop and the transmembrane domain. In summary, bFGF-induced cell death in Ewing's sarcoma cell lines and decreased tumour growth *in vivo*. We have identified an FGFR-3 splice variant, which may play a role in bFGF-induced apoptosis and decreased tumour growth. We are currently investigating the effects and expression of this previously undescribed receptor.

**#44  $\alpha$ -amidating enzyme, peptidylglycine  $\alpha$ -amidating monooxygenase (PAM): a potential new target to inhibit glial tumor cell proliferation and development.** Ouafik L.H., Boudouresque F., Chinot O., Deifino C., Sauze S., and Martin P.M. *Laboratoire de cancérologie expérimentale, faculté de Médecine Nord, Marseille, France.*

Normal glial cell development and proliferation are regulated by many elements. Glioma brain tumor are characterized by particular invasiveness and angiogenic properties which participated to the aggressiveness of these tumors. Autocrine and paracrine signals are thought to accelerate glial tumor cell proliferation including REGF, PDGF and FGF signals. Among these regulatory factors, bioactive peptides have attracted significant interest because of their diverse roles not only as hormones/transmitters in endocrine and nervous systems, but also as trophic factors with critical roles in cell proliferation and maturation during development, growth and regeneration. Many studies have demonstrated elevated levels of bioactive peptides expression in a variety tumors. Since bioactive peptides are synthesized from precursor molecules by a complex series of posttranscriptional processing events, one efficient means of blocking the production of multiple growth promoting peptides is to inhibit key peptide biosynthetic enzymes. Instead of focusing on endoproteases or carboxypeptidases, which represent families of related enzymes with functional redundancy, we have chose to target the unique  $\alpha$ -amidating enzyme, peptidyl  $\alpha$ -amidating monooxygenase (PAM), the only enzyme identified to date capable of catalyzing the synthesis of bioactive  $\alpha$ -amidated peptides from their inactive precursors. In our preliminary studies, total RNA from surgically resected human gliomas and normal brain tissue was prepared to assess steady-state levels of PAM transcripts by Northern blot analysis. We have identified high levels of PAM expression particularly in human glioblastoma, while no expression was detected in normal brain. The same results were found in glioma cell lines. Moreover, the amount of PAM mRNA appeared to correlate with malignancy stage. Accordingly, to test the role of PAM in glial tumors, we are using pharmacological inhibitors, neutralizing antibodies and adenoviral mediated expression of PAM antigens RNA to eliminate PAM function *in vitro* and *in vivo*. These techniques are developed using human glioma cell lines to assess their abilities to suppress glial tumor cell proliferation and migration. The same strategies will be used to evaluate inhibition of glioma proliferation/progression in nude mice. The studies may provide an efficient means of suppressing tumor cell development and growth, and have important implications for therapeutic intervention.

**#45 Hormonesensitivity index: expression of 5 $\alpha$ -réductase isoforms and peptidylglycine  $\alpha$ -amidating monooxygenase enzyme in human prostate cancer.** Rocchi P., Boudouresque F., Ouafik L.H., Karsenty G., Bledou F. and Martin P.M. *Laboratoire de cancérologie expérimentale, Faculté de Médecine Nord, Marseille, France.*

**Introduction:** In the prostate, two 5 $\alpha$ -réductase (5 $\alpha$ -R) isoenzymes, type 1 and 2 have been described. The 5 $\alpha$ -R 2 isoform is expressed primarily in the stroma and in androgeno-dependent epithelial cells has been considered as being predominant isoform in both normal and diseased human prostate. Evidence for the 5 $\alpha$ -R 1 isoform is much more recent. It is expressed essentially in the epithelium and associated with neuroendocrine differentiation (NED). Studies suggest that NED is associated with an unfavorable prognosis and androgen-independent progression. Recently, a variety of neuropeptides have been shown to be expressed in prostatic carcinoma; these peptides are secreted by local areas of neuroendocrine differentiated cells. These are  $\alpha$ -amidated at their carboxyl terminus a structural modification that is essential for their biological activity. This posttranslational modification is catalyzed by the bifunctional enzyme, peptidylglycine  $\alpha$ -amidating monooxygenase (PAM). We therefore decided to measure both 5 $\alpha$ -R and PAM expression in cultured epithelial cells from malignant human prostate and a human xenograft model.

**Methods:** Methods used were northern blot, enzyme assays, RT-PCR, Immunohistochemistry.

**Results:** In this study, high expression of 5 $\alpha$ -R1 and PAM was found in PC3, DU145 cells lines, and LuCaP 23.1 whereas it was barely detectable in LNCaP (androgeno-dependant) cells. Enzymes expression (5 $\alpha$ -R1 and PAM) was higher in DU145 and PC3 cells compared with LNCaP cells. It was expressed in LuCaP 23.1 after castration, in hormone-independent stage. Similar data were obtained with prostate carcinoma samples.

**Conclusions:** We conclude that neuroendocrine differentiation is associated with: 1/changes in androgen metabolism pathway; 2/expression of PAM suggests the synthesis of  $\alpha$ -amidated peptides that could play a fundamental role in androgeno-insensitivity.

**Objectives:** To test directly the role of PAM in hormone-independent stage, we will use pharmacological inhibitors, neutralizing antibodies and adenoviral mediated expression of PAM antisense RNA to eliminate PAM



function *in vitro* and *in vivo*. These studies represent a novel approach to understanding prostate cell proliferation after castration and have important implications for therapeutic intervention.

**#46 National Cancer Institute: Connections with commercial partners for technology development.** Gabrielsen, B., Carrol, K., Lovoy, E., Marquis, S., Stackhouse, T., Twomey, P., Maurey, K., and Sybert, K. *NCI-Technology Development & Commercialization Branch.*

The Technology Development and Commercialization Branch (TDCB) of the National Cancer Institute (NCI) negotiates Cooperative Research and Development Agreements (CRADAs) with commercial partners to facilitate the development and utilization of new technologies emanating from the NCI programs and laboratories. This poster provides a brief but representative composite of successful collaborations from the NCI Divisions of: Basic Sciences (DBS), Clinical Sciences (DCS), and, Cancer Treatment and Diagnosis (DCTD) including the Developmental Therapeutics Program (DTP) and the Cancer Therapy Evaluation Program (CTEP). New cooperative research (CRADA) opportunities with NCI scientists will also be presented.

**#47 Vaccination against poor immunogenic self-peptide using toxin receptor binding domain-conjugated peptide repeats.** Hwang, J., Hsu, C.-T., Ting, C.-Y., Ting, C.-J., Chen, T.-Y., Lin, C.-P., and Whang-Peng, J. *Inst. Mol. Biol., Academia Sinica, Taipei, Taiwan.*

To overcome the difficulty of inducing immune response against poor immunogenic self-peptide, an immunogen was designed to contain an efficient antigen delivery vehicle and multiple copies of self-peptide. The receptor binding domain of pseudomonas exotoxin A was used as an antigen delivery vehicle because it could deliver antigen into antigen presenting cells through receptor-mediated endocytosis, which is known to be more efficient than phagocytosis. To increase the copy numbers of small peptide, we have developed a novel technique named template repeated polymerase chain reaction. Using this technique, we are able to construct a DNA fragment encoding a tandem repeated peptide. In this study, we have constructed a fusion protein containing receptor binding domain of pseudomonas exotoxin A and 12 repeats of gonadotropin releasing hormone in linear alignment (PEIa-GnRH12). After immunization with PEIa-GnRH12, all four female rabbits produced anti-PE and anti-GnRH antibodies. The produced anti-GnRH antibody was shown to effectively neutralize GnRH activity *in vivo* as evidenced by the degeneration of the ovary of the PEIa-GnRH12 immunized rabbits. Thus, we expect that vaccination with PEIa-GnRH12 may be useful in the treatment of GnRH-associated disease, such as ovarian cancer.

**#48 Expression of angiogenic factors and plasminogen converting enzymatic activity by cervical cancer patient-derived cells.** Chopra, V., Dinh, T.V. and Hannigan, E.V. *Department of Obstetrics and Gynecology, The University of Texas Medical Branch at Galveston, Galveston, TX 77555-0587.*

We investigated the production of angiogenic factors by peripheral blood-derived mononuclear cells (PBMC, n=8) and tumor-derived epithelial cells (n=6) from patients with cervical cancer during different stages (FIGO, Stages I-IV) of cancer progression. The production of angiogenic factors was studied by using human umbilical vein-derived endothelial cell (HUVEC) proliferation (MTT) and migration (wound healing and Boyden chamber) assays as compared to basic fibroblast growth factor (bFGF) as positive control and transforming growth factor- $\beta$  (TGF- $\beta$ ) as negative control. The angiogenic factors (IL-2, IL-6, IL-8, angiogenin, bFGF, angiogenin and vascular endothelial growth factor) were identified by using ELISA. An increase in expression of message levels of bFGF, TNF- $\alpha$ , angiogenin, VEGF and its receptor *flt-1*, and KDR was observed by HUVEC in presence of tumor-derived, conditioned medium (TCM) collected from patient-derived cells. The TCM collected from cancer cells also increased the expression of ICAM-1 and VCAM adhesion molecules on the surface of HUVEC. We also observed that human cervical cancer-derived epithelial cells expressed enzymatic activity that could generate bioactive angiotensin from purified human plasminogen. Thus it can be concluded that the production of angiogenic factors by patient-derived cells was independent of FIGO-Stage of cancer progression, but the serum levels of angiogenic factors varied during different stages of cancer progression. These experiments indicated that angiogenic factors are not only produced by tumor-derived epithelial cells and PBMC, but also by ascitic fluid derived epithelial and mononuclear cells as compared with control epithelial cells, epithelial cells from benign tumors, and PBMC from normal control subjects.

### SECTION 3: METASTASIS AND INVASION TARGETS

**#49 Inhibition of matrix metalloproteinase-2 (MMP-2) expression and bladder carcinoma metastasis by halofuginone.** Elkin Michael, Reich Rouven, Angorn Elena, and Vlodavsky Israel. *Dapt. of Oncology, Hadassah-Hebrew University Hospital, Jerusalem 91120, Israel.*

Matrix metalloproteinase-2 (MMP-2) plays a critical role in tumor cell invasion and metastasis. Inhibitors of this enzyme effectively suppress tumor metastasis in experimental animals and are currently being tested in clinical

trials. MMP-2 transcriptional regulation is a part of a delicate balance between the expression of various extracellular matrix (ECM) constituents and ECM degrading enzymes. Halofuginone, a low molecular weight quinazolinone alkaloid, is a potent inhibitor of collagen type I ( $\beta$ ) gene expression and ECM deposition. We now report that expression of the MMP-2 gene by murine (MBT2-t50) and human (5637) bladder carcinoma cells is highly susceptible to inhibition by halofuginone. Fifty percent inhibition was obtained in the presence of as little as 50 ng/ml halofuginone. This inhibition is due to an effect of halofuginone on the activity of the MMP-2 promoter, as indicated by a pronounced suppression of CAT activity driven by the MMP-2 promoter in transfected MBT2 cells. There was no effect on CAT activity driven by SV40 promoter in these cells. Halofuginone treated cells failed to invade through reconstituted basement membrane (Matrigel) coated filters, in accordance with the inhibition of MMP-2 gene expression. A marked reduction (80-90%) in lung colonization of MBT2 bladder carcinoma cells was obtained following intravenous inoculation of halofuginone treated cells as compared to the high metastatic activity exhibited by control untreated cells. Under the same conditions there was almost no effect of halofuginone on the rate of MBT2 cell proliferation. These results indicate that the potent anti-metastatic activity of halofuginone is due primarily to a transcriptional suppression of the MMP-2 gene, resulting in a decreased enzymatic activity, matrix degradation and tumor cell extravasation. This is the first description of a drug which inhibits experimental metastasis through inhibition of MMP-2 at the transcriptional level. Combined with its known inhibitory effect on collagen synthesis and ECM deposition, halofuginone is expected to exert a profound anti-cancerous effect by inhibiting both the primary tumor stromal support and metastatic spread.

**#50 Inhibition of renal cell carcinoma growth and metalloproteinase activity by NF681, a phosphonic acid diphenylurea.** Gliagardi, A.R.T., Bittencourt, M., Nickel, P., Collins, D.C. *VAMC and University of Kentucky Medical Center, UNICAMP, Campinas-SP, Brazil and University of Bonn, Bonn, Germany.*

Treatment for renal cell carcinoma remains a major challenge. Renal cell carcinoma is characterized by uncontrolled angiogenesis, hypervascularity and a high frequency of invasion and metastasis. The results of systemic therapy for metastatic renal cell carcinoma are disappointing and currently available chemotherapeutic agents have not been effective. We have synthesized and characterized a phosphonic acid diphenylurea, NF681, that is less bound to plasma proteins, less toxic and has a shorter half-life than suramin. In this study, we showed that NF681 is a potent inhibitor of cell growth and metalloproteinase (MMP) activity in renal cell carcinoma (A-498) cells and primary renal adenocarcinoma (786-0) cells. The MTT assay was used to determine the effect of NF681 on cell proliferation. MMP activity was determined in culture media by gelatin gel zymography. The 50% inhibitory concentration (IC<sub>50</sub>) for NF681 was < 30  $\mu$ M for both cell lines. Metalloproteinase activity (MMP-2) was expressed in the culture media of 786-0 cells. Epidermal growth factor stimulated this activity in both A-498 and 786-0 cells. NF681 was a potent inhibitor of MMP-2 activity in a dose-dependent manner on both cell lines. In summary, NF 681 is a potent inhibitor of renal carcinoma growth and MMP-2 activity that is important for invasion and metastasis. This phosphonic acid diphenylurea may be an effective new therapeutic agent for renal cell carcinoma.

(Supported by the Department of Defense Grant DAMD17-98-1-8467 and Department of Veterans Affairs.)

**#51 Inhibition of endothelial cell sprout formation and extracellular matrix invasion by a small molecule MMP inhibitor.** Manthey, C.L., Zhou, Z., Hasiwo, K., Maragan, J.J., Laltanze, J., Green, D., and Molloy, C.J. *3-Dimensional Pharmaceuticals, Exton, PA.*

Tumor angiogenesis involves the "colonization" of tumors by host endothelial cells (EC). EC invasion of the tumor matrix requires pericellular proteolysis, and the relevant proteases are attractive anticancer drug targets. In this regard, migrating EC express urokinase, which through the conversion of plasminogen to plasmin is thought to aid EC migration through fibrin deposits commonly encountered in tumor matrix. Matrix metalloproteinases (MMPs), including MMP-1, -2, and -14, are also expressed by migrating EC and facilitate movement through extracellular matrices. We performed *in vitro* assays to examine the effects of a plasmin inhibitor (aprotinin) and a synthetic hydroxamic acid MMP inhibitor (AG3430) on microvessel formation/invasion in fibrin, type 1 collagen, and basement membrane (Matrigel). Rings cut from rat aortas were cultured in 3-dimensional gels of type 1 collagen leading to the formation of capillary-like outgrowths of EC and smooth muscle cells. AG3430 (5  $\mu$ M) completely inhibited the formation of these microcapillary "sprouts." In contrast, aprotinin (10  $\mu$ g/ml) had no effect on vessel formation. In an alternative assay, human microvascular EC were plated onto fibrin gels. Over 72 h, many cells escape the monolayer and invade the fibrin gel. We found that AG3430 (IC<sub>50</sub> = 30 nM), but not aprotinin, completely inhibited the ability of ECs to invade fibrin. Finally, AG3430 (5  $\mu$ M), but not aprotinin (10  $\mu$ g/ml), inhibited EC invasion through either fibrin or Matrigel-coated transwell filters. These data are consistent with the recently described fibrinolytic activities of MMPs, underscore a relative importance of MMPs in EC migration, and support MMPs as important drug targets in tumor angiogenesis.



**#52 Antitumor efficacy and longterm sensitivity to prinomastat (AG3340) after extended *in vivo* treatment.** Zou, H., Brekken, J., Feeley, R. and Shalinsky, D.R. Dept. of Research Pharmacology, Agouron Pharmaceuticals, Inc., 4245 Sorrento Valley Blvd., San Diego, CA 92121.

Prinomastat, a potent inhibitor with pM affinities for inhibiting the activities of MMP-2, -9, -13, and -14, markedly delays the growth of many human tumor xenografts (Ann. N. Y. Acad. Sci. 878:236-270, 1999). We are now assessing effects of prinomastat on the enzyme activities of MMP-2 and -9, key mediators of angiogenesis and metastasis, in human colon tumor cells (line COLO-320DM) *in vitro* and *in vivo*. Cells were cultured *in vitro* and the conditioned medium from these cells was collected for zymographic studies. Prinomastat suppressed gelatinase activities potently at 1-10 nM. Zymography was also conducted in colon tumors after s.c. implantation of tumor cells into nude mice. Proteolysis of gelatin and collagen IV was evident in tumors; studies are underway to assess effects of prinomastat on this proteolysis. Prinomastat dose-dependently decreased the growth of these tumors while producing marked antiangiogenic and antiproliferative activities (*ibid.*). Following a period of tumor growth suppression, tumor volumes increase despite continued treatment. To test whether tumors became resistant to prinomastat, viable tumor pieces from prinomastat-pretreated mice were serially-passaged into naive mice. Mice were then dosed orally with vehicle (acidified H<sub>2</sub>O) or prinomastat. In vehicle-treated mice, tumors readily regrew. In contrast, profound growth delays were observed in prinomastat-treated animals, even when pretreated tumors were passaged into naive mice and treated for over a year with prinomastat. Corroborating growth sensitivity data have been generated in prostate and lung cancer tumor models (Proc. Amer. Assoc. Cancer Res 40:A4686, 1999). Prinomastat markedly inhibits colon tumor angiogenesis after three serial passages (>200 days of treatment) as was observed during initial drug treatment. Histological and immunohistochemical analyses of tumor angiogenesis and proliferation over the full series of experiments are in progress. In summary, these results demonstrate that human colon COLO-320DM tumor cells secrete gelatinases and prinomastat potently inhibits gelatinase activities *in vitro*, and the antitumor efficacy of prinomastat is evident after longterm treatment of human tumor xenografts.

**#53 The effect of food on the pharmacokinetics of oral MMI270B (CGS 27023A), a novel matrix metalloproteinase inhibitor.** Eskens, F.A.L.M., Levitt, N.C., Sparreboom, A., Choi, L., Mather, R., Verweij, J., Harris, A. Departments of Medical Oncology and Clinical Pharmacology, Rotterdam Cancer Institute (Daniel den Hoed Kliniek) and University Hospital, Rotterdam, The Netherlands, ICRF Clinical Oncology Unit, Oxford, England, Novartis Pharma, East Hanover, NJ, USA, Novartis Pharma AG, Basel, Switzerland.

**Purpose:** MMI270B is a matrix metalloproteinase inhibitor (MMPi) with *in vitro* and *in vivo* activity against several MMPs and human tumor xenografts. As this type of drug will be given chronically, oral bioavailability is important. We performed a clinical study to evaluate the effect of food intake on pharmacokinetic parameters of MMI270B.

**Patients and methods:** Seventeen patients entered the study. Doses of MMI270B were 150, 400 and 600 mg. The first day, patients ingested the drug in a fasted state and were not allowed to eat for 2 hours. The second day, patients ingested the drug 30 minutes after a light breakfast. Pharmacokinetic parameters that were compared with AUC<sub>0-8h</sub>, C<sub>max</sub>, and T<sub>max</sub>.

**Results:** Pharmacokinetic parameters showed large interpatient variability, both in the fasted and fed state. AUC<sub>0-8h</sub> was 10% lower in the fed versus fasted state. The 90% confidence interval for the ratio of means fed/fasted (0.816-0.986) lies within the range (0.8-1.25), indicating no significant effect of food intake on AUC<sub>0-8h</sub>. In both the fed and fasted state, plasma levels were well above the IC<sub>50</sub> of MMP 1, 9, and 3 for considerable periods of time. C<sub>max</sub> in the fed state was about 40% lower than in the fasted state. The 90% confidence interval for the ratio of means fed/fasted (0.457-0.778) almost falls entirely outside of the range (0.7-1.43), indicating some effect of food intake on C<sub>max</sub>. T<sub>max</sub> was significantly (0.34 hrs or 20 minutes) increased after food intake (P = 0.042; 95% confidence limits for the mean difference: 0.04 h < 8 < 0.65 h).

**Conclusion:** Food intake did not result in a significant change in exposure to MMI270B (AUC<sub>0-8h</sub>), but did result in a significant decrease in peak plasma levels of the drug. Time to peak was increased. No specific guidelines concerning the ingestion of MMI270B in either the fed or fasted state are recommended.

**#54 BAY 12-9566: A selective matrix metalloproteinase inhibitor (MMPi) with distinct pharmacologic and toxicity profiles: update on NCIC CTG experience in 5 phase I and III trials.** Goel R, Hirte H, Chouinard E, Moore M, Ottaway J, Sadura A, Coppleters S, Elias I, Schwartz B, Seymour L. NCI-Canada Clinical Trials Group, Bayer Inc and Bayer AG.

Unlike other MMPi's in development, BAY 12-9566 is non-peptidic, selective, does not inhibit MMP-1, and has a toxicity profile notable for the absence of troublesome dose limiting musculoskeletal effects as well as the presence of dose related but usually clinically insignificant effects on peripheral platelet counts. Occasional maculopapular rashes have been

described. The compound is also being developed in a parallel program for osteoarthritis. A dose-seeking phase I study (NCIC CTG IND.107) was completed in 1998; 800 mg bid po was defined as the recommended dose for further study. Recognizing the difficulty in designing appropriate phase II trials with drugs of this class, 2 phase III trials and 2 dose seeking trials (cross-over design) in combination with doxorubicin (DOX) or modulated 5-fluorouracil (FU) were simultaneously initiated early in 1998. NCIC CTG PA.1 is a randomized phase III study comparing BAY 12-9566 to gemcitabine for patients with advanced or metastatic pancreatic cancer. 277 of a planned 350 patients have been enrolled. NCIC CTG OV.12 is a randomized phase III study comparing BAY 12-9566 to placebo in patients who have completed initial surgical- and chemo-therapy (paclitaxel and platinum containing) for stage III or IV ovarian cancer and are in complete or partial response. 167 of 730 planned patients have been accrued to this trial to date. In NCIC CTG IND.113, patients were able to receive full single agent doses of DOX and BAY 12-9566 although there was some evidence of a modest PK interaction; in the BAY 12-9566 plus FU + leucovorin arm, there was some evidence of a clinical (mild thrombocytopenia) but not pharmacokinetic interaction, necessitating reduction of BAY 12-9566 to 400 mg bid; this trial will be completed in the summer. Final results from the phase I trials will be presented as well as an overview of safety experience to date.

**#55 Real time quantitative RT-PCR for determination of MMP-7 mRNA in colorectal mucosa and tumors.** Yan Jiaming, Heslin Martin J, Shao Lingning, Johnson Martin and Diasio Robert B. University of Alabama at Birmingham, AL 35294.

The matrix metalloproteinases (MMPs) are a family of enzymes responsible for the degradation of extracellular matrix components. MMP-7 (matrilysin), is responsible for hydrolyzing proteoglycans and extracellular matrix glycoproteins. The overexpression of MMP-7 gene has been reported in various tumors, including colon, breast, stomach, prostate cancer, and some of colon adenomas with a potential for malignancy. MMP-7 may play a role in tumor growth, invasion, metastasis and tumorigenesis. The previous methods for measurement of MMP-7 mRNA are not sensitive enough to detect MMP-7 levels in all tissues. We report a sensitive, reproducible and real time quantitative RT-PCR method for determination of MMP-7 mRNA in tissues using the ABI Prism Sequence Detector. This system utilizes a unique fluorescent oligonucleotide probe which contains 5'-end fluorescent reporter dye and 3'-end quencher dye and eliminates the need for post PCR processing. MMP-7 mRNA levels are quantitated by measurement of increased fluorescence separating the reporter dye from quencher during PCR. Our preliminary results showed that the fluorescent signal is directly proportional to the starting copy numbers of MMP-7 with a linear range over 250 to 10,000,000 copies (r<sup>2</sup>=0.997). Within-day and between-day coefficients of variation were less than 7%. This method has been applied in 10 patients with colon adenoma and 5 patients with colon carcinoma. The MMP-7 mRNA levels (median) were 87.88 copies/ng GAPDH RNA with a range from 26.20 to 1070.89 in normal mucosa, 1462.11 copies/ng GAPDH RNA with a range from 690.49 to 6200.80 in adenoma and 2784.25 copies/ng GAPDH RNA with a range of from 1083.05 to 14640.36 in colon carcinoma, respectively. The expression of MMP-7 was significantly higher in adenoma and carcinoma compared with normal mucosa (P < 0.02). These results suggest that overexpression of MMP-7 may be an important step in the tumorigenesis and malignant progression of colon cancer and may be a useful target for new therapies. The method we developed is rapid, sensitive and reliable for quantitating MMP-7 mRNA in various tissues and will be very useful in evaluation the effect of MMP-7 expression on tumor invasion, metastasis and tumorigenesis.

**#56 Inhibition of pericellular urokinase plasminogen activator activity and basement membrane cell invasion by novel small molecule urokinase inhibitors.** Molloy, C.J., Sharp, C., Manthey, C.L., Zhou, Z., Randle, T., Green, D., Hoffman, J., Subasinghe, N., Rudolph, J., Wilson, K., Deckman, I., Bone, R., Illig, C. 3-Dimensional Pharmaceuticals, Exton, PA, 19341.

Angiogenesis and tumor cell metastasis are critical processes involved in cancer progression. In this regard, invasion of cells through tissue requires pericellular proteolysis and predominant among cell surface-localized proteases is urokinase plasminogen activator (uPA). This enzyme mediates the conversion of plasminogen to plasmin leading to matrix degradation either directly or through subsequent activation of matrix metalloproteinases. Using an iterative structure-based drug design process, we have developed non-peptidic, potent (K<sub>i</sub>'s ~ 20-100 nM), low molecular weight (MW < 500) uPA inhibitors with selectivity vs. other serine proteases, including tPA, thrombin, trypsin, and plasmin. Cell-based assays were performed using 3DP-49215 (K<sub>i</sub> ~ 20 nM) as a representative compound. Treatment of PC-3 human prostate carcinoma cells with 3DP-49215 reduced uPA-receptor bound uPA activity with IC<sub>50</sub> < 100 nM. The ability of 3DP-49215 to inhibit cell invasion also was evaluated using a basement membrane (Matrigel)-coated Transwell filter system. We found that 3DP-49215 blocked uPA-mediated invasion of basement membrane by PC-3, M24met (human melanoma), THP-1 (human monocytic cells), and rat vascular smooth muscle cells in a concentration-dependent manner,



with IC<sub>50</sub> values in the range of 0.3–3 μM. Taken together, these results support uPA inhibitors as a new class of chemotherapeutic agent with potential utility against a variety of human tumors. Studies are ongoing to evaluate the *in vivo* efficacy of these compounds in tumor xenograft models as well as related diseases involving tissue remodeling.

**#57 Prognostic significance of PAI1 and EGFR expression in adult glioma tumors.** Muracciole, X., Palmari, J., Dufour, H., Romain, S., Chinot, O., Ouafik, L., Grisoll, F., and Martin, P.M. *Laboratoire de Cancérologie Biologique, Faculté Nord, Marseille, France - CHU La Timone, rue St Pierre, Marseille, France.*

**Background:** In malignant gliomas, high levels of uPA and PAI1 were expressed and not in normal brain tissue. Also EGFR was found to be amplified, overexpressed, and altered in 40% of glioblastoma multiforme. A correlation was found between an EGFR gene mutation and a poor prognosis. **Objective:** We studied the Epidermal Growth Factor Receptor (EGFR), urokinase type Plasminogen Activator (uPA) and Plasminogen Activator Inhibitor type-1 (PAI1) expression levels in 60 glioma tumors and the correlation with tumor histology. We have evaluated the prognostic significance of these biological parameters and the clinical factors (age, performance status, pathological WHO classification) in a multivariate analysis. **Methods:** We analysed 10 grade I and II tumors, and 50 malignant gliomas (grade III–IV). Median cytosolic levels of uPA, PAI1 and EGFR, as determined by ELISA, were respectively 0.03 ng/mg protein, 7 ng/mg protein, and 67.5 fmole/mg protein. Treatment in all patients consisted of surgery and for malignant tumors adjuvant chemotherapy and radiotherapy. The median follow-up was 40 months in the alive population (38 deaths and 22 censored data). **Results:** PAI1 level was correlated positively with histological grade ( $p < 0.001$ ) and the age ( $p = 0.035$ ). Univariate analysis demonstrated that high levels of PAI1 and of EGFR were associated with a shorter survival for overall population and for malignant gliomas (respectively  $p = 0.0013$  and  $p = 0.0018$ ). In contrast, uPA expression had no influence on the clinical outcome. In a multivariate analysis, only the PAI1 and the EGFR levels remained highly significant ( $p < 0.0001$  and  $p = 0.0045$ ; respectively) and not other clinical parameters. The Overall Survival rate at 5 years were respectively: 73% for patients with PAI1 level less than 1.3 ng/mg protein (Group I), 25% with level between 1.4 and 99 ng/mg protein (Group II) and 0% with level upper than 99 ng/ml protein (Group III) ( $p < 0.0001$ ). In a second step, the histological grade (grade 1–2–3 versus 4) for the group I and the EGFR expression in the group II have allowed to define three classes of patients: A (favorable outcome), B (intermediate outcome), C (with unfavorable outcome) with a significant difference in OS rate at 2 and 5 years concerning all tumors and also the malignant tumors ( $p < 0.0001$ ). **Conclusion:** These results must be confirmed in a larger series and underlines the major impact of PAI1 expression to define more accurately the prognosis of glioma tumors and to help therapeutic decision.

**#58 Combination therapy with tamoxifen (TAM) and an inhibitor of invasion and angiogenesis (A6) leads to significant inhibition of hormone-dependent breast cancer cell growth *in vivo*.** Guo, Yongling, Mazar, Andrew P. and Rabbani, Shafaat A. *Royal Victoria Hospital, McGill University, Montreal CA and Angstrom Pharmaceuticals, San Diego, CA.*

Aggressive breast tumors are characterized by their increased expression of urokinase plasminogen activator (uPA) and its receptor (uPAR) relative to normal tissue or benign tumors. We previously described the ability of a small, 8 amino acid peptide (A6), derived from the connecting peptide region of uPA, to prevent growth and metastasis of several hormone dependent and independent breast cancer lines *in vivo*. In this study, we have examined the more likely scenario of using A6 in combination with anti-estrogens to treat established, hormone-responsive tumors *in vivo*. A6 was tested in combination with tamoxifen (TAM), an anti-estrogen used in the treatment of hormone dependent breast cancer. A6 or TAM alone inhibited the invasion of hormone-dependent breast cancer lines in a dose-dependent manner in a Transwell invasion assay. The degree of inhibition was increased significantly when A6 and TAM were used in combination. The effects of this combination treatment were then examined *in vivo*. Mat B-III ( $7 \times 10^5$ ) cells were inoculated orthotopically into the mammary fat pads of female Fisher rats. Tumors were staged to 40 mm<sup>3</sup> (7 days after inoculation) and treatment was initiated at this time. A6 (75 mg/kg, b.i.d.) and TAM (3 mg/kg/day, q.d.) were injected i.p. for 11 days. Animals were euthanized on day 19 and evaluated for primary tumor growth and the presence of macroscopic metastasis. Control animals receiving vehicle alone developed large tumors and macroscopic metastases to axillary lymph nodes. Both tumor growth and metastasis were suppressed by 50% in the groups receiving either A6 or TAM alone. Most strikingly, combination treatment with both TAM and A6 inhibited tumor growth by 75% and completely inhibited the formation of macroscopic metastases. We conclude that combination therapy using an anti-angiogenic/anti-invasive agent (A6) and an anti-estrogen significantly inhibits the progression of hormone-dependent breast cancer. This conclusion has implications for both prophylaxis as well as the treatment of early stage, hormone-dependent breast cancer in the clinical setting.

**#59 External Optical Imaging Of Green Fluorescent Protein-Expressing Metastatic Tumors.** Yang, M.,<sup>1,2,3</sup> Baranov, E.,<sup>1</sup> Sun, F.X.,<sup>1</sup> Chishima, T.,<sup>3</sup> Moossa, A.R.,<sup>2</sup> Hoffman, R. M.<sup>1,2</sup> *1)AntiCancer, Inc., San Diego, CA 92111, USA; 2)Dept. of Surgery, Univ. of Calif., San Diego, CA 92103 USA; 3)Dept. of Surgery, Yokohama City Univ. School of Med., Yokohama, Japan.*

We report here the establishment of an external high-resolution real-time optical imaging system of internally growing tumors in intact live mice. Stable high-level green fluorescent protein (GFP)-expressing human and rodent cancer cells enable tumors and metastasis formed from them to be externally imaged. B16F0 mouse melanoma cells and AC3488 human colon cancer tissue were transduced with a retroviral vector containing the green fluorescent protein (GFP) and neomycin resistance genes, *in vitro* and *in vivo*, respectively. The selected B16F0-GFP cells were injected into the tail vein of 6-week-old C57BL/6 and nude mice. External optical images of internally-growing tumors and metastatic lesions in the brain, liver, and bone were obtained. Real-time tumor growth was externally imaged in each of these organs. The *in vivo* selected GFP-expressing AC3488 human colon cancer tissues were transplanted into nude mice orthotopically. External optical images of internally-growing tumors and metastatic lesions in the liver, spleen, lymph nodes and bone were obtained. Real-time tumor growth also was externally imaged in each of these organs. With the use of a transilluminated fluorescence microscope and thermoelectrically cooled CCD camera, the minimum size of tumors imaged at the indicated depth in the various tissues were:  $\phi \sim 250 \mu\text{m}$  at a depth of 0.8 mm in the brain;  $\phi \sim 500 \mu\text{m}$  at a depth of 1 mm in the liver, and  $\phi \sim 250 \mu\text{m}$  at a depth of 0.8 mm in the various parts of the skeletal system. If the size of the tumor was greater than 1 mm in diameter, the maximum depth of tumors imaged increased up to  $\sim 1.5$  mm. Non-invasive real time fluorescence optical tumor imaging allows study of the tumor growth and metastasis, inhibition by experimental agents of all types in the intact animal.

**#60 Mutant thrombin receptor increases the metastatic potential of the human colorectal tumor cell line HCT-8 *in vitro*.** Feng Xue-sheng, Karpalkin Simon. *Department of Molecular and Cellular Biology, Roswell Park Cancer Institute, Buffalo, NY 14226 (X.F.); NYU Medical Center, NYC, NY 10016 (S.K.).*

It is well documented that thrombin can increase the metastatic potential of some tumor cell lines such as murine melanoma cells by binding to a unique protease-activated receptor (PAR-1). PAR-1 is a member of the seven transmembrane domain receptor family. To investigate which part of the receptor involved in this phenotype, we transferred a mutant thrombin receptor (muPAR-1) into human colorectal tumor cell line, HCT-8 and observed its effects on cell growth and metastatic potential. MuPAR-1 was made by substitution of eight amino acids from the Xenopus receptor's second extra cellular loop (XECL2B) for the cognate sequence in the human thrombin receptor. Comparing with wild type human thrombin receptor-transfected cell line, HCT8-WI, mutant thrombin receptor-transfected cell line, HCT8-Mu, has more adhesion ability to fibronectin (1.5–2.0 fold) *in vitro*. HCT8-Mu formed aggregates in culture while HCT8-WI does not. The doubling time for HCT8-Mu cell is less than that of HCT8-WI cells (27.7 hrs vs. 33.3 hrs). The tyrosine phosphorylation signaling in HCT8-Mu without thrombin stimulation is same as that in HCT8-WI and HCT8 with thrombin stimulation. These results suggest that mutant thrombin receptor can constitutively activate thrombin receptor and the mutant part of thrombin receptor, XECL2B, is responsible for the enhancement of human colorectal cancer metastatic potential by thrombin.

**#61 Mammalian heparanase: a novel gene involved in tumor progression and metastasis.** Elkin Michael, Pecker Iris, Friedmann Yael and Vlodavsky Israel. *Department of Oncology, Hadassah-Hebrew University Hospital, Jerusalem 91120, and InSight Ltd. POB 2128, Rehovot 76100, Israel.*

Heparan sulfate proteoglycans (HSPGs) attached to cell surfaces and in the extracellular matrix (ECM) interact with a multitude of ECM constituents, growth factors and enzymes via their heparan sulfate (HS) side chains. Degradation of HS by limited endoglycosidic heparanase cleavage affects a variety of biological processes and may play a decisive role in the extravasation of metastatic tumor cells. We have purified a 50 kDa heparanase from human hepatoma and placenta, and now report cloning of the cDNA and gene encoding this enzyme. Expression of the cloned cDNA in insect and mammalian cells yields 65 kDa and 50 kDa recombinant proteins, displaying heparanase activity. The 50 kDa enzyme represents an N-terminal processed enzyme which is  $\sim 100$ -fold more active than the full length 65 kDa form. The heparanase mRNA and protein are preferentially expressed in metastatic cell lines and specimens of human breast, colon and liver carcinomas. We show that non-metastatic murine T-lymphoma cells transfected with the heparanase gene acquired a highly metastatic phenotype *in vivo*, reflected by a high rate of mortality due to massive liver infiltration of subcutaneously inoculated lymphoma cells. Increased metastatic potential was also obtained with low metastatic mouse melanoma cells transfected with the heparanase cDNA. This represents the first cloned mammalian heparanase and provides direct evidence for its role in



tumor metastasis. Cloning of the heparanase gene enables the development of specific molecular probes and inhibitors for early detection and treatment of cancer metastasis and autoimmune disorders.

**#62 SR-45023A: a novel bisphosphonate ester inhibits both frequency and volume of bone metastasis *in vivo* in a nude mouse model.** Gailwitz, W.E., Mundy, G., Bentzen, C.L., Niesor, E., Hunter, C. and Schmid, S.M. Osteoscreen, Inc., San Antonio, TX 78229, Symphar, Geneva, Switzerland, and Ilex Oncology, Inc., San Antonio, TX, 78230.

SR-45023A is a novel bisphosphonate ester currently in Phase I clinical trials. Previous studies have demonstrated that SR-45023A activates the FXR nuclear receptor decreasing the rate of tumor cell proliferation and inducing apoptosis. Although SR-45023A is not a bisphosphonic acid and does not chelate  $Ca^{++}$ , it inhibits osteoclastic bone resorption induced by high doses of Vit D3 in Wistar rats (50 mg/kg/day for 5 days). The potential activity of SR-45023A on bone metastases formation was studied in a nude mouse model using intracardiac injection of human breast adenocarcinoma MDA-MB-231 cells. The cells were injected on Day 0 in female nude mice ( $n = 12/\text{group}$ ). The mice were treated with SR-45023A by gavage at dose levels of 50, 100, and 200 mg/kg daily from Days 1-14. The bone lesions were identified by faxitron radiography with image analysis along with animal weight recorded on Days 14, 21 and 28. Hind limb long bones were taken at terminal sacrifice, fixed, decalcified, mounted and stained with H&E and examined for both lesion number and lesion area. SR-45023A treatment reduced both the number and lesion area of bone metastases in a dose dependent fashion that was significant at Days 21 and 28 in the 200 mg/kg dose group. Microscopic examination of individual lesions indicated SR-45023A caused reduced cell proliferation and bone resorption. By Day 28, only 7 of 12 (58%) of the control animals were surviving compared with 11 of 12 (92%) in the high dose group. On Day 28, no lesions were detected in 7 of 11 of the surviving animals in the high dose group while 5 of the 7 surviving control animals had lesions. Although weight loss for the animals in the 200 mg/kg dose group was 7% during therapy, they unexpectedly recovered completely during the 2 week follow-up period without therapy. In contrast, a loss in body weight of 10.8% was measured in the surviving untreated animals during the follow-up period (Days 21-28). These data demonstrate that SR-45023A has potential for reducing both the incidence and progression of bone metastases to a degree that may be of clinical importance.

**#63 Inhibition of glioma invasivity and tumor formation by manipulation of specific glycosyltransferase gene expression.** Yamamoto, H., Oviedo, A., Kersey, D., Sweeley, C., Huh, J., Kroes, R., Mkrdichian, E., Leestma, E., Cerullo, L. and Moskal, J. The Chicago Institute of Neurosurgery and Neuroresearch, Chicago, IL 60614.

The invasive properties of malignant glioma cells are primarily responsible for the poor prognosis of patients with glioblastomas, for which there are no effective therapies. Changes in cell adhesion and the remodeling of the extracellular matrix play a critical role in the invasion of malignant tumors. The increased expression of aberrantly glycosylated adhesion molecules plays a major role in glioma invasion. We have previously reported that gliomas express integrins with terminal  $\alpha$ 2,6-linked sialic acids but not  $\alpha$ 2,6-linked sialic acids. The expression of  $\alpha$ 2,6-linked sialic acids on  $\alpha$ 3 $\beta$ 1 integrins by the stable transfection of the  $\alpha$ 2,6-sialyltransferase ( $\alpha$ 2,6-ST) gene resulted in inhibition of U-373MG glioma invasivity *in vitro*. An intracranial brain tumor model using SCID mice was employed to evaluate this transfectant *in vivo*. While U-373MG cells and vector-transfected control cells formed intracranial tumors,  $\alpha$ 2,6-ST transfected U-373MG showed virtually no tumor formation. These results suggest that altered sialylation of cell-surface adhesion molecules by  $\alpha$ 2,6-ST gene transfection can alter cell-extracellular interactions and block glioma cell invasion and tumor formation.

To further evaluate the feasibility of expressing the  $\alpha$ 2,6-ST gene in gliomas for therapeutic purposes, a replication-deficient adenovirus containing the  $\alpha$ 2,6-ST gene was developed. Infection of U-373MG cells with this viral construct resulted in dose and time dependent: (a) expression of cell-surface  $\alpha$ 2,6-linked sialic acids, (b) alterations in focal adhesions, and (c) inhibition of invasion *in vitro*. Taken together, these data suggest that if the  $\alpha$ 2,6-ST gene can be effectively delivered to gliomas, the resulting alterations in cell-surface glycosylation can lead to an inhibition of invasivity.

**#64 The PHSCN sequence as a potent anti-tumorigenic and anti-metastatic agent.** Livant, D. L., Brabec, R. K., Plenta, K. J., Allen, D., Kurachi, K., Markwart, S., and Upadhyaya, A. Departments of Anatomy and Cell Biology, Surgery and Internal Medicine, and Human Genetics, University of Michigan, Ann Arbor, MI.

Plasma fibronectin (pFn) was necessary and sufficient to stimulate serum-free (SF) basement membrane invasion by metastatic DU145 human and MATLyLu (MLL) rat prostate carcinoma cells. The PHSCRN sequence stimulated SF basement membrane invasion by DU145 or MLL cells whether on fragments of the pFn cell-binding domain or as a peptide. The P1D6 blocking monoclonal antibody showed that the  $\alpha$ 5 $\beta$ 1 integrin fibronectin receptor was involved. PHSCRN inhibited both PHSCRN-induced and serum-induced invasion *in vitro*. Acetylated, amidated PHSCRN (Ac-

PHSCRN-NH<sub>2</sub>) was 30-fold more potent; but, Ac-HSPNC-NH<sub>2</sub>, failed to inhibit DU 145 or MLL invasion. Rats injected subcutaneously with 100,000 MLL cells were intravenously treated thrice weekly with 1 mg Ac-PHSCRN-NH<sub>2</sub> or Ac-HSPNC-NH<sub>2</sub> beginning 24 hours later, or thrice weekly with 1 mg Ac-PHSCRN-NH<sub>2</sub> beginning only after the removal of large (2 cm) MLL tumors, or were left untreated. MLL tumors grew equally rapidly in Ac-HSPNC-NH<sub>2</sub>-treated and untreated rats. However, MLL tumor growth in the presence of systemic Ac-PHSCRN-NH<sub>2</sub> was reduced by more than 99.9% during the first 16 days of treatment, although subsequent growth occurred. Analysis of MLL tumor cryosections immunostained with anti-PECAM-1 showed that Ac-PHSCRN-NH<sub>2</sub> reduced tumor vasculature by 12-fold during this time. Relative to untreated MLL cells, Ac-PHSCRN-NH<sub>2</sub>-treated cells showed no apoptosis or reduction of S phase percentage. Thus, angiogenesis inhibition probably accounted for the reduced tumor growth observed. After administering 6 Ac-PHSCRN-NH<sub>2</sub> or Ac-HSPNC-NH<sub>2</sub> doses over the 14 days following surgery, all rats were euthanized. Metastases were scored at 10-fold magnification on lung surfaces, and micro-metastases at 400-fold magnification in sectioned, hematoxylin/eosin-stained lung tissue. The mean number of surface MLL lung metastases per Ac-PHSCRN-NH<sub>2</sub>-treated rat was 1, irrespective of when therapy was initiated. In contrast, the mean number of MLL lung metastases per rat was 81 in the untreated rats and 239 in rats treated with Ac-HSPNC-NH<sub>2</sub>. Analyses of micrometastases in sections of lung tissue were consistent with these results. Thus at sufficient dosages, Ac-PHSCRN-NH<sub>2</sub> may be an effective anti-angiogenic agent, and appears to be a potent anti-metastatic agent even if administered only after metastatic tumor removal.

**#65 Inhibition of proteasome-mediated I $\kappa$ B degradation blocks hepatic metastasis via downregulation of NF $\kappa$ B-dependent endothelium-stimulating factor production from melanoma cells.** Mendoza L., Carrascal T., Marín JJ, de Luca M, Fuentes AM, Anasagasti MJ, and Vidal-Vanaclocha F. Dpt. Basque Country Univ. Sch. Med, 48940-Vizcaya, Spain; INBIOMED Fund, San Sebastian Technol Park, 20009-Gipuzkoa, Spain.

The rising incidence of melanoma and the lack of curative therapies for metastatic disease represent a therapeutic challenge. Interleukin-1 $\beta$  (IL-1 $\beta$ ) and tumor necrosis factor- $\alpha$  (TNF $\alpha$ ) that are released from host and cancer cells have been involved in the mechanism of cancer-endothelial cell adhesion and metastasis in animal models. However, most disseminated melanoma spontaneously metastasize without clinical evidence of proinflammatory cytokine augmentation and how cytokine-dependent adhesion is upregulated during the capillary period of melanoma metastasis is unclear. We first studied whether non-IL-1 $\beta$ - and TNF $\alpha$ -producing disseminated melanoma cells are able to activate capillary endothellium cells and to metastasize via cytokine-induced endothelial adhesion. Cultured mouse hepatic sinusoidal endothellium (HSE) cells were treated or not with non-TNF $\alpha$ - and IL-1 $\beta$ -producing B16 melanoma (B16M) cell-conditioned medium (CM), and their secretion of IL-1 $\beta$  and TNF $\alpha$  and adhesiveness determined. B16M-CM significantly ( $P < .01$ ) increased *in vitro* HSE production of TNF $\alpha$  and IL-1 $\beta$  (as checked by RT-PCR and ELISA), and their adhesiveness for B16M. B16M given TNF $\alpha$  for only 30 min increased (by 2-fold) endothelium-stimulating activity in the B16M-CM. Complete abrogation of B16M-CM-dependent adhesion was found when HSE received TNF soluble receptor p55 plus IL-1 receptor antagonist together with B16M. Anti-mouse VCAM-1 antibody abolished B16M-dependent HSE adhesion *in vitro*, and inhibited almost all hepatic metastasis, indicating that VCAM-1-independent adhesion little contributed to metastasis. We next studied whether inhibition of proteasome-mediated I $\kappa$ B degradation may limit metastasis via the attenuation of NF $\kappa$ B-dependent cytokine and cell adhesion molecule expression. HSE given 0.5  $\mu$ g/ml MG-132 proteasome inhibitor for 30 min did not significantly increase VCAM-1 expression and adhesiveness in response to B16M-CM. MG-132 also suppressed constitutive production of endothelium-stimulating activity from B16M and abrogated its upregulation in TNF $\alpha$ -treated B16M. B16M cells given 0.5  $\mu$ g/ml MG-132 for 30 min prior to intrasplenic injection also decreased by 90% hepatic metastasis, indicating that, despite constitutive B16M production of endothelium-stimulating activity, almost all metastases depended on its cytokine-induced upregulation by liver microenvironmental factors *in situ*. Metastatic melanoma induced VCAM-1 expression via TNF $\alpha$  and IL-1 $\beta$  production from HSE. This cytokine-stimulating activity represents an unknown metastasis-promoting feature of disseminating melanoma. Importantly, both melanoma-derived endothelium-stimulating activity and adhesion molecule expression from tumor-activated endothelium were NF $\kappa$ B-dependent, suggesting that proteasome inhibitors may arrest cancer-endothelial cell interaction at capillary sites, offering a novel approach to treat metastatic melanoma.

**#66 BrMS1—A human breast cancer metastasis-suppressor gene encoded on chromosome 11q13.1-q13.2.** Welch, D.R., Seraj, M.J., Samant, R.S., Leonard, T.O., Harms, J.F., Verderame, M.F. Jake Gittlen Cancer Research Institute, Penn State University College of Medicine, Hershey, PA 17033-2390.

Introduction of normal human chromosome 11 reduces the metastatic capacity of MDA-MB-435 human breast carcinoma cells without affecting tumorigenicity [Phillips et al. (1996) Cancer Res. 56: 1222-7]. This suggests



the presence of a metastasis suppressor genes on human chromosome 11. Differential display was done to identify mRNAs with increased expression in neo11/435 hybrids compared with their metastatic counterparts. Six cDNA fragments were consistently differentially expressed in replicate amplifications and RNA analyses at levels at least 5-fold greater in metastasis-suppressed neo11/435 hybrids. Three of the six candidates were homologous to known cDNAs. The remaining three had minimal homology to known sequences or ESTs. We isolated a full-length cDNA for one of the novel genes, designated *BRMS1* (Breast-cancer Metastasis Suppressor 1), which maps to human chromosome 11q13.1-q13.2 by fluorescence *in situ* hybridization. *BRMS1*-transfected human breast carcinoma cell lines MDA-MB-435 and MDA-MB-231 formed significantly fewer metastases in athymic mice than parental or vector-only controls in an expression-dependent manner. Like the neo11/435 hybrids, *BRMS1* transfectants remain tumorigenic. These results provide functional evidence that *BRMS1* is a metastasis-suppressor. *BRMS1* predicted protein sequence contains regions with homology to DNA binding domains, coiled-coil, leucine zipper, nuclear localization and some consensus phosphorylation sites. These homologies suggest that *BRMS1* may function in a signaling cascade as a transcription factor. The mechanism by which *BRMS1* suppresses metastasis is not fully elucidated, but does not involve upregulation of Nm23-H1, KISS1 or KAI1 metastasis-suppressor genes.

Support: U.S. Army Medical Research and Materiel Command DMD-96-1-6152; RO1-CA62168; National Foundation for Cancer Research and the Jake Gittlen Memorial Golf Tournament.

**#67 P-glycoprotein: A novel target for antimetastatic therapies.** Yang, Jin-Ming, Medina, Daniel J., Vassil, Andrew D., and Hait, William N. *The Cancer Institute of New Jersey, UMDNJ-Robert Wood Johnson Medical School, New Brunswick, New Jersey 08901.*

The prognosis of patients with tumors expressing P-glycoprotein (P-gp), the *MDR1* gene product, is generally poor. It is assumed that this is due to decreased tumor responsiveness that results from decreased drug accumulation. We observed that treatment of animals bearing *MDR1*-transfected P388 tumor cells with P-gp substrates (i.e., drugs that are transported by P-gp) enhanced metastases compared to treatment with vehicle or non-P-gp substrates. This effect was seen with cancer chemotherapeutic agents (paclitaxel and vincristine), and with the multidrug resistance (MDR) modulator, *trans*-flupenthixol. We postulated that the interaction of P-gp substrates with P-gp might lead to membrane changes which might favor metastases. To explore this possibility, we tested the effect of drugs on invasion of several MDR cell lines through a hepatocyte monolayer, and membrane ruffling, an early indicator of enhanced cellular motility. The invasive capacity of cancer cells was assessed on a murine hepatocyte layer in a cell culture insert contained within a blind-well chamber, and with Chemicon QCM™-FN cell migration assay kit. Membrane ruffles were examined by staining with phalloidin-tetramethyl-rhodamine isothiocyanate. P-gp(+) cells were more invasive after treatment with P-gp substrates (paclitaxel, vincristine, and *trans*-flupenthixol) than when treated with vehicle or non-P-gp substrate (mechlorethamine). In contrast, the invasiveness of P-gp(-) cells was not affected by drug treatment. P-gp substrates increased membrane ruffling in P-gp(+) cell lines, while this effect was not seen with non-P-gp substrate, or in P-gp(-) cell lines. We further demonstrated that these pro-metastatic features of P-gp(+) cells treated with P-gp substrates were associated with the activation of phosphatidylinositol-3 kinase (PI-3K), an enzyme involved in membrane trafficking. Wortmannin, a specific inhibitor of PI-3K, appeared to inhibit the invasion induced by P-gp substrates. These results suggest that P-gp may be a novel target and use of PI-3K inhibitors may be a new strategy, for antimetastatic therapies in the treatment of patients with P-gp(+) tumors.

**#68 Thymosin  $\beta$ 15 predicts for distant failure in patients with clinically localized prostate cancer.** Chakravarti, Arnab; Zehr, Elizabeth M.; Zietman, Anthony L.; Shipley, William U.; Goggins, William B.; Finkelstein, Dianne M.; Young, Robert H.; Wu, Chin-Lee. *Departments of Radiation Oncology, Pathology and Urology, Biostatistics, Massachusetts General Hospital, Harvard Medical School.*

Background: Because a significant proportion of patients with clinically localized prostate cancer will eventually fail with distant metastases, it is important to identify at the time of initial presentation which patients are at high-risk for harboring occult systemic metastases so that appropriate systemic therapy can be incorporated into their treatment regimens. As up to 80% of patients present with moderately differentiated tumors, histologic grade is of limited prognostic value for most patients. Laboratory data suggest that an actin-binding protein called thymosin  $\beta$ 15 (T $\beta$ 15) enhances metastatic potential in prostate cancer cell lines (*Nature Medicine* 12(2): 1322-1328). This is the first reported clinical study to determine if T $\beta$ 15 staining intensity of the initial biopsy specimen from patients with moderately differentiated, clinically localized prostate cancer has value in predicting PSA and bone failure.

Methods: Thirty-two patients treated by radical radiotherapy alone with clinically localized moderately differentiated (Gleason 6/10) prostate cancer were evaluated for this pilot study. Their corresponding biopsy specimens were stained for T $\beta$ 15, which was then correlated with clinical

outcome. Staining, interpretation of staining, and correlation with clinical outcome were all done in a blinded manner. The median follow-up time was 6 years (range 1 year to 19 years).

Results: The outcomes of the 32 patients can be grouped into 3 categories: 1) 11 patients with no evidence of disease 2) 11 patients with PSA failure without documented bony failure and 3) 10 patients with PSA failure with documented bony failure. T $\beta$ 15 staining intensity strongly correlated with clinical outcome. Of those patients who stained 3+ (strongest staining), 62% developed bony failure, compared to 13% of those patients that stained 1+ (weakest staining),  $p = 0.01$ . The 5-year freedom from PSA failure was only 25% for those patients that stained 3+, compared to 83% for those who stained 1+,  $p = 0.02$ . The 5-year positive predictive value of a stain of 3+ (with biochemical failure as endpoint) was 86%, and the 5-year negative predictive value (with freedom from biochemical failure as endpoint) of a stain of 1+ was 71%.

Conclusions: These results demonstrate that T $\beta$ 15 intensity of 3+ identifies patients with moderately differentiated, clinically localized prostate cancer who are at high risk for subsequent PSA and bony failure.

**#69 Sensitive PCR probe for the detection of human cells in xenotransplantation system.** Becker, M., Neumann, C., Goan, S.-R., Jung-hahn, I., Fichtner, I.

The sensitive detection of human cells in immunodeficient rodents is a prerequisite for the monitoring of  
-micrometastases of solid tumors,  
-dissemination of leukemic cells, or  
-engraftment of hematological cells.

For such purpose tumor-associated markers (CEA), specific surface proteins (HLA-DR) of human cells or artificially transfected genes (LacZ) can be determined by appropriate PCR, FACS or immunohistochemical methods. But, if specific markers are lacking or yet unknown or if transfection is hampered by any reason, a general detection principle for human cells in xenotransplantation systems is necessary.

Therefore, we developed a PCR method for the detection of a human-specific 850-bp DNA fragment of the  $\alpha$ -satellite DNA on chromosome 17. This method detecting reliably 1 human cell in  $10^5$  murine cells was used for the following xenotransplantation systems in SCID and NOD/SCID-mice:

1. In a limiting dilution assay cells of the MDA-MB-435 breast carcinoma were injected into the mammary fat pad (mfp) of NOD/SCID-mice. It could be shown that 10 cells/mouse were sufficient to induce a positive PCR signal in liver and lung 30 days after transplantation as a sign for micrometastases. At this time a palpable tumor was not yet detectable in the mfp-region.
2. Cells of a newly established human acute lymphatic leukemia (ALL) were administered i.p. to SCID-mice. These cells apparently disseminated and were detectable as early as day 50 in the peripheral blood of living mice, while the leukemia manifestation was delayed by day 140.
3. In a transplantation experiment using mature human lymphocytes we wanted to standardize conditions for a successful survival of these cells in NOD/SCID-mice. We learned that a least  $5 \times 10^7$  cells given i.v. were necessary and that the mice had to be conditioned by 2 Gy body irradiation to get a positive PCR band.
4. Engraftment studies with blood stem cells originating from cytokinesis samples of tumor patients or from cord blood were undertaken in NOD/SCID-mice in order to define conditions of successful engraftment and to use this model for further optimization strategies. The PCR method presented allowed a reliable prediction of positive engraftment.

All together, the PCR method developed allows a sensitive and reliable detection of low numbers of human cells in immunodeficient hosts. As this procedure can be performed in the living animals, follow up studies for the estimation of therapeutic interventions are possible in which the survival time of mice as evaluation criteria can be omitted.

**#70 The LNCaP progression model of human prostate cancer: androgen independence and osseous metastasis.** Thalmann G.N., Sikes R.A., Wu T.T., Hyytinen E., Pathak S., Studer U.E., Chung L.W.K. *Department of Urology, University of Bern, Switzerland and Molecular Urology and Therapeutics Program, Department of Urology, UHSC, Charlottesville, Virginia and Department of Cell Biology, University of Texas, M. D. Anderson Cancer Center, Houston, TX.*

RATIONALE: The lethal phenotypes of human prostate cancer (PCa) are characterized by their androgen-independence (AI) and their propensity to form osseous metastases. We previously reported on the establishment of AI human PCa cell lines derived from androgen-dependent (AD) LNCaP cells. The C4-2 subline was found to be AI, highly tumorigenic and metastatic with osteoblastic bone metastases. From these bone metastases we established the AI and bone metastatic cell lines B2, B3, B4, and B5. We determined their biologic behavior in vivo and in vitro and their molecular and cytogenetic characteristics.

METHODS: We evaluated the biologic (intrinsic growth, soft agar colony formation, prostate-specific antigen production on the protein and mRNA level, invasion assay) and genetic (karyotyping, comparative genomic hybridization) properties of these lineage-derived cell lines.



**RESULTS:** The LNCaP progression model shares remarkable similarities with human PCa and a comparable metastatic pattern of metastasis (osteoblastic). Genetic and biochemical characterizations also indicate close similarities between human PCa and the LNCaP progression model. Most AI sublines expressed higher basal steady-state levels of prostate-specific antigen (PSA) than the parental AD LNCaP cells but were less inducible by androgens. The LNCaP derivative cell line expressed osteomimetic properties, including the synthesis and deposition of osteocalcin, osteopontin, osteonectin and bone sialoprotein. LNCaP sublines derived from C4-2 bone metastases were found to acquire further chromosomal changes and enhanced osseous metastatic potential.

**CONCLUSIONS:** The LNCaP progression model of human PCa closely reflects the biologic and genetic properties of human metastatic PCa. We have developed a unique LNCaP human PCa progression model that may serve to improve our understanding of the mechanisms of androgen-independence, osseous metastasis and osteoblastic reactions. This animal model may serve as a model to evaluate both local therapy and therapy for prostate cancer bone metastasis.

**#71 Clinical relevance of human tumor metastasis models.** Fodstad, Øystein; Brøsetøl, Knut; Engebraaten, Olav; Department of Tumor Biology, Institute for Cancer Research, The Norwegian Radium Hospital, N-0310 Oslo, Norway.

The use of human tumor models for in vivo drug evaluation has largely been restricted to *sc* xenografts. It is known, however, that the biochemical characteristics of tumor cells are influenced by microenvironmental factors and that cells with metastatic potential may differ from those capable of local growth only. Orthotopic models help reduce these problems, but since drug therapy mainly aim at killing metastatic cells and tumors, increased use of appropriate metastasis models seems logical. Such models should as closely as possible mimic clinical situations for the relevant types of cancer, and also be practical in use. We have developed a number of metastasis models involving human malignant melanomas, sarcomas, breast and lung cancers. The similarities between the experimental metastases and their clinical counterparts include morphological features as well as organ-preferred metastasis formation and scintigraphic growth patterns. The observed intertumor heterogeneity in biology and biochemical characteristics cautions against generalizations commonly seen in the literature. The data emphasize the importance of choosing models and therapeutic approaches typical for the clinical situation in which the drugs are intended to be used. Results obtained in therapy experiments including new and established chemotherapeutic agents, prodrugs of doxorubicin and cytarabine, as well as immunotoxins, demonstrate the relevance and usefulness of the models for drug evaluation.

**#72 Primary thoracoscopic evaluation of pleural effusion under local anesthesia an alternative approach.** Sadir J. Alrawi MD, Norman M. Rowe MD, Ira Shaywitz BS, Edward Kosoy BS, Azza Abo deeb MD, Ramanathan Raju MD, Joseph N. Cunningham MD., Anthony J. Aclapura MD and Jeffrey Cane MD.

**Purpose:** The development of a thoracoscopically assisted technique to be performed under local anesthesia for both diagnostic and therapeutic purposes when treating pleural effusions and empyemas.

**Methods:** Twenty patients with the finding of a pleural effusion or empyema who were also determined to be at high risk for complications following an open thoracotomy, pleural biopsy and/or general anesthesia underwent a placement of a thoracoscope under local anesthesia, followed by thoracic fluid drainage, in addition to a pleural biopsy and pleurodesis, as required. Patients were retrospectively evaluated for a variety of factors including personal history, pre-existing medical conditions, pre and postoperative course and details of the thoracoscopic procedure.

**Results:** The average age of the patients was 59 years old (18-89) with a 55% male/45% female sex distribution. Patients had this procedure as a consequence of malignancy (60%), empyema (30%), spontaneous pneumothorax (10%), bronchiectasis (5%) or heart failure (5%). The average duration of the procedure was 62 minutes (20-190) with an average of 861 ml (0-1800) of fluid drainage and 114 ml (0-1200) of estimated blood loss. The chest tube was usually removed on the sixth (0-13) post procedure day. The procedures were well tolerated by the patients with the majority of pain management being achieved with patient controlled analgesia (56%). The complication rate was 15%, with 10% of patients requiring endotracheal intubation and 5% suffering a post procedure infection.

**Conclusions:** This novel thoracoscopic procedure represents an acceptable alternative to the traditional treatment of pleural effusions and empyema with comparable outcome parameters and morbidity. This technique may eventually become the standard of care for the treatment of pleural effusions.

**#73 Disease stabilization in patients with advanced refractory disease treated with BAY 12-9566, a matrix metalloprotease inhibitor.** Gurtler Jayne, Meddow Jodie, Kumar Karen. East Jefferson Hospital, Metairie, LA and Bayer Corp., West Haven, CT.

Degradation of extracellular matrix and stimulation of angiogenesis are mandatory for tumor invasion and metastases. Matrix metalloprotease inhibitors (MMPI) can potentially inhibit growth and metastatic spread of a broad range of tumors. BAY 12-9566 is a well-tolerated MMPI of MMP-2 and MMP-9.

Treatment with BAY 12-9566 has resulted in stable disease in some of the 22 pts with advanced refractory disease treated in a single center PK study. The study enrolled 24 pts over a period of 15 months, from Feb 98 to March 99; 2 pts had less than 3 days therapy and are excluded from analysis. The running median survival (July 99) for the group is 138 days (average 192 days); the median time to discontinuation of the drug (progression or other reason) is 125 days (average 170 days). Twelve pts have died; 10 continue on BAY 12-9566 treatment. Eight pts received therapy for 270 days or more; seven of these are alive with stable disease and are continuing treatment. One pt with glioblastoma multiforme has been treated for 13+ months; one pt with pancreatic carcinoma for 11+ mos, one pt with malignant mesothelioma for 11+ mos, one pt with malignant thymoma 11+ mos, and one pt with metastatic chondrosarcoma for 9+ mos. Except for the pt with mesothelioma, these pts had failed more than one previous therapy.

Adverse events have been generally attributable to disease progression. One pt received only 5 doses of BAY 12-9566 and experienced Gr III nausea, vomiting and diarrhea. Another pt had progression of thrombocytopenia that was present prior to BAY 12-9566 treatment and associated with marrow metastases and extensive radiation therapy and chemotherapy. The pt with thymoma experienced anemia, which improved by temporarily withholding the MMPI treatment and subsequently dropping the treatment to half doses.

In summary, we have seen encouraging stabilization of disease in pts treated with BAY 12-9566 who have a wide variety of advanced and refractory malignancies.

## SECTION 4: FAS PATHWAYS/GROWTH FACTORS: BIOLOGY AND THERAPEUTICS

**#74 Simultaneous presence of FasR-FasL in childhood brain tumors: the major apoptotic pathway is switched to enhance neoplastic cell proliferation and immune escape.** Bela Bodey, Bela Bodey Jr, Stuart E. Siegel, and Hans E. Kaiser. University of Southern California, Los Angeles, CA, USA and University of Vienna, Vienna, Austria.

FasR (APO-1/CD95) is a member of the nerve growth factor/tumor necrosis factor (NGF/TNF) receptor superfamily. The coexpression of both FasR and FasL in a number of neoplastically transformed cell types represent a mechanism of tumor escape from the cellular immune response of the host. Childhood astrocytomas (ASTRs) and primitive neuroectodermal tumors (PNETs)/medulloblastomas (MEDs) express FasR whereas normal cells in the central nervous system (CNS) do not. Immunocytochemical screening for FasR in 42 ASTRs: 6 WHO grade I or pilocytic ASTRs; 14 WHO grade II or low grade ASTRs; 16 WHO grade III or anaplastic ASTRs and 6 WHO grade IV or glioblastoma multiforme (GBM), as well as 34 primary PNETs/MEDs defined expression (intensity of staining: "A", the highest possible; number of stained ASTR cells: ++ to +++++, between 20% and 90%; number of stained PNET/MED cells: +++ to +++++, between 50% and 90%) of FasR, employing 4 µm, formalin fixed, paraffin-wax embedded tissue slides. FasR was present on 70% to 90% of tumor cells in pilocytic ASTRs, 50% to 60% in low grade ASTRs, between 30% to 40% in anaplastic ASTRs and rarely (20% to 35%) in GBM tissues. The control panel of normal tissues demonstrated presence of FasR in the prenatal thymus, tonsils and colon epithelium. The indirect, four step enzyme conjugated, streptavidin-biotin based antigen detection technique provided excellent immunocytochemical results. Concurrently, ASTRs and MEDs produce their autocrine FasL, and may even become capable of switching the signal transduction of the FasR from programmed cell death (PCD) related signaling to a neoplasm proliferative pathway. Presence of FasL also ensures the possibility of autoregulatory PCD (intratumoral autocrine suicide during the microevolution of tumor cell clones) in childhood ASTRs and MEDs. The therapeutic use of FasR-FasL, as molecules of the major mammalian apoptotic pathway, represents a new exciting possibility in the alternative treatment of primary childhood brain tumors, as the classical three modalities of cancer therapy have not led to major improvements in the prognosis of CNS malignancies.

**#75 Activation of protein kinase C inhibits ceramide synthesis in inostamycin-induced apoptosis in human small cell lung carcinoma cell lines.** Kawatani, M., Simizu, S., Imoto, M. Department of Applied Chemistry, Faculty of Science and Technology, Keio University, 3-14-1 Hiyoshi, Kohoku-ku, Yokohama 223-8522, Japan

In the present study, we have examined the involvement of protein kinase C (PKC) in anticancer drug-induced apoptosis. Treatment of cells with TPA suppressed apoptosis induced by inostamycin, a phosphatidylinositol synthetase inhibitor but not that by other anticancer drugs including camptothecin and adriamycin. Activation of protein kinase C by TPA suppressed inostamycin-induced activation of caspase-3(-like) proteases without affecting inostamycin-inhibited phosphatidylinositol synthesis. Furthermore, although inostamycin induced the release of cytochrome c from mitochondria resulting in caspase-3(-like) proteases via caspase-9 activation, TPA inhibited it. Ceramide synthesis is also thought to be involved in some types of apoptosis. Inostamycin induced elevation of



Intracellular ceramide levels, and this was inhibited by fumonisin B1. Fumonisin B1 also inhibited inostamycin-induced cytochrome c release and caspase-3(-like) protease activation, indicating that ceramide synthesis acted upstream of cytochrome c release and subsequent activation of caspase-3(-like) protease in the pathway of inostamycin-induced apoptosis. TPA treatment inhibited inostamycin-induced ceramide synthesis. Ceramide synthesis was not detected during camptothecin- and adriamycin-induced apoptosis. Furthermore, TPA did not inhibit C2-ceramide-induced cytochrome c release and activation of caspase-3(-like) proteases. Taken together, ceramide synthesis caused activation of caspase-3(-like) proteases through cytochrome c release in inostamycin-induced apoptosis. In addition, protein kinase C suppressed inostamycin-induced apoptosis by inhibiting ceramide synthesis.

**#76 Molecular determinants of enhanced apoptosis of prostate cancer cells induced by a combination of Taxol and death ligand TRAIL.** Perkins, Charles; Orlando, Marlangelli; Fang, Guofu; Wen, Jinghai; Jing, Xin and Bhalla, Kapil. *University of Miami Sylvester Comprehensive Cancer Center, Miami, FL 33136.*

In the present studies we demonstrate that the TNF $\alpha$  related death ligand TRAIL induces apoptosis of the human prostate cancer PC-3, DU-145 and LNCaP cells in a time and dose dependent (0.1 to 1.0  $\mu$ g/ml) manner. Exposure of PC-3 cells to TRAIL caused the processing of caspase 8 and 10, through a death inducing signaling complex (DISC) involving the death receptors DR4 and DR5, as well as, for the first time, was demonstrated to produce the mitochondrial permeability transition (MTP), the cytosolic accumulation of cytochrome c (cyt c) and the processing of procaspase 9 and 3. Without significantly engaging DISC, taxol (20 to 500 nM, 24 hrs) also caused MTP, cytosolic cyt c and the processing of caspase 9 and 3. Consequently, in PC-3 cells in caspase-8 inhibitor IETD, or transient transfection of dominant negative (DN) caspase 8 or 10, or DR4; Fc markedly inhibited TRAIL but not taxol-induced apoptosis. Also, transient transfection with Crm A or FLAME-1 (FADD like antiapoptotic molecule) cDNA had a similar effect. In contrast, as compared to the control, Apaf-1 $-/-$  mouse embryonic fibroblasts were markedly resistant to taxol but only partly resistant to TRAIL-induced apoptosis. Surprisingly, treatment with taxol (4 to 24 hrs) increased (5 to 8 fold) DR4 protein expression in PC3 and DR5 in LNCaP cells. A similar effect was also observed after treatment of PC-3 cells with taxotere (100 nM). There was no change in Fas receptor or ligand levels. Consistent with this, as compared to a combined treatment, sequential exposure to taxol, followed by TRAIL, induced significantly more apoptosis of PC-3 cells (52 vs 70%, by Annexin V staining). Combined treatment with TRAIL and taxol produced at least additive apoptotic effect. Treatment with taxol and TRAIL was also associated with the processing of cIAP and XIAP, without significant effect on Flame-1 (c-FLIP) levels. These preclinical, in vitro data indicate that due to the engagement of predominantly different molecular pathway of apoptosis, taxol and TRAIL have additive apoptotic effects against human prostate cancer cells. The superior apoptotic effect of the sequential treatment with taxol followed by TRAIL may be determined by the upregulation of DR4 and DR5 levels and/or downregulation of the IAP family of proteins.

**#77 Targeting up-regulated TRAIL receptors following chemotherapy enhances neuroblastoma cell killing.** Schmelder Nathah, Rosebrook Joshua, Wen Judy, Takamizawa Shigeru, Bishop Warren, Kimura Ken, and Sandler Anthony. *Department of Surgery, University of Iowa Hospitals, Iowa City, IA.*

Programmed pathways of cell death (apoptosis) are used by immune effector cells and chemotherapeutic agents during destruction of target cells. This study was undertaken to evaluate the presence of apoptotic mediators in a Neuroblastoma (NB) cell line (SK-N-MC) and to explore the effect of chemotherapeutic agents on expression and function of these apoptotic regulators. **METHODS:** Doxorubicin (1  $\mu$ g/ml; 12 hour duration) and Etoposide (50  $\mu$ g/ml; 12 hour duration) treated NB cells were screened for expression of 19 different mRNA species using an RNase protection assay (RPA) and compared to untreated controls. The effect of recombinant TRAIL (20 ng/ml) and Fas Antibody (500 ng/ml) were tested on untreated and treated NB cells in an attempt to correlate functional effects with apoptosis receptor expression. A cell viability assay (MTT) and an apoptosis assay (Annexin V) were used to evaluate cell killing. **RESULTS:** The pro-apoptotic factors DR4 and DR5 were abundantly expressed in untreated NB (11% and 132% of GAPDH respectively), while Fas mRNA was barely detectable (3.5%). TRAIL treatment induced apoptosis of the NB cells ( $p = 0.01$ ), while Fas Ab failed to induce cell death ( $p = 0.4$ ). Doxorubicin and Etoposide treatment both induced marked NB apoptosis and down-regulated most pro- and anti-apoptotic mRNA species screened, except for the pro-apoptotic TRAIL receptors; DR4 and DR5, which were up-regulated. This receptor up-regulation was associated with an enhanced killing effect when Doxorubicin or Etoposide were combined with TRAIL treatment ( $p = 0.05$ ). **CONCLUSIONS:** Doxorubicin, Etoposide and TRAIL alone or in combination induced apoptosis of the NB cell line tested. Both Doxorubicin and Etoposide up-regulated expression of DR4 and DR5, making the tumor cell more susceptible to TRAIL induced killing.

These findings suggest that such agents may not only intensify the cytotoxic effect of immune effectors in vivo, but that adjuvant immune therapy with TRAIL may enhance NB tumor cell killing.

**#78 2-Methoxyestradiol upregulates DR5 and induces apoptosis independently of p53 in endothelial and tumor cells.** LaVallee, T.M., Hambrough, W.A., Papatianasslu, A., Pribluda, V.S., Swartz, G., Williams, M., and Green, S.J. *EntreMed, Inc., Rockville, MD 20850 and American Red Cross, Department of Immunology, Rockville, MD 20855*

2-Methoxyestradiol (2ME<sub>2</sub>), a metabolite of estradiol that lacks several of the effects normally associated with estrogens, is a potent antitumor and antiangiogenic agent. At nanomolar and low micromolar concentrations 2ME<sub>2</sub> inhibits the proliferation of a wide variety of tumor and nontumor cell lines, including endothelial cell lines. The mechanism of the inhibitory action of 2ME<sub>2</sub> is unclear. It has been reported that 2ME<sub>2</sub> requires functional p53 protein for its antiproliferative and cytotoxic activities. Using an endothelial cell line, HUVEC, and two tumor cell lines, ECV and HL60, we demonstrate that all three cell lines have a similar antiproliferative and apoptotic response to 2ME<sub>2</sub>. However, p53 protein is upregulated only in HUVECs in response to 2ME<sub>2</sub> treatment, suggesting that 2ME<sub>2</sub> induced apoptosis can occur independently of p53. While DR5 has been reported to be a p53 response gene, we observe upregulation of DR5 protein in all three cell lines after exposure to 2ME<sub>2</sub>. DR5 induces cell death by the activation of intracellular caspases and consistent with this, the ability of 2ME<sub>2</sub> to induce apoptosis is inhibited by treatment with zVAD-fmk, a broad-spectrum caspase inhibitor. RNase protection analysis and western blot experiments demonstrate that HUVEC cells activate a different set of caspases as compared to ECV cells in response to 2ME<sub>2</sub> treatment. These data indicate that 2ME<sub>2</sub> upregulation of DR5 is independent of p53 and 2ME<sub>2</sub> induced activation of the caspase cascade is cell type specific.

**#79 Inhibition of BTK by LFM-A13 abrogates BTK-Fas association and renders resistant leukemic cells sensitive to Fas mediated apoptosis.** Vassilav A.O., Ozer Z., Navara C., Tibbles H.E., Ghosh S., Zhang Y., Mahajan S., and Uckun F.M. *Parker Hughes Cancer Center and the Hughes Institute, St. Paul, MN.*

Fas/APO-1 (CD95), a 45-kD surface protein belonging to the tumor necrosis factor receptor family, is known to be a key player in the apoptosis of cells of immune system, function as effector molecules of cytotoxic T lymphocytes, and function in the elimination of activated lymphocytes during the downregulation of the immune response. The critical roles of the Fas-Fas ligand system in apoptosis suggest that its inactivation may be involved in malignant transformation. Inappropriate apoptosis may also contribute to the development as well as chemotherapy resistance of human leukemias and lymphomas.

We obtained biochemical and genetic evidence that Fas/APO-1 death inducing signaling complex (DISC) is inhibited by BTK. BTK associates with Fas via its kinase and PH domains and prevents the Fas-FADD interaction, which is essential for the recruitment and activation of FLICE by Fas during the apoptotic signal. BTK-deficient RAMOS-1 human Burkitt's leukemia cells underwent apoptosis after Fas ligation, whereas BTK-positive NALM-6-UM1 human B-cell precursor leukemia cells expressing similar levels of Fas did not. Treatment of the anti-Fas-resistant NALM-6-UM1 cells with a LFM-A13, a potent inhibitor of BTK which was designed using a homology model for the kinase domain of BTK, abrogated the BTK-Fas association without affecting the expression levels of BTK or Fas and rendered them sensitive to Fas-mediated apoptosis.

**#80 New sensitivity test to docetaxel by early detection of apoptosis and new therapeutic approach through the Fas-FasL system which CDDP acts as an apoptosis inducer in combination with LAK cell.** Hiroyuki Suzuki, Ikuo Matsuzaki, Hirohide Moriyama, Reijiro Saito, Satoru Motoyama, Manabu Okuyama, Hiroshi Imano, Jun-ichi Ogawa. *Second department of Surgery, Akita University School of Medicine.*

**Aim:** In order to gain insight into the cancer therapy, the new approaches both in sensitivity test to chemotherapeutic agents and in immunotherapy for esophageal cancer were made utilizing the mechanism of apoptosis. The early detection of apoptosis induced by docetaxel closely related to sensitivity for docetaxel and a new therapeutic approach through the Fas-Fas ligand (FasL) system was established, which CDDP acts as an apoptosis inducer. Conventional immunotherapies activate only the effector cells (T-cells). In this study, we investigated an alternative mechanism for sensitizing target cells to effector cells, with the intent of establishing for treatment of human malignancies.

**Methods and Results:** The susceptibility of apoptosis measured by flow cytometric analysis after double staining with Annexin V and propidium iodide was accorded to the conventional sensitivity test to docetaxel using MTT. While MTT assay needs 24 hrs reaction, ten minutes was enough to react with docetaxel. Analysis by flow cytometry indicated that five out of six esophageal cancer cell lines expressed Fas antigen at various levels (26.2%–61.5%). Fas expression increased after CDDP (not docetaxel) treatment and the degree of increase was independent of cell sensitivity to CDDP. The anti-tumor effect of anti-Fas antibody on the esophageal cancer cell line was enhanced by pretreatment with CDDP. In the thera-



peutic model of the interaction between lymphocytes and cancer cells through Fas/FasL system, the anti-tumor effect of LAK cells activated by IL-2 was enhanced in only Fas positive cells by pretreatment with CDDP and an anti-Fas neutralizing antibody inhibited this cytotoxicity. Therefore, CDDP's role is not only that of a chemotherapeutic agent, but also a Fas inducer. These results suggest that apoptosis in esophageal cancer cells is controlled by CDDP and by a cytokine, such as IL-2.

**#81 Apoptotic Induction via CPP32/caspase-3 pathway of chemoresistant HCC exhibiting MRP-2 and EGFR after treatment with humanized anti-EGFR mAb fusogenic liposomal vinorelbine.** Giannios J. Dept. of Molecular Oncology, Peripheral Hospital of Patras, Greece.

**Aim:** We aim to circumvent MRP-2 drug-efflux action by delivering cytostatic vinorelbine intracellularly.

Furthermore, missile therapy with humanized Mab fragments linked by diazotization process in the surface of liposomes was targeted at EGFR of tumour cells.

Finally, we use liposomal constituent hexadecyl-PC as a PKC inhibitor. **Material/methods:** HCC tissue was obtained by percutaneous biopsy under radiological guidance from a patient. IHC analysis has exhibited over expression of EGFR, MRP-2, PKC and CPP32/caspase-3.

Tumour cells were derived by the collagenase method. Post-treated cells were analysed immunocytochemically with specific antibodies for the proteins mentioned above. SUV Immunoliposomes were prepared with hexadecyl-PC chol and fusogenic PEG. Humanized fragments of anti-EGFR mAb were examined morphologically by SEM and TEM. Cell cycle was monitored by flow-cytometry. Cytotoxicity assays were performed such as BrdU for DNA synthesis and MTT for metabolic activity.

**Results:** After treatment of HCC with vinorelbine loaded immunoliposomes in a shaking bath incubator for six (6) hours at 37°C, we observe immunocytochemically upregulation of CPP32/caspase-3 and down-regulation of EGFR and PKC, due to hexadecyl-PC.

Flow cytometry has exhibited blockage of cell-cycle at stage G2/M, due to vinorelbine's action. Morphological examination by TEM exhibited fusion of immunoliposomes with the plasma membrane of tumour cells binding anti-EGF Mab to their respective receptor inducing PCd via activation of the CPP32/caspase-3 pathway. Furthermore, the anti-EGFR Mab induced ADCC via accumulation and activation of NK cells and monocytes. Seventy-two (72) hours post-treatment we observed irreversible apoptotic signs of D2 stages forming apoptotic bodies which are phagocytosed by adjacent tumour cells, implying a bystander killing effect. Finally, DNA synthesis and metabolic activity of tumour cells exhibited great reduction compared to control tumour cells, which were incubated with empty liposomes.

**Conclusion:** We have induced apoptosis of chemoresistant HCC cells by upregulation of CPP32/caspase-3 and downregulation of PKC and EGFR, while liposomal vinorelbine blocks cell cycle of phase G2/M circumventing MRP-2.

**#82 Inhibition of Tumor Growth by a Monoclonal Antibody Targeting to Microvasculature.** Xiyun Yan, Dongling Yang, Xiaoping Wu, Xiaodong Zhu (Institute of Microbiology, Chinese Academy of Sciences, Beijing 100080) Pelyu Li, Mei Yuan, Li Li, Lihua Fei, Yongxin Fong, Honglian Xia (Cancer Res. Lab. General Hospital of PLA, Beijing, 100853)

**Objective.** To generate a monoclonal antibody specially reacted with proliferating vascular endothelial cells, and to apply it for tumor therapy and novel target identification. **Methods.** The specificity of mAb AA98 was evaluated immunohistochemically with tumor frozen sections. The biological effects of the mAb *in vitro* were examined by MTT assay. The retardation of tumor growth *in vivo* was performed with xenografted human tumors in nude mice. **Results.** The antibody AA98 bound specifically to microvasculature in both human and mouse tumors, but not normal tissues, except for ovary during menstruation. The target recognized by antibody AA98 is expressed in human umbilical vein endothelial cells (HUVEC) using confocal immunofluorescence microscopy. In immunoblots prepared with stimulated HUVEC extracts, a single >100 kDa protein band was stained by the antibody. The antibody inhibited the proliferation and sprouting of vascular endothelial cells, and also mediated CDC and ADCC on proliferating endothelial cells. Animal experiments showed that the antibody itself inhibited the growth and metastasis of xenografted human leiomyosarcoma, liver and pancreatic cancers in nude mice. **Conclusion.** Monoclonal antibody AA98 is a promising agent for tumor therapy and its related antigen might be a novel target on vascular endothelial cells, which play an important role in tumor angiogenesis.

**#83 Therapy of metastatic transitional cell carcinoma of the bladder with the anti-vascular endothelial cell growth factor receptor (flk1/KDR) monoclonal antibody DC101 and paclitaxel.** Inoue, Keiji, Slaton, Joel W., Davis, Darren W., Hicklin, Daniel J., McConkey, David, Karashima, Takashi, Radinsky, Robert, and Dinney, Colin P. N. at The University of Texas M.D. Anderson Cancer Center.

Vascular endothelial cell growth factor (VEGF) regulates angiogenesis and metastasis of bladder cancer (TCC) following binding to its receptor type I (flk1) or II (flk1/KDR). In this study, we evaluated whether the anti-flk1

monoclonal antibody Mab DC101 in combination with paclitaxel inhibited tumorigenesis, angiogenesis, and metastasis of human TCC growing within the bladder of athymic nude mice. *In vitro*, Mab DC101 therapy inhibited endothelial cell proliferation. *In vivo* therapy with Mab DC101 and paclitaxel induced significant regression of bladder tumors compared with either therapy alone. The median bladder weight was reduced from 601 mg (range: 482-964 mg) in untreated controls to 422 mg (range: 240-599 mg) and 361 mg (range: 127-501 mg) following paclitaxel or DC101 alone ( $p < 0.005$ ), and 113 mg (range: 96-264 mg) following combination therapy ( $p < 0.0005$ ). Spontaneous lymph node metastasis were significantly reduced by combination therapy. Only 1/9 mice developed metastasis compared with 7/7 of untreated controls ( $p < 0.0005$ ), 6/8 after DC101, ( $p < 0.01$ ), and 5/8 following paclitaxel, ( $p < 0.05$ ). Therapy with paclitaxel and DC101 inhibited tumor induced neovascularity compared to all other groups ( $p < 0.005$ ), but there was no change in the expression of VEGF or flk1. Mab DC101 and paclitaxel enhanced apoptosis in the tumor and endothelial cells compared with other therapy ( $p < 0.005$ ). These studies indicate that therapy targeting VEGF has significant efficacy against human TCC, especially when combined with chemotherapeutic agents such as paclitaxel. The antitumor effect is mediated by inhibition of angiogenesis and induction of apoptosis.

**#84 Complete regression of advanced colon carcinoma xenografts and basis for selectivity of SB-408075, an antibody-directed small-molecule cytotoxic agent.** Johnson, Randall K, McCabe, Francis L, Whitacre, Margaret, Chen, Yi-Jiun, Jonak, Zdenka L and Mattern, Michael R. Oncology Research, SmithKline Beecham Pharmaceuticals, King of Prussia, PA USA

SB-408075 is a conjugate of a humanized mAb, huC242, with a potent semisynthetic maytansinoid DM1. The mAb recognizes the CanAg antigen that has been reported to be expressed on 70+% of colon cancer. Our immunocytochemical studies have confirmed high level expression of this antigen in colon cancer biopsies; antigen was expressed in a significant proportion of NSCLC samples as well. Selectivity for tumor vs. normal tissue for this agent appears to be due to expression of the antigen only on the luminal surface of normal gastrointestinal tissue and secretory epithelium of the pancreas and salivary glands. We confirmed results obtained with SB-408075 by ImmunoGen, Inc. in advanced human colon cancer xenografts. In athymic mice bearing established antigen-positive HT-29 and Colo-201 human colon tumors, treatment with the murine version of SB-408075 at doses well below an MTD resulted in complete and long-term regressions. Colon carcinoma SW-620 appeared to be negative for expression of CanAg by immunocytochemistry. Treatment of mice bearing SW-620 with SB-408075 resulted in only partial regressions and tumor growth delay at high doses of SB-408075, suggesting low level expression of CanAg. In many tumor specimens, including HT-29 and Colo-201, expression of antigen is heterogeneous, with only 20-50% of cells demonstrating reactivity with the C242 mAb. An important question is why tumors with heterogeneous antigen expression respond to SB-408075 with complete regression as opposed to brief tumor growth delay before outgrowth of antigen-negative cells. This was addressed *in vitro* comparing the homogeneous high expressing Colo-205 with HT-29. In a colony-forming assay, SB-408075 had a subnanomolar  $IC_{50}$  in both cell lines. The  $IC_{50}$  for SB-408075 in Colo-205 cells was identical when evaluated in a monolayer XTT assay but, in this assay format, the  $IC_{50}$  was shifted 3 orders of magnitude higher for HT-29 cells. This suggests that there is likely a bystander effect in which SB-408075 binds to and is internalized by antigen-positive cells with intracellular release and activation of DM1. The activated drug is then passively or actively effluxed and kills neighboring antigen-negative cells.

**#85 Patent anti-tumor activity of ABX-EGF, a fully human monoclonal antibody to the epidermal growth factor receptor.** Xiao-Dong Yang, Xiao-Chi Jia, Jose R.F. Corvalan, Ping Wang, C. Geoffrey Davis. Department of Research, Abgenix, Inc., 7601 Dumbarton Circle, Fremont, CA 94555, USA.

Overexpression of epidermal growth factor receptor (EGFR) has been found on many human tumors and the increase in receptor expression levels has been reported to be associated with a poor clinical prognosis. Blocking the interaction of EGFR and the growth factors could lead to the arrest of tumor growth and possibly result in tumor cell death. To this end, using Xenomouse™ technology, we have generated ABX-EGF, a human IgG2 monoclonal antibody (mAb) specific to human EGFR. ABX-EGF exhibits high binding affinity ( $5 \times 10^{-11}$  M) to the receptor, blocks completely the binding of both EGF and transforming growth factor- $\alpha$  to various EGFR-expressing human carcinoma cell lines, and abolishes EGF-dependent tumor cell activation, including EGFR tyrosine phosphorylation, increased extracellular acidification rate and cell proliferation. The antibody prevents completely the formation of human epidermoid carcinoma A431 xenografts in athymic mice. More importantly, administration of ABX-EGF without concomitant chemotherapy results in complete eradication of established tumors, as large as 1.2 cm<sup>3</sup>. No tumor recurrence was observed for more than 8 months following the last antibody injection, further indicating complete tumor cell elimination by the antibody. Inhibition of human pancreatic, renal, breast and prostate tumor xenografts which express



different levels of EGFR by ABX-EGF was also achieved. The potency of ABX-EGF in eradicating well established tumors without concomitant chemotherapy indicates its potential as a monotherapeutic agent for treatment of multiple EGFR-expressing human solid tumors, including those where no effective chemotherapy is available. Being a fully human antibody, ABX-EGF is expected to exhibit minimal immunogenicity and a longer half life, as compared to mouse or mouse-derivatized mAbs, thus allowing repeated administration, including in immunocompetent patients. These results suggest ABX-EGF as a good candidate for assessing the full therapeutic potential of anti-EGFR antibody in therapy of multiple patient populations with EGFR-expressing solid tumors.

**#86 Selective tumor sensitization to paclitaxel with SGN-15, a mAb BR96-doxorubicin conjugate.** Wahi, A.F., Donaldson, K.L., Trail, P.A. and Siegall, C.B. *Seattle Genetics, Inc., Bothell, WA 98021 and Bristol Myers Squibb Research Institute, Princeton, NJ 08543 (P.A.T.).*

The monoclonal antibody (mAb) BR96 is actively internalized following binding to Lewis Y antigen (Le<sup>Y</sup>) expressed on a wide variety of human carcinomas. Endocytosis of a BR96-doxorubicin conjugate (SGN-15) by Le<sup>Y</sup> carcinoma cells is followed by cleavage and release of free Dox from the endocytic vesicles into the cytosol. Cell cycle analysis indicated that BR96-Dox is most effective against S-phase cells yet cells exposed to even subtoxic levels progress to and arrest in G<sub>2</sub>/M. Cell cycle positioning is likely due to Dox-induced inhibition of topoisomerase II and resultant accumulation of target cells in G<sub>2</sub> phase. The anticancer agent paclitaxel stabilizes microtubule formation resulting in maximum cytotoxicity in G<sub>2</sub>/M phase. As active endocytosis also requires functional microtubules, internalization of SGN-15 and resultant Dox-induced apoptosis are antagonized by coincident treatment with paclitaxel. However, delayed treatment facilitates selective sensitization to paclitaxel. Sequential exposure of tumor cells with SGN-15 followed by paclitaxel at progressively delayed times up to 24 h produces progressively increasing synergy between the two agents in effecting tumor cell killing. Optimal sensitization is a function of population doubling time and SGN-15 internalization rate. The synergy obtained by staged administration *in vitro* is reflected in antitumor efficacy *in vivo* against xenograft models of human lung and colon tumors that cannot be achieved by either agent alone. The staged combination elicited complete regression of established human tumor xenografts using levels that are achievable in human. Taken together these data demonstrate a mechanistic approach to the selective elimination of Le<sup>Y</sup> tumors incorporating a mAb targeted cytotoxic/sensitizing agent and small molecule taxanes.

**#87 Mutant E-cadherin as basis for cancer specific immunotoxins.** K.-F. Becker<sup>1,4</sup>, J. Mages<sup>1</sup>, G. Handschuh<sup>1</sup>, E. Kremmer<sup>2</sup>, Q.C. Wang<sup>3</sup>, L. Pastan<sup>3</sup>, H. Höfler<sup>1,4</sup>. *GSF-Forschungszentrum, <sup>1</sup>Institut für Pathologie und <sup>2</sup>Institut für Molekulare Immunologie, D-85764 Neuherberg, <sup>3</sup>NIH, NCI, Laboratory of Molecular Biology, Bethesda, USA, <sup>4</sup>Technische Universität, Klinikum rechts der Isar, Institut für Pathologie, D-81675 München-Germany.*

E-cadherin is a homophilic cell adhesion molecule that is mutated in half of diffuse-type gastric cancer patients. Since these mutations generally affect the extracellular portion of the transmembrane molecule and do not interrupt the reading frame, altered E-cadherin protein is an excellent target for selective clinical interventions. In-frame deletions of exon 9 from the E-cadherin messenger RNA due to different splice site gene mutations are a mutational hot spot. The aim of our study was to generate and functionally analyze an immunotoxin against the exon 9-deleted E-cadherin variant.

Modified *Pseudomonas* exotoxin was coupled to a mutation-specific monoclonal antibody reacting with exon 9-deleted E-cadherin. Various concentrations of the resultant immunotoxin were added to L929 fibroblasts stably transfected with mutant or normal E-cadherin cDNA, respectively.

The immunotoxin was shown to be exclusively cytotoxic for cells that express E-cadherin lacking exon 9 as determined by XTT metabolism (LD<sub>50</sub>: 220 ng/ml); cells expressing normal E-cadherin were not affected. Moreover, this effect was demonstrated to be concentration dependent and could be blocked by free E-cadherin mutation-specific monoclonal antibody. Annexin-V-propidium iodide staining prior to FACS analysis indicated that the toxin induced apoptosis.

E-cadherin mutation-specific monoclonal antibodies are attractive candidates for diagnosis of malignant cells. Our study demonstrates that immunotoxins targeting mutant E-cadherin expressed exclusively on the surface of tumor cells may be used as a novel approach to treat small tumor deposits.

**#88 Combining radiation with molecular blockade of the EGF receptor in cancer therapy.** Harari, Paul M.; Huang, Shyhmin; Li, Jing—*University of Wisconsin School of Medicine and Comprehensive Cancer Center, Madison, WI 53792.*

**Aim:** The primary objective of this work is to examine the capacity of molecular blockade of the epidermal growth factor receptor (EGFR) to modulate the effects of ionizing radiation in epithelial tumors. The chimeric monoclonal antibody C225 is examined using *in vitro* and *in*

*vivo* model systems of squamous cell carcinomas (SCCs) derived from head and neck (H&N) cancer patients. **Methods:** *In vitro* and *in vivo* investigations regarding the capacity of EGFR blockade with C225 to modulate SCC tumor growth characteristics and response to radiation are described. Cell culture and xenograft model systems are utilized to examine specific molecular and growth modulating effects. **Results:** Experimental studies identify C225 as a potent antiproliferative agent in human SCCs capable of inhibiting tumor cell growth kinetics. EGFR blockade with C225 induces G<sub>1</sub> cell cycle arrest with an associated decrease in the S-phase fraction. The mechanism of cell cycle arrest and growth inhibition induced by C225 involves accumulation of the G<sub>1</sub> cyclin-dependent kinase (CDK) inhibitor p27<sup>KIP1</sup> and inhibition of CDK-2 activity with subsequent accumulation of hypophosphorylated retinoblastoma protein. Exposure of SCCs to C225 enhances *in vitro* radiosensitivity using both single dose and fractionated radiation schemes. Amplification of radiation induced apoptosis (approximately 3-fold) is also observed in the presence of C225. The capacity of C225 to augment the *in vivo* radiation response of SCC tumor xenografts in athymic mice is demonstrated with complete regression of fully established tumor xenografts in animals receiving the combination of C225 and radiation. Preliminary data regarding the capacity of C225 to inhibit angiogenic response of human SCC tumor xenografts in athymic mice are presented with examination of VEGF and Factor VIII immunohistochemical staining. The design, rationale and preliminary observations from the Phase III multicenter trial examining C225 plus radiation therapy for advanced H&N cancer patients will be provided. **Conclusions:** Molecular blockade of the EGF receptor represents a promising investigational area in cancer therapy. The chimeric EGFR monoclonal antibody approach advanced by Mendelsohn and colleagues shows particular promise for several epithelial malignancies. The current data suggests targeting the EGF receptor in combination with radiation therapy for EGFR-rich tumors such as SCC of the H&N may be particularly fruitful.

**#89 Clustered CD20 induced apoptosis: Src-family kinase, the proximal regulator of tyrosine phosphorylation, calcium influx and caspase 3 dependent apoptosis.** Hofmeister, Joseph K., Cooney, Damon S., Coggshall, K. Mark. *Division of Hematology and Oncology, The Ohio State University Comprehensive Cancer Ctr.—The Arthur G. James Cancer Hospital and Richard J. Solove Research Institute.*

**Aim:** To determine the signal transduction events induced by clustered anti-CD20 stimulation leading to B cell apoptosis.

**Methods:** The human Ramos B cell line was stimulated with 3 different anti-CD20 antibodies (humanized chimeric Rituximab, murine 2H7, or murine 1F5) and clustered with goat anti-mouse Ig (GAM). Apoptosis was analyzed by annexin V-FITC/PI staining. Intracellular signal transduction events were evaluated for tyrosine phosphorylation of general and specific targets, calcium influx and caspase 3 activity.

**Results:** Rituximab alone and clustered (Rituximab + GAM) induces a 3.3 and 3.4, fold increase in apoptosis, respectively. Murine antibodies require clustering with GAM but induce an 8.4 (2H7) and 4.0 (1F5) fold increase in apoptosis. PP2 (a specific Src-family kinase inhibitor) and EGTA/Bapta-AM (extracellular and intracellular calcium chelators, respectively) inhibit apoptosis induced by clustered 2H7. These findings indicate a role for Src-family kinases and alterations in cytosolic calcium for anti-CD20-induced cell death. Supporting this notion, we observed an influx of calcium only upon clustering 2H7, which was sensitive to PP2 pretreatment. B cells stimulated via CD20 reveal increased tyrosine phosphorylation of PLC-γ2 and of a p125/p130 KD protein, yet to be characterized. Additional studies revealed that 2H7 and GAM alone failed to induce caspase 3, while clustered 2H7 increased caspase 3 activity two-fold. Similar to apoptosis and calcium influx, PP2 blocked CD20-mediated induction of caspase 3.

**Conclusion:** Our studies of clustered anti-CD20 induced apoptosis establishes a model in which Src-family kinase activation acts proximal to tyrosine phosphorylation of PLC-γ2 and to an uncharacterized p125/p130 KD phosphotyrosyl protein. These early events induce calcium influx and caspase 3 activity, which results in B cell apoptosis.

**#90 An anti-HER2/neu RANTES fusion protein induces effector cell infiltration to the site of HER2/neu expressing tumors.** Chalhita-Eid, Pia M., Hilschey, Shannon P., and Rosenblatt, Joseph D. *Hematology-Oncology Unit, University of Rochester Cancer Center, Rochester, NY.*

The successful eradication of cancer cells in the setting of minimal residual disease may require targeting of metastatic tumor deposits that evade the immune system. We combined the targeting flexibility and specificity of a monoclonal antibody with the immune effector function of the chemokine RANTES to target established tumor deposits. RANTES is a potent chemoattractant of T cells, NK cells, monocytes and dendritic cells. Expression of RANTES has been shown to enhance immune responses against tumors in murine models. We have developed an antibody fusion molecule with variable domains directed against the tumor-associated antigen HER2/neu, linked to sequences encoding the chemokine RANTES (RANTES.her2.IgG3). In this study, we demonstrate specific localization of RANTES.her2.IgG3 to HER2/neu expressing tumor cells within



24 hrs of antibody administration in SCID as well as B-cell deficient mice. We also show that specific localization of RANTES.her2.IgG3 is associated with increased macrophage as well as CD8+ T-cell infiltration within the HER2/neu expressing tumors. Recruitment of effector cells within the tumor vicinity can provide an enhanced repertoire of T-cells capable of being activated and generating a systemic anti-tumor immune response. T-cell activation can occur through direct effect of the RANTES domain in RANTES.her2.IgG3 on T-cells, or through the recruitment of antigen-presenting cells by RANTES.her2.IgG3. Alternatively, co-administration of cytokine or costimulatory antibody fusion proteins could activate the effector cells recruited by RANTES.her2.IgG3.

**#91 Targeting and therapy of a human lung cancer xenograft using Lutetium-177-labeled MAb RS7.** Stein, Rhona, Govindan, Serangulam V., Griffiths, Gary L., Hansen, Hans J., and Goldenberg, David M. Garden State Cancer Center, Belleville, NJ 07109, and Immunomedics, Inc., Morris Plains, NJ 07950.

Rapid and high-yield Lu-177 labeling of MAbs has rendered radioimmunotherapy with this nuclide practical. In this study the potential of Lu-177-labeled RS7 was evaluated by performing preclinical targeting and therapy studies. In a paired label biodistribution study of Lu-177-DOTA-RS7 and Y-88-DOTA-RS7 in nude mice bearing human non-small cell carcinoma of the lung xenografts, the accretion of the two isotopes in tumor and normal organs was nearly identical. Mean %ID/g for Lu-177 and Y-88 (in parentheses) in tumor were 38.3 (39.1), 63.0 (66.0), 63.0 (65.8), and 34.0 (34.9), on days 1, 3, 7, and 14, respectively. Calculated mean cumulative absorbed radiation dose to tumor due to Lu-177 and Y-88 were 6202 and 2966 cGy, respectively, when normalized to 1500 cGy to blood, an estimate of the maximum tolerated dose (MTD). Doses of Lu-177-DOTA-RS7 up to 275  $\mu$ Ci were tolerated in the nude mice. Elimination of established tumors was demonstrated using doses of Lu-177-DOTA-RS7 ranging from 150–250  $\mu$ Ci/nude mouse, with no significant difference in response rate noted between the doses in this range. At 14 weeks post radioimmunotherapy, 11 of 25 animals with established tumors (mean tumor volume = 0.23 cm<sup>3</sup>) experienced complete remissions. The remaining 14 animals had partial responses with remaining tumors averaging 82% reduction in volume. Specificity of the therapeutic effect was shown in an isotope-matched control experiment, where Lu-177-DOTA-RS7 was markedly more effective than the Lu-177-DOTA control antibody. In conclusion, dosimetry calculations based on the longer half-life of Lu-177 relative to Y-88, 6.7 vs. 2.7 days, respectively, and the near identical biodistribution of MAb labeled with the two isotopes predict that Lu-177-labeled MAbs should be able to deliver higher doses to tumor at the MTD. The therapy studies presented confirm the predicted efficacy of Lu-177-DOTA-RS7. A direct comparison of the therapeutic efficacy of Lu-177-DOTA-RS7, Y-88-DOTA-RS7, and I-131-labeled RS7 is in progress.

(Supported in part by grant CA60039 from the NIH.)

**#92 Targeting of breast tumors with scFv antibodies selected for internalization from a phage display library.** Nielsen, U.B., Poul, M.A., Pickering, E.M., Kirpoltin, D., Shalaby, R., Hong, K., Park, J.W., Papahadjopoulos, D., Benz, C.C., and Marks, J.D. University of California, San Francisco, and California Pacific Medical Center, San Francisco, CA 94110.

Many targeted therapeutic approaches to cancer require endocytosis of the targeting molecule and delivery of the drug into the tumor cell. To rapidly generate single chain Fv (scFv) antibody fragments capable of triggering receptor mediated endocytosis we developed a method to directly select phage antibodies for internalization by recovering infectious phage from the cytosol. To generate internalizing antibodies to breast tumor cells, we used this methodology to select from a non-immune phage antibody library, antibodies which were internalized by the breast tumor cell line SKBR3. After three rounds of selection more than 40 scFv's which internalized SKBR3 cells were identified. To target immunoliposomes (ILs) to SKBR3 cells, we selected one of these scFv's (F5) which recognized ErbB2. The F5 scFv was re-engineered with a C-terminal cysteine for coupling to sterically stabilized liposomes and expressed at high levels by fermentation in *E. coli*. The immunoreactivity of F5 ILs was determined by surface plasmon resonance and cellular uptake determined on a number of tumor cell lines. F5 targeted liposomes containing doxorubicin produced significant reduction in tumor size and a greater cure rate in a tumor xenograft model than non-targeted liposomes. We believe this selection methodology will be generally applicable to generate scFv capable of delivering drugs or other agents directly into tumor cells.

**#93 Combined radioimmunotherapy (RAIT) and chemotherapy (CH) in patients with medullary thyroid cancer (MTC): first clinical results.** Juweid, Malik, Rubin, Arnold D., Hajjar, George, Stein, Rhona, Sharkey, Robert M. and Goldenberg, David M. Garden State Cancer Center, Belleville, NJ (USA).

Preclinical studies support the combination of RAIT and CH for treatment of MTC. This phase I study was initiated to clinically determine the safety, dose-limiting toxicity (DLT) and maximum tolerated dose (MTD) of humanized <sup>90</sup>Y-MN-14 (hMN-14) anti-CEA MAb combined with CH with doxorubicin (dox) and peripheral blood stem cell rescue (PBSCR) in patients with metastatic MTC. Escalating doses of <sup>90</sup>Y-hMN-14 were given

with a fixed dose of dox (60 mg/m<sup>2</sup>), administered 24 hours post RAIT, followed by PBSCR. All patients had a tracer study with <sup>111</sup>In-hMN-14 (as <sup>90</sup>Y surrogate) 1 week prior to RAIT. PBSCR were re-infused when the <sup>90</sup>Y total body activity was  $\leq$ 3 mCi/m<sup>2</sup>, corresponding to an <sup>90</sup>Y blood level of  $\sim$ 0.4  $\mu$ Ci/ml. DLT was defined as a grade 3 non-hematologic toxicity of  $>$ 2 weeks, or a grade 4 non-hematologic toxicity of any duration, except a grade 4 GI toxicity and hyperbilirubinemia up to 6 mg/dl where a duration of 1 week and 10 days, respectively, was allowed. To date, eleven patients were entered, 3 at 20 mCi/m<sup>2</sup>, 3 at 30 mCi/m<sup>2</sup>, 3 at 40 mCi/m<sup>2</sup> and another 2 at 50 mCi/m<sup>2</sup> of <sup>90</sup>Y-hMN-14. The MAb scan was positive in all 11 patients and the calculated average tumor dose was  $51 \pm 34$  cGy/mCi and was 5.9, 4.9, and 7.5-fold higher than that of the lung, liver, and kidney, respectively. PBSCR could be re-infused at day 7–12 post therapy in all patients. Nine patients are currently evaluable for toxicity. Grade IV myelotoxicity (transient grade IV neutropenia/thrombocytopenia) was seen in 2/3 patients at 30 mCi/m<sup>2</sup>, and in 2/3 patients at 40 mCi/m<sup>2</sup>. The peripheral blood counts returned to normal levels within 3–6.5 (median = 5.5 weeks) in all patients. Only grade I or II non-hematologic toxicity (cardiopulmonary and gastrointestinal) was observed, except in 1/3 patients at 30 mCi/m<sup>2</sup>, and in 1/3 patients treated at 40 mCi/m<sup>2</sup>. Both patients had a grade III nausea/vomiting for 5 and 1 days. No renal or hepatic toxicity was seen. Of the 9 currently evaluable patients, 2 had a minor response to 12+ months, and three stable disease for 2.5, 6+, and 10+ months. Four patients progressed. In conclusion, the initial results of this trial demonstrate the feasibility of concurrent RAIT and single-agent CH (dox) with PBSCR, with only moderate non-hematologic toxicity and relatively rapid marrow reconstitution. Dose escalation continues to determine the MTD of this combination. (Supported in part by grant FD-R-001555 from the FDA and grant CA-39841 from the NIH.)

**#94 Tumor-specific targeting of wtp53 by anti-transferrin receptor single chain antibody: a new therapeutic strategy for cancer treatment.** Xu, Liang, Alexander, William A., Tang, Wen-Hua, Huang, Cheng-Cheng and Chang, Esther H. Lombardi Cancer Center, Georgetown University Medical Center, Washington, DC 20007.

We have previously demonstrated that cancer cells *in vivo* can be sensitized to both chemotherapy and radiotherapy, resulting in long-term tumor regression, via efficient restoration of p53 function. This was accomplished using a systemically delivered, cationic liposomal p53 delivery system targeted specifically to tumors and their metastases by the addition into the complex of a ligand such as folic acid or transferrin (Tf). The Tf receptor is elevated on the surface of cells in a variety of tumor types. We designed and produced an immunoliposome which uses a recombinant single-chain fragment derived from an anti-transferrin monoclonal antibody (TfRscFv) to target the complex to tumor cells. Because it is a recombinant protein, not a blood product, in addition to its small size and lack of iron, the use of TfRscFv is advantageous over Tf itself as a targeting ligand. The addition of the TfRscFv also successfully directed the liposome complex specifically to tumor cells *in vitro* yielding high level expression of either a reporter gene or exogenous wtp53. More significantly, the systemically administered TfRscFv liposome complex also delivered wtp53 selectively to human prostate xenograft tumors. Therefore, the TfRscFv strategy is a viable method of targeting the cationic liposome complex and delivering wtp53 to tumor cells, thereby increasing the efficacy of functional p53 restoration gene therapy.

**#95 Ionizing-radiation (x-ray) co-administered with complexes of vinorelbine, rhu anti-Her2/neu (c-erbB2) MAbs and hexadecyl-PC induce PC in human MBRCA via antibody dept. cell cytotoxicity (ADCC), apoptotic-induced-drug-delivery (AIDD), radiation-induced-apoptosis (RIA) and PKC-inhibition.** Giannios John N, Glinopoulos P. Dept. of Molecular & Clinical Oncology, Peripheral Hospital of St. Andreas, Patras, Greece.

Purpose: To induce apoptosis in human metastatic breast carcinoma cells overexpressing c-erbB2, bcl-2 and PKC.

Materials & methods: We pretreated disaggregated metastatic breast carcinoma cells from freshly dissected tissues with complexes consisting of rhu-anti c-erbB2 (HER2/neu) mAbs, hexadecyl-phosphocholine and vinorelbine. Then, these cells were irradiated with 8 Gy <sup>60</sup>Co or not irradiated. Pre- and post treatment ICC analysis was performed for c-erbB2, bcl-2 and PKC. Caspase-3/CPP32 and its substrate PARP were measured by Western immunoblotting. Cytotoxicity assays measured BrdU incorporation into cellular DNA, cleavage of tetrazolium salt and LDH leakage while GSH levels were measured by a fluorometric assay. Cell cycle was monitored by flow cytometry and apoptotic signs were examined by TEM.

Results: Rhu anti-HER2-2/neu mAbs have downregulated c-erbB2 gene, hexadecyl-PC has inhibited PKC activity and vinorelbine has downmodulated expression of bcl-2; furthermore, it has depolymerized cytoplasmic microtubules blocking tumour cells at the radiosensitive window of G2/M. Ionizing radiation (IR) has augmented cleavage of caspase-3/CPP32, and generation of its poly (ADP-ribose) polymerase (PARP) cleavage activity. BrdU was not incorporated into cellular DNA indicating inhibition of DNA synthesis and tetrazolium salt was not cleaved to formazan salt revealing inhibition of metabolic activity. The reaction of GSH with OPT exhibited



depletion of GSH due to oxidative stress and lipid peroxidation. The enzyme catalysed reaction of pyruvate with NADH to form lactate and NAD has exhibited enhanced leakage which is proportional to the cellular membrane's rupture. Transmission electron microscopy has revealed attraction on the tumour cell surface of cells that possess receptors for the Fc portion of IgG such as macrophages, T-lymphocytes and natural killer cells; they release free radicals, peroxides and cytolytic lymphokines participating in antibody dependent cell mediated cytotoxicity (ADCC). Finally, TEM has revealed signs of radiation induced apoptosis (RIA) of irreversible stage D2 such as formation of apoptotic bodies which were phagocytosed by adjacent tumour cells leading to bystander killing. Not irradiated tumour cells have not exhibited proteolytic cleavage limiting apoptotic cell death (ACD).

Conclusion: Activation of caspase-3/ CPP32 may cause radiation induced apoptosis (RIA) leading to bystander killing of human metastatic breast carcinoma cells in G2/M phase after downregulation of c-erbB2, bcl-2 and PKC. In addition, antibody dependent cell cytotoxicity (ADCC) contributes to the completion of apoptotic cell death (ACD).

**#96** A phase I clinical study of <sup>111</sup>Indium-labeled NovoMab-G2-scFv, a recombinant human monoclonal antibody fragment, in patients with non-Hodgkin's lymphoma. Percheson Paul B., Connors Joseph M., Dan Michael D., Reilly Raymond M., Kaplan Howard A., Malil Pradip K., St-Onge Jean-Maurice, Novopharm Biotech Inc., Toronto, Canada; British Columbia Cancer Agency, Vancouver, Canada; The Toronto General Hospital, Toronto, Canada

NovoMab-G2-scFv is a single-chain Fv fragment of the multicarcinoma-specific human IgM monoclonal antibody H11, which is expressed in *E. coli*, and contains the variable region sequences from the parent IgM heavy ( $\mu$ ) and light ( $\kappa$ ) chains, constructed in a V<sub>L</sub>-V<sub>H</sub> orientation. The objective of this Phase I trial was to evaluate the tumor and normal tissue localization, pharmacokinetics, radiation dosimetry and overall safety following administration of NovoMab-G2-scFv to patients with non-Hodgkin's lymphoma. Five patients (3 male, 2 female) with follicular small cell non-Hodgkin's lymphoma received a single i.v. injection of 5 mCi (2 mg) of <sup>111</sup>Indium-DTPA-labeled NovoMab-G2-scFv. Whole body planar images were obtained at 0.25, 1, 4, 12, 24, and 48 hours post-injection (p.i.). Blood samples were collected for pharmacokinetic analysis at 5, 10, 15, 30, 45, and 60 minutes and 2, 4, 8, 12, 24, and 48 hours p.i. Patients were followed up at days 14 and 28. NovoMab-G2-scFv was well tolerated at this subtherapeutic dose (2 mg) with only one adverse event (left arm tenderness) possibly related to the drug. Significant changes in hematology from baseline were observed in one patient but these are thought to be due to lymphoma progression, initiation of chemotherapy, and development of pneumonia during the study. Performance status deteriorated by one ECOG grade in 3 patients and remained the same in 2 patients at the end of the study. Imaging demonstrated that NovoMab-G2-scFv localized to known tumor sites in 4 patients. The mean whole body radiation dose was estimated to be 1.86 (SD 0.33) rads/mCi. The radiation dose to the tumor could not be calculated since tumor volumes were not measured. Most normal organs received low radiation doses. Highest doses were delivered to the spleen (71.56 [SD 41.49] rads/mCi), a possible disease site, and the kidneys (33.78 [SD 5.49] rads/mCi), due to renal excretion. The mean terminal half-life in blood and plasma was 33.4 and 32.2 hours respectively. Tumor assessment at day 28 was determined as progressive disease in 3 patients and no change in 2 patients. With demonstrated safety and tumor uptake, a dose escalation clinical study is being planned.

**#97** A Pilot Trial of Vitaxin, an Anti-angiogenic Humanized Antibody in Patients with Advanced Solid Tumors. James Posey<sup>1</sup>, Alma Del Grosso, M.B. Khazaeli, Mansoor Saleh, Daniel Macey, Kamellia Salavy, David Cheresch<sup>2</sup>, William Huse<sup>3</sup>, Albert LoBuglio<sup>1</sup>, University of Alabama at Birmingham Cancer Center<sup>1</sup>, Scripps Research Institute<sup>2</sup>, LaJolla, CA, IXSYS, Inc., San Diego, CA<sup>3</sup>.

Vitaxin is humanized monoclonal antibody which targets the  $\alpha v\beta 3$  integrin. This receptor is integrally involved in tumor angiogenesis. LM609, the murine counterpart to Vitaxin has been shown to inhibit tumor growth in animals. This pilot effort was conducted to assess tumor targeting, pharmacokinetics, toxicities and anti-tumor activity associated with the infusion of this antibody on a days 0 and 21. A previous Phase I trial suggests that this agent is tolerable in doses up to 4 mg/kg on a weekly schedule. We have treated nine patients, three per cohort at 10, 50 and 200 mg. Grade 2 fever was observed in 3 patients and 1 patient developed grade 2 transaminitis after the day 0 dose of 200 mg. There was no change in human anti-humanized antibody formation. We were able to image index lesions in 3 patients. Two at the 200 mg dose and one at the 50 mg dose. Vitaxin pharmacokinetics based on an anti-idiotypic radiometric assay is described in Table 1.

Dose	C <sub>max</sub>	t <sub>1/2</sub> (hrs)	AUC	CL (mL/hr/kg)
10 mg	1.45 ± 0.4	13.8 ± 2.7	29 ± 10	6.4 ± 1.8
50 mg	10.3 ± 2.2	161 ± 40	1073 ± 290	0.57 ± 0.16
200 mg	81.4 ± 11.8	173 ± 37	8664 ± 197	0.40 ± 0.02

The kinetics for patients receiving 200 mg are consistent with other genetically engineered chimeric or humanized intact monoclonal antibodies. Serum levels fit a two-compartment model with a  $\beta$  half-life of about one week. At the 10 mg doses the T<sub>1/2</sub> was about 14 hours with increased clearance and a larger volume of distribution. These data suggest that there is a  $\alpha v\beta 3$  pool which causes rapid clearance of lower doses that can be exceeded at higher doses (200 mg). At 200 mg the dose schedule of every three weeks can maintain circulating levels in excess of 5  $\mu$ g/ml.

## SECTION 5: KINASE INHIBITORS

**#98** Efficacy of cytotoxic agents against human tumor xenografts is markedly enhanced by co-administration of ZD1839 (Iressa™), an inhibitor of EGF receptor tyrosine kinase. Sirotnak F.M., Miller V.A., Scher H.I. and Kris M.G. Memorial Sloan-Kettering Cancer Center, New York, NY 10021.

Blockade of EGFR function with monoclonal antibodies (Mab's) has major antiproliferative effects (Fan, Z., Mendelsohn, J., Current Opin. Oncol. 10:67, 1998) against human tumors *in vivo*. Similar antiproliferative effects against some of these same tumors have also been obtained (Lawrence, D.S., Nul, J., Pharmacol. Ther. 77:81, 1998) by specific inhibitors of the EGFR associated tyrosine kinase. One such inhibitor, the orally active ZD1839 (Woodburn, J.R. et al, Proc. Amer. Assoc. Cancer Res. 38:633, 1997) has pronounced antiproliferative activity against human tumor xenografts. We now show that co-administration of ZD1839, as with anti-EGFR Mab's, will enhance the efficacy of cytotoxic agents against human lung (A549 and SK-LC-16 NSCL and LX-1 SCL) and prostate (PC-3 and TSU-PR1) tumors. Oral ZD1839 (qd  $\times$  5)  $\times$  2 and cytotoxic agents (ip q3-4d  $\times$  4) were given for a period of 2 weeks to mice with well established tumors. On this schedule the MTD (150 mg/kg) of ZD1839 was 40-60% growth inhibitory. In contrast, most combinations of ZD1839 with cytotoxic agents were highly effective but dose reduction of ZD1839 below its single-agent MTD was required for optimum tolerance. This reduction was 2 fold for adriamycin (ADR), edatrexale (EDX) and platinum (CDDP, CBDCA) and 3-fold for paclitaxol (PTXL), docetaxol (DTXL) and gemcitabine (GEM). ZD1839 with navebine was toxic at a 6-fold dose reduction and proved ineffective as was dose-reduction of cytotoxic agents with the MTD of ZD1839. The pronounced growth inhibitory action of CDDP and CBDCA against A549 and LX-1 lung and TSU-PR1 and PC-3 tumors was increased 3-4 fold with ZD1839 with some regression seen with PC-3. While PTXL and DTXL markedly inhibited the growth of LX-1, SK-LC-16, TSU-PR1 and PC-3, with ZD1839 there was either partial or complete regression. Against A549 the growth inhibition of ADR was increased 10 fold (>99%) with ZD1839. EDX was highly growth inhibitory to A549, LX-1 and TSU-PR1, while EDX with ZD1839 resulted in partial or complete regression. In contrast, ZD1839 did not enhance the highly growth inhibitory action of GEM against A549 or SK-LC-16 tumors. Overall, these results portend significant clinical potential for ZD1839 in combination with many cytotoxic agents. Support: NCI CA08748 and CA56517, The Simon Benlevy Cancer Fund and the Pepsico Foundation.

**#99** Phase I study of oral ZD1839 (Iressa™), a novel inhibitor of epidermal growth factor receptor tyrosine kinase (EGFR-TK): evidence of good tolerability and activity. Kris M, Ranson M, Ferry D, Hammond L, Averbuch S, Ochs J, Rowinsky E. Memorial Sloan Kettering Cancer Center, New York, USA; Christie Hospital, Manchester, UK; Cancer Therapy & Research Center, San Antonio, USA; Queen Elizabeth Hospital, Birmingham, UK; AstraZeneca Pharmaceuticals.

ZD1839 (Iressa™) is a potent and selective, oral EGFR-TK inhibitor. The aim of this phase I dose-escalation trial was to evaluate the tolerability, safety and activity of ZD1839 in patients (pts) with advanced solid tumors. To date, 60 pts with NSCLC (14), breast (7), colorectal (7), ovarian (7), renal (4), esophageal (4), pancreatic (3), mesothelioma (3), or miscellaneous (11) tumors have been recruited. Escalating doses of ZD1839 (50-700 mg once daily, 4-8 patients per dose level) were given orally for 14 consecutive days followed by 14 days without treatment. In the absence of progression or significant toxicity ZD1839 was reinitiated at the same dose and intermittent 14-day schedule. In total, 94 14-day treatment periods were completed. Mean C<sub>max</sub> and AUC<sub>0-24h</sub> at 50 to 525 mg/day after 14 days ranged from 113-933 ng/ml and 4.5-51.3 ug·h/ml, respectively. The mean elimination half-life was 44.0 hrs, consistent with once-daily administration. The most frequent adverse events (AEs) [NCI-CTC grades] included grade 1-2 nausea/vomiting (20%), skin changes (16%), and infection (10%). Grade 3-4 AEs were rare, non-mechanism based, or related to disease progression, except for transient transaminase elevation (n = 1) and skin rash (n = 1). Skin rash frequency occurred dose-dependently, rashes were usually grade 1-2, reversible, pustular and involved the face and/or upper torso. One pt (525 mg), withdrawn with grade 3 pruritic pustular rash, had complete resolution of this lesion two weeks later. Fourteen NSCLC patients were evaluable for response (WHO criteria). Rapid symptom improvement with significant anti-tumor response occurred, including 1 partial response (50% shrinkage bidimensionally and 30% unidimensionally for 4+ months at 300 mg). Another pt at 400 mg had 50% shrinkage



bidimensionally and 25% unidimensionally on CT scan at 28 days; one month later he progressed with symptomatic brain metastases. Almost complete resolution of a large pleural effusion with probable hilar tumor area necrosis was detected in a pt at 525 mg. Accrual is ongoing and updated results will be available November 1999.

**Summary:** in this ongoing phase I study, ZD1839 (a novel EGFR-TK inhibitor) has shown generally mild, reversible toxicity and potentially significant anti-tumor activity in NSCLC when given as monotherapy.

**#100 Preclinical profile of PK1166 – a novel and potent EGFR tyrosine kinase inhibitor for clinical development.** P. Traxler, E. Buchdunger, P. Furet, H.-P. Geschwind, P. Ho, H. Mett, T. O'Reilly, U. Pfahr, H. Thomas. *Novartis Pharmaceuticals, Therapeutic Area Oncology, Novartis Limited, CH-4002 Basel, Switzerland, Phone: +41-61-696-5286, FAX: +41-61-696-3429.*

The EGFR protein tyrosine kinase is a promising target for the rational design of anticancer drugs. PK1166, a new chemical entity of the pyrrolopyrimidine class of compounds, was designed using a pharmacophore model of the ATP-binding site of the EGFR kinase.

PK1166, a selective and potent inhibitor of the EGFR tyrosine kinase *in vitro* ( $IC_{50} = 1$  nM), preferentially inhibited signalling through the ligand-activated EGFR signal transduction pathway. EGF-mediated EGFR autophosphorylation, *c-fos* mRNA expression and cell proliferation were inhibited in the sub-micromolar range. At higher concentrations, the compound also inhibited cellular *c-ErbB2* autophosphorylation ( $IC_{50}$ : 0.1–1  $\mu$ M).

PK1166 showed good oral bioavailability in mice, rats and dogs after single oral administration, the estimated bioavailability in dogs being approximately 47%. Plasma levels were above cellular  $IC_{50}$  values for more than 8 h.

The compound showed potent and selective *in vivo* antitumor activity in several EGFR expressing xenograft tumor models in nude mice following oral administration of 10–100 mg/kg/day. Proof of concept was obtained by measuring the effect of PK1166 on EGF-stimulatable kinase activity in A431 tumors from treated mice. Administration of EGF *in vivo* to mice produced a marked autophosphorylation of the EGFR in the tumor which was potently inhibited by pretreatment with 100 mg/kg of PK1166 *p.o.*

In *in vitro* and *in vivo* toxicity studies, PK1166 exerted a favorable toxicity profile.

PK1166 will enter Phase I trials in patients in the second half of this year.

**#101 ErbB receptor tyrosine kinases as regulators of cytoprotective and cytotoxic radiation responses of carcinoma cells.** Schmidt-Ullrich RK, Bowers G, Dent P, Reardon D, Contessa J, Valerie K. *Virginia Commonwealth University/Medical College of Virginia, Richmond, VA, USA.*

ErbB receptor Tyr kinases (RTKs) in autocrine growth regulated human carcinoma cells have been identified as a critical response network after exposure to ionizing radiation (IR). This 5-fold activation of ErbB1 is essential for the activation of the MAPK pathway and a cytoprotective proliferation response, known as accelerated repopulation. The inhibition of MAPK results in compensatory activation of the JNK pathway via Ras, a stress response associated with increased apoptosis. Based on the widely varied levels of ErbB RTK expression, we demonstrate that, due to the indiscriminate activation of ErbB receptors by IR the ErbB expression profile of a given tumor cell is critical for the response to IR and overrides the effects of growth factor (GF) ligands.

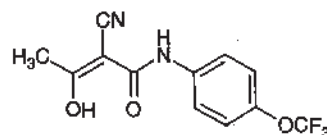
The findings are described for two breast carcinoma cell (BCC) lines, MDA-MB-231 and T47D, expressing different levels of ErbB1/2/3 and ErbB2/3/4. The biological effects of GFs are compared to those of IR under conditions of selective inhibition of ErbB RTK function by the tyrosine phosphatase AG1478 and AG825. The activation profiles after GF and IR exposure are linked to MAPK/JNK stimulation and cellular responses of proliferation, survival, and apoptosis.

The selective inhibition of ErbB1 and ErbB3/4 function demonstrates the critical role of these receptors on MAPK/JNK activation in response to IR exposure. Importantly, the activation of ErbB RTKs after GF or IR treatment are markedly different and explain differences in cytoprotective and stress responses as involving p21Cip-1 and Elk, G1 cell cycle arrest, DNA synthesis, and rates of apoptosis. While ErbB1 and ErbB4 may have similar effects, their functions are critically modulated by ErbB2 resulting in fundamentally different responses of cells to IR and GFs, such as transient vs. prolonged MAPK activation.

For the first time, we demonstrate that the IR and GFs in carcinoma cells induce fundamentally different activation responses which are most likely based on the nondiscriminating activation of ErbB receptors by IR. Differences in signalling responses as a result of selective inhibition of ErbB1/2/3/4 and ErbB2 function demonstrate the importance of these receptors as potential targets for the modulation of carcinoma cell IR responses.

**#102 Specificity of leflunomide derivative LFM-A12 for inhibiting epidermal growth factor receptor (EGFR) tyrosine kinase.** Ghosh, S.; Zheng, Y.; Jun, X.; Naria, R. K.; Mahajan, S.; Navara, C.; Mao, C.; Sudbeck, E.; Uckun, F. M. *Parker Hughes Cancer Ctr., Str. Biol, Chem, Biochem, Exp. Oncol., Hughes Institute, St. Paul, MN.*

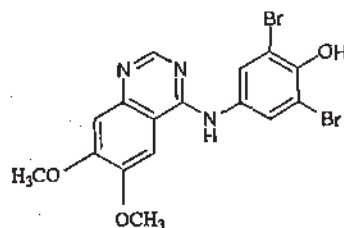
The epidermal growth factor receptor (EGFR) tyrosine kinase has an essential function for the survival of human breast cancer cells. In a systematic effort to design potent and specific inhibitors of this receptor family protein tyrosine kinase as anti-breast cancer agents, we recently reported the construction of a 3D homology model of the EGFR kinase domain. Our lead compound LFM-A12 inhibited EGFR kinase *in vitro* with an  $IC_{50}$  value of 1.7  $\mu$ M. LFM-A12 was also discovered to be a highly specific inhibitor of the EGFR. Even at concentrations ranging from 175 to 350  $\mu$ M, this inhibitor did not affect the enzymatic activity of other protein tyrosine kinases such as, the Janus kinases JAK1 and JAK3, the Src family kinase HCK, the Tec family member Bruton's tyrosine kinase (BTK), and the receptor family PTK insulin-receptor kinase (IRK). This observation is in contrast to the activity of a quinazoline inhibitor tested as a control (4-(3-Bromo, 4-hydroxyanilino)-6,7-dimethoxyquinazoline), which was shown to inhibit EGFR, and other tyrosine kinases such as HCK, JAK3, and SYK. In addition, LFM-A12 inhibited the proliferation ( $IC_{50} = 26.3$   $\mu$ M) and *in vitro* invasiveness ( $IC_{50} = 28.4$   $\mu$ M) of human breast cancer cells in a concentration-dependent fashion. At concentrations  $\geq 100$   $\mu$ M, LFM-A12 rapidly induced apoptosis in multidrug-resistant human breast cancer cells and killed >99.9% of their clonogenic fraction.



LFM-A12

**#103 Potent 4-Anilinoquinazoline inhibitors of epidermal growth factor receptor (EGFR) tyrosine kinase.** Ghosh, S.; Lu, X.-P.; Naria, R. K.; Jun, X.; Mao, C.; Uckun, F. M. *Parker Hughes Cancer Center, Structural Biology, Chemistry, Biochemistry, Experimental Oncology, Hughes Institute, St. Paul, MN.*

Epidermal growth factor receptor (EGFR) tyrosine kinase is known to be overexpressed in several malignancies and is an important target for anti-cancer drug design. A structure-based approach was used to design and synthesize potent 4-anilinoquinazoline derivatives targeting the EGFR catalytic site. The compounds were designed based on a constructed 3D homology model of the EGFR kinase domain. A model of the EGFR binding pocket was used in combination with docking procedures to predict the favorable placement of chemical groups with defined sizes at multiple modification sites on the parent compound, 4-anilinoquinazoline. The model indicated that EGFR inhibition may be significantly improved by increasing the size of the ligand by appropriate substitutions at the 3', 4' and 5' positions on the anilino ring. This approach has led to the successful design of a dibromo quinazoline derivative, WHI-P97, which had an estimated  $K_i$  value of 0.09  $\mu$ M from modelling studies, and a measured  $IC_{50}$  value of 2.5  $\mu$ M in EGFR kinase inhibition assays. WHI-P97 effectively inhibited the *in vitro* invasiveness and proliferation of EGFR positive human cancer cells in a concentration-dependent manner. The reported studies may provide the basis for the development of clinically useful anti-cancer agents.



P97

**#104 The tyrosine kinase inhibitors CEP-751 (KT-6587) and CEP-701 (KT-5555) lead to apoptosis in prostate cancer cells via the elevation of intracellular free calcium and inhibition of the PI-3Kinase/PKB pathway.** Weeraratna, Ashari T., Tombal, Bertrand, and Isaacs, John T. *Johns Hopkins Oncology Center, Johns Hopkins School of Medicine, Baltimore, MD 21231 and Department of Physiology, Catholic University of Leuven, Brussels, Belgium.*

The neurotrophins and their high-affinity tyrosine kinase (trk) receptors have been linked to prostate cancer progression, and may represent molecular targets for therapeutic intervention. Ligand-occupied trk receptors signal via several pathways, including *ras/raf/meck* and the PI-3 kinase/Akt pathways. This latter pathway is important in the phosphorylation of the pro-apoptotic protein Bad, sequestering it in the cytoplasm, and in phosphorylation-dependent inactivation of pro-caspase-9. CEP-751 and CEP-701, two trk inhibitors, impede the growth of prostate cancers in various animal models in a cell-cycle independent fashion via



induction of apoptosis. CEP-751/701 induce prostate cancer apoptosis by inhibiting kinase activity of the *trk* receptor, preventing its autophosphorylation. This prevents the activation of *Trk*-associated *ras* and *PI-3* kinase pathways. Using dominantly activated *ras* mutants, induction of apoptosis by CEP751/701 was demonstrated not to require inhibition of the *ras/raf/meck* pathway. Other proteins such as those of the *p38* MAP Kinase and *JNK/STAT* pathways also appear to be unaffected by these agents. In contrast, *Trk* inhibition resulted in the nearly complete inhibition of *AKT* phosphorylation. This was unexpected since *PI-3* kinase activation and subsequent *Akt* phosphorylation can be induced by a large series of ligand-occupied receptor kinases (eg, *PDGFR*, *bFGFR*, *IGFR*, etc.) besides *Trk*. Using specific *PI3* kinase inhibitors, which also inhibit *Akt* phosphorylation, it was demonstrated that this inhibition of *Akt* phosphorylation was insufficient to induce prostate cancer cell death. CEP701/751 also led to a delayed (>18 h) elevation in intracellular free  $Ca^{2+}$  ( $\geq 10 \mu M$ ), which is associated with the induction of morphological changes and the loss of clonogenic ability, but not leakiness of the plasma membrane. This  $Ca^{2+}$  rise via binding to calmodulin activates calcineurin, leading to the dephosphorylation of *BAD*, and thus its translocation to the mitochondria and downstream activation of caspases and cell death. These results demonstrate that the apoptosis of prostate cancer cells induced by CEP-751/701 requires the inactivation of survival signalling in conjunction with the delayed elevation of  $Ca^{2+}$ . (This work was partially supported by Cephalon Inc. and TAP Holdings Inc.)

**#105 INHIBITION by CEP-751 (KT-6587) of human neuroblastoma (NBL) & medulloblastoma (MBL) xenografts in nude mice.** Evans, A.E., Kisselbach, K.D., Ikegaki, N., Camoratto, A.M., Dionne, C.A. and Brodeur, G.M. Div. of Oncology, Children's Hosp. of Phila., Cephalon, Inc., West Chester, PA, & Univ. of Penna. Cancer Center.

**Introduction:** This study was designed to determine the effect of CEP-751 on the growth of NBL and MBL cell lines as xenografts. CEP-751 (KT-6587), an indolocarbazole derivative, is an inhibitor of *Trk* family tyrosine kinases at nanomolar concentrations.

**Methods:** *In vivo* studies were conducted on four NBL (IMR-5, CHP-134, NBL-S and SY5Y) and three MBL (D283, D341 and DAOY) cell lines using two treatment schedules: (1) treatment was started after the tumors were measurable (therapeutic study); or (2) four to six days after inoculation, before tumors were palpable (prevention study). CEP-751 was given at 21 mg/kg/dose administered twice a day, seven days a week; the carrier vehicle was used as a control.

**Results:** In therapeutic studies, a significant difference in tumor size was seen between treated and control animals with IMR-5 on day 8 ( $p = 0.01$ ), NBL-S on day 17 ( $p = 0.016$ ) and CHP-134 on day 15 ( $p = 0.034$ ). CEP-751 also had a significant growth inhibitory effect on MBL line D283 (on day 39,  $p = 0.031$ ). Inhibition of tumor growth of D341 did not reach statistical significance, and no inhibition was apparent with DAOY which lacks *TrkB* receptors. In prevention studies, CEP-751 showed a modest growth inhibitory effect on IMR-5 ( $p = 0.062$ ) and CHP-134 ( $p = 0.049$ ). Furthermore, inhibition of growth was greater in the SY5Y cell line transfected with *TrkB* compared to the untransfected parent cell line expressing no detectable *TrkB*. TUNEL studies showed CEP-751 induced apoptosis in treated CHP-134 tumors, whereas no evidence of apoptosis was seen in control tumors. Finally, there was no apparent toxicity identified.

**Conclusion:** These results suggest that CEP-751 may be a useful therapeutic agent for NBL or MBL.

**#106 EFFECT of CEP-751 (KT-6587) on human neuroblastoma (NBL) xenografts expressing *Trk B*.** Evans, A.E., Kisselbach, K.D., Ikegaki, N., Eggert, A., Camoratto, A.M., Dionne, C.A., and Brodeur, G.M. Div. of Oncology, Children's Hosp. of Phila., Cephalon, Inc., West Chester, PA, and U. Penn Cancer Ctr.

**Introduction:** *TrkB* has been suggested to play a crucial role in the growth and survival of advanced NB tumors. In these experiments, we studied the effect of *TrkB* on the growth of NB xenografts in nude mice and the effect of CEP-751 (KT6587), a potent and selective inhibitor of *Trk* family tyrosine kinases, on that growth.

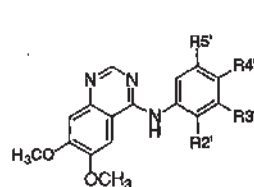
**Methods:** SY5Y, a human NB cell line with no detectable level of *Trk* expression, was transfected with *TrkB*, and resulting clones, G8 and G12, expressed moderate and high level, respectively, of *TrkB* mRNA and protein. These *TrkB* expressing subclones and the parental line were then grown as xenografts in nude mice. CEP-751 was used to inhibit *TrkB* in these xenografts. Animals were treated (bid) with CEP-751 (21 mg/kg/day), or with the carrier vehicle as a control. *TrkB* expression in the resultant tumors was examined by quantitative RT-PCR. The effect of CEP-751 on *TrkB* activation by BDNF was examined in G12 cells in culture by immunoprecipitation with anti-pan *Trk* antibodies, followed by Western blot analysis using antiphosphotyrosine antibodies.

**Results:** Activation of *TrkB* in G12 cells by BDNF was inhibited by CEP-751 in a dose dependent fashion. CEP-751 had no effect on the growth of SY5Y tumors, but did slow the rate of the G8 and G12 tumor growth in proportion to their level of *TrkB* expression. RT-PCR analysis confirmed the expression of *TrkB* in G8 and G12 but not in SY5Y tumors.

**Conclusions:** These data support an important role of *TrkB* expression in the growth of advanced NB tumors, and suggest that the potent and selective inhibitor of *Trk* kinases, such as CEP-751, may be effective in retarding the growth of advanced stage NB tumors in humans.

**#107 Structure-based design of specific inhibitors of Janus kinase 3 (JAK3) as apoptosis-inducing anti-leukemic agents.** Sudbeck, E. A.; Liu, X.-P.; Narla, R. K.; Mahajan, S.; Ghosh, S.; Mao, C.; Uckun, F. M. Parker Hughes Cancer Center, Structural Biol., Chemistry, Drug Discovery Program, Hughes Institute, St. Paul, MN.

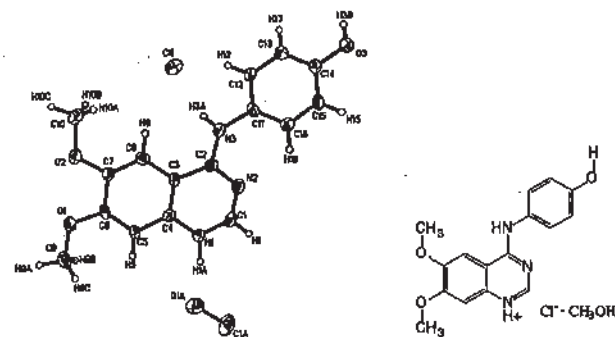
A homology model of the kinase domain of Janus kinase 3 (JAK3) was constructed and used for structure-based design of dimethoxyquinazoline compounds with potent and specific inhibitory activity against JAK3. The JAK3 model revealed a 530 Å<sup>3</sup> volume available for inhibitor binding and was useful for identifying a quinazoline derivative, WHI-P131, predicted to inhibit JAK3. An analysis of the catalytic site of JAK3 revealed six nonconserved residues which can interact more favorably with WHI-P131 and enhance binding relative to other tyrosine kinases. *In vitro* kinase assays showed that WHI-P131 inhibited JAK3 ( $IC_{50} \sim 9 \mu M$ ) but did not show inhibition of JAK1, JAK2, SYK, BTK, LYN, or IRK. WHI-P154 and WHI-P97 also showed activity against JAK3 ( $IC_{50} \sim 28 \mu M$  and  $1.1 \mu M$ , respectively) whereas WHI-P79, WHI-P111, WHI-P112, WHI-P132, and WHI-P258 did not show any significant JAK3 inhibition. WHI-P131 induced apoptosis in JAK3 expressing human leukemia cell lines NALM-6 and LC1;19, but not in melanoma (M24-MET) or squamous carcinoma (SQ20B) cells. Leukemia cells were not killed by dimethoxyquinazoline compounds which were inactive against JAK3. WHI-P131 inhibited the clonogenic growth of JAK3 positive leukemia cell lines DAUDI, RAMOS, LC1;19, NALM-6, MOLT-3, and HL-60 (but not JAK3-negative BT-20 breast cancer, M24-MET melanoma, or SQ20B squamous carcinoma cell lines) in a concentration-dependent fashion. Potent and specific inhibitors of JAK3 such as WHI-P131 may provide the basis for the design of new treatment strategies against acute lymphoblastic leukemia, the most common form of childhood cancer.



R = H except for:  
 WHI-P79: R3'=Br  
 WHI-P97: R3'=Br, R4'=OH, R5'=Br  
 WHI-P111: R3'=Br, R4'=CH3  
 WHI-P112: R2'=Br, R5'=Br  
 WHI-P131: R4'=OH  
 WHI-P132: R2'=OH  
 WHI-P154: R3'=Br, R4'=OH  
 WHI-P258: R2'-5' = H

**#108 Crystal structure of WHI-P131, a dimethoxyquinazoline inhibitor of Janus kinase 3 (JAK3).** Sudbeck, E. A.; Jennissen, J. D.; Liu, X.-P.; Uckun, F. M. Parker Hughes Cancer Center, Drug Discovery Program, Departments of Structural Biology and Chemistry, Hughes Institute, St. Paul, MN.

The crystal structure of the methanol solvate of 4-(4'-Hydroxyphenyl)-amino-6,7-dimethoxyquinazoline-HCl (WHI-P131, an inhibitor of Janus kinase 3) was determined. The structure contains four hydrogen bonds, two of which are within the asymmetric unit. One interaction is formed between WHI-P131 and Cl<sup>-</sup> and another occurs between methanol and Cl<sup>-</sup>. A third interaction is formed between WHI-P131 and Cl<sup>-</sup> (related by a 2<sub>1</sub> screw) and a fourth is formed between WHI-P131 and methanol (related by an n-glide). The conformation of crystalline WHI-P131 was comparable to an energy-minimized model of WHI-P131 used in molecular docking studies to predict how the inhibitor would bind to JAK3.



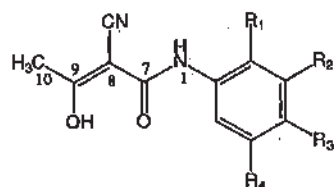
WHI-P131

**#109** A tyrosine kinase inhibitor and interleukin-12 synergize to inhibit tumor growth in mice. Burdelya Lyudmila, Catlett-Falcone Robyn, Levitzki Alexander\*, Jove Richard, and Yu Hua. H. Lee Moffitt Cancer Center & Research Institute, Tampa, FL, \*Institute of Life Sciences, The Hebrew University, Jerusalem, Israel.

Constitutive activation of signal transducer and activator of transcription 3 (STAT3) has recently been found in the majority of human myeloma specimens. In this study, we investigated the effect of blocking the Janus kinase (JAK)/STAT pathway upon myeloma cell survival and cytokine-mediated immune responses in a syngenic murine model. Blocking JAK/STAT signaling in vitro by a specific tyrosine kinase inhibitor, AG-490, suppressed STAT3 DNA-binding activity and induced apoptosis of the murine myeloma cell lines which harbored constitutively activated STAT3. Treatment of subcutaneously growing murine myeloma tumors with AG-490 resulted in complete but transient tumor regression, mediated by tumor cell apoptosis. In contrast to AG-490, cytokine-based immunotherapy usually generates long-term antitumor immunity but fails to induce regression of established tumors. While IL-12 has been shown to be one of the most effective cytokines for immunotherapy, its signaling is mediated by JAK kinases. Our results, however, demonstrate that in vivo administration of AG-490 had no detectable effect on both IL-12-mediated activation of macrophage cytotoxicity and IFN- $\gamma$  production by splenocytes. Furthermore, while tumor regression induced by AG-490 was transient and IL-12 alone had little effect in inhibiting tumor growth, combination therapy of the two resulted in prolonged tumor regression. These results suggest that AG-490 possesses clinical potential as an effective adjuvant for cancer immunotherapy.

**#110** Crystal structures of leflunomide metabolite analogs. Ghosh, Sutapa; Zheng, Yaguo; Uckun, Fatih M. Parker Hughes Cancer Center, Drug Discovery Program, Departments of Structural Biology and Chemistry, Hughes Institute, St. Paul, MN.

Leflunomide metabolite analogs were recently shown to exhibit tyrosine kinase inhibiting activity. Crystal structures of seven leflunomide analogs, LFM-A1, LFM-A7, LFM-A9, LFM-A10, LFM-A11, LFM-A12, and LFM-A13 are reported. The compounds are analogs of A77 1726, the active metabolite of the immunosuppressive drug leflunomide. The molecular structures of the reported compounds are very similar and they display similar crystal packing and hydrogen bonding networks. All three molecules are approximately planar; the dihedral angles between the phenyl ring and the plane defined by the atoms N1, C7, C8, C9 and C10 are 4.76(83)°, 12.54(17)°, 6.21(58)°, 5.54(30)°, and 4.42(28)° for LFM-A1, LFM-A7, LFM-A9, LFM-A10, and LFM-A11, respectively. In all of the structures the hydroxyl group is involved in an intramolecular hydrogen bond with the carbonyl oxygen. Two intermolecular hydrogen bonds are observed between the amine group (N1) and the cyano nitrogen of the centrosymmetrically related molecule, and between the hydroxyl group and the centrosymmetrically related carbonyl oxygen.



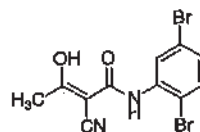
R=H except for:

LFM-A1: R3=Br  
 LFM-A7: R1=F  
 LFM-A9: R2=Br  
 LFM-A10: R2=Cl  
 LFM-A11: R2=F  
 LFM-A12: R3=OCF<sub>3</sub>  
 LFM-A13: R1, R4=Br

**#111** Rational design of leflunomide derivatives as anti-leukemic agents which target Bruton's tyrosine kinase. Sudbeck, E., Ghosh, S., Mahajan, S., Zheng, Y., Downs, S., Hupke, M., Uckun, F.M., Parker Hughes Cancer Center, Structural Biol., Chemistry, Biochem., *Experiml. Oncology, Hughes Institute, St. Paul, MN.*

In a systematic effort to design potent inhibitors of the anti-apoptotic tyrosine kinase BTK as antileukemic agents with apoptosis promoting and chemosensitizing properties, we constructed a 3D homology model of the BTK kinase domain. Our modeling studies revealed a distinct rectangular binding pocket near the hinge region of the BTK kinase domain with Leu<sup>460</sup>, Tyr<sup>476</sup>, Arg<sup>525</sup> and Asp<sup>539</sup> residues occupying the corners of the rectangle. Advanced docking procedures were employed for the rational design of leflunomide metabolite (LFM) analogs with a high likelihood to bind favorably to the catalytic site within the kinase domain of BTK. The lead compound LFM-A13 inhibited human BTK *in vitro* with an IC<sub>50</sub> value of 17.2 ± 0.8  $\mu$ M. Similarly, LFM-A13 inhibited recombinant BTK expressed in a baculovirus expression vector system with an IC<sub>50</sub> value of 2.5  $\mu$ M. The predicted position of LFM-A13 in the binding pocket of BTK directs its aromatic ring toward Tyr<sup>476</sup>, and its substituent group to be between residues Arg<sup>525</sup> and Asp<sup>539</sup>. LFM-A13 is capable of favorable hydrogen bonding interactions with BTK via Asp<sup>539</sup> and Arg<sup>525</sup> residues. Besides its remarkable potency in BTK kinase assays, LFM-A13 was also discovered to be a highly specific inhibitor of BTK. Even at concentrations as high as 100  $\mu$ g/ml (~278  $\mu$ M), this novel inhibitor did not affect the enzymatic activity of other protein tyrosine kinases, including JAK1, JAK3, HCK, EGF-Receptor Kinase (EGFR), and Insulin-Receptor Kinase (IRK). In

accordance with the anti-apoptotic function of BTK, treatment of BTK<sup>+</sup> B-lineage leukemic cells with LFM-A13 enhanced their sensitivity to ceramide- or vincristine-induced apoptosis.



LFM-A13  
 IC<sub>50</sub> = 17  $\mu$ M

**#112** The cyclin-dependent kinase (CDK) inhibitor flavopiridol (flavo) potentiates radiotherapy (RT) induced apoptosis in association with loss of p21<sup>waf1/cip1</sup>. Jung, Christoph P, Motwani, Monica V, Halmovitz-Friedman, Adriana, Schwartz, Gary K. Memorial Sloan-Kettering Cancer Center, New York, NY 10021, USA.

We have previously reported that the CDK inhibitor, flavo, potentiates mitomycin C and paclitaxel induced apoptosis in human breast and gastric cancer cells. The results of a clinical trial with flavopiridol in combination with chemotherapy appear very promising. There have been no reports on the effect of flavo on RT-induced apoptosis. Therefore, we explored the effect of flavo on  $\gamma$ -radiation induced apoptosis in the human MKN74 gastric and HCT-116 colorectal carcinoma cell lines. These cells were treated under the following series of conditions: drug free media (ND<sub>24</sub>), flavo for 24 hours (F<sub>24</sub>, 300 and 150 nm), RT alone (20/10 Gy), flavo + RT, or sequential combinations of these conditions (RT  $\rightarrow$  F<sub>24</sub> and F<sub>24</sub>  $\rightarrow$  RT). The extent of apoptosis was determined by staining the cells with DAPI and scoring the percentage of apoptotic nuclei by fluorescence microscopy. In the MKN-74 cells, flavo enhanced the induction of apoptosis from 2 ± 1% and 11 ± 1%, respectively, with RT and flavo alone to 24 ± 3% with RT  $\rightarrow$  F<sub>24</sub>. In RT  $\rightarrow$  F<sub>24</sub> there was 80% cleavage of the PARP proenzyme and this was associated with the activation of caspase 3, as shown by western blot. In contrast there was almost no PARP cleavage with RT alone and only 10% PARP cleavage with flavo alone. The mechanism of enhanced apoptosis by flavo on RT treated cells remains unknown. It has been reported that HCT-116 cells which lack p21<sup>waf1/cip1</sup> (p21<sup>-/-</sup>) are more sensitive to RT than HCT-116 cells which express p21 (p21<sup>+/+</sup>). Therefore, we tested the effect of RT and flavo on HCT-116 p21<sup>+/+</sup> and HCT-116 p21<sup>-/-</sup> cells. Our results indicate that in the p21<sup>-/-</sup> cells RT alone induces a 2-fold greater increase in apoptosis than in the p21<sup>+/+</sup> cells. However, when the p21<sup>+/+</sup> cells are treated with RT  $\rightarrow$  F<sub>24</sub>, the induction of apoptosis is 3-fold greater than the p21<sup>-/-</sup> cells treated with RT alone. Western blot analysis of the p21 status of these cells indicates that the potentiation of apoptosis by flavo is associated with a loss of p21 protein expression in the p21<sup>+/+</sup> cells, despite the induction of p53. This data suggests that flavo sensitizes a p21<sup>+/+</sup> cell to RT by virtue of loss of p21 protein. The potentiation of RT induced apoptosis by flavo represents a new therapeutic strategy in the treatment of human cancer and may be in part mediated by a loss of p21.

**#113** Phase I trial of combination bryostatatin-1 and vincristine in B-cell malignancies. Dowlati A, Robertson K, Ksenich P, Jacobberger J, Whitacre C, Schnur G, Cooper B, Spiro T, Lazarus H, Gerson S, Murgu A, Sedransk N, Remick SC. Developmental Therapeutics Program, Ireland Cancer Center, Case Western Reserve University, Cleveland, OH and NCI, Bethesda, MD.

Bryostatatin-1 (NSC 339555) is a macrocyclic lactone originally isolated from the marine animal *Bugula neritina*. It has both antitumor and immunomodulatory activity. It is proposed that modulation of protein kinase C (PKC) activity plays a major role in mediating these effects. In preclinical models, bryostatatin-1 has been shown to enhance the antitumor effects of a variety of other antitumor agents including vincristine and that this synergistic activity is sequence dependent. Preclinical models have shown significant activity in B-cell malignancies. We have undertaken a phase I trial of a 24-hour infusion of bryostatatin-1 followed immediately by a bolus injection of vincristine. Bryostatatin-1 was dose escalated (12.5, 16.5, 22, 30, 40  $\mu$ g/m<sup>2</sup>/24-hour continuous infusion) while the dose of vincristine was fixed at 1.4 mg/m<sup>2</sup> (max. dose of 2.0 mg). Eleven patients (1 CLL, 6 MM, 4 NHL) have been treated to date. Enrollment on dose level 4 is continuing. No dose limiting toxicity has been seen to date. Grade 1/2 myalgia is frequently seen and has occurred at all dose levels. Grade 1 neuropathy is common with prolonged therapy and is due to vincristine. Grade 3 lymphocytopenia occurs frequently. Prolonged stable disease (SD) and a partial response have been seen in 2 patients with pretreated (1 post-transplant) NHL (6 mos with SD and then progressed, 7 mos with PR and bone marrow infiltration resolved), and SD in 2 patients with transplant-failed myeloma (6 and 7 mos). Peripheral blood lymphocytes were obtained at several time points during the bryostatatin infusion as well as 6 hours after the vincristine infusion. When bone marrow was involved a pretreatment and post-vincristine marrow sample was obtained as well. Preliminary data with acridine orange staining and Western blot analysis of cleavage of poly (ADP-Ribose) polymerase (PARP cleavage) shows no increase in apoptosis during or after treatment. Furthermore, flow cytometric analysis of tumor cells from the bone marrow pre-treatment and 6 hours post vincristine showed no change in the percentage of tumor cells



undergoing apoptosis. Samples are being kept for analysis of different cytokines including IL-2, IL-2 receptor, IL-6 and TNF alpha. The trial is ongoing. (Supported by NIH grant nos. 2 U01 CA62602-06)

**#114 Structure-based discovery and development of selective protein kinase inhibitors.** Rose, P.E., Begley, M., Boucher, C.E., Carney, D., Daniel, T., Kim, J., Morgenstern, K., Stovar, D., Toledo, L., Zhao, H., Zhu, X. *Kinetix Pharmaceuticals Inc., 200 Boston Avenue, Medford, MA 02155 USA.*

Protein kinases are widely found in signal transduction pathways, play central roles in diverse biological processes such as control of cell growth, metabolism, differentiation, and apoptosis and are likely to be involved in the development and/or progression of many cancers. Solutions of the X-ray crystal structures of a variety of protein kinases in complex with small molecule inhibitors and recent pre-clinical successes have shown that selective, high affinity inhibitors can be tailored to a variety of kinase targets. The ATP binding pockets of serine/threonine and tyrosine kinases are the targets of our search for novel, selective inhibitors. Using a structure based approach, we have discovered novel inhibitor scaffolds which are being optimized against a number of oncology targets including c-Met, Kdr, Tek, EGFR/erbB2, Akt, and IGF-1R. Initial three-dimensional structures of multiple inhibitors bound to the active site of Lck have allowed the development of methods for virtual screening of available compound databases ( $>2 \times 10^9$  molecules). Virtual "hits" obtained from this search were then screened using our Kinase Assay Array which consists of a panel of ~70 human kinase domains expressed and purified from insect cells infected with recombinant baculovirus. A variety of chemical scaffolds with submicromolar  $IC_{50}$ s have been identified. Cell-based assays, X-ray crystal structures of inhibitors complexed with kinase domains and optimization of lead compounds are in progress.

**#115 An in-vivo system for the study of CDK inhibitors.** Dawson, Mark A., Robinson, William A., Do, Cuong, Brady, Benjamin, Asimakis, Maria, and Lieschke, Graham. *The Ludwig Institute for Cancer Research, Melbourne, Australia.*

P16 and its protein product p16<sup>INK4A</sup> are important cell cycle regulators. Through the inhibition of Cyclin Dependent Kinases (CDK) 4 and 6, the phosphorylation of the retinoblastoma protein is controlled and hence progression at the restriction point in G1. Mutations and/or deletions of P16 have been documented in a variety of human malignancies, most notably malignant melanoma, pancreatic and esophageal carcinoma, lymphoid malignancies and malignant gliomas. While numerous missense variations of p16 have been described the functional significance of each of these is not clear. We have recently developed an in-vivo system for the functional evaluation of CDK inhibitors using the zebrafish. Initial studies have shown that microinjection of wildtype human p16 mRNA into one cell fertilized embryos leads to marked perturbation in development, which results in a highly reproducible and characteristic phenotype. This includes severe melanocyte dysgenesis, suppression of blood formation, bradycardia, jaw agenesis and death at, or before, 120 hours. In contrast, injection of mRNA from 3 inactive forms of p16 had no effect on development. This data indicated the presence of p16 interacting partners in zebrafish and suggested that this system may be useful for the study of pharmacological inhibitors of the CDKs as well as for separating mutants of this gene from polymorphisms and variants which have no effect on function. To examine the latter we then injected, in a blinded study, mRNA from 13 wildtype and previously characterized p16 variants. Western analysis of embryos 10 hours after mRNA injection showed that all lead to protein translation. On the basis of the phenotype that developed we correctly identified all of these as either wildtype, polymorphisms or true mutants of p16. Recent studies have centered on the use of this system to examine the growing class of pharmacological anti-neoplastic CDK inhibitors. The results of these studies will be described.

**#116 Use of a novel, high-throughput screening-compatible kinase assay to identify inhibitors of the human AIK serine/threonine kinase.** Rodems, Steven M., Woollenwaber, Leslie A., Hamman, Brian H., and Pollok, Brian A. *Aurora Biosciences Corp., 11010 Torreyana Rd., San Diego, CA 92121*

Dysregulation of protein kinases involved in cell division and mitotic checkpoint control can lead to certain genetic abnormalities found in human cancer such as incorrect chromosome segregation and aneuploidy. The human serine/threonine kinase AIK (Aurora/PL1-related kinase; also referred to as Aurora2, STK15, or BTAk) is overexpressed in many types of cancers. Consistent with a role in tumor formation, overexpression of AIK in tissue culture cells also results in a transformed phenotype. AIK localizes to the mitotic spindles and may be involved in proper chromosome segregation. Mitotic kinases, such as AIK, are excellent targets for the development of anti-cancer drugs, and drug discovery companies have placed considerable effort into developing screens and identifying inhibitors of these kinases. A major roadblock in serine/threonine kinase screen development has been the lack of an inexpensive, generic, high-throughput screening-compatible kinase assay. We have developed a biochemical, homogeneous (addition-only), high-throughput kinase assay with a development step that distinguishes phosphorylated from non-phosphorylated fluorescent-peptide substrates. To date, this assay platform has been validated for five different serine/threonine kinase targets including AIK. As part of the AIK assay validation, we have completed both kinetic and

inhibitor analyses. This assay is currently being used to screen small-molecule compound libraries for inhibitors of AIK activity that could eventually be developed into anti-cancer drugs.

**#117 The protein kinase C inhibitor chelerythrine activates c-jun expression through protein kinase C, Raf-1, p42/44 MAP kinase, and p38 MAP kinase signaling pathways.** Taher, M. M., Hershey, C. M., Oakley, J. D., Grant, S., and Valerie, K. *Department of Radiation Oncology, Massey Cancer Center, Medical College of Virginia, VCU, Richmond, VA 23298.*

Inhibition of protein kinase C (PKC) has been proposed as a means to block cell proliferation, tumor promotion and metastasis. Several natural product inhibitors of PKC have been identified, including staurosporin, bis-Indolylmaleimide, Ro31-8220 UCN-1028C, calphostin C, hypericin, isquinoline-sulfonamide H-7, and chelerythrine (CE). Recent studies have demonstrated that CE activates PKC, and expression of c-jun and promotes apoptosis. The upstream signaling events triggered by CE leading to these processes have not been identified. We found that in HeLa cells stably transfected with the luciferase gene under control of the human c-jun promoter, CE increased c-jun expression in the presence and also in the absence of PMA, rather than inhibiting PMA-mediated c-jun expression. Other PKC inhibitors, such as bis-Indolylmaleimide and Ro31-8220 inhibited c-jun expression activated by either PMA or CE. The MEK-1/2 inhibitor PD98059 and the p38 MAP kinase inhibitor SB203580 both abrogated CE activation of c-jun expression, suggesting that the p42/44 MAP kinase and p38 MAP kinase pathways are triggered by CE. In line with this result, CE significantly activated p42/44 MAP kinase and p38 MAP kinase as determined by Western blot analysis using phospho-specific antibodies. CE also caused significant activation of Raf-1, and JNK. Furthermore, CE increased phosphorylation of the CREB, ATF-1, and ATF-2 transcription factors positioned downstream of the JNK and p38 MAP kinases. As a result, CE also activated AP-1 and CREB DNA binding activity, but not NF- $\kappa$ B. Based on these results we conclude that CE activates c-jun expression via PKC, Raf-1, p42/44 MAP kinase and/or p38 MAP kinase pathways, most likely through increased AP-1 activity. Supported by CA53199 (KV).

**#118 Growth inhibition of tumor cells by epidermal growth factor receptor tyrosine kinase inhibitor ZD1839 is associated with upregulation of p27 and p21 cyclin-dependent kinase inhibitors.** Di Gennaro Elena, Barbarino Marcella, Bruzese Francesca, De Lorenzo Sonia, Pepe Stefano, Caponigro Francesco, and Budillon Alfredo. *Istituto Nazionale Tumori-G. Pascale; Università Federico II; Napoli, Italy.*

Overexpression of epidermal growth factor receptor (EGF-R) has been implicated in the development of head and neck squamous carcinomas (HNSCC) and, hence, is a potential target for antitumor intervention in this disease. ZD1839, an anilinoquinazoline, is a specific EGF-R tyrosine kinase inhibitor with powerful antitumor activity both *in vitro* and *in vivo* and is currently under clinical evaluation. We have demonstrated that ZD1839 induced growth arrest in KB, CAL27, SCC15 and CAL33, human HNSCC cell lines by inhibiting basal and EGF-induced EGF-R mediated signaling. Moreover the growth inhibitory effect induced by ZD1839 is associated with a dose-dependent upregulation of p27<sup>Cip1</sup> and p21<sup>Cip1/Waf1</sup> cyclin-dependent kinase (CDK) inhibitors. The increase in p27 and p21 protein expression was evident after 12 hr and maximal stimulation was reached after 24 hr of ZD1839 treatment. Furthermore, we found a dose-dependent decrease in CDK2 activity after 24 hr of ZD1839 treatment. Cell cycle kinetic analysis by bromodeoxyuridine (BrdU) incorporation revealed that ZD1839 induced a delay in cell cycle progression. In particular we demonstrated by DNA-flow cytometry an increase in the percentage of cells in S phase, which was evident after 24 hr of treatment. These results suggest that p27<sup>Cip1</sup> and p21<sup>Cip1/Waf1</sup> can play a key role in ZD1839-induced cell cycle perturbation by decreasing CDK2 activity and leading to growth arrest. Moreover this data add new insight in the regulation of cell cycle machinery by growth factor receptor-mediated signal transduction pathways. The potential application of these findings for combination study involving ZD1839 with conventional drugs or biological agents utilized in advanced HNSCC therapy, such as IFN $\alpha$  or RA, is currently under investigation.

**#119 UCN-01 selectively enhances mitomycin C-cytotoxicity in p53 defective cells which is mediated through S and/or G2 checkpoint abrogation.** Sugiyama K., Shimizu M., Akiyama T., Tamaoki T., Inoue K., Yamaguchi K., Takahashi R., Eastman A. and Akinaga S. *Pharmaceutical Research Laboratories, Kyowa Hakko Kogyo Co. Ltd., Kyoto University, Graduate School of Medicine National Cancer Center Research Institute Japan, Dartmouth Medical School, USA.*

UCN-01 (7-hydroxystaurosporine) is a protein kinase inhibitor which is under clinical trials as an anti-cancer agent in the USA and Japan. We previously reported that UCN-01 enhanced the antitumor activity of mitomycin C (MMC) *in vitro* and *in vivo*. Subsequent studies from other laboratories revealed that UCN-01 could selectively enhance cytotoxicity of DNA damaging agents in p53 defective cells, and this was mediated by abrogation of S and/or G2 arrest by UCN-01. In this study, we report for the first time that UCN-01 also selectively enhanced the cytotoxicity of MMC in human p53 mutant human cell lines such as A431 epidermoid carcinoma and PSN-1 pancreas carcinoma. In contrast, UCN-01 showed little, if any, effect on MMC-cytotoxicity in human p53 wild-type MCF-7 breast carci-

noma and HCT116 colon carcinoma cell lines. Terminal deoxynucleotidyl transferase (TdT)-mediated dUTP-nick end labeling (TUNEL) assay revealed that the combination of MMC with UCN-01 increased DNA breaks consistent with apoptosis in p53 defective cells. In p53 wild-type cells, the cyclin-dependent kinase inhibitor protein, p21/WAF1 was markedly induced after the treatment with MMC alone, although this response was significantly delayed from the time of MMC-treatment. Detailed cell-cycle studies revealed that UCN-01 abrogated S and G2 phase accumulation induced by MMC in p53 defective cells and to a lesser extent in p53 wild-type cell lines. The abrogation of arrest in p53 wild-type cells was observed prior to significant induction of the p53 response. Furthermore, the combination of MMC with UCN-01 up-regulated cdc2 kinase activity in both cell lines as compared to MMC alone, confirming that UCN-01 abrogated S and G2 phase arrest induced by MMC both in p53 defective and p53 wild-type cell lines. Since MMC was less effective against p53 defective cell lines than against p53 wild-type cell lines, and UCN-01 selectively enhanced MMC-cytotoxicity in p53 defective cell lines, UCN-01 may provide a new modality of MMC-based cancer chemotherapy, particularly in p53 defective cancer patients.

**#120 Mechanisms of S-phase arrest induced by fludarabine and its modulation by the kinase inhibitor, UCN-01.** Sampath, Deepa and Plunkett, William. *University of Texas M.D. Anderson Cancer Center, Houston, TX.*

Treatment of human ML-1 cells with cytotoxic levels of F-ara-A (10  $\mu$ M), the nucleoside of fludarabine elicits a rapid apoptotic response in S phase cells. However lower, cytostatic concentrations of F-ara-A (1  $\mu$ M) result primarily in an S phase arrest; where the population of S phase cells increased to over 70% from the approximately 30% observed in exponentially growing cells. Subsequent exposure of S-phase arrested cells to non toxic concentrations (50 nM) of UCN-01, a kinase inhibitor, resulted in an increase in the sub-G1 population, which was associated with a decrease in the number of S-phase cells. This investigation was directed at understanding the mechanisms involved with F-ara-A-induced S phase arrest and its modulation by UCN-01. Immunoprecipitates of cdk2 from extracts of exponentially growing cells had little or no immunoprecipitable p21 detected by immunoblots. Conversely, immunoprecipitates of p21 from these extracts did not reveal any associated cdk2 kinase activity, indicating minimal association between the two proteins in normally growing populations. Upon F-ara-A-induced S-phase arrest however, there was a three-fold increase in the amounts of p21 that associated with immunoprecipitated cdk2. Further experiments using genetically defined HCT116 cells differing in their p21 status confirmed the importance of p21 in inducing S-phase arrest by F-ara-A because cells lacking p21 were unable to institute an S-phase arrest in response to F-ara-A. In addition to p21, cdk2 can also be regulated by phosphorylation on specific residues. In F-ara-A-induced S-phase arrest, the cells had an increase in the level of inhibitory tyrosine-15 phosphorylation on cdk2. Consequently, the cdk2 function, as measured by cyclin-A associated kinase activity as well as cdk2 kinase activity was inhibited by 2-fold in S-phase cells in comparison to the values obtained for these same kinase activities in an S-phase enriched population.

Addition of UCN-01 to S-phase arrested cells caused a decrease in the level of inhibitory phosphorylation at the tyrosine-15 residue and a corresponding activation of the cyclin A associated and cdk2 associated kinase activities. However, UCN-01 treatment did not have an effect on the F-ara-A-induced association between p21 and cdk2. Thus, F-ara-A treatment appears to induce S-phase arrest by increased association of p21 with cdk2 as well as by an increase in the inhibitory phosphorylation on cdk2 at the tyrosine-15 residue, which together, result in an inhibition of this essential S-phase transit regulator. Exposure of F-ara-A arrested S-phase cells to UCN-01 may generate conflicting signals leading to cell death, because UCN-01 decreases the inhibitory phosphorylation on cdk2 but does not affect the inhibitory association between p21 and cdk2.

**#121 The cyclin-dependent kinase inhibitor flavopiridol inhibits glycogen phosphorylase and affects glucose metabolism.** Astrid U. Kalsner, Kayoko Nishi, Donal A. Walsh, Fred A. Gorin, E. Morton Bradbury, Joachim B. Schnler. *University of California Davis, Department of Biological Chemistry, Tupper Hall, Department of Neurology, Davis CA 95616.*

The synthetic flavone flavopiridol, known as an inhibitor of cyclin-dependent kinases, showed antitumor effects in patients with renal, prostate and colon cancer and non-Hodgkin's lymphoma. Using affinity chromatography, we isolated two proteins of about 100 kDa and of 40 kDa present in various human cell lines. The larger protein was identified by mass spectroscopy as a mixture of glycogen phosphorylases (GP) from brain and liver, when HeLa cell extract was used for chromatography. Purified muscle GP also bound tightly to the flavopiridol affinity column. Muscle GP-b, which is activated by AMP, was inhibited by flavopiridol with an  $IC_{50}$  of 1  $\mu$ M. Lowering the AMP concentration lowered also the  $IC_{50}$  value for inhibition by flavopiridol indicating competition between flavopiridol and AMP. GP-a, the phosphorylated active form of GP, was less inhibited by flavopiridol and AMP-activated GP-a was nearly insensitive to inhibition by flavopiridol. Phosphorylation of GP-b by phosphorylase kinase was also inhibited at high flavopiridol concentrations indicating interference of the kinase with flavopiridol-bound GP. A comparison of the two prostate cancer cell lines PC3 and LNCaP showed a correlation between GP activity

and resistance of cells to the cytotoxicity of flavopiridol. Thus PC3 cells with about three times higher GP activity compared to LNCaP cells were more resistant to cytotoxicity by flavopiridol. Treatment of the flavopiridol sensitive LNCaP cell line with flavopiridol led to an increase in pyruvate and a decrease in deoxyglucose uptake suggesting a stimulation of glycolytic activity. Treatment of PC3 and LNCaP cell lines with flavopiridol led to an increase in GP activity as a possible result of glucose shortage. The results suggest that flavopiridol affects glycogen and glucose metabolism. High GP-a levels may contribute to resistance of cells to flavopiridol.

**POSTER SESSION 2  
SECTION 1: CELL CYCLE TARGETS: P53, CYCLINS,  
CYCLIN-DEPENDENT KINASES**

**#122 Phase I trial of sequential paclitaxel and cisplatin in combination with the cyclin dependent kinase inhibitor flavopiridol (flavo) in patients with advanced solid tumors.** Schwartz GK, Kaubisch A, Saltz L, Ilson D, O'Reilly E, Barazzuol J, Endres S, Stoltz M<sup>1</sup>, Tong W, Kelsen DP, Spriggs D. *Memorial Sloan-Kettering Cancer Center, New York, NY; <sup>1</sup>Hoechst Marion Roussel, Inc., Kansas City, MI.*

Flavopiridol/HMR 1275 (flavo) is a semi-synthetic flavone that inhibits cyclin dependent kinases. Our in vitro studies have shown that flavo significantly enhances paclitaxel and cisplatin-induced apoptosis in a sequence dependent manner. We initiated a Phase I study of 24 hour (and later 3 hour) paclitaxel on day #1, followed on day #2 both by escalating doses of 24 hour flavo, and later by 20 minute cisplatin, repeated every 21 days. Fifty-four patients with advanced solid tumors are evaluable for toxicity, best response, and pharmacokinetics. The results are summarized below:

Paclitaxel, mg/m <sup>2</sup>	Flavo, mg/m <sup>2</sup>	Cisplatin, mg/m <sup>2</sup>	n	Gr 4 tox (n)/DLT	Best Response
135 (24 hr)	10	—	3	ANC: 3/DLT	1 CR, 2 SD
100 (24 hr)	10	—	3	0	1 SD
100 (24 hr)	20	—	6	ANC: 3/DLT	3 SD
100 (3 hr)	20	—	3	0	None
100 (3 hr)	40	—	3	0	None
100 (3 hr)	53	—	3	0	1 PR, 1 SD
100 (3 hr)	70	—	3	0	1 SD
135 (3 hr)	70	—	3	0	1 MR, 1 SD
135 (3 hr)	80	—	3	0	1 SD
135 (3 hr)	94	—	6	ANC: 2/DLT dyspnea: 3	4 SD
175 (3 hr)	70	—	6	dyspnea: 1	1 MR, 2 SD
175 (3 hr)	80	—	6	0	1 MR, 3 SD
175 (3 hr)	80	30	3	0	2 SD
175 (3 hr)	80	50	3	ANC: 1	too early

With 24 hour paclitaxel at either 135 or 100 mg/m<sup>2</sup>, flavo could not be escalated above 10 mg/m<sup>2</sup> without dose-limiting neutropenia. With 3 hour paclitaxel, dose-limiting pulmonary and hematologic toxicity occurred with 135 mg/m<sup>2</sup> paclitaxel and 94 mg/m<sup>2</sup> flavo. Paclitaxel could be further escalated to 175 mg/m<sup>2</sup> with 80 mg/m<sup>2</sup> of flavo without DLT, representing the recommended phase II dose. A dose escalation of cisplatin to 50 mg/m<sup>2</sup> with fixed doses of paclitaxel and flavopiridol is being evaluated. Clinical responses have been observed in patients with taxane refractory esophagus, lung and prostate cancer. These flavo combinations are well-tolerated and show promising clinical activity, even in patients who have received prior paclitaxel.

**#123 Flavopiridol disrupts PMA-induced differentiation and CDK1 expression and significantly enhances apoptosis in human leukemia cells (U937).** Carter, L. and Grant, S. *Dept. of Medicine, Division of Hematology/Oncology, Medical College of Virginia, MCV Station Box 980230, Richmond, VA 23298-0230.*

The present studies were undertaken to test the hypothesis that the CDK inhibitor, flavopiridol, would interfere with cell cycle progression and enhance PMA-induced differentiation in human leukemia cells (U937). Contrary to expectations, flavopiridol opposed, rather than promoted, PMA-related maturation and dramatically induced apoptosis. PMA (1–10 nM) or flavopiridol (10–100 nM) treatment alone for 24 h was marginally toxic to U937 cells ( $\leq 10\%$  apoptotic in all cases), while co-administration of 10 nM PMA and 100 nM flavopiridol for 24 h was highly synergistic with respect to apoptosis induction ( $57 \pm 3.8\%$  apoptotic; combination index  $< 0.01$ ). The enhanced apoptosis following PMA/flavopiridol treatment, manifested by characteristic morphology, cleavage of procaspase 3, degradation of PARP, and loss of mitochondrial membrane potential ( $\Delta\psi_m$ ), was accompanied by a parallel decline in leukemic cell clonogenicity. Co-administration of flavopiridol markedly inhibited PMA (10 nM; 24 h)-induced maturation in U937 cells manifested by decreased plastic adherence and CD11b expression. In addition, 100 nM flavopiridol substantially antagonized the



ability of PMA to induce the CDKs, p21<sup>CIP1</sup> and p27<sup>KIP1</sup>, which are associated with cell cycle arrest and anti-apoptotic actions. Despite blocking CDK1 induction, flavopiridol failed to inhibit the PMA-induced dephosphorylation of pRb, which accompanies cell cycle arrest. Thus, flavopiridol co-administration may promote apoptosis by disrupting certain cell cycle events (i.e., CDK1 induction) associated with PMA-induced differentiation. These findings also raise the possibility that co-administration of differentiation inducers with pharmacological inhibitors of cyclin-dependent kinases may represent a novel therapeutic approach for the treatment of leukemia.

**#124 Antiproliferative cyclin dependent kinase inhibitors with distinct molecular interactions and tumor cell growth inhibition profiles.** Newell DR, Arris CE, Boyle FT, Calvert AH, Curlin NJ, Dewsbury P, Endicott JA, Garman EF, Gibson AE, Golding BT, Griffin RJ, Johnson LN, Lawrie A, Noble MEM, Sausville EA, Schultz R. *Univ. Newcastle & Oxford, UK; AstraZeneca Pharms., UK; NCI, USA.*

Cyclin dependent kinases (CDKs) are central to the function of cell cycle checkpoints, and CDK control is frequently disrupted in human tumours. CDKs are therefore important targets for cancer therapy; however, available CDK inhibitors lack potency and/or specificity. Novel guanidine- and pyrimidine-based CDK inhibitors were synthesized and tested for their ability to inhibit cyclin B1/CDK1 and cyclin A/CDK2. Active inhibitors were soaked into crystals of monomeric CDK2. Inhibitor-protein interactions were identified in the CDK2/inhibitor complex structures determined by X-ray crystallography. The structural information was used to design inhibitors to probe the impact of specific hydrogen bonding interactions on the ability of compounds to inhibit CDK activity and cell growth. The *in vitro* activity of the CDK inhibitors was compared to that of standard anticancer agents and known CDK inhibitors in the NCI cell line panel using the COMPARE analysis. 6-O-cyclohexylmethylguanidine (NU2058) was shown to be a competitive inhibitor of CDK1 and CDK2 with respect to ATP ( $K_i$  values = CDK1  $5 \pm 1 \mu\text{M}$ , CDK2  $12 \pm 3 \mu\text{M}$ ), via formation of a triplet of hydrogen bonds (i.e. NH-9 to Glu 81, N-3 to Leu 83 and 2-NH<sub>2</sub> to Leu 83). Removal of the 2-NH<sub>2</sub> group or methylation at N-9 reduced activity. The triplet of hydrogen bonding and CDK inhibition seen with NU2058 was reproduced by 6-amino-4-cyclohexylmethoxy-5-nitro-opyrimidine (NU6027,  $K_i$  values = CDK1  $2.5 \pm 0.4 \mu\text{M}$ , CDK2  $1.3 \pm 0.2 \mu\text{M}$ ), the 5-nitroso group forming an intramolecular hydrogen bond with the 6-amino group, constraining it in the correct orientation. Against human tumour cells, NU2058 and NU6027 were growth inhibitory *in vitro* (mean GI<sub>50</sub> values 5–19  $\mu\text{M}$ ) with a pattern of cellular sensitivity distinct from that of the established CDK inhibitors flavopiridol and olomoucine. The enzyme inhibition, structural and *in vitro* chemosensitivity data indicate that the distinct mode of binding of NU2058 and NU6027 to CDKs has direct consequences for CDK and cell growth inhibition, and their differential activity with respect to other CDK inhibitors. NU2058 and NU6027 represent important leads for the development of CDK inhibitors, and these studies illustrate how high-throughput cell growth inhibition studies can be successfully interfaced with structural biology in rational drug discovery.

**#125 Diaminotiazoles: Potent, selective cyclin-dependent kinase inhibitors with anti-tumor efficacy.** Lundgren, K., Price, S.M., Escobar, J., Huber, A., Chong, W., Li, L., Duvadie, R., Chu, S.S., Yang, Y., Nonamiya, J., Tucker, K., Knighton, D., Ferre, R., and Lewis, C. *Agouron Pharmaceuticals, Inc.*

Cyclin-dependent kinases (CDKs) play a critical role in regulation of the eukaryotic cell cycle. Different CDK/cyclin complexes function during different phases of the cell cycle and drive cell cycle progression by phosphorylating key substrates. The important role of CDKs in cellular proliferation is underscored by the frequent occurrence of mutations in cancerous tissue that result in an increase in CDK activity. These mutations occur in a variety of different tumors and through several distinct mechanisms. Such findings highlight these kinases as important targets for novel chemotherapeutic intervention. We have developed a novel series of CDK inhibitors—diaminotiazoles—using combinatorial chemistry and structure-based drug design. Two sub-classes have evolved: compounds that are equipotent for CDK4, CDK2 and CDK1 inhibition and compounds that show over 100-fold selectivity for CDK4. These molecules bind within the ATP binding site and display low nanomolar binding affinities to CDKs. Inhibition of several unrelated serine/threonine and tyrosine protein kinases occurs within the micromolar concentration range. Treatment of tumor cells with these diaminotiazoles results in decreased phosphorylation of the substrate retinoblastoma protein in a time- and dose-dependent manner and a cell cycle block in G1 and G2 phases. The CDK4-selective diaminotiazoles display a G1 block that is dependent on the presence of functional retinoblastoma protein. Selected compounds inhibit the proliferation of several human tumor cell lines at sub-micromolar concentrations and in a clonogenic survival assay these compounds irreversibly inhibit the formation of cancer cell colonies. Furthermore, the diaminotiazoles delay tumor growth and time to progression in human colon tumor xenografts *in vivo*.

**#126 The role of p53 in determining chemosensitivity of two novel aminopurine based cyclin dependent kinase inhibitors.** Pestell KE, Walton MI, Tiley JC, Kelland LR, Lane D and Workman P. *CRC Centre for Cancer Therapeutics, Institute of Cancer Research, Sutton, SM2 5NG, UK and Cyclacel Ltd, 5 Whitthall Crescent, Dundee, DD1 4AR, UK.*

The p53 gene is involved in the regulation of multiple cell cycle checkpoints including the G1/S and G2/M following various stresses. We have therefore studied the role of p53 in governing the chemosensitivity of the novel aminopurine, cyclin dependent kinase inhibitors Roscovitine (ROS) and Bohemine (BOH) *in vitro*. A panel of human ovarian cancers cell lines with different p53 functional status and the A2780 cell line transfected with HPV16 E6 were employed. Cytotoxicity was determined by 96 h SRB growth delay and clonogenic assay. The cell lines A2780 and LK2 (wild type p53) showed lower IC<sub>50</sub>s than A2780 E6, SKOV-3, HX62, 59M (mutant p53). Values were 19 and 23  $\mu\text{M}$  for ROS and BOH, respectively for wt p53 versus 35 and 34  $\mu\text{M}$  for the mt p53 lines. Clonogenic assays were carried out following 16 h drug exposure (minimum cytotoxic exposure time). Survival curves were linear for vector control A2780 lines (IC<sub>50</sub> 8  $\mu\text{M}$  for both ROS and BOH) but were biphasic in A2780 E6 lines with IC<sub>50</sub> values of 16 and 29  $\mu\text{M}$  for ROS and BOH, respectively. Equitoxic drug treatment ( $5 \times \text{IC}_{50}$ ) induced p53 during drug exposure in A2780 control lines but not following drug removal. By contrast p21<sup>WAF1/CIP1</sup> was not induced during drug exposure but increased immediately following drug removal. There was slight induction of MDM-2 following drug removal. CDK1 protein was stably expressed up until 40 h post treatment when some depletion may have occurred. By comparison in A2780 E6 lines there was no detectable p21 or MDM-2 expression throughout the time course (0–40 h). However there was evidence of induction of p53 during drug treatment. Further studies showed that the E6 mRNA was depleted by both drugs after 8 h continuous exposure in A2780 E6 cell lines. Both drugs gave slightly fewer cells in G1 and correspondingly more in S and G2 following 16 h exposure in A2780 E6 compared to vector controls. There were more detached cells in the control A2780 lines following ROS and BOH treatment than in the E6 transfected line and there was evidence of apoptosis in both populations by DAPI staining. In conclusion the drugs ROS and BOH appear to be somewhat more cytotoxic towards p53 wild type expressing tumour cell lines and cause apoptosis in both populations. Moreover these drugs may deplete HPV16E6 offering the exciting possibility of novel cervical cancer targeted drugs. We are currently developing assays of various proteins as molecular markers of drug action for preclinical and clinical studies.

**#127 Development of cell cycle inhibitors for cyclin D1/cdk4: benzothioopyranes and quinolinedisulfides.** Shih C, Al-Awar R, Brooks S, Patel B, Schultz R, Menon K, Ray J, Rao N, Grossman S, Watkins S, Stamm N, Dempsey J, Ogg C, Teicher BA. *Lilly Research Labs, Lilly Corporate Center, Indianapolis, IN 46285.*

Cell replication is recognized to be controlled by the transient, sequential, highly-regulated expression of a series of cyclins which associate with specific cyclin-dependent kinases (cdk's), which are serine/threonine protein kinases, to compose an active enzyme and initiate a cascade of phosphorylations allowing the cell to progress to the next stage of replication. The Rb protein, pRb, a substrate for the cyclin-cdk's is frequently missing or mutated in human tumors. Coordinate with this are the cyclin-dependent kinase inhibitors (CKIs) that block the actions of specific cyclin-cdk complexes. The cdk inhibitors halt cell cycle progression and cause cells to enter the quiescent G<sub>0</sub> phase. The cdk inhibitors of the INK4 group including p15, p16, p18 and p19 block the cyclin-cdk4 and cyclin-cdk6 complexes. The most frequent alteration in human malignant disease, thus far recognized, is the overexpression, mutation and/or dysregulation of cyclin D. Therefore, the development of agents that mimic the effects of CKIs could be predicted to be useful anticancer agents. A series of benzothioopyranes were micromolar (1.0–1.6) inhibitors of cyclin D1/cdk4 using a peptide model substrate and were almost as potent when a 21kD fragment of pRb was used as the substrate. These compounds inhibited the proliferation of MCF-7, HCT116 and H460 human tumor cells expressing pRb at micromolar concentrations and also inhibited the growth of pRb negative MB468 cell line with equal potency. The quinolinedisulfides showed a marked variation in potency against cyclin D1/cdk4 with IC<sub>50</sub>'s ranging from 0.15 to 8.2 micromolar with the peptide substrate and 0.6 to 4.4 micromolar with the pRb substrate. The quinolinedisulfides were potent inhibitors of cell proliferation with IC<sub>50</sub>'s from 0.1 to 2.2 micromolar. Several compounds had effects on cell cycle progression. The antitumor activity of the compounds was assessed using HCT116 colon carcinoma xenografts. Each of the benzothioopyranes were active antitumor agents while the antitumor activity of the quinolinedisulfides was highly dependent upon the substituents on the ring system.

**#128 The p16 status of tumor cell lines identifies small molecule inhibitors specific for cyclin dependent kinase (CDK) 4.** Kubo, A., Nakagawa, K., Varma, R.K., Conrad, N.K., Cheng, J.Q., Lee, W.-C., Testa, J.R., Johnson, B.E., Kaye, F.J., Kelley, M.J. *MB & DTP, National Cancer Institute; Dept of Med Onc, Fox Chase Cancer Ctr; Dept of Med, Duke University Medical Ctr.*

Loss of p16 functional activity leading to disruption of the p16/cdk4:cyclin D/Rb pathway is a very common event in human tumorigen-

esis, suggesting that compounds with CDK4 kinase inhibitory activity may be useful to regulate cancer cell growth. To identify such inhibitors, the 60 cancer cell lines of the NCI drug screen panel were examined for alterations of p16 (biallelic deletion, intragenic mutations, or absent p16 protein), cyclin D1 (gene amplification), and CDK4 (gene amplification, intragenic mutations). The growth inhibitory activity of more than 50,000 compounds against these 60 cell lines was compared with their p16 status. One compound, 3-amino thioacridone (3-ATA; NSC 680434), whose growth inhibitory activity correlated with the p16 status of the cell lines had an  $IC_{50}$  (50% inhibitory concentration) of 3.1  $\mu$ M. In a CDK4 kinase assay using immunopurified baculovirus-expressed CDK4: cyclin D1. In addition, four compounds structurally-related to 3-ATA inhibited CDK4 kinase with  $IC_{50}$ 's ranging from 0.2 to 2.0  $\mu$ M. All five of these compounds were less potent inhibitors of CDK2 and CDK2 kinases with  $IC_{50}$ 's 30- to 500-fold higher than that for CDK4. ATP competition experiments demonstrated a non-competitive mode of inhibition for 3-ATA ( $K_i = 5.5 \mu$ M) and a linear mixed mode for benzothiadiazine (NSC 645787;  $K_i = 0.73 \mu$ M), while flavopiridol was confirmed to be a pure ATP-competitor. Cyclin D1 and CDK4 genetic alterations were found in 13 and 3 of the 60 cell lines, respectively. We have successfully demonstrated a novel approach to identify specific CDK4 kinase inhibitors that may selectively induce growth inhibition of p16-altered tumors. Further correlation of alterations of the p16/cdk4: cyclin D/Rb pathway with drug activity is expected to identify additional compounds with specificity for targets in the pathway.

**#129 Inhibition of cyclin-dependent kinase 1 (cdk1) by Indirubin derivatives in human tumor cells.** Marko D, Schätzle S, Eisenbrand G, Div. of Food Chemistry/Environmental Toxicology, University of Kaiserslautern, Erwin-Schroedinger Str., D 67663 Kaiserslautern, Germany.

The bisindole indirubin has been described more than 30 years ago as being clinically active in the treatment of human chronic myelocytic leukemia. However, the underlying mechanism of action has remained unclear. We have reported previously that indirubin and its analogues are potent and selective inhibitors of cyclin-dependent kinases (cdk). In this study, we investigated the influence of indirubin and derivatives on cdk1/cyclin B kinase in human tumor cells at concentrations known to induce growth inhibition. Treatment of the human mammary carcinoma cell line MCF-7 with growth inhibitory concentrations of Indirubin-3'-monoxime induces dose-dependent inhibition of the cdk1/cyclin B activity in the cell. After 24 h treatment, a strong decrease of the active cdk1/cyclin B complex is observed. Cells synchronized by serum deprivation are arrested in the  $G_1/G_0$  phase of the cell cycle, when treated after serum repletion for 24 h with 2  $\mu$ M indirubin-3'-monoxime. At higher drug concentrations ( $\geq 5 \mu$ M) an increase of the cell population in the  $G_2/M$ -phase is additionally observed. Cells synchronized in  $G_2/M$  phase by nocodazole remain arrested in the  $G_2/M$ -phase after release. In the presence of indirubin-3'-monoxime at concentrations  $\geq 5 \mu$ M. After 24 h treatment with 10  $\mu$ M Indirubin-3'-monoxime a sub- $G_2$  peak appears, indicative for the onset of apoptotic cell death. Taken together, the results of this study strongly suggest that inhibition of cdk activity in human tumor cells is a major mechanism by which Indirubin derivatives exert their potent antitumor efficacy.

**#130 A common polymorphism in the cyclin D1 gene influences survival of colorectal cancer patients: lack of correlation with cyclin D1 protein and other key G1/S proteins.** McKay Judith A, Douglas Joy J, Ross Val G, Curran Stephanie, Murray Graeme I, McLeod Howard L. Departments of Medicine & Therapeutics, & Pathology, University of Aberdeen, Foresterhill, Aberdeen, Scotland UK.

Cyclin D1, encoded by the *CCND1* gene, is a key regulator of the cell cycle which elicits its effects at the G1/S checkpoint. Overexpression of cyclin D1 protein has been associated with prognosis in a number of tumor types, and more recently a common A/G polymorphism at nt870 of *CCND1* has been related to outcome in non-small cell lung cancer and squamous cell carcinoma of the head and neck. In addition, *in vitro* studies have shown cyclin D1 can affect sensitivity of cancer cells to certain antineoplastic drugs and chemopreventive agents. We have investigated the *CCND1* nt870 polymorphism and cyclin D1 protein expression in 100 colorectal cancer patients. Genotyping was achieved using polymerase chain reaction—restriction fragment length polymorphism analysis for genomic DNA, while protein expression was determined by immunohistochemical staining of paraffin-embedded tumour sections. *CCND1* genotype was not correlated with standard clinicopathological data (i.e. Dukes' stage, differentiation grade, sex, site). However, patients homozygous for the G allele showed significantly improved overall survival when compared with patients displaying an AA or AG genotype ( $P = 0.035$ ). In addition, while the absence of cyclin D1 immunoreactivity was not associated with prognosis ( $P = 0.81$ ), patients demonstrating a high level of cyclin D1 protein overexpression ( $>50\%$  of tumor cells immunostaining) were found to have significantly shorter survival ( $P < 0.001$ ). *CCND1* genotype was unrelated to either the level of expression of cyclin D1 protein or its localisation (nuclear +/- cytoplasmic,  $P > 0.05$ ), and was not associated with the G1/S proteins p21, p27, p53, retinoblastoma or proliferation, as measured by proliferating cell nuclear antigen. This suggests that although both cyclin D1 genotype and protein overexpression are related to survival in colorectal cancer, they are not interrelated and the impact of genotype<sup>42</sup>

is not through influences on other G1/S checkpoint proteins or tumor proliferation. The new, as yet undefined, mechanism of interaction between the *CCND1* polymorphism and behaviour of colorectal cancer may modify sensitivity to anticancer drugs.

Acknowledgements: This work was carried out on behalf of the Aberdeen Colorectal Cancer Initiative.

**#131 Exogenous inhibitors of cyclin-dependent kinases induce the expression of endogenous inhibitor of cyclin-dependent kinase p21<sup>waf1/cip1</sup> in prostate cancer cells.** Silvy, M., Prévost, G.P., Meijer, L., Vlossat, I., Thuriel, C., and Calvo, F. INSERM EPI 9932, Pharmacology Laboratory, Hôpital St Louis, Paris, France (SM, FC); Institut Henri Beaufour, Les Ulis, France (PG, VI, TC); CNRS, Station Biologique, Roscoff, France (ML)

Cyclin-dependent kinases (CDK) and their regulators control the cell cycle progression and are frequently deregulated in human tumours. The activity of such CDKs can be inhibited by (i) endogenous inhibitors (p21<sup>waf1/cip1</sup>) and/or (ii) exogenous inhibitors (purine analogues: olomoucine, roscovitine and purvalanol A). In this study, the effects of exogenous CDK inhibitors on the expression of endogenous CDK inhibitor p21<sup>waf1/cip1</sup> and on the tumor growth have been analyzed in human epithelial prostate cancer cell lines. Olomoucine showed little effect on LN-CaP(p53<sup>+/+</sup>; Rb<sup>+/+</sup>) cell growth, whereas roscovitine and purvalanol A were more potent inhibitor. Using an ELISA assay, we observed an increase of p21<sup>waf1/cip1</sup> in LN-CaP cells exposed to 50  $\mu$ M olomoucine, 10  $\mu$ M roscovitine or 1  $\mu$ M purvalanol A. Maximal effects (6-fold increase compared to the basal level) were observed in the presence of 50  $\mu$ M olomoucine or 10  $\mu$ M purvalanol A. Iso-olomoucine, a structural analog of olomoucine which fails to inhibit CDKs, did not modify cell growth or expression of p21<sup>waf1/cip1</sup>. This suggests that the induction of p21<sup>waf1/cip1</sup> by exogenous CDK inhibitors may be linked to their ability to inhibit CDK activity, rather than to their purine structures. In addition, olomoucine, roscovitine and purvalanol A also induce p21<sup>waf1/cip1</sup> expression in another prostate cancer cell line PC3 characterized by a p53<sup>-/-</sup>; Rb<sup>+/+</sup> genotype. This result suggests that such a rise of p21<sup>waf1/cip1</sup> level is p53-independent. Induction of p21<sup>waf1/cip1</sup> by 50  $\mu$ M olomoucine was associated with the presence of both hypo- and hyperphosphorylated Rb measured by Western blotting whereas, induction of p21<sup>waf1/cip1</sup> by 50  $\mu$ M roscovitine or 10  $\mu$ M purvalanol A was associated with the accumulation of hypophosphorylated Rb, suggesting a dual mechanism of induction.

Our data show that exogenous CDK inhibitors are also inducers of endogenous CDK inhibitor p21<sup>waf1/cip1</sup> through a p53-independent pathway. Such observations reinforce the rationale for using CDK inhibitors in cancer treatment.

**#132 Cell cycle arrest induced by anticancer prostaglandin and its modulation by MRP1/GS-X pump inhibitor.** ISHIKAWA Toshitsugu<sup>1</sup>, FURUTA Kyoji<sup>2</sup>, SUZUKI Masaaki<sup>2</sup>, and NOYORI Ryoji<sup>3</sup> <sup>1</sup>M.D. Anderson Cancer Center, Houston, TX, USA; <sup>2</sup>Gifu University, Gifu, Japan; <sup>3</sup>Nagoya University, Nagoya, Japan.

The A and J series of prostaglandins (PGA and PGJ) suppress proliferation of cancer cells without affecting intracellular cAMP levels. These PGs are actively transported into cells and accumulated in their nuclei. To gain insight into the molecular mechanism of antitumor PG-mediated inhibition of cell cycle and proliferation, we have studied the phosphorylation state of the RB gene product (pRB) and expression of cyclin-dependent kinase inhibitors in HL-60 cells. We here demonstrate evidence that  $\Delta^7$ -PGA<sub>1</sub> methyl ester specifically induces p21 (*Sd1/CIP1/WAF1*) without any effect on the expression of p27, p18, p16, or p14, and that the induction of p21 results in accumulation of hypophosphorylated pRB and suppression of *c-myc* expression in HL-60 cells treated with this anticancer PG. These changes were closely linked to cell-cycle arrest in the  $G_1$ -phase. Since the p53 gene is completely deleted in HL-60 cells, the induction of p21 by  $\Delta^7$ -PGA<sub>1</sub> methyl ester is independent of p53.

Unlike in HL-60 cells, growth inhibition and cell cycle arrest by  $\Delta^7$ -PGA<sub>1</sub> methyl ester were minimal in HL-60/R-CP cells which overexpress the MRP1/GS-X pump. When HL-60/R-CP cells were incubated with  $\Delta^7$ -PGA<sub>1</sub> methyl ester in the presence of G1F-0019, an MRP1/GS-X pump-specific inhibitor, cells became sensitive to the anticancer PG. These results suggest that the MRP1/GS-X pump may play a critical role in modulating cell growth arrest induced by the anticancer PG.

**#133 Polyamine biosynthetic pathway as a cell cycle target for breast cancer therapy.** Shah, N., Thomas, T.J., and Thomas, T. Departments of Medicine and Environmental & Community Medicine, UMDNJ-Robert Wood Johnson Medical School, New Brunswick, NJ 08903.

Ornithine decarboxylase (ODC) and S-adenosylmethionine decarboxylase (SAMDC) are two key enzymes in the biosynthesis of polyamines, the cellular oligocations with multiple functions in cell proliferation. Increased levels of ODC and polyamines are found in breast cancer tissues compared to normal tissues. We examined the effects of DFMO, an inhibitor of ODC, and CGP 48664, an inhibitor of SAMDC on cell cycle progression, and the expression of cyclins D1 and E in MCF-7 breast cancer cells. Cells were synchronized at G1 phase by isoleucine starvation (36 h), and cell cycle was initiated by the addition of complete medium in the presence of



estradiol, DFMO (1 mM) and CGP 48664 (1  $\mu$ M) produced cell growth inhibition and accumulation of cells in G1 phase. DFMO treatment led to depletion of cellular putrescine and spermidine with no significant change in spermine. CGP 48664 produced a reduction of spermidine and spermine and an increase in putrescine. Western blot analysis showed that DFMO treatment led to a 50% decrease in cyclin D1, whereas CGP 48664 induced a 3-fold increase. In contrast, cyclin E was down-regulated by CGP 48664, but not by DFMO. Similar effects on cyclin D1 and E were observed at 4, 8, 12, 16, and 24 h time points after the initiation of cell cycle. Effects of DFMO and CGP 48664 were reversible by the addition of exogenous putrescine or spermidine, respectively. Our results show that G1 arrest could occur, in some cases, with high levels of cyclin D1. Our results also indicate that polyamine biosynthetic pathway is intimately linked to cell cycle checkpoints and that reduction of putrescine and spermine may affect different cell cycle targets, in spite of G1 arrest in both cases.

**#134 p53 is associated with cytoplasmic and spindle microtubules and requires functional microtubules for nuclear accumulation.** Gianakakou Paraskevi, Sackett Dan L., Ward Yvona, Blagosklonny Mikhail and Fojo Tito. *Medicine Branch, NCI and Laboratory of Integrative and Medical Biophysics, NIDDK, NIH, Bethesda, MD.*

The tumor suppressor p53 is a multifunctional protein involved in cell cycle control, differentiation and apoptosis. Variations in the subcellular localization of p53 have been observed in different types of tumors and correlated with tumor response to DNA damage and prognostic factors. The cellular mechanism(s) regulating p53 subcellular localization and shuttling are still not well defined, and may include tethering to cytoplasmic structures. Here, we examined the interaction of p53 with tubulin/microtubules and found that both wild type (wt) and mutant p53 proteins are physically associated with tubulin *in vivo* and *in vitro*. The p53/tubulin association was abolished by microtubule (MT)-depolymerizing agents, suggesting a preference of p53 for MTs over soluble  $\alpha/\beta$ -tubulin dimers. Consistent with this, *in vitro* polymerization experiments showed p53 associated with polymerized and not soluble tubulin. Using four human cancer cell lines of distinct origin, we demonstrated by confocal microscopy, that p53 localized to cellular and spindle microtubules. Following treatment with DNA-damaging agents or the nuclear export inhibitor Lepomycin B (LPM), wt p53 translocated to the nucleus inducing p53-target genes. Disruption of the microtubule cytoskeleton whether by stabilization with paclitaxel or depolymerization with vincristine inhibited p53 nuclear accumulation following DNA-damage or LPM treatment. The reduced nuclear accumulation of p53 was also evidenced by impaired mdm2 and p21 induction. We propose that functional microtubules are necessary for p53 trafficking, nuclear accumulation and execution of p53 tumor suppressor activity. These data also identify p53 as an additional target for tubulin active agents.

**#135 Novel phosphorylation sites in domains necessary for mediating apoptosis by p53.** Tanaka, T., Choi, S., Obata, T., Taya, Y. (*Biology Div., National Cancer Center Research Inst., Tsukiji 5-1-1, Chujo-ku, Tokyo 104-0045, Japan*); Tamai, K. (*Ina Lab., MBL, Nagano, Japan*).

A newly found transcriptional activation domain (43-63) and the proline-rich domain (64-92) are recently suggested to be needed for apoptosis induction by p53 because deletion of either of these two domains abolishes this activity. We now found that phosphorylation of Ser46 and Ser90 is induced after DNA damage. However, phosphorylation of these two sites was observed only at the late stage after DNA damage by several different agents compared to Ser15 or Ser20 of MDM2-binding domain. Since the time course of phosphorylation of these sites and apoptosis induction is similar, these results suggest a intriguing possibility that phosphorylation of Ser46 and Ser90 regulates the transcriptional activation of an apoptosis-inducing gene by p53. We have detected kinase activities to phosphorylate Ser46 and Ser90, and we are trying to purify and identify these kinases by column chromatographies. These kinases could be good targets for cancer therapeutics.

**#136 Programmed cell death by c-Myc: Evidence of a caspase-independent effector signaling role for the c-Myc-interacting adaptor protein Bin1.** D. Sakamuro, K. Elliott, K. Ge, J. DuHadaway, D. Ewert, and G.C. Prendergast. *The Wistar Institute, Philadelphia, PA USA 19104; Glenolden Laboratory, Dupont Pharmaceuticals, Glenolden, PA USA 19036.*

**INTRODUCTION.** Defining how c-Myc triggers programmed cell death (PCD) may offer new therapeutic targets in advanced cancer where c-Myc is often activated. Current evidence suggests that c-Myc kills cells through some caspase-independent process. Here we identify a potential effector role for the c-Myc-interacting adaptor protein Bin1 in mediating a caspase-independent PCD process. Notably, while Bin1 is often functionally disrupted in cancer cells, the downstream components of the pathway engaged by Bin1 remain intact.

**RESULTS.** In primary chick fibroblasts or rat kidney epithelial cells transformed by c-Myc, inhibition of Bin1 by antisense or dominant inhibitory methods did not affect transformation but suppressed apoptosis elicited by serum deprivation. In particular, overexpression of the c-Myc-binding domain of Bin1 rendered cells resistant to c-Myc (but not to the

cytotoxic agent staurosporine), implying that protein-protein interaction is required and that Bin1 may have a specific effector role. In clonogenic survival assays, inhibition of Bin1 blocked the cytotoxic effects of c-Myc as potently as Bcl-2, allowing productive cell proliferation under low serum conditions. Conversely, Bin1 was sufficient to induce PCD in human carcinoma cells where c-Myc is overexpressed and Bin1 is missing. Adenoviral vectors elicited PCD within 24-36 hr of infection of malignant liver, breast, and melanoma cell lines but did not affect diploid IMR90 fibroblasts, nonmalignant HBL100 breast cells, or fetal melanocytes. Cells undergoing PCD displayed substratum detachment, cell shrinkage, vacuolated cytoplasm, positive TUNEL reaction, and DNA degradation. p53 status did not affect response. Interestingly, caspases were not activated and ZVAD.fmk had no effect. Consistent with the lack of caspase involvement, nucleosomal DNA cleavage, chromatin collapse, and disruption of the nuclear lamina were not apparent in dying cells, although chromatin condensation at focal sites and on the nuclear lamina ('margination') occurred. In support of a link with c-Myc, the serine protease inhibitor AEBSF which specifically blocks PCD by c-Myc also impeded PCD by Bin1. Results of ongoing analysis of molecular markers of PCD (e.g. cytochrome c release, etc.) affected by Bin1 as well as progress in identifying downstream components of the relevant signaling mechanism will be reported.

**#137 Selective Induction of fas mediated apoptosis by p53 peptide in human cancer cells.** Raffo, Anthony J., Kim, Arianna L., Drew, Lisa, Petrylak, Daniel P., Brandt-Rauf, Paul W., and Fine, Robert L. *Experimental Therapeutics Program, College of Physicians and Surgeons of Columbia Univ., Div. of Med. Oncol., 650 W. 168 St., New York, NY 10032.*

The C-terminus of p53 (aa 360-393) has been identified as an auto-inhibitory region, which regulates p53 into active states. Antibodies to the C-terminal epitope (aa 371-380) can induce sequence specific DNA binding of certain p53 mutants and the same effect occurs when the C-terminus is cleaved from certain mutant p53 forms. Thus, wild type p53 phenotype can be restored in certain mutant forms. We explored a structure-activity study in various C-terminal p53 peptides and correlated them to *in vitro* DNA binding activity and their ability to induce apoptosis in the MDA-MB-468 human breast cancer line which carries an endogenous null/273 p53 mutation of arg to his. This is the most commonly mutated hot spot in p53 in human cancer. The peptide with the greatest ability to induce apoptosis, aa 361-382, was covalently linked to a highly efficient transmembrane transporter, a truncated *Drosophila* antennapedia protein (17aa) and called Ant-p53pep. Ant-p53pep selectively induced rapid apoptosis in multiple cancer lines with mutant p53: DU145 prostate, MDA-MB-468 and MDA-MB-231 breast, as well as in a wt p53 prostate cancer line (LNCaP) and a wt p53 breast cancer cell line (MCF-7). Two non-malignant cell lines, MCF 10/2A (breast epithelium) and sk 27 (fibroblast) both with wt p53 were not affected by the Ant-p53pep. Furthermore, we found that the Ant-p53pep did not alter Bax, Bcl-2, Bcl-X<sub>L</sub> or Bcl-X<sub>s</sub> levels, but rapidly induced the cell surface expression of Fas and FasL and the activation of caspase 3 (CPP32) and 8 (FLICE) within 30 minutes of exposure. The increased Fas/FasL expression was not through a translational process since total protein content of Fas/FasL did not change in Westerns and cycloheximide pre-exposure did not alter the apoptotic response from Ant-p53pep through Fas. Binding experiments showed that the peptide bound to mutant and wt p53 but the lack of toxicity in non-malignant cells may be related to low expression of p53 in non-malignant cells. Thus, our work shows that this novel and exciting peptide can rapidly induce Fas/FasL mediated apoptosis in human cancer cells which overexpress mutant or wt p53.

**#138 Apoptotic-induced-vinorelbine-delivery (AIDD) mediated by electrochemotherapy (ECT), and radiation-induced-apoptosis (RIA) caused by radiation-enhanced-wtp53cDNA gene-transfer (REGT) eradicated radioresistant NSCLC cells with mutant p53.** Giannios, John N., Glinopoulos, P. *Dept. of Molecular & Clinical Oncology, Peripheral Hospital of St. Andreas, Patras, Greece.*

**Purpose:** To induce PCD in human radioresistant NSCLC possessing mutations in exon 6 of p53 by transfection of wtp53cDNA gene under exposure to ionizing radiation and electroporation combined with vinorelbine administration.

**Materials & methods:** NSCLC cells were obtained by FNA biopsy from the lung of a patient. Tumour cells were electroporated (900V, 8x99us pulses) with simultaneous administration of vinorelbine tartrate. Intracellular concentration of the drug was determined by HPLC. Subsequently, tumour cells were irradiated with  $\gamma$ -rays (8Gy) produced by Cobalt-60, while plasmid wtp53cDNA gene of pCMV-Neo-Bam vector was administered. The recombination between plasmid and cellular genome was monitored by ICC using Pab240 IgG1 monoclonal antibodies whose epitope maps in the middle region (AA212-217) of p53 and reacts with only its mutant form. Cell cycle was monitored by flow cytometry and cytotoxicity was determined by assays such as MTT, BrdU, GSH and LDH. Apoptotic signs were examined by TEM. Control cells were not electroporated and irradiated.

**Results:** After electroporation, HPLC analysis exhibited enhanced intracellular concentration of vinorelbine compared to controls. This resulted in

blockage of the tumour cell cycle at the radiosensitive phase G2/M according to flow cytometry. Also, there was enhanced cytotoxicity and reduction of IC50 value for pulsed tumour cells in the presence of vinorelbine compared to the drug only treatment. Furthermore, TEM has exhibited enhanced phagocytosis of drug loaded apoptotic bodies by a portion of adjacent tumour cells (AIDD). However, the majority of tumour cells did not exhibit apoptotic signs. ICC analysis of these cells exhibited enhanced expression of p53 due to sustained mutation in exon 6. Ionizing radiation has mediated gene transfer by enhancing recombination between plasmid wtp53cDNA gene of pCMV-Neo-Bam vector and the cellular DNA compared to controls. Subsequently, ICC analysis has exhibited no p53 expression of the irradiated cells indicating normal function of wtp53, compared to nonirradiated tumour cells which sustained mutations between AA212-217. Also, cytotoxicity assays exhibited for irradiated tumour cells reduced metabolic activity (MTT), reduced DNA synthesis (BrdU), depleted GSH and enhanced leakage of LDH compared to controls. Finally, TEM exhibited for all tumour cells irreversible D2 stage of radiation induced apoptosis (RIA) leading to bystander killing after phagocytosis of apoptotic bodies by adjacent tumour cells.

**Conclusion:** We have achieved to enhance intracellular concentration of vinorelbine by electroporation (ECT) blocking cells at the radiosensitive phase G2/M, and re-establish wtp53 function of NSCLC cells by radiation-enhanced-gene-transfer (REGT). Most importantly, we have eradicated radioresistant NSCLC cells by apoptotic-induced-vinorelbine-delivery (AIDD) combined with radiation-induced-apoptosis (RIA) which lead to bystander killing of adjacent tumour cells after phagocytosis of apoptotic bodies.

**#139 The efficacy of ionizing radiation combined with adenoviral p53 therapy in EBV-positive nasopharyngeal carcinoma.** Li, J.-H., Huang, D., Sun, B.-F., Klamul, H., Takada, K., Liu, F.-F. *University of Toronto, Chinese University of Hong Kong, and Hokkaido University School of Medicine.*

We have previously demonstrated the efficacy of Ad5CMV-p53 gene transfer, either alone, or delivered concomitantly with ionizing radiation (XRT), which resulted in cytotoxicity, mediated by apoptosis, in two nasopharyngeal carcinoma (NPC) cell lines (Li et al 1997, & Li et al 1999). We have now expanded this work to evaluate the interaction of Ad5CMV-p53 gene therapy plus XRT, in a NPC cell line, which harboured the latent gene products of Epstein Barr Virus (EBV), a virus which is almost universally present in NPC. Using the C666-1 cell line, originally derived from a Hong Kong patient with NPC, we confirmed the presence of LMP1 and EBNA-1 using RT-PCR. Western blotting demonstrated that Ad5CMV-p53 gene therapy resulted in the rapid expression of biologically active p53 protein, shown by induction of p21<sup>WAF1/CIP1</sup>. XRT had little effect on p53 expression, although there appeared to be a slight induction of p21<sup>WAF1/CIP1</sup> expression. There was no alteration in the expression of the Bcl-2 protein under any of the experimental conditions. There was a more than additive interaction in the cytotoxic effects of Ad5CMV-p53 gene therapy plus XRT in the C666-1 cells, with less than 0.4% survival when 50 pfu/cell of Ad5CMV-p53 was combined with 6 Gy XRT. Using morphologic criteria, we demonstrated that <10% of C666-1 cells underwent apoptosis when exposed to either XRT or Ad5CMV-β-gal. However, treatment with Ad5CMV-p53 (10 pfu/cell) increased the apoptotic rate up to 20%, which was further enhanced to 58% when combined with 6 Gy XRT. Therefore, despite the presence of EBV in NPC, gene transfer therapy using wtp53 is still efficacious, which hopefully will ultimately translate into improved survival when combined with XRT, for patients with this disease.

(Supported by a grant from the Medical Research Council of Canada).

**#140 Cancer gene therapy with a modified p53 overcomes mdm2-mediated oncogenic transformation.** Page Carmen, Lin Huey-Jen, Sondak Vernon, Jiang Gulhua, Castle Valerie, Changery Jennifer, Reynolds Kevin, and Lin Jlayuh. *Departments of Obstetrics and Gynecology, Pediatrics, and Surgery. University of Michigan Cancer Center, Ann Arbor, MI 48109.*

The anti-proliferative activities of wild-type (wt) p53 are inhibited by mdm2 oncogene product. The presence of mdm2 gene amplification was observed in 19 tumor types. We tested growth suppression activity of p53 14/19, which contains double substitutions at amino acid residues Leu-14 and Phe-19. The p53 14/19 retains wild-type p53 functions. Furthermore, the transcriptional activation, stability, and G1 growth arrest functions of p53 14/19, unlike wt p53, is completely resistant to the specific inhibition by mdm2 oncoprotein. Importantly, p53 14/19, in contrast to wt p53, suppresses sarcomas and neuroblastoma cells that contain amplified mdm2 very efficiently by DNA transfection or adenovirus gene transfer. In addition, p53 14/19 also inhibits the sarcoma, cervical, prostate, and lung cancer cells without mdm2 gene amplification as efficient as wt p53 but has no significant inhibitory effect on normal human fibroblasts.

We further examined the anti-oncogenic potencies of p53 14/19 in the rat embryo fibroblast (REF) co-transformation assay against various oncogene combinations. Addition of wt p53 failed to cause a statistically significant decrease in ras plus mdm2 foci counts. In contrast, co-transfection of p53 14/19 with ras/mdm2 significantly reduced foci number. In the similar experiments, co-transfection of wt or 14/19 p53 both resulted in

significant inhibition of ras/myc, ras/E1A, or ras/HPV E7 transformation in REF. Therefore, these results strongly suggested that p53 14/19 could be a very potent therapeutic agent to inhibit human cancers with or without mdm2 amplification, as well as cancers containing activated ras, myc, and E7 oncogenes.

**#141 The role of p53 on nitric oxide synthase-2 (NOS-2) expression in human tumors.** Yoon, S. J., Park, J. S., Kang, J. O., Kim, N. K., and Heo, D. S. *Cancer Research Center, College of Medicine, Seoul National Univ.; Dept. of Internal Medicine, Seoul National Univ. Hospital, Seoul, Korea*

Nitric oxide (NO) has been found to either inhibit or stimulate tumor growth according to p53 status (wild or mutant types). However, the relationship of NO and p53 in carcinogenesis is uncertain. We examined whether the effect of NO on tumor growth is p53-dependent and exogenously transduced p53 inhibits the growth of NOS-2 expressing tumor. We studied the expression of NOS-2, p53, and p27 in seven stomach cell lines (SNU-16, 464, 601, 620, 638, 668, and 719) and investigated the role of NOS-2 in tumor growth using lymphoma cell line (HL-60) genetically engineered to produce p53 constitutively. Among seven stomach cells, NOS-2 protein was found only in SNU-719 cell despite of the presence of NOS-2 gene in all cells by Southern blot analysis. After treating human recombinant IFN-γ (300 U/ml for 5 hrs.), NOS-2 protein was induced only in SNU-668 and SNU-719 cells. Through Western blot, SSCP, and sequencing analysis, we confirmed that p53 was mutated in SNU-16, 464, 601, 638, and 668 cells, and homozygously deleted in SNU-620. However, SNU-719 cell showed the wild type expression of p53, and the slower growth rate than other cells which do not express NOS-2 in normal conditions. These results suggest that endogenously produced NO and p53 are related each others on tumor growth, and especially, NO might play a major role in tumor growth inhibition induced by p53 expression. Transduction studies with NOS-2 and/or p53 genes need to be done to determine the relationship between these two genes.

**#142 Multi step approach to augment drug induced apoptosis in Hela cells.** Reddy Vijay G, Dhawan Deepika and Singh Neeta. *Department of Biochemistry, All India Institute of Medical Sciences, New Delhi, INDIA*

The action of the chemotherapeutic drugs is not specific for tumor cell, with increasing dose normal cells are also affected since the drugs primarily act on rapidly dividing cells. This constitutes the primary side effect as well as the dose-limiting factor for most anti cancer drugs. In cervical cancer derived cell line like Hela the cellular tumor suppressor protein p53 is present in very low amounts. This is due to ubiquitin mediated degradation of p53 by the E6 proteins derived from tumor associated papillomavirus. Dietary antioxidant like vitamin C has been found to inhibit the E6 mediated p53 degradation. The accumulation of p53 subsequently causes cell cycle arrest at G1-S level. Cancer cell lines that were negative for HPV did not show similar effects. The treatment of the antioxidant primed Hela cells with anti cancer drugs like cisplatin and adriamycin showed increased apoptosis when compared to unprimed Hela cells. This dual step approach has the potential to reduce the dose and increase the specificity of chemotherapy of cervical cancer.

## SECTION 2: CELLULAR THERAPY, VACCINES, AND IMMUNOLOGIC TARGETS

**#143 Priming cellular immunity against a normal tissue antigen in a phase I trial of hormone refractory prostate cancer.** Burch, P.A., Breen, J., Buckner, J.C., Gaslineau, D.A., Kaur, J.A., Laus, R.L., Padley, D.J., Peshwa, M.V., Pitot, H.C., Richardson, R.L., Smits, B., Strang, G., Valone, F.H., and Vuk-Pavlovic, S. *Mayo Clinic, Rochester, MN, and Dendreon Corporation, Seattle, WA.*

Dendritic cells (DC) are the only antigen presenting cells which prime naive T-cells and initiate an immune response. Studies in rats indicate that DC exposed to rat prostatic acid phosphatase (PAP) fused to rat GM-CSF induced cellular anti-PAP immunity. When the same antigen was subsequently injected s.c., it raised a strong humoral response. Accordingly, in a phase I trial of 13 patients (pts) with advanced hormone-refractory prostate cancer, we administered DC, exposed ex vivo to human PAP fused to human GM-CSF, in 2 doses (each approximately 150 × 10<sup>6</sup> cells/m<sup>2</sup>), spaced by a month. This was followed by 3 monthly injections of the same soluble antigen (SA) for 3 months. Pts were grouped by SA dose (0.3 mg, 0.6 mg, and 1.0 mg). We monitored T cell and antibody responses. Twelve pts were evaluable. Five patients developed mild fever (grade 1-2) and/or chills within 1 hour after infusion, 5 patients mild (grade 1-2) myalgia or pain, usually one to two days after treatment with DC. Six pts reported grade 1-2 fatigue and one prolonged grade 3 fatigue. One developed a mild local reaction after injection of SA. We evaluated the proliferation of patients' T cells upon in vitro stimulation by SA and PAP. SA stimulated T cell proliferation up to 100 fold over the baseline, while PA stimulated it up to 10 fold indicating that treatment successfully raised cellular immunity against PAP. All pts developed antibodies to SA de novo or increased the



pre-existing titers. Most antibodies were directed at the GM-CSF component of SA. Five pts developed PAP-specific antibodies; in three, the titer was equal or less than 1/20. One pt had a low titer (1/10) of PAP-specific antibody before treatment; it did not change after treatment. The median time to development of PAP-specific antibodies was 12 weeks. In two pts, PSA levels were reduced to below one half of the level prior to treatment (baseline) although in one of them the disease rapidly clinically progressed. Other two pts experienced a less than 50% PSA reduction. The median time to disease progression was 135 days after registration (range 30 to 274 days). Three of the six patients treated at the highest dose of SA remained progression-free for 206, 253 and 274 days, respectively. We conclude that the treatment was well tolerated and that it broke tolerance to PAP, a normal tissue protein.

**#144 Phase I-study on patients with inoperable pancreatic carcinoma with encapsulated cells producing cytochrome P 450 CYP 2B1 that activates ifosfamide.** A. Hoffmeyer, J. Kröger, A. Holle, P. Müller, J. Hahn, R. Saller, T. Wagner, W. Günzburg, B. Salmons, K.-H. Hauenstein, S. Liebs, M. Löhr. *Abt. Gastroenterologie, Klinik f. Innere Medizin und Institut f. Diagn. & Intervent. Radiologie, Univ. Rostock; Med. Klinik, Abt. Onkologie, MH Lübeck; Bavarian Nordic Research Inst., München; Inst f. Virologie, VMU, Wien.*

**Background.** Conventional chemotherapy of pancreatic carcinoma is only marginally effective. Substances such as ifosfamide, registered for the treatment of pancreatic cancer, have not been followed up due to a high toxicity at therapeutic doses. **Hypothesis.** The local conversion of ifosfamide into its active compounds, phosphoramide and acrolein, should be feasible for treatment employing low systemic concentrations of the drug. **Rationale.** Transfection of CYP2B1 in cells with subsequent microencapsulation. **Experimental work.** The enzyme activity (resorufin-assay) remains stable for weeks in vitro and in vivo within the microencapsulated CYP2B1-expressing cells. We could demonstrate a significant antitumor effect of the intratumorally injected capsules on xenotransplanted human pancreatic carcinomas on the nude mouse (*Gene Therapy* 1998, 5: 1070-1078). Angiographic experiments in pig assured the feasibility of an intra-arterial placement of the capsules into the pancreas (*Ann NY Acad Sci* 1999, 88: in press). A clinical protocol was established and approved (*J Mol Med* 1999, 77: 393-398). **Patients, Material and Methods.** L293-cells were transfected with CYP2B1-gene, microencapsulated (diameter 0.5 mm) under GMP-conditions and packed sterile. Patients with confirmed inoperable adenocarcinoma of the pancreas underwent angiography and capsules were injected into a vessel leading into the tumor. The patients were monitored for 48 hrs to exclude allergic reactions or pancreatitis. A day later, ifosfamide was administered at 1000 mg/m<sup>2</sup> BS for three consecutive days to be repeated day 21-23. The patients were followed-up for 5 months. **Results.** The study was opened 7/98. A total of 17 patients were enrolled. In 14/17 patients the capsules could be administered as planned. In one patient, this was technically impossible, 2 had to be excluded due to acute infection. The 14 patients treated tolerated the procedure without any complications. No allergic reactions or pancreatitis was encountered. Chemotherapy was uneventful. **Conclusion.** The intra-arterial application of microcapsules for targeted chemotherapy was well tolerated. The anti-tumor effect can't be judged at present time.

**#145 Treatment of therapy-refractory B-lineage acute lymphoblastic leukemia with an apoptosis-inducing CD19-directed tyrosine kinase inhibitor.** Messinger, Y.; Chen, C.-L.; O'Neill, K.; Myers, D.E.; Goldman, Fred.; Hurvitz, C.; Casper, J.T.; Levine, A.; Uckun, F.M.; *Parker Hughes Cancer Center, Hughes Institute, St. Paul, MN; Biotherapy Program, University of Minnesota Academic Health Center, Minneapolis, MN; Kenneth Norris Cancer Center, University of Southern California, Los Angeles, CA; University of Iowa Hospitals and Clinics, Iowa City, IA; Cedar Sinai Medical Center, Los Angeles, CA; University of Wisconsin, Milwaukee, Wisconsin.*

Seven children and eight adults with CD19<sup>+</sup> B-lineage acute lymphoblastic leukemia (ALL) as well as one adult with chronic lymphocytic leukemia (CLL) were treated with the CD19 receptor-directed tyrosine kinase inhibitor B43-Genistein. All patients had failed previous chemotherapy regimens and six patients had relapsed after bone marrow transplantation (BMT). The Phase I dose escalation study was initiated at a cumulative dose level of 1.0 mg/kg, which is 10-fold lower than the well-tolerated dose level of 10 mg/kg in cynomolgus monkeys and 100-fold lower than the nontoxic dose level of 100 mg/kg in mice. B43-Genistein was administered as a one-hour intravenous infusion at 0.1 mg/kg/day-0.32 mg/kg/day dose levels for 10 consecutive days or 3 consecutive days weekly for a total of 9 doses. B43-Genistein was well tolerated by all patients with no life-threatening side effects. There were seven episodes of grade 2-3 fever, one episode each of grade 3 myalgia, grade 2 sinus tachycardia, and grade 2 vascular leak syndrome. Two ALL patients who had failed bone marrow transplantation and were in second or greater relapse with an M3 marrow prior to B43-Genistein therapy achieved a bone marrow remission with an M1 marrow status by day 28. One therapy-refractory adult ALL patient in first relapse showed a lytic response with reduction of the bone marrow blast fraction from 53% to 25% and disappearance of circulating pe-

ripheral blasts. Pharmacokinetic analyses in 12 patients revealed a plasma half-life of 20 ± 5 hours, mean residence time of 24 ± 5 hours, and a systemic clearance rate of 20 ± 3 mL/h/kg. The average (mean ± SEM) values for the maximum plasma concentration C<sub>max</sub>, central volume of distribution at steady state (V<sub>ss</sub>), and area under curve (AUC) were 1009 ± 290 ng/ml, 332 ± 45 mL/kg, and 9711 ± 2787 μg·h/L, respectively. No human anti-mouse antibodies (HAMA) were detected in any of the day 7 or day 14 posttreatment blood samples or any of the pretreatment (negative control) blood samples. However, moderate levels of HAMA ranging from 20 ng/ml to 87 ng/ml were detected in the day 28 blood samples from 3 of 9 cases examined. Based on its acceptable toxicity profile and its ability to elicit objective responses at nontoxic dose levels, B43-Genistein may provide the basis for an effective treatment strategy for B-lineage ALL patients who have failed standard therapy.

**#146 Induction of hepatoma-specific immunity with dendritic cell immunization results in complete tumor regression.** Holowachuk, Eugene W., Ruhoff, Mary S., Dauchy, Robert T., Sauer, Leonard A., and Blask, David E. *Research Institute, The Mary Imogene Bassett Hospital, Cooperstown, NY 13326.*

Dendritic cells (DCs) are professional antigen (Ag)-presenting cells that are being considered as potential immunotherapeutic agents to promote host immune responses against tumor Ags. Bone-marrow-cell (BMC) derived DCs, newly differentiated with GM-CSF plus IL-4 for 8-10 days, were tested for their ability to induce an immune response against a tissue-isolated Morris hepatoma, 7288CTC, implanted in male Buffalo rats on the tip of a vascular stalk formed from the superficial epigastric artery and vein. The tumor implant and vascular stalk were enclosed within a parafilm envelope, placed in the inguinal fossa and the incision closed. Vascularization of the implant was limited to new vessel connections with the epigastric artery and vein. Subsequent subcutaneous tumor size was estimated every 2 days from measurements made through the skin.

Hepatoma growth was measured for 2-5 weeks following implantation and hosts, with hepatomas varying in size from 2-16 grams, were injected with DCs (2.5-40 × 10<sup>3</sup> DCs). BMC DCs were pulsed for ≤14 hours with a membrane fraction (HepAg) prepared from 7288CTC, washed twice, enumerated, suspended in 100 μl PBS (with 1% normal rat serum) and injected via the tail vein. Size-matched hepatoma-bearing control rats were injected with non-pulsed DCs or liver-membrane-pulsed DCs. In all cases of HepAg-pulsed DC treatment, the hepatoma was found to completely regress by 14-18 days post injection, with no evidence of remaining hepatoma tissue. No effect on hepatoma growth was observed in tumor-bearing rats injected with non-pulsed DCs or liver membrane-pulsed DCs. In addition, no effect upon liver function (serum levels of 3 liver enzymes) was detectable in any DC-injected rats. Moreover, a single injection of HepAg-pulsed DCs completely prevented subsequent hepatoma implantation. Finally, hepatoma-specific cytotoxic T cells were detected and assayed using the HTC hepatoma cell line as target and splenic T cells purified from hepatoma-bearing hosts injected with HepAg-pulsed DCs. These results strongly support the concept of cancer immunotherapy using antigen-pulsed DCs.

**#147 A less costly method for obtaining dendritic cells from peripheral blood adherent mononuclear cells using low doses of GM-CSF + IL-4 + IFN-γ.** Goldman, Lisa A., Frischmann, Kevin J., Gizas, Lisa C., Blumenthal, Rosalyn, Goldenberg, David M. *Garden State Cancer Center, Belleville, NJ USA.*

The cytokine combination that is most commonly used to generate DCs from human peripheral blood monocytes is GM-CSF (800 U/ml) + IL-4 (500-1000 U/ml). Other labs have also been able to generate DCs using cytokine combinations such as GM-CSF (500 U/ml) + IL-13 (10 ng/ml) or GM-CSF (500 U/ml) + IFN-α (5000 U/ml).

DCs are becoming increasingly more useful in cancer immunotherapy making the study of less costly methods for generating DCs more desirable. In 1995, Xu, H. et al. [*Adv. Exper. Med. Biol.* 1995. 378:75-78] showed that it was possible to generate cells with a DC phenotype using low doses of GM-CSF (100 U/ml) + IL-4 (50 U/ml) + IFN-γ (50 U/ml). The cost of the cytokines using this low dose, triple cytokine combination is significantly reduced (~8.5-fold) compared to methods using high doses of GM-CSF + IL-4.

In the current study, we directly compare the phenotype and the antigen uptake and antigen presenting functions of DCs differentiated from peripheral blood adherent monocytes using both low dose and high dose cytokine combinations. Morphologically, DC cultured using low doses of GM-CSF + IL-4 + IFN-γ are more elongated compared to DC cultured in high doses of GM-CSF + IL-4 without IFN-γ; both populations are large and irregularly shaped and form the characteristic DC star-shaped clusters. Cell recovery was comparable using both culture methods. Phenotypically, both DC populations are CD14 negative and express many of the typical surface markers found on immature DC such as high levels of HLA-DR and CD86 and moderate levels of CD4, CD80, and CD1a. The cells do not express CD83, a marker for mature DC. Both DC populations are capable of antigen uptake via mannose receptor-mediated endocytosis, as measured using FITC-Dextran. Moreover, both populations are capable of in-

ducing proliferation of allogeneic T cells in a mixed lymphocyte reaction (MLR). In conclusion, we have found that it is possible to generate functional DCs from peripheral blood adherent monocytes using significantly lower doses of cytokines. (Supported in part by USPHS grant CA39841 from the NIH.)

**#148 Activity of the MHC-nonrestricted T-cell line TALL-104 in the treatment of Central Nervous System tumor xenografts.** Geogerger, Birgit, Tang, Cheng-Bi, Cesano, Alessandra, Visonneau, Sophie, Marwaha, Sunil, Judy Kevin D., Sutton, Leslie N., Santoli, Daniela and Phillips, Peter C. *Children's Hospital of Philadelphia, Division of Neuro-Oncology, Department of Neurosurgery; The Wistar Institute; Hospital of the University of Pennsylvania, Department of Neurosurgery; Philadelphia, PA 19104.*

Malignant glioma in adults, and primitive neuroectodermal tumors/medulloblastoma (PNET/MB) in childhood are the most common malignant primary brain tumor, which either respond poorly to current treatment or tend to relapse. Adoptive therapy with irradiated TALL-104 cells, an IL-2 dependent MHC-nonrestricted T-cell line, has demonstrated significant cytotoxic activity in a broad range of various tumors and may be envisioned as an effective approach for adjuvant cancer treatment. To evaluate the role of TALL-104 cell therapy in the treatment of brain tumors we investigated the distribution of systemically and locally administered TALL-104 killer cells and their efficacy on survival in a human brain tumor model. *In vitro*, measured by  $^{51}\text{Cr}$ -release assay and  $^3\text{H}$  thymidine proliferation assay, TALL-104 cells showed significant cytotoxic activity when added to the human glioblastoma cell lines U87-MG, U251 and A1690, the medulloblastoma cell lines DAOY, D283 and D341, and the epidermoid cancer cell line A431. Biodistribution studies in two brain tumor xenograft models were performed after intracarotid, intravenous and intracranial injections of fluorescent-labeled TALL-104 cells (Hoechst 33342 dye). In brain tumor bearing rats, detection of TALL-104 cells in brain was increased following intracarotid injection in comparison to intravenous administration. However, TALL-104 cells rapidly decreased to low levels within 1 hour after injection. Repetitive local treatment with TALL-104 cells injected into the tumor bed increased survival significantly in the human brain tumor model (A431 carcinoma xenografts in athymic nude rats). Therefore, we propose local therapy with TALL-104 cells as a novel adjuvant treatment for malignant brain tumors. (Supported by the National Institute of Health (Grant: P01-NS 34514), the Jeffrey Miller Neuro-Oncology Research Fund and the Deutsche Krebshilfe e.V.).

**#149 Murine non-pulsed bone marrow-derived dendritic cells generated in presence of normal mouse serum induce tumor resistance.** Dworacki Grzegorz, Cioinatti Vito R., Hoffmann Thomas, Beckebaum Susanna, Whiteside Teresa L. and DeLeo Albert, *University of Pittsburgh Cancer Institute, Pittsburgh, PA 15213.*

We evaluated the efficacy of vaccines consisting of tumor peptide-pulsed bone marrow (BM)-derived dendritic cells (DC) generated in the presence of FBS or BALB/c mouse serum (NMS) in the BALB/c Meth A tumor model. Lymphocyte-depleted BM cells were cultured for 7 days in presence of IL-4/GM-CSF in medium containing 10% (v/v) FBS or 1.5% (v/v) NMS. The number and MLR activity of DCs generated in both cultures were similar. 3-color flow cytometry analysis indicated 50–60% of the cells were DC (CD11c<sup>+</sup>/GR-1<sup>-</sup>), with over 60% considered immature DC (B7.1<sup>low</sup>/B7.2<sup>low</sup>). Flow cytometry and confocal microscopy analyses indicated that immature DC had a high capacity to uptake apoptotic cells present in the culture, which was confirmed by annexin and TUNEL staining. DC ( $2.5 \times 10^5$  cells) pulsed with the H2-K<sup>d</sup>-restricted Meth A mutant p53 232–240 peptide were used to immunize BALB/c mice subcutaneously. A booster immunization was given 7 days later. All groups of mice ( $n = 3/\text{group}$ ) were challenged subcutaneously with Meth A cells ( $4.2 \times 10^5$ ) one week later. Peptide-pulsed DC generated in the presence of NMS or FBS were equally effective in inducing tumor resistance and rejection. Interestingly, "naked" (non-pulsed) DCs generated in the presence of NMS induced significant inhibition of tumor growth, but not rejection. Pulsing "naked" DC with KLH or an irrelevant H2-K<sup>d</sup>-binding peptide abrogated this effect. Immunization of mice with DCs generated in FBS did not induce inhibition of tumor growth. These observations suggest that DCs generated in NMS are presenting "self" determinants, some of which may be derived from apoptotic cells present in the BM cell culture. Further studies on the nature of this "anti-self, anti-tumor" immune response induced by the "naked" DC vaccine and its relevancy to other tumors are in progress.

**#150 Impact of DNA and peptide-pulsed dendritic cell-based vaccines targeting wild-type sequence p53 epitopes on chemically induced carcinogenesis in mice.** Cioinatti Vito R., Dworacki Grzegorz, Töling Thomas, Albers Andreas and DeLeo Albert B., *University of Pittsburgh Cancer Institute, Pittsburgh, Pennsylvania 15213.*

p53 is frequently altered in cancers, and it is an attractive candidate for development of vaccines capable of inducing anti-tumor cytotoxic T lymphocytes (CTL) and rejection. While vaccines targeting p53 missense mutations for immune recognition would be tumor specific, they would be restricted to individual tumors and further limited by the constraints of antigen presentation. In contrast, tumors have the potential of processing

and presenting multiple class I MHC-restricted wild-type sequence epitopes for immune recognition. Vaccines targeting these epitopes, therefore, would have broader applicability. The wild-type sequence mouse p53<sub>232–240</sub> peptide is an H2-K<sup>d</sup> and H2-D<sup>b</sup>-restricted CTL-defined epitope. As a preclinical model of p53 immunotherapy, we evaluated in mice the efficacies of dendritic cell (DC)-based and DNA vaccines targeting the p53<sub>232–240</sub> epitope on induction of sarcomas by methylcholanthrene (MCA). Most MCA-induced sarcomas express p53 mutations. To maximize vaccine efficacy, the study was done in CB6F1(H2<sup>d/b</sup>) mice, which express H2-K<sup>d</sup> and -D<sup>b</sup> molecules. Groups of 10 female mice each were treated with the non viral plasmid, pCI, expressing the p53<sub>232–240</sub> peptide linked to an endoplasmic reticulum insertion sequence (ERIS) to enhance its class I presentation. The DNA immunization was performed by particle-mediated biobalistic gene transfer (gene gun). In addition, groups of mice were immunized with autologous bone marrow-derived DC pulsed with the p53<sub>232–240</sub> peptide injected subcutaneously in the inguinal lymph node area. Control groups were untreated or immunized with pCI backbone or non-pulsed DCs. A total of three weekly treatments were administered, and all groups of mice were challenged with MCA two weeks later. Four weeks later, treatment of the mice resumed. To date, mice immunized with either the pCI-ERIS-p53<sub>232–240</sub> DNA vaccine or peptide-pulsed DC vaccine show a significant inhibition in induction of tumors relative to untreated and treated control groups of mice.

**#151 Characterization of T/Tn antigen-pulsed dendritic cells and subsequently activated T lymphocytes.** Wang, Bao-Le., Harwick, Larissa C., H.M. Bligh. *Cancer Research Laboratories, Department of Microbiology and Immunology, FUHS/The Chicago Medical School, North Chicago, IL 60064.*

T (Gal  $\beta 1 \rightarrow 3$  GalNAc- $\alpha$ -Q-Ser/Thr) and Tn (GalNAc- $\alpha$ -Q-Ser/Thr) epitopes (EPs) are Q-linked carbohydrate structures in carcinoma-associated glycoconjugates and detectable in ~90% of human adenocarcinomas. Skin tests of carcinoma patients with T/Tn antigen (Ag), prepared from human blood group O, MN glycoproteins of red blood cell membrane, have demonstrated that delayed-type hypersensitivity reaction can be elicited by T/Tn Ag after intradermal administration. To further study the cellular immune response mechanism induced by T/Tn Ag, we prepared human dendritic cells (DC) from peripheral blood. After being loaded with T/Tn Ag either in solid or in liquid phase, these DC were applied to stimulate the autologous peripheral blood lymphocytes (PBL). Activated T lymphocytes could be detected by proliferation assay and cytotoxicity assay after 5–10 days co-culture of T/Tn Ag-pulsed DC and PBL. These activated T lymphocytes showed tumor cell-killing capability when co-cultured with homologous T/Tn Ag-expressing breast carcinoma cells. Immunocytochemical staining revealed that T/Tn EPs were present on the T/Tn Ag-pulsed DC surface in a disseminated dot pattern. The DC pulsed by solid phase of T/Tn Ag resulted in stronger positive staining than those pulsed by liquid phase, and the T/Tn Ag-expressing tumor cell-killing T lymphocytes were more frequently obtained with solid phase T/Tn Ag-pulsed DC and are being further characterized for their Ag-specificity. These results suggested that as carbohydrate structures in glycoprotein, T/Tn EPs can be processed and presented by DC, which subsequently can induce naive PBL differentiation into functionally activated T lymphocytes. The physical state of T/Tn Ag may affect the efficacy of antigen presenting by DC and the subsequent immune response.

**#152 Maturation of dendritic cells (D.C.) from ovarian cancer patients.** Zavadova, E., Savary, C., and Freedman, R.S. *Department of GYN/Oncology, and Department of Surgery, M.D. Anderson Cancer Center, Houston, TX 77030.*

Dendritic cells are the most potent antigen-presenting cells of the immune system. We have shown that D.C. from ascites of patients with peritoneal carcinoma have low maturity (Clin Cancer Res 4:799–809, 1998). Here we examined the effects of the *in vitro* treatment of D.C. with cytokines or proteolytic enzymes (polyenzyme preparation Wobe-Mugos®, Garetsried, Germany) on the phenotype and function of D.C. This preparation has been used successfully in an additive therapy of some cancer patients. D.C. from ascitic fluid of 16 untreated ovarian cancer patients were cultured either with RPMI medium alone or with medium containing granulocyte-macrophage colony-stimulating factor (GM-CSF), tumor necrosis factor alpha (TNF- $\alpha$ ) and Interleukin-4 or with medium containing papain, trypsin and chymotrypsin (Wobe-Mugos) for 5–7 days. After washing, phenotypic analysis of DC on culture day 7 resulted in a higher proportions of CD83<sup>+</sup>, CD40<sup>+</sup> and CD80<sup>+</sup> cells when incubated with cytokines or enzymes than D.C. incubated only with medium alone. Mixed lymphocyte reactions resulted in stimulation of allogeneic T-cells. This investigation shows that D.C. from peritoneal cavity of patients with untreated ovarian cancer can be matured. This may be of relevance for the modulation of D.C. functions in cancer patients by therapeutic measures. (Supported in part by Firma MUCOS).



**#153 Identification of HLA-A\*03, A\*011 and B\*07-restricted melanoma-associated peptides that are immunogenic *in vivo* by vaccine-induced immune response (VIR) analysis.** Reynolds, Sandra R., Cells, Esteban, Sette, Alessandro, Oratz, Ruth, Johnston, Dean, Shapiro, Richard L. and Bystry, Jean-Claude. *Kaplan Cancer Center, New York, NY, Mayo Clinic, Rochester, MN and Epimune, Inc., San Diego, CA.*

In order to effectively construct cancer vaccines from individual antigens or peptides, there is a need to identify those antigens and peptides that can stimulate anti-tumor immune responses *in vivo* in humans. One way to do so is to use vaccine-induced immune responses (VIR) as probes to identify immunogenic tumor-associated antigens. Novel immunogens can be identified by immunizing patients to vaccines that contain a broad range of potential immunogens and identifying the individual antigens in the vaccine that trigger immune responses. In this study, we used this approach to identify multiple melanoma-associated peptides that are immunogenic in humans, and presented by HLA-A\*03, A\*11 or B\*07. Thirty-one patients with melanoma were immunized to a polyvalent shed antigen vaccine that contains Melan A/MART-1, gp100, tyrosinase and MAGE-1, -2 and -3 as well as other antigens. Peripheral blood was assayed before and after immunization by ELISPOT assay for peptide-specific CD8+ T cell responses to a panel of 20 peptides derived from these antigens and presented by at least one of these 3 alleles. The peptides were selected for their immunogenic potential based on strong binding affinity to HLA-A\*03, A\*11 or B\*07 and their ability to stimulate a CD8+ T cell response *in vitro*. Seventeen (85%) peptides stimulated a vaccine-induced CD8+ T cell response *in vivo*. At least one, and usually several, of the immunogenic peptides was derived from each of the antigens; at least one immunogenic peptide from each antigen was presented by each of the 3 HLA class I molecules. None of these peptides were previously known to be immunogenic *in vivo* in humans. Thus, VIR analysis is an effective strategy to directly identify novel immunogenic peptides and antigens that are good candidates for vaccine construction.

**#154 Prostate Stem Cell Antigen (PSCA): A Target for Cancer Immunotherapy.** Arthur B. Raitano<sup>1</sup>, Igor Vivanco<sup>1</sup>, James Kuo<sup>1</sup>, Rene S. Hubert<sup>1</sup>, Robert E. Reiter<sup>2</sup>, Owen N. Witte<sup>3</sup>, Aya Jakobovits<sup>1</sup>, Daniel E.H. Afar<sup>1</sup>, and Douglas C. Saffran<sup>1</sup>. <sup>1</sup>*UroGenesys, Inc., 1701 Colorado Ave., Santa Monica, CA 90404.* <sup>2</sup>*Department of Urology, University of California, Los Angeles, CA 90095.* <sup>3</sup>*Howard Hughes Medical Institute and Department of Microbiology and Molecular Genetics, University of California, Los Angeles, CA 90095.*

PSCA is a newly described member of the Ly-6 family of GPI-linked cell surface antigens (Reiter *et al*, PNAS 95:1735-1740, 1998). Human tissue analysis shows that PSCA is expressed in normal prostate, prostate cancer, and in prostate cancer xenograft models. Screening of a panel of cell lines of multiple cancer types revealed expression of PSCA in pancreatic and bladder cancer. These results suggest that PSCA is an attractive target for cancer immunotherapy. Recently, monoclonal antibodies (mAbs) have been derived which specifically recognize PSCA. The antibodies react with PSCA protein by ELISA and Western blot, and recognize PSCA on the surface of prostate cancer xenografts and transfected cell lines by flow cytometry. Anti-PSCA mAbs also stained normal prostate, prostate cancer tissue, and xenografts and cell lines by immunohistochemical analysis. The ability of the mAbs to bind PSCA on the cell surface has suggested their potential utility as modulators of tumor cell growth. Experiments to study the effect of anti-PSCA mAbs on the growth of PSCA-positive prostate cancer cells *in vitro* and *in vivo* will be presented.

**#155 Anti-GM2 antibodies in melanoma patients induced by the ganglioside-conjugate vaccine GM2-KLH/QS-21 (GMK) demonstrate binding to melanoma cells, complement-mediated cytotoxicity (CMC), and antibody dependent cellular cytotoxicity (ADCC).** Morrissey, Donna M., Hamilton, W. Bradley, Zhan, Cenchen, Owens, Kristina, Israel, Robert J. *Progenics Pharmaceuticals, Inc., 777 Old Saw Mill River Road, Tarrytown, New York 10591*

We have studied the serum from 52 patients who recently completed a dose-response study of GMK vaccine to characterize the humoral response and to provide insight into the possible mechanisms of action of vaccine-induced antibodies. GMK contains the ganglioside GM2 linked to the carrier protein Keyhole Limpet Hemocyanin (KLH) and adjuvanted with QS-21. Phase II studies show that GMK, at GM2 doses > 3 µg, consistently induces IgM and IgG anti-GM2 antibodies in melanoma patients when given subcutaneously at weeks 1, 2, 3, 4, 12, 24, and 36. Flow cytometry on GM2 expressing tumor cells (SK-Mel-31, Saos-2) and GM2 negative tumor cells (SK-Mel-24, SK-Mel-28) as well as assays for complement-mediated cytotoxicity (CMC) and antibody-dependent cellular cytotoxicity (ADCC) were performed. Flow cytometry demonstrated high affinity and specific binding of anti-GM2 IgM and IgG. CMC was assessed by an LDH assay using GM2-expressing tumor cells with a GM2-negative cell line as a control. Potent and specific CMC was detected at anti-GM2 IgM antibody titers as low as 1:80. The percentage of specific complement-mediated killing increased with increasing IgM antibody titer. At titers of 1:320, 1:640, and 1:2560, specific killing was approximately 25%, 50%, and 65% respectively. CMC did not appear to correlate independently with the dose of GM2. Anti-GM2 IgG was subtyped as predominantly IgG1 and

IgG3. ADCC assays demonstrated specific killing of GM2-expressing tumor cells at anti-GM2 IgG antibody titers as low as 1:160. The percentage of specific ADCC killing increased with increasing anti-GM2 IgG titers and did not appear to correlate independently with the dose of GM2. We conclude that the ganglioside-conjugate vaccine GMK induces antibodies that may be effective in reducing melanoma recurrence by both CMC and ADCC. Ongoing randomized phase III adjuvant trials in melanoma will define the clinical utility of this compound.

**#156 Identification of a novel prostate-specific cell surface antigen highly expressed in human tumors.** Igor Vivanco, Rene S. Hubert, Emily Chen, Shiva Rastegar, Kahan Leong, Steve C. Mitchell, Rashida Madraswala, Yanhong Zhou, James Kuo, Arthur B. Raitano, Aya Jakobovits, Douglas C. Saffran and Daniel E.H. Afar. *UroGenesys Inc., Santa Monica, CA 90404.*

In search of novel genes expressed in metastatic prostate cancer we subtracted cDNA isolated from benign prostatic hyperplasia (BPH) from cDNA isolated from a prostate cancer xenograft model that mimics advanced disease. One novel gene that is highly expressed in advanced prostate cancer encodes a protein with potential membrane-spanning domains. The gene is predominantly expressed in human prostate tissue and is up-regulated in multiple cancer cell lines, including prostate, bladder, colon, ovarian, pancreatic and Ewing sarcoma. Polyclonal antibodies (pAbs) were raised towards a peptide derived from the open-reading frame. Using the pAbs for immunohistochemical analysis of clinical specimens, significant protein expression was detected at the cell-cell junctions of the secretory epithelium of prostate and prostate cancer cells. Little to no staining was detected in non-prostate normal human tissues, except for bladder, which expressed low levels of the protein at the cell membrane. Protein analysis located the protein to the cell surface of cancer cell lines. Our results support this novel marker as a cell surface tumor antigen target for cancer therapy and diagnostic imaging.

**#157 A Critical Analysis of Murine Models used in Studies of Host Immune Responses to Progressive Tumor Growth.** Manson, L.A. *Dept. of Biology University of Pennsylvania, Philadelphia, PA 19104.*

The initial tumor mass in an autochthonous tumor system is one cell, therefore model system that are designed to analyze the role of the host immune responses during progressive tumor growth should attempt to approach this state as closely as possible. Thus, working with transplantable murine tumors, we initially investigated whether our tumors (L5178Y, EL4, P815Y) would grow in their syngeneic hosts from small inocula. In all 3 cases, fatal tumors could be initiated with as few as a 10 cell inoculum. We standardized on Initiating I.p or s.c. tumor growth with an inoculum of 10<sup>3</sup> tumor cells grown in tissue culture. It was in such studies that we reported that tumor cells became resistant to the killer cells found in the tumor mass. Later studies found that anti-tumor IgM, bound to the growing tumor cells *in vivo*, was the modulating agent. The oncotopes of MCA-105, an H-2<sup>b</sup> sarcoma, were immunologically cross-reactive with those of EL4 and P815Y, but not with those of L5178Y. (Oncotopes are epitopes that are unique to the tumor, and that are recognized by the immune systems of the syngeneic host; for details, see abstract Oncotopes...) MCA-105 has been used by a number of laboratories as a model to develop immunotherapeutic treatments to eliminate the tumor. The initial studies in which an implanted tumor was eliminated by treatment with TIL or other agents, indicated that treatment was commenced on day 3 after tumor inoculation. (*Science* 239, 1318, 1986). Such studies encouraged experimenters to draw inappropriate conclusions as to the efficacy of the treatment, as they subsequently learned when therapy was applied to autochthonous tumors in human patients. Not enough time had been allowed for killer cell resistance to form prior to the commencement of treatment in the murine experiments. (*JAMA*, 272, 1827, 1994). In the human patient, tumor growth has been ongoing for months, and killer cell resistance has had ample time to be established. This criticism has been overlooked by other investigators as is evident in a recent publication (*J. Immunol.* 160, 334, 1998). In this latest study, tumor MCA-105 eradication was claimed after treatment, and here as well, the protocol indicated that treatment was initiated on day 3 after tumor inoculation.

**#158 BCG-cell wall skeleton plays a critical role in preventing the tumor escape.** Hayashi, Akira, Seya, Tsukasa, Toyoshima, Kumao, Azuma, Ichiro. (*Osaka Medical Center for Cancer & Cardiovascular Diseases, and Institute of Immunological Science, Hokkaido University.*)

Since 1975, more than 600 patients have been treated by immunotherapy with BCG-cell wall skeleton (CWS) alone, usually just after or occasionally before surgical operation. In this pilot study we noticed the important clinical features. First, this therapy proved especially effective for the immunologically eligible patients who expressed positive interferon (IFN)-γ induction in their peripheral blood after BCG-CWS inoculation. Second, its clinical effect was observed in most kinds of cancer patients, regardless of the presence of lymphnode metastasis, of histological types, and of differentiation state. These facts suggest that this therapy may be related to the fundamentals of our immune surveillance system.

Recently we confirmed that BCG-CWS directly worked both on the innate (natural) and on the adaptive (acquired) immunity; *in vitro* study, we

found that BCG-CWS activated human monocytes and/or macrophages, and stimulated the maturation of dendritic cells, concomitantly down-regulating the expression of a human homologue of chicken MD-1. Further we also found *in vivo* that in the presence of cancer cells the activated T cells, on which CD28 or CD152 (CTLA-4) signals were strongly expressed, infiltrated around necrotic cancer cells along with dendritic cells expressing CD86 (B 7.2) signals in metastatic lymphnodes only after, but not before, BCG-CWS immunotherapy. These results strongly suggest that BCG-CWS links the innate immunity with the adaptive one and prevents the tumor escape.

These properties of BCG-CWS have been reflected to the results of clinical trial: For instance, the 5 years survival rates of the postoperative primary lung cancer patients (total 117; adeno-ca. 90, squamous cell-ca. 18, large cell-ca. 9) treated with BCG-CWS alone were 93.8% (n = 45) [control, 76.1% (n = 315)] in Stage I, 88.9% (n = 20) [control, 61.0% (n = 82)] in Stage II, 51.6% (n = 52) [control 39.6% (n = 126)] in Stage III, and statistically significant in Stage II and III.

**#159 Locally applied recombinant mistletoe lectin (rML) Inhibits urinary bladder carcinogenesis *in vivo*.** Mengs U., Schwarz T., Elsässer-Belle U., Freudenberg N., and Weber K. *Madaus AG, Köln; University of Freiburg, Germany; RCC, Itingen, Switzerland.*

The  $\beta$ -galactoside-specific recombinant mistletoe lectin (rML) is a type II ribosome-inactivating protein with cytotoxic and immunostimulating potencies. In the present studies the influence of locally applied rML on urinary bladder carcinogenesis was investigated in two different rodent models.

In the first experiment, MB49 urinary bladder carcinoma cells were implanted into the urinary bladder of female C57BL/6J mice and from day 11 onwards, the animals were treated three times weekly for 4 weeks with doses of 3, 30 or 300 ng/0.1 ml intravesically. As a result, rML had a significant impact on the tumour growth at all dose levels. At termination, 27% to 33% of the mice receiving rML had urinary bladder carcinomas, compared to 80% of the control group.

In the second model, female Fischer 344 rats received four biweekly 1.5 mg doses of N-methyl-N-nitrosourea (NMU) intravesically to induce tumor development. The animals were treated intravesically with rML twice weekly after tumor induction with 30 or 150 ng/0.1 ml from week 8 to 13 or from week 14 to 19. The animals were sacrificed at week 21 after tumor initiation and the urinary bladders were evaluated histologically. Malignant transformation (44% flat atypia and 36% transitional cell bladder tumors) were found in 82% of the controls. In the groups treated with 30 or 150 ng rML (week 8 to 13), malignant transformation was found only in 50% and 52% of the animals. In animals treated with rML from week 14 to week 19, malignant changes were seen in 45% and 42% of the rats. The differences were statistically significant. To conclude, intravesical instillation of rML showed inhibitory activity in two different models of urinary bladder carcinoma *in vivo*.

Supported by the grant 0311183 of BMBF, Germany.

**#160 Recombinant mistletoe lectin (rML) is a potent anticancer agent in experimental murine and human tumor models *in vivo*.** Burger, A.M., Mengs, U., Gerstmayr, B., Weber, K., Fiebig, H.H., and Lentzen, H. *Tumor Biology Center, Freiburg; Madaus AG; Memorec GmbH, Köln, Germany; RCC, Itingen, Switzerland.*

Recombinant mistletoe lectin (rML) is a ribosome inactivating protein which has been previously described as a potent inhibitor of tumor cell growth *in vitro* and as a modulator of immune response. In this study, we examined whether rML treatment would confer tumor growth inhibition in a variety of experimental animal tumor models *in vivo*. The antitumor activity of rML was studied in 4 subcutaneously growing and 3 intravenously inoculated syngeneic murine models as well as in 4 human tumor xenografts. The maximum tolerated rML dose was established at 3  $\mu$ g/kg/d in a Qdx5 schedule, when administered i.p. The transplantable syngeneic murine tumor models Lewis lung, Renca, C 8 colon 38 and F9 were treated for 2-4 consecutive weeks in doses ranging from 3  $\mu$ g-0.3 ng/kg/d. Significant antitumor activity ( $p < 0.005$ ) as compared to control was seen at 3 and 0.3  $\mu$ g rML/kg/d in all 4 models examined. T/Cs ranged from 1-32%. rML was more effective than the standard therapies cisplatin in the F9 testicular and adriamycin in the Renca renal carcinoma at their MTDs. Significant tumor growth inhibition was also seen in 1/4 subcutaneously growing human tumor xenografts, the LXFS 538 lung carcinoma, with a T/C of 26% ( $p < 0.001$ ) at the 3  $\mu$ g/kg/d dose level.

In 3 syngeneic murine metastasis models, the B16 melanoma, the L-1 sarcoma and the RAW117-H10P lymphosarcoma, rML was also potently active. Given i.v. or s.c. at doses ranging from 0.3 to 300 ng/kg/d, rML showed antimetastatic activity as measured by reduction in lung or liver metastases.

By using immunoperoxidase staining with anti-rML antibodies, the presence of rML in tumor tissues could be demonstrated. Whilst this would reflect direct rML cytotoxicity, in the sarcoma models rML activity was accompanied by enhancement of peripheral blood immunocytes suggesting an additional immunomodulation.

In conclusion, the present data indicate that rML is a new therapeutic entity and good candidate for clinical development.

Supported by the grant 0311183 of BMBF, Germany.

**#161 Recombinant mistletoe lectin (rML): A cytotoxic immune response modifier *in vitro*.** Schwarz, T., Elsässer-Belle, U., Möckel, B., Hirt, W., Mengs, U., and Lentzen, H. *Madaus AG, Köln; University of Freiburg, BRAIN GmbH, Zwingenberg; Orpegen Pharma GmbH, Heidelberg, Germany.*

The recombinant mistletoe lectin (rML) is a new biological entity under development for cancer therapy. rML consists of a cytotoxic A chain linked by a disulphide bridge to a lectinic B chain, and has affinity for galactopyranosyl residues. The A chain inactivates protein biosynthesis by enzymatic modification of 28S rRNA. The objective of this study was to analyze, firstly, immunostimulatory actions of rML which can initiate immune signaling cascades and responses against cancer cells and, secondly, the putative relationship with its cytotoxic potency. rML concentration-dependently increased the release of IFN- $\gamma$  from human peripheral blood mononuclear cells (PBMC), of IL-1 $\beta$  from PBMC and THP-1 cells as well as of IL-6 and IL-15 from the human HaCaT keratinocyte cell line. The expression of IL-1 $\beta$  mRNA in THP-1 and HL-60 cells and of mRNA for IL-6 was enhanced in HaCaT, THP-1 and HL-60 cells by rML. Furthermore, the lectinic cytotoxin up-regulated the expression of CD25 on human PBMC surface and primed the rML-induced granulocyte oxidative burst in an human whole blood bioassay. The natural killer cell activity of mouse splenocytes against YAC-1 lymphoma target cells was augmented by rML. In most of these bioassays, rML was immunopharmacologically active at cytotoxic concentrations only. The agent induced apoptosis at low and necrosis at high concentrations. In conclusion, these observations indicate a relationship between the cytotoxic and the immunostimulatory effects of rML. The release of cytokines from rML-treated apoptotic cells may trigger a bystander activation of hyporesponsive or tolerant immune cells with subsequent elimination also of distant cancer cells.

Supported by the grant 0311183 of BMBF, Germany.

**#162 Oncotopes—targets for immunotherapeutic attack.** Manson, L. A. and Snyder, A. K. *Dept. of Biology, University of Pennsylvania, Philadelphia, PA 19104.*

Progressive growth of lymphoid murine tumors (EL4, P815Y, L5178Y) in the ascites of the syngeneic host from small inocula ( $10^3$  cells) occurs because the tumors become resistant to killer cells that are found in the tumor bed. Progressively-growing resistant tumor cells were coated with IgM, whereas tissue culture-grown tumor cells are IgM-free. The IgM was secreted by ascitic B cells. By day 8 after tumor inoculation, hybridomas producing anti-oncotopes IgM could be generated from the B1.B cell fraction, none were found with the B2.B cell fractions. Examination of ascitic lymphoid populations during early tumor growth by flow cytometry analysis observed the appearance of CD8 $^+$  killer cells, and IgM was detected on the tumor cells. Oncotopes are tumor-unique epitopes which generate a T-independent response within days of the introduction of the tumor. The oncotopes of EL4, P815Y and MCA-105 (a sarcoma) were found to be cross-reactive, but not with the L5178Y oncotope. Cross reactivity across an MHC barrier was initially determined by growing a tumor in an F1 hybrid and testing activity of spleen CTL with tissue culture-grown targets in  $^{51}$ Cr release assay with the two targets, e.g. EL4 (H-2 $^b$ ) and P815Y (H-2 $^d$ ). Cross-reactivity was confirmed using cold target inhibition assays. The oncotope-bearing molecules were found on the surface of the tumor cells to be hydrophobically-associated with the Class I gene product. Early experiments showed that syngeneic mice immunized with anti-oncotope IgM, eluted from *in vivo* grown tumor cells, were incapable of supporting tumor growth, perhaps due to the formation of an anti-idiotypic antibody. It is important to emphasize that in our model, progressive tumor growth is initiated with small numbers of tumor cells, similar to what occurs spontaneously in autochthonous growth, where the initial tumor load is one cell.

**#163 Expression of Bcl-2, CK20, and p53 in Merkel cell carcinoma: Quantitative and Qualitative study.** Iram Rafique MD, Sadir J Alrawi MD, Gabriel Levi MD, Azza A Abo deeb MD, Mohamed Abdalla MD, Anthony J Acinapura MD, and Ramanathan Raju MD.

**BACKGROUND:** Merkel Cell Carcinoma (MCC) is a rare but highly aggressive neuro-endocrine skin carcinoma with poor patient outcome. Immunohistochemical expression of certain tumor markers may suggest the aggressiveness of the tumor. It could also be a tool of differentiation from other neoplasms (metastatic small cell lung carcinoma and lymphoma).

**MATERIAL AND METHODS:** Clinicopathological features of seven resected specimens of MCC were evaluated qualitatively and quantitatively. Immunohistochemical analysis was performed using five tumor markers (CK20, p53, Bcl-2, Her-2-Neu and Cyclin-D1).

**RESULTS:** Age range of patients in our study was 39-83 years with male:female ratio of 3:4. The size range of resected specimens was 0.5-21 cm. Tumors were mostly located at the trunk, head and the neck. Clinical gross appearance was hemangiomatous in 3 cases while others were simple nodular masses. The immunohistochemical profile showed that 85% of our patients were positive for Bcl-2 with average % age expression of 64.2%. 85% of patients were positive for CK-20 with average % age



expression of 82.1%. p53 was positive in 85% of the patients with % age expression of 53.5%. However all of them were negative for Her-2/neu and Cyclin D1.

**CONCLUSION:** Our study shows that expression of Bcl-2, CK-20 and p53 is very useful in the diagnosis of MCC. Although initial quantitative analysis shows some promising results regarding the aggressiveness of this tumor, further quantitative studies of these tumor markers are recommended.

**#164 Peptide-MHC monomers bound to tumor cell surfaces via an antibody-avidin bridge can mediate tumor killing by peptide-specific CTL.** Zaremba, Sam, Siccardi, Antonio, Paganelli, Giovanni, and Schlom, Jeffrey. *National Cancer Institute, USA; San Raffaele Scientific Institute, and European Institute of Oncology, Italy.*

The ability of cytotoxic T lymphocytes (CTL) to lyse target cells is restricted by the expression of appropriate antigenic peptide and class I major histocompatibility (MHC) molecules on the target cell surface. In this report we show that tumors which do not endogenously express antigen or MHC can bind peptide-MHC monomers, thereby becoming sensitized for lysis by peptide-specific CTL. Our *in vitro* experiments employ human tumor cells that are negative for HLA-A2 and therefore resistant to lysis by A2-restricted CTL. However, they express tumor-associated antigens (TAA) such as carcinoembryonic antigen (CEA) which is found on a high percentage of human epithelial tumors *in situ*. We sequentially incubated tumor cells with biotinylated MAb to TAA, avidin, and biotinylated MHC monomer folded about an antigenic peptide. Treated tumor cells are now sensitive to lysis by A2-restricted, peptide-specific CTL. Cells that do not express antigen and do not bind biotinylated MAb are not lysed.

Attempts at CTL elimination of tumors are often hindered by mechanisms that limit successful recognition and activation. These mechanisms include: (1) absence from the tumor of a sufficiently immunogenic peptide or adequate costimulation for priming a CTL response; (2) failure to positively select high affinity CTL to self oncofetal proteins, thereby leading to holes in the repertoire; (3) evolution of the tumor leading to down-regulation or absence of the MHC or; (4) a phenotype capable of inactivating or anergizing the relevant CTL. The attachment of competent peptide-MHC complexes to tumor cells via MAbs can bypass some of these problems. The need to generate a response directly to the tumor is eliminated, as is the requirement for surface expression of MHC on the target. Instead the possibility opens of recruiting autologous pre-existing anti-viral CTL specifically to the tumor. Moreover, this strategy can be broadened by exploiting MAb to other tumor-associated antigens or to viral antigens.

**#165 Immunocytologic detection of cell-adhesion antigens on carcinoma cells.** Valladares-Ayerbes M, Iglesias P, Rendal E, Yebra MT, Lema B, Calvo L, Alonso G, Antolón S, Antón L, Andión C. *Medical Oncology, Cribology, Pathology, Juan Canalejo Hospital, Medicine Dept. Univ. La Coruña, Spain.*

**Introduction and objectives:** Isolated tumor cells (ITC) could be better immunotherapeutic targets on solid cancer than overt metastases. Most of the studies about ITC detection have been done by immunocytochemistry (ICC). We have therefore studied expression of cell adhesion antigens (Ag) using ICC on several tumors cell lines and on samples from metastatic epithelial cancer patients (pt). **Material and Methods:** Breast cancer (BC) PM1 and T47D, small-cell lung cancer (SCLC) H-146, and colon cancer (CC) SW480 cell lines were used. In addition, a new pancreatic adenocarcinoma (PC) cell-line established in our laboratory and capable of multicellular spheroid growth on agarose-coated flask was studied. Monoclonal antibodies (mAb) MOC-31 and MOC-1 were assessed. They recognize a 35-40 kD epithelial glycoprotein (EGP2) and neural cell adhesion molecule (NCAM) respectively. Ag-mAb reaction was developed with avidin biotin complex-alkaline phosphatase (ABC-AP) system. Mononuclear cells from malignant effusions, smears and cytopins of fine-needle aspirations of metastatic lesions from SCLC and a variety of epithelial tumors were stained by the same method. Non-effusions samples were also stained with Fab-fragment of pan-cytokeratin (CK) mAb A45-B/B3 and AP. **Results:** BC, CC and PC cells shown a homogeneous expression for EGP2 and CK. The majority of samples from epithelial tumors displayed a homogeneous staining for MOC-31 and A45-B/B3. H146 was positive for MOC-31, MOC-1 and A45-B/B3 but SCLC specimens were more heterogeneous on CK and cell-adhesion Ag expression. **Conclusions:** Anti-EGP2 mAb could be useful for ITC target on epithelial cancers. Sensitive target of ITC in SCLC could require the use of a panel of mAb due to Ag expression heterogeneity.

Supported in part by a research grant from Amgen.

**#166 Effect of Adenovirus Humoral Immunity on Anti-tumor Efficacy of an Oncolytic ARCA™ Following Intravenous Administration** Yu Chen, De-Caho Yu, and Daniel R. Henderson *Calydon, Inc. 1324 Chesapeake Terrace, Sunnyvale, CA 94089*

Use of an oncolytic attenuated replication competent adenovirus (ARCA™) for cancer therapy holds promise, but there are a number of significant barriers to its effectiveness. Two of the major limitations of virus-based vectors as therapeutic vehicles are 1) the inactivation of virus by pre-existing circulating antibodies to the virus, and 2) the reduced

efficacy of repeat dosage by primary or secondary induction of humoral immunity. In order to evaluate the effect of anti-adenovirus immunity on the outcome of ARCA™ based cancer therapy *in vivo*, we have developed an animal xenograft model, in which we are able to adjust the level of anti-adenovirus neutralizing activity by passively injecting the purified anti-adenovirus IgG that was raised in a rabbit. The experiments on this animal model show that pre-existing neutralizing antibodies significantly reduced the efficacy of IV administered virus; however, a higher viral dosage could achieve anti-tumor effectiveness. Antitumor activity of our virus was not compromised when a high level of neutralizing activity in the blood circulation was established one week after virus administration, indicating that post-immune response would not inhibit virus antitumor efficacy. Toxicity studies were conducted in the animals in the presence or absence of pre-existing antibodies. It was shown that animals with pre-existing antibodies could tolerate a higher viral dosage and the number of infectious virus particles in circulation was significantly reduced. Interestingly, it was demonstrated that pre-existing antibodies did not alter virus biodistribution; the majority of administered virus went to the liver. It is the first time, as far as we are aware, that an animal model was developed to evaluate the effect of anti-adenovirus antibody on the efficacy of the anti-tumor activity of a tumor-specific adenovirus.

**#167 Psychoneuroimmunology in Breast Cancer Patients.** Lakshmi Rao (1), Ashok Khar (2), Gopal Pande (2), Brinda Sitaraman (3), (1) CDFD (2) CCMB (3) BRCA.

Taking Breast Cancer as a model for psychoneuroimmunology (PNI) study to explore the mind body nexus in cancer patients, is grouped into (I) Breast cancer patients, (II) Spouses of group I, (III) Female caregivers of group I, and (IV) Normal subjects assessed at three or more points of time (Pre-surgery, Pre-radiation and Pre-chemotherapy) for various psychological and neuroimmunological measures. The highlights of our findings are: (1) **psychological:** (a) Patients experienced more negative life changes, depression, anxiety and neuroticism than spouses and normals. They were more extroverted and expressed greater satisfaction with their social supports. (b) Amongst psychological factors, COPING emerged as most outstanding psychological parameter that was different in patients, their husbands and in normals. (2) **Neuroimmune parameters:** (a) Significant differences seen among immune parameters at various points of assessment. (b) While surgery, radiation and cortisol levels had no impact on immune parameters, a definite correlation, in both normals and in patients was seen between psychological factors and immune functions. Positive psychological factors enhanced NK cell activity, total T, B cell % and Ig A levels. Likewise, negative psychological factors suppressed total immunoglobulin levels, T cell levels, CD4 and CD8 %, and Con A activity. NK activity and SIL-2R levels on other hand, enhanced by negative psychological factors.

**#168 Proteolytic enzymes (Wobe-Mugos®) reduce Immuno-suppression in cancer patients via a reduction of TGF-β expression.** Deßer, L., Herbagek, L., Mohr, T., and Wrba, H. *Institute for Tumorbiology, Cancer Research, University Vienna, Austria.*

Proteolytic enzymes (Wobe-Mugos E®) have been subject to various clinical investigations in several malignant tumors. Additive treatment with WM obtained orphan drug status by FDA in 1999.

Retrospective studies showed that additive therapy with Wobe-Mugos® (WM) leads to a prolonged remission time in patients with breast cancer and multiple myeloma (Hanisch & Bock, *in press*) and a prolonged survival in patients with certain stages of colon cancer (Popiela et al. *in press*) and multiple myeloma (Sakalova et al. 1998). An excessive production of TGF-β is believed to be the main cause of immunosuppression and accelerated progression in multiple myeloma and several other malignancies. Therefore, TGF-β might be a target for therapeutic interference. *In vitro* studies with melanoma cells or tumor associated macrophages (isolated from patients with breast or ovarian cancer) demonstrated that treatment with WM reduces TGF-β production on protein and mRNA-level (Zavadova et al. 1997) via interruption of the autocrine loop.

It is well documented that TGF-β is eliminated out of the blood circulation by a mechanism involving the transformation of α2Macroglobulin from the so-called slow-form into its fast-form, and the subsequent capture and inactivation of TGF-β by this isoform of α2Macroglobulin (Hall et al. 1993).

We propose a model that the response to enzyme treatment is to a certain degree related to the enzyme induced elimination of excess TGF-β via the α2Macroglobulin-pathway.

### SECTION 3: NEW INTRACELLULAR TARGETS

**#169 Surprising homology of DNA (cytosine-5) methyltransferases.** Quada, James C., Jr., Rashidi, Hooman H., Izbička, Elzbieta, Von Hoff Daniel D. *Institute for Drug Development, CTRC, San Antonio, TX, 78245.*

DNA (cytosine-5) methyltransferase (DCMTase) is frequently elevated in cancer cells, and is believed to mediate the silencing of genes that interfere

with cancer progression. Inhibition of DCMTase (Dnmt1) has been shown to dramatically impair carcinogenesis. Therefore, Dnmt1 is a promising target for anticancer therapy. Our approach is to develop structural models of Dnmt1 based on sequence similarity to bacterial DCMTases of known structure, which can then be used for computer-assisted inhibitor design. Bacterial *M. HhaI* is the most studied DCMTase, with several X-ray crystal structures, while the mammalian DCMTases have not yet been crystallized. We assessed sequence similarity between *M. HhaI* and mammalian DCMTases in the three families identified to date (Dnmt1, Dnmt2, and Dnmt3) using multiple and pairwise sequence alignments of the protein catalytic domains and also the unique signatures (Prosite signature PS00094) within their catalytic sites. Dnmt1 and *M. HhaI* are 62% identical and 79% similar (Clustal W multiple sequence alignment) in the PS00094 signature, whereas, *M. HhaI* and Dnmt2 are only 38% identical and 50% similar, and *M. HhaI* and Dnmt3a and Dnmt3b1 are 38% identical and 44% similar. Another Prosite signature, PS00095, which contains residues found in the catalytic site of *M. HhaI* crystal structures, is present in Dnmt1 but absent in Dnmt2 and the Dnmt3 family. Despite the striking homology of Dnmt1 and *M. HhaI* within their catalytic domains, large structural differences also exist. We have characterized two novel sequence motifs with putative regulatory functions present only within the catalytic domain of higher eukaryotic Dnmt1 DCMTases. These data indicate that the *M. HhaI* crystal structures comprise the most effective starting point for developing a structural model of Dnmt1 for design of specific inhibitors.

**#171** Generation of phosphatidic acid by lysophosphatidic acid acyl transferase- $\beta$  is implicated in tumorigenesis, loss of "contact inhibition," reduced actin filaments, and activation of Raf-1 kinase. Tang, N.M., Morrison, D., Leung, D.W., Bonham, L., Hollenback, D.M., and Finney, R.E. *Cell Therapeutics, Inc., Seattle, WA 98119* and *Frederick Cancer Research Development Center, Frederick, MD.*

Augmented production of phosphatidic acid (PA), a key precursor for biomembrane synthesis and a second messenger in signal transduction pathways with targets that include PLC- $\gamma$ , Ras-Gap and the serine/threonine kinase, Raf-1, has been associated with neoplastic transformation. Lysophosphatidic acid acyl transferase(s) (LPAAT) catalyze the *de novo* biosynthesis of PA. Using *in situ* hybridization with anti-sense cDNA, we demonstrated that expression of the  $\beta$  isoform of this enzyme (LPAAT- $\beta$ ) was augmented in human tumor tissue in 10/11 ovarian, 14/20 breast, and 3/16 prostate biopsies as compared to normal adjacent tissues. In contrast, no tumor specific expression was observed with the  $\alpha$  isoform of LPAAT (LPAAT- $\alpha$ ). When ectopically expressed in ECV-304 cells (a derivative of T24 bladder carcinoma cells), LPAAT- $\beta$  allowed cells to continue to grow after reaching confluency where they attained densities that were approximately 2-fold over cultures over-expressing green fluorescent protein or enzymatically inactive LPAAT- $\beta$ . At confluent densities, growth arrest in G1 was reduced in LPAAT- $\beta$  expressing cells, the cells assumed a rounded morphology, and they no longer exhibited well-defined actin stress fibers. Biochemically, LPAAT- $\beta$ , but not LPAAT- $\alpha$  or enzymatically

inactive LPAAT- $\beta$ , augmented MAPK activation and germinal vesicle breakdown in *Xenopus* oocytes when co-expressed with either activated Ras or Raf-1, whereas no effect on Mos signaling was observed. The enhanced signaling effect of LPAAT- $\beta$  appears to be functioning at the level of Raf-1. Because LPAAT- $\beta$  expression is associated with human tumors, induces phenotypes characteristic of neoplastic cells, e.g. loss of contact inhibition and actin stress fibers, and because it participates in signal transduction pathways induced by known oncogenes, we conclude that LPAAT- $\beta$  may be a target for anti-cancer drug development.

**#172** The DNA polymerase/processivity factor complex of Kaposi's sarcoma-associated herpesvirus: a novel target for high-throughput drug screening. Kal Lin<sup>1</sup>, Judy A. Milkovits<sup>2</sup>, Robert H. Shoemaker<sup>3</sup>, Edward A. Sausville<sup>1</sup>, and Robert P. Ficciardi<sup>1</sup>. <sup>1</sup>Department of Microbiology, School of Dental Medicine, and Department of Biochemistry and Biophysics, School of Medicine, University of Pennsylvania, and <sup>2</sup>SARC-Frederick Cancer Research and Development Center, <sup>3</sup>Developmental Therapeutics Program, National Cancer Institute.

Kaposi's sarcoma-associated herpesvirus (KSHV) or human herpesvirus 8 (HHV-8) is a newly identified herpesvirus with tumorigenic potential. The 140 kb dsDNA genome of KSHV has been sequenced, which reveals that KSHV encodes all its own proteins required for viral replication, including a viral DNA polymerase (Pol-8) and a processivity factor (PF-8). We have cloned Pol-8 and PF-8 and expressed both proteins *in vitro*. Although PF-8 has no catalytic activity, the processivity of DNA synthesis by Pol-8 strongly depends on the presence of PF-8; while Pol-8 itself can only efficiently incorporate several nucleotides before dissociating from the DNA template, PF-8 specifically forms a complex with Pol-8 and allows it to processively synthesize fully-extended DNA. Since both Pol-8 and PF-8 are apparently essential for viral DNA replication and since they cannot be substituted by cellular or other viral proteins, they are potentially excellent antiviral targets. Here, we describe a rapid plate assay which is suitable for robotic high throughput screening of antiviral agents against Pol-8 and PF-8. The assay allows the measurement of not only the total DNA synthesis activity but also the processivity of the DNA synthesis. Any inhibitory effect by the screened compounds against the total DNA synthesis activity and/or the processivity would reflect potential antiviral activity targeting against Pol-8 and/or PF-8. Particularly, since PF-8 is highly specific for Pol-8, the discovery of antiviral agents against PF-8 may lead to more specific antiviral therapies with minimal toxicity to host cells as compared to the use of available anti-herpesvirus drugs.

**#173** Inhibition of translation initiation in cancer therapy. Aktas Huseyin, Palakurthi Sangeetha S, Fluckiger Rudolf, Changolkar Arun, and Halperin Jose A. *Laboratory for Membrane Transport, Harvard Medical School, 240 Longwood Ave., Boston, MA 02115.*

Translation initiation plays a critical role in regulation of cell growth because most oncogenes are encoded by mRNAs with highly structured 5'UTRs and their translation is highly dependent on translation initiation factors. Thus, translation initiation factors represent excellent targets for anticancer drugs. We present here evidence that the anti-cancer effect of two distinct compounds, clotrimazole (CLT) and the n-3 PUFA eicosapentaenoic acid (EPA), is mediated by inhibition of translation initiation. Intracellular  $Ca^{++}$  measurements show that CLT and EPA partially deplete intracellular  $Ca^{++}$  stores. This activates the protein kinase R (PKR) which phosphorylates and inhibits the translation initiation factor eIF2 $\alpha$ . This was demonstrated directly by immunoprecipitation of <sup>32</sup>P-labeled eIF2 $\alpha$ , and by experiments in cells expressing either a dominant negative PKR or a non-phosphorylatable mutant of eIF2 $\alpha$  (eIF2 $\alpha$ -51A). Phosphorylation of eIF2 $\alpha$  inhibits translation initiation, as demonstrated by a shift in the ribosomal profile of CLT- and EPA-treated cells from heavy to lighter polysomes. Inhibition of translation initiation by CLT and EPA preferentially reduces synthesis and expression of growth-promoting proteins such as G1 cyclins and Ras, but not of  $\beta$ -actin or ubiquitin, as demonstrated by Northern and Western blot analysis, and by <sup>35</sup>S-met-cys pulse labeling experiments. Consistently, CLT and EPA blocked cell cycle progression in G1, without affecting the expression of cyclin D1 mRNA. Further, we confirmed the potent anti-cancer effect of both CLT and EPA in mouse models of experimental cancer. In tumors, both compounds abrogate the expression of cyclin D1 and increase the fraction of cells in G1-G0 phase of the cell cycle. Epidemiological studies show that populations consuming diets rich in EPA-containing fish oils have a remarkably low incidence of cancer. Thus, our work strongly supports the notion that inhibitors of translation initiation represent a promising new class of agents for treatment and perhaps prevention of cancer.

**#174** Inhibition of translation initiation mediates anti-cancer effects of Clotrimazole. Aktas Huseyin, Fluckiger Rudolf, Changolkar Arun, Palakurthi Sangeetha, S and Halperin Jose A. *Laboratory for Membrane Transport, Harvard Medical School, 240 Longwood Ave., Boston, MA 02115.*

Clotrimazole (CLT) inhibits cell proliferation *in vitro* and tumor growth *in vivo*. Because of its potential use in cancer therapy we investigated the molecular basis of anti-proliferative activity of CLT. CLT depletes  $Ca^{++}$  stores by releasing  $Ca^{++}$  from intracellular stores and inhibiting store



regulated  $Ca^{++}$  influx. Depletion of  $Ca^{++}$  stores inhibits translation initiation (TI). Because TI plays a critical role in cell growth, we hypothesized that inhibition of TI through depletion of  $Ca^{++}$  stores mediates the anti-cancer effects of CLT.

CLT inhibits protein synthesis by 50%. Inhibition of protein synthesis is caused by depletion of  $Ca^{++}$  stores because cells cultured with CLT and then washed and pulse-labeled in  $Ca^{++}$  containing media synthesize protein at a rate comparable to untreated cells while similarly treated cells labeled in  $Ca^{++}$  free media synthesize protein at 50% of control level. Treatment with CLT shifts the polysome profile from heavy polyribosomes toward lighter ones confirming that CLT inhibits protein synthesis at the level of TI. CLT causes phosphorylation and inactivation of eIF2 $\alpha$ . This effect of CLT is abrogated by overexpression of dominant negative mutant of the eIF2 $\alpha$  kinase (PKR-K296) or constitutively active mutant of eIF2 $\alpha$  (eIF2 $\alpha$ -51A). Cells over-expressing eIF2 $\alpha$ -51A and PKR-K296 are also resistant to inhibition of protein synthesis and cell growth by CLT. These results indicate that depletion of  $Ca^{++}$  stores by CLT causes inhibition of TI by activating PKR. Inhibition of TI preferentially blocks translation of mRNAs with complex 5' UTRs, including those coding for oncogenes and G1 cyclins. Consistently, CLT inhibits synthesis and expression of G1 cyclins and block cell cycle in G1. In animal models of cancer, CLT inhibits tumor growth, increases fraction of cancer cells in G0-G1 and inhibits expression of cyclin D1 and cyclin E in tumors, all with minimal toxicity. These results define TI as a potentially useful target for cancer therapy.

**#175 Calcium depletion, eIF2 $\alpha$  phosphorylation and cell cycle inhibition mediate the anti-cancer effect of eicosapentaenoic acid.** Palakurthi Sangeetha S, Fluckiger Rudolf, Aktas Huseyin, Changolkar Arun, Halperin Jose A. *Harvard Medical School, 240 Longwood Ave., Boston, MA 02115.*

Epidemiological evidence suggest that populations consuming marine diets rich in the n-3 PUFA eicosapentaenoic acid (EPA) have a low incidence of cancer. A potential anti-cancer activity of EPA is further supported by *in vitro* and *in vivo* experimental studies. In this work we define the molecular basis for the anti-cancer activity of EPA. EPA affects cell growth by inhibiting translation initiation. This is a consequence of the ability of EPA to release  $Ca^{2+}$  from intracellular stores while inhibiting their refilling via capacitative  $Ca^{2+}$  influx through the plasma membrane, as shown in Fura-2 loaded 3T3 cells to follow EPA-induced changes in cytosolic  $Ca^{2+}$ . This dual effect of EPA partially depletes intracellular  $Ca^{2+}$  stores which activates the eIF2 $\alpha$  kinase, protein kinase R (PKR). PKR phosphorylates and thereby inhibits eIF2 $\alpha$ , a rate limiting step in translation initiation. This results in partial inhibition of protein synthesis at the level of translation initiation, as demonstrated by pulse-labeling with  $^{35}S$ -met/cyst and by the shift in the polysome profile from heavy to light polyribosomes. EPA-induced phosphorylation of eIF2 $\alpha$ , as well as inhibition of both protein synthesis and cell growth were reversed by over expression of dominant negative mutant of PKR (PKR-K296) or a constitutively active nonphosphorylatable mutant of eIF2 $\alpha$  (eIF2 $\alpha$ -51A). EPA-mediated inhibition of translation initiation preferentially reduces the synthesis and expression of proteins coded for by mRNAs with highly structured 5'-UTR including cyclin D1, cyclin E and Ras. This abrogates the activity of cdk's necessary for progression into S phase and causes cell cycle arrest in G1. Consistently, EPA inhibits tumor growth in an animal model of experimental cancer causing reduction in the expression of cyclin D1. These results define EPA as an inhibitor of translation initiation, an emerging new class of compounds for the treatment and perhaps prevention of cancer.

**#176 Elongation factor-2 kinase: A unique calmodulin-dependent kinase as a potential therapeutic target.** Parmer, T.G., Vyas, V., Ward, M.D., Hua, S., Kearney, T.J. and Halt, W.N. *The Cancer Institute of New Jersey, Dept. of Medicine and Pharmacology UMDNJ-Robert Wood Johnson Medical School, New Brunswick, N.J.*

Protein kinases are attractive targets for anticancer therapies since they often lead to uncontrolled growth of cancer cells. Yet, the utility of protein kinases as targets may be limited by their structural similarities. We describe a protein kinase whose activity is markedly increased in cancer cells, and one that has characteristics distinct from most other kinase families.

Elongation factor-2 kinase (EF-2 kinase) is a calcium/calmodulin-dependent enzyme that phosphorylates a single known substrate, elongation factor-2. Purification and cloning of the kinase (Hait et al., *FEBS Lett.* 397:55-60, 1996; Ryazanov et al., *PNAS*, 94:4884-4889, 1997) revealed its unique amino acid sequence, defining it as representing a new superfamily of protein kinases.

EF-2 kinase activity is increased in a variety of malignant cell lines and in human cancer (Bagaglio et al., *Cancer Res.*, 53:2260-2264, 1993; Parmer et al., *Brit. J. Cancer*, 79:59-64, 1999). Its activity is regulated by serum and growth factors. In human breast cancer specimens EF-2 kinase activity is markedly increased compared to that of adjacent normal tissue and normal mammary epithelium obtained during mammoplasty.

Rottlerin, (R), a 5,7-dihydroxy-2,2-dimethyl-6-(2,4,6-trihydroxy-3-methyl-5-acetylbenzyl)-8-cinnamoyl-1,2-chromone, isolated from the pericarp of *Mallotus philippinensis*, was used in medieval times to treat cancers and is an inhibitor of EF-2 kinase. Treatment of cancer cells with R blocks cells

at  $G_0/G_1$ -S, produces cell death ( $IC_{50}$  = 2-5  $\mu$ M), and blocks IGF-I- and EGF-induced cell proliferation. In glioblastoma, the effects of R were augmented by BCNU and geldanamycin (an inhibitor of Hsp90). Studies are in progress using EF-2 kinase antisense to further define the potential of EF-2 kinase as a therapeutic target.

**#177 Three key active site residues in the C-terminal domain of human folypoly- $\gamma$ -glutamate synthetase identified by active site labeling and site-directed mutagenesis.** Sanghani, Sonal P., Sanghani, Parash C., and Moran, Richard G.

We have identified a region of the active site of human folypolyglutamate synthetase (FPGS). Three reactive cysteines in cytosolic FPGS from CEM cells were located in peptides that were highly conserved across species. The functions of the ionic amino acids in two of these peptides, located in the carboxy terminal domain, were studied by site-directed mutagenesis. When cDNAs containing mutations in on these peptides were transfected into AUXB1 cells, a CHO cell lacking FPGS activity, one mutant (D335A) did not complement the auxotrophy, and another (R377A) allowed only minimal growth. Recombinant baculoviruses were constructed and enzyme species were expressed in Sf9 cells; FPGS activity could not be detected in insect cells expressing abundant levels of these two mutant proteins nor in cells expressing a H338A mutant FPGS. The recombinant enzymes were purified to homogeneity. The major kinetic change detected for the H338A mutation was a 600-fold increase in the  $K_m$  for glutamic acid. For D335A, the binding of all three substrates (aminopterin, ATP, and glutamic acid) was affected. The  $k_{cat}$  of these two enzymes were not changed. For R377A, the  $K_m$  for glutamic acid was increased by 1500-fold, and there was a ~20-fold decrease in the  $k_{cat}$  of the reaction. The binding of  $K^+$  ion, a known activator of FPGS, was decreased by the D335A and H338A mutations. We conclude that D335, H338, and R377 all participate in the alignment of glutamic acid in the active site and that R377 is also involved in the mechanism of the reaction. (Supported by CA-39687.)

**#178 Tissue-specific expression of functional isoforms of folypoly- $\gamma$ -glutamate synthetase: a basis for targeting folate antimetabolites.** Turner, F.B., Andreassi, J.L., Ferguson, J.K., Titus, S.A., Taylor, S.M., Moran, R.G. *Departments of Pharmacology and Toxicology, Microbiology and Immunology, Medical College of Virginia, Virginia Commonwealth University*

Folates and folate antimetabolites are metabolically trapped in mammalian cells as polyglutamates, a process catalyzed by folypoly- $\gamma$ -glutamate synthetase (FPGS). Any difference in the active site of FPGS between tissues could potentially be used to direct cytotoxic antifolates or to change the pattern of toxicity from such drugs. We now demonstrate that such differences exist, at least in mouse tissues. Utilizing 5'-rapid amplification of cDNA ends, ribonuclease protection assays, transfection of cDNAs into FPGS deficient cells, and kinetic analysis of recombinant enzymes expressed in insect cells, it was determined that the species of active FPGS in mouse liver and kidney was different from that in several types of mouse tumor cells, bone marrow, and intestine. The amino terminal peptide of hepatic enzyme contained 18 amino acids not found in enzyme from dividing tissues. Each of the species of FPGS differing in initial sequence proved to encode functional enzyme, as judged by complementation of the FPGS-null phenotype in AUXB1 cells. Expression of these different FPGS species in insect cells and subsequent kinetic analysis revealed differences in substrate specificity for antifolates which matched the effects seen with crude enzyme isolates. In most tissues, the expression of one isozyme or the other was an all-or-nothing event. The tissue-specific selection of initial coding exons in different tissues underlies this phenomenon, suggesting the design of antifolates specific for activation by individual FPGS isoforms and, hence, tissue-selective targeting of antifolate therapy.

**#179 Relationship between NAD(PH):Quinone Oxidoreductase 1 (NQO1) levels in a series of stably transfected cell lines and susceptibility to antitumor quinones.** Wlinski, Shannon L., Swann, Elizabeth, Hargreaves, Robert, H.J., Butler, John, Moody, Christopher J. and Ross, David; *Univ. CO Hlth. Sci. Cntr., Denver, CO; Univ. Exeter, Exeter, UK; CRC, Manchester, UK; Salford Univ., Salford, UK.*

To investigate the importance of NQO1 activity in bioactivation of anti-tumor quinones, we have established a series of stably transfected cell lines derived from BE human colon adenocarcinoma cells. BE cells have no NQO1 activity due to a polymorphism in the NQO1 gene. The new cell lines, BE-NQ, stably express wild-type NQO1. BE-NQ7 cells that stably expressed the highest level of NQO1 were more susceptible to new and existing antitumor quinones as determined by MTT and colonogenic survival assays. BE and BE-NQ7 cells demonstrated no significant difference in toxicity when treated with ES936, a selective NQO1 inhibitor. Inhibition of NQO1 protected BE-NQ7 cells from toxicity induced by streptonigrin, ES921 (an indolequinone) and RH1 (an azlindylbenzoquinone). These three compounds were the most selectively toxic to BE-NQ7 cells and were further evaluated in a panel of 5 BE-NQ cell lines expressing a range of NQO1 activities. Streptonigrin, RH1 and ES921 demonstrated a threshold effect with no significant increase in toxicity to BE-NQ2 cells with NQO1 activity of 23 nmol/min/mg. In four BE-NQ cell lines with NQO1

actively levels between 77 and 433 nmol/min/mg, streptonigrin and RH1 exhibited maximal toxicity suggesting a sharp dose response curve between the no effect level (22 nmol/min/mg NQO1) and maximal effect level (>77 nmol/min/mg NQO1). These data provide unequivocal evidence that NQO1 can bioactivate antitumor quinones in this system and suggest that a threshold level of NQO1 activity is required to initiate toxic events. This work was supported by National Institutes of Health Grant CA51210 and The Cancer Research Campaign.

**#180 Interleukin-13 receptor as a specific molecular target for cytotoxic therapy of human renal cell carcinoma in a xenograft model.** Husain, S.R., and Puri, R.K. *Laboratory of Molecular Tumor Biology, Division of Cellular and Gene Therapies, CBER, FDA, Bethesda, Maryland 20892.*

Renal cell carcinoma (RCC) is the seventh leading cause of malignant tumors with an estimated incidence of >30,000 new cases per year in the US. Because of limited anti-tumor activity of chemo- and/or immunotherapy, an alternative receptor-mediated targeted tumor therapy was sought. We have discovered that the interleukin-13 receptor (IL-13R) is abundantly expressed in many RCC cell lines and is an excellent target for a chimeric protein composed of IL-13 and truncated *Pseudomonas* exotoxin (IL-13 toxin). MA-RCC, a tumorigenic cell line in nude mice, expressed a large number (~5013 sites/cell) of high affinity IL-13R and was highly sensitive to IL-13 toxin *in vitro*. In an *in vivo* model, six intratumoral injections of IL-13 toxin (250 µg/Kg) on alternate days (QOD) resulted in complete elimination of established subcutaneous human RCC tumors (40 mm<sup>3</sup>) in all six mice. The tumors also regressed completely by twice a day intraperitoneal injections of 50 µg/kg of toxin for five days in three out of six mice. Five daily intravenous injections of 50 µg/Kg of toxin suppressed tumor growth by 60 ± 15% in all mice (n = 6). The incomplete disappearance of tumors may be due to the short half-life of IL-13 toxin in serum (t<sub>1/2α</sub> 8 min, t<sub>1/2β</sub> ~90 min). This promising novel IL-13 receptor targeted cytotoxin is being developed for the treatment of advanced RCC.

**#181 Molecular motors as targets of drug development.** Middleton, Kim M., Nelson, Joshua and Davis, Ashley. *Cytoskeleton, Inc. 1650 Fillmore Street, #240, Denver, CO 80206, USA.*

Microtubule based motors of the eukaryotic kinesin family represent an important class of cytoskeletal proteins. They have been shown to be essential for many biological functions, including cellular organization and motility, intracellular trafficking, axonal transport and cell division. At Cytoskeleton Inc. we are exploring the possibility that the kinesins would make excellent targets for the therapeutic intervention in a number of human conditions, including cancer. This poster describes the progress that we have made in the development of a novel, inexpensive and robust HTS assay (CytodyNAMIX-KI screens). These screens comprise one aspect of our anti-kinesin drug discovery program and constitute part of our general technology platform aimed at targeting a range of cytoskeletal proteins for therapeutic drug discovery. This research was sponsored by the NIH Small Business Innovative Research Program.

**#182 Novel antitumor 2-cyanoaziridines bind thiols, perturb mitochondrial membrane potential and induce apoptosis in solid tumors.** Dorr, R., Dvorakova, K., Iyengar, B., Remers, W., *Colleges of Medicine and Pharmacy, Arizona Cancer Center, The University of Arizona, Tucson, AZ 85724, U.S.A.*

A series of 2-cyanoaziridines-1-carboxamides were synthesized with substitutions of the carboxamide nitrogen with various alkyl and aryl substituents to yield a group of potent antitumor agents. These agents inhibit the growth of human cancer cell lines *in vitro* with IC<sub>50</sub> values in the low µM range for continuous exposures using the SRB protein assay. More lipophilic substituents had greater potency (r<sup>2</sup> = 0.49), with the exception of bulky groups such as *t*-butyl. Sensitive cell lines included parental and multidrug resistant (MDR) human MCF-7 breast cancers, 8226 myelomas, WiDr colon cancers, and L-1210 murine leukemias. Analogs with halogenated phenyl substituents were substantially more potent in solid tumors over leukemic cell lines. The simple phenyl-substituted compound, was also active in fresh human tumors in colony forming assays in soft agar, with particular activity in fresh melanoma and ovarian cancer cells. This agent, at a dose of 100 mg/Kg, produced antitumor activity *in vivo* in SCID mice bearing human MDR 8226 myeloma and there was no evidence of myelosuppression, a feature shared with the cyclized aziridine compound, imexon. Mechanistic studies with these agents have shown binding to sulfur moieties of endogenous thiols, but not to nucleophilic atoms in DNA. With unsubstituted 2-cyanoaziridine-1-carboxamide, sulfur binding occurs via the aziridine, whereas substituted compounds bind via the cyano nitrogen. As a result of this binding, apoptosis is induced evidenced by morphologic criteria, annexin V binding and DNA strand breaks. Treated cells also show pronounced mitochondrial swelling and loss of mitochondrial membrane potential, detected by CMXros labeling in flow cytometry assays. Overall, there are several unique features of these agents. These include activity in MDR tumors, lack of myelosuppression, and thiol binding with mitochondrial perturbation leading to apoptosis. These findings

suggest that substituted 2-cyanoaziridine-1-carboxamides comprise intriguing agents for clinical development as novel agents for resistant solid tumor therapy.

**#184 Prostate carcinoma cell death induction by inhibiting the activity of the 26S proteasome complex using PS-341 a novel dipeptidyl boronate.** Herrmann, J.L., Yang, H., Logothetis, C.J., Elliot, P., Adams, J., McConkey, D., and Papandreou, C.N. *Departments of Genitourinary Medical Oncology and Cell Biology, The University of Texas, M.D. Anderson Cancer Center, Houston, TX 77030 and ProScript, Inc., Boston, MA 02139.*

The ubiquitin-proteasome system regulates the proteolytic destruction of key inhibitors of cell cycle progression that either have either genuine tumor suppressor activity or those having potential tumor suppressor function. Recent evidence indicates that a unique mechanism of inactivating the cyclin-dependent kinase inhibitor p27<sup>Kip1</sup>, a candidate tumor suppressor, is "selective" degradation of p27<sup>Kip1</sup> by the proteasome complex. For these reasons, the 26S proteasome complex has emerged as a novel target for anti-cancer therapy development. Here we investigate the unique activities of PS-341, a novel dipeptidyl boronate inhibitor of the chymotrypsin site of the 26S proteasome, which is being evaluated clinically. PS-341, but not an inactive enantiomer, blocked the activation of NF-κB by blocking the proteasomal-mediated proteolysis of IκBα, the endogenous inhibitor of NF-κB nuclear import. Treatment of DU145 cells with pharmacologically achievable concentrations of PS-341 effectively stabilized the levels of cyclin-dependent kinase inhibitors p21<sup>Waf1</sup> and p27<sup>Kip1</sup>. Stabilization of these proteasome substrates preceded the onset of DU145 cell death. Treatment of LNCaP cells with PS-341 substantially stabilized wild type p53 protein while down-regulating the level of the anti-apoptotic bcl-X<sub>L</sub> protein. These events preceded PS-341-induced LNCaP cell death induction through a pathway that could be inhibited by z-VAD-FMK, a broad-spectrum inhibitor of caspases. In addition, ectopic expression of bcl-2, a pro-survival factor implicated in prostate cancer progression and resistance to cytotoxic therapy, inhibited the kinetics of cell death induction by PS-341. Unlike PS-341, its inactive enantiomer PS-398 was incapable of inducing cell death, underscoring the molecular specificity of PS-341. Treatment of LNCaP and DU145 cells with PS-341 activated two stress kinases c-jun N-terminal kinase-1 (JNK1) the p38 implicated in apoptosis signaling. The potential role of JNK1 and p38 in cell death induction following the inhibition of proteasomal activity is under investigation. These studies are designed to help us refine the clinical application of proteasome inhibitors for prostate cancer. This work was supported by awards from the Association for the Cure of Cancer of the Prostate (CaP CURE) to C.N.P. and C.J.L.

**#185 Cellular pharmacology of novel inhibitors of ras protein palmitoylation.** De Vos, Mackenzie L., Lawrence, David S., and Smith, Charles D. *Dept. of Pharmacology, H078, Pennsylvania State University, College of Medicine, Hershey, PA 17033.*

Post-translational processing of ras proteins involves a series of modifications at the C-terminus which is required for targeting the protein to the plasma membrane. For proteins encoded by H- and N-ras, this includes attachment of a palmitoyl moiety through thioester linkages. We have found that the natural product cerulenin inhibits protein palmitoylation, and have synthesized a series of analogs as a potential new class of anti-ras drugs. The compound *cis*-2,3-epoxy-4-oxononadecanamide (16C) was designed as a palmitoyl analog of cerulenin and inhibits protein palmitoylation without affecting fatty acid synthase. In contrast, the cerulenin analog *cis*-2,3-epoxy-4-oxododecanamide (9C) effectively inhibits both



protein palmitoylation and fatty acid synthase. To study the cellular pharmacology of these compounds, tritium-labeled 9C and 16C were prepared by catalytic incorporation of  $^3\text{H}_2$  into unsaturated precursors. Equilibrium dialysis studies demonstrated that [ $^3\text{H}$ ]9C is extensively bound by serum proteins associated with covalent alkylation of serum albumin. This presumably involves interaction of the epoxy moiety with sulfhydryls of albumin as has been demonstrated for interaction of cerulenin with fatty acid synthase. In contrast, albumin binding and alkylation by [ $^3\text{H}$ ]16C is considerably lower. Cellular accumulation of [ $^3\text{H}$ ]9C by T24 bladder carcinoma cells was reached a plateau by 30 min, whereas [ $^3\text{H}$ ]16C continued to accumulate for at least 120 min, resulting in 3-fold higher intracellular levels of [ $^3\text{H}$ ]16C at that time. Uptake of [ $^3\text{H}$ ]9C and [ $^3\text{H}$ ]16C were markedly reduced by the presence of 50% serum in the medium. Both [ $^3\text{H}$ ]9C and [ $^3\text{H}$ ]16C alkylated proteins in T24 cells; however, the labeling patterns were much different for the two compounds. Whereas [ $^3\text{H}$ ]16C alkylated only a few proteins, predominantly proteins of approx. 250, 67, 57, 22 and 7 kDa, [ $^3\text{H}$ ]9C alkylated a large number of proteins, some of which overlap with those alkylated by [ $^3\text{H}$ ]16C. Since both compounds inhibit p21 acylation, the commonly labeled proteins are candidates for the heretofore uncharacterized human protein palmitoyltransferase. Efforts to isolate and sequence the targets of [ $^3\text{H}$ ]16C are currently underway.

**#186 Synthetic and natural activators of the nuclear receptor FXR are inhibitors of tumor cell proliferation and induce apoptosis.** Niesor Eric J., Flach Jean, Guyon-Gellin Yves and Bentzen Craig L. *Symphar 243 Route des Fayards 1290 Versoix Geneva Switzerland*

The hypothesis that the activation of the nuclear receptor FXR is biochemically linked to the induction of apoptosis was investigated using derivatives of synthetic and natural activators of FXR. Bile acids have been recently found to be natural ligands and activators of FXR (Science 284, 1362-1368, 1999). We have previously shown that a potent synthetic FXR agonist SR-12813 (18 fold at 5  $\mu\text{M}$ ) is antiproliferative (Drugs of the Future 24(4), 431-438, 1999). We tested analogs of SR-12813 [2-(3,5-di-*t*-butyl-4-hydroxyphenyl)-ethylidene-1,1-bis-phosphonate] and various bile acids in the colon carcinoma cell line SW620 in an attempt to correlate FXR activation with antiproliferative and apoptotic activities. Substitution of the *t*-butyl moiety of the bisphosphonate ester by methoxy groups led to a complete loss of FXR activation (0.94 fold at 5  $\mu\text{M}$ ) and antiproliferative activity (IC50 > 100  $\mu\text{M}$ ) and shortening the ethylidene linker also led to suppression of both activities. We compared the natural FXR activators chenodeoxycholic acid (CDCA), deoxycholic acid (DCA) and lithocholic acid (LCA) with cholic acid (CA), which unexpectedly does not activate FXR. A direct correlation was observed between FXR activation and antiproliferative activity with IC50s of about 50  $\mu\text{M}$  for CDCA, DCA, LCA and >200  $\mu\text{M}$  for CA. As expected the lauro and glyco conjugates of CDCA, DCA and CA did not affect SW620 cell proliferation (IC50 > 200  $\mu\text{M}$ ). CDCA and DCA but not CA induced apoptosis in tumor cells. The structure-activity relationships observed with both the synthetic and natural FXR agonists support the hypothesis that FXR plays a key role in the control of cell proliferation and in the induction of apoptosis. SR-45023A, which is the most potent antiproliferative analog of SR-12813 (IC50 5  $\mu\text{M}$ ), rapidly induces apoptosis and was chosen for clinical development.

**#187 Protein hydroxylations as molecular targets for cancer therapeutics: Deferiprone is a candidate for probing multitargeted inhibition.** Hanauske-Abel, Hartmut M.; Slowinska, Bozena; McCaffrey, Timothy M.; Cracchiolo, Bernadette M.; Hanauske, Axel-R. *Weill Med. Coll. of Cornell University, New York, NY; University of Med. and Dent., Newark, NJ; Ctr. for Hematol./Oncol., Munich, Germany.*

At least three criteria identify a molecular target for cancer therapeutics: 1. Its steric and electronic architecture must be known; 2. It must be of strategic importance in cancer biology, preferentially serving several non-redundant functions; 3. Its failure should trigger aggregate deficiencies in the tumorigenic cascade. We hypothesize that the enzymes prolyl 4-, aspartyl 3-, and deoxyhypusyl hydroxylase (P4H, A3H, DOHH, respectively), which mediate posttranslational protein hydroxylations, represent such a molecular target. Collagens and fibrillins, key proteins for angiogenesis, rely on P4H and A3H; DOHH enables cell cycle progression via translation factor eIF-5A. These non-heme iron dioxygenases display very similar active site pockets and catalytic cycles, a fact we used for the modeling-assisted identification of the iron decarboxation drug deferiprone as a putative inhibitor, multitargeted against human P4H, A3H, and DOHH. Deferiprone inhibited recombinantly expressed P4H and A3H, and cellular DOHH at concentrations achieved in patients (serum peaks, ~250  $\mu\text{M}$ ). As determined by metabolic labeling and mass spectroscopy, deferiprone completely blocked cellular formation of peptidyl hydroxyproline (ID<sub>50</sub>, 120  $\mu\text{M}$ ) and peptidyl hypusine (ID<sub>50</sub>, 100  $\mu\text{M}$ ), and at 250  $\mu\text{M}$  half-maximally inhibited peptidyl hydroxyaspartate, all without affecting overall protein synthesis. P4H and A3H inhibition caused quantitative deficiency of collagen-like and functional deficiency of fibrillin-like matrix proteins, DOHH suppression caused cell cycle arrest at the G1-S boundary. Ultrastructurally, P4H and A3H inhibition in fibroblasts exclusively affected the appearance of the rough endoplasmic reticulum, the Golgi, and the lysosomes, consistent with intracellular rerouting of underhydroxylated material. eIF-5A deficiency due to deferiprone-mediated DOHH inhibition in IM-9

cells caused marked changes in the polysomal mRNA populations, as shown by RT-PCR-based differential display. A 386 bp sequence of the first deferiprone-sensitive mRNA, which we termed 'Transit Enabler 1', had two matches in the NCBI database, one in the human cervical carcinoma cell line HeLa 3 and one in the human epitheloid lung cancer Lu1. Thus, the DOHH-dependent, deferiprone-sensitive Transit Enabler 1 is lineage-independent. Our findings with the pilot compound deferiprone establish that multitargeted suppression of protein hydroxylation is feasible, and represents a promising target for the discovery of novel cancer therapeutics.

**#188 Malonyl-Coenzyme-A is a potential mediator of cytotoxicity induced by fatty acid synthase inhibition in human breast cancer cells and xenografts.** Pizer, Ellen S., Thupari, Jagan, Han, Wan Fang, Pinn, Michael L., Chrest, Francis J., Townsend, Craig A., and Kuhajda, Francis P. *The Johns Hopkins University and The National Institute on Aging.*

A biologically aggressive subset of human breast cancers and other malignancies are characterized by elevated fatty acid synthase enzyme expression, elevated fatty acid synthesis and selective sensitivity to pharmacologic inhibition of fatty acid synthase activity by cerulenin or the novel compound, C75. Excess ambient fatty acid does not substantially ameliorate the cytotoxicity of fatty acid synthase inhibitors, suggesting an alternative mechanism to fatty acid withdrawal. In this study, inhibition of fatty acid synthesis at the physiologically regulated step of carboxylation of acetyl-CoA to malonyl-CoA by 5-(tetradecyloxy)-2-furoic acid (TOFA) was not cytotoxic to breast cancer cells in clonogenic assays. Fatty acid synthase inhibitors induced a rapid increase in intracellular malonyl-CoA to several fold above control levels, while TOFA reduced intracellular malonyl-CoA by 60%. Exposure of breast cancer cells to FAS and ACC inhibition in combination resulted in substantially reduced cytotoxicity and apoptosis compared to FAS inhibition alone, suggesting that malonyl-CoA accumulation may be an important mediator of the cytotoxic effects of FAS inhibitors. Subcutaneous xenografts of MCF7 breast cancer cells in nude mice treated with C75 showed fatty acid synthesis inhibition, apoptosis, and inhibition of tumor growth to less than one eighth of controls, without comparable toxicity in normal tissues. The data suggest that differences in intermediary metabolism render tumor cells susceptible to toxic fluxes in malonyl-CoA, both *in vitro* and *in vivo*.

**#189 Novel lysine-spermine conjugate alters *in vitro* and *in vivo* tumor cell growth through inhibition of polyamine transport.** Weeks, Reitha S., Vanderwerf, Scott M., Carlson, C. Lance, Burns, Mark R., O'Day, Christine L., Cal, Feng and Webb, Heather K. *Oridigm Corp., Seattle, WA.*

Because polyamines are ubiquitous molecules with an important role in regulating cell growth, they are a target for cancer therapeutic development. To effectively inhibit cell growth through polyamine depletion, one needs to inhibit both polyamine synthesis and import. We have identified ORI 1202, an N<sup>1</sup>-spermine-L-lysine amide, as an effective polyamine transport inhibitor. ORI 1202 inhibits polyamine transport in the MDA-MB-231 human breast carcinoma cell line with K<sub>i</sub> values in the 20-100 nM range. ORI 1202 does not accumulate in cells but it prevents the cellular accumulation of spermidine. After a 1 h exposure to ORI 1202, spermidine transport activity recovers slowly over 24 h. ORI 1202 effectively inhibits cell growth when used in conjunction with the polyamine synthesis inhibitor  $\alpha$ -difluoromethylornithine (DFMO). Human breast, prostate, and bladder cell lines show ORI 1202 IC<sub>50</sub> values in the low micromolar range when tested in a six day growth assay with DFMO. Cells retain  $\geq 90\%$  viability. The cytostatic effect can be attributed to an ~90% reduction in the intracellular levels of putrescine and spermidine. ORI 1202 with DFMO was able to inhibit human prostate and breast murine xenograft growth by ~80%. ORI 1202 was given i.p., 3x/day (135 mg/kg/day) with 3% DFMO in the drinking water. Polyamine depletion therapy provides a cytostatic therapy that could be useful against cancer and other diseases resulting from uncontrolled cell growth.

**#190 Pharmacological induction of phosphatidylinositol accumulation is associated with cytotoxicity of neoplastic cells.** Finney, R.E., Nudelman, E., Shaffer, S.A., White, T., Burslen, S., Leer, L.L., Wang, N., Waggoner, D., Singer, J.W., and Lewis, R.A. *Cell Therapeutics, Inc., Seattle, WA 98119.*

Enhanced trafficking of phospholipids through phosphatidic acid (PA) in tumor cells has been cited among the effects of certain oncogenes (e.g. *ras*, *fos*, and *src*) and growth factors (e.g. PDGF, EGF, FGF, Insulin). PA, in turn, has direct targets implicated in neoplastic transformation (e.g. PLC- $\gamma$ , Ras-Gap, and Raf-1) and is a key intermediate for biosynthesis of other biologically active phospholipids that include the intracellular signaling molecules diacylglycerol and phosphatidylinositol (PI) polyphosphates as well as the mitogen, lysophosphatidic acid. PA is also precursor for prevalent anionic phospholipids that include PI and cardiolipin. We demonstrate that the dysregulation of phospholipid metabolism in neoplastic cells can be exploited pharmacologically to produce a two-to-three fold elevation in the cellular concentration of PI in tumor cell lines, with attendant cytotoxicity. CT-2584, a cancer chemotherapeutic drug candidate currently in Phase II clinical trials, induced PI accumulation at cytotoxic concentrations and well prior to tumor cell death. Cytotoxicity was observed in a broad spectrum of tumor cell lines including those resistant to

multiple drugs. In contrast to the effects of CT-2584, cisplatin did not induce accumulation of PI in NCI-H23, a non-small cell lung carcinoma cell line, indicating that PI elevation by CT-2584 is not a general consequence of chemotherapy-induced cell death. The induced PI appears to be derived from PC, as indicated by reduced PC mass in CT-2584 treated cells and by mass spectrometric analyses which indicates that acyl chain compositions of bulk PC and CT-2584 induced PI are similar. Propranolol, an inhibitor of PA phosphohydrolysis, augments PI accumulation in tumor cell lines and is synergistic with CT-2584 in cytotoxicity assays. Consistent with the expected biophysical effects of anionic phospholipids on cellular membranes, especially those rich in calcium, CT-2584 was associated with disruption and swelling of endoplasmic reticulum and mitochondria. We conclude that CT-2584 effects a novel tumor-selective mechanism of action involving modulation of phospholipid metabolism.

**#191 The angiostatic sterol squalamine is a calmodulin chaperone.** Chen Q., Williams J.L., Anderson M., Kinney W.K., and Zasloff M. *Magainin Pharmaceuticals, Plymouth Meeting, PA, USA*

Squalamine is a cationic sterol initially isolated from tissues of the dogfish shark as a broad spectrum antimicrobial. Subsequent studies have shown it to exhibit potent anti-angiogenic activity in animal systems. Squalamine has recently entered a Phase II trial for the treatment of patients with stage IIIb or IV NSCLC, in concurrent therapy with paclitaxel and carboplatin. We report here the results of elucidating the mechanism of action for squalamine. Purification and partial sequencing of a proteinaceous squalamine binding activity isolated from human placenta revealed its identity to be calmodulin (CaM). Studies on the interaction between squalamine and calmodulin demonstrate that specific interaction between sterol and protein occurs with a  $K_d$  of about 5  $\mu$ M for both calcium-free and calcium-bound forms of CaM. The site of physical interaction between squalamine and CaM does not overlap with that for a number of known CaM antagonists, but a peptide substrate for CaM can displace squalamine from CaM. Fluorescently tagged squalamine rapidly accumulates in the Golgi/ER membrane system following exposure of HUVECs and immunofluorescent techniques reveal a similar rapid relocalization of CaM from a homogeneous distribution to the perinuclear Golgi/ER system. F-actin stress fibers in HUVECs are disrupted subsequent to squalamine treatment, and a profound alteration in cell shape also occurs through inhibition of CaM dependent enzymes. We propose that squalamine's mechanism of action involves specific entry of squalamine into endothelial cells and intracellular redistribution of CaM that depletes CaM in certain cellular compartments and enriches CaM in others, but without necessarily inhibiting CaM function. Squalamine therefore represents the first of a new class of biological modifiers that act as CaM chaperones, altering cellular responses to stimuli that increase intracellular calcium concentrations.

**#192 Inhibition of tumor growth in treatment of human colon cancer and non-small cell lung cancer xenografts by novel dibenzazepines, NC381 and NC384.** Liu, C.N., Mao, H., Wang, X.J., Halperin, J., Ferdnandi, E.S., and Ely, G. *University of Nebraska Medical Center, Omaha, NE; Harvard Medical School, Boston, MA; Lorus Therapeutics, Inc., Markham, Ontario, Canada.*

NC381 and NC384 are novel dibenzazepine compounds which showed potent anti-cell proliferation activity against a panel of human cancer cells. Similar to colrimazole, NC381 and NC384 block cell cycle progression in G1 through  $Ca^{2+}$  store-mediated inhibition of translation initiation. In an *in vitro* study using HT-29 (colon cancer) and Calu-6 (non-small cell lung cancer) cells, the  $IC_{50}$  of NC381 and NC384 ranged from 0.5–0.9  $\mu$ M. In an *in vivo* HT-29 model study, NC384 and NC381 were administered by s.c. injection at a dose of 80 mg/kg/day (three cycles of 5 daily doses/week for 3 weeks) and orally by gavage (NC384 only) at the same dose level for 21 consecutive days. 5-FU (15 mg/kg/daily  $\times$  5, i.p.) and CPT-11 (20 mg/kg/daily  $\times$  5, i.p.) were used as positive controls. Based on tumor volume measurements, NC384 significantly inhibited HT-29 tumor growth with T/C values of 45.3% and 55.6%, respectively. Tumor growth inhibition was somewhat higher for CPT-11 (T/C, 37.6%) while inhibition by 5-FU (T/C = 87%) was not significant. Tumor growth inhibition was highest for the combination treatment of NC384 with CPT-11 (T/C, 29.8%) suggesting a possible additive effect. In a Calu-6 xenograft model, NC381 inhibited tumor growth (T/C, 62.3%;  $P = 0.02$ ) after s.c. injection at a dose of 80 mg/kg/day. Based on body weight observations and histology, there was no significant toxicity related to the treatments. These data indicated that NC384 was an effective and relatively non-toxic inhibitor of tumor growth in an HT-29 colon cancer xenograft model after both s.c. and oral administration. Although lower efficacy was shown in the Calu-6 model, both NC381 and NC384 represent a new class of compounds that may have potential efficacy in the treatment of cancer.

**SECTION 4: TUMOR PHYSIOLOGY: HYPOXIA, RADIOSENSITIZATION, AND NEW EXTRACELLULAR TARGETS**

**#193 Farnesyltransferase mediated radio-sensitization of human tumor xenografts expressing mutant H-ras.** Cohen-Jonathan, E.<sup>1</sup>, Muschel, R.J.<sup>1,2</sup>, McKenna, W.G.<sup>1</sup>, Hamilton, A.D.<sup>4</sup>, Sebti, S.M.<sup>5</sup>, Gibbs J.<sup>6</sup>, Oliff, A.<sup>6</sup>, Cerniglia, G.<sup>1</sup>, Knight, L.<sup>1</sup>, Mick, R.<sup>3</sup> and Bernhard, E.J.<sup>1</sup> *Depts. of Radiation Oncol., <sup>2</sup>Pathology and Lab. Med. and <sup>3</sup>Biostat. and Epidemiology; <sup>4</sup>Yale University; <sup>5</sup>University of South Florida; <sup>6</sup>Merck Research Laboratories.*

Ras activity depends upon membrane binding which is mediated by post-translational farnesylation of ras and can be blocked by farnesyltransferase inhibitors (FTI). FTI have been shown to radiosensitize H-ras transfected rodent cells and human tumor cells expressing activated H- or K-ras in tissue culture.

In order to determine whether treatment with FTI has clinical potential as a radiosensitizing agent, we studied the effect of farnesyltransferase inhibitor treatment on the radiosensitivity of two human tumor xenografts in nude mice: T24 bladder carcinoma cells expressing a mutated H-ras and HT-29 colon carcinoma cells expressing wild-type ras.

Ras prenylation was inhibited by intraperitoneal injection or osmotic pump administration of two different FTI (FTI-276 or L744,832). The effect of FTI on tumor cell radiation survival was determined by clonogenic survival comparing the plating efficiency of tumor cells from mice treated with FTI + radiation to mice receiving either FTI or radiation. FTI treatment resulted in significant radiosensitization in T24 tumors causing a 20–50 fold reduction in clonogenicity over radiation alone. The survival of HT-29 tumor cells was reduced by FTI treatment, but no synergistic effect was seen. These results were confirmed by tumor regrowth delay experiments. In comparison to control T24 tumors, tumors irradiated with 6 Gy showed a 12 day delay in attaining a size of 500 mm<sup>3</sup>. Animals treated with 30 mg/kg/day L744,832 alone exhibited a 6 day delay, while the combination of L744,832 plus radiation resulted in a 35 day regrowth delay. In contrast to increased tumor radiosensitivity, no alteration of the normal tissue response to radiation was detected.

These data demonstrate that FTIs are capable of radiosensitizing human tumors *in vivo*. Our studies also indicate that treatment with FTI+ irradiation does not increase radiation damage to cells expressing wild-type ras. These results suggest that FTI could act as a radiosensitizer of human tumors expressing mutated ras.

**#194 Preferential radiosensitization of MMR-deficient tumors by halogenated thymidine analogs.** Barry, Suzanne; Davis, Thomas; Schupp, Jane; Kinsella, Timothy. *Department of Radiation Oncology, Case Western Reserve University School of Medicine/University Hospitals of Cleveland, Cleveland, Ohio.*

Deficiency in DNA Mismatch Repair (MMR), particularly in MLH1 and MSH2 protein expression has recently been shown to impart cellular resistance to multiple types of chemotherapy agents. The observed drug resistance in MMR-deficient cells may be attributed to "damage tolerance", an inability of the cell to detect or respond to drug-induced DNA damage. The purine analog, 6-Thioguanine (6-TG) is used experimentally to define this phenotype.

Genetically matched cell systems differing in expression of either MLH1 (human IIC7116 colon cancer cells and murine MEF's) or MSH2 (human HEC endometrial cancer cells and E1a immortalized murine ES cells) proteins were used. Differential responses of these genetically matched MMR<sup>+</sup> and MMR<sup>-</sup> cell lines to either 6-TG or to the halogenated thymidine (dThd) analogs, IdUrd and BrdUrd were compared. These dThd analogs are used clinically as experimental sensitizing agents in radioresistant human cancers, and there is a direct correlation of levels of dThd analog-DNA incorporation and tumor radiosensitization. In contrast to a marked increase in cytotoxicity (>1 log cell kill) found with 6-TG exposures in MMR<sup>+</sup> (MLH1<sup>+</sup>, MSH2<sup>+</sup>) cells compared to MMR<sup>-</sup> cells, we found only modest cytotoxicity (<20% cell kill) in both MMR<sup>+</sup> and MMR<sup>-</sup> cell lines when treated with IdUrd or BrdUrd. However, the levels of halogenated dThd analogs in DNA were significantly lower (2–3x) in MMR<sup>+</sup> human and murine cells compared to MMR<sup>-</sup> cells. We also found no differences in the cellular metabolic pathways for dThd-analog-DNA incorporation, in both MMR<sup>-</sup> and MMR<sup>+</sup> cells. The higher DNA incorporation increased the radiation sensitivity in MMR-deficient cells, but not in MMR-proficient cells following pretreatment with IdUrd or BrdUrd, when compared to radiation alone.

These data suggest that the MMR system may participate in the recognition and subsequent removal of halogenated dThd analogs from DNA. Consequently, while MMR-deficient cells and tumor xenografts have shown intrinsic resistance to a large number of chemotherapeutic agents, the 5-halogenated dThd analogs appear to selectively target such cells for potential enhanced radiation sensitivity, while having little to no radiosensitization in normal MMR-proficient tissues.



**#195 Enhancement of the chemotherapeutic index of weakly-ionizing drugs by acute alterations of tumor pH.** Raghunand, N., Mahoney, B., Galons, J.-P., and Gillies, R. *University of Arizona Health Sciences Center, Cancer Center Division, Tucson, AZ 85724-5024, U.S.A.*

The extracellular pH ( $pH_e$ ) and intracellular pH ( $pH_i$ ) of tumors influence the effectiveness of chemotherapy by influencing drug uptake kinetics and the ionic equilibrium of weak acid and weak base drug molecules: weak-base drug molecules like mitoxantrone will tend to be retained in the more acidic compartments within a tumor, while weak-acid species like chlorambucil will tend to concentrate in the more alkaline compartments. We have recently shown that the chemotherapeutic effectiveness of doxorubicin, a weak-base, in a SCID mouse model of human breast carcinoma can be enhanced by subjecting the host mouse to chronic (>9 days)  $NaHCO_3$ -induced metabolic alkalosis concomitant with the drug therapy (Raghunand et al., *Br. J. Cancer*, 80, 1005-1011, 1999). Chronic administration of  $NaHCO_3$  to mice is undesirable due to potential hyponatremia and other metabolic disorders. The lifetime of free drug in a mouse is on the order of 1 hour following drug injection via the i.v. route. Thus, acute metabolic alkalosis, induced for durations of only 1-2 hours, may suffice to obtain the enhancement in efficiency of chemotherapy with a weak-base drug.  $^{31}P$  Magnetic Resonance Spectroscopy (MRS) allows the non-invasive measurement of  $pH_i$  and  $pH_e$  from the chemical shifts of endogenous inorganic phosphate and exogenous 3-aminopropylphosphonate (3-APP), respectively. We have measured  $pH_e$  and  $pH_i$  in C3H mammary adenocarcinoma tumors grown in syngeneic C3H/He host mice, as well as in control normal hind leg muscle tissue. Acute metabolic alkalosis or acidosis were demonstrably induced by bolus intraperitoneal injection or gavage administration of  $NaHCO_3$  or  $NH_4Cl$  to the host mice. Acute acidification induced by  $NH_4Cl$  is of the same magnitude in normal and tumor tissue. The intraperitoneal delivery of  $NaHCO_3$ , however, produced a far greater alkalization in tumor tissue as compared to control normal tissue. Consequently,  $NaHCO_3$  therapy is predicted to enhance the effectiveness of weak-base drugs like mitoxantrone. Our results predict that the optimum delay between intraperitoneal administration of  $NaHCO_3$  and drug injection is about 2 hours. Experiments combining  $NaHCO_3$ -induced acute alkalosis with chemotherapy using mitoxantrone are currently underway.

**#196 Tumor oxygenation during hormone ablation and chemotherapy.** N. Hansen-Aigenstaedt, P. Aigenstaedt, E.G. Achilles, B.R. Stoll, T.P. Padera, D. Fukumura, R. Kothe, W. R  ther and R.K. Jain *Massachusetts General Hospital, Children's Hospital, Harvard Medical School, Boston, MA, 02114, USA, University Hospital Hamburg, Dep. of Orthopaedic Surgery and Dep. of Hepato-Biliary Surgery, 20246 Hamburg, Germany.*

**Background:** Tumor oxygenation is the most important factor not only for tumor survival but also for successful tumor therapies since most therapies are oxygen dependent. Hormone ablation therapy lead to vessel regression but has also shown beneficial effects when combined with radiation therapy and chemotherapy. These findings are counterintuitive since vessel regression should reduce oxygen tension ( $pO_2$ ) in tumors, decreasing the effectiveness of radiotherapy and chemotherapy. To analyze tumor oxygenation under conditions of vessel regression, we have developed a novel *in vivo* system to measure  $pO_2$  and calculate oxygen consumption rates. The effects of hormone ablation on tumor oxygenation was compared with those of chemotherapy, an anti-neoplastic treatment that is not known to cause vessel regression. **Methods:** Androgen-dependent male mouse mammary carcinoma (Shionogi) was implanted into transparent skinfold chambers in male SCID mice. Thirteen days after the tumors were implanted, mice were treated with hormone ablation by castration, or continuous chemotherapy (doxorubicin, 6.5 mg/kg and cyclophosphamide, 100 mg/kg every seven days). **Results:** Tumors treated with hormone ablation led to tumor and vessel regression followed by an increase in  $pO_2$  coincident with regrowth. Chemotherapy led to tumor growth arrest characterized by constant oxygen consumption rate and elevated  $pO_2$ . Surprisingly we found improved tumor oxygenation during hormone ablation therapy. Furthermore we observed normalized vascular functions, vessels became less tortuous and had regular diameters. **Conclusions:** The improved tumor oxygenation and the effect on vascular functions may explain the observed beneficial effects of combined therapies.

**#197 Cytotoxic and radiosensitizing activity of anti-CD30-pokeweed antiviral protein immunotoxin against Hodgkin's lymphoma cells.** Narla, R.K., Meyers, D.E., Kils, D., and Uckun, F.M. *Drug Discovery Program, Parker Hughes Cancer Center, Hughes Institute, St. Paul, MN 55113.*

Reed-Sternberg cells of Hodgkin's disease express CD30 on their cell surface and provides unique opportunity to target antibody driven delivery of immunotoxin. This study aimed to determine the extent of Ber-H2 (anti-CD30)-pokeweed antiviral protein (PAP) immunotoxin induced cytotoxicity when used in combination with ionizing radiation in Hodgkin's lymphoma cells. Immunotoxin was prepared by covalently linking the anti-CD30 monoclonal antibody Ber-H2 to the plant hemitoxin PAP. Internalization of immunotoxin was demonstrated using confocal laser scanning microscopy. The cytotoxic activity of Ber-H2-PAP was assessed with MTT assays, clonogenic assays and *in situ*

TUNEL assays. To characterize the cell killing, specific mitochondrial dyes JC-1, DiIC1(5) and NAO were used to assess changes in mitochondrial membrane potential. For experiments in combination with radiation, cells were exposed to Ber-H2-PAP for 24 h prior to irradiation and cell survival was determined by clonogenic assays. Ber-H2-PAP selectively bound to CD30 cell surface receptors present on the Hodgkin's lymphoma cells and induced the internalization of receptor-immunotoxin complex. Ber-H2-PAP killed Hodgkin's lymphoma cells at picomolar concentrations, whereas no cytotoxicity against CD30-negative leukemic cells was observed. Treatment with 100 ng/ml of Ber-H2-PAP resulted in 99.0% and 98.7% inhibition of clonogenic growth of HS445 and RPMI6666 cells with  $IC_{50}$  values of 7.89 pM and 7.06 pM, respectively. Ber-H2-PAP depolarized the mitochondrial membranes of both cell lines in a dose- and time-dependent fashion. When the cells were exposed to 10 ng/ml or 25 ng/ml for 24 h prior to ionizing radiation, the radiation-induced killing was significantly enhanced in a dose-dependent fashion. The  $SF_2$  values (0.61 for control vs. 0.18 for treated in HS445; 0.54 for control vs. 0.12 for treated in RPMI6666) were significantly reduced when the cells were treated with Ber-H2-PAP (25 ng/ml) prior to radiation. In conclusion, Ber-H2-PAP has potent cytotoxic and radiosensitizing activities against Hodgkin's lymphoma cells. The present study establishes Ber-H2-PAP as a radiosensitizing cell-type specific cytotoxic agent against Hodgkin's lymphoma cells.

**#198 MGI 114 is an effective radiosensitizing agent against pancreatic carcinoma.** Eishihabi, Said, Kirkpatrick, John, Wang, Weixin, Freeman, James W., Herman, Terry, Sadeghi, Amir, Waters, Stephen J., MacDonald, John R., Miller, Alexander R. *Departments of Surgery, Division of Radiation Oncology, University of Texas Health Science Center at San Antonio, San Antonio, TX; MGI PHARMA, INC., Minnetonka, MN.*

Locally advanced pancreatic cancer is incurable by current multimodality therapy. In an effort to develop a clinically relevant therapeutic strategy, we evaluated the combination of MGI 114 (6-HMAF, irafulven), a semi-synthetic analog of illudin-S, with ionizing radiation using human pancreatic cancer cell lines (MiaPaCa-2, AsPC-1, and Hs766t). Cancer cells were treated with varying concentrations of MGI 114 (0-5  $\mu M$ ) for 8-24 hours. Following drug treatment, cells were exposed to ionizing radiation (0-7.5 Gy) using a  $^{60}Co$  source with a focus-surface distance of 30 cm at room temperature. Cell survival was assessed by clonogenic assay (50 cells/well, in triplicate), and curves were fit using the mean inactivation dose (MID), or linear area under the cell survival curve. The radiation enhancement ratio (RER) was defined as  $(MID_{control}/MID_{MGI 114})$ . A ratio > 1 indicated radiation sensitization. All three pancreatic cell lines tested demonstrated radiosensitivity. In the relatively radioresistant cell line MiaPaCa-2, the mean MIDs for cells treated with 0, 0.2, and 0.5  $\mu M$  MGI 114 were  $4.47 \pm 1.8$ ,  $4.07 \pm 1.8$ , and  $1.7 \pm 0.6$ , respectively. Maximal radiosensitization was observed in MiaPaCa-2 cells treated with 0.5  $\mu M$  MGI-114 for 24 hrs followed by ionizing radiation. The optimal radiation dose was determined to be 5 Gy. The mean RER for this dosing scheme was  $2.6 \pm 0.14$ . These data suggest the efficacy of a chemoradiation combination including MGI 114 in the treatment of human pancreatic cancer. The results encourage investigation in an *in vivo* model to study the effect of this combination prior to initiating clinical trials.

**#199 Tumor Regression in Rat Pancreatic (AR42J) Tumor-Bearing Mice with Re-188 P2045—A Somatostatin Analog.** R. Manchanda, M.T. Azur, J. Lister-James, L.R. Bush, K.R. Zinn, R. Baggs and R.T. Dean. *Diatide, Inc., Londonderry, NH 03053; University of Alabama, Birmingham, AL 35294 and University of Rochester, Rochester, NY 14543, USA.*

Somatostatin is a neuropeptide implicated in the inhibition of certain growth factors and hormones. Somatostatin receptors (SSTRs) are over-expressed on tumors including lung cancer, breast cancer, lymphoma and melanoma. Natural somatostatin is enzymatically degraded *in vivo* and as such cannot be utilized for binding to SSTR-expressing tumors. A somatostatin analog, P2045, is a cyclic peptide that shows high affinity for SSTRs *in vitro*. When complexed with rhenium, Re-P2045 bound to SSTRs *in vitro* with equally high affinity as P2045. Based on *in vitro* binding of Re-P2045 to SSTR-expressing tumor membranes, Re-188 P2045 was investigated *in vivo* in rat pancreatic (AR42J) tumor-bearing nude mice. Rhenium-188 is a beta-ray emitting isotope ( $\beta_{max}$  2.1 MeV, 17 h half-life) of rhenium ideally suited for radiotherapy of tumors. Re-188 P2045 showed an *in vivo* tumor uptake of 9.8 %ID/g. There was rapid renal clearance of Re-188 P2045 affording a favorable tumor-to-kidney ratio of 1.8. Treatment of nude mice afflicted with AR42J tumor with a repeat (2 doses per week) dose regimen of three levels of Re-188 over 3 weeks was undertaken. As the dose of Re-188 was increased, tumor volume decreased correspondingly indicating a dose response in tumor regression. Histopathology of the organs and tissues showed no radiation-related effects. In addition, blood analysis indicated no myelosuppression in mice treated with Re-188 P2045. Thus, tumor-regression data using Re-188 bound to a novel synthetic somatostatin analog will be discussed. Comparison of Re-188 P2045 to another somatostatin analog, DOTATOC labeled with Yttrium-90 will also be presented.

**#200 Radiotherapy of Tumor Using Re-188 P2045, A Somatostatin Analog, in Conjunction with Chemotherapy in Human Small Cell Lung (NCI-H69) Tumor-Bearing Mice.** M.T. Azure, R. Manchanda, J. Lister-James, L.R. Bush, R. Beggs and R.T. Dean. *Diastide Inc., 9 Delta Drive, Londonderry, NH 03053 and University of Rochester, Rochester, NY 14543, USA.*

P2045, a somatostatin (SST) analog, was radiolabeled at specific activities using the dual gamma/beta emitter, Rhenium-188 ( $P_{max}$  2.1 MeV, 17 h half-life) for the radiotherapeutic application. The radiochemical purity of Re-188 P2045 was >90%. Radiolysis products were minimized via addition of stabilizing agents. Radiotherapy was conducted in female nude mice implanted with human small cell lung cancer (NCI-H69) cells. The tumors were allowed to grow for 42 days prior to initiating therapy. Re-188 P2045 at two different doses (3.7 and 14.8 MBq) was compared to the commonly used chemotherapeutic combination of carboplatin/taxol; in addition, a combination of radiotherapy and chemotherapy was also investigated. Five groups of mice (5-6/group) were injected i.v. either with unlabeled P2045 (control), Re-188 P2045 (3.7 and 14.8 MBq) every 3 or 4 days for 7 cumulative doses. One group was administered carboplatin/taxol (2.5 mg carboplatin/200  $\mu$ L, 500  $\mu$ L 5-fold dilution taxol suspension) interperitoneally. The last group received a chemotherapeutic dose (bolus interperitoneally) along with a repeat dose of Re-188 P2045 (3.7 MBq/dose every 4 days). Normalized tumor volumes (NTV) were calculated as % size relative to the tumor volume at initiation of therapy. Tumor measurements were monitored for 37 days post-initiation. Both Re-188 P2045 doses inhibited tumor growth with low dose Re-188 P2045 (3.7 MBq) demonstrating increased regression. Chemotherapy alone (carboplatin/taxol) demonstrated efficacy at injection but tumor growth subsequently resumed to near normal. In the combination group (chemotherapy and radiotherapy) tumor growth showed initial decrease. Low *in vivo* tumor uptake of 2.5 %ID/g for Re-188 P2045 is attributed to low SST receptor population in the NCI-H69 tumors. Re-188 P2045 showed good renal clearance with 80% of the injected dose excreted in urine 90 minutes post-injection. No deleterious effects were observed for either of the Re-188 P2045 groups due to radiation treatment. Detailed tumor regression, biodistribution and histopathology data will be presented.

**#201 TX-1920: Designed anti-angiogenic hypoxic cell radio- and chemo-sensitizer.** Hori, H.; Kasai, S.; Yamashita, M.; Nagasawa, H.; Uto, Y. *Dept Biol Sci & Tech, Fac Engg, Univ Tokushima, Tokushima Japan*; Shlmamura, M. *Dept Mol Oncol, Tokyo Metro Inst Med Sci, Tokyo, Japan.*

Hypoxia-initiated angiogenesis is a critical problem on the design of hypoxic cell radio- and chemo-sensitizer. Previously we developed anti-angiogenic hypoxic cell radiosensitizer haloacetylcarbonyl-2-nitroimidazoles (Hori, H. *et al.*, *Bioorg. Med. Chem.*, 5, 591-599, 1997). Recently our designed BRM (biological response modifier)-functional hypoxic cell radiosensitizer 2-nitroimidazole acetamide, TX-1877 (Kasai, S. *et al.*, *Int. J. Radiat. Oncol. Biol. Phys.*, 42, 799-802, 1998) was found to have anti-angiogenic activity using rat lung endothelial (RLE) cells proliferation assay and chorioallantoic membrane (CAM) assay. We present here on the synthesis, and potent anti-angiogenic activity of a new hypoxic cell radiosensitizer TX-1920 among the TX-1877 derivatives designed.

**Materials and Methods:** TX-1877 derivatives including TX-1920 [1-(4-methylpiperazino)-2-(2-nitro-1H-1-imidazolyl)-1-ethanone] were selected based on their molecular orbital calculation (LUMO level and its coefficients) as well as the effect of nitro group, length of amide side-chain, logP, pKa, and then synthesized in our laboratory. *In vitro* radiosensitizing ability [ER (enhancement ratio)] was measured in EMT6/KU cells under hypoxic conditions. Anti-angiogenic activity was measured in RLE assay *in vitro* and CAM assay *in vivo*.

**Results:** Ten TX-1877 derivatives including TX-1920 were designed, and synthesized in higher yield. Almost TX-1877 derivatives showed their radiosensitizing ability having ER of more than 1.6. 2-Nitroimidazole methylpiperazinoacetamide TX-1920 showed the most potent inhibition of RLE cells proliferation with a  $IC_{50}$  of 90  $\mu$ M and a similar potent anti-angiogenic activity to that of TX-1877 in CAM assay.

**Summary:** We found the new anti-angiogenic hypoxic cell radiosensitizer TX-1920, the detail evaluation of which is now being investigated.

**#202 Effect of hypoxiradiotherapy on immune function in tumor-bearing BALB/c mice.** Zhongling Feng, Gao Feng. *Cancer Research Institute and Department of Cell Biology, China Medical University, Shenyang LN, 110001, P. R. China.*

**Objective:** To study the activity level of TNF and IL-2 in host of sarcoma-bearing mice after hypoxiradiotherapy. **Methods:** The level changes of TNF and IL-2 were studied in BALB/c sarcoma-bearing mice after breathing 10.5% oxygen during radiotherapy by MTT colorimetric method and crystal violet staining. The data were analyzed using SPSS software package. **Results:** 1) The activity level of IL-2 of mice in tumor-bearing alone group were lower than control group on detecting time ( $P < 0.001$ ). Those in hypoxiradiotherapy were higher than other tumor-bearing study groups on the 7th day after hypoxiradiotherapy, but lower than radiotherapy alone group and were higher than tumor-bearing alone group on days 7, 14 after treatment, respectively ( $P < 0.001$ ); 2) TNF activity level in tumor-bearing alone group were higher than control on detecting time

( $P < 0.001$ ). Those in hypoxiradiotherapy alone group were lower than tumor-bearing alone group on the 7th day ( $P < 0.001$ ), but little higher on the 14th day ( $P > 0.05$ ). **Conclusion:** Hypoxiradiotherapy increase IL-2 and TNF activity in host, and may preserve and enhance immune function of host.

**#203 Radiosensitization of human glioblastoma cells by 4-(3'-bromo-4'-hydroxyphenyl)-amino-6,7-dimethoxy-quinazoline (WHI-P154).** Naria, R.K., Liu, X.-P., and Uckun, F.M. *Drug Discovery Program, Parker Hughes Cancer Center, Hughes Institute, St. Paul, MN 55113.*

WHI-P154 is a novel quinazoline which exhibits substantial activity against glioblastoma (Naria RK, Liu X, Myers DE, Uckun FM. *Clin. Cancer Res.* 4:1405-14, 1998; Naria RK, Liu X, Klis D, Uckun FM. *Clin. Cancer Res.* 4: 2463-71, 1998). The aim of this study was to determine the combined effects of WHI-P154 plus ionizing radiation against U373 and T98 glioblastoma cells. The cytotoxic activity of the combined regimen was assessed by the mitochondrial-based MTT (3-[4,5-dimethylthiazol-2-yl]-2,5-diphenyl tetrazolium bromide) assays, clonogenic assays and *in situ* TUNEL assays. Cell cycle perturbations were assessed by bromodeoxy uridine (BrdU) labeling and flow cytometry. Treatment of U373 glioblastoma cells with WHI-P154 alone for 24 hr, 48 hr, 72 hr, and 96 hr resulted in dose- and time-dependent cytotoxicity with  $IC_{50}$  values of 144  $\mu$ M, 63.1  $\mu$ M, 27.8  $\mu$ M and 15.8  $\mu$ M, respectively. Cell cycle perturbations were consistent with the presence of a mitotic block after WHI-P154 treatment. Treatment of U373 cells with 100  $\mu$ M or 150  $\mu$ M WHI-P154 for 24 hr prior to ionizing radiation caused an induction of apoptosis and decrement in clonogenic survival with significant reduction of  $SF_2$  values (0.44 for control Vs. 0.12 for 150  $\mu$ M treatment) and  $\alpha$  values (0.22 for control vs. 0.021 for 150  $\mu$ M treatment). Furthermore, *in vitro* growth delay assays were used to examine the effect of WHI-P154 and/or ionizing radiation on established glioblastoma colony growth. Growth of established colonies was severely impaired when treated with a single dose of WHI-P154 in combination of radiation than either one of the modalities. The invasive potential of glioblastoma cells in Matrigel matrix-coated Boyden chamber assays was significantly diminished when pretreated with WHI-P154 in followed by ionizing radiation. In conclusion, WHI-P154 has potent cytotoxic and radiosensitizing activities against glioblastoma cells. The present data further provide a radiobiological basis for using WHI-P154 as a radiosensitizer in brain tumor cells.

**#204 Enhanced induction of prostate carcinoma cell death by inhibition of proteasomal activity using the novel dipeptidyl boronate PS-341 in combination with ionizing radiation: modulation by bcl-2.** Yang, H., Herrmann, J.L., Logothetis, C.J., Elliot, P., Adams, J., McConkey, D., and Papanicreou, C.N. *Departments of Genitourinary Medical Oncology and Cell Biology, The University of Texas M.D. Anderson Cancer Center, Houston, TX 77030 and ProScript, Inc., Boston, MA 02139.*

The ubiquitin-proteasome pathway is responsible for the properly timed proteolytic destruction of key inhibitors of cell cycle progression that either have tumor suppressor activity or are considered candidate tumor suppressors. Recent evidence indicates that a unique mechanism of inactivating the cyclin-dependent kinase inhibitor p27<sup>Kip1</sup>, a candidate tumor suppressor, is "selective" degradation of p27<sup>Kip1</sup> by the proteasome. For these reasons, the 26S proteasome complex has emerged as a novel target for anti-cancer therapy development. Here we investigate the activity of PS-341, a novel dipeptidyl boronate inhibitor of the chymotrypsin site of the 26S proteasome, which is being evaluated clinically. Treatment of LNCaP cells with PS-341 substantially stabilized the level of cellular wild type p53 protein. This suggested the possibility that the inhibition of proteasomal activity might be used to pre-set the apoptotic threshold to a lower level. In consideration we investigated whether we might achieve enhanced cytotoxic activity of PS-341 by combining it with ionizing radiation. We report that pretreatment of LNCaP cells with pharmacologically achievable concentrations enhances LNCaP cell death induction by ionizing radiation (1-2 Gy). Preliminary data indicates that prior radiation followed by PS-341 treatment does not result in enhanced cell death induction. We also find that the kinetics of cell death induction following combined PS-341/radiation treatment of LNCaP was inhibited by bcl-2, a cell survival protein implicated in prostate cancer progression. These studies are designed to help us refine the clinical application of proteasome inhibitors for prostate cancer. (Supported by awards from the Association for the Cure of Cancer of the Prostate [CaP CURE] to C.N.P. and C.J.L.)

**#205 Activity of pH-sensitive salicylic acid derivatives against human tumors *in vivo*.** Burger, A.M., Steidle, C., Fiebig, H.H., Frick, E., Schömerich, J., and Kreuz, W. *Institut für Biophysik und Strahlenbiologie, University of Freiburg, D-79104 Freiburg; Tumor Biology Center, D-79106 Freiburg, Department of Internal Medicine, University Hospital Regensburg, D-93042 Regensburg, Germany.*

The salicylic acid derivatives aspirin (acetylsalicylic acid), PAS (4-amino-salicylic acid), diflunisal (5-[2,4-difluorophenyl]-salicylic acid) and DHSA (4,6-dihydroxysalicylic acid) selectively inhibit human tumor cell growth *in vitro* independent of tumor type, but dependent of extracellular pH. These agents exert their cytotoxic activity selectively in an acidic environment (pH



6.0–6.8) and thus might be activated in the interstitial fluid of solid tumors (pH 6.5–6.8) but not in normal tissue or blood at physiological pH. To test this hypothesis we examined the *in vivo* antitumor activity of aspirin, PAS, diflunisal and DHSA alone or in combination in mammary (MX-1), lung (LXFL 529) and pancreas (PAXF 736) human tumor xenograft models. The MTD for this class of agents in nude mice was established between 20–400 mg/kg given twice daily (0, 8h) into the tail vein for two consecutive weeks. This schedule assured that the required interstitial drug concentrations of 10 mM for PAS, 1 mM for aspirin, 0.5 mM for diflunisal and 5 mM for DHSA were reached, which reflect the clinically effective doses used to treat other diseases in men. In combination drugs were administered at precise time points in order to obtain optimal synergism and to respect plasma clearance times. In marked contrast to the *in vitro* results, we found that aspirin, PAS and diflunisal given as monotherapies were inactive *in vivo*. The combinations of aspirin+PAS and diflunisal+PAS however, did inhibit tumor growth in all 3 human tumor xenografts examined. Aspirin+PAS were capable to inhibit the growth of the chemosensitive mammary carcinoma MX1 and the chemoresistant PAXF 736 pancreas tumor with T/Cs of 45%. The combination of diflunisal+PAS was more potent (T/Cs 37–43%) in the MX1, LXFL 529 and PAXF 376 models. The best antitumor activity was seen against PAXF 736, where tumor regression was paralleled by an increase in histologically occurring necrosis. Moreover, all treatments were well tolerated and thus prompted an exploratory clinical study with the combination of the registered drugs aspirin+PAS in two patients with pancreatic carcinomas. The patients received 5 cycles of a 4 day treatment while monitoring tumor growth by sequential CT-scanning. After completion of treatment, the primary tumor as well as lymph node metastasis were completely necrotic. A patient receiving PAS alone, responded only marginally. These data indicate that phase I clinical trials should be initiated to test the potential of salicylic acid derivatives for cancer chemotherapy.

**#206 A biophysical approach to cancer treatment: selective pH-dependent membrane poration and inhibition of energy supply in human tumor cells.** Kreuz, W., Müller, B., Fischer, B., Heun, J. and Etzkorn, M. *Institut für Biophysik und Strahlenbiologie, University of Freiburg, Freiburg D-79104, Germany.*

A physiological characteristic of solid tumors and distant metastasis derived thereof is the relative lower pH (6.5–6.8) in their interstitial fluids as compared to that of adjacent normal tissue and blood. Thus, the acidic extracellular pH milieu can be considered a target for cancer therapy. In a biophysical approach to inhibit tumor cell growth, we screened over 220 compounds *in vitro* which would exist as polar/hydrophilic salts at physiological pH (7.2–7.4), but would be protonated in the acidic tumor compartment and as such show selective cytotoxicity against cancer cells. The compounds were evaluated in 8 human tumor cell lines (RT112, Capan-1, SK-MEL-30, MCF-7, HepG2, LS174T, Colo-699, SK-N-MC) and in human mononuclear cells (MNC) cultured in media at a pH ranging from 6.0–7.4. Combinations of the salicylic acid derivatives acetylsalicylic acid (aspirin), 4-aminosalicylic acid (PAS), 4,6-dihydroxysalicylic acid (DHSA) and 5-[2,4-difluorophenyl]-salicylic acid (diflunisal) were the most potent and selective agents. In the protonated form, these compounds confer a pH-dependent poration of cell membranes as determined by propidium iodide assay and block the cellular energy supply by inhibition of the respiratory chain (XTT assay, Roche) and lactate transport (lactate kit, Sigma). Given alone aspirin, PAS, diflunisal and DHSA were cytotoxic toward tumor cells, combinations of aspirin+PAS, aspirin+diflunisal, diflunisal+PAS and diflunisal+DHSA however, were synergistic in their action and did more effectively inhibit respiration, lactate transport and induced poration of tumor cell membranes at a pH of 6.0–6.8 in concentrations ranging from 0.5–10 mM—levels which are achieved with therapeutic doses of these drugs in men. On the contrary, normal cell types (MNC) were not affected at physiological pH.

Aspirin, PAS and diflunisal are registered drugs and are currently in use for the treatment of other diseases. Our data however indicate that these drugs should be clinically re-evaluated under the view of their potential use in cancer chemotherapy.

**#207 Cell Adhesion Mediated Drug Resistance (CAM-DR): A New Molecular Target for Drug Discovery.** Dalton WS, Hazlehurst L, Damiano J, Shih A. *Clinical Investigations Program, Moffitt Cancer Center and Research Institute, University of South Florida, Tampa, Florida.*

We recently reported that myeloma cells interact with fibronectin (FN) via  $\beta 1$  integrin receptors and that this interaction regulates survival and response to chemotherapy (Damiano et al. BLOOD, 93: 1658, 1999). We have now expanded upon this initial observation by studying numerous other cell lines and environmental matrices, including collagen I and IV. In all cases, cell adhesion mediated by integrin receptors reduced apoptosis induced by drugs or radiation. Classical mechanisms of drug resistance, such as upregulation of MDR1 genes or Bcl-2 family members, does not explain the reduction in apoptosis. We hypothesized that the tumor micro-environment influences cytotoxic drug response by utilizing signal transduction pathways initiated by cell surface adhesion molecules. Experimental evidence now shows that  $\beta 1$  integrin mediated adhesion of tumor cells to FN results in a G1 cell cycle arrest. Associated with the cell cycle arrest

is an increase in p27<sup>kip1</sup> protein levels which is post-translationally regulated. When tumor cells are released from FN, they promptly re-enter the cell cycle and synthesize DNA, p27<sup>kip1</sup> protein levels decrease, and the cells become drug sensitive. Using an anti-sense approach to reduce p27<sup>kip1</sup> protein levels, we demonstrated a causal relationship between, cell adhesion, p27<sup>kip1</sup> protein levels and drug response. Given the observation that tumor cell adhesion mediated by integrin receptors reduces treatment related apoptosis, we are now searching for molecules that either reduce  $\beta 1$  integrin mediated cellular adhesion or interrupt integrin mediated signaling pathways so that the efficacy of cytotoxic drugs and radiation treatments may be enhanced.

**#208 Selective Inactivation of decay-accelerator activity of Factor H by monoclonal antibodies: implications for bladder cancer therapy.** Corey, Michael J., Hass, G. Michael, Vessella, Robert L., and Kinders, Robert J. *Bion Diagnostic Sciences, Redmond, WA and Urology Department, University of Washington, Seattle, WA.*

A number of cancers have been shown to express cell-surface regulators of complement. However, our recent characterization of the expression of complement Factor H in bladder cancer is the first report of dramatic upregulation of a soluble complement regulator in cancer. Subsequent to this discovery, monoclonal antibodies (MAbs) specific for Factor H were tested for effects on complement-mediated lysis *in vitro*. Two of the tested antibodies, X52.1 and X13.2, are used in the BTA stat<sup>®</sup> and BTA TRAK<sup>®</sup> assays for detection and monitoring of transitional cell carcinoma of the bladder. X52.1 exhibits both very strong enhancement of complement cytotoxicity and an unusual mechanism of action. This MAAb has no effect on the Factor H/Factor I-mediated solution-phase cleavage of C3b, yet is capable of enhancing complement-mediated lysis of various cell types, including cancer cells, by as much as 15-fold at concentrations of 10–300 nM (depending on the concentrations of complement proteins present). The effects are absent in serum depleted of Factor H and are evidently limited to activation of the alternative pathway of complement. The other antibody used in the BTA stat and BTA TRAK sandwich assays, X13.2, inhibits the solution-phase "cofactor" activity of Factor H in cleavage of C3b, yet this antibody actually blocked complement-mediated lysis even at concentrations under 10 nM. Results of hemolysis kinetics, zymosan fixation reactions, measurements of dissociation constants with and without C3b, and comparisons of hemolysis mediated by the classical and alternative pathways of complement are all consistent with a model in which X52.1 protects the C3 convertase from the decay-accelerator activity of Factor H. If correct, this hypothesis has important implications for cancer therapy based on inhibition of complement regulators, in that reagents such as X52.1 may be able to enhance the lytic activity of complement at the cell surface without causing inappropriate activation of complement in the bloodstream. At present we consider X52.1 to be a lead compound within this therapeutic approach and are seeking means of testing our hypothesis in an animal model.

**#209 Monoclonal antibody antagonists of RHAMM, a hyaluronan receptor that is highly expressed in human tumor cell lines, and required for activation of MAP kinase.** Jackson, Jeffrey R.; Gilmartin, Aidan; Abrahamson, Julie; Holmes, Stephen D.; Ho, Maureen L.; Malico, Rosalie; Formwald, James; and Winkler, James D. *SmithKline Beecham Pharmaceuticals, King of Prussia, PA.*

Hyaluronan (HA) plays an important role in the extracellular environment, providing structural support, serving as an osmotic regulator and an attachment factor for cells. Through cellular receptors, HA can play a role in signaling both growth and migration. Tumors often contain very high levels of HA, which is thought to be involved in both the proliferative and invasive properties of tumor cells. Murine RHAMM is a previously described receptor for hyaluronan mediated motility, and has been shown to be required for ras transformation of fibroblasts. In these studies, we characterized the expression and function of human RHAMM. In several tumor cell lines, RHAMM expression was very high at the mRNA level. This is in contrast to many normal tissues, which demonstrated low RHAMM expression. To further study the function of human RHAMM, we generated monoclonal antibodies, and identified neutralizing antibodies that could block the binding of HA to RHAMM. We used PDGF activation of p42/44 MAP kinase (Erk) in normal fibroblasts to test whether RHAMM was required for signaling downstream from ras. The RHAMM neutralizing monoclonal antibody was able to inhibit PDGF-stimulated activation of Erk. These studies suggest that RHAMM and its signaling functions can be antagonized by a monoclonal antibody. This provides a potential means of therapeutic intervention in an important growth regulator in cancer.

**#210 Combined treatment of experimental brain tumors with dibromodulcitol and X-irradiation.** Hidvégi, E.J., Mangel, L.C., Gazsó, L.G., Dám, A.M., Sárány, G., Institoris, L. *National Research Institute for Radiobiology and Radiohygiene, Budapest 1775, Hungary.*

In multicenter study, directed by EORTC Brain Tumor Group, the adjuvant chemotherapeutic combination of 1,8-dibromodulcitol (DBD) and BCNU with radiotherapy, performed postoperatively, produced a significantly better survival in patients with malignant gliomas than radiotherapy alone (Hildebrand, J., et al. Neurology 44, (1994) 1479). We have studied

the effect of combined treatment of X-irradiation and DBD on experimental brain tumors. DBD increased the survival of ependymoblastoma bearing mice in dose and time dependent manner, while X-irradiation alone lead to slight effect. The two modalities produced opposite result in glioma 261 transplanted mice. Combination, however, provided supraadditive effect in both tumors. DBD treatment on human U373 astrocytoma-glioblastoma cells, grown on nude mice, was ineffective but after combination with X-irradiation 80% of mice remained tumor free. In model experiment DBD acted like a moderate radiosensitizer. From the study of pulse radiolysis of DBD the conclusion can be drawn that the hydroxyl free-radical, evolved by radiation, reacts with bromide-ion of DBD and results in dibromide radical/ anion which is a strong oxidizing agent. In conclusion: the appropriate combination of X-irradiation and DBD may produce supraadditive effect. DBD, in addition to the widely proved chemotherapeutic attribute, may possess radiosensitizer property as well.

## SECTION 5: PHASE II STUDIES WITH MOLECULAR ENDPOINTS

**#211 Efficacy of p53-directed ONYX-015 therapy in hepatobiliary tumors.** Makower D, Rozenblit A, Edelman M, Augenlicht L, Kaufman H, Haynes H, Zwiebel J, Wadler S. *Depts of Oncology, Radiology and Pathology, Albert Einstein Cancer Center, Bronx, NY and IDB, CTEP, NCI, Bethesda, MD.*

ONYX-015, a Group C adenovirus with a deletion in the region coding for the E18 55 kD protein, preferentially replicates *in vitro* in cells lacking functional p53. To test the clinical efficacy of ONYX-015, a Phase IIb trial was initiated in patients (pts) with primary hepatobiliary tumors. Treatment was delivered via CT-guided intratumoral injection every 3 weeks. Pts with ascites received intraperitoneal ONYX-015. Pts were enrolled without knowledge of their tumor's p53 status; tumor samples were acquired prior to treatment for p53 analysis by both immunohistochemistry (IHC) and single strand conformation polymorphism (SSCP) analysis with DNA sequencing. Viral shedding was analyzed by plaque titration. Antibody titers to ONYX-015 were determined by ELISA prior to treatment, and at 1 and 3 weeks. 8 pts with advanced disease were enrolled on this protocol. Pt characteristics are as follows: tumor histology = cholangiocarcinoma (6 pts), gallbladder (1), ampullary (1); median age = 67.5 years (range 44-78); sex: male = 5, female = 3; prior treatments = 0 (2 pts), 1 (4 pts), 2 (2 pts); performance status = 0 (1 pts), 1 (7 pts); number of ONYX-015 treatments = 1 (4 pts), 2 (2 pts); 3 (1 pt), 4 (1 pt); number of sites injected = 1 (2 pts), 2 (2 pts), 3 (2 pts), 4 (1 pt), 6 (1 pt). The first two pts received ONYX-015 at an initial total dose of  $6 \times 10^8$  pfu; subsequently pts were treated with  $10^{10}$  pfu per lesion. Grade 2-4 toxicities include: transaminitis (2 pts), anemia (1), leukopenia (1), and atrial fibrillation (1). No radiographic responses were observed. However, 3/7 pts assessable for response exhibited >50% decline in CA125, and 2/7 exhibited 25-50% decline in CA19-9. p53 overexpression by IHC was noted in 4/8 pts, 2 of whom demonstrated a biochemical response. SSCP results are pending. Urine (8 pts), sputum (8), and bile (1) were collected daily for viral shedding analysis. Results are pending. Conclusions: 1) ONYX-015 may be safely administered percutaneously and intraperitoneally to pts with hepatobiliary tumors; 2) treatment is well-tolerated; 3) biochemical evidence consistent with response is seen; 4) responses may be observed in pts without p53 overexpression by IHC.

**#212 Targeting somatostatin receptor subtype 2 with SomatoTher<sup>SM</sup>: discordancy between predicted and observed renal radiation exposures in a phase II clinical trial.** McCarthy K., Wollering E., Cronin M., Espanan G., Sartor O., Maloney T., Anthony L. *Louisiana State Health Sciences Center and Bayou Nuclear, Inc., New Orleans, LA.*

Indium-111 pentetreotide is a widely used diagnostic agent (OctreoScan®) in patients with tumors expressing the somatostatin receptor. This radiolabeled compound is internalized with nuclear translocation and is primarily excreted through the kidney. Renal toxicity has been proposed as a dose-limiting side effect of high-dose Indium-111 pentetreotide (SomatoTher<sup>SM</sup>) therapy. Between February 1997 and July 1999, 35 patients were treated with multiple, sequential 180 mCi doses of SomatoTher<sup>SM</sup> as therapy for somatostatin receptor-positive tumors. Twelve patients have been evaluated for the development of renal toxicity more than 12 months after their last therapy dose. These patients received two to eight courses of therapy and the total number of mCi administered ranged from 360 to 1,480 mCi (mean 645 mCi  $\pm$  291 mCi) per patient. The cumulative kidney radiation doses ranged from 142 to 3,438 cGy by standard MIRD calculations with classical limits placed at 2,300 cGy. When the auger component is added, the tumor dose increases to 3,000-6,000 cGy per 180 mCi treatment. The mean pre-therapy creatinine clearance in these patients was  $120 \pm 67$  ml/min. The mean post-therapy creatinine clearance was  $118 \pm 48$  ml/min ( $p = NS$ ). These data suggest significant limitations in conventional measurements and models of therapeutic radiation toxicity when delivered by auger emitting, internalizing radiopeptides. The renal

effects of additional SomatoTher<sup>SM</sup> doses and schedules are being evaluated. (Supported in part by NIH-GCRC-RR05096-07 and the LSUMC Foundation).

**#213 Targeting somatostatin receptor subtype 2 with SomatoTher<sup>SM</sup>: a phase II clinical trial in advanced gastroenteropancreatic malignancies.** Anthony L, Wollering E, Cronin M, Espanan G, Maloney T, McCarthy K. *LSUMC and Bayou Nuclear, Inc., New Orleans, LA; O'Dorisio T, The Ohio State University, Columbus, OH.*

Indium-111 pentetreotide is a somatostatin receptor subtype 2 (sst 2) preferring radioligand that can induce radiographic responses in gastroenteropancreatic (GEP) tumors such as carcinoid and islet cell malignancies (*Ca J Sci Am* 4:94-102, 1998). We hypothesized that high-dose In-111 pentetreotide therapy (SomatoTher<sup>SM</sup>) would induce receptor-specific biochemical responses and prolong survival in patients with GEP malignancies. To test this hypothesis, GEP tumor patients who had failed all conventional therapy, with expected survivals of <6 months and were set positive as determined by the uptake on a 6.0 mCi <sup>111</sup>In-pentetreotide scan (OctreoScan®), were treated with at least two monthly 180 mCi intravenous injections of SomatoTher<sup>SM</sup>. Baseline plasma pancreastatin levels were measured and repeated prior to each SomatoTher<sup>SM</sup> treatment. From 2/97 to 12/97, 27 GEP (24 carcinoid syndrome and 3 pancreatic islet cell) patients were entered with 26 patients evaluable for biochemical assessment and 27 patients evaluable for survival analysis. Pancreastatin levels decreased by 50% or more in 85% of the patients. NCI Common Toxicity Criteria were used to assess toxicity in these 27 patients treated with >100 SomatoTher<sup>SM</sup> doses: 3 hepatic Grade 4; 2 grade IV platelets; 1 grade IV WBC; 1 grade III neurologic. The median survival was 18 mos (range = 3 to 29+ mo). Monthly 180 mCi SomatoTher<sup>SM</sup> doses resulted in an 85% biochemical response rate, were well tolerated and prolonged survival in patients with end-stage GEP malignancies. SomatoTher<sup>SM</sup> dose escalation and alternative dosing intervals are being investigated. (Supported in part: NIH-GCRC-RR05096-07/LSUMC Foundation).

**#214 Circulating erbB-2 and resistance to chemotherapy in advanced breast cancer.** Colomer, R.,<sup>1</sup> Montero, S.,<sup>1</sup> Lluch, A.,<sup>2</sup> Ojeda, B.,<sup>3</sup> Barnadas, A.,<sup>4</sup> Casado, A.,<sup>5</sup> Massutell, B.,<sup>6</sup> Lloveras, B.,<sup>7</sup> Cortés-Funes, H.,<sup>1</sup> <sup>1</sup>Hospital 12 de Octubre, Madrid; <sup>2</sup>Hospital Clínic, Valencia; <sup>3</sup>Hospital de la Santa Creu i Sant Pau, Barcelona; <sup>4</sup>Hospital Germans Trias i Pujol, Barcelona; <sup>5</sup>Hospital Clínic, Madrid; <sup>6</sup>Hospital General, Alicante; <sup>7</sup>Inst Català d'Oncologia, Barcelona.

**Purpose:** Several retrospective studies have suggested that the expression of the erbB-2 oncogene is associated with resistance to chemotherapy in breast carcinoma. To test this hypothesis, we performed a prospective assessment of the predictive value of circulating erbB-2 in patients with advanced breast carcinoma, in the setting of a multicenter phase II trial.

**Methods:** Serum samples were collected in 58 patients with metastatic breast carcinoma before first-line chemotherapy treatment with a combination of paclitaxel and doxorubicin, and the levels of circulating erbB-2 were measured using an enzyme immunoassay. Immunohistochemistry with anti-erbB-2 monoclonal antibody CB11 was used to assess the overexpression of the protein in the primary tumors.

**Results:** Using 450 fmol/ml as a cut-off, 24 cases (41%) had elevated erbB-2 levels. Elevated levels of circulating erbB-2 were associated with the expression of erbB-2 in the primary tumor tissue and with the metastatic tumor burden (evaluated with the marker CA 15-3) ( $p = 0.032$  and  $p = 0.002$ , respectively), but not with variables such as menopausal status, stage at diagnosis, previous adjuvant therapy, or the number of metastatic sites. The levels of circulating erbB-2 correlated inversely with the response to treatment. The probability of obtaining a complete response to chemotherapy was significantly lower ( $p = 0.021$ ) in patients with elevated erbB-2 levels (0%; 95% CI: 0%-13%) when compared with patients with non-elevated erbB-2 (26%; 95% CI: 12%-45%). In addition, the duration of clinical response was significantly shorter in patients with elevated erbB-2, in comparison with the cases with non elevated erbB-2 (7.5 months vs. 11 months,  $p = 0.03$ ).

**Conclusions:** Elevated levels of circulating erbB-2 in patients with metastatic breast cancer correlate with a reduced efficacy of chemotherapy. Since the poor response rate was observed with paclitaxel and doxorubicin, drugs previously thought to be more active in erbB-2 positive cancer, we suggest that the resistance to chemotherapy associated with erbB-2 expression is not drug-specific.

**#215 Safety, toxicity and antitumor efficacy of the modulated oral fluoropyrimidine derivative S-1 in patients with metastatic colorectal cancer: preliminary results of an early phase II study.** Schöffski P, Vermorken J, Schellens J, Aapro M, Bruntsch U, Wanders J, de Boer R and Hanauke AR for the EORTC Early Clinical Studies Group (ECSG)/NDDO Oncology (supported by Taiho Pharmaceuticals)

**Introduction:** S-1 combines the 5-FU prodrug Tegafur with 5-chloro-2,4-dihydropyridine (CDHP) and K<sup>+</sup>-oxonate (oxonic acid) at a molar ratio of Tegafur:CDHP:oxonic acid = 1:0.4:1. CDHP decreases the degradation of 5-FU by inhibiting dihydropyrimidine dehydrogenase, resulting in pro-



longed maintenance of active concentrations of 5-FU. Oral oxonic acid mainly inhibits the intestinal phosphorylation of 5-FU by interacting with pyrimidine-phosphoribosyl-transferase, thus reducing toxicity while preserving the antitumor activity of 5-FU. The ECGS is conducting an early phase II study to determine the efficacy, safety, toxicity, and pharmacokinetics of S-1 in pts with metastatic colorectal cancer and bidimensionally measurable disease. **Accrual:** 36 pts (14♀, 22♂), median age 63 (37-75) yrs, WHO PS 0-1, entered the trial. Pretreatment included adjuvant chemo-(2), radio-(4), or radiochemotherapy (2). **Treatment:** S-1 was taken twice daily within 1 h after meals, the first 16 pts were treated at a starting dose of 40 mg/m<sup>2</sup>. Due to gastrointestinal toxicity, the starting dose was reduced to 35 mg/m<sup>2</sup> and further 20 pts were enrolled. **Results:** 36 pts (119 crs) are currently evaluable for toxicity, 26 for response; kinetics are pending. A median no. of 4.5 (1-8) crs have been administered. At the 40 mg/m<sup>2</sup> dose level (16 pts), the most common side effects possibly, probably or definitely related to S-1 were nausea (12 pts), diarrhea (11), fatigue (10), vomiting (7), stomatitis (7), anorexia (6); grade 3/4 toxicity included diarrhea (6), nausea (2), stomatitis (2) and fever (2). At the 35 mg/m<sup>2</sup> level (20 pts), the most common side effects were diarrhea (14), fatigue (9), nausea (7) and anorexia (6); grade 3/4 toxicity was diarrhea (5) and dehydration (2). Serious adverse events occurred in 6/16 pts (40 mg/m<sup>2</sup>) and 5/20 pts (35 mg/m<sup>2</sup>) during the 1st crs, and were to some degree center-dependent. Response evaluation: PR (confirmed) 4, SD 10, PD 5; early PD 3, too early 3. A >50% tumor size reduction in another 4 pts was not confirmed in consecutive cycles. **Summary:** S-1 is active in colorectal cancer, the recommended dose and optimal handling of the compound requires further investigation, including food intake relationship, pharmacokinetic and pharmacodynamic studies.

**#216 CPT-11 is an active agent in patients with advanced gastric cancer.** Kähne C-H, Catane R, Klein H, Peretz T, Preusser P, Niederle N, Ducreux M, Wilke H and Jacques C. Rostock, Leverkusen, Münster, Essen Germany; Jerusalem, Israel; Paris, France.

To evaluate the activity of CPT-11 in chemo-naïve pts with metastatic gastric cancer a phase II trial was initiated. Inclusion criteria: metastatic gastric adenocarcinoma, bidimensionally measurable lesion, adequate bone marrow, normal hepatic and renal function; PS 0-2; no prior chemotherapy; no contraindications to CPT-11. Pts with locally advanced disease only were not accepted. Pts received CPT-11 350 mg/m<sup>2</sup> day 1/q 3 week (w) until progression (PD), unacceptable toxicities or in case of no change (NC) without subjective improvement of tumor related symptoms. Responses were reviewed by an Independent Expert Committee. 40 pts were included from 18/03/96 to 04/06/98; M/F: 70%/30%; median age: 58 yrs; weight loss >5%: 16 pts; PS 0/1/2: 32%/58%/10% pts; primary tumor 63% pts; with tumor related symptom(s): 70%. Median number of organs involved: 2. Metastatic sites: liver 53%; lymph nodes: 55%; abdominal mass: 25%; lung: 20%. All pts were evaluable for toxicity: one pt died early (diarrhea, tachyarrhythmia, congestive cardiac failure possibly related to treatment). 1 pt was ineligible due to non-gastric cancer; 4 pts were unevaluable for efficacy: 2 pts had inadequate staging, 2 pts had early treatment discontinuation due to toxicity. Grade 3-4 toxicity: neutropenia: 33.3% pts—14.7% cycles (cy); Diarrhea: 20% pts—5.6% cy; febrile neutropenia: 7.5% pt—1.8% cy; infection without neutropenia: 2.5% pt—0.6% cy. Among 35 evaluable pts for efficacy: 3 CR, 3 PR, 17 NC, 12 PD. 37.5% of pts had subjective improvement of tumor related symptoms after cycle 2. Median progression free survival was 3.8 months (95% CI: 2.3-4.4 months) and median survival 6.8 months (95% CI: 5.2-9.0 months). **Conclusion:** CPT-11 is well tolerated and active as single agent in gastric cancer which deserves further investigation in this setting. Randomised phase II-III studies in combination treatment are ongoing.

**#217 Aminopterin (AMT), an "old dog with new tricks": therapeutic and pharmacodynamic results of early phase II trials for patients with acute leukemia and endometrial cancer.** Kamen, Barton A., Fliniewicz, Katarzyna, Holenberg, John S., Larson, Richard, Miller, David S., Muller, Carolyn Y., Ratliff, Arleen F., and Coleman, Robert L. UTSouthwestern Med Ctr, Univ WA and Univ Chicago.

Aminopterin (AMT), an antifolate used before methotrexate (MTX), fell out of favor because of variable and unpredictable toxicity even though it is 25-50 times more potent than MTX. With nearly 50 years of cumulative knowledge regarding antifolate transport, metabolism and resistance and the development of better preparative and analytical techniques coupled with the empiric success of MTX, it seemed time to investigate AMT again. Based upon studies of freshly isolated lymphoblasts *in vitro* and a phase I study which included pharmacokinetics (Clin Cancer Res 2:1-5, 1996 and J Clin Oncol 16:1458-1464, 1998), AMT was approximately 25 times more potent than MTX and had greater and more consistent bioavailability. We also saw a complete remission in a woman with endometrial cancer and stable disease in other patients. Therefore, we are doing phase II trials of AMT in acute leukemia and endometrial cancer. The dose of AMT is 4 mg/m<sup>2</sup>/week given as 2 mg/m<sup>2</sup> B.I.D. orally on a single day. Treatment is continued as long as the patient is responding (or stable). Thus far, 17 patients with leukemia and 8 patients with endometrial cancer have been treated. Toxicity has been primarily mucositis and then myelosuppres-

sion. One patient with AML experienced tumor lysis syndrome after only the first day's dose. A unique biochemical toxicity was finding a marked increase in plasma homocysteine in two patients (from 5 μM to >50 μM in one). Since venous thrombosis can be caused by or exacerbated by folate deficiency, and there is a common genetic predisposition to homocysteinemia, this phenomena needs further attention. Of the 17 patients with leukemia, in addition to the tumor lysis, there have been 3 significant responses, all in patients with T-lineage disease (one CR and two stabilized at M2 marrow). There has also been stable disease in 1 patient with endometrial cancer. One patient demonstrated a 75% reduction in a hepatic mass. Based upon limited sampling, bioavailability remains as published (>75%). The two trials continue to accrue patients.

**#218 Docetaxel (DTX) + cisplatin (CDDP) in locally advanced or metastatic head and neck cancer (HN).** A phase II study. Caponigro F, Avallone A, Rivellini F, Squitti C, Manzione L, De Luca L, Biglietto M, Massa E, Cornella P, Mantovani G, Comella G. Southern Italy Cooperative Oncology Group (SICOG) c/o National Tumor Institute of Naples; \*Rhône-Poulenc Rorer, Origgio, Italy.

**Purpose:** DTX is among the most promising new drugs in HN, while CDDP is acknowledged as probably the most active single agent. Since the combination of the two drugs has proven feasible and has shown clinical activity in HN in a previous phase I study, we started a phase II study in patients (pts) with locally advanced and metastatic HN.

**Patients and methods:** Eligible pts, never pretreated with chemo- (CT) or radiotherapy (RT), received a combination of DTX 75 mg/m<sup>2</sup> and CDDP 100 mg/m<sup>2</sup> every 3 weeks. After 3 cycles, pts were re-evaluated; responding pts with locally advanced HN underwent RT, while metastatic responding pts received further CT.

**Results:** 46 pts (median age 59; M/F = 39/7) were accrued. 45 pts had locally advanced disease, while 1 pt had lung metastases. 5 complete responses (CR) and 16 partial responses (PR) have been observed, for an overall response rate of 46% (95% C.I., 32% to 60%), according to intention-to-treat analysis. In 2 pts with PR and 1 pt with SD after CT, a CR was achieved after subsequent RT. Neutropenia (grade 3-4 in 23 pts) and diarrhea (grade 3-4 in 5 pts) were the main side effects. Ten pts died before completion of 3 courses of treatment; in 6 cases (grade 4 diarrhea in 4, and neutropenic sepsis in 2) this was considered probably CT-related.

**Conclusion:** DTX + CDDP is an active, but toxic regimen in HN. Careful selection of pts is needed for further trials.

**#219 Clinical and pharmacokinetic study of three times daily oral etoposide in patients with advanced AIDS-related Kaposi's sarcoma (AIDS-KS).** Schwartsmann, G., Sprinz, E., Di Leone, L., Stefani, S., Cancella, A.I., Caldas, A.P.F., Mans, D.R.A. South-Am. Off. Anticancer Drug Dev. (SOAD), Luth. Univ., Canoas, RS, Brazil; Dept. Oncology, Hosp. Clinicas Porto Alegre, Porto Alegre, RS, Brazil.

Compared with administration of higher dosages at once, low-dose, fractionated etoposide may provide more prolonged tumoricidal plasma levels and more sustained topoisomerase II inhibition, while avoiding excessively toxic peak concentrations. Indeed, such schedules produced significant response rates in patients with (etoposide-refractory) small cell lung cancer, lymphoma, and ovarian cancer. We previously reported that oral etoposide at the dose of 25 mg/m<sup>2</sup> BID q 12 hours q 7 days exhibited encouraging efficacy in patients with advanced AIDS-KS while producing relatively mild toxicity. Parallel pharmacokinetic analyses showed the achievement of apparently cytotoxic plasma concentrations for prolonged periods of time. In this study, we report on a follow-up trial with etoposide TID 20 mg/m<sup>2</sup> q 8 hours q 7 days in a similar patient population. The intermediate data from this trial are compared with those from the previous study. Thus far, 18 patients were accrued, 12 of whom were evaluable for response and toxicity. They had a median age of 36 years (31-50), a median WHO performance status of 0 (0-3), and adequate liver, renal, and bone marrow function (thrombocytes > 75,000/mm<sup>3</sup> and granulocytes > 1,500/mm<sup>3</sup>). Two patients had received previous chemo- or immunotherapy, but none had undergone prior treatment with anti-retroviral agents. Plasma pharmacokinetic analyses were performed in 8/12 patients. Thus far, 1 CR and 7 PR (67% objective responses) as well as 2 SD were documented. Response duration varied from 1 to 24 months. The main side-effects were granulopenia and leukopenia (CTC-NCI grades 3 and/or 4). Non-hematological toxicity was insignificant, mainly consisting of grade 1 or 2 alopecia, and nausea and vomiting. In addition, one case of grade 3 anorexia was noted. No cases of severe thrombocytopenia or life-threatening drug-related infection were observed. Pharmacokinetic analyses showed the achievement of AUCs of 13.5 ± 6.1 μg·h/mL, peak levels of 2.2 ± 1.0 μg/mL at about 2 h, and t<sub>1/2</sub> of 4.1 ± 2.4 h. Comparison with the data from our previous trial suggests that etoposide at this 20% more dose-intensive schedule produced about 30% greater cumulative AUCs, not more toxicity, but significantly more objective responses. The study remains open for accrual.

**#220 A Phase II Study of Marimastat in Patients with Previously Treated Advanced Lung Cancer.** K. Nakagawa, M. Fukuoaka and the TA-2516 Lung Cancer Study Group *Kinki University School of Medicine, Osaka, Japan.*

Matrix metalloproteinases appear to be essential for cancer cells to grow and spread in cancer patients. Marimastat is a broad-spectrum matrix metalloproteinase inhibitor which has shown activity in various cancer models, including small or non-small cell lung cancer. To determine feasibility and dose dependent antitumor activity, and to compare pharmacokinetic parameters between Japanese and non-Japanese patients, a phase II study of marimastat was conducted in patients with advanced lung cancer. The patients, with PR or CR for previous chemotherapy or chemoradiotherapy, adequate main organ functions, PS 0-2, age range 20-74 years old, and more than 3 months of life expectancy, were eligible for this study. Thirty-nine patients entered in this study were randomized to 10 mg (14 pts), 20 mg (12 pts), and 40 mg (13 pts)/body/day (bid) of oral administration for 3 months. Three patients withdrew from the study before the treatment due to tumor progression (2 pts) and to patient refusal (1 pt). Thirty-six patients were evaluable for toxicity and tumor activity (28 male, 8 female). Sixteen patients had an ECOG score of 0 at baseline, 20 had a score of 1. Median age was 61 years (range: 38-72). Primary tumour types were adenocarcinoma (n = 18), squamous cell carcinoma (n = 10), and small cell carcinoma of the lung (n = 8). Eleven patients (28%) have discontinued the study, 6 (56%) due to unacceptable musculoskeletal (M/S) pain, 3 (27%) for disease progression, 1 (9%) due to allergic skin reaction, and 1 (9%) for patient refusal. Complete study results, including pharmacokinetic parameters, will be presented. Supported by Tanabe Ph. Co. LTD.

**#221 AE-941, an inhibitor of angiogenesis: Rationale for a phase III study on AE-941 in combination with induction chemotherapy/radiotherapy in patients with non small cell lung cancer (NSCLC).** Evans WK, Latreille J, Battist G, Falardeau P, Champagne P, Dupont E, *Ottawa Regional Cancer Centre, Ottawa, Canada K1H 8L6, CHUM, Montréal, Canada H2W 1T8, Jewish General Hospital, Montréal, Canada H3T 1E2, Aeterna Laboratories Inc., Québec, Canada G1P 4P5.*

AE-941, a standardized complex of antiangiogenic inhibitors, shows antiangiogenic and antimitotic activities *in vitro* and *ex vivo*. It was selected by the US National Cancer Institute to investigate its efficacy in advanced NSCLC patients. This double-blind placebo-controlled study will evaluate the effect on survival of AE-941 in addition to induction chemotherapy/radiotherapy combined modality treatment in inoperable stage III patients. The preclinical rationale for this trial is based on the antimetastatic activity of AE-941 in the Lewis Lung Carcinoma mouse model where a 30 and 58% reduction in pulmonary metastases was observed with 7 and 30 ml/kg/day of AE-941, respectively. AE-941 (30 ml/kg) was additive to cisplatin 4 mg/kg (82% reduction compared to 75% with cisplatin alone) in reducing the number of lung metastases. No treatment related mortality or loss of body weight were observed at 30 ml/kg, the highest dose of AE-941 administered. Toxicology studies in monkeys at very large doses (up to 60 ml/kg/day orally) demonstrated no dose-limiting toxicity or target organ damage after 1 year chronic exposure. During a phase I/II trial, 80 lung cancer patients (64% with distant metastases, 88% ECOG 0-1) received AE-941 monotherapy in an open-label trial. Seven percent of non serious adverse events were possibly related to AE-941, most commonly gastrointestinal symptoms (nausea, vomiting). Retrospective survival analysis performed in 45 patients with a primary diagnosis of unresectable stage IIIA, IIIB and IV NSCLC indicated that AE-941 given orally at a dose higher than 3 ml/kg/day significantly improved survival (P = 0.028) in these patients compared to patients receiving doses lower than 3 ml/kg/day (median = 6.6 vs 4.6 months, respectively). Additionally, patients receiving more than 3 ml/kg/day of AE-941 had an approximately three fold decreased risk of death as compared to those receiving less than 3 ml/kg/day (p = 0.016). Phase III clinical studies will evaluate the effect of AE-941 on survival when given in combination with standard therapy in various tumors, including inoperable stage III NSCLC.

**#222 The use of the growth modulation index to evaluate the activity of oxaliplatin added to a 5FU-based regimen in fluoropyrimidine-resistant colorectal cancer.** Bonelli A, Zaninelli M, Leone R, Brienza S, Pasini F, Franceschi T, Pavarana M, Bassetto MA, Cetto GL. *From the Department of Oncology, Verona, Italy, and Debiopharm S.A., Paris, France (B.S.).*

Oxaliplatin (L-OHP) is an interesting new drug for the treatment of colorectal cancer patients. In this cancer the correlation between response rate and patient's survival is poor. It has recently been suggested by von Hoff that the growth modulation index (GMI = the ratio of TTP with a drug used as a second line treatment compared with the TTP with prior therapy) can help in identifying drugs that can change the natural history of tumors; any result >1.33 is unexpected for second-line therapy and is considered excellent. Patients entering this study were treated according to a two-step protocol. In the first step patients chemotherapy-naïve or progressing more than six months from the completion of a 5FU-based adjuvant regimen received the LV-5FU2 chemotherapy program until disease progression. Patients progressing during the first step, or patients relapsed

less than six months from the completion of a 5-FU-based adjuvant regimen, entered the second step of the protocol, in which L-OHP was added to the LV-5FU2 program. Thus far 30 advanced colorectal cancer patients (pts) entered the second step of the protocol. Responses were exclusively evaluated by CAT scans (repeated every 2 months) using standard WHO criteria. Thirty pts (M/F: 20/10; median age: 60 years) received 247 cycles of chemotherapy (median number of cycles/pt: 8; range 2-18). Responses: partial responses in 2 pts (6%), disease stabilization in 23 pts (77%), progressive diseases in 5 pts (17%). Twelve pts (40%), showed a GMI  $\geq 1.33$ , 7 pts (23%) showed a GMI  $\leq 1.33$ -1, while the remaining 11 pts (37%) presented a GMI <1. By the Kaplan Meier method median TTP during the first step of the protocol was 4 months, while on the second step was 7 months (7 patients are still progression-free). Median overall survival from the beginning of the second step was 11.3 months (17 patients are still alive). These data confirm the good results of the LV-5FU2-LOHP regimen in advanced colorectal cancer and suggest that the determination of GMI may be a useful parameter in the clinical evaluation of drugs activity.

**#223 A phase II study of CI-980 in previously untreated small-cell lung cancer: An Ohio State University phase II research consortium study.** Thomas, Jason P; Moore, Timothy; Kraut, Eric H; Balcerzak, Stanley P. *Division of Hematology/Oncology, The Ohio State University, Arthur G. James Cancer Hospital and Solove Research Institute, Columbus, Ohio; Grant Medical Center, Columbus, Ohio.*

CI-980, [ethyl(S)-(5-amino-1,2-dihydro-2-methyl-3-phenylpyrido[3,4-b]pyrazine-7-yl)carbamate 2-hydroxyethanesulfonate (1:1)], is a water-soluble mitotic inhibitor. It acts by binding to the colchicine binding site on tubulin, a site different from that of the vinca alkaloids, inhibiting tubulin polymerization. Cells exposed to CI-980 accumulate in M phase and die. In preclinical tumor models, CI-980 showed a broad spectrum of activity, including in multi-drug resistant tumors, with activity at least equal to that of vincristine.

As a result of the preclinical data, a phase II study of CI-980 was initiated in extensive small-cell lung cancer, a disease considered incurable with conventional chemotherapy. Twelve patients were enrolled in the study and underwent a total of 16 cycles of chemotherapy. Median age of the patients was 54 years (range 34-71 years), and performance status was ECOG 1 (9 patients) and ECOG 2 (3 patients). Peripheral blood samples were collected during the 3 day continuous intravenous infusion at times 0, 24, 48, 72 and 96 hours (24 hours post-infusion) for evaluation of effects on peripheral blood leukocytes. There were a total of 61 significant (grade 2 or >) adverse reactions reported during the 16 cycles. The most common significant adverse reactions were granulocytopenia (9), anemia (7), leukopenia (6), nausea, constipation, fatigue and vomiting (3). Eleven of 12 patients were removed from the study due to progressive disease, three of the eleven having undergone two cycles of therapy. The twelfth patient was removed from study after a second cycle because of stable disease. Only two patient's peripheral blood samples were adequate for interpretation and they showed microtubule depolymerization in both granulocytes and monocytes. This effect was most pronounced at 72 hours and was reversible, with resolution by 24 hours post-infusion.

We conclude that despite antitumor activity demonstrated in preclinical studies, CI-980 does not have biological activity in previously untreated extensive small-cell lung cancer at this dose and infusion protocol.

Supported by NCI grant # 401 CA63185.

**#224 Dolostatin-10 in patients with hepatobiliary cancer: A University of Chicago Phase II Consortium study.** Kindler, H.L., DeMario, M., Abbruzzese, J., Sciorino, D., Pall, Y., Mani, S., Shilsky, R.L., Vokes, E.E. *University of Chicago, MD Anderson Cancer Center, and the University of Chicago Phase II Consortium.*

There is no effective standard therapy for patients with advanced cancers of the hepatobiliary tree; agents with novel mechanisms of action deserve evaluation. Dolostatin-10 is a potent antimitotic agent, derived from the sea hare *Dolabella auricularia*, which binds to tubulin, inhibiting microtubule assembly, polymerization of purified tubulin, and GTP hydrolysis. A phase II multicenter study evaluated the safety and efficacy of Dolostatin-10 in patients with hepatobiliary malignancies. Eligibility criteria included no previous chemotherapy, measurable disease, and adequate hematopoietic, hepatic, and renal function. Thirteen patients (pts) were enrolled between 1/99 and 5/99; enrollment is ongoing. One patient was ineligible for assessment of response or toxicity and is not included in this analysis. Patient characteristics: 8M/4F, median age 64 years (range 47-83), hepatocellular carcinoma (5 pts) cholangiocarcinoma (3 pts), gallbladder carcinoma (4 pts); CALGB performance status: 0 (4 pts), 1 (7 pts), 2 (1 pt). A total of 22 courses of Dolostatin-10 were administered (median 2, range 1-3) at a dose of 400 mcg/m<sup>2</sup> by intravenous bolus once every 3 weeks. There have been no objective responses; 17% of patients have had stable disease for a median of 63 days (range 58-68 days). Grades 3-4 leukopenia developed in 42% pts (27% courses), grades 3-4 neutropenia in 67% pts (41% courses), neutropenic fever in 33% pts (18% courses). One patient each experienced grade 2 thrombocytopenia and grade 3 anemia. Dose reductions for hematologic toxicity were required in 23% of courses. Grade 3 nonhematologic toxicities were infrequent and included



anorexia (1 pt), fatigue (2 pts), diarrhea (1 pt), elevated alkaline phosphatase (2 pts), and elevated SGOT (1 pt). Conclusion: Dolastatin-10 in this dose and schedule does not have significant activity in patients with hepatobiliary cancers. Myelosuppression is the principal toxicity.

**#225 Pre-operative gemcitabine and radiation for resectable adenocarcinoma of the pancreas—preliminary report of a phase II multi-institution trial.** Wolff RA, Madary AR, Pisters PWT, Lee JE, Lenzi R, Vauthey JN, Janjan NA, Crane CH, Staley C, Termuhlen P, Cleary K, Chamsangavej C, Abbruzzese JL, Evans DB: *UT MD Anderson Cancer Center, Emory University School of Medicine and University of Nebraska Medical Center*

Gemcitabine (gem) is an active drug for the treatment of pancreatic cancer and a potent radiosensitizer *in vitro*. In a Phase I study conducted at UT MD Anderson, patients with locally advanced adenocarcinoma of the pancreatic head were treated with weekly gem for 7 weeks concurrently with 2 weeks of external-beam radiation therapy (EBRT) to a dose of 3,000 cGy (300 cGy/fraction/per day; M-F). The maximal tolerated dose of gem was determined to be 400 mg/m<sup>2</sup>. A multi-center Phase II trial of pre-operative gem and EBRT is currently underway for patients with resectable pancreatic cancer. Patients are eligible for treatment if there is a pancreatic mass visualized on contrast-enhanced computed tomography (CT) or endoscopic ultrasound. There must be cytologic or histologic confirmation of adenocarcinoma, no evidence of tumor involvement of the superior mesenteric artery or celiac axis, a patent superior mesenteric-portal vein confluence, and no radiographic evidence of distant metastatic disease. Treatment includes 7 weekly doses of gemcitabine (400 mg/m<sup>2</sup>) and EBRT (3000 cGy) during weeks 1 and 2. Four to 6 weeks after completion of chemoradiation, patients undergo restaging CT and chest x-ray. If there is no interval development of metastatic disease and the primary tumor remains resectable, patients go on to pancreaticoduodenectomy. To date, 18 patients have been enrolled in the trial, 9 have completed all treatment and 9 are in the chemoradiation phase of the treatment plan. Of the 9 patients that have completed all treatment, 3 (33%) required admission for supportive care, typically intravenous hydration and antiemetics. Grade 3 neutropenia developed in 44% and grade 3 thrombocytopenia in 11%. Following chemoradiation, 3 patients were found to have metastatic disease (1 at restaging, 2 at laparotomy) and 6 underwent successful pancreaticoduodenectomy. A complete histologic response to preoperative chemoradiation was seen in 2 of the 6 resected specimens. One other surgical specimen contained only microscopic nests of viable tumor cells. In conclusion, gemcitabine combined with EBRT delivered in this manner has acceptable toxicity and can produce pathologic complete responses. Accrual to this protocol continues.

**#226 A phase I-II study of cisplatin (CDDP) + tomudex (TOM) + levofolinic acid (LFA) + 5-fluorouracil (5-FU) in locally advanced or metastatic head and neck cancer (HN).** Caporigno F, Budillon A, Avalone A, Rivellini F, Di Gennaro E, Ionna F, Mozzillo N, Marcolin P, Guida C, Comella P, Comella G. *National Tumor Institute—Naples, ITALY*

**Purpose:** In a previous phase I study, the combined administration of TOM on day 1, and LFA + 5-FU on day 2, every 14 days, showed manageable toxicity and high activity in locally advanced or metastatic HN. With the above schedule, TOM dose intensity was higher than that achievable with standard every 3 week schedule. CDDP is the most active single agent in HN, and has shown at least additive growth inhibitory effects in a panel of human tumor cell lines, when combined with TOM.

Based on the above observations, we started a phase I-II study of CDDP + TOM + LFA + 5-FU in locally advanced or metastatic HN.

**Patients and methods:** Eligible pts, never pretreated with chemo- or radio-therapy, received a combination of CDDP + TOM on day 1, and LFA + bolus 5-FU on day 2, every 2 weeks. Doses of CDDP, TOM, 5-FU were alternately escalated up to maximum tolerated dose (MTD), which was defined as the dose level at which at more than a third of patients had dose limiting toxicity.

**Results:** Available clinical data are summarized below.

Step	TOM/CDDP/LFA/5-FU	Pts	DLT	Type*	Response
1	2.0/40/250/750	6	2	F3; N4	3/6 (PR)
2	2.5/40/250/750	6	1	Febrile N	1/6 (CR)
3	2.5/40/250/900	6	2	N4	4/6 (2CR, 2PR)
4	2.5/50/250/900	6	2	N4	3/6 (1CR, 2PR)
5	3.0/50/250/900	6	4	N4	4/6 (PR)
5bis	2.5/60/250/900	11	3	N4	5/5 (1CR, 4PR) (6TE)
Total		41	14		20/35

\* F = Fatigue; N = Neutropenia; TE = Too early

**Conclusion:** CDDP + TOM + LFA + 5-FU is a well tolerated and active regimen in advanced HN. MTD has been reached at 5<sup>th</sup> dose level; 5 bis dose level has been selected for phase II evaluation and very preliminary response data show impressive clinical activity.

**#227 Irinotecan as a second line chemotherapy in advanced and metastatic colorectal cancer. Is that appropriate regimen?** Chilikid, K.Y., Lazarev, A.F., Doty, I.N. *Altai Regional Oncological Center, Barnaul, Russian Federation*

Chemotherapy in colorectal cancer is an open question required future investigations, especially second line chemotherapy. We evaluated response rate and survival in 86 patients with Dukes'B3,C2,D advanced and metastatic colorectal cancer after failed 5-fluorouracil based chemotherapy. 32 patients received Irinotecan 125 mg/sq.m intravenously weekly for 4 weeks followed up to 2 weeks rest up to tumor progression or an acceptable toxicity (group A). 54 patients received supportive therapy (group B). There were no complete responses, 12.5% partial responses, 34.4% stable disease and 59.4% disease progressions. Toxicity rate included 15.6% leucopenias, 21.9% gastrointestinal (1-grade 4) and 12.5% liver toxicities, 15.6% hyperthermias in group A. Overall survival was 15.4 months in group A and 13.7 months in group B (P=.054). Thus: there is no statistically significant increase of survival, though response rate was not pure. This fact together with large toxicity rate and highly expensive treatment cost lead to doubt that such Irinotecan regimen is appropriate for advanced and metastatic colorectal cancer.

**#228 Phase II clinical trial design for noncytotoxic anticancer agents for which time to disease progression is the primary endpoint.** Mick, Rosemarie, Crowley, John J., and Carroll, Raymond J. *University of Pennsylvania School of Medicine, Philadelphia, PA and Fred Hutchinson Cancer Research Center, Seattle, WA*

Historically, the primary Phase II endpoint for cytotoxic agents has been tumor response rate, the percentage of patients whose tumors shrink >50%. In contrast, cytostatic agents are expected to delay tumor growth, such that the primary Phase II endpoint is likely to be time to progression (TTP). Currently, Phase II trials with TTP endpoints are designed as single arm comparisons to historical control estimates. It may be difficult to interpret the relative merit of TTP estimates from single arm trials, for which there is no active control group. Through computer simulation, we examined power properties of a novel Phase II design that determines clinical efficacy by comparing sequential failure times within each patient. Assuming patients eligible for Phase II study have failed previous treatment, their most recent prior time to progression is TTP<sub>1</sub>. Time to progression after the cytostatic agent, TTP<sub>2</sub>, may or may not be censored at analysis. This design is motivated by a "growth modulation index" (TTP<sub>2</sub>/TTP<sub>1</sub>) and the proposition that a cytostatic agent be considered effective if the index >1.33. Degree of correlation between (TTP<sub>1</sub>, TTP<sub>2</sub>) pairs is a key component of this design. Power of the test was evaluated by 1,000 simulated trials at varied sample and clinical effect sizes and correlations. Clinical effect was measured by the hazard ratio (HR). For example, null and alternative hypotheses of TTP<sub>2</sub> = TTP<sub>1</sub> (no benefit) vs. TTP<sub>2</sub> > TTP<sub>1</sub> (benefit) were tested by HR = 1.0 vs. HR = 1.3 or HR = 1.5, respectively.

		Power of the test of paired failure times				
		Null Hazard ratio = 1.0	N = 30	N = 40	N = 50	N = 60
		Alternative Hazard ratio = 1.3	pairs	pairs	pairs	pairs
Correlation	r = 0.3		.169	.185	.254	.306
	r = 0.5		.315	.364	.463	.522
	r = 0.7		.612	.743	.828	.886
Alternative Hazard ratio = 1.5						
Correlation	r = 0.3		.316	.417	.488	.542
	r = 0.5		.505	.571	.680	.762
	r = 0.7		.823	.909	.950	.966

These results clearly demonstrate efficiency of the trial design, assuming moderate to strong correlation between paired failure times.

**#229 Clinical pharmacodynamics of topoisomerase-1 inhibitor therapy: lessons and issues for future studies.** Howard Hochster, Leonard Liebes, Scott Wadler\*, C. Runowicz\*, Milan Polmesil, James Speyer, and Franco Muggia; *Kaplan Comprehensive Cancer Center, New York University School of Medicine, New York, NY 10016 and the Albert Einstein College of Medicine, Bronx NY*

We investigated the interaction of topotecan (10-hydroxy-9-dimethylaminomethyl-camptothecin, TPT), a semi-synthetic camptothecin analog and topoisomerase-1 (topo-1) in endoscopic biopsies and in peripheral blood mononuclear cells (PBMCs) in several clinical studies by SCL-70 antibodies and improved Western blot allowing measurements in <10 mg of tissue. Endoscopic biopsy of patients with Upper GI cancers who received topotecan 1.5 mg/m<sup>2</sup>/day x 5 days over 30 minutes q 28 days were correlated with TPT drug levels were obtained on days 1 and 4. In 14 patients post-treatment topo-1 ranged from 0.36 to 18.3 x 10<sup>6</sup> copies/cell (median 7.36). Five specimens allowed cleavable complex measurement, showing 18-91% (median 49%) inhibition of topo-1 and fit a sigmoid inhibition model of pharmacodynamic interaction.

We also determined topo-1 levels weekly in PBMCs in phase I and II studies of 21-day prolonged topotecan administration (Clinical Ca Res,

1997 and JCO, 17:2553, 1999). In 58 samples (21 patients) with ovarian cancer given TPT 0.4 mg/m<sup>2</sup>/day × 21 days, we found a strong correlation of decrease in topo-1 level with topotecan AUC (Wilcoxon  $p < 0.01$ ), and a good fit to the pharmacodynamic inhibitory effect model (Emax CV = 15% with EC50 = 950 ng/ml-hr). Median values of topo-1 decreased weekly from baseline ( $8.0 \times 10^5$  copies/cell) to 6.2, 3.8, and 5.0 at weeks 1, 2 and 3 respectively ( $p < 0.001$  all three). ANC nadir strongly correlated with change in PBMC topo-1 level also (Spearman  $\rho = 0.66$ ,  $p < 0.02$ ).

These observations demonstrate increased topo-1 inhibition with prolonged TPT administration (AUC). We are currently investigating similar correlations in 1) previously untreated ovarian cancer pts treated with 14-day TPT and cisplatin and 2) with oral topo/cisplatin; 3) phase I/II studies of doxil and 14-day TPT and 4) daily × 5 TPT with the FTI, R115777. These combinations will shed light on factors other than TPT exposure which contribute to topo-1 depletion and pharmacodynamics.

## POSTER SESSION 3 SECTION 1: GENOMICS AND HIGH THROUGHPUT SCREENS FOR TARGET DISCOVERY (ARRAYS AND CHIPS)/SIGNAL TRANSDUCTION (RELATED TO GENE EXPRESSION)

**#230 DNA array technology in the molecular pharmacology of 17-allylamino geldanamycin.** Clarke, Paul A., Hostein, Isabelle, Maloney, Allison, Walton, Mike and Paul Workman, Paul. CRC Centre for Cancer Therapeutics, ICR, Sutton, Surrey, UK.

Exposure of cells to anticancer agents can result in altered gene expression. In general, only a single gene or a small number of genes are studied. In order to improve the efficiency and value of such experiments, we are interested in using DNA array technology to identify, on a genome wide scale, drug responsive genes which might serve both as surrogate markers for drug action and as future targets for drug development. In this study we have examined gene expression following treatment of colon adenocarcinoma cells with a novel benzoquinone ansamycin, 17-allylamino geldanamycin (17-AAG), an agent that is about to enter clinical trial in our centre and elsewhere. This agent inhibits hsp-90 activity, a protein required to maintain the stability of a number of signalling proteins, including c-Raf-1. Two colon adenocarcinoma cell lines, HCT116 and HT29, were selected for initial *in vitro* studies. In both cell lines a single 500 nM dose of 17-AAG was sufficient to reduce c-Raf-1 protein levels detected by western blotting at 24 hours. In addition, 17-AAG inhibited the high levels of constitutive MAP kinase phosphorylation detected in HCT116 cells. However, 48 hours after treatment c-Raf-1 levels recovered in the HCT116 cells, but remained depressed in HT29 cells. This difference was also reflected in the different patterns of gene expression detected with an array corresponding to approximately 5000 cDNAs of known identity. Only a few transient changes in gene expression were detected at 24 hours following treatment of HCT116 cells, these included decreased expression of a number of c-myc regulated genes. In contrast, the pattern of gene expression in 17-AAG treated HT29 cells underwent a far greater alteration. Data detailing changes in gene expression in response to 17-AAG treatment of both HT29 and HCT116 cells will be presented.

**#231 Mechanisms of Raf-independent Ras transformation.** Shields, Daniel M., and Der, Channing. Department of Pharmacology, Lineberger Cancer Center, University of North Carolina, Chapel Hill, NC 27599.

The proto-oncogene Ras utilizes a complex, multitude of diverse effector targets to transduce signals to the nucleus including the Raf/MAPK pathway. The understanding of Ras signaling is further complicated when different cell types are examined. For example while both Ras and Raf can transform fibroblasts, only Ras can fully transform epithelial cells. Numerous studies have demonstrated that Raf-independent pathways are crucial for Ras transformation in epithelial cells. In particular, analysis of effector domain mutants of Ras containing a 40C or a 37G mutation rendering them unable to bind Raf are still capable of transforming epithelial cells.

To understand better the Raf-independent mechanisms by which Ras transforms cells, genes that are either up or down regulated in response to Ras but not Raf expression in rat intestinal epithelial cells were identified by representational difference analysis. Examples include tropomyosin, connexin, and TLSF beta which were downregulated and protease nexin which was upregulated by Ras but not Raf. We found that some of these genes are also dysregulated in human tumor cell lines containing Ras mutations but not in the same cells where mutant Ras has been genetically deleted. This suggests that the expression patterns observed in the RIE cells are not cell line specific. In addition, we found the dysregulation also occurred in matched pairs of human breast and colon tumor samples as compared to the normal marginal tissue. These results suggest that some of these genes may represent potential new targets for cancer therapy.

**#232 Integrated proteomics technologies in molecular medicine.** Rohlf Christian, Townsend Reid, Page Martin and Parekh Raj. Oxford GlycoSciences, Abingdon Science Park, 10 The Quadrant, Abingdon, OX14 3YS

The advances in the human genome project joined with the availability of an increasing number of methods for gene expression analysis have led to new strategies in drug discovery. However, it is becoming apparent that purely gene-based expression analysis is not sufficient. Proteomics-based studies add additional information on abundance, post-translational modifications, processing and subcellular/extracellular locations of proteins and heteroprotein complexes. Although proteins reflect the physiology of normal and diseased tissue more closely, the demands on proteomic technology of reproducibility, sensitivity and throughput have hampered the fast and direct access to this information. Based on several significant technological advances, OGS has implemented a high-sensitivity highly reproducible, high throughput platform for proteomics analysis of human tissue, cells and body fluids. Applications of the platform will be discussed to (i) breast tumor cells, (ii) to identify tumor-specific plasma membrane proteins, (iii) to characterize the distribution of post-translational modification status of key regulatory proteins in tissues and cell lines, and (iv) to identify and characterize proteins involved in key signaling pathways.

**#233 Exploring Putative Molecular Determinants of Cytotoxicity and Antiproliferative Effects in the NCI Anticancer Drug Screen Using Pattern Analysis Tools.** Myers TG, Holbeck SL, Bell P, Rubinstein L, Monks A, Drake JC, Sausville EA. Developmental Therapeutics Program, DCTD, National Cancer Institute, NIH, Bethesda, MD.

The NCI cancer screen has now tested over 70,000 compounds for cytotoxicity in 60 human tumor cell lines. The same cell lines have been characterized for gene mutations or expression at the RNA, protein, or enzyme activity level by numerous investigators to mine the database of selective cytotoxicity patterns for compounds that might interact with the "molecular target" of interest. More than 300 molecular factors have been measured individually. A database resulting from the mRNA quantitation of the 60 human tumor cell lines using a 10,000 cDNA microarray will soon be released. The retrospective correlation analysis of these data, using, for example, the COMPARE program, is capable of producing very provocative hypotheses relating the action of particular compounds to particular molecular targets. Evaluating the multiple hypotheses that such tools generate requires an assessment of biological plausibility as well as statistical significance of each. We have developed new WWW-enabled interfaces to a ChemoDB (chemotherapy database) system that allow for dynamic exploration of automatically-generated hypotheses. We will illustrate the capacity of this system to generate hypotheses regarding experimental cancer pharmacology by defining groups of molecular targets that appear to determine the cell line selective potency of the same compounds. This tool has the potential to reveal signalling pathways and interacting cellular components that are being targeted by the compounds.

**#234 Genetic approaches to cancer drug discovery.** Dunstan, Heather M., Szankasi, Philippe, Lamb, John L., Simon, Julian A., Hartwell, Leland H. and Friend, Stephen H. The Seattle Project, Fred Hutchinson Cancer Research Center

Anti-cancer drug discovery is driven by the need to identify agents that are differentially toxic to tumor cells by exploiting differences in the biology of normal and tumor cells. Several of the alterations found in human tumors can be modeled in systems that are amenable to genetic alteration, such as the yeast *Saccharomyces cerevisiae*. We are using yeast mutant models of the tumor context of genetic instability—including DNA repair defects, chromosome transmission fidelity defects, checkpoint defects, and cell cycle control defects, to identify known and novel agents that target these alterations. The primary goals of this research are: 1) to identify agents that target unexploited alterations in tumors, 2) to identify new agents acting against currently targeted alterations with different biological limitations, and 3) to build an information base toward the treatment of tumors based on molecular defects rather than tissue of origin. We have assembled an isogenic panel of yeast mutants with defined defects, and use these in cell-based assays to identify agents with differential toxicity toward cells defective in particular pathways governing genetic stability. In collaboration with the National Cancer Institute, we have determined the relative toxicity of FDA-approved anticancer agents to a large panel of yeast mutants. In an ongoing program, we are screening the compounds in the NCI/DTP repository for new agents that target genetic instability. From these yeast screens, we have identified several classes of compounds that may be clinically useful, including new structural classes of topoisomerase poisons and compounds that are differentially toxic to yeast defective for mitotic spindle assembly checkpoint function.

**#235 Gene expression profiles associated with antiestrogen responsive versus resistant human breast cancer cells.** Gu, Z., Davis, N., Hanfelt, J., Hurley, C., Xiao, H., Gray, F., Flessate-Harley, D. and Clarke, R. Georgetown University, Departments of Oncology, Physiology & Biophysics, Lombard Cancer Center, 3970 Reservoir Rd., NW, Washington, DC 20007.



Anti-estrogen therapy is a major approach used in the treatment of breast cancer. Approximately 80% of breast tumors that express estrogen and progesterone receptors will initially respond to anti-estrogen therapy. However, most of these tumors will develop an acquired resistance phenotype. We hypothesize that this resistance is due to the altered expression and/or activity of specific genes, which were previously regulated by the transcriptional regulatory activities of estrogen receptors. The identification and modulation of those pathways that confer anti-estrogen resistance could provide new approaches for the prevention or treatment of anti-estrogen resistance.

We have used serial analysis of gene expression (SAGE) and gene microarray analyses to identify changes in gene expression patterns between anti-estrogen responsive and anti-estrogen resistant breast cancer cells. Our data suggests that cAMP response element (CRE), NF- $\kappa$ B, and AP-1 exhibit differences in their gene expression patterns and/or transcriptional regulatory activities between anti-estrogen responsive and anti-estrogen resistant breast cancer cells. Regulation of these changes in gene expression/activity may prevent acquired resistance or restore responsiveness to resistant cells. Additional studies are in process to test these hypotheses. These studies will aid in the development of novel approaches for the management of acquired anti-estrogen resistance.

**#236 Retinoid regulated genes in breast cancer cells.** Skear, Todd, C., Bouker, Kerrie, B., Clarke, Robert Lombardi Cancer Center, Dept of Physiology and Biophysics, Georgetown University.

Retinoids are vitamin A analogs that have shown effectiveness in pre-clinical and clinical breast cancer studies. Although breast cancer cells frequently respond to retinoid treatment, the development of resistance to these drugs is common. A better understanding of the signaling pathways that mediate retinoids in the retinoid sensitive or resistant cells could identify new molecular targets for the development of drugs that will be effective in retinoid resistant tumors. We have identified two genes, nucleophosmin (npm) and interferon regulatory factor-1 (IRF-1), that are regulated by 9-cis retinoic acid (9cRA) in the MCF-7 breast cancer cells. IRF-1 is a tumor suppressor gene that is involved in growth arrest and apoptosis in response to several anticancer agents. Npm can transform cells, possibly through its ability to inhibit IRF-1 activity. Npm protein expression is suppressed >40% by 9-cRA in MCF-7 cells. We have previously shown that npm is also suppressed by antiestrogens and elevated by estradiol in MCF-7 cells. IRF-1 RNA levels are induced 7-fold by 9-cRA in the MCF-7 cells. Preliminary experiments indicate that this induction occurs very rapidly, <1 hr. In order to understand the role of IRF-1 in breast cancer cells, we have made MCF-7 cell lines that constitutively overexpress IRF-1. During the selection of the G418 resistant transfected MCF-7 cells, we obtained 40% less colonies in the IRF-1 transfectants than in the empty vector control transfectants. Furthermore, of the 24 IRF-1 transfectant clones that were isolated, we were able to establish only 4 clonal cell lines that stably express IRF-1. The IRF-1 expression levels in these 4 lines was variable and growth assays showed an inverse correlation between the IRF-1 expression levels and the growth rates of the cells. These data indicate that the IRF-1/npm signaling pathway may be involved in mediating the effects of retinoids on breast cancer cells and that they may be targets for future drug development. This research was supported by American Cancer Society grant IRF-97-1520-01-IRG (TS), NIH grants P50 CA58185 (RC), R01 CA58022 (RC), DOD grant BC980586 (KB).

**#237 Interferon Regulatory Factor-1: A Putative Mediator of Anti-estrogen Responsiveness in Breast Cancer.** Bouker, Kerrie B., Skear, Todd C., and Clarke, Robert. Georgetown University, Departments of Oncology and Physiology & Biophysics, and Lombardi Cancer Center, Washington, DC 20007.

The causes of anti-estrogen resistance in breast cancer are currently unclear. However, our data provides several lines of evidence suggesting that the tumor suppressor Interferon Regulatory Factor-1 (IRF-1) may be involved in cellular responsiveness to antiestrogens. We have previously shown that treatment with interferon synergizes with antiestrogens to inhibit breast cancer cell growth. Additionally, we have shown that IRF-1 expression is induced more than 50% by the antiestrogen ICI 162,780, which inhibits proliferation, and repressed 56% by estradiol, which stimulates proliferation in these cells. Interestingly, basal IRF-1 mRNA expression is higher in the antiestrogen responsive MCF-7 cells compared to the antiestrogen resistant MCF-7/LCC9. We have recently created a dominant negative IRF-1, by deleting amino acids 150-326 of the IRF-1 cDNA, to evaluate the role of IRF-1 in breast cancer cells. Using transient transfection assays we have shown that this dominant negative IRF-1 inhibits basal IRF-1 activity more than 2-fold and completely blocks interferon- $\gamma$  induced IRF-1 activity. We will use this construct to determine the role of IRF-1 in the response of breast cancer cells to antiestrogens. The inhibition of IRF-1 activity will ultimately allow us to determine if this tumor suppressor and its subsequent signaling pathways are required for the induction of growth arrest and apoptosis by antiestrogens in breast cancer cells. Furthermore, this dominant negative approach may lead to the identification of novel molecular targets for breast cancer gene therapy. This work was sup-

ported by DOD grant BC980586 (KB), American Cancer Society grant IRF-97-1520-01-IRG (TS), NIH grants P50 CA58185 (RC), R01 CA58022-07 (RC), NRSA CA-09686 (LCC)

**#238 Trichostatin A activates immediate c-jun gene expression by a mechanism involving MEK/MAPK signaling and increased AP-1 activity that is separate from histone acetylation.** Taher, M. M., Bullock, S. K., Palk, D. S., Hershey, C. M., Allis, D. C., and Valerie, K. University of Virginia, Charlottesville, and Department of Radiation Oncology, MCV-VCU, Richmond, VA 23298.

Numerous studies have demonstrated that histone deacetylase (HDAC) inhibitors are effective transcriptional activators. However, it is not clear whether HDAC inhibitors affect transcription through modulation of chromatin alone or upstream signaling events are also required. In this study we investigated the functional link between histone acetylation (HA) and the activation of c-jun expression after trichostatin A (TSA) treatment and any involvement of specific signal transduction pathways. Incubation of cells with TSA (1-50 nM) significantly activated c-jun expression ( $\leq 49$ -fold) in a dose- and time-dependent manner in HeLa cells stably transfected with the luciferase reporter gene driven by the human c-jun promoter. Increased gene expression correlated with rapid induction of AP-1 DNA binding activity. Then, examining upstream signaling events required for this increase, we found that TSA-mediated c-jun expression was inhibited 60% using the MEK-1/2 inhibitor PD98059 whereas the p38 MAP kinase inhibitor SB203580 did not affect c-jun expression. Western blot analyses with phospho-specific antibodies confirmed the rapid and transient activation (10-20 min) of p42/44 MAP kinase and the lack of p38 MAP kinase activation in response to TSA, and the inhibition of the former with PD98059. As expected, TSA treatment also resulted in rapid acetylation of histones H3 and H4, but PD98059 did not affect this process. Furthermore, TSA did not increase Ser-10 phosphorylation of histone H3. We conclude that TSA primarily activates immediate c-jun expression via the p42/44 MAP kinase pathway and increased AP-1 activity, a process that is separated from HA. Opening of chromatin by HA may cooperate with activated AP-1 transcription factor to increase promoter accessibility and subsequent c-jun gene expression. Supported by CA53199 (KV).

**#239 Trichostatin A is a histone deacetylase inhibitor with potent antitumor activity against breast cancer *in vivo*.** Vigushin DM, All S, Pace P, Ito K, Adcock I and Coombes RC. Departments of Cancer Medicine and Thoracic Medicine, Imperial College of Science, Technology & Medicine, London W6 8RF, United Kingdom.

Trichostatin A (TSA), an antifungal antibiotic with cytostatic and differentiating properties in mammalian cell culture, is a potent and specific inhibitor of histone deacetylase (HDAC) activity. TSA inhibited proliferation of six breast carcinoma cell lines with mean  $\pm$  SD  $IC_{50}$  of  $134.2 \pm 125.3$  nM (range 26.4-308.1 nM). In MCF-7 cells, antiproliferative potency ( $IC_{50}$  = 27.7 nM) and HDAC-inhibitory activity ( $IC_{50}$  = 9.3 nM) of TSA were comparable, and TSA caused pronounced histone H4 hyperacetylation. In randomized controlled efficacy studies using the N-methyl-N-nitrosourea (NMU) carcinogen-induced rat mammary carcinoma model, TSA had pronounced antitumor activity *in vivo* when administered to 5 animals at a dose of 500  $\mu$ g/kg by subcutaneous injection daily for 4 weeks compared with 4 control animals. Furthermore, TSA did not cause any measurable toxicity in doses of up to 5 mg/kg by subcutaneous injection. Eight tumors from 6 animals were examined by histology. Tumors from 2 rats refractory to TSA treatment and from a third control animal were all adenocarcinomas. In contrast, 4 tumors from 3 rats that responded to TSA had a benign fibroadenoma phenotype, suggesting that the antitumor activity of TSA is due to induction of differentiation. The present studies confirm the potent dose-dependent antitumor activity of TSA against breast cancer *in vitro* and *in vivo*, strongly supporting histone deacetylase as a molecular target for anticancer therapy in breast cancer.

**#240 Gene therapy with dominant-negative STAT3 induces apoptosis and suppresses growth of the murine melanoma B16 tumor *in vivo*.** Niu Guilian<sup>1</sup>, Heller Richard<sup>2</sup>, Callett-Falcone Robyn<sup>1</sup>, Coppola Domenico<sup>1</sup>, Jaroszeski Mark<sup>2</sup>, Dalton William<sup>1</sup>, Jove Richard<sup>1</sup>, and Yu Hua<sup>1</sup>. <sup>1</sup>H. Lee Moffitt Cancer Center & Research Institute, Tampa, FL. <sup>2</sup>University of South Florida College of Medicine, Tampa, FL.

While signal transducers and activators of transcription (STATs) were originally discovered as mediators of normal cytokine signaling, constitutive activation of STAT proteins, including STAT3, has been found in increasing numbers of human cancers. Recently, a causal role for STAT3 activation in oncogenesis has been demonstrated, suggesting that STAT3 represents a novel target for cancer therapy. We report here that *in vitro* expression of a STAT3 variant with dominant-negative properties, STAT3 $\beta$ , induced cell death in murine B16 melanoma cells that harbor activated STAT3. By contrast, expression of STAT3 $\beta$  had no effect on normal fibroblasts or the STAT3-negative murine tumor, MethA, suggesting that only tumor cells with activated STAT3 have become dependent on this pathway for survival. Significantly, gene therapy by electroinjection of the STAT3 $\beta$  expression vector into pre-existing B16 tumors caused inhibition of tumor growth and tumor regression. This STAT3 $\beta$ -induced antitumor effect is associated with apoptosis of the B16 tumor cells *in vivo*. These findings

demonstrate for the first time that interfering with STAT3 signaling induces potent antitumor activity *in vivo*, and thus identify STAT3 $\beta$  as a potential molecular target for therapy of human cancers harboring activated STAT3.

**#241 Regulation of proliferation of squamous cell carcinoma of the head and neck (SCCHN) by CD40.** Tillman, Karl; Cavaclini, Lisa; Hinds, Phillip; Mungler, Karl; Rheinwald, James; and Posner, Marshall. *Beth Israel Deaconess Medical Center, Brigham and Women's Hospital and Harvard Medical School, Boston, MA 02215.*

The TNF $\alpha$  related cell surface receptor, CD40, has been identified on a variety of cells in malignant and normal tissues including normal basal keratinocytes. Receptor ligation is associated with varying effects on cell proliferation and cell-associated processes in different tissues as well as in B cells. Previously, we demonstrated that CD40 is expressed *in vitro* on SCCHN cell lines and *in vivo* on tumors. Furthermore, CD40 ligation by trimeric CD40 ligand (CD40L) inhibited the proliferation of 3 out of 7 SCCHN cell lines. In this report, we demonstrate that inhibition of SCCHN proliferation is not mediated by apoptosis, differentiation or senescence. As measured by annexin V binding, there was no significant change in apoptosis following incubation with either CD40L, anti-CD95 (Fas) or both. Involucrin expression was used as a marker of differentiation following CD40 ligation for 24 or 48 hours. Changes in Involucrin expression were not induced by CD40L. Senescence, as measured by senescence-associated  $\beta$ -galactosidase was also not altered following exposure to CD40L. After exposure to CD40L for 24-72 hrs, no significant changes were observed in the cell cycle status of any of the seven SCCHN lines tested. From these results we conclude that the inhibition of proliferation of SCCHN by CD40 ligation does not occur by mechanisms that cause apoptosis, differentiation, or senescence. Further, if cell cycle perturbations occur, they do so by a mechanism that subtly effects cell cycle. Although the mechanisms by which CD40 act remain to be established, these results suggest that CD40, in SCCHN, acts in a manner that is distinct from its traditional means associated with B cell activation pathways.

**#242 Retinoid cross-resistance to 9-cis-RA and 4HPR is not associated with the loss of RAR $\alpha$  and RXR $\alpha$  RNA expression.** Lee, Richard Y., Skaar, Todd C., Gu, Zhiping, Leonessa, Fabio, and Clarke, Robert. *Georgetown Univ., Dept. of Physiology & Biophysics, Lombardi Cancer Center, Washington, DC 20007.*

Retinoids, analogs of Vitamin A, inhibit breast cancer cell proliferation and are useful chemopreventive agents for postmenopausal women. These compounds have varied selectivity for retinoid receptors in the super-family of nuclear transcriptional factors. 9-cis-retinoic acid (9-cis-RA) is a retinoid pan agonist that activates both RAR and RXR isoforms. N-(4-hydroxyphenyl) retinamide (4HPR) has unclear receptor selectivity, but shows promising clinical activity and is presently used in phase II clinical trials. One issue with retinoid chemoprevention is the acquisition of resistance and possible cross-resistance, but no established *in vitro* model has been developed to study the problem of acquired retinoid resistance for postmenopausal breast cancer patients.

We established an *in vitro* model by generating two stable retinoid resistant cell lines, MCF-7/LCC20<sup>4HPR</sup> and MCF-7/LCC21<sup>9cis</sup>. They were generated through selection of an estrogen independent MCF-7 variant (LCC1) against increasing concentrations of 4-HPR and 9-cis-RA. Anchorage-dependent growth assays confirm that MCF-7/LCC20<sup>4HPR</sup> is stably and consistently 3-5 fold resistant to the drug 4-HPR, but surprisingly shows a half log cross-resistance to 9-cis-RA after growing more than 30 passages without the drug. However, MCF-7/LCC21<sup>9cis</sup> maintains its resistance to 9-cis-RA (100-fold), but exhibits no cross-resistance to 4-HPR. RNase Protection Assay was used to measure retinoid receptor RNA levels. RAR $\alpha$  and RXR $\alpha$  RNA levels of these retinoid resistant cell lines are unaltered with respect to the parental cells. A cDNA atlas array is being used presently to identify molecular pathways and biomarkers of acquired retinoid resistance and cross-resistance. The information from the arrays will find known genes that may play a role in acquired resistance to retinoids.

**#243 Inhibition of DNA methyltransferase stimulates the expression of STATs 1, 2 and 3 genes in colon tumor cells: implications for tumor suppression.** Karpf, Adam R., Petersen, Peter W., Rawlins, Joseph T., Dalley, Brian K., Yang, Q., Albertsen, Hans M. and Jones, David A. *The Huntsman Cancer Institute, Salt Lake City, UT 84108.*

Inhibitors of DNA methyltransferase (DNMTase), typified by 5-aza-2'-deoxycytidine (5-Aza-CdR) induce the expression of genes transcriptionally downregulated by *de novo* methylation in tumor cells. Clinical trials have demonstrated promise in the use of 5-Aza-CdR (decitabine) for treating leukemia and current trials are evaluating 5-Aza-CdR for the treatment of lung and prostate cancers. In view of the clinical interest in methyltransferase inhibition and our incomplete understanding of the cellular consequences of inhibiting DNA methylation, we have utilized gene expression microarrays to probe the effects of treating HT29 colon adenocarcinoma cells with 5-Aza-CdR. HT29 cells were dramatically growth-inhibited following treatment with 5-Aza-CdR, and the kinetics of the growth inhibition suggested that gene activation could account for the

inhibition. Microarray expression analysis revealed that nineteen of 4608 genes (0.4%) were upregulated by greater than 2 standard deviations above the mean expression ratio following 5-Aza-CdR treatment. The composition of this gene set implicated a role for the stimulation of interferon response genes in the molecular action of 5-Aza-CdR. Extended investigations revealed that the induction of this gene set correlated with the transcriptional induction of STATs-1, 2, and 3 and their subsequent activation by endogenous stimuli. Consistent with this response was our finding that 5-Aza-CdR treatment sensitized HT29 cells to growth inhibition mediated by exogenous Interferon- $\alpha$ 2a. These observations suggest that 5-Aza-CdR should be investigated as a potentiator of Interferon-responsiveness in certain interferon-resistant tumors. This study demonstrates that microarrays can successfully interrogate the cellular consequences of drug treatment.

**#244 MICROMAX™: A complete system for rapid high sensitivity gene expression analysis.** Brown, Beverly A. and Killian, Jeffery. *NEN Life Science Products, Inc.*

The rapid parallel study of the entire panorama of mRNA expression in a wide range types of samples, from cell culture to clinical micro-metastasis has been enabled by the development of differential gene expression analysis on cDNA microarrays and related chip technology utilizing oligonucleotides. However, full acceptance of this technology has been hindered by a number of factors, unavailability of genes and spotting capability, lack of adequate sensitivity, poor reproducibility, complex lengthy protocols and cost. NEN, in collaboration with AlphaGene, has introduced MICROMAX; a complete cDNA microarray system for high through put, high sensitivity differential gene expression, available to all researchers. NEN brings extensive assay development capability and Tyramide Signal Amplification (TSA) to provide unparalleled sensitivity and convenience to cDNA microarrays. Utilizing the first product, an array of 2400 known human genes, collaborators have been able to reduce the amount of starting total RNA from the typical 100 ug to as little as 1-4 ug while gaining the capability of detecting a single copy mRNA from samples as small as 10<sup>5</sup> cells without the need to amplify the mRNA. The linear range of the response in MICROMAX is over 2 orders of magnitude. Comparative studies with human tissue samples and cell lines give results that agree with two color hybridization and published Northern analysis. The reproducibility is such that significant changes in expression levels are around 2-3 fold. The reading of a MICROMAX slide is by standard microarray scanners as it is developed with the traditional cyanine 3 and cyanine 5 tyramides. A slide reading service is available for those who do not have access to scanners.

Additional products, including focus arrays of specific gene families and screening arrays with genes from non-human sources are in development. With the introduction of MICROMAX, any researcher can take advantage of the potential of microarray analysis of differential gene expression without upfront fees, large capital investment in instrumentation or the investment in the time required for optimization.

**#245 Towards a definition of the molecular processes associated with tumor progression.** Bozic Christophe, Pillof-Brochet Céline, Malinge Sophie, Wagner Sarah, Gaultier Aurélie, Gadal Franck, Crépin Michel, Iris François, Buffat Laurent and Treich Isabelle. *VallGene SA, Tour Neptune, 92086 Paris-La-Défense, France and Laboratoire de Recherche Oncologie Moléculaire Humaine (EA 445) UFR Léonard de Vinci, Université Paris-nord, 93012 Bobigny, France.*

It is well established that spontaneous malignant tumors initially arise from clonal expansion of a transformed cell. However, during tumor evolution a wide variety of histological phenotypes often are concurrently present within a neoplastic focus and understanding the molecular phenomena associated with tumor progression is of primary importance.

The experimental system constituted by the cell lines MCF7 and MCF7-ras is one of the most extensively studied model mimicking two stages of human breast tumor progression. MCF7 is regarded as a good model of hormone-dependent, relatively well differentiated, breast cancer (SRB II). When transfected with constitutively activated h-ras (MCF7-ras), an oncogene over-expressed in 40% of breast cancers, the cell line acquires the SRB III invasive phenotype. These cell lines constitute a rich experimental model for identification of the genes whose expression (induction/repression) is specifically associated with progression from non-invasive to invasive tumoral states.

VallGene's Gene Identification (VGID™) technology is independent of complex probe arrays and directly isolates over-expressed and under-expressed transcripts associated with the transition from one defined phenotypic state to another defined phenotypic state within a congenic system. VGID was applied to the MCF7-MCF7-ras model system in order to identify the genes specifically involved in the transition from non-invasive to h-ras-associated invasive phenotype.

The transcripts isolated correspond to known as well as unknown genes. The known genes belong to the expression classes II and III (from 100 transcripts to less than 20 transcripts per cell) and define a limited set of physiological pathways. Several previously characterized genes are dem-



onslated to play unexpectedly important roles in the transition from non-invasive to h-ras-associated invasive phenotype, as defined by the MCF7-MCF7-ras experimental model.

**#246 Use of cDNA microarray and competitive template reverse transcription-polymerase chain reaction analysis to identify genes associated with carboplatin chemoresistance in non-small cell bronchogenic carcinoma cell lines.** Willey, James C., Weaver, David A., Crawford, Erin L., Wu, Ding, and Zahorchak, Robert, *Department of Medicine, Medical College of Ohio, Gene Express National Enterprises, Inc. and Research Genetics, Inc.*

Non-small cell lung cancer (NSCLC) is poorly responsive to current chemotherapeutic regimens with an overall regression rate of only 30-50%. The mechanisms of resistance are likely to involve multiple gene products. In an effort to identify these genes, NSCLC carcinoma cell lines were assessed for carboplatin resistance by MTT assay. The H1435 carcinoma cell line had a 60-fold higher IC<sub>50</sub> for carboplatin (300 µM) compared to H460 (5 µM). RNA samples from H1435 and H460 then were compared for differences in gene expression by 6000 gene cDNA microarray (GeneFilters GF200, Research Genetics, Inc., Huntsville, AL) and quantitative competitive template reverse transcription polymerase chain reaction (CT RT-PCR) analysis. GF200 microarray analysis revealed 5-fold lower levels in H1435 compared to H460 for 4 known genes (transferrin receptor protein, alpha (1,2)fucosyl transferase, translational initiation factor 2 gamma subunit and KIAA0231) and 46 expressed sequence tags (ESTs). In addition, 5-fold higher gene expression levels were observed for four known genes (glutathione transferase [GST] P1, distal-less homeobox 4, heterogeneous nuclear ribonucleoprotein C, and KIAA0112). Quantitative CT RT-PCR analysis of 20 genes putatively associated with carboplatin chemoresistance based on previous studies revealed that GST P1, p21, E2F1, bax alpha, and GADD45 genes are expressed at 21, 8, 5, 4, and 4-fold higher levels respectively in H1435 compared to H460. Further, bcl-2 was expressed at a 9-fold lower level in H1435 compared to H460. GSTP1 was the gene with the greatest difference in gene expression between the two lines as measured both by microarray (8-fold) and by CT RT-PCR analysis. These data demonstrate the value of combining cDNA microarray analysis as a screening tool followed by CT RT-PCR analysis for confirmation and rigorous quantification. The genes discovered by microarray analysis may be investigated in small biopsy samples from primary NSCLC tumors using the more sensitive CT RT-PCR.

Authors JCW and RZ each have significant equity interest in GENE, Inc. which prepares reagents for CT RT-PCR.

**#247 High throughput screening of differentially expressed genes by combining suppression subtractive hybridization (SSH) and cDNA expression array technology.** Desai, S.H., Hill, J.E., Diatchenko, L., Htun, S., Hyder, K., Chenchik, A., Siebert, P.D. *CLONTECH Laboratories, Inc. Palo Alto, CA 94303*

The purpose of this research project was to identify differentially expressed genes in various tumors in a high throughput manner. Two different approaches were used: 1) suppression subtractive hybridization and 2) differential screening analysis of cDNA chip containing 20,000 cDNA clones (ESTs from Image consortium). For subtractive hybridization, we used our SSH technique. Poly A+ RNAs were isolated from lung, breast, prostate and liver tumor samples along with their matching normal counterparts and subjected to suppression subtractive hybridization to obtain differentially expressed cDNAs. These differentially expressed cDNAs were cloned, amplified and arrayed onto nylon membranes. The membranes were hybridized with equivalent amounts of p32-labeled cDNA from subtracted and unsubtracted tumor and normal tissues. By this method, we isolated 285 independent cDNA clones up or down regulated in various tumors when compared with their normal counterparts. Differential expression of thirty two out of thirty five randomly selected candidate cDNAs were confirmed on the virtual northern blot. These differentially expressed cDNA clones were arrayed on to nylon membrane together with another 152 clones differentially expressed in bladder and prostate tumor by differential screening approach. This cDNA array was subjected to the high throughput screening by using radiolabeled cDNA probes from a panel of various tumor and normal samples. Results are compared to find a set of genes differentially expressed in various tumor samples used in this study.

**#248 A novel transforming growth factor-β1-regulated gene in lung cancer.** Ozbun, Laurent L., and Jakowlew. *Sonia B. National Cancer Institute, Medicine Branch, Department of Cell and Cancer Biology, Rockville, MD 20850.*

Transforming growth factor-β (TGF-β) is a growth modulator which inhibits the proliferation of many epithelial cells through interaction with its receptors, the TGF-β type I and II receptors. Tumors of epithelial origin frequently lose the ability to respond to TGF-β-mediated growth inhibition. Altered receptor proteins and deregulation of the TGF-β1 signaling cascade contribute to resistance to TGF-β growth inhibition. Identification of genes involved in TGF-β1 growth inhibition may identify targets for therapeutic intervention of lung cancer. Addition of exogenous TGF-β1 to the non-small cell lung cancer (NSCLC) cell line NCI-H727 inhibited proliferation and induced TGF-β1 mRNA expression by 15-fold. H727 cells were

used as a model system for epithelial cancers to identify genes involved in TGF-β1 growth inhibition. The differential mRNA display method was used to generate comparative cDNA expression patterns between H727 cells treated with TGF-β1 or with vehicle alone, and revealed several potential differentially regulated cDNA fragments; one of these cDNA fragments of 500 bp was recovered, cloned and sequenced. This cDNA fragment was differentially increased 5-fold by TGF-β1 treatment and hybridized to a 3.0 Kb mRNA species in NCI-H727 cells by northern analysis. Sequence homology searches of this cDNA fragment revealed no significant match to any known gene sequence. The mRNA transcript of this novel gene which we have named Lung Cancer Differential Gene (LCDG), is expressed in several normal human tissues, with highest expression in brain. Screening of a human brain cDNA library yielded longer LCDG cDNA fragments which still share no significant homology with any known gene sequence. Additional NSCLC cell lines sensitive to TGF-β1 growth inhibition showed differential LCDG mRNA expression when treated with TGF-β1. In contrast, LCDG mRNA expression was not affected by TGF-β1 treatment of normal human bronchial epithelial cells or of NSCLC cells resistant to TGF-β1 growth inhibition. Our data suggest LCDG may be a novel gene in normal and malignant lung cells which contributes to inhibition of NSCLC cell proliferation by TGF-β1.

**#249 Multiparametric high content screening for apoptotic signals.** Woo, Elizabeth S., Larocca, Greg, Lapets, Oleg, and Bright, Gary R. *Cellomics, Inc., 635 William Pitt Way, Pittsburgh, PA 15238.*

Apoptosis is a complex network of metabolic pathways and processes that are dynamic, interconnected and often redundant. However, it is clear that significant divergence within apoptotic pathways occurs with inducer and cell type. We have developed multiparameter, High Content Screening (HCS) assays for apoptosis that monitor, quantify, and correlate several apoptotic targets simultaneously, automatically, and in individual cells. These spatial measurements provide a definitive approach to screening because many archetypal apoptotic responses are morphological in nature. Multiparameter assays assess nuclear condensation, nuclear fragmentation, plasma membrane blebbing, changes in mitochondria, including mass and membrane potential, and changes in the cytoskeleton, quantifiable by the amount of f-actin present, in various combinations. Additionally, we have developed a molecular based biosensor for caspase activation, one of the definitive steps in many apoptotic pathways. This biosensor can also be analyzed in a multiparameter format, and shows a robust signal that is apoptosis specific. All measurements are automatically acquired from multicolor fluorescent images of intact cells grown in standard microarray formats. Our results show dependency on apoptotic inducers staurosporine and taxol, as well as cell types MCF-7, BHK, and L929. In some cases, we are able to detect dose dependent differential responses within the same cell line. The results of the study support the growing realization that every cell line/apoptotic inducer pair responds differently. It also reinforces the need for a portfolio of apoptotic measures that can be effectively combined and cross-correlated to give a definitive basis on which to screen compounds for any cell, any inducer, and in any part of the cascade.

**#250 A mammalian two-hybrid system for high throughput screening of inhibitors of the interaction between human herpesvirus 8 (HHV-8) polymerase and HHV-8 processivity factor.** Fletcher, Thomas M., Halliday, Susan M., Ptak, Roger G., Ward, Priscilla A., Shoemaker, Robert H., Mikovits, Judy A., Sausville, Edward, A., Lin, Kai, Ricciardi, R. P., and Buckeit, Robert W. *Developmental Therapeutics Program, DCTD, NCI, University of Pennsylvania, Philadelphia, PA and Southern Research Institute, Frederick, MD.*

Human herpesvirus 8 (HHV-8) has been associated with the development of Kaposi's sarcoma, body cavity-based lymphoma, multifocal Castleman's disease, and multiple myeloma. The HHV-8 genome encodes a DNA polymerase (Pol-8) and a processivity factor (PF-8). In order for processive viral DNA synthesis to occur, Pol-8 must physically associate with PF-8. Finding inhibitors of this interaction therefore represents a potential means for treating the diseases associated with HHV-8. We have verified the intracellular binding of Pol-8 to PF-8 using the CheckMate mammalian two-hybrid system (Promega). This system allows for the *in vitro* detection of protein-protein interactions using a luciferase reporter gene. To detect the interaction of these proteins, Pol-8 and PF-8 were cloned into both pACT and pBIND from the CheckMate system using standard molecular biology techniques. The resulting plasmid constructs were co-transfected into cells. At 48 hours post transfection, cells were washed, lysed and monitored for luciferase activity. Using this system, the interaction of Pol-8 with PF-8 was easily detectable. Initial experiments revealed levels of luciferase activity in the Pol-8/PF-8 co-transfection which were 15 fold higher than the background levels found in control samples. Transfection conditions are currently being optimized and adapted to a robotic platform for use in high throughput screening for inhibitors of the interaction. Initial screening results for a panel of natural product extracts will be presented. This system represents a novel assay for use in identifying inhibitors of this interaction. Such compounds could prove efficacious in treating the diseases associated with HHV-8 infection.

**#251 Genetically engineered repressors of the MDR1 gene promoter.** Bartsevich Victor V. and Juliano R.L. *Department of Pharmacology, School of Medicine, University of North Carolina, Chapel Hill, NC 27599.*

The ability to selectively regulate the expression of genes implicated in cancer or other diseases could have important ramifications for both basic research and for therapy. Using peptide combinatorial libraries expressed in yeast, we have screened for novel zinc finger proteins that selectively bind to a target site in the promoter of the MDR1 multi-drug resistance gene. The target site in MDR1 overlaps an SP1 binding site; however, the novel zinc finger proteins emerging from our screen do not bind to SP1 consensus sites. When the novel zinc finger proteins are coupled to mammalian transactivator or repressor domains, they can very effectively activate or repress transcription from model promoters containing the DNA target. They can also repress transcription from the native MDR1 promoter. These results indicate that the yeast combinatorial library approach can be used to identify novel transcriptional regulators with high affinity and substantial selectivity for unique sequences in virtually any gene of interest. This work was supported by NIH grant CA77340 to R.L.J.

**#252 Imaging and quantitating the actions of taxol and vinblastine on microtubule dynamics and kinetochore movements in living human tumor cells.** Jordan, Mary Ann; Kelling, Jonathan; Sullivan, Kevin; and Wilson, Leslie. *Dept. Mol. Cell. & Devel. Biol., Univ. California Santa Barbara, CA, 93106 and The Scripps Research Institute, LaJolla, CA 92037.*

Taxol and vinblastine (as well as novel anticancer drugs that work primarily by binding to tubulin and/or microtubules (MTs)) have been studied extensively in cell-free MT/tubulin systems and in fixed cells. It is well established that both taxol and vinblastine suppress MT dynamics at low concentrations (nM) both in cell-free systems and in living cells in interphase (Yvon *et al.*, 1999, *Mol. Biol. Cell.*, 10: 947-959, Dharmodharan *et al.*, 1995, *Mol. Biol. Cell.*, 6: 1215-1229). (At high concentrations ( $\mu$ M), the two drugs alter the overall mass of cellular MTs in opposite ways.) However, the actions of antimetabolic drugs on MT dynamics in living cells during mitosis, when cells are the most sensitive to MT-targeted drug action, have been difficult to study and thus have not been well characterized. We are employing a green fluorescent protein-labeled kinetochore protein (GFP-CENP-B) as a reporter for MT ends to analyze the effects of antimetabolic drugs on the dynamic behavior of mitotic spindle MTs by quantitative high resolution confocal video microscopy in living human osteosarcoma cells (U2Os). The spindle MT (+)-ends attached to the chromosomes are marked by the fluorescent kinetochores. By confocal video microscopy, the kinetochores of sister chromatids can be seen to oscillate back and forth during prometaphase as the chromosomes gradually move to the metaphase plate, and the sister chromatids and kinetochores are rhythmically stretched apart and relaxed together by the attached dynamic MTs. We are quantitating the effects of taxol, vinblastine, and other drugs on these dynamic movements. We find that taxol dampens the oscillations and stretching/relaxation movements in a concentration-dependent manner, in concert with blockage of mitosis. For example, 100 nM taxol reduces the time in stretching and relaxation of sister kinetochores by 95% and 98%, respectively, and reduces the mean kinetochore separation distance by 15%. Taxol also blocks progression from metaphase into anaphase by 98% at the same concentration. The results support the hypothesis that the metaphase/anaphase transition depends on the development of tension on kinetochores and that the most sensitive molecular mechanism of taxol during mitosis involves reduction of spindle tension by suppression of MT dynamics. Supported by NIH CA57291.

## SECTION 2: STRUCTURE-BASED DRUG DESIGN/ AGENTS WITH UNKNOWN OR UNCERTAIN TARGETS

**#253 Molecular insights into the origin of the acute human leukemias revealed from the three-dimensional structure and sub-cellular localization of AML1.** Werner, M.H., Nagata, T., Gupta, V., Goger, M., Chait, B.T., Sali, A., Kim, W.-Y., Shigesada, K., Ito, Y. *The Rockefeller University and Virus Research Institute, Kyoto University.*

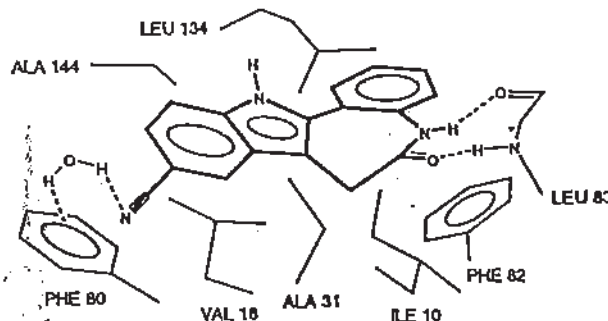
AML1 is a heterodimeric transcription factor essential for genetic regulation of hematopoiesis and osteogenesis. DNA-binding by AML1 $\alpha$  is accomplished by a highly conserved DNA-binding domain, the runt-domain (RD), whose structure we have determined to be an S-type immunoglobulin fold when bound to DNA. The supplementary subunit  $\beta$ , known as PEBP2/CBF $\beta$ , enhances DNA-binding by the RD *in vitro*, but its role in the control of gene expression has remained largely unknown *in vivo*. The three-dimensional structure of PEBP2/CBF $\beta$  has also been determined and is shown to adopt a fold related to the  $\beta$ -barrel oligomer binding motif.

The onset of the acute human leukemias is causally associated with the presence of chimeric gene products in which either the RD or PEBP2/CBF $\beta$  has been fused in-frame with a second protein as a result of chromosomal translocation. Analysis of the sub-cellular localization of normal and chimeric forms of AML1 demonstrates that the chimeric gene

products sequester the normal subunits of AML1 in a manner that leaves them unavailable to stimulate gene expression of AML1-dependent genes. Molecular insights into the mechanism of sequestration have been revealed by direct analysis of a 43.6kD ternary RD/ $\beta$ /DNA complex in which the heterodimerization interface has been identified. The identified heterodimerization interface forms the basis for developing pharmaceutical agents which can disrupt heterodimerization by the chimera, thereby disrupting an early step in leukemogenic transformation. Chromosome 16 inversion, in which PEBP2/CBF $\beta$  is fused to a portion of the smooth muscle myosin heavy chain (PEBP2/CBF $\beta$ -SMMHC), is discussed as a specific example for structure-based drug design.

**#254 Optimization of the paullone molecular scaffold for cyclin-dependent kinase inhibition: a structure-based, three-dimensional, quantitative structure activity relationship (3D QSAR) approach.** Gussio, R., Zaharevitz, D.W., McGrath, C.F., Pattabiraman, N., Kellogg, G.E., Schultz, C., Link, A., Kunick, C., Leost, M., Meijer, L., and Sausville, E.A. *DTP, DCTD, National Cancer Institute, Frederick, USA. Institut für Pharmazie, Univ. of Hamburg, Hamburg, Germany, Centre National de la Recherche Scientifique, Station Biologique, Roscoff, France.*

A congeneric series of paullones were characterized using a 3D QSAR with cyclin dependent kinase 1 (CDK1) inhibition data. First, a homology model of CDK1/cyclin B was formed. Each paullone was then docked into the ATP binding site of the CDK1/cyclin B models and optimized with molecular mechanics. Quality of interaction between each docked ligand and the side chains of the binding site was assessed by hydrophobic analysis. Next, electronic properties of the ligands were calculated using quantum mechanical methods (QM), and were combined with the hydrophobic descriptors (HDs) using multivariate statistical techniques to predict their IC50 data. The results indicate that (HDs) with molecular mechanics geometries are sufficient to help design overt steric and chemical complementarity of the ligands. However, the electronic properties derived from QM helped direct synthetic chemistry efforts to produce ligands that promote better charge transfer and strengthen hydrogen bonding through resonance facilitation. For example, our method predicted that substitution of the paullone with a 9-cyano group (shown below) will hydrogen bond with a water molecule, enable the ring system to accept charge density from the electron rich aliphatic side chains of CDK1 (i.e., A144, L134, I10, A31, and V16) and increase hydrogen bonding strength due to the greater charge delocalization. This prediction was confirmed when 9-cyano-paullone demonstrated an IC50 of 24 nanomolar in inhibiting CDK1.



**#255 Homology models for CDK1 and CDK1/cyclin B.** McGrath C.F., Pattabiraman, N., Gussio, R., Zaharevitz, D.W., Sausville, E.A. *Advanced Biological Computing Center, Frederick, MD, DTP, DCTD, National Cancer Institute, Frederick, MD, USA.*

We have constructed a molecular model of a CDK1/cyclin B complex that can be used in a target structure-based drug design strategy. A preliminary model was formed from the homologous regions of the published CDK2/cyclin A crystal structure. Initial placement of the non-homologous residues was performed using LOOK 3.0 software. Further refinement of the CDK1/cyclin B complex was accomplished using molecular mechanics and hydrophobic analysis with a protocol of constraints and local geometry searches. The refinements did not result in any significant deviations from the homologous regions in CDK2/cyclin A. Using similar techniques, a model was constructed for CDK1 alone based on a CDK2 crystal, without a bound cyclin. The CDK1/cyclin B model was used to successfully model the binding of the paullone series of inhibitors. These compounds, like all CDK inhibitors described to date, bind at the ATP-site and the two models were compared to assess changes at this site upon cyclin binding. The adenine binding portion of the pocket still retains its general character. Phe80 and Phe82 maintain their positions as do the contributors to hydrogen bonding in this portion of the pocket. One region of the pocket, however, showed a significantly reduced volume in the non-cyclin-bound form. The aliphatic portions of the Asp145 and Lys33 sidechains were in steric clash with the 10-bromo-paullone inhibitor in this case. These results suggest that the difference in the ATP-site caused by cyclin binding may be relevant to the understanding of inhibitor binding.



The CDK-cyclin interfaces produced in the models presented here were also analyzed and the significance of these results for the understanding CDK-cyclin specificity is discussed.

**#256 Rationalization of the selective inhibition of VEGF-tyrosine kinase by the anglogenesis inhibitor, PTK787/ZK222584 (†) on the basis of shape complementarity to hydrophobic domains within the ATP-binding site.** Manley, Paul W.; Bold, Guido; Cozens, Robert; Furet, Pascal; Hofmann, Francesco; Mestlan, Jürgen; Wood, Jeanette M. *Oncology Research, Novartis Pharma AG, CH-4002 Basel, Switzerland*

Vascular endothelial growth factor (VEGF) regulates angiogenesis primarily via interaction with two receptor tyrosine kinases, KDR and Flt-1, located on the surface of endothelial cells. On binding VEGF, KDR and Flt-1 undergo autophosphorylation, thus becoming activated to phosphorylate further proteins leading to a signal transduction cascade. Thus selective inhibition of either KDR or Flt-1 is an attractive strategy towards modulating the activity of VEGF and hence angiogenesis.

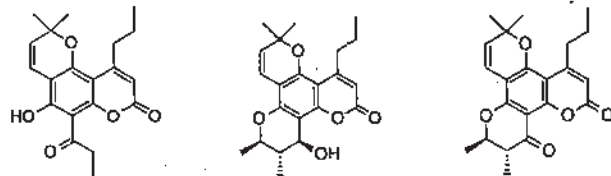
From high-throughput screening we identified a series of phthalazines as Flt-1 kinase inhibitors. The structure-activity trends observed for these compounds was rationalised using our published homology model for the ATP-binding domain of tyrosine-kinases.

N-4-Chlorophenyl-4-(4-pyridylmethyl)-1-phthalazinamine (†), emerged from this series as a potent, selective inhibitor of KDR kinase. Based on our hypothesis, the activity of † is attributable to its good topological fit to hydrophobic regions within the ATP-binding site of KDR. Such a binding mode differs from that of ATP and many known kinase inhibitors, which interact with tyrosine kinases through H-bonds to the peptide backbone of the hinge region of the enzyme. Whereas the ATP-binding motif is highly conserved across tyrosine kinases, heterogeneity exists in the size and shape of the flanking hydrophobic regions. Consequently, favourable interactions with these latter regions provides potential for improved kinase inhibitor selectivity.

As a result of favorable selectivity, physicochemical and pharmacokinetic properties, † has an attractive *in vivo* profile, inhibiting VEGF-mediated angiogenesis in mice (12.5–50 mg/kg/day) and has been selected to enter Clinical Trials.

**#257 Structure-based drug design of calanolide derivatives targeting Bruton's tyrosine kinase.** Sudbeck, Elise A., Venkatachalam, T.K., Ghosh, Sutapa, Mahajan, Sandeep, Uokun, Fatih M., Parker Hughes Cancer Center, Structural Biology, Chemistry, Biochemistry, Hughes Institute, St. Paul, MN.

Calanolide derivatives were evaluated for their ability to inhibit Bruton's Tyrosine Kinase (BTK), an anti-apoptotic protein. A constructed homology model of BTK was used to facilitate protein/inhibitor docking studies and inhibitor binding estimations. Compound WHI-D12 was predicted to bind to the BTK catalytic site. *In vitro* kinase assays showed that WHI-D12 inhibited BTK with an  $IC_{50}$  ~29 $\mu$ M, 4 times better than the activity of calanolide derivatives WHI-D63 and WHI-D86. WHI-D12 did not inhibit Janus kinases JAK1, JAK2, or JAK3, Src kinase HCK, Zap/Syk kinase family member SYK, or insulin receptor kinase (IRK). Molecular modeling showed that WHI-D12 can form favorable interactions with specific amino acid residues in the catalytic site of BTK, which can enhance binding. The less potent compounds WHI-D63 and WHI-D86 are less planar molecules which may not fit into the binding site as well and were predicted to form fewer hydrogen bonds with BTK residues. The identification of BTK inhibitors such as WHI-D12 which can promote apoptosis cell death in human leukemia cells may lead to the development of potent new anti-cancer agents.



WHI-D12

WHI-D63

WHI-D86

**#258 Structure-activity relationships of the Hsp90 inhibitor 17-allylamino 17-demethoxy geldanamycin analogues (17AAG).** Maloney Alison; Walton Mike I.; Sharp Sweet; Kelland Lloyd R.; Jarman Mike; Prodromou Chrisostomos; Pearl Laurence and Workman Paul. *CRC Centre for Cancer Therapeutics, Institute of Cancer Research, Cotswold Rd, Belmont, Sutton, Surrey, UK. SM2 5NG. Department of Biochemistry and Molecular Biology, UCL, Gower St, London. UK. WC1E 6BT.*

The benzoquinone ansamycin, 17AAG is just entering phase 1 clinical trial as a first-in-class Hsp90 inhibitor. Inhibition of Hsp90 results in a depletion of oncogenic client proteins including tyrosine kinases, mutant p53 and other signalling molecules e.g. Raf-1. 17AAG sensitivity was shown to correlate with DT-diaphorase (DTD) activity in a panel of ovarian and colon tumor cell lines and is enhanced in BE cells transfected with the

DTD NQO1 gene. A structure activity relationship study was conducted to identify the molecular features of 17AAG required for its activity and its enhanced sensitivity in DTD-expressing cell lines. Hsp90 ATPase inhibition, growth inhibition (measured by 96hr SRB), and depletion of Raf-1 by the 17AAG analogues were compared to 17AAG and geldanamycin. The DTD potentiation effect was examined in BE cells and BE cells transfected with the DTD NQO1 gene. Geldanamycin was the most potent inhibitor of Hsp90 ATPase activity (50% inhibition) with 17AAG and 17-n-propyl-, -dimethylaminoethyl and -dimethylaminopropyl analogues (26-18% inhibition) > analogues with various acyl substituents on the 11-OH group on the ansamycin ring or bulky substituents at position 19 on the quinone ring (<5% inhibition). In contrast, the aforementioned 17-substituted analogues inhibited growth  $\geq$  geldanamycin > the 11- and 19-substituted analogues. Raf-1 depletion was observed with analogues which inhibited growth and Hsp90 ATPase activity. Potentiation in high DT-diaphorase cells is associated with specific substitutions at the 17-position, particularly the allylamino moiety or to a lesser extent -propyl-, -dimethylaminoethyl and -dimethylaminopropyl. In conclusion, the substitutions at the 11- and 19-positions prevent Hsp90 ATPase inhibition and growth inhibition. The 17-alkylamino substitution seems to confer DTD potentiation. The lower inhibition of Hsp90 ATPase activity by 17AAG and similar analogues compared to geldanamycin suggests that these analogues may be metabolised to more potent compounds, perhaps via DTD metabolism or that another mode of action is contributing to their antiproliferative effect.

Supported by the Cancer Research Campaign and the Institute of Cancer Research.

**#259 Structural modification of model bioreductive antitumor agents: effects on DT-diaphorase dependent bioreduction and cytotoxicity.** Fourie, Jeanne, Oleschuk, Curtis; Wang, Xiaowei; Guziec, Frank, Jr, Guziec, Lynn; Begleiter, Asher. *Manitoba Institute of Cell Biology, University of Manitoba and Dept. of Chemistry, Southwestern University.*

DT-diaphorase (DTD) is a cytosolic flavoenzyme that mediates NAD(P)H-dependent two-electron reduction of quinone and N-oxide bioreductive elements: DTD is overexpressed in neoplastic tissues and may contribute to variability in response to bioreductive antitumor drugs. DTD activates mitomycin C, but decreases the activity of tirapazamine and the model agent, benzoquinone mustard (BM). We studied the effect of different functional groups on DTD reduction of the quinone in BM, and on drug cytotoxicity. Reduction of BM and three analogs with different [electron-donating (MBM), electron-withdrawing (CBM) and bulky (PBM)] functional groups by DTD was compared under hypoxic and aerobic conditions. Nitrogen or air were bubbled through the reaction buffer containing the cofactors NADH and FAD for 3 hr. BM analogs and purified DTD were added and gassing was continued for up to 120 min. Reactions were terminated by adding the DTD inhibitor, dicoumarol. NADH consumption, an index of quinone reduction by DTD, was measured by HPLC. The  $t_{1/2}$  for quinone reduction had a rank order of BM < MBM ~ CBM < PBM under hypoxia. Under aerobic conditions, there was redox cycling with MBM, CBM and PBM, but not with BM. For cytotoxicity studies, SK-MEL-28, human melanoma cells, were treated with BM analogs for 1 hr with, or without, dicoumarol, and cytotoxic activity was determined by MTT assay. DTD decreased BM and CBM cytotoxicity, but increased MBM cytotoxicity. Thus, structural modifications can alter the rate of quinone reduction by DTD; may effect the ability of the quinone to redox cycle, and may alter the effect of DTD on cytotoxicity. [Supported by MRC of Canada and the American Institute for Cancer Research]

**#260 Structure-based drug design targeting Bcl-2-mediated apoptosis.** Wang, J.-L., Zhang, Z.-J., Liu, D.X., Shan, S., Han, X., Croce, C.M., Alnemri, E., and Huang, Z. *Kimmel Cancer Center, Jefferson Medical College, Thomas Jefferson University, Philadelphia, PA*

Members of the Bcl-2 family play a critical role in regulating the process of apoptosis and are implicated in the resistance of cancer cells to many of the currently available drugs. The goal of this study is to develop a chemical approach to regulate the process of apoptosis and discover potential therapeutic agents for the treatment of cancer. Since Bcl-2 family proteins mediate apoptotic pathways involved in cancer and chemoresistance, small molecule agents blocking or mimicking the biological function of Bcl-2 family members could be used as novel regulators of apoptosis and potential anticancer agents. We designed and synthesized various peptide analogs derived from functional regions of Bcl-2 family proteins. Chemical modifications were made to these analogs to improve their activity and cell-permeability. In addition, we used a computer-based technique to discover novel non-peptidic organic inhibitors of Bcl-2 function. Using a Bcl-2 ligand binding assay recently developed in our laboratory, we confirmed the specific-binding of these synthetic peptides and computer-selected compounds to the designated Bcl-2 functional pocket. In a series of subsequent biological and biochemical studies, we demonstrated that these analogs potently blocked the biological function of Bcl-2 and induced apoptosis in human cancer cells. These findings strongly suggested the therapeutic potential of these compounds as promising leads for the development of a new class of anticancer drugs. Furthermore, these chemical reagents are useful probes of mechanisms and signaling pathways underlying apoptosis.

**#261 Novel channel blockers as cytostatic cancer agents.** Heady, Tiffany, N., Haverstick, Doris M., Gray, Lloyd S., and Macdonald, Timothy L. *Departments of Chemistry and Pathology, University of Virginia, Charlottesville, VA.*

There are currently three classes of calcium channel blockers classified by their binding to specific sites on the four subunit calcium channel protein; dihydropyridines, phenylalkylamines and benzothiazepines. Many structural attributes are important for the activity of these compounds and have been incorporated into a novel class of channel blockers recently synthesized by us containing proline and ethyl nipecotate cores. These are first generation targets developed through examination of existing channel blockers (CB). CBs share a number of structural similarities such as a basic tertiary nitrogen, varying regions of hydrophobicity (or log P), core heterocycles, substituted aryl rings, and ether linkages. Our proline and nipecotate targets incorporate these features and are typically N- and O-dialkylated. As with dihydropyridines, orientation and ortho, meta, para substitution of the aryl ring(s) affect the activity of these compounds as does varying degrees of hydrophobicity in benzothiazepines. Like phenylalkylamine derivatives, activities of these compounds vary with the enantiomer as well as with the type of group substituted on the aryl rings. Screening consists of an initial cell proliferation assay to determine cytostatic potential, followed by measurement of intracellular  $[Ca^{2+}]$  by spectrofluorometry. Details of the activity of one compound is shown in the companion abstract: Inhibition of human prostate cancer proliferation *in vitro* and in a mouse model by a compound synthesized to block  $Ca^{2+}$  entry, Haverstick *et al.* We have also developed a Comparative Molecular Field Analysis (CoMFA), which correlates biological activity with chemical structure to predict  $IC_{50}$  values of future synthetic targets for each cell line.

**#262 Structure-based drug design of thymidine phosphorylase/platelet-derived endothelial cell growth factor inhibitors and their application for an antitumor agent.** Tada, Y., Yano, S., Kazuno, H., Satoh, T., Fukushima, K., Asao, T. *Hanno Research Center, Taiho Pharmaceutical Co., Ltd., Hanno, Saitama, 357-8527 Japan.*

Thymidine phosphorylase (TP) is an enzyme which converts thymidine to thymine and 2-deoxyribose-1-phosphate. Certain antitumor nucleosides are good substrates of TP. Herein, 2'-deoxy-5-fluorouridine and 5-trifluoromethyl-2'-deoxyuridine ( $F_3dThd$ ) are inactivated, and tegafur and 5'-deoxy-5-fluorouridine are activated by TP. There is a good correlation between the TP expression and the malignancy of solid cancers such as colon, mammary and pancreatic cancer. Recently, it has been shown that human TP is identical to platelet-derived endothelial cell growth factor (PD-ECGF). We have designed a series of 5- and/or 6-substituted uracils as TP inhibitors on the basis of the 3D structure model of human TP. Among the compounds we synthesized, 6-aminoalkyl-5-halogenouracils were found to be a specific and potent inhibitor of TP. 5-Chloro-6-(2-iminopyridinyl)methyluracil (TPI),  $K_i = 2 \times 10^{-9}$  M, has been selected by QSAR analysis for further development. TPI inhibited angiogenesis caused by PD-ECGF *in vivo* and showed antitumor activity *in vivo*. Furthermore, when TPI was co-administered orally with  $F_3dThd$ , significant antitumor activities were observed in not only human colon carcinoma DLD-1, but also 5-fluorouracil resistance DLD-1/5-FU xenografts.

**#263 Modulation of bcl-2 and cytotoxicity of licochalcone-A, a novel estrogenic flavonoid.** Rafi, M.M., Rosen, R.T., Vassil, A., Ho, Chi-Tang, Zhang, H., Ghai, G., Lambert, G., DiPaola, R.S. *The Cancer Institute of New Jersey/Robert Wood Johnson Medical Center/UMDNJ, New Brunswick, N.J.*

We recently demonstrated that the herbal combination PC-SPES, which contains licorice root, has potent estrogenic activity *in vitro*, in animals, and in patients with prostate cancer (DiPaola *et al.* *N Engl J Med* 339:785-791, 1998). Licochalcone-A (LA) is one flavonoid extracted from licorice root with antiparasitic and antitumor activity, but the effect on the human estrogen receptor and mechanism of anti-tumor activity is unknown. LA belongs to a class of chalcone structures, in which some compounds have both estrogenic and anti-tumor activity. Recent studies demonstrated that the mechanism of cytotoxic effect by some estrogens may involve modulation of bcl-2. In the present study, we determined if LA has estrogenic activity, anti-tumor activity, and modulates bcl-2 in human cell lines derived from acute leukemia, breast cancer, and prostate cancer. A yeast growth-based assay under the control of the human estrogen receptor (HER) demonstrated that LA is a phytoestrogen. LA had anti-tumor activity in HL-60, MCF-7, PC-3, and DuPro-1 tumor cells. LA induced apoptosis in HL-60 (15  $\mu$ M) and MCF-7 (15  $\mu$ M) cell lines as demonstrated by PARP cleavage. Immunoblot analysis demonstrated that LA (15  $\mu$ M) decreased the expression of bcl-2 and decreased the bcl-2/bax ratio. In contrast, the parent compound chalcone (15  $\mu$ M) or estradiol did not modulate bcl-2 protein expression. Therefore, these data demonstrate that LA is a phytoestrogen with anti-tumor activity against hormone responsive and unresponsive tumors and is capable of modulating bcl-2 protein expression. The effects on bcl-2 may be dependent on specific structural differences between LA and the parent compound chalcone and independent of LA estrogenicity.

**#264 Exploring the mechanisms of action of FB642 at the cellular level.** Hammond Lisa H., Izbicka Elzbieta, Davidson Karen, Lawrence Richard, Camden James, Von Hoff Daniel D., Weitman Steve. *Institute for Drug Development, Cancer Therapy and Research Center, San Antonio, TX; University of Texas Health Science Center, San Antonio, TX; Procter and Gamble, Cincinnati, OH.*

FB642 (methyl-2-benzimidazolecarbamate, carbendazim) is a systemic fungicide with antitumor activity against a broad spectrum of tumors *in vitro* and *in vivo* such as pancreas, prostate, colon, and breast. To determine the prospects and utility of FB642 as a potentially clinically relevant antineoplastic agent, we conducted a series of experiments to further define the properties of FB642 with regards to its mechanism of action, its effect on apoptosis, its cross-resistance with known antitumor agents, and its ability to kill p53 abnormal or p53-negative tumor cells. FB642 had a concentration dependent effect on apoptosis in MCF7, HT29, B16, SK-MES, and SKOV-3 human tumor cell lines. Flow cytometry evaluation of human tumor cell lines (MCF7, HT29, SK-MES, and SKOV3) and murine melanoma B16 treated in culture with FB642 for 4 days revealed an increased accumulation of cells in the G0/G1 phase in all but the SK-MES cell line and suggests a possible effect on the G2/M phase. FB642 at 1  $\mu$ g/mL decreased the number of DLD1 cells (abnormal p53) and HCT 116 (normal p53) to 63% and 80% of control, respectively, suggesting that FB642 may selectively kill p53 abnormal cells. FB642 was equally effective in retarding growth in most drug sensitive and drug resistant cells (MES SA, MES SADX5; MCF7M, MCF7Adr; P388, P388Adr; HL60, HL60Adr; CEM, CEM/C2). RT-PCR analysis of RNA from HCT 116 (expresses MDR-1), indicates that FB642 had no effect on the expression of MDR-1. FB642 was equally effective in retarding growth in the MES SADX5 (MDR) cell line when compared to its parent line, MES SA. This study demonstrates that FB642 mitigates the effect of an abnormal p53 and induces apoptosis, may induce G2/M uncoupling, and exhibits antitumor activity in drug and multidrug resistant cell lines making it an excellent candidate for clinical trials.

**#265 A unique structural aspect of the staurosporine analog, Ro-31-8220, is associated with its apoptotic activity.** Han, Z., Hendrickson, E.A., Pantazis, P., and Wyche, J.H. *Department of Molecular Biology, Cell Biology, and Biochemistry, Brown University, Providence, RI 02912.*

A series of bisindolylmaleimide (Bis) compounds were designed analogs of the natural compound staurosporine (STS), a potent inducer of apoptosis. The Bis analogs appeared to be highly selective inhibitors of protein kinase C (PKC). In this report we describe the effects of several Bis analogs, including Bis-I, Bis-II, Bis-III and Ro-31-8220 on HL-60 cells, which have been widely used as model cells for studying the biological roles of PKC. Treatment of HL-60 cells with Bis-I, Bis-II, Bis-III, or Ro-31-8220 blocked phosphorylation of PKC target proteins such as Raf-1 with equal potency but did not appear to affect phosphorylation of proteins by other kinases. However, their biological effects were different: Bis-I and Bis-II had no observable effects on either cell survival or proliferation; Bis-III inhibited cell proliferation but not survival, whereas Ro-31-8220 induced apoptosis. These results indicated that PKC activity inhibitable by the Bis analogs was not required for survival and proliferation of HL-60 cells. Cells treated with Ro-31-8220 showed that the apoptotic activity of this compound was mediated by a well-characterized early transduction process of apoptotic signals, i.e., mitochondrial cytochrome c efflux, and activation of caspase-3 in the cytosol. The ability of Ro-31-8220 to induce activation of this mechanism was completely blocked by over-expression of the apoptotic suppressor gene, bcl-2, in cells. Interestingly, proliferation of the cells were sensitive to the presence of Ro-31-8220, suggesting that the inhibitory effects of Ro-31-8220 on viability and cell proliferation were mediated by different mechanisms. Finally, the apoptotic effect of Ro-31-8220 on cells was not altered by the presence of an excess amount of the other Bis analogs, suggesting that this effect was mediated by a factor(s) other than PKC, or mechanism which was not saturable by the other Bis analogs. Furthermore, structure-function analyses of compounds related to Ro-31-8220 revealed a unique aspect of the structure of Ro-31-8220, which was associated with its apoptotic activity.

**#266 MGI 114 induces a multiple caspase activation cascade in human pancreatic cancer.** Wang, Weixin, Elshihabi, Said, Von Hoff, Daniel D., Waters, Stephen J., MacDonald, John R., Miller, Alexander R. *Departments of Surgery and Medicine, University of Texas Health Science Center at San Antonio, San Antonio, TX; MGI PHARMA, INC., Minnetonka, MN.*

Chemotherapy-induced apoptosis appears to involve the activation of caspase proteases. MGI 114 (6-HMAF, iruloven) is a novel sesquiterpene analogue known to induce apoptosis in multiple tumor models. We sought to determine the molecular effectors responsible for the induction of apoptosis in human pancreatic cancer cell lines by this agent. Eight-24 hour MGI 114 treatment resulted in cytotoxicity against all 6 human pancreatic cancer cell lines tested (MiaPaCa-2, AsPC-1, Hs768L, CAPAN-2, CFPAC-1, and Panc-1;  $IC_{50}$  1-18  $\mu$ M) as demonstrated by MTT assay. Flow cytometric analysis using both TUNEL assay and propidium iodide staining for the subG<sub>1</sub> population demonstrated 10-fold (4%  $\pm$  2 vs. 41%  $\pm$  5) induction of apoptosis in MiaPaCa-2 cells treated with MGI 114 compared with untreated or sham-treated controls. Apoptosis was also



documented by the demonstration of poly-ADP-ribose polymerase (PARP) cleavage. The addition of Z-VAD-fmk, a broad-spectrum caspase inhibitor, reduced apoptosis to baseline levels ( $5\% \pm 2$ ). Western blot analysis demonstrated that caspases 3, 7, 8, and 9 were activated, as evidenced by the observation of cleavage bands of anticipated size in MGI 114 treated cells. Z-VAD-fmk treatment prevented caspase activation. These results indicate a profound induction of apoptotic molecules in human pancreatic cancer cells by MGI 114, and provide insights into the mechanism of action of this agent and a basis for its clinical activity in patients with pancreatic cancer.

**#267 Development and characterization of two human tumor sublines expressing high grade resistance to the new antitumoral cyanoguanidine CHS 828.** Gullibo, J., Dhar, S., Öberg, F., Binderup, L., Lukinits, A., Nilsson, K., and Larsson R. *Clinical Pharmacology/Pathology, Uppsala University Hospital, SE-75185 Uppsala, Sweden. Leo Pharmaceutical Products, Denmark.*

CHS 828 is a newly developed cyanoguanidine exerting promising antitumoral properties with unknown mechanism of action. The CHS 828 activity showed little or no apparent dependence on P-glycoprotein, multidrug-resistance associated protein (MRP), tubulin, GSH or topoisomerase II associated drug resistance when investigated in a panel of human tumor cell lines representing defined mechanisms of resistance. In order to establish CHS 828 resistance two cell lines were cultured under continuous exposure to gradually increasing concentration of CHS 828 for 6 months. The final concentration was 0.1  $\mu\text{M}$  for the histiocytic lymphoma cell line U-937 GTB and 0.5  $\mu\text{M}$  for the myeloma line RPMI 8226/S. The sublines demonstrate high grade resistance to CHS 828 (>1000 and >200-fold difference in IC50 respectively) and cross resistance to eight other cyanoguanidine analogues. Activity pattern of the resistant sublines for nine standard drugs and two known cytotoxic guanidines, MIBG and MGBG, revealed low to moderate resistance factors (RF; IC50 resistant/IC50 parental cell line). The highest RFs were observed for Taxol® and vincristine (3–6) whereas RFs for topoisomerase inhibitors, antimetabolites, alkylating agents and the guanidines were low (<3). The resistant phenotype has been stable for approximately 6 months and no differences in growth rate, ultrastructural or morphologic appearance in the sublines compared to their normal counterparts has been shown. No changes in cell cycle distribution or differentiation could be detected. The relatively low level of cross resistance to standard drugs may indicate development of specific cellular alterations leading to CHS 828 resistance. Further studies to investigate these alterations may reveal the antitumoral mechanism of action for this novel compound.

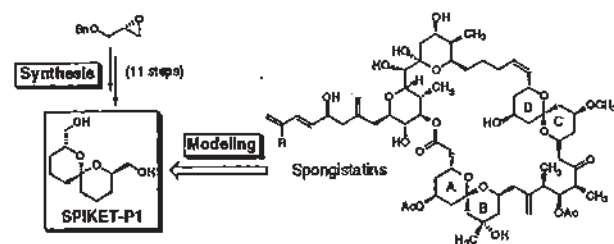
**#268 A Binding Protein of Tumor Tissue-Accumulative Water-soluble Porphyrin and Its Application to Cancer Therapy.** Nakajima, S., Sakata, I., Takemura, T. *Central Division of Surgery, Asahikawa Medical College, Photochemical Co. Ltd, University of Hokkaido, Japan.*

Although it is well recognized that porphyrin accumulates in cancer tissue, the whole picture has not yet been clarified. Based on our 20 years of experiences in the synthesis and evaluation of 1,200 porphyrin derivatives, we report the tumor-tissue accumulating mechanism of porphyrin derivatives clarified to date, focusing on binding proteins and application of porphyrins to cancer therapy.

**Mechanism of accumulation in tumors:** Accumulation of porphyrin derivatives in tumors was shown to be attained by specific physico-chemical properties of porphyrin, that is, affinity for proteins due to enriched  $\pi$  electrons and amphipathic properties due to stacking phenomenon, and by lack of lymphatic tissue in tumor tissues. It was revealed that the major binding protein of water soluble porphyrins accumulating in tumor tissues was not the currently suggested low density lipoprotein (LDL), but a glycoprotein similar to hemopexin with a molecular weight of approximately 70,000. It is very likely that this protein is involved in invasion, and vascularization of cancer tissue.

**Application to cancer therapy:** a) Photosensitizer ATX-S10(Na) (molecular weight 878.2), which is a photochlorin, was synthesized, and its applicability for fluorescence diagnosis of tumors and the effect on tumor destruction in interstitial photodynamic therapy using a diode laser were investigated. ATX-S10(Na) generated a unique red fluorescence, which was useful in endoscopic tumor diagnosis. Photoirradiation using a diode laser attained a higher radical cure rate than the usual radiotherapy in radiation-resistant cancer-bearing animals. b) KADTF (molecular weight 855.9) was synthesized by adding a fluorinated nitazole to the side chain group of STA-R12, which is an Mn porphyrin used as a tumor scintigram agent due to its superior accumulation in tumors, and the effect of KADTF on MR tumor imaging and sensitization of radiotherapy were investigated. Because of the trivalent Mn in the backbone, the tumor-accumulating radiation sensitizer KADTF showed a high ability to shorten the  $T_1$  time on MRI, and facilitated the visualization of a clear tumor shadow. Furthermore, in an experimental radiation-resistant cancer, a rate of healing higher than that usually achieved by radiotherapy was obtained.

**#269 Synthetic spiroketal pyrane (SPIKET-P) as a novel class of tubulin-depolymerizing anti-cancer agents.** Uckun, F.M., Mao, C., Jan, S-T. *Drug Discovery Program and Parker Hughes Cancer Center, Hughes Institute, St. Paul, MN 55113.*



Spongistatin 1 (SP) is a potent tubulin depolymerizing natural product which has been isolated from an Eastern Indian Ocean sponge in the genus *Spongia*. In a rational drug design effort intended to determine the minimal molecular architecture of the SP structure necessary for biological activity, we used the 3-D atomic model of the  $\alpha\beta$  tubulin dimer for the identification of the potential tubulin binding sites for SP. The search resulted in the discovery of a unique candidate binding pocket on the tubulin surface. The docking simulation results indicated that the putative SP binding pocket which is located on the surface of tubulin is approximately 8Å wide  $\times$  18Å long  $\times$  11Å deep and is in close proximity to the GDP exchange site on the  $\beta$  subunit of the tubulin heterodimer. This binding pocket contacts the longitudinal interdimer interface of the microtubule; the existence of bound SP in this binding pocket may therefore hinder interdimer interactions of tubulin and contribute to the tubulin depolymerizing activity of SP. Advanced modeling studies indicated that the two spiroketal groups of SP likely serve as the critical binding components of SP. The spiroketal group of SPIKET-P1 has a molecular surface of 218 Å<sup>2</sup>, 75% of which would be covered by the aforementioned two aromatic rings. Following its retro-synthetic analysis, SPIKET-P1 was prepared as an SP pharmacophore using a versatile multi-step synthetic scheme in a stereocontrolled fashion. SPIKET-P1 at nanomolar concentrations caused tubulin depolymerization and prevented tubulin polymerization in standard *in vitro* tubulin turbidity assays. SPIKET-P1 prevented normal mitotic spindle formation in BT20 human breast cancer cells at nanomolar concentrations and killed >99.9% of MDA-MB-231 as well as BT20 human breast cancer cells at concentrations  $\geq 100$  nM. SPIKET-P1 treated human breast cancer cells showed destruction of the microtubule organization, membrane blebbing, and nuclear fragmentation consistent with apoptosis. We are in the process of completing the deconvolution of a SPIKET-P1-based pilot 59-member combinatorial library with potent anti-cancer activity.

**#270 Two vanadium compounds stop cell proliferation and effect mitotic and meiotic spindle formation.** Navara, C.S., Ghosh, P., Benyumo, A., Naria, R.K., and Uckun, F.M. *Drug Discovery Program, Department of Experimental Oncology, Chemistry, Hughes Institute, St. Paul, MN, 55113.*

We have examined the anti-proliferative effects of two vanadium compounds, Vanadocene Dichloride and Vanadocene Diacetate. These compounds halt cell proliferation in several cancer cell lines and also in a zygotic system, zebrafish embryos. We used immunocytochemistry and laser scanning confocal microscopy to determine the mechanism of action of these compounds. When these cells were examined a pleiotropic mechanism was discovered. These compounds cause apoptosis and also cause monopolar mitotic spindle formation (19.52% in treated cells vs. 0.57% in control cells). When cells containing monopolar spindles were examined for the distribution of the mitotic spindle pole markers gamma-tubulin we observed two centrosomes at the single spindle pole. It appears that monopolar spindle formation is not caused by failure to replicate the centrosome but rather failure to separate replicated centrosomes. Meiotic spindles are formed in a different fashion than mitotic spindles and therefore we wanted to examine the effects of these compounds on meiotic spindle formation. Treated bovine oocytes arrested during the first meiotic division. When spindle formation was examined approximately 60% had abnormal spindle formation. Therefore these vanadium compounds stop proliferation by causing apoptosis and blocking cell division by disrupting normal bipolar spindle formation.

**#271 Arsenic trioxide-mediated cytotoxicity in prostate and ovarian carcinoma lines.** Uslu, R., Sezgin, C., Karabulut, B., Sanli, U.A., Tobu, M., Saydam, G., Buyukkececi, F., Omay, S.B., Goker, E. *Department of Medical Oncology and Hematology, School of Medicine, Ege University, 35100 Bornova/Izmir/Turkey.*

The arsenic compounds have been reported to have cytotoxic effect on several cancer cell lines including promyelocytic leukemia, esophageal carcinoma, megakaryocytic leukemia, and malignant lymphocytic cell lines. Recent studies showed that arsenic trioxide (As<sub>2</sub>O<sub>3</sub>) can induce

clinical remission in patients with acute promyelocytic leukemia via induction of differentiation and programmed cell death (apoptosis). We have examined the cytotoxic effects of  $As_2O_3$  on ovarian carcinoma cell line MDAH 2774 and hormone and drug resistant prostate carcinoma cell lines DU145 and PC3. Cytotoxicity was tested by "Trypan Blue Dye Exclusion test" and "MTT assay". For the first time our results demonstrated that the growth and survival of tumour cells were markedly inhibited by  $As_2O_3$ . Cytotoxicity was dose and time dependent. The half dose effect (ED50) was at the concentration of  $10^{-4}$  M at 24 hours. Flow cytometry analyses showed that apoptotic peak was identified in  $As_2O_3$  treated cells but not in the control. We will investigate the mechanisms of cytotoxic effect of  $As_2O_3$  on these cell lines and relationship between  $As_2O_3$  and other therapeutic agents on these cell lines.

**#272 Novel multitargeted deaza-antifolate SND47.** Stoicescu Dan, Rotaru Maria, Badea Irinel, Murgoci Elena from Sinda, Bucharest, Romania and Stancovski Iliana-Pfizer Cincinatti, Connecticut, US.

SND47 is a new generation deaza antifolate with multi-enzyme inhibition (including dihydrofolate reductase DHFR) and favorable structure features leading to unexpectedly good *in vivo* results using standard panel of mouse tumors. There was little toxicity during the treatment, mainly hematological and several cases of long time survivors and "cures". The general pre-clinical activity compares favorably with both Methotrexate (MTX) and newer analogues like LY231514 from Eli Lilly. The rationale behind design is presented together with its synthesis and structure-activity relationship based on several sets of products from the database of more than 600 prepared in our laboratories. These pre-clinical data will be used in the Phase I trial starting Q4 1999.

**#273 New binding regions of tubulin and microtubule models as anti-cancer drug design targets.** Mao, Chen, and Uckun, Fatih M. Parker Hughes Cancer Center, Drug Discovery Program, Structural Biology Department, Hughes Institute, St. Paul, MN, U.S.A.

A high-resolution model of the microtubule structure was constructed based on the  $\alpha\beta$  tubulin dimer structure which was recently solved by electron crystallography data from zinc-induced tubulin sheets. Based on the available structural information, systematic modelling studies of the interface between tubulin dimers within the microtubule structure led to the identification of two previously unidentified regions as potential binding pockets for several potent tubulin inhibitors including vinca alkaloids and spirogastatin. Our modeling strategies involved "cavity searching" and sequence "patch" analysis of the tubulin surface, docking procedures using inhibitor models, and a calculation of inhibitor binding constants using a modified score function. Our modeling efforts were extended to search a chemical database at the Hughes Institute in order to identify small molecules which would target the same binding pocket. The database search relied on a defined pharmacophore which was identified based on an analysis of each binding region of tubulin and was aided by the use of the Cerius2 program. Our final efforts were focused on the design of a combinatorial library based on a template molecule which would bind with the characterized binding site. Several successful applications of the reported strategy will be presented.

**#274 Isolation of bone marrow endothelium targeting peptides by random peptide bacteriophage display.** G.N. Thalmann, A. Finger, A. Wetterwald, L.W.K. Chung, U.E. Studer, M.G. Cecchini Gene Therapy Laboratory, Dept. of Urology and Dept. of Clinical Research, University of Berne Switzerland, Molecular Urology and Therapeutics, Dept. of Urology, Charlottesville, VA

Rationale: Organ specific receptors expressed on the luminal surface of the endothelium play an essential role in leukocyte intra- and extravasation at precise anatomical sites. Equivalent receptors specific for the bone marrow endothelium are involved in homing hematopoietic stem cells during embryogenesis and after bone marrow transplantation. However, similar or identical homing receptors may mediate preferential colonization of the bone marrow by certain cancer cell types. The identification of molecules specific for the luminal surface of the bone marrow endothelium represents the basis for a better understanding of the process of hematopoietic stem cell homing in the marrow and, possibly, bone metastasis.

Methods: To identify such surface molecules, a phage library expressing random 6 amino-acid linear peptides was screened by panning *in vivo*, in mice. The animals were sacrificed shortly after intravenous injection of the phage library and perfused with Hank's salt solution in order to remove unbound phages from circulation. Subsequently, the bone marrow was flushed out from long bones and the high affinity and/or internalized phages were amplified *in vitro* and further re-injected *in vivo*.

Results: Five consecutive cycles of selection *in vivo* and amplification *in vitro* were performed. Sequencing of the insert from bone marrow-enriched phage libraries after the fourth and fifth panning *in vivo* revealed two dominant amino-acid sequence motifs. Single phage clones, each expressing one of the dominant peptides, were further injected *in vivo* and the whole animal fixed by perfusion through the left ventricle. Immunohistochemistry showed that two phage clones localized exclusively in endo-

thelial cells of bone marrow, bone and spleen red pulp. This binding was specifically mediated by the peptide insert, since insertless phages injected at the same concentration did not exhibit any specific binding.

Conclusions: The two peptide motifs binding to marrow endothelium may allow the bone marrow-selective delivery of cells, hematopoietic cytokines, and drugs or genes.

**#275 Clinical disease suppression and reduction in acute myeloid leukemia and solid tumors by very high dose of L-ascorbic acid: a new concept and in search of molecular targets.** Park CH, Kim WS, Park C, Lee MH, Boo YC, Yoon S-S, Park MH, Lee H, Lee SJ, Riordan NH, Rubin D, Kimler BF. Samsung Med Ctr & Sungkyunkwan Univ Korea. RECNA, Phoenix, AZ and Kansas Univ Med Ctr, Kansas City, KS.

There have long been a number of studies indicating that L-ascorbic acid (LAA) modulates the growth of human malignant cells *in vitro* (e.g., Park, et al. Science 174: 720, 1971). However clinical studies have not generally substantiated the effect of LAA (e.g., Moertel, et al. New Engl. J. of Med. 312: 137, 1985). This may be due to the studied dose being too low, i.e. 10 gm/day. We have used doses of LAA up to 100 gm/day, and have seen beneficial effects without significant toxicities. We are now in search of molecular targets to explain these effects of LAA. A 52-year-old female patient with acute myeloid leukemia who received chemotherapy twice and presented at the 2<sup>nd</sup> relapse can illustrate clear evidence of disease suppression by LAA. The leukemic blast counts in the peripheral blood rose rapidly during the 1<sup>st</sup> relapse: from 2,182/ $\mu$ l to 16,564/ $\mu$ l over a 12-day period. The increased blast count was reduced by chemotherapy. Seven months later she had a 2<sup>nd</sup> relapse and was treated only with oral LAA, escalating doses up to 72 gm/day. The disease progression was halted with blast counts held under 10,000/ $\mu$ l over a ten-week period. There was no chemotherapy or other treatment whatsoever during this period. There are multiple cases of other solid tumors: breast; colorectal; renal cell; and pancreatic cancers; as well as lymphoma, in which remarkable reduction in size of tumors including complete responses has been noted (Riordan, et al. Med. Hypotheses 44:207, 1995). Although we need controlled clinical studies for precise delineation of response rates and magnitude of survival advantage, there are simply too many undeniable cases to make it impossible to escape the assertion that this very high dose of LAA is beneficial. We have performed DDPCR to identify molecular mechanisms for LAA effects with test results indicating differences between cultivated cells with and without LAA. In conclusion, very high dose LAA is an effective new concept in the treatment of human malignancies, requiring further studies with DDPCR as well as newer technologies such as microchip array for elucidation of its molecular mechanisms.

### SECTION 3: NEW AGENTS

**#276 Enhancement of apoptosis: a potential therapeutic strategy for EBV-associated nasopharyngeal carcinomas.** Khebir A., Ardila-Osoyo H., Clause B., Jilidi R., Busson P. UMR 1598, Inst. Gustave Gustave Roussy, Villejuif, France. Labo. Ana. Path., CHU Habib Bourguiba, Sfax, Tunisia.

Nasopharyngeal carcinoma (NPC) is unique among epithelial malignancies because of some remarkable epidemiological and biological characteristics. NPC is rare in most countries but it occurs at a high incidence in South China and North Africa. In its typical undifferentiated form, it is constantly associated with the Epstein-Barr virus (EBV). In addition, at the initial stage of the treatment, NPCs are generally more sensitive to radio- and chemotherapy than other head and neck carcinomas. Despite their short doubling time, there is often a high rate of spontaneous apoptosis among malignant cells on tissue sections (Harn et al., *Histopathology* 33, 117-122, 1998). Biological and pharmacological investigations of NPCs have long been hampered by the absence of malignant NPC cells propagated *in vitro*. We have used xenografted NPC tumor lines to investigate apoptotic processes in this malignancy. We have shown that the malignant NPC cells consistently express the Fas-receptor (CD95) at a very high level. In contrast with many other types of carcinoma cells, NPC cells are exquisitely sensitive to Fas-mediated apoptosis (Sohi-Lammali et al., *Cancer Research* 59, 924-930, 1999). To investigate the possibility to induce or facilitate NPC cell apoptosis with small diffusible molecules, we have tested several pharmacological agents on short term *in vitro* cultures of xenografted NPC cells. Preliminary experiments have shown a rapid and strong cytotoxic effect of a farnesyl-transferase inhibitor, FTI 277 (Calbiochem) in the range of 10  $\mu$ M. This suggests that farnesyl-transferase inhibitors could be useful drugs in the treatment of NPCs. Additional investigations are planned to explore the molecular basis of their cytotoxic effect and a possible synergy with other drugs.



**#277 Targeting HMG-CoA reductase induces a pronounced apoptotic response in a subset of tumor derived cell lines: A potential therapeutic approach in a variety of retinoid responsive cancers.** Dimitroulakos, J., Kamel-Reid, S., Yeager, H., and Penn, L.Z. *Department of Cellular and Molecular Biology, the Ontario Cancer Institute, Toronto, Canada.*

Our previous work has focused on the identification of retinoid responsive genes as an approach to uncover potential mediators of their biological and anti-tumor effects. Using differential expression methodologies, we identified the enzyme HMG-CoA reductase as a potential retinoid responsive gene. HMG-CoA reductase is the rate limiting enzyme of the mevalonate pathway whose diverse array of endproducts are vital for a variety of cellular functions including cholesterol synthesis and cell cycle progression. We re-evaluated HMG-CoA reductase as a potential therapeutic target in a variety of retinoid acid responsive cancers that had not been adequately surveyed previously. In initial studies, we demonstrated that inhibiting HMG-CoA reductase with lovastatin, a potent competitive inhibitor of this enzyme, induced pronounced apoptotic responses in neuroblastoma and acute myeloid leukemic cells. We have now extended this work and evaluated a number of retinoid responsive cancers with respect to sensitivity to lovastatin-induced apoptosis. A total of 79 cell lines have been evaluated for lovastatin sensitivity. These cell lines were exposed to a wide range (0–100  $\mu$ M) of lovastatin for 2 days and assayed for cell viability using the MTT assay and the induction of apoptosis by flow cytometric analysis. Lovastatin induced a pronounced apoptotic response in the pediatric, acute myeloid leukemias, juvenile monomyelocytic leukemia and squamous cell carcinomas of the cervix and the head and neck tumor derived cell lines. Therefore, we have identified HMG-CoA reductase as a potential therapeutic target of these retinoid responsive cancers.

**#278 Mannosylerythritol lipid is a potent inducer of apoptosis and differentiation of mouse melanoma cells in culture.** X. Zhao, T. Nakahara, and K. Yokoyama. *RIKEN 3-1-1 Koyadai, Tsukuba, Ibaraki 305-0074, Japan and Institute of Applied Biochemistry, University of Tsukuba, 1-1-1 Tennodai, Tsukuba, Ibaraki 305-0006, Japan.*

Malignant melanomas are tumors that are well known to respond poorly to treatment with chemotherapeutic reagents. We report here that an extracellular glycolipid, mannosylerythritol lipid (MEL), from yeast inhibited the growth of mouse melanoma B16 cells markedly in a dose-dependent manner. Exposure of B16 cells to MEL at 10  $\mu$ M and higher concentrations caused the condensation of chromatin, DNA fragmentation and sub-G1 arrest, all of which are hallmarks of cells that are undergoing apoptosis. Analysis of the cell cycle also suggested that both the MEL-mediated inhibition of growth and apoptosis were closely associated with growth arrest in the G1 phase. Moreover, exposure of MEL stimulated the expression of markers of the differentiation of melanoma cells such as tyrosinase activity and the enhanced production of melanin, an indication that MEL triggered both apoptotic and cell-differentiation programs. Forced expression of Bcl-2 protein in stably transformed B16 cells had a dual effect: it interfered with MEL-induced apoptosis but increased both tyrosinase activity and the production of melanin as compared with these phenomena in vector-transfected MEL-treated control B16 cells. These results provide the first evidence that growth arrest, apoptosis and the differentiation of mouse malignant melanoma cells can be induced by a microbial extracellular glycolipid.

**#279 Specific induction of apoptosis and cytotoxicity of recombinant mistletoe lectin (rML) in human tumor cells in vitro.** Mückel B., Burger, A.M., Mengers, U., Zinke H., Fiebig, H.H., Lentzen, H. *BRAIN GmbH, Zwingenberg; Tumor Biology Center, Freiburg; Madaus AG, Köln, Germany.*

The type II ribosome inactivating protein (RIP) mistletoe lectin I (ML I) plant isolate has previously been shown to induce apoptosis in human tumor cells in vitro. Precise mechanistical studies, however, were hampered by the heterogeneity of plant extracts. Thus, we have developed recombinant mistletoe lectin (rML) and genetically engineered variant forms to investigate the mechanism of ML-induced cell death. We found that: i) 10 to 100 ng/ml concentrations (0.01–10 ng/ml) of rML were sufficient to induce apoptosis in human tumor cell lines; ii) RIP activity was essential for induction of apoptosis, whereas the isolated lectin component had no effect; iii) the cell death cascade was specifically regulated by caspases and mitogen activated protein kinases; iv) highly toxic rML concentrations caused a direct and fast necrotic cell death.

rML was found to be potentially cytotoxic in human tumor cell lines and xenograft derived fresh human tumor specimens in vitro. The mean IC70 values were 0.4 ng/ml in panel of 20 permanent cell lines derived from different tumor types and 3 ng/ml in 48 human tumor xenografts as determined by clonogenic assay. The standard therapeutic agent adriamycin was tested for comparison in the same experimental system and found to be approximately 10-times less active than rML. Moreover, the pattern of cell lines being more or less sensitive to rML or adriamycin compared at the respective median IC70 value was completely different for the two cytotoxic agents. In addition, rML was efficiently inhibiting a vincristin resistant mesothelioma cell line, PFX 1118, and MCF-7/ADR, suggesting that multidrug resistance mechanisms do not affect rML activity.

Our findings indicate that rML is a potent cytotoxic agent with a novel mode of action, namely RIP mediated induction of apoptosis through the caspase cascade, and that this potential should be exploited for cancer therapy. Supported by the grant 031183 of BMBF, Germany.

**#280 Bcl-2 overexpression inhibits lonidamine induced apoptosis in breast cancer lines.** Del Bufalo, D., Ricca, A., Bircocco, A., Bruno, T., Floridi, A. and Zupi, G. *Regina Elena Cancer Institute, Rome, Italy [D.B.D., R.A., B.A., B.T., Z.G.]; University of L'Aquila, L'Aquila, Italy [F.A.].*

Lonidamine (LND), a selective inhibitor of the energy metabolism of tumor cells used in breast cancer therapy, plays a crucial role in reversing drug resistance. We have previously demonstrated that LND induces apoptosis selectively in drug resistant cells independently of the p53 gene. In this study we evaluated whether the different susceptibility to LND-induced apoptosis of resistant and sensitive cells might be due to different expression of the bcl-2 protein. To this aim we have investigated the ability of LND to induce apoptosis in several breast cancer lines (MCF7 W, MCF7 ADR, CG5, LS175, ZR75, SKBR3, MM2). LND was used at a concentration employed in clinical treatment. The apoptosis evaluated in terms of sub-diploid populations, cytochrome c release, and ROS generation, was more pronounced in the cells with a low bcl-2 protein level. In addition, the transfection of bcl-2 in the resistant MCF7 ADR line prevents the LND-induced apoptosis by altering the energy metabolism and reducing the ATP content. These results provide insights into the relationship between apoptosis and the metabolic status in cancer cells suggesting LND as a good candidate in combination trials for treatment of tumors resistant to conventional chemotherapeutic agents.

Partially supported by Ministero della Sanità.

**#281 3-bromoacetyl amino benzoic acid ethyl ester (3-BAABE): a cancericidal agent which acts as an activator of apoptosis effector caspase-9.** Schlesinger, Michael, Jiang, Jian-Dong, Denner, Larry and Bekasi, J. George. *Department of Medicine, Mount Sinai School of Medicine, New York, N.Y. 10016.*

The mechanisms underlying the cancericidal activity of 3-bromoacetyl amino benzoic acid ethyl ester (3-BAABE) were investigated. 3-BAABE exerted a strong cancericidal effect on human leukemia and lymphoma cells ( $ID_{50} < 0.2 \mu$ g/ml) and on cell lines of prostate, colon, ductal and kidney cancer ( $ID_{50}$  0.8–0.88  $\mu$ g/ml). Multiple drug resistance had no effect on the susceptibility of human lymphoma cells to 3-BAABE, since Daudi/MDR20 cells and wild type Daudi cells had a similar susceptibility to the cytotoxic effect of 3-BAABE. The cancericidal effect of 3-BAABE, which was not associated with changes in the cell cycle, was mediated by apoptosis. Thus, cells exposed to 3-BAABE displayed the DNA fragmentation ladder characteristic for apoptosis, associated with a marked increase of the level of apoptosis effector caspases -3 and -6, which was followed by activation of DFF and proteolytic cleavage of PARP. Exposure of tumor cells to 3-BAABE increased the level of apical caspase-9, but had no effect on the level of caspase-8. Complete inhibition of 3-BAABE-induced apoptosis was exerted by LEHD-FMK, a caspase-9 inhibitor. DEVD-FMK, a caspase-3 inhibitor, and VEID-FMK, a caspase-6 inhibitor partially inhibited 3-BAABE-induced apoptosis, while exposure to IETD-FMK, a caspase-8 inhibitor, had no effect. The elevated level of caspase-9 in 3-BAABE-treated cells and the fact that only an inhibitor of caspase-9 abrogated apoptosis, indicate that 3-BAABE is a distinctive compound that elicits apoptosis through a pathway that is specifically limited to activation of apical caspase-9.

Acknowledgment: This work was supported by the T.J. Martell Foundation for Leukemia, Cancer and AIDS Research.

**#282 MT-21 induces the direct release of cytochrome c from mitochondria.** Watabe, M. and Osada, H. *(Antibiotics Laboratory, Riken Institute, Japan).*

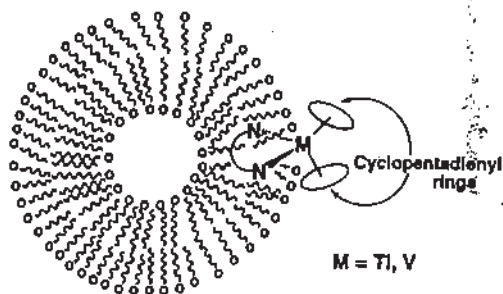
We previously reported that one of our synthetic compounds, MT-21, induced apoptosis by the activation of c-Jun-NH<sub>2</sub>-terminal kinase via the Kras/MST protein, which is activated by caspase-3 cleavage depending on reactive oxygen species production. We examined herein the activation mechanism of caspase-3, an important cysteine aspartic protease during MT-21-induced apoptosis. We found that MT-21 activated caspase-3 via caspase-9, but not via caspase-8. In addition, MT-21 induced the release of cytochrome c from mitochondria that is necessary to activate caspase-9 and this release occurred prior to change of membrane potential. This initiation process of MT-21-induced apoptosis was suppressed by the overexpression of Bcl-2 that is known to prevent cells from undergoing apoptosis in response to a variety of stimuli. Moreover, when we treated mitochondria isolated from the cells with MT-21, the direct release of cytochrome c from mitochondria was observed and this effect was not observed in mitochondria isolated from the cells overexpressed Bcl-2. Other apoptosis-inducing agents known to induce apoptosis via the cytochrome c release from mitochondria failed to release directly from isolated mitochondria. These findings indicate that MT-21 is a good synthetic compound which is able to induce apoptosis via the direct release of cytochrome c from mitochondria.

**#283 CHML suppresses cell growth and induces apoptosis in multiple human tumor lines.** Qimin Zhan,<sup>1</sup> Zheng Xu,<sup>2</sup> <sup>1</sup>Pittsburgh Cancer Institute, University of Pittsburgh School of Medicine, Pittsburgh, PA 15213 and <sup>2</sup>Glory F & D Co. Ltd, Arlington, VA 22203.

In the present study, we have investigated the effect of cytotoxic heterogeneous molecular lipid (CHML), a new anticancer agent, on growth suppression in a variety of human tumor cell lines. At a non-toxic concentration (a range from 25 µg/ml to 100 µg/ml), CHML has shown to strongly inhibit tumor cell growth by using a typical colony survival assay. At a treatment of concentration of 50 µg/ml for 6 hours, CHML is able to suppress 50% of the tumor cell colony formation. At a concentration of 100 µg/ml (the therapeutic dosage in the clinical trial), more than 90% of the cells were killed in human breast carcinoma MCF-7, colorectal carcinoma RKO, kidney carcinoma G410, lung carcinoma and human myeloid leukemia ML-1 lines. In contrast, growth suppression of non-cancerous human skin fibroblasts by CHML was observed much less than that seen in tumor lines. These results indicate that CHML is an efficient inhibiting agent in tumor cell growth and is able to generate greater suppression in tumor cells than in non-cancerous cells. With the use of DNA fragmentation assay, CHML was found to induce apoptosis in MCF-7, ML-1, H1299 and RKO lines after treatment at a concentration of 75 µg/ml for 8 hours. Following the CHML treatment, the tumor suppressor p53 protein elevated in RKO cells at 2 h posttreatment. The induction of p53 reached a peak at 4 hr and returned to normal level 16 hr later. Consistent with this result, Bax, which is regulated by p53 and is able to promote apoptosis, was also found to increase in a same kinetic manner as p53. These results suggest that the p53-pathway is activated by CHML and the activation of p53 may contribute to CHML-induced apoptosis in some tumor cells, such as MCF-7, RKO and ML-1. Considering that CHML is able to induce apoptosis in H1299 cells, which are of p53-negative status, it is speculated that CHML induces programmed cell death through both the p53-dependent and -independent pathways.

**#284 Interactions of apoptosis-inducing vanadocene complexes with artificial membranes.** Kotchevar, Ann T.; Ghosh, Phalguni; DuMez, Darin D.; Ghosh, Sutapa; Uckun, Fatih M. *Parker Hughes Cancer Center, Departments of Chemistry and Structural Biology, Hughes Institute, St. Paul, MN.*

Several vanadocene(IV) complexes have been shown to induce apoptosis. Depolarization of mitochondrial membranes is a critical event in apoptotic cell death leading to the leakage of cytochrome C and proteolytic enzymes. To gain further insight into the vanadocene-membrane interactions, physico-chemical studies of three structurally characterized vanadocene complexes and the titanium analogues with zwitterionic liposomes as artificial membranes are presented. We show that the ability of metallocenes to enhance the permeability of a liposomal membrane depends on the hydrophobicity as well as the size and planarity of the ancillary chelated ligands but not the nature of the central metal ion. Also provided is evidence that vanadocene complexes but not titanocene complexes induce lipid peroxidation and that lipid peroxidation does not correlate to permeability changes in artificial membranes.



**#285 Potent Growth Inhibition and Induction of Apoptosis by Oxovanadium(IV) Complexes of 1,10-Phenanthroline Against Human Ovarian Cancer Cell Lines In Vitro.** D'Cruz Osmond J., Dong Yanhong, and Uckun Fatih M. *Drug Discovery Program, Departments of Reproductive Biology and Chemistry, Hughes Institute, St. Paul, Minnesota.*

The coordination complexes of transition metal vanadium(IV) with a square pyramidal geometry and the oxo ligand in the axial position are potent inducers of oxidative DNA damage via the generation of hydroxyl radicals in a Fenton-like reaction. We have synthesized and tested the ability of 15 oxovanadium(IV) [VO] complexes stabilized with 5-membered *mono* and *bis* ancillary ligands of 1,10-phenanthroline, 2,2'-bipyridyl, 5'-bromo 2'-hydroxyacetophenone, and bipyrimidine to inhibit the growth and induce apoptosis in human ovarian carcinoma cell lines. Confluent monolayers of three ovarian cancer cell lines (ES-2, PA-1, and SKOV-3) in 96-well plates were incubated for 24 h in RPMI media with 10% fetal calf serum in the presence of increasing two-fold concentrations (0.7 µM to 100 µM) of 15 VO complexes, cisplatin as well as control solvent (DMSO) and cell proliferation was measured by the MTT assay. The ability of VO complexes to trigger apoptosis was evaluated by the two-color flow cy-

tometric terminal deoxyribonucleotidyl transferase-based assay that labels 3'-hydroxy ends of DNA fragments (TUNEL assay), confocal laser scanning microscopy, flow cytometric analysis of DNA content/cell cycle distribution, and DNA laddering. Only VO complexes with *bis* 5-chloro, 4,7-methyl and 5-nitro-linked 1,10 phenanthroline as ancillary ligands dose-dependently inhibited the growth of all three cell lines with IC<sub>50</sub> values ranging from 6.5 µM to 25 µM when compared with cisplatin (IC<sub>50</sub> values: 2.5 µM to 35.2 µM). TUNEL assay showed marked increase in FITC-digoxigenin-UTP incorporation in VO-treated cells. By confocal microscopy, VO complexes were found to induce morphological changes consistent with apoptosis in ovarian cancer cells, including apoptotic bodies. Cells treated with cytotoxic VO complexes demonstrated DNA laddering, typical of apoptosis. Cell cycle analysis of VO-treated cells revealed that growth inhibition was preceded by accumulation of the cells in the G<sub>2</sub>/M phase of cell cycle. We conclude that the ability of VO complexes to inhibit the growth of human ovarian cancer cell lines via the induction of apoptosis has the potential effectiveness in the treatment of human ovarian carcinoma.

**#286 Potent Growth Inhibition and Induction of Apoptosis by Cyclopentadienyl Complexes of Vanadium(IV) Against Human Testicular Cancer Cells In Vitro.** D'Cruz Osmond J., Ghosh Phalguni, and Uckun Fatih M. *Drug Discovery Program, Departments of Reproductive Biology and Chemistry, Hughes Institute, St. Paul, Minnesota.*

Metallocenes containing early transition elements in oxidation state IV are a novel family of potent antitumor organometallic agents. We have synthesized and tested the ability of 4 non-vanadium metallocene dihalides with hafnium, molybdenum, titanium or zirconium as metal ions (IV) and 19 cyclopentadiene complexes of vanadium(IV) or vanadocenes to inhibit the growth and induce apoptosis in human testicular cancer cells. Confluent monolayers of two testicular cancer cell lines (NTERA and TERA-2) in 96-well plates were incubated for 24 h in McCoy's 5A media with 10% fetal calf serum in the presence of increasing two-fold concentrations (1.9 µM to 250 µM) of 4 metallocenes and 19 vanadocenes as well as control solvent and cell proliferation was measured by the MTT assay. The ability of vanadocenes to trigger apoptosis was evaluated by the two-color flow cytometric terminal deoxyribonucleotidyl transferase-based assay that labels 3'-hydroxy ends of DNA fragments (TUNEL), confocal laser scanning microscopy, flow cytometric analysis of DNA content/cell cycle distribution, and DNA laddering. The effect of vanadocenes on intracellular Ca<sup>2+</sup> concentration ([Ca<sup>2+</sup>]) was determined by a fluorescent Ca indicator Fluo-3 and digital fluorescence microscopy. Only vanadium(IV)-containing complexes induced dose-dependent cytotoxicity at micromolar concentrations (IC<sub>50</sub> range 9 µM to 211 µM). Vanadocenes with di-pseudohalide substitution containing selenium and thiocyanate as ancillary ligands were the most active cytotoxic agents (IC<sub>50</sub> 9 µM and 17 µM, respectively). Vanadocenes elicited a dose-dependent increase in [Ca<sup>2+</sup>]. TUNEL assay showed marked increase in FITC-digoxigenin-UTP incorporation in vanadocene-treated cells. By confocal microscopy, vanadocenes were found to induce morphological changes consistent with apoptosis in testicular cancer cells, including apoptotic bodies. Cells treated with vanadocenes demonstrated DNA laddering, typical of apoptosis. Cell cycle analysis of treated cells revealed that growth inhibition was preceded by accumulation of the cells in the G<sub>2</sub>/M phase of cell cycle. We conclude that the ability of vanadocenes to inhibit the growth of human testicular cancer cell lines via the induction of apoptosis has the potential effectiveness in the treatment of testicular cancer.

**#287 Oxovanadium(IV) Complexes of 1,10-Phenanthroline are Potent Anti-Cancer Agents Against Human Testicular Cancer Cell Lines In Vitro.** D'Cruz Osmond J., Dong Yanhong, and Uckun Fatih M. *Drug Discovery Program, Departments of Reproductive Biology and Chemistry, Hughes Institute, St. Paul, Minnesota.*

The oxovanadium(IV) complexes with a square pyramidal geometry and the oxo ligand in the axial position are potent inducers of oxidative DNA damage via the generation of hydroxyl radicals in a Fenton-like reaction. We determined the ability of 15 oxovanadium(IV) [VO] complexes stabilized with 5-membered *mono* and *bis* ancillary ligands of 1,10-phenanthroline, 2,2'-bipyridyl, 5'-bromo 2'-hydroxyacetophenone, and bipyrimidine to inhibit the growth and induce apoptosis in human testicular cancer cell lines. Confluent monolayers of four testicular cancer cell lines (833-K, 64cp5, TERA-2, and NTD1) in 96-well plates were incubated for 24 h in RPMI media with 10% fetal calf serum in the presence of increasing two-fold concentrations (0.7 µM to 100 µM) of 15 VO complexes, cisplatin as well as control solvent and cell proliferation was measured by the MTT assay. The ability of VO complexes to trigger apoptosis was evaluated by the two-color flow cytometric terminal deoxyribonucleotidyl transferase-based assay that labels 3'-hydroxy ends of DNA fragments (TUNEL assay), confocal laser scanning microscopy, flow cytometric analysis of DNA content/cell cycle distribution, and DNA laddering. The VO complexes stabilized with *mono* and *bis* 1,10-phenanthroline dose-dependently inhibited the growth of all four cell lines with IC<sub>50</sub> values ranging from 0.9 µM to 57.6 µM when compared with cisplatin (IC<sub>50</sub> 9.7 µM to 21.6 µM). Oxovanadium(IV) complexes with *bis* 5-chloro, 4,7-methyl and 5-nitro-linked 1,10 phenanthroline as ancillary ligands were the most active cytotoxic agents.



TUNEL assay showed marked increase in FITC-digoxigenin-UTP incorporation in VO-treated cells. By confocal microscopy, VO complexes were found to induce morphological changes consistent with apoptosis in testicular cancer cells, including apoptotic bodies. Cells treated with cytotoxic VO complexes demonstrated DNA laddering, typical of apoptosis. Cell cycle analysis of VO-treated cells revealed that growth inhibition was preceded by accumulation of the cells in the G<sub>2</sub>/M phase of cell cycle. We conclude that the ability of VO complexes to inhibit the growth of human testicular cancer cell lines via the induction of apoptosis has the potential effectiveness in the treatment of testicular cancer.

**#288 Anticancer activity of oxovanadium(IV) complexes of 1,10-phenanthroline and 2,2'-bipyridyl derivatives.** Narla, R.K., Dong, Y., and Uckun, F.M. *Drug Discovery Program, Parker Hughes Cancer Center, Hughes Institute, St. Paul, MN 55113.*

In a systematic effort to identify a cytotoxic agent with potent anticancer activity, we synthesized 15 oxovanadium(IV) complexes and their structure-activity relationships were evaluated using a panel of human cancer cell lines including pre-B Acute lymphoblastic leukemia (ALL) (NALM-6), T-ALL (MOLT-3), acute myeloid leukemia (HL-60), plasma cell leukemia (ARH-77), Hodgkin's lymphoma (HS445), multiple myeloma (U266BL, HS-SULTAN). The oxovanadium compounds include *mono* and *bis* ancillary ligands of 1,10 phenanthroline (phen) and 2,2'-bipyridyl (bipy) with chloro, dimethyl and nitro substitutions. All of the 15 oxovanadium(IV) complexes elicited concentration-dependent apoptosis at micromolar concentrations. The methyl derivatives of *mono*- and *bis*-phenanthroline complexes of oxovanadium(IV), VO(Me<sub>2</sub>-phen) and VO (Me<sub>2</sub>-phen)<sub>2</sub> were the most active. In clonogenic assays, VO(Me<sub>2</sub>-phen) and VO (Me<sub>2</sub>-phen)<sub>2</sub> inhibited NALM-6 cell colony growth with EC<sub>50</sub> of 154 nM and 31 nM, respectively. The lead compounds VO(Me<sub>2</sub>-phen) and VO (Me<sub>2</sub>-phen)<sub>2</sub> generated reactive oxygen species and depolarized the mitochondrial membrane potential without effecting the mitochondrial mass at nanomolar concentrations. Furthermore, VO(Me<sub>2</sub>-phen)<sub>2</sub> caused cell-cycle perturbations by arresting the cells at G<sub>1</sub>. In conclusion, our results provide unprecedented evidence that the apoptosis-inducing activities of oxovanadium(IV) complexes are determined by the oxidation state of vanadium, their geometry and the ancillary ligands present on them. Because of its potent apoptosis-inducing activity, further preclinical development of our lead compound VO (Me<sub>2</sub>-phen)<sub>2</sub> may provide the basis for the development of more effective adjuvant chemotherapeutic programs.

**#289 Fluorine-containing dimethoxyquinazolines: A Novel group of quinazoline derivatives with potent cytotoxic activity against cancer cells.** Narla, R.K., Liu, X.-P., and Uckun, F.M. *Drug Discovery Program, Parker Hughes Cancer Center, Hughes Institute, St. Paul, MN 55113.*

In a systematic effort to identify a cytotoxic agent with potent anti-tumor activity against cancer cells, we synthesized several novel fluorine-substituted dimethoxy quinazoline derivatives and examined their activity against human pre-B acute lymphoblastic leukemia (ALL) (NALM-6), T-ALL (MOLT-3), breast cancer (BT-20), prostate cancer (PC3) and brain tumor (U373) cell lines. Several of the fluorine-containing dimethoxy quinazolines with multiple fluorine groups showed significant cytotoxicity. Notably, two compounds, WHI-P353 and WHI-P364 exhibited highest activity causing apoptotic cell death at micromolar concentrations with IC<sub>50</sub> values of 6.1 μM and 7.9 μM for NALM-6, 17.4 μM and 25.3 μM for MOLT-3 cells, respectively. The *in vitro* anti-cancer activity of these two compounds was confirmed by assessing the adhesive and invasive activity of tumor cells treated with these compounds. At non-cytotoxic concentrations, these compounds inhibited (a) integrin-mediated tumor cell adhesion to the extracellular matrix proteins laminin, type IV collagen, and fibronectin, and (b) migration of tumor cells from multicellular spheroids as well as invasion through Matrigel-coated Boyden chambers in a dose-dependent fashion. Furthermore, fluorine-substituted dimethoxy quinazolines derivatives depolymerized the actin stress fibers and microtubules in intact cells and also prevented the fetal bovine serum-stimulated polymerization of actin in serum starved cells. WHI-P353 and WHI-P364 were very active in the SCID mouse xenograft model of human breast cancer and brain tumors. The *in vivo* administration of fluorine-substituted dimethoxyquinazolines resulted in delayed tumor progression of MDA-MB-231 breast cancer and U373 brain tumor subcutaneous xenografts and improved survival of nude mouse intracranial glioblastoma model. Further preclinical development of these fluorine-substituted dimethoxyquinazolines derivatives may provide the basis for the design of more effective adjuvant chemotherapy programs.

**#290 PS-341: A new agent with activity in prostate and pancreatic cancer.** C. Bruns, M.T. Harblson, R.J. Bold, P. Elliott<sup>†</sup>, J. Adams<sup>‡</sup>, J. Abbruzzese, and C. Pettaway, and D.J. McConkey, U.T. M.D. Anderson Cancer Center, Houston, Texas 77030 and ProScript, Inc., Cambridge, MA 02139

The proteasome is a multisubunit protease complex that mediates the degradation of a number of proteins involved in cell cycle regulation and survival. The dipeptide boronate, PS-341, is a potent dipeptide boronate inhibitor of the proteasome that was developed by ProScript, Inc. for use in cancer therapy. Preliminary work demonstrated that PS-341 triggers

apoptosis in a variety of human pancreatic cancer cell lines, including those engineered to overexpress the anti-apoptotic protein, BCL-2. We therefore conducted studies in nude mice bearing orthotopic human pancreatic tumors to determine the drug's efficacy *in vivo*. *Methods:* Human PC-3 prostatic or Mia-PaCa-2 pancreatic adenocarcinoma cells (1 × 10<sup>6</sup>) were implanted orthotopically in nude mice. After 7–14 days, animals were treated with various doses of PS-341 (0.3–1 mg/kg i.v., once or twice weekly) for up to 4 weeks. Tumors were harvested, and proliferation, apoptosis, and angiogenesis endpoints were analyzed in paraffin sections by immunohistochemistry. *Results:* Treatment of established tumors with PS-341 resulted in central tumor necrosis associated with increased apoptosis and decreased proliferation. Analysis of tumor vascularity by anti-CD31 immunohistochemistry revealed a marked, dose-dependent reduction in microvessel density associated with decreased expression of vascular endothelial growth factor (VEGF). The effects of PS-341 were associated with inhibition of the transcription factor, NFκB, and parallel experiments with a molecular inhibitor of NFκB (IκBαM) confirmed that it was required for VEGF expression. *Conclusions:* PS-341 is effective in established orthotopic human tumors. Its effects involve induction of tumor cell apoptosis and suppression of angiogenesis, and its mechanism of action involves inhibition of NFκB. A Phase I trial of PS-341 in patients with advanced solid tumors is currently underway at our institution.

**#291 Novel oxime derivatives of radicicol induces erythroid differentiation associated with preferential G1 phase accumulation against chronic myelogenous leukemia cells through destabilization of bcr-abl with hsp90 complex.** Shiotsu Y., An G.W., Shulle T.W., Neckers L.M., Soga S., Murakata C., Tamaoki T., Inoue K., and Akinaga S. *Pharmaceutical Research Laboratories, Kyowa Hakko Kogyo Co. Ltd., 1188 Shimotogari, Nagazumi-cho, Sunto-gun, Shizuoka Japan 411-8731 and Clinical Pharmacology Branch, National Cancer Institute, Bethesda, MD 20892.*

Chronic myelogenous leukemia (CML) is a clonal disorder of a pluripotent hematopoietic stem cell characterized by a chimeric bcr-abl gene giving rise to a p210<sup>Bcr-Abl</sup> protein with dysregulated tyrosine kinase activity. On the other hand, we have reported that radicicol, a macrocyclic anti-fungal antibiotic, binds to N-terminal of Heat shock protein 90 (Hsp90) and destabilizes Hsp90 associated proteins such as Raf-1. In this study we investigated the effect of radicicol, novel oxime derivatives of radicicol (KF25706, KF58333), and Herbimycin A (HA), a benzoquinone ansamycin antibiotic, on growth and differentiation of human K562 CML cells. The concentration of drug required for 50% inhibition of cell growth (IC<sub>50</sub>) of HA, radicicol, KF25706 and KF58333 against K562 was 0.27 μmol/L, 0.20 μmol/L, 0.28 μmol/L and 0.025 μmol/L respectively. While KF25706 and KF58333 induced the expression of erythroid specific surface marker Glycophorin A in K562 cells at the concentration of over IC<sub>50</sub> value, radicicol and HA showed transient erythroid differentiation. While treatment of K562 cells with KF25706 or KF58333 showed G1-phase accumulation at the concentration of over IC<sub>50</sub> value, HA or radicicol showed transient G1-phase accumulation. KF58333 treatment depleted p210<sup>Bcr-Abl</sup>, Raf-1 and cellular tyrosine phosphorylated proteins in K562 cells, whereas radicicol and HA showed transient depletion of p210<sup>Bcr-Abl</sup>, Raf-1 and tyrosine phosphorylated proteins. KF58333 also down-regulated the level of Cdk4, Cdk6 and phosphorylated form of Erk and up-regulated Cdk inhibitor p27<sup>Kip1</sup> protein without effect on the level of Erk and Hsp90 protein. Immunoprecipitation study showed that p210<sup>Bcr-Abl</sup> protein was co-precipitated with Hsp90 and treatment with KF58333 dissociated p210<sup>Bcr-Abl</sup> protein from Hsp90. These data suggest that KF58333 destabilize p210<sup>Bcr-Abl</sup> protein by association with Hsp90 and eventually induce G1 phase accumulation and erythroid differentiation. Furthermore, treatment of K562 cells with KF58333 induced cleavage of PARP protein that was concomitant with an increase of apoptotic (Annexin V positive) cells. Administration of KF58333 prolonged the survival time of SCID mice inoculated with K562 cells. Our results suggest that KF58333 may have therapeutic potential for the treatment of CML that involve abnormal cellular proliferation induced by p210<sup>Bcr-Abl</sup>.

**#292 Enzyme Catalyzed Therapeutic Agents Targeting Thymidylate Synthase.** Shepard HM, Boyer C, Li Q, Lackey D (NewBlotics, Inc, San Diego, CA), Grozlek M (SRI International, Menlo Park, CA), Wahl GM (Salk Institute, La Jolla, CA), Pegram M and Slamon D (UCLA School of Med., Los Angeles, CA).

Thymidylate synthase is a well-characterized target for treatment of cancer and infectious disease. Pharmaceutical development has focused on inhibitors. The rationale for the inhibitors has been that most tumor cells divide more frequently *in vivo* than most normal cells. As a result, the average amount of TS in tumor cells is higher than in their normal counterparts. Limited efficacy has been observed with such compounds, accompanied by significant dose-limiting toxicity. This result is anticipated since normal cells have lower levels of TS and should, therefore, be more sensitive to inhibitors of this enzyme. Little or no increase in cancer survival has occurred with the continuing development of alternative dosing strategies or new approaches to inhibition of TS activity. Because treatment with fluoropyrimidines or Tomudex both result in increased levels of TS, a significant cross-resistance is observed. Fluoropyrimidine failures are re-

fractory to Tomudex as well. The work to be described focuses on the design and testing of new chemical entities which are activated to cytotoxic compounds by thymidylate synthase (TS), an enzyme overexpressed in a majority of cancers, and especially in cancers that have been exposed to fluoropyrimidine therapeutics (5FU, 5FdUR, Xeloda) or other TS inhibitors (e.g., Tomudex). These compounds are based on a novel technology called Enzyme Catalyzed Therapeutic Agents (ECTA). Preferential activation in tumor cells will lead to inhibition of tumor cell growth, or death of the target cell population.

We have successfully synthesized a TS ECTA candidate compound, called NB101.1. This compound has demonstrated *in vitro* activity, especially on fluoropyrimidine/Tomodex-resistant human breast and colon cancer cell lines. Significantly more activity is observed on tumor cells which express at least 4-fold the normal level of TS protein. Unlike the natural TS substrate, dUMP, or the inhibitor, 5FdUMP, NB101.1 is not co-factor dependent. This allows the potential therapeutic to more efficiently exploit total cellular TS. Recently, we have made preliminary determinations of maximum tolerated dose and successfully demonstrated therapeutic activity in nude mouse models of fluoropyrimidine-resistant human colon cancer. NB101.1 is a promising new candidate therapeutic for cancers which express elevated levels of thymidylate synthase.

**#293 HSP90 inhibitors block the mitotic checkpoint and are synergistically toxic with spindle poisons.** Susan Hurst, John Lamb and Julian Simon. Program in Molecular Pharmacology, Fred Hutchinson Cancer Research Center, 1100 Fairview Avenue North, Seattle, WA, 98109.

The mitotic spindle checkpoint monitors the proper attachment of kinetochores to spindle microtubules. In the presence of microtubule poisons, the checkpoint blocks the metaphase to anaphase transition thus preventing inaccurate chromosome segregation. Recent studies suggest that mutations that compromise the effectiveness of the mitotic checkpoint may sensitize cells to the action of spindle poisons. We set out to identify compounds that inhibit the mitotic spindle checkpoint and, potentially increase the effectiveness of clinically important spindle poisons (e.g. paclitaxel). A screen of over 8,000 compounds from the NCI/DTP yielded 13 "hits" that allowed cells to overcome an MPS1 overexpression-induced arrest in the absence of spindle damage. Two of the hits were compounds related to the ansamycin antibiotic geldanamycin. Geldanamycin is an inhibitor of the yeast and mammalian HSP90 chaperones. Inhibition of HSP90 by geldanamycin has been previously shown to destabilize and inactivate a number of signal transduction proteins in yeast and mammalian cells. In addition to the compounds that were identified in the screen, we tested a number of geldanamycin derivatives, including mabecein I and II, herbimycin and radicicol—all known HSP90 inhibitors. Here, we present the results of the screen. Compounds that overcome the MPS1-induced arrest in yeast reduce the activity of the MPS1 kinase. Additionally, treatment of wild type yeast cells with radicicol accelerates the rate of rebudding in the presence of a spindle poison. Also in wild type cells, HSP90 inhibitors cause a synergistic growth inhibition in the presence of a spindle poison. These results provide pharmacological support the recently identified genetic interaction between MPS1 and HSC82, the yeast homologue of mammalian HSP90. Finally, we show that treatment of mammalian cells with colcemid or taxol in the presence of HSP90 inhibitors leads to a synergistic toxicity. Thus, HSP90 inhibitors are a new class of checkpoint-inhibiting drugs that may act as therapeutic modifiers of existing anticancer agents. The results underscore the value of yeast as a model system for anticancer drug discovery.

**#294 Novel screens for potential drugs against cervical cancer identify zinc ejecting inhibitors of the HPV-16 E6 oncoprotein.** Beerheide Walter, Bernard Hans-Ulrich, Tan Yee-Joo, Ganesan Arasu, Rice William G., Ting Anthony E. Institute of Molecular and Cell Biology, Singapore [B. W., B. H.-U., T. Y.-J. G. A., T. A. E.]; and Laboratory of Antiviral Drug Mechanisms, SAIC Frederick, National Cancer Institute-Frederick Cancer Research and Development Center, Maryland [R. W. G.].

The E6 gene encodes one of the three oncoproteins of human papillomavirus type 16 (HPV-16), the principal agent in the etiology of cervical cancer. Structural and mutational studies had identified two zinc fingers as critical for E6 protein function. Here, we describe high-throughput assays to identify compounds that interfere with the binding of zinc to E6. Thirty-six compounds, selected on the basis that they may perform sulfhydryl residue specific redox reactions, were tested for their ability to release zinc from HPV-16 E6 protein. The zinc-ejecting compounds were then tested for their ability to inhibit E6 binding to E6 associated protein (E6AP) and E6 binding protein (E6BP), two coactivators of E6-mediated cellular transformation. The binding of E6 to these two cellular coactivators were measured by surface plasmon resonance technology and *in vitro* translation assays. The compounds were also tested for their effects on HPV-containing cell lines. 9 out of the 36 compounds ejected zinc from E6. Two of these compounds inhibited the interaction between E6 and the cellular proteins. One of these compounds selectively inhibited cell viability and induced p53 levels in tumorigenic HPV-containing cells. We propose that the assay systems described here can be employed to identify compounds that

interfere with HPV biology and pathology, and that these compounds may be useful for the development of drugs against cervical cancer, genital warts and asymptomatic infections by genital HPVs.

**#295 Oligonucleotide inhibitors of DNA methyltransferase for cancer therapeutics.** Sufirin, Janice R., Brank, Adam, Marasco, Canio and Christman, Judith K. Roswell Park Cancer Institute, Buffalo, NY 14263 and University of Nebraska Medical Center, Omaha, NE 68198

DNA methylation is a posttranscriptional mechanism that plays a key role in gene expression. The alterations in normal DNA methylation patterns that occur during tumorigenesis and tumor progression are known to contribute significantly to the genetic reprogramming of cancer cells. Aberrant DNA methylation in tumors is a pervasive feature that has recently revitalized the search for DNA methylation inhibitors with therapeutic potential. The validity of this approach is substantiated by earlier clinical findings with the 2'-deoxycytidine analogs, 5-aza-2'-deoxycytidine (5azadC) and 5-fluoro-2'-deoxycytidine (5FdC). When these agents are incorporated into CpG sequences of DNA, they become potent mechanism based inhibitors of DNA methyltransferase. However, both nucleosides are cytotoxic and have other sites and mechanisms of action that are distinct from their inhibition of DNA methylation. In efforts to dissociate nonspecific cytotoxicity/genotoxicity from therapeutic effects specifically associated with inhibition of DNA methylation, oligodeoxynucleotides (ODNs) containing 5-FdC were designed, synthesized and evaluated for *in vitro* activity against mammalian as well as bacterial DNA methyltransferases. A series of single stranded 24-mer DNA analogs with potent *in vitro* substrate and/or inhibitory DNA methyltransferase (DNA MTase-dnmt1) activity were identified (Christman et al., Proc. Natl. Acad. Sci., USA 92, 7347, 1995). These 24-mer ODNs have novel structural features that enable a 5-methylcytosine (5MeC) residue at position 5 to direct downstream methylation of a CpG target site at least 13 bp distant. The observation that 5MeC stimulates methylation of CpG sites *in cis* can be attributed to the ability of these ODNs to form a looped structure that presents the classical molecular recognition motif for DNA MTase-dnmt1. Using the initial series of 24-mer ODN substrates/inhibitors of DNA MTase as lead structures, new ODNs have been designed, synthesized and evaluated for their *in vitro* and cellular effects on mammalian DNA MTase. Several "second generation" ODN inhibitors of DNA MTase with improved biological activity have now been identified. The rationale for their design will be discussed. (Supported by DAMD/BC971827; S.G. Komen Breast Cancer Fund, and Nebraska Dept. of Health).

**#296 Cytotoxic effects of rapamycin in human medulloblastoma cell lines and xenografts: as single agent or in combination chemotherapy.** Georger, Birgit, Kerr, Karol, Tang, Cheng-Bi, Janss, Anna J., Sutton, Leslie N. and Phillips, Peter C. The Children's Hospital of Philadelphia, Division of Neuro-Oncology, Department of Neurosurgery, Philadelphia, PA 19104.

Rapamycin has significant antitumor activity and specific advantages for brain tumor therapy: relative lipophilicity; unique mechanisms of cytotoxicity; absence of cross-resistance to other effective drugs; and minimal systemic toxicity. To evaluate the role of rapamycin in the treatment of medulloblastoma we examined *in vitro* cytotoxicity of rapamycin in medulloblastoma cell lines and *in vivo* activity of CCI 779, a rapamycin analog, in athymic nude mice bearing DAOY medulloblastoma subcutaneous flank xenografts.

*In vitro* cytotoxicity studies demonstrated  $IC_{50} \leq 10$  ng/ml in 4/7 medulloblastoma cell lines. By contrast, a glioblastoma cell line (U251) was highly resistant ( $IC_{50} > 1000$  ng/ml). Furthermore, rapamycin's cytotoxic effects were assayed in drug combination experiments with cisplatin (CDDP) or camptothecin (CPT) and showed significant additive effects.

To evaluate *in vivo* cytotoxicity in athymic mice bearing medulloblastoma flank xenografts, CCI 779 was administered i.p., daily x5 for 1, 2 or 4 weeks. CCI 779 1- or 2-week treatments yielded significant tumor growth delays; i.e., the time to 5x initial tumor volume increased by 160% and 240%, respectively, compared to controls. Extended treatment did not further increase its effects, nevertheless, significant side effects as dermatitis and weight loss in the animals could be seen. Prolonged growth delay (>50 days) was observed in 20% of the 2- and 4-week groups, but not in the 1-week group. Retreatment of large tumors with CCI 779 restored growth inhibition, but did not yield tumor regression. Simultaneous treatment with CCI 779 and CDDP increased tumor growth delay by 125% compared to CDDP alone.

Our results indicate that prolonged treatment with CCI 779 causes significant growth delay in DAOY medulloblastoma, has additive effects with CDDP and CPT, and suggests that this rapamycin analog has major cytotoxic activity in neuroectodermal tumor. (Supported by the National Institute of Health (Grant: PO1-NS 34514), the Jeffrey Miller Neuro-Oncology Research Fund and the Deutsche Krebshilfe e.V.).

**#297 Establishment Of Cell Based Assays For Evaluation Of Compounds Against HCV NS2-3 Protease and Internal Ribosomal Entry Site (IRES).** Huang, Mingjun; Wenzel, Michelle; Troxell, Jason and Buckheit, Robert Jr. Infectious Disease Research Department, Serquest, Southwestern Research Institute, Frederick, Maryland 21701-4756.



In most patients, HCV infection results in chronic hepatitis, which can progress to hepatocellular carcinoma. Development of an effective therapy will eradicate infection early in the course of disease and thereby to prevent progression to end stage.

Due to lack of efficient HCV in vitro replication system, molecular targets-based assays have been used for development of anti-HCV drugs. In this study, we report two cell-based assays targeting, respectively, at HCV NS2/3 proteinase and HCV IRES.

The cleavage at the NS2-3 junction of HCV polyprotein involves a viral protease which resides within the NS2 and NS3 domain. Development of a biochemical assay for NS2-3 protease is hindered by its autocatalytic nature. Here, we reported a cell-based luciferase reporting system for assaying the activity of NS2-3 protease. We observed an induction of luciferase expression when we introduced the wild type construct into cells. Such induction was not detected after a mutation is introduced to NS2 domain at His952, but a similar level of induction was observed when a mutation at Ser1165 of NS3 domain was introduced, suggesting strongly that the induction of luciferase expression is NS2-3 cleavage dependent. To evaluate the system, we tested several commercial available protease inhibitors. We observed the reduction of luciferase expression in a dose-dependent manner with some of the compounds. Inhibition of protease, however, is due to the toxicity of the compounds. The only exception is Pepstatin A which demonstrated an activity with a therapeutic index of approximately 10.

The 5' untranslated region of the HCV genome contains an IRES as demonstrated by functional and structural analysis. Since specific macromolecular interactions are involved in a cap-independent initiation of translation, IRES is speculated to be an antiviral target. To screen the activity of the compound against HCV IRES target, a dual luciferase reporting system was utilized. In the system, the translation of the first cistron, renilla luciferase from a bicistron mRNA is cap-dependent while the expression of the second cistron, luciferase, from this mRNA is IRES-dependent. The system is evaluated with oligos derived from antisense and sense region of IRES and the results will be presented.

**#298 RAS endoprotease inhibitors are potent antileukemic agents.** Perrey, D.A., Naria, R.K., Navara, C.S., and Uckun, F.M. *Drug Discovery Program, Parker Hughes Cancer Center, Hughes Institute, St. Paul, MN 55113.*

Oncogenic ras is associated with a wide range of human malignancies. The posttranslational modification of the Ras protein involves sequential prenylation, proteolytic cleavage and methylation, which assists its association with the cell membrane. A series of 55 cysteine chloromethyl ketone derivatives and 9 diazomethyl ketone derivatives designed as inhibitors of the Ras endoprotease were synthesized and evaluated against pre-B acute lymphoblastic leukemia (ALL) (Nalm-6) and T-ALL (Molt-3) cell lines. As a new class of anticancer drugs, the compounds showed high cytotoxicity against leukemic cell lines with  $IC_{50}$  values in low micromolar range. N-Acetyl-S-dodecyl-Cys chloromethyl ketone (HI-131) exhibited potent activity with  $IC_{50}$  values of 2.0 and 2.3  $\mu$ M against Nalm-6 and Molt-3 cell lines, respectively. Variation of the S-alkyl chain length from methyl to docosyl (1-22 carbons) showed the best compounds to be N-acetyl-S-undecyl-Cys chloromethyl ketone (HI-321) ( $IC_{50}$  = 1.7  $\mu$ M against Nalm-6) and N-acetyl-S-hexyl-Cys chloromethyl ketone (HI-357) ( $IC_{50}$  = 0.7  $\mu$ M against Molt-3). HI-131 was further evaluated as the lead compound and was found to inhibit the production of active Ras using the Ras-binding domain (RBD) of Raf1 as an activation specific probe for Ras. HI-131 induced apoptosis in leukemia cells, as determined by confocal laser scanning microscopy with multi-photon imaging, flow cytometry, TUNEL assays and DNA gels. HI-131 was very active in the Nalm-6 SCID mouse model of human ALL; whereas all of the 10 PBS-treated control SCID mice died of disseminated human leukemia within 60 days after i.v. inoculation of  $1 \times 10^6$  Nalm-6 cells, 6 out of 7 SCID mice treated with HI-131 according to a 10 mg/kg/day  $\times$  5 days  $\times$  4 weeks schedule remained alive free of leukemia >120 days. HI-131 was also found to be very active against primary leukemic cells from ALL and AML patients (N = 11) at nanomolar concentrations.

**#299 Inhibitors of Calpain as Novel Chemotherapeutic Agents for Prostate Cancer.** G.F. Eilon, J. Gu, K. Hara, and J.W. Jacobs. *Hitech Chemical Research Center, Irvine, CA and Nippon Chemiphar Co., Ltd., Tokyo, Japan.*

NCO-700 and TOP-008, epoxide-containing calpain inhibitors, displayed cytotoxicity against the androgen receptor-negative prostate cancer cell lines, PC-3 and DU-145, with  $ED_{50}$  values in the 5-20  $\mu$ M range. Cytotoxicity against the hormone receptor-positive LN prostate cancer cell lines occurred at 10-20 fold higher concentrations. In dose-response studies in nude mice bearing DU-145 prostate tumor xenografts, 50 mg/kg doses of the two compounds either stopped tumor growth (TOP-008) or significantly slowed (NCO-700) growth. The mechanism of cytotoxicity was shown to be through apoptosis by a) confocal microscopy studies revealing nuclear fragmentation, b) mitochondrial studies revealing disruption of the mitochondrial membrane and release of the cationic dye, JC-1, into the cytoplasm and c) protein immunoblot assays indicating that over a 6 h period, TOP-008 induced a significant accumulation of the pro-apoptotic

protein, bak, in the mitochondrial fraction of DU-145 prostate cancer cells, accompanied by activation, at 2.5 h, of CPP32 (caspase-3). Finally, using the Clontech Atlas cDNA array for apoptosis genes, significant up-regulation of bak mRNA occurred in TOP-008 treated cancer cells. Previous toxicology studies in rodents and dogs, as well as a Phase I study in humans, showed NCO-700 to be a well-tolerated, non-toxic compound. Taken together with our current findings, these results suggest that these calpain inhibitors have the potential to be relatively safe, new chemotherapeutic agents for refractory prostate cancers.

## SECTION 4: MARINE COMPOUNDS AND OTHER NATURAL PRODUCTS, SYNTHETIC APPROACHES

**#300 Dolastatin 10 (dola 10) administered with G-CSF allows substantial escalation of the maximum tolerated dose (MTD) in patients (pts) with advanced solid tumors.** Madden, T., Tran, H.T., Felix, E., Newman, R.A., and Abbruzzese, J.L. *Depts. of Clinical Investigation, Pharmacy, and Gastrointestinal Medical Oncology and Digestive Diseases, U.T.M.D. Anderson Cancer Center, Houston, TX 77030.*

Dola 10 is a pentapeptide isolated from the mollusc *Delabella auricularia* with promising antitumor activity. In a previous study the MTD was reached at 300  $\mu$ g/m<sup>2</sup> with granulocytopenia the dose-limiting toxicity (DLT). Available preclinical and clinical data suggest that for dola 10 to have meaningful anti-cancer activity the time whereby plasma levels exceed 1 ng/ml should be maximized. The objective of this Phase I study was dola 10 dose-escalation to extend the period of drug exposure above 1 ng/ml to 24-48 hours, while adding G-CSF to manage granulocytopenia. Doses of dola 10 were given by iv push every 21 days. Beginning 24 hours after dola 10, G-CSF was administered daily for up to 14 days. Nineteen pts have been treated. Pt characteristics: median age-53; sex: male-12, female-7; malignancy: colorectal-13; head + neck-2; one each pancreas, breast, ovary and esophagus; prior therapy: chemotherapy-19, radiation-9. At doses of 300, 375, and 469  $\mu$ g/m<sup>2</sup>, no episodes of grade 3 or 4 granulocytopenia or thrombocytopenia were observed. At 585 and 730  $\mu$ g/m<sup>2</sup> 1/6 pts and 3/3 pts experienced grade 4 granulocytopenia, respectively. Using ESI-LC/MS we examined dola 10 disposition in 16 of these 19 pts. The mean values are summarized below:

Dose ( $\mu$ g/m <sup>2</sup> )	Cl <sub>p</sub> (L/hr/m <sup>2</sup> )	T <sub>1/2<math>\alpha</math></sub> (hrs)	Time > 1 ng/ml (hrs)
<300*	4.5		4.2
300	3.6	16.4	18.0
>300	1.6	12.8	31.5†

†, value is for patients treated at 585  $\mu$ g/m<sup>2</sup>. \*, pts NOT receiving G-CSF.

Plasma clearance was 3-fold lower at higher dola-10 doses versus lower dola 10 doses and those without G-CSF. At 585 and 730  $\mu$ g/m<sup>2</sup> the mean (n = 3) time above a dola 10 plasma concentration of 1 ng/ml was 31.5 and 60.1 hrs respectively. Patient accrual continues at the anticipated MTD of 660  $\mu$ g/m<sup>2</sup>. With G-CSF, the MTD of dola 10 can be doubled; the anticipated DLT is granulocytopenia, but at higher doses (730  $\mu$ g/m<sup>2</sup>) thrombocytopenia begins to emerge. Phase II trials of dola 10 should be conducted using this optimized dosing strategy. (Supported in part by the U.S. Public Health Service [2 U01 CA62461]).

**#301 Interference of transcriptional activation by the anti-neoplastic drug ET-743.** Minuzzo Mario and Mantovani Roberto; *Dip. Genetica e Biologia dei Microrganismi, Università degli Studi di Milano, Milan, Italy.* Faircloth Glynn T.; *PharmaMar USA, Inc., Cambridge, MA, USA.* D'Incalci Maurizio, *Istituto Mario Negri, Milan, Italy.*

ET-743 is an alkaloid isolated from the marine tunicate *Ecteinascidia turbinata*, currently under Phase II clinical trials for its potent anti-cancer activity, that was shown to bind DNA in the minor groove and form covalent adducts with some sequence-specificity. We show that ET-743 selectively inhibits *in vitro* CCAAT-box binding of NF-Y, a trimeric transcription factor targeting the regulatory NF-YA subunit. We assayed ET-743 function *in vivo* by deriving stable NIH3T3 lines with integrated HSP70 promoter, which is dependent on NF-Y, and on the Heat Shock Factor (HSF). Upon heat induction, the drug blocks transcription rapidly, at pharmacological concentrations (2-30 nM) and in a CCAAT-dependent way. The Distamycin-like alkylating compound Tallimusline has no effect, even in the microM range. The activity of the CCAAT-less SV40 promoter is not affected, indicating that ET743 is not a general Pol II inhibitor. Extracts of drug-treated cells showed normal NF-Y and increased HSF binding, suggesting that inhibition of activator(s) binding is not responsible for lack of promoter activity. We hypothesize that this new marine compound is a promoter specific transcriptional interfering agent.

**#302** The antitumor agent Ecteinascidin 743 (ET743), inhibits transcriptional activation of the MDR1 Gene by multiple inducers. Jin, Shangkan, Hu, Zhen and Scott, Kathleen W. Memorial Sloan-Kettering Cancer Center, New York, New York 10021.

Ecteinascidin 743 (ET-743), a natural product isolated from the marine organism *Ecteinascidia turbinata*, exhibits strong anti-tumor activity against several cancers, and is currently entering Phase II trials. Previous studies have shown that ET743 binds to the minor groove of DNA and specifically blocks the *in vitro* interaction of the transcription factor NF-Y with its cognate binding site. We have recently shown that NF-Y is required for the activation of the human P-glycoprotein gene (MDR1) by inducers that including trichostatin A (TSA), butyrate and ultraviolet light. To determine whether ET743 could block activation of this NF-Y-dependent promoter *in vivo*, we evaluated its impact on expression of both the endogenous MDR1 gene and MDR1 promoter/luciferase constructs stably transfected into the human colon carcinoma cell line SW620. While no significant effect on basal MDR1 promoter activity was observed, concentrations of as little as 10 nM inhibited activation of both the endogenous and transfected promoters; 50 nM ET743 was sufficient to abolish response to all three transcriptional inducers. Since NF-Y is required for the regulation of several cell cycle-related genes, we next evaluated the effect of TSA and ET743 on SW620 cell cycle progression. Following a 24 hour exposure, ET743 had no apparent effect on cell cycling. However, TSA caused a strong G2/M block which was abolished in the presence of ET743, suggesting a model in which ET743 blocks TSA-regulated cell cycle genes. Taken together, our data suggest that this promising antitumor agent blocks transcription of a subset of promoters through a novel mechanism. Moreover, its effect on MDR1 transcription makes it a candidate for a new class of sensitizing agents for MDR drugs.

**#303** Importance of DNA repair mechanisms for the sensitivity of tumor cells to ET-743. Damia Giovanna, Silvestri Simonetta, Filiberti Laura, Brogini Massimo and D'Incalci Maurizio; Istituto Mario Negri, Milan, Italy. Faircloth Glynn T.; Pharma Mar USA, Inc., Cambridge, MA, USA.

ET-743 is a tetrahydroisoquinoline alkaloid extracted from the tunicate *Ecteinascidia turbinata* and poses striking antitumor efficacy in pre-clinical systems and promising activity in the initial clinical investigations.

It binds to the minor groove of DNA and alkylates the N2 position of guanine. In order to better define the mechanisms of ET-743 interaction with DNA, its sensitivity was evaluated in different cellular systems characterized by defined deficiencies in DNA repair pathways. Defects in mismatch repair pathway, that are usually associated with an increased resistance to methylating agents and cisplatin, did not affect the cytotoxic activity of ET-743. On the contrary ET-743 displayed an unusual pattern of potency in UV-sensitive NER (nucleotide excision repair) deficient mutant CHO cell lines, being eight and six fold less potent in ERCC1 (excision repair cross-complementing) and in XPB (xeroderma pigmentosum) deficient cell lines respectively. The DNA-double-strand break (DSB) repair pathway was also investigated using human glioblastoma cell lines MO59K and MO59J, proficient and deficient in DNA-dependent protein kinase (DNA-PK), respectively. ET-743 was found to be more effective, with a two fold decrease in IC50, in cells lacking DNA-PK. An increase in ET-743 sensitivity was also observed in AT (Ataxia telangiectasia, mutated) cells.

Although the molecular mechanisms underlying these effects have not been elucidated yet, the data strongly suggest that ET-743 has a unique mechanism of interaction with DNA.

**#304** *In vitro* effect of the tetrahydroisoquinoline alkaloid Ecteinascidin-743 (ET-743) on chondrosarcoma (CHSA) cells. Hornicek, Francis J., Weissbach, Lawrence, Nielsen, G. Petur, Fondren, Gertrude, Harmon, David, Jimeno, Jose, Chabner, Bruce A., Faircloth, Glynn T. Massachusetts General Hospital and PharmaMar, Inc.

Tumors of cartilage comprise the most common primary connective neoplasms of the skeleton. They have a variety of presentations and behave unpredictably. Treatment modalities have included radiation therapy (XRT) and chemotherapy but have yielded disappointing results except in patients with dedifferentiated and mesenchymal CHSAs. Currently, the most effective treatment for CHSA is surgical resection.

As a first step in developing more effective treatments we have established CHSA cell lines from surgically resected specimens that have not been exposed to chemotherapy or XRT. We have performed RT-PCR analysis on these cells after isolating total RNA. Both type II and type IV collagen mRNA have been detected. The fact that the expression of the type II collagen gene, a classical marker for cartilage differentiation, is found in these cultured cells suggests the retention of a chondrocytic character.

ET-743, a tetrahydroisoquinoline alkaloid isolated from the marine ascidian *Ecteinascidia turbinata*, is highly cytotoxic to various tumor cells, but bone and cartilage tumor cells have not been tested for their sensitivity to this compound. Due to the lack of effective treatments currently available for CHSA, we tested the effect of ET-743 on cultured CHSA cells, established from explants and grew exponentially in monolayers. At a concen-

tration of 1 nM, ET-743 was cytotoxic for these cells, and flow cytometry of the treated samples indicated an inhibition of progression through the cell cycle. There was a dose-dependent toxicity in the range of 1 to 100 nM, and S + G<sub>2</sub> + M phase cells decreased correspondingly. The morphology of the cells changed concomitantly, with a loss of spindle shape and the development of fewer intercellular connections or bridges. The cell cycle block was at the G<sub>2</sub>/S interface. These results support earlier data on the cellular toxicity of ET-743 against cancer cells.

Except for surgery none of the conventional treatments are successful in managing patients with CHSA. The reasons for this poor response to chemotherapy and XRT remain unknown. New approaches seem warranted in the treatment of CHSA. The demonstration that ET-743 inhibits proliferation of these cells lends itself to further investigation as a new option for treatment of CHSA.

**#305** Potent antitumor activity of ET-743 against human soft tissue sarcoma cell lines. Li Weiwei, Jhanwar Suresh, Elisseyeff Yaroslav, and Bertino Joseph, R. Memorial Sloan-Kettering Cancer Center, New York, NY 10021.

We examined the antitumor activity of ET-743, a novel marine natural product, in human soft tissue sarcoma (STS) cell lines. Nine cell lines (4 previously described in Int. J. Cancer 68:514, 1996, 4 new cell lines and HT-1080 a fibro-sarcoma cell line) were exposed to ET-743 at different concentrations for 72 h and IC50 values of ET-743 for these cell lines were determined using a SRB cytotoxicity assay. Results showed that IC50's are particularly low for HT-1080 and for malignant fibrous histiocytoma (MFH) cell lines, HS-90, M-8805, M-9110 and M-9005 (<0.1 μM). IC50's determined in four other HSTS cell lines, HS-16 (mesenchymal chondrosarcoma), HS-18 (liposarcoma), HS30 (malignant hemangiopericytoma) and HS-42 (malignant mesenchymoma) ranged from 4 μM to 100 μM. Antitumor activity of ET-743 is also observed to be time-dependent and p53-independent in these STS cell lines. In contrast, ET-743 was less potent against other types of tumor; higher IC50's were observed in colon cancer cell lines such as HCT-8 (10 nM), HT-29 (3 nM) and HCT-116 (3 nM) and a breast cancer cell line, MCF-7 (20 nM). We conclude that ET-743 is highly active against STS cells, especially against MFH cells, and encourage trials of this drug in patients with STS.

**#306** Enhancing the preclinical *in vivo* antitumor activity of Ecteinascidin 743, a marine natural product currently in Phase II clinical trials. Jimeno, José M., PharmaMar, S.A., Madrid, Spain, Grant, Wendy, Faircloth, Glynn T. PharmaMar USA, Inc., Cambridge, MA.

The potent antineoplastic drug Ecteinascidin 743 (ET-743) is a tris, tetrahydroisoquinoline alkaloid isolated from the marine tunicate *Ecteinascidia turbinata* and currently in Phase II clinical trials. The present studies were undertaken to provide clinically relevant information on the effect that (i) 2 representative infusion schedules or (ii) the use of an anti-emetic has on the biological efficacy of ET-743.

The schedule-dependent antitumor activity of ET-743 has been well documented against NSCL, melanoma and ovarian tumors. In the first study, an *in vivo* inoculated B16 murine melanoma model was used to compare survival in male rats (RH-rnu) receiving a total dose (TD) of 90 μg/kg ET-743 administered by 3-hr or 24-hr infusion. Initial results indicate that both infusion schedules caused increase life extension (ILS) well beyond the saline control; however, the 3-hr infusion was more effective (±68% ILS) than the 24-hr infusion (±28% ILS). In addition, body weight loss was generally greater in the 24-hr infusion group from 2 wks after drug delivery until death or at the day of sacrifice for long-term survivors.

In the second study, the *in vivo* B16 tumor model in male rats was used to compare dexamethasone (DEX) pre-treated (3 mg/kg TD; -15 min), ET-743 (90 μg/kg TD) animals (DEX<ET743) to ET-743 alone on a q2dx5, iv, schedule. The choice of DEX has more than one implication for the current clinical trials. Many patients exhibit emesis during their course of treatment. An effective anti-emetic would greatly benefit these patients. On the other hand, DEX enhances the enzymatic activity of the hepatic P450 3A subfamily, the isoform primarily responsible for induction of ET-743 metabolism. Initial results indicate that DEX pre-treatment greatly enhances the efficacy of ET-743 (±132% ILS) compared to ET-743 alone (±55%). Moreover, upon necropsy at death or the day of sacrifice there were no visible lung mets in 2 animals (2 CR/1 PR per 5) in the DEX<ET743 group. This compared to 1 CR/1 PR per 5 in the ET-743 group. It was also apparent that the DEX<ET743 animals seemed more 'robust' than ET-743 animals during the course of their treatments. Further studies are underway to confirm and extend these findings as well as to identify and characterize any bioactive ET-743 metabolites.

**#307** A Phase I and Pharmacokinetic (PK) study of ET-743 evaluating a 3 hours (h) intravenous (iv) infusion (i) in patients (pts) with solid tumors. Twelves, C., Hoecckman, H., Bowman, A., Beijnen, J.H., Faber, M., Guzman, C., Anthony, A., Smyth, J., Hanauske, A. R., and Jimeno, J. <sup>1</sup>ECSG/EORTC (Glasgow) and Edinburgh<sup>2</sup>, UK; Amsterdam<sup>3</sup>, NL; <sup>4</sup>Stofervaart Hospital, (Amsterdam, NL); <sup>5</sup>NDDO (Amsterdam, NL) <sup>6</sup>PharmaMar R&D (Tres Cantos, Spain).

ET-743 is a marine derived compound currently in phase II using an iv infusion (i) for 24 h q 3 weeks. In this dose finding study pts with advanced/



resistant solid tumors received ET-743 as an iv 3 h l every 3 weeks. Thirty two pts (median age=55 y., PS=1, male/female 14/17) have been treated. The starting dose of 1000 mcg/m<sup>2</sup> is the recommended dose of ET-743 given as a 1 h l. The following dose levels have been assessed (pts/cycles): 1000 (3/8), 1300 (6/16), 1500 (6/17), 1800 (4/5) and 1650 (13/29) mcg/m<sup>2</sup>. The maximal tolerated dose (MTD) is 1800 mcg/m<sup>2</sup> with grade (G) 4 thrombocytopenia and severe fatigue the dose limiting toxicities. There were no toxic deaths. The 1650 mcg/m<sup>2</sup> dose level was generally well tolerated with G3-4 neutropenia in 3/13 pts and thrombocytopenia in 2/13 patients; 1 pt had febrile neutropenia. Transient, non-cumulative rises in serum transaminases were observed in 9/13 pts at 1650 mcg/m<sup>2</sup>.

Pharmacokinetic analysis (LC/MS/MS/ES) is ongoing; initial data confirm high clearance (median 38.34 L/h m<sup>2</sup>) and volume of distribution (1231 L/m<sup>2</sup>). AUCs achieved with the 1650 mcg/m<sup>2</sup>-3 h l are similar to those using the 1500 mcg/m<sup>2</sup>-24 h l (median 43.20 and 43.32 h\*ug/l, respectively). At the 1500 mcg/m<sup>2</sup> dose level, a pt with relapsed, metastatic leiomyosarcoma previously treated with chemotherapy and pelvic RT had a complete remission; (8+ cycles, time to progression=32+wks); a further 8 pts are ongoing at 1650 mcg/m<sup>2</sup>, with tumor assessment awaited. Our results indicate that the 3 h l is an active, feasible out-patient schedule for ET-743. The proposed phase II dose for good risk pts is 1650 mcg/m<sup>2</sup>.

**#308 Exploratory evaluation of the potential predictors for dose-limiting toxicities (DLTs) in patients treated with Ecteinascidin-743 (ET-743) as a 24-h intravenous (iv) infusion every 3 weeks and its relationship to pharmacokinetics (PK).** López-Lázaro, L.<sup>1</sup>, Guzmán, C.<sup>1</sup>, Taamma, A.<sup>2</sup>, Cvilkovic, E.<sup>2</sup>, Missel, J.L.<sup>2</sup>, Brain E.<sup>3</sup>, Beijnen, J.H.<sup>4</sup> and Jimeno J.<sup>1</sup>. <sup>1</sup>Pharmamar R & D., Tres Cantos, Madrid, Spain; <sup>2</sup>Paul Brousse Hospital, Villejuif, France; <sup>3</sup>René Huguenin Hospital, Paris, France, <sup>4</sup>Slotervaart Hospital, Amsterdam; The Netherlands.

We evaluated the potential predictors of ET-743 DLTs and its relationship to PK. Evaluation was performed with data from the 24 h iv infusion q 3 weeks Phase I study. DLT was defined as any grade ≥3 non-hematological toxicity (excluding reversible transaminitis, alopecia and emesis), grade 4 neutropenia longer than 5 days, febrile (>38°C) neutropenia or grade 4 thrombopenia. Two analysis were performed, one without PK including all 105 treatment courses, and other including PK parameters of the 2 initial courses. In both cases, 3 dose levels (34pts) were considered; 1200 (5pts), 1500 (25pts) (RD) and 1800 mcg/m<sup>2</sup> (4pts) (MTD). The considered PK parameters were terminal half-life (t<sub>1/2</sub>), clearance (Cl), area under the curve (AUC) and volume of distribution (Vd) calculated by non-compartmental methods. Pts characteristics were: sex (14/20; M/F), age (median 59 yrs, range: 19-75). Other potential predictors were: previous treatment (more than 2/1-2 previous lines), liver metastases (yes/no), bone metastases (yes/no), cycle number, dose, and baseline performance status, prothrombin time, partial thromboplastin time, albumin, bilirubin, alkaline phosphatase (AP), AST and ALT. For the initial univariate analysis Fisher's exact test for dichotomous variables, Mann-Whitney test for ordinal variables and Student's t-test for continuous variables were used. Variables with a p value <0.20 were entered in a backward stepwise logistic regression model.

All observed DLTs (16 cycles/13 pts) were neutro- (9 cycles/7 pts) or thrombopenia (7 cycles/6 pts) related. The DLT likelihood increased with dose (p=0.012) and baseline AP (p=0.0026). 62 (34 1st/28 2nd) treatment courses given to 34 pts were included in the analysis including PK. DLT risk correlated with increasing baseline AP (p=0.081), and number of cycles given (p=0.052). Moreover, it correlated with PK features: increased AUC (p=0.044) and decreased Cl and Vd (p=0.047 and 0.043 respectively) in the multivariate analysis.

Increased baseline AP is a potential prospective predictor of ET-743 induced DLTs, but its value should be validated in further studies. The risk of DLT is higher on cycle 2 than in cycle 1. Increased AUC increases the risk of DLTs and both low Cl and low Vd are independent predictors of DLT.

**#309 Ecteinascidin-743 (ET-743) in heavily pretreated refractory sarcomas: early results of the French experience.** Taamma A, Missel J.L, Delalage S, Guzman C, Di Palma M, Yovine A, Brain E, Cottu P, Riefrio M, Jimeno J.M, Cvilkovic E. Hop Paul Brousse, Centre René Huguenin, Hop Saint Louis, France. Pharma Mar, Très Cantos, Spain.

ET-743 is a new minor groove DNA binding agent of marine origin, currently in early phase II development. During the phase I trial testing the 24 hours continuous infusion given every 3 weeks the maximal tolerated dose was 1800 mcg/m<sup>2</sup> and the recommended dose was 1500 mcg/m<sup>2</sup>. The limiting toxicities were neutropenia and thrombopenia. Fatigue and reversible transaminitis were also frequent. We report our current experience in treatment of refractory advanced sarcoma patients.

**Patients characteristics:** Twenty four patients received ET-743, 23 at recommended dose and schedule and 1 at the maximum tolerated dose. Niné of them were treated in the phase I study, 9 in an early phase II and 6 received this treatment in a compassionate use basis. Sex: 14 women/10 men; median age 46 (16-71); histology: leiomyosarcoma 6, liposarcoma 6, fibrosarcoma 4, angiosarcoma 1, rhabdomyosarcoma 1, osteosarcoma 2, other types 4; median number of previous chemotherapy regimens 2 (1-4), (all patients previously treated with anthracycline and alkylators); median

PS 1 (0-2); median number of metastatic sites 1 (1-3). Toxicity is evaluable for 84 given cycles. Median number of cycles/patient 3 (1-8). Grade 3-4 (NCI-CTC) toxicities are acute reversible transaminitis (46%), neutropenia (34%), thrombopenia (6%) nausea/vomiting (9%). Febrile neutropenia occurred in 2 cycles (2%). Grade 1-2 asthenia were observed in 42% of cycles. Antitumor activity 22 patients evaluable (2 patients too early for evaluation). Four PR (18%) (3.5, 6+, 6+, 6+ months), 3 MR (2+, 3+, 4+) and 7 disease stabilization (3 ongoing) were observed. Both osteosarcoma patients achieved a PR, the other two PR were observed in liposarcoma and fibrosarcoma. Median time to progression for the overall cohort is 10 weeks (2-25). ET-743 is a promising agent with a Phase II program in patients with pretreated soft tissue sarcomas actively accruing.

**#310 Changes in gene expression in tumor cells exposed to the two marine compounds, ET-743 and Aplidine, by using cDNA microarrays.** Broggnini Massimo, Marchini Sergio and D'Incalci Maurizio; Istituto Mario Negri, Milan, Italy. Faircloth Glynn T. and Jimeno José; Pharma Mar, Cambridge, USA and Tres Cantos, Spain.

The present study was undertaken to investigate whether and to which extent two natural products (ET-743 and Aplidine) with poorly understood modes of action could induce early changes in the expression of genes encoding for proteins having a crucial role in signal transduction, proliferation, cell cycle or apoptosis. Igrov-1 cells were exposed to active concentrations of ET-743 and total RNA was isolated after 0, 6 and 24 hours of treatment. For Aplidine, total RNA was isolated from MOLT-4 cells at 0, 1, 6 and 24 hours after treatment. Total RNA (1 µg) was retrotranscribed in the presence of <sup>32</sup>P-ATP using a mixture of specific primers (Clontech) and MMLV reverse transcriptase. Equal amounts of <sup>32</sup>P labeled RNA were hybridized to cDNA expression arrays (Clontech, human cancer) containing 588 human cDNAs. Hybridization and washing of the filters were performed according to manufacturer's instructions. Analysis was carried out using ATLAS IMAGE 1.0 software (Clontech). Preliminary results revealed changes in the expression of genes playing important roles including for p21/WAF, GADD45 and killer/DR5 for ET-743 and c-fms, ETR-1, FLT-1 topoisomerase II α, DNA-PK and ATM for Aplidine. Studies are currently underway to confirm the observed changes of expression using other methods and to evaluate the relevance of these findings for the antitumor activity of these drugs.

**#311 A correlation of selective antitumor activities of the marine-derived compound Aplidine using different model systems.** Jimeno, José M. PharmaMar S.A., Madrid, Spain, Smith, Brendan, Grant, Wendy, Faircloth, Glynn T. PharmaMar USA, Inc., Cambridge, MA.

Aplidine (APL) is a cyclic depsipeptide isolated from a Mediterranean tunicate, *Aplidium albicans*, and currently in Phase I clinical trials. Selective antitumor activities were seen against two histologically different solid tumors: human gastric and prostate carcinomas. Potent *in vitro* activity to primary gastric tumor specimens or Hs746T gastric tumor cells is evident with IC<sub>50</sub> values of 146 and 450 pM, respectively. A less potent, but no less selective, IC<sub>50</sub> activity of 3.4 nM was determined against PC-3 prostate tumor cells. *In vivo* activities were evaluated in nude rodents using sc implanted tumor fragments or hollow fibers (HF) containing tumor cells.

Table 1. Optimal Dose and *In Vivo* Activities of APL

Tumor	Line	Regimen	sc Model	Animal	Dose (mg/kg)	Activity (%T/C)
Gastric	MRI-H254	qd9, ip	xenograft	mouse	2.1	19%
					1.05	17%
		q4dx3, ip	xenograft	mouse	1.25	18%
Prostate	PC-3	24 hr, iv inf.	HF	rat	0.7	20%
		qd9, ip	xenograft	mouse	1.25	25%
					0.62	30%
		q4dx3, ip	xenograft	mouse	2.10	34%
					1.05	38%
		24 hr, iv inf.	HF	rat	0.70	31%
		5 day, iv inf.	HF	rat	0.70	33%

Optimal activities were observed in xenografted gastric (17-20%) and prostate (25-38%) tumors following ip administration. Follow-up studies necessitated using rats for *iv* infusions. With this variation, a 24-hr *iv* infusion schedule produced similar activities against HF gastric (20%) and HF prostate (31%) tumor cells. Cytotoxicity was also found using a 5-day *iv* infusion schedule against HF prostate tumor cells (33%). The extended *in vivo* evaluations not only show that there is a strong relative correlation to the *in vitro* cytotoxic profile, but also a strong correlation with *in vivo* models used to characterize the tumor selectivity that identified APL as a candidate for clinical development.

**#312 Is Aplidine acting as an Ornithine Decarboxylase (ODC) inhibitor?** Erba Eugenio, Baesano Lucia, Di Liberti Giacchino, Muradore Ivan, Codegioni Anna Maria, Celli Nicola and D'Incalci Maurizio; *Istituto Mario Negri, Milan and Mario Negri Sud, Chieti, Italy*. Desiderio Alfonso; *Ist. Patol. Gen., Univ. Milan, Milan, Italy*. Faircloth Glynn T. and Jimeno José; *Pharma Mar, Cambridge, USA and Tres Cantos, Spain*.

Aplidine is a marine depsipeptide isolated from the Mediterranean tunicate *Aplidium albicans*, which has shown potent *in vitro* activity in several cancer cell lines, *in vivo* efficacy in human xenografts and is currently in Phase I clinical trials. The mechanism of action of Aplidine is not yet fully elucidated. In Molt-4 leukemia cells Aplidine at concentrations of 10–20 nM causes a G1 blockade and apoptosis 6h after 1 h drug exposure. The G1 block does not appear to be related to a direct effect on DNA synthesis nor to inhibition of Cdk2-cyclin A or Cdk2-cyclin E kinases. However, Aplidine (10–20 nM) causes a strong inhibition of ODC with a depletion of putrescine already evident by the end of 1 h treatment without any change in the intracellular levels of spermidine or spermine. At the same time no inhibition of DNA, RNA nor protein synthesis was observed. The addition of external putrescine causes an increase in intracellular levels of this polyamine in Aplidine treated cells, which are even higher than those found in untreated control cells. Moreover, Aplidine-induced cell cycle perturbations and apoptosis were reduced but not abolished by putrescine treatment. These data suggest that ODC is one but not the main target of Aplidine action.

**#313 A phase I and Pharmacokinetic (PK) study of Aplidine (APL) given as a weekly (w) 24 hours (h) infusion (I) in patients (pts) with advanced solid tumors.** L. Pronk<sup>1</sup>, C. Twelves<sup>2</sup>, H. Cortes-Funes<sup>1</sup>, A. Anthony<sup>2</sup>, S. Kaye<sup>3</sup>, S. Alonso<sup>1</sup>, N. Celli<sup>4</sup>, C. Guzman<sup>1</sup>, J. Jimeno<sup>1</sup>, L. Paz-Ares<sup>1</sup>. <sup>1</sup>Hospital 12 Octubre (Madrid-Spain), <sup>2</sup>Beatson Cancer C. (Glasgow, UK), <sup>3</sup>I.M. Negri (Milano, Italy) and <sup>4</sup>PharmaMar R&D (Tres Cantos, Spain).

APL is a new marine derived antitumor depsipeptide discovered in the Mediterranean tunicate *Aplidium albicans*. Its mode of action relates to a GTP dependent inhibition of the elongation factor 1 $\alpha$  (a tRNA transition component of protein elongation). APL interferes with the cell cycle progression at G1 and has *in vitro* and *in vivo* activity (A) in human tumor models. *In vivo* studies revealed that A increased by prolonging I duration. In this study 16 pts were treated. Pts characteristics: median age 55 years, median PS 1, male/female 11/5, tumor types being as follows: Head and neck 6, kidney 2, colon 3, rectum 2, sarcoma 1 and melanoma 3, all pretreated with chemotherapy (median 2 lines).

APL was administered as a 24 h I at the following dose levels (DLs): 133 (3 pts), 266 (3 pts), 532 (3 pts), 1000 (3 pts), 2000 (3 pts) and 3000 (1 pt) mcg/m<sup>2</sup>/wk x 3 every 28 days.

No dose limiting toxicities (DLTs) were observed. Only mild nonhematological toxicities consisting of nausea g 1, mucositis g 1, asthenia g 1 were reported. Phlebitis of the infusion arm was common and concentration-dependent. PK analysis was performed in all pts, showing plasma levels at the DLs 1000 mcg/m<sup>2</sup>/w and 2000 mcg/m<sup>2</sup>/w equivalent to the active *in vitro* concentration (1 ng/ml). At DL 532 mcg/m<sup>2</sup>/w clinical improvement was observed in 1 pretreated pt with advanced melanoma.

Accrual of pts will be continued until maximum tolerated dose (MTD) is determined.

**#314 ES-285, a marine natural product with activity against solid tumors.** Jimeno José M., Garcia-Gravalos, D. *PharmaMar, S.A., Madrid, Spain*, Avila, Jesús, *CSIC-UAM, Madrid, Spain*, Smith, Brendan, Grant, Wendy, Faircloth, Glynn T. *PharmaMar USA, Inc., Cambridge, MA*.

The novel marine natural product ES-285, isolated from the clam *Spisula polynyma*, has been shown to promote the disassembly of actin stress fibers by inhibition of Rho activity, a small GTP binding protein.

An evaluation of cytotoxicity against a human tumor cell line panel containing solid tumors, lymphomas and leukemias revealed selectivity for certain solid tumors (i.e. colon, gastric, pancreas pharynx, renal) with IC<sub>50</sub> potencies in the nM range and a specificity to SK-HEP-1 hepatoma tumor cells with an IC<sub>50</sub> of 0.562 pM. The activities against the solid tumor cell lines were generally 1 log more potent than against the leukemias and lymphomas. Among the solid tumors, the more slowly growing (adherents) seemed to be more sensitive to ES-285. To initiate an *in vivo* profile for ES-285, five representative tumors (i.e. leukemia, melanoma, renal, prostate and hepatoma) were chosen. The single bolus MTD<sub>ip</sub> established for ES-285 in mice (30 mg/kg) was used as the total dose for all regimens. There was no *in vivo* activity observed against *ip* inoculated P388 murine leukemia or *iv* inoculated B16 murine melanoma. However, there was significant tumor growth inhibition (TGI) by ES-285 against sc implanted PC-3 human prostate (<1% T/C) and MHI-H-121 human renal (28% T/C) tumor xenografts administered on a q4dx3, *ip*, schedule. There were complete and near-complete remissions against the prostate xenografted tumors at the highest dose. Although the overall TGI was less than that seen against prostate tumors, there was a prolonged effect on renal tumor volume by ES-285 that lasted up to 3 weeks after the last dose. In a hollow fiber model, ES-285 was very active against sc implanted SK-HEP-1 hepatoma tumor cells at the MTD (14% T/C) and 1/2 MTD (19% T/C) administered on a qdx5, *iv*, schedule.

Taken together, the data shows that ES-285 has remarkable *in vivo* activity against certain slow-growing solid tumors in a manner that may be a direct consequence of its action on Rho protein factor. Other preclinical studies are underway to look at the possible anti-metastatic and/or anti-vascular effects of ES-285.

**#315 Preclinical pharmacology studies with the marine natural product Kahalalide F.** Supko, Jeffrey G., Lu, Hong, *Massachusetts General Hospital, Harvard Medical School, Boston, MA*. Jimeno, José M., *PharmaMar S.A., Madrid, Spain*. Grant, Wendy, Faircloth, Glynn T., *PharmaMar USA, Inc., Cambridge, MA*.

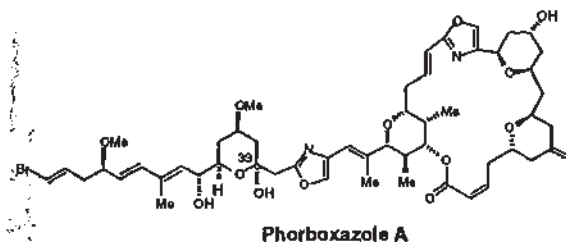
Kahalalide F (KF) is a peptide toxin isolated from the Hawaiian mollusk *Elysia rubefescens*. The compound is under advanced preclinical development for its selectivity to prostate tumors and is known to target lysosomes as its possible primary mechanism of action, among other effects. The maximum tolerated dose (MTD) of KF in female mice following a single bolus *iv* injection was determined to be 280  $\mu$ g/kg. Whereas single doses just above the MTD<sub>iv</sub> were extremely toxic, with animals exhibiting signs of neurotoxicity followed by death, 280  $\mu$ g/kg KF could be administered repeatedly, according to a once daily times five schedule, without any apparent evidence of acute toxicity. A sensitive and specific assay based upon reversed-phase high performance liquid chromatography with electrospray ionization mass spectrometric detection was developed for measuring KF in mouse plasma.

Preliminary pharmacokinetic (PK) studies were performed following administration of 280  $\mu$ g/kg KF to mice by bolus *iv* and *ip* injection. In mice treated by the *iv* route, plasma levels of KF declined from a peak concentration near 1.0  $\mu$ M with a 35 min. biological half-life. Estimates of the total body clearance and apparent volume of distribution were 3.8 ml/min/kg and 199 ml/kg, respectively. There was no accumulation upon repeated *iv* injection at an interval of 24 hrs. In contrast, *ip* administration of the same dose, which afforded excellent *in vivo* antitumor activity, provided a much lower peak concentration of 0.3  $\mu$ M occurring approximately 1 hr after dosing.

This preliminary data indicates that KF is rapidly eliminated from plasma with limited binding to extravascular tissues. Additional studies will be performed to further delineate the influence of systemic drug exposure upon toxicity and efficacy.

**#316 Synthetic phorbaxazole A as a potent anticancer agent.** Uckun, F.M., Nara, R.K., Navara, C., Forsyth, C. *Drug Discovery Program and Parker Hughes Cancer Center, Hughes Institute, St. Paul, MN; Department of Chemistry, University of Minnesota*.

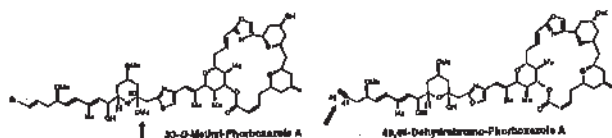
Phorbaxazole A is marine sponge-derived natural product with potent anti-cancer activity (Searle, P. A et al., *Journal of the American Chemical Society* 117, 8126-8131, 1995).



We have recently completed the total synthesis of phorbaxazole A using a convergent, tri-component coupling strategy that has taken advantage of several existing and reliable methods, as well as several new tactics and methodologies (Forsyth, C.J. et al., *Journal of the American Chemical Society* 120, 5597-5598, 1998). In standard MTT assays, synthetic phorbaxazole A exhibited potent cytotoxicity against a panel of 9 multidrug resistant human cancer cell lines, including NALM-6 acute lymphoblastic leukemia cells (IC<sub>50</sub>[MTT] = 1.7 nM), BT-20 breast cancer cells (IC<sub>50</sub>[MTT] = 3.4 nM), PC3 prostate cancer cells (IC<sub>50</sub>[MTT] = 14.2 nM), DU-145 prostate cancer cells (IC<sub>50</sub>[MTT] = 15.0 nM), U373 glioblastoma cells (IC<sub>50</sub>[MTT] = 6.7 nM), ARH77 multiple myeloma cells (IC<sub>50</sub>[MTT] = 7.5 nM), HS-SULTAN multiple myeloma cells (IC<sub>50</sub>[MTT] = 14.9 nM), and RPMI-18226 multiple myeloma cells (IC<sub>50</sub>[MTT] = 55.9 nM). The anti-cancer activity of synthetic phorbaxazole A was confirmed by confocal laser scanning microscopy. BT-20 breast cancer cells, DU-145 prostate cancer cells as well as U373 brain tumor cells showed a marked shrinkage 4 days after treatment with 50 nM phorbaxazole A concomitant with nuclear fragmentation and complete destruction of the well organized microtubule cytoskeleton, which is consistent with apoptotic cell death. Apoptosis was also confirmed by TUNEL assays. At concentrations  $\geq$ 10 nM, synthetic phorbaxazole A completely abrogated breast cancer, prostate cancer, and glioblastoma cell invasion through the Matrigel matrix in Boyden chambers and inhibited clonogenic growth by 99.9%. This study provided the first evidence that synthetic phorbaxazole A is a potent anticancer agent.



**#317** Biologically active synthetic analogs of phorbosazole A as potent anticancer agents. Uckun, F.M. and Forsyth, C. Drug Discovery Program and Parker Hughes Cancer Center, Hughes Institute, St. Paul, MN; Department of Chemistry, University of Minnesota.



In a preliminary effort aimed at determining the minimal molecular architecture of the phorbosazole A structure necessary for its biological activity, we studied in a side by side comparison the antiproliferative activity of synthetic phorbosazole A and 8 distinct synthetic analogs against the human B-lineage acute lymphoblastic leukemia NALM-6, breast cancer BT-20 and brain tumor U373 cell lines using MTT assays. All three cell lines were inhibited by synthetic phorbosazole A as well as its analogs 45,46-dehydrobromo-phorbosazole A, which bears an alkyne in place of the C45-C46 terminal bromide, and 33-O-methyl-phorbosazole A, which has a mixed methyl ketal instead of the C33 hemiketal, (but not by any of the other 6 synthetic analogs) in a concentration-dependent fashion with low nanomolar  $IC_{50}$  values. The rank order of sensitivity was NALM-6 > BT-20 > U373. Phorbosazole A was 2.8-fold more potent against NALM-6 cells ( $IC_{50}$  values: 1.7 nM vs. 4.8 nM), 3.7-fold more potent against BT-20 cells, and 4.1-fold more potent against U373 cells than its dehydrobromo analog. Phorbosazole A was 3.1-fold more potent against NALM-6 cells, 3.3-fold more potent against BT-20 cells ( $IC_{50}$  values: 3.4 nM vs. 11.3 nM), and 4.4-fold more potent against U373 cells than its analog 33-O-methyl-phorbosazole. The  $IC_{50}$  values for the remaining 6 synthetic analogs were >2,000 nM. The 3 active compounds also inhibited the clonogenic growth of all 3 cancer cell lines. Apparently, the macrolide, central oxazole, polyene side chain, and acrylate moiety of phorbosazole A are necessary for potent activity. Molecular modeling indicates that the conformation of 2,3-dihydrophorbosazole A is similar to that of the parent compound. The potent activities of the 45,46-dehydrobromo- and 33-O-methyl-analogs allows simplification of the preparative chemistry required to access novel cytotoxic agents. The high yield of C29-C31 oxazole formation and opportunities for terminal carbon-carbon bond formation via Sonogoshira type-couplings make the dehydrobromo-analog particularly attractive for development as an anti-cancer drug.

**#318** Bryostatin 1 Induced XIAP mRNA expression in apoptosis resistant THP-1 cells. Chen, Catherine, Chen, Ben D.-M. Program in Cell Biology, Division of Hematology/Oncology, Department of Internal Medicine, Barbara Ann Karmanos Cancer Institute, Wayne State University, Detroit, MI.

THP-1, human promonocytic leukemia cells, can be induced to undergo apoptosis by Z-LLL-CHO, a cell permeable reversible 20S proteasome inhibitor. The pathway of apoptosis induced by Z-LLL-CHO proceeded through cytochrome c release from mitochondria and caspase 9 activation. Upon induction by bryostatin 1 (bryol), a natural PKC activator from bryozoan *Bugula neritina*, THP-1 become differentiated and also resistant to Z-LLL-CHO induced apoptosis. The mechanism of this resistance was investigated. It was found that the activation of XIAP, human X-chromosome-linked inhibitor of apoptosis protein, might be responsible for the prevention of apoptosis in differentiated THP-1. IAP family inhibits cell death cysteine protease family by blocking distinct caspases, which are responsible for the activation of apoptosis. RNase protection assay showed that upon bryol addition, differentiated THP-1 cells increased its XIAP mRNA while IAP-1, IAP-2, survivin, and TRPM-2 had no changes in mRNA expression. In apoptotic cells, XIAP, IAP-1, IAP-2, survivin, and NAIP mRNA expression were decreased, while TRPM-2 was increased slightly. At 12 hrs, decrease in mRNA expression was more than at 6 hrs. THP-1 treated with bryol first then with Z-LLL-CHO showed higher increase in XIAP and TRPM-2 than bryol alone. Western blots with XIAP antibody also show increase of XIAP protein in a time and dose dependent manner when treated with bryol. We conclude that XIAP is the major inhibitor of caspases responsible for the resistance to apoptosis in differentiated THP-1 cells.

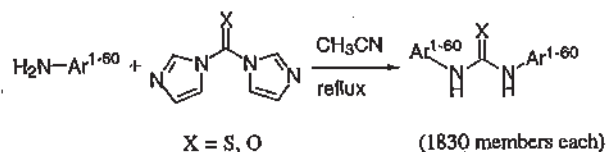
**#319** A phase I and pharmacokinetic (PK) study of the novel mushroom-derived cytotoxin, MGI 114, in combination with irinotecan in patients with advanced cancer. Eokhardt SG, Kuhn JG, Britten CD, Weltman S, Baker SD, MacDonald JR, Newman A, Smith S, Von Hoff DD, Rowinsky EK. Cancer Therapy and Research Center, San Antonio, TX and MGI PHARMA, Minnetonka, MN.

HMAF (6-hydroxymethylacylfulvene; MGI 114) is a semisynthetic analog of illudin S, a sesquiterpene isolated from the *Omphalotus* mushroom. Previous combination studies of MGI 114 and irinotecan revealed enhanced activity compared to either agent alone in the HT29 human colon carcinoma xenograft model. The combination of these agents (MGI 114: i.p. daily x 5; irinotecan: i.p. days 1, 12, 19) at 50% of the MTD resulted in

2/9 complete and 6/9 partial responses [Canc Res 59: 1049-1053, 1999]. This phase I study was performed to evaluate the feasibility of administering MGI 114 as a 5 min infusion daily for 5 days every 4 weeks in combination with irinotecan on days 1 and 15, in adults with advanced cancer, and to study the PK behavior of the combination. The following dose levels were selected (MGI 114/irinotecan): 5/100, 5/125, 8/125, 8/175, 11/175, 11/200, and 11/250 mg/m<sup>2</sup>. Thus far, 7 pts (median age, 59 [range, 43-67]; median PS 0; prior therapy: chemo, 3; RT + chemo, 4) have received 12 courses. Of the 6 pts enrolled to the first dose level, grade 3 or 4 neutropenia has been observed in 4 pts, whereas 4 of 11 day 15 doses of irinotecan were omitted due to persistent neutropenia. Nonhematologic toxicities have been mild and include grade 1/2 nausea/vomiting (3 pts), grade 1/2 diarrhea (4 pts), and grade 1/2 fatigue (4 pts). Additional pts are being accrued with stratification for prior therapy to determine if further dose escalation is feasible. Preliminary noncompartmental PK analysis of irinotecan on day 1 indicates PK parameters within published ranges for the first dose level (median ± SD): elimination  $t_{1/2}$  10.8 ± 5.43 hrs.,  $Cl$  15.4 ± 3.14 L/hr/m<sup>2</sup>,  $AUC_{0-24}$  6507 ± 1884 ng·hr/mL, and  $Vd_{ss}$  135.9 ± 44.89 L/m<sup>2</sup>. The median SN-38/irinotecan ratio in 4 evaluable patients on day 1 is 0.033 ± 0.11 and on day 15 (or 22) is 0.028 ± 0.006. These data suggest that the combination of MGI 114 and irinotecan results in augmented myelosuppression, whereas further analysis of irinotecan and MGI 114 pharmacokinetics will elucidate whether there are pharmacological interactions between the two agents.

**#320** N,N'-Bis-substituted thiourea and urea liquid-phase combinatorial libraries: synthesis and apoptosis induction. Zhu, Zhaohai; Naria, Rama Krishna; Mao, Chen; Uckun, Fahim M. Parker Hughes Cancer Center, Departments of Chemistry, Experimental Oncology, and Structural Biology, Hughes Institute, St. Paul, MN.

An efficient synthetic procedure was developed to generate thiourea and urea combinatorial libraries in liquid phase for apoptosis screening. The reaction was accomplished under reflux for 1 h in acetonitrile. The concentrated reaction mixture was re-dissolved in chloroform and purified by aqueous acid wash/extraction. The libraries were characterized by <sup>1</sup>H NMR and MS. Several apoptosis-inducing lead compounds with potent cytotoxic activity against leukemic cells and breast cancer cells were identified.



**#321** Benzopyrone combinatorial libraries for identification of selective agents for molecular targets in breast cancer. Brueggemeier, R.W.; Whelstone, J.L.; Bhat, A.S.; Joonprabutra, S. College of Pharmacy, OSU Comprehensive Cancer Center, The Ohio State University, Columbus, OH 43210.

Molecules with a benzopyrone ring system include a number of natural products such as flavonoids found widely in higher plants. The class of flavonoids encompasses the flavones, isoflavones, flavanones, and flavonols. Compounds in this class have shown activity as protein tyrosine kinase inhibitors, estrogen receptor agonists/antagonists, or inhibitors of steroidogenic enzymes. The low molecular weight, fairly rigid benzopyrone nucleus contains multiple sites of potential chemical diversity, and this chemical structure should serve as an ideal template for producing combinatorial libraries. Our hypothesis is that the design, synthesis, and screening of substituted benzopyrone combinatorial libraries would allow us to harvest the biological potential of these molecules and develop more selective agents for molecular targets in breast cancer. Our initial medicinal chemistry efforts developed synthetic methods for constructing benzopyrones that are accomplished under mild reaction conditions, allow for flexibility in substitutions, and provide for moderate to high yields. Our novel synthetic route utilizes readily available salicylic acids and terminal alkynes as starting materials to construct the benzopyrone nucleus. Substituted salicylic acids are coupled with various terminal alkynes via a one-pot acid chlorination-Sonogoshira coupling to give the desired alkyne in excellent yields. Conversion of the alkyne to enamino-ketones and subsequent cyclization to the benzopyrone ring can be effected in a single step. Synthetic approaches for diversifying the benzopyrone skeleton have been developed, and solution phase combinatorial chemistry is utilized to construct small flavonoid libraries. Bioassay determinations on synthetic benzopyrones include evaluation of effects on breast cancer cell proliferation, estrogen receptor agonist/antagonist properties, and inhibition of aromatase. This work was supported in part by NIH grants NCI R21 CA66193, USAMRMC DAMD17-96-1-6136, and USAMRMC DAMD17-99-1-9342.

**#322** Extending the scope of *Vinca* alkaloids with superacid chemistry. Duflos A., Jacquesy J.-C., Kruczynski A., Etievant C., Barret J.-M., Hill B.T., Fahy J. *Centre de Recherche Pierre Fabre, Castres, France. Université de Poitiers, Poitiers, France (J.C.J.)*

The unusual use of superacid chemistry applied to complex structures such as *Vinca* alkaloids has permitted the synthesis of a series of compounds modified at a non-activated site of the molecule according to classical chemistry. Halogenated solvents, peroxides, or cycloalkanes in superacidic media led to the formation of superelectrophilic species able to introduce selectively substituents such as fluorine, chlorine, oxygen or hydrogen at the piperidine ring of the «catharanthine» moiety.

	n	R <sub>1</sub>	R <sub>2</sub>	R <sub>3</sub>	T/C max.* (Dose)
	2	H	H	O	[VLB] 143% (10 mg/kg)
	1	F	F	H	200% (40 mg/kg)
	2	F	F	H	157% (80 mg/kg)
	1	OH	H	H	inactive
	1	OH	F	F	inactive
	1	Cl	H	H	214% (80 mg/kg)

\*: data obtained from *in vivo* P388 (i.v./i.p.) experiments.

Among these derivatives, vinflunine (n = 1, R<sub>1</sub> = R<sub>2</sub> = F, R<sub>3</sub> = H) exerted unprecedented antitumor properties against murine and human *in vivo* tumor models compared to vinblastine (VLB) and vinorelbine (Navelbine®) used as reference compounds. Vinflunine is currently being evaluated in Phase I clinical trials in Europe.

**#323** Cloning, recombinant expression and biochemical characterization of mistletoe lectin. Langer, M., Eck, J., Möckel, B., Zinke, H., and Lentzen, H. *B · R · A · I · N GmbH, Zwingenberg, Germany; MADAU AG, Köln, Germany.*

The heterodimeric plant protein mistletoe lectin (ML), consisting of an enzymatically active A- and a lectin like B-chain, represents the active component of mistletoe extracts widely used in cancer therapy. In order to reveal the genomic organization of ML and for recombinant production of homogeneous ML the full length sequence of the Intron-less ML gene of 1923 nt was cloned. Expression vectors containing the coding region of the A- or the B-chain were constructed and the single chains were expressed separately. Expression in *E. coli* resulted the proteins to be made as inclusion bodies (IBs). In a co-association process, A- and B-chain IBs were natively assembled in a single step yielding 10% of active recombinant ML (rML).

The biological activities of the rML and the plant derived mistletoe lectin (pML) were compared. The IC<sub>50</sub> values of the two proteins were 30 µg/ml (rML) and 20 µg/ml (pML) in a cytotoxicity assay with MOLT-4 cells. The rRNA N-glycosidase activity of the A-chain was measured in a coupled transcription/translation assay. 50% translation inactivation was achieved with ML concentrations of 52 pM (rML) and 64 pM (pML). Carbohydrate binding specificity of the B-chain was analysed in a competitive binding assay. 50% competition of lectin binding was achieved at lactose concentrations of 1.6 mM (rML) and 1.8 mM (pML). Hence, using three different assays no significant differences comparing the activities of the *E. coli* derived rML and the glycosylated pML were found, which led to the conclusion that glycosylation is not a prerequisite for cytotoxicity. Furthermore, we speculate that both lectin activity and the rRNA N-glycosidase activity are prerequisites for the cytotoxic action against target cells. This work was supported by grant 0311183 of BMBF, Germany.

**#324** *Phallus impudicus* in experimental inhalant antimetastatic treatment of Lewis lung carcinoma. Kuznecova Galina V., Kuznecovs S.J. *Health Research Laboratory, Riga, Latvia.*

The present study is aimed to examine the possibilities of inhalant antimetastatic treatment of Lewis lung carcinoma using *Phallus impudicus* concentrated extract (Ph.i.ex) 30% w/w in small particle spray and to investigate the mechanism of action and the possible targets of this remedy. The experiments were carried out on C57BL/6 strain male mice (n = 80) with Lewis lung Carcinoma after surgical ablation on 14<sup>th</sup> day after carcinoma inoculation. The volume and number of metastases in the lungs were determined by Lucke method (1952). Ph.i.ex was injected subcutaneously in a dose of 5.0 mg/kg on the 7<sup>th</sup> day after inoculation of tumor cells and inhaled for 28 days in concentration 50 ppm with pH 6.5 starting from day 5 after injection. Alveolar macrophages were extracted by Fidler method (1980). Adenosine deaminase (AD) and 5' nucleotidase (5'N) activity was estimated in lysate by ascending paper chromatography. 28 days inhalation after immunization with Ph.i.ex was beneficial for reducing the number of metastases by 8.3 times, depressing the metastases volume by 13.2–14.9 times. The studies of the enzyme activity of adenosine metabolism in alveolar macrophages reveal that by inhalation of Ph.i.ex the activity of AD increased up to 255–286%, while that of 5'N decreased up to 79–105% against the values in nontreated animals. The obtained results suggest that the action of Ph.i.ex gives rise to restoration of the alveolar

macrophage antitumor activity after surgical distress. The features noted make it possible to offer *Phallus impudicus* extract inhalation for pre and postoperative antimetastatic therapy in lung cancer.

## SECTION 5: PHASE I CLINICAL TRIALS: DERIVATIVES, NEW FORMULATIONS, AND COMBINATIONS

**#325** Phase I study of NX211 given as an intravenous infusion on days 1, 2 & 3 every 3 weeks in patients (pts) with solid tumors—an NCIC Clinical Trials Group study. Gelmon KA, Eisenhauer E, Reyno L, Fisher B, Ayers D, Lee U, Hirtle H, D'Aloisio S, Hurak S, Hamilton M, Ptaszynski M, Onetto N. *BC Cancer Agency Vancouver Clinic, Hamilton Regional Cancer Centre, NCI Canada Clinical Trials Group, NaXstar Pharmaceuticals.*

NX211 is a liposomal formulation of lurtotecan, a water soluble analogue of camptothecin. It is an effective inhibitor of topoisomerase I *in vitro* and *in vivo*. In preclinical studies the liposomal formulation had greater potency and a higher therapeutic index compared to other topo I inhibitors. Pre-clinical toxicology showed dogs to be the most sensitive species and suggested marrow and/or GI toxicity will be dose limiting. Extrapolating from studies with other topo I inhibitors, the maximum tolerated dose (MTD) in man is estimated to be about 3–4 mg/m<sup>2</sup> total dose. A phase I trial was initiated by the NCIC CTG to determine the MTD and the recommended dose (RD) of NX211 when given as a 30-minute infusion d 1, 2 & 3 q 3 weeks in pts with solid tumors. Secondary objectives are to describe the pharmacokinetic profile of NX-211 and to investigate preliminary evidence of anti-tumour activity. Three pts are to be treated at dose levels that first double, then revert to modified Fibonacci escalation following observation of gr 2 toxicity. At least 3 pts each have been treated at 0.15, 0.30 and 0.6 mg/m<sup>2</sup>/day with full data available on the 6 pts at the first 2 levels. Pt characteristics are as follows: female 4, male 2, ECOG performance status 0-1, 1-4, and 2-1. No neutropenia or thrombocytopenia have been seen and non-hematologic effects have generally been grade 1. One instance of grade 2 skin rash and grade 2 fatigue at the 0.15 and 0.30 dose levels, respectively, have been seen but these were not thought to be definitely drug related. Pharmacokinetics are performed using non-compartmental analysis.

Dose (mg/m <sup>2</sup> /day) (hr)	C <sub>max</sub> (ng/mL) (L/hr/m <sup>2</sup> )	AUC (ng/hr/m <sup>2</sup> )		
0.15	61.3	223	2.31	1.19
0.30	141	1292	6.56	0.623

Data in the same patients on days 1 and 3 show little intra-patient variation and no evidence of accumulation but considerable inter-patient variation has been seen. Both the AUC and C<sub>max</sub> are increasing with dose and are significantly greater than those found with free drug. Dose escalation continues and updated clinical and pharmacokinetic data will be presented.

**#326** Phase I study and pharmacology of DX-8951f, a new camptothecin derivative, administered over 30 minutes every 3 weeks. Minami H, Sasaki Y, Shigeoka Y, Onozawa Y, Fujii H, Igarashi T, Itoh K, Tamarai K, Kajimura T, Oguma T. *National Cancer Center Hospital East, Kashiwa, Japan; Daiichi Pharmaceutical Co, Ltd, Tokyo, Japan.*

DX-8951f (DX), a new water-soluble camptothecin derivative, has greater antitumor activity and less toxicity than other camptothecins in preclinical models. A phase I study of DX infused over 30 minutes every 3 weeks was completed, and pharmacokinetics and pharmacodynamics in humans were compared to those in dogs, the most sensitive animal to DX. Dose was escalated from 3 mg/m<sup>2</sup>, 1/3 dog toxic dose low, to 5 and 6.65 mg/m<sup>2</sup>. Fifteen patients (age 40–73, median 58 years; female/male, 8/7; PS 0 in one patient, 1 in others) were treated; 3 at 3 mg/m<sup>2</sup>, 6 at 5 mg/m<sup>2</sup> and 6 at 6.65 mg/m<sup>2</sup>. Grade 4 neutropenia lasting 5 days or more, which was dose limiting, was observed in one patient, respectively, at 5 and 6.65 mg/m<sup>2</sup>. No grade 4 thrombocytopenia was observed. Dose limiting but transient grade 3 hyperbilirubinemia and transaminase elevation were observed in two patients at 6.65 mg/m<sup>2</sup>. No grade 2 or worse diarrhea was observed. Dose limiting factors were neutropenia and abnormal liver function tests and the recommended dose for phase II study was 5 mg/m<sup>2</sup>. Area under the time-concentration curves (AUC) of lactone and total (lactone + carboxylate) DX were measured. AUC of both lactone and total DX were linearly increased according to dosage, and the relationship between AUC and the decrease of neutrophils was explained by a sigmoid Emax model. For the comparison of pharmacokinetics and pharmacodynamics between human and dogs, protein-unbound AUC of lactone and total



(lactone + carboxylate) DX were estimated by multiplying measured AUC (bound + unbound) by the unbound fraction of the total DX in plasma (2.5% for humans and 14% for dogs). When protein-bound and unbound DX were combined, clearance of lactone and total drug in humans was 8.5- and 15.4-fold smaller, respectively, than in dogs. However, the interspecies difference of clearance was decreased to 1.5-fold for lactone and 2.7-fold for total drug when only unbound AUC was considered. Similarly, interspecies difference of the relationship between total AUC and the decrease of neutrophils was substantially reduced when protein-unbound AUC was used. Interspecies variability of protein binding partially explains the interspecies difference of pharmacokinetics and pharmacodynamics of DX.

**#327 Phase I and Pharmacokinetic (PK) Study of DX-8951f, a Novel Camptothecin Analog, Given as 30 Minute Infusion Daily for 5 Days.** Kamiya Y, Yamamoto N, Yamada Y, Kusaba H, Shimada Y, Tamura T, Tamanoi K, Oguma T. *National Cancer Center Hospital, Tokyo, Japan; Daiichi Pharm. Co., Ltd., Tokyo, Japan.*

DX-8951f (DX), a synthetic water-soluble camptothecin analog, is a new topoisomerase I inhibitor. DX showed a broader spectrum of activity than other camptothecins and lack of esterase-dependent activation. The major toxicity was myelosuppression in animals. We conducted a phase I study of 30 minute infusion daily for 5 days every 3 weeks in patients (pts) with solid tumors, because more frequent dosing schedules reported superior antitumor effects in preclinical models. The starting dose was 0.1 mg/m<sup>2</sup>/day (1/3 dog toxic dose low) and dose escalation was based on a dose-doubling method until grade (gr) 1 toxicity (nausea/vomiting; gr 2) followed by the modified Fibonacci method. Thus far, 24 pts with a median age of 56 years (range: 32-66), PS 0 (5 pts) or 1 (19 pts) have been enrolled at dose levels of 0.10 (6 pts), 0.17 (3 pts), 0.25 (4 pts), 0.35 (3 pts), 0.45 (6 pts) and 0.40 (2 pts). Dose limiting toxicity (transient gr 3-elevation of GOT) was observed in a pt of esophageal cancer with liver metastasis at the initial dose level. Myelosuppression was observed dose dependently. At the 0.45 level, dose limiting toxicities were observed in two pts, which were gr 4 neutropenia lasting 5 days or more and gr 4 thrombocytopenia. Since this dose level was beyond maximum tolerated dose (MTD), the dose was reduced to 0.40 mg/m<sup>2</sup>/day. At this level, dose-limiting neutropenia occurred in one pt to date. Other toxicities were mild to moderate (gr 1/2) including nausea, vomiting, diarrhea and malaise. Antitumor activity was observed in one with non-small-cell lung cancer which had been refractory to cisplatin, vindesine and docetaxel. No drug accumulation was suggested from AUC and Cmax of total and lactone form of DX during day 1 to 5. PK parameters (day 1, mean±SD) for total and lactone form were CL(1/hr/m<sup>2</sup>): 2.47±0.81, 6.45±1.88; elimination t1/2(hours): 6.19±1.49, 4.18±2.13; Vss(l/m<sup>2</sup>): 15.81±3.43, 19.65±5.65, respectively. Lactone/total ratio of AUC was 0.39±0.08 (day 1) and 0.31±0.10 (day 5). Percentage of urinary excretion of DX and its metabolite was 7.94±3.12 and 14.39±4.52. This study is ongoing and the MTD and recommended dose will be 0.40 mg/m<sup>2</sup>/day or lower.

**#328 Phase I pharmacokinetic study of MEN-10755 in solid tumors.** Vermorken JB<sup>1</sup>, Bos AME<sup>2</sup>, Schrijvers D<sup>1</sup>, Dyck J<sup>1</sup>, Roelink M<sup>3</sup>, Wanders J<sup>3</sup>, Hanauke AR<sup>4</sup>, Bortini S<sup>5</sup>, Capriall A<sup>6</sup>, Uges DRA<sup>6</sup>, De Vries EGE<sup>2</sup>, Departments of Medical Oncology of the Univ. Hosp. Antwerp, Belgium<sup>1</sup> and the Univ. Hosp. Groningen, The Netherlands<sup>2</sup>, New Drug Development Office, Amsterdam, The Netherlands<sup>3</sup>, EORTC Early Clinical Studies Group<sup>4</sup>, Menarini Ricerche SpA<sup>5</sup>, Department of Pharmacology, Univ. Hosp. Groningen, The Netherlands<sup>6</sup>.

**Aims:** To assess a) the maximum tolerated dose (MTD) of MEN-10755, when given weekly x3 q 4 weeks, b) its safety, c) its pharmacokinetics, and d) to document any antitumor activity. MEN-10755 is the most promising third generation anthracycline (ANT), with improved efficacy over doxorubicin, e.g. in breast, ovarian & lung cancer.

**Patients & methods:** Eligible patients (pts) had incurable cancer, ECOG performance status ≤2, no prior ANT or anthracenediones and a LVEF (MUGA) ≥50%. MEN was administered iv over 15 min. Starting dose was 15 mg/m<sup>2</sup> per infusion. Doses were escalated to 30 mg/m<sup>2</sup> and up to 45 mg/m<sup>2</sup> per infusion. Plasma and urinary MEN levels were measured by HPLC with fluorescent detection.

**Results:** The first 14 pts (16 entered) had variable solid tumors, a median age of 63.5 years (range: 45-74) and a median performance status of 1 (0-2). Prior treatment included radiotherapy 1, chemotherapy 2, both 5, none 2 and unknown 4. Dose limiting toxicity was observed at 45 mg/m<sup>2</sup>: in 2/2 the 3<sup>rd</sup> infusion on day 15 could not be given because of an absolute neutrophil count (ANC) ≤1000/mm<sup>3</sup> (both had also leukopenia grade 3). For that reason next pts were treated with 40 mg/m<sup>2</sup>/infusion: so far 1/4 developed grade 4 neutropenia (+ fever: pneumonia). Anemia grade 1-2 occurred in 6 pts; 1 grade 4 at 30 mg/m<sup>2</sup>. Thrombocytopenia grade 1 was found in 1 patient at 30 mg/m<sup>2</sup>. Grade 3 (or severe) nonhematologic toxicities included anorexia (1 patient at 15 mg/m<sup>2</sup>), nausea + asthenia + depression (1 at 45 mg/m<sup>2</sup>), fatigue (1 at 40 mg/m<sup>2</sup>). Two pts had flushing and sweating grade 2 during infusion, 1 developed a "hypersensitivity-like" reaction after the 1<sup>st</sup> infusion at 40 mg/m<sup>2</sup>, which precluded further therapy. So far, 1 patient had a drop in LVEF from 54% to 45% (measured shortly after 2<sup>nd</sup> infusion of 3<sup>rd</sup> cycle at 45 mg/m<sup>2</sup>). Preliminary PK data:

AUC correlated with dose; mean AUC<sub>0-∞</sub> for 30 mg/m<sup>2</sup> = 6.0 mg/L.h.; t<sub>1/2β</sub> (all doses) = 15.2 ± 3.6 h; Cl = 5.6 ± 0.9 L/h/m<sup>2</sup>; Vss = 81.2 ± 23.5 L/m<sup>2</sup>; renal clearance = 4.4 ± 2.1%.

**Conclusion:** Neutropenia on day 15 is dose limiting at 45 mg/m<sup>2</sup>/week x3 q 4 wks. Evaluation at the 40 mg/m<sup>2</sup> dose level continues.

**#329 BBR2778 a new anthracenedione analogue with no preclinical cardiac toxicity: Results from 3 phases I studies.** Faivre S, Borchmann P, Jodrell D, Camboni G, Bamareggi A, Raymond E, Imadidou K, Engert A, Diehl V. *Institut Gustave Roussy, Villejuif, France; University of Köln, Germany, Western General Hospital, Edinburgh, UK; Novuspharma, Monza, Italy; C&AC, Kremlin-Bicêtre, France.*

BBR2778, namely 6,9-bis-([(2-amino)ethyl] amino) benzo[g] isoquinoline-5,10-dione dimaleate, is a novel aza-anthracenedione with activity in experimental tumours and devoid of delayed cardiotoxicity in animal models.

Three phases I studies including a total of 80 patients with refractory solid tumors (ST) or hematological lymphoid malignancies (HLM) were performed, using a weekly schedule for 3 consecutive weeks (AZAI-02, AZAI-03) or a once q3wk schedule (AZAI-01). Neutropenia was the limiting toxicity in all 3 studies. The MTDs were determined at 240 mg/m<sup>2</sup> for the q3wk schedule, 150 mg/m<sup>2</sup> and 84 mg/m<sup>2</sup> x 3 for the weekly schedule for ST and HLM, respectively. No grade 3-4 gastrointestinal toxicities were observed. Alopecia, transient blue skin and urine coloration were common. A decrease of LVEF > 20% was noted in only 2/80 patients: one patient (AZAI-01) experienced a decrease of 31% after 3 cycles at dose 120 mg/m<sup>2</sup> q3w, the other experienced a decrease of 32% (AZAI-02) after 2 cycles at dose 75 mg/m<sup>2</sup>/wk q4wk. These events were not significant because none of the two patients were symptomatic and LVEF value never decreased below 45%.

BBR2778 pharmacokinetic parameters results in animals (mice, rats, and dogs) and in patients have proved to be linear in a wide dose range. The drug showed a large volume of distribution, a high plasma clearance and a long elimination half-life. Renal excretion did not represent the major elimination route. Metabolism and excretion in the bile probably contribute significantly. A significant antitumor activity was observed in solid tumors and lymphomas. Three partial responses were seen in one SCLC, one metastatic cylindroma of the nasopharynx and one breast cancer. Minimal change (about 50%, resolution of pericardial and fluid effusion) in another SCLC. Responses occurred in 6/16 heavily pretreated Lymphoma patients.

**Conclusion:** The safety profile of BBR2778 is well evaluated among 3 phases I studies using 2 different schedules. Neutropenia was the main treatment limiting toxicity. No cardiac toxicity was seen. An interesting antitumor activity was observed, and has to be confirmed by further phase II studies. A clinical trial is planned in NHL.

**#330 Initial phase I trial of a new liposome-encapsulated doxorubicin formulation in patients with refractory solid tumors.** Izquierdo MA, Balañá C, Fabregat X, García M, Martíns M, Llorens MA, Gimeno M, Masía R, Rosell R, Germá JR. *Instituto Catalán Oncología, Hosp Germans Trias Pujol, Hosp Mar, Barcelona; Tedec-Melji Farma Madrid, Spain.*

A new formulation of liposome-encapsulated doxorubicin (LD-TM), under clinical development by Tedec-Melji, incorporates an antioxidant agent in the phospholipid bilayer that provides chemical advantages. A phase I study of LD-TM given as a 1 hr iv. infusion every 21 days is being conducted in patients (pts) with advanced and refractory solid tumors. Based on pre-clinical data with LD-TM and clinical studies with other liposomal doxorubicin, the starting dose was 30 mg/m<sup>2</sup>. Dose was escalated in increments of 10 mg/m<sup>2</sup>. Thus far, 20 pts have received 51 cycles of LD-TM. All pts but five had received prior chemotherapy (no anthracyclines). The dose of LD-TM has been escalated up to 80 mg/m<sup>2</sup> but the MTD has not been reached yet. Nonhematological toxicity (tox) was moderate. The most frequent tox was fever and chills that occurred 8-12 hrs after the first drug administration in 12 pts (60%) and resolved within 2-3 hrs without treatment or after treatment with acetaminophen and antihistaminics. In subsequent cycles, these pts received pre-medication without recurrence. Other gr 1-2 nonhematological tox included: asthenia in 12 pts, mucositis in 8 pts, palmar-plantar erythrodysesthesia in 2 pts (gr 1, dose unrelated). Nausea and vomiting were very mild. Complete alopecia was observed in 2 pts, at 70 mg/m<sup>2</sup>. Hematological tox in the 51 evaluable cycles was: anemia gr 3 in 2 (4%), thrombocytopenia gr 3 in 3 (6%); at 70 mg/m<sup>2</sup> and neutropenia gr 3 and 4 in 12 (24%) and 11 (22%) cycles, respectively. 1/6 pts at 70 and 1/3 pts at 80 mg/m<sup>2</sup> had DLT (neutropenia gr 4 > 7 days, neutropenia gr 4 and fever). Accrual continues at 80 mg/m<sup>2</sup>. 4 pts showed minor response (1 melanoma, 1 chondrosarcoma) or stable disease (1 head and neck, 1 colon). It seems that the DLT of LD-TM will be neutropenia. The tox varies from other liposomal doxorubicin (i.e. Caelyx<sup>®</sup>) and shows also differences with free doxorubicin. At the recommended dose for further clinical studies, a comparative pharmacokinetic analysis between free doxorubicin and LD-TM is planned in a group of 9 pts using each pt as his/her own control.

**#331 A phase I study of BMS-188797, a new taxane analogue.** Sullivan, D., Fago, R., Garland, L., Dellaportas, A.M., Mahany, J.J., Lush, R.M., Skillings, J., Bulanhagui, C., and Dalton, W.S. *H. Lee Moffitt Cancer Center & Research Institute and Bristol-Myers Squibb, Inc.*

A phase I study of BMS-188797 was initiated to determine the maximum tolerated dose and pharmacokinetics. The drug is one of several new analogues of TAXOL® currently being evaluated in phase I studies. BMS-188797 was chosen for clinical testing because of its increased activity in preclinical models compared to paclitaxel. The drug is administered as a one-hour infusion every 21 days. Dosing started at 3.75 mg/m<sup>2</sup> and has been escalated in cohorts of patients. A total of 28 patients have been enrolled onto seven dosage tiers. Enrollment of patients at the 110 mg/m<sup>2</sup> dosage is currently underway. Non-hematologic toxicity at all lower dosage tiers have been minor, with only grade 2 or lower toxicities (neutropenia, fever, diarrhea, nausea, myalgia, arthralgia and edema) observed that were considered possibly related to drug administration. Several pretreated patients have experienced grade 3 or 4 hematologic toxicity, however none were of sufficient duration to be considered a dose-limiting toxicity. Pharmacokinetic parameter estimates are similar to that of TAXOL® and are as follows: Clearance = 156 ml/min/m<sup>2</sup>, Volume of distribution = 198 L/m<sup>2</sup> and Half-life = 27 hr. Interpatient variability in the pharmacokinetic parameter estimates is approximately 30% for the patients studied. No routine premedication has been administered to date, and no hypersensitivity reactions have been reported, despite the cremaphor in this formulation. Patient cohorts at increased dose levels will be evaluated until the maximum administered dose is reached, at which time a phase II dose will be determined.

**#332 A PHASE I AND PHARMACOKINETIC (PK) STUDY OF THE TAXANE ANALOG, BMS 184476, ADMINISTERED AS A 1-HOUR IV INFUSION EVERY 3 WEEKS.** M. Hidalgo, C. Aylesworth, S. Baker, G. Weiss, C. Britten, A. Patnalk, J. Stephenson, L. Hammond, K. Molpus, D. Sonnichsen, S. Dlab, A. Tortora, J. Skillings, D. Von Hoff and E. Rowinsky. *Cancer Therapy and Research Center, San Antonio, TX; and Bristol-Myers-Squibb, Wallingford, CT.*

BMS184476, a novel taxane analog, with potential advantages over paclitaxel, including a higher potency and a wider spectrum of preclinical activity. The agent also has higher aqueous solubility requiring 68% less Cremophor EL® which might result in better tolerability of short intravenous infusions and avoidance of premedications for hypersensitivity reactions (HSR). This study evaluated the feasibility and PK behavior of BMS184476 administered as a 1-hour IV infusion every 3 weeks in patients with advanced cancer without the use of HSR premedications. Thirty-two patients (median age 59, range 27-78; median ECOG PS-1) received 68 courses of treatment at doses ranging from 20-80 mg/m<sup>2</sup>. Dose-limiting toxicities (DLTs), which consisted of febrile neutropenia (5 pts) associated with gr. 3 mucositis (3 pts), and abdominal cramps gr. 3 with diarrhea gr. 2 (1 pt), were observed in 6 out of 9 minimally pretreated pts at doses >60 mg/m<sup>2</sup>. A total of 14 pts were treated at the 60 mg/m<sup>2</sup> dose level at which 1 heavily pretreated subject developed febrile neutropenia gr. 3 diarrhea, and gr. 3 thrombocytopenia and 1 pt developed neutropenia gr. 3 associated with mucositis gr. 3. Other individuals tolerated treatment well irrespective of prior treatment. In addition, 1 pt at the 40 mg/m<sup>2</sup> dose level developed a gr. 2 HSR during the second course of treatment. Based on these results, the MTD of BMS 184476 on this administration schedule is 60 mg/m<sup>2</sup>. PKs (n=24) appear dose-independent with a Cl of 184±50 ml/min/m<sup>2</sup> and a proportional increment in the AUC<sub>0-24</sub> from 1532±1292<sub>0-24</sub> nmLh to 6628±2093 nmLh at doses ranging from 20-80 mg/m<sup>2</sup>. The calculated Vd, and t<sub>1/2</sub> averaged 412±215 L/m<sup>2</sup> and 44±19 h, respectively. Equivalent parameters for paclitaxel administered at doses of 135-175 mg/m<sup>2</sup> as a 3-h IV infusion include a Vd of 74-98 L/m<sup>2</sup> and a t<sub>1/2</sub> of 6-16 hours. One pt with cholangiocarcinoma achieved a PR and an one pt with esophageal adenocarcinoma attained a minor response. These data indicate that BMS184476 is 2-3 fold more potent than paclitaxel and has a larger volume of distribution and longer elimination half-life.

**#333 A phase I study of a novel, trinuclear, platinum analogue, BBR3464, in patients with advanced solid tumors.** Calvert, P.M., Highley, M.S., Hughes, A.N., Plummer, E.R., Azzabi, A.S.T., Verrill, M.W., Camboni, M.G., Verdl, E., Bernareggi, A., Zucchetti, M., Robinson, A.M., Carmichael, J., Calvert, A.H. *Newcastle upon Tyne, UK; Novuspharma SpA, Italy; Nottingham, UK.*

**Introduction:** BBR3464 is a novel trinuclear platinum compound which demonstrates significantly greater potency than cisplatin. Preclinical studies showed non-cross-resistance to cisplatin and activity in a broad spectrum of tumours including cisplatin-refractory tumours such as gastric and non-small cell lung cancer. Toxicology showed significantly less emesis and nephrotoxicity with BBR3464, but focal lung lesions were seen in rats.

**Aims:** Determine the maximum tolerated dose (MTD), Dose-limiting toxicity, and toxicity profile of BBR3464 given as a 1 hour infusion every 28 days in patients with advanced solid tumour malignancies.

**Methods:** Patients (pts) recruited in single patient cohorts until grade 2 toxicity seen. 100% dose increase until toxicity seen, then cohorts expanded and doses calculated using modified Fibonacci scheme. Starting dose 0.2 mg/m<sup>2</sup>.

**Results:** 11 pts (6 M: 5 F) have been recruited with a median age 56 years (range 26-74). 8 had received prior chemotherapy regimens (median 2, range 1-3). Primary tumours included colorectal 3, upper GI 3 and 1 each of renal, melanoma, NSCLC, mesothelioma and STS. Total cycles of BBR3464 administered: 22, (median per pt 1; range 1-6). Dose levels (mg/m<sup>2</sup>): 0.2 n = 1, 0.4 n = 2, 0.8 n = 3, 1.1 n = 6. Significant toxicity was confined to the 1.1 mg/m<sup>2</sup> dose level with diarrhoea; grade II (2 pts) and grade III (3 pts) and neutropenic sepsis; grade III in 1 pt and grade IV, lasting 7 days in 1 pt. There has been no significant nephrotoxicity or neurotoxicity and no evidence of pulmonary toxicity. An encouraging partial response, measured using CT imaging and CA19.9 tumour marker, was seen in a patient with metastatic pancreatic cancer.

**Conclusions:** BBR3464 has shown signs of activity in this phase I study and has a different toxicity profile to that of cisplatin. Dose-limiting haematologic toxicity was seen at the current dose level and recruitment is continuing. Pharmacokinetic analyses are being performed.

**#334 A preliminary report of L-NDDP (platar), liposomal cisplatin analog, in patients with refractory peritoneal carcinomatosis or sarcomatosis: a phase I study.** CF Verschraegen, M Royce, P Mansfield, B Feig, K Hunt, Z Siddik, T Nelson-Taylor, R Perez-Soler, AP Kudelka, JJ Kavanagh, G Lopez-Berstein, A Khokhar. *University of Texas, M.D. Anderson Cancer Center, Houston, Texas.*

We initiated a study of intraperitoneal administration of L-NDDP at increasing doses for patients [pts] with refractory peritoneal carcinomatosis or sarcomatosis. The starting dose was 200 mg/m<sup>2</sup>, and doses were increased to 300, 350, 400, and 450 mg/m<sup>2</sup> per cohort of 3 to 6 pts. Treatment was repeated every 4 weeks if pts benefited from it. The first 2 courses were given during a laparoscopic evaluation, the 4 last courses through a subcutaneous port inserted during the second laparoscopy (maximum of 6 courses). One dose escalation was permitted per pt, if no > grade 2 toxicity was observed. A pharmacology study was performed on plasma and ascites. Pts with altered hematopoietic, renal, or hepatic function, and pts with peritoneal adhesions were not eligible. **Results:** Twenty-six patients were treated, of whom 10 received more than one course. Three patients are pending their second course. Twenty-three pts are evaluable for toxicity. Median age was 53 years (26-76), median Zubrod 1 (0-2). Three pts each were treated at 200 and 300 mg/m<sup>2</sup>, and 6 at 350, 400 or 450 mg/m<sup>2</sup>. Six patients were also treated at 350 mg/m<sup>2</sup> immediately after tumor debulking surgery. Of these, 2 had surgical complications necessitating reintervention, and 2 other pts developed adhesions preventing retreatment after 1 and 2 courses. Of the pts treated solely by laparoscopy, dose-limiting toxicity was adhesions at 450 mg/m<sup>2</sup> (3 pts), and in 2 other pts, dose had to be reduced to 400 mg/m<sup>2</sup> for excessive fatigue and anorexia. The MTD is therefore 400 mg/m<sup>2</sup>. Additional pts will be added at 400 mg/m<sup>2</sup> to better define the toxicity profile. Grade 3 toxic effects were abdominal pain (2 pts), anorexia (1 pt), and neutropenia in 1 pt who had had a bone marrow transplant. Other ≤ grade 2 toxic effects included: fatigue (52%), abdominal pain (43%), nausea/vomiting (39%), anorexia (26%), and cumulative neuropathy (13%). Median survival has not been reached. Activity was noted in pts with mesothelioma, pseudomyxoma peritonei, and ovarian cancer. **Conclusion:** L-NDDP is well tolerated intraperitoneally at 400 mg/m<sup>2</sup>. The study continues to better define the toxicity and pharmacology profile. A phase 2 study is planned in pts with mesothelioma.

**#335 Mild copper deficiency induced by tetrathiomolybdate as an antiangiogenic strategy in the treatment of metastatic cancer: phase I study and preliminary evidence of efficacy.** Marajver, Sofia D. and Brewer, George J. *Departments of Internal Medicine and Human Genetics, University of Michigan, Ann Arbor, MI.*

Pre-clinical and *in vitro* studies have determined that copper is an important co-factor for angiogenesis. Tetrathiomolybdate, (TM) was developed as an effective anti-copper therapy for the initial treatment of Wilson's disease, an autosomal recessive disorder that leads to abnormal copper accumulation. Given the potency and uniqueness of the anti-copper action of TM and its lack of toxicity, we hypothesized that TM would be a suitable agent to achieve and maintain mild clinical copper deficiency in order to impair neovascularization in metastatic solid tumors. Following pre-clinical work which showed efficacy for this anti-copper approach in mouse tumor models, we carried out a Phase I clinical trial in 18 patients with 11 different types of metastatic cancer. Patients were enrolled 3 dose levels of oral TM (90, 105, and 120 mg/day) administered in 6 divided doses with and in-between meals. Serum ceruloplasmin (Cp) was used as a surrogate marker for total-body copper and measured weekly. As anemia is the first clinical sign of copper deficiency, the goal of the study was to reduce Cp to 20% of baseline value, without reducing hematocrit by more than 80% of baseline. Cp is a reliable and sensitive measure of copper status, and TM was non-toxic when Cp was reduced to 15-20% of baseline, with only one case of mild, reversible anemia observed. The level III dose of TM of 120 mg/day was effective in reaching the target Cp, without added toxicity, in 14/18 patients, before progression. After achieving the target Cp reduction, the TM doses were individually tailored for each patient to maintain the Cp within a window of 20 ± 10% of baseline. Thirty-three percent (6/18) of these patients with advanced



disease have been copper deficient at the target range (Cp ~20% of baseline) for over 90 days. TM-induced mild copper deficiency achieved stable disease by standard criteria in 5 out of 6 patients who have been copper deficient at the target range for at least 90 days, with a remarkable average duration of stabilization of disease of 249 days, for this patient population with advanced, previously progressive disease.

Work supported by NIH RO1-CA77612 (SDM) and RO3-CA77122 (SDM) and FDA Orphan Products grant (GJB).

**#336 Clinical, pharmacokinetic (PK) and pharmacodynamic evaluation of the colloidal dispersion formulation of 9-aminocamptothecin (9-ACCD) administered orally to patients (pts) with refractory solid tumors.** Tran, H.T., Madden, T., Xiong, Q., Zahman, S., Newman, R.A., and Abbruzzese, J.L. Depts. of Experimental Therapeutics, Pharmacy, and GI Medical Oncology and Digestive Diseases, U.T.M.D. Anderson Cancer Center, Houston, TX 77030.

9-ACCD is a water-insoluble derivative of camptothecin, which has been prepared in a colloidal dispersion for iv administration. We investigated the utility of administering this compound orally in a Phase I trial to determine the maximum tolerated dose (MTD), dose-limiting toxicities (DLT) and pharmacokinetic profile, including absolute bioavailability. Data is available from 29 evaluable pts with refractory solid tumors treated with 9-ACCD. To determine the absolute bioavailability of this formulation, the first dose of 9-ACCD was administered intravenously. Pt characteristics: median age: 52 yrs; gender: male 17, female 12; cancer types: colorectal-14; lung-3; head + neck-3; pancreas-3, sarcoma-2, others-4. The starting dose was 0.1 mg/m<sup>2</sup>/d × 5 days (M-F) × 2 weeks. After establishing the safety of the two week schedule, the duration of 9-ACCD administration was increased to 0.1 mg/m<sup>2</sup>/d × 5 days (M-F) × 4 weeks, with subsequent dose escalations to 0.2, 0.3, 0.45, 0.56, and 0.7 mg/m<sup>2</sup>/d. At 0.7 mg/m<sup>2</sup>/d, 2/3 pts developed grade 3 to 4 granulocytopenia and thrombocytopenia. Six episodes of grade 3 anemia were seen at the two highest dose levels. Non-DLT effects included transient elevation of the total bilirubin, nausea, vomiting, and fatigue. Pts are currently being treated at the anticipated MTD of 0.63 mg/m<sup>2</sup>/d × 4 weeks. No objective responses have been observed. Blood samples for PK analysis were obtained in 16 of these 29 pts. Mean PK parameters for total 9-ACCD are as follows: Terminal t<sub>1/2</sub> = 10.1 ± 8.3 hrs, V<sub>c</sub> = 17.7 ± 20.6 L, Cl/F = 45.8 ± 30.5 ml/min/m<sup>2</sup> (apparent oral clearance). There was moderate correlation between both drug dose and total drug exposure (r<sup>2</sup> = 0.52) and between total drug exposure and percent decrease in the absolute neutrophil count (r<sup>2</sup> = 0.59). The median percent bioavailability of 9-ACCD was 87.3 ± 31% (range = 25.7–100%). Despite good tolerance when 9-ACCD is administered orally, the lack of clinical responses and the variable absorption of this formulation suggest that further development is not warranted. (Supported in part by the U.S. Public Health Service [2 U01 CA62461]).

**#337 Clinical pharmacokinetics of liposomal lurtotecan (NX211) in whole blood, plasma and urine.** Kehr D., Bos A., Sparreboom A., Loos W., Hamilton M., Ptaszynski M., De Vries E., and Verweij J. Rotterdam Cancer Institute and University Hospital Groningen, the Netherlands; Nexstar Pharmaceuticals, Boulder, CO.

Lurtotecan [7-(4-methylpiperazinomethylene)-10,11-ethylenedioxy-20-(S)-camptothecin] is a totally synthetic analogue of the topoisomerase-I inhibitor camptothecin, with substantial antitumor activity in both preclinical and Phase II studies. Liposomal lurtotecan (NX211) was developed in an attempt to prolong systemic drug exposure. In an ongoing Phase I study, NX211 was administered as a single 30-min i.v. infusion to 6 patients with solid tumors at dose levels of 0.4 or 0.8 mg/m<sup>2</sup>. No drug-related toxicity was reported. Here, we report on the clinical pharmacokinetics. Serial whole blood, plasma and urine samples were collected before and up to 96 h after drug administration, and analyzed for the presence of total lurtotecan by a new HPLC method with fluorescence detection (lower limit of quantitation: 1 ng/mL). A mono-exponential decline was observed for the total drug in plasma and blood, with peak drug levels at the end of infusion. The pharmacokinetic profile in plasma was characterized by a slow systemic clearance of 1.38 ± 1.01 L/h/m<sup>2</sup> (mean ± SD) and a steady state volume of distribution of 3.74 ± 1.74 L/m<sup>2</sup>, thus approximating the blood volume. The blood to plasma AUC ratio averaged 0.73 ± 0.26, indicating limited drug distribution to erythrocytes. Urinary excretion was limited to 10.2 ± 6.23% (range, 5.2–18.7%) of the delivered dose, indicating that renal clearance was a minor route of drug elimination. As compared to non-liposomal lurtotecan (Gerrits et al., Br. J. Cancer, 73: 744–750, 1996), NX211 demonstrates significantly increased plasma residence time and terminal disposition half-life, which may be a potential advantage with pharmacodynamic importance. Data from additional dose levels will be available at the time of the meeting.

**#338 Phase I/Pharmacokinetic trial of the taxane analogue BMS-184476 in combination with carboplatin (CBDCA) or cisplatin (CDDP) administered as an IV infusion every 3 weeks.** Stevenson, J.P., Gallagher, M., Ryan, W.F., Vaughn, D.J., Algazy, K., Tortora, A., Skillings, J., O'Dwyer, P.J. University of Pennsylvania Cancer Center, Philadelphia, PA, and Bristol-Myers Squibb, Wallingford, CT.

The taxane BMS-184476 displays potency against paclitaxel-resistant cell lines with the MDR phenotype *in vitro* and exhibits antitumor efficacy superior to paclitaxel in human tumor xenograft models *in vivo*. Toxicology studies in rats suggest that BMS-184476 is less neurotoxic than paclitaxel. In an ongoing Phase I study, 14 patients have received BMS-184476 at an initial dose of 40 mg/m<sup>2</sup> as a 1-hour infusion followed by CBDCA (AUC 5) or CDDP (75 mg/m<sup>2</sup>) on day 1 every 21 days. Eleven pts are evaluable for preliminary assessment of toxicity. Toxicity in the CBDCA stratum has included neutropenia (2 pts, gr 4), thrombocytopenia (1 pt, gr 3), nausea/vomiting (5 pts, gr 1–2), and peripheral neuropathy (2 pts, gr 1). Neutropenia (1 pt, gr 4), thrombocytopenia (1 pt, gr 3), nausea/vomiting (5 pts, gr 1–2), and uremia (1 pt, gr 2) have been observed in the CDDP stratum. Two hypersensitivity reactions have occurred (2 pts, gr 2–3) but did not recur following premedication with H1/H2 blockers and dexamethasone. Two pts with NSCLC maintained stable disease for > 4 cycles (1 in each stratum) and 1 pt with mesothelioma attained a PR in a lung mass with resolution of a malignant pleural effusion (CDDP stratum). The combination of BMS-184476 and CBDCA or CDDP is active and well-tolerated on this schedule. BMS-184476 dose is currently being escalated to 50 mg/m<sup>2</sup>. BMS-184476 pharmacokinetic data and updated results will be presented.

**#339 A Phase I and pharmacokinetic study of the matrix metallo-protease (MMP) inhibitor BAY 12-9566 in combination with doxorubicin and docetaxel in patients with advanced cancer.** Grathlein S.J., Lathia C., Humphrey R. SUNY Health Science Center, Syracuse, NY; Bayer Corporation, Pharmaceutical Division, West Haven, CT.

**Introduction:** BAY 12-9566 (BAY) is a selective, non-peptidic inhibitor of MMPs 2 & 9, which have been correlated with poor prognosis in a variety of cancers. In preclinical studies, BAY has shown activity against invasion, metastasis and angiogenesis.

**Methods:** This phase I study of oral BAY is being performed to evaluate the safety and pharmacokinetics (PK) of escalating doses of BAY in combination with doxorubicin and docetaxel in subjects with advanced cancer. Cohort 1 (n = 3) will receive full doses of doxorubicin (50 mg/m<sup>2</sup>) and docetaxel (100 mg/m<sup>2</sup>). Daily treatment with BAY (400 mg p.o. qd) will be initiated 1 week later. Each subsequent cohort will receive increasing doses of BAY (400 mg p.o. bid and 800 mg p.o. bid), as tolerated, to a maximum of 800 mg bid. Dose limiting toxicity (DLT) is toxicity ≥ grade 3; symptomatic, dose limiting or ≥ 7 days grade 2. Maximum tolerated dose (MTD) will be declared if ≥ 2 pts experienced DLT. A PS 0–2 and acceptable organ function are required for eligibility.

**Results:** To date, 7 patients (pts) have been enrolled with a variety of tumor types. 3 pts in cohort 1 completed therapy, and 4 completed at least 2 cycles of therapy in cohort 2. After 2 cycles, 3 pts had progressive disease, 3 stable disease, and 1 a response that has not yet reached the level of PR (Ca 27–29 falling, multiple lesions reduced by 30–44%). To date 19 cycles of therapy have been administered. The only observed toxicity of grade 3 or higher has been neutropenic fever (5 episodes; 3 in a single pt). No episodes of fluid retention were observed in the 7 pts treated to date.

**Conclusions:** Administration of BAY with doxorubicin and docetaxel is well tolerated. Drug level analyses of BAY, doxorubicin, and docetaxel are ongoing and will be presented.

**#340 A Phase I and pharmacokinetic study of the selective, non-peptidic inhibitor of matrix metalloproteases (MMPs) BAY 12-9566 in combination with etoposide and carboplatin.** Alberts, S., Reid, J., Erlhman, C., Lathia, C., Agarwal, V., Humphrey, R., Saifon, S. Mayo Clinic, Rochester, MN; Bayer Corporation, West Haven, CT.

**Introduction:** BAY 12-9566 (BAY) is a non-peptidic biphenyl inhibitor of MMPs, with nanomolar inhibitory activity against MMPs 2, 3 & 9, and anti-invasive, anti-metastatic and anti-angiogenic activity in a variety of tumor models.

**Methods:** This phase I study of BAY is being conducted to evaluate safety and pharmacokinetics (PK) of BAY when administered with etoposide or etoposide/carboplatin in subjects with advanced cancer. The first cohort of patients (pts) (n = 8) received a cycle of etoposide 60 mg/m<sup>2</sup> followed one week later by a fixed daily oral dose of BAY 800 mg bid, to which 3 potential doses of etoposide (low dose: 60 mg/m<sup>2</sup>, mid dose: 90 mg/m<sup>2</sup>, high dose: 120 mg/m<sup>2</sup>) were added every 3 weeks as tolerated. The second cohort is currently being enrolled (n = 6) and will receive etoposide (120 mg/m<sup>2</sup>) and carboplatin (AUC = 5) followed one week later by a fixed daily oral dose of 800 mg bid BAY, to which etoposide (120 mg/m<sup>2</sup>) and carboplatin (AUC = 5) will be added. In the final 2 cycles, pts will receive carboplatin AUC = 6. Dose limiting toxicity (DLT) is toxicity ≥ grade 3. Maximum tolerated dose (MTD) will be declared if ≥ 2 pts experienced DLT. A PS 0–2 and acceptable organ function are required for eligibility.

**Results:** 8 eligible pts with a variety of tumor types (median age 64 yrs, range 44–76 yrs) have been enrolled in the first cohort; 6 have completed all 3 levels of etoposide. Progressive disease has occurred in 5 of the 8 pts; 3 pts continue on study with treatment. Drug level analyses of etoposide are ongoing. PK parameters (C<sub>max</sub>, t<sub>max</sub> and AUC) of BAY did not change upon concomitant administration of 60 and 90 mg/m<sup>2</sup> of etoposide indicating a lack of PK interaction between BAY and etoposide. The combi-

nation of BAY and etoposide was tolerable in the first cohort, permitting enrollment of the second cohort. A detailed review of toxicities will be presented.

**Conclusion:** The PK analysis, safety, and response data will be presented for the combination of BAY and etoposide. (Supported in part by a grant from the Bayer Corporation.)

**#341 Hepatic artery infusion of ONYX-015 in combination with 5-FU/Leukovorin for metastatic gastrointestinal cancer metastatic to the liver: A Phase I/II study.** T. Reid, J. Rubln, E. Galanis, J. Abbruzzese, A. Lowe, D. Sze, L. Romel, D. Kimm. *Stanford Univ, Stanford, CA, Mayo Clinic, Rochester, MN, MD Anderson, Houston, TX, ONYX Pharmaceuticals, Richmond, CA.*

ONYX-015 is an adenovirus engineered to selectively replicate in and lyse p53-deficient cancer cells. ONYX-015 was administered by hepatic artery infusion into patients with measurable gastrointestinal cancer involving the liver, with KPS > 70% and LFT values not more than 3 times the upper limit of the normal range. ONYX-015 was administered on days 1, 8, 22 and 50. The infusions on days 22 and 50 were followed by standard dose 5-FU/Leukovorin daily for 5 days. Treatment was initiated at  $10^6$  pfu/infusion and escalated in 0.5 log increments to  $10^{11}$  pfu/infusion. To date, no dose-limiting toxicities have been observed. Grade I/II fevers have been observed in most patients and 2 of 4 patients treated at  $10^{11}$  developed rigors starting 1 to 2 hours after the infusion that responded rapidly to treatment with demerol and phenergan. Preliminary response data is available for 4 patients treated at  $10^{11}$  pfu/infusion, three of whom had failed prior 5-FU/leukovorin therapy. These patients had extensive liver involvement, with 30 to 45% of the liver replaced by tumor and moderate to markedly elevated LFTs, LDH and CEA. Two of the 4 patients have had >50% reduction in tumor mass, with evidence of extensive necrosis of the residual tumor. These patients had complete resolution of LDH and LFT abnormalities and CEA was normalized (25 to 1.8) in one patient and reduced almost 50% (358 to 187) in the other. The other two patients had significant reductions in LDH and transaminases levels and radiographic evidence of extensive tumor necrosis. Viral replication will be assessed on normal liver and tumor biopsies post-treatment. Despite the extensive tumor necrosis observed in these patients, treatment resulted in only minor and transient >increases in serum transaminase levels, confirming the safety and selectivity of ONYX-015 administered by hepatic artery infusion.

**#342 A Phase I clinical study of the sequential administration of paclitaxel (P) followed by oral topotecan (T) and etoposide (E) in patients with solid tumors.** Rocha Lima, C.M.S., Catapano, C.V., Sherman, C.A., Mushtaq, C.M., Pacheco, D., Harper, M., Lightcap, K.D., Fields, S.Z. and Green, M.R. *Medical University of South Carolina (MUSC), Charleston, SC.*

Synergistic anti-tumor activity has been observed in pre-clinical studies when a topoisomerase (topo) I inhibitor is administered before a topo II inhibitor, and when a taxane is administered before a topo I inhibitor. The synergistic effects of these drug combinations were strictly sequence-dependent and, apparently, relates to up-regulation of topo I and topo II protein levels induced by taxanes and topo I inhibitors, respectively. We have evaluated the feasibility of the sequential administration of a taxane (P), a topo I inhibitor (T), and a topo II inhibitor (E) in a phase I clinical study. The drugs were given in the sequence P→T→E, with P i.v. over 3 hours on day 1 (D1), followed 24 h later by oral T for 3 days (D2-4), and oral E for 3 days (D5-7) starting 24 h after the last dose of T. P and T were escalated in alternating steps from the initial doses of 50 mg/m<sup>2</sup> and 0.6 mg/m<sup>2</sup>, respectively, while E was given at a fixed dose of 160 mg/m<sup>2</sup>. Treatment was repeated every 21 days. Blood samples were collected on day 1 (before P), day 2 (before T), and day 5 (before E) to measure topo levels in peripheral blood lymphocytes (PBL) by immunoblotting. Nineteen patients (pts), 14 males/5 females, median age 55, Zubrod PS 1/2 (14/5), were accrued. Fifty-three cycles of chemotherapy (mean: 2.8 cycles/patient) were delivered. The DLT was neutropenia lasting ≥4 days in 2 out of 6 pts in cohort 5 (P 110 mg/m<sup>2</sup>, T 1.5 mg/m<sup>2</sup> and E 160 mg/m<sup>2</sup>). In addition, one episode of febrile neutropenia and 2 episodes of uncomplicated grade III thrombocytopenia of short duration were observed at cohort level 5. Non-hematological toxicity was mild, with grade II nausea in 2 pts and grade II skin rash in one pt. One pt expired during cycle 1 due to an unrelated cause. The MTD for the PTE regimen are P 80 mg/m<sup>2</sup> D1, T 1.5 mg/m<sup>2</sup> D2-4, and E 160 mg/m<sup>2</sup> D5-7. Further dose escalation continues using G-CSF starting on day 8. Among the 18 pts with measurable disease, two radiological PR (1 SCLC and 1 NSCLC), one unconfirmed bone marrow PR in a pt with a neuroendocrine tumor, and a continuing minimal response in a pt with NSCLC have been observed. All responders had been previously treated with ≥2 different chemotherapy regimens. Measurements of topo I levels have been performed in 14 pts. Seven pts had substantial increases (2- to 15-fold) and 2 pts had minor increases (≤50%) of the topo I levels 24 h after P. In all these pts, topo I levels decreased by day 5, probably reflecting DNA binding or degradation of topo I induced by T. The remaining 5 pts did not show any change (2 pts) or had a slight decrease (3 pts) of topo I on day 2. In these pts, however, topo I increased 2- to 4-fold on day 5 compared to day 2. To our knowledge, these data represent the first evidence of modulation of topo I levels following treat-

ment with P in clinical samples and provide a rationale for design and further clinical investigation of chemotherapy regimens that include combinations of taxanes and topo I inhibitors.

Supported by SmithKline Beecham Pharmaceuticals.

**#343 A Phase-I study of the combination of interferon alfa-2b (IFN-2b) with paclitaxel (PCTX) and carbo-platin (CBP) on weekly schedule in advanced cancer patients (pts).** Obrocea, Mihail; Ernstoff, Mark S.; Beaulieu, Bernard B.; MacKay, Katherine; Fisher, Jan; Waugh, Mary; Truman, Debra; Perez, Ray P.; Lewis, Lionel D. *Dept of Medicine & The Norris Cotton Cancer Center, Dartmouth-Hitchcock Medical Center, Lebanon, NH, USA.*

**Introduction:** Interferons modulate chemotherapeutic cytotoxicity, enhance monocyte/macrophage immune function and downregulate hepatic CYP450 drug metabolizing isoenzyme activity. We therefore combined IFN-2b with weekly PCTX + CBP and investigated the pharmacokinetics and pharmacodynamics of the combination. **Objectives:** to define (i) the safety and tolerance of PCTX + CBP/IFN-2b administered on a weekly basis (ii) the effect of combining IFN-2b on the pharmacokinetics of weekly PCTX. (iii) the effect of IFN-2b + PCTX/CBP on peripheral blood monocyte (PBM) phagocytic activity. **Methods:** We studied the regimen of weekly PCTX 80 mg/m<sup>2</sup> + CBP AUC 2 for 3 weeks, with a two week break followed by IFN-2b TIW + weekly PCTX 60 mg/m<sup>2</sup>/CBP AUC 2 for 3 weeks in advanced cancer patients. Blood samples for PCTX pharmacokinetics were obtained on weeks 1, 3, 5 and 7 and analyzed by HPLC. PBMs were harvested pre-treatment (baseline) and 24 h post-PCTX/CBP infusion on weeks 3 and 7. PBM phagocytic activity was measured by dual color flow cytometry. **Results:** 7 pts with advanced stage solid tumors and median age 63 yrs (range 56-74) have, so far been enrolled in the study at the lowest IFN-2b dose tier (1 MIU/m<sup>2</sup> TIW). 3 pts have completed the study (1 pt voluntarily withdrew; 1 pt developed grade 4 thrombocytopenia and 2 pts are only on study for 2 weeks). PCTX + CBP combination was well tolerated; addition of IFN-2b (1 MIU/m<sup>2</sup>) TIW has not yet affected the toxicity of the combination. There was no change in the mean (n = 3) PCTX clearance on week 1, 16.9 (SD ± 2.6); week 3, 19.5 (SD ± 1.8), week 5, 19.4 (SD ± 0.4), and week 7, 18.9 (SD ± 3.9) L/h/m<sup>2</sup> (MANOVA p = 0.4). Mean (±SD) n = 3 baseline, week 3 and week 7 maximum PBMA phagocytic activity was 91.1 ± 8.2%; 914 ± 10.9% and 82.2 ± 12.3 respectively (MANOVA p = 0.02). **Conclusions:** The regimen appears well tolerated. The data suggest that "low dose" IFN-2b did not significantly affect PCTX clearance, but that IFN-2b impaired monocyte phagocytic activity compared to baseline. The study is ongoing and higher dose of IFN-2b (5 MIU/m<sup>2</sup>) TIW will be studied with weekly PCTX + CBP, toxicity permitting.

**#344 The pharmacokinetics of paclitaxel (P) are unaffected by the multidrug resistance (MDR) reversing agent SDZ PSC 833 (PSC) in patients (pts) with metastatic breast cancer (BC) despite an improvement in overall response rate.** Synold TW, Spicer D, Muggia F, Tettef M, Ganjara D, Groshen S, Lenz H-J, Newman EM, Johnson K, and Doroshow JH. *City of Hope Cancer Ctr, Duarte, CA; USC/Norris Cancer Ctr, Los Angeles, CA; and Univ. of Calif. Davis Cancer Ctr, Sacramento, CA.*

PSC is a non-immunosuppressive, non-nephrotoxic derivative of cyclosporine and a potent MDR-reversing agent. Previous clinical trials of PSC in combination with etoposide and doxorubicin have demonstrated that, like cyclosporine A, PSC interferes with the elimination of chemotherapeutic agents, leading to higher than expected systemic exposures. While phase I trials of the combination of PSC and P have shown that the dose of P must be reduced by 60% in order to avoid unacceptable toxicity, there are no published pharmacokinetic data indicating that PSC affects P clearance. The current randomized phase II study was designed to evaluate the response rate, time to treatment failure, and pharmacokinetics of paclitaxel with and without PSC 833. Pts were eligible if they had either evaluable or measurable BC, had received prior anthracycline-based adjuvant chemotherapy and recurred within 2 years, or had failed one prior anthracycline-based regimen. Pts were randomized to receive either P alone at 175 mg/m<sup>2</sup> as a 3-hour infusion every 21 days (Arm I), or P at 70 mg/m<sup>2</sup> as a 3-hour infusion with PSC 5 mg/kg po qid × 12 doses every 21 days (Arm II). Serial blood samples were collected during the first cycle for determination of P plasma levels by HPLC. P plasma concentration versus time data were analyzed using model-independent methods to determine the maximum P plasma concentration (C<sub>max</sub>), P area-under-the-curve extrapolated to infinity (AUC), apparent systemic clearance (CL<sub>app</sub>), and the time the P concentration was above 0.5 μM (T > 0.05 μM). To date, 39 female pts have been randomized—18 to Arm I and 21 to Arm II. P pharmacokinetics have been studied in 30 pts; 12 from Arm I and 18 from Arm II, and the results are shown in the table below. Pharmacokinetic data are means ± standard deviations.

	# of patients	C <sub>max</sub> (μM)	AUC (μMxhr)	CL <sub>app</sub> (L/hr)	T > 0.05 μM
Arm I	12	4.9 ± 1.3	17.9 ± 9.7	13.2 ± 3.8	38.3 ± 51
Arm II	18	1.2 ± 0.3	7.0 ± 2.8	12.9 ± 3.5	21.2 ± 5.6
p-value		<0.00001	0.003	0.8	0.3



Pts in Arm I have significantly higher mean  $P C_{max}$  and AUC than those in Arm II. Mean  $P C_{L_{50\%}}$  is unchanged by the addition of PSC. The ratio of the AUCs in Arms I and II is exactly the same as the ratio of the administered doses (1:2.5), further suggesting a lack of effect of PSC on P pharmacokinetics. Interestingly, clinical responses to date have been greater in Arm II (2 CR/5 PR) than in Arm I (0 CR/4 PR), with equivalent levels of toxicity, suggesting that PSC may be potentiating the therapeutic effect of P without affecting its systemic exposure. (Supported by CA 63265).

**#345 Phase I and pharmacokinetic trial of Irinotecan (CPT-11) and Tomudex administered as sequential IV infusions, D1 and D2, repeated every 21 days.** Sun W., Stevenson J.P., Gallagher M., Hiller K., Rose L., Mitchell E.P., Algazy K., Gianantonio B., Haller D.G., Blair I.A., O'Dwyer P.J. *Thomas Jefferson University, Philadelphia, PA, and the University of Pennsylvania Cancer Center, Philadelphia, PA.*

Sequential exposure of human colon cancer cell lines to the CPT-11 metabolite SN-38 followed 24 hours later by the thymidylate synthase inhibitor Tomudex is maximally synergistic *in vitro* (Aschele et al, Clin Cancer Res, 1998). We therefore performed a phase I study of CPT-11 administered as a 60-minute IV infusion on D1 followed by Tomudex given IV over 30 minutes on D2, repeated every 3 weeks. CPT-11 doses have ranged from 100–350 mg/m<sup>2</sup>, Tomudex 1.0–4.0 mg/m<sup>2</sup>. 38 pts with advanced solid tumors and good performance status have been treated to date. Toxicities at varying dose levels have included neutropenia (3 pts, gr 4), diarrhea (6 pts, gr 3; 2 pts, gr 4), fatigue (5 pts, gr 3), and AST/ALT elevation (2 pts, gr 3). Tomudex at 4.0 mg/m<sup>2</sup> was poorly tolerated because of asthenia and was deescalated while CPT-11 escalation continued. Activity has been observed in this pretreated population, including PRs lasting > 6 months in 2 pts with esophageal ca and disease stabilization lasting > 4 months in 6 pts (5 colon ca, 1 gastric ca). CPT-11/SN-38 pharmacokinetic data will be presented. Doses recommended for phase II evaluation are CPT-11 350 mg/m<sup>2</sup> and Tomudex 3.0 mg/m<sup>2</sup>. CPT-11 and Tomudex can safely be administered at full doses on this schedule, and the combination is active in a range of gastrointestinal malignancies.

**#346 Extended phase I study of a weekly schedule of Irinotecan (CPT-11), leucovorin and infusional 5-FU as first-line chemotherapy in metastatic colorectal cancer.** Vanhoefler, U., Harstrick, A., Achterhath, W., Lipp, R., Mayer, S., Schöffski, P., Köhne, C.H., Hossfeld, K.D., Wilke, H., and Seeber, S. *University of Essen Medical School; University Clinics Hamburg; University of Hannover Medical School; University Hospital Rostock; Rhône-Poulenc Rorer, Cologne; Germany.*

In the first part of the study the maximum tolerated dose (MTD) and recommended dose (RD) of a weekly schedule of CPT-11, leucovorin (LV) and infusional 5-FU were investigated as first-line chemotherapy in 26 patients (pts) with metastatic colorectal cancer. The RD was defined as follows: CPT-11 80 mg/m<sup>2</sup> (90 min i.v. infusion), LV 500 mg/m<sup>2</sup> (2-h i.v. infusion) and 5-FU 2.6 g/m<sup>2</sup> (24-h i.v. infusion) weekly for 6 weeks followed by one week rest period (J. Clin. Oncol. 17: 907–913, 1999). At the MTD (CPT-11 100 mg/m<sup>2</sup>, LV 500 mg/m<sup>2</sup> and 5-FU 2.6 g/m<sup>2</sup> weekly for 6 weeks) the dose-limiting toxicity was diarrhea NCI-CTC grade 4 in 3 out of 6 pts. In the second—not previously published—part of this study the safety and efficacy of this regimen was assessed at the RD in additional 21 pts. So far, a total of 24 pts. received 78 cycles (median 3 cycles per pt.) at the RD and are evaluable for toxicity and response. Worst toxicities per patient according to NCI-CTC: Diarrhea grade 3 and 4: 21% and 13% respectively, vomiting grade 4: 4%, pneumonia grade 4: 4%, and neutropenia grade 3: 8%. Eighteen pts. (75%) achieved a partial response (95% confidence interval: 53%–90%) and five pts. (21%) had no change (NC) resulting in a tumor growth control rate of 96% (95% confidence interval: 79%–100%). **Conclusions:** The results of the extended phase I study demonstrate that the combination of CPT-11 and LV/5-FU can be administered at the recommended dose of weekly CPT-11 80 mg/m<sup>2</sup>, LV 500 mg/m<sup>2</sup> and 5-FU 2.6 g/m<sup>2</sup> with acceptable side-effects. The antitumor activity of this regimen as first-line chemotherapy is promising in terms of tumor response rate.

**#347 Dose escalation of the combination of Topotecan (T) and Oxaliplatin (OXA): Preliminary results of an ongoing phase I study.** M. Gross-Goupil, G. Lopez, D. Roman, J.-L. Misset, and F. Goldwasser. *Cancérologie, Hôpital Paul Brousse, Villejuif, SmithKline Beecham Pharmaceuticals, Nanterre, France.*

Given as single agents using an every 3 weeks schedule, the dose limiting toxicities (DLT) and the recommended doses (RD) of T and OXA are respectively neutropenia using 1.5 mg/m<sup>2</sup>/d for 5 days for T and a cumulative neurosensory toxicity with 130 mg/m<sup>2</sup> for OXA. The non-overlapping clinical toxicity and the synergy reported *in vitro* led to this dose escalation study of the combination using an every 3 weeks schedule in advanced cancer patients (pts). OXA is given as a 2h infusion on day 1, prior to T which is given as a 30 min daily infusion from day 1 to 5. Presently, 4 dose levels (DL) have been studied: 65mg/m<sup>2</sup> OXA + 0.5, 0.75, or 1 mg/m<sup>2</sup> T, were the 3 first DL. The 4th DL was: 110 mg/m<sup>2</sup> OXA + 1 mg/m<sup>2</sup> T. **Results:** 22 pts enrolled and 106 cycles (cy) evaluable for toxicity. M/F: 9/13. Median age (years): 51 (34–73). Primary tumor was hepatocellular (7 pts), ovarian (4 pts) and renal carcinoma (3 pts), or miscellaneous (8 pts). 1st DL:

6 pts/33 cy; 2nd DL: 6 pts/40 cy. DLTs were: 1 septic shock with Gr4 febrile neutropenia (1 pt/1 cy), Gr4 thrombocytopenia (4 pts/4 cy). All DLTs were observed in pts with at least one of the following parameters: PS = 2, >2 previous chemotherapy regimens, Creatinin clearance <60 ml/min, (CRP × orosomucoid)/(albumin × pre-albumin) >1. Only pts who fit the above inclusion criteria were included at the 3rd (4 pts/20 cy) and 4th (6 pts/13 cy) DLs, and only one DLT occurred (Gr 4 neutropenia for more than 7 days). One partial response has been observed in an ovarian cancer patient pretreated with carboplatin and paclitaxel. **Conclusion:** We will now explore 110 mg/m<sup>2</sup> OXA + 1.25 mg/m<sup>2</sup> T. The RDs should be in selected pts close to the doses given as single agents.

**#348 Phase I Study of CAELYX® Prior to Daily × 5 TOPOTECAN q4w In Patients with Advanced Solid Tumors. Early Results of an Ongoing Phase I study.** N. Germann\*, M. Gross-Goupil\*, R. Jourdan\*, P. Pautier\*, C. Lhomme\*, K. Djazouli\*, M.E. Boutin-Tranchant\*, J.-P., Armand\*, E. Raymond\*. *Department of Medicine\*, Institut Gustave-Roussy, Villejuif, France, Schering-Plough\*, Levallois-Perret, France, SmithKline Beecham\*, Nanterre, France.*

**Rationale:** Unlike TOPOTECAN (TPT), CAELYX (Stealth stabilized liposomal doxorubicin - Doxil® - KLX) has a mild hematologic toxicity. Therefore, the nonoverlapping toxicity and the potential benefit of combining Topoisomerase I and II inhibitors made the KLX-TPT combination suitable for a phase I study. **Objectives:** The objectives were: (1) to determine the maximal tolerated dose (MTD), (2) to describe the dose limiting toxicity (DLT), (3) to recommend doses, and (4) to identify tumor types for phase II studies. **Treatment:** 100mg hydrocortisone and 300mg cimetidine were given prior to KLX. 5-HT3 antiemetic regimen was given daily 30 min. prior to chemotherapy. KLX was given on day 1, as a 60 min infusion, prior to TPT. TPT was administered as a 30 min. infusion daily × 5 days. Cycles were repeated every 4 weeks (d1=d28). The starting daily doses were 0.5 and for TPT and 35 mg/m<sup>2</sup> for KLX. **Results:** From 01/99, 9 patients (pts) were entered in this monocenter phase I clinical trial (M/F: 4/5; age 46–61, median: 55; WHO Performance status 0/1/2/4/2/3). Tumor types included: ovarian (2 pts), esophagus (1 pt), unknown primary (5 pts), and small cell lung carcinoma (1 pt). 3 pts received ≥ 2 prior lines of chemotherapy. 4 pts presented locally advanced diseases in the peritoneum and 1 in the lung. Metastatic sites were the lung in 3 pts, the pleura in 1 pt, the liver in 1 pt, lymph nodes in 1 pt, the spleen in 1 pt, and the adrenal gland in 1 pt. Febrile neutropenia and/or neutropenia lasting more than 7 days were DLTs observed in 3/6 pts at the dose level II which defined the MTD. One pt at dose level II experienced both grade 4 neutropenia, thrombocytopenia, and anemia requiring transfusions.

Dose level (DL)	Doses (mg/m <sup>2</sup> ) TPT/KLX	Pts/Cycles	Nb. of pts with dose reduction	Neutropenia		Thrombocytopenia Gr4
				Gr3	Gr4	
I	0.5/35	3/7	1	1	0	0
II	0.5/40	6/14	1	3	3	1

Other toxicities included gr. 2 nausea and vomiting in 1 pt and a gr 2 asthenia in 1 pt at dose level II. Two pts developed mild acute hypersensitivity reactions at the start of the 1<sup>st</sup> infusion of 40 mg/m<sup>2</sup> KLX (flushing, shortness of breath, facial swelling, tightness in the chest and throat) which resolved within few min. and required to slow down the infusion of KLX. Neither palmo-plantar erythrodysesthesia nor cardiotoxicity was observed. One minor response was observed in a pt with ovarian carcinoma refractory to cisplatin and paclitaxel. The study is ongoing to determine the dose to be recommended for phase II.

**#349 New HPLC method using UV detector for the estimation of Treosulfan in biological samples.** S Poondru, V Purohit, RE Parchment, RD Baynes, CK Grieshaber and BR Jasti. *Karman Cancer Institute and Dept. of Pharmaceutical Sciences, Wayne State University, Detroit, MI 48201.*

**Introduction:** Treosulfan, L-threitol 1,4-Bis(methanesulfonate), is a water soluble prodrug that gets converted to alkylating monooxides and diepoxides in physiological environment by non-enzymatic mechanisms. This drug is registered for ovarian cancer under the trade name Ovastat®. Currently the drug is in clinical trials for other cancer indication(s). **Purpose:** To develop a new high performance liquid chromatographic method using UV detector for the quantification of Treosulfan in biological samples such as plasma and urine and compare it with the existing methods. **Methods:** Aqueous solution (500 µL) of treosulfan (concentration range 100–1000 µg/mL) was treated with 0.5 mL of 1.17 M sodium diethylthiocarbamate in presence of 0.5 mL 100 mM ammonium acetate for ten minutes. The mixture was heated for 30 minutes at 50°C to facilitate the derivatization reaction. The reaction mixture was then extracted with 3 mL of ethyl acetate and dried under nitrogen. The residue was reconstituted in 200 L of methanol and 100 µL of it was injected on to the column. A high performance liquid chromatography system LC-HP 1100 series (Hewlett Packard Corporation) equipped with G1311A pump, G1313A auto sampler, G1315A diode array detector and Chemstation software was used in

the study. The samples were analyzed using methanol: water (80:20) mobile phase, at a flow rate of 1 mL/minute. A  $\mu$ -bondpak (250 $\times$ 4.6 mm) column was used for elution and the analytes were monitored at 254 nm wavelength using an UV detector. Biological samples were also processed similarly. **Results:** The retention times of treosulfan was found to be 12.8. The method showed excellent linearity for the detection of treosulfan in the range of 100  $\mu$ g/mL to 1000  $\mu$ g/mL. The reproducibility of the method was checked by analyzing the samples 5 times and the coefficient of variation was found to be less than 10% at all concentrations. Reproducibility and sensitivity of this method for treosulfan were similar to the published refractive index method. Urine samples collected from a patient treated with treosulfan were analyzed using published RI method and current UV methods. Concentrations obtained from both methods were similar. **Conclusions:** Based on the above results, this method can be used for the assay of treosulfan in biological samples.

**#350 Pharmacologic Issues for Fenretinide Chemotherapy (4HPR, NSC-374551)** RE Parchment, BR Jasli, TA Kocarek, RA Wiegand, J Kassab, W Wurster, KA Keyes, CK Grieshaber, and PM LoRusso. *Div of Hematology-Oncology, Karmanos Cancer Institute, Detroit, MI 48201 USA*

4HPR is a synthetic vitamin-A analog that has shown clinical promise in chemoprevention trials. It also induces apoptosis in cultured human tumor cells at low nanomolar concentrations and exerts anti-proliferative effects independent of differentiating effects, prompting clinical evaluation as a chemotherapeutic agent. During a Phase I dose escalation trial of oral 4HPR daily  $\times$  7 every 3 weeks, several pharmacological characteristics have emerged that could confound its clinical potential as a cytotoxic/cytostatic agent. Peripheral venous blood levels did not increase as dose increased from 1200 to 1700 mg/m<sup>2</sup> bid, nor did it change from 1200 mg/m<sup>2</sup> bid to tid. 4HPR interfered with CYP2D6 metabolism of oral dextromethorphan when co-administered on day-1 of treatment, but not when dextromethorphan was delayed 9-hours relative to the last dose of 4HPR, when highest peripheral blood levels were achieved from accumulating drug. This result is consistent with hepatic portal vein levels immediately following drug dosing not only exceeding the K<sub>i</sub> for CYP2D6 determined *in vitro*, but also exceeding peripheral venous blood levels. Either saturable absorption or a low affinity, high capacity, first-pass phenomenon during which liver extracts excess 4HPR from hepatic portal venous blood can explain these results. Further study of dosage [peak portal vein concentration] effects on peripheral plasma concentration, CYP2D6 inhibition, all-trans-retinol (ATROL) levels and nyctalopia [the likely dose-limiting toxicity when retinoids decline] is required to distinguish these alternatives. *In vitro* studies of 4HPR on normal myeloid progenitors (CFU-GM) showed that several physiological substances antagonize 4HPR cytotoxicity, including thymidine, folates, and ATROL. Thus, levels of these endogenous compounds must be considered when relating *in vitro*, preclinical and clinical findings. Thymidine and leucovorin antagonism indicate that pyrimidine metabolism is one target of 4HPR in proliferating cells. Supported by grant UO1-CA 62487.

## POSTER SESSION 4 SECTION 1: SIGNAL TRANSDUCTION/SIGNALING TARGETS

**#351 Phase I trial of SU101 in combination with mitoxantrone in the treatment of patients with hormone refractory prostate cancer.** Kabinavar, F.; Hannah, A.; Rosen, P.; Sawyers, C.; Prager, D.; Baker, C.; DePaoli, A.; and Cropp, G. *UCLA School of Medicine - Jonsson Comprehensive Cancer Ctr., Los Angeles, CA SUGEN, S. San Francisco, CA.*

There are no current approved effective systemic therapies for hormone refractory prostate cancer (HRPC). Consistently elevated expression of the platelet-derived growth factor (PDGF) alpha-receptor in human metastatic prostate cancer bone marrow samples has been reported. In Phase 1 and 2 studies, SU101, an inhibitor of PDGF-mediated signaling, has shown potential clinical activity as a single agent in HRPC patients, resulting in amelioration of bone pain and decreases in PSA. These observations led to a Phase 1 dose escalating trial of SU101 in combination with mitoxantrone. HRPC patients receive once weekly SU101 infusions (200, 300 or 400 mg/m<sup>2</sup>) for 12 weeks with mitoxantrone (12 mg/m<sup>2</sup>) administered at 3-week intervals and prednisone 5 mg po twice daily. Patients are followed for pain assessment, PSA, PAP, bone scan, measurable/evaluable disease, SU101 pharmacokinetics and safety parameters. Enrollment is ongoing with 18 patients enrolled to date: median age 72 years; median KPS 90%; median PSA 126 ng/mL; half of the patients had one prior cytotoxic therapy. Of the 18 patients, 7 patients have completed 12 weeks of therapy; of these, 3 are receiving extended therapy. Seven patients are off-study: 3 due to adverse events, 2 due to disease progression, 1 due to death, and 1 due to patient request. Four patients are continuing at this time. Nine patients are currently evaluable for PSA responses after 6 or 12 weeks of therapy: 4 PR (>50% decrease), 1 MR (25%-50% decrease), 2 SD (<25% increase), and 2 PD (>25% increase). Of the 16 patients with

pain symptoms at baseline on the Brief Pain survey, 10 patients are evaluable at this time, 6 of whom have a 2 point or greater decrease in pain on a 10 point scale without an increase in pain medications. The four patients with a PSA partial responses all reported pain relief. Neutropenia is the primary toxicity, occurring as Grade 1 in 2.5% of mitoxantrone cycles, Grade 2 in 18%, Grade 3 in 36% and Grade 4 in 41%; no instances of febrile neutropenia have been observed. A Phase 3 study using SU101 in combination with mitoxantrone and prednisone is underway.

**#352 Farnesyltransferase Inhibitors: Mechanism of antineoplastic action and basis for cytostatic versus cytotoxic response.** W. Du, A. Liu, and G.C. Prendergast. *The Wistar Institute, Philadelphia, PA USA 19104; Glendolen Laboratory, Dupont Pharmaceuticals, Glendolen, PA USA 19036.*

**INTRODUCTION.** Farnesyltransferase inhibitors (FTIs) are in clinical trials, yet the exact basis for their antineoplastic effects and for their cytotoxic versus cytostatic actions remain obscure. Here we provide evidence that the altered prenylation of RhoB which is elicited by FTI treatment is sufficient to mediate growth inhibition in human carcinoma cells, and that the status of the P13<sup>K</sup>-AKT survival pathway determines whether cells respond to this event by apoptosis or cell cycle inhibition.

**RESULTS.** We showed previously that FTI treatment causes an elevation in the levels of geranylgeranylated species of RhoB (RhoB-GG) and that this event is sufficient to mediate phenotypic reversion and growth inhibition in Ras-transformed fibroblasts. In this study, we observed that elevation of RhoB-GG is also sufficient to mediate growth inhibition in FTI-sensitive but not FTI-resistant human carcinoma cell lines. Similar to FTIs, Ras or p53 status was not correlated with response. p21<sup>WAF1</sup> was neither consistently induced nor required, suggesting this effect of FTIs or RhoB-GG may be correlative rather than causative. Consistent with this likelihood, some cells exhibited increased apoptotic index or accumulation in G2/M phase.

While FTIs are cytostatic to Ras-transformed cells they can rendered cytotoxic if cells are deprived of either IGF-1 or substratum attachment. Since each of the latter activates the P13<sup>K</sup>-AKT pathway, we examined a role for it in dictating the response. LY294002, a P13<sup>K</sup> kinase inhibitor, shifted the response of Ras-transformed cells from arrest to apoptosis. Similar treatments did not affect normal or Raf-transformed Rat1 cells, pinpointing a difference in survival mechanism. Constitutive activation of AKT blocked FTI-induced death under appropriate conditions. These findings (1) confirm the growth inhibitory action of RhoB-GG in human malignant epithelial cells and explain how FTIs block growth of such cells lacking Ras mutations, and (2) suggest that combinatorial inhibition of Rho signaling by FTIs and AKT signaling by other agents may improve clinical response and widen therapeutic index.

**#353 Effects of prenyltransferase inhibitors, FTI-277 and GGTI-298, on human lung cancer cells.** Iizuka Masayoshi, Inoue Shoichi, Hamilton Andrew, and Sebti Said. *Dept. Environ. Med. and Informat., Graduate sch. Environ. Earth Sci., Hokkaido Univ. and Dept. Biochem. and Molecul. Biol., H. Lee Moffitt Cancer Ctr and Res. Inst., Univ. South Florida*

Ras prenylation is essential for Ras to be localized on the cytoplasmic membrane and to play its role in signal transduction. Therefore, the inhibition of Ras prenylation may induce cell kill effects by disturbing signal transduction. To test the effects of two Ras prenylation inhibitors, FTI-277 and GGTI-298, we investigated expression levels and localization of four kinds of Ras in nine human lung cancer cells and evaluated cell growth-inhibitory effects of FTI-277 and GGTI-298.

**Material and method.** Nine human lung cancer cell lines were used. Ras expression levels were detected by western blotting. Ras localization was observed by confocal laser scanning microscopy. Cell viability was evaluated by MTT assay. Proportions of apoptotic cells and cell cycle phases were analyzed by flow cytometry.

**Results.** The cells tested expressed mainly K-Ras 4B and N-Ras by Western blotting. However, confocal laser scanning microscopic observation showed that K-Ras 4B was localized as a granule around the cytoplasmic membrane, in the cytosol, and near the nucleus, whereas N-Ras was localized diffusely in the cytosol. GGTI-298 was more effective to inhibit cell growth in all human lung cancer cell lines tested than FTI-277. GGTI-298 induced apoptosis gradually with increasing concentrations, whereas FTI-277 induced apoptosis at more than 10  $\mu$ M. From these results we concluded that GGTI-298 was more effective on human lung cancer cell lines than FTI-277. Localization of Ras is an important factor to evaluate effects of prenyltransferase inhibitors, because localization of Ras may be changed in each cell cycle phase.

**#354 The farnesyltransferase inhibitor, FTI-277 targets the phosphatidylinositol 3-kinase/AKT2 pathway to induce apoptosis.** Jiang, Kun, Coppola, Domenico, Crespo, Nichole C., Nicolsa, Santo V., Hamilton, Andrew D., Cheng, Jin Q. and Sebti, Said M. *Drug Discovery Program, Department of Pathology and Department of Biochemistry and Molecular Biology, College of Medicine and H. Lee Moffitt Cancer Center, University of South Florida, Tampa, Florida 33612, and Department of Chemistry, Yale University, New Haven, CT 06511.*



The mechanism by which FTIs inhibit tumor growth is not well understood. Previous work showed that FTIs induce apoptosis only when Ras-transformed cells are deprived of serum or attachment. Here we demonstrate that FTI-277 induces apoptosis of attached human cancer cells in presence of serum. Furthermore, we demonstrate that FTI-277 inhibits PI 3-kinase/AKT2 mediated growth factor- and adhesion-dependent survival pathways and induces apoptosis in human cancer cells that overexpress AKT2. Overexpression of AKT2, but not oncogenic H-Ras, sensitizes NIH 3T3 to FTI-277; and high serum level prevents FTI-277-induced apoptosis in H-Ras but not AKT2 transformed NIH 3T3 cells. A constitutively active AKT2 rescues human cancer cells from FTI-277-induced apoptosis. FTI-277 inhibits IGF1-induced PI 3-kinase and AKT2 activation and subsequent phosphorylation of the pro-apoptotic protein BAD. Integrin-dependent activation of AKT2 is also blocked by FTI-277. Thus, one mechanism by which FTIs induce apoptosis is by inhibiting the PI 3-kinase/AKT2 pathways.

**#355 Constitutive kinase activity and survival of non-small cell lung cancer cells: new molecular determinants of therapeutic resistance in lung cancer.** Brognard, J., Clark, A., Oppolner, A., and Dennis, P. Department of Developmental Therapeutics, Medicine Branch, NCI, NIH, Bethesda, MD 20889.

Lung cancer is the most lethal form of cancer in the U.S. The most common form of lung cancer, non-small cell lung cancer (NSCLC), is quite resistant to both chemotherapy and irradiation, and the biochemical basis for this resistance is not well understood. To study the role of kinase activation in NSCLC cells survival, we chose 10 NSCLC cell lines that varied histologically and in p53, ras, and Rb status. Initial studies showed that all 10 cell lines were resistant to apoptosis caused by serum starvation,  $\gamma$  irradiation, and chemotherapy, as measured by the formation of sub 2N DNA. Because growth factors offered no additional protection from apoptosis, we hypothesized that NSCLC cells constitutively activate kinases that enhance cellular survival. Immunoblot analysis using antibodies raised against native and phosphorylated forms of Akt/PKB, MAPK, and PKC $\delta$ , kinases previously shown to promote cellular survival in other systems, demonstrated that 10/10 cell lines maintain phosphorylation of MAPK and PKC $\delta$  under serum starvation conditions (0.1% FBS for 48 hr). 6 of 10 cell lines maintain Akt/PKB phosphorylation under identical conditions. Phosphorylation of MAPK and Akt in serum starvation correlated with increased kinase activity as assessed by *in vitro* kinase assays with relevant substrates (GSK $\alpha$  for Akt, MBP for MAPK).

To demonstrate the role of activated MAPK, Akt, and PKC $\delta$  in NSCLC survival, inhibitors of each pathway were used singly and in combination with  $\gamma$  irradiation or chemotherapy. PD98059 completely inhibited phosphorylation of MAPK and increased the fraction of cells in G1 in all 5 cell lines tested, but had no effect on apoptosis caused by irradiation or chemotherapy. In contrast, LY294002, which completely inhibited Akt phosphorylation, increased apoptosis 4–5 fold in 4 of 5 cell lines when combined with either  $\gamma$  irradiation or chemotherapy. Rottlerin, an inhibitor of PKC $\delta$  activity, did not inhibit PKC $\delta$  phosphorylation, but increased apoptosis 10 fold in all 5 cell lines. Together, these studies indicate that NSCLC cell lines endogenously activate at least 3 kinases known to promote survival, and that inhibitors of Akt and PKC $\delta$  dramatically increase apoptosis caused by irradiation and chemotherapy. Targeting pathways involving Akt and PKC $\delta$  in patients with NSCLC may therefore provide therapeutic benefit by increasing the effectiveness of conventional therapy.

**#356 Serum deprivation activates Na<sup>+</sup>/H<sup>+</sup> exchanger and invasion via PKA-dependent phosphorylation of RhoA in human breast cancer cells.** Reshkin S.J., Bellizzi A., Paradiso A., Tommasi S., Casavola V. Dept. Gen. and Environ. Physiology, Univ. Bari, and Lab. Clin. Exp. Oncology, Oncol. Inst. Bari, Bari, Italy.

The acidic extracellular pH of tumors plays a crucial role in the invasive process while the alkaline intracellular pH characteristic of cancer cells stimulates movement. We have previously shown that low nutrient conditions, i.e. serum deprivation, stimulates the Na<sup>+</sup>/H<sup>+</sup>-exchanger (NHE) in human breast cancer cells and also confers increased tumor motility and invasive ability that were abrogated by specific inhibition of the NHE. A reversal of normal phosphoinositide 3-kinase (PI3K) action found in serum replete conditions is involved in this up-regulation of the NHE. The regulation of this event is probably orchestrated by a complex system involving several other signaling pathways such as MAP kinases, serine/threonine kinases, small G-proteins, etc. These signaling pathways could have a role in the pathophysiological response of tumor cells to the tumor microenvironment. While much has been learned of the kinetics and action at all the levels of these cascades in normal cells, very little is known about their actual regulation in neoplastic cells and their role in neoplastic processes and malignant progression. The stimulation in the tumor cell NHE activity by serum deprivation was potentiated by pharmacological inhibition of PI3K and of p38 MAP kinase while inhibition of Protein Kinase A abrogated the stimulation. C3 exotoxin and N19RhoA mimicked the effects of activation of PKA on NHE activity while CNF-1 and V14RhoA mimicked inhibition of PKA on NHE activity. Serum deprivation increased the PKA-dependent phosphorylation of RhoA with a time course similar to that for the activation of the NHE. A phosphorylation deficient mutant of RhoA

abrogated the stimulation of the NHE. These results are consistent with a model in which RhoA is phosphorylated by PKA upon serum deprivation leading to its inactivation with subsequent inhibition of PI3K and p38 MAPK leading to the stimulation of the NHE.

**#357 Adenosine Acts as a chemoprotective agent by stimulating G-CSF production: A role for A1&A3 adenosine receptors.** Fishman P., Bar-Yehuda S., Farbstein T., Barer F. and Ohana G. Laboratory of Clinical and Tumor Immunology, The Felsenstein Medical Research Center, Tel-Aviv University, Rabin Medical Center, Petach-Tikva, Israel.

In this study, we demonstrated the capability of adenosine to act as a chemoprotective agent by preventing myelosuppression. Adenosine, a purine nucleoside present in plasma and other extracellular fluids, interacts with cell membranes by binding to three different classes of cell-surface receptors, A1, A2 and A3. In this study, we showed that adenosine stimulates the proliferation of murine bone marrow cells *in vitro*. Using three adenosine receptor antagonists, DPCPX, anti-A1, DMPX, anti-A2 and MRS-1220, anti-A3, we verified that adenosine induced bone marrow cell proliferation through binding to its A1 and A3 receptors.

This result was further corroborated by showing that the two selective A1 and A3 receptor agonists (CPA and IB-MECA, respectively), induced bone marrow cell proliferation in a similar manner to adenosine.

Adenosine was shown to induce this stimulatory effect on bone marrow cells, through the induction of G-CSF production, which was also mediated via the interaction of adenosine with the A1 and A3 receptors. These receptors are functionally coupled with decreased intracellular cAMP levels which may be responsible for the G-CSF production and bone marrow cell proliferation.

*In vivo* studies demonstrated that low dose adenosine (0.25 mg/kg) administered after chemotherapy, restored the number of leukocytes and neutrophils to normal levels, compared with the decline in these parameters after chemotherapy alone. It is suggested that low dose adenosine, which is being used clinically, may be applied as a chemoprotective agent.

**#358 PHOSPHORYLATION OF CYCLIC-AMP RESPONSE ELEMENT BINDING PROTEIN (CREB) UPON CHRONIC EXPOSURE TO MORPHINE IN HEK-293 CELLS.** Mazarakou, G., Merkouris, M., and Georgoulas Z. Institute of Biology, N.C.S.R. "D", 153 10 Ag. Paraskevi, Athens, Greece. University of Chicago, Dept. of Pediatrics, Chicago, USA.

Opioid receptors belong to the large superfamily of G protein coupled receptors and modulate a variety of physiological responses in the nervous system. Opioid receptors are classically described as coupling to members of the G $\alpha$ /G $\alpha$  family, and their activation results in the inhibition of adenylate cyclase and/or the regulation of a variety of ion channels and other effector systems. Adenylate cyclase regulation represents an important part of the opioid response. It has been implicated in the control of expression levels of various transcription factors (CREB, AP1, etc), as well as in the modification of components of the intracellular signal transduction cascades that regulate the expression of target genes. In this regard, we have found that chronic morphine treatment of EE-tagged HEK 293 cells stably transfected with the  $\mu$ -opioid receptor results in an upregulation of adenylate cyclase activity and stimulation of cAMP response element binding protein (CREB) phosphorylation, which is thought to be mediated by protein kinase A (PKA) activation. By contrast, acute exposure to morphine causes a decrease in adenylate cyclase inhibition and attenuation of CREB phosphorylation. These results provide novel information on the mechanisms through which administration to opiates alters gene expression in specific target neurons and thereby induces tolerance and dependence. Supported by YPER06 and CHRX-CTS 1-0689 grants to ZG.

**#359 Selective loss of response to activators or inhibitors of PKC in prostate cancer cells: p21/cyclin D1 balance.** Blagosklonny M.V., Dix6n S.C., Figg, W.D. Medicine Branch, Division of Clinical Sciences, National Cancer Institute, NIH, Bethesda, MD.

Resistance of human metastatic prostate cancer to chemotherapy and multifarious role of PKC in cell growth and differentiation has prompted investigation of two opposite approaches: activation of PKC by phorbol ester (PMA) or inhibition of PKC by UCN-01. While LNCaP cancer cells were very sensitive to growth inhibition by PMA (IC<sub>50</sub> = 0.5–1 nM), DU145, PC3, and PC3M, more advanced cancer cells, were resistant (IC<sub>50</sub> > 5000 nM). The growth of PMA-resistant cells but not LNCaP was inhibited by UCN-01 with an IC<sub>50</sub> of 200–400 nM. Low doses (25–50 nM) of UCN-01 abrogated PMA-induced p21<sup>WAF1/CIP1</sup> and growth arrest in LNCaP cells, indicating that PMA-induced growth arrest is due to activation and not by "inhibition" of PKC. On the other hand, low doses of UCN-01 were not growth inhibitory, indicating that basal levels of PKC activity is dispensable for proliferation of prostate cancer cells. 200–400 nM UCN-01 downregulated cyclin D1, and induced p21 and morphological differentiation of PMA-resistant cancer cells. This is conceivable that combining the induction of p21 with the down-regulation of cyclin D1 resulted in growth arrest by UCN-01, whereas, like wt p53, PMA induces growth arrest due to a dramatic induction of p21 in cell-type selective manner. Proliferating normal prostate epithelium cells were sensitive to both PMA and UCN-01. Therefore, loss of sensitivity to activators or to inhibitors of PKC accompanies progression of prostate cancer.

Our data suggest either inhibition or activation of PKC may be utilized in the treatment of prostate cancer. Although this strategy would require criteria to predict PMA- or UCN-01 sensitivity, initial treatment with PMA and treatment with UCN-01 of relapse cancer warrant investigation.

**#360 Regulation of ornithine decarboxylase (ODC) expression in human glioblastoma cell lines involves through distinct protein kinase C (PKC)- and epidermal growth factor receptor (EGFR)-mediated mechanisms.** Brondani da Rocha, A., Mans, D.R.A., Lenz, G., Fernandes, K., de Lima, C., Gonçalves, D., Ruschel, C., Schwartsmann, G. *South-Am. Off. Anticancer Drug Dev. (SOAD), Luth. Univ., Canoas, Dept. Biochem., Fed. Univ. Rio Grande do Sul, Porto Alegre, RS, Brazil.*

We examined in the U-373, U-138, and U-87 human glioblastoma cell lines the involvement of EGFR-, PKC-, and mitogen-activated protein kinase/extracellular-signal-regulated kinase (MEK)-mediated mechanisms in ODC induction. To this end, 2-days serum-starved cells were stimulated with recombinant human EGF (rhEGF) 25 ng/ml or phorbol 12-myristate 13-acetate (PMA) 100 nM in the absence or presence of DL- $\alpha$ -difluoromethylornithine (DFMO), PD 098059 (20  $\mu$ M), and/or GF 109203X (5  $\mu$ M) or calphostin C (40 nM). PKC and MEK activities were determined by histone phosphorylation and an in-gel kinase assay, respectively, and related to ODC mRNA and activity levels as well as cell growth rates, as assessed by Northern blotting, a  $^{14}$ C release assay, and a  $^3$ H-thymidine incorporation assay, respectively. Whereas only 5% of control cells were radiolabeled at 48 h, this was the case with 90 and 60% of rhEGF- or PMA-treated cells, respectively. DFMO inhibited the cell growth promotion in a dose-dependent manner, supporting a direct involvement of ODC in this phenomenon. Stimulation of the cells with rhEGF led further to a 2-fold increase in peak MEK activity levels which was accompanied by a 2-3-fold increase in peak ODC mRNA and activity levels. No significant changes were observed in PKC activity levels. The rhEGF-stimulated ODC expression decreased by 2/3 in the presence of PD 098059, by 1/3 with GF 109203 X, and almost completely with these compounds together. These data suggested the participation of MEK in the rhEGF-stimulated ODC expression, but also that of additional mechanisms. PMA considerably mimicked the stimulatory effects of rhEGF on ODC mRNA and ODC and MEK activity levels, but caused in addition a 2-fold increase in those of PKC. PD 098059, GF 109203X, or calphostin C, either alone or together, completely abolished the PMA-stimulated ODC expression. Thus, both PKC and MEK were probably involved in the PMA-inducible ODC expression. Together, our data suggest that ODC gene transcription in the presently used model was activated through the stimulation of a MEK-mediated module that in its turn, received input from EGFR- as well as PKC-mediated mechanisms.

**#361 Inhibition of human prostate cancer proliferation *in vitro* and in a mouse model by a compound synthesized to block  $Ca^{2+}$  entry.** Haverstick, Doris M., Heady, Tiffany N., Macdonald, Timothy L., and Gray, Lloyd, S. *Departments of Pathology and Chemistry, University of Virginia, Charlottesville, VA.*

Accelerated  $Ca^{2+}$  entry may be one component of the pathway regulating the proliferative phenotype of some types of cancer. Thus, a pharmacological agent with the ability to retard  $Ca^{2+}$  influx in susceptible cancers might inhibit proliferation by a cytostatic mechanism rather than by inducing cytotoxicity. Extensive screening of existing inhibitors of  $Ca^{2+}$  entry demonstrated the merit of this approach. Based on these known compounds, we have developed a small library of novel compounds that block  $Ca^{2+}$  entry induced by occupancy of the P2 receptor in two prostate cancer cell lines and inhibit proliferation of these cells *in vitro* to various degrees. Details of the syntheses of these compounds are shown in the companion abstract: Novel channel blockers as cytostatic cancer agents, Heady *et al.*

One of these agents, named TH-1177, was used to treat SCID mice inoculated with the human prostate cancer line PC-3. Although the doses used and treatment schedule were chosen arbitrarily, treatment extended the mean lifespan of mice bearing tumors by 38%. Treatment of mice without cancer at doses 18 times that used in mice bearing tumors was not associated with any obvious toxicity either grossly or on histological examination. These results suggest that novel, cytostatic agents with efficacy against human prostate cancer cells can be developed by chemical synthesis of agents directed at the  $Ca^{2+}$  entry pathway.

**#362 Regulation of Raf-1 by the p21 activated protein kinases (PAK).** Marshall, Mark T., Sun, Huaiyu, Diaz, Bruce T., Barnard, Darlene and King, Alastair. *Lilly Research Laboratories, Indianapolis, IN, USA 46285f. Indiana University School of Medicine, Indianapolis, IN, USA 46202.*

We have shown previously that a p21-activated protein kinase (PAK) specifically phosphorylates Raf-1 on serine 338 and that a constitutively active PAK mutant can activate Raf-1 in COS7 cells in a serine 338-dependent manner. In this study, the contribution of small GTPases to Raf-1 activation through PAK was determined. Cdc42V12 and Rac1V12, but not RhoAV14, modestly increased Raf-1 activity. When co-transfected with PAK3, Cdc42V12 significantly stimulated Raf-1 as well as the membrane-targeted form of Raf-1, Raf-CaaX. Raf-1 mutants defective in Ras binding were also found to be activated by Cdc42V12 and PAK3, suggest-

ing that the activation of Raf-1 by Pak is independent of a physical interaction between Ras-GTP and Raf-1. Moreover, we observed that RasV12 was capable of stimulating the activity of membrane localized Raf-CaaX mutant proteins which were defective for Ras association, suggesting that Ras-GTP triggers an alternative Raf-1 activation pathway distinct from a physical Ras-Raf interaction. This pathway requires membrane association of Raf-1 in order to function. The activation of these Raf-CaaX mutants by RasV12 was found to be dependent upon PAK. We will also show evidence that PI3-kinase function lies upstream of PAK for Raf-1 activation, supporting our hypothesis that the Ras-dependent Raf-1 pathway is co-regulated by the parallel Ras-dependent PI3-kinase pathway through PAK. These findings provide a mechanism for the observation that inhibition of PAK function reverses oncogenic Ras transformation (Field, J. 1998). Therefore the p21-activated protein kinases appear to be valid targets in proliferative diseases.

**#363 Localization of the novobiocin binding site on heat shock protein 90 (Hsp90) to the carboxyl terminal dimerization domain: Implications for alternative inhibition of Hsp90 activity.** Marcu, Monica G., Schulte, Theodor W. and Neckers, Leonard M. *Department of Cell and Cancer Biology, Medicine Branch, National Cancer Institute, NIH, 9610 Medical Center Drive, Rockville, MD 20850.*

Heat shock protein 90 (Hsp90), one of the most abundant chaperone proteins in eukaryotes, is involved in the folding of signal-transducing molecules such as steroid hormone receptors and protein kinases. Sequence alignment and functional studies suggest that Hsp90 is composed of two highly conserved domains (N- and C-terminal chaperone sites) separated by a charged region. Recently, it was shown that the N-terminus contains a non-conventional binding site for ATP/ADP, which is closely related to the ATP-binding site of bacterial gyrase I. The antitumor agents geldanamycin (GA) and radicicol bind specifically at this site, competing with ATP and inducing destabilization and depletion of Hsp90-dependent client molecules. We have previously demonstrated that the gyrase I inhibitor novobiocin is also able to interact with Hsp90, altering the chaperone's affinity for immobilized GA and causing *in vitro* and *in vivo* depletion of key regulatory Hsp90-dependent kinases including Raf-1 and p185erbB2. Due to its low toxicity and established pharmacokinetics, novobiocin may be a promising therapeutic adjuvant for specific tumors over-expressing Hsp90-dependent oncogenic molecules. Using deletion/mutation analysis and immobilized novobiocin, GA and ATP, we now demonstrate that the novobiocin binding site on Hsp90 overlaps the chaperone's C-terminal dimerization domain, where, surprisingly, GA and ATP are also found to interact and to compete for binding with novobiocin. This binding site is partially masked in the full-length wild type protein, but is readily apparent in Hsp90 constructs either containing point mutations in the amino terminal nucleotide binding domain, or comprised solely of the carboxyl terminal portion of the protein. Additionally, novobiocin interferes with association of several co-chaperones (Hsp70, p23) known to bind to Hsp90 in the vicinity of its dimerization domain. These results suggest that the two chaperone domains of Hsp90 are functionally more related than was previously appreciated. Further, these data identify a second site on Hsp90 where the binding of small molecule inhibitors can significantly impact the chaperone's ability to bind to and stabilize its client proteins.

**#364 Induction of differentiation and apoptosis in human breast cancer cell lines by modified geldanamycin derivatives (17-AAG).** Münster, Pamela N.; Zheng, Fuzhong F.; Srethapakdi, Mary; Sausville, Edward; Rosen, Neal. *Memorial Sloan-Kettering Cancer Center, New York, NY 10021 and National Cancer Institute, Bethesda, MD 20892.*

The ansamycin antibiotic geldanamycin (GM) is novel cytotoxic drug that binds to a specific pocket of the protein chaperone hsp90. Occupancy of this pocket by drug results in the proteasomal degradation of several key signaling proteins including steroid receptors, Raf kinase and transmembrane tyrosine kinases. HER2 is one the most sensitive targets. GM causes G1 cell cycle arrest and subsequent differentiation and apoptosis. We found that this block is Rb dependent, Rb negative cells block in mitosis and undergo apoptosis. However, unacceptable toxicity of GM required the development of a less toxic compound. A derivative of GM, 17-allylaminoGM (17-AAG), is less toxic and equally effective in cell lines and tumor models. Phase I trials of 17-AAG are currently ongoing. We evaluated the effects of 17-AAG on several breast cancer cell lines with various levels of HER2 expression. 17-AAG inhibited cell growth in all cell lines, but cell lines with HER2 amplification were 10-100 fold more sensitive. 17-AAG caused near complete degradation of Her2/neu protein within 24 h, Rb hypophosphorylation and rapid decrease of D cyclins. Cells underwent profound morphological changes including flattening and enlarging of the cytoplasm resulting in an increased cytoplasmic:nuclear ratio. Exposure to 17-AAG caused significant intracellular lipid accumulation and the induction of milk fat globule proteins. This transient differentiation was followed by apoptosis. In cells with high HER2 expression, apoptosis occurred earlier and at lower concentrations. In cells that lack Rb, cells underwent apoptosis, but differentiation was not observed. However, when these cells were transfected with Rb, 17-AAG caused G1 block and differentiation followed by apoptosis. These data suggest that 17-AAG inhibits proliferation and causes apoptosis of breast cancer cells with both wild type and mutated Rb, but the mechanism is different. Breast cancer cell



lines that overexpress HER2 are much more sensitive. These findings will be instrumental for the selection of patients who are most likely to benefit from this drug and the design of combinations of 17-AAG with other cytotoxic agents that induce apoptosis by a cell cycle specific block.

**#365** A small molecule, erbB kinase inhibitor blocks growth and invasion of human breast cancer cells and sensitizes them to ionizing radiation. Woods Ignatoski, Kathleen M., Rao, Geetha, and Ethier, Stephen P. Department of Radiation Oncology, University of Michigan Medical School, University of Michigan Comprehensive Cancer Center. Ann Arbor, MI 48109

Amplification and overexpression of receptor tyrosine kinases occurs in many human breast cancers (HBC). The activity of these receptors appears to play a role in the etiology of the disease. Our laboratory isolated a series of HBC cell lines and oncogene transformed human mammary epithelial cell lines that overexpress activated forms of different erbB receptors, including SUM-149PT (EGFR+/erbB-2-) and H16N2-erbB-2 (EGFR+/erbB-2+). These cell lines grow in a growth factor-independent and anchorage-independent manner and invade naturally occurring basement membranes. PD183805, a small molecule tyrosine kinase inhibitor that is erbB-specific, blocked growth of HBC cells and inhibited their ability to invade basement membranes. The compound had no effect on erbB-negative HBC cells.

Because PD183805 inhibits HBC cell growth and invasion, it has potential therapeutic value. Therefore, we tested its effect on HBC cells in conjunction with ionizing radiation (IR). IR had only a modest effect on the clonogenic survival of SUM-149PT cells. To examine the interaction of PD183805 and IR on SUM-149PT cells, cells were exposed to three 5 Gy fractions of  $\gamma$ -radiation over a five day period in the presence or absence of the compound. Exposure of SUM-149PT cells to 15 Gy (3 fractions) decreased the clonogen number by a factor of 100 compared to nonirradiated cells. The same radiation dose delivered to cells exposed continuously to PD183805 decreased clonogen number by an additional factor of 70 over that obtained with radiation alone.

These data show that PD183805, an irreversible inhibitor of the erbB tyrosine kinases, is a potent inhibitor of EGFR-mediated growth and invasion and potently enhances radiation-induced cell killing.

**#366** Dominant-negative MEKK1 blocks cisplatin-induced apoptosis but does not alleviate cell cycle blocks in 12V-Ras transformed fibroblasts. Viktorsson, K., Helden, T., Molln, M., Akusjärvi, G., Linder, S. and Shoshan, M. Cancer Center Karolinska, Karolinska Institute and Hospital, S-171 76 Stockholm, Sweden. Dept. of Microbiology, Uppsala University, S-751 23 Uppsala, Sweden.

Mutationally activated Ras is involved in tumor progression and likely also in resistance to anticancer therapy. Short-term viability assays showed that Ras2:3 cells were more sensitive to cisplatin than were FR3T3. By contrast, Ras2:3 showed higher clonogenic survival. This discrepancy could be explained by a higher cisplatin sensitivity of FR3T3 cells at low cell densities, i.e. conditions used for clonogenic assays. Cisplatin induced apoptosis was approximately 2-fold higher in Ras2:3 cells than in FR3T3. Cell cycle progression was differentially affected by cisplatin in normal and transformed fibroblasts. FR3T3 cells showed a G2 arrest 24 hrs after cisplatin treatment, while Ras2:3 showed a prominent S-phase delay. Whereas apoptosis was in both cell lines blocked by a dominant-negative mutant of MEKK1, this mutant did not affect either cell cycle block. The results indicate that cisplatin sensitivity of Ras2:3 cells is due to increased activation of a specifically apoptotic response which involves MEKK1 signalling. By contrast, cisplatin-induced cell cycle blocks do not depend on MEKK1 signalling.

**#367** Analysis of the mechanism of inhibition of apoptosis by a dominant negative mutant of MEKK1. Mandic, A., Viktorsson, K., Linder, S. and Shoshan, M. Cancer Center Karolinska, R8:03, Karolinska Institute and Hospital, S-171 76 Stockholm, Sweden.

A recombinant adenovirus was constructed which expresses a dominant negative mutant of MEKK1 under the control of an inducible promoter. dnMEKK1 was found to block cisplatin induced apoptosis of human melanoma cell lines. dnMEKK1 did not, however, block the induction of JNK1/2 observed after cisplatin treatment. Experiments where dnMEKK1 expression was induced at different times after cisplatin treatment showed that dnMEKK1 expression was not required during the early phases after treatment to block apoptosis. Analyses of caspase activation dnMEKK1 expressing cells are ongoing. Preliminary results indicate that dnMEKK1 blocks apoptosis at a late stage.

**#368** Activation of JNK1 correlates to cisplatin sensitivity in a panel of human melanoma cell lines. Viktorsson, K., Mandic, A., Linder, S. and Shoshan, M. Cancer Center Karolinska, R8:03, Karolinska Institute and Hospital, S-171 76 Stockholm, Sweden.

A panel of human melanoma cell lines was characterized with respect to sensitivity to the DNA damaging anticancer agent cisplatin. Signalling in the JNK and ERK pathways was investigated in cisplatin sensitive and resistant cell lines. Cisplatin was found to induce an activation of JNK1/2 and ERK1/2 in some, but not all, cell lines. JNK was activated during the

first few hours after cisplatin treatment, and during late phases during the onset of apoptosis. Neither early or late activation of JNK was observed in cisplatin resistant melanoma cell lines. JNK activation did not correlate to induction of c-jun mRNA expression. Furthermore, we demonstrate that cisplatin induces apoptosis in a resistant melanoma cell line can be increased by infection with a recombinant adenovirus expressing a dominant positive mutant of MEKK1.

**#369** The effect of the S-alkyl chain length on the anti-leukemic potency of cysteine chloromethyl ketone derivatives. Perrey, D.A., Narla, R.K., Navarra, C.S., and Uckun, F.M. Drug Discovery Program, Parker Hughes Cancer Center, Hughes Institute, 2665 Long Lake Road St. Paul, MN 55113.

Cysteine chloromethyl ketone derivatives display significant cytotoxicity toward both pre-B acute lymphoblastic leukemia (ALL) (Nalm-6) and T-ALL (Molt-3) cell lines. These compounds were designed to act as inhibitors of Ras endoprotease, an enzyme involved with one of the vital posttranslational events which leads to active Ras protein. Following the discovery of our lead compound, N-acetyl-S-dodecyl-Cys chloromethyl ketone (HI-131) which exhibited potent anti-leukemic activity *in vitro* as well as *in vivo*, we sought to determine the effect variation of this S-alkyl chain length would have on the efficacy of the compounds. We have synthesized 19 cysteine chloromethyl ketone derivatives, systematically varying the S-alkyl substituent from methyl to dodecyl (1-22 carbons long). *In vitro* evaluation of activity of these compounds against Nalm-6 and Molt-3 cell lines showed that compounds with a side chain of 5-15 carbons was highly effective as an anti-leukemic agent, giving  $IC_{50}$  values in the range of 1-10  $\mu$ M. The best compounds were N-acetyl-S-undecyl-Cys chloromethyl ketone (HI-321) ( $IC_{50}$  = 1.7  $\mu$ M against Nalm-6) and N-acetyl-S-hexyl-Cys chloromethyl ketone (HI-357) ( $IC_{50}$  = 0.7  $\mu$ M against Molt-3) which showed slightly better activity than HI-131. The biological effect of these compounds *in vitro* is characterized by destruction of the cytoskeleton, mitochondrial membrane depolarization and apoptosis as determined by confocal laser-scanning microscopy with multi-photon imaging, flow cytometry, TUNEL assays and DNA gels.

**#370** Ras-mediated anolks resistance of RIE-1 cells is independent of Raf and PI3K activation. McFall, A.J., Lambert, Q., Rogers-Graham, K. and Der, C.J. Department of Pharmacology, Lineberger Comprehensive Cancer Center, University of North Carolina, Chapel Hill, NC 27599.

Activation of the Ras protein contributes to the development of a wide variety of human cancers. In addition to its growth-promoting properties Ras has recently been identified as a potent inhibitor of anolks, or suspension-induced apoptosis. Anolks represents a physiologically appropriate response of normal epithelial cells to loss of matrix attachment. Circumventing the anolks response and acquiring anchorage independence is a key step in the development of carcinomas. The current model of Ras-mediated anolks resistance implicates a single Ras effector, PI3K, and its downstream target Akt, as both necessary and sufficient for resistance. Yet, studies performed to date have relied almost exclusively on findings obtained with a single cell line, namely the MDCK canine kidney epithelial cell line. To test the relevancy of this model in other epithelial cell lines, we have identified an alternative model for anolks studies. RIE-1 cells, a rodent intestinal epithelial cell line, are anolks sensitive. Expression of oncogenic variants of H-, N- and K-Ras inhibited anolks of these cells. Surprisingly, however, we have been unable to implicate the Ras effector PI3K in Ras-mediated anolks resistance of RIE-1 cells. Treatment with the PI3K inhibitor LY294002 fails to block K-Ras-mediated anolks resistance nor does it substantially inhibit growth of K-Ras transformed cells in soft agar. Furthermore, expression of the H-Ras effector domain mutant C40, that activates PI3K, or activated PI3K (PI3K-CAAX) itself, failed to protect RIE-1 cells from anolks. The Ras effector Raf has also been evaluated for its ability to promote anolks resistance in these cells. Expression of constitutively activated Raf kinase (Raf22W) or the H-Ras effector domain mutant 35S, that activates Raf, failed to block anolks. Furthermore, treatment with the chemical inhibitor U0126 that targets the Raf/MEK/MAPK pathway failed to inhibit anolks resistance of K-Ras transformed cells. These results suggest that the mechanism(s) of Ras-mediated anolks resistance may differ depending on cellular context and underscore the complex nature by which oncogenic Ras promotes carcinogenesis.

**#371** Genetic Targets for c-myc oncogene in proliferation and apoptosis. Benvenisty, Nissim\*, Eden, Amir, Schuldiner, Oren, Ben-Yosef, Tamar, Ben-Porath, Ilal and Yanuka, Ofra. Department of Genetics, The Hebrew University of Jerusalem, Israel.

The c-myc proto-oncogene is a key regulator of cell growth and death and is involved in malignant transformation. Myc proteins function as transcription factors activating expression of other genes. Identification of such target genes may help to understand the mechanism by which Myc proteins exert their various effects. We have identified two targets for c-Myc regulation, one (named *Eca39/Bcat1*) is associated with apoptosis and the other (named *Tmp*) is involved in oncogenic transformation. *Eca39/Bcat1* is a target for c-Myc regulation in man and mouse. It codes for the cytosolic branched chain amino acid aminotransferase, an enzyme cata-

lyzing the first step of branched-chain amino-acid catabolism. *Eca39/Bcat1* is highly conserved in evolution and disruption of its yeast homolog affects cell growth. To assess the role of *Eca39/Bcat1* in mammalian cells, we transfected murine cells with an *Eca39/Bcat1* expression vector. Overexpression of *Eca39/Bcat1* led to a decrease in cell viability and apoptosis. The branched-chain keto acids, the metabolic products of *Eca39/Bcat1* activity, can also induce rapid apoptotic cell death when added to growth medium. This observation suggests that the growth inhibitory effect of *Eca39/Bcat1* and its apoptosis promoting effect may be mediated by the metabolic effects of this enzyme. We have also isolated the tumor-associated membrane protein gene, *Tmp*, as a target for *c-myc*-activity. *Tmp* is highly expressed in tumors which develop in *c-myc* transgenic mice, and it is induced upon serum-stimulation of fibroblasts. In a time-course closely correlated with *c-myc* expression. We have isolated the *Tmp* promoter region, and identified a putative *c-myc* binding element, CACGTG, located in the first intron of the gene. We show that constructs containing the *Tmp* regulatory region fused to a reporter gene are activated by *c-myc* through this CACGTG element, and that the *c-myc*/Max protein complex can bind this element. Moreover, an inducible form of *c-myc*, the MycER fusion protein, can activate the endogenous *Tmp* gene. We also show that *Tmp* overexpressing fibroblasts induce rapidly growing tumors when injected into nude mice, suggesting that *Tmp* may possess a tumorigenic activity. Thus, *TMP*, a member of a novel family of membrane glycoproteins with a suggested role in cellular contact, is a *c-myc* target, possibly involved in *c-myc*-induced transformation.

\*Tel: 972-2-6586774; Fax: 972-2-6586975; e-mail: nissimb@iconardo.lshuj.acil

**#372 Enhanced expression of c-kit, c-myc, N-myc, c-Ha-ras 1, c-erb B-2/neu, c-fos and c-jun in human germ cell tumors.** Röhler<sup>1</sup>, U., Nunnensiek<sup>2</sup>, C., Müller<sup>3</sup>, H.A.G. and Scheller<sup>1</sup>, A. <sup>1</sup>Fachklinik, "Leonards," Kornwestheim, Germany, <sup>2</sup>Ärztliche Praxis, Reutlingen, Germany, <sup>3</sup>Zentrum für Laboratoriumsmedizin, Klinik am Eichert, Göppingen, Germany.

The presence of c-kit, c-myc, N-myc, c-Ha ras 1, c-erb B-2/neu, c-fos, and c-jun was investigated in biopsy specimens from 20 patients with various types of germ cell tumors. The expression of the oncogenes was demonstrated *in situ* hybridization. C-kit-ligand was found in 14/20 of tumors including 7 seminomas, in 2 embryonal carcinomas, in 1 embryonal carcinoma with seminoma, in 1 embryonal carcinoma with teratoma, in 1 immature teratoma with choriocarcinoma. C-myc oncogene expression was found in 10/20 of tumors including 2 embryonal carcinomas, in one Leyding cell tumor, in 3 embryonal carcinomas with seminomas, in one immature teratoma with choriocarcinoma, in one embryonal carcinoma with immature teratoma, and in one mature teratoma. N-myc was observed in 8/20 of tumors including 2 embryonal carcinomas, in 3 embryonal carcinomas with seminomas, in one embryonal carcinoma with immature teratoma, in one immature teratoma with choriocarcinoma, and one immature teratoma with seminoma.

C-Ha-ras 1 oncogene expression was found in 7/20 tumors including 2 embryonal carcinomas, in one mature teratoma, in the benign Leyding cell tumor, in 2 embryonal carcinomas with seminomas, and in one embryonal carcinoma with immature teratoma. Expression of c-erb B-2/neu oncogene could be identified in benign Leyding cell tumor only.

C-fos was expressed in 12/20 tumors including in the benign Leyding cell tumor, in 4 pure seminomas, in 3 embryonal carcinomas with seminomas, in 2 immature teratomas, and in one immature teratoma with choriocarcinoma. C-jun expression was observed in 14/20 tumors including in 6 pure seminomas, in the benign Leyding cell tumor, in 2 immature teratomas, in one mature teratoma, in 2 embryonal carcinomas with seminomas, in one immature teratoma with choriocarcinoma, and in one embryonal carcinoma with immature teratoma.

The presence of activated c-kit and oncogenes only in tumor DNA and not in normal DNA from the same individual further suggests, that oncogenes have a fundamental role in tumorigenesis of testicular germ cell tumors. Further molecular analysis should be done and correlation between detectable alterations of c-kit and of oncogenes and clinical characteristics of testicular cancer be sought.

## SECTION 2: CYTOKINES

**#373 Prediction of response to interleukin-2 treatment in renal cell carcinoma based on modulation of lymphocyte proliferation.** Håkansson Leif, Bratthäll Charlotte, Clinchy Birgitta, Hagström Thomas, Håkansson Annika, Isaksson Annika and Fähræus Bengt. *Depts of Oncology and Urology, The University Hospital, Linköping, Sweden.*

The remission rate in metastatic renal cell carcinoma (RCC) after administration of recombinant IL-2 is generally low (15–20%). As the treatment is associated with severe side effects and high cost it would be of value if patients that benefit from this treatment could be identified in advance. The objective of this study was to investigate a possible correlation between

the efficacy of IL-2 treatment and the effect of immunomodulating drugs on PHA-induced proliferation and cytokine production of peripheral blood mononuclear cells (PBMC) from RCC patients.

PBMC were isolated from 23 patients with metastatic RCC immediately before start of treatment with subcutaneous rIL-2 (Proleukin, Celus/Farmos). Proliferation (<sup>3</sup>H-thymidine uptake) of PBMC was determined after culture with PHA for 72 hours in the presence or absence of chlorambucil, indomethacin or cimelidine. The production of cytokines (TNF- $\alpha$ , IFN- $\gamma$ , IL-1, IL-2, IL-4) was evaluated in culture supernatants.

Tumor regressions were observed 10 patients, 4 had stable disease and 9 had progressive disease. Chlorambucil had no effect on the proliferative response of PBMCs from patients with progressive disease, whereas the proliferative response was significantly inhibited ( $p > 0.005$ ) in patients with tumor regressions. A clear correlation was observed when the modulation of TNF- $\alpha$  production by chlorambucil was compared to the modulation of proliferation. Furthermore, patients where chlorambucil induced a strong inhibition of the proliferative response had a longer time to progression compared to those where chlorambucil showed no or little modulating effect.

**#374 Interleukin-4 targets therapeutic toxins to human head and neck cancer cells.** Kawakami, Koji, Leland, Pamela, and Puri, Raj K. *Laboratory of Molecular Tumor Biology, Division of Cellular and Gene Therapies, CBER, FDA, Bethesda, Maryland 20892.*

Head and neck cancer comprises >4% of all human cancers worldwide. Despite advances in diagnosis and treatment, survival rates for patients with head and neck cancer have remained unchanged for the last 30 years. In an attempt to develop novel therapeutic agents, we have found that a variety of murine and human carcinoma cells express receptors for interleukin-4 (IL-4R) *in vitro* and *in vivo*. Although, the importance of expression of these receptors on solid tumor cells is not known, others and we have observed that solid tumor cells including head and neck squamous cell carcinoma (HNSCC) cells respond to IL-4. Here we show that seventeen HNSCC cell lines established from tumors obtained from various anatomic regions, express high levels of IL-4R. These receptors are functional as a chimeric fusion protein comprised of circularly permuted IL-4 and a mutated form of *Pseudomonas* exotoxin (IL-4 cytotoxin) is highly cytotoxic to these cells. The IC<sub>50</sub> protein concentration mediating 50% inhibition, ranged between 0.1 ng/ml to 600 ng/ml. Ten of 17 cell lines were extremely sensitive to IL-4 toxin with IC<sub>50</sub> below <2 ng/ml. The cytotoxicity of IL-4 toxin was specific as excess of recombinant IL-4 neutralized the cytotoxicity. Since IL-13, an IL-4 related cytokine, also blocked the cytotoxicity of IL-4 toxin, it is proposed that IL-4R and IL-13R are related in HNSCC cell lines. These studies suggest that IL-4R may be useful target to exploit for head and neck cancer therapy.

**#375 Identification and characterization of IL-13 and IL-4 receptor complex in Pancreatic carcinoma cells.** Joshi, Bharat H., and Puri, Raj K. *Laboratory of Molecular Tumor Biology, Division of Cellular and Gene Therapies, CBER, FDA, Bethesda, MD 20892.*

In order to understand the complexities and ambiguous nature of different solid tumors, we have investigated the structure and function of IL-13 and IL-4 receptors belonging to the cytokine superfamily. In the present study, we have examined pancreatic carcinoma cell lines for the expression and function of these receptors. Reverse transcriptase-PCR of RNA from five different cell lines showed that transcripts of IL-13 receptor (R)  $\alpha 1$  chain, IL-4 R p140 (termed  $\beta$ ) and IL-2R common  $\gamma$  ( $\gamma c$ ) chains are present in three of the five highly metastasizing pancreatic carcinoma cell lines (Panc-1, BxPC-3 and CFPAC-1). However, two other cell lines (SU 86.86 and COLO-587), only expressed IL-13R  $\alpha 1$  transcripts and mRNA for the other three chains was below the limits of detection. IL-13R  $\alpha 2$  chain was either absent or present in very low levels in same three lines. We further observed that these three cell lines that express IL-13R  $\alpha 1$ , IL-4R  $\beta$  and IL-2R  $\gamma c$  chains also express high-affinity surface IL-4R. Using a chimeric protein composed of circularly permuted IL-4 and a truncated form of *Pseudomonas Exotoxin* [IL-4(36-37)-PE38KDEL], we found that IL-4 toxin is highly cytotoxic (killing 50% of the cell population at <10 ng/ml of IL-4 toxin) to these three IL-4R positive cell lines. The cytotoxicity was receptor specific because excess IL-4 neutralized the cytotoxicity. IL-4 toxin was not cytotoxic to cells that did not express IL-4 R chains (SU86.86 and COLO 587). Our results suggest that some of the pancreatic tumors express functional IL-4R and this property may be exploited for targeting IL-4 toxin for antitumor activity.

**#376 Molecular targeting with engineered Interleukin 13 for imaging and treatment of human high-grade gliomas.** Deblinski Waldemar, Thompson Jeffrey P., Gibo Denise M., Slagle Becky. *Section of Neurosurgery/H110, Department of Surgery, Penn State University College of Medicine, 500 University Drive, Hershey, PA 17033-0850.*

Human high-grade gliomas (HGG) represent a significant medical problem, since they are considered incurable. We uncovered that the vast majority of patients with HGG over-express a receptor (R) for interleukin 13 (IL13) *in situ*. Other brain tumors do not seem to possess IL13 receptor to any significant degree. This receptor is more restrictive, since it is IL-4 independent and thus different from the IL13/4-R of normal tissue that is



signaling and shared with IL4. To exploit the difference that exists in physiology and malignancy, we determined the sites involved in the interaction of IL13 with the IL13/4-R and/or the HGG-R. We identified thus far three regions in IL13 that are needed for signaling through the IL13/4-R and they were localized to  $\alpha$ -helices A, C and D of IL13. These regions were mainly separate from the region(s) needed to bind the HGG-R. We also found a single residue within  $\alpha$ -helix D that is essential for IL13 interaction with the HGG-R. Subsequently, in order to abolish IL13 affinity towards the physiological receptor we introduced variety of mutations into regions crucial for IL13 interaction with the IL13/4-R, but not HGG-R. Next, we equipped the cytokine with an additional tyrosine residue for higher specific activity radiolabeling by substituting amino acids important for activation of the IL13/4-R. We have also made cytotoxins based on IL13 mutants, which are arguably the most potent growth inhibitory agents on HGG cells.

IL13 is a small endogenous protein (~12 kDa) and appears not to be sensitive to a variety of genetic modifications. Because of these, IL13 mutants should penetrate solid tumors relatively well, be of little immunogenicity and amenable to further engineering, if desired. All these factors make IL13 mutants attractive vehicles for the specific delivery of, e.g., imaging tracers or cytotoxicity to HGG. In our unique approach we are able to change a naturally occurring compound for the purpose of specific targeting of HGG without the need to raise separate antibodies or adding other reagents.

**#377 Phase I study with Interleukin-12 Intratumorally in patients with recurrent head and neck squamous cell carcinoma.** Van Herpen Carla M.L., Adema Gosse J., Marres Henri A.M., De Wilde Peter, De Mulder Pieter H.M. *University Hospital Nijmegen, Nijmegen, The Netherlands*

The main biological activities of Interleukin-12 (IL-12) are promotion of the  $T_{H1}$  response, regulation of the cytokine response, i.e. upregulation of Interferon- $\gamma$  and activation and proliferation of cytotoxic T-cells and Natural Killer (NK) cells. Therefore IL-12 is tested in oncology in phase I and II studies in which IL-12 was administered subcutaneously, intravenously or intravasically. In this study we have treated patients with head and neck squamous cell carcinoma (HNSCC) with IL-12 intratumorally (i.t.) to get a relatively high concentration of the cytokine in the tumor and draining lymph nodes. After this phase I study patients with HNSCC will be treated with IL-12 i.t. pre-operatively to investigate the effects of IL-12 on the cellular immunity. IL-12 (Wyeth-Ayers/Genetics Institute) was given i.t. once a week for 8 weeks. In case of stable disease (SD) or response administration of IL-12 was continued to a maximum of 24 injections. The primary objective was to determine the toxicity profile of IL-12 with this route of administration. Secondary objectives were to evaluate pharmacokinetic and pharmacodynamic parameters and possible anti-tumor activity. IL-12 was administered on 2 dose levels: 100 and 300 ng/kg. Six patients, 3 per dose level, who had a local recurrence of HNSCC, that was not amenable for surgery or radiotherapy, were treated. The toxicity of the treatment was mild. All patients developed fever after 4-8 hours till 24 hours after administration of IL-12 i.t. One patient had a grade 4 lymphopenia. No other grade 3 and 4 toxicities were seen. In all patients we saw a rapid decrease of total number and almost all subclasses of lymphocytes (CD3+, CD4+, CD8+ and CD56+ cells). The decrease started after 4 hours, was maximal after 12-24 hours and was nearly normalised after 96 hours. Data on the expression of cytokines in time after IL-12 i.t. administration both on protein level and on mRNA level will be presented. Of the 5 evaluable patients (one has started recently) 2 patients (one on 100 and the other on 300 ng/kg) had SD (one had 40% regression) and received the maximum of 24 injections. In conclusion: IL-12 i.t. on both dose levels is well tolerated in HNSCC.

**#378 Subcutaneously administered Interleukin-12 induces activation of coagulation and fibrinolysis in humans.** Portielje Johanna EA, Eerenberg Anke JM, Kruit Wim HJ, Schuler Martin, Sparreboom Alex, Beck Joachim, Stoter Gerrit, Huber Christoph, Aulitzky Walter E and Hack C Erik. *Rotterdam Cancer Institute (Daniel den Hoed Kliniek) and University Hospital Rotterdam, The Netherlands, Central Laboratory of the Red Cross Blood Transfusion Service, Amsterdam, The Netherlands and Johannes Gutenberg University Mainz, Germany.*

Interleukin-12 (IL-12) is a cytokine with potential therapeutic efficacy in malignant diseases. It stimulates cellular immunity by promoting T-helper 1 responses and induces production of IFN- $\gamma$ . Administration of IL-12 to chimpanzees was complicated by disseminated intravascular coagulation. As part of a phase I study, we studied the coagulative and fibrinolytic response after the first subcutaneous (s.c.) injection of recombinant human IL-12 (rhIL-12) in patients with advanced renal cell carcinoma treated at the maximum tolerated dose. Patients had normal haematologic, cardiopulmonary and hepatic function. Eighteen patients were studied after s.c. injection of 0.5  $\mu$ g/kg rhIL-12. Blood samples were drawn before and 4, 8, 12, 24, 48, 72, 96 and 168 hours after injection.

IL-12 induced a coagulative response, demonstrated by increased thrombin-anti-thrombin III complexes (TATc), in 7 patients (39%). Their TATc increased from  $48 \pm 67$  to a mean maximum of  $522 \pm 301$  ng/ml, 12 hours (median) after IL-12 injection, thereafter declining to baseline. Of note, all 4 patients with strongly elevated TATc before therapy showed a

further increase. A fibrinolytic response was demonstrated by plasmin- $\alpha$ 2-antiplasmin complexes (PAPc) increasing from  $12 \pm 6.8$  to a mean maximum of  $23 \pm 10.2$  nmol, reached after 72 hours. Although PAPc increased in all patients, the response appeared strongest for patients with a coagulative response. Levels of tissue plasminogen activator (tPA) and plasminogen-activator inhibitor-1 (PAI) were increased in the majority of patients before treatment. After initial decrease, tPA started to rise after 12 hours, ending above baseline. PAI decreased with a minimum after 12 hours, remaining below baseline. The rise of PAPc after IL-12 injection correlated with elevation of tPA and reduction of PAI ( $p = 0.0042$ ). Patients with and without coagulative response did not differ with regard to peak levels of IFN- $\gamma$ , reached after 24 hours. Routine coagulation tests (prothrombin time, activated partial thromboplastin time) were unaffected and none of the patients experienced venous thrombo-embolic complications.

This study indicates that IL-12 induces activation of coagulation and fibrinolysis. A fibrinolytic response does also occur in the absence of a coagulative response, suggesting independent stimulation by IL-12. Besides IFN- $\gamma$ , other mediators must contribute to the observed effects.

**#379 IL-12/pulse IL-2 induces endothelial injury, inhibits tumor neovascularization, and induces complete tumor regression via mechanisms dependent on CD8<sup>+</sup> T cells and FAS-L.** Wigginton, J.M., Back, T.C., Gieselhart, L., Willtrout, T.A., Sayers, T., McCormick, K., and Willtrout, R.H. *POB, DCS, NCI, Bethesda; IRSP, SAIC; LEI, DBS, NCI, Frederick.*

We have reported previously that daily systemic administration of IL-12 in combination with intermittent, weekly pulse doses of IL-2 induces complete regression of established murine renal carcinoma (Renca) in up to 98-100% of treated mice. Induction of tumor regression occurs in conjunction with a reduction in vascularity observable at the light microscopic level. More recently, utilizing a novel quantitative latex-radiotracer infusion method, we have demonstrated significant reductions in overall vascularization of intrarenal Renca tumors after treatment with IL-12/pulse IL-2 versus vehicle alone. Ultrastructural studies utilizing electron microscopy demonstrate that after as little as five days of administration, IL-12/pulse IL-2 induces ultrastructural changes indicative injury and/or apoptosis in both endothelial and tumor cell populations, including nuclear condensation and fragmentation, vacuolization, and in some instances, swelling/degeneration of the endo-plasmic reticulum. In vitro, flow cytometry studies demonstrate that IL-12 and IL-2 may additively or even synergistically enhance cell surface expression of FAS-L on lymph-node derived T cells, while in vivo, treatment with IL-12/pulse IL-2 enhances local expression of the genes encoding FAS and FAS-L (as assessed by RT-PCR), and induces infiltration of CD8<sup>+</sup> T cells into the tumor site. In turn, the anti-tumor activity of IL-12/pulse IL-2 is ablated in mice depleted of CD8<sup>+</sup> T cells, and in mice with mutated FAS-L. Collectively, these studies provide direct evidence of the ability of IL-12/pulse IL-2 to induce endothelial injury and inhibit tumor neovascularization, and implicate CD8<sup>+</sup> T cells, FAS-L and the induction of tumor and/or endothelial apoptosis in the anti-vascular/anti-tumor activity of this combination.

**#380 Intraperitoneal administration of human recombinant interleukin-12 (rhIL-12) for the treatment of ovarian and GI cancer patients with progressive disease after standard chemotherapy (T97-0034).**

Lenzi, R., Kudelka, A., Verschraegen, C., Nash, M., Loercher, A., Zhang, H.Z., Kalz, R.L., Abbruzzese, J.L., Kavanagh, J.J., Platsoucas, C.D., Rosenblum, M., Freedman, R.S. *M.D.A.C.C., Houston, TX, Temple U, Philadelphia PA.*

Clinical, pharmacologic and correlative laboratory finds are reported from the first human trial of intraperitoneal rhIL-12 in patients with peritoneal carcinomatosis from Mullerian and gastrointestinal malignancies. The trial was designed as a standard Phase I study, with cohorts of three patients being treated at escalating weekly doses of the drug, starting at the dose of 3 ng/kg. At the time of this report three patients had been treated at the fourth escalation level of 100 ng/kg and two patients demonstrated pathologically complete responses while a third patient had stable disease. The highest dose level achieved is 300 ng/m<sup>2</sup> and the trial is proceeding. No significant drug related toxicities were observed at these dose levels. Immunobiologic effects of IP rhIL-12 detected even at the initial dose level of 3 ng/kg, included an increase in expression of IFN- $\gamma$ , and increased expression of HLA Class I on tumor cells. With escalation in dose peritoneal exudates from additional patients demonstrated increased levels of the antiangiogenic  $\alpha$  chemokine IP10 and decreased levels of expression of the angiogenic factors VEGF and FGF2. Immunohistochemistry studies were quantitated by computerized image analysis. The pharmacologic concentrations of IP rhIL-12 from serial sampling of peritoneal fluid and of peripheral blood will be shown. This study provides detailed observations in vivo on the clinical and biologic behavior of IP rhIL-12 in humans: Absence of significant drug related toxicity, evidence of significant clinical activity, enhancement of TH-1 type immune response and favorable modulation of angiogenesis related factors in the peritoneal

tumor microenvironment. Accrual of patients continues to determine the MTD and to define clinical activity and biologic correlations at higher dose levels and to further define the biological effects of the drug.

**#381 The antitumor activity of IL-18/IL-2: mechanisms accounting for the induction of complete tumor regression.** Wigginton, J.M., Wiltrout, T.A., Smith, J., Back, T.C., and Wiltrout, R.H. *POB, DCS, NCI, Bethesda, MD; IRSP, SAIC; LEI, DBS, NCI, Frederick, MD.*

Increasing attention has focused recently on the use of rationally-designed combinations of immunomodulatory agents, including various cytokines, as a means of therapeutically enhancing the host-antitumor immune response. We have now shown that in combination, the antitumor cytokines IL-18 and IL-2, possess synergistic immunomodulatory and antitumor activity *in vitro* and *in vivo*. *In vitro*, IL-18 and IL-2 synergistically enhance the production of IFN- $\gamma$  by murine splenocytes. *In vivo*, daily system administration of IL-18 in combination with twice weekly split pulse IL-2 induces complete regression of established SQ 3LL lung carcinoma tumors in 82% of treated mice versus 40% or 10% complete responses among mice treated with IL-18 or IL-2 alone respectively. The majority of mice cured of their original tumor are resistant to rechallenge, suggesting that immunological memory is generated in these mice. Utilizing immunodeficient SCID mice, as well as those with targeted disruption of the genes encoding IFN- $\gamma$ , TNFR1, IL12p40, perforin, FAS or FAS-L, we have found that the ability of IL-18/IL-2 to prolong survival and induce complete tumor regression is dependent on intact T/B cell function, IFN- $\gamma$ , the type 1 TNF receptor, FAS and FAS-L, but is independent of IL-12 and perforin production in mice. Collectively, these studies demonstrate the potent antitumor activity and novel mechanisms engaged by this combination, and given its therapeutic activity, suggest that clinical evaluation of IL-18/IL-2 may be warranted.

**#382 Preclinical development of Interleukin-18 for cancer therapy.** Jonak Zdenka L., Ho Yen Sen, Trulli Stephen, McCabe Francis L., Maier Curtis, Kirkpatrick Robert, Elafante Louis, Chen Yi-Jun, Herzyk Danuta, Johanson Kyung, Rose Matico, Whitacre Margaret, Abdel-Meguid Sherin S., Johnson Randall K. *SmithKline Beecham Pharmaceuticals, 709 Swedeland Rd., King of Prussia, PA 19406.*

Interleukin-18 (IL-18) was initially identified as an interferon  $\gamma$  (IFN- $\gamma$ ) inducing factor that enhances natural killer (NK) cell activity and elicits protective anti-tumor activity *in vivo*. The goal of our study was to demonstrate the use of IL-18 for cancer immunotherapy. Purified human and murine mature IL-18 was for bioactivity in human myelomonocytic KG-1 cells and in human, murine and Cynomolgus PBLs. IL-18 alone and in combination with cytotoxic agents was profiled in advanced syngeneic murine MOPC-315 plasmacytoma, B16F10 melanoma and Lewis lung carcinoma. In MOPC-315, IL-18 alone regressed established tumors at a dose of 0.5 and 5 mg/kg. Co-administration of IL-18 with topotecan at MTD doses (15 mg/kg) and suboptimal dose (9 mg/kg) markedly enhanced the activity. Treated mice that regressed their tumors, retained immunological memory since re-implantation of MOPC-315 resulted in tumor rejection. To address IL-18 mechanism of action, NK activity, the phenotypic profile of lymphocytes by flow cytometry and the expression of cytokines (TaqMan and Elisa) from IL-18 treated mice/human PBLs was analyzed. NK bioactivity correlated with upregulation of CD56/CD16-positive cells and expression of IFN- $\gamma$  and GM-CSF, at message and protein level. In the MOPC-315 plasmacytoma T cells were essential for IL-18 activity since regressions were not seen in syngeneic SCID mice. Upregulation of IFN- $\gamma$  demonstrated functional activity for human IL-18 in Cynomolgus PBLs. In conclusion, 1) IL-18 alone or as an adjunct to cytotoxic agents is a potential agent for the treatment of cancer and 2) markers and bioassays that could be used in the clinic to monitor IL-18 induced immunotherapeutic responses have been developed.

**#383 Phase I/II Evaluation of Beta LT™ as an antilymphoma agent and enhancer of DTH in lymphoma patients.** Taub, F.; Mayerson, S.; McQuillan, A.; Caplan, S.; Shustik, C.; Miller, W. *LifeTime™ Pharmaceuticals, Davetail Technologies, McGill University.*

Preclinical studies of beta-alethine (Beta LT™ or BETATHINE™) have suggested a potential anti-tumor effect in myeloma, melanoma and breast cancer models that may be immune mediated (Knight et al. 1994; Pontzer et al. submitted; and abstracts by Fichtner et al. 1998 and Mokyr et al.). Preclinical data revealed low toxicity and high therapeutic margins. Initial Phase I/II studies in humans with lymphoma previously treated with chemotherapy noted a lack of toxicity and apparent modulation of immune cell surface cytokines and receptors (Miller et al., IMF abstract, 1999). The hypothesis that Beta LT™ acts by an immune mechanism predicts Beta LT™ would increase T-cell activity and that T-cell activity would correlate with any reductions in cancer. In order to measure T-cell activity *in vivo*, a validated multi-antigen delayed type hypersensitivity (DTH) test of response to 7 common antigens was used (Multitest CMI). To date, five patients and 19 masses have been evaluated, thus data is insufficient to be conclusive. However, both patients who had a response to any of the seven test antigens pre-study have shown a reduction in tumor size by CAT scan. In one patient all four tumor masses decreased, and in another all five tumor masses decreased. In contrast, none of the ten tumors seen

In the three patients who were anergic pre-study decreased in size. One patient who was initially anergic developed responses to four out of seven antigens and a second patient developed responses to 5 out of 7 antigens. Both have "stable disease". The third initially anergic patient remained anergic throughout the 12-week treatment period and has progressed. Thus, initial observations indicate 1) DTH has been predictive of anticancer response and 2) DTH in some patients increased. However, while anergic patients showed an increase in DTH while on drug, those patients who had DTH responses pre-therapy and are showing tumor shrinkage do not show an increase in DTH responses while on study. Available data will be discussed to confirm or refute observations that suggest pre-study DTH responses may predict the anti-cancer potential of Beta LT™ and Beta LT™ may increase DTH in anergic patients.

**#384 Phase I-II study of CRM197 administration to 50 advanced cancer patients.** Buzzi Silvio, Baccini Cesare, Rubboli Diego, Monti Giuseppe, Buzzi Giorgio, and Buzzi Anna Maria. *Centro Medico TRIS and Ospedale S.M. delle Croci, Ravenna, 48100, Italy.*

CRM197 is an immunogenic, nontoxic mutant of diphtheria toxin (DT). The molecule binds to both membrane anchored and secreted forms of heparin-binding epidermal growth factor (proHB-EGF and HB-EGF, respectively). ProHB-EGF is the specific cell receptor for DT and a juxtacrine mitogen with frequent overexpression in cancer. HB-EGF is an autocrine and paracrine mitogen and an adhesion factor. This study aimed to determine whether the binding of CRM197 to the growth factor inhibits its mitogenic effect and elicits an immune reaction affecting the tumor. CRM197 was injected s.c. in the abdominal wall of 50 advanced outpatients subdivided in three groups receiving 20, 40 or 60 Lf at a time for 6 times at 3 days' intervals. Main side effects were: mild inflammatory skin lesions, tolerable systemic reaction in hypersensitive patients, and hypotension. There were 3 complete responses (6%) lasting 88+, 80+, and 64 weeks, respectively. Partial response was achieved in 11 patients (22%) with a median duration of 8 weeks. A patient condition of cell-mediated hypersensitivity to DT/CRM197 and an increase in neutrophils, fibrinogen and C3c complement fraction after injection of the mutated toxin seemed to be predictive of a possible tumor response. At relapse, responders had no further improvement by a new systemic cycle. However, if CRM197 was administered by peritumoral injections to a s.c. lesion, the mass shrank again. We suggest that CRM197 can be given safely on an outpatient basis and that the molecule exerts antitumor activity.

**#385 Interferon- $\gamma$  (IFN- $\gamma$ ) upregulates expression of the MUC1 tumor antigen in epithelial cancer cell lines.** Burton, Jack D., Mishina, Dina, Krupkin, Ruvim and Goldenberg, David M. *Garden State Cancer Center, Belleville, NJ.*

Mucin-1 (MUC1) antigen is a favorable tumor target antigen that is expressed by a wide range of epithelial cancers and derivative cells, such as breast, ovarian, prostate and non-small cell lung cancer. We have also confirmed MUC1 expression in multiple myeloma (MM) with the MA5 mAb (anti-VNTR specificity). We tested the effect of interferons ( $\alpha$  and  $\gamma$ ) on the level of expression of this antigen, since these cytokines are known to upregulate other tumor antigens such as CEA. A panel of MUC1+ epithelial cell lines including breast, lung and colon Ca were tested along with a panel of MM cell lines. Using both flow cytometry and <sup>125</sup>I-MA5 binding, we found that IFN- $\gamma$  (over a range of 125-500 U/ml) upregulated MUC1 in 5/6 epithelial cell lines (>25% increase in either specific radiolabel binding or %+ cells in flow cytometry) tested. IFN- $\alpha$ , on the other hand, showed a markedly decreased effect in that 0/6 of these epithelial cell lines showed MUC1 upregulation beyond this cutoff value ( $p = 0.03$ , IFN- $\gamma$  vs IFN- $\alpha$ ). With MM lines, this IFN- $\gamma$  effect was less frequent, such that 2/5 cell lines had this degree of MUC1 upregulation. As with the epithelial lines, 0/5 MM lines showed a response to IFN- $\alpha$ . To study the mechanism of this effect, IFN binding (using <sup>125</sup>I-IFNs) was determined. In all epithelial cell lines tested, either no specific IFN- $\alpha$  binding or levels that were lower than those with IFN- $\gamma$  were observed. 5/5 of the panel of epithelial cell lines that were tested showed specific binding for <sup>125</sup>I-IFN- $\gamma$ . In the MM panel of cell lines, there was a correlation of IFN- $\gamma$  binding and IFN- $\gamma$  response in that 2/2 lines showing specific binding also showed a MUC1 upregulatory effect upon IFN- $\gamma$  exposure, while the MM lines exhibiting no specific IFN- $\gamma$  binding showed no MUC1 response. Thus, these studies demonstrate: 1) upregulation of MUC1 to IFN- $\gamma$  (analogous to CEA and sialyl-T<sub>n</sub>) is seen in epithelial cell lines and to a lesser extent in MM lines; 2) IFN- $\gamma$  consistently shows a much greater effect than IFN- $\alpha$  and 3) some of the selectivity for an IFN- $\gamma$  versus an IFN- $\alpha$  effect appears to depend upon the presence of detectable, specific, whole-cell IFN binding. (Supported in part by NIH grant CA39841.)

**#386 Increased epithelial cadherin expression in SiHa cervical carcinoma cell line by anti-proliferative agents interferon and retinoic acid.** Arrastia, Concepcion Diaz, Arany, Istvan, Whitehead, William E., Salas, Sonia C., Hannigan, Edward V., and Tying, Steven K. *Departments of Obstetrics & Gynecology and Microbiology & Immunology, The University of Texas Medical Branch at Galveston, Galveston, TX 77555-0567.*

Epithelial cadherin (e-cadherin) is a cell-cell adhesion molecule that connects epithelial cells via homotypic calcium-dependent interactions.



The e-cadherin cell adhesion molecule is important in the maintenance of normal epithelial structures, and its altered expression may be important in epithelial tumor carcinogenesis, particularly in the process of invasion and metastasis. Abnormalities of e-cadherin expression have been described in cervical dysplasia and in invasive squamous cervical carcinomas. Therapeutic agents, such as interferons, which are cytokines with known anti-proliferative activity and retinoic acids, known regulators of gene expression, are being evaluated for their anti-tumor activity.

**Aim:** To study the effect of anti-proliferative agents on e-cadherin expression in cervical cancer cell lines.

**Methods:** SiHa, an HPV positive cervical cancer cell line, was separately exposed to: interferon alpha, beta, and gamma, in addition to all trans retinoic acid, 13 cis retinoic acid and retinol, an inactive form of retinoic acid. Eight samples were collected at time increments between 30 minutes and 3 days. RNA was extracted and reverse transcriptase PCR was performed on the samples. E-cadherin expression was calculated in a semi-quantitative fashion, expressed as a ratio of e-cadherin to alpha tubulin expression.

**Results:** SiHa cells treated with interferon alpha, interferon gamma, or 13 cis retinoic acid have a marked increase (5-24X) in e-cadherin expression over baseline untreated cells after 48 hours of treatment. Cells treated with all trans retinoic acid had a moderate increase (2.5X) in e-cadherin expression. There was no apparent effect of exposure to interferon beta or retinol.

**Conclusion:** Our findings are clinically relevant because they suggest a novel mechanism of the anti-proliferative effects of interferons and retinoids, with e-cadherin as the molecular target and further provides a convenient *in vitro* model to study these effects.

**#387 Effects of Bacillus Calmette-Guérin (BCG) and Interferon  $\alpha$ -2b on Superficial Bladder Cancer.** Zhang Y., Khoo H.E., Gan Y.H., R. Mahendran and K. Esuvaranathan. *Departments of Surgery and Biochemistry, National University of Singapore, Singapore*

**Introduction:** Although intravesical BCG therapy for superficial bladder cancer is the most successful example of immunotherapy today, a significant proportion of patients fail therapy. Therefore, in this study, we investigated the anti-tumor effects of combining BCG with interferon  $\alpha$ -2b, *in vitro* and *in vivo*.

**Methods:** Five human bladder cancer cell lines with different histopathological tumor grades were studied. The cytolytic and anti-proliferative effects of BCG and/or IFN $\alpha$ -2b were determined by [<sup>14</sup>C]-thymidine release and incorporation assay. The release of eleven cytokines from these cancer cell lines was measured by ELISA assays, and mRNA expression of IL-6 and GM-CSF were determined by RT-PCR as well. The cell cycle stage of these cells after treatment was determined by flow cytometric analysis. *In vivo*, mice implanted subcutaneously with MB49 murine bladder cancer cells, were given intravesical treatments with BCG and/or IFN $\alpha$ . Tumor size was measured and T cell subset distribution in spleen was determined by flow cytometric analyses while cytokine expression was measured by RT-PCR.

**Results:** BCG had direct dose-dependent cytolytic and anti-proliferative effects on all three grade 3 cell lines and increased the production of IL-6, IL-8 and GM-CSF dramatically from these cells. The addition of IFN $\alpha$ -2b had additive anti-proliferative effects on three of these five cell lines and had marked additive or synergistic effect on production of IL-6, IL-8 and TNF- $\alpha$ . *In vivo*, the combination of BCG and IFN $\alpha$  had superior and earlier anti-tumor activity than BCG alone whereas IFN $\alpha$  had no effect. The cure rate was 14/15 in the combination group versus 8/17 with BCG alone. BCG and the combination increased IFN $\gamma$  expression. BCG increased CD4+ and CD8+ populations in spleens while the  $\alpha\beta$ + population was increased by IFN $\alpha$ . The combination increased both  $\alpha\beta$ + and CD4+/CD8+ populations significantly.

**Conclusion:** Both *in vitro* and *in vivo* studies suggest that the combination of BCG and IFN $\alpha$ -2b may represent a more efficacious therapy than BCG alone for superficial bladder cancer.

**#388 Iron-responsive element-dependent sustained production of nitric oxide.** Son, K.K., Wang, X. and Hall, K. *Department of Pharmaceutics, Rutgers, The State University of New Jersey, College of Pharmacy, Piscataway, NJ 08854.*

We have found that liposomal interferon-gamma (IFN $\gamma$ ) or liposomal inducible nitric oxide synthase (iNOS) gene was effective in treating cisplatin-resistant human ovarian carcinoma through production of nitric oxide (NO). To develop a high and sustained transgene expression system, it was our hypothesis that the expression of iNOS gene could be controlled by iron-responsive element (IRE) (33 nucleotides) located at 3'-end of the gene. We have synthesized Wild type IRE (5'-ATAATTATCGGAAGCAGT-GCCTCCATAATTAT-3') having the highest binding activity to iron-responsive element binding protein (IRE-BP) and constructed mammalian expression vectors pcDNA3-IFN $\gamma$ -IRE and pcDNA3-iNOS-IRE. To test the IRE-dependent IFN $\gamma$  or iNOS level and the subsequent NO production, A2780CP cells were transfected with pcDNA3, pcDNA3-IFN $\gamma$ , pcDNA3-iNOS, pcDNA3-IFN $\gamma$ -IRE or pcDNA3-iNOS-IRE using the standard *in vitro* lipofection protocol and grown in the presence of SNAP (0 to 100  $\mu$ M). The results showed that the level of IFN $\gamma$  as determined by the RAW264.7

method and iNOS expression by the Griess reaction increased in the cells transfected with pcDNA3-IFN $\gamma$ -IRE or pcDNA3-iNOS-IRE as compared to the cells transfected with pcDNA3-IFN $\gamma$  or pcDNA3-iNOS. These results indicate that IRE at the 3'-end of IFN $\gamma$  or iNOS gene can directly or indirectly regulate translation by NO. The NO-mediated cytotoxicity was also significantly enhanced in the pcDNA3-IFN $\gamma$ -IRE or pcDNA3-iNOS-IRE cells as compared to the pcDNA3-IFN $\gamma$  or pcDNA3-iNOS cells. It is thus concluded that both pcDNA3-IFN $\gamma$ -IRE and pcDNA3-iNOS-IRE construct sustained the high level of NO production and can thus be more effective in treating the drug-resistant ovarian carcinoma than the constructs with IRE, pcDNA3-IFN $\gamma$  and pcDNA3-iNOS.

This work is supported by NIH R29 CA75249.

**#389 The antioxidant agents alpha lipoic acid and N-acetyl cysteine are able to correct *in vitro* several functional defects of PBMC from advanced stage cancer patients.** Mantovani G., Maccio A., Mellis G., Mura L., Lai P., Massa E. and Mudu M.C. *Department of Medical Oncology and Internal Medical Sciences and Department of Obstetrics and Gynecology, University of Cagliari, Cagliari, Italy.*

We studied the ability of ALA and NAC, two powerful antioxidant agents, to correct *in vitro* the most significant functional defects of peripheral blood mononuclear cells (PBMC) from advanced stage cancer patients. In particular, we assessed the proliferative response of cancer patient PBMC to anti-CD3 monoclonal antibody (mAb). We also studied the expression of CD25 (IL-2R) and CD95 (Fas) on unstimulated and anti-CD3 mAb-stimulated PBMC: all these assays were performed with and without ALA and NAC. Moreover, we assessed the serum levels of proinflammatory cytokines IL-1, IL-6, TNF $\alpha$  as markers of pro-cachectic activity in cancer patients and the serum levels of IL-2 and sIL-2R. Twenty patients (pts) (mean age 64.6 years, range 40-72; M/F ratio 11/9) with lung cancer, ovarian cancer, endometrial cancer, head and neck cancer, all in advanced (III, IV) stage of disease, were studied. The serum levels of IL-1 $\beta$ , IL-2, IL-6, TNF $\alpha$  and sIL-2R were significantly higher in cancer patients than in normal subjects. The PBMC response to anti-CD3 mAb was significantly lower than that of controls. The addition of either ALA or NAC in the PBMC cultures stimulated with anti-CD3 mAb significantly increased the response of both cancer patient and normal subject PBMC. After 24 and 72 hr of culture with anti-CD3 mAb, CD25 expression on cancer patient PBMC was significantly lower than that of normal subject PBMC. The addition of either ALA or NAC into cultures of cancer patient PBMC significantly increased the percentage of cells expressing CD25, whereas in normal subject PBMC cultures the addition of ALA or NAC did not change the percentage of cells expressing CD25. After 24 and 72 hr of culture with anti-CD3 mAb, CD95 expression on cancer patient PBMC was significantly lower than that of normal subject PBMC. The addition of either ALA or NAC into cultures of cancer patient PBMC significantly increased the percentage of cells expressing CD95, whereas in normal subject PBMC cultures the addition of ALA or NAC did not change the percentage of cells expressing CD95. The results of the present study seem to confirm the favourable effect of antioxidant agents, such as ALA and NAC, on several important T cell functions *in vitro* in advanced stage cancer patients. Potentially this may lead to a more effective control of tumor cell growth and prevention/reversal of cancer cachexia also *in vivo*.

This work was supported from C.N.R., Rome, A.P. "Clinical Applications of Oncological Research" Contract Number 96.00588.PF39.

**#390 Sphingomyelin enhances chemotherapy of colonic tumor xenografts.** Modrak, David E., Lew, Walter, Blumenthal, Rosalyn D., Goldenberg, David M. *Garden State Cancer Center, 520 Belleville Ave., Belleville, NJ, USA 07109.*

**Background:** It has been shown in the literature that, 1) ceramide appears to be involved in drug-induced apoptosis, 2) alterations in ceramide metabolism *in vitro* can lead to resistance to anticancer therapies, 3) sphingomyelin (SM) levels are altered in tumor cells *in vivo*, 4) distinct signalling pools of SM appear to exist in cells and 5) lowering of the apoptotic threshold can result in greater induction of apoptosis in radio-resistant cells. Thus, one manifestation of altered SM metabolism within tumor cells could be reduced sensitivity to anticancer therapies because of an inability to produce a sufficient apoptotic signal via SM hydrolysis to ceramide. **Aim:** To determine if SM administration may reverse this effect and increase the tumors' sensitivity to chemotherapy. **Methods:** GW39 and HT29 colonic tumor bearing nude mice were treated with SM (2 or 10 mg/d for 7 days) in conjunction with the maximum tolerated dose of 5-fluorouracil (5FU, 0.45 mg/day for 5 days). Liver and kidney function and white cell counts were measured by blood analysis 3 and 7 days after the initiation of treatment. *In vitro* cell viability assays were performed using the MTT reagent. **Results:** SM alone had no effect on HT29 or GW39 tumor growth and 5FU alone slightly inhibited GW39 but not HT29 tumor growth. The intravenous co-administration of SM (10 mg/d) significantly enhanced 5FU induced tumor growth delay. Use of 2 mg/d SM resulted in no enhancement of therapy. Liver and kidney toxicity above that seen with 5FU alone was not noted at any SM level. Reduction in white cell counts was not enhanced by the co-administration of SM. *In vitro*, HT29 cells were not sensitized to either 5FU or adriamycin when SM was added to the media at 1 mg/ml. HCT15, however, were sensitized 2.4- and 4.1-fold, respec-

tively. Conclusions: Sphingomyelin administration appears to be a safe and effective method to increase chemo-therapeutic efficacy. Enhancement of potency is postulated to result from an increased ability of the tumor cell to initiate apoptosis. Current work is aimed at verifying this hypothesis and determining the applicability of these findings to other colonic tumor models and tumor types. Supported in part by USPHS grants R23 CA39841 and P01 54425 from the NIH.

**#391 Tumor suppression and sensitization to tumor necrosis factor  $\alpha$ -induced apoptosis by p202 in breast cancer cells.** Wen, Y., Yan, D.-H., Spohn, B., Deng, J., Lin, S.-Y., and Hung, M.-C. Department of Cancer Biology, Section of Molecular Cell Biology, The University of Texas M.D. Anderson Cancer Center

p202, an interferon (IFN)-inducible protein, interacts with several important regulatory proteins, resulting in transcription repression, growth arrest or differentiation. Our previous studies have shown that p202 can inhibit the growth of prostate cancer cells. In this report, we demonstrate that, in addition to inhibiting *in vitro* cell growth and transformation, p202 can also suppress the tumorigenicity of breast cancer cells *in vivo*. The expression of p202 in MDA-MB-453 and MCF-7 cells caused marked growth inhibition as measured in a colony-forming assay. The retarded growth rate caused by p202 is due to the inhibition of cell replication. The colony formation in soft agar of the p202 expression cells also significantly reduced. The loss of *in vitro* transformation phenotype correlated well with a suppression of tumorigenicity *in vivo*. The p202 transfection caused a drastic reduction of tumorigenicity of MCF-7 cells in nude mice as compared with the controls. The anti-tumor activity of p202 was also observed in prostate cancer cells. Furthermore, we found that p202 expression could sensitize breast cancer cells to apoptosis induced by TNF- $\alpha$ . TNF- $\alpha$  induces three-fold more apoptosis in p202 expressing cells than that in the parental cells. The sensitization correlates with the inactivation of NF- $\kappa$ B by a NF- $\kappa$ B/p202 interaction. In response to TNF- $\alpha$ , p202 can physically interact with p65, which impedes the active p65/p50 heterodimer formation in the nucleus and suppresses NF- $\kappa$ B transactivation activity. These results provide a scientific basis for a novel therapeutic strategy that combines p202 and TNF- $\alpha$  treatment against breast cancer.

**#392 Application of Tumor Necrosis Factor  $\alpha$  in Local and Systemic Treatment of Solid Tumors in Combination With Anti-Tumor Agents: Old Cytokine, New Opportunities.** ten Hagen, Timo L.M., van Tiel, Sandra T., Seynhaeve, Ann, L.B., de Wilt, Johannes H.W., van der Veen, Alexander, H., de Vries, Marc R., and Eggemont, Alexander M.M. Department of Surgical Oncology, University Hospital Rotterdam, the Netherlands.

Recently Tumor Necrosis factor- $\alpha$  (TNF) has been registered in Europe for the treatment of extremity soft tissue sarcoma by isolated limb perfusion (ILP). We have developed rat tumor models to study the anti-tumor activity of TNF in regional (e.g. ILP or isolated liver perfusion (ILP)) or systemic setting. Next to that *in vitro* studies are performed to examine the working mechanism of TNF in more detail.

Combination of TNF with melphalan (or doxorubicin) in ILP for the treatment of sarcomas in the rat demonstrated tumor responses comparable to the clinic. In this model we were able to demonstrate that addition of high dose TNF to the perfusate results an increased uptake of melphalan and doxorubicin (resp. 6- and 3-fold) in tumors. Moreover, systemic application of low dose TNF in combination with liposomal formulated doxorubicin (DOXIL) improved tumor response dramatically. Also in this setting enhanced intratumoral drug levels were demonstrated as compared with DOXIL alone. Both in high dose as well as in low dose treatment setting TNF is speculated to improve drug accumulation in tumor specifically by increasing permeability of the tumor associated vasculature (TAV). *In vitro* studies revealed no or marginal direct effect of TNF on tumor cells (cell growth arrest or induction of apoptosis), and no direct enhancement of the cytotoxicity of doxorubicin and melphalan. Moreover, TNF had also no effect on the cell cycle of the cells, ruling out possible negative effects of the cytokine on cell cycle specific drug like doxorubicin.

TNF most likely has strong effects on the TAV explaining the observed strong synergy with cytotoxic drugs *in vivo* and the absence of synergy *in vitro*. TNF could therefore very well be an useful addition to several therapies.

**#393 Gene Therapy By Isolated Limb Perfusion Results in High Local Transfection And Is The Only Modality Capable of Inducing Tumor Response With An Adeno Virus IL-3 Construct.** de Wilt, Johannes H.W., ten Hagen, Timo L.M., Eggemont, Alexander M.M., Bout, Abraham, de Roos, Wilfried K., Valerio, Dingo, and van der Kaaden, Marieke E. Dept. Surg. Oncol., Univ. Hospital Rotterdam, and Integene BV, Leiden, the Netherlands.

Selective transfection of tumor cells is a major problem in cancer treatment using gene therapy. In the first place the present study compares transfection efficacy of different routes of administration. Systemic, regional and intratumoral (IT) administration was compared with isolated limb perfusion (ILP) using adenoviruses harbouring the luciferase or LacZ gene. Secondly, an adenovirus construct carrying the gene for IL-3 was used to study antitumor effects in established tumors in rats using above mentioned routes of administration.

No specific transfection of tumor cells was found after systemic or regional administration. After ILP and IT injection high luciferase expression was demonstrated in tumor cells. Systemic contamination of luciferase was minimal after ILP but not IT. Histological slides showed only expression of LacZ around the needle track after IT administration, whereas ILP demonstrated a homogenous distribution through the tumor. After ILP with the adenovirus construct IG.Ad.CMV.rIL-3 $\beta$  a significant anti-tumor effect was demonstrated in two different tumors (BN175 and ROS1). This anti-tumor effect could not be demonstrated after IT or systemic administration with a similar dose. Dose finding studies showed that doses below  $1 \times 10^9$  i.u. IG.Ad.CMV.rIL-3 $\beta$  resulted in loss of anti-tumor effect. A weaker adenoviral vector (MLP) was not able to evoke an anti-tumor response with a similar dose of rIL-3 $\beta$ .

In conclusion, the present studies show that ILP results in selective gene transfection without systemic contamination, which is superior to IT treatment. Cytokine gene therapy using an rIL-3 $\beta$  construct results in a significant anti-tumor effect after ILP only, whereas other treatment modalities are without effect on the tumor.

**#394 The effect of Taxol treatment on serum interleukin-8 (IL-8) levels in patients with ovarian carcinoma.** Uslu, R., Ozsaran, A., Sanli, U.A., Dikmen, Y., Goker, E.N.T., Goker, E. Department of Medical Oncology and Department of Obstetrics and Gynecology, School of Medicine, Ege University, 35100 Bornova Izmir/Turkey.

Paclitaxel or Taxol is the most important chemotherapeutic agent used in ovarian cancer treatment. It is known that paclitaxel stabilizes microtubules, and this characteristic is the presumed primary mechanism for its antitumor activity. Recently, however, paclitaxel's other therapeutic effects has been reported by several groups. Lee LF et al have shown that paclitaxel can induce IL-8 promoter activation in subgroups of ovarian cancer through the activation of both AP-1 and NF $\kappa$ B. Further analysis of paclitaxel analogs indicated that the degree of IL-8 induction by analysis correlates with the extent of cell death; however, IL-8 itself is not the cause of cell death.

In this study, the effect of Taxol on serum IL-8 levels in patients with ovarian cancer was investigated. Twenty three patients were included to the study. The mean age was 53 years (26-72). Twelve of 23 patients have received Taxol treatment as an adjuvant therapy after optimal debulking surgery, 11 of 23 patients have received Taxol treatment because of metastatic disease. Serum IL-8 levels was analyzed before Taxol treatment (day 0) and 8 days after Taxol treatment with ELISA.

In patients who received Taxol as an adjuvant treatment after optimal debulking surgery, the mean IL-8 level was 31.01 pg/ml on day 0 and 52.02 pg/ml on day 8 and the difference was not significant ( $p > 0.05$ ). In patients with existing tumor bulk, the mean IL-8 level was 82.19 pg/ml on day 0 and 523.46 pg/ml on day 8 of Taxol treatment. The difference was statistically significant ( $p < 0.05$ ).

IL-8 is a pleiotropic molecule that has several pro-inflammatory properties including chemotactic effects on neutrophils, T cells and basophils, adhesive effects on monocytes, proliferative activation effect on endothelial cells. In addition to its direct toxic effect of Taxol, the increased proinflammatory response may contribute to the success of Taxol in patients with ovarian cancer. In present study, we have shown that serum IL-8 levels were increased at day 8 of Taxol treatment in patients with metastatic ovarian carcinoma. The prognostic significance and influence on treatment strategy of this increased serum IL-8 levels will be studied.

### SECTION 3: ANTIANGIOGENESIS/ANTIVASCULAR AGENTS

**#395 Localized activation of coagulation by engineered TF thrombogen targeted to cell surfaces through an N-terminally fused docking structure.** Liu, C., Dickinson, C.D., Shobe, J., Ruf, W., Yao, J., Doflate, F., and Edgington, T.S. Departments of Immunology and Vascular Biology, The Scripps Research Institute, La Jolla, California; Nuvas LLC, San Diego, California.

Anti-angiogenic and anti-vascular interventions have received increasing interest as potential cancer therapy strategies. Work published from this laboratory and collaborators demonstrated selective thrombotic infarction of tumors through selective targeting of the Tissue Factor (TF) extracellular domain to tumor vessels (Huang, et al. Science, 1997). TF is the cell surface initiator of the thrombotic cascade. The extracellular domain of TF is responsible for binding of Factor VII(a) to form the bimolecular protease TF-VIIa to proteolytically activate Factors X and IX. However efficient activation of the thrombotic cascade also requires the approximation of this complex to phospholipid membranes. Native transmembrane TF is 100,000-fold more active than soluble TF extracellular domain. In order to achieve site-specific induction of thrombosis to occlude undesired vessels under pathologic conditions using TF, a soluble TF molecule that retains coagulative function upon proper positioning onto a cell surface facilitator structure is necessary. Based on the crystal structure of TF and



factor VII complex as well as mutagenesis studies of both TF and factor VII, it is apparent that the N-terminus of TF will tolerate a fused docking protein domain. When binding to a membrane surface protein through that fused docking structure, the TF molecule might mimic the function of native cell surface TF. To test this hypothesis, a recombinant protein that contains the TF extracellular domain was fused at its N-terminus to fibronectin domains 8–11. This fusion protein efficiently initiated the coagulation cascade on Integrin-expressing cells that otherwise do not support this function. Synthetic peptides containing the RGD sequence blocked the binding of the fibronectin TF fusion protein to the integrin-positive cell and also prevented the activation of coagulation. These data demonstrate that the coagulation cascade can be efficiently activated through proper positioning of a soluble TF domain via a docking structure fused at its N-terminus. Based on the current understanding of the mechanism of cellular thrombosis, TF provided us with a unique opportunity to design selective vascular thrombogens to target a variety of specific endothelium and to thrombotically occlude undesired vessels.

**#396 Inhibition of endothelial cell function and induction of apoptosis by the anti-vascular agent 5,8-dimethylxanthenone-4-acetic acid (DMXAA),** Ching, Lal-Ming; Cao, Zhilun and Baguley, Bruce C. *Auckland Cancer Society Research Center, Auckland University Medical School, Auckland, New Zealand.*

DMXAA, a synthetic, low molecular weight compound, currently in clinical trials, has excellent activity against transplantable murine tumors with an established vasculature. It halts tumour blood flow and induces hemorrhagic necrosis, effects similar to that obtained with tumor necrosis factor (TNF). DMXAA stimulates the infiltrating host cells as well as some tumor cells to synthesise TNF *in situ*, and the anti-vascular effects of DMXAA can be partially reduced by the administration of antibodies to TNF. To determine whether its anti-vascular action is mediated entirely through the production of TNF, or whether DMXAA can target endothelial cells directly, we examined the effect of DMXAA on the ECV-304 human endothelial cells in culture. Between 3–100 µg/ml, doses that had no effect on cell viability, DMXAA inhibited tube formation by the ECV-304 cells, indicating that DMXAA may be capable of angiogenesis inhibition. At concentrations above 100 µg/ml, DMXAA induced, in a time and dose-dependent manner, endothelial cell apoptosis as determined using the TUNEL assay. The effects of DMXAA on ECV-304 cells in culture were independent of TNF, interferons or IP-10 production, and appeared to be as a result of a direct action of DMXAA. A single administration of DMXAA at the maximal tolerated dose inhibited by nearly 100%, bFGF-induced neo-vascularisation of matrigel plugs in an *in vivo* model for angiogenesis. An inactive analogue that does not have antitumor activity or induces cytokines, 8-methylxanthenone-4-acetic acid, did not inhibit endothelial cell invasion in the same assay. DMXAA induced synthesis of the anti-angiogenic cytokines, IP-10 and interferon- $\alpha$ , interferon- $\gamma$ , but not IL-12. These results indicate that DMXAA may possess both anti-vascular and anti-angiogenic properties through its ability to target tumor endothelial cells. The direct effects may be amplified *in vivo* by the production of anti-vascular and anti-angiogenic cytokines.

**#397 Regulation of tumor angiogenesis by p53-induced ubiquitin-mediated degradation of hypoxia-inducible factor-1 $\alpha$ .** <sup>1</sup>Ravi, Rajani, <sup>2</sup>Mookerjee, Bijoyesh, <sup>1</sup>Bhujwala, Zaver M., <sup>1</sup>Hayes-Sufter, Carrie, <sup>1</sup>Artemov, Dmitri, <sup>1</sup>Zeng, Q., <sup>1</sup>Dillehay, L. E., <sup>2</sup>Madan, Ashima, <sup>1</sup>Semenza, Gregg L., and <sup>1</sup>Bedi, Alul. <sup>1</sup>Johns Hopkins University School of Medicine, <sup>2</sup>University of Maryland Greenebaum Cancer Center, <sup>3</sup>Stanford University School of Medicine.

Regions of vascular deficiency or defective microcirculation in growing tumors are deprived of O<sub>2</sub>, glucose, and other nutrients. Clonal evolution of tumor cells in these hypoxic microenvironments results from selection of sub-populations that not only resist apoptosis, but also promote neovascularization. The switch to an angiogenic phenotype is considered to be a fundamental determinant of neoplastic growth and tumor progression. This realization has fueled a search for the molecular mechanisms by which the "angiogenic switch" is activated during tumorigenesis. In this study, we demonstrate that genetic inactivation of p53 in cancer cells provides a potent stimulus for tumor angiogenesis and identify a novel mechanism by which loss of p53 function contributes to the angiogenic phenotype of tumors. We find that homozygous deletion of p53 via homologous recombination in a human colorectal carcinoma cell line (HCT116) promotes the neovascularization and growth of tumor xenografts in nude mice. We show that p53 promotes the ubiquitination and proteasomal-degradation of the HIF-1 $\alpha$  subunit of hypoxia-inducible factor-1 (HIF-1), a heterodimeric transcription factor that regulates cellular energy metabolism (glucose transport and glycolysis) and angiogenesis in response to O<sub>2</sub> deprivation. HIF-1 binds to the 5' flanking sequence of the vascular endothelial growth factor (VEGF) gene and is required for transactivation of VEGF in response to hypoxia. We show that loss of p53 in tumor cells enhances HIF-1 $\alpha$  levels and DNA binding activity, and augments HIF-1-dependent transcriptional activation of the VEGF gene in response to hypoxia. We further demonstrate that forced expression of HIF-1 $\alpha$  in p53-expressing HCT116 cells promotes VEGF expression and neovascularization of tumor xenografts. HIF-1 $\alpha$  is frequently overexpressed in common human cancers and there

is a statistically significant correlation between the presence of mutant p53 and HIF-1 $\alpha$  overexpression. Therefore, amplification of normal HIF-1-dependent responses to hypoxia via loss of p53 function may contribute to activation of the angiogenic switch in a broad array of human cancers.

**#398 Squalamine and cisplatin block angiogenesis and growth of human ovarian cancer cells with and without overexpression of HER-2/neu oncogene.** Pielras, Richard J., Li, Diane and Williams, Jon I. *UCLA School of Medicine, Division of Hematology-Oncology, Los Angeles, CA 90095; and Magalain Pharmaceuticals, Plymouth Meeting, PA 19462.*

Angiogenesis appears to be essential for the growth of solid tumors and their metastases. Squalamine is a natural antiangiogenic steroid originally isolated from the dogfish shark *Squalus acanthias*; it is synthesized as a 7-24-dihydroxylated-24-sulfated cholesterol steroid conjugated to a spermidine at C3. Squalamine has potent antitumor effects (Cancer Res., 58: 2784–2792, 1998), and its potential role in the treatment of ovarian cancer with or without standard cisplatin chemotherapy was assessed. Since overexpression of HER-2 oncogene is associated with poor prognosis and enhanced promotion of tumor angiogenesis *in vitro*, human ovarian cancer cells 2008 without (2008 PAR) or with (2008 HER-2) HER-2 gene overexpression were grown as subcutaneous xenografts in nude mice. After growth of tumors to 150–200 cu. mm, animals were treated by intraperitoneal injection with control solution, cisplatin (4 mg/kg, day 1), squalamine (2 mg/kg, days 1–10) or cisplatin in combination with squalamine. By 28 days, both 2008 PAR and 2008 HER-2 tumors showed resistance to therapy with cisplatin alone, but squalamine alone elicited partial reduction in tumor size as compared to control (P<0.01). More profound regression of primary tumors to 5–6% of controls was elicited by combined treatment with squalamine and cisplatin (P<0.001). Immunohistochemistry revealed a blockade of angiogenesis assessed by quantitation of vessel density, and this was accompanied by increased apoptosis in tumor cells as determined with TUNEL assays. Although 2008 HER-2 ovarian tumors displayed more angiogenic activity (P<0.001) and less apoptotic activity (P<0.001) than 2008 PAR cancers, growth of both tumor types was suppressed by treatment with squalamine combined with cisplatin. Using *in vitro* studies, we find that squalamine does not directly affect proliferation of 2008 PAR or 2008 HER-2 cells but does block vascular endothelial growth factor (VEGF)-activated growth and migration of human umbilical vein endothelial cells. These results suggest that squalamine is antiangiogenic for human ovarian cancer cells with or without HER-2 overexpression and appears to enhance the cytotoxic effects of cisplatin chemotherapy, a phenomenon that may benefit patients who fail standard therapy. [Supported by NIH grants.]

**#399 Quantitative analysis of endothelial cell shape change after treatment with combretastatin A4 phosphate.** Galbraith SM, Lee F, Vojnovic B, Tozer GM, Chaplin D. *Tumour Microcirculation Group, Gray Laboratory Cancer Research Trust, Northwood, U.K.*

The tubulin binding agent combretastatin A4 phosphate has a tumour vascular targeting action. It has been shown that this drug produces a rapid increase in vascular resistance in tumours, with no increase in vascular resistance in the isolated hindlimb. This increase in vascular resistance occurred even using a cell free perfusate, so intravascular coagulation was not the primary event. Combretastatin has also been shown to increase permeability across endothelial cell monolayers, with an associated disruption of the cytoskeleton and endothelial cell shape change.

**Aim** To quantify the shape change produced by combretastatin and identify possible explanations for its tumour selective action.

**Methods** Confluent and proliferating cultures of HUVECs were exposed to the drug at varying concentrations and times, then fixed. Fixed cells were stained with anti- $\beta$  tubulin primary mouse antibody, and FITC linked anti-mouse secondary antibody. Images were acquired at  $\times 20$  magnification using in-house image acquisition software from randomly selected areas of slides, and then analysed using Visilog v4 software (Noesis, France), adapted in-house. A light pen was used to draw around each cell outline, and the cell areas (in pixels) contained by the outlines was calculated. At least 200 cells were outlined in this way for each slide.

**Results** There was a significant decrease in cell size with increasing concentration for both proliferating and confluent cells after 10 minutes (Spearman rank correlation coefficient  $-0.481$  and  $-0.238$  respectively), but the strength of the correlation was significantly greater for proliferating cells (p < 0.001), and the decrease in cell size began at least 1 log lower concentration for proliferating than for confluent cells.

**Conclusions** The time course of endothelial cell shape change is very rapid, with reduction in cell area visible by 10 minutes. This is the same time course as that seen for increases in vascular resistance in an ex-vivo model. This supports the hypothesis that it is the change in endothelial cell shape which is the initiating event leading to tumour vascular shutdown. The large difference in concentration at which shape change occurs in proliferating versus confluent cells could partly explain the wide therapeutic window seen for this drug in pre-clinical studies.

**#400 Development and characterization of monoclonal antibodies to the human VEGF receptors Flt-1 and KDR: Analysis of signals and functions of Flt-1 and KDR.** Kenya Shitara. (Tokyo Research Lab., Kyowa Hakko Kogyo Co. Ltd., Japan), Yasutomi Sato (Inst. of Development, Aging and Cancer, Tohoku Univ., Japan), Masabumi Shibuya (Inst. of Medical Science, Univ. Tokyo, Japan).

VEGF is thought to be a principal regulator of tumor angiogenesis. VEGF mediates its effects through two high affinity receptor kinases, Flt-1 and KDR. To gain a better understanding of physiological and pathological roles of VEGF receptors, we established and characterized monoclonal antibodies (mAbs) reactive with extracellular domain of human Flt-1 and KDR. Both mAbs could detect the cell surface VEGF receptors on human umbilical endothelial cells (HUVECs) by FACS analysis. Neutralizing activity of these mAbs was confirmed by the inhibition of VEGF binding to VEGF receptors and the suppression of VEGF-induced autophosphorylation of VEGF receptors. VEGF elicits cell migration and proliferation of HUVECs. The pattern of inhibition of two mAbs indicated that cell migration is regulated by the Flt-1, which is responsible for actin reorganization. A distinct signal is generated by KDR. This signal influences cell migration by regulating cell adhesion via phosphorylation of focal adhesion kinase (FAK) and paxillin, and the assembly of vinculin in focal adhesion plaque. Moreover, this latter signal regulates DNA synthesis.

These results suggest that both anti-Flt-1 mAb and anti-KDR mAb may have the potential for treatment and diagnosis of human cancers.

**#401  $\beta$  pep-25, a designer peptide cytokine, that potently inhibits angiogenesis.** Van der Schaft, Daisy W.J., Hillen, Harry F.P., Mayo, Kevin H., Griffioen, Aryan W., Wagstaff, John. Tumor Angiogenesis Laboratory, Section of Haematology & Oncology, Dept. of Internal Medicine, University Hospital Maastricht, P.O. Box 5800, 6202 AZ Maastricht, The Netherlands and the Dept. of Biochemistry, University of Minnesota, Health Sciences Center, Minneapolis, MN 55455.

$\beta$  pep-25, a de novo designer peptide 33mer, derived from the platelet factor 4 (PF4) molecule is a potent anti-angiogenic agent. Biophysical data (Nuclear Magnetic Resonance and Circular Dichroism) show that  $\beta$  pep-25 forms a stable, anti-parallel  $\beta$ -sheet structure in aqueous solution. At 100  $\mu$ g/ml  $\beta$  pep-25 specifically inhibits vascular endothelial cell (EC) proliferation >95% in 3 day cultures. Half maximal effects were obtained at 10–30  $\mu$ g/ml. The peptide induces apoptosis in 80% of EC as indicated by TUNEL-analysis and by the presence of propidium iodide-labeled subdiploid cells in FACS analysis. These *in vitro* effects were more potent than those of PF4, endostatin & angiostatin. A related peptide, over 80% homologous to  $\beta$  pep-25, did not have any inhibitory activity.  $\beta$  pep-25 also inhibits EC adhesion to extracellular matrix components which leads to inhibition of EC migration. Inhibition of angiogenesis was demonstrated in the *in vitro* collagen gel tube formation assay and *in vivo* in the CAM assay. Treatment of xenograft tumor models with  $\beta$  pep-25 inhibited tumor growth by approximately 70%.  $\beta$  pep-25 produced no significant toxicity in mice at a total dose of 1 mg.

This is the first designer peptide cytokine with well-defined biological functions which may be an effective anti-angiogenic agent for therapeutic use against various pathological disorders such as neoplasia, rheumatoid arthritis, diabetic retinopathy and re-stenosis. Phase I clinical trials with this agent are planned for the near future.

**#402 Soluble VEGF-receptor sflt-1 in conditioned medium from uveal melanoma cells inhibits VEGF-induced migration, invasion and differentiation of endothelial cells.** Rota Rossella, Ricconi Teresa, Petrucci Romina, Biasi Maria A., Marullo Michele, Capogrossi Maurizio, Balesstrazzi Emilio. Department of Ophthalmology, University of L'Aquila, Italy; I.D.I., Roma, Italy.

**Aim:** To test the effect of media conditioned by OCM-1 uveal melanoma cells infected with a replication-deficient adenovirus vector (Ad) carrying a recombinant soluble-flt-1 cDNA (Ad.sflt-1) on human endothelial cells (HUVEC) functions *in vitro*. **Methods:** OCM-1 cells were either infected with Ad.sflt-1 or Ad.null (100 pfu/cell) or not infected. HUVEC cell counting was performed by an hemacytometer. Cell migration and invasion were assessed in modified Boyden chambers, through gelatin or Matrigel-coated filters, respectively. HUVEC differentiation was performed on reconstituted basement membrane proteins (Matrigel)-coated plates. **Results:** OCM-1 cells either Ad.null-infected or uninfected produced  $3.6 \pm 0.5$  and  $3 \pm 0.3$  ng of VEGF in 24 hours/ $10^6$  cells respectively. In contrast Ad.sflt-1 infection completely prevented VEGF detection in OCM-1 conditioned medium. HUVECs exhibited inhibition of growth rate when cultured in conditioned medium from Ad.sflt-1 infected OCM-1 cells (at 5 days: 62% and 70% of Ad.null infected or uninfected cells respectively). HUVEC migration and invasion were reduced when performed in the presence of media conditioned by Ad.sflt-1 infected OCM-1 cells (80% and 85% of reduction vs Ad.null-infected cells for migration and invasion respectively). HUVEC resuspended in Ad.sflt-1 infected OCM-1 conditioned medium also failed to form capillary-like structures on Matrigel coated plates. **Conclusions:** Secretion of soluble flt-1 receptor in the media conditioned by OCM-1 melanoma cells infected with Ad.sflt-1 affects endothelial cell functions through depletion of VEGF.

**#403 Antivascular effects and antitumor activity of NSC 643314 *in vitro* and *in vivo*.** Burger, A.M., McGown, A., Kelland, L., Fiebig, H.H., Härter, M., Sausville, E.A. Tumor Biology Center, Freiburg, FRG; Patterson Institute for Cancer Research, Manchester, UK; The Institute of Cancer Research, Sutton, UK; Bayer AG, Wuppertal, FRG; National Cancer Institute, DTP, Bethesda, MD, USA: on behalf of the CRC/EORTC Committee on European NCI compounds.

Since November 1993 the CRC/EORTC Committee on European NCI compounds has reviewed nearly 1,000 agents in 10 sets which have originated in Europe and were tested for activity in the NCI 60 cell line screening program. NSC 643314 was selected from set 1 as a compound which was potentially active (mean  $GI_{50} = 275$  nM) and which showed differential cytotoxicity towards colon and ovarian cancer cell lines. Thus, the compound was subsequently referred for formulation, pharmacokinetics, and time course experiments in sensitive cell lines. These parameters were favorable in that the duration of exposure required to establish cytotoxic drug effects at the  $GI_{50}$  was 1h and the peak plasma drug levels achieved *in vivo* were 10-times higher (10–14  $\mu$ g/ml after 15 min.) than the  $GI_{50}$  concentrations needed *in vitro*. The compound was therefore forwarded for xenograft testing and mechanistic studies. We found marked *in vivo* antitumor activity in 2 ovarian cancer xenografts (OVXF 1023 and OVCFAR-3) if drug was given i.p. at doses of 100 mg/kg in a Q7Dx3 schedule. T/Cs were approximately 40% with regressions seen in the OVXF 1023 model. In 2 colon carcinomas (SW-620 and CFX 280) however, the drug was inactive (T/Cs 73–92%).

COMPARE analysis based on  $GI_{50}$  data indicated that NSC 643314 might be related to tubulin binding agents, which is also reflected in its flat dose response curves. Thus, NSC 643314 was tested for inhibition of tubulin assembly and for antivascular effects—a characteristic of many tubulin binders. The drug was able to displace  $^3H$ -labeled colchicine to 75% at its binding site and did affect permeability and growth of HUVEC cells more potently than the angiogenesis inhibitor TNP-470 and to a similar extent as the antivascular agent combretastatin. Moreover, NSC 643314 was more potent in HUVEC cells with a mean  $GI_{50}$  of 35 nM than in the sensitive ovarian cancer cell line A2780 with a  $GI_{50}$  of 70 nM.

Our data indicate that NSC 643314 is an interesting new anticancer agent and particularly its antivascular effects will warrant further investigations and the exploitation of NSC 643314 as a candidate for clinical development.

**#404 Characterization of the anti-angiogenic activity of human endostatin.** Ziche Marina, Donnini Sandra, Morbidelli Lucia, Granger Harris J. and Rehn Marko. CIMMBA, Univ. Florence, Florence, Italy, Microcirculation Res. Inst. and Dept. Med. Physiology, Texas A&M Univ., College Station, TX and La Jolla Cancer Research Center, The Burnham Institute, La Jolla, CA, USA.

Endostatin, a 20 kDa C-terminal fragment of collagen XVIII, is a specific inhibitor of endothelial cell proliferation and angiogenesis. The aim of the present study was to assess the activity of human endostatin preparation both *in vitro* and *in vivo*. Endostatin was obtained by expression in *E. coli* with a His-tag tail. After a first purification step using Ni-column under reducing and denaturing conditions, endostatin was refolded *in vitro*. The soluble fraction was collected and processed by anion exchange chromatography and heparin affinity chromatography. To remove any residual bacterial endotoxins it was run through polymyxin B-agarose.

The inhibitory effect of human endostatin was tested in two different experimental settings: 1) in cultured postcapillary venular endothelial cells stimulated with fibroblast growth factor-2 (FGF-2) and vascular endothelial growth factor (VEGF); 2) in the angiogenesis process produced in the avascular rabbit cornea by VEGF. Our results indicate that low concentrations (10–300 ng/ml) of human endostatin were able to specifically inhibit the proliferation and migration of endothelial cells, while it was devoid of any effect on other cell lines. Endostatin differentially affected the functions of endothelial cells in response to FGF-2 and VEGF. When tested *in vivo* in the avascular rabbit cornea assay endostatin exerted a differential behaviour depending on the experimental design (endostatin added simultaneously to angiogenic factor vs the tissue enrichment with the angiogenic factor, vs the enrichment with the inhibitor).

These findings taken together suggest that the angiogenic profile of a tumor may have an influence on the efficacy of antiangiogenic/antitumor therapy with endostatin.

**#405 Effect of combination of phenylbutyrate and 13-cis retinoic acid on tumor cell proliferation, *in vivo* growth and angiogenesis.** Pili, R., Kruszewski, M., Hager, B., Plette, C., Isaacs, J.T., and Carducci, M.A. Johns Hopkins Oncology Center, Baltimore, MD 21231.

Differentiation inducing agents such as retinoids and butyric acid derivatives have been shown to have an inhibitory effect on tumor cell proliferation and tumor growth in preclinical studies. Clinical trials involving single agents have been suboptimal in terms of antitumor activity or clinical benefit. The purpose of this study was to evaluate the combination of phenylbutyrate (PB) and 13-cis retinoic acid (CRA) as a treatment of cancer. Mechanistically it has been suggested that this combination may have synergistic activity based on the modulation of retinoid receptors and



retinoid response elements by PB. The cytostatic activity of the drugs was evaluated using proliferation assays utilizing the human (TSU-Pr1, PC-3, LNCaP) and rat (Dunning rat-G cell) prostate carcinoma (PCA) cell lines, the human glioblastoma (U-87 MG) and breast carcinoma (MCF-7) cell lines. Program cell death (PCD) was determined using flow cytometry analysis (FACS) and *in vivo* antitumoral activity of PB and CRA was evaluated on TSU-Pr1, PC-3, LNCaP and Dunning rat-G cell xenograft tumors in nude mice. The agents alone showed inhibition of PCA cell proliferation *in vitro* (PB 52–68%; CRA 11–38%) with additive effect when combined together (PB + CRA 62–84%). Similar results were obtained with U-87 MG and MCF-7 cell lines, though with lesser inhibition. FACS analysis detected increased apoptosis in the combined groups of PCA when compared to control (~11–16% vs 0.5–0.6%). Combination of PB and CRA had a statistically significant and greater inhibition of tumor growth *in vivo* as compared with single agents, more evident for the hormone-sensitive cell lines LNCaP and G cell lines (82–92% inhibition). Histological examination of the xenografts for microvessel density showed a reduced number of blood vessels in the animals treated with combined drugs (62% reduction) suggesting also a direct effect on tumor angiogenesis. The effect of PB and CRA was tested on bovine and human endothelial cells. Single agents had an inhibitory effect on cell proliferation and clonogenic capability of endothelial cells and combination had an additive effect (60–80% and 70% inhibition, respectively). The Matrigel angiogenesis assay showed inhibition of neovascularization in the animals treated with combined drugs (59% inhibition). This study showed the additive inhibitory effect of combination of differentiation agents PB and CRA on several tumor cell type proliferation. We also demonstrated inhibition of tumor growth and angiogenesis, suggesting an inhibitory activity of these two agents on both the tumor and the vasculature compartments. Phase I clinical trial is planned for later this year.

**#406 Cyclo-oxygenase and nitric oxide synthase inhibitors inhibit murine mammary tumor growth and metastasis by blocking tumor cell migration, invasion and angiogenesis.** Lala Peeyush K., Jadeski Lorraine, Hum Kathleen, Rozic Jerry and Chakraborty Chandan. *Department of Anatomy and Cell Biology, The University of Western Ontario, London, Ontario, Canada N6A 5C1.*

Productions of prostaglandins (PG) ascribed to cyclo-oxygenase-2 (COX-2) and nitric oxide (NO), ascribed to endothelial type (e) NO synthase (NOS) expression by tumor cells were both found to promote tumor growth and metastasis in a murine breast cancer model, which could be mitigated with respective treatments with the COX-inhibitor indomethacin (Indo) or NOS inhibitors NMMA or L-NAME. Present study explored the underlying mechanisms, utilizing two mammary adenocarcinoma cell lines, clonally derived from a single C3H/HeJ spontaneous tumor, which differed in metastatic phenotype (C3L5-highly metastatic, high eNOS and high COX-2 expressing; C10-weakly metastatic, low eNOS and moderate COX-2 expressing). Cellular migratory ability *in vitro*, quantitated with a transwell migration assay, was found to be similar in both cell lines, and was suppressed by treatments with Indo (C3L5 cells) as well as L-NAME (C3L5 and C10 cells) and respectively restored with addition of PGE<sub>2</sub> or L-Arginine indicating that endogenous PGE<sub>2</sub> and NO had migration-stimulating effects. Cellular ability to invade Matrigel *in vitro* was higher in C3L5 than in C10 cells. However, using similar experiments as in the migration assay, endogenous NO was shown to promote invasiveness of both cell lines. Invasion stimulation by NO was found to be due to an upregulation of matrix metalloproteinase (MMP)-2 mRNA and downregulation of tissue inhibitor of metalloproteinases (TIMP)-2 and -3 mRNA in C3L5 cells. Finally, endogenous NO was shown to promote tumor-induced angiogenesis *in vivo* quantitated in sc implants of tumor cells suspended in growth factor-reduced Matrigel: (a) angiogenesis was lower with low-eNOS-expressing C10 than with high eNOS-expressing C3L5 cells; (b) L-NAME therapy of C3L5 but not C10 implant-bearing mice substantially reduced tumor angiogenesis as compared to control mice receiving D-NAME the inactive enantiomer. Similarly, endogenous PG was shown to be angiogenic in C3L5 implants; Indo therapy dramatically reduced angiogenesis. However, a combination of L-NAME and Indo therapy failed to produce any additive or synergistic effect, indicating that angiogenic stimulus by PG and NO may be mediated by a final common pathway. Thus antitumor and antimetastatic effects of COX/NOS inhibitors were due to inhibition of migration, invasion and angiogenesis in this tumor model. Since COX-2 and iNOS expression are positively correlated with human breast cancer progression, selective COX-2 and iNOS inhibitors may prove useful in human breast cancer therapy. (Supported by the US Army Grant DAMD 17-96-6069 and the Breast Cancer Society of Canada).

**#407 Inhibition of bladder carcinoma angiogenesis, stromal support and tumor growth by halofuginone.** Elkin Michael, Miao Huan-Qua, Ariel Ilana and Vlodavsky Israel. *Departments of Oncology and Pathology, Hadassah-Hebrew University Hospital, Jerusalem 91120, Israel.*

We have previously demonstrated that halofuginone, a widely used alkaloid coxidiostat, is a potent inhibitor of collagen a1(I) and matrix metalloproteinase 2 (MMP-2) gene expression. Halofuginone also suppresses extracellular matrix (ECM) deposition and cell proliferation. We investigated the effect of halofuginone on transplantable and chemically

induced mouse bladder carcinoma. In both systems, oral administration of halofuginone resulted in a profound anti-cancerous effect, even when the treatment was initiated at advanced stages of tumor development. While halofuginone failed to prevent proliferative pre-neoplastic alterations in the bladder epithelium, it inhibited further progression of the chemically induced tumor into a malignant invasive stage. Histological examination and *in situ* analysis of the tumor tissue revealed a marked decrease in blood vessel density, and in both collagen a1(I) and H19 gene expression. H19 is regarded as an early marker of bladder carcinoma. The anti-angiogenic effect of halofuginone was also demonstrated by an almost complete inhibition of microvessel formation at the periphery of aortic rings embedded in a collagen gel. Oral administration of halofuginone also inhibits neovascularization in the mouse corneal micropocket assay. We attribute the profound anti-tumoral effect of halofuginone to its combined inhibition of the tumor vascularization, stromal support, invasiveness and cell proliferation.

**#408 Vascular growth factor and vascular growth receptor expression after radioimmunotherapy.** Taylor, Alice P., Osorio, Louis, Goldenberg, David M., Blumenthal, Rosalyn D. *Garden State Cancer Center, Belleville, NJ 07109.*

Tumor-recovery and regrowth after therapy may depend on regulation of vascular growth factor and vascular growth factor-receptor expression. To determine how expression of vascular growth factors and their receptors is altered after RAIT, mice bearing Calu-3 (human lung), LoVo, GW-39, or HT-29 human colon tumor xenografts were treated with one dose (1500 cGy) of <sup>131</sup>I-MN-14 anti-CEA IgG (RAIT). Afterwards at one week intervals tumors were removed up to 6 weeks and sections were immunohistochemically stained (n = 4–6 samples/time point/2 independent experiments) for: vascular endothelial growth factor (VEGF), VEGF receptors, flk-1 and flt-1, angiotensin-1 and -2 (angio), their receptor, Tie-2, and endothelial cell-associated, Tie-1, NOS-3 and CD 31. LoVo and Calu-3 expression of VEGF and its receptors, flk-1 and flt-1, remained near untreated levels. However, LoVo and Calu-3's expression of Tie-1 and Tie-2 rose significantly above untreated controls at weeks 3 and 4. LoVo and Calu-3 also demonstrated concomitant significant rise in Tie-2 ligands, angio-1 and -2. On the other hand, HT-29 and GW-39 displayed significant VEGF upregulation (weeks 3, 4; week 1, respectively). Enhanced VEGF expression was paralleled by concomitant upregulation of flk-1 expression for HT-29 (1.5, 2.0-fold, weeks 1, 3), and flt-1 for GW-39 (significantly above untreated, weeks 1, 2). Unlike LoVo and Calu-3, Tie-2 expression in HT-29 and GW-39 did not rise appreciably after RAIT. Lysates from all 4 tumor lines were also subjected to immunoassay for VEGF; only HT-29 showed upregulation of VEGF. Tumors, HT-29 and GW-39, with the highest increases in VEGF concomitantly increased either flk-1 or flt-1. LoVo and Calu-3, on the other hand, increased Tie-1, Tie-2 and angiotensin expression, but VEGF production, and VEGF receptor expression remained near untreated levels. These results suggest that tumors differentially regulate angiogenic factors and their receptors after RAIT, and that different mechanisms of recovery from RAIT may dominate recovery in different tumors. It may be possible to employ these changes in a combination therapy approach utilizing RAIT and VEGF, angiotensins or their receptors as targets. (Supported in part by USPHS grant #CA60764 from the NIH.)

**#409 Intravenous cationic liposome endostatin gene therapy for spontaneous canine cancer.** MacEwen, EG; Thamm, DH; Medberry, P; Elmajli, RE; Dow, SW. *Univ. of Wisconsin (EGM, DHT), Madison, WI; Valentis, Inc. (PM), Veterinary Cancer Specialists (REE), and National Jewish Medical and Research Center (SWD), Denver, CO.*

Recently, a large body of data has been generated regarding the anti-tumor efficacy of endogenous angiogenesis inhibitors such as angiostatin and endostatin in a variety of preclinical models. The spontaneous canine cancer model offers several unique advantages for preclinical drug development, including relatively large size, spontaneous tumor development, a shared environment with humans, and similarities in terms of the biological behavior of canine and human tumors. This study evaluates the safety of intravenously administered endostatin cationic liposome-DNA complexes in dogs with refractory tumors. Data regarding antitumor efficacy and gene expression has also been generated.

Client-owned dogs with cancer, for which standard treatment had failed or been declined, received 90-minute intravenous infusions of the cDNA encoding murine or canine endostatin complexed to DOTIM-cholesterol (Endo-CLDC), at a starting dose of 20 mcg DNA per kg. Vital signs were monitored and serum collected during the first 48 hours, and samples of tumor tissue were obtained prior to and 24 to 48 hours following the first Endo-CLDC administration, for assessment of systemic endostatin levels and gene expression in tumor tissue. Responses were assessed according to standard criteria. Endo-CLDC infusions were continued on a weekly basis until there was evidence of progressive disease.

To date, 19 dogs with various tumor types have been enrolled. The median number of treatments received was 3 (1 to 8). Two dogs died within 3 days of receiving the first Endo-CLDC infusion: one apparently from gastrointestinal perforation and one from septicemia. Other side effects have been limited to moderate thrombocytopenia and fever, which typi-

cally resolved within 48 hours. One dog with malignant melanoma experienced a complete response, and another experienced stabilization of disease for 4 months. Detectable levels of endostatin protein have been measured in canine lung tissue. Additional data regarding *in vitro* canine tumor cell transfection and *in vivo* gene expression will be presented.

**#410** SU6668, a broad spectrum angiogenesis inhibitor, exhibits potent anti-tumor activity in xenograft models, including regression of established tumors. Laird, AD, Sukbuntherng, J, Antonian, L, Shawver, LK, Strawn, LM, Shenoy, N, Blake, R, Sun, L, Tang, C, Tang, F, Wagner, GS, Hirth, P, McMahon, G, Cherrington, JM. *SUGEN, Inc., South San Francisco, CA 94080.*

SU6668, a novel tyrosine kinase angiogenesis inhibitor, is currently being evaluated in Phase I studies for the treatment of advanced malignancies. SU6668 competitively inhibited (with regard to ATP) the kinase activities of Flk-1/KDR, PDGFR and FGFR. Pharmacokinetic parameters of SU6668 were determined in mice following delivery by the intravenous, intraperitoneal and oral routes and indicated a long ( $\approx$ 5 hours) plasma half life, high plasma AUC and essentially 100% bioavailability. Plasma levels of SU6668 were above the IC50 for inhibition of VEGF- and FGF-stimulated endothelial cell proliferation for at least 16 hours following oral administration. As expected for an inhibitor of Flk-1/KDR, FGFR and PDGFR, SU6668 potently inhibited the growth of a variety of human tumor xenografts in athymic mice. In these experiments, greater than 75% inhibition of tumor growth was readily achieved with SU6668 dosed by either the intraperitoneal or oral route. Furthermore, SU6668 treatment induced regression of very large (approximately 1000 mm<sup>3</sup>) established tumors in several tumor xenograft models. The rate of regression was rapid and independent of tumor size prior to the start of treatment. Further experiments to determine the mechanism of tumor regression with this angiogenesis inhibitor are ongoing. Importantly, in spite of its broad target profile, SU6668 is well tolerated, exhibiting no toxicity to date in short term preclinical chronic dosing studies. Data are forthcoming regarding the safety and efficacy profiles of this inhibitor in human clinical trials.

**#411** Activity profile of SU5416, a small molecule Flk-1/KDR inhibitor, in tumor xenograft models. Cherrington, JM, Laird, AD, Strawn, L, Shenoy, N, Tang, F, Blake, R, Yamada, Y, Yonekura, K, McMahon, G and Shawver, L. *SUGEN, Inc., South San Francisco, CA 94080, and Taiho Pharmaceutical, Cancer Research Laboratories, Hanno Research Center, Japan.*

SU5416 is currently in Phase III studies for the treatment of advanced malignancies administered twice weekly by the intravenous (IV) route. SU5416 is a novel, competitive (with regard to ATP), small molecule inhibitor of the receptor tyrosine kinase Flk-1/KDR (K<sub>i</sub> = 0.16  $\mu$ M) and has been shown to inhibit VEGF-stimulated endothelial cell mitogenesis *in vitro*. SU5416 inhibits growth of a panel of tumor xenografts (lung, melanoma, epidermoid, prostate) in athymic mice when administered intraperitoneally (IP). In addition to these activities, oral (PO) and subcutaneous (SC) administration of SU5416 have also demonstrated efficacy in tumor xenograft models. SU5416 delivered PO daily inhibited the growth of several tumor xenografts by 55-79%. As well, infrequent (weekly or monthly) SC administration of SU5416 resulted in >80% growth inhibition of tumor xenograft models. SU5416 also has been shown to inhibit the growth of established (50-200 mm<sup>3</sup>) tumor xenografts in athymic mice by 45-75%, demonstrating that SU5416 does not have to be present during very early tumor establishment and initial growth to be efficacious. Finally, SU5416 has shown potent inhibition of A549 (NSCLC) experimental lung metastases in athymic mice. These data suggest that SU5416 may demonstrate broad efficacy against human cancers and that additional routes of administration may be feasible for clinical use.

**#412** Constitutive expression of vascular endothelial growth factor correlates with growth and metastasis of human pancreatic adenocarcinoma. Wang, B., Shi, Q., Le, X., Huang, S., Abbruzzese, J.L., and Xie, K. *The University of Texas M. D. Anderson Cancer Center, Houston, TX 77030.*

The most deadly aspect of pancreatic adenocarcinoma is the ability of this disease to metastasize early and widely. The aggressive nature of this disease has been related to overexpression of several growth factors and their receptors. In the present study, we determined the role of vascular endothelial growth factor (VEGF) in the growth and metastasis of human pancreatic cancer cells. A series of human pancreatic cancer cell lines were grown *in vitro*. Ten of fifteen (67%) of human pancreatic cancer cell lines constitutively secreted high levels of VEGF as determined by an enzyme-linked immunosorbent assay. To determine whether VEGF expression correlated with *in vivo* growth and metastasis, various clones were established from PANC-1 human pancreatic cancer cells. PANC-1W1, W2, and W3 expressed low levels of VEGF, whereas PANC-1W4, W5 and W6 expressed high levels of VEGF. High and low VEGF-expressing cell lines were injected into the pancreas of nude mice. High VEGF-expressing cell lines produced large pancreatic tumors and numerous liver metastases, whereas low VEGF-expressing cell lines did not. Examination of the tumors demonstrated that aggressive local growth and metastasis correlated with the high vascular density. Collectively, our data demonstrate that

constitutive overexpression of VEGF plays an important role in tumor angiogenesis and the aggressive biology of human pancreatic cancer. As a potential therapeutic target for pancreatic cancer, understanding the mechanism of constitutive VEGF overexpression may lead to novel treatment strategies.

**#413** Preclinical evaluation of antiangiogenic therapy with TNP-470 for human neuroblastoma. Shusterman Suzanne, Grupp Stephan A, Maris John M. *Children's Hospital of Philadelphia, The University of Pennsylvania Cancer Center, Philadelphia, PA, USA.*

Neuroblastoma (NB) is a pediatric malignancy in which tumor vascularity is highly correlated with disease outcome. Thus, novel therapeutics that target the vascular endothelium are candidates for incorporation into neuroblastoma clinical trials. TNP-470 (TAP Pharmaceuticals) is a specific angiogenic inhibitor with a broad spectrum of activity that could be used for this purpose. We therefore examined the efficacy of TNP-470 on NB xenograft growth in athymic (nu/nu) mice. Sixty mice were inoculated with  $1 \times 10^7$  CHP-134 cells (*MYCN* amplification, 1p deletion, 17q gain) in 0.2 ml of Matrigel®, and treated with either TNP-470 (100 mg/kg/dose) or saline subcutaneously 3 times a week. Three experiments were performed with treatment initiated: a) when tumor volumes reached 250 mm<sup>3</sup>; b) 12 hours after tumor inoculation; or c) 10 days following 450 mg/kg cyclophosphamide (CPM), which was initiated when tumor volume reached 300 mm<sup>3</sup>. Angiogenesis inhibition by TNP-470 was assayed separately using a Matrigel® implant model. Tumor growth rate was markedly inhibited in mice receiving TNP-470 administered alone as compared to mice receiving saline with a treatment to control (T/C) ratio at day 21 = 0.4 (p = .007). TNP-470 also significantly inhibited tumorigenicity when administered shortly after xenograft inoculation (minimal residual disease model; T/C at day 30 = 0.1, p < .0001), and when administered following CPM (T/C at day 30 = 0.1, p < .0001). Histopathologic evaluation of tumors treated with TNP-470 showed an increased apoptotic index with no change in the proliferative index. Preliminary Matrigel assay results showed decreased hemoglobin content of TNP-470 treated implants compared to controls, consistent with specific inhibition of angiogenesis. These data show that TNP-470 is a potent inhibitor of human NB growth rate and tumorigenicity both alone and when given in sequential fashion with conventional chemotherapy. We speculate that TNP-470, or other antiangiogenic agents may be useful adjuvant therapy for high-risk NB patients, particularly when used in the setting of minimal residual disease.

**#414** Proteasome inhibitor PS-341 Effective as an anti-angiogenic agent in the treatment of human pancreatic via the inhibition of NF- $\kappa$ B and subsequent inhibition of vascular endothelial growth factor production. Harbison, M.T., Bruns, C.J., Bold, R.J., Elliot, J.P., Adams, J., Abbruzzese, J., and McConkey, D.J. *U.T.M.D. Anderson Cancer Center, Houston, Texas 77030 and Proscript, Inc., Cambridge, MA 02139.*

PS-341, a boronate inhibitor of the multisubunit protease complex, blocks the degradation of regulatory proteins involved in cell cycle regulation and cellular survival. The proteasome is required for the activation of NF- $\kappa$ B via the degradation of the inhibitory protein, I $\kappa$ B. NF- $\kappa$ B triggers survival pathways in a variety of cells via the upregulation of inhibitors of apoptosis. Recent reports indicate that NF- $\kappa$ B is constitutively activated in pancreatic carcinoma. Treatment of Pancreatic tumors implanted orthotopically in nude mice with PS-341 showed a decrease in angiogenic endpoints. We therefore investigated PS-341's effects on NF- $\kappa$ B mediated survival and VEGF production in human pancreatic cancer cell lines.

**Methods:** Human pancreatic cell lines Mia-PaCa1 and L3.6pl were injected orthotopically in nude mice. After 14 days the tumors were treated bi-weekly with various doses of PS-341 for up to 4 weeks. The tumors were then harvested and evaluated for apoptosis, proliferation, NF- $\kappa$ B activity, and angiogenic markers. *In vitro* analysis of NF- $\kappa$ B activity was analyzed using gel shift techniques, and dual Luciferase using a NF- $\kappa$ B consensus sequence and a full length VEGF promoter.

**Results:** Treatment of established tumors resulted in the marked decrease in viability and proliferation. In addition, there was a decrease in NF- $\kappa$ B activity, VEGF production, and microvessel density in the treated tumors. *In vitro* analysis demonstrated a marked decrease in NF- $\kappa$ B activity via gel shift and NF- $\kappa$ B driven Luciferase. PS-341 also decreased the production of VEGF in the cell lines as measured by full length VEGF promoter in front of a Luciferase construct. The effects of PS-341 mimicked transient transfection of the super repressor of NF- $\kappa$ B, I $\kappa$ B with serine to alanine mutations at the regulatory residues.

**Conclusions:** PS-341 is an effective therapy against human pancreatic carcinoma. These tumors apparently rely on NF- $\kappa$ B mediated survival pathways. Treatment reduces proliferation and increases tumor cell apoptosis via the blockade of NF- $\kappa$ B activation. The reduction in NF- $\kappa$ B activity reduces the production of VEGF which acts as a survival factor for tumor endothelial cells resulting in a reduction of tumor vascularity.

**#415** Heterogeneity of angiogenic activity in a human liposarcoma. Eike-Gert Achilles, Nils Hansen-Algenstaedt, Antonio Fernandez, Elizabeth N. Alfred, Oliver Kisker, Xavier Rogiers and Judah Folkman *Children's Hospital, Harvard Medical School, Boston MA, 02115, USA, University Hospital Hamburg, Dep. of Hepato-Biliary Surgery and Dep. of Orthopaedic Surgery, 20246 Hamburg, Germany.*



**BACKGROUND:** Tumor heterogeneity has been demonstrated for metastasis, proliferation rate and enzymatic activity. However, the angiogenic heterogeneity of tumors has been little investigated.

**METHODS:** To study angiogenic heterogeneity in a single tumor we have developed an *in vivo* model of subcutaneous xenotransplants from a human liposarcoma cell line (SW-872) in SCID-mice. Tumor growth was recorded over a period of up to 6 months. Tissues were analyzed for tumor cell apoptosis, microvessel density and proliferation.

**RESULTS:** Isolated and re-transplanted tumor pieces or clones of SW-872 were either highly angiogenic and fast growing, or weakly angiogenic and slow growing, or appeared not to be angiogenic and remained stable. Increasing tumor volume correlated positively with microvessel density and inversely with tumor cell apoptosis. However, rate of tumor volume was less strongly, but positively, associated with tumor cell proliferation *in vivo* and *in vitro*.

**CONCLUSIONS:** Tumor cells appear to be heterogeneous for angiogenic activity. This suggests that clinical progression of human cancer may be mediated in part by selection of clones with higher angiogenic activity. This heterogeneity provides a possible mechanism to explain why microvessel density is an independent prognostic indicator of tumor recurrence or metastatic risk in many different tumor types.

**#416 Angiogenesis inhibitors given during stem cell transplant: safety in a preclinical model.** Stern, J., Fang, J. and Grupp, S.A. Children's Hospital of Philadelphia, Philadelphia PA.

**Purpose:** To explore the safety of treatment with the antiangiogenic agent TNP-470 during stem cell transplant. **Background:** High-dose therapy with stem cell rescue is a treatment option for patients with advanced solid tumors. Though this approach has promise for some pediatric cancers, especially neuroblastoma, it is limited by the risk of relapse post treatment, as well as concern about possible reinfused tumor cells in autologous stem cell products. We have postulated that anti-angiogenic agents given during recovery from high-dose therapy with stem cell rescue may inhibit establishment of foci of disease arising from reinfused tumor cells, as well as prevent regrowth of minimal residual disease. TNP-470 is an anti-angiogenic agent now in Phase II clinical trials in adults that significantly inhibits growth of bone marrow colony-forming cells *in vitro*, though no significant hematologic toxicity has been seen in phase I trials. **Results:** In order to design a treatment strategy that uses such agents during the period of post-transplant hematopoietic engraftment, we have developed a model of stem cell transplant in mice, testing the safety of antiangiogenic agents given in this setting. In this model, FVB mice were lethally irradiated with 900 cGy and then infused with bone marrow from FVB mice that express a detectable transgene expressed in the hematopoietic lineage (human IgM). Mice were then treated with TNP-470 or placebo, and assessed for engraftment kinetics. Analysis of engraftment included both flow cytometric determination of transgenic IgM expression in B lymphocytes, as well as polymerase chain reaction detection of the transgene (detectable in all cells) in spleen, peripheral blood, bone marrow, and specific cell lineages. We measured hematologic parameters in the peripheral blood as well as bone marrow cellularity. Both treated and control mice demonstrated reliable multilineage engraftment as well as normal B cell maturation with no excess mortality in the treated group. Bone marrow cellularity was unaffected by treatment. WBC were lower but still within the normal range at day 28 in the treated group. These data indicate that inhibitors of angiogenesis do not adversely impact engraftment after stem cell transplant.

**#417 Recombinant human Endostatin™ in Cynomolgus monkeys produces no toxicological effects following i.v. administration for 28 consecutive days.** Fortier, A.H., Fogler, W.E., Tomaszewski, J.E., DuVall, M., Schwelkart, K.M., Covey, J.M., Paolotti, G.F., Ruiz, A., and Sim, B.K.L. EntreMed Inc., Rockville, MD, Toxicology and Pharmacology Branch, DTP, NCI, Bethesda, MD, Covance Laboratories, Vienna, VA, Cytimmune Sciences, Inc., College Park, MD.

Soluble, recombinant human (rhu) Endostatin™ protein expressed in *Pichia pastoris* was assessed for safety following i.v. injection to Cynomolgus monkeys for 28 days. Doses of rhu Endostatin™ protein were derived from pharmacodynamic assessments in preclinical murine tumor models, and bridging pharmacokinetics and dose-range finding studies in Cynomolgus monkeys. Male and female monkeys were assigned to four treatment groups comprised of control, formulation vehicle (17 mM citric acid, 66 mM sodium phosphate, 59 mM sodium chloride, pH 5.2) or rhu Endostatin™ protein at 4.5, 150, or 300 mg/m<sup>2</sup>/day. All doses were administered in an equivalent volume (3.12 mL/kg) at an infusion rate of 2 mL/min. Physical examinations were performed once weekly and blood samples were collected for hematology, coagulation, chemistry, and serum drug and antibody determinations prior to study initiation and on study days 2, 15, and 28. There were no mortalities or unscheduled sacrifices during the course of the study. In addition, there were no adverse clinical observations that were related to the administration of rhu Endostatin™ protein. No rhu Endostatin™ protein-related effects were noted on any of hematology, coagulation, or blood chemistry parameters. A slight reversible decrease in total and ionized serum Ca<sup>2+</sup> was seen in both treated and control monkeys without corresponding alterations in ECG recordings.

Anatomic pathology was unremarkable in all monkeys treated with rhu Endostatin™ protein. Circulating levels of rhu Endostatin™ protein were dose-dependent with mean values on day 28 of 226, 8225, and 20745 ng/mL 20-min post injection of 4.5, 150, and 300 mg/m<sup>2</sup>/day, respectively. Serum trough level determinations of circulating rhu Endostatin™ protein during the course of the study revealed drug accumulation. Low titer anti-Endostatin™ protein IgM and IgG antibodies (<1:800) were elicited in 4/20 and 16/20 monkeys, respectively. These studies are currently being extended out to 90 consecutive days of i.v. and 28 days of s.c. dosing with rhu Endostatin™ protein in additional cohorts of Cynomolgus monkeys. These data indicate that rhu Endostatin™ protein administered intravenously daily for 28 days to Cynomolgus monkeys is without profound significant toxicological effects and supports the initiation of clinical trials.

**#418 Detection of bone marrow derived endothelial cells in mouse subcutaneous matrigel implants and tumor vasculature.** Dutta, Sanjoy K., Marl, Mary R., Warren, Robert S. Dept. of Surgery, University of California School of Medicine, San Francisco, California 94143

Tumor angiogenesis requires the recruitment of endothelial cells from adjacent vessels, but may also involve the recruitment of circulating endothelial cell progenitors. Using a model of murine bone marrow transplantation, we were able to demonstrate that circulating endothelial cell precursors derived from donor bone marrow will contribute cells to newly formed tumor endothelium. Donor bone marrow was obtained from C57BL/6-ROSA26 transgenic mice which express the lacZ gene in a variety of tissues including endothelium, and from FVB/N-Tie2LacZ transgenic mice which express the lacZ gene on endothelium only. Subcutaneous MCA207 fibrosarcoma and Lewis lung carcinoma tumors were grown in C57BL/6 mice reconstituted with bone marrow from C57BL/6-ROSA26 transgenic mice. Compared to wild type controls, tumor endothelium of ROSA26 reconstituted mice demonstrated a significant number of donor derived endothelial cells ( $p < 0.001$ ) and immunohistochemistry with endothelial cell specific markers (CD31) demonstrated that these cells were incorporated into the tumor microvasculature. The pattern of donor bone marrow derived endothelial cell incorporation in bone marrow transplant recipients resembled the pattern observed in control ROSA26 donor mice, but occurred at a lower vascular density in two tumor models: MCA207 (43.6±28.8 lacZ-expressing vessels/cm<sup>2</sup> in bone marrow transplant recipients vs. 102.5±96.3 lacZ-expressing vessels/cm<sup>2</sup> in donor control) and Lewis lung (42.6±50.1 lacZ-expressing vessels/cm<sup>2</sup> in bone marrow transplant recipients vs. 154.4±114.9 lacZ-expressing vessels/cm<sup>2</sup> in donor control). In FVB/N mice reconstituted with bone marrow from FVB/N-Tie2LacZ transgenic mice, comparable results were observed in the endothelium of subcutaneous breast carcinoma tumors (7.4±10.8 lacZ-expressing vessels/cm<sup>2</sup> in bone marrow transplant recipients vs. 28.2±23.1 lacZ-expressing vessels/cm<sup>2</sup> in donor control) and vascular endothelial growth factor (VEGF) containing matrigel plugs (17.2±14.7 lacZ-expressing vessels/cm<sup>2</sup> in bone marrow transplant recipients vs. 52.4±61.9 lacZ-expressing vessels/cm<sup>2</sup> in donor control). These findings support the hypothesis that circulating progenitors derived from the bone marrow may contribute endothelial cells to the process of tumor angiogenesis.

**SECTION 4: CELL BIOLOGY-BASED STRATEGIES: APOPTOSIS AND DIFFERENTIATION**

**#419 Towards Bax-mediated gene therapy: adenovirus-mediated delivery of Bax consistently induces apoptosis in human tumor cell lines and primary cells, sensitizes refractory cells to the effects of chemotherapy and radiation, and appears to be selectively toxic against cancer.** Xiang, Jialing, Arafat, Waleed O., Gomez-Navarro, Jesus, Buchsbaum, Donald, and Curjel, David T. Gene Therapy Center [J.X., W.O.A., J.G-N., D.T.C.], and Radiation Oncology [D.B.], University of Alabama at Birmingham, Birmingham, AL 35233.

Bax, a member of the Bcl-2 family that can act as a tumor suppressor, potentially induces apoptosis. We sought to explore its therapeutic potential. **Firstly**, we constructed a recombinant adenoviral vector encoding Bax (Ad/Bax) without compromising the survival of virus-packaging cells. To this end, we used the inducible Cre-loxP system, whereby expression of Bax occurs when Cre recombinase is induced by a second adenovirus (Ad/Cre). **Secondly**, we evaluated the cytotoxicity of Bax in a panel of cancer cell lines representing a variety of tissues. We infected the cells with increasing multiplicities of infection (moi), and measured cell viability 48 hours later by a quantitative MTS assay. Expression of Bax resulted in apoptotic cell death in most human cancer cells, although the sensitivity of each cell line varied. Frequently, 80-90% of cell killing was achieved with 100 moi (+++), although occasionally higher doses were needed (+) or resistance was observed (Table).

Tumor	Cell line	Bax cytotoxicity	Sensitization to paclitaxel	Sensitization to radiation
Ovary	SKOV3.ip1	+	+++	+++
"	OVCAR3	+++		N.D.
"	OV4	+++		N.D.
"	PA-1	+++		N.D.
"	SW626	+	+++	+++
"	Primary	++		N.D.
Colon	SW626	++	N.D.	N.D.
"	LS174T	++	N.D.	N.D.
"	SW1116	+	N.D.	N.D.
Lung	A427	++	N.D.	N.D.
"	H1299	++	N.D.	N.D.
Pancreas	BXPC	++	N.D.	N.D.
"	ASPC	++	N.D.	N.D.
Cholangio.	SKCHA	++	N.D.	N.D.
Liver	HepG2	+++	N.D.	N.D.
"	Hep3B	+++	N.D.	N.D.
Glioma	DG54	-	N.D.	+++
"	U373	+	N.D.	+++
SCCHN	UM-SCC-1	-	N.D.	++
Cervix	HeLa	+++	N.D.	+++

Differential sensitivity did not correlate with cell infectibility by Ad. Importantly, Bax-mediated cell death was observed in pure populations of primary patient-derived ovarian cancer cells but did not occur when normal human peritoneal mesothelial cells were infected and expressed Bax. This apparent specificity was supported by a preliminary *in vivo* experiment, whereby Ad/Bax and Ad/Cre were administered intravenously into SCID mice at a total dose of  $1 \times 10^8$  pfu. After 72 hours, high levels of Bax were detected in the liver by Western blot, but no evidence whatsoever of toxicity was microscopically evident. Thirdly, to establish the dependence of Bax-mediated cytotoxicity on other mediators of the apoptosis pathways, we determined in the ovarian cancer panel by Western blot the endogenous levels of both Bcl-2 and Bax proteins and p53 status. We found no correlation with any of those parameters. Interestingly, a similar percentage of cells were killed in the cells with wild-type p53 (PA-1), or mutant or null p53 (OV4 and OVCAR3). Fourthly, to evaluate the potential of Bax for sensitizing refractory tumors to conventional chemotherapy and radiotherapy, we tested the combined treatments and determined dose-response curves and cell colony formation assays in several cell lines and primary ovarian cancer cells, and found very significant enhancement of cytotoxicity in cells particularly refractory to both chemo and radiotherapy (Table). Thus, production and delivery of Bax via a recombinant adenovirus vector is feasible, induces apoptosis robustly and preferentially in human cancer cells, and augments the efficacy of both chemotherapy and radiotherapy in otherwise refractory tumor cells. The independence of these biological effects of the Bcl-2, Bax, and p53 status suggests its potential utility for overcoming tumor heterogeneity.

**#420 Apoptosis-promoting bax gene transfer enhances chemotherapy in head and neck squamous cell carcinoma *in vitro* and *in vivo*.** Sugimoto, Chizuru, Fujieda, Shigeharu, Seki, Mizue, Sunaga, Hiroshi, Fan, Guo-Kang, Tsuzuki, Hideaki, Borner, Christoph, Saito, Hitoshi, Matsukawa, Shigeru. Department of Otorhinolaryngology and Central Research Laboratories, Fukui Medical University, Fukui, Japan; Institute of Biochemistry, University of Fribourg, Switzerland.

Bax, an apoptosis-promoting member of the bcl-2 family may be a key factor influencing the chemosensitivity of tumor cells, however, its involvement in cellular sensitivity to anti-cancer drugs remains uncertain in squamous cell carcinoma (SCC). Modulation of apoptosis may potentiate the sensitivity of tumor cells to chemotherapeutic drugs, thus improving the clinical outcome of cancer treatment. To investigate the role of bax gene expression in modulating cisplatin (CDDP)-induced apoptosis *in vitro*, an established CDDP-resistant cell line of human head and neck SCC was transfected with bax gene-bearing mammalian expression vector. Overexpression of the bax gene in CDDP-resistant IMC-3 cells elevated the CDDP susceptibility of tumor cells to a level similar to that of the parental IMC-3 cells. In an *in vivo* study, percutaneous transfer of bax gene by particle-mediated (gene gun) delivery caused overexpression of Bax in SCC, which was confirmed by immunohistochemical staining, and inhibited the growth of mouse CDDP-resistant SCC. Furthermore, combination therapy with bax gene transfer and subcutaneous administration of CDDP at 3-day intervals clearly inhibited the growth of mouse SCC. Thus, overexpression of bax in SCC by a gene gun system appears to be a rational approach to improving the efficacy of chemotherapy and treatment outcome. We suggest that exogenous bax expression may have therapeutic applications for enhancing chemotherapy in SCC.

**#421 Bcl-2 mediates resistance to flavopiridol-induced apoptosis that is dependent upon the level of Bcl-2 protein expression and is negatively regulated by elements within the N-terminal loop.** Decker, R., and Grant, S. Departments of Biochemistry and Medicine, Division of Hematology/Oncology, Medical College of Virginia, MCV Station Box 230, Richmond, VA 23298-0230.

Flavopiridol (FP) is an inhibitor of cyclin dependent kinases 1 and 2 that has been shown to induce apoptosis in hematopoietic cell lines. The purpose of these studies was to characterize events accompanying FP-induced apoptosis in human myeloblastic leukemia cells (U937), and to assess the effects of Bcl-2 on this process. Exposure to FP (100–300 nM; 24 h) potently induced apoptosis in U937 cells, a process accompanied by characteristic morphological changes, loss of the inner mitochondrial membrane potential, release of cytochrome C, and processing of procaspases 3, 6, and 9. Inhibition of caspase processing by general inhibitors zVAD-fmk and Boc-fmk significantly reduced the loss of mitochondrial membrane potential and decreased morphological apoptosis. To assess the influence of Bcl-2 on FP-mediated cell death, U937 cells were stably transfected with a plasmid containing the cDNA for full-length Bcl-2 as well as that of an N-terminal phosphorylation loop deletant ( $\Delta$ 32-80). A cell line (G3) expressing approximately a 7-fold excess of Bcl-2 displayed virtually no resistance to FP relative to the empty vector control, whereas a cell line (D9) overexpressing Bcl-2 to a considerably higher degree was significantly more resistant. Interestingly, Bcl-2 loop deletant expressing cells ( $\Delta$ Bcl-2 B9) exhibited a high degree of FP resistance despite relatively low levels of protein expression. Collectively, these findings indicate that the ability of Bcl-2 to block FP-mediated apoptosis is highly dependent upon the degree of Bcl-2 expression and is also influenced by putative negative regulatory factors residing within the N-terminal phosphorylation loop domain.

**#422 Taxol-induced apoptosis and BCL-2 degradation inhibited by rapamycin.** Calastretti A., Rancati F., Viganò S., Carli G., Schiavone N., Capaccioli S., Nicolini A. Department of Pharmacology, University of Milan, Institute of General Pathology, University of Florence, Italy.

We have found that the human follicular B cell lymphoma lines were growth inhibited, arrested in the G2M phase of the cell cycle and protected from apoptosis by very low doses of rapamycin. The immunophilin binding compound was able to increase four fold the cellular level of both the antiapoptotic BCL-2 and the cell-cycle inhibitor p27 proteins. Because of the relevance of the protein BCL-2 for the tumor cell response to chemotherapeutic agents, we studied the mechanisms by which rapamycin increases the cellular level of the protein BCL-2 and protects cells from apoptosis induced by antitumor compounds. In the rapamycin-treated cells the cellular level of the bcl-2 mRNA was not modified suggesting a post-translation mechanism regulating the BCL-2 degradation pathway. Rapamycin was very effective to inhibit taxol-induced BCL-2 phosphorylation in a dose response manner, to protect cells from apoptosis and to inhibit DNA synthesis. Moreover, taxol-induced endoreplication (hyperdiploid cells) was completely abrogated in the cells pretreated with rapamycin. In addition, cells exposed to the same treatments were synchronized in the G2M phase. In contrast, rapamycin was unable to overcome the G2M arrest and to protect microtubules from stabilization. These studies show that rapamycin can protect cells from taxol-induced apoptosis by preserving BCL-2 from degradative phosphorylation. Moreover, in these studies rapamycin seems to uncouple BCL-2 phosphorylation from G2M and microtubule stabilization suggesting that the two events are mediated by two mechanisms not directly related. Alternatively, it might not be ruled out that G2M cells cannot phosphorylate BCL-2 because a specific kinase or the kinase cascade starting from mTOR are inhibited by rapamycin. In conclusion, rapamycin was able to increase the cellular level of BCL-2 and to protect cells from apoptosis by hampering BCL-2 phosphorylation. The present study demonstrates that in the t(14;18) cells the degradation of both p27 and BCL-2 proteins can be regulated by rapamycin.

**#423 Inhibition of calcineurin-mediated Fas signaling activation and apoptosis by Bcl-2 in antitumor drug-treated cells.** Simizu, S. and Osada, H. (Antibiotics Laboratory, Riken Institute, 351-0198, Japan).

Bcl-2 is known to be a negative regulator of apoptosis, however, the exact biochemical functions remain unclear. We demonstrated that apoptosis induced by antitumor drugs such as proneurin, vinblastine, paclitaxel, camptothecin, adriamycin and etoposide was mediated by Fas/Fas ligand (FasL) system through the increase of Fas and FasL expression in Baby Hamster Kidney (BHK) and human lung fibroblast WI-38 cells. Moreover, calcineurin was imported to nucleus in response to the drug treatment, and cyclosporin A inhibited the drug-induced calcineurin nuclear import and FasL expression in BHK cells. Overexpression of Bcl-2 also inhibited the drug-induced calcineurin nuclear import and FasL expression, resulting in inhibiting apoptosis. Although a caspase inhibitor suppressed the drug-induced apoptosis, the inhibitor failed to inhibit the drug-induced expression of Fas and FasL. The FasL-neutralizing antibody suppressed the drug-induced caspase activation. These findings suggest that the Fas/FasL system is activated by calcineurin-dependent transcription and then the downstream caspase-cascade is activated in antitumor drug-induced apoptosis.



**#424 Bcl-2 is located predominantly in the inner membrane and crista of mitochondria in rat liver.** Satoru Motoyama, Satoshi Saito, Hiroyuki Suzuki, Reijiro Saito, Manabu Okuyama, Hiroshi Imano, Jun-ichi Ogawa. *The second Department of Surgery, Akita University School of Medicine.*

Bcl-2 is now recognized as a potent inhibitor of apoptotic cell death. It has been reported that Bcl-2 is located in the mitochondria, endoplasmic reticulum, and nuclear membrane in some cell lines, and it is not expressed in normal human and rat liver. An earlier study showed that Bcl-2 is an inner mitochondrial membrane protein. On the contrary, the following investigations using immunoelectron microscopy demonstrated that Bcl-2 resides predominantly in the mitochondrial outer membrane. In this study, using a cryo-sectioning immunogold labeling technique and an immunoblotting, we carefully determined the subcellular localization of Bcl-2. Here we present that Bcl-2 is expressed in normal rat liver, and located predominantly in the inner membrane and crista rather than in the outer membrane of mitochondria.

**#425 Bcl-2 overexpression and exogenous glutathione prevent adriamycin-induced necrosis, but not apoptosis, in CC531 rat colorectal cancer cells.** Hoetelmans, R.W.M., Vahrmeijer, A.L., Van de Velde, C.J.H., and Van Dierendonck, J.H. *Department of Surgery, Leiden University Medical Center, The Netherlands.*

After depletion of their glutathione (GSH) content, CC531 rat colorectal cancer cells rapidly die in a non-apoptotic (necrosis-resembling) fashion, a phenomenon involving reactive oxygen species (ROS). By continuous exposure of CC531 cells to increasing concentrations of GSH synthesis inhibitor buthionine sulfoximine (BSO) we selected a cell line (CCBR25) that is 50 times more resistant to BSO treatment. We observed a much higher level of the anti-apoptotic protein Bcl-2 in these CCBR25 cells. Stable transfection of CC531 cells with human *bcl-2* resulted in a cell line (CCBcl2) with 9 times higher resistance to BSO compared to the parental line. This indicates that Bcl-2 indeed is responsible for protection to this type of cell death. Our data also indicated that Bcl-2 does not prevent, but apparently acts downstream ROS generation.

The anthracyclins adriamycin (A) and epi-adriamycin (E) are potent and widely used anticancer drugs. In contrast to A, E does not generate ROS, a feature believed to be responsible for its relatively low cardiotoxicity. In a clonogenic assay, both A and E were equally effective in all CC531 variants (as based on their IC50 values). High concentrations of A (25 times IC50 values) within 12 hrs induced necrosis-like death in CC531, but not in CCBR25 or CCBcl2 cells. However, an equimolar amount E did not induce necrosis, but after 24 hr had resulted in massive apoptosis both in CC531 cells and, although to a lesser extent, in the Bcl-2 overexpressing variants. Whereas co-incubation with 1 mM GSH inhibited A-induced necrosis, it did not affect induction of apoptosis.

We conclude that in CC531 cells, Bcl-2 overexpression can prevent ROS-related necrosis and retards, but does not prevent, A- or E-induced apoptosis. However, this has no significant impact on clonogenic survival. Because in CC531 cells a relatively high concentration of A rapidly triggers necrosis, this may explain why treatment with A may lead to a higher proportion of apoptotic cells in case of Bcl-2 overexpression, despite the possibility that Bcl-2 retards the apoptotic process.

**#426 Bcl-2 phosphorylation in a human breast tumor xenograft: a common event in response to effective DNA-interacting drugs.** Polizzi, D., Perago, P., Zunino, F. and Pratesi, G. *Istituto Nazionale Tumori, 20139 Milan, Italy.*

Bcl-2 phosphorylation has been reported to be implicated in apoptotic response of different cell lines to microtubule-interacting drugs. The involvement of bcl-2 in drug resistance remains unclear. In this study we have compared efficacy, apoptosis induction and Bcl-2 phosphorylation in the Bcl-2 overexpressing MX-1 human tumor xenograft after treatment with cytotoxic agents characterized by different mechanisms of action (antimicrotubule drugs, platinum compounds and topoisomerase inhibitors). Our results showed that MX-1 tumor was very sensitive (i.e. complete tumor regression) to some drugs of all classes investigated, in spite of Bcl-2 overexpression. Moreover, when agents belonging to the same mechanistic class were compared, antitumor activity correlated with drug ability to induce phosphorylation of Bcl-2 and to induce apoptosis (assessed as apoptotic index by TUNEL reaction). In conclusion, overexpression of Bcl-2 did not counteract the apoptotic effects of drugs belonging either to taxanes, platinum-containing agents or anthracycline and Bcl-2 phosphorylation was a common event in response to different types of cytotoxic stress, including DNA damage.

**#427 Functional activity of chimeric molecules containing a death signal against neuroblastoma.** Lin Huey-Jen L, Holman Peter, Lu Jinyi, Finniss Susan, Dickinson Chris, and Castle Valerie P. *The University of Michigan Comprehensive Cancer Center, Ann Arbor Michigan and the University of California at San Diego, San Diego CA.*

Neuroblastoma (NB) is the most common extracranial malignancy of childhood. Despite aggressive modern treatment strategies the survival rate for patients with high risk NB remains poor. Although the molecular genetic defects responsible for NB are not well understood the resist-

ance of this disease to contemporary treatment modalities is consistent with a fundamental defect in the apoptotic mechanism. Moreover, intracellular delivery of a death signal to NB cells using a Bcl-x<sub>L</sub> adenoviral expression system suggests direct targeting of apoptotic pathways may provide a novel approach for treating this disease. To obviate the need for viral delivery we are exploring the potential to deliver a death signal by receptor mediated internalization of death inducing polypeptides. Five NB cell lines (Shep-1, SK-N-AS, SH-SY5Y, IMR-32, and SK-N-MC) were initially tested for their susceptibility to undergo apoptosis in response to expression of Bax, Bcl-x<sub>L</sub>, granzyme B or Harakiri (HRK). NB cells were most sensitive to expression of HRK. Over 95% of transfected cells were apoptotic as demonstrated by luciferase and lac-z reporter assays, morphologic assessment and TUNEL staining. To achieve delivery of these death molecules in a virus-independent manner, expression vectors were constructed by overlapping RT-PCR reactions fusing functional elements of Bax, Bcl-x<sub>L</sub> or HRK to the receptor-binding domain of somatostatin (SST). The SST fusion partner was chosen as NB express high levels of specific SST receptors known to internalize their ligand. Correct sequence was verified and fusion protein production was determined by western analysis of transfected 293T cells. Each construct produced protein of the expected molecular weight and immunoreactivity. Importantly, confocal microscopy demonstrated that the fusion proteins localized as predicted to the cytoplasmic compartment. NB cells transfected to express the fusion proteins showed similar apoptotic rates when compared to native Bax, Bcl-x<sub>L</sub> or HRK protein. Control experiments with empty vector or SST alone resulted in no loss of viability. Thus the pro-apoptotic activity of these bcl-2 family members was retained after fusion with SST making them useful candidates for further development. These new protein reagents are being tested for specificity of binding to the SST receptor and cytotoxicity when applied to NB cells.

**#428 Role of STAT5, STAT3 and Bcl-2 family members in mammary epithelial cell proliferation and apoptosis during normal physiology and tumorigenesis in mouse models.** Li, M., Schorr, K., Ren, S., Lewis, B., Almiroudis, D., Laucirica, R., Capuco, A. and Furth, P.A. *Institute of Human Virology, Med & Phys, UMD, Baltimore, MD; USDA, Beltsville, MD; Baylor & Methodist Hospital, Houston, TX.*

The aims of this study are to determine the in vivo role of phosphorylated STAT5 and STAT3 in mammary epithelial cell proliferation and apoptosis during normal physiology and tumorigenesis, to identify factors which regulate phosphorylation of STAT5 and STAT3, and to investigate possible links between activation of STAT proteins and Bcl-2 family member survival and death factors.

Combinations of wild-type, transgenic and knock-out mouse models at different stages of normal physiology and tumorigenesis were studied using histological, biochemical and molecular techniques. In previous experiments we have shown that changes in expression levels of Bax and Bcl-2 alter survival of mammary epithelial cells during mammary gland involution (*Cancer Research* 59: 2541-2545, 1999) and that Bcl-2 overexpression can modify the rate of both cell proliferation and apoptosis during breast carcinogenesis (*Oncogene*, in press). Loss of STAT5 activation and gain of STAT3 activation during involution correlate with apoptosis of normal mammary epithelial cells and up-regulated expression of death factors Bax, Bad and Bak (*Proc Natl Acad Sci USA* 94: 3425-3430, 1997; *J Mam Gland Biol Neoplasia* 4: 153-164, 1999).

Here we demonstrate that phosphorylation of STAT3 by itself, however, was not sufficient to induce apoptosis in normal mammary epithelial cells during involution. In the presence of exogenous glucocorticoid, STAT3 remained phosphorylated although Bax expression was down-regulated and apoptosis was inhibited. Expression of the survival factor Bcl-x<sub>L</sub> was maintained although glucocorticoids did not increase STAT5 phosphorylation and cell proliferation was not induced. In contrast to the biology of the normal mammary epithelial cells, glucocorticoids did increase STAT5 phosphorylation in pre-malignant mammary epithelial cells. Phosphorylation of STAT5 in these cells was associated with a dramatic increase in cell proliferation, the appearance of tetraploidy, premature development of irreversible hyperplasia and the early appearance of breast cancer. In the pre-malignant cells expression levels of Bcl-2 family members were unaffected by exogenous glucocorticoids.

**#429 Antimycin A Mimics A BH3 Domain-Containing Peptide And Selectively Induces Apoptosis In Cell Lines Overexpressing Bcl-x<sub>L</sub>.** Shia-Pon Tzung<sup>1</sup>, Kristine M. Kim<sup>2</sup>, Gorka Basanez<sup>3</sup>, Joshua Zimmerberg<sup>3</sup>, Kam Y.J. Zhang<sup>2</sup> & David M. Hockenbery<sup>1,4</sup>. <sup>1</sup>Division of Gastroenterology, Department of Medicine, University of Washington, <sup>2</sup>Divisions of Basic Science and <sup>3</sup>Clinical Research, Fred Hutchinson Cancer Research Center, Seattle, Washington 98109, <sup>4</sup>NICHD, NIH, Bethesda, MD, 20892, USA.

The anti-apoptotic members of the Bcl-2 family confer resistance to a wide range of apoptotic triggers. We established isogenic clones of the tumorigenic hepatocyte TAMH cell line expressing Bcl-x<sub>L</sub> cDNA in sense and antisense orientations. TABX2S cells, transfected with SFFV-sense Bcl-x<sub>L</sub> vector, expressed 5-6 fold higher levels of Bcl-x<sub>L</sub> compared to the antisense-generated TABX1A cell line. TABX2S cells were resistant to TNF, doxorubicin and cisplatin, but had markedly increased sensitivity to treat-

ment with antimycin A, an inhibitor of mitochondrial electron transfer complex III, compared to TABX1A cells. Similar results were found with two other hepatocyte cell lines, AML-12 and NMH. Oxidative phosphorylation was inhibited in both high and low-Bcl-x<sub>L</sub>-expressing cell lines to a similar degree, as shown by reduction in ATP levels and generation of reactive oxygen species.

Antimycin A induced mitochondrial swelling in isolated mitochondria prepared from TABX2S, but not TABX1A cells. By computational molecular docking analysis, antimycin A is predicted to bind at the BH3-binding hydrophobic groove of Bcl-x<sub>L</sub>. We show that antimycin A binds to recombinant Bcl-2 protein and demonstrate competitive binding with a synthetic 16-amino acid BH3 peptide. Antimycin A and a pro-apoptotic BH3 domain peptide both trigger loss of mitochondrial  $\Delta\Psi_m$  and mitochondrial swelling selectively in Bcl-x<sub>L</sub>-expressing mitochondria. Finally, the channel activity of Bcl-x<sub>L</sub> measured by leakage of fluorescent calcein dye from synthetic lipid vesicles was inhibited in the presence of antimycin A. These results demonstrate that small non-peptide ligands can directly influence the function of Bcl-2-type proteins. Non-peptidyl compounds related to antimycin A may be useful clinically to target drug-resistant tumor cells overexpressing Bcl-x<sub>L</sub>.

**#430 Selective inhibition of Cyclooxygenase-2 enhances Mitomycin-C-induced apoptosis.** Hsueh, Chung-Tsen<sup>1</sup>; Kelsen, David P., Schwartz, Gary K. <sup>1</sup>China Medical College Hospital, Taichung, Taiwan; Memorial Sloan-Kettering Cancer Center, New York, New York 10021, U.S.A.

**Background.** Cyclooxygenase-2 (COX-2) is involved in anti-apoptosis signaling, and its induction may require activation of protein kinase C (PKC). Safligol (SAF), a PKC inhibitor, has been shown to enhance mitomycin-C (MMC)-induced apoptosis in human gastric cancer MKN-74 cells (J. Natl. Cancer Inst. 87:1394-1399, 1995).

**Purpose.** The aim of this study is to identify the role of COX-2 in MMC-induced apoptosis in MKN-74 cells.

**Materials and Methods.** Protein expression of COX-2 and Bcl-2 and activation of PKC $\alpha$  were examined by Western blot analysis. Apoptosis induction was examined by staining with bisbenzimidazole trihydrochloride (Hoechst-33258) of condensed chromatin, which characterizes the cells undergoing apoptosis. COX-2 mRNA levels were examined by Northern blot analysis.

**Results.** After 1- to 2-hour exposure to 1  $\mu$ g/ml MMC, up-regulation of COX-2 and Bcl-2 protein expression was noted. The activation of PKC $\alpha$  occurred within 1 hour after MMC exposure, and temporally preceded the induction of COX-2. Similar results were observed in cells exposed to the PKC activator, 3-phorbol 12-myristate 13-acetate. Co-treatment of SAF with MMC abolished the induction of COX-2 by MMC. Furthermore, NS-398, a selective COX-2 inhibitor, significantly enhanced MMC-induced apoptosis by 5 fold from  $4 \pm 2\%$  (MMC alone) to  $20 \pm 2\%$  (MMC plus NS-398) as determined by quantitative fluorescent microscopy. Northern blot analysis for COX-2 mRNA levels revealed no discernible change after 2-hour exposure to MMC but a 2-fold increase after 24-hour exposure.

**Conclusion.** MMC up-regulates COX-2 expression, which appears to be an anti-apoptotic signal downstream of PKC. Selective inhibition of COX-2 can therefore provide a novel way to enhance MMC-induced apoptosis independent of inhibiting PKC.

**#431 Molecular basis for 2-CdA action: interactions with the apoptosome.** Joya Chandra, Lina Goldschmidt, Frelidou Albertoni, and Sten Orrenius. Departments of Toxicology and Clinical Pharmacology, Karolinska Institute, Stockholm, SWEDEN.

Previous studies have shown that the nucleoside analog, 2-chlorodeoxyadenosine (2-CdA), clinically known as cladribine, induces apoptosis in lymphocytes both *in vivo* and *in vitro*. This drug has been used in the treatment of hairy cell leukemia and chronic lymphocytic leukemia and has shown greater activity than other clinically relevant nucleoside analogs. This observation is surprising because DNA incorporation of these analogs is thought to require cell cycle progression in target cells. However, lymphocytes from CLL and HCL patients, as well as human thymocytes, are sensitive to 2-CdA-induced apoptosis despite the fact that they accumulate in the G1 phase of cell cycle. This suggests that 2-CdA may be using an alternate mechanism, other than DNA incorporation, to induce apoptosis in lymphocytes. Programmed cell death or apoptosis has been shown to involve the formation of a complex called the apoptosome, which consists of Apaf-1, cytochrome-c, dATP, and caspase 9. The possibility that 2-CdATP, the *in vivo* phosphorylated form of 2-CdA, may be capable of substituting for dATP during apoptosome assembly is likely and has been demonstrated by others, providing an attractive explanation for this compound's high activity. However, in cells resistant to 2-CdA, it is not known whether there is a defect in apoptosome assembly, or if 2-CdA binding to the apoptosome is hindered. In the present study we utilize a number of human lymphocytic cell lines, including several with acquired resistance to 2-CdA, in order to explore this question. Quantitation by PCR of levels of dCK, the enzyme responsible for phosphorylating the drug *in vivo*, show that resistant cell lines vary between normal and very low levels of dCK, yet are equally resistant to 2-CdA. This suggests that the defect in these cells does not involve transport or intracellular accumulation of the active drug. In parental cells, release of cytochrome c upon 2-CdA treat-

ment is observed, indicating a role for mitochondria in the mechanism of action of 2-CdA. Experiments utilizing cytosols isolated from resistant cells will be incubated with 2-CdATP or dATP and cytochrome c and tested for activation of caspases, in order to assess the functionality of the apoptosome in these cells. Elucidation of the molecular defect in cells resistant to 2-CdA will aid in the design of more effective treatment strategies for leukemia.

**#432 Anti-tumor therapy alters expression of key apoptosis-related factors in MCF-7 xenografts.** Taylor, Alice P., Lew, Walter, Goldenberg, David M., Blumenthal, Rosalyn D. Garden State Cancer Center, Belleville, NJ 07109.

Treatment-induced cytotoxicity commonly depends on apoptosis or programmed cell death. Susceptibility to therapy may rely on suppression or induction of apoptosis-related factors such as fas, bcl-2, or bax. Similarly, treatment may induce alterations in apoptosis factor expression that leads to resistance. To determine if regulation of these factors may be a mechanism of tumor susceptibility or resistance to cytotoxicity, and to maximize cytotoxic effects of combined treatments, mice bearing xenograft human breast carcinoma, MCF-7, were treated once with radio-antibody (250  $\mu$ Cl <sup>125</sup>I-MN-14 anti-CEA IgG (RAIT)), taxol (375  $\mu$ g/mouse/i.v.) or doxorubicin (100  $\mu$ g/mouse/i.v.). Changes in fas, bcl-2, and bax expression during the first 72 hours after treatment were determined by immunohistochemistry and immunoblot. Results were compared to untreated controls. None of the treatments altered bcl-2 expression over untreated controls in the first 72 hours. However, after RAIT and Taxol therapy, a retarded band, characteristic of phosphorylated bcl-2, appeared in immunoblots, and this band became the dominant bcl-2 band at 72 hours after RAIT. Doxorubicin treatment did not induce the retarded bcl-2 variant. Surprisingly, bax, a proapoptotic factor, was downregulated for 24 hours and 72 hours by doxorubicin and RAIT, respectively. Fas, a cell surface molecule which transmits apoptotic signals when bound to its ligand, was upregulated by doxorubicin at 6 hours, while at the same time point, Taxol down regulated fas. By 72 hours after treatment, fas expression returned to baseline levels for all treatments. MDR1 expression, which may alter delivery of drugs into tumor cells, was also analyzed in this study. All three treatments downregulated MDR-1 for the first 24 hours. By 48-72 hours expression had returned to baseline in RAIT and Taxol treated tumors. These results suggest that different treatments modify the expression of apoptosis-related factors and therefore that timing and sequence of combined treatment may optimize proapoptotic cytotoxicity in tumors. (Supported in part by grants CA54425 and CA99841 from the NIH.)

**#433 Kinetics of tamoxifen-induced cell death in rat mammary tumors.** Christov, K., Shilkaitis, A., Green, A., Grubbs, C., Kelloff, G., and Lubet, R. Department of Surgical Oncology, University of Illinois, Chicago, IL, Institute of Chemoprevention, Birmingham, AL, NCI, Division of Chemoprevention, Bethesda, MD.

Most preclinical *in vivo* studies that justified the use of tamoxifen for treatment and prevention of breast cancer were performed on DMBA or MNU mammary carcinogenesis models in rats. These tumors are ER+, and they are similar to human breast cancer in morphology, origin (ductal cells), and development. This study examined the time-dependent alterations in programmed (apoptotic) cell death (ACD) and the expression of cell death-related genes/proteins Bcl-2 and Bax in mammary tumors of rats treated with tamoxifen. Rats with palpable (5-10 mm) tumors were given tamoxifen (1.0 mg/kg in diet) and sacrificed 2, 4, 10, and 20 days after initiation of treatment. The percentage of apoptotic cells (AI) was evaluated by the TUNEL assay. Bcl-2 and Bax expression was estimated semiquantitatively by immunocytochemistry (ICH) as well as by Western blot, and the number of proliferating cells was estimated by labeling them with BrdU. Tamoxifen given for 2 days did not significantly affect AI or cell proliferation. In the animals treated for 4, 10, and 20 days, AI increased from  $0.6 \pm 0.2\%$  in control (n=20) to respectively  $1.3 \pm 0.7\%$  (n=10),  $2.0 \pm 0.8\%$  (n=20), and  $4.5 \pm 1.1\%$  (n=10). In 4- and 10-day-treated animals, apoptotic cells increased either randomly among tumor parenchyma or close to the basal membrane that separates tumor cells from the stroma. BrdU-labeled cells decreased from  $22.7 \pm 5.2\%$  in control tumors to  $14.1 \pm 8.5\%$  in 4-day- and to  $11.0 \pm 8.3\%$  in 10-day-treated animals, respectively. In 20-day-treated animals, focal ACD with disintegration of tumor parenchyma predominated. The increase in apoptotic cells in tamoxifen-treated animals was associated with a decrease in Bcl-2 [score  $2.9 \pm 0.8$  in control (n=10) vs.  $1.7 \pm 0.5$  in treated tumors (n=10),  $p < 0.001$ ] but, with limited effect on Bax expression (score  $3.1 \pm 0.7$  in control vs.  $2.8 \pm 0.6$  in treated tumors,  $p < 0.1$ ), as evaluated by ICH. By double-labeling of apoptotic cells (TUNEL assay + staining for Bcl-2 or Bax expression), both Bcl-2 and Bax increased in apoptotic cells, suggesting a dual role of both proteins in the early and terminal phase of apoptosis. Thus, tamoxifen given in the diet suppresses mammary tumor growth both by increasing ACD and decreasing cell proliferation, and both cellular phenomena occur concomitantly and relatively early (4 days) after initiation of treatment.



**#434 Induction of apoptosis by mifepristone, tamoxifen and the combination of both in human LNCaP prostate cancer cells in culture.** El Etreby, M. Fathy, Llang, Yayun and Lewis, Ronald W. *Medical College of Georgia, Augusta, GA.*

**Background:** Antiprogesterins are a promising new class of mammary tumor inhibitors. Published data also indicate that antiprogesterins and antiestrogens could inhibit prostate cancer cell growth in vitro and in vivo. The main objective of the present studies is to explore the role of  $bcl_2$  and TGF $\beta_1$  for induction of apoptosis in LNCaP prostate cancer cells growing in culture as a treatment response to the antiprogesterin, mifepristone, the antiestrogen, 4-hydroxytamoxifen and the combination of both.

**Methods:** In vitro cell viability (cytotoxicity), DNA fragmentation and changes in the expression of  $bcl_2$  and TGF $\beta_1$  proteins were assessed using the sulforhodamine B protein dye-binding assay, specific ELISA and competitive inhibition assays.

**Results:** Both steroid antagonists induced a significant time- and dose-dependent cell growth inhibition (cytotoxicity). This inhibition of cell survival was associated with a significant increase in DNA fragmentation (apoptosis), downregulation of  $bcl_2$ , and induction of TGF $\beta_1$  protein. The effect of a combination of mifepristone and 4-hydroxytamoxifen on cell growth inhibition, on the increase in DNA fragmentation,  $bcl_2$  downregulation and induction of TGF $\beta_1$  protein was additive or synergistic and significantly different ( $P < 0.05$ ) from the effect of monotherapy. Abrogation of the mifepristone- and 4-hydroxytamoxifen-induced cytotoxicity by TGF $\beta_1$  neutralizing antibody and by the addition of mannose-6-phosphate confirms the correlation between induction of active TGF $\beta_1$  and subsequent prostate cancer cell death.

**Conclusions:** Our data suggest that mifepristone and tamoxifen are effective inducers of apoptosis and may represent non-androgen ablation, novel therapeutic approaches to overcome a potential intrinsic apoptosis resistance of androgen-independent prostate cancer cells.

**#435 Phenylbutyrate in myeloid malignancies: relationship between inhibition of histone deacetylase, cytostasis and differentiation.** Gore, Steven D., Weng, Li-Jun, Yu, Kenneth, and Fu, Shen. *The Johns Hopkins Oncology Center, Baltimore, Maryland.*

Sodium phenylbutyrate (PB) leads to induction of expression of  $p21^{WAF1/CIP1}$ , cell cycle arrest, and differentiation in the ML-1 myeloid leukemia cell line and has led to modest hematologic improvement in Phase I clinical trials of patients with hematologic malignancies. Recent attention has focused on the potential utility of PB as an inhibitor of histone deacetylase (HD). We compared the dose response characteristics of PB for changes in histone acetylation to its pharmacodynamic effects, and examined the pharmacodynamic effects of Trichostatin A (TSA), a specific inhibitor of histone deacetylase. ML-1 cells were cultured in the presence or absence of TSA, PB, or TSA + PB for 1-3 days before evaluation of terminal differentiation (CD11b expression), cell cycle parameters (bromodeoxyuridine/propidium iodide), apoptosis (Annexin V binding), and induction of  $p21^{WAF1/CIP1}$ . Unlike PB, treatment with TSA did not lead to induction of CD11b expression in ML-1 cells. Like PB, TSA led to rapid induction of expression of  $p21^{WAF1/CIP1}$ . This was accompanied by cell cycle arrest; however TSA led to G2/M arrest, whereas PB is associated with G1 arrest. Incubation of ML-1 cells with PB induced detectable histone acetylation at doses ranging from 0.25 to 5 mM, encompassing doses which induce all measured pharmacodynamic endpoints. In normal peripheral blood and normal and AML bone marrow mononuclear cells, PB induces acetylation of histones H3 and H4 at doses ranging from 0.25 mM to 1 mM. TSA was a strong inducer of apoptosis (ED50 ~0.2 nM); in contrast, the ED50 for apoptosis induction by PB is two times greater than the ED50 for CD11b induction and cell cycle arrest. While PB leads to induction of histone acetylation in ML-1 cells and normal hematopoietic cells, these data suggest that inhibition of histone deacetylase in myeloid leukemia cells may not account for all of the pharmacodynamic actions of PB. However, doses of PB which are clinically sustainable (0.3-1 mM) clearly lead to increases in histone acetylation, making PB a reasonable model for the clinical development of HD inhibitors.

**#436 The cyclin-dependent kinase inhibitor (CDKI)  $p21^{CIP1}$  regulates leukemic cell differentiation and apoptosis induced by low concentrations of 1- $\beta$ -D-arabino-furanosylcytosine (ara-C).** Zhiliang Wang, Paul Fisher, Paul Dent, and Steven Grant. *Departments of Medicine and Radiation Oncology, Medical College of Virginia, Richmond, VA, and College of Physicians and Surgeons, N.Y., N.Y.*

While it is known that low concentrations of cytotoxic drugs such as ara-C can induce leukemic cell differentiation, the factors responsible for this phenomenon remain obscure. To assess the functional role of the CDKI  $p21^{CIP1}$  in this process, we have examined human leukemia cells (U937) expressing  $p21^{CIP1}$  in the antisense configuration. In contrast to high, cytotoxic concentrations of ara-C (e.g.,  $\geq 1 \mu\text{M}$ ), which did not induce  $p21^{CIP1}$ , chronic exposure of wild-type cells (pREP4) to a low concentration of ara-C (e.g., 50 nM) resulted in delayed (e.g.,  $\geq 48$  hr) but unequivocal induction of  $p21^{CIP1}$ , accompanied cell maturation (i.e., increased CD11b expression). In marked distinction, low concentrations of ara-C failed to induce  $p21^{CIP1}$  or trigger a differentiation program in U937/ $p21^{CIP1}$  antisense-expressing cells. Instead, such exposures were associated

with a marked increase in apoptosis, manifested by the appearance of characteristic morphologic features, DNA fragmentation, loss of mitochondrial membrane potential ( $\Delta\psi_m$ ), cytochrome c release, processing/activation of caspases 9 and 3, and degradation of PARP.  $p21^{CIP1}$  antisense-expressing cells exposed to low concentrations of ara-C also displayed marked degradation of the retinoblastoma protein (pRb) and attenuation of the p42/p44MAPK response. Finally, whereas treatment of wild type cells with 50 nM ara-C led to a marked increase in cytosolic  $p21^{CIP1}$ , a phenomenon recently associated with anti-apoptotic effects (EMBO J 18: 1223, 1999),  $p21^{CIP1}$  antisense-expressing cells treated in this manner failed to display cytosolic accumulation of this CDKI. Together, these findings indicate that chronic exposure of U937 cells to low ara-C concentrations leads to a clear, albeit delayed, induction of  $p21^{CIP1}$  in association with cellular maturation. Furthermore, disruption of the  $p21^{CIP1}$  response blocks ara-C-mediated differentiation while dramatically promoting apoptosis, possibly by preventing accumulation of  $p21^{CIP1}$  in the cytosol.

**#437 Differentiation of human breast tumor cell lines by quinolines.** Johnson, David N., Melkoumian, Zara K., Lucktong, Ann, Strobl, Jeannine S. *Department of Pharmacology & Toxicology, R.C. Byrd Health Sciences Center, West Virginia University.*

Our goal is the design of novel compounds that cause differentiation of human breast tumor cells. Based upon evidence that quinidine caused differentiation of MCF-7, MCF-7ras, MDA-MB-231, and MDA-MB-435 human breast tumor cell lines, we screened a series of quinolines and other antimalarials for induction of a more differentiated phenotype of MCF-7 cells. Oil Red O (ORO) is a histochemical stain that detects accumulated lipid droplets, a marker of differentiation in breast epithelial cells. Normal human mammary epithelial cells (HMEC) are 97% ORO-positive, however, less than 3% of control MCF-7 cells are ORO-positive. The differentiating agent, retinoic acid (10  $\mu\text{M}$ ), was used as the positive control. The most active agents tested were quinidine (maximum effective concentration, 90  $\mu\text{M}$ ), quinidine (90  $\mu\text{M}$ ) and primaquine (10  $\mu\text{M}$ ), and these caused positive ORO staining in 79-89% of MCF-7 cells by 72 hours. Quinolone (50  $\mu\text{M}$ ) and chloroquine (10  $\mu\text{M}$ ) were less active, and 20-23% of cells were ORO-positive by 72 hours. Quinolonic acid (50  $\mu\text{M}$ ), mefloquine (1  $\mu\text{M}$ ) and halofantrine (1  $\mu\text{M}$ ) were inactive as differentiating agents (<8% ORO-positive). All agents tested, except quinoline and quinolonic acid, caused apoptosis of MCF-7 cells at concentrations greater than those which elicited a maximum ORO response. Our results demonstrate that a subset of quinolone antimalarial agents cause differentiation and apoptosis in human breast tumor cell lines. Primaquine was the most potent differentiating agent identified, and may be of use as a lead compound in the design of breast tumor differentiating agents. Support: WVU School of Medicine, USARMC, BC981114, and Edwin C. Spurlock Cancer Research Fellowship.

**#438 Interconnections between P-glycoprotein activation, differentiation and apoptosis in the cultured blood cells Rybalkina, E., Stromskaya, T., Zabolina, T., Logacheva, N., Stavrovskaya A. *Institute of Carcinogenesis, Russian Cancer Research Center of Academy of Russian Academy of Medical Sciences, Moscow, Russia.***

The anticancer drugs induce different processes in the tumor cells: arrest of cell proliferation, cell differentiation, apoptosis, necrosis. Under influence of these drugs cell defence systems also can be activated. In particular, anticancer drugs influence the functional activity of the multidrug resistance protein, P-glycoprotein (Pgp) and expression of MDR1 gene encoding Pgp (Choudhary, Roninson, 1993). The mechanisms underlying the connections between apoptosis, cell differentiation and activation of cell defense systems remains unclear. The aim of this study is to elucidate the participation of signal transduction pathway controlled by retinoids in coordinated regulation of Pgp, apoptosis and cell differentiation. Various human cell lines were used: K-562 (chronic myeloid leukemia), H9 (T-cell leukemia) and KG-1 (stem cell leukemia). cDNA of RAR $\alpha$  gene (retinoic acid receptor) was introduced into these cells by retroviral vector LRARSN in packing line P317 and stable transfectants expressing transgene were isolated. The time course of constitutive and induced expression of MDR1 gene was studied by semi-quantitative RT-PCR technique and Pgp functional activity was evaluated by Rh123 efflux and FACScan flow cytometry. These data were compared with the number of apoptotic cells as well as cell differentiation alterations induced by anticancer drugs. For the studies of cell differentiation monoclonal antibodies to leukocyte differentiation antigens and flow cytometry will be used. The data show that RAR-controlled signaling pathway influence both MDR1/Pgp activity, apoptosis and differentiation but its effects depend on cell lineage.

**#439 All-trans retinoic acid, a possible agent in the treatment of hepatocellular carcinoma.** Egedy Miklós, Rumi György, Puskás Attila, Horváth Gyula, Viskl Anna. *Kaposi Mór County Hospital, Kaposvár, Hungary*

A 44 yr. old female patient is reported suffering of hepatocellular carcinoma for 40 months. Symptoms were upper abdominal discomfort, right upper quadrant pain. She had lost 12 kg during three months. Paleness, hepatomegaly and ascites were noted. Ultrasonography and CT-scan showed multiple liver lesions with partial portal vein thrombosis. Increased alpha fetoprotein, ASAT, ALAT were found (2x normal). Histology proved

hepatocellular carcinoma. Liver transplantation was denied because of portal vein thrombosis. Patient's status was worsening rapidly, she reached ECOG 4 stadium, became cachectic and needed parenteral nutrition. Severe gastrointestinal bleeding episodes were observed due to duodenal ulcer and stomach erosions. All-trans retinoic acid (ATRA) treatment was started (45 mg/sq.m/day on alternated weekly base) on the basis of the assumption that hepatocellular carcinoma and acute promyelocytic leukemia share similar oncogenic pathway, i.e. they modify the structure of retinoic acid receptor  $\alpha$  and  $\beta$  8 days after starting the therapy highly elevated transaminases were observed (10x normal). Since then she has gained 15 kg and has resumed her work as a teacher for the last three years. Abdominal CT-scan showed a complete regression of the intrahepatic tumor and simultaneously the serum AFP value had normalized. After 2 years of complete remission the patient relapsed. It was considered ATRA resistant. Roferon was given 3 MU/day for three months followed by ATRA reinvention. The patient is still stable; she shows the clinical status of ECOG zero.

**#440 Phenylarsonic acid containing compounds induce cytotoxicity and apoptosis in human cancer cells.** Liu, X.-P., Naria, R.K., and Uckun, F.M. *Drug Discovery Program, Parker Hughes Cancer Center, Hughes Institute, St. Paul, MN 55113.*

Arsenic trioxide ( $As_2O_3$ ) exhibits significant anti-leukemic activity. Because of its toxicity and poor solubility, arsenic trioxide is not optimally suitable for therapeutic use. In a systematic effort to identify a cytotoxic agent with potent anti-tumor activity against cancer cells, we synthesized several phenylarsonic acid substituted compounds and examined their *in vitro* effects on human leukemic cells using NALM-6, MOLT-3, ALL1, RS4;11 and breast cancer (BT-20) cells. The cytotoxic activity was measured using MTT [(3-[4,5-dimethylthiazol-2-yl]-2,5-diphenyl tetrazolium bromide)]. Apoptosis was detected with *in situ* apoptosis assay which allows the detection of exposed 3'-hydroxyl groups in fragmented DNA by TdT-mediated dUTP nick-end labeling (TUNEL). The *in vitro* anti-cancer activity of these compounds were further tested using highly sensitive clonogenic assays. Four lead compounds, WHI-P273, WHI-P370, WHI-P371 and WHI-P380 induced apoptosis in leukemic cells as determined by TUNEL assay. In clonogenic assays, these phenylarsonic acid substituted compounds inhibited human pre-B Acute lymphoblastic leukemic NALM-6 cell colony growth with  $EC_{50}$  in low micromolar range. Furthermore, WHI-P370 and WHI-P371 were also found to be active in inducing apoptosis in primary leukemic cells from 9 out of 10 ALL patients. Further preclinical development of these phenylarsonic acid substituted compounds may provide basis for the design of more effective adjuvant chemotherapy programs.

**#441 Inhibition of the Sp1-mediated activity of the E2F promoter by the promyelocytic leukemia protein, PML.** Vallian, Sadeq; and Chang, Kun-Sang. *Division of Biology, Faculty of Sciences, Isfahan University, Isfahan, Iran; Division of Laboratory Medicine, The University of Texas MD Anderson Cancer Center, Houston, Texas, USA.*

The PML gene was first identified in the breakpoint region of the t(15q-17q) translocation in acute promyelocytic leukemia (APL). Several reports indicate that PML encodes a nuclear phosphoprotein with growth and transformation suppressing ability. We have previously demonstrated that PML is a transcriptional repressor and inhibits transcription of a number of target genes involved in cellular growth, particularly, the epidermal growth factor receptor (EGFR) gene promoter. It was also found that PML directly interacted with the Sp1 transcription factor, a major regulator of the EGFR promoter, thus inhibiting its Sp1-mediated transcriptional activity. Here, we show that PML can repress transcription of the E2F1 promoter, that is, regulated by Sp1. In transient transfection studies in mammalian cells (e.g. U2OS and HeLa cells), PML significantly repressed the activity of the promoter. The E2F1 promoter contains DNA-binding sites for E2F and Sp1 transcription factors. Transient transfections into the Sp1-negative *Drosophila melanogaster* SL2 cells, indicated that the repression of the E2F promoter activity by PML is achieved through the Sp1, but not the E2F DNA-binding sites of the promoter. When the Sp1 DNA-binding sites were replaced with an unrelated DNA-binding site (GAL4), the repressive effects of PML were lost, confirming the necessity of the Sp1 DNA-binding sites for PML's repressive effects. Furthermore, PML were found to inhibit transcription of thymidine kinase (TK) and dihydrofolate reductase (DHFR) promoters, which are also regulated by Sp1. These data demonstrated that PML could function as a negative regulator of the E2F1 and other Sp1-regulated promoters, which may represent a novel mechanism for the known repressive effects of PML on the cell cycle progression and cellular growth.

**#442 Invasin, a Yersinia outer membrane protein, induces apoptosis/necrosis in different human tumour cell lines.** Arencibia, Ignacio and Sundqvist, Karl-Gösta. *Dept. Clinical Immunology, University of Umeå, 90185 Umeå, Sweden.*

Yersinia invasin binds to various beta-1-integrin receptors in phagocytic and non-phagocytic cells through the 192 a-a at the carboxyl-terminal end of the protein and facilitates bacterial penetration into animal cells. Previous studies have shown that Invasin induces cell motility-migration and apoptosis of human T lymphocytes and lymphoid cell lines. Both functions

(motility-migration and apoptosis) seem to be differentiated by the length of the protein. In the present study we show that a MBP-Inv fusion protein (Inv-740) and a glutaraldehyde fixed Yersinia enterocolitica preparation (Intact bacteria) induce apoptosis/necrosis in a number of tumour cell lines such as melanoma, prostatic cancer, malignant glioma and lung cancer. Cell death develops very fast within 30-60 minutes and shows no DNA fragmentation neither the characteristic apoptotic nuclear condensation although the cells expose phosphatidylserine in the outer leaflet of the cell membrane as shown by the Annexin assay. The TUNEL assay demonstrated positive labelling nevertheless the process is not inhibited by the typical caspase inhibitors. Our data point to a possible novel apoptotic pathway. Analysis of the Invasin effect on cell death using antibody blocking experiments and a beta-1-integrin negative cell line show a beta-1-integrin mediated signaling. With further work these results suggest that Invasin may be useful in the treatment of cancer diseases.

**#443 Hepatitis B virus activity and its impact on liver histology and tumor biological features in hepatocellular carcinoma.** Tao Chen, Siu-Tim Cheung, Irene OL Ng, Chung-Mau Lo, Wen-Ching Yu, Sheung-Tai Fan. *Center of Liver Diseases and Department of Surgery, University of Hong Kong, Queen Mary Hospital, Hong Kong.*

Objective: This study aims at defining the activity of hepatitis B and its impact on liver histology and tumor biological features in HCC. Materials and Methods: 40 consecutive HCC patients were studied. The preoperative serum samples were detected for HBsAg, HBeAg, HBeAb, HBcAb (Abbott), HBV DNA (by PCR and bDNA) and liver functions; HBsAg and HBeAg immunohistochemical staining were also performed on adjacent nontumor tissue. Hepatitis activities in adjacent liver tissues were scored by Knodell scoring system; Liver tumor differentiation was scored by Edmondson grading system. RESULTS: (1). The positive rates for HBsAg, HBeAg, HBeAb and HBcAb were 85%(34/40), 28%(11/40), 70%(28/40), 97%(37/38), respectively. HBV DNA were positive in 75% (30/40) and 55% (22/40) of patients by PCR and bDNA, respectively. All sero-HBeAg positive patients were HBV DNA positive both by PCR and bDNA and with higher titer of HBV DNA ( $p = 0.003$ ). HBV DNA titer was significantly higher in patients with positive adjacent non-tumor tissue HBcAg staining than that in negative ones ( $P = 0.036$ ). 29 patients were with sero-HBeAg-, of which HBV DNA could be detected in 19 (66%) by PCR (2). CAH and cirrhotic patients had higher HAI scores (7.6(3.08 and 9.4(2.59);  $p = 0.00$ ,  $p = 0.00$ ). The positive rate and titer of HBV DNA in CAH and cirrhotic patients were significantly higher than those in normal adjacent liver group were ( $p = 0.002/p = 0.004$  for positive rates;  $p = 0.003/p = 0.001$  for HBV DNA titers). HAI score in HBcAg staining + patients was significantly higher than that in negative ones ( $p = 0.022$ ). (3). 76% (31/40) of patients were with poorly differentiated tumors. Tumor size correlated well with Edmondson scores (correlation coefficients = 0.4792,  $p = 0.002$ ) and negatively correlated with HAI scores. More patients in poorly differentiated group were likely to present low HAI scores but large tumors. CONCLUSION: HBV chronic infection was high and more than half of them were with active infection in HCC in Hong Kong; 48% of all patients might be infected with mutant viruses. HBV chronic infection did poorly impact on the remaining liver tissue; Most patients had poorly differentiated tumors and were likely to have fine liver histology in adjacent non-tumor liver tissue but large tumors in size. The study suggested that more attention should be paid to HBV activity during the treatment of HCC. Anti-viral treatment may be worthwhile in patients with elevated HBV DNA to avoid reactivation of hepatitis enhanced by chemotherapy or surgery. Relationship between tumor differentiation and HBV DNA status needs further study.

Key words: Hepatocellular Carcinoma (HCC); Hepatitis B virus; Polymerase chain reaction; Branched DNA assay (bDNA), Histology activity index (HAI score); Edmondson grading system.

## SECTION 5: DRUG DELIVERY, PRODRUGS, AND TOXICOLOGY

**#444 An isogenic human colon model for NQO1 and its application in determining the role of DT-diaphorase in the antitumor activity of a range of quinone-based agents.** Kelland, Lloyd R., Sharp, Sweeney Y., Valenti, Melanie R., Brunton, Lisa A., and Workman, Paul. *CRC Centre for Cancer Therapeutics, Institute of Cancer Research, Sutton, Surrey SM2 5NG, UK.*

The obligate 2-electron reducing enzyme DT-diaphorase (DTD) catalyzes the reduction of a range of quinones. Because some tumor types (e.g. colon and nonsmall cell lung) have been shown to possess relatively high levels, this may allow the selective bio-reduction of prodrugs to cytotoxic species in these tumors. In order to aid in the discovery of improved DTD activated agents and elucidate the role of DTD in the growth inhibitory and antitumor properties of prototype drugs such as mitomycin C and the indoloquinone EO9, we have established an isogenic human colon model for DTD expression. The BE cell line (which contains a disabling point mutation in the NQO1 gene encoding DTD) was stably transfected with



human *NGO1* resulting in the DTD expressing F397 subline. The DTD activity in the F397 was 1400 compared to <2 nmoles/min/mg in the parent BE line. These cell line and parallel *in vivo* xenograft models, differing only in DTD expression, were then used to study the antitumour properties of a range of quinone-containing agents. Using a 96 hour continuous exposure sulforhodamine B growth inhibition assay, a range in potentiation was observed in the high DTD expressing F397 versus the vector control lines. The growth inhibitory properties of the known DTD substrates streptonigrin and EO9 were potentiated by 132-fold and 17-fold respectively. In contrast, mitomycin C and RH1 (a more water soluble derivative of MeDZQ scheduled for phase I trial) showed less potentiation (7.3 fold and 4-fold respectively whereas MeDZQ itself showed no difference in potency). However, at shorter exposure times (24 hours) both RH1 and MeDZQ exhibited greater potentiation (maximum of 20-fold for RH1 and 13-fold for MeDZQ). The geldanamycin analog, 17 allylamino-17 demethoxygeldanamycin (17AAG) which is now in phase I trial, was 32-fold more potent against F397 versus vector control BE cells. *In vivo* xenograft studies revealed no difference in the antitumour activity of mitomycin C between the BE vector control and F397 tumours. In contrast, 17AAG (administered at the maximum tolerated dose of 80 mg/kg/day ip on days 0-4 and 7-11) exhibited greater antitumour efficacy against the F397 xenograft than the BE vector control (growth delays of 11.4 days for the BE F397 xenograft versus 5.8 days for the vector control). This *in vitro* cell line and parallel *in vivo* xenograft human colon model is of value in the discovery of improved DTD-activated prodrugs.

**#445 EO9 and bladder cancer: Biochemical and pharmacological studies suggest a novel strategy for therapeutic intervention.** Phillips RM, Choudry GA, Hamilton Stewart PA, Brown JE, Doubie JA. *Clinical Oncology Unit and Department of Pharmacy, University of Bradford, Bradford BD7 1DP, Bradford NHS Trust, Bradford, BD9 6RJ.*

EO9 is an indolequinone which requires enzymatic activation by reductases to generate cytotoxic species. DT-diphorase (DTD) plays a central role in the activation of EO9 under aerobic conditions and a good correlation between DTD levels and chemosensitivity *in vitro* exists. Despite the fact that EO9 is pharmacodynamically a good drug, it failed to demonstrate activity in phase II clinical trials primarily because of poor drug delivery to tumours as a result of rapid pharmacokinetic elimination ( $t_{1/2} < 10$  min) and poor penetration through avascular tissue. These properties may be advantageous in terms of treating cancers which arise in a third compartment (such as the bladder) as intravesical drug administration removes the problem of drug delivery and EO9's short half life in plasma would reduce the risk of systemic side effects. The aims of this study were twofold: firstly to characterise the levels of DTD in bladder tumours and normal bladder mucosa and, in view of the fact that EO9's activity is influenced by extracellular pH (pHe) the second aim of this study was to determine the relationship between DTD and chemosensitivity in cell lines exposed to EO9 under acidic pHe conditions. Paired tumour (G1pTa to G2/3pT4) and normal bladder biopsies were taken at transurethral resection (cold pinch biopsy) and the presence of DTD determined by both biochemical and immunohistochemical methods. A broad spectrum of DTD activity exists in tumour material (ranging from 571 nmol/min/mg to undetectable,  $n = 18$  patients) with a subset of patients (8/18) having significantly higher levels of DTD activity in tumour tissue compared with normal bladder mucosa (ranging from 63 nmol/min/mg to undetectable). Immunohistochemical analysis of DTD in tumour tissue confirmed biochemical analysis. No staining of the urothelium was observed. A good correlation between DTD and chemosensitivity exists in tumour cell lines exposed to EO9 at both pHe values of 7.4 and 8.0. In conclusion, intravesical administration of EO9 in an acidic vehicle may generate selective antitumour activity (based on elevated DTD in tumour compared with normal tissue) with minimal systemic toxicity as any drug which reaches the blood would be relatively inactive (due to a rise in pHe) and rapidly cleared. A further clinical study of intravesical EO9 against bladder cancer is therefore warranted on the basis of these results.

**#446 Quantitation of Cytosine Deaminase and Adenovirus by Real Time RT-PCR: A Novel Method for Assessing Expression Levels in Gene Therapy.** Johnson Martin R, Gustin Allen N, Wang Kangsheng, High Lisa, Stockard Cecil R, Vickers Selwyn M, Grizzle William E, Buchsbaum Donald J and Diasio Robert B. *Depts of Pharmacology and Toxicology, Surgery, Radiation Oncology, Pathology and the Comprehensive Cancer Center, University of Alabama of Birmingham.*

One of the most promising strategies for cancer gene therapy uses recombinant adenovirus (Ad) expressing *E. coli* cytosine deaminase (CD) for molecular chemotherapy. Solid tumors expressing CD have been shown to convert the non-toxic prodrug 5-fluorocytosine into 5-fluorouracil. Current studies focusing on increasing specific tissue targeting and improving low *in vivo* transduction efficiencies require a sensitive method for quantitation of Ad and CD levels. We report the development and validation of a real time quantitative PCR method based on the addition of a third fluorogenic oligonucleotide (probe). This system eliminates the need for post PCR processing, since the fluorescence emitted from each reaction is continuously monitored using the ABI PRISM 7700 thermal cycler. Using this system, we have demonstrated that the fluorescence signal is

directly proportional to the starting copy number of Ad and CD molecules with a linear dynamic range of  $10^0$  to 250 and an intra-assay variation of <5%. Analysis of LS174T (colon adenocarcinoma) and BXP-3 (pancreatic adenocarcinoma) infected with an E1A/B replication incompetent Ad encoding *E. coli* CD (at a multiplicity of infection of 100) demonstrated a significant correlation ( $R^2=0.95$  and  $R^2=0.98$  respectively) between Ad and CD levels. Cell pellets were analyzed at different time points post infection (6, 18, 30 and 48 h). CD mRNA levels increased with time (LS174T increased 47-fold from 6 to 48 h while BXP-3 cells increased 233-fold from 6 to 30 h). Peak CD mRNA levels were detected at 48 h post infection in the LS174T ( $471 \pm 37$  CD copies/pg GAPDH RNA) and at 30 h post infection in the BXP-3 cells ( $361 \pm 8$  CD copies/pg GAPDH RNA). Protein expression levels of CD in the infected cells (as determined by immunostaining with a CD specific monoclonal antibody) correlated with CD mRNA levels in both cell lines. Lastly, both cell lines demonstrated increasing levels of Ad DNA with time (LS174T increased 4.8-fold from 6 to 48 h while BXP-3 cells increased 6.1 fold from 6 to 30 h) suggesting autoraplication of the vector genome in these cell lines. This quantitative RT-PCR assay is a significant improvement over existing methods and will be useful for quantitation of gene transfer in future *in vivo* studies.

**#447 Phase I study of Caelyx (doxorubicin HCL, pegylated liposomal) in recurrent head and neck cancer (HN).** Caponigro F, Avallone A, Rivellini F, Budillon A, Di Gennaro E, Ionna F, Mozzillo N, Marcolin P, Comella P, Comella G. *National Tumor Institute—Naples—ITALY.*

**Purpose:** Caelyx is a long-circulating pegylated-liposome containing doxorubicin (DOX), which was developed to target delivery of DOX to cancer cells. Biodistribution studies using  $^{111}\text{In}$ -DTPA-labelled STEALTH liposomes have demonstrated a positive tumor uptake in patients (pts) with advanced HN, with minimal localization in surrounding tissues. Based on the above observation, a phase I study of Caelyx in recurrent HN was started.

**Patients and methods:** Pts with recurrent HN were treated with Caelyx administered at the starting dose of 30 mg/m<sup>2</sup> every 3 weeks. Doses were escalated by 5 mg/m<sup>2</sup>/step up to maximum tolerated dose (MTD), which was defined as the dose level at which at more than a third of patients had dose limiting toxicity. Response was evaluated after 4 courses of chemotherapy.

**Results:** Available clinical data are summarized below.

Step	Caelyx (mg/m <sup>2</sup> )	Pts	DLT	Type	Response
1	30	3	0		1/3 (PR)
2	35	3	0		0/3
3	40	6	0		2/6 (1CR, 1PR)
4	45	6	2	N4, Sk4	2/6 (PR)
5	50	5	1	S3	0/0 (too early)
Total		23	3		5/18 (5 too early)

\* N = neutropenia; Sk = skin toxicity; S = stomatitis.

**Conclusion:** Pegylated liposomal doxorubicin is a safe and effective palliative outpatient treatment for recurrent HN patients at the doses tested thus far. Patient accrual is continuing up to MTD.

**#448 Pegylated liposomal doxorubicin (CAELYX®), administered intravenously at conventional dosages, penetrates into the brain.** Czeglak M, Braunsdorfer M, Strauch S, and Dittlich Ch. *Dept. of Pharmacokinetics and Drug Metabolism, Institute of Pharmaceutical Chemistry, University of Vienna; LBI for Applied Cancer Research (LBI-ACR VIE), KJF-Spital, Vienna, Austria.*

Aim of this investigation was to determine whether intravenously (i.v.) administered CAELYX® penetrates into the brain. In a patient with a primitive neuro-ectodermal tumor (PNET) in the cerebrum, having progressed under conventional chemoradiotherapy, two cycles of CAELYX® at the dosages of 40 mg/m<sup>2</sup> and 50 mg/m<sup>2</sup>, respectively, were administered as i.v. infusion at a three-weekly interval. The patient died 16 days after the second infusion due to tumor progression. CAELYX® was quantified in post-mortem tumor tissue by means of homogenization, solid phase extraction and reversed phase HPLC (external standard method). CAELYX® could be detected in each tissue sample analyzed at the following concentrations: brain right side: 33 ng/g, brain left side: 13 ng/g, brain tumor: 37 ng/g, brain tumor adjacency: 21 ng/g, liver: 39 ng/g, kidney: 34 ng/g, lung: 31 ng/g, and bone marrow: 4 ng/g. The results give evidence that a) CAELYX® penetrates into the brain after i.v. application; b) the distribution of CAELYX® from the blood seems to be independent of the kind of tissue except bone marrow; c) the main serum metabolite doxorubicinol was not detectable in the tissue samples; this is in accordance with data that CAELYX® is not metabolized; d) unknown peaks from tissue samples, not originating from the tissue matrix, could be observed in the chromatograms; these observations have yet to be verified.

**#449 Comparative antitumor activity of a novel injectable emulsion of paclitaxel (QW8184) and Taxol® in the B16 melanoma and IGROV1 human ovarian tumor xenograft in nude mice.** Constantinides P.P., Kessler D., Tustian A.K., Lambert K.J., Worah D., Quay S.C., Weltman S., and Rowinsky E.K. *SONUS Pharmaceuticals, Bothell, WA 98021 and Cancer Therapy and Research Center, San Antonio, TX 78229.*

The antitumor activity of QW8184, an injectable emulsion of paclitaxel, against the B16 melanoma and the human ovarian tumor xenograft IGROV1 was evaluated using Taxol® as a reference formulation. B6D2F mice (8 per group) were s.c. implanted with B16 tumor cells and iv therapy begun at day 4 with bolus QW8184 at 20, 40 and 60 mg/kg on q3dx5 or q4dx5 schedules or slow infusion of Taxol® at its MTD of 20 mg/kg following a 10-fold dilution with saline. The administered volume of saline and drug-free emulsion (vehicle) controls were 7 or 8 ml/kg. Nude mice were implanted s.c. by trocar with fragments of IGROV1 human ovarian carcinomas harvested from s.c. growing tumors in nude mice hosts. When tumors were approximately 5 × 5 mm in size, the animals were paired matched into treatment and control groups containing 9 tumor-bearing mice per group. QW8184 was administered i.v. on a q3dx5, q4dx5, and qdx5 schedule at 20, 40 and 60 mg/kg. Taxol® was administered i.v. on the same schedules at 20 mg/kg, its MTD. Mice were weighed (twice weekly) and tumor measurements were taken starting Day 1. In the B16 melanoma model, log-kill cell values of 1.8 and 3.0 were observed with QW8184 at 20 and 40 mg/kg, respectively, as compared to 0.5 obtained with Taxol® at 20 mg/kg. A significant reduction in tumor growth and an increase in survival was observed with QW8184 which was found to be more efficacious and less toxic than Taxol®. Administration of QW8184 in IGROV1 tumor-bearing mice at 20, 40 and 60 mg/kg on a q3dx5 or q4dx5 schedule resulted in nearly 100% tumor growth inhibition at all doses with 2, 8, and 7 and 3, 9, and 8 complete tumor responses, respectively. In comparison, administration of Taxol® resulted in 3 complete tumor responses on both schedules. On a qdx5 schedule, the antitumor activities of QW8184 and Taxol® were similar. QW8184, however, was better tolerated with no toxic deaths, whereas six drug-related deaths were noted with Taxol®. QW8184 was highly active against the IGROV1 in a dose-dependent fashion, regardless of the dosing schedule and it was better tolerated than Taxol®. The improved antitumor activity of QW8184 in both tumor models may well be related to its preferential uptake by tumor cells due to the extremely small particle size of the emulsion droplets (mean diameter of about 60 nm).

**#450 Taxane derivatives for targeted therapy of cancer: Design and synthesis of a soluble paclitaxel-peptide conjugate with enhanced antitumor activity.** Safavy, Ahmad, Raisch, Kevin P, Khazaell, MB, Buchsbaum, Donald J, Bonner, James A, *Departments of Radiation Oncology and Medicine, University of Alabama at Birmingham, Birmingham, AL 35294.*

The diterpenoid molecule paclitaxel (PTX) is considered to be one of the most important and promising anticancer drugs currently in clinical use for breast and ovarian cancers with potential for the treatment of skin, lung, and head and neck carcinomas. The aim of this study was to develop water-soluble prodrugs of PTX with tumor-recognizing abilities through conjugation to a peptide that binds to a receptor on tumor cells. Such molecules should be able to 1) eliminate the allergenic solubilizers, 2) provide efficient delivery of the drug to micrometastatic tumors, and 3) reduce the administered dose as a result of site-specific delivery of the drug. In this report, the synthesis of a ternary molecule consisting of PTX, poly(ethylene glycol) (PEG), and a peptide recognizing the bombesin/gastrin releasing peptide receptor (BBN/GRPr), is described. The 7-amino acid peptide, BBN[7-13], was synthesized by solid-phase methods and was conjugated to the PTX-2'-hydroxy function by a heterobifunctional PEG linker to afford the target conjugate, designated as PTXPEGBBN[7-13]. Cell-binding and cytotoxicity assays were performed on BBN/GRPr-positive NCI-H1299 cells. The PTXPEGBBN[7-13] conjugate was readily soluble in aqueous buffers and completely retained the receptor binding properties of BBN[7-13]. The drug release kinetics was studied in both PBS (pH 7.4) and human serum (HS) at 37°C for the cleavage of PTX pharmacophore from the conjugate. These studies showed release half-lives of 154 min and 113 min in PBS and HS, respectively. Cytotoxicity assays with NCI-H1299 cells showed that cytotoxicity of PTXPEGBBN[7-13] at a 15 nM dose was enhanced by a factor of 17 for 24-h and 10 for 96-h exposure times, relative to unconjugated paclitaxel at equimolar concentration. The IC<sub>50</sub> of the conjugate was lower than the free drug by a factor of 2.5 for both 24-h and 96-h exposures. These results describe, for the first time, the design and synthesis of a water-soluble tumor-directed PTX prodrug which may establish a new mode for the utilization of this drug in cancer therapy.

**#451 Optimization of the anti-tumor activity of water-soluble poly L-glutamic acid (PG)—paclitaxel (TXL) conjugates.** de Vries Peter, Kumar Anil, Heasley Eveline, Singer Jack. *Cell Therapeutics, Inc., 201 Elliott Avenue West, Seattle, WA, 98119.*

Stable conjugation to polymers makes hydrophobic drugs water-soluble and increases relative distribution to tumor tissues because the tumor vasculature is relatively permeable to macromolecules. The con-

jugate is retained in the tumor bed, undergoes pinocytosis, and slowly releases the active drug. TXL conjugated by ester linkage to the  $\gamma$  carboxylic acid residues of PG forms a stable inactive conjugate in plasma with a MTD in TXL equivalents of 160 to 320 mg/kg in mice, versus 80 mg/kg for TXL in cremophor/ethanol, and superior anti-tumor activity against a variety of tumor types (Li *et al.*, *Cancer Res.* 58: 2404, 1998 and *Clin. Cancer Res.* 5:891, 1999). At equivalent doses, >6-fold more TXL is delivered to subcutaneous (SC) OCA-1 tumors with PG-TXL than with TXL. We examined two critical parameters, average MW and percent substitution of TXL (loading), that may affect the efficacy of PG-TXL using the growth of SC implanted murine Lewis lung cancer (LL/2) tumors as a bioassay. Groups of 10 mice each received a single intraperitoneal injection of PG-TXL when tumors were less than 50 mm<sup>3</sup> and the effect on TGD to 500 mm<sup>3</sup> was determined. Comparison of PG-TXL conjugates made with PG of different MW (33-, 49- and 74-kD) showed that all three were more effective than TXL: 4.1, 5.3, and 7.2 days at 240 mg/kg TXL equivalents, respectively, versus 2.1 days for TXL at its MTD of 80 mg/kg ( $p < 0.05$  for each). The MTD for the TXL conjugates with 33-, 49-, and 74-kD were, respectively,  $\geq 240$ ,  $\geq 240$ , and 160 mg/kg TXL equivalents. Using 33 kD PG, the TXL loading was then varied. TGD to 500 mm<sup>3</sup> at 160 mg/kg TXL equivalents were 3.0, 4.1, and 5.1 days, for 25, 37.5 and 50% loading (w/w), respectively. When PG-TXL (37.5% TXL; 33 kD PG) was given every 3 days for 3 doses of 160 mg/kg TXL equivalents, TGD was extended to 7.2 days with no mortality among 10 animals. These data confirm the superior efficacy of PG-TXL over free TXL and indicate that limiting PG MW and increasing TXL loading can enhance the MTD and relative efficacy.

**#452 Modulating recognition of anticancer agents at the large, neutral amino acid transporter of the blood-brain barrier: Implications for brain tumor targeted drug therapy.** Killian D and Chikhale P. *Department of Pharmaceutical Sciences, 20 North Pine Street, School of Pharmacy, University of Maryland, Baltimore, MD 21201, USA.*

Using bioreductively-activated, anticancer prodrugs (as drug delivery systems; DDS), we demonstrate interconversion between passive and the large, neutral amino acid (LNAA) carrier-mediated drug transport mechanisms at the BBB. Such strategies could be used to optimize brain tumor targeted drug therapy. The amino acid functionality of melphalan and acivicin was "blocked" using bioreductive prodrugs, to form M-DDS and A-DDS respectively, whereas, mercaptopurine was derivatized using L-Cys, to form MP-DDS. The physiologically relevant, *in situ* rat brain perfusion technique was used to demonstrate affinity of the DDS for the LNAA transporter as well as to determine passive brain uptake. Brain levels of analytes were determined using either liquid scintillation counting of appropriate radiotracers or by brain parenchymal tissue sampling, followed by homogenization, extraction and reverse-phase UV-HPLC analysis of the supernatant. Our results showed that M-DDS and A-DDS do not enter the brain via the LNAA transporter, as determined by their lack of competition for brain uptake of [<sup>14</sup>C]-Leu. The intrinsic, passive BBB permeability-surface area (PA) product for M-DDS containing various substituents was in the range of 3 to 6 × 10<sup>-3</sup> ml/s/g, which is about 3-fold higher compared to PA for the parent melphalan, and is about 10-fold lower compared to PA for diazepam, a lipophilic marker for the BBB. On the other hand, MP-DDS and IBM-DDS (a model compound) showed high affinity for the LNAA transporter of the BBB, thus inhibiting [<sup>14</sup>C]-Leu brain uptake by 63% and 92%, respectively. The IBM-DDS showed potent affinity (K<sub>i</sub> = 11  $\mu$ M) for the LNAA transporter. Therefore, recognition for the LNAA transporter at the BBB can be altered by chemical modifications at the amino acid terminal of anticancer agents. Furthermore, the level of passive as well as carrier-mediated brain uptake of the DDS can be influenced using substituents. Such methods in manipulating BBB permeability for enhancing brain uptake of anticancer drugs could be useful in the effective treatment of brain tumors. [Supported by NIH].

**#453 Evaluation of the sequencing of cranial irradiation and enhanced antibody targeted chemotherapy delivery for efficacy in a rodent human lung cancer brain xenograft model.** Neuwell, Edward A.; Remsen, Laura G.; Pearce, Harper D.; Garcia, Raymond; *Oregon Health Sciences University, Portland, Oregon.*

**Introduction:** Delivery targeting and sequencing of chemotherapy and radiotherapy need to be assessed in the treatment of CNS metastatic disease. **Methods:** Nude rats with intracerebral human small cell lung carcinoma (LX-1) xenografts were randomly assigned to the following treatment groups on tumor day 6. Radiation (2000 cGy) was administered as a single fraction, by using parallel opposed portals; 6 days before chemotherapy, 24 hours before chemotherapy, 6 days after chemotherapy, alone day 6, or alone day 12. Chemotherapy consisted of intrarterial BR96-DOX (a tumor specific mAb-doxorubicin immunconjugate) delivered after osmotic blood-brain barrier disruption (BBBD) and was done in combination with the radiotherapy, alone day 6, or alone day 12. Animals were followed until condition necessitated sacrifice.



Groups (n = 10/group)	Survival Days
no treatment	14.8 ± 1.9
Radiation (d6) before BBBB (d12)	29.5 ± 1.9
Radiation (d6) before BBBB (d7)	27.1 ± 2.1
BBBB (d6) before Radiation (d12)	34.0 ± 2.0
Radiation only (d6)	20.0 ± 1.6
Radiation only (d12)	17.4 ± 2.4
BBBB only (d6)	25.9 ± 2.1
BBBB only (d12)	23.2 ± 2.5

**Results:** All groups had increased survival ( $p < .05$ ) when compared to untreated controls ( $14.8 \pm 1.9$  days). No significant difference was found in either radiation only groups, but chemotherapy day 6 was significantly better than radiotherapy on either day. The best survival was antibody targeted delivery on day 6 and radiation on day 12 ( $34.0 \pm 2.0$  days), albeit this was not statistically better than radiation on day 6 and BR96-DOX on day 12 ( $29.5 \pm 1.9$ ). **Conclusion:** Combined-modality therapy improved survival in the LX-1 rodent brain tumor model when compared to either radiotherapy or chemotherapy alone. There was a strong trend for increased survival when antibody targeted chemotherapy was delivered prior to radiotherapy.

**#454 Application of chronotherapy principles to cell-mediated immunotherapy: IL-12-based therapy in the MCA38 murine colon cancer model grown in syngeneic C57BL/6 mice.** Alisauskas, Rita, Glzas, Lisa C., Goldenberg, David M., and Blumenthal, Rosalyn D. Garden State Cancer Center, Belleville, NJ 07109.

The aim of these studies was to extend the concept of chronotherapy from chemotherapy to IL-12-based immunotherapy. The goal was to determine the optimal time of day to administer IL-12. The tumor model for these studies was the MCA38 murine colonic s.c. xenograft grown in C57BL/6 male mice. Mice were dosed with  $0.5 \mu\text{g}$  IL-12 daily for 5 days. Seven groups of mice were included with each a fixed dosing time for each group for all 5 days. The time points of treatment were 3, 7, 10, 13, 17, 20, and 23 Hours After Light Onset or HALO or 10 AM, 2 PM, 5 PM, 8 PM, 12 AM, 3 AM and 6 AM. Changes in therapeutic outcome (tumor growth) as a function of HALO have been determined and optimal dosing time was found to be between 13–17 HALO. The poorest outcome was between 23 and 7 HALO. To attempt to understand the mechanism governing periodicity of IL-12 immunotherapy, we used flow cytometry to evaluate the rhythm of lymphocyte expression of IL-12-R & IFN- $\gamma$ -R expression in tumor-bearing mice. Peak IL-12-R and IFN- $\gamma$ -R expression occurred at 23 HALO with 28%+ cells for IL-12R and 16%+ cells for IFN- $\gamma$ -R. Additional studies ongoing include periodicity of IFN- $\gamma$  production, and induction of IP-10, RENA, and Mlg, known mediators of IL-12 activity. We are also evaluating the periodicity of IL-12-induced T and NK cell proliferation and cytotoxicity. Finally, we have also looked at an angiogenic explanation for the optimal chronotherapy with IL-12 and found that peak BF to this tumor occurs at 17 HALO possibly resulting in the highest tumor delivery of IL-12. Results of these studies should permit more effective use of cellular-based therapies and should impact dose planning. (Supported in part by USPHS OIG grant R23 CA39841 from the NIH and a NJCC grant.)

**#456 Regulation of tumor targeting by small molecule (5-FU) or macromolecule (I-131-anti-CEA IgG) using principles of blood flow, chronobiology.** Blumenthal, Rosalyn D., Osorio, Louis, Ochakoskaya, Rita, Ying, Zhiliang, Goldenberg, David M. Garden State Cancer Center, Belleville, NJ & Dept of Statistics, Rutgers University, Piscataway, NJ.

The efficacy of many forms of therapy is governed in part by local blood flow (BF). Transient reductions in tumor BF can be used to enhance the activity of drugs that are more cytotoxic in a hypoxic environment. Transient increases in tumor BF can influence local  $\text{pO}_2$  concentration and thereby affect radiotherapy. Similarly, BF plays an important role in delivery of appropriate agents for chemotherapy, immunotherapy and gene therapy.

The chronobiology of many physiological phenomena that impact tumor targeting with nonspecific and specific agents has not yet been established. Preliminary results by Hori et al. (*Cancer Res.* 1992; 52:912–916) have demonstrated fluctuations in tumor blood flow in s.c. rat tumors with a higher rate at 15–21 HALO compared with the rate at 3–9 HALO.

We used GW-39 and LS174T human colon carcinoma xenografts grown s.c. in nude mice for these studies. BF was determined at 3, 7, 10, 13, 17, 20, and 23 Hours After Light Onset or HALO. In separate studies, dosing of  $^3\text{H}$ -5FU or  $^{131}\text{I}$ -131-MN-14-anti-CEA IgG was done at each of the same 7 HALO points noted and uptake was determined in each group.

Using cosinor analysis of BF data, we have found that the acrophase (peak) for tumor BF occurs at ~17 HALO in both tumor xenografts while maximal liver BF occurred at 10–13 HALO. Tumor BF ranged from the lowest value of  $1.34 \pm 0.54 \mu\text{l/g/min}$  at 20 HALO to the highest value of  $2.79 \pm 0.57 \mu\text{l/g/min}$  at 17 HALO. Thus, the rhythm of tumor and normal tissue BF are different, creating a window of opportunity when tumors can be targeted with a therapeutic agent. At 3 hrs post injection, the %ID/g of 5FU in tumor at 10 HALO was  $0.14 \pm 0.09$  and at 17 HALO was  $0.32 \pm 0.21$  ( $p < 0.02$ ). In liver at 10 HALO, uptake was  $0.134 \pm 0.08$  and at 17 HALO was  $0.071 \pm 0.03$  ( $p < 0.05$ ). At 24 hrs post injection, the %ID/g of  $^{131}\text{I}$ -MN-14 IgG in tumor at 10 HALO was  $11.5 \pm 1.58$  and at 17 HALO was 1.5-fold higher at  $16.96 \pm 2.35$  ( $p < 0.001$ ). In liver at 10 HALO, uptake was  $6.47 \pm 0.49$  and at 17 HALO was 1.3-fold lower at  $5.04 \pm 0.81$  ( $p < 0.001$ ). These results suggest that small shifts in the chronobiology of BF in tumor and in normal tissue can have a sizeable impact on the distribution of chemotherapeutics and antibody-based drugs. (Supported in part by USPHS OIG grant R23 CA39841 and RO1 CA 60641 from the NIH.)

**#457 Positive interaction between 5-fluorouracil and FdUMP[10] in the inhibition of human colorectal tumor cell proliferation.** Gmelner, William H., Liu, Jinqian, Lawson, Terence A., Talmadge, James. UNMC Eppley Cancer Center, Omaha, NE 68198-6805

Interaction between 5-fluorouracil (5-FU) and FdUMP[10], a novel pro-drug formulation of the thymidylate synthase (TS) inhibitory nucleotide 5-fluoro-2'-deoxyuridine-5'-O-monophosphate (FdUMP), was investigated to evaluate the feasibility of using these two forms of fluorinated pyrimidine in combination chemotherapy regimens. 5-FU and FdUMP[10] are expected to differ in their relative intracellular distribution of active metabolites, and their combined administration may result in either a positive or a negative interactive effect. The dose-response behaviors of 5-FU and FdUMP[10] towards H630 and H630-10 (human colorectal tumor) cells were first investigated separately. Effects on cell viability were measured using an assay for 3-(4,5-dimethylthiazol-2-yl)-2,5-diphenyltetrazolium bromide (MTT), while cytotoxicity and apoptosis were investigated using clonogenic and TUNEL assays, respectively. Exposure of H630 cells to concentrations of FdUMP[10] insufficient to inhibit cell proliferation as a single agent markedly increased the cytotoxicity of single-agent 5-FU. The results indicate that 5-FU and FdUMP[10] interact in a positive manner in killing cultured human tumor cells. These results, in conjunction with previous studies from our laboratory indicating that FdUMP[10] is extremely well-tolerated *in vivo* (maximum tolerated dose in

Balb/c mice greater than 200 mg/kg/day (qdx3) compared to 45 mg/kg/day (qdx3), demonstrate that combining these two forms of fluorinated pyrimidine may be clinically superior to 5-FU in combination chemotherapy regimens.

**#458 Tumor-directed delivery and amplification of tumor-necrosis factor- $\alpha$  (TNF) by attenuated *Salmonella typhimurium*.** Lin, S.L., Spinka, T.L., Le, T.X., Pianta, T.J., King, I., Belcourt, M.F., Li, Z. *Vion Pharmaceuticals, Inc. 4 Science Park, New Haven, CT 06511.*

TNF expression, preferential tumor accumulation, and antitumor efficacy of attenuated *S. typhimurium*, bearing a single-copy, chromosomally-integrated TNF gene, were evaluated. Chromosomal integration of a *trc* promoter-driven TNF gene, expressing the mature form of human TNF, was achieved by transposon-mediated insertion into an attenuated strain of *S. typhimurium* (*msbB*<sup>-</sup>, *purF*<sup>-</sup>, *serC*<sup>-</sup>). Western blot analysis of three independent colonies revealed that mature TNF was expressed by all three clones at levels exceeding 10 ng/10<sup>7</sup> colony forming units (cfu) of bacteria. Intravenous administration of Clone 2 (the highest TNF-expressing clone) at a dose of 1 × 10<sup>6</sup> cfu/mouse, to B16F10 melanoma tumor-bearing C57BL/6 mice (n = 3), revealed bacteria accumulation levels of 5.4 × 10<sup>8</sup> ± 1.8 × 10<sup>8</sup> cfu/g tumor vs. 1.3 × 10<sup>6</sup> ± 0.8 × 10<sup>6</sup> cfu/g liver, when examined 5 d following bacteria inoculation. PCR analysis of 125 recovered colonies revealed retention of the TNF gene in all colonies tested. In preliminary studies using a Colon 38 tumor model, where tumors were staged to between 0.25 and 0.3 g prior to treatment, a single intravenous inoculation of 1 × 10<sup>6</sup> cfu/mouse resulted in complete tumor regression in 6 of 7 mice. Replicate administration of the parental strain resulted in tumor stasis, with little or no regression. No significant weight loss occurred following administration of either parental or TNF-expressing *Salmonella*, indicating that cytoplasmic expression of TNF did not enhance bacterial toxicity. Results indicate that selective tumor delivery of potent cytokines, of limited utility due to dose-limiting toxicity, can be achieved using attenuated *Salmonella*, and that such cytokine delivery can markedly enhance the antitumor efficacy of *Salmonella*.

**#459 Activation of cyclophosphamide by tumor-targeting *Salmonella typhimurium*.** Belcourt, M.F., Waxman, D.J., Goss, K., King, I., Bermudes, D., and Lin, S. *Vion Pharmaceuticals, Inc., 4 Science Park, New Haven, CT 06511; Department of Biology, Boston University, Boston, MA 02215.*

Attenuated *Salmonella typhimurium* are capable of selective amplification within solid tumors and inhibiting tumor growth in murine tumor models following intravenous or intratumoral administration. To further exploit the tumor-targeting ability of these microorganisms, we have engineered bacteria to express the P450 monooxygenase enzyme CYP2B1, which is capable of activating cyclophosphamide, a widely used anticancer prodrug. The rat CYP2B1 gene was obtained from a rat liver cDNA library and subcloned into a *trc* promoter-dependent expression plasmid. The human NADPH P-450 oxidoreductase cDNA, which is required for efficient CYP2B1 enzyme function in bacteria, was positioned immediately 3' to the CYP2B1 gene to create a bicistronic cassette that expresses both genes from a single transcript. Expression of each gene was confirmed by immunoblot analysis. The oxidoreductase activity was measured at approximately 2000 nmol/min/mg protein (cytochrome c reduction). Incubation of intact bacteria with the CYP2B1 substrate 7-ethoxy-4-trifluoromethylcoumarin resulted in its conversion to 7-hydroxy-4-trifluoromethylcoumarin, demonstrating the functionality of the P450 enzyme system in these bacteria. Similarly, the intact CYP2B1/P450 oxidoreductase expressing bacteria were capable of activating cyclophosphamide to its cytotoxic, anti-cancer metabolite 4-hydroxycyclophosphamide. Interestingly, these bacteria were resistant to cyclophosphamide concentrations as high as 10 mM. These results imply that tumor-localized conversion of cyclophosphamide to its cytotoxic intermediate may be achieved by tumor-targeting *Salmonella* carrying the CYP2B1 gene. [Supported in part by NIH grant CA49248 (to D.J.W.).]

**#460 A novel strategy for gene therapy delivery to brain tumors: Genetically modified neural stem cells (NSCs) display tropism for intracranial gliomas.** Aboody KS<sup>1</sup>, Bower KA<sup>1</sup>, Shivji S<sup>1</sup>, Brown A<sup>2</sup>, McDonough CB<sup>1</sup>, Rainov NG<sup>2</sup>, Black PM<sup>3</sup>, XO Breakfield<sup>2</sup> and EY Snyder<sup>1</sup>. <sup>1</sup>Depts of Neurology, Pediatrics, & Neurosurg., Children's Hosp., HMS, Boston, MA; <sup>2</sup>Molecular Neurogenetics Unit, Dept of Neurology, Mass. Gen. Hosp., HMS, Boston, MA; <sup>3</sup>Brain Tumor Svc., Dept. of Neurosurg., Brigham & Women's Hospital & Children's Hospital, HMS, Boston, MA.

One of the main reasons primary human brain tumors (e.g., gliomas) are largely refractory to currently available treatments is the degree to which they expand, infiltrate surrounding tissue, and migrate widely in normal brain. We demonstrate that inherently migratory NSCs, when implanted into experimental intracranial gliomas, will distribute themselves rapidly and extensively throughout the tumor and migrate in juxtaposition to widely expanding and aggressively advancing tumor cells while continuing to stably express a foreign reporter gene. Furthermore, when implanted at even distant sites from the tumor bed (e.g., into adjacent normal tissue, into the contralateral hemisphere, or into the lateral ventricles), the donor NSCs migrate through normal tissue and specifically target the tumor cells.

Preliminary data suggest that both murine and human NSCs retrovirally transduced to express the prodrug cytosine deaminase behave in a similar manner. Additionally, pilot cell culture studies suggest an oncolytic effect of these genetically modified NSCs, both human and murine, on surrounding brain tumor cells when exposed to 5-fluorocytosine. These results support the use of NSCs as an effective delivery vehicle for targeting therapeutic genes and vectors to invasive brain tumor cells. Potential approaches made feasible by NSC-mediated gene delivery may include not only the direct dissemination of cytotoxic gene products, but also the more efficacious delivery of viral vectors encoding therapeutic genes to be incorporated by tumor cells (e.g. suicide genes).

**#461 HuN901-DM1: A tumor-activated prodrug that eradicates large xenografts of small cell lung cancer in mice and shows minimal toxicity in cynomolgus monkeys.** Chari, Ravi V.J., Derr, Susan M., Ferris, Cynthia A., Steeves, Rita M., and Widdison, Wayne C., *ImmunoGen, Inc., 148 Sidney Street, Cambridge, MA 02139, U.S.A.*

The maytansinoid drug DM1, a potent anti-mitotic agent, was converted into the tumor-activated prodrug (TAP) huN901-DM1 by linking it to the humanized monoclonal antibody huN901. Upon binding to the target small cell lung cancer (SCLC) cell, through the CD56 antigen, and internalization, this TAP is converted to the active drug inside the cancer cell. *In vivo*, huN901-DM1 is exceptionally active as a single agent. Treatment of SCID mice bearing large (average size 420 mm<sup>3</sup>) SCLC SW2 xenografts with huN901-DM1 resulted in cures, lasting greater than 200 days. In order to examine the effects of combination therapy, SCID mice bearing subcutaneous SCLC xenografts, established with NCI N417 cells were treated with a low, non-curative dose of huN901-DM1 combined with optimal doses of either Taxol or cis-platin + VP-16, the most effective therapeutic agents in SCLC. Treatment with Taxol alone, or with huN901-DM1 alone resulted in tumor growth delays of 5 days in each case. In animals treated with a combination of the two agents, the tumors disappeared, with complete regressions lasting 58 days, indicating that the anti-tumor efficacy of the combination was synergistic. The combination of cis-platin + VP-16 with huN901-DM1 was also more efficacious than the respective agents used alone.

HuN901 cross-reacts with some normal human tissues, notably adrenal glands, cardiac tissue and peripheral nerve. The cross-reactivity pattern in cynomolgus monkeys is similar to that seen in human tissues. In an effort to gauge the relevance of this *in vitro* cross-reactivity to the *in vivo* situation, a pilot toxicology study was conducted in monkeys. Monkeys were treated with huN901-DM1 at doses equivalent to 42% and 126% of the mouse LD<sub>50</sub>. At these doses, there were no significant clinical, hematological or pathological abnormalities observed, indicating that there was little or no toxicity. Thus, huN901-DM1 has exceptional anti-tumor activity in mice, and low toxicity in monkeys, and is a promising candidate for the treatment of patients with SCLC.

**#462 SB 408075: A tumor-activated prodrug with exceptional activity against colon, pancreatic and lung tumor xenografts.** Chari, Ravi V.J., Derr, Susan M., Widdison, Wayne C., Steeves, Rita M. and Lambert, John M., *ImmunoGen, Inc., 148 Sidney Street, Cambridge, MA 02139, U.S.A.*

SB 408075 is a tumor-activated prodrug (TAP) created by linking the maytansinoid drug DM1, a potent anti-mitotic agent, to the humanized monoclonal antibody huC242. The C242 antibody binds to the CanAg antigen expressed on human colon tumors. We have previously shown that, *in vitro*, SB 408075 is 1000-fold more specific for killing antigen-expressing cells as compared to non-target cells. *In vivo*, a murine version of SB 408075 was shown to cure mice bearing large (500 mm<sup>3</sup>) human colon tumor xenografts.

We evaluated the binding of huC242 with tissue sections of other human tumors, using immunohistochemical methods. The antibody was found to react with most pancreatic tumors (95% of tested tissues were positive). The antibody also stained 77% of non-small cell lung adenocarcinomas and squamous cell carcinomas (20 out of 26 tested tissues were positive in each case). In order to determine whether *in vitro* reactivity with tumor tissues could be correlated with *in vivo* efficacy, the anti-tumor activity of the murine version of SB 408075 was evaluated in xenograft models of pancreatic and non-small cell lung cancers. SCID mice bearing three different human pancreatic tumor xenografts (average tumor size at treatment was 100 mm<sup>3</sup>) established subcutaneously with the tumor cell lines SW1990, BXP-3, and SU.8686 were treated with SB 408075 at doses ranging between 35 to 60% of the maximum tolerated dose (MTD). In all three models, SB 408075 caused complete tumor regressions lasting 50 days for SW1990, 28 days for BXP-3, and 92 days for 50% of the animals bearing the SU.8686 tumor. The remaining 50% of the animals in the SU.8686 group were cured. The efficacy of this TAP was also evaluated in mice bearing human lung adenocarcinoma H441 xenografts. Treatment with SB 408075, at a dose of about 30% of the MTD, resulted in complete tumor regression lasting 84 days. These studies demonstrate that SB 408075 has exceptional anti-tumor activity in animal models, at non-toxic doses. Thus, in addition to colon cancer, SB 408075 is a promising therapeutic candidate for the treatment of patients with pancreatic and non-small cell lung cancers.



**#463 Signaling pathways that regulate apoptosis and the MDR1 gene activation are similar but not identical.** Kakpakova, E.S., Kltorova, O.V., Vinogradova, M.M., Zabolina, T.N., Ilyina, E.N., Stavrovskaya, A.A., Shill, A.A. *Institute of Carcinogenesis, N. Blokhin Cancer Research Center, Moscow, Russia*

The rapid up-regulation of the MDR1/P-glycoprotein in the course of exposure of tumor cells to chemotherapeutic drugs can diminish the anticancer effect of therapy. We investigated the association between programmed death of human leukemia cells treated with different agents and the MDR1 gene activation. We show that, in H9 cells, cytarabine (Ara C) (25–50  $\mu$ M) and C<sub>2</sub>-ceramide (25–50  $\mu$ M) induced both apoptosis (as determined by sub-G1 peak of flow cytometrical profiles of propidium iodide-treated nuclei and morphological examination of the cells) and the MDR1 gene activation (as determined by semi-quantitative RT-PCR) within 18 hrs. In addition, in K562 cells, C<sub>2</sub>-ceramide induced both apoptosis and MDR1 activation whereas AraC caused neither cytotoxicity nor MDR1 activation. Moreover, prevention of C<sub>2</sub>-ceramide-induced apoptosis with z-VAD, a broad spectrum caspase inhibitor, abrogated the MDR1 activation. These data suggested an association between apoptosis and MDR1 up-regulation. However, D-erythro-sphingosine (15  $\mu$ M, 18 hrs) was toxic for K562 cells whereas the MDR1 activation was not observed. Thus, we provide evidence that triggering the apoptotic signaling pathways could be necessary but not sufficient for the MDR1 activation in human leukemia cells. The search for the point(s) of divergence of signaling mechanisms that execute apoptosis and those that govern the MDR1 activation would be important for directed pharmacological and/or genetic inhibition of drug-induced MDR1 up-regulation without targeting death pathways.

**#464 An Experimental Study of Efficacy and Related Gene Expression of Continuous Hyperthermic Peritoneal Perfusion (CHPP) on Nude Mice bearing Human Colonic Cancer Cells.** Qing Sanhua, Hou Baohua. *Department of General Surgery, Nan Fang Hospital, The First Military Medical University, Guangzhou 510515, P.R. China.*

Aims to study the efficacy and mechanism of biological molecule of CHPP preventing and treating postoperative peritoneal recurrence of colorectal cancers. Methods applying CHPP with 5-Fu, MMC and DDP to treat 35 nude mice bearing human colonic cancer cells (LoVo line) which simulate the two periods after colorectal cancers resection (free cancer cell period and visible peritoneal plant period in peritoneal cavity) and observe the effect of CHPP preventing peritoneal plant, assay the expression of MDR and bcl-2 gene. Results the rates of developed peritoneal plants: 4/10 mice in early CHPP group ( $P < 0.05$ ), 6/10 mice in late CHPP group, 4/5 and 4/5 mice in alone chemotherapy and hyperthermia group, 5/5 mice in control. Mortality: 59.4  $\pm$  4.9 days in early CHPP group ( $P < 0.01$ ), 41.4  $\pm$  7.9 days in late CHPP group ( $P < 0.01$ ), 36.2  $\pm$  8.5 days and 35.6  $\pm$  8.1 days in alone chemotherapy and hyperthermia group ( $P < 0.01$ ), 24.8  $\pm$  8.1 days in control group. CHPP can significantly increase the survival rate, delay the emerge of ascites, inhibit the growth of tumor than alone chemotherapy and hyperthermia, reduce the expression of MDR gene and bcl-2 gene. Conclusion CHPP, especially early CHPP, has significant efficacy of preventing developed peritoneal implants of HCC in nude mice and the low expression of MDR bcl-2 gene, HCC apoptosis may be one of mechanism of CHPP inhibiting the growth of HCC.

**#465 Human pharmacokinetics of T138067, a novel antimicrotubule agent, given as a 3-hour infusion once every 21 to 26 days.** Berg, William; Vongphrachanh, Phothisath; Walling, Jackie; Wright, Matthew; Ye, Qiuping; Peterson, Karen; Motzer, Robert; Thoolen, Martin; Timmermans, Pieter; Solignet, Steven; Spriggs, David. *Memorial Sloan Kettering Cancer Center, NY, NY and Tularik Inc, South San Francisco, CA.*

T138067-sodium (2-fluoro-1-methoxy-4-(pentafluorophenyl-sulfonamide) benzene, sodium salt) is a novel antitumor agent that covalently binds to  $\beta$ -tubulin and inhibits microtubule formation. It has antitumor efficacy against a variety of xenografted tumors in mice. Here we report the pharmacokinetic behavior of T138067 in cancer patients in a Phase I study. T138067-sodium was administered as an intravenous infusion over 3 hours, at doses of 11, 22, 36, 55, 110, 220, 440 and 585 mg/m<sup>2</sup>. Patients treated at the first 7 dose levels received T138067 every 28 days, and subsequent patients were treated every 21 days. Plasma concentrations during the i.v. infusion, and AUC increased linearly with dose. Total plasma clearance ranged from 0.85 to 2.3 (1.43  $\pm$  0.43, mean  $\pm$  S.D., n = 16) L/kg/h. Volume of distribution (V<sub>dss</sub>) ranged from 0.27 to 1.26 L/kg (0.52  $\pm$  0.25, mean  $\pm$  S.D., n = 16). Following termination of the infusion, plasma concentrations of T138067 declined rapidly with an apparent elimination half-life of 25.6  $\pm$  16.3 min (mean  $\pm$  S.D., n = 16). DLT has not been reached but at 585 mg/m<sup>2</sup> the most severe toxicity observed has been CTC grade III (G3) leukopenia, G1 neutropenia and G2 nausea, emesis and diarrhea. Steady state plasma concentrations at this dose were approximately 5.5  $\mu$ g/mL. These data show that T138067 is very rapidly eliminated after i.v. infusion, and that total plasma clearance approximates hepatic blood flow. In comparison rats given a 4-hour infusion of 20 mg/kg/hour T138067 (a myelosuppressive but non-lethal dose) had plasma concentrations at steady state of 5.34  $\pm$  0.64  $\mu$ g/mL (mean  $\pm$  S.D., n = 12). The plasma concentrations associated with myelosuppression in patients appear to be predictable based on animal data.

**#466 The toxicology of recombinant mistletoe lectin (rML), a novel anticancer agent.** Mengs U., Weber K., Hamann H.J., and Corney S.J. *Madaus AG, KÖln, Germany; RCC, Iltingen, Switzerland.*

The recombinant mistletoe lectin (rML), which has cytotoxic and immunostimulatory properties, was shown to possess anticancer activity in a variety of animal tumor models. rML was intensively investigated for its toxicological profile according to actual GLP and ICH guidelines, and is currently in clinical trials for treatment of cancer.

**Single dose toxicity:** Studies on rats and mice of either gender revealed LD50 values in the  $\mu$ g-range (rat: 50  $\mu$ g/kg i.v., 150  $\mu$ g/kg s.c.; mouse: 10  $\mu$ g/kg i.v., 50  $\mu$ g/kg s.c.). The animals died within 4 days p.a., the cause of death being unclear so far.

**Repeated dose toxicity:** Studies on rats and dogs were carried out over a period of max. 90 days using the i.v. or s.c. administration route. There was no systemic target organ toxicity obvious up to 1  $\mu$ g/kg/day. Due to local intolerance at the injection sites, higher doses/concentrations were not feasible. The presence of rML-antibodies has been shown.

**Local tolerance:** From the above mentioned studies, local lesions occurred at concentrations higher than 50 ng/ml, both with i.v. or s.c. application. Intravesical instillations (3x/week for 14 days) were well tolerated up to 1  $\mu$ g/ml.

**Genotoxicity:** rML gave negative responses in the Ames test with five different strains of *S. typhimurium*. The mouse lymphoma assay and the mouse micronucleus test revealed also negative results under non-toxic conditions.

**Conclusion:** Taking into consideration that rML has antitumor potencies in several animal models at doses <100 ng/kg, a sufficiently wide safety margin has to be expected regarding clinical use.

Supported by the grant 0311183 of BMBF, Germany.

**#467 Toxicity of the polyamine analogue CI-1006 (N<sup>1</sup>, N<sup>11</sup>-diethylnorspermine) in rats following multiple injection or continuous intravenous infusion.** Graziano, M.J., Courtney, C.L., and Bergeron, R.J. *Dept. of Pathology and Experimental Toxicology, Parke-Davis Pharmaceutical Research, Ann Arbor, MI and Dept. of Medicinal Chemistry, University of Florida, Gainesville, FL.*

CI-1006 is a dysfunctional polyamine analogue that suppresses cell growth through depletion of endogenous intracellular polyamines. CI-1006 has in vivo activity in a number of murine and human tumor xenograft models when administered by multiple daily injections (3 times/day every 8 hours; TID dosing) or continuous infusion. To assess the preclinical toxicity of these two schedules, rats were given total daily doses of CI-1006 at 20, 40, 80, or 100 mg/kg (120, 240, 480, or 600 mg/m<sup>2</sup>) for 7 days by TID or continuous intravenous infusion (CI). All but one animal at 80 and 100 mg/kg either died or were sacrificed in moribund condition on days 3 to 7. Clinical signs included hypoactivity, irritability, prostration, hypothermia, ptosis, chromatocryorrhea, tremors and convulsions. Convulsions were not temporally associated with dosing and occurred just prior to death. No deaths or significant clinical signs were observed at 20 or 40 mg/kg. Weight gain was decreased in the 20 and 40 mg/kg males on the CI schedule. Bone marrow erythroid cells were decreased 32% to 62% at 40 mg/kg on the TID schedule and at 20 and 40 mg/kg on the CI schedule. Serum glucose and urea nitrogen were increased by more than 2-fold at 40 mg/kg on both schedules. Serum phosphorus and creatinine were also increased up to 2.5-fold at 40 mg/kg on the CI schedule. The same clinical biochemistry changes, but of a greater magnitude, were seen in the 80 and 100 mg/kg animals sacrificed in moribund condition. Renal tubular necrosis and/or degeneration were observed in one animal at 20 mg/kg on each schedule and almost all animals at  $\geq$ 40 mg/kg. The severity of the renal lesions was dose-related and was minimal at 20 mg/kg. Tissue concentrations of drug were generally highest in the kidney, followed in decreasing order by liver, small intestine, heart, and brain. In some animals, CI-1006 concentrations in the liver were equal to or greater than the kidney. In conclusion, there was no difference in the toxicity of CI-1006 when administered intravenously to rats by TID dosing or CI. The kidney was identified as the target organ for both dosing regimens. Only minimal effects were noted at 20 mg/kg (120 mg/m<sup>2</sup>).

**#468 Possible links between the products of oil fires and increased brain tumors in Kuwait.** Hayat, Lamya H. J. *Associate Prof. Biochemistry-Biological Sc. Dept. Faculty of Sc. Kuwait University.*

The burning of the 736 oil fields by the Iraqi invaders in 1991 produced 15,000 Km<sup>2</sup> of smoke containing 3000 tons of mono- & poly-aromatic hydrocarbons (MAH & PAH), and soluble Ni & V salts. The people in Kuwait were inhaling the air saturated with the above particulates for 9 months. MAH comprise 16.4% of the Kuwait #2-diesel. Inhalation of toluene was correlated with lipid concentration in the brain. It inhibits cytochrome P450 metabolizing enzymes which results in reduced metabolic detoxification of xenobiotics which may exacerbate carcinogenic effects of Benzo (a) pyrene (Bap) and delay the reduction of vanadate to the nontoxic tetravalent form of vanadyl. This will lead to inhibition of enzymes like Ca<sup>2+</sup>-ATPase, adenylate kinase... and consequently cause the toxicity of the cells.

Examining actual brain tumors collected after operation on patients exposed to the fumes of the blazed oil wells (1991-1995) or the brain tumors collected between 1996-1998, which represent an exposure to the

deposited products of the blazed oil wells, showed increased Ni & V in malignant relative to benign tumor brain tissue compared to the control. The trace element determination was done using inductively coupled plasma (ICP).

It was reported and proved that through inhalation elements levels is elevated in the blood. V & Ni have been proven definitely to exist as vanadyl and nickel porphyrins in crude oils. Accordingly it is concluded that these heavy metals overcome the blood brain barrier by possible replacement of the iron of the heme group of the blood supply to the tissue affected.

Oral consumption of trace elements is another route to elevate their levels. Locally grown samples of fruits and vegetables collected 6 months after the start of oil well fires, showed increased levels of Ni and V.

In 1997 a study of % frequency of PAH's occurrence in food commodities illustrated that phenanthrene (ph) has the highest % occurrence in the food basket tested. Ph can function as a precursor for cholesterol, which might help in promoting the tumor formation in individuals exposed to carcinogens. These factors and others might possibly explain the drastic increase in brain tumor rates after 1990 in Kuwait.

## POSTER SESSION 5 SECTION 1: MOLECULAR MARKERS AND TUMOR IMAGING: DIAGNOSIS, PROGRESSION, AND DRUG RESPONSES

**#469 High levels of biologically active vascular endothelial growth factor (VEGF) in a subpopulation of patients with pleural effusion (PE) or ascites.** Verheul, H.M.W., Hoekman, K., Jorna, A.S. and Pinedo, H.M. Department of Medical Oncology, Academic Hospital Vrije Universiteit Amsterdam, The Netherlands.

PE and ascites formation is a common problem in advanced stage cancer patients. In preclinical models, it has been demonstrated that VEGF plays a pivotal role in the accumulation of PE or ascites. In order to determine the role of VEGF in PE and ascites formation in patients (pts), we determined the VEGF concentration by Elisa (R&D Systems) and its biological activity in these fluids. In 50 pts (34 pts with PE and 16 pts with ascites), VEGF concentrations varied from 67–6245 pg/ml. No significant differences of VEGF concentrations between different diagnoses or between PE and ascites were detected, but the highest levels were measured in histologically proven malignant fluids. Biological activity of PE and ascites was determined in an endothelial cell (EC) proliferation assay with human umbilical vein endothelial cells. 30 of the 50 PE and ascites samples were biologically active, based on a 2–4 fold stimulation of EC-proliferation in 72 hours. VEGF concentrations were significantly higher in the biologically active samples compared to the 20 non-active samples (2215 versus 1051 pg/ml,  $p = 0.03$ ). In addition, 10 samples were co-incubated with a neutralizing antibody against VEGF (1  $\mu$ g/ml, R&D Systems) in the EC-proliferation assay. The antibody inhibited the stimulation of EC-proliferation maximally for 57%. Interestingly, a significant correlation ( $r = 0.7$ ,  $p < 0.05$ ) between the biological activity and the % inhibition of the neutralizing antibody was found, indicating that VEGF was mainly responsible for the EC-proliferation. Currently, we are studying the biological activity of PE and ascites in an *in vitro* permeability assay as well. In conclusion, one may expect that in a subpopulation of patients with high concentrations of biologically active PE- or ascitic-VEGF, this endothelial growth factor is responsible for the fluid accumulation. For these patients, anti-VEGF therapy should be investigated clinically.

**#470 K-ras codon 12 mutation and expression in a series of transplantable tumors of the mouse colon.** Thompson, M.J., O'Sullivan, M., Bibby, M.C. and Double, J.A. Clinical Oncology Unit, University of Bradford, West Yorkshire BD7 1DP.

The murine colorectal adenocarcinoma (MAC) tumour models consist of a series of mismatch proficient tumours having known angiogenic potential, chemotherapy profiles and genetic stability. This work represents the further characterization of this group of tumour models.

K-Ras is a membrane bound 21kD oncoprotein involved in a signal transduction pathway concerned with cell proliferation and differentiation. It is suggested that a K-ras mutation could be an early event in the carcinogenesis of colorectal adenocarcinomas. Ras mutations are detected in up to 50% of clinical colorectal tumours. Mutations of the Ras oncogene are thought to give a selective growth advantage and so play a role in carcinogenesis.

Ras expression was determined using immunohistochemistry in both tumours and normal tissues. SSCP & RFLP were used to determine the presence of mutations at codon 12, where approximately 45% of clinical K-ras mutations occur. DNA was extracted from nine MAC tumour models and restricted with BstNI following the PCR amplification of the codon 12 region. Restriction occurs in wild type DNA at codon 12 (5' CC TGG 3'). However, mutant DNA will not restrict. Two tumour models, the well differentiated MAC 30T and the poorly differentiated MAC 15A, were found

to contain mutations. When K-ras expression was examined in these models, MAC 30T exhibited membrane staining in a small proportion of cells and MAC 15A did not demonstrate any significant staining within the tumour. In normal murine colonic epithelial tissue, pronounced cytoplasmic K-ras expression was found in the more differentiated cells towards the tips of the villi, particularly on the luminal membrane of these cells. Of the more differentiated tumours, MAC 29 and 15 demonstrated membrane expression. MAC 26 and 13 showed both membrane and cytoplasmic staining, while membrane expression was restricted to the luminal surface in MAC 13. Poorly differentiated MAC 16 demonstrated membrane staining in limited areas of the tumour.

These tumour models will contribute to studies involving the control and manipulation of Ras expression. The MAC tumour series therefore represents a relevant and useful tool for the study of K-ras as an anti-tumour target.

This work was supported by War on Cancer.

**#471 A mutation (V104M) in the reduced folate carrier (RFC1) results in impaired methotrexate (MTX) transport and resistance but without cross resistance to DDATHF which is transported by the same carrier.** Zhao, Rongbao and Goldman, I. David, Albert Einstein College of Medicine, Comprehensive Cancer Center, Bronx, New York.

The carrier mediated transport of antifolates is a key determinant of cytotoxicity and resistance is often associated with altered RFC1 expression or kinetic properties. This laboratory has developed a panel of clonal cell lines resistant to MTX by virtue of a transport defect, each with a defined mutation(s) in RFC1. One such cell line, L1210-G2, selected with leucovorin as the folate substrate, was 30-fold resistance to MTX but was not significantly cross-resistant to the GARFT inhibitors DDATHF or LY309867. This disparity in resistance could be explained entirely on the basis of the mutation in RFC1 as established by transfection of the V104M carrier cDNA into an MTX-resistance cell line (MTX<sup>r</sup>A) which lacks functional RFC1 to obtain the MTX<sup>r</sup>A-V104M cell line. Influx of tritiated DDATHF, MTX, or leucovorin in the transfectant was increased by factors of 32, 4 and 6, respectively, as compared to the transport-null recipient. This was similar to the decreases in IC<sub>50</sub> by factors of 18 and 2, and EC<sub>50</sub> of 4, respectively. Hence, the mutated carrier had substantially more transport activity for DDATHF than for MTX or leucovorin as substrates. Of particular interest, preservation of steady-state levels of DDATHF substantially exceeded the preservation of influx. When cells were grown in leucovorin, the level of DDATHF accumulation after 3 days was the same in the L1210, L1210-G2 and the MTX<sup>r</sup>A-V104M cell lines. However, the endogenous folate pools were markedly decreased in the lines with the V104M carrier. With folic acid as the growth substrate, (folic acid is transported, largely, by an RFC1-independent pathway), DDATHF accumulation was decreased by ~40%, the folate pools only minimally decreased, and the IC<sub>50</sub> for DDATHF was increased in the cell lines carrying the mutant carrier.

Hence, preservation of DDATHF sensitivity in the MTX resistant cell lines is due to (1) partial and selective preservation of RFC1-mediated DDATHF transport activity, and (2) enhanced DDATHF polyglutamylation and DDATHF inhibitory activity at the target enzyme due to the accompanying marked decline in leucovorin transport resulting in low levels of competing tetrahydrofolate cofactors at enzyme sites within the cell. Hence, resistance to one antifolate, due to a loss of RFC1 activity, need not be accompanied by cross-resistance to another antifolate that utilizes the same carrier. This work was supported by Grant CA-39807 from the National Cancer Institute.

**#472 Ki-67 expression as proliferation index in surgically resected stage I and II non-small cell lung cancer (NSCLC) and its correlation with survival.** Huang C.H., Langer C.J., Liu S.C., Schilder R., Klein-Szantos A.J.P. Temple University/Fox Chase Cancer Center, Philadelphia PA.

Ki 67 is a nuclear antigen expressed in proliferating cells. Its usefulness as a prognostic marker has been reported in several types of cancer. In NSCLC there are controversial reports regarding its prognostic value. Nevertheless, proliferation index could be a useful tool in distinguishing cases with worse prognosis, which would be clinically relevant in making decisions regarding adjuvant treatment. We studied Ki 67 expression of the tumor by immunohistochemistry using MIB-1 monoclonal antibody and correlated it with survival. 89 cases of surgically resected stage I and II NSCLC from 1990 to 1992 were obtained from the Fox Chase Cancer Center tumor registry. 67 patients (pts) had stage I NSCLC and 22 pts had stage II NSCLC. 29 pts had squamous cell, 45 had adenocarcinoma and 15 had other histologic subtypes. 56 were male and 33 were female. 39 pts were 70 years old (yo.) or younger and 50 pts were above 70 yo. 38 pts are alive and 51 are deceased. We counted 500 cells in five 100x high power fields using a light-microscope and calculated a MIB-1 index as a percentage of the positive staining cells. Overall the group had 21.6% mean positive staining cells (range 0 to 68%). In stage I NSCLC the MIB-1 index was 22% and 19% in stage II ( $p = 0.6$ ). In squamous cell it was 27%, 17% in adenocarcinoma and 24% in other subtypes ( $p = 0.001$ ). Male pts had 23.6% and female pts had 18% ( $p = 0.08$ ). In pts 70 yo or younger it was 24.4% and pts above 70 yo. was 19.4% ( $p = 0.043$ ). In alive pts it was 19.7% and 22.9% in deceased pts ( $p = 0.07$ ). In the subgroup of 45 pts



with adenocarcinoma, MIB-1 Index in 17 pts who are alive was 15% and 28 pts who are deceased was 27% ( $p = 0.0036$ ). There was no statistical difference in other histologic subtypes. We conclude that squamous cell carcinoma and other subtypes have a higher proliferation Index by Ki 67 compared with adenocarcinoma subtype. Ki 67 expression appears to predict progression in the adenocarcinoma subtype.

**#473 Ki-67 Nuclear Antigen and P53 protein correlate with squamous cell carcinoma (SSC) recurrence.** Mohamed Abdalla M.D., Sadr J Alrawi M.D., Norman M Rowe M.D., Koff Abbensetts M.D., Christian Oreda M.D., Anthony J Acinapura M.D., Joseph N Cunningham M.D. and Ramanathan Raju M.D.

**PURPOSE:** Tumor growth depends on a balance between cellular proliferation and cellular death, including apoptosis. The purpose of this study was to investigate the relationship between these two processes in recurrent SSC.

**METHODS:** Tissue samples from four resected SSC cases along with a sample from a recurrence in one patient 12 months after resection (the remaining patients did not have recurrence of disease; follow up 18-36 months). The five samples were immunohistochemically stained with monoclonal antibodies for the proliferative antigen Ki-67, tumor suppressor protein p53 and the apoptotic marker protein BCL-2. The percentages of positive staining cells on representative slides of each sample were determined via optical densitometry.

**RESULTS:** There was on average 37% expression of Ki-67 in the basal skin layer of the patients with no recurrence whereas there was 75% expression in all skin layers in the patient with recurrence. There was minimal expression of p53 in the basal layer of the first resected specimen of the patient who eventually developed recurrence. The p53 expression was much higher (95%) and present in all layers of the skin after recurrence. This finding was similar to those samples with no recurrence.

**CONCLUSIONS:** This study demonstrates for the first time that the proliferative protein Ki-67 is upregulated while the tumor suppressor protein p53 is initially downregulated in SSC which may recur. P53 expression increases after the recurrence. These findings may help identify those patients at risk for recurrence and benefit from a more aggressive surgical approach.

**#474  $\beta$ -tubulin mutations in serum DNA of non-small-cell lung cancer patients receiving first or second line chemotherapy.** Mariano Monzó, Aurora O'Brate, José Miguel Sánchez, Mónica Guillot, José Javier Sánchez, Carmen Aracil, Rafael Rosell. Hospital Germans Trias i Pujol, Badalona, Barcelona, Spain.

Based on our previous experience, we thought that amino acid substitutions of GTP tubulin binding sites could play a role in drug resistance. We have studied the feasibility of detecting tubulin mutations in the circulation of patients with advanced non-small-cell lung cancer (NSCLC). We hypothesized that tubulin genotypes could be found in non-responding patients. We extracted DNA from the peripheral blood serum of 30 NSCLC patients. Two different sets of primers were designed for the PCR assay to amplify GTP binding sites at exon 4. We carried out sequence comparisons using BLAST. (<http://www.ncbi.nlm.nih.gov>).  $\beta$ -tubulin mutations were found in 10/30 patients. The median amount of DNA was 48.5 (35-139) for responding patients and 117 (35-289) for non-responders ( $P = 0.04$ ). Tubulin mutations were found in 8/21 (38%) Stage I, IIIB and IV patients and in 2/9 Stage I-IIIA patients who also had circulating DNA. Overall median survival time was 5.4 months (95% CI, 2.4-8.5) for patients with mutations and 9 months (95% CI, 4.3-13.7) for patients without mutations. Five additional patients had tubulin mutations detected in a second DNA analysis, three of whom received second- and third-line chemotherapy. These results suggest that circulating NSCLC DNA is easily detected and could serve for screening genetic abnormalities. In conclusion, in the future, sequentially checking serum DNA could be useful in ruling out circulating micrometastases, and drug resistant genotyping assessment in DNA could lead to selecting second line chemotherapy.

**#475 Elevated egression of cGMP from transformed cells—Another form of acquired resistance?** G. Sager, E. Boadu, E. Sundkvist, R. Jaeger and A. Ørbo. Dept. of Pharmacology and Dept. of Pathology, Institute of Medical Biology, Medical Faculty, University of Tromsø, N-9037 Tromsø, Norway.

Several clinical studies have revealed elevated levels of cGMP in extracellular fluids from patients with various types of malignancies and increase in the daily urinary excretion of cGMP appears to predict relapse after treatment of certain cancer types. In vitro studies have shown that it is possible to mimic the growing tumor bulk in vivo since the extracellular cGMP levels and cell densities increase in parallel. Furthermore, it is a distinct difference in this cell-density effect between normal and transformed cells. Our hypothesis is that increased cellular efflux from malignant cells is a type of acquired resistance against cGMP's ability to modulate growth. The present work was performed to characterize the cGMP transporter as a potential target for drug development. The cGMP pump is a glycoprotein of about 85 kDa (monomeric form). Both transport and ATPase activity are restored when the membrane transport protein is reconstituted in proteoliposomes. The transporter is energized by an

ATPase which has characteristics similar to that of P-glycoprotein. It is an anion transporter inhibited by probenecid, but not by LTC<sub>4</sub> (a MRP-substrate) or cAMP. The ability of glutathione S-conjugates to inhibit cGMP efflux suggests that this is a type of GS-X pump. The well-known membrane transport modulators verapamil, progesterone and forskolin showed a concentration-dependent inhibition. The transporter was inhibited by cGMP analogues in a concentration-dependent manner and discriminated between stereoisomers. These results make it valid to conclude that the cGMP transporter is a potential target for drug development.

**#476 Methods for in vitro genotyping of drug-sensitive and drug-resistant subsets of primary tumors.** Fruehauf JP, Shahbahrami B, Tee L, Yeh T, Torres C, Mechetner M. Oncotech, Inc. Irvine, CA.

Drug discovery methods have evolved from empirical screening models to targeted therapeutics. However, the complex genomic response to rationally designed agents is beyond the horizon of most screening processes. We are developing methods to characterize the genomic response of primary tumors to various classes of anti-tumor agents. Our focus has been on the selection of malignant cells from the tumor background after in vitro drug exposure in order to clarify the source of mRNA signals detected on gene arrays. Towards this end, we developed cell-sorting techniques that enable us to purify tumor cells from the stromal background using flow cytometry. Freshly resected tumors are initially processed into fixed sections and cell suspensions. Suspensions are cultured in non-adherent cytophobic plates in the presence of selected anticancer agents for varying lengths of time. Tissue sections are analyzed by immunohistochemical staining with various monoclonal antibodies that identify tumor-specific markers. At set intervals, tissue culture aliquots are removed from the drug exposure environment, washed, and stained with fluorescently conjugated antibodies for flow cytometric analysis. Cells are also labeled with annexin V to identify cells undergoing apoptosis. Based on the specificity of double labeling for malignant cells and cells undergoing apoptosis, two populations of malignant cells are sorted: drug sensitive and drug resistant. Sorting also serves to eliminate the non-malignant components present in the primary tissue culture. Sensitive and resistant cells from the same genetic background are then compared by extracting and amplifying mRNA, which is evaluated by micro-array display. Kinetics of mRNA expression after drug exposure are evaluated and informatics studies relating these changes to drug sensitivity or resistance are carried out.

**#477 Identification of genes associated with human glioma tumorigenesis.** Kroes, R.A., Jastrow, A., McLone, M., Kersy, D., Hawkins, E., Sweeley, C., Yamamoto, H., and Moskal, J.R. Chicago Institute of Neurosurgery and Neuroresearch, Chicago, IL 60614.

Current therapies for the treatment of glioblastoma multiforme (GBM) are ineffective, in that 80% of patients die within the first year following diagnosis. To identify novel therapeutic targets, a 2-step strategy coupling DDRT-PCR with reverse Northern screening was developed and differentially expressed genes in malignant gliomas were characterized. A malignant human glioma cell line, U373MG, and primary cultures of human fetal astrocytes were used for the DDRT-PCR analysis and freshly resected specimens of human GBM and normal human brain were used for the reverse Northern analyses. Utilizing this strategy, we identified a panel of genes that have clear-cut diagnostic value, are likely to play a role in glioma development and should be further evaluated for their therapeutic potential in the treatment of brain tumors. Among the genes identified in this panel was the *dek* oncogene. *dek* encodes a nuclear protein that has been found as the N-terminus of several fusion proteins in specific subtypes of acute myeloid leukemia. Its carboxy-terminus can partially reverse the transformation-prone phenotype of patients with ataxia-telangiectasia. *dek* has also been shown to be an autoantigen in juvenile rheumatoid arthritis. However, the function of *dek* in brain tumors is unknown. Northern analyses revealed that *dek* is limited to brain tumors of glial origin since it is expressed at very high levels in most glioma cell lines, but not in most neuroblastoma cell lines. Moreover, *dek* mRNA is robustly expressed in primary high grade gliomas, but is expressed at low levels in most meningiomas, brain metastases and normal brain. *dek* also can function as a DNA binding/transcription factor via interactions at TG-rich peri-*o*s (pets) elements (5'-TTGGTCAGGG-3') in genomic DNA. EMSA analysis demonstrated sequence-specific protein binding to radiolabeled pets sequences in glioma cell extracts. Additionally, CAT-reporter gene transfection analyses revealed that single and multimerized pets element(s) significantly enhanced SV40-mediated transcription in U373MG glioma cells. The fact that *dek* functions as a transcriptional enhancer in tumors of glial origin suggests that it is important in regulating glioma-associated gene expression and provides a potential therapeutic target for the treatment of gliomas.

**#478 Differential Increase in Copy Number For PIK3CA in Non-Small Cell Lung Cancers.** Massion PP, Kuo W-L, Treseler PA, Basas J, Riedell L, Gray JW. Cancer Genetic Program, UCSF Cancer Research Center, San Francisco, California 94143 (PPM, W-LK, JB, LR, JWG) and Department of Pathology, UCSF, San Francisco, California 94143 (PAT).

Amplification of the alpha catalytic subunit of phosphatidylinositol 3 kinase (PIK3CA) which localizes to chromosome 3q28 has been implicated as an

early oncogenic event in ovarian cancer. Analyses using comparative genomic hybridization have shown that 3q26 also is amplified in non-small cell lung cancer. Thus, we are now evaluating whether amplification of *PIK3CA* is involved in non-small cell lung cancer development. To test this, we have applied fluorescence in situ hybridization (FISH) to tissue microarrays to enable efficient assessment of *PIK3CA* copy number relative to that for *RhoA*, a reference gene located on 3p. Fifty-one squamous cell carcinomas and 42 adenocarcinomas of the lung were prepared as tissue arrays using cores taken from formalin-fixed paraffin embedded tissues. Five micron-thin sections were cut from the tissue arrays, deparaffinized, dehydrated and hybridized with a BAC clone for *PIK3CA* directly labeled with Cy3 and with a BAC clone for *RhoA* indirectly labeled with digoxigenin and stained with an anti-digoxigenin FITC-labeled antibody. We found that the *PIK3CA/RhoA* copy number ratio was greater than 2 in 29 of 51 squamous carcinomas and greater than 4 in 9/51 of squamous carcinomas. In contrast, none of the 42 of adenocarcinomas showed a ratio greater than 2. Morphological differences could not be found between tumors with increased copy number of the *PIK3CA* from those without. This data suggests that *PIK3CA* may be involved in the development of squamous cell carcinomas but not adenocarcinomas of the lung. Further investigations on P13 Kinase pathway genes are under way to determine the functional significance of the *PIK3CA* copy number increase in lung cancer development and progression.

(Supported in part by a Parker B. Francis Fellowship)

**#480 Role of progesterone receptor as a prognostic molecular marker for gall bladder carcinoma.** Vij, U., Bhaskaran, V., Sahani, P. and Nundi, S. Departments of *Reproductive Biology and Gastrointestinal Surgery*, All India Institute of Medical Sciences, Ansari Nagar, New Delhi-110029.

In order to improve the prognosis of carcinoma gall bladder disease (CaGB) the search for a more rational and sensitive molecular marker, based on better understanding of its pathology is required. As both CaGB and cholelithiasis are more common in female, ovarian sex hormones may play a crucial role in the genesis of gall bladder disease-through their specific receptors at the molecular level. Since, the expression of progesterone receptor (PR) is dependent on estrogen interplay for its genesis, evaluation of PR appeared to be a better molecular marker which can be implicated for the prognosis of CaGB. In this study PR expression was assessed in 21 CaGB patients 20 gall stone patients and in 5 patients who had undergone incidental cholecystectomy. PR was estimated by enzyme immunoassay (EIA) using monoclonal antibodies. The results revealed that 72% of the CaGB patients and only 33% of the gall stone patients expressed PR while in none of the normal gall bladders, PR was above the sensitivity of the detective system which was 1.7 fmol/mg cytosol protein. This indicated a specific role of progesterone and PR in CaGB. In a follow up study, PR negative and PR positive CaGB patients were evaluated for the disease free survival. In the PR positive patients the survival was significantly better than in PR negative patients being 301 days and 52 days respectively. The results suggested that PR may be involved in the pathophysiology of gall bladder carcinoma and appears to have strong clinical implication as a prognostic marker for the CaGB disease.

**#481 Polymorphisms in the human 5 $\alpha$ -reductase gene and breast cancer.** Scorilas, A., Bharu, B., Gial, M., Diamandis, E.P. Department of Pathology and Laboratory Medicine, Mount Sinai Hospital and Department of Laboratory Medicine and Pathobiology, University of Toronto, Toronto, Ontario, M5G 1X5, Canada [A.S., B.B., E.P.D.], Department of Gynecologic Oncology, Institute of Obstetrics and Gynecology, University of Turin, Turin, 10128, Italy [MG].

There is an increasing amount of evidence that androgens play a significant role in the development and progression of breast cancer. The SRD5A2 (5 $\alpha$ -reductase) gene harbors two frequent polymorphic sites, one in the coding region, at codon 89 of exon 1, where valine is substituted by leucine (V89L) and the other in the 3' untranslated region where a variable number of dinucleotide TA repeat lengths exists. Both polymorphisms are known to alter the activity of this enzyme which is expressed in androgen dependent tissues and it catalyses the reduction of testosterone to its more bioactive form dehydrotestosterone which transactivates a number of genes. The aim of this study was to evaluate the role of these polymorphisms in breast cancer prognosis. We examined 144 sporadic breast tumors from Italian patients as well as the whole blood of 70 women without cancer for the V89L and TA polymorphisms by sequence and fragment analysis, respectively. Tumor extract prostate-specific antigen concentration as well as a number of well-established clinical and pathological parameters were evaluated. The results showed that TA(0) repeats were found in tumors with VV, LL and VL genotypes. TA(9) repeats were only found in VV homozygotes and were totally absent from either LL homozygotes or VL heterozygotes. PSA expression was significantly elevated in tumors with VV genotype. We found that the LL genotype was also associated with earlier onset and more aggressive forms of breast cancer. The presence of LL alleles in breast tumors was associated with earlier onset and shorter disease-free (RR = 2.65; P = 0.013) and overall survival (RR = 3.06; P = 0.014) rates. Patients with long TA repeats and VV genotype appeared to have more favorable prognosis. We are currently pursuing the significance of the above polymorphisms in breast cancer susceptibility.

**#482 Molecular characterization, mapping, tissue expression and hormonal regulation of KLK-L2, a new member of the kallikrein gene family.** Yousef, G.M., Luo, L.Y., Black, M.H., Diamandis, E.P. Department of Pathology and Laboratory Medicine, Mount Sinai Hospital, Toronto, Ontario, Canada.

Since in rodents the kallikreins are represented by a large multi-gene family, the restriction of this family in humans to three genes is somewhat surprising. In an effort to identify new human kallikrein genes, we examined a genomic area of about 300 Kb on chromosome 19q13.3-q13.4, a region that contains most of the currently known kallikreins. By using the positional candidate approach, we were able to identify a new gene named KLK-L2 (for kallikrein like gene 2). Screening of human EST libraries allowed us to delineate the full genomic and cDNA structure of the new gene. KLK-L2 consists of 5 coding exons and 4 introns and has significant similarities to other members of the kallikrein multi-gene family. Homology studies suggest that the protein is likely secreted. KLK-L2 is expressed mainly in breast, brain and testis and to a lesser extent in many other tissues. We further demonstrated that KLK-L2 is up-regulated by estrogens and progestins in the breast cancer cell line BT-474. Based on information on other kallikrein genes that are localized in the same region (PSA, KLK2, zyme and NES1), we speculate that this gene may be involved in the pathogenesis and/or progression of prostate, breast and possibly other malignancies.

**#483 The ratio of human glandular kallikrein (hK2) to free PSA improves the discrimination between prostate cancer and benign prostatic hyperplasia in patients with moderately elevated total PSA levels.** Magklara A., Scorilas, A., Catalona, W.J., Diamandis E.P. Department of Pathology and Laboratory Medicine, Mount Sinai Hospital and Department of Laboratory Medicine and Pathobiology, University of Toronto, Toronto, Ontario, Canada. [A.M., A.S., E.P.D.], Division of Urologic Surgery, Department of Surgery, Washington University School of Medicine, St Louis, MO, USA. [C.W.G.]

Prostate specific antigen (PSA) is the most reliable tumor marker available and is widely used for the diagnosis and management of prostate cancer. Unfortunately, PSA cannot distinguish efficiently between benign and malignant disease of the prostate, especially within the range of 4-10  $\mu$ g/L. However, it has been established lately that the free/total PSA ratio is useful in discriminating between the two diseases within the diagnostic "gray-zone". Recent data indicate that human glandular kallikrein (hK2), a protein with high homology to PSA, may be an additional serum marker for the diagnosis and monitoring of prostate cancer. We undertook this study to investigate the potential role of hK2 in the discrimination between benign prostatic hyperplasia and prostate cancer patients. We analyzed 206 serum samples from men with histologically confirmed benign prostatic hyperplasia (BPH; N = 100) or prostatic carcinoma (CaP; N = 106) with total PSA in the range of 2.5-10  $\mu$ g/L. Total and free PSA and hK2 levels were measured with non-competitive immunological procedures. Statistical analysis was performed to investigate the potential utility of the various markers or their combinations in discriminating between BPH and CaP. Our results showed that the hK2 levels were not statistically different between the two groups of patients. There was a strong positive correlation between hK2 and free PSA levels in the whole population. hK2/free PSA ratio (AUC = 0.69) was stronger predictor of prostate cancer than the free/total PSA ratio (AUC = 0.64). At the level of 95% specificity, the hK2/free PSA ratio identified 30% of patients, with total PSA between 2.5-10  $\mu$ g/L and 25% of patients, with total PSA between 2.5-4.5  $\mu$ g/L.



who had cancer. The combination of the two ratios, though, was able to discriminate even better between BPH and CaP patients (AUC = 0.72). Our data suggest that hK2 in combination with free and total PSA can enhance the biochemical detection of prostate cancer in patients with moderately elevated total PSA levels. More specifically, the hK2/free PSA ratio appears to be valuable in identifying a subset of patients with total PSA between 2.5–4.5 µg/L who have high probability of cancer and who should be considered for biopsy.

**#484** The new kallikrein-like gene, *Protease/KLK-L1*, is expressed in prostate and breast tissues and is hormonally regulated. Yousef G.M., Obiezu C.O., Luo L.Y., Black M.H., Diamandis E.P. Department of Pathology and Laboratory Medicine, Mount Sinai Hospital, Toronto, Ontario, Canada.

By using the positional candidate gene approach, we were able to identify a novel serine protease gene that maps to chromosome 19q13.3–q13.4. Screening of ESTs allowed us to establish the expression of the gene and delineate its genomic organization (Genbank Accession # AF135023). We named this gene *KLK-L1*. Another group, by using a subtraction hybridization method, cloned the same gene and named it *protease* (Genbank Accession # AF113140 and AF113141). In this paper we describe the precise mapping and localization of the *protease-KLK-L1* gene between the known genes *KLK2* (human glandular kallikrein) and *zyme* (also known as *protease M/neurosin*). *Protease-KLK-L1* transcribes in the same direction as *zyme* and opposite to the direction of *KLK2* and *PSA* genes. Contrary to the initial impression, *protease-KLK-L1* is expressed at high levels not only in prostate tissue but also in testis, mammary gland, adrenals, uterus, thyroid and salivary glands. We have further demonstrated with *in-vitro* experiments with the breast carcinoma cell line BT-474 that this gene is expressed and that its expression is up-regulated by androgens and progestins. Based on information on other genes that are localized in the same region (prostate specific antigen, *KLK2*, *zyme* and normal epithelial cell-specific 1 gene), we speculate that *protease-KLK-L1* may be involved in the pathogenesis and/or progression of prostate, breast and possibly other malignancies.

**#485** Rapid *in vivo* monitoring of tumor response to chemotherapy, with sodium magnetic resonance imaging employing an inversion recovery pulse sequence, weights for intracellular sodium. Kline, Richard; Wu, Edward; Petrylak, Daniel; Szabolcs, Matthias; Christov, Konstantin; Weisfeldt, Myron; Cannon, Paul; Katz, Jose. Medicine & Radiology, Columbia U; Pathol., U. Minn; Surg. Oncol., U. Illinois, Chicago

*In vivo* assessment of antineoplastic activity is limited by the length of time required for a change in size in a measurable soft tissue lesion to occur. Apoptosis and related changes, however, can be observed within hours of exposure of cancer cells to antineoplastic agents. We describe an *in vivo* assay of chemotherapeutic efficacy based on these rapid changes, and using sodium (Na)-MRI. By employing an inversion recovery (IR) pulse sequence (25 msec inversion time), we can suppress sodium with long longitudinal relaxation times (T1)—e.g. primarily unbound. This technique (without use of reagents) weights the image for a responsive population of sodium nuclei which show increased signal following chemotherapy.

PC3 human prostate cancer cells were propagated in nude mice. Gradient-echo images (3D; 24 slices) were acquired on a high field (4.23 Tesla) whole body MRI (Hatch Center) employing a small quadrature birdcage r.f. coil (50 mm ID, Morris) and high strength gradient insert coil (30 mT/m, Bruker, G-33). Following control tumor image acquisition, Taxotere (40 mg/kg; n=5) or VP-16 Etoposide (1.2 mg/kg; n=7) was administered *i.v.* At 24 hrs, taxotere induced a 32% (p<0.001) and VP-16 a 38% (p<0.0005) increase in IR image intensity. Saline induced a 4% (NS) decrease (n=2). Comparable results were obtained with a different cell line (DU145), and a non-xenograph rat mammary tumor model (MNU Induced).

In cell culture experiments (PC3), we measured with ratometric ion sensing fluorescent dyes (Molecular Probes) the Taxotere (10 nM) and VP-16 etoposide (10 µg/ml) induced [Na], elevations (10–20 mM; SBFI/AM dye) and also [Ca], elevations (150 µM; Fura II/AM dye) starting at 2–6 hrs and peaking by 24 hrs. Ion responses occurred earlier than apoptotic markers (DNA fragmentation using fluorescent end-labelling; reorientation of membrane phosphatidylserine using annexin V/FITC conjugated antibody). Postmortem analysis (histology; *in situ* TUNEL assay, n=10 tumors) showed cancer cells had decreased mitotic figs in treated vs untreated tumors (2.2 vs 8.6/field; p<0.0001). Mitotic suppression correlated with increased IR image intensity for individual tumors (p<0.02). Central necrosis and fluid were dark on IR image, while enhanced image intensity correlated with active apoptosis, where cells, as shown, presumably have elevated [Na].

**#486** Two-photon microscopy as a useful tool for elucidating the mode of action of novel potential cancer therapeutics. Navara, C.S. and Uckun, F.M. Departments of Experimental Oncology and Drug Discovery Program Hughes Institute, St. Paul, MN 55113.

Multiphoton microscopy allows us to follow specific cellular structures (i.e. nuclei, mitochondria, and the plasma membrane) in a high resolution three dimensional and time resolved fashion. We have used multiphoton confocal microscopy to evaluate the cellular effects of potential cancer

therapeutics. Cancer cells were plated onto coverslips and labeled with either the vital DNA dye Hoechst to image the nuclei and chromosomes or the lipid dye DiI to label the plasma membrane. Both of these dyes can be imaged with several sections without affecting cell viability as assessed by cell motility and the ability to undergo mitosis and cytokinesis. We have used this technology to show that one compound (DDE131) rapidly induces in cancer cell lines the hallmarks of apoptosis; DNA hypercondensation, nuclear fragmentation and rapid membrane blebbing. In a leukemic cell line these changes take place within 20 minutes of treatment. In contrast to the very dynamic effects of DDE131 another compound (DDE061) affects breast cancer cells in a strikingly different fashion. After treatment cells lose membrane structures such as membrane ruffles and filopodia eventually rounding up on the coverslip. These initial changes are not characteristic of apoptosis (no immediate effect is observed on the DNA) but do later induce apoptosis in treated cells.

**#487** Magnetic resonance spectroscopy studies of ifosfamide *in vivo*. Payne GS, Pinkerton CR, Leach MO. CRC Clinical Magnetic Resonance Research Group and Paediatric Oncology Unit, Institute of Cancer Research and Royal Marsden Hospital, Sutton; Surrey, UK.

**Introduction.** The structural isomer of cyclophosphamide, ifosfamide, is widely used in the treatment of sarcomas and a variety of paediatric cancers. Information regarding individual variation in the hepatic metabolism of this drug to active and inactive forms is of importance in understanding both normal organ toxicity and antitumour activity. Ifosfamide and its metabolites have previously been studied *in vitro* using MRS and the drug has been detected *in vivo* in rats.

**Aim of study.** To detect ifosfamide and its metabolites *in vivo* during infusions of the drug in patients receiving combination chemotherapy.

**Method.** Unlocalised spectra were acquired using a 5.12 ms BIR4 45 degree adiabatic pulse and a 8 cm 31P surface coil over the liver. Most spectra were acquired with 1024 acquisitions at TR = 1 s (ie a total of 17 minutes). Later studies incorporated 1H decoupling which had been developed *in vitro* using a 25 ml sphere containing 1g ifosfamide. Optimum decoupling was achieved for a 1H frequency offset of (-150 Hz) relative to that of water. With this offset a B1 decoupling field of 100 Hz was sufficient to yield good decoupling and an amplitude of enhancement of a factor of 4 was achieved.

**Results.** To date, 8 studies have been performed on 5 patients, mainly children and young adults. They were receiving infusional doses of ifosfamide of between 1200 and 5700 mg. Peaks at the position of ifosfamide (18.4 ppm relative to Pcr) were detected in 5 studies. In one spectrum there was also a peak at the position of the metabolite carboxy ifosfamide (21.5 ppm from Pcr).

**Conclusions.** These preliminary observations indicate that it is feasible to detect this drug *in vivo* in liver at conventional dose administration.

**#488** Tracking and correlation of adenovirus and adeno associated virus with stealth and non-stealth iron oxide MR contrast agents after transvascular delivery to brain. Neuweil, Edward A., Pagel, Michael A., McCown, Thomas, and Muldoon, Leslie L., Oregon Health Sciences University, and University of North Carolina.

**Introduction:** Transvascular delivery of adenovirus or adeno-associated virus (AAV) using osmotic disruption of the blood-brain barrier (BBB), may provide a mechanism for global delivery to the brain or to intracerebral tumors. However, the extent of delivery of virus-mediated gene expression cannot currently be determined in live animals. We investigated the localization and distribution of adenovirus and AAV in normal rat brain after transvascular delivery and evaluated whether MR contrast agents consisting of viral-sized stealth and non-stealth iron particles (Combidex & Feridex) could be used to demonstrate virus delivery (AJNR, 20:217–222, 1999). **Methods:** Osmotic BBB disruption was performed in normal rats by intracarotid infusion of hyperosmotic mannitol. Iron particle delivery was assessed with MR imaging, iron histochemistry, and electron microscopy (EM). Virus delivery was assessed by fluorescence microscopy of AAV virions labeled with Cy3 or immunocytochemistry for beta-galactosidase. **Results:** Within 2 hr after delivery of Cy3-labelled AAV virions across the BBB, fluorescence was detected in neuronal cells throughout the disrupted hemisphere. In contrast, after delivery of adenovirus, expression of beta-galactosidase was found primarily in perivascular glial cells. When assessing delivery of the stealth Combidex iron particles, iron histochemistry and EM showed the iron intracellularly in neurons in the disrupted hemisphere. With the non-stealth iron Feridex particles, iron histochemistry was detected in capillaries of the disrupted hemisphere, and EM localized the iron particles between the capillary endothelial cells and the basal lamina. **Conclusion:** The pattern of delivery of Feridex particles seems to correlate with Adenovirus, while the Combidex particles correlate with AAV, although no difference was detected between the two agents at the level of whole brain MR imaging.

**#489** Assessment of ovarian cancer treatment response using a Hypoxic Marker: <sup>99m</sup>Tc-EC-NIM. Yang, David J., Kim, Edmund E., Liu, Chun-Wei, Yu, Dong-Fang and Podoloff, Donald A. The University of Texas MD Anderson Cancer Center.

**Alms:** To radiosynthesize a  $^{99m}\text{Tc}$ -ethylenedicycysteine-nitroimidazole ( $^{99m}\text{Tc}$ -EC-NIM) and non-invasively identify the diagnostic potential in tumor-bearing animal models with  $^{99m}\text{Tc}$ -EC-NIM by planar scintigraphy before and after chemotherapy. **Methods:** Scintigraphic images, using a gamma camera equipped with low-energy, parallel-hole collimator, were obtained 0.5, 1, 2 and 4 h ( $n = 2/\text{time interval}$ ) following i.v. injection of 100  $\mu\text{Ci}$  of  $^{99m}\text{Tc}$ -EC-NIM. To ascertain whether the  $^{99m}\text{Tc}$ -EC-NIM uptake altered after chemotherapy, ten mice will be treated with paclitaxel (40 mg/kg, single injection, iv). On day 5,  $^{99m}\text{Tc}$ -EC-NIM was administered to the mice and planar imaging was conducted at 2 h. Computer outlined region of interest (ROI) was used to measure tumor to nontumor tissue ratios. Intratumoral  $\text{pO}_2$  measurements were performed using the Eppendorf computerized histographic system. Twenty to twenty-five  $\text{pO}_2$  measurements along each of two to three linear tracks were performed at 0.4 mm intervals on each tumor (40–75 measurements total). **Results:** ROI indicated that there was a marked difference of tumor/background ratios at pre- and post-paclitaxel treatment of ovarian tumors with  $^{99m}\text{Tc}$ -EC-NIM uptake ( $4.4 \pm 0.27$  vs.  $2.8 \pm 0.03$ ). Tumor oxygen tension of tumors was measured to be 3–6 mmHg compared to 40–60 mmHg of normal tissue at the tumor volume of 0.8–1.0 cm. Histopathology findings revealed that extensive necrosis was observed after paclitaxel treatment. The findings suggest that tumor hypoxia may be an important determinant in the treatment of ovarian cancer.

**#490 Dynamic contrast enhanced MR imaging in the evaluation of antiangiogenesis therapy.** Padhani Anwar, Hayes Carmel, Judson Ian, Workman Paul, Langecker Peter, Leach Martin, Husband Janet. *CRC Magnetic Resonance Research Group, Clinical Pharmacology and Centre for Cancer Therapeutics, Institute of Cancer Research and The Royal Marsden NHS Trust, London.*

**Purpose:** To evaluate the dose-related effects of an antiangiogenic compound (SU5416) on tumour permeability in patients with metastatic solid tumours, using quantitative contrast enhanced MR techniques.

**Methods:** SU5416 (2-[3-[2,4-dimethylpyrrol-5-yl)methylidene]-2-indolinone), a potent inhibitor of vascular endothelial growth factor (VEGF) signalling is being evaluated in a phase I dose-escalation trial in patients with metastatic solid tumours. Thirteen patients receiving escalating doses twice weekly (28 cycles; dose 48–145 mg/m<sup>2</sup>) have been evaluated to date. Accrual is ongoing. Quantitative 5 slice dynamic contrast-enhanced turbo-FLASH MR imaging was performed following the bolus administration of intravenous Gd-DTPA. Examinations were performed before treatment, 2–3 hours after first dose, at 2–4 weeks and then as required. Serial measurements of tumour capillary permeability, extracellular leakage space and Gd-DTPA accumulation were compared using histogram analysis and correlated with clinical response.

**Results:** Forty MR examinations have been performed in 13 patients (9F: 4M), median age 49 years old (range, 25–74 yrs.). In five of eight patients with progressive disease, a significant increase in permeability from baseline was observed with no change in two (median increase 20%; range, 8–93%). In one patient with alveolar soft part sarcoma, the tumour permeability could not be computed because of tumour hypervascularity. In four of five cases with tumour stabilisation, a decrease in permeability was seen (median decrease 27%; range, 14–46%) with one patient showing no change from baseline ( $p = 0.006$ ). Four of these patients also showed a decrease in leakage space (median 16%; range, 3–21%) and tissue Gd-DTPA concentration (median 11%; range, 6–14%). Permeability decreases in stable patients were observed even at the lowest dose of SU5416 (48 mg/m<sup>2</sup>).

**Conclusions:** Tissue permeability to Gd-DTPA measured by MRI can be used to quantify the effects of anti-VEGF inhibitors on tumour vascular permeability. Findings to date suggest that permeability changes correlate with clinical response.

**Acknowledgement:** The support of The Cancer Research Campaign, UK is gratefully acknowledged.

**#491 Development of novel pharmacokinetic and pharmacodynamic technologies for phase I clinical trials: The UK CRC experience and future plans.** Workman Paul, Aboagye Eric, Burtles Sally, Griffiths John, Leach Martin, Maxwell Ross, McSheehy Paul, Price Pat and Verdon Veronica. *CRC Pharmacokinetic/Pharmacodynamic Technologies Group, \*CRC Centre for Cancer Therapeutics, ICR, Sutton, Surrey, UK.*

As we move into the era of clinical evaluation of molecular therapeutics that target specific oncogenic molecular abnormalities in signal transduction, cell cycle, apoptosis and angiogenesis, there is a clear and urgent need to put in place assays that can answer specific questions about the pharmacokinetic and pharmacodynamic effects achieved. Our Working Group has been established under the auspices of the CRC Phase I/II Clinical Trials/New Agents Committee to ensure that novel technologies and assays are available in a timely way and used appropriately. Systemic pharmacokinetics and metabolism are generally well described by techniques such as HPLC-UV and LC-MS-MS. However, there is a need for more information on tissue distribution (in Phase I) and this can be provided by surgically non-invasive PET and MR imaging methods. PET may

also be useful when carried out in a clinical 'Pre-Phase I' setting, an example being the CRC study of DACA (Harte et al., Proc. 9<sup>th</sup> NCI-EORTC meeting, pg 50, #167, 1996).

Both PET and MR studies will be carried out in the clinical evaluation of SAR 4554, a nitroimidazole marker which labels hypoxic tumour cells. Of particular importance are methods that provide information on mechanism of action and proof of principle. Early information on whether the intended molecular target or biochemical target is being inhibited and whether the desired biological effect (anti-proliferation, apoptosis, anti-angiogenesis) is being achieved are of particular value. PET and MR methods are being used to investigate such effects as combretastatin A4 affecting tumour blood flow and AG337 inhibiting thymidylate synthase.

Although non-invasive imaging studies are preferred, most molecular biological readouts of drug effect will require tumour biopsies or analysis of surrogate normal tissues such as peripheral blood lymphocytes. It is important that DNA microarray technology is evaluated in Phase I trials because of the rich database that can be established for immediate and future use. A variety of molecular readouts are being employed in the Phase I evaluation of 17-allylamino 17-demethoxy geldanamycin, an agent that depletes oncogenic kinase through specific inhibition of Hsp 90.

**#492 Treatment of colorectal cancer: The challenge of perioperative blood transfusion and postoperative infectious complications.** Nielsen, Hans J, Christensen, Ib J, Myrner T. *Dept. of Surgical Gastroenterology, Hvidovre University Hospital, and The Finsen Laboratory, State University Hospital, Copenhagen, Denmark.*

**Background:** Cancer growth related bioactive substances, such as VEGF, PAI-1, MPO, and histamine, are accumulated in blood components for transfusion. In addition, release of these substances are induced by E-coli LPS. We therefore evaluated the effect of perioperative blood component transfusion and development of postoperative infectious complications on recurrence and survival of patients operated for colorectal cancer. **Methods:** 720 consecutive patients undergoing elective operation were included in this prospective study. Of the patients 538 underwent curative resection, while 182 underwent palliative resection. Among 167 variables recorded, preoperative albumin, tumor location, tumor stage according to Dukes, intraoperative blood loss, perioperative blood transfusion, postoperative infectious complication development, recurrence, and survival were included. None of the patients received adjuvant treatment. Recurrence and survival data were separated into four groups: I) patients without blood transfusion and postoperative infections; II) patients receiving blood transfusion, but without postoperative infections; III) patients without blood transfusion, but developing postoperative infections; IV) patients receiving blood transfusion and subsequently developing postoperative infections. **Results:** Median observation time was 6.8 (5.7–7.9) years. In a survival analysis there was no statistical significant difference between groups I, II and III, while patients in group IV ( $n = 135$ ) had a poor prognosis ( $p = 0.0002$  vs. group I, II or III, respectively). Similarly, curative resected patients in group IV ( $n = 95$ ) had the highest risk of local and distant recurrence ( $p = 0.0013$ ). In a multivariate analysis the combination of perioperative blood component transfusion and subsequent development of postoperative infectious complications independently identified patients with reduced recurrence free as well as long term survival. **Conclusion:** When developing new adjuvant treatment regimens to patients with colorectal cancer it should be considered, that side-effects following operation may influence the risk of recurrence and reduce overall survival. Blood component transfusion and bacterial contamination may increase the levels of various cancer growth related bioactive substances, which may challenge the optimal therapeutic selectivity.

## SECTION 2: TELOMERASE AND GENE THERAPY-BASED TECHNOLOGY

**#493 Identification of genes activating and repressing the telomerase RNA gene promoter: Implications for genetic therapies.** Keith, W. Nicol., Islvan, Steven., Zhao, Jlanglin. *CRC Dept. of Medical Oncology, CRC Beatson Labs., Garscube Estate, Switchback Road, Bearsden, Glasgow G61 1BD, UK.*

Telomerase gives unlimited replicative capacity to cancer cells. Telomerase activity is due to the expression of two genes, the telomerase RNA component gene, hTR, and the protein component gene hTERT. hTR gene expression is activated during cancer progression. Therefore, the hTR gene promoter may be exploited in gene and transcription based therapeutics. This requires an understanding of the transcriptional regulation of the hTR promoter. **Methods:** Electrophoresis mobility shift assay (EMSA) were used to identify protein complexes binding to the hTR promoter. Mutagenesis of the hTR promoter and transient transfection analysis in cell lines were used to identify functional regulatory domains. Candidate genes were co-transfected with the hTR Luc-reporter construct to test their ability to modulate hTR promoter activity. **Results:** The hTR promoter contains a consensus sequence for the CCAAT-binding protein complex, NF-Y, as



identified by EMSA. Mutation of the CCAAT site abolished hTR promoter activity. The critical role for NF- $\kappa$ B in regulating the hTR gene was confirmed by co-transfection with a dominant negative mutant of NF- $\kappa$ B resulting in abolition of hTR promoter activity. The hTR promoter region contains 4 Sp1 motifs. Mutation of the Sp1.1 element increased activity of the hTR promoter by 4–5-fold suggesting this site may be the target for a repressor molecule. Mutation of all 4 Sp1 sites abolishes the ability of the Sp1 transcription factor to stimulate promoter activity on co-transfection, suggesting Sp1 is an activator of the hTR promoter requiring multiple Sp1 sites. In contrast, the Sp3 transcriptional modulator is a potent repressor of hTR promoter activity. Interestingly, co-transfection of the retinoblastoma gene, pRb, with the hTR promoter construct resulted in a 5–10 fold induction of promoter activity strongly supporting a role for pRb in the normal regulation of hTR expression. The identification of hTR transcription factor complexes offers direct targets for developing hTR inhibitory molecules. In addition, the hTR promoter may be used in gene therapy to target suicide genes to cancer cells.

**#494 Telomerase activity and hTERT mRNA expression in preinvasive bronchial lesions detected by LIFE-lung system.** Fujisawa, T., Shibuya, K., Baba, M., Saitoh, Y., Iizasa, T., Sekine, Y., Suzuki, M., Otsuji, M., Motohashi, S., Hoshino, H., Haga, Y., Yamaji, H., Hiroshima, K., and Ohwada, H. *Departments of Surgery and Pathology, Institute of Pulmonary Cancer Research, Chiba University School of Medicine, Chiba, Japan.*

**Background:** Telomerase activation is thought to be a critical event responsible for cell immortalization and carcinogenesis. Human telomerase catalytic subunit (hTERT) is correlated with telomerase activity. Most human tumors express telomerase activity, including lung cancer, but is undetectable in normal somatic cells except for proliferative cells of renewal tissues. **Aims:** To analyze telomerase activity and hTERT mRNA of preinvasive bronchial lesions using the biopsied specimens detected by fluorescence bronchoscopy (LIFE-lung system). **Methods:** Bronchial biopsy specimens obtained by fluorescence bronchoscopy were studied. The intensity of telomerase activity was analyzed by fluorescence-based TRAP method in 64 specimens (22 normal bronchial epithelium or bronchitis, 12 squamous metaplasia, 19 dysplasia and 11 squamous cell carcinoma), and the levels of hTERT mRNA were analyzed in 38 specimens (11 normal bronchial epithelium or bronchitis, 11 squamous metaplasia, 9 dysplasia and 7 squamous cell carcinoma) by real-time PCR. **Results:** When 21 units of telomerase activity (mean  $\pm$  2SD of normal bronchial epithelium or bronchitis) were evaluated as the cut off value for the practical application, none of 22 normal bronchial epithelium or bronchitis, 5 of 12 squamous metaplasia (42%), 5 of 19 dysplasia (32%) and all squamous cell carcinoma (100%) exhibited more than 21 units. Especially 2 dysplasias expressed strong telomerase activity similar to squamous cell carcinoma. The mean levels of hTERT mRNA in normal bronchial epithelium or bronchitis, squamous metaplasias, dysplasias and squamous cell carcinomas were  $1954 \pm 1640$  copies/ $\mu$ g total RNA,  $2384 \pm 1726$ ,  $3495 \pm 2592$  and  $6739 \pm 8111$ , respectively. Especially 2 dysplasias expressed strong hTERT mRNA expression similar to squamous cell carcinoma. **Conclusions:** A strong telomerase activity and elevated hTERT mRNA suggested cell immortalization in some of squamous dysplasias.

**#495 Is Small Cell Lung Cancer the Perfect Target for Anti-Telomerase Treatment?** Evans, T.R. Jeffrey, Sarvesvaran, Joseph, Golig, James J., Milroy, Robert, Kaye, Stanley B., Keith, W. Nicol. *CRC Dept. of Medical Oncology, CRC Beatson Labs., Gartcube Estate, Swilchback Road, Glasgow G61 1BD, UK.*

Small cell lung cancer is common in men and women, has a very poor prognosis, and is therefore a major cause of premature mortality. As such, any prospects for improved therapy are of great significance. The promise of telomerase as a therapeutic target is now close to realization with extremely encouraging preclinical studies aimed at the RNA component, (hTR), of telomerase. The rational integration of telomerase therapeutics into clinical trials will therefore require tumours to be well characterised for hTR expression. Despite the large number of cancer types now characterised for telomerase or telomerase component gene expression only a handful of small cell lung cancer samples have been analysed. Given the major clinical problem with treating SCLC, we specifically set out to address the issue of hTR expression in neuroendocrine tumours. Our study covers 91 pulmonary neuroendocrine tumours, (62 SCLC and 29 carcinoid tumours). hTR gene expression was analysed by RNA *in situ* hybridisation to tissue sections from formalin fixed, paraffin embedded tissue blocks. Immunohistochemical evaluation of p53 and BCL2 expression on serial sections used monoclonal antibodies DO7 (p53) and 124 (BCL2). 98% of SCLC had detectable levels of hTR gene expression. Interestingly, a high percentage of carcinoid tumours also express detectable levels of hTR although at a significantly lower frequency than SCLC (59%,  $\chi^2=25.52$ ,  $df=1$ ,  $p<0.01$ ). Carcinoid tumours are not associated with smoking and are also less aggressive in their biological behaviour than SCLC. Importantly, we compare hTR expression in this series to the well characterised biological targets for therapy, p53, (69%), and BCL2, (67%), and show hTR to be more frequently expressed. Therapies directed at the RNA component

of human telomerase are in active development and these data suggest that the telomerase RNA component may currently represent the best available candidate for targeted therapy in SCLC.

**#496 Inhibition of telomerase by tea catechins: A mechanism for tea anticancer and chemopreventive effects.** Naasani Imad and Tsuruo Takashi. *Cancer Chemotherapy Center, Japanese Foundation for Cancer Research, Kami-Ikebukuro, Toshima-ku, Tokyo 170-8455 [N. I., T. T.], and Institute of Molecular and Cellular Biosciences, University of Tokyo, Yayoi, Bunkyo-ku, Tokyo 113-0032 [N. I., T. T.], Japan.*

Maintenance of telomeres mainly by telomerase is essential for permitting unlimited proliferation of cancer cells. We have recently demonstrated that epigallocatechin gallate (EGCG), a major tea catechin, is a potent telomerase inhibitor that can induce progressive telomere shortening and senescence/crisis-like features in cancer cells after prolonged cultivation (Naasani et al, *BBRC*, 249, 391–396, 1998). Here we show that EGCG, even at a concentration comparable to the plasma levels of catechins after drinking a few cups of green tea (5  $\mu$ M), is still effective in inducing telomere shortening and senescence/crisis-like properties in the telomerase positive U937 leukemia cells. Meanwhile, EGCG was unable to induce similar effects on the telomerase negative osteosarcoma cells, Saos-2, and on normal human fetal fibroblast cells, confirming our view that telomerase is the main cellular target for tea catechins. To establish a proper nude mouse model with inoculated human tumors for testing the specificity of EGCG on telomerase, it was necessary to establish a control cell line that has inoculation, growth and drug accumulation properties similar to the cell line under examination. For this purpose, a mass culture of the colon carcinoma cell line HCT-116 (telomerase positive) was used to derive single cell subclones. The average telomere lengths of the isolated subclones varied from 2 to 7 kb. All subclones had similar proliferation rates and were telomerase positive when tested with the TRAP assay. Subclones with the shortest (HCT-S, 2 kb) and the longest (HCT-L, 7 kb) telomeres were selected and subjected to EGCG prolonged treatment at 2, 5, and 10  $\mu$ M in culture dishes. During the initial days of passage, parallel treated and untreated control cultures grew normally without detectable changes in viability or morphology. However, from approximately day 20 and thereafter, treated HCT-S cells alone started to show, in a dose dependent manner, senescence/crisis-like changes characterized by a dramatic growth arrest, loss of cell viability, size enlargement, and increased staining with the senescence marker, acidic  $\beta$ -galactosidase. Experiments with these two subclones inoculated in nude mice are undergoing to test whether EGCG prolonged treatment is able to affect the growth of HCT-S cells before HCT-L cells, which would then provisionally serve as an internal negative control.

**#497 Inhibitory effect of gemcitabine on telomerase in a human pancreatic cancer cell line.** Rha, Sun Y., Sun, Daekyu, Davidson, Karen K., Izbicka, Elzbieta, Von Hoff, Daniel D. *Cancer Therapy & Research Center, Institute for Drug Development, San Antonio, Texas, 78229.*

Changes of telomerase activity correlate with proliferative activity and have been used as a marker for responsiveness to chemotherapy (Faraoni et al. *Clinical Cancer Res.* 3:579, 1997). Some chemotherapeutic agents and nucleotides which bind to DNA may inhibit telomerase activity *in vitro* (Yegorov et al. *Biochemistry* 62:1296, 1997; Burger et al. *Eur J Cancer* 33:638, 1997). We evaluated the effect of gemcitabine which has a broad spectrum antitumor activity on telomerase activity in human pancreatic cancer cell line. This was done to obtain more information to enable the optimal design of preclinical and clinical studies for combinations of gemcitabine and telomerase inhibitors. We treated MIA-Paca-2 pancreas cancer cells with gemcitabine (2',2'-difluorodeoxydylidine) at concentration of 0.5, 1, 2, and 5 ng/ml. Cells were harvested daily. We counted the total cell numbers and evaluated the cell viability using a trypan blue dye exclusion test. We measured the telomerase activity by a non-PCR based conventional assay. All the viabilities of the control and drug treated cells were more than 90% at the time of harvest. Gemcitabine inhibited telomerase activity in MIA-Paca-2 cells after 48 hours of drug treatment. Inhibition was substantial at 92%. Telomerase inhibitory effects of these agents were maintained for 7 days after treatment. We also observed dose-dependent telomerase inhibitory effects with gemcitabine. These results indicated that gemcitabine itself inhibits telomerase and it would be of interest to combine with other telomerase inhibitors. Supported by NCI #CA67760 from the NCI, DHHS.

**#498 Methylation of the Telomerase RNA Gene Promoter and its Role in Resistance to Telomerase Therapeutics.** Keith, W. Nicol., Hoare, Stacey., Wiseman, Bea., Trueman, Lisa., van der Zee, Ate. *CRC Dept. of Medical Oncology, Beatson Labs, Glasgow, UK. Dept. Obstetrics & Gynecology, University Hospital, Groningen, Netherlands.*

The immortal phenotype of most human cancers is due to telomerase expression. However, a number of immortal cell lines and tumours achieve telomere maintenance in the absence of telomerase via alternative mechanisms known as ALT, (alternative lengthening of telomeres). At present the ALT pathways lack a molecular basis and it is unclear why the ALT pathway is selected for in preference to telomerase activation. Due to this lack of knowledge, it has not been possible to induce ALT activity in order to identify the genes responsible. The presence of alternative telomere lengthening mechanisms in tumours may be important in proposals to treat

cancers with telomerase inhibitors as resistance to telomerase therapeutics may select for the ALT phenotype. Thus it is important to define the molecular events which may force the ALT pathways to be activated in cancer cells. Northern blot analysis cell lines for telomerase RNA gene, (hTR), expression identified 3 ALT lines which did not express hTR. The hTR gene lies within a CpG island and is therefore a potential target for methylation. Thus, we used Southern blot analysis to investigate the methylation status of the hTR gene in cell lines. Interestingly, all 3 ALT, hTR negative cell lines, had complete methylation of the hTR promoter resulting in repression of hTR gene expression. Screening 107 tumour samples from cervix, colon, breast, lung and ovary identified 7 ovarian tumours to be hemizygous for hTR promoter methylation. This suggests that although the selective pressure is against fully methylating the hTR promoter in cancer cells, they have the potential to activate the ALT pathway via promoter methylation. Analysis of normal tissues for hTR gene expression and promoter methylation showed hTR expression was only detectable in normal adult testis. However, examination of promoter methylation in 25 normal tissues including brain, lung, colon, and muscle showed no evidence of methylation, suggesting regulation of hTR gene expression by methylation may be specific to a subgroup of immortal cells. In conclusion, methylation of the telomerase RNA gene promoter in telomerase-negative immortal cells activates alternative mechanisms of telomere length measurement.

**#499 Cytostatic effects of porphyrins in hormone-refractory cancers.** Izbička, Elzbieta, Davidson, Karen K., Lawrence, Richard, Hurley, Laurence H., Von Hoff, Daniel D. *Institute for Drug Development, CTRC, San Antonio, TX 78229 and Drug Dynamics Institute UT Austin, Austin, TX 78712.*

Hormone-refractory forms of breast and prostate cancer are difficult to manage using standard chemotherapy and new therapeutic approaches are urgently needed. G-quadruplex DNA is a novel target for anticancer drugs. A G-quadruplex interactive porphyrin TMPyP4 has recently been shown to inhibit telomerase in human tumor cells (*Cancer Res* 59:639-644, 1999). In this study we investigated the effects of TMPyP4 in human prostate cancer cell lines PC3 and DU145 (both androgen receptor negative), and in breast cancer cell lines MCF7 (estrogen receptor positive) and BT20 (estrogen receptor negative). These cells all express telomerase activity except for BT20. The continuous presence of 5  $\mu$ M TMPyP4 ( $\ll$  IC<sub>50</sub> values in all cell lines) did not affect cell viability and decreased the growth rates by 10-30% in the cells maintained in liquid cultures up to 30 population doublings. To examine the effects of exposure to 5  $\mu$ M TMPyP4 on clonogenic cell growth, the tumor cells were removed at predetermined times from the liquid cultures, plated in soft agar, and the number of colonies quantitated after 10-14 days. The acute exposure (TMPyP4 absent in the liquid culture, and added only to the cells in soft agar) had little effect, however colony formation was greatly decreased in a time-dependent fashion upon a longer exposure of tumor cells to TMPyP4. A significant inhibition of colony formation was observed as early as 3 population doublings and could be reversed by removing TMPyP4 from the cultures for >7 days. Equimolar TMPyP2, a non-planar positional isomer of TMPyP4 that does not show stacking interaction with G-quadruplex, had a significantly less effect against cells both in culture and in soft agar.

Our results with TMPyP4 against hormone refractory human breast and prostate cancer cells suggest that the porphyrin TMPyP4 is an effective agent in decreasing the clonogenic potential of tumor cells regardless of their hormone receptor status. A time-dependent effect of the drug on clonogenic growth in agar suggests that the cells exposed to TMPyP4 might gradually acquire more differentiated phenotype with a decreased ability to grow in anchorage-independent mode. Our results support further development of porphyrins as agents for hormone refractory tumors. Supported in part by the NCCDG grant CA67760 and by Bristol Myers Squibb.

**#500 Multiple allelic losses in gastric carcinoma are composed of initial loss on chromosomes 5q and 17p and progressive loss on chromosome 18q.** Kim Kyoung-Mee, Chung Yuen-Jun, Rhyu Mun-Gan. *Department of Microbiology and Clinical Pathology, The Catholic University of Korea.*

To assess the temporary order of allelic loss involved in the development of gastric carcinoma, allelic loss was categorized into two patterns: initial loss uniformly observed in all tumor areas and additional loss localized in a part of tumor tissue. One-hundred sixty-seven tumor sites, each of which was histo-topographically distinct, obtained from 42 gastric carcinoma tissues were examined for loss of heterozygosity (LOH) on chromosome 5q, 9p, 13q, 17p, and 18q, all of which have been well known to be lost non-randomly in gastric tumors. A polymerase chain reaction-based LOH assay using two or three microsatellite markers per chromosome arm showed that a total of the 42 gastric tumors had LOH in 33.8% of the informative cases on the five arms, 17p (41.9%), 18q (40.9%), 9p (32.4%), 5q (30%), and 13q (22.8%). All the allelic losses on 5q (100%) were detected uniformly in all tumor sites tested, whereas the intratumoral uniformity of LOH was noted less frequently on 17p (86.1%), 9p (82.6%), 13q (77.8%), and 18q (59.3%). In gastric carcinomas (35.7%, 15 of 42) harboring high-levels of LOH on

three or more chromosome arms, most LOH cases (89.4%, 84 of 94) were found to be shared in all tumor sites tested, thus initiated by concurrent losses. When comparing the incidence rate of LOH between early and advanced cancers, LOH of 5q and 17p were similar, while LOH of 9p, 13q, and 18q were frequent in advanced cancers for more than twofold. Taken together, the progression of allelic loss in gastric carcinomas appeared to be composed of obligatory initial losses on 17p and on 5q, obligatory progressive loss on 18q, and optional losses on 9p and 13q.

**#501 VNP20009, a genetically modified *Salmonella typhimurium*: anti-tumor efficacy, toxicology, and biodistribution in preclinical models.** Clairmont, C., Bermudes, D., Low, K.B., Pawelek, J., Pike, J., Ittensohn, M., Li, Z., Lou, X., Margitich, D., Lee, K., Zheng, L.M., and King, I. *Vion Pharmaceuticals, Inc., New Haven, CT; Yale University, New Haven, CT; Oread Inc., Farmington, CT.*

VNP20009 is a genetically modified *Salmonella typhimurium* designed for potential use as an antitumor agent and/or delivery vector in humans. VNP20009 possesses an excellent safety profile including genetic stability, attenuated virulence, reduction of septic shock potential, and antibiotic sensitivity in animal studies. VNP20009 contains two highly attenuating mutations, *purI* and *msbB*. Disruption of *purI* results in a high degree of attenuation and disruption of the *msbB* gene results in an altered lipid A on the bacteria surface that dramatically lowers induction of TNF $\alpha$ . VNP20009 administered systemically to tumor bearing mice at  $1-2 \times 10^9$  cfu/mouse accumulates preferentially in tumors over livers at a ratio of 1000:1. In normal mice, VNP20009 is rapidly cleared from the blood in 24 hours and from all organs by 3 months. LD<sub>50</sub> analysis in normal mice demonstrates that VNP20009 is more than 10,000 fold less virulent than wild type *Salmonella*. VNP20009 is able to dramatically inhibit tumor growth up to 95% in both murine and human tumor xenograft models. To develop VNP20009 for use in humans, preclinical toxicology studies were carried out using non-human primates (cynomolgus monkeys). Intravenous administration of VNP20009 to cynomolgus monkeys at  $1 \times 10^9$  cfu/monkey also shows rapid clearance from the blood in 24 hours. VNP20009 accumulates predominantly in the liver, spleen and bone marrow of cynomolgus monkeys and is completely cleared from all organs by Day 41. Pre-clinical toxicology studies in monkeys demonstrate that VNP20009 at doses as high as  $1 \times 10^{10}$  cfu/monkey did not cause mortality. Body temperature, body weight, and all ophthalmic examinations were normal. Toxicity was mild and confined predominantly to changes in liver enzymes. Our results demonstrate that VNP20009 is safe and efficacious as an antitumor agent and warrants clinical development.

**#502 Tumor-targeted gene delivery by ligand-PEG "post-coated" cationic liposomes.** Xu, Liang and Chang, Esther H. *Lombardi Cancer Center, Georgetown University Medical Center, Washington, DC, 20007.*

A novel strategy, designated as the ligand-PEG "post-coating" method, to prepare ligand-PEG-liposomes for targeted gene delivery *in vivo* has been developed in our laboratory. DNA is complexed and condensed first with cationic liposomes which contain a sulfhydryl-reacting molecule conjugated to a lipid, MPB-DOPE. In their formulation for use in subsequent conjugation. A dihydropyridine (PDP) group is first introduced at one end of polyethylene glycol (PEG). A ligand, e.g. folic acid, is then bonded to the other end. Subsequently, the folate-PEG-PDP is reduced to free sulfhydryl to obtain folate-PEG-SH, which can then react with the maleimide group of MPB on the surface of the DNA-liposome complex to link folate-PEG to the DNA-liposomes. Since ligand-PEG is linked after the DNA has been condensed inside the liposomes, the PEG layer will only coat the outside of the DNA-liposome and won't interfere with the internal structure of the DNA-liposome complex. The ligand-PEG "post-coating" method takes advantage of the reported protective and long-circulating properties of PEG-liposomes such as the "sterically stabilized" liposomes or "Stealth" liposomes, which have enhanced stability in serum and prolonged shelf-life. The liposomes prepared by the ligand-PEG "post-coating" strategy have a defined size, a PEG coating outside, and the ligand at the distant end of PEG accessible to corresponding receptors for receptor-mediated endocytosis. These ligand-PEG "post-coated" liposomes were shown to deliver the complexed genes selectively to the tumor *in vivo* after systemic administration, and gave sustained gene expression in the tumor, with an *in vivo* transfection efficiency of 25-40% (single i.v. injection) in human tumor xenografts in nude mouse. This strategy is a useful and promising way to design and develop targeted gene delivery systems for systemic gene therapy.

**#503 Construction of tetracycline-regulatable system for use in gene therapy.** Siamak Agha-Mohammadi (*University of Pittsburgh Medical Center*)

The basic principle of gene-based therapies is the efficient delivery of therapeutic genes adequate transgene expression and transgene regulation in a dose-dependent and reversible manner for certain genes. For effective gene delivery, the regulatory system must be contained on a single vector and it must display high levels of transgene expression on induction and low levels of basal expression on repression. We have investigated several self-contained tetracycline-regulatable vectors containing both the tetracycline-controlled transactivator (tTA) and a poten-



tially therapeutic gene (mGM-CSF) in transient studies. Maximal expression from a single vector (pSialI) carrying both the tTA expression cassette and a tTA-responsive mGM-CSF gene was comparable to that of intact CMV IE promoter in A431, Vero, NIH3T3 and 293 cells, but significantly lower in HeLa cells. The degree of regulation from pSialI was predominantly dependent on the cell type used. In these cells, the degree of regulation ranged from 5- to 24-fold at 60 hours in transient studies. Similar results were obtained in stable transformants. The modest degree of regulation from pSialI appears to be dependent on the activity of CMV IE promoter and the basal expression which may be influenced by the enhancers present on the vector. To achieve high transgene induction and low basal expression, a novel tetracycline-controlled positive feedback regulatory vector (PFRV) was constructed and characterized. An enhancerless positive feedback regulatory vector (pSialV) transcribing both tTA and mGM-CSF from a modified tTA-responsive bidirectional promoter demonstrated over 200-fold gene regulation in HeLa cells. This was comparable to the degree of regulation obtained on co-transfection of vectors expressing tTA and tTA-responsive mGM-CSF. The maximal transcriptional activity of pSialV was comparable to that of CMV IE promoter in several commonly used cell lines, and its basal activity was similar to the leakiness of the tetracycline-responsive promoter in all the cell types tested, allowing 47- to 328-fold regulation. Furthermore, an analogous plasmid (pSialV.tTA) carrying reverse tTA produced over 200-fold regulation in transient studies of the tet-on system. pSialV also showed enhanced regulation relative to pSialI in stable cells. Overall, the positive feedback regulatory system offers efficient gene regulation that is suitable for most intra- and extra-chromosomal applications, especially gene therapy.

**#504 Superior efficacy of a selectively-replicating adenovirus, ONYX-015/CD, expressing the cytosine deaminase gene.** Heise Carla, Hatfield Mike, Lemmon Marilyn, Nye Julie, Weber Suzette, Kim David, Hermiston Terry. *Onyx Pharmaceuticals, Richmond, CA 94806.*

ONYX-015 is an engineered adenovirus that can replicate in and selectively lyse tumor cells deficient in p53-pathway functions. Tumor-selective replication and necrosis was seen in clinical trials. Clinical benefit was significantly improved when combined with 5-FU-containing regimens. To enhance the anti-tumor activity of ONYX-015 we inserted the cytosine deaminase (CD) gene, the prodrug-activating enzyme that converts 5-FC to 5-FU, into the E1B 55kD region which has been deleted in ONYX-015. Human MB231 breast tumor xenografts in nude mice were directly injected with  $2 \times 10^8$  pfu of ONYX-015/CD (015/CD) or a non-replicating E1-deleted CD containing adenovirus (E1-CD) on study days 1-5. Several different 5-FC treatments were evaluated; the most effective dosing regimen in the MB231 model was 500 mg/kg, injected iP twice daily on study days 5-18. Tumors treated with 015/CD showed significant tumor growth inhibition compared to the equivalent E1-CD treatment groups and controls ( $p < 0.01$ ). Five complete responses and three partial responses were achieved (8 of 11 total). Similar results were seen in the MiaPaCa pancreatic tumor xenograft model, but no prodrug effect was seen in the HT29 colon cancer model. These studies suggest that the anti-tumor activity of ONYX-015 can be enhanced by the concomitant expression of the CD gene from the virus genome, and administration of the prodrug 5-FC. These studies also provide a rationale for the selective amplification of prodrug activating enzymes within the tumor tissue, in combination with administration of their respective prodrugs, as an anti-cancer therapeutic strategy.

**#505 Redox-Dependent GDEPT: Combining Hypoxia-Responsive Transcriptional Control With Oxygen-Sensitive Prodrug Metabolism.** Adam V. Patterson and Ian J. Stratford. *Experimental Oncology, Dept. of Pharmacy, University of Manchester, M13 9PL, UK.*

Transcriptionally-targeted gene expression in neoplastic tissues can be achieved using tissue- or disease-specific promoters or alternatively, enhancer elements responsive to the physiological conditions that distinguishes a solid tumor mass from normal tissues<sup>1</sup>. The most conspicuous of these micro-environmental differences is hypoxia, which arises through both diffusion- and perfusion-limited oxygen availability<sup>2</sup>. Hypoxia responsive elements (HREs), found within a number of genes involved in energy metabolism and angiogenesis<sup>3</sup> can specifically regulate transcription in response to tissue hypoxia. Utilizing these HREs to drive expression of therapeutic "suicide" enzymes is a potential approach to exploiting the unique tumor characteristic, hypoxia<sup>4</sup>. In addition to the transcriptional response to oxygen-deprivation, the hypoxia-signaling pathway can also be constitutively activated by oncogenic transformation<sup>5</sup> and loss of tumor suppressor gene function<sup>6</sup>. Immunohistochemical analysis of a spectrum of human solid tumors has revealed that 70% express the oxygen-regulated transcription factor HIF-1 that is known to trans-activate HRE containing genes<sup>7</sup>. Gene-directed enzyme-prodrug therapy (GDEPT) requires the transfer of therapeutic DNA into target cells in order to facilitate the expression of metabolic "suicide" enzymes. Most GDEPT paradigms utilize non-mammalian enzymes in combination with selective prodrug substrates to restrict metabolism to genetically modified cells. Agents that require bioreduction can also be considered as prodrugs. Enzymes present in both tumor and normal tissues activate these bioreductive prodrugs, but cytotoxicity is restricted to hypoxic tissues by the presence of

oxygen. We have demonstrated that the redox-sensitive flavoprotein, NADPH: Cytochrome P450 reductase (P450R), is an important endogenous bioactivator of multiple hypoxic cytotoxins (i.e. tirapazamine, mitomycin C, EO9, RSU1069). P450R will donate single-electron to any prodrug with appropriate one-electron reduction potential<sup>8</sup> including many nitro-aromatic, aromatic N-oxide and quinone "triggered" agents<sup>9-13</sup>. A therapeutic vector containing human P450R cDNA under the control of the HRE from the PGK-1 gene (pHRE-P450R) was stably transfected into a human fibrosarcoma cell line, HT1080. The oxlic levels of P450R activity were 6.5 and 160 nmol cytc reduced/mg/mln in the parental and transfected cell line, respectively. Upon exposure to 18h hypoxia (>10 ppm O<sub>2</sub>), P450R activity was suppressed to 4.2 nmol/min/mg in the parental cell line, but upregulated to 740 nmol/min/mg in the clonal cell line. Both cell lines were assessed for sensitivity to the bioreductive alkylating agent, RSU1069, under normoxic and hypoxic conditions. The hypoxic cytotoxicity ratio (HCR; IC<sub>50</sub> ratio under oxidic and hypoxic conditions) in the parental HT1080 cell line was 31-fold (43 μM versus 1.4 μM) and this was increased to over 300-fold in the pHRE-P450R transfected cell line (37 μM versus 0.12 μM). Thus expression and up-regulation of P450R confers hypoxia-selective sensitivity to RSU1069. A novel strategy to target oxygen-deprived tumor cells using gene therapy has been achieved through combining an oxygen-inhibited prodrug activation step with a hypoxia-selective expression strategy. Such an HRE-regulated gene therapy strategy could be applied to a broad range of cancers of variable tissue origin and histology.

**REFERENCES**

1. Dachs et al. *Oncol. Res.* 1998; 9:313.2.
2. Vaupel P. In: Teicher BA, ed. *Drug Resistance in Oncology*; New York: M. Dekker, 1993:59.
3. O'Rourke et al. *Oncol. Res.*, 1997; 6-7:327.
4. Dachs et al. *Nature Med.*, 1997; 3:515.
5. Jiang et al. *Cancer Res.*, 57:5328.
6. Maxwell et al. *Nature*, 1999:399:271.
7. Semenza et al. *AACR 90<sup>th</sup> Ann. Meet.* 1999. Absc1.
8. Butler & Hoey. *Biochim. Biophys. Acta.* 1993;1161:73.
9. Patterson et al. *ACDD*, 1998;13:541.
10. Patterson et al. *BJC*, 1997;76:1338.
11. Denny & Wilson. *Can. Met. Rev.*, 1993;12:135.
12. Denny et al. *BJC*, 1996;74:(Suppl. 27):32.
13. Jaffer et al. *ACDD*, 1998;13:593.

**#506 Specific targeting of inducible nitric oxide synthase (iNOS) gene to CEA-expressing tumor cells by a retroviral vector displaying a single-chain variable fragment (scFv) antibody.** Kuroki, Ma., Khare, P.D., Liao, S., Kuroki, Mo., and Arakawa F. *First Department of Biochemistry, School of Medicine, Fukuoka University, Fukuoka 814-0180, Japan.*

The goal of this study is to deliver the inducible nitric oxide synthase (iNOS) gene, a suicidal gene, to carcinoembryonic antigen (CEA)-expressing tumor cells by the use of a retroviral vector displaying an anti-CEA scFv/envelope chimeric protein.

An anti-CEA scFv gene, which was derived from hybridoma clone 11-39 generated by ourselves, was constructed and inserted into the ecotropic expression vector pEnv 20.22 (kindly provided by Dr. Somia, N.V., Salk Institute) to obtain a chimeric envelope expression construct, pscFv-env. The construct was transfected into a ecotropic retroviral packaging cell line (CRL9642) and a permanent clone with the highest expression of scFv, termed CRL-scFv-env, was selected. The iNOS gene, obtained from Oxford Biomedical Research, Inc., was inserted into a retroviral vector (pLNCX) and the resultant vector pLNC-iNOS was transfected into a amphotropic packaging cell line (PA317). The transient virus thus obtained was infected to the CRL-scFv-env packaging cells. The stable transduced packaging cell clones were selected by drug selective media and expanded. The retrovirus harvested were screened for chimeric envelope and infected to CEA-producing and nonproducing gastric carcinoma cell lines. The results obtained from virus binding assay and virus infection assay showed that the retrovirus binds specifically only to the CEA-expressing gastric carcinoma cell lines and introduce the iNOS gene specifically to these cell lines.

This approach offers a significant cell specific retroviral vector delivery of iNOS gene and a step towards the cell and tissue specific suppression of tumorigenicity.

**#507 Examination of the gene delivery capabilities of a replication competent adenovirus.** T. Hemiston, L. Hawkins, J. Nye, L. Johnson, D. Castro, J. Holt, and G. Kitzes. *Onyx Pharmaceuticals, Richmond, California, USA.*

To date gene delivery from viruses has been limited primarily to replication incompetent viruses. With our enhanced understanding of both tumor and viral biology, the potential for using replication competent viruses to selectively destroy tumors in the clinical setting is being realized with viruses such as ONYX-015, a mutant adenovirus that selectively replicates in and destroys cancer cells. To maximize the utility of ONYX-015 and viruses like it, we have begun to explore the gene delivery capabilities of a replication competent adenovirus. In these studies, we have used the endogenous adenoviral promoters to drive therapeutic transgene expression, taking advantage of the replication competence of the viral system. In

addition, we have engineered restriction enzyme sites into the transcription units of the E1B and E3 regions of the viral genomes to allow selective removal of specific genes from these multi-gene transcription units. We have inserted the pro-drug activating enzyme cytosine deaminase (CD) and the cytokine, tumor necrosis factor (TNF) into these sites and will show that the timing and expression of the transgenes mimics that of the native adenoviral genes. We will also show that this can be done without affecting the expression of the surrounding genes in the transcription unit. We believe that this represents a powerful new methodology for therapeutic gene expression that will extend the utility and potency of tumor selective oncolytic viruses.

**#508 Ligand-targeted, liposome-mediated p53 gene therapy in combination with radiation or chemotherapy leads to prostate tumor regression.** Pirolo, Kathleen F., Xu, Liang, Tang, Wen-Hua, Rait, Antonina, and Chang, Esther H. *Lombard Cancer Center, Georgetown University Medical Center, Washington, DC 20007.*

Abnormalities in tumor suppressor gene p53 are found in the majority of human cancers. Many tumors lacking wtp53 function are relatively resistant to chemotherapeutic agents, and/or show increased resistance to radiotherapy, possibly due to lack of p53 mediated apoptosis. Introduction of wild-type p53 by means of an adenoviral vector was able to restore chemosensitivity or radiosensitivity via apoptosis in xenograft tumors carrying mutant p53. However, the use of adenoviral vectors has limitations in tumor-specificity and gene delivery. A ligand-liposome system was optimized in our laboratory to systemically deliver the wt p53 gene efficiently, both *in vitro* and *in vivo*. Our data demonstrate that the restoration of wtp53 function via this tumor-targeting liposomal delivery system can sensitize prostate tumor cells to radiation and chemo-therapeutic agents *in vitro* and *in vivo*. Thus, the incorporation into currently used cancer treatment regimens of a new systemically delivered component resulting in radiosensitization or chemosensitization would have immense clinical relevance as a more effective prostate cancer treatment modality not only for primary tumors, but also for metastases and recurrent disease.

**#509 Virus-directed enzyme prodrug therapy (VDEPT) with CPT-11 and rabbit carboxylesterase for purging of tumor cells from stem cells for autologous transplant of patients with neuroblastoma.** Mack, Mandy M., Harris, Linda C., Potter, Phillip M., Danks, Mary K. *St. Jude Children's Research Hospital, Memphis TN 38105.*

Children with Stage III or IV neuroblastoma (NB) are commonly treated with surgery, chemotherapy, and stem cell rescue. Gene marking studies have shown that reinfusion of autologous stem cells contaminated with a level of tumor cells that is undetectable morphologically contributes to relapse. We are developing a VDEPT-based method to eliminate NB cells from stem cell preparations. An adenovirus-based method was chosen, first, because adenovirus is more toxic to NB cells than to hematopoietic cells. A multiplicity of infection (moi) of 50 of a replication-deficient virus decreases the clonogenic potential of SK-N-SH and SJNB-1 NB cells by 50% but is nontoxic to human peripheral hematopoietic progenitor cells. Further, an moi of 50 transduces 100% of NB cells and 0% hematopoietic cells, suggesting that this moi could be used to deliver a drug-activating enzyme to produce tumor cell-specific toxicity. CPT-11 was chosen as an appropriate prodrug for this VDEPT approach to purging because preclinical studies and early clinical trials have suggested that NBs are relatively sensitive to this agent. *In vitro* clonogenic and progenitor cell assays determined that a 4-hour exposure to 100 micromolar CPT-11 abolishes the clonogenicity of SK-N-SH, SJNB-1, and primary NB cells, but allows 70% survival of human hematopoietic progenitor cells. The combined selective toxicity of adenovirus, CPT-11, and adenovirus encoding a rabbit liver carboxylesterase which efficiently converts CPT-11 to its active form SN-38 is being evaluated as a clinically useful purging method. (Supported in part by CA23099, CA63512, CA79763, and ALSAC.)

**#510 Non viral vectors for gene therapy of Small Cell Lung Cancer (SCLC).** Albæk C<sup>1</sup>, Abel KL<sup>1</sup>, Frederiksen KS<sup>1</sup>, Abrahamson N<sup>1</sup>, Cristiano RJ<sup>2</sup>, Poulsen HS<sup>1</sup> <sup>1</sup>Section of Radiation Biology Copenhagen University Hospital, Denmark <sup>2</sup>M.D. Anderson Cancer Center, Department of Genitourinary Oncology, Houston, USA

The incidence of lung cancer is increasing. Especially small cell lung cancer (SCLC) has a high risk of metastasis mostly to liver, bone tissue and brain. The 5-year overall survival rate of 5-15% in treated patients is still very low. This makes it of great interest to develop new therapeutic approaches such as gene therapy. Gene therapy will be a potential method to target the cancer cells. One approach is to use receptor mediated endocytosis. Using a complex of cell specific ligands coupled to a plasmid containing the therapeutic gene the cells can be specifically targeted. In the case of SCLC an apoptosis inducing gene could show promising effects. We report that SCLC cell lines show susceptibility to Epidermal Growth Factor (EGF)-receptor mediated gene transfer. Our vector construct containing EGF as ligand and a plasmid carrying the LacZ gene showed transduction efficiencies ranging from 41% to 73% in the EGF-receptor positive SCLC cell lines. However, the EGF-receptor has been found to be expressed in only 10 of 21 SCLC cell lines and is expressed in a wide variety of normal tissue. For this reason it is necessary to find new and more specific receptors. We used RT-PCR to elucidate the

receptor status of our cell lines and normal human tissue. Investigating 10 receptors we found two to be very promising. To increase the specificity and the security of our vector system we propose to use a bidimensional approach. To find genes higher expressed in SCLC cells than in normal lung tissue we are using Serial Analysis of Gene Expression (SAGE) to compare the transcription level. Combining the promoter of one of those genes with the above mentioned receptors we can specifically target the cancer cells and increase the security of our vector system. Earlier results suggested that 90% of our SCLC cell lines show mutations in the p53 cDNA. For this reason we suggest to include an apoptosis inducing gene in our vector to erase the cancer cells.

**#511 Apoptotic induction of radioresistant malignant glioma tumor cells exhibiting mtp53 after combined adm. of liposomal plasmid wtp53cDNA gene of PCMV-Neo-Bam vector and radiotherapy.** Gianrios J., Voumvourakis K. *Peripheral Hospital of Patras, Eginition Hospital, Greece.*

Approximately 80% of malignant glioblastomas express elevated levels of p53 protein due to mutations or deletions which lead to functional loss of its activity causing inhibition of apoptosis after radiotherapy. Glioma tumor cells were derived by the collagenase method and they were analysed immunocytochemically with Pab240 IgG1 monoclonal antibodies whose epitope maps in the middle region (AA212-217) of p53 and reacts with only its mutant form. The results were positive exhibiting p53 over-expression. Tumor cells were irradiated with  $\gamma$ -rays (8Gy) produced by Cobalt-60, while plasmid wtp53cDNA gene of pCMV-Neo-Bam vector encapsulated in liposomes was administered. Tumor cells were incubated with liposomal wtp53 for 6 hours at 37 C. The recombination between plasmid and cellular genome was monitored by ICC using Pab240 IgG monoclonal antibodies. Cytotoxicity was determined by assays such as MTT, BrdU, GSH and LDH. Apoptotic signs were examined by TEM. Control cells were treated with empty liposomes. After treatment, immunocytochemical analysis has exhibited no p53 expression of the irradiated cells indicating normal function of wtp53. TEM has exhibited irreversible D2 signs of radiation induced apoptosis (RIA) forming apoptotic bodies which are phagocytosed by adjacent tumour cells indicating a bystander killing effect. Also, cytotoxicity assays exhibited for treated cells reduced metabolic activity (MTT), reduced DNA synthesis (BrdU), depleted GSH and enhanced leakage of LDH compared to controls. Liposomal wtp53 has mediated gene transfer by recombining plasmid wtp53cDNA gene of pCMV-Neo-Bam vector into the cellular DNA inducing apoptosis to glioma tumour cells after DNA damage caused by radiation.

### SECTION 3: DRUG RESISTANCE/MODIFIERS

**#512 An oral and intravenous Phase I clinical trial of a potent P-glycoprotein modulator, XR9576, in healthy volunteers.** Steiner J, Mellows G, Stewart A.J., Norris D, Bevan P. *Xenova Ltd, 240 Bath Road, Slough SL1 4EF, UK.*

XR9576 is a novel selective and potent modulator of P-glycoprotein (P-gp)-dependent multidrug resistance (MDR) *in vitro* and *in vivo* against MDR xenografts (Mistry *et al*, 1999, *Proc. Amer. Assoc. Cancer Res.* 2079, p313). A Phase I clinical trial of XR9576, administered both orally (p.o.) and intravenously (i.v.), was undertaken to assess the tolerability, pharmacokinetics and effect of XR9576 on a surrogate marker of efficacy. The studies were rising single dose, randomised, double-blind, placebo controlled design in healthy volunteers. Here, we report data on the pharmacokinetic (PK) and clinical parameters which complement the surrogate marker assay in CD56<sup>+</sup> lymphocytes where XR9576 was able to give complete inhibition of P-gp (Stewart *et al*, 1999, *Proc. Amer. Soc. Clin. Oncol.* 704, p183a).

XR9576 was administered i.v. in 250 ml over 30 minutes or p.o. in hard gel capsules in up to five subjects per dose level. The doses were 0.1, 0.2, 0.5, 1.0 and 2 mg/kg i.v. and 50, 100, 200, 500 and 750 mg (per volunteer) p.o. In addition, the highest doses (i.v. and p.o.) were administered twice, separated by 24 h. Plasma PK parameters are shown below for the higher doses. In addition to the terminal half life of ~24 hours the volume of distribution was in excess of 6 L/kg after i.v. administration indicating extensive tissue distribution. Higher daily systemic exposure was observed after the second of the two successive daily doses of either 750 mg po or 2 mg/kg iv.

Dose	C <sub>max</sub> (ng/ml)	T <sub>max</sub> (h)	AUC <sub>(0-∞)</sub> (ng.h/ml)	t <sub>1/2</sub> (h)
0.5 mg/kg i.v.	268	0.17	1464	20.0
1.0 mg/kg i.v.	602	0.33	2673	20.0
2.0 mg/kg i.v.	1517	0.33	10879	25.9
200 mg p.o.	62.7	10.5	2088	24.5
500 mg p.o.	100	9.0	3161	22.2
750 mg p.o.	142	8.5	5911	28.5



Both the oral and intravenous formulations were well tolerated and no drug related abnormalities were noted in any of the haematological or clinical chemistry parameters including the double doses.

These data together with the surrogate marker of efficacy have been used to select the XR9576 doses (150 mg i.v. and 500 mg p.o. as single daily doses) for Phase II clinical trials which are underway. In conclusion, XR9576 is a potent MDR modulator in man, which completely inhibits P-gp for in excess of 24 h at the projected therapeutic dose as assessed by a surrogate marker.

**#513 A clinical pharmacodynamic (Pd) and pharmacokinetic (Pk) phase I study of I.V. R101933, an inhibitor of MDR1 P-glycoprotein (Pgp) given alone and in combination with Taxol in patients with solid tumors.** Awada A, Bourgeois P, Cornez N, Bleiberg H, McCabe S, Gill T, Lehmann F, de Valeriola D, Di Leo A, Van de Loempt E, Bol K, Palmer P, Piccart M. *Jules Bordet Institute, Brussels; Janssen Research Foundation, Brussels.*

**Introduction:** R101933 (R) is a new MDR reversing agent. Oral R (200 mg bid daily  $\times$  5) did not alter the Pd and Pk of Taxol (T) (AACR 1999 abstr. 4373). A study in healthy volunteers receiving oral or I.V. R suggests that the maximum tolerated dose (MTD) of I.V. R would be much higher. Thus a phase I study was designed using the I.V. formulation. **Study design:** A phase I dose escalation study of I.V. R in combination with a fixed dose of T was conducted in patients (pts) with advanced solid tumors. In cycle 1, pts received I.V. R (125, 250, 500, 750 mg; 1 h inf.) immediately followed by T (175 mg/m<sup>2</sup> I.V.; 3 h inf.). In cycle 2, pts received T alone. In cycle 3 and subsequently, pts received R+T. Pharmacokinetics were performed in cycles 1 & 2. In 6 pts, the effect of I.V. and oral R (administered alone 40 hours apart) on the hepatic uptake and clearance of 99m Tc labelled sestamibi (MIBI); a substrate of Pgp 170 in liver) was also studied before cycle 1 + 2 using gamma camera techniques. **Pts' characteristics:** 16 pts; median age 49 ys (32-69); sex 7 M/9 F; prior CT/RT/CT + RT: 5/1/10; med. PS: 1. **Clinical results:** Median no. of cycles (Cy) per pt: 4 (1-10). No unexpected toxicity was observed. As foreseen, neutropenia (gr 3/4), neuropathy (gr  $\leq$  2), asthenia (gr  $\leq$  2) and myalgia (gr 2/3) were the main toxicities of T. No toxicities related to R were observed. No significant differences in toxicity were reported between Cy 1 & 2. Antitumor activity was evident at each dose level in 10 out of 13 evaluable pts. No Pk interaction of I.V. R with T was found at doses of 125, 250 and 500 mg R. Accrual is ongoing at 750 mg I.V. R. Preliminary results of MIBI study suggest that R increases the uptake and decreases the clearance of MIBI in the liver. **Conclusion:** I.V. R + Taxol is safe. The MTD has not been reached at 500 mg I.V. R. No Pk interaction was observed between T and I.V. R up to the dose level 500 mg R.

**#514 Identification of signal transduction components as potential therapeutic targets for circumvention of multidrug resistance mediated by P-glycoprotein.** Yang, Jin-Ming, Vassil, Andrew D., and Halt, William N. *The Cancer Institute of New Jersey, UMDNJ-Robert Wood Johnson Medical School, New Brunswick, New Jersey 08901.*

The discovery of P-glycoprotein (P-gp), the MDR1 gene product that functions as an energy-dependent drug transporter, provided a tantalizing target for developing new methods to sensitize tumor cells to chemotherapy. However, attempts to overcome multidrug resistance (MDR) with P-gp modulators, i.e., drugs that block P-gp function, have had limited success. To explore alternative approaches to the MDR problem, we investigated the role of the phospholipase C (PLC)-mediated signaling pathway in regulating the expression of MDR1 gene. Transfection of NIH3T3 cells with a pMJ30-PLC- $\gamma$ 1 expression vector increased the activity of PLC, as evidenced by the increased production of inositol trisphosphate. When cells were co-transfected with pMJ30-PLC- $\gamma$ 1 and MDRCAT, a MDR1 promoter-chloramphenicol acetyltransferase construct, the activity of the MDR1 promoter increased 2-10 fold in a dose-dependent manner, as compared with the cells transfected with MDRCAT alone. Treatment of co-transfected cells with platelet-derived growth factor (PDGF), an activator of PLC- $\gamma$  via receptor-mediated tyrosine kinase, further enhanced the activity of the MDR1 promoter. The induction of MDR1 expression by PDGF was also demonstrated in human kidney carcinoma cell line, HTB-46, using Northern blot analysis. U-73122, a PLC inhibitor, blocked the effect of activation of PLC on MDR1 expression. To define components involved in the regulation of MDR1 expression by PLC, the role of c-Raf, a serine/threonine kinase that phosphorylates and activates MEK1 and MEK2, was determined. The stimulatory effect of PLC on the MDR1 promoter was enhanced by co-transfection with v-raf, a constitutively activated Raf kinase. c-Raf-C4, a dominant negative Raf mutant, blocked the activation of MDR1 promoter by PLC- $\gamma$ 1. Inhibition of mitogen-activated protein kinase (MAPK) by U0126 and PD98059, two specific inhibitors of MAPK, also decreased the activity of the promoter. These results suggest that the expression of MDR1 gene is modulated by PLC-Raf-MAPK pathway, and that the enzymes involved in this pathway may be targets for the prevention and treatment of P-gp-mediated drug resistance.

**#515 Resistance of mouse cells lacking the poly(ADP-ribose) polymerase to anti-cancer therapy due to upregulation of multidrug-resistance gene product P-glycoprotein.** Wurzer Gabriele, Herceg Zdenko and Wesiarska-Gadok Jozefa. *Institute of Tumorbology-Cancer Research, University of Vienna, A-1090 Vienna, Austria and International Agency for Research on Cancer, F-69372 Lyon, France.*

We have recently found a clearly reduced basal level of wt p53 protein in PARP-/- mouse embryo fibroblasts (MEFs). Interestingly, PARP deficiency affected only regularly spliced (RS) form of wt p53 protein, whereas alternatively spliced p53 remained unchanged. Treatment with doxorubicin at concentrations activating RS p53 in normal MEFs, failed to induce wt p53 protein in PARP knock out cells. Therefore, we tested increasing doxorubicin concentrations to induce p53 response and simultaneously monitored the cytotoxic action. As expected, doxorubicin at higher concentrations was highly cytotoxic for normal MEFs and only negligibly elevated the p53 level. Surprisingly, the viability of PARP-/- cells remained unaffected even after the treatment with the highest doxorubicin concentrations. The lack of doxorubicin cytotoxicity resembled an unique phenomenon known as multidrug resistance (MDR). This assumption was substantiated by the observation that the uptake of <sup>3</sup>H-daunomycin was clearly reduced in PARP-deficient cells and that the enhanced activity of P-glycoprotein (P-gp) was down-regulated by MDR modulators. Pretreatment with Verapamil but not with Probenesid reversed the MDR phenotype. Consequently, <sup>3</sup>H-daunomycin uptake increased to that of normal MEFs and cells died upon doxorubicin application. Moreover, PARP-deficient cells showed an elevated level of P-gp compared with normal counterparts. Interestingly, reconstitution of cells lacking the PARP gene with the human counterpart restored cell susceptibility to doxorubicin. This was accompanied by down-regulation of P-gp. Our results indicate that up-regulation of P-gp in PARP-/- cells was due to the loss of p53 mediated negative regulation of the MDR gene at the transcriptional level and identify the mechanism of the resistance of PARP-deficient cells to chemotherapy. This model offers an explanation of the lack of development of streptozotocin-induced diabetes in PARP deficient mice.

**#516 Frontal chromatographic analysis of drug interactions with immobilized P-glycoprotein.** Lu Lili, Leonessa Fabio, Clarke Robert and Wainer Irving W. *Departments of Pharmacology, Physiology & Biophysics and Oncology, Georgetown University School of Medicine, Washington, DC 20007.*

The membrane protein P-glycoprotein (PGP) confers a multidrug resistant phenotype by actively effluxing several anticancer drugs from cells. We evaluated the possibility of using affinity chromatography as a means to define the affinity of PGP substrates for PGP. PGP was extracted from the membranes of MDA435/LCC6 human breast cancer cells transfected with the PGP gene, and immobilized onto Immobilized Artificial Membranes (IAM) particles in a 0.5  $\times$  0.8 cm column. The interactions between vinblastine, verapamil and PGP were measured on-line by quantitative frontal affinity chromatography. In two separate evaluations, the dissociation constant ( $K_d$ ) of vinblastine was measured to be  $19 \pm 20$  nM and  $71 \pm 11$  nM respectively (Zhang et al., submitted to *J. Chromatogr. A*). The activity of PGP was irreversibly blocked at 250 nM vinblastine (100  $\mu$ l injection). The  $K_d$  for verapamil was determined to be 44.0  $\mu$ M. We will next evaluate the affinity of other PGP substrates (e.g., doxorubicin and taxol) and their reciprocal interaction with vinblastine and verapamil at PGP's binding sites). Moreover, we will evaluate the effect of ATP on substrate affinity. PGP-IAM provide a rapid method to measure the affinity of ligands for PGP and their interactions. These columns also may be useful for the identification and characterization of novel PGP ligands.

**#517 The UIC2 Shift Assay, a new technique for high throughput screening of MDR1 inhibitors.** Mechetter E, Tee L, Fruhauf JP *Oncotech, Inc., Irvine, CA*

In 1992, we described a monoclonal antibody, UIC2, that reacts with the extracellular domain of P-glycoprotein (Pgp) and inhibits Pgp-mediated efflux of all tested MDR1 drugs. The conformational epitope recognized by UIC2 can be distinguished from the epitopes of the other anti-Pgp mAbs by differential reactivity with a mutant Pgp that carries a deletion in the first extracellular loop. We found that UIC2 reactivity with MDR1-positive cells was enhanced in the presence of Pgp-transported drugs, or in Pgp double mutants in the ATP-binding domains, or in ATP-depleted cells. These data indicated that UIC2 recognized a functionally active Pgp conformation associated with ATP hydrolysis and active drug efflux (Mechetter et al., *Proc. Natl. Acad. Sci.*, 94: 12908, 1997).

UIC2-based flow cytometry staining provides a new, highly specific and sensitive method for the detection of functional Pgp and MDR1 inhibitors, the UIC2 Shift Assay. It allows for simultaneous determination of two end-points: enhanced detection of Pgp expression on the cell membrane and information on the functional status of Pgp-mediated drug efflux. The test is specific for MDR1-related drug resistance and can be used to distinguish the Pgp membrane pump from other mechanisms of multidrug resistance, such as MRP or LRP. Functional data generated by the UIC2 Shift Assay closely correlated with the DiOC<sub>2</sub> efflux test in normal MDR1-positive cells and clinical tumor specimens. Drug-induced UIC2 s-shift is

more pronounced in MDR1-positive cells with relatively low, clinically relevant levels of Pgp expression (Mechtner et al., *Clin. Cancer Res.*, 4: 389, 1998).

We screened 163 solid tumor and leukemia/lymphoma specimens using the UIC2 monoclonal antibody, a Pgp probe, and vinblastine as the UIC2 shift inducer in parallel to DiOC<sub>2</sub> efflux studies. A 2–10-fold increase in sensitivity was observed, as compared to conventional staining. Oncotech's Extreme Drug Resistance (EDR™) or Differential Staining Cytotoxicity (DISC™) assays were performed on each specimen to assess the relationship between Pgp function determined by the UIC2 Shift Assay and in vitro drug response to doxorubicin (MDR1 drug) and 4-HC (non-MDR1 drug). Doxorubicin drug resistance was significantly associated with the UIC2 Shift Assay, while no such association was found in 4-HC-treated specimens.

When applied to high throughput screening of MDR1 inhibitors, the UIC2 Shift Assay successfully identified new drugs transported by Pgp and provided new information on MDR1 substrate specificity of commonly used chemotherapeutic agents.

**#518 Role of Intestinal MDR1 P-glycoprotein in the plasma disposition and fecal elimination pathways of docetaxel in humans.** Van Zuylen L., Verweij J., Nooter K., Brouwer E., Slotter G., and Sparreboom A. *Department of Medical Oncology, Rotterdam Cancer Institute, 3008 AE Rotterdam, the Netherlands*

P-glycoprotein (Pgp) is a drug-transporting protein that is abundantly present in biliary ductal cells and epithelial cells lining the gastrointestinal tract. In preclinical studies performed in mice lacking *mdr1a* Pgp, it has been shown that Pgp is not essential for normal hepatobiliary secretion of paclitaxel (Sparreboom, et al., *Proc. Natl. Acad. Sci. U.S.A.*, 94: 2031–2035, 1997). On the other side it has been found that the absorption of Pgp substrate drugs from the intestine can be increased by concomitant administration with Pgp inhibitors (Van Asperen, et al., *Pharmacol. Res.*, 37: 429–435, 1998). To further elucidate the role of Pgp in the metabolic disposition of anticancer drugs in humans, we administered i.v. docetaxel, one of the best known substrates of Pgp, alone and in combination with oral R101933, a new potent inhibitor of Pgp activity with metabolic routes independent of cytochrome P450 activity, which has a major role in the docetaxel metabolism. Pharmacokinetic profiles were evaluated in 5 cancer patients receiving treatment cycles with docetaxel alone (100 mg/m<sup>2</sup> i.v. over a 1-h period) and in combination with R101933 (200–300 mg b.i.d.). The terminal disposition half-life and total plasma clearance of docetaxel were not altered by treatment with oral R101933 ( $P = 0.27$ ). The cumulative fecal excretion of docetaxel, however, was markedly reduced from  $8.47 \pm 2.14\%$  (mean  $\pm$  SD) of the dose with the single agent to less than 0.5% in the presence of R101933 ( $P = 0.0016$ ). Levels of the major cytochrome P450 3A4-mediated metabolites of docetaxel in feces were significantly increased following combination treatment with R101933 ( $P = 0.010$ ), indicating very prominent and efficient detoxification of re-absorbed docetaxel into hydroxylated compounds before reaching the systemic circulation. It is concluded that intestinal Pgp plays a principal role in the fecal elimination of docetaxel by modulating reabsorption of the drug following hepatobiliary secretion. In addition, the results indicate that inhibition of Pgp activity in normal tissues by effective modulators, and the physiological and pharmacological consequences of this treatment, cannot be predicted based on plasma drug monitoring alone.

**#519 Blockade of HER-2/neu restores estrogen responsiveness and Tamoxifen sensitivity.** Witters, Lois M., Lipton, Allan, Leltz, Kim E., and Slikowski, Mark. *Penn State College of Medicine, Hershey, PA 17033 and Genentech, Inc., San Francisco, CA 94080.*

HER-2/neu overexpression is evident in 10–40% of breast cancers. The response rate of women with ER-positive breast tumors to endocrine therapy is reduced in patients with elevated serum HER-2/neu levels. The aim of this study is to show that reducing HER-2/neu expression restores estrogen sensitivity and response to hormonal therapy. We used a parental human breast cancer cell line which is estradiol (E2)-stimulated and growth inhibited by Tamoxifen (TAM) and the HER-2/neu transfected clone of this line which shows a minimal response to E2 and TAM. Cells plated in estrogen-depleted media were exposed to E2 and/or TAM with or without the 4D5 HER-2/neu antibody. Cell growth was determined using the tetrazolium dye (MTT) assay. In the parental line,  $10^{-11}$  M E2 increased cell growth by 160%, and the addition of 0.5  $\mu$ M TAM prevented E2-stimulated growth. In the HER-2/neu transfected line, growth was not stimulated by E2 nor affected by TAM in the absence of the 4D5 Ab; but in the presence of the Ab, E2 enhanced growth by 180%. TAM treatment resulted in total blockade of this E2-induced growth. These results suggest that HER-2/neu blockade can restore E2 sensitivity and response to TAM.

**#520 Potentiation of temozolomide and topotecan growth inhibition by novel potent benzimidazole poly(ADP-ribose) polymerase (PARP) inhibitors.** Curtin, N.J., Kyle, S., Wang, L.-Z., Durkacz, B.W., White, A.J., Srinivasan, S., Griffin R.J., Golding, B.T.G., Newell D.R., Calvert, A.H., Maegley, K., Hostomsky, Z. *University of Newcastle-upon-Tyne, UK, and Agouron Pharmaceuticals, USA*

PARP is an NAD<sup>+</sup> utilising nuclear enzyme which promotes DNA strand break repair and cell survival following genotoxic insult. PARP inhibitors enhance the cytotoxicity of monofunctional DNA methylating agents, topoisomerase I inhibitors and ionising radiation. LoVo (colon carcinoma) cells have been used to investigate the efficacy of four novel benzimidazole-4-carboxamides with potent PARP inhibitory activity ( $K_i < 10$  nM). These were 14-019, 14-032, 14-163, and 14-238. Growth inhibition (SRB assay) was determined following 5 days continuous exposure to increasing concentrations of temozolomide (TM) or topotecan (TP) in the presence or absence of 0.4  $\mu$ M PARP inhibitor. The potentiation factor PF<sub>50</sub> was given by the IC<sub>50</sub> values for TM or TP alone + IC<sub>50</sub> values for TM or TP + PARP inhibitor. The IC<sub>50</sub> for TM and TP alone were  $926 \pm 87$   $\mu$ M and  $15.5 \pm 4.7$  nM, respectively. 14-019, 14-032, 14-163, and 14-238 significantly potentiated TM-induced growth inhibition ( $p < 0.05$  paired Student's t-test), PF<sub>50</sub> values were  $1.5 \pm 0.3$ ,  $1.5 \pm 0.3$ ,  $1.2 \pm 0.1$  and  $4 \pm 1$ , respectively. Significant potentiation of TP-induced growth inhibition was only observed with 14-238 (PF<sub>50</sub> =  $1.5 \pm 0.4$ ). An analogue of 14-019 which should be unable to bind to PARP, due to substitution of a methyl group on the carboxamide nitrogen, failed to potentiate TM or TP (PF<sub>50</sub> =  $0.9 \pm 0.2$  and  $1.1 \pm 0.1$ , respectively). 14-238 potentiated a sub-cytostatic concentration of TM (400  $\mu$ M  $\approx$  20% growth inhibition) in a concentration-dependent manner, significant potentiation was observed with 10 nM and maximum potentiation with 1  $\mu$ M 14-238. The IC<sub>50</sub> of 14-238 alone was  $43 \pm 3$   $\mu$ M. Inhibition of PARP in whole cells by 14-238 was confirmed by the demonstration of the prevention of NAD<sup>+</sup> depletion following MNNG exposure. These data demonstrate that the activity of TM and TP can be significantly enhanced by sub-micromolar concentrations of novel benzimidazole PARP inhibitors.

**#521 ALTERATION OF STAT1 EXPRESSION IN RELATION TO DRUG RESISTANCE IN GLIOMA CELL LINES.** Rebbaa A., Mirkin BL and Chou PM. *Cancer Biology and Chemotherapy, Children's Memorial Institute for Education and Research, Children's Memorial Hospital, Northwestern University, Chicago, IL.*

It has been shown that in certain tumor types, development of drug resistance is accompanied by reduction in cell proliferation and enhanced differentiation. Certain signaling molecules such as signal transducers and activators of transcription (STAT) were found to play a pivotal role in both differentiation and proliferation. Therefore, STAT molecules may be implicated in development of drug resistance. In order to verify this hypothesis we examined the expression of both differentiation markers and STAT molecules in six glioma cell lines: U373 wild type, U373 cisplatin-selected, U87 wild type, U87-MDR1-transfected and subsequently selected with vinblastine; U251 wild type and U251-MDR1-transfected and selected with vinblastine. All the drug resistant cell lines were found to proliferate at a slower rate as compared to the wild type. The resistant cells also showed a more differentiated phenotype accompanied with an increase in the expression of differentiation markers such as neuron specific enolase (NSE) and glial fibrillary acidic protein (GFAP). In addition, expression of STAT molecules particularly STAT1 was strongly enhanced in all the resistant cell lines, whereas expression of another transcription factor (NF- $\kappa$ B) was similar in both the parental and drug resistant cell lines. Taken together these results suggest that enhanced expression of STAT1 may play a pivotal role in the development of drug resistance and may explain its association with reduced proliferation and enhanced differentiation in response to chemotherapeutic agents.

**#522 Dolichyl phosphate deficiency as a possible mechanism of drug resistance: effect of polyprenol on P-388 leukaemia cells.** Kuznetsov Sergejs J., *Health Research Laboratory Riga, Latvia.*

The investigations reveals that drug resistance correlates with MDR1 gene expression and accumulation of P-glycoprotein (P-GP) in plasma membrane. The recent results are in favour of the idea that glycoprotein synthesis and proliferation in tumour cells is limited by Dolichyl Phosphate (DoIP). The aim of the present study is to investigate this molecular mechanism by DoIP stimulation. P-388 leukemia cells with induced resistance to Doxorubicin (Dox) (P-388/Dox) were obtained by selection from P-388 sensitive leukaemia cells (P-388/0) when treating animals with low doses of Dox. Polyprenol (Pol) (BioLat, Latvia) concentration in the culture medium made up  $10^{-3}$  –  $10^{-5}$  M. P-GP extraction from plasma membranes was performed by Riordan and Ling (1979) method. MDR1 expression was assessed by an immunohistochemical technique. DoIP and P-GP fractions were analysed by HPLC methods. Pol in concentration  $10^{-3}$  –  $10^{-4}$  M induced apoptosis in leukemia cells within 3–4 hours with nuclear fragmentation and cleavage of genomic DNA. It is confirmed that plasmatic membranes of P-388/Dox cells contain 5.6 – 6.4% of P-GP (the total protein amount) as a resistance marker. Resistant P-388/Dox cells differ from sensitive ones (P-388/0) in Pgp content by 10–12 times. The study showed 3.5-fold DoIP decrease in P-388/Dox cells. The investigations demonstrate that the situation can be changed by resistant cells treatment with Pol. The DoIP concentration in P-388/Dox cells was returned to the normal level. It is established that polyprenol in the concentration 10<sup>-6</sup> M and 7–9-fold reducing P-GP in membranes of P-388/Dox cells. The P-388/Dox cells cultivation in medium with polyprenol proceeded to give lowered P-GP content in membranes no over 0.4–0.6%, which amount was con-



sistent with the level of P-GP in P-386/0 cells. These results indicate that noncontrollable biosynthesis of P-GP, after MDR1 expression in P-386/0 Dox cells can be modified using DoIP stimulation.

**#523 Intrinsic antitumor activity of PSC 833 (Valspodar) and Cyclosporin A (Sandimmune) as a single agent and synergistic effects in combination with other drugs.** Krels W, Calabro A, Budman DR. *North Shore University Hospital, New York University, Manhasset, NY 11030.*

Cyclosporin A (CSA) and its non-immunosuppressive congener PSC 833 are classically thought as not useful cytotoxic agents. However, *in vivo* antitumor activity of CSA in a variety of mouse tumors was previously demonstrated (Krels et al, *Experientia* 35:1506, 1979). Antiproliferative effects of CSA were also reported in tissue cultures derived from a variety of malignancies. As CSA is associated with significant clinical toxicity and PSC 833 may be better tolerated in man, we evaluated the effect of PSC 833 in culture as a single agent and in combination with more classical antitumor drugs. The solid tumor cell lines were LnCaP, DU 145, PC 3, MCF<sub>7</sub>, MCF<sub>7</sub>/adr (resistant to anthracyclines), and the leukemia cell lines CCRF-SB, MOLT-4 and AML-193. Cytotoxicity was evaluated by the MTT assay and antagonism, additive effect, or synergism determined by median effect analysis as previously described (*Brit J Urol* 79:196, 1997). The mean ID<sub>50</sub> values for CSA was 4.4 ± 2.2 μM; for PSC 833 the value was 3.4 ± 1.8 μM. Combinations of PSC 833 with other antitumor agents were evaluated in the three prostate cancer cell lines. Drug interactions as measured by the combination index (CI) were evaluated at the fa 50 (50% of cells affected). Synergism was observed in all prostate cell lines with estramustine (CI: 0.46–0.51), Suramin (CI: 0.71–0.86), vinorelbine (CI: 0.61–0.86), and ketoconazole (CI: 0.39–0.85). Synergistic response restricted to 2/3 or 1/3 cell lines was observed with bicalutamide (CI: 0.87 + 0.89), Liarozole (CI: 0.69 + 0.76), trans retinoic acid (CI: 0.66 + 0.82), and dexamethasone (CI: 0.50). Triple combinations of PSC 833 with estramustine, and trans retinoic acid demonstrated schedule dependent synergy when trans-retinoic acid followed estramustine and PSC 833 (CI: 0.15–0.66) but not with the reverse sequence. The actions of PSC 833 on tumor cells may be complex. Several new combinations of drugs with this agent need to be tested clinically.

Support: Don Monti Memorial Research Foundation.

**#524 Dexrazoxane significantly impairs the induction of doxorubicin resistance in the human leukaemia line, K562.** Sargent, Jean M; Williamson, Christine, J; Taylor, Collin G; Hellmann, Kurt. *Haematology Research, Pembury Hospital, Pembury, Kent TN2 4QJ, UK. Windlesham House, Withyham, Sussex TN7 4DB, UK.*

Dexrazoxane (DXRz) combined with doxorubicin (+ 5-fluorouracil + cyclophosphamide—the FAC regime) leads to a significant decrease in doxorubicin cardiotoxicity and a significant increase in median survival time for patients with advanced breast cancer. The reasons for this increase in survival are unclear. They may be related to a reduction in the emergence of multidrug resistance (MDR). In order to test this hypothesis, we induced resistance to doxorubicin (DOX) in the K562 cell line by growing cells in increasing concentrations of DOX (10–40 nM) in the presence (20 and 200 nM) and absence of DXRz. The DOX sensitivity of all cell lines was measured using the MTT assay. Flow cytometry was used to assess the MDR phenotype, measuring Pgp expression with MRK 16 plus indirect immunofluorescence and drug accumulation in the presence and absence of PSC 833 for functional Pgp. Long-term growth in DOX increased the cellular resistance (IC<sub>50</sub>) of K562 cells in a concentration dependent manner ( $r^2 = 0.999$ ). This was reduced approximately 2-fold by the addition of DXRz ( $p = 0.005$ ). Likewise, both the induction of Pgp expression and attendant function were reduced in the presence of DXRz ( $p < 0.0001$  and  $p = 0.003$  respectively).

	K562 <sub>40</sub>	K562 <sub>40</sub> + DXRz (20 nM)
DOX IC <sub>50</sub> (μM)	4.9	2.2
Pgp (ratio: fluorescence test/control)	15.6	9.0
Drug accumulation (ratio: fluorescence +PSC/-PSC)	6.48	3.87

These results suggest that DXRz may prevent the development of MDR, thus allowing responders to the FAC regime to continue to respond.

**#525 Berberine Overcome the drug Resistance of Leukemic Cells K562/A02.** Cui, Shuxiang, QU, Xianjun, XIE, Yanying, HOU, Jinling, ZHOU, Ling, ZHANG, Q, XU, Xueming. (Dept. Pharmacology, Institute of Materia Medica, Shandong Academy of Medical Science, Jinan 250062 P.R. China).

**ABSTRACT:** We had studied the characteristics of berberine in overcoming the drug resistance of leukemic cells K562/A02 *in vitro* and *in vivo*. K562/A02 cells were resistant to adriamycin by 83-fold. The mechanisms of resistance of K562/A02 cells are over-expression mdr-1 and P-glycoprotein which can pump out drugs from inside-cells. *In vitro* tests, berberine overcame the drug resistance of K562/A02 cells by 20-fold. The IC<sub>50</sub> of adriamycin remarkably decreased from 25.70 μg/ml to 1.25 μg/ml while coexisting berberine. The administration dosage of berberine was 20 μg/

ml, under this condition there were non-cytotoxicology to K562/A02 cells and had strongest ability to overcome the drug resistance. Another test showed that berberine could inhibited glycoprotein(P170) or sealed up the efflux pump in membrane of K562/A02 cells. The number of P170 in cell membrane decreased from 86.02% to 40.05% and accumulated adriamycin inside K562/A02 cells. The analysis of cell cycle showed that proportion of G<sub>0</sub>/G<sub>1</sub> was increased when treated with berberine. In addition, berberine also made K562/A02 cells apoptosis. *In vivo* tests, berberine had the ability to increase sensitivity to adriamycin in K562/A02 cells which bearing in nude mice. Inhibition rates were 60.2% and 98.0% respectively when treated with berberine alone or plus adriamycin in nude mice.

**#526 Effect of multidrug resistance reversing agents on the transporting activity of human canalicular multispecific organic anion Transporter (cMOAT).** Chen, Z.S., Kawabe, T., Ono, M., Sumizawa, T., Furukawa, T., Uchiyama, T., Wada, M., Kuwano, M., and Akiyama, S. *Inst. for Cancer Res., Faculty of Med., Kagoshima Univ., 8-35-1 Sakuragaoka, Kagoshima 890 and Dept. of Biochem., Kyushu Univ. Sch. of Med., 3-1-1 Maidashi, Fukuoka 812, Japan.*

The canalicular multispecific organic anion transporter (cMOAT), also termed MRP2, is a recently identified ATP-binding cassette (ABC) transporter. We have established stable human cMOAT cDNA transfected cells, LLC/cMOAT-1, and LLC/CMV cells which were transfected with an empty vector alone, from LLC-PK1 cells previously and found that LLC/cMOAT-1 cells have increased resistance to vincristine (VCR), 7-ethyl-10-hydroxy-camptothecin (SN-38) and cisplatin but not to etoposide. The aims of this study were to investigate whether some Pgp and MRP inhibitors can modulate the drug resistance conferred by cMOAT. We found that the multidrug resistance (MDR)-reversing agents, cyclosporin A (CsA) and PAK-104P, almost completely reversed the resistance to VCR, SN-38 and cisplatin of LLC/cMOAT-1 cells. CsA and PAK-104P at 10 μM enhanced the accumulation of VCR in LLC/cMOAT-1 cells near to the level in LLC/CMV cells without the agents. The efflux of VCR from LLC/cMOAT-1 cells was enhanced compared with LLC/CMV cells and it was inhibited by CsA and PAK-104P. Transport of leukotriene C<sub>4</sub> (LTC<sub>4</sub>) and S-(2,4-dinitrophenyl) glutathione (DNP-SG) was also studied using membrane vesicles prepared from these cells. LTC<sub>4</sub> and DNP-SG were actively transported into membrane vesicles prepared from LLC/cMOAT-1 cells. The  $K_m$  and  $V_{max}$  for the uptake of LTC<sub>4</sub> by the LLC/cMOAT-1 membrane vesicles were 0.26 ± 0.05 μM and 7.48 ± 0.67 pmol/min/mg protein, respectively. LTC<sub>4</sub> transport was competitively inhibited by PAK-104P, CsA, MK571 and PSC833, with  $K_i$  values of 3.7, 4.7, 13.1, and 28.9 μM, respectively. These findings suggest that CsA and PAK-104P are useful for reversing cMOAT-mediated drug resistance in tumors.

**#527 Reversal of MRP- and Glutathione related multi drug resistance (MDR) in chemo-selected prostate cancer (PC) models by buthionine sulfoximine (BSO) and leukotriene D<sub>4</sub> receptor antagonist MK-571.** Mickisch, Gerald H, Van Brussel, Jérôme P. *Erasmus University Rotterdam, The Netherlands.*

**INTRODUCTION:** Advanced PC is resistant to treatment with chemotherapy. We studied whether MDR mechanisms, such as the multidrug resistance associated protein (MRP; a drug transporter) and glutathione-S-transferase- $\pi$  (GST- $\pi$ ; an enzyme involved in the detoxifying glutathione pathway) are involved in the resistant phenotype of PC.

**METHODS:** The PC cell lines PC3 and DU145 were cultured in the presence of increasing concentrations of Etoposide (VP-16). Resistance to VP-16, Doxorubicin (Dox) and Vincristine (VCR) was measured with the MTT assay. Cloning of resistant cells was done with the limiting dilution technique. Expression of MDR proteins was assessed by immunohistochemistry. The MRP blocking agent MK-571, a leukotriene D<sub>4</sub> receptor antagonist, and the glutathione depleting agent BSO were combined with the cytotoxic drugs and reversal of drug resistance was measured with the MTT assay. Inhibition of the MRP1-pump by MK-571 was assessed by flow cytometry using the MRP1 specific fluorescent carboxyfluorescein.

**RESULTS:** Resistance to cytotoxic drugs of PC3 and DU145 increased by approximately 100% after continuous exposure to VP-16. Expression of MRP and GST- $\pi$  was markedly increased in the resistant clones of both PC3 (PC3-R) and DU145 (DU-R). Treatment with MK-571 and VCR completely reverted resistance of PC3-R, whereas resistance of DU-R was reduced with 70%, MDR reversal with BSO was complete in DU-R. Of note is that the concentration of MK-571 needed for chemosensitization was 20 times less than clinically achievable. The concentration of VCR was in the range of reported peak plasma levels in men.

**DISCUSSION:** Overexpression of MRP and GST- $\pi$  in our models appears to result in MDR, which can adequately be reverted with specific agents. Further characterization of MDR mechanisms in PC models and study of MDR reversal may result in a more effective treatment of chemotherapy-resistant PC.

**#528 Co-administration of probenecid, an inhibitor of a cMOAT/ MRP-like plasma membrane ATPase, greatly enhanced the efficacy of a new 10-deazaaminopterin against human solid tumors *in vivo*.** Sirotnak F.M., Bornmann W.G.B., Miller V.A., Scher H.I. and Kris M.G. *Memorial Sloan-Kettering Cancer Center, New York, NY 10021.*

Earlier studies from this laboratory have shown (Schlemmer, S.R. and Sirotnek, F.M., *J. Biol. Chem.* 267:14746, 1992) that the uricosuric agent, probenecid (PBCD), will inhibit the extrusion of folate analogues from tumor cells mediated by a ubiquitous plasma membrane ATPase resembling the cMOAT/MRP family of ABC cassette transporters. This inhibition of this previously unidentified, outwardly-directed membrane ATPase had already been shown (Sirotnek, F.M. et al., *Cancer Res.* 41:3944, 1981) to favorably impact upon the cellular pharmacokinetics and cytotoxicity of MTX *in vitro* and on its efficacy *in vivo*. In an extension of these earlier studies, that had focused only on murine ascites tumors, we now report that co-administration of PBCD, either parentally or orally, will inhibit ATP dependent extrusion from tumor cells and markedly enhance the efficacy of a new folate analogue, 10-propargyl-10-deazaaminopterin (PDX), against well established murine and human lung neoplasms and human prostate and mammary neoplasms growing as solid tumors in mice. In these studies, PBCD (125 mg/kg ip or 500 mg/kg po) could be given with the MTD of PDX (60 mg/kg) on a schedule of q3-4d without toxicity. The therapeutic enhancement obtained was manifested as tumor regression where PDX alone was only growth inhibitory (A549 NSCL tumor) or as a substantial increase (3-4 fold) in overall regression and (or) number of complete regressions (Lewis and LX-1 lung, PC-3 and TSU-PR1 prostate and MX-1 mammary tumors) compared to PDX alone. Also, only in the case of PDX with PBCD, a significant number of mice transplanted with LX-1 or MX-1 tumors that experienced complete regression did not have regrowth of their tumor. In view of these results, clinical trials of this therapeutic modality appear to be warranted especially in the case of new potentially more efficacious folate analogues such as PDX that are also permeants for this cMOAT/MRP-like plasma membrane ATPase. A phase I trial of this therapeutic modality is now underway at MSKCC. Support: NCI CA08748 and CA56517, The Simon Benlevy Cancer Fund and the PepsiCo Foundation.

**#529** Detection of chemotherapeutic synergism through pre-clinical testing and its application in the design of a Phase I human clinical trial. Ishmael, D. Richard, Nordquist, John A., Hamilton, Stephen A. and Nordquist, Robert E.

The BQT-2 breast cancer cell line was used to determine synergism between chemotherapeutic agents using the MTT assay. If additive or synergistic activity was detected, there was an attempt to maximize synergism through various timing schedules. Serial dilutions of various drugs were made to determine kill curves. Non-cytotoxic doses of drugs were used. Serial dilutions of drugs in combination were used to determine the extent of dose kill. If additive or synergistic activity was found, then optimal scheduling of drug was studied. Delivery was given sequentially or concurrently. Drugs given sequentially were tested at 24, 48 and 72 hrs. Results revealed that three drugs had synergism (mitoguzone, gemcitabine and docetaxel). Mitoguzone given concurrently with gemcitabine gave minimal additive effect. Mitoguzone given 24 hours before gemcitabine showed 100% cell killing at gemcitabine concentrations of  $3.8 \times 10^{-8}$   $\mu\text{g/ml}$ . A second synergistic combination was that of gemcitabine and docetaxel. If the drugs were given concurrently the kill curve for gemcitabine was improved one log. The curve for docetaxel was worsened by 3 logs. Gemcitabine and docetaxel needed separation by at least 72 hours to achieve maximal synergism. Log kill was improved by 2 for docetaxel and 6 logs for gemcitabine. A combination mitoguzone and gemcitabine was studied in a rat breast cancer model to determine any unexpected untoward effects. There were no additional toxic effects seen with the combination vs. gemcitabine alone. In a group of six animals treated with a single treatment of mitoguzone plus either 1000 or 1250 mg/m<sup>2</sup> of gemcitabine, there were 3 cures, and after more than 150 days there was no evidence of tumor. In the animals treated with gemcitabine alone, mitoguzone alone or with gemcitabine doses lower than 1000 mg/m<sup>2</sup>, i.e. 250 to 750 mg/m<sup>2</sup>, no cures were seen. Based on the results, a Phase I clinical trial was undertaken with mitoguzone day 1 (starting dose 500 mg/m<sup>2</sup>) and gemcitabine day 2 (starting dose 1500 mg/m<sup>2</sup>) given every two weeks. Three to six patients were added at each dose levels until the maximally tolerated dose was determined. Preliminary Phase I data will be presented.

**#530** A Phase II study of Incel™ (bircodar, VX-710) + paclitaxel in women with advanced ovarian cancer refractory to paclitaxel therapy. Seiden M, Swenerton K, Matulonis U, Rose P, Battist G, Verma S, Oza A, Popadiuk C, Bessette P, Angers E, Ette E, Harding MW, Charpentier D. Massachusetts General Hospital, Boston MA, BCCA, Vancouver, BC, Dana Farber Cancer Institute, Boston MA, Macdonald Women's Hospital, Cleveland, OH, Jewish General Hospital, Montreal QC, ORCC, Ottawa, ON, Princess Margaret Hospital, Toronto, ON, H Bilts Murphy Cancer Center, St John, NF, CUSE, Fleurimont, QC, BioChem Pharma, Laval, QC, Vertex Pharmaceuticals Incorporated, Cambridge MA, CHUM, Pavillon Notre-Dame, Montreal, QC.

Incel™/VX-710 is a potent inhibitor of multidrug resistance mediated by P-glycoprotein (P-gp) and MRP expression. Varying levels of P-gp and MRP are expressed (40 and 60%, respectively) in patients (pts) with advanced ovarian cancer. We initiated a Phase II study to evaluate safety, pharmacokinetics and efficacy of Incel + paclitaxel (P) in advanced ovarian

cancer pts refractory to prior P therapy. Inclusion criteria:  $\geq 2$  prior regimens for pts with advanced ovarian carcinoma; progressive disease on P, or documented progressive within 4 months of prior P therapy; bi-dimensional measurable disease; ECOG performance status  $\leq 2$ ; normal renal, liver and bone marrow function. Pts receive a 24-hr Incel infusion (120 mg/m<sup>2</sup>/hr) with 3-hr P at 60 mg/m<sup>2</sup> (P AUC and time  $> 0.05 \mu\text{M}$  comparable to 3 hour 175 mg/m<sup>2</sup> P). Endpoints: response rate, response duration and CA125 levels. As of July 1999, 34 patients have enrolled and  $> 100$  cycles of Incel/P have been administered. Safety data is available for 22 pts. Incel/P has been well tolerated. Myelosuppression is the principal toxicity. Median (range) cycle 1 WBC and ANC nadirs were 2.05 (0.7-6.3) and 0.49 (0.02-3.85)  $\times 10^9/\text{L}$ , respectively. The most frequent non-hematological toxicities (nausea, vomiting, asthenia, neuropathy, fever, diarrhea) were mild to moderate. Among the 1<sup>st</sup> 25 evaluable pts, 14/25 received 4-9 treatment cycles and only 7 pts terminated with PD after 1-2 cycles. Significant CA125 decreases (ranging from 40-90%) were observed in 56% of pts (14/25; 4 pts with  $> 50\%$  and 9 with  $> 75\%$  reductions, respectively) that were sustained for up to 18 weeks. One CR, 2 PRs and 2 MRs ( $> 30\%$  tumor shrinkage) have been observed thus far and 9 pts continue on therapy. Incel/P therapy results in objective responses in strictly defined P refractory ovarian carcinoma pts and in sustained CA125 reductions in a high percentage of pts.

**#531** A Phase II study of the safety, pharmacokinetics and efficacy of Incel™ (bircodar, VX-710) in combination with mitoxantrone (M) and prednisone (P) in hormone refractory prostate cancer (HRPC). Einstein Jr A, Lush R, Rago R, Ko Y-J, Buble G, Henner WD, Beer T, Chatta G, Shepard R, Unger P, Merica EA, Ette E, Harding MW, Dalton WS. Moffitt Cancer Center, Tampa, FL, Beth Israel Deaconess Hospital, Boston MA, Oregon Health Sciences University, Portland OR, Arkansas Cancer Research Ctr, Little Rock, AR, Greater Baltimore Medical Ctr, Baltimore, MD, Vermont Ctr Cancer Medicine, Burlington, VT, and Vertex Pharmaceuticals Incorporated, Cambridge, MA.

Incel™ is a potent inhibitor of multidrug resistance (MDR) mediated by P-glycoprotein (P-gp) and MRP expression. Prostate tumors have a high incidence of MRP expression and a variable incidence of P-gp. Since mitoxantrone (M) and prednisone (P) are both substrates for MDR transporters, we initiated a Phase II study of Incel + M/P in HRPC patients (pts). Endpoints: primary—serum PSA response rate; secondary—response duration, pain reduction, analgesic consumption and QOL measures. Inclusion criteria: progressive HRPC (defined as new lesions, new disease related pain, or a 50% increase in PSA within 6 weeks of study entry); testosterone  $< 30 \text{ ng/ml}$ ; no prior chemotherapy; ECOG performance status 0-3; adequate organ function. Pts receive Incel (120 mg/m<sup>2</sup>/hr) as a 72 hr CIVI with M (12 mg/m<sup>2</sup>) administered 4 hrs after starting Incel and P (5 mg bid) administered throughout study treatment. As of July 1999, 40 pts have been enrolled and  $> 130$  courses of Incel + M/P have been administered. Six pts received a cycle of M/P alone then Incel + M/P with intensive pharmacokinetics sampling. Pharmacokinetic analysis (n = 6) shows that Incel does not alter M clearance [median (range) of 0.35 (0.13-0.97) and 0.38 (0.11-0.54) L/h/kg for M/P alone and Incel + M/P, respectively]. Incel + M/P has been well tolerated. Transient Gr 1/2 nausea & vomiting and Gr 1/2 neutropenia are the principal treatment toxicities: 5 pts experienced an uncomplicated febrile neutropenic episode, 3 pts had Gr 3 nausea/vomiting, and 1 pt had Grade 3 ataxia. Among 25 evaluable pts, 10 achieved PSA responses: 8 with  $> 80\%$  PSA reductions sustained for up to 27 wks, and 2 active pts at  $> 50\%$  with PSAs continuing to decline. Twenty evaluable pts have discontinued therapy (6 with PD and 9 with SD, 5 PSA response pts are in follow-up), 14 pts are too early to assess, and 6 non-evaluable pts discontinued prematurely. Incel + M/P can produce substantial and prolonged PSA reductions in HRPC pts and may improve responses and response duration compared to M/P alone.

**#532** Hyperthermia could inhibit the expression of multidrug resistance gene (MDR1) and GSTpi gene in bladder carcinoma cells and increase the intracellular accumulation of Daunorubicin. Song, Yan Shuang; Memorial Sloan-Kettering Cancer Center, NY 10021; Jia, Wei Ying; Lee, Wen Lu; Liu, Hong Yin; Wang, Li Mei; Yang, Yi; Tianjin Cancer Institute & Hospital, Tianjin 300060, P.R. China.

Our previous study has shown that hyperthermia may contribute to reversal of multidrug resistance of human colon adenocarcinoma cell line-THC-8908 *in vitro* by inhibiting the expression of multidrug resistance gene (MDR1) and GSTpi gene, and increasing the intracellular accumulation of Daunorubicin. In this study, we investigated the effect of hyperthermia on expression of multidrug resistance gene (MDR1) and GSTpi gene and intracellular accumulation of Daunorubicin of cells from fresh resected bladder carcinoma tissues *in vitro*.

METHOD: 68 bladder cancer specimens were obtained, all cases underwent chemotherapy and were diagnosed with transitional cell carcinoma. Single cell suspensions were prepared; Cells in test group were exposed to hyperthermia ( $42.5 \pm 0.5$  degrees C in water bath for 60 minutes) at the beginning of 48 hr culture, cells exposed to 37 C degree for the same period served as controls. An immunohistochemical analysis was performed with monoclonal antibodies against P-glycoprotein and GSTpi



to analyse the expression level of MDR1 gene and GSTp1 gene, flow cytometry was performed to detect the intracellular accumulation of Daunorubicin. All experiments were done in triplicate.

**RESULT:** 1) Out of the 68 specimens of bladder cancer, 39 (57%) were found positive MDR1 expression, including 18 high expression with >70% of cells stained, 14 moderate expression and 7 low expression with <30% of cells stained. 66 of 68 specimens (97%) were found positive GSTp1 expression: 30 were high expression and 31 were moderate expression and 5 low expression. After exposed to hyperthermia, 27 of 39 MDR1 positive expression and 38 of 66 GSTp1 positive expression in the test group became significantly inhibited compared with that of control group with regard to the proportion of positive stained cells and staining intensity. Flow cytometry showed that intracellular concentration of Daunorubicin (ICD) in test group were significantly higher than that of control group ( $P < 0.01$ ). 2) The extent of increase in intracellular concentration of Daunorubicin (It was determined by test group ICD-control group ICD) was compared between MDR1 positive expression specimens and negative expression specimens, the biggest increase of intracellular Daunorubicin was found in 15 cases which were high expression of MDR1 gene but turned out low level expression or negative expression after hyperthermia. The smallest increase of intracellular Daunorubicin was found in 16 cases, which were negative expression of MDR1 gene. These findings strongly suggested that multidrug resistance of cancer cells might be overcome by hyperthermia.

**#533 Chemo-Immunotherapy In advanced and metastatic colorectal cancer: three agents for 5FU biomodulation started in early postoperative period.** Chilikidi, K.Y., Lazarev, A.F., Sholhet, J.N., Tchilklidi, N.Y., Doty, I.N. *Altai Regional Oncological Center, Barnaul, Russian Federation.*

We evaluated results of 5FU biomodulation regimen started in early postoperative period compare to 5FU monotherapy in advanced and metastatic colorectal cancer. 113 patients with Dukes' C2 and D after palliative surgery were observed. Performance state was 0-2.50 patients (group A) received IFNa2b 6 MU, methotrexate (MTX) 30 mg/sq.m, 5FU 2400 mg/sq.m and oral leucovorin (LV) 30 mg/sq.m. First course started in early postoperative period through intraperitoneal route (except for LV) followed by next courses with subcutaneous IFNa2b, intravenous bolus MTX, protracted venous infusion (PVI) 5FU and oral LV with 6 weeks interval. 63 patients (group B) received PVI 5FU monotherapy 2400 mg/sq.m. Chemotherapy was administered up to disease progression or unacceptable toxicity. Overall survival was 14.3 months in group A and 9.1 months in group B ( $P < .01$ ), one-year survival—52% and 27% ( $P < .01$ ), two-years survival—18% and 4.8% ( $P = .03$ ), time to disease progression—8.4 months and 4.3 months ( $P < .01$ ) correspondingly. No toxicities grade 3-4. No increase of postoperative morbidity. No decrease of immunity after early postoperative chemo-immunotherapy course. No differences in elder patients versus others. Therefore: proposed regimen of chemo-immunotherapy improves survival with acceptable toxicity, no increase of morbidity and no decrease of immunity in early postoperative period. The drugs are not expensive. Such combination can be used for patients with advanced and metastatic colorectal cancer, including elder.

**#534 Reconstitution of nonirradiated mice with donor marrow cells transduced with a fusion construct encoding the Phe22/Ser31 double mutant of human dihydrofolate reductase (dm DHFR) and Green fluorescence protein (GFP).** Zhao, Shi-Cheng, Barberjee, Debabrata, Takebe, Naoko, and Barlino, Joseph, R. *Sloan Kettering Institute for Cancer Research, New York, NY 10021.*

Transplantation of bone marrow cells transduced *ex vivo* with genes of interest has been successfully carried out in myeloablated recipient animals. Bone marrow ablation either by total body irradiation or by use of chemical agents is associated with considerable risk of marrow failure and therefore methods for transplantation that avoid this preparative regimen need to be developed. We have been investigating bone marrow transplantation without prior irradiation in animals using bone marrow cells transduced with drug resistant genes. In the present study, we report the use of a fusion gene construct encoding the double mutant (F22S31) of human DHFR and GFP in a retroviral vector for transduction of murine bone marrow cells.

Nonirradiated recipients were transplanted with  $2 \times 10^7$  transduced cells and the recipients were treated once a week with 300 mg/kg of methotrexate (MTX) on the 4th and 5th week posttransplant and 600 mg/kg on the 7th and 8th week posttransplant. We have previously shown that transplant recipients receiving dm DHFR transduced bone marrow cells are protected from MTX lethality administered posttransplant. Control animals were transplanted with bone marrow cells transduced with either a vector containing the GFP cDNA alone or vector not containing GFP or DHFR. Following the last MTX treatment, 6 of 8 animals in the GFP transduced group and 7 of 8 in the mock transduced group died while 7 of 8 animals in the experimental group survived the entire MTX treatment. Recovery of wbc counts, reticulocyte counts, platelet counts and emergence of MTX resistant CFU-GM colonies indicated engraftment of donor marrow cells. Green fluorescent cells were detected by FACS analysis in bone marrow preparations from recipients and in CFU-GM colonies by 23

fluorescence microscopy. Integration of the vector derived fusion gene was further demonstrated by PCR amplification of regions from the DHFR and the GFP cDNA from genomic DNA isolated from 11 day CFU-S colonies obtained from secondary transplant recipients. Our data suggests that low level engraftment can be achieved in nonirradiated recipients, and encourages clinical studies using this approach.

**#535 Chemosensitization of tumor cells by systemically delivered, ligand-directed, cationic liposome mediated wtp53 gene therapy.** Xu, Liang, Tang, Wen-Hua, Pirolo, Kathleen F., Xiang, Lalman, Ullick, David and Chang, Esther H. *Lombardi Cancer Center, Georgetown University Medical Center, Washington, DC 20007.*

Abnormalities in the p53 gene are found in over 60% of human cancers. A direct link has been suggested between the lack of functional p53 and resistance to chemotherapeutic agents. Restoration of wtp53 function has been shown to sensitize tumors to chemotherapy. However, due to limitations of delivery, current gene therapy methodologies are not able to effectively reach metastatic disease, a leading cause of cancer deaths. We have optimized transferrin or folic acid ligand-targeted cationic liposome delivery systems which efficiently delivers wtp53 preferentially to tumor cells. *In vitro* studies with various tumor cell types, including head and neck, breast, and prostate, showed a 5-fold to over 50-fold increase in sensitization to conventional chemotherapeutic agents after treatment with the ligand-liposome-p53 complex. More significantly, this systemically delivered complex was shown to specifically and efficiently target metastases, as well as primary tumors, in nude mouse xenograft models. The combination of this *in vivo* administered, targeted p53 delivery system and conventional chemotherapeutics led to significant tumor growth inhibition, even tumor regression, in multiple tumor types. Additionally, in a syngenic B<sub>16</sub> mouse melanoma model, *in vivo* administration of the ligand-liposome-p53 complex markedly sensitized the melanoma cells to cisplatin, leading to virtually complete inhibition of these lung metastases. Therefore, the use of this systemically administered highly efficient tumor cell targeted delivery system for wtp53 in combination with chemotherapy represents a more effective treatment modality for both primary tumors and metastatic cancers.

## SECTION 4: PRECLINICAL PHARMACOKINETICS/ PHARMACODYNAMICS

**#536 Pharmacokinetics of 17-allylamino(17-demethoxy)geldanamycin in SCID mice bearing MDA-MB-453 xenografts and alterations in the expression of p185<sup>erb-B2</sup> in the xenografts following treatment.** Eisenman, J., Grimm, A., Sentz, D., Lessor, T., Gessner, R., Zuhowski, E., Nemieboka, N., Egorin, M., Hamburger, A. *U of MD GCC & Dept of Path., Balto., MD 21201 & U of Pitt CI, Dept of Med. & Pharmacol., Pittsburgh, PA 15213*

17-Allylamino(17-demethoxy)geldanamycin (17-AAG) is an analogue of geldanamycin which is entering Phase I clinical trials. 17-AAG is thought to alter the expression of a number of signal transduction proteins and inhibit their transport by binding to the carrier protein, HSP90. In this study, we examined the pharmacokinetics of 17-AAG and its major metabolite, 17-aminogeldanamycin (17-AG) in normal SCID mice and in SCID mice bearing MDA-MB-453 human breast cancer xenografts following a single intravenous dose of 40 mg/kg 17-AAG. We also examined the time course of the expression of p185<sup>erb-B2</sup>, Raf-1, HSP90 and HSP70 in the tumors and in normal tissues from these mice. Plasma and tissue concentrations of 17-AAG and 17-AG were measured using an isocratic HPLC method with detection at 313 nm. The concentration times time data for 17-AAG and 17-AG were examined in normal SCID mice and in mice bearing human tumor xenografts and the data were best fit using either a one or two compartment open linear model. The concentrations of both 17-AAG and 17-AG were below detection at times greater than 7 h in normal tissues, but remained at ~0.5-1 µg/g in tumor for longer than 48 h. p185<sup>erb-B2</sup> was initially detected in the xenografts by immunohistochemistry and scored as +3. Using Western blot analysis, we determined that the concentrations of p185<sup>erb-B2</sup> in xenografts from 17-AAG treated mice were 2-fold higher than control at 2 h, but fell to below 30% of control at 7, 24 and 48 h after treatment. Tumor Raf-1 followed a similar pattern, but was much less affected. Tumor HSP70 and HSP90 were lower than control concentrations at 4 and 7 h after treatment with 17-AAG, but were elevated at 48 and 72 h. Changes in tumor volume were minor 72 h after 17-AAG treatment. Raf-1, HSP70 and HSP90 in lungs, livers, kidneys, and spleens of the animals following 17-AAG treatment were less affected. We will determine if the changes in these proteins are observed after multiple doses of 17-AAG and whether such changes are associated with tumor regression. (Supported by NCI Contract: N01-CM-57199)

**#537 2-Imidazolyl disulfides (DS): A new class of thioredoxin (Trx) reactive antitumor agents with a novel mechanism of action.** Powis G., Kirkpatrick D.L., Hashash A., Egorin M., Vogt A., & Lazo J. *Arizona Cancer Center, Tucson AZ, Proix Pharmaceuticals LP, Pittsburgh, University of Pittsburgh, Pittsburgh PA.*

The DS are a new class of antitumor agents soon to enter clinical trial. They have as their primary target the redox protein Trx which is found over-expressed by a number of human primary tumors. Experimental and clinical correlative studies have shown Trx to be associated with increased rates of tumor growth and inhibited apoptosis. A synthetic program using parallel synthesis identified the 2-imidazolyl DS from a library of over 700 mono-DS and bis-DS as the most potent antitumor agents and inhibitors of Trx. DS distribution was investigated using [ $^{14}$ C] benzyl 2-imidazolyl DS (PX-36). When added to fresh human blood, 99% of the radioactivity was bound irreversibly to plasma protein. Female Balb/C mice were injected i.v. with [ $^{14}$ C] PX-36. The peak radio-activity fell with an initial half life of 2 hr. There was also acid soluble radioactivity in the plasma which peaked at 15 min and fell with a half life of 2 hr and had almost completely disappeared by 8 hr. In 24 hr 36.1% of the administered radioactivity was excreted in the urine. In a separate study [ $^{14}$ C]PX-36 was administered to mice with 1 g s.c. A549 lung tumors. Tumor showed higher  $^{14}$ C-radioactivity than lung and heart at 3–48 hr but when corrected for plasma content of the tissue none of the  $^{14}$ C-radioactivity was tissue associated. Additional studies in which PX-36 and 1-methylpropyl 2-imidazolyl DS (PX-12) were administered i.v. to mice at doses of 30 and 25 mg/kg failed to detect any unchanged drug in the plasma ( $>0.1$   $\mu$ g/ml) at 5 min using a sensitive HPLC method. The results suggest that the DS binds irreversibly to plasma proteins and then *in vivo* is slowly removed from this binding to give an acid soluble form which is excreted in the urine. Since no  $^{14}$ C-radioactivity could be found in the tumor it is anticipated that a reaction product of PX-36 in the plasma or an alteration of the plasma redox status through thioalkylation of Trx is responsible for antitumor activity.

**#538 Metabolic and mechanistic aspects of 8-chloro-adenosine and 8-chloro-cAMP-mediated cytotoxicity in multiple myeloma cells.** Gandhi, Varshat, Ayres, Maryt, Krett, Nancy L.,\* and Rosen, Steve T.\* (University of Texas M.D. Anderson Cancer Center, Houston, TX and \*Lurie Comprehensive Cancer Center, Northwestern Univ., Chicago, IL.

Our previous studies demonstrated that both 8-chloro-cAMP (8-Cl-cAMP) and 8-chloro-adenosine (8-Cl-Ado) induce apoptosis in a number of multiple myeloma (MM) cell lines that are resistant to traditional chemotherapeutic agents (Clin. Cancer Res. 3:1781, 1997). Additional studies showed that 8-Cl-cAMP-mediated cytotoxicity was due to its conversion to the free nucleoside 8-Cl-Ado (Blood 92:2893, 1998). These data suggested that the mechanism of action of 8-Cl-cAMP or 8-Cl-Ado is via a separate route than either the glucocorticoid or protein kinase A signaling pathway. Because 8-Cl-Ado is a ribonucleoside analog, we investigated its metabolic conversion in the MM cell lines. When MM.1 cells were incubated with different concentrations of 8-Cl-Ado, the drug was transported to cells and metabolized to its triphosphate, 8-Cl-ATP. Cells accumulated mean of 25, 50, 124, 145  $\mu$ M 8-Cl-ATP after a 3-hr incubation with 1, 3, 10, and 30  $\mu$ M 8-Cl-Ado, respectively. The accumulation of the analog triphosphate was also dependent on time and reached  $>400$   $\mu$ M by 12 hr. Parallel to accumulation, there was a decline in the endogenous level of ATP pool, which was decreased to  $<40\%$  of control values after a 12-hr incubation with 8-Cl-Ado. Although DNA synthesis was not affected at these concentrations or time, there was a time-dependent decrease in RNA synthesis reaching  $<50\%$  of control value by 12 hr. Cells incubated with 8-Cl-cAMP in a medium containing serum that had not been heated (to maintain phosphodiesterase) also accumulated 8-Cl-ATP albeit at a 50% slower rate than that observed with 8-Cl-Ado. The formation of 8-Cl-ATP from 8-Cl-cAMP was inhibited  $>85\%$  by 3-isobutyl-1-methylxanthine, which blocks the action of phosphodiesterase, indicating that 8-Cl-cAMP was converted to 8-Cl-Ado followed by its phosphorylation to make 8-Cl-ATP. Taken together these data suggest that in MM cells the cytotoxic action of 8-Cl-Ado or 8-Cl-cAMP seems to be due to accumulation of 8-Cl-ATP which is associated with a decrease in the ATP pool and inhibition of RNA synthesis.

**#539 Dog pharmacokinetics and oral bioavailability of BN80915, a novel topoisomerase I inhibitor.** Prufionosa J., Lopez S., Basart D., Celma C., Vilagellu J., Obach R., Peraire C., Principe P. Lasa Laboratorios, Barcelona, Spain (Beaufour-Ipsen Group). CIDA, Barcelona, Spain. Institut Henri Beaufour, Les Ulis, France.

Homocamptothecins (hCPT) are a novel family of anticancer agents developed on the concept of topoisomerase-1 inhibition and characterized by the unique feature of a 7-membered  $\beta$ -hydroxylactone ring that results in enhanced stability of the molecule in plasma. BN80915 has been selected for clinical development. The objective of the present study was to investigate, in male Beagle dogs, the pharmacokinetic parameters and the oral bioavailability of BN80915 administered, according to a cross-over design, at the dose of 0.2 mg/kg. A drug solution ( $\sim 130$   $\mu$ g/ml) was used both for a short intravenous infusion (10 min) and oral gavage. Blood samples were obtained at time intervals from 0 to 720 min after administration. The plasma levels of BN80915 and its corresponding lactone open ring analogue (BN80942) were measured using a validated LC-MS/MS analytical method. This technique consists in a prior extraction of the two analytes with acidic methanol and refers to a  $^{13}$ C-labelled analogue as the internal standard. The limit of quantitation is equivalent to 2 ng/ml for both analytes. A noncompartmental pharmacokinetic analysis was carried out

Plasma profiles of the lactone open ring compound (BN80942) were in parallel to those observed for BN80915, both after iv and oral administration. The following results have been obtained (expressed as mean  $\pm$  SD,  $n = 6$ ): plasma clearance  $21.5 \pm 7.5$  ml $\cdot$ min $^{-1}\cdot$ kg $^{-1}$ , distribution volume ( $V_{d_{0-1}}$ )  $2.1 \pm 0.5$  l $\cdot$ kg $^{-1}$ , terminal half-life  $1.5 \pm 0.3$  h. The compound showed a peak level equivalent to  $42 \pm 17$  ng $\cdot$ ml $^{-1}$  after 0.7  $\pm$  0.6 h after oral administration. The ratios  $AUC_{BN80942}/AUC_{BN80915}$  were equivalent to 0.3 and 0.4, after iv and oral administration, respectively. Oral absolute bioavailability in dogs has been found equivalent to  $60 \pm 12\%$ .

**#540 Biotransformation of  $^{14}$ C-BN80915, a novel e-ring modified topoisomerase I inhibitor, after single dose administration in rats.** Celma C., Lopez S., Solà J., Prufionosa J., Vilagellu J., Obach R., Peraire C., Principe P. Lasa Laboratorios, Barcelona, Spain (Beaufour-Ipsen Group). CIDA, Barcelona, Spain. Institut Henri Beaufour, Les Ulis, France.

BN80915 is a novel homocamptothecin (hCPT) characterized by the unique feature of a 7-membered  $\beta$ -hydroxylactone ring that results in enhanced stability of the molecule in plasma. The compound is a new synthetic topoisomerase-I analogue whose pharmacological activity is being extensively investigated as it undergoes clinical development.

The main excretion routes of the compound have been studied in male and female Sprague-Dawley rats after short (10 minutes) intravenous (iv) infusion and oral administration of 1 mg/kg (100  $\mu$ Ci/kg). Urine and faeces were collected at different time intervals from 0 to 120 h; bile samples were collected at time intervals between 0 and 48 h and blood plasma sample between 0 and 24 h. The results indicate that 1) after iv and oral administrations the compound is mainly recovered in faeces (69–74%); 2) urinary recovery is approximately 16%. The remaining radioactivity was found in wash-outs (about 5%), GI tract (1–7%), carcass (0.4–1%) and skin (0.4–0.6%). In faeces and urine, the elimination of  $^{14}$ C-BN80915 is produced mainly through bio-transformation to a non active metabolite (P-20). This same metabolite has been found after metabolic transformation of the compound by liver microsomes isolated from several species. In parallel, minor quantities of BN80915 and its corresponding open lactone ring analogue (BN 80942) were also present but in minor quantities. In faeces two minority metabolites appears also to be present. Spectroscopic analysis conducted with the P-20 metabolite suggests that this compound is characterised by a modified 7-membered  $\beta$ -hydroxylactone ring. LC-MS/MS analysis is in progress to elucidate the chemical structure of the P-20 metabolite.

**#541 Pharmacokinetics of the cyclin dependent kinase inhibitors Olomoucine, CYC201 and CYC202 in Balb C mice after iv administration.** Raynaud, F., Nutley, B.P., Goddard P., Fisher P., Marriage H., Lane D., Workman P. CRC Centre for Cancer Therapeutics Institute of Cancer Research Cotswold Road Sutton Surrey SM2 6AT United Kingdom, Cyclacel Limited, Dundee Technopole, James Lindsay Place, Dundee DD1 5JJ, United Kingdom.

Olomoucine, CYC201 and CYC202 are inhibitors of cyclin dependent kinase 2. Studies have shown that the cytotoxicity of these compounds in ovarian carcinoma cell lines A2780 depends upon the length of exposure and is optimal after 16 h (1 cell cycle). In this study, we determined the maximum tolerated dose and pharmacokinetic properties of the 3 compounds in female Balb C mice. Olomoucine was tolerated at 100 mg/kg iv in 50 mM HCl saline and the other 2 analogs at 50 mg/kg. Liquid chromatography with mass spectrometry on a triple sector instrument with selected reaction monitoring provides a specific and sensitive method to measure all these analytes with a limit of detection of 1 ng/ml. Pharmacokinetics performed at 50 mg/kg iv in 50 mM HCl saline were analysed with Winnonlin compartmental analysis. Results showed very rapid plasma clearance for all 3 compounds. The clearance was lowest for CYC202 (2.24 ml/g/h) when compared with Olomoucine (4.06 ml/g/h) and CYC201 (11.3 ml/g/h). Tissue distribution was evaluated for Olomoucine, CYC201 and CYC202 in animals bearing the colon 26 murine tumour. Liver, kidney, spleen and tumour showed very rapid drug uptake for all 3 analogs. However, CYC202 showed the best tissue distribution with tumour to plasma ratio of 0.71 compared to 0.45 for Olomoucine and 0.18 for CYC201. Tissue  $C_{max}$  levels and clearance observed for CYC202, when considered in the light of the length of exposure needed for *in vitro* activity, suggests that continuous or repeated administration will be needed to achieve optimal *in vivo* antitumour activity.

This work was supported by the Cancer Research Campaign and by Cyclacel Limited

**#542 Normal-phase separation of XK469 enantiomers (R: NSC-698215; S: NSC-698216) applied to preclinical pharmacology.** RA Wiegand, TD Doyle<sup>1</sup>, CK Grieshaber, PM LoRusso, J Kassab, BR Jasli, and RE Parchment. Karmanos Cancer Institute, Wayne State University, Detroit MI 48201 and <sup>1</sup>Product Quality Research, CDER, US FDA, Rockville, MD.

XK469 is a water soluble member of a novel quinoxaline family that is broadly active against murine and human tumors. XK469 exists as two stereoisomers that differ in toxicity to normal myeloid progenitors in human and animal bone marrow. Given this stereo-specific pharmacology, a method was developed to quantify R and S isomers in biological fluids. The Phenomenex Chirex 3005 column, a "Brush" or Pirkle type of chiral sta-



tionary phase (CSP) made from an optically pure amino acid derivative covalently bonded to gamma-aminopropyl-silicized silica gel, was selected to provide at least these points of interaction with the aromatic nitrogens and carboxylic acid group in XK469. Optimized mobile phase consisted of 47.5:47.5 heptane:isopropanol:formate buffer (0.4% formic acid and 0.6% ammonium hydroxide). Autosampler and column temperatures were set at 4° and 25°C, respectively, injection volume 100 µL, and run-time 60 minutes at 1.0 mL per minute. Plasma samples were treated with methanol (1:2, v/v) and microfuged to remove protein, the methanol-plasma solution mixed into 3 mL 0.2 M ammonium acetate (pH 5.0), and XK469 extracted with a 1 cc Waters C18 Sep-Pack column. The methanol eluent from the SPE was dried under N<sub>2</sub> at 50°C, reconstituted with mobile phase, clarified by microcentrifugation (10 minutes, 10,000 rpm), and analyzed by HPLC using detection at 335 nm. Both isomers are stable for 1 hour in whole blood at 37°C. Standard curves, prepared in human plasma by spiking standards dissolved to 500 µg/mL in ethanol, were linear over the range of 0.1–50 µg/mL ( $r = 0.99$ ). At efficacious dose levels (150 mg/m<sup>2</sup>), BDF<sub>1</sub> mice rapidly and extensively converted (S)XK469 into R, but (R)XK469 is cleared from plasma with a beta t<sub>1/2</sub> ~4–8 hours with little conversion to S. Rat, dog, and monkey also converted (S)XK469 to R in pilot PK studies by the NCI. Therefore, administration of (S)XK469 actually results in exposure to the R isomer, so the S isomers cannot be studied *in vivo* unless its conversion to R is blocked. Furthermore, the *in vivo* biological activities of (R) and (S)XK469 should be identical in these species but unknown at this time in the human.

**#543 Preclinical pharmacology of novel substituted benzimidazole-potent inhibitors of poly (ADP-ribose) polymerase.** Calabrese C.R, Thomas H.D, Batey M.A., Boritzki T., Zhang K., White A.W., Curtin N.J., Griffin R.J., Golding B.T., Hostomsky Z., Calvert A.H., Newell D.R.—University of Newcastle upon Tyne, UK and Agouron Pharmaceuticals, San Diego, USA.

The nuclear enzyme poly (ADP-ribose) polymerase (PARP) is an attractive target for potentiation of DNA damaging chemo- and radiotherapy due to its involvement in DNA repair. The benzimidazole-4-carboxamides are a novel class of PARP inhibitors shown to effect potent inhibition of the enzyme *in vitro* and potentiate the activity of DNA damaging agents in a number of human tumour cell lines. Preliminary *in vivo* studies with the benzimidazole NU1085 (K<sub>i</sub> = 6 nM using recombinant human PARP) required a vehicle of 40% PEG<sub>300</sub> in saline to achieve a maximum dose of 40 mg/kg i.p. In order to increase the aqueous solubility of NU1085, a phosphate pro-drug of the compound has been synthesized and evaluated *in vitro* for release to parent compound using fresh human plasma. Also, two novel benzimidazole compounds bearing solubilising substitutions have been synthesized (compounds III and IV, K<sub>i</sub> values of 7.5 and 4.5 nM). For the phosphate prodrug of NU1085, cleavage (HPLC analysis) proceeded slowly (t<sub>1/2</sub> value for cleavage of 400 ± 48 min in fresh human plasma) with limited conversion (<1% by 24 h) observed in controls. Both of the substituted benzimidazoles were soluble in saline and pharmacokinetic studies performed at 25 mg/kg i.p. In female C57/B16 mice, compound III was eliminated rapidly but compound IV more slowly (t<sub>1/2</sub> values of 18 and 134 min, respectively) compared with NU1085 (t<sub>1/2</sub> 30 min). Tissue distribution studies (in CD-1 nude mice bearing LoVo human colorectal cancer xenografts) 30 and 60 min after treatment (50 mg/kg i.p) demonstrated that distribution into brain was limited (<1.5 µM) for both compounds III and IV at 30 min, consistent with that observed for NU1085. Tumour penetration was high for both of the substituted benzimidazoles in comparison with NU1085 (8, 32 and 6 µM, respectively, at 30 min). In conclusion, although the developed NU1085 phosphate prodrug showed unfavourable characteristics (poor rate of cleavage to parent compound *in vitro*) the compounds substituted with an effective solubilising group maintained potent PARP inhibitory activity without compromising pharmacological distribution and are currently undergoing further evaluation.

**#544 Pharmacokinetics of the antileukemic immunotoxin, TXU (anti-CD7)-pokeweed antiviral protein, in chimpanzees and adult patients.** Chen, Chun-Lin; Bellomy, Kelly; O'Neill, Karen; Messinger, Yoav; Johnson, Trisle; Myers, Dorothea; Uckun, Fatih M., Parker Hughes Cancer Center, Hughes Institute, St. Paul, MN.

The purpose of the present study was to evaluate the toxicity and pharmacokinetics of the CD7 antigen directed antileukemic agent TXU-PAP in chimpanzees and adult patients. At a total dose level of 100 µg/kg, TXU-PAP was well tolerated by 6 chimpanzees. The only side effects were a transient elevation of the liver enzyme ALT between days 2 and 14 without a concomitant rise in total bilirubin levels and a decrease of the serum albumin levels between days 1 and 5 without any concomitant weight gain or peripheral edema. TXU-PAP showed favorable pharmacokinetics in chimpanzees with a plasma elimination half life of 5.1–12.0 hours and a systemic clearance of 5.8–15.1 mL/h/kg. TXU-PAP was well tolerated by adult volunteers who received a single 5 µg/kg iv infusion of TXU-PAP. TXU-PAP showed very favorable pharmacokinetics in these individuals with a relatively long plasma elimination half life of 12.4 ± 1.4 h; mean residence time of 17.9 ± 2.0 h and a slow systemic clearance of 2.7 ± 0.7 mL/h/kg. To our knowledge, this is the first report of a clinical pharmacokinetics study of an anti-CD7 PAP immunconjugate in chimpanzees and human subjects.

The favorable pharmacokinetic characteristics of TXU-PAP in combination with its low toxicity provides the basis for further investigation of TXU-PAP as a potential anti-leukemic agent.

**#545 Cellular determinants for the interactions of 5-fluorouracil (5-FU) and Irinotecan (CPT-11) in human colon carcinoma cell lines.** Mans, D.R.A., Grivklich, I., Peters, G.J., Neumann, J.M., Sporleder, H., Schwartzmann, G. South-Am. Off. Anticancer Drug Dev. (SOAD), Luth. Univ., Canoas, RS, Brazil; Dept. Biochem., Fed. Univ. Rio Grande do Sul, Porto Alegre, RS, Brazil; Dept. Med. Oncol., Free Univ. Hosp., Amsterdam, The Netherlands; Transpl. Unit, Hosp. Santa Casa, Porto Alegre, RS, Brazil.

Assessing combinations of 5-FU and CPT-11 for their anti-proliferative effects in the SW620, HT-29, and SNU-C4 human colon carcinoma cell lines, we observed additive to synergistic interactions with 2 h IC<sub>20</sub> CPT-11 preceding 5-FU. The reversed sequence as well as simultaneous drug treatment acted antagonistic to additive. These results could be partially related to the introduction of more persistent DNA lesions with the former sequence. To better understand the molecular basis for these interactions, we assessed the effects of CPT-11 or 5-FU on cellular determinants relevant to drug cytotoxicity. Thus, cells were exposed for 2 or 24 h to IC<sub>20</sub>, IC<sub>60</sub>, or IC<sub>90</sub> 5-FU or CPT-11, after which they were assessed for possible changes in DNA-topoisomerase complex formation, plasma membrane integrity, DNA excision repair capacity, and cell cycle phase distribution. For these purposes we made use of an SDS precipitation assay, lactate dehydrogenase (LDH) leakage into the culture medium, a [<sup>3</sup>H-methyl]thymidine incorporation assay, and fluorescence-activated cell sorting, respectively. Data with untreated cells were used as control values. None of the drug treatments caused significant alterations in DNA-topoisomerase complex formation, LDH release, or cell cycle phase distribution. However, [<sup>3</sup>H-methyl]thymidine incorporation in CPT-11-treated cells increased with more prolonged exposure times and higher drug concentrations, suggesting a time- and dose-dependent introduction of DNA damage by CPT-11 that was amenable to excision repair mechanisms. Significant incorporation of [<sup>3</sup>H-methyl]thymidine in 5-FU-treated cells was only seen after exposure to IC<sub>20</sub> for 2 h, suggesting that excision repair mechanisms were only operative on the damage introduced by low doses of, and short exposure periods to this drug. Together, our data suggest that interference with the DNA repair machinery is an important determinant for the sequence-dependent anti-proliferative effects of CPT-11–5-FU, providing a possible explanation for our previous findings. Studies on the involvement of alterations in relevant enzyme activities are in progress.

**#546 Pharmacokinetics of S(-)-XK469 (NSC 698216) in CD1F2 mice and Fischer 344 rats.** Chen, Kenneth K., Jiang, Chun, Zheng, Helen, H., Chiu, Ming H., and Joseph M. Covey. Colleges of Pharmacy, Medicine, & Comprehensive Cancer Center, The Ohio State University, Columbus, OH 43210; The National Cancer Institute, Bethesda, MD 20892.

XK469 (NSC 697887), (±)-2-[4-[(7-Chloro-2-quinoloxalyl)oxy]phenoxy]propionic acid, is an analog of the herbicide Assure<sup>®</sup>, which has been found to possess antitumor activity especially against murine solid tumors and human xenografts. Both the R(+) (NSC 698215) and S(-) isomers are equally cytotoxic. The titled study was carried out using a newly developed reversed-phase HPLC method. Drug along with the added 7-fluoro-XK469 as the internal standard in plasma was isolated by solid-phase extraction and the mixture was eluted isocratically on a 10 µm 4.6 × 250 mm C18 column with a mobile phase consisting of 70% methanol in 10 mM, pH 4.1 potassium phosphate buffer. The analytes were detected by UV at 330 nm with retention times of 16.8 and 9.8 min, respectively. The assay was validated in both mouse and rat plasma which showed a LOQ of 0.2 and 0.1 µg/ml, using 200 and 500 µL samples, respectively. The within day CVs in mouse plasma were 7.7, 4.8, and 5.0% (n = 6) for 0.2, 0.5, and 1.5 µg/ml, respectively, and similar values in rat plasma. The between day CVs were 6.0 and 7.3% for mouse and rat plasma, respectively (n = 6). XK469 was stable in plasma and binds to animal plasma proteins to the extent of 95%. There was a slight enrichment in plasma (70–90%) over red blood cells. Plasma concentration-time profiles in both mice and rats displayed biphasic declines and their pharmacokinetics (PKs) were describable by a two compartmental model. In mice at 10 mg/kg i.v. dose, plasma levels >40 µg/ml were produced at 0.5 hr, which increased to 475 µg/ml (1.4 mM) at 100 mg/kg dose. The initial t<sub>1/2</sub> was short (<3 m) and the terminal t<sub>1/2</sub> values fluctuated with a mean value of 8.1 h (5.4–15.1 h). MRT values were rather constant with a mean value of 5.9 h (5.6–6.2 h). AUC and Cmax values increased linearly with an increase in dose. PKs of XK469 in the rat given i.v. doses of 10–50 mg/kg showed similar PK properties with a longer mean terminal t<sub>1/2</sub> of 43.6 h (31.4–66.7 h). Thus, PKs of XK469 show linearity within the dose range studied and pharmacologically active plasma levels were achievable. Supported by NCI Contract CM-57201.

**#547 Preclinical study of antitumor Prostaglandin<sub>13</sub>,14-dihydro-15-deoxy-Δ<sup>7</sup>-PGA<sub>1</sub> methyl ester (TEI-9826) *in vitro* and *in vivo*.** Fukushima S.<sup>1</sup>, Shirakawa S.<sup>1</sup>, Kishimoto S.<sup>1</sup>, Takeuchi Y.<sup>1</sup>, Suzuki M.<sup>2</sup>, Furuta K.<sup>2</sup>, Noyori R.<sup>3</sup>, Sasaki H.<sup>4</sup>, Yamori T.<sup>5</sup>, Kurozumi S.<sup>6</sup>, and Fukushima M.<sup>7</sup> <sup>1</sup>Kobe-Gakuin Univ., Kobe 651, <sup>2</sup>Gifu Univ., Gifu 501, <sup>3</sup>Nagoya Univ., Nagoya 464, <sup>4</sup>Jikei Univ., Sch. Med., Tokyo 105, <sup>5</sup>Jpn. Fdn. Cancer Res., Tokyo 170, <sup>6</sup>Teijin LTD., Tokyo 100, <sup>7</sup>Aichi Cancer CTR, Nagoya 464, Japan.

13,14-Dihydro-15-deoxy- $\Delta^7$ -PGA<sub>1</sub> methyl ester (TEI-9826) is one of the candidate antitumor prostaglandin analogs for clinical use. We have studied preclinically on biological stability *in vitro*, antitumor activity *in vitro* and *in vivo*, toxicity, and pharmacokinetics of this compound. TEI-9826 was rapidly hydrolyzed to carboxylic type (TOK-4528) ( $t_{1/2} < 30$  sec.), but TOK-4528 was stable as well as  $\Delta^7$ -PGA<sub>1</sub> in rat and mouse serum. These two analogs exhibited the same antitumor activity as other analogs including  $\Delta^7$ -PGA<sub>1</sub> and  $\Delta^7$ -PGA<sub>1</sub> *in vitro* against Colon 26 tumor cells. TEI-9826 exhibited unique antitumor profiles with the COMPARE program using 38 human tumor strains *in vitro*. Furthermore, TEI-9826 showed only little cross-resistance against CDDP resistant ovarian cancer cells: IC<sub>50</sub> against A2780 and A2780<sup>CDDP</sup> (resistant) were 0.072 and 1.7  $\mu$ g/ml for CDDP, 0.7 and 1.4  $\mu$ g/ml for TEI-9826, respectively. For clinical dosage form, TEI-9826 was integrated in lipid microspheres (Lipo TEI-9826). Growth inhibition effect by Lipo TEI-9826 against Colon26 tumor inoculated sc in mice depended on administration route. Namely, at 80 mg/kg, no activity was observed at daily bolus iv, but significant activity was observed at daily ip, daily sc, every other day sc, and 4 times a day continuous (5 min) iv. PK study suggested that maintaining blood level of TEI-9826 and/or TOK-4528 was essential for antitumor effect. At constant rate iv infusion over 5 days, Lipo TEI-9826 exhibited tumor growth suppressive effect against Walker 256 tumor sc inoculated in rat. (growth rate at the day after end of infusion: non-treatment, 950%; 80 mg/kg/day, 470%; 160 mg/kg/day, 170%). Lipo TEI-9826 also exhibited significant antitumor effect against A2780<sup>CDDP</sup> *in vivo* (Cancer Res., In press). These tumor suppressive effects might be cytostatic at these dose. Although fatal dose was 300 mg/kg at bolus iv, all rats (n=5) were survived even at this dose in the case of 60 min. Continuous infusion. (Supported by a grant from MHW of JAPAN).

**#548** *In vivo* toxicity and pharmacokinetic features of the Janus kinase 3 (JAK3) inhibitor WHI-P131 [4-(4'-hydroxyphenyl)-amino-6,7-dimethoxyquinazoline]. Uckou, Falh M.; Ek, Orur; Liu, Xing-Ping; Chen, Chun-Lin. *Parker Hughes Cancer Center, Oncology, Pharmaceut. Sci., Chemistry, Immunology, Drug Discovery Prog., Hughes Institute, St. Paul, MN.*

WHI-P131 [4-(4'-hydroxyphenyl)-amino-6,7-Dimethoxyquinazoline] is a potent and selective inhibitor of the Janus kinase 3 (JAK3) which triggers apoptosis in human acute lymphoblastic leukemia (ALL) cells. In this preclinical study, we evaluated the pharmacokinetics and toxicity of WHI-P131 in rats, mice, and cynomolgus monkeys. Following intravenous (i.v.) administration, the terminal elimination half-life of WHI-P131 was 80.9  $\pm$  23.1 min in rats, 103.4  $\pm$  61.6 min in mice and 45.0 (41.4, 48.5) min in monkeys. The intravenously administered WHI-P131 showed a very wide tissue distribution in mice. Following intraperitoneal (i.p.) administration, WHI-P131 was rapidly absorbed with  $t_{1/2\alpha}$  of 8.4  $\pm$  0.7 min in rats and 7.4  $\pm$  0.7 min in mice, and the time to reach the maximum plasma concentration ( $t_{max}$ ) was 24.7  $\pm$  1.7 min in rats and 10.0  $\pm$  0.6 min in mice. Subsequently, WHI-P131 was eliminated with a terminal elimination half-life of 45.6  $\pm$  5.5 min in rats and 123.6  $\pm$  48.8 min in mice. The estimated intraperitoneal bioavailability was 95% for rats as well as mice. WHI-P131 was quickly absorbed after oral administration in mice with a  $t_{max}$  of 5.8  $\pm$  1.1 min but its oral bioavailability was relatively low (29.6%). The elimination half-life of WHI-P131 after oral administration was 297.6  $\pm$  46.4 min. WHI-P131 was not acutely toxic to mice at single intraperitoneal bolus doses ranging from 0.5 mg/kg to 250 mg/kg. Two cynomolgus monkeys treated with 20 mg/kg WHI-P131 and one cynomolgus monkey treated with 100 mg/kg WHI-P131 experienced no side effects. Plasma samples from WHI-P131-treated monkeys exhibited potent antileukemic activity against human ALL cells *in vitro*. To our knowledge, this is the first preclinical toxicity and pharmacokinetic study of a JAK3 inhibitor. Further development of WHI-P131 may provide the basis for new and effective treatment programs for relapsed ALL in clinical settings.

**#549** Preclinical assessment of PSP-94 for the treatment of hormone refractory prostate cancer. Garde, S.V., Fraser, J.E., Chambers, A.F., Illichuk, T.T. *Procyon Biopharma Inc., 746 Baseline Rd., London, ON, Canada N6C 5Z2, London Regional Cancer Centre, Cancer Research Labs, London, ON, Canada N6A 4L6.*

Procyon BioPharma's PSP-94 prostate cancer therapeutic development program is based on the discovery that the 94 amino acid protein, prostate secretory protein (PSP-94), has pro-apoptotic properties and can inhibit the growth of hormone refractory prostate cancer. PSP-94 is a small cysteine rich protein and is one of three major proteins found in human seminal plasma. The protein is produced by prostatic epithelial cells and its expression is decreased during hormone ablation therapy. Our goal has been to demonstrate the feasibility of using PSP-94 in clinical trials. The results of our preclinical assessment are presented here.

PSP-94 can induce apoptosis *in vitro* in PC-3 and DU145 prostate cancer cell lines, but not in CHO or human primary fibroblast culture cells. Apoptosis was demonstrated by DNA fragmentation, Bax/Bcl-2 levels and the Cell Death Detection ELISA<sup>PLUS</sup> assay system, and a dose dependent effect was seen. PSP-94 also produced a dose dependent decrease in cell number as detected by the MTS cell proliferation assay.

Pharmacokinetic (PK) analyses and *in vivo* efficacy studies were also conducted. The data from PK analysis showed that PSP-94 has a slow clearance rate (30 ml/hr/kg) from blood and a terminal half-life between 22-29 hours in rats. Efficacy studies, in which nude mice with human hormone refractory prostate cancer tumours (PC-3) were treated once a day with PSP-94, showed a significant reduction in tumour growth with no evidence of toxicity. In conclusion, Procyon Biopharma Inc. has demonstrated the feasibility of using PSP-94 in clinical trials for treatment of hormone refractory prostate cancer. It is suggested that PSP-94 may function to regulate prostate growth by an autocrine pathway which is lost during hormone ablation therapy and can be replaced by providing an external source of PSP-94. The most likely method of action is induction of apoptosis with notable specificity and negative potential for toxicity.

**#550** Interrelationships of paclitaxel disposition, infusion duration and Cremophor EL kinetics in cancer patients. Sparreboom A., Van Zuylen L., Verweij J., Moss K., Brouwer E., and Gianni L. *Rotterdam Cancer Institute, The Netherlands; Tumor Biology Center Freiburg I. Br., Germany; Istituto Nazionale Tumori, Milan, Italy.*

Cremophor EL (CrEL) is a castor oil surfactant used as a vehicle for formulation of a variety of poorly water-soluble agents, including paclitaxel. Recently, we found that CrEL can influence the *in vitro* blood distribution of paclitaxel by reducing the free-drug fraction, thereby altering drug accumulation in erythrocytes (A. Sparreboom et al, Cancer Res., 59: 1454-1457, 1999). The purpose of this study was to investigate the clinical pharmacokinetics of CrEL, and to examine interrelationships of paclitaxel disposition, infusion duration and CrEL kinetics. The CrEL plasma clearance, studied in 17 patients for a total of 28 courses, was time-dependent and increased significantly with prolongation of the infusion duration from 1 to 3 to 24 h ( $P < 0.034$ ). The blood:plasma ratio of paclitaxel was independent of the concentration at the lowest dose tested (135 mg/m<sup>2</sup>), but significantly decreased from 0.99  $\pm$  0.12 to 0.68  $\pm$  0.08 toward the end of 3-h infusions at 175 or 225 mg/m<sup>2</sup>. An indirect response model, applied based on use of a Hill function for CrEL concentration-dependent alteration of *in vivo* blood distribution of paclitaxel, was used to fit experimental data of the 3-h infusion ( $r^2 = 0.733$ ;  $P < 0.001$ ). Simulations for 1- and 24-h infusions using predicted parameters and superposition of CrEL kinetic data revealed that both short and prolonged administration schedules induce a low relative net change in paclitaxel blood distribution. Our pharmacokinetic/pharmacodynamic model demonstrates that CrEL causes disproportional accumulation of paclitaxel in plasma in a 3-h schedule, but is unlikely to affect drug pharmacokinetics in this manner with alternative infusion durations.

**#551** Investigation of bioavailability and pharmacokinetics of treosulfan capsules in patients with relapsed ovarian cancer. Hilger R.A., Jacek G., Oberhoff, C., Kredtke S., Baumgart J., Seeber S., Scheulen M.E. *Dept. Int. Medicine, West German Cancer Center, University of Essen; medac, Hamburg; Germany.*

*Purpose:* Treosulfan (L-threitol-1,4-bis-methanesulfonate, Ovastat®) is a prodrug of a bifunctional alkylating agent with activity in ovarian carcinoma and other solid tumors. For a pharmacological study of the bioavailability of treosulfan capsules, patients with relapsed ovarian carcinoma were treated with alternated doses of oral and intravenous treosulfan of 1.5 or 2.0 g daily for 5 to 8 days. *Methods:* A sensitive method for the determination of treosulfan in plasma and urine by reversed-phase high-performance liquid chromatography had been developed previously. In twenty plasma and urine courses pharmacokinetic analyses of treosulfan were carried out after intravenous dosing in comparison with twenty courses of oral administration. *Results:* The bioavailability

$$f = \frac{AUC_{po} \times D_{iv}}{AUC_{iv} \times D_{po}} = 0.96 \pm 0.17$$

(mean  $\pm$  SD) was calculated with  $AUC_{po} = 82.1 \pm 39.4 \mu$ g/ml  $\times$  h and  $AUC_{iv} = 85.4 \pm 30.3 \mu$ g/ml  $\times$  h. The peak plasma concentration  $C_{max}$  (29  $\pm$  14  $\mu$ g/ml vs 65  $\pm$  23  $\mu$ g/ml) was significantly ( $p < 0.01$ ) higher after intravenous administration and a  $t_{max} = 1.5 \pm 0.34$  h was calculated after oral dosing. Terminal half-life of treosulfan was in the range of 1.8 h. Mean urinary excretion of the parent compound was about 15% of the administered total dose during 24 h (range 6-26%). *Conclusions:* According to its high and relatively constant bioavailability treosulfan capsules guarantee a sufficient noninvasive treatment alternative. The feasibility of a reliable oral administration of treosulfan may be the basis for the development of long-term low-dose outpatient treatment of patients with malignant diseases.

**#552** Pharmacokinetics and oral bioavailability of BN80915, a novel topoisomerase I inhibitor, after single dose administration in rats. Menologos A., Celma C., Cordero J.A., Basat D., Obach R., Peraire C., Principe P. *Lasa Laboratorios, Barcelona, Spain (Beaufour-Lassen Group). Institut Henri Beaufour, Les Ulis, France.*

Homocamptothecin (hCPT) are a novel family of anticancer agents developed on the concept of topoisomerase-1 inhibition, with camptothecin as the original prototype. hCPT are characterised by the unique feature of a 7-membered  $\beta$ -hydroxylactone ring that results in enhanced



stability of the molecule in plasma. Among the newly synthesised compounds, BN80915 has been selected for clinical development and the pharmacological activity of this hCPT being extensively studied. The pharmacokinetic parameters and oral bioavailability of BN80915 have been evaluated in Sprague-Dawley male rats at the dose of 1 mg/kg. The compound was given by intravenous route (iv) as a short infusion (10 minutes) and by oral gavage as a suspension. Nine to twelve blood samples from 0 to 720 min were obtained from each animal from the retro-orbital plexus under light anaesthesia. Both BN80915 and its corresponding open lactone ring analogue (BN80942) were used for a LC-MS/MS analytical measurement (100 µl plasma samples). This analytical method consists in a prior extraction of the analytes with acidic methanol and refers to the <sup>13</sup>C-labelled analogue as the internal standard. The quantitation limit is 2 ng/ml for BN80915 and BN80942. The following parameters have been obtained using a non-compartmental pharmacokinetic analysis of plasma levels (results expressed as mean ± SD, n = 6): plasma clearance 23 ± 0.2 ml·min<sup>-1</sup>·kg<sup>-1</sup>, distribution volume (V<sub>dss</sub>) 2 ± 0.5 l·kg<sup>-1</sup>, terminal half-life 103 ± 27 min and mean residence time 88 ± 29 min. Plasma concentrations of the parent compound were predominant for six hours after iv route. The ratio AUC<sub>open form</sub>/AUC<sub>BN80915</sub> was equal to 0.3, reflecting the high plasma stability of the compound. The compound is rapidly absorbed after oral administration. Peak plasma level was reached after 30 min. Maximum plasma concentration was 79.4 ± 26.6 ng·min<sup>-1</sup> and mean residence time 251 ± 170 min. Oral absolute bioavailability in rats is equivalent to 30 ± 6.9%.

**#553 A Preliminary Pharmacokinetic Evaluation of Intravenous FR901228 (Depsipeptide) Given Over 4 Hours.** Min H. Kang, Zhaoyang Li, Kenneth K. Chan, Victor Sandor, Susan Bakka, Eben Tucker, Stanley Balcerzak, Jonathan Bender, Lee Peng, Tito Fojo, William D. Figg, Susan E. Bates. *Medicine Branch, NCI, Bethesda, MD; Hematology-Oncology, Ohio State University, Columbus, OH.*

FR901228 (Depsipeptide) is a novel anticancer agent isolated from the fermentation broth of *Chromobacterium violaceum* which inhibits histone deacetylase. FR901228 is currently under phase I investigation. Toxicities to date have included neutropenia and thrombocytopenia, fatigue and nonspecific EKG changes. The purpose of this study is to characterize the pharmacokinetics of FR901228 given as a 4-hour intravenous infusion to patients with refractory solid tumors on days 1 and 5 of a 21 day cycle. Pharmacokinetic parameters were determined in 26 patients at 8 dose levels (1, 1.7, 2.5, 3.5, 6.5, 9.1, 12.7, 17.8, 24.9 mg/m<sup>2</sup>). Serial blood samples were obtained during and up to 48 hours after the infusion, and FR901228 was measured using a LC/MS/MS method. Using the ADAPT II program, four pharmacokinetic models were evaluated to describe the data. The plasma disposition of FR901228 was well described by a first-order, two-compartment pharmacokinetic model as well as a two-compartment model that incorporated saturable distribution. There was no statistical difference between the models, although the Akaike Information Criteria was slightly better in the saturable distribution model. With the first-order, two compartment model the mean volume of distribution, clearance, distribution t<sub>1/2</sub>, and elimination t<sub>1/2</sub> were 9.13 L/m<sup>2</sup>, 18.25 l/h/m<sup>2</sup>, 0.40 h, and 11.80 h, respectively. Maximum plasma concentrations for the first eight dose levels were 35.6, 42.0, 47.7, 129.9, 211.8, 235.3, 513.7, and 472.6 ng/ml, respectively. In addition, the data showed that the steady state concentration and area under the concentration-time curve of FR901228 increased in proportion to the increase in dose within the entire dose range. We concluded that the disposition of FR901228 in humans follows a first-order, two-compartment model. This pharmacokinetic model should be a useful tool in predicting FR901228 disposition, and allowing pharmacodynamic correlations in further studies.

**#554 A novel two-part phase I, dose seeking pharmacokinetic and pharmacodynamic study of ZD1839, a potent and specific inhibitor of epidermal growth factor receptor (EGFR) tyrosine kinase.** Goss, G., Hirt, H., Stewart, D., Batist, G., Miller, W., Lorimer, I., Averbuch, S., Ochs, J., Blackledge, G., Feld, R., Matthews, S. and Seymour, L. *NCI-Canada CTG IND Program. Kingston, Canada and Astra Zeneca.*

ZD1839 (Iressa™) an achiral compound with an aminoquinazoline and morpholine group, has potent, specific and reversible inhibitory effects on EGFR tyrosine kinase. Dose and time dependent effects on downstream markers of EGFR activation (c-fos mRNA) were demonstrable *in-vivo*. Preclinical toxicology suggested target organs would include skin, cornea and kidney. Early clinical and pharmacokinetic (PK) studies with limited duration of exposure (14 days) suggest the compound is suitable for daily oral administration; only mild dermal and gastrointestinal effects have been reported to date (Hammond, ASCO 1999). Phase I studies provide a unique opportunity to test dose-response and to initiate validation of surrogate efficacy endpoints. Given the high degree of interest in the compound, the feasibility of designing correlative studies for compounds of this type, and the well described difficulty in dose-selection for such compounds, we have initiated a phase I dose seeking study with ZD1839. The study incorporates traditional endpoints such as PK, toxicity, efficacy and mandatory pharmacodynamic (PD) assessment. In stage 1, patients who have undergone initial tumor-sampling (paracentesis, needle biopsy) receive escalating daily doses of ZD1839 for 28 days (3-6 patients per

dose level; 150-1000mg/day). Full toxicity, PK assessments and repeat biopsy (after 28 days) are also performed. Treatment is continued in the absence of disease progression or unacceptable toxicity. Tumor samples are examined for EGFR expression, mutations, phosphorylation and for apoptosis to derive evidence of 'biologic effect'. In stage 2, two 'active' (defined by anti-tumor or biologic effect) dose levels will be expanded by 10-15 patients with a single tumor type to better assess dose-response (anti-tumor and PD). Interim clinical and PD results will be presented.

## SECTION 5: DRUG DESIGN, METABOLISM, AND PHARMACOGENETICS

**#555 Molecular modelling based design of novel anticancer therapeutics that target the active sites of polymorphic GSTP1 proteins.** Ali-Osman, F., Buolanwini, J. *Dept. of Neurosurgery, MD Anderson Cancer Center, Houston, Texas; Univ. of Mississippi, Oxford, MS.*

The human glutathione S-transferase-pi (GSTP1), product of a polymorphic gene locus, is frequently over-expressed in human cancers and is associated with more aggressive biological behavior and therapeutic failure. A major cellular function of the GSTP1 protein is the metabolism and inactivation of electrophiles, including, several anticancer agents. In this study, we applied molecular dynamic modelling to examine the binding of anticancer agents to the 3-dimensional, crystal structure-derived active H-sites of the polymorphic GSTP1 proteins to the design as novel anticancer agents directed against these active sites. And chemical ligands. Using 4-hydroxyflorophamide (4-HIF) as a model, we observed significant differences in binding energy between the different GSTP1 proteins and 4-HIF that were consistent with the orientations of 4-HIF in the different protein-ligand complexes. Extensive hydrophobic interactions were observed between a) 4-HIF and the side chain aromatic rings of Phe8 and Tyr108 in the H-site, b) the OH of 4-HIF and the α-carbonyl oxygen of Glu in GSH and c) the P=O of 4-HIF and the OH group of Tyr108. Important van der Waals interactions included those between a) the Phe8 and the N2-chloroethyl group of 4-HIF, b) both Ile104/Val104 (involved in the GSTP1 polymorphism) and Tyr108 and the C5-C6 edge of the ring in 4-HIF, c) the proximal γ-CH<sub>3</sub> of Val35 and α-CH<sub>2</sub> of Gly205, and the chlorine of the 2-chloroethyl group of 4-HIF, and d) the NH of Gly in GSH and the proximal CH<sub>2</sub> of the chloroethyl group of the ring nitrogen of 4-HIF. By docking chemical fragments into the GSTP1 active sites, we obtained lead ligands that specifically inhibited the different GSTP1 proteins. Two of the active ligands demonstrated antitumor activities against human glioma cells and induced both cell cycle checkpoint (G2) arrest and apoptosis. We have used the ligands as leads for the production and screening of combinatorial libraries for the discovery of novel GSTP1-targeted cancer therapeutics.

**#556 Structure-Based Drug Design Of Novel Urokinase Plasminogen Activator Inhibitors.** Subasinghe, N., Hoffman, J., Rudolph, J., Soll, R., Wilson, K., Randle, T., Green, D., Lewandowski, F., Zhang, M., Bone, R., Spurlino, J., Deckman, I., Manthey, C., Zhou, Z., Sharp, C., Kratz, D., Grasberger, B., DesJarlais, R., Molloy, C.J., Illig C. *3-Dimensional Pharmaceuticals Inc., 665 Stockton Drive, Exton, PA 19341.*

The serine protease urokinase plasminogen activator (uPA) is thought to play a central role in tumor metastasis and angiogenesis. Thus, specific uPA inhibitors may be of therapeutic potential in the treatment of many types of malignancy. Ideally, a small molecule uPA inhibitor should exhibit high affinity and selectivity for uPA, be competitive, reversible, stable, and orally bioavailable with a favorable pharmacokinetic profile. We have determined a high-resolution X-ray crystal structure of a recombinant form of uPA and developed a generalized structure-based library approach for exploring S1 specificity determinants using synthetic small molecules. Novel, non-peptidic, small molecule (MW < 500) S1 templates were identified exhibiting KI's for uPA in the range of 0.1-0.8 µM. Selected S1 fragments were further optimized using iterative chemical methods to generate potent uPA inhibitors with selectivity towards a panel of related proteases, including IPA, trypsin, and thrombin. 3DP-49215 is one example in this series, with potent (KI ~ 20 nM) activity against uPA. This compound is a reversible, competitive inhibitor of uPA with no active site modifying groups and no chiral centers. 3DP-49215 and related uPA inhibitors represent a new class of chemotherapeutic agents with potential utility against a variety of human tumors.

**#557 Novel mustard analogues of EO9: DT-diaphorase inactivators and increased specificity to hypoxic tissue.** Jaffar M, Phillips RM, Lookyer SD & Stratford IJ. *School of Pharmacy and Pharmaceutical Sciences, University of Manchester, Oxford Road, Manchester, UK and Clinical Oncology Unit, University of Bradford, Bradford, West Yorkshire, UK.*

**Introduction** The indolequinone prodrug EO9<sup>1</sup> was developed as a hypoxia-selective agent. The observed hypoxic cytotoxicity *in vitro* has been related to its reductive activation to active species utilising one-electron reductive enzymes. The aerobic toxicity of EO9 has been attrib-

uted primarily to its aziridinyl function. However, a significant proportion of the aerobic toxicity may be due to metabolism by DT-diaphorase (DTD), since EO9 is a good substrate for this enzyme.<sup>2</sup> Aim To design and synthesize novel analogues of EO9 whereby the 5-aziridinyl substituent is replaced by a mustard moiety and the *di*-ol substituents are replaced by bulkier groups (e.g., Cl) to facilitate inhibition by DTD.<sup>3</sup> This study was devised to ascertain the importance of the bulky substituents at the C-2 and C-3 positions of the EO9 backbone to inhibit DTD activation under aerobic conditions, but maintain the hypoxic potency that is observed with EO9. In this way, a more hypoxia-selective agent can be generated. **Results** We report the synthesis of a series of novel analogues of EO9. These analogues were evaluated in A549 human tumour cell lines (a high expressing DTD cell line) against EO9 under aerobic and hypoxic conditions. Of particular interest, one of the compounds was approx. 1500 times less potent than EO9 (IC<sub>50</sub> EO9 0.13 µM; IC<sub>50</sub> analogue 200 µM) under aerobic conditions and only 160-fold less potent (IC<sub>50</sub> EO9 0.06 µM; IC<sub>50</sub> analogue 10 µM) under hypoxic conditions. The analogue was at least 10 times more selective to hypoxic tissue. In all cases, the *di*-chloro derivatives synthesised showed no specificity to DTD. **Conclusions** These results suggest that the presence of the mustard moiety renders the C-5 position unavailable for DNA alkylation under aerobic conditions. However, under hypoxic condition, the lone pair is free to form the alkylating aziridinyl species. However, this alone may not account for the surprisingly large decrease in aerobic toxicity. This observation, was in part, accredited to the fact that the novel analogues were not substrates for DTD and hence are not predominantly activated under aerobic conditions. Overall, we have synthesised novel bioreductive inhibitors of DTD which display a marked increase in hypoxia-selectivity. **References** <sup>1</sup>Speckamp & Oostveen USP 5079257 (1992); <sup>2</sup>Jaffer et al., (1998) *Anti-cancer drug des.*, 13, 105; <sup>3</sup>Phillips et al., *J. Med. Chem.*, (1999), in press.

**#558 Structure activity relationships for aryl/heterocyclic-2,4'-nitrophenylhydrazone anticancer activities.** Morgan, L.R., Thangaraj, K., Le Blanc, B.W., Rodgers, A.H., Boue, S.M. and Cole, R.B. *DEKK-TEC, Inc. and Chem. Dept., University of New Orleans, New Orleans, Louisiana, 70119 and 70112, resp.*

4,4'-Dihydroxybenzophenone-2,4-dinitrophenylhydrazone (A-007) demonstrated objective responses in patients with advanced cancer during a recent Phase I clinical trial. A-007 is an interesting molecule composed of a dihydroxy-*gem*-diphenyl methane, a hydrazone, and a dinitrobenzene moiety. The active pharmacophores present in A-007 have not been optimized. The present study reviews our recent experience with A-007 analogs.

Using a monolayer tissue culture assay, 13 fresh human breast cancer tissues were grown as explants in tissue culture (with a MTT assay) and used to document IC<sub>50</sub> activities for the analogs. Fusion of the *gem*-diphenyl rings produced coplanar systems, improved activities in breast cancer—[1,8-diacetoxanthraquinone-10-(2,4-DNP) and 7-hydroxy fluorenone-9-(2,4-DNP)], IC<sub>50</sub> 0.005 & 0.05 µg/ml, resp. vs references A-007 3 µg/ml & DOX 0.3 µg/ml]. Fusing A-007's =N-NH-moiety into an azapyrazidone similarly improved activity; IC<sub>50</sub> 0.5 µg/ml. A single 2- or 4-nitro group in the phenylhydrazone ring slightly improved activity (~0.02 µg/ml); absence of which or replacement with a Tosyl group reduced activity (5 µg/ml). A 2-hydroxyl or 2,2'-dihydroxyl on A-007's diphenylmethane moiety improved activity (>0.5 µg/ml). Other isosteric/functional group substitutions in any of the aryl rings (Cl, F, CH<sub>3</sub>, OCH<sub>3</sub>, COCH<sub>3</sub>) reduced activity; >5 µg/ml. Blocking the -NH (N-benzyl fluorenone-2-(2-DNP) reduced activity; IC<sub>50</sub> > 10 µg/ml.

1,8-Diacetoxanthraquinone-10-(2,4-DNP) was administered i.p. (10 mg/kg/d) on days 1 & 5 to C-57 mice bearing measurable B-16 melanomas. Responses noted were 75% TGI and 175% ILS vs 35% and 75% for A-007, resp. Minimal toxicity will be reviewed.

A model for future aryl phenylhydrazone analogs will be presented.

**#559 1-aldophosphamide-perhydrothiazines: Inverse correlation of in vivo antitumor activity and in vitro cytotoxicity and in vivo antitumor activity compared to ifosfamide.** Voelcker Georg, Pfeiffer Barbara, Schnee Annette, Hohorst Hans-Jürgen, *Gustav-Erbsen Zentrum der Biologischen Chemie, Institut für Biochemie II, Theodor-Stern Kai 7, D 60590 Germany.*

1-aldophosphamide-perhydrothiazines were developed according to our working hypothesis: the reason of cancerselectivity of oxazaphosphorine cytostatics is toxicogenation to the alkylating agent in vicinity of the target molecule DNA by exonucleases subsites of DNA polymerase  $\beta$  and/or  $\epsilon$ . To fulfill the kinetic requirements of these enzymes and to reduce overall toxicity due to toxicogenation by ubiquitous phosphodiesterases, it is necessary to establish low but long lasting steady state concentrations of activated oxazaphosphorines. This is managed by aldophosphamide-perhydrothiazines which spontaneously but slowly hydrolyse to the corresponding aldophosphamide derivatives. When equitoxic dosages of ifosfamide and 1-aldophosphamide perhydrothiazine (IAP) were tested for antitumor activity in the P388 mice leukaemia model, 80% long-time survivors (ILS > 100 d) were achieved with IAP—whereas in the ifosfamide group all mice died due to tumor growth within 60 days. Superior antitumor activity of IAP when compared with ifosfamide was even more increased in

an IAP derivative (SUM-IAP) in which one 2-chloro-ethyl-group of the alkylating function is substituted by a mesyl-ethyl group. Evaluation of tumor growth curves in mice by the back extrapolation method after treatment with IAP and SUM-IAP demonstrates a four to five log increase in antitumor activity of SUM-IAP when compared with IAP. Contrary to the results of these in vivo experiments IAP, was more cytotoxic against P388 mice leukaemia cells in vitro than SUM-IAP. The inverse correlation of in vivo antitumor activity and in vitro cytotoxicity indicates that the reasons for the increase in antitumor activity induced by chemical modulation of IAP are others than those involved in cytotoxicity on the cellular level. In therapy tests with curative schedules of SUM-IAP a four fold increase in WBC was measured in s.c. transplanted P388 tumor bearing mice. The findings suggest immunostimulating activity as the reason for the increase in in vivo activity of SUM-IAP compared to IAP.

**#560 Novel A,B,E-ring modified camptothecins displaying high lipophilicity and markedly improved human blood stabilities.** Bom, David,<sup>1</sup> Du, Wu,<sup>1</sup> Gabarda, Ana,<sup>1</sup> Curran, Dennis P.,<sup>1</sup> Chavan, Ashok J.,<sup>2,3</sup> Kruszewski, Stefan,<sup>2</sup> Zimmer, Stephen G.,<sup>4,5</sup> Fraley, Kimberly A.,<sup>2</sup> Bing-cang, Alexander L.,<sup>2</sup> Wallace, Vincent P.,<sup>6</sup> Tromberg, Bruce J.,<sup>6</sup> and Burke, Thomas G.,<sup>2,3,5</sup> <sup>1</sup>Department of Chemistry, University of Pittsburgh, Pittsburgh, PA 15260, <sup>2</sup>Tigen Pharmaceuticals, Inc., Lexington, KY 40506, <sup>3</sup>Division of Pharmaceutics Sciences, College of Pharmacy, <sup>4</sup>Department of Microbiology and Immunology, College of Medicine, <sup>5</sup>Markey Cancer Center, University of Kentucky, Lexington, KY 40506, and <sup>6</sup>Backman Laser Institute, Univ. of California-Irvine, Irvine, CA 92612.

Camptothecins such as topotecan (TPT), CPT-11, Lurtotecan (GI147211), 9-aminocamptothecin (9-AC), 9-nitrocamptothecin (9-NC), DX-8951f, and the parent compound (CPT) are known to undergo relatively rapid hydrolysis in blood. It is a key  $\alpha$ -hydroxy- $\delta$ -lactone pharmacophore that undergoes facile acyl cleavage at physiological pH, yielding biologically inactive and potentially toxic carboxylate forms. For CPT, 9-AC, and 9-NC the extent of hydrolytic ring opening is promoted by preferential carboxylate binding by human albumin (HSA). Interestingly, this effect is not observed in lesser vertebrates (i.e. mice) where the lactone levels in blood are 10 to 100-fold higher than in humans. In this abstract we describe the rational design and total synthesis of highly lipophilic, A,B,E-ring modified camptothecins that are the most blood-stable camptothecins displaying intrinsic anticancer potencies yet to be identified. In our approach to the design of blood-stable camptothecins, we sought to: 1) include structural modifications that eliminate highly preferential binding of carboxylate over lactone forms by HSA, thereby enhancing plasma stability; 2) include a convenient structural means of enhancing compound lipophilicity, thereby promoting the reversible partitioning of active lactone forms into red cell membranes; and 3) expand the E-ring to a 7-membered system by insertion of a methylene spacer between the 20-OH moiety and the carboxyl functionality, a change which has been shown previously to enhance the solution stability of CPT without loss of topoisomerase I inhibitory activity (Lavergne et al., *J. Med. Chem.* 41: 5410-5419 (1998)). Our new homolactecan (hST) derivatives containing silyl groups at position 7, and in some cases modifications at the 10-position, were prepared by total synthesis using the cascade radical annulation approach. The figure to the right depicts the superior human blood stabilities of four novel homolactecans (DB38, DB81, DB90, and DB91). In all cases, the agents displayed markedly enhanced human blood stabilities relative to clinically-relevant analogs such as TPT and SN-38. The greater than 80% lactone levels following 3 hrs. of incubation for the hSTs compare very favorably relative to the corresponding % lactone levels in whole human blood for 9-AC (0.3%), CPT (5%), TPT (16%), CPT-11 (20%), and SN-38 (30%). The IC<sub>50</sub> cytotoxicity values of the new hSTs against MDA-MB-435 tumorigenic metastatic human breast cancer cells following 72 hr. exposure times were in the 2 to 50 nM range. Thus, our results clearly indicate that rational design efforts can lead to the development of new analogs with markedly improved blood stabilities and high intrinsic potencies. Preclinical evaluation of the lead hST compounds is now underway.

**#561 4-epi-Brefeldin A: probing new structural requirements of brefeldin A for inducing activity of differentiation and apoptosis in human colon cancer cell HCT 116.** Zhu, J.-W., Nagasawa, H., Nagura, F., Mohamad, S. B., Uto, Y., Ohkura, K., Hori, H. *Dept of Biol. Sci. & Tech., Fac. of Engg., Univ. Tokushima, Tokushima, Japan.*

Brefeldin A (BFA) is a macrolide antibiotic that could induce a wide variety of human cancer cells to differentiation and apoptosis and is in development as an anticancer agent. To elucidate the structural requirements of BFA for differentiation and apoptosis inducing activity, we designed and synthesized BFA derivatives which were evaluated with cytotoxicities, DNA fragmentations, and morphological changes in human colon cancer cell HCT 116. 4-epi-BFA, differing from BFA in configuration at only one chiral center (C4), was synthesized and its cytotoxicity (IC<sub>50</sub> = 60 µM) was 300 times lower than that of BFA (IC<sub>50</sub> = 0.2 µM). Besides, 4-epi-BFA was unable to induce DNA fragmentation and morphological changes. On the other hand, 7-acetyl BFA, 4-acetyl BFA, and diacetyl BFA exhibited potential activities in cytotoxicity and inducibility of apoptosis. These results indicated that the configuration of 4-hydroxyl group played a more important role than other structural determinants such as the C1-C4



moleity and conformational rigidity, which we suggested previously (Zhu, J.-W., *et al.*, *Bioorg. & Med. Chem. Letter*, 7:139-144, 1997). In addition, we presented the results of the molecular modelling of 4-*epi*-BFA and discussed the reactivities of BFA and 4-*epi*-BFA in Michael addition.

**#562** Construction of a human epidermal growth factor (hEGF)-immunoglobulin (C<sub>H</sub>1) fusion protein for targeting breast cancer. Sandu, J.S., Wang, J., Bray, M., Yang, S., Hendler, A., Vallis, K., Cameron, R., Reilly, R.M. *University Health Network and Samuel Lunenfeld Research Institute; University of Toronto.*

Overexpression of the epidermal growth factor receptor (EGFR) is present in the majority of hormone-resistant and poor prognosis breast cancers. hEGF is a potential targeting vehicle for delivery of radionuclides to EGFR-positive breast cancer for imaging and radiotherapy, but its rapid blood clearance results in low tumour uptake. Our objective was to construct an hEGF-C<sub>H</sub>1 fusion protein which may exhibit slower blood clearance and improved tumour localization. The gene for hEGF was amplified from plasmid pADH59 by PCR using oligonucleotides encoding a flexible peptide linker [(GGGG)<sub>3</sub>] and inserted into pASK84 which contained the genes for C<sub>H</sub>1 and C<sub>K</sub> of IgG<sub>1</sub>. The hEGF-linker-C<sub>H</sub>1 gene was amplified from pASK84 by PCR and inserted into expression plasmid pGEX2T for expression in *E. coli*. Conditions for expression were optimized. The hEGF-C<sub>H</sub>1 fusion protein was isolated using non-denaturing conditions and purified by affinity chromatography on an anti-GST column. The GST domain was subsequently cleaved from the fusion protein using thrombin. SDS-PAGE and Western blot using an anti-EGF antibody demonstrated a single band with the expected molecular weight (18 kDa). Flow cytometry against MDA-MB-468 breast cancer cells (>10<sup>6</sup> EGFR/cell) and ELISA against purified EGFR demonstrated that the hEGF-C<sub>H</sub>1 fusion protein exhibits preserved receptor-binding properties. Experiments are planned to evaluate the hEGF-C<sub>H</sub>1 fusion protein for targeting MDA-MB-468 human breast cancer xenografts hosted in athymic mice.

Supported by U.S. Army Breast Cancer Research Program and Susan G. Komen Breast Cancer Foundation.

**#563** SR 16234, a novel steroidal tissue selective antiestrogen: selective estrogen receptor modulator (SERM). Tanabe, M., Peters, R., Chao, W., Ryan, K., Jong, L., Johansson, J., Olsen, C., Sato, B., Liu, J., *SRI International, Menlo Park, CA, and Yamada, Y., Toko, T., Asao, T., Yano, S., Eshima, K., Taiho Pharm. Co., Hanno, Japan.*

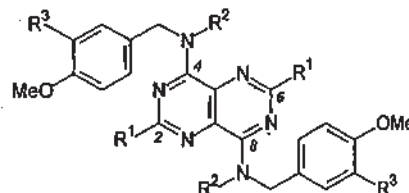
Effective treatment of hormone-dependent breast tumors has primarily been antihormonal therapy, with tamoxifen being the drug of choice. Although tamoxifen appears to be a highly effective antiestrogen, its effectiveness as a chemotherapeutic agent decreases with time as breast tumors acquire resistance to the drug. Similar resistance has been shown with many of the non steroidal tamoxifen analogs. The recent finding that the intramuscularly injected steroidal antiestrogen faslodex does not show cross resistance with tamoxifen in nude mice and in clinical studies lends support to the hypothesis that a similar novel class of steroidal antiestrogens will also be devoid of this cross resistance. We have designed and synthesized a novel class of steroidal antiestrogens that are orally active against tamoxifen resistant breast cancer cells and exhibit pure antitumor activity, devoid of partial agonist activity, in vitro and in vivo. The most potent compound of this new steroidal class of tissue selective antiestrogenic SERM is SR 16234. Unlike faslodex, SR 16234 demonstrates improved tissue selective agonist activity in the bone and cardiovascular systems. The initial molecular modification of critical significance arose from our finding that several C-17 desoxy estrogen analogs retained modest affinity for the estrogen receptor along with antiestrogenic activity as shown in Ishikawa endometrial and MCF-7 breast tumor cells. The C-17 oxygen functionality is not required for receptor binding and antiestrogenic activity. SR 16234, the most potent of these novel steroidal C-17 desoxy SERM, is more active than faslodex against tamoxifen resistant tumor cells. The effects of varied molecular modifications of this novel class of SERMs on uterotrophic, antitumor activity, and  $\alpha$  and  $\beta$  estrogen receptor binding (quantitative structure-activity relationships, QSAR) will be presented, along with the general synthesis for these new compounds. SR 16234 is a highly promising candidate for initial evaluation in a Phase I clinical trial for the treatment and management of breast cancer patients.

**#564** 2,6-Disubstituted-4,8-dibenzylaminopyrimido[5,4-d]pyrimidines as nucleoside transport inhibitors: Structure-activity relationships for binding to  $\alpha_1$ -acid glycoprotein (AGP). Griffin, Roger J; Barlow, Hannah C; Curtin, Nicola J; Calvert, A Hilary; Golding Bernard T; Newell, David R; and Smith, Peter G. *Chemistry Dept. and Cancer Research Unit, University of Newcastle upon Tyne, UK.*

Resistance to antimetabolite antitumor agents may arise by a number of mechanisms, including salvage of extracellular nucleobases and nucleosides via carrier-mediated plasma membrane transport. Avid binding of dipyridamole (DP), a nucleobase/nucleoside transport (NNT) inhibitor, to the plasma protein  $\alpha_1$ -acid glycoprotein (AGP), is thought to account, at least in part, for the disappointing clinical activity of DP as a resistance-modifier. In order to develop potent NNT inhibitors with reduced AGP binding, we have elucidated structure-activity relationships for a new series of 4,8-dibenzylaminopyrimidopyrimidines.

Table 1. Inhibition of <sup>3</sup>H-thymidine transport into L1210 cells

No	% Inhibition at 1 $\mu$ M		IC <sub>50</sub> ( $\mu$ M)
	-AGP	+5 mg/ml AGP	
DP	89	4	0.37
1	56	46	0.25
2	71	53	0.25
3	75	40	0.91
4	85	73	0.40
5	73	57	—
6	40	28	0.94
7	73	17	0.55



Compounds 1 ( $R^1 = N(CH_2CH_2OH)_2$ ,  $R^2 = R^3 = H$ ) and 2 ( $R^1 = N(CH_2CH_2OH)_2$ ,  $R^2 = H$ ,  $R^3 = OMe$ ) were equipotent with DP (Table 1). However, the activity of these compounds was not significantly reduced by 5 mg/ml AGP, a concentration which essentially abrogated the activity of DP. By contrast, the corresponding bis-*N*-methyl derivative 3 ( $R^1 = N(CH_2CH_2OH)_2$ ,  $R^2 = Me$ ,  $R^3 = H$ ) exhibited a significant reduction in potency in the presence of AGP. A similar trend was also observed for the pairs of compounds 4 ( $R^1 = NHCH_2CH(OH)CH_3$ ,  $R^2 = H$ ,  $R^3 = OMe$ ), and 5 ( $R^1 = NHCH_2CH(OH)CH_3$ ,  $R^2 = Me$ ,  $R^3 = OMe$ ), and 6 ( $R^1 = OCH_2CH_2OH$ ,  $R^2 = H$ ,  $R^3 = H$ ), and 7 ( $R^1 = OCH_2CH_2OH$ ,  $R^2 = Me$ ,  $R^3 = H$ ). These results indicate that tertiary amino groups at the 4,8-positions of the pyrimidopyrimidine may be a critical determinant of AGP binding.

**#565** The potential role of the  $\alpha$ -isoform of the folate receptor ( $\alpha$ -FR) in the transport of two cyclopenta[*g*]quinazoline-based thymidylate synthase (TS) inhibitors with low affinity for the reduced-folate carrier (RFC). Jackman Ann, Mellin Camille, Yafai Farid, Theil Davinder, Skelton Lorraine, Jansen Gerrit, Bavetsias Vassilios. *CRC Centre for Cancer Therapeutics, Inst. of Cancer Res; Sutton, Sy, UK. Vrije University, Amsterdam, Netherlands.*

The  $\alpha$ -FR is a glycosylphosphatidylinositol linked transmembrane protein with high affinity for folic acid (K<sub>d</sub> 0.1-1 nM) and reduced folate co-factors. The  $\alpha$ -FR can function as a low capacity transporter of folates in the upregulated or constitutively expressed state. Some solid tumours, particularly ovarian, constitutively express high levels of the  $\alpha$ -FR compared with normal tissues, making it an attractive target for the selective delivery of novel antifolates which in turn will inhibit intracellular targets such as TS. Inhibitors of TS such as raltitrexed (RTX) and ZD9331 have high affinity for the  $\alpha$ -FR although transport into cells is believed to proceed predominantly via the RFC when the two transporters are co-expressed. Therefore, in order to obtain tumour selectivity it is necessary that affinities for the RFC and  $\alpha$ -FR are very low and high respectively. Thus, a series of *N*<sup>10</sup>-propargyl, cyclopenta[*g*]quinazoline (pure *S*-isomers) analogues of folic acid with modified glutamate ligands were synthesised which were potent TS inhibitors without the necessity for polyglutamation, and had low affinity for the RFC. Two examples are CB300638 which has an L-glu- $\gamma$ -D-glu ligand, and CB300907 which is similar but has a tetrazole moiety replacing the  $\alpha$ -carboxyl of the D-glutamate. Kiapps for TS inhibition are 0.52 and 0.16 nM respectively but IC<sub>50</sub>s for L1210 (RFC+/FR-) growth inhibition are relatively high (300 and 500 nM) and explained by their low affinity for the RFC (K<sub>m</sub>s > 100  $\mu$ M). The potential role of the  $\alpha$ -FR in the activity of these compounds was investigated using L1210-FBP (RFC-/FR+ + +) cells with an upregulated  $\alpha$ -FR. Binding affinities for the  $\alpha$ -FR were similar to RTX and ZD9331 and slightly lower than for folic acid (~0.5 relative to folic acid). Growth inhibition assays were performed in 2 nM LV and IC<sub>50</sub> values were 0.64 and 0.8 nM for CB300638 and CB300907 respectively, representing a 470 and 630-fold increase in activity over L1210 cells. In comparison, RTX and ZD9331 had IC<sub>50</sub>s of 0.45 and 0.8 nM respectively, which are only ~25-fold lower than in L1210 cells. In conclusion, CB300638 and CB300907 are representative examples of a class of TS inhibitor that have the potential to be preferentially transported via the  $\alpha$ -FR and further studies are in progress to define their activity in cells co-expressing both transporters.

**#566** The human A431-FBP cell line transfected with the  $\alpha$ -isoform of the folate receptor ( $\alpha$ -FR) is highly sensitive to CB300907 and CB300638 in physiological folate concentrations. Theil Davinder, Mellin Camille, Bavetsias Vassilios, Skelton Lorraine, Jackman Ann. *CRC Centre for Cancer Therapeutics, Institute of Cancer Research, Sutton, Surrey, UK.*

Selective targeting of antifolates to solid tumours that overexpress the  $\alpha$ -FR potentially could be achieved with folic acid analogues such as the cyclopenta[*g*]quinazoline-based antifolates that inhibit thymidylate synthase (TS) (Jackman et al, accompanying abstract). Mouse cell lines, including one with a highly upregulated  $\alpha$ -FR (L1210-FBP), have been useful in the selection of candidate compounds. Studies have now been extended to the human vulvular tumour cell line transfected with the  $\alpha$ -FR (A431-FBP; generous gift of Dr. Tomassetti). Compounds tested included examples of the cyclopenta[*g*]quinazolines (CB300638 and CB300907) and for reference some quinazolins-based TS inhibitors (CB3717, raltitrexed (RTX) and ZD9331) and methotrexate (MTX). With the exception of MTX, all these compounds bind to the  $\alpha$ -FR with high affinity in the order CB3717 > folic acid > ZD9331 = RTX = CB300907 = CB300638. Cells were cultured in a physiological folate concentration (20 nM leucovorin; LV). Consistent with the low affinity of MTX for the  $\alpha$ -FR no growth inhibition difference was observed between the neo-transfected and transfected cell lines ( $IC_{50}$ s ~ 30 nM). A431-FBP cells were only ~4 to 8-fold more sensitive to CB3717, RTX and ZD9331 than the A431 cells (A431-FBP  $IC_{50}$ s = 270 nM, 0.7 nM, 11 nM respectively). However, these transfected cells were ~150 and 250-fold more sensitive to CB300907 and CB300638 respectively (15 nM and 4 nM). Lowering the folate concentration to sub-physiological levels (1 nM LV) resulted in some further sensitisation ( $IC_{50}$  = 4 nM and 2 nM respectively), that was more marked for CB3717 ( $IC_{50}$  = 4 nM). Consistent with uptake via the  $\alpha$ -FR, co-addition with 1  $\mu$ M folic acid largely returned the sensitivity to that seen in the A431 neo-transfected cells. In summary, A431-FBP cells are highly sensitive to CB3717, CB300907 and CB300638 when cultured in 1 nM LV. This is consistent with these compounds preferentially using the  $\alpha$ -FR rather than the reduced-folate carrier for internalisation. Only CB300907 and CB300638 displayed the same level of activity in physiological folate conditions (20 nM LV) suggesting an advantage over CB3717.

**#567 MDR1-reversal by C-7 progesterone analogs: potency and structure-activity relationships.** Kim, Ji-Hyun, Leonessa, Fabio, Green, Geneene, Singh, Harmeet, and Clarke, Robert. *Depts. of Physiology & Biophysics and Oncology, Georgetown University Medical Center, Washington, D.C. 20007.*

Among the natural steroids, progesterone is the most potent inhibitor of the multidrug resistant phenotype conferred by the membrane transporter and MDR1 gene product, P-glycoprotein (PGP). We have previously demonstrated that substitution of a bulky moiety, containing one or two aromatic rings and a urea group, in the C7 position of progesterone significantly increases its MDR1-reversing activity, while also inhibiting its hormonal (progestational and glucocorticoid) activity. In order to help optimize the MDR1-reversing potency and define structure-activity relationships of these agents, we have so far generated 24 different analogs by stepwise modification of the C7 substituent. The activity of these compounds was evaluated on MDA435/LCC6 human breast cancer cells transfected with the MDR1 gene, in terms of reversal of the PGP-related differential in doxorubicin accumulation. The C7 progesterone analogs tested so far are up to 166-, 15-, and about 2-fold more potent than respectively the parental compound progesterone, verapamil and cyclosporin A. A second aromatic ring (F-ring) positively affects the analog's potency, but only when directly substituted on the urea group. Substitution on the F-ring with electron-withdrawing groups, which make the ring relatively electron deficient, appears detrimental. The potency of the different analogs does not appear to correlate with their hydrophobicity. In conclusion, we have used a step-wise analog-design approach to generate novel MDR1-reversing agents that are up to 180 fold more potent than the lead compound progesterone, and that are more potent than other classical PGP-inhibitors.

This study was supported by a DOD grant (WAMD17-96-1-6231).

**#568 Synthetic analogs of green tea catechins and their *in vitro* cell growth inhibition activity.** Zaveri, Nurulain T., and Chao, Wan-Ru. *Pharmaceutical Discovery Division, SRI International, Menlo Park, CA.*

Green tea and its constituent polyphenols have received increasing attention as potential cancer chemopreventives and are currently undergoing Phase I dose-escalation trials and toxicology studies. (-)-Epigallocatechin-3-gallate (EGCG) is the most abundant polyphenolic catechin and the most potent chemopreventive principle in green tea. Although the mechanism of action of EGCG is not fully elucidated, its chemopreventive activity has been attributed to its antioxidant properties, inhibition of signal transduction pathways, and induction of apoptosis. A recent study demonstrated that the trihydroxyphenyl B ring of EGCG is the principal site of antioxidant action of EGCG. However, significant problems with the use of EGCG and green tea as chemopreventives are the extremely low oral bioavailability of EGCG and its extensive metabolic conjugation. We have devised a versatile chemical synthesis of EGCG and other catechins that allows us to vary different portions of the EGCG molecule to study the structure-function relationship of EGCG. We have synthesized several novel analogs of EGCG and other catechins in green tea and tested these compounds in *in vitro* growth inhibition assays against human breast

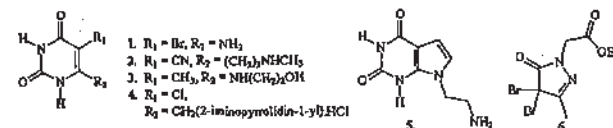
cancer and other cell lines. Interestingly, racemic analogs modified in the galloyl ring of EGCG were less active than EGCG in growth inhibition assays. The new analogs were also tested in *in vitro* chemopreventive assays such as the inhibition of anchorage-independent growth of A427 human lung cancer cells. The inhibition of colony formation in these assays by the EGCG analogs, along with their structure-activity relationships, will be further discussed.

**#569 The closed conformation of human thymidine phosphorylase/platelet-derived endothelial cell growth factor (PD-ECGF): a tool for rationalizing inhibitor design.** Cole, Christian; Douglas, Kenneth T; Jaffar, Mohammed; Stratford, Ian J & Freeman, Sally. *School of Pharmacy and Pharmaceutical Sciences, University of Manchester, Oxford Road, Manchester M13 9PL, UK*

Thymidine phosphorylase (TP, EC 2.4.2.4) catalyses the phosphorylation of thymidine to thymine and 2-deoxyribose-1-phosphate. TP is identical to platelet-derived endothelial cell growth factor (PD-ECGF), an important angiogenic factor for neovascularisation in several tumour types.<sup>1, 2</sup> The enzymatic activity of TP is necessary for angiogenesis, as the dephosphorylated 2-deoxyribose is proposed to be angiogenic.<sup>1</sup> Inhibition of TP has been proposed to decrease tumour angiogenesis and metastases, and promote apoptosis.

To this end a similarity model of human TP was built using Swiss-Pdb Viewer 3.1<sup>3</sup> and Swiss-Model,<sup>4</sup> based on the crystal structure of pyrimidine nucleoside phosphorylase (PyNP) from *Bacillus stearothermophilus*.<sup>4</sup> Human TP and *B. stearothermophilus* PyNP have a sequence identity of 36% and a sequence similarity of 53%, both enzymes are homodimers with subunit molecular weights of between 46 and 55 kDa.<sup>4, 5</sup> Only strand 8 of PyNP was used to model human TP as this was the most closed of the two monomers.<sup>4</sup>

This new structure, compared with a previous model,<sup>6</sup> is in the closed/active conformation giving a better model for inhibitor design. Using the ligand-docking program Autodock 2.4 (Scripps Research Institute), the model was used to rationalise the binding of several known inhibitors (1-6) and a comparison was made with respect to open-conformation binding.<sup>1</sup> Brown, NS & Bicknell, R. (1998). *Biochem. J.*, 334, 1-8. <sup>2</sup>Griffiths, L &



Stratford, IJ. (1997). *Br. J. Cancer*, 76, 689-693. <sup>3</sup>Guex, N & Peitsch, MC (1997). *Electrophoresis*, 18, 2714-2723. <sup>4</sup>Pugmire, MJ & Ealick, SE. (1998). *Structure*, 6, 1467-1479. <sup>5</sup>Desgranges, C et al. (1981). *Biochim. Biophys. Acta*, 654, 211-218. <sup>6</sup>Cole, C. et al. (1999). *Anti-Cancer Drug Design*, in press.

**#570 Novel mathematical approaches for understanding gene expression data and its role in anticancer drug development and target selection.** Sunil Sharma, MD. *Division of Gastrointestinal Oncology, Memorial Sloan-Kettering Cancer Center, 1275 York Avenue, New York (NY) 10021*

Gene expression data is now widely available for various cellular processes. Various techniques like cDNA microarrays, TaqMan quantitative PCR analysis, serial analysis of gene expression (SAGE) etc. offer an opportunity to reliably measure expression of multiple genes on a real time-basis. Examples of such data are widely available in several recent publications and include gene expression in yeast cells in conditions of switch to anaerobic conditions, transcriptional response of human fibroblasts to serum, and comparison of expression profiles in tumorigenic and non-tumorigenic cell lines. In most of the experiments that analyze genome wide data, a clustering analysis has been used to display similarity of gene expression. This type of analysis computes a similarity score for the expression profiles for all pairs of genes studied. By repeating the process  $n-1$  times for a set of  $n$  genes, a similarity matrix or a hierarchical cluster is generated. It has been shown that genes with similar functions cluster together in this type of analysis. However the limitation of this analysis is that it does not fully elucidate the overall interdependence and temporal pattern of expression of genes in response to a stimulus. We demonstrate, using various alternative mathematical techniques that primarily utilize non-linear mathematics and set theory that a more meaningful analysis of genomic data can be obtained. The advantage of these techniques is that it can be used to complement the clustering analysis that can outline similarities of gene expression. We demonstrate the limitations in current understanding of genomic expression data and offer guidance on design of more meaningful experiments to study response to stimuli. Lastly, we offer mathematical models to use this approach to validate target selection and analyze effects of anticancer drugs on overall gene expression.



**#571 Dihydropyrimidine dehydrogenase gene promoter: Functional characterisation and species comparison.** Collier-Duguid Elaine SR, Johnston Stephen J, Powrie Robin H, Watson Gillian, McLeod Howard L. Department of Medicine and Therapeutics, University of Aberdeen, Aberdeen, Scotland, UK.

5-Fluorouracil (5FU) is commonly used in the treatment of solid tumours. However, response rates to 5FU remain relatively low due to the narrow therapeutic index of this drug. Dihydropyrimidine dehydrogenase (DPD) degrades over 80% of an administered dose of 5FU, thereby regulating the clinical efficacy and cytotoxicity of this antimetabolite. DPD activity is highly variable (8–21 fold) in healthy and cancer populations. Control of DPD activity in cancer patients receiving 5FU therapy would standardise the levels of active metabolites in different individuals and provides a target for improving 5FU response rates.

DPD is encoded by the *DPYD* gene and 13 variant alleles have been reported. However, these variants do not fully explain low DPD activity and 5FU toxicity in cancer patients. Although DPD activity and mRNA levels are differentially regulated in human tissues, very little is known about transcriptional regulation of DPD expression. We have cloned 1.85 kb of sequence upstream of exon 1 in the human *DPYD* gene (–1751 to +103). This 5' flanking region was sufficient to initiate and up-regulate transcription by 4 fold in PANC3 cells, when cloned upstream of a luciferase reporter gene. A truncated fragment (–1406 to +103) was not transcriptionally active. We have also determined the 5' flanking sequences of the rhesus monkey (–1751 to +75), cynomolgus monkey (–1751 to +52), beagle dog (–796 to +97) and sprague-dawley rat (–796 to +52) *DPYD* genes. These 5' flanking regions have over 96% homology with the human *DPYD* promoter. A region from –421 to +52 has 100% identity in all five species, indicating that this region may have functional importance. Putative C/EBP and HNF-4 binding sites, liver-enriched transcription factors involved in regulating the expression of many hepatic proteins, were identified in all five species. A putative interferon (IFN) response element was identified in the human *DPYD* promoter and IFN has been reported to down-regulate DPD activity. IFN has been used with limited success to modulate 5FU therapy probably due to its lack of specificity. Further insight into the molecular mechanisms regulating *DPYD* transcription may identify novel factors that modulate DPD expression specifically within the tumour.

**#572 High thymidylate synthase gene expression in gastrointestinal mucosa is associated with gastrointestinal tract toxicity following treatment with raltitrexed.** Ford Hugo ER, Farrugia David, Cunningham David, Aherne Wynne, Hardcastle Anthea, Mitchell Fraser, Danenberg Peter, Danenberg Kathleen, Jackman Ann. CRC Centre for Canc. Therapeutics, ICR, & Royal Marsden Hosp, Sutton, UK; USC, CA.

Raltitrexed is a folate-based thymidylate synthase (TS) inhibitor which is rapidly polyglutamated by polyglutamate synthetase (FPGS). Polyglutamates are more potent than parent compound and are retained intracellularly. Thymidine phosphorylase (TP) may reduce thymidine available for salvage, and high levels enhance raltitrexed cytotoxicity *in vitro*. Despite a good toxicity profile, some patients treated with raltitrexed develop diarrhoea and myelosuppression, which may be life-threatening. This study examines tissue factors associated with toxicity. Patients with advanced colorectal cancer undergoing treatment with raltitrexed have pre-treatment and day 5 biopsies of tumour and normal GI mucosa. Blood is taken on days 1, 5, 14, 21 and before each treatment cycle. Pre-treatment tissue samples were analysed for levels of TS, FPGS and TP mRNA by RT-PCR, and for TS protein by immunohistochemistry (IHC). Post-treatment biopsies were assayed for drug levels. Plasma was assayed for drug levels and deoxyuridine, a surrogate marker of TS inhibition. 27 patients have been recruited, of whom 25 are evaluable for toxicity. Five patients experienced NCI-CTC grade 2–4 diarrhoea. There was no association between drug levels in plasma or bowel and toxicity. Interim analysis of expression markers shows that GI tract TS/ $\beta$ -actin ranged from 2.2–20  $\times 10^3$  (median 5.9  $\times 10^3$ ). 5/6 patients with gut TS/ $\beta$ -actin  $>5.9 \times 10^3$  experienced NCI-CTC grade 2 or greater GI tract toxicity, as compared to 0/6 patients with TS/ $\beta$ -actin  $<5.9 \times 10^3$  ( $p = 0.015$ , Fisher's exact test). More toxicity was also seen in those with strong TS staining on IHC (4/11 strong staining patients and 1/7 with weak staining experienced toxicity). TP/ $\beta$ -actin ranged from 3.6–60  $\times 10^3$  (median 8.4  $\times 10^3$ ). There were no significant differences in toxicity between high and low TP expressers, and 0/3 patients with very high TP (TP/ $\beta$ -actin  $>20 \times 10^3$ ) experienced toxicity. Gut FPGS/ $\beta$ -actin ranged from 10.5–320  $\times 10^3$  (median 36  $\times 10^3$ ) with no correlation to toxicity. By contrast with previously reported tumour response data from the same cohort, patients with high levels of gut TS appear more prone to GI tract toxicity. This may enable prediction of patients at high risk of toxicity, allowing tailoring of therapy.

**#573 Is tumor-specific CYP1B1 expression an unrecognized source of drug resistance?** Rochat Bertrand, McFadyen Morag CE, Murray Graeme I, McLeod Howard L. Departments of Medicine & Therapeutics and Pathology, Institute of Medical Sciences, University of Aberdeen, Foresterhill, Aberdeen AB25 2ZD, United Kingdom.

Intrinsic resistance to chemotherapy remains a major obstacle to successful cancer treatment. Classical *in vitro* or model system approaches have identified a number of putative resistance factors, but none have yet proven to

be of high impact in human solid tumours. Murray *et al* (Cancer Res 1998;57:3026) demonstrated frequent protein overexpression of the P450 enzyme CYP1B1 in a variety of human tumours, but not adjacent normal tissue. As this metabolizing enzyme is down regulated in tissue culture and not found in human liver, it will have escaped evaluation of clinical relevance in the standard analytical approaches. Therefore, we evaluated the ability of commonly used anticancer agents to interact with CYP1B1. 7-Ethoxycoumarin deethylase activity was used for the initial screening using cDNA expressed CYP1B1 enzyme (Geneset Supersomes). Dixon and Cornish-Bowden plots were constructed to identify the nature of any observed interaction. Paclitaxel ( $K_i = 31.6 \mu\text{M}$ ), docetaxel ( $K_i = 28 \mu\text{M}$ ), flutamide ( $K_i = 1.0 \mu\text{M}$ ), and mitoxantrone ( $K_i = 11.6 \mu\text{M}$ ) were competitive inhibitors of CYP1B1 activity, while tamoxifen, daunomycin, and doxorubicin were either mixed or noncompetitive inhibitors. 5-Fluorouracil, cyclophosphamide, vincristine, vinblastine, and etoposide had no inhibitory activity against CYP1B1. Biotransformation studies identified by HPLC analysis that CYP1B1, as CYP1A2, is able to 2-hydroxylate flutamide with similar  $K_m$  (18.6  $\mu\text{M}$  versus 18.0  $\mu\text{M}$ , respectively). Similar studies are now underway with paclitaxel and docetaxel. Cytotoxicity studies identified a 3 to 5-fold resistance to docetaxel in cell lines overexpressing CYP1B1. Together, this data supports a role for CYP1B1 in resistance through tumor specific drug inactivation. Approaches are now needed to utilize the tumour selectivity of CYP1B1 expression for modulation of existing chemotherapy or as an *in situ* directed enzyme prodrug therapy strategy.

**#574 Evaluation of NQO1 Gene Expression and Point Mutations in Patients Receiving Mitomycin-C and Irinotecan.** Kolesar J, Hillman L, Drenkler R, Hammond L, Diab S, Felton S, Monroe P, Schaaf L, Von Hoff D, Kuhn J, Rowinsky E, Villalona-Calero M. School of Pharmacy, University of Wisconsin-Madison, Madison WI and the Cancer Therapy and Research Center, San Antonio, TX

NQOR (NAD(P)H:Quinone oxidoreductase) is a flavoprotein that catalyzes the two-electron reduction of quinones and their derivatives. Since mitomycin-C (MMC) contains a quinone structure and is activated by NQOR, our hypothesis is that NQOR activity may predict efficacy or toxicity of MMC. The purpose of this study was to evaluate NQOR activity by gene expression and mutation status in peripheral blood samples of patients undergoing chemotherapy with MMC and Irinotecan as part of a phase I clinical trial. Peripheral blood lymphocytes were obtained in 6 patients on Day 1 prior to infusion, 5 minutes into the MMC infusion, end of infusion and 3 hours after the end of infusion. On Day 2 samples were obtained 24 hours after the end of infusion (5 minutes prior to start of irinotecan infusion), at the end of the irinotecan infusion, and at 2, 4 and 24 hr after the end of irinotecan. RNA was extracted by standard techniques and quantitated spectrophotometrically. Gene expression was quantitated by RT-PCR (reverse transcription-polymerase chain reaction) with a competitive, reaction specific internal standard with analysis by capillary electrophoresis with laser induced fluorescence (CE-LIF). Mutation at bp609 was evaluated by restriction fragment polymorphism (RFLP) with analysis by CE-LIF. The mean gene expression prior to MMC infusion was  $5.66 \times 10^{-13}$  ng/mL  $\pm 2.88$ . Mean gene expression decreased to  $0.70 \times 10^{-13} \pm 0.56$  ng/mL 5 minutes into the MMC infusion, but was induced to  $1.65 \times 10^{-13}$  ng/mL  $\pm 21.63$  by 24 hours after the infusion. Gene expression was inhibited to  $1.16 \times 10^{-13}$  ng/mL  $\pm 0.72$  five minutes into the irinotecan infusion. By 24 hours after the irinotecan infusion, gene expression was approaching baseline at  $2.61 \times 10^{-10}$  ng/mL  $\pm 1.21$ . Three of six patients had NQO1 mutations, one with breast cancer and two with stomach cancer diagnosed at ages 22 and 27. In summary, inhibition of NQO1 mRNA appears to be a nonspecific and rapid effect of MMC or irinotecan, while induction appears specific to MMC. Additionally, the NQO1 mutation frequency appears high in young patients with stomach cancer, encouraging further study in this malignancy. (Supported by the Pharmacia & Upjohn Company).

**#575 P450-enhanced cytotoxicity of the bioreductive drug tirapazamine: combination with cyclophosphamide for P450/P450-reductase-based cancer gene therapy.** Youssef Jounaidi and David J. Waxman. Division of Cell and Molecular Biology, Department of Biology, Boston University, Boston, MA 02215.

Tirapazamine (TPZ) is a promising bioreductive drug that exhibits greatly enhanced cytotoxicity in hypoxic tumor cells, which are frequently radiation resistant and chemoresistant. TPZ exhibits particularly good activity when combined with alkylating agents such as cyclophosphamide (CPA). The present study examines the potential of combining TPZ with CPA in a cytochrome P450 (CYP)-based gene therapy strategy. Recombinant retroviruses were used to transduce 9L gliosarcoma cells with the genes encoding P450 2B6, P450 reductase, or both genes in combination. Intratumoral co-expression of P450 2B6 and P450 reductase sensitized 9L tumor cells to CPA equally well under normoxic (19.6%  $\text{O}_2$ ) and hypoxic (1%  $\text{O}_2$ ) conditions. The P450 2B6/P450 reductase combination sensitized 9L tumor cells to the combination of TPZ and CPA to a greater extent than to either CPA or TPA alone, indicating a synergistic action of CPA and TPZ. TPZ at noncytotoxic concentrations exerted a striking growth inhibitory effect on CPA-treated 9L/2B6/P450 reductase cells, particularly under hypoxic conditions. 9L tumors transduced with P450 2B6 and P450 reductase and grown as solid tumours in *scid* mice showed little or no

response to TPZ treatment. However, tumor growth was significantly delayed when TPZ was combined with CPA compared to CPA treatment alone. These studies demonstrate the potential benefit of incorporating the bioreductive drug TPZ into a P450/P450 reductase-based prodrug activation gene therapy strategy for cancer treatment. [Supported in part by grant CA49248 from the N.I.H.]

**#576 Aldo-keto reductases confer resistance to carbonyl containing anticancer drugs.** Hyndman, David J. and Flynn, T. Geoffrey Dept. of Biochemistry, Queen's University, Kingston CANADA K7L 3N6.

The aldo-keto reductases (AKRs) are a growing group of monomeric oxidoreductases that metabolize the reduction of a wide variety of aldehyde and ketone containing small molecules. These compounds include steroids, products from biogenic amine metabolism and lipid peroxidation in addition to carcinogenic xenobiotic compounds such as aflatoxin B<sub>1</sub>. The ability of some AKRs to metabolize anticancer drugs such as daunorubicin and the bioactive form of cyclophosphamide may indicate that AKRs are involved in drug resistance. To examine this issue we have used a normal CHO cell line and one that overexpresses an AKR. Overexpression of the CHO reductase confers resistance to daunorubicin, hydroperoxy-cyclophosphamide but not vincristine. This resistance is partially reversed by the addition of AKR inhibitors. In addition we have screened the NCI tumour cell line panel and a lung cell line panel for the expression of aldose reductase and HSI reductase to determine the relative abundance of these human AKRs. Based on this screen two non-small cell lung cancer lines, A549 and LC-T, were selected and were also shown to be resistant to daunorubicin consistent with the level of AKR expression. This work strongly suggests that AKR expression can influence the cellular level of some commonly used anticancer drugs and thus may play a role in resistance to these compounds.

Supported by the Medical Research Council and the National Cancer Institute of Canada.

**#577 Pharmacokinetics of Irinotecan (CPT-11) in patients treated with neomycin to diminish  $\beta$ -glucuronidase activity in the intestines.** Sparreboom A., Kehrner D., Verweij J., De Bruijn P., and De Jonge M.J.A. Rotterdam Cancer Institute, 3008 AE Rotterdam, The Netherlands.

Exposure of the intestinal lumen to the active metabolite SN-38 is considered to play a key role in CPT-11-induced diarrhea. In line with this hypothesis, we have recently found high fecal concentrations of SN-38 accompanied by a virtual disappearance of a detoxified SN-38 glucuronide form (SN-38G) in patients who suffered from severe diarrhea (Clin. Cancer Res. 4: 2747-2754, 1998). In this study, we test the hypothesis that  $\beta$ -glucuronidases from intestinal microflora mediate the hydrolysis of SN-38G to the active compound in patients, and we determined the effect of the broad-spectrum antibiotic neomycin on the metabolism and plasma pharmacokinetics of CPT-11. Until now, 3 patients received CPT-11 at 350 mg/m<sup>2</sup> (90 min i.v.) on day 1 alone in the first course and in combination with oral neomycin at 1000 mg t.i.d. (days -5 to 2) in the second course. CPT-11, SN-38 and SN-38G were determined in serial samples by HPLC. Administration of neomycin significantly changed fecal  $\beta$ -glucuronidase activity from 6.30  $\pm$  1.96 (course 1) to 0.581  $\pm$  0.194  $\mu$ g/h/mg (course 2;  $P = 0.036$ ), as measured by a colorimetric phenolphthalein microassay, and coincided with decreased fecal SN-38 concentrations. The CPT-11 terminal plasma half-life (13.7  $\pm$  4.62 vs 14.8  $\pm$  5.46 h) and AUC<sub>0-12h</sub> (46.6  $\pm$  22.6 vs 57.3  $\pm$  24.1  $\mu$ M.h), however, were very similar between courses. The relative extents of metabolism to SN-38 (0.022  $\pm$  0.020 vs 0.036  $\pm$  0.012) and glucuronidation to SN-38G (7.11  $\pm$  4.48 vs 5.88  $\pm$  3.40) were also unaltered by neomycin treatment. Our findings indicate that microbial  $\beta$ -glucuronidases contribute to the fecal disposition of CPT-11, without affecting enterocycling and systemic SN-38 levels. Currently, we are evaluating the potential of oral neomycin to modulate CPT-11-induced diarrhea in patients with metastatic colorectal cancer.

**#578 In vivo modulation of antitumor activity of 5-FU by 2'-deoxyinosine in human colorectal xenograft model.** Clocolini Joseph, Paillard Laurent, Evrard Alexandre, Cucq Pierre, Pelegrin Andre, Aubert Claude and Catalin Jacques. Toxicocinétique et Pharmacocinétique, Faculté de Pharmacie, Marseille, France, Toxicologie, Faculté de Pharmacie, Montpellier, France and \*CRLCC Val D'Aurelle, Montpellier, France.

5-FU antiproliferative activity depends on its intracellular activation to cytotoxic metabolites FdUMP, FdUTP, FUTP interfering with TS, DNA and RNA respectively. We showed in a previous study that deoxyinosine (d-ino), a deoxyribose 1-phosphate donor involved in thymidine phosphorylase (TP) activity, can greatly affect 5-FU activation in various human colorectal cell lines by triggering the DNA pathway, thus leading to an intracellular accumulation of FdUMP. Combining d-ino to 5-FU proved to increase by 20 up to 700 times the sensitivity of HT29 and SW620, but no improvement was observed in CaCo2 cells. We suggested then that involvement of Fas system in the apoptosis induced by the association d-ino/5-FU could explain the discrepancy between the cells although high levels of FdUMP and higher TS inhibition were observed in all of the cell lines exposed to this association. The aim of this present work was to study the feasibility of combining high dose d-ino to 5-FU in vivo. We investigated antitumor effect of the association in human tumor xenograft

models. Swiss-nude mice were subcutaneously transplanted with fragments of 5-FU-resistant SW620 tumors and split into 4 groups (n=10) receiving either saline, d-ino (1.6 g/kg twice daily, IP), 5-FU (35 mg/kg, daily IP) or combination of both for 5 days. Treatment started by day 11, after tumor became measurable, tumor growth was evaluated 3 times a week and experiment was terminated when tumors in control animals reached a size of about 1.5 gr. Anova analysis performed on final tumor weights showed that while 5-FU alone has no effect on SW620 xenografts ( $p > 0.05$ , Tukey test), associating d-ino significantly reduced the tumor growth by 57% ( $p < 0.05$ ). These data suggest that it is possible to reverse both in vitro and in vivo the resistance to 5-FU by modulating the way the drug is activated after cellular uptake. Increasing TP yield by providing co-factors donors such as d-ino appears to be a convenient way for reaching high levels of TS-directed FdUMP metabolite. Although TP activity has been described as a potential tumor growth factor by enhancing angiogenesis, animals receiving d-ino alone didn't exhibit higher tumor growth compared with control group ( $p = 0.459$ ). Further animal studies will have to be carried out to confirm the exact mechanism of action of d-ino when associated to 5-FU in vivo and to optimize the administration schedule.

**POSTER SESSION 6  
SECTION 1: DNA-TARGETED STRATEGIES:  
OLIGODEOXYNUCLEOTIDES AND MODULATION OF  
REPAIR PATHWAYS**

**#579 Phase I trial of the c-Raf-1 antisense oligonucleotide (ODN) ISIS 5132 administered as a 21-day continuous IV infusion in combination with 5-fluorouracil (5-FU) and leucovorin (LV) as a daily x 5 IV bolus.** Stevenson, J.P., Gallagher, M., Ryan, W.F., Fox, K., Algazy, K., Schueter, L.M., Haller, D.G., Holmlund, J., Dorr, F.A., Yao, K-S., O'Dwyer, P.J. University of Pennsylvania Cancer Center, Philadelphia, PA, ISIS Pharmaceuticals, Carlsbad, CA.

The kinase c-Raf-1 is a downstream effector of Ras in the MAP kinase signaling pathway. ISIS 5132, a 20-base antisense ODN targeted to c-Raf-1 mRNA, is active in human tumor xenograft models and was nontoxic as a single-agent at doses up to 6.0 mg/kg/day in Phase I trials. In an ongoing study, 14 pts with refractory cancers have received ISIS 5132 doses of 1.0-3.0 mg/kg/day as a 21-day IV infusion in combination with 5-FU (425 mg/m<sup>2</sup>) and LV (20 mg/m<sup>2</sup>) as an IV bolus on days 1-5 every 4 weeks. Dose-limiting toxicity in the form of neutropenia (3 pts, gr 4), thrombocytopenia (1 pt, gr 4), and mucositis (2 pts, gr 4) at the 3.0 mg/kg/day dose level precluded further ISIS 5132 escalation. Eight pts have been treated at the 2.0 mg/kg/day dose level and toxicities have included neutropenia, thrombocytopenia, diarrhea, and mucositis but these were not dose-limiting. Disease stabilization lasting  $\geq 6$  cycles occurred in 3 pts (1 renal cell ca, 1 colon ca, 1 pancreatic ca). ISIS 5132 at a dose of 2.0 mg/kg/day is active and well-tolerated in combination with full doses of 5-FU/LV on this schedule. Phase II evaluation at these doses is recommended. Pharmacokinetic data and updated results will be presented.

**#580 A phase I trial of ISIS 3521 (ISI641A), an antisense inhibitor of protein kinase C alpha, combined with carboplatin and paclitaxel in patients with cancer.** Yuen A, Silic BI, Advani R, Fisher G, Halsey J, Lum B, Geary R, Kwok TJ, Holmlund JT, Dorr A. Oncology Division, Stanford University, Stanford CA and Isis Pharmaceuticals, Carlsbad CA.

Inhibitors of protein kinase C (PKC) have demonstrated anti-tumor activity in a variety of cancers. ISIS 3521, a 20-base phosphorothioate DNA oligonucleotide, specifically depletes PKC- $\alpha$  mRNA and protein *in vitro*, and has demonstrated anti-tumor activity in patients. In this phase I study, 17 patients (age 32-74, median 54) with metastatic cancer received fixed doses of carboplatin (AUC 6) and paclitaxel (175 mg/m<sup>2</sup> over 3 hours) on cycle 1. With cycle 2 and beyond, patients received ISIS 3521 by continuous intravenous infusion on days (d) 1-14, with carboplatin and paclitaxel on d 4. Treatment was repeated every 21 d until maximum benefit. Doses of ISIS 3521 (1.0, 1.5, 2.0 mg/kg/d) and carboplatin (AUC 5 or 6) were escalated among 4 patient cohorts starting with cycle 2. Tumor types were non-small cell lung (NSCLC) (11), unknown primary (2), small cell of the cervix (2), esophageal (1), and sarcoma (1). Eleven patients had not received chemotherapy before study entry (range 0-2 regimens). Seventy-seven cycles (range 1-7) have been administered. Toxicity between cycles 1 and 2 (without and with ISIS 3521) did not differ. The mean plasma concentrations of ISIS 3521 did not change significantly during infusion of either carboplatin or paclitaxel. Areas under the curve of paclitaxel or carboplatin were not significantly altered by the addition of ISIS 3521. No episodes of grade 3 or 4 toxicity were observed during treatment at the maximum doses of ISIS 3521, carboplatin and paclitaxel. Of 16 patients evaluable after cycle 3, 7 have attained a partial response, with all 7 responses occurring among 10 patients with NSCLC. An expanded phase of this study combination is ongoing in patients with untreated advanced NSCLC. In this phase II portion, patients receive ISIS 3521 (2.0 mg/kg/d for 14 days), and carboplatin (AUC 6) and paclitaxel (175 mg/m<sup>2</sup>) on day 4. The



overall response rate among all 13 patients with NSCLC treated on both phases of the study is 62% (95% CI 33–83%). The combination of ISIS 3521, carboplatin and paclitaxel is well tolerated, and has promising activity in NSCLC.

**#581 Induction of apoptosis via the CPP32/caspase-3 pathway of glioblastoma-multiforme (GBM) after administration of fusogenic immunoliposomes composed of PKC inhibitor hexadecyl-PC with linked anti EGFR Mab and entrapped bcl-2 phosphorothioated antisense oligodeoxynucleotides (ODNs).** Giannios J, Vournvourakis K. *Peripheral Hospital of Patras, Eginition Hospital, Greece.*

Human glioblastoma multiforme (GBM) is characterized by a 801-bp deletion mutation of the EGFR resulting in its amplification which inhibits PCD of GBM cells after radio- and/or chemotherapy. EGFR is a transmembrane glycoprotein of the tyrosine kinase family which regulates proliferation of cells; mEGFR is a suitable target for active immunotherapy of GBM, since it is expressed in human gliomas and not in normal tissues. GBM are the most common human brain tumours and they are extremely lethal. Immunocytochemical analysis exhibits enhanced expression of EGFR, bcl-2 and PKC. We treat tumour cells for 6 hours at 37 C with fusogenic anti-EGFR Mab immunoliposomes (SUV) composed of hexadecyl-PC. In addition, bcl-2 antisense phosphorothioated antisense oligodeoxynucleotides were encapsulated intraliposomally. After treatment, immunocytochemical analysis exhibits upregulation of CPP32/caspase-3 and downregulation of EGFR, bcl-2 and PKC. TEM has exhibited accumulation of NK cells and monocytes implying ADCC. Seventy-two hours post-treatment TEM exhibited irreversible D2 apoptotic signs of tumour cells forming apoptotic bodies which were phagocytosed by adjacent tumour cells implying a bystander killing effect. Thus, missile therapy targeted at EGFR-GBM with anti-EGFR Mab combined with bcl-2 antisense ODN and PKC inhibitor hexadecyl-PC resulted in apoptotic cell death of chemoresistant GBM via activation of the CPP32/caspase-3 pathway.

**#582 Antisense Bcl-2 oligonucleotide uptake and Bcl-2 protein expression in human bladder transitional cell carcinoma.** B J Duggan, K E Williamson, P W Hamilton, J Kelly, F E Cotter, P F Keane, S R Johnston. *Department of Pathology, Royal Victoria Hospital, Belfast, N.I., Department of Urology, Belfast City Hospital, Belfast, N.I., and Institute of Child Health, London, U.K.*

Antisense oligonucleotides are a novel gene therapy for preventing the production of disease causing proteins. The Bcl-2 protein is known to inhibit apoptosis and increase the metastatic potential of bladder cancer. In this study we explore uptake of antisense Bcl-2 oligonucleotides in human superficial bladder tumours and also tumour expression of the Bcl-2 protein. Samples of superficial bladder cancer (Ta, T1, G1-3) were obtained fresh after trans-urethral resection. The tissue was incubated in a specially designed *ex vivo* model.

In this model tumour samples were maintained in a homeostatic environment while FITC-labelled antisense Bcl-2 oligonucleotides were infused onto them for one hour. Uptake at four hours post infusion was assessed using fluorescence microscopy and immunohistochemistry in six tumours while flow cytometry was used to assess uptake every 4 hours within the first 24 hour incubation period in eight tumours. Tissue was retrieved for snap freezing and also for single cell suspensions to assess expression of Bcl-2 using immunohistochemistry and flow cytometry respectively.

All tumours tested in the *ex vivo* model had detectable intracellular FITC-antisense by flow cytometry, fluorescence microscopy and immunohistochemistry at 4 hours. Over the 24 hour incubation period there was some variation in the intracellular level of antisense Bcl-2 oligonucleotides. Most tumours had a monotonic increase in intracellular antisense until a peak intracellular level was detected at 16 hrs post infusion. Frozen section immunohistochemistry for Bcl-2 was positive in 9 out of 16 tumours (56%) while flow cytometric Bcl-2 analysis was positive in 8 out of 16 tumours (50%). Antisense Bcl-2 oligonucleotides are readily taken up by superficial bladder cancer cells but the variable tumour uptake over time needs to be considered when assessing the bioavailability of these drugs. As Bcl-2 is expressed in a significant proportion of bladder tumours, antisense oligonucleotides represent a possible therapeutic strategy to manipulate both Bcl-2 expression and apoptosis in human transitional cell carcinoma.

**#583 Downregulation of BCL-2 expression by the antisense oligonucleotide G3139 enhances paclitaxel chemosensitivity in the androgen-independent prostate cancer LNCaP xenograft model.** Tolcher, A.W., Miyake, H., Gleave, M. *The Institute for Drug Development, Cancer Therapy and Research Center, San Antonio, TX and The Prostate Center, Vancouver Hospital, Vancouver, Canada.*

The development of androgen-independent (AI) prostate cancer is accompanied by a marked increase in BCL-2 protein expression in patient tumor samples. AI prostate cancer also represents an intrinsically chemoresistant disease. In our LNCaP xenograft model BCL-2 is overexpressed in subcutaneously implanted tumors following castration during AI growth. We previously demonstrated that G3139 antisense oligonucleotide (ASODN) to bcl-2 downregulates bcl-2 mRNA and protein in a dose-dependent, and nucleotide sequence-dependent manner and delays the development of AI LNCaP growth *in vivo*. In this model we determined the

effect of bcl-2 downregulation on the chemosensitivity of LNCaP tumors to paclitaxel. Subcutaneously implanted LNCaP tumors cell were grown in Intact nude mice until established and then the mice castrated. Cohorts of mice were treated with 1) G3139 and paclitaxel, 2) G3139 alone, 3) paclitaxel alone. At 14-weeks post castration mean tumor volumes for G3139 and paclitaxel were 66% of baseline versus 2.5 and 2.9 fold greater than baseline for paclitaxel alone and G3139 alone. Mean PSA values mirrored tumor volume at 14-weeks for cohorts 1, 2, and 3. Since murine tolerability for the combination of paclitaxel and G3139 (human bcl-2 sequence) would not be assessed in the LNCaP xenograft model, the combination of paclitaxel and a murine sequence bcl-2 ASODN was administered to mice bearing the AI Shionogi tumor. Paclitaxel plus murine antisense oligonucleotide were tolerable at effective doses. These results demonstrate that downregulation of BCL-2 expression by ASODN markedly enhances paclitaxel chemosensitivity in the LNCaP xenograft model, is a tolerable combination for the host animal when a BCL-2 species specific model is used, and represents a potential clinical strategy to enhance paclitaxel chemosensitivity in AI prostate cancer.

**#584 Oral antisense targeting protein kinase A type I causes anti-tumor and apoptotic effect in human cancer cells *in vitro* and *in vivo* and has a cooperative activity in combination with antisense bcl-2.** Tortora G., Caputo R., Damiano V., Bianco R., Pepe S., De Paolillo S., Bianco A.R., Agrawal S., Ciardiello F. *Cattedra di Oncologia Medica, Università di Napoli Federico II, Napoli, Italy. Hybridon, Inc, Millford, USA.*

Protein kinase A type I (PKA) plays a key role in neoplastic transformation and conveys mitogenic signals of different growth factors and oncogenes. Inhibition of PKA by different tools results in cancer cell growth inhibition *in vitro* and *in vivo*. We have recently shown that a novel class of mixed-backbone oligonucleotides (MBOs) targeting the PKA subunit R1 $\alpha$  exhibits improved pharmacokinetic properties and antitumor activity *in vitro* and *in vivo* in several human cancer types accompanied by increased apoptosis. The role of bcl-2 in the control of apoptosis has been widely documented and inhibition of bcl-2 expression and function may have important therapeutic implications. In fact, oligonucleotides antisense bcl-2 have shown antitumor activity in animal models and have successfully completed clinical trials. Recent studies have demonstrated a direct role of PKA in the phosphorylation and modulation of bcl-2-related targets and bcl-2-dependent apoptotic pathway. In this study we report that a novel hybrid DNA/RNA MBO antisense R1 $\alpha$ , containing 2-O-methyl ribonucleotides, following oral administration was able to inhibit the growth of human colon cancer xenografts in nude mice and showed a cooperative antitumor effect with taxol which significantly prolonged mice survival. Histochemical analysis of tumor specimens showed inhibition of R1 $\alpha$  and of growth factors expression, inhibition of angiogenesis and increase in p27 expression. We then investigated whether the double blockade of PKA and bcl-2 by antisense oligonucleotide may exert any cooperative effect. Combination of the antisense R1 $\alpha$  with the antisense bcl-2 inhibited the expression of the target proteins and determined a cooperative effect on both inhibition of growth and induction of apoptosis in different human cancer cell lines. When we administered oral antisense R1 $\alpha$  in combination with antisense bcl-2 given i.p., we observed a significant cooperative antitumor effect and a prolongation of survival of nude mice bearing human cancer xenografts. In absence of toxicity. This study demonstrates the activity of an oral MBO targeting PKA and that the combined blockade of PKA and bcl-2 by antisense strategy may have a therapeutic potential, which deserves evaluation in a clinical setting.

**#585 Clinical pharmacokinetics and pharmacodynamics of G3139 (Genta Incorporated) antisense oligonucleotide targeting BCL-2.** Fingert, Howard J. and Klem, Robert E. *Genta Incorporated, Lexington, MA.*

G3139 (Genta Incorporated) is a 18mer phosphorothioate oligonucleotide targeting the first 6 codons of the BCL-2 mRNA. Coupled with potent antitumor activity in several preclinical models, used alone or in combination with cytotoxic drugs, G3139 bioactivity has been demonstrated by the reduction of BCL-2 protein in human tumor xenografts, using systemic treatments leading to steady-state concentrations (C<sub>ss</sub>) in plasma > 1  $\mu$ g/ml (170 nM). Infusions of radiolabeled G3139 in mice produced stable steady-state plasma concentrations, and wide distribution with high tissue/plasma ratios in major organs except brain (F. Raynaud, JPET 281: 420, 1997). Using G3139 by IV or SC routes, recent clinical studies demonstrate that multiple treatment cycles of 2–5 mg/kg/day are tolerable in patients with advanced solid tumors, and rapidly achieve C<sub>ss</sub> > 1  $\mu$ g/ml. C<sub>ss</sub> was linear with delivered dose, and unchanged by combined treatment with a cytotoxic agent. Evidence for systemic bioactivity in patients has been reported from independent clinical studies by 1) the demonstration of reduced intracellular BCL-2 protein content from multiple organ sites, assayed before and during G3139 therapy, including peripheral blood lymphocytes and malignant disease in bone marrow, lymph nodes or subcutaneous metastases; and indirectly by 2) objective responses or stabilization of metastatic cancer in multiple organs, including bone, liver, lung, abdomen, and skin, observed in patients with lymphoma, melanoma, prostate, and renal cell cancers (Waters, Proc. ASCO. 18:4a; Jansen, Proc. ASCO 18:531a; Morris, Proc. ASCO 18:323a, 1999). Using flow cytometry, Western blots, and immunohistochemistry, reductions of BCL-2 protein

have been observed within 5-7 days of G3139 administration, relevant to rational scheduling in combination with cytotoxic agents. Taken together, the data from Phase 1-2a studies indicate favorable safety, pharmacokinetics, and pharmacodynamics of G3139 in patients with diverse malignancies; provide a rational basis for Phase 2-3 trials; and support its further development in cancer therapy.

**#586 Antisense TRPM-2 oligodeoxynucleotides delay progression to androgen independence and enhance chemosensitivity in prostate cancer tumor models.** Mlyake H, Chi KN, Gleave ME. *The Prostate Research Centre, Vancouver General Hospital and the BC Cancer Agency, Vancouver, Canada.*

**Background:** Testosterone-repressed prostate message-2 (TRPM-2) expression is highly upregulated in normal and malignant prostate cells after androgen withdrawal. Studies have suggested a protective role of TRPM-2 expression against apoptosis in several experimental models.

**Objectives:** To define the functional role of TRPM-2 in apoptosis, the development of androgen independence and chemosensitivity in prostate cancer, and test whether antisense (AS) TRPM-2 oligodeoxynucleotide (ODN) therapy enhances apoptosis, delays time to androgen independent (AI) recurrence, and improves chemosensitivity.

**Results:** Immunostaining of 20 radical prostatectomy specimens confirmed that TRPM-2 is highly expressed in specimens after neoadjuvant hormone therapy, but low or absent in untreated specimens. In Shionogi tumors, TRPM-2 mRNA and protein levels increase >10 fold post-castration. Pretreatment of mice bearing Shionogi tumors with calcium channel blockers inhibit castration-induced apoptosis, tumor regression, and TRPM-2 gene upregulation, illustrating that TRPM-2 is an apoptosis-associated gene and not an androgen-repressed gene. LNCaP cells transfected to overexpress TRPM-2 were highly resistant to androgen ablation and chemotherapy through the inhibition of apoptotic cell death. Treatment of mouse Shionogi and human PC3 tumor cells with species specific AS TRPM-2 ODN inhibited TRPM-2 gene expression in a dose-dependent, sequence-specific manner. Combined treatment with AS TRPM-2 ODN enhanced the cytotoxic effects of paclitaxel or mitoxantrone in both cell lines *in vitro*, reducing the IC50 by 60-80%. Systemic administration of AS TRPM-2 ODN in mice bearing Shionogi tumors resulted in a more rapid regression of tumors and a significant delay of emergence of AI recurrent tumors. This effect was more pronounced when ODN therapy was combined with paclitaxel. Enhanced chemosensitivity was also observed in mice bearing PC3 tumors treated with AS TRPM-2 ODN combined with either paclitaxel or mitoxantrone.

**Conclusions:** These findings demonstrate that TRPM-2 is a cell survival gene upregulated by androgen ablation that confers resistance to hormonal and chemotherapy. AS TRPM-2 ODN treatment enhances cell death, improves treatment efficacy of androgen ablation and cytotoxics, and has potential as a new therapeutic modality for the treatment of prostate cancer.

**#587 Antisense oligodeoxynucleotides targeting the human papilloma-virus type 16 (HPV-16) E6 gene inhibits proliferation of cervical carcinoma cells.** Alvarez-Salas, L.M. and DiPaolo, J.A. *Laboratory of Gene Therapy, Dept. of Molecular Biology, Center of Research and Advance Studies of NIP, Mexico D.F. 07300, Mexico and DCS, National Cancer Institute, National Institute Health, Bethesda, MD 20892-4255.*

Over 50% of invasive cervical carcinomas worldwide as well as many cervical carcinomas-derived cell lines express DNA from human papillomavirus type 16 (HPV-16). The E6 and E7 genes are required for immortalization and maintenance of a transformed phenotype in several cell types. Therefore, the E6/E7 genes can be considered relevant targets for anti-cancer therapy. Furthermore, the E6 gene based on analysis of 78 HPV-16 isolates had low variability as indicated by single stranded conformational polymorphism. Based on our previous research with anti-HPV ribozymes we developed a 16 nt antisense oligodeoxynucleotide (AntiE6) able to direct RNase H activity on full-length HPV-16 E6/E7 mRNA. Although the precise mechanism is not completely understood, addition of 50  $\mu$ M AntiE6 oligodeoxynucleotide caused a significant decrease in the growth rate of CaSki and QGU tumor cell lines. In contrast, addition of a mismatched mutant M4 oligodeoxynucleotide did not affect cell growth after 72 h. Treatment with AntiE6 resulted in intracellular destruction of E6/E7 mRNA in CaSki and QGU cells and an increase in p53 levels in QGU cells. To determine the inhibitory effect of AntiE6 *in vivo*, CaSki tumor cells were injected subcutaneously and when palpable tumors were treated with 2 mg of AntiE6 or M7 S-ODNs in sterile water for 14 days using constant delivery by Alzet osmotic pumps. Tumors treated with AntiE6 were significantly (>10 folds) smaller in weight than those treated with water or a mutant ODN. No major pathologic difference was observed indicating that the differences were due to growth inhibition. The present results confirm the validity of using antisense oligodeoxynucleotides which act as effective inhibitors of HPV-16 E6/E7 immortalization and as therapeutic agents against cervical carcinomas.

**#588 Antibody mediated delivery of antisense oligonucleotides to prostate tumors *in vivo* and *in vitro*.** Mirochnik, Y., Rubenstein, M. and Guinan, P. *Haktoen Institute for Medical Research, Rush Presbyterian St. Lukes Medical Center.*

New pharmaceuticals, particularly antisense oligonucleotides, must be capable of specific delivery and entry into targeted tumor cells. Antitumor effects of oligonucleotides (oligos) directed to transforming growth factor- $\alpha$  (TGF- $\alpha$ ) and the epidermal growth factor receptor (EGFR) have been previously demonstrated against prostate cancer.

In this study we describe the targeting of the biotinylated oligos to prostate tumor cells utilizing delivery vehicles derived from monoclonal antibodies specific against prostate specific antigen (PSA) and prostate specific membrane antigen (PSMA).

Two delivery vehicles were prepared and characterized: 1) A bispecific heteroconjugate, recognizing both PSA and biotin; and 2) CYT-356 (Cytogen Corporation), specific for PSMA, conjugated to avidin.

Both delivery vehicles retained immunoreactivity and were able to target biotinylated horseradish peroxidase to the glandular regions of human prostate tissue in paraffin embedded sections. Complex formation between delivery vehicles and biotinylated oligos was confirmed by mobility shift assay.

Cellular uptake of oligos was demonstrated by fluorescence. LNCaP cells, expressing PSA and PSMA, were incubated with FITC labeled oligonucleotides in the presence or absence of the heteroconjugate delivery vehicle. Targeting by heteroconjugate delivery vehicle improved cellular uptake and showed increased intracellular fluorescence.

*In vivo* study <sup>35</sup>S labeled oligos alone or with delivery vehicle were administered to nude mice bearing LNCaP tumors. We found increased radioactivity in serum and at the LNCaP tumor site 24 hours after i.p. injection, when the injected oligo was attached to either delivery vehicle. Increases in serum were more profound with the heteroconjugate delivery vehicle, while increases at tumor site were higher with the CYT-356 delivery vehicle. Although both delivery vehicles were able to direct oligos to targeted tissue *in vitro* and *in vivo*, the Cytogen vehicle seemed to be more efficient.

**#589 Sensitization of tumors to radiotherapy and chemotherapy by systemic delivery of anti-HER-2 oligonucleotides.** Rait, Antonina, Pirolo, Kathleen F., Tang, Wen-Hau, Xu, Liang, Hao, Zheng-Mei, Xiang, Lalman, and Chang, Esther H. *Lombardi Cancer Center, Georgetown University Medical Center, Washington DC, 20007 and Stanford University, Stanford, CA 94305 (Z-M.H.)*

Failure to respond to therapy is an unmet medical need in the treatment of cancer. The incorporation into current cancer therapies of a new component that increases sensitization would have immense clinical relevance. The anti-sense (AS) strategy involves short oligonucleotides that selectively bind to specific nucleic acids modulating the expression of the targeted gene product. The attractiveness of the AS therapeutic approach is its potential for high specificity. However, one limitation is the lack of an efficient delivery system. We used a ligand-directed, cationic liposomal systemic gene delivery system in our laboratory to deliver an AS HER-2 oligonucleotide to sensitize tumor cells to radiotherapy and chemotherapeutic agents *in vitro* and *in vivo*. The introduction of AS HER-2 via the ligand-liposome system significantly sensitized these cancer cell lines to radiation and chemotherapeutics *in vitro*. More significantly, *in vivo* systemic delivery of ligand-liposome-AS-HER-2 was able to sensitize breast cancer xenograft tumors to chemotherapy, resulting in significant tumor growth inhibition. These findings demonstrate the potential of this tumor-directed, ligand liposome delivery system for AS HER-2 as a new component in a more effective treatment for primary and metastatic cancer.

**#590 Determination of the accessibility of antisense oligonucleotides to native MDM2 RNAs in cell extracts.** Li J.R., Momand J., Wang J.M., Li H.T., Westaway S., Caslanotto D., and Rossi J. *Department of Molecular Biology (L.J.R., L.H.T., W.S., C.D., R.J.) and Department of Cell and Tumor Biology (M.J.), Beckman Research Institute, 1450 E. Duarte Road, Duarte, CA 91010, U.S.A.; Department of Clinical Laboratory, the Great Wall Hospital, 28 Fu-Xing Road, Beijing 100853, P.R. China (W.J.M.)*

MDM2 (murine double minute chromosome clone number 2) is an oncogene initially cloned from a spontaneously transformed mouse cell line. It forms a complex with the p53 tumor suppressor gene product and can inactivate p53. Several types of tumors and malignancies appear to overexpress MDM2 protein. In model systems, it has been demonstrated that inhibition of MDM2 through MDM2 antisense oligonucleotides or antibodies directed against MDM2 can lead to upregulation of p53 growth suppression activity. Such results indicate that anti-MDM2 reagents may be useful as anti-neoplastic agents for some cancers. At this point it is not clear what reagent will prove to be the most efficient in eliminating MDM2 *in vivo*. Therefore, we have pursued a strategy to build a set of ribozymes against MDM2 transcripts that could be used, in the future, as a form of gene therapy. Ribozyme cleavage efficiency usually parallels the efficiency of antisense-mediated RNase H cleavage in a cell extract assay in which all endogenous protein functions remain, including RNase H cleavage activity. To select potential sites for efficient ribozyme cleavage, four antisense oligonucleotides were designed: 1) Antisense (AS) 1: 5'-CTCGTCA-



GAGGGGTCGC-3'; 2) AS 2: 5'-ACGGGGACTGACTACTGC-3'; 3) AS 3: 5'-CACCTTCAAGGTGACAC-3'; and 4) AS 4: 5'-GATCACTCCACCTTCAAGG-3'. The scrambled oligonucleotide 5'-CGCTGGGGAGACTGCTC-3' was used as a negative control because it won't form a hybrid with the MDM2 mRNA and RNase H cannot cleave the MDM2 mRNA in the absence of a hybrid. Antisense-mediated RNase H cleavage experiments in an osteosarcoma cell (SUSA-1) extracts showed that 67.1% of MDM2 transcript was cleaved at AS1 site compared to that of control; 13.5% at AS2; 14.3% at AS3; and 100% at AS4. These results indicated that AS1 and AS4 might encode potential cleavage sites for ribozymes to down-regulate MDM2 expression. Ribozyme oligonucleotides corresponding to the AS1 and AS4 will be synthesized for Ribozyme cleavage tests of MDM2 transcripts in the cell extract and cell culture.

**#591 Mouse strain differences affect the antitumor activity of ISIS 2503, an antisense phosphorothioate oligodeoxynucleotide targeted to Ha-ras, against the MDA-MB-231 breast carcinoma.** Orr Rosanne M, Valenti Melanie R, Brunton Lisa A, Carnochan Paul, Brooks Robert C, Wanciewicz Edward, Monia Brett P, Workman Paul. *CRC Centre for Cancer Therapeutics, The Institute of Cancer Research, Surrey, UK and Isis Pharmaceuticals Inc., CA, USA.*

ISIS 2503 is a fully thioated 20 mer targeted to the translation initiation region of human Ha-ras RNA and is currently in a multicenter phase I trial in the US against a broad spectrum of solid tumor types. In this current study, 2 colonies of athymic nude mice, ICR (a closed outbred colony) and Balb-C, have been used to assess the antitumor activity of ISIS 2503 against the human MDA-MB-231 breast tumor implanted subcutaneously. ISIS 2503 was injected at 25 mg/kg i.v. for 21 days. The control doubling times of the MDA-MB-231 tumors in ICR and Balb-C mice were 4.1 and 3.4 days respectively. After 21 days the tumors were 36% of control tumour volumes in the treated Balb-C mice whereas no growth delay was observed in the ICR mice (113% of controls). Significant thrombocytopenia ( $P=0.0015$ ) was observed in the Balb-C mice with a concurrent decrease in RBC counts ( $P=0.01$ ) on Day 22. There were no changes in PT, PTT or fibrinogen following antisense treatment in either mouse strain, indicative of no other clotting abnormalities. Vascular volume and permeability of tumor, lung, brain, muscle and small bowel were equivalent in the 2 strains of mice, as analyzed using radiolabeled mouse albumin. However, Ha-ras message decreased to 66% (Day 8) and 68% (Day 22) of control tumors in Balb-C mice whereas no decrease was seen in the treated tumors in ICR mice. On Day 8, tumor-associated full length ISIS 2503 concentrations, as measured by CGE, were  $0.6 \mu\text{M} (\pm 0.14)$  and  $1.02 \mu\text{M} (\pm 0.28)$  in the ICR and Balb-C mice respectively.

In conclusion, the strain of athymic nude mouse affects the sensitivity of the MDA-MB-231 breast tumor to ISIS 2503. This is an important factor in experimental chemotherapy with antisense oligodeoxynucleotides.

**#592 Identification of genes showing altered expression in antisense K-ras-transduced pancreatic cancer cells with suppressed tumorigenicity.** Aoki Kazunori<sup>1</sup>, Ohnami Shumpel<sup>2</sup>, Nakano Masafumi<sup>2</sup>, Terada Masaaki<sup>2</sup>, and Yoshida Teruhiko<sup>2</sup>. <sup>1</sup>Section for Studies on Host-Immune Response, <sup>2</sup>Genetics Division, National Cancer Center Research Institute

We previously reported that the liposome-mediated transduction of an antisense K-ras RNA expression vector was effective and safe to treat the peritoneal dissemination of pancreatic cancer (*Cancer Res.* 55: 3810-6, 1995). To enhance the transduction efficiency of antisense K-ras, we constructed an antisense K-ras expressing adenovirus vector (Ax-AS). The infection of Ax-AS induced an apoptosis in pancreatic cancer cells AsPC-1. The intravenous injection of Ax-AS suppressed the hepatic growth of AcPC-1, and intratumoral injection of Ax-AS inhibited subcutaneous tumor growth of HCT15 colon cancer cells in nude mice. Antisense K-ras adenovirus may be a promising vector for cancer gene therapy.

K-ras point mutation is found in pancreatic cancer at characteristically high frequency of 70-80%, and pancreatic cancer cells with activated K-ras appear to depend heavily on a K-ras-mediated growth signaling pathway for their growth (*Mol. Carcinog.* 20: 251-8, 1997). One possible explanation for the unusual dependency of pancreatic ductal carcinogenesis on K-ras activation is that K-ras mutation leads to activation of a special set of cancer-related genes in pancreatic duct epithelium. The RNA differential display method (DD) was employed to compare the mRNA expression profile of AsPC-1, and that of the antisense K-ras-transduced, growth retarded AsPC-1 cells. cDNA fragments were isolated from 20 bands on the DD gel, and their differential expression between two cell lines was confirmed. A sequence analysis revealed that all of the 11 clones up-regulated in the antisense transduced cells were mitochondrial genes such as 16s rRNA, cytochrome oxidase and NADH dehydrogenase gene. The other 9 cDNA clones which were down-regulated in the antisense transduced AsPC-1 cells included an oncogene *PTI-1* (prostate tumor inducing-1) and matrix metalloproteinase (MMP)-7. These genes may be novel targets of gene therapy for pancreatic cancer.

**#593 Disruption of ceramide metabolism by transfection with glucosylceramide synthase antisense reverses adriamycin resistance in human breast carcinoma cells.** Yong-Yu Liu, Tie-Yan Han, Armando E. Giuliano and Myles C. Cabot. *John Wayne Cancer Institute at Saint John's Health Center, 2200 Santa Monica Blvd., Santa Monica, CA 90404*

Ceramide, a critical messenger in the apoptotic signaling pathway, is generated in cells in response to chemotherapy and radiotherapy. Cellular resistance to apoptosis has been linked to metabolic dysfunction of ceramide production. Previous evidence from our laboratory shows that increased proficiency to glycosylate ceramide confers adriamycin resistance in breast cancer cells (*J. Biol. Chem.* 274:1140-1146, 1999). With this, we hypothesized that decreasing the cellular glycosylation potential would result in heightened drug sensitivity, a novel way to overcome adriamycin resistance. The enzyme, glucosylceramide synthase (GCS) converts ceramide to glucosylceramide, and, hence, is a natural pathway for down-shifting cellular ceramide levels. By transfecting adriamycin resistant human breast cancer cells (MCF-7-AdrR) with GCS antisense (asGCS), using pcDNA 3.1/hisA, we developed a new cell line, MCF-7-AdrR/asGCS. RT-PCR and Western blot revealed a marked decrease in both GCS mRNA and protein in MCF-7-AdrR/asGCS cells, compared with the MCF-7-AdrR parental cells. MCF-7-AdrR/asGCS cells exhibited 30% less GCS activity, *in vitro*, ( $19.73 \pm 1.06$  vs.  $27.37 \pm 2.27$  glucosylceramide pmol/h/ $\mu\text{g}$ ) and were 28-fold more sensitive to adriamycin ( $\text{EC}_{50}$ ,  $0.44 \pm 0.01$  vs.  $12.4 \pm 0.68 \mu\text{M}$ ,  $p < 0.0001$ ). GCS antisense transfected cells were also 2.4-fold more sensitive to  $\text{C}_6$ -ceramide ( $\text{EC}_{50}$ ,  $4.03 \pm 0.03$  vs.  $9.58 \pm 0.49 \mu\text{M}$ ,  $p < 0.0005$ ), compared to the parental cell line. This work shows that transfection of asGCS tempers the expression of GCS and restores cell sensitivity to adriamycin.

**#594 p21WAF1/CIP1 antisense therapy radiosensitizes human colon cancer by converting growth arrest into apoptosis.** Tian H, Wittmack EK, Jorgensen TJ. *Department of Radiation Medicine, Lombardi Cancer Center, Georgetown University Medical Center, 3970 Reservoir Road, N.W., Washington DC 20007-2197, USA.*

Resistance to radiotherapy is common clinical problem for human malignant tumors. For wild type p53 expressing tumors, radiation-induced cell cycle arrest caused by p53-mediated transactivation of p21, as an alternative to apoptosis, may be a major component of resistance mechanism. Substantial evidence exists supporting the concept that loss of cellular p21WAF1/CIP1 results in significantly increased apoptotic killing by ionizing radiation. We hypothesized that a p21-antisense oligodeoxynucleotide (ODN) could be used to sensitize cancer cells to radiotherapy. *In vitro* treatment of colon cancer cells (HCT116/p21+/+) with p21-antisense-ODN (200 nM) led to inhibition of radiation-induced p21 expression (> 95% inhibition, 0-30 Gy), resulting in loss of G1 arrest and enhancement of apoptosis to comparable levels and with similar kinetics to HCT116/p21-/- cells (~60% apoptotic cells at 96 h following 10 Gy). *In vivo*, p21-antisense-ODN in combination with radiation (intraperitoneally 6 days at 20 mg/kg/day ODN and 15 Gy) increased apoptosis in subcutaneous p21+/+ tumors in nude mice to levels similar to p21-/- tumors (2-fold at 24 h post-irradiation) and improved radiocurability of p21+/+ tumors into levels comparable to p21-/- tumors (p21+/+, 2/8 cures vs. p21-/-, 2/9 cures). Our findings suggest that p21 treatment may be a rational approach to improve conventional radiotherapy outcomes.

**#595 The mutations of gene Bax are an infrequent event in the low grade lymphomas.** Martini M., D'Ald F., Pierconti F., Ricci R., Leone G., Larocca L. M. *Istituto di Pathologia and Hematologia of Università Cattolica del Sacro Cuore, Rome.*

The gene Bax is one of the most important genes in the apoptosis regulation. Recently, it has been proposed that inactivating mutations of this death agonist may contribute to the pathogenesis of human tumors. In particular, among the hematological malignancies, Bax mutations have been detected at a certain frequency in Burkitt lymphomas, LLA-T, and in a 20% of cell lines derived from hematological malignancies. This study aimed at defining the status of the Bax gene in 60 paraffin-embedded low grade lymphomas biopsies, including centroblastic/centrocytic lymphomas (15), mantle cell lymphomas (15), marginal cell lymphomas (15) and small lymphocytic lymphomas (15). All six Bax exons and flanking sequences were subjected to mutational analysis by polymerase chain reaction-single strand conformation polymorphism (PCR-SSCP) followed by direct sequencing of positive cases. CEM cell line was used as mutated control and DNA of a normal donor as wild type control. All analysed cases showed wild type Bax gene alleles, independently of histological subtyping. In order to investigate whether Bax inactivation in these samples may occur through mechanism other than gene mutation, Bax protein expression was investigated by immunohistochemical analysis. A normal expression of Bax protein was present in all samples analysed. Overall, this study indicates that deregulation of apoptotic control in low grade lymphomas is not caused by Bax mutations and that other molecular mechanisms are implicated. Moreover, the discrepancy between the high frequency of Bax mutations detected in cell lines and the low incidence in primary biopsies, would be explained with a selective "in vitro" growth advantage of tumor clones harboring inactivated Bax gene.

**#596 Enhanced antitumor efficacy by combining a new nucleoside analogue FMdC [(E)-2'-deoxy-2'-(fluoromethylene)cytidine] and cisplatin in A549 human lung xenografts.** Yu, Ning Y., Patawan, Montesa B., Peña, Rhoneil, L.S., Chen, Joy Y., Tressler, Robert J., and Jones, Richard E. *Matrix Pharmaceutical, Inc., Fremont, CA.*

FMdC is a novel nucleoside analogue of deoxycytidine. After intracellular phosphorylation, FMdC irreversibly inhibits ribonucleotide reductase activity, resulting in a reduction in dNTP pools. FMdCTP competes with dCTP for incorporation into DNA, resulting in DNA chain termination and cell death. FMdC as a single agent has demonstrated a broad spectrum of antiproliferative activity in vitro and antitumor activity in vivo. Currently FMdC is in Phase II trials in patients with non-small-cell lung cancer (NSCLC) and colorectal cancer. The purpose of this study was to evaluate the effect of FMdC when combined with the DNA-damaging agent cisplatin (CDDP). CDDP-mediated induction of DNA repair should result in an increase of FMdCTP incorporation into DNA and an enhancement of cell death. Athymic mice with subcutaneously implanted A549 human lung cancer xenografts were treated when tumors reached approximately 100 mm<sup>3</sup> in size. FMdC or gemcitabine at a dose of 20 mg/kg was administered intraperitoneally 2 times a week for 2 weeks, and CDDP at 4 mg/kg once a week for 2 weeks. The time for tumors to quadruple (4x) in size was determined. The median tumor volume quadrupling time was 18.8 days for untreated controls, and 18.9, 19.7, and 18.2 days for FMdC, gemcitabine, and CDDP treatment groups, respectively. Combining FMdC and CDDP extended the 4x endpoint to 25.8 days, a greater than additive effect, whereas the 4x endpoint for the gemcitabine/CDDP combination was 18.9 days, which was no better than single agents. The enhancement of efficacy by combining FMdC and CDDP appeared to be synergistic. Another study evaluating the effect of dosing sequence and time interval between FMdC and CDDP showed that the degree of synergism of the FMdC/CDDP combination was sequence- and time-dependent. In conclusion, FMdC/CDDP combination therapy results in a synergistic antitumor effect in the A549 NSCLC tumor xenograft model that is dependent on both dosing sequence and time interval.

fmol/mg protein) and IPC227 (AGT activity = 40 fmol/mg protein), were examined for their sensitivity to 3 families of alkylating agents: i) 4 nitrogen mustards: glufosfamide mustard (D-19575), a new compound synthesized by ASTA Medica (Frankfurt, Germany) less toxic and more efficient than ifosfamide *in vivo*, phosphoramide and ifosfamide mustards (D-18846 and D-18847, active metabolites of cyclophosphamide and ifosfamide), and melphalan; ii) 2 nitrosoureas: carmustine (BCNU) and cystemustine (CMOEN<sub>2</sub>); iii) 2 compounds belonging to the platinum family, carboplatin and cisplatin. Additionally, depletion of AGT activity with O<sup>6</sup>-benzyl-N<sup>2</sup>-acetylguanosine (BNAG) at 300 μM during 4 hours was performed to evaluate the relationship between AGT and resistance to these treatments. Cytotoxicity assays used were: sulforhodamine B test (SRB), Alamar Blue test and a DNA fluorimetric assay using Hoechst 33342. Based on IC50s determined by SRB, the IPC227 cell line was 1.95-times more sensitive to CMOEN<sub>2</sub> and 1.83-times more sensitive to BCNU, but not to D-19575 (ratio = 1.07) than M3Dau cell line. In M3Dau cell line, according to the cytotoxicity assay employed, potentiation of CMOEN<sub>2</sub> cytotoxicity by BNAG was between 1.87 and 2.19-fold, with a statistically validated difference (0.01 < p < 0.05) between IC50s with or without BNAG. This potentiation exceeded that of BCNU (1.42 to 2.15-fold 0.03 < p < 0.18). No potentiation of all others alkylating agents cytotoxicity was observed (0.73 to 1.12-fold, p > 0.05). These results confirmed a direct relationship in melanoma cells between AGT activity level and sensitivity to the two nitrosoureas tested; and that this relationship was more pronounced for CMOEN<sub>2</sub> than for BCNU. Thus, the use of an AGT inhibitor could have a clinical incidence in the treatment by nitrosoureas of chemoresistant tumors. For other alkylating agents (nitrogen mustards, notably D-19575, and platinum derivatives) no correlation was found between AGT activity and the cytotoxicity of these treatments, thus, resistance would be multifactorial and dependent on other factors than AGT activity level.

**#599 Cellular determinants of Oxaliplatin sensitivity in a panel of human colon cancer cell lines.** S. Gulchard, S. Arnould, J. Hennabille, R. Bugat, P. Canal. *Institut Claudius Regaud, Laboratoire de Pharmacologie, Toulouse, France.*

Oxaliplatin (L-OHP) is a new platinum derivative that showed antitumor activity in colon carcinoma in preclinical studies, now used in the chemotherapeutic treatment of metastatic colorectal carcinoma. By contrast, cisplatin (CDDP) is barely cytotoxic in colon cell lines. The difference in cytotoxicity profiles between L-OHP and cisplatin, demonstrated by the NCI cytotoxicity screening, implies a different mechanism of action. Intracellular accumulation of the drug, detoxification by glutathione and glutathione-related enzymes, and DNA adducts formation and repair are major factors involved in cellular sensitivity to platinum compounds. We determined these cellular parameters and evaluated their relationship with LOHP sensitivity on a panel of 7 colon cancer cell lines. The IC50s of L-OHP and CDDP were determined by sulforhodamine B technique. Detoxification was evaluated by determining glutathione and glutathione-S-transferase cellular levels. Adducts formation and repair were determined by atomic absorption spectrophotometry. Expressions of transcripts of DNA repair genes, hMSH2 and hMSH6 for mismatch repair (MMR), and ERCC1 and XPAC for nucleotide excision repair (NER) were evaluated by RT-PCR. Results were expressed as ratio with β-actin expression.

IC50s after 1-h exposure of the different cell lines ranged from 18 to 77 μM and 12 to 46 μM for CDDP and LOHP, respectively. No clear relationship was found between detoxification process and LOHP sensitivity. A different pattern of gene expression seemed to be probably related to the difference between CDDP and L-OHP sensitivity: we confirmed that hMSH2 expression was related to cisplatin sensitivity (r<sup>2</sup>=0.45); moreover, we found a linear relationship between both hMSH6 and XPAC expressions and L-OHP IC50s (r<sup>2</sup>=0.30 and 0.47, respectively). Investigations are ongoing to determine the regulation of MMR and NER gene expressions during L-OHP treatment.

**#600 Differences in repair of tandem oxidative damage lesions by endonuclease III homologs.** Carlton D. Donald, Rhadika Venkateraman, Hou J. You, Paul W. Doelsch, Robinindra Roy and Yoke W. Kow. *Department of Radiation Oncology (CDD, RV, YWK) and Biochemistry (HJY, PWD), Emory University, Atlanta, GA; 30335 Sealy Centre for Molecular Science, University of Texas Medical Branch (RR), Galveston, TX 77555.*

Ionizing radiation and other free radical-generating systems induce a great variety of oxidative damage to DNA bases including base modifications, abasic sites, strand breaks, crosslinks and tandem base damage. The removal of oxidative damage from DNA is thought to be conducted primarily through the base excision repair pathway. The Escherichia coli endonuclease III (Nth) is a N-glycosylase-associated apurinic/apyrimidinic (AP) lyase that recognize a wide variety of damaged pyrimidines. We have investigated the capacity of E. coli Nth protein to cleave 32mer DNA duplexes containing single and tandem dihydrouracil (DHU) residues. In addition, we compared the activity of Nth from E. coli to homologs from human (Nth1) and S. cerevisiae (Ntg1 and Ntg2) as well as to E. coli endonuclease VIII. The results show that E. coli Nth recognizes single DHU lesions well in the sequence context used, however, tandem lesions are recognized very poorly. Endonuclease VIII preferentially removes lesions at position 20 of the tandem lesion when DHU is present at position 19 and 20. Reaction of human Nth1 with the 5' labeled

**#598 Role of O<sup>6</sup>-Alkylguanine-DNA alkyltransferase depletion on sensitivity to glufosfamide (D-19575) and other alkylating drugs in human melanoma cells.** Marchenay, Cécilia, Debiton, Eric, Rolhion, Christine, Maurizis, Jean-Claude, Cellarier, Eric, Pohl, Jörg, Madelmont, Jean-Claude, and Chollet, Philippe. *Centre J Perrin, Inserm U484, Clermont-Ferrand, France; ASTA Medica AG, Frankfurt, Germany.*

The DNA repair protein, O<sup>6</sup>-alkylguanine-DNA-alkyltransferase (AGT), removes alkyl groups from the O<sup>6</sup>-position of guanine, and appears as the main mechanism protecting cells against alkylating agents, notably nitrosoureas. To determine the involvement of this protein on toxicity of different treatments, two melanoma cell lines, M3Dau (AGT activity = 300/136



DHU substrate results in only one band corresponding to the product of a cut at position 19. However, 3' labelling of the same substrate shows equal cutting at both positions 19 and 20 of the substrate oligomer. These results are indicative of 3' processing of the substrate cleaved at position 20. Ntg1 preferentially cleaves at position 19 of the tandem lesion, but Ntg2 shows equal cutting of 5' labeled DHU substrate. Furthermore, when the substrate was 3' labeled, Ntg2 shows more of a product corresponding to a cut at position 20. These results suggest 5' processing of the substrate cleaved at position 19 compared to Ntg1 which showed no processing. These results demonstrate differences in cleavage and processing abilities of various endonucleases.

**#601 Re-expression of hMLH1 in vivo by the demethylating agent 5-aza-2-deoxycytidine sensitises a mismatch repair deficient ovarian tumour xenograft to cisplatin, temozolomide and epirubicin.** Plumb, Jane A, Sludden, Julieann, Strahdee, Gordon and Brown, Robert. *Department of Medical Oncology, University of Glasgow, CRC Beatson Laboratories, Garscube Estate, Glasgow G61 1BD, UK.*

Loss of DNA mismatch repair due to hypomethylation of the hMLH1 gene promoter occurs at a high frequency in a number of human tumours. In cell lines *in vitro* loss of hMLH1 expression results in resistance to some cytotoxic drugs including cisplatin (CP), temozolomide (TEM) and epirubicin (EPI). We have shown that re-expression of hMLH1 by chromosome 3 (C3) transfer or by treatment with the demethylating agent 5-aza-2-deoxycytidine (DAC) sensitises the hMLH1 negative ovarian tumour cell line A2780/CP70 to CP *in vitro*. We have now investigated whether DAC can be used *in vivo* to sensitise tumours where hMLH1 loss is due to promoter hypomethylation. Cells were grown as xenografts in athymic nude mice. Mice were treated with a single dose of cytotoxic drug (CP 6 mg/kg ip; TEM 200 mg/kg ip; EPI 10 mg/kg iv) once tumours reached a mean diameter of 1 cm and response is expressed as time (days) to double the initial volume.

The doubling time of the hMLH1 positive drug sensitive A2780 tumour was increased from 2.1 to 3.8 by CP. For A2780/CP70 tumours the doubling time (2.4) was not significantly affected by CP (2.0) or TEM (1.9) but was increased by EPI (2.8). In contrast, B1 tumours (CP70+C3) which retained expression of hMLH1 *in vivo*, were sensitive to CP (doubling time increased from 2.9 to 5.1), TEM (4.7) and EPI (4.8). Tumour bearing mice were treated with DAC (5 mg/kg ip x 3 at 3 hr intervals). After 6 days significant re-expression of hMLH1 in A2780/CP70 cells could be observed, which was associated with a decreased in hMLH1 promoter methylation. Therefore, this time point after DAC treatment was used to treat mice with a cytotoxic drug. The doubling time (2.4) was not affected by DAC alone (2.5). However, DAC treatment sensitised the drug resistant A2780/CP70 tumours to CP (3.8), TEM (3.6) and EPI (6.1). AZA treatment did not increase the growth delay observed in hMLH1 positive B1 tumours for these cytotoxic drugs.

These results show clearly that DAC can induce re-expression of hMLH1 *in vivo* and sensitise drug resistant tumours. Thus, DAC could have a role in increasing the efficacy of chemotherapy for patients whose tumours lack hMLH1 expression due to promoter methylation.

## SECTION 2: DNA-INTERACTIVE AGENTS

**#602 Multidrug Resistance Induced by DNA Minor Groove Alkylation of Ecteinascidin 743 (Et743).** Takebayashi Yuji, Urasaki Yoshimasa, Pourquier Philippe, Zimonjic Drazen B., Popescu Nicholas C., and Pommier Yves. *Labs. Mol. Pharmacology and Exp. Carcinogenesis, Division of Basic Sciences, NCI, NIH, Bethesda, Maryland.*

Ecteinascidin 743 (Et743, NSC 648766) isolated from the Caribbean tunicate *Ecteinascidia turbinata* is a potent antitumor agent presently in phase I/II clinical trials. Et743 has recently been shown to alkylate selectively guanine N2 in the DNA minor groove (Biochemistry, 1996, 35: 13303-9). We have also found that DNA minor groove alkylation by Et743 induces topoisomerase I (top1)-mediated protein-linked DNA breaks and that top1 is a target for Et743 *in vitro* and *in vivo* (Proc. Natl. Acad. Sci., 1999, 96: 7196-201). We have generated a resistant cell line (ER5) against Et743 by continuous drug exposure using HCT116 cells. The IC50 of Et743 in ER5 is thirty times higher than in parental HCT116, and resistance is stable. ER5 cells are cross-resistant to other DNA damaging agents including doxorubicin, etoposide and camptothecin and its derivatives. Although top1 is a target of Et743, expression of top1 and formation of top1 cleavage complex are not different in ER5 and HCT116 cells. Expressions of Pgp, MRP, LRP and topoisomerase II do not differ significantly between the two cell lines. Interestingly, the survival rate of ER5 is higher than that of HCT116 after UV treatment. ER5 cells are tetraploid, and replication errors are increased in ER5 cells, as determined by microsatellite instability analysis. These results indicate that the mechanism of resistance to Et743 in ER5 cells is downstream of top1 and is associated with cell cycle checkpoint alterations.

**#603 Differential recognition of minor groove Et 743-DNA adducts by UvrABC nuclease.** Zewall-Foote, M., and Hurley, L.H. *Department of Chemistry and Biochemistry and Division of Medicinal Chemistry, The University of Texas at Austin, Austin, TX 78712.*

Ecteinascidin 743 (Et 743), a natural product derived from a marine tunicate, is a potent antitumor agent in phase II clinical trials. Et 743 binds in the minor groove of DNA and alkylates N2 of guanine. The Et 743-DNA adduct is unique in that it is the first example of a minor groove alkylator that bends DNA toward the major groove. The sequence selectivity of Et 743 is governed by the different patterns of hydrogen bonding. Through NMR studies, we have shown that the highly reactive sequences 5'-PuGC or 5'-PyGG is stabilized by a hydrogen bonding network while the low reactive sequences 5'-NG(A/T) are much less stabilized due to the loss of hydrogen bonds. In this study, we have used the multisubunit endonuclease UvrABC to provide a possible rationale for the antitumor activity of Et 743. The Et 743-DNA adducts are indeed recognized and incised by the UvrABC repair proteins, however, the pattern of recognition is unexpected. First, the DNA sequences that are weakly reactive toward Et 743 are generally incised to a higher degree than the highly reactive sequences. In addition, within the same Et 743 recognition sequence, the level of incision varies, indicating that the flanking regions may contribute to the differential incision efficiency. Second, cleavage on the 5' side of the Et 743-DNA adduct is sometimes aberrant and third, at high Et 743 concentrations, repair of the DNA lesions is inhibited. These results suggest that the highly reactive and biologically relevant Et 743 recognition sequences are not repaired readily and this may contribute to the mode of action of Et 743. (Supported by grant CA-49751 from NCI.)

**#604 Comparative NMR and modeling study of Et 743, Et 736, and Et 729 adducts of DNA duplexes containing either the favored or less-favored target sequences.** Seaman, F.C., Moore, B.M., Foote, M.Z., and Hurley, L.H. *College of Pharmacy, The University of Texas at Austin, Austin, Texas.*

Ecteinascidin 743 coexists with biosynthetically related marine natural products that differ primarily in the nature of the C-subunit (e.g., Et 743: tetrahydroisquinoline; Et 736: tetrahydro- $\beta$ -carboline) or the N12 substituents (e.g., Et 743: Me & H; Et 729: 2H). Et 743 is currently in phase II clinical trials involving different solid tumor types. We undertook parallel structural and modeling studies of Et 743, Et 736, and Et 729 guanine N2-adducts of a 12-mer containing the favored target sequence, 5'-AGC, in order to compare these adducts' conformations and to investigate possible correlations between structural and biological properties. The results show that all agents alkylated the 12-mer's central guanine without radically distorting the DNA duplex. Et 729 is unique in that it is less rigidly held in the minor groove of the adduct. It shows more conformational flexibility than either Et 743 or Et 736. Et 736 is distinct in that it generates backbone distortion of the covalently modified DNA strand in a region opposite the agent's C-subunit. This capacity to produce recognizable backbone distortion may influence the binding of proteins at the drug attachment site and contribute to Et 736's lower biological activity relative to Et 743 and Et 729. Our current study of Et 743 adducts of DNA duplexes containing less-favored targets (e.g., 5'-AGT) reveal a much higher level of duplex distortion leading in the case of 5'-AGT to disruption of base pairing. Presumably, this disruption results from the inability of the drug-DNA complex to form the same stable hydrogen bonding complex produced between Et 743 and 5'-AGC. (Supported by grant CA-49751 from NIH.)

**#606 Interaction of synthetic fluoroquinolones with telomeric G-quadruplex DNA.** Rangan, A., Fedoroff, O.Y., and Hurley, L.H. *Division of Medicinal Chemistry, The University of Texas at Austin, Austin, TX 78712.*

The telomeric DNA has many unique features with regard to its sequence and secondary structures. It has an ability to form hairpins and G-quadruplexes. Our laboratories have already identified and characterized G-quadruplex interactive compounds that inhibit telomerase. In the present study, we demonstrate that quinobenzoxazines, synthetic analogues of fluoroquinolones, interact with G-quadruplex DNA. Although quinobenzoxazines were originally designed to be topoisomerase II inhibitors, the extended planar moiety indicated that these compounds may also interact with G-quadruplex DNA. We have used DNA polymerase extension assay, photocleavage mediated strand breakage reaction and solution NMR to evaluate the interaction of these ligands with G-quadruplex DNA. The results indicate that the quinobenzoxazines bind to and stabilize G-quadruplex DNA. They may serve as lead compounds that possess possible activity against both telomerase and topoisomerase II and achieve anti-neoplastic activity through a dual mechanism of action. (Supported by OIG and NCI grants from NCI).

**#607 PIPER, a G4 DNA-interactive compound, prevents the unwinding of G-quadruplex DNA by yeast Sgs1 helicase.** Han, H., Bennett, R.J., and Hurley, L.H. *Drug Dynamics Institute, The University of Texas at Austin, Austin, TX 78712 and Department of Molecular and Cellular Biology, Harvard University, Cambridge, MA 02138 USA.*

PIPER, a perylene derivative, is a very potent G-quadruplex (G4) DNA-interactive agent. It has been shown to inhibit DNA polymerase and telomerase by interacting with G4 structures formed within their DNA substrates. Recently, we have demonstrated that this small molecule also accelerates the assembly of G4 structures *in vitro*. Here, we present data showing that this compound prevents the unwinding of G4 structures by yeast Sgs1 helicase. Sgs1 belongs to the RecQ DNA helicase family whose members include other G4 DNA unwinding helicases such as human BLM and WRN helicases. PIPER specifically prevents the unwinding of G4 DNA but not the duplex DNA by Sgs1. Competition experiments indicate that this inhibitory activity is due to the interaction of PIPER with G4 structure rather than the helicase itself. These results combined with previous studies suggest a possible mechanism of action for these G4-interactive agents inside cells: They might induce the G-quadruplex formation in G-rich regions on genomic DNA, stabilize these structures and prevent them from being cleared by enzymes like helicases. The G-quadruplex structures, in turn, disrupt some critical cellular events such as DNA replication, transcription and telomere maintenance.

**#608 Selective interaction of cationic porphyrins with different types of G-quadruplex structures.** Han, H., Rangan, A., and Hurley, L.H. *Division of Medicinal Chemistry and Drug Dynamics Institute, The University of Texas at Austin, Austin, TX 78712.*

G-quadruplex (G4) DNA presents a potential target for the design and development of novel anticancer drugs. G-quadruplex DNA exhibits polymorphism. Hence it is critical to achieve selectivity against different types of G-quadruplexes with G4-interactive agents. In this study, we compare the interaction of three cationic porphyrins, TMPyP2, TMPyP3, and TMPyP4 with different types of G-quadruplexes using polymerase and helicase assays. Taq DNA polymerase primer extension assay indicates that TMPyP3 and TMPyP4 stabilize intramolecular foldover G-quadruplex to about the same extent, whereas TMPyP2 has much lesser stabilization effect. Yeast Sgs1 unwinding assay shows that TMPyP3 prefers parallel tetrameric G-quadruplex and TMPyP4 prefers anti-parallel dimeric G-quadruplex. TMPyP2 does not appear to affect the unwinding of either structure by Sgs1. To rationalize the difference in the enzymatic assays, gel shift and photocleavage experiments were carried out. The results not only reveal the binding modes of these porphyrins to G-quadruplex structures but also provide insight on achieving selectivity. (Supported by OIG and NCI grants from NCI).

**#609 Design, synthesis, and evaluation of second-generation cationic porphyrin analogs as telomerase inhibitors.** Lu, T., Shi, D.-F., Rangan, A., Sun, D., and Hurley, L.H. *Drug Dynamics Institute, University of Texas at Austin, Austin, TX, and Institute for Drug Development, San Antonio, TX.*

Cationic porphyrins have been reported to inhibit telomerase by interacting with G-quadruplex (G4) DNA. On the basis of the structural data and modeling studies, we designed and synthesized novel cationic porphyrins with quinolyl substituents on the porphyrin core. A series of cationic porphyrins with various combinations of pyridyl and quinolyl substituents were synthesized. The 3-quinolyl substituted porphyrins were synthesized using traditional methods by condensation of the pyrrole and aryl aldehydes. The 6-quinolyl substituted porphyrins were synthesized by a novel approach in which the 6-quinolyl substituents were assembled on a 4-acetamidophenyl porphyrin scaffold by Skraup cyclization. These compounds were evaluated for telomerase inhibition and G4 interaction. The results indicate that quinolyl substituted porphyrins exhibit better telomerase inhibition than the pyridyl substituted porphyrins. We also evaluated these compounds for

their interaction with different types of G4 structures. Interestingly, some of the compounds preferentially facilitated the formation of either the dimeric hairpin G4 or tetrameric parallel G4 structures.

**#610 Interaction of a cationic porphyrin with I-motif DNA.** Fedoroff, O.Y., Rangan, A., Chemeris, V.V., Salazar, M., and Hurley, L.H. *Drug Dynamics Institute, College of Pharmacy, The University of Texas at Austin, Austin, TX 78712.*

Telomeric C-rich strands can form a noncanonical intercalated DNA structure known as an I-motif. We have studied the interactions of tetra-(methyl-4-pyridyl)porphyrin (TMPyP4) with the I-motif forms of several oligonucleotides containing human telomeric sequences. TMPyP4 was found to promote the formation of the I-motif DNA structure. On the basis of <sup>1</sup>H-NMR studies, we have created a model of the I-motif-TMPyP4 complex that is consistent with all the available experimental data. The two-dimensional NOESY data prompted us to conclude that TMPyP4 binds specifically to the edge of the intercalated DNA core by a nonintercalative mechanism. Recently we have shown that TMPyP4 binds to and stabilizes the G-quadruplex form of the complementary G-rich telomeric strand. This result, combined with the present study, raises the intriguing possibility that TMPyP4 can trigger the formation of unusual DNA structures in telomeres and other regions of the genome that may in turn explain the recently documented inhibitory effect of TMPyP4 in cancer cells. (Supported by an NCI grant from NCI).

**#611 Illudin DNA damage is exclusively removed by transcription-coupled nucleotide excision repair due to failure of recognition by XP-C.** Jaspers Nicolaas G.J., Raams Anja, Hooijmakers Jan H.J., McMorris Trevor C., and Kelner Michael J. *Erasmus University, Rotterdam, The Netherlands and The University of California, San Diego, U.S.A.*

The agent MGI 114 (6-hydroxymethylacylfulvene, 6HMAF) is a novel semi-synthetic illudin derivative which is demonstrating antitumor activity against a variety of solid tumors in phase I and phase II trials. MGI 114 has also demonstrated activity against MDR1/gp170 and MRP/gp180 xenograft models that are not responsive to conventional agents. Early studies indicated illudins strongly inhibited DNA synthesis at <10 nM, and produced an unusual type of DNA damage. After exposure to illudins, there is a block at the G1/S interphase and cells eventually undergo apoptosis. To further investigate the mechanisms of toxicity, we studied the effect of illudin S on human fibroblast strains from patients with known defects in the nucleotide excision repair (NER) pathway (XP or CS). Cell strains with a defect in transcription-coupled NER were sensitive to illudin S. The XP-C and XP-E cells, which are deficient in global genome repair, are two exceptions in that their sensitivity to illudin S is normal. The normal response of XP-C cells to illudin S was also confirmed by UDS and RNA synthesis recovery. Thus, illudin-induced DNA adducts are not recognized by the global genome repair subpathway of NER and are repaired by the NER only in sites with stalled transcription complexes. These results are consistent with the emerging notion that blocked transcription forks are a strong signal for apoptosis. In summary, illudin-induced DNA damage is distinct from other known DNA damaging agents, such as cisplatin, which utilize the XP-C and XP-E global genome repair proteins. In contrast to UV-induced lesions, the illudin lesions appear to complete the spectrum of DNA damage by being of very low to undetectable affinity. In this condition, a stalled transcription complex evading the need for early XP-C or XP-E involvement, would be the only signal left for NER of illudin damage. Supported by the Tobacco-Related Disease Research Program, Award 7RT-0002.

**#612 Preclinical antitumor activity of a series of acylfulvene analogs.** McMorris, Trevor C., Kelner, Michael J., Daws, Robin, MacDonald, John R., Waters, Stephen J. *The University of California, San Diego, CA; MGI PHARMA, INC., Minnetonka, MN.*

The acylfulvenes are a new class of potent antitumor agents developed via rational structural modification of illudin S, a sesquiterpene product of the mushroom *Omphalotus olearius*. The lead agent in this series, MGI 114 (6-HMAF, irifulven), has demonstrated promising antitumor activity, including profound tumor shrinkage and cures, in a variety of human xenograft models. It demonstrates differential cytotoxicity and induction of apoptosis, with greater activity in tumor versus normal cells. Presently, MGI 114 is undergoing Phase II clinical trials for a variety of solid tumors. This report focuses on the preclinical activity of other patented acylfulvene analogs. Consistent with the activity shown by MGI 114, the acylfulvene analogs demonstrate a potent, broad-spectrum activity across many of the tumor cell lines represented in the NCI 60-cell panel, with the majority of GI<sub>50</sub> values below 10<sup>-6</sup> M. Mouse hollow fiber test results have demonstrated good activity (total scores ranging from 18-46), activity across a variety of tumor types and positive net cell kill (9/9 analogs tested). *In vivo* activity has been demonstrated in the drug resistant MV522 mdr1/gp170+ human lung carcinoma xenograft model in which acylfulvene analogs have led to increased life span and/or tumor shrinkage and tumor growth inhibition. Three acylfulvene analogs, NSC-690179, NSC-690180 and NSC-688985, have displayed significant activity, each producing tumor cures in the early stage NCI-H23 non-small cell lung tumor, the early stage OVCAR 3 ovarian tumor, and the early stage RXF 393 renal tumor xe-



nograft models. The broad-based antitumor activity of these acylfulvene analogs suggests that this class of compounds demonstrate the potential to produce additional clinical development candidates. (The authors gratefully acknowledge studies performed by the Development Therapeutics Program, NCI.)

**#613** A phase I with accelerated titration design (ATD) and pharmacokinetic (PK) study of BBR3464, a novel cationic triplatinum complex. Sessa Cristiana, Capri Giuseppe, Gianni Luca, Peccatori Fedro, Grasseil Giacomo, Zucchetti Massimo, Ronchi Anna, Minola Claudio, Liati Paola, Bernareggi Alberto, Camboni Gabriella, Marsoni Silvia. *Fondazione Maugeri, Pavia; Novuspharma, Monza and SENDO, Milan, Italy.*

BBR3464 is approximately 10-fold more potent than cisplatin (P), is active *in vivo* in both P-resistant and insensitive xenografts and more active in p-53 mutant tumors. Compared to P, BBR 3464 achieves a higher proportion of major DNA adducts and its interaction with DNA is not recognized by the HMG-proteins. We conducted a daily times 5 (dx5) phase I with modified ATD 4 (JNCI 1997), investigating the drug PK. Total and free Pt concentrations were assessed by ICP-MS. So far 11 pts with solid tumors were treated with available PK data in 6; the starting dose was 0.03 mg/sqm/day. Two levels of escalation have been tested in the accelerated phase (0.06, 0.12) and 2 in the standard phase (0.14, 0.17). The maximum tolerated dose appears to be 0.17 mg/sqm/day. Currently pts are entered at 0.14 mg/sqm/day. Neutropenia, complicated by fever in 2 pts, and diarrhea (D), mostly occurring on day 14, were dose limiting. D occurred unexpectedly also at lower doses. No objective responses were observed. Total and free Pt plasma level could be fitted to a bi-exponential model with a rapid distribution of 1 hour and a terminal half-life of several days. Cmax and AUC\* determined on day 5 at the highest dose were higher than those on day 1, indicating drug accumulation after repeated administration (see table). Approximately 10% of the equivalent dose of BBR3464 (2.2–13.4%) was recovered in urine in 24 hrs.

Pt. Dose Level	Cmax free Pt (ng/ml)		AUCexp free Pt (ng/ml/h)		
	D-1	D5	D1	D5	D5/D1
0.03	0.025	0.019	—	—	—
0.06	0.131	0.136	1.72	—	—
0.06	0.120	0.125	1.81	1.43	0.8
0.12	0.219	0.230	3.22	2.73	0.8
0.17	0.400	0.560	3.54	5.45	1.5
0.17	0.430	0.590	3.24	5.23	1.6

\* D = day, Cmax = Maximum plasma concentration, AUC = 24 hrs-area under the plasma concentration-time curve.

**Conclusions:** the unexpected GI toxicity does not recommend further clinical development of the dx5 schedule. Minor renal excretion and lack of nephrotoxicity suggest that hydration is not needed and that further clinical development should be done with the intermittent schedule.

**#614** A phase I clinical and pharmacokinetic trial of oxaliplatin and irinotecan (CPT-11) given every two weeks to patients with refractory solid tumors. Rothenberg ML, McClinney J, Hande KR, Dorminy C, Berlin J, Boeing A, Johnson DH, Purvis JD. *Vanderbilt University Medical Center, Vanderbilt-Ingram Cancer Center, Nashville, TN and Sanofi Pharmaceuticals, Inc., Malvern, PA.*

Oxaliplatin (oxali) is a diamminocyclohexane (DACH) platinum with structural, functional, and clinical differences that distinguish it from cisplatin and carboplatin. Irinotecan (CPT-11) is a camptothecin derivative that converts topoisomerase I into a cellular poison. Preclinical studies have demonstrated synergy between the platinum and irinotecan. This Phase I trial was designed to identify the MTD, DLT, qualitative and quantitative toxicities, and pharmacokinetic behavior of oxaliplatin and irinotecan when administered on the same day once every two weeks. To date, 13 patients (5 M, 8 F) have been treated. Median age: 58 (range: 35–77). Ten patients have had recurrent colorectal cancer, and one patient each has had soft tissue sarcoma, appendiceal carcinoma, and renal cell carcinoma. Clinical data to date:

Dose Level	Oxali mg/m <sup>2</sup>	CPT-11 mg/m <sup>2</sup>	n	Cycle 1 Gr 3–4 Tox		% Dose Delivered Cycle 1–3
				NA/D	ANC	
1	70	125	3	0/0/0	0	100%
2	70	150	3	0/0/0	0	94%
3	85	150	6	1/1/1	0	91%
4	85	175	1	0	0	Too Early

Cold-sensitive fingertip paresthesias have been observed in all patients, but have not been associated with functional impairment. Cumulative Grade 2 fatigue is common by the end of 12 cycles. DLT has not been reached and dose escalation continues. Of 10 patients with colorectal cancer: 3 PR, 3 SD, 1 PD, 3 TE. Pharmacokinetic and pharmacodynamic data for both drugs will be presented. This combination appears to be

active and well-tolerated at doses up to oxali 85 mg/m<sup>2</sup> and CPT-11 150 mg/m<sup>2</sup> q 2 weeks. These results are consistent with those reported by Goldwasser and colleagues (Proc ASCO 1998;17:242a). This trial was supported by a grant from Sanofi Pharmaceuticals, the Ingram Charitable Trust, NCI Cancer Center Support Grant P30 CA68485 and NIH CRC Grant 5M01 RR00095.

**#615** Mechanism of synergy between oxaliplatin and the topoisomerase I inhibitor SN-38. Erlichman Charles, Boerner Scott, Kaufmann Scott H. *Department of Oncology, Mayo Clinic, Rochester, MN 55905 USA.*

Irinotecan and oxaliplatin have promising activity in metastatic colorectal cancer. We examined the effects of combining SN-38 (the active metabolite of irinotecan) and oxaliplatin on HCT-8 human colon cancer cells using a colony-forming assay. The IC<sub>50</sub>'s, after 24-hour exposure to single agent SN-38 and oxaliplatin, were 1.25 nM and 1.25 μM, respectively. Analysis, using the median effect method of Chou and Talalay, revealed that when HCT-8 cells were exposed to oxaliplatin and SN-38 simultaneously for 24 hours or to the sequence of oxaliplatin → SN-38 sequence, there was antagonism. In contrast, the SN-38 → oxaliplatin sequence showed marked synergy. Cell cycle analysis demonstrated that SN-38 caused an initial S phase retardation with a subsequent arrest in G2/M. Oxaliplatin caused a small G1/S arrest. When HCT-8 cells were exposed to SN-38 followed by oxaliplatin for 24 hours each, a marked G2/M phase arrest was observed. The effects of SN-38 on oxaliplatin platinum-DNA adduct formation and removal were examined. No significant difference in the total platinum-DNA adducts formed or the rate of their removal was observed when oxaliplatin was used alone or in combination with SN-38. The effect of oxaliplatin on formation of topoisomerase (topo I)-DNA covalent complexes was assessed using a band depletion assay. Oxaliplatin at IC<sub>50</sub>'s did not alter topo I levels or increase SN-38 stabilized topo I-DNA complexes. These results indicate that the synergy observed between SN-38 and oxaliplatin cannot be attributed to altered platinum-DNA adduct formation, depletion of topoisomerase I but that there is an increased G2/M checkpoint arrest. Supported by CA73700-01 and CA69912-05 and CA15083-25.

**#616** *Schizosaccharomyces pombe* as a model system for identification of determinants of sensitivity to platinum drugs. Perago P., Gatti L., Carenini N., Howell S.B. and Zunino F. *Istituto Nazionale Tumori, 20133 Milan, Italy [P.P., N.C., F.Z.]; University of California, San Diego, CA, USA [S.B.H.]*

The fission yeast *S. pombe* has been widely used for studying basic cellular processes of eukaryotic cells, including DNA repair mechanisms and cell cycle control. In this organism, crucial physiological processes like mitosis and cell division are very similar to those of human cells. Based on these considerations, in this study we used *S. pombe* mutants as a model system for identification of determinants of sensitivity to platinum drugs, with particular reference to the role of genes involved in checkpoint control, in nucleotide excision repair and in recombinational repair. All the mutants with defects in checkpoint control (rad1, rad3, rad9, rad17, rad24–rad27) were hypersensitive to cisplatin. Also the nucleotide excision repair mutants, including strains deficient in the nuclease homologue of hERCC5 (rad13), and in an alternative nucleotide excision repair pathway (rad18), were hypersensitive to cisplatin. A similar behavior was found for recombinational repair mutants (rad21, rad22, rhp51). Epistasis analysis indicated that rad13 and rad17 were synergistic in sensitizing to cisplatin, suggesting that the two mutations are likely to affect different pathways. Differently, double mutants of rad13 and rad18 did not exhibit increased sensitivity to cisplatin. We suggest that several genes are involved as determinants of cisplatin sensitivity in yeast and multiple independent pathways, including nucleotide excision repair and checkpoint control, are responsible for regulation of cellular sensitivity to cisplatin.

**#617** Anticancer activity of alcohol amines and diamminocyclohexane derivatives of cis-diamminedichloroplatinum (II) (cisplatin). Dong Y., Narta R.K., and Uckun F.M. *Drug Discovery Program, Parker Hughes Cancer Center, Hughes Institute, St. Paul, MN 55113.*

Cisplatin (cis-diamminedichloroplatinum(II)) has potent antitumor effects on various human tumors. However, it has serious toxic side effects such as nephrotoxicity, nausea and vomiting. In attempts to develop more effective platinum-based antitumor agents with less toxicity and broad spectrum of activity, we have synthesized five alcohol amines or trans-1,2-diaminocyclohexane containing cis-platinum (II) complexes. The new compounds were characterized by <sup>1</sup>H NMR and elemental analyses, and evaluated for their *in vitro* anticancer activity using a panel of human cancer cell lines including pre-B acute lymphoblastic leukemia (ALL) (NALM-6), T-ALL (MOLT-3), multiple myeloma (U266BL, HS-SULTAN), breast cancer (MDA-MB-23 and BT-20), prostate cancer, (PC3) and brain tumor (U373) cells. The cytotoxic activity was measured using MTT ([3-(4,5-dimethylthiazol-2-yl)-2,5-diphenyl

tetrazolium bromide) assay. Apoptosis was detected with *in situ* apoptosis assay which allows the detection of exposed 3'-hydroxyl groups in fragmented DNA by TdT-mediated dUTP nick-end labelling (TUNEL). The *in vitro* anti-cancer activity of these compounds were further tested using highly sensitive clonogenic assays. Among the compounds tested, our lead compound DDE250 showed potent *in vitro* anti-cancer activity by inducing apoptosis in leukemic cells with IC<sub>50</sub> values of 456 nM and 666 nM for Molt-3 and Nalm-6, respectively. As compared to cisplatin, our lead compound was more potent (1.13 μM vs. 666 nM for Nalm-6 cells and 1.04 μM vs. 456 nM for Molt-3). This compound was also active against multiple myeloma cell lines with low micromolar IC<sub>50</sub> values. Further preclinical development of these alcohol amines and diaminocyclohexane derivatives of cis-platinum (II) containing compounds may provide basis for the design of more effective adjuvant chemotherapy programs.

**#618** A novel strategy for the design of selective genotoxins as potential cancer therapeutics. Croy, Robert G., Park, Hyun-Ju, Bevers, Susan and Essigmann, John M., Division of Bioengineering and Environmental Health, Massachusetts Institute of Technology, Cambridge, MA 02139

We have developed a concept for the design of selective genotoxins in which any of a variety of molecular changes present in tumor cells are exploited to target the lethal effects of the toxin. The compounds produce unique DNA adducts that attract proteins specifically present in tumor cells. Selective toxicity in the target cells results from the fact that the DNA adducts of these novel toxins are camouflaged by their association with the tumor-specific proteins. Persistence of DNA damage leads to greater toxicity in tumor cells than in non-tumor cells. An advantage of this strategy for the development of selective toxins is that such repair-blocking proteins need not be directly responsible for the malignancy.

The soundness of this drug design strategy was tested by the preparation of bifunctional compounds that produce DNA adducts with high affinity for the estrogen receptor (ER). The new compounds consist of an aniline mustard joined to a ligand for the ER by a stable linker. The toxicities of these compounds were evaluated in ER-positive and ER-negative breast cancer cell lines. Greater lethality was observed in cell lines that express the ER at high levels. The results of biochemical investigations supported the intended mechanism of selective toxicity. The ER was found to bind avidly to oligonucleotides containing damaged sites produced by a 2-phenylindole-linked mustard. Investigation of the repair of DNA adducts produced by this compound in breast cancer cells revealed a slower repair of interstrand DNA crosslinks in ER-positive cells than in ER-negative cells. Substitution of the phenylindole by a 7α-linked estradiol moiety produced a bifunctional compound with greater affinity for the ER and increased toxicity toward ER-positive breast cancer cells. The bifunctional 2-phenylindole-mustard and estradiol-mustard compounds are currently being evaluated in human tumor xenograft models in nude mice. Similar bifunctional compounds are being developed that may have potential for the treatment of prostate cancers.

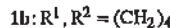
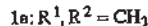
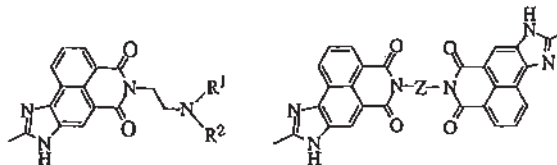
**#619** Crystal structure of the topoisomerase II poison 9-amino-[N-(2-dimethylamino)ethyl]acridine-4-carboxamide bound to the DNA hexanucleotide d(CGTAAG)<sub>2</sub>. Adams, Adrienne; Guss, J. Mitchell; Collyer, Charles A.; Denny, William A.; Wakelin, Laurence P.G. Department of Biochemistry, University of Sydney, Australia, Auckland Cancer Society Research Centre, Auckland, New Zealand, School of Physiology and Pharmacology, University of New South Wales, Australia.

The structure of the complex formed between d(CGTAAG)<sub>2</sub> and the anti-tumor agent 9-amino-[N-(2-dimethylamino)ethyl]acridine-4-carboxamide has been solved to a resolution of 1.6 Å using X-ray crystallography. The complex crystallised in space group P6<sub>4</sub> with unit cell dimensions a = b = 30.2 Å and c = 39.7 Å, α = β = 90°, γ = 120°. The asymmetric unit contains a single strand of DNA, one and a half drug molecules and 29 water molecules. The final structure has an overall R factor of 19.3%. A drug molecule intercalates between each of the CpG dinucleotide steps with its sidechain lying in the major groove and the protonated dimethylamino group partially occupies positions close to (~3.0 Å) the N7 and O6 atoms of guanine G2. A water molecule forms bridging hydrogen bonds between the 4-carboxamide NH and the phosphate group of the same guanine. Sugar rings adopt the C2'-endo conformation except for cytosine C1 which moves to C3'-endo, thereby preventing steric collision between its C2' methylene group and the intercalated acridine ring. The intercalation cavity is opened by rotations of the mainchain torsion angles a and g at guanine G2 and G6. Intercalation perturbs helix winding throughout the hexanucleotide compared to B-DNA, steps 1 and 2 being unwound by 8° and 12° respectively whereas the central TpA step is overwound by 17°. An additional drug molecule, lying with the two-fold axis in the plane of the acridine ring is located at the end of each DNA helix linking it to the next duplex to form a continuously stacked structure. The protonated NN-dimethylamino group of this "end-stacked" drug hydrogen bonds to the N7 atom of guanine G6. In both drug molecules the 4-carboxamide group is internally hydrogen bonded to the protonated N-10 atom of the acridine ring. The structure of the intercalated complex enables a rationalisation of the

known structure-activity-relationships for inhibition of topoisomerase II activity, cytotoxicity and DNA-binding kinetics for 9-aminoacridine-4-carboxamides.

**#620** Novel DNA Intercalators based on the 9-methylbenz[de]imidazo-[4,5-g]isoquinoline-4,6-dione system: Synthesis, molecular modeling and DNA binding properties. Cacho, M., López Padrola, P., Ramos, A., DePascual-Teresa, B., Braña, M.F., Abradelo, C. and Rey-Stolle, M.F. Facultad de CC. Exp. y Tecn. Univ. San Pablo-CEU. 28668-Madrid (Spain).

Mono and bis-naphthalimides are a class of intercalating agents, which have shown significant antitumor activity. Amonafide, mitonafide and elinafide have been entered into clinical trials. We now report the synthesis of a new series of mono- and bis-intercalators 1 and 2, containing an imidazo-naphthalimide chromophore, designed in order to enhance their affinity and selectivity for the DNA molecule.



Studies of viscosimetric titration with sonicated calf thymus DNA as well as UV-VIS spectrometry indicate that compounds 1 and 2 behave as mono- and bis-intercalators, respectively. Evaluation of the biological activity has shown that compounds 2 are less active than 1 and considerably less active than the parent bis-intercalating compound, elinafide. This result could be explained by the steric hindrance caused by the methyl group in position 9 of the chromophore system. Molecular mechanics and dynamics techniques have been used in order to rationalize this hypothesis.

**Acknowledgments:** We thank Knoll AG (BASF Pharma), Fundacion Ramon Areces and University San Pablo-CEU for financial assistance.

**#621** Antitumoral activity of new sesquiterpene lactones derivatives. Angelina Quintero, José Solano, Eduardo Díaz and Angel Guzmán. Facultad de Química e Instituto de Química. Universidad Nacional Autónoma de México. 04510 México.

Recently, it was reported the Michael addition of dipeptide L-Cys-L-Ala;OCH<sub>3</sub> to alantolactone which provided compounds with a biological activities. From these findings it seemed interesting to explore the 1,4-addition of 6-amino-1,3-dimethyl-2,4-pyrimidinedione to the α,β-unsaturated system of the dehydrocostus lactone, valin acetate and zalanine diacetate. The products of these reactions were submitted to biological evaluation. In the present report we describe the effects of seven modified sesquiterpene lactones previously synthesized, in order to evaluate the cytotoxic activity in several cancer cell lines using the MTT technique. The new compounds were tested in HeLa, C-33, CALO, VIPA, SW 480, MCF-7 and CHO. From all the tested compounds, two of them, III (JLNZ-106) and IV (EDAG-IV-SMe), revealed toxicity against the cancer cell lines used. The inhibition of proliferation in the different cell lines is showed. The IC<sub>50</sub> values of the cytotoxic activity for these modified sesquiterpene lactones, III (JLNZ-106) and IV (EDAG-IV-SMe), were about 16 μM and 30 μM respectively, in HeLa cell lines. In addition, we carried out assays of <sup>14</sup>C-thymidine incorporation to DNA, in the cancer cell lines. The results of these experiments showed inhibition of <sup>14</sup>C-thymidine incorporation into DNA synthesis. From these experiments we concluded that drugs III (JLNZ-106) and IV (EDAG-IV-SMe) inhibited DNA replication. In Conclusions, we demonstrated antitumoral activity of two drugs, III (JLNZ-106) and IV (EDAG-IV-SMe) in HeLa, C-33, CALO, INBL, VIPA, SW480, MCF-7 and CHO cancer cell lines. Both compounds presented cytotoxic activity and inhibited of <sup>14</sup>C-thymidine incorporation to DNA.

**#622** Small-Ring Heterocyclic Polyamine Analogues as Potential Anticancer Agents. Callery, Patrick S.; Egorin, Merrill J.; Eisman, J.L.; Li, Yanlong; Yuan, Zhi-min; Rogers, Faye A.; Kyprianou, N. West Virginia University and University of Maryland Baltimore.

**Purpose.** The objective of this work is to design and develop novel agents for the treatment of cancer based on the incorporation of small-ring nitrogen-containing heterocyclic moieties into polyamine structures that show tumor or tissue selectivity. **Methods.** Aziridine-containing spermine analogues were synthesized as described previously (U.S. Patent 5,612,329). An azetidine-containing spermine analogue was synthesized in four steps from beta alanine ethyl ester and succinic acid. Growth inhibitory activity was assessed *in vitro* against human, non-small cell lung cancer (H23 cells); human, androgen-independent prostate cancer (PC3



cells); and a panel of 60 cell lines assessed by the National Cancer Institute. An aziridine polyamine analogue was effective against PC-3 and DU-145 tumor xenografts by induction of apoptosis (Cancer Res., 58, 4664, 1998). *In vivo* efficacy studies of antitumor activity were performed in Ncr nu/nu mice bearing established H23 tumor xenografts. The polyamine analogues were administered intravenously 2 or 3 doses/week. **Results.** *In vitro* IC<sub>50</sub> values of 229 ± 52 μM to 0.72 ± 0.12 μM were obtained against PC3 cells; and 74 ± 17 μM to 1.6 ± 0.2 μM against H23 cells. In the NCI screen, the cytotoxicity profile of the aziridine analogues differed from that of the azetidine analogue which suggests that the analogues inhibit growth by different mechanisms. The azetidine analogue was a less potent inhibitor of cell growth and was less acutely toxic in mice than were the aziridine analogues. The aziridine analogues were effective inhibitors of tritiated spermidine uptake by L1210 cells, suggesting that these polyamine analogues interact with the polyamine uptake system (Cancer Res., 57, 234-239, 1997). In the efficacy studies, prolonged median tumor volume doubling times (5.5 to 10.6 days) were observed as a result of treatment with the analogues. A group of untreated control mice had a median doubling time of 3.1 days. **Conclusions.** Spermine analogues containing aziridine or azetidine functional groups have potential as agents for the treatment of cancer.

**#623 Mechanism of Camptothecin resistance in human prostate carcinoma cell lines.** Urasaki Yoshimasa, Takebayashi Yuji, Pourquier Philippe, Kohlhagen, Glenda., Chatterjee Devasis, Pantazis Panayolis, Pommier Yves. Lab. Mol. Pharmacology, DBS, NCI, Bethesda, MD. Department MCB, Brown University, Providence, RI, USA.

DNA topoisomerase I (top1) is essential for cellular metabolism and survival. It is also an important target for anti-cancer agents including camptothecins (CPT). Defining the mechanism of CPT resistance is important because CPT is a key drug for cancer chemotherapy and novel mutations could define the CPT-top1 interactions further. In this study we characterized new CPT-resistant prostate cancer cell lines, RC0.1 and RC1. Both cell lines were selected by continuous exposure of DU145 cells to increasing concentrations of 9-nitro CPT. RC0.1 and RC1 cells grow in 0.1 and 1 μM 9-nitro CPT, respectively. The RC0.1 and RC1 cells have high cross-resistance to CPT derivatives including SN38 and topotecan and are not cross-resistant to etoposide, doxorubicin or vincristine. Top1 protein levels were increased approximately 2-fold in the resistant cells compared to parental cells. Experiments with nuclear extracts demonstrated normal top1 catalytic activity in SV40 DNA relaxation assays. However, CPT-induced DNA cleavage was markedly reduced in nuclear extracts from RC0.1 and RC1 cells. RT-PCR analysis showed a point mutation resulting in a R364H mutation in the top1 of both RC0.1 and RC1. No normal top1 RNA was detectable.

In conclusion, we found a novel point mutation of top1 leading to CPT resistance.

**#624 Oncogenes as molecular targets within active chromatin.** Frenster, John H. Physicians' Educational Series, Atherton, California 94027-5446.

Active oncogenes play an important role in the pathogenesis of human neoplasms, and are found within the active portion of euchromatin in the cell nucleus (Exp. Cell Res. 93: 484 (1975)). Nuclear species of RNA, protein, and lipids are also found at these active sites, and provide possible molecular targets for imaging (Cancer Res. 31: 1128 (1971)), for analysis (Nature 248: 334 (1974)), and for therapy (Clin. Res. 26: 434 (1978)). Nuclear RNA species activate DNA transcription (FASEB J. 13: A1506 (1999)), while nuclear protein and lipid have less activity (Nature 206: 680 (1965)). Nuclear RNA species can form stable RNA-RNA duplexes (Europ. J. Cancer 11: 117 (1975)) that are resistant to RNase, are transmitted to the daughter cells during mitosis, and are more stable to strand-separation than are comparable DNA-DNA duplexes. Single-stranded RNA species have been reported to reverse the human leukemic state (Nature 197: 1077 (1963)), and may do so by forming RNA-RNA duplexes with activator RNA at oncogene sites. An analysis of activator RNA at oncogene sites and of the effects of binding such RNA with complementary RNA may provide a form of gene-specific therapy. Supported in part by USPHS Research Grant CA-10174 from the National Cancer Institute.

**#625 Antiproliferative effects of a c-myc-targeted triple helix-forming oligonucleotide (TFO) alone and in combination with chemotherapeutic drugs.** McGuffie, E.M., and Catapano, C.V. Department of Experimental Oncology, Medical University of South Carolina, Charleston, SC 29425.

TFOs bind in a sequence-specific manner to purine-rich target sequences in double stranded DNA. TFOs directed to sequences in the promoter region of a gene can interfere with transcriptional initiation, offering a means to downregulate expression of a specific gene. This strategy may have therapeutic applications in diseases where deregulated gene expression is an important pathogenic factor. The c-myc gene is an attractive target for triplex DNA-mediated transcriptional inhibition since expression of this gene is essential for proliferation and survival of many human cancer cell types. Reduced c-myc expression is also associated with induction of cell differentiation, growth arrest, and cytotoxicity by

various agents, including many currently used anticancer drugs. We have designed a TFO directed to a sequence immediately upstream of the P2 promoter of the c-myc gene. The target sequence overlaps with cis-regulatory elements important for the activity of the P2 promoter, which is the major c-myc transcriptional initiation site. The phosphorothioate (PS) TFO formed triplex with an affinity comparable to that of the corresponding phosphodiester TFO, as shown by gel mobility shift assay and DMS footprinting. Fluorescence microscopy and polyacrylamide gel analysis showed that the fluorescein-labeled PS-TFO accumulated in CEM leukemia cells at 24 h to concentrations approximately tenfold higher than the starting concentration in the extracellular medium, and remained intact in cells for up to 72 h. Incubation of CEM cells with 10 μM PS-TFO for 24 h reduced c-myc RNA levels by 40%, and c-Myc protein levels by at least 75%. A control oligonucleotide with scrambled sequence had minimal effects in these assays. A single exposure of human leukemia cells to the c-myc PS-TFO was sufficient to induce dose-dependent growth inhibitory effects as determined by MTT assays, with IC<sub>50</sub> concentrations of about 3 μM. Furthermore, when given in combination with either paclitaxel, etoposide or topotecan, the PS-TFO had additive/synergistic effects, reducing the dose of anticancer drug required to inhibit cell growth. These data indicate that the c-myc TFO has antiproliferative activity in leukemia cells, and can augment the effects of chemotherapeutic drugs, suggesting novel possible strategies for cancer treatment.

### SECTION 3: TUBULIN-INTERACTIVE AGENTS

**#626 IDN5109, a new taxane with oral bioavailability and antitumor activity.** Nicoletti, Maria L., Colombo, Tina, Monardo, Caterina, Rossi, Cosmo, Zucchetti, Massimo, Bombardelli, Ezio, Riva, Antonella, D'Incalci, Maurizio and Glavazzi, Raffaella, Mario Negri Institute, Bergamo and Milan; Mario Negri Sud, Santa Maria Imbaro; Indena S.p.A., Milan, Italy.

1 $\beta$ -hydroxy-10-deacetylpaclitaxel III derivatives is a new class of taxanes with improved pharmacological properties. IDN5109 is a new compound in this series, which has been shown to be active on tumor cell lines expressing the MDR phenotype. It has been suggested that IDN5109 is a poor substrate for P-glycoprotein, therefore we hypothesized that IDN5109 given orally could have improved bioavailability compared to paclitaxel. In this study, we investigated the oral (po) and intravenous (iv) pharmacokinetics of IDN5109, and its antitumor activity on human tumor xenografts.

IDN5109 and its 7-epi-form IDN5140 were determined in plasma of nude mice after po and iv administrations by the HPLC method. The bioavailability of IDN5109 resulted in 48%. After oral delivery of IDN5109 both C max and plasma AUC values were linear related to the dose. The antitumor efficacy of IDN5109 was determined on 1A9, HOC18 and MNB-PTX1 ovarian carcinoma xenografts transplanted sc in nude mice. IDN5109 was given po every 4 days for 3 injections (Q4x3), at three dose levels. For iv treatments, IDN5109 and paclitaxel were administered Q4x3 at their MTDs. IDN5109 given orally was highly active against the two paclitaxel responsive 1A9 and HOC18 xenografts, causing 90-100% tumor regressions, and showed significant activity on the resistant MNB-PTX1 (10% tumor regressions). The oral administration was as efficient as the intravenous route at doses reflecting the pharmacokinetic profile. IDN5109 is the first taxane showing both good oral bioavailability and potent oral antitumor activity.

**#627 3-(Iodoacetamido)-benzoylurea: A novel cancericidal tubulin ligand that inhibits microtubule polymerization, phosphorylates bcl-2, and induces apoptosis in tumor cells.** Jiang, Jian-Dong\*, Davis, Ashley\*, Middleton, Kim M\*, Ling, Yi-He\*, Perez-Soler, Roman\*, Holland, James F\*, and Bekesi J. George\*. \*Cytoskeleton, Inc. 1650 Fillmore Street, #240, Denver, CO 80206. USA. \*T.J. Martell Laboratory for Leukemia, Cancer and AIDS Research, Department of Medicine, Mount Sinai School of Medicine, New York, NY 10029. USA. \*Kaplan Comprehensive Cancer Center, New York University Medical School, New York, NY 10016. USA.

† - These authors contributed equally to this work.

3-(Iodoacetamido)-benzoylurea (3-IAABU) is a newly synthesized anti-tubulin compound with a molecular weight of 347. 3-IAABU exhibited anticancer activity in a variety of tumor cell lines with ID<sub>50</sub> in the range 0.015 to 0.29 μM for leukemic cells and 0.06 to 0.92 μM for solid tumors. Higher selectivity against malignant cells was observed with 3-IAABU than that with vinblastine and paclitaxel. It inhibits microtubule assembly in tubulin systems either with or without microtubule associated proteins (ID<sub>50</sub> was 0.1 μM and 1.2 μM respectively) and microtubule depolymerization was not affected, indicating an inhibition of polymerization by binding of 3-IAABU to the heterodimeric subunit of tubulin. 3-IAABU was shown to inhibit the binding of colchicine, a subunit binding compound, but did not inhibit the binding of vinblastine or GTP, indicating that 3-IAABU binds at or near to the colchicine site of tubulin. Tumor cells treated with 3-IAABU showed scattered chromosomes in metaphase.

Normal microtubule architecture or spindle apparatus was absent in these cells; instead, punctuated aggregates of tubulin were found by immunofluorescent staining. Cell cycle analyses showed an accumulation of tumor cells at M phase after a 4h treatment with 3-IAABU. The phosphorylated bcl-2 representative of an inactivated form of the oncoprotein was found in the cells 12h after treatment with 3-IAABU. These cells progressed to apoptosis within 16h. As a new tubulin ligand, 3-IAABU could be a promising agent in cancer chemotherapy. This work was supported by the TL Martell Foundation and NIH Small Business Innovative Research Awards.

**#628 Suicide ligands of tubulin reveal a novel mechanism of cancer cell apoptosis.** Davis, Ashley<sup>1\*</sup>, Jaing, Jain-Dong<sup>1\*</sup>, Middleton, Kim M<sup>2</sup>, Wang, Yue<sup>3</sup>, Weisz, Imra<sup>4</sup>, Ling, Yi-He<sup>5</sup>, and Bekesi J. George<sup>6</sup>. <sup>1</sup> - Cytoskeleton, Inc. 1650 Fillmore Street, #240, Denver, CO 80206. USA. <sup>2</sup> - T.J. Martell Laboratory for Leukemia, Cancer and AIDS Research, Department of Medicine, Mount Sinai School of Medicine, New York, NY 10029. USA. <sup>3</sup> - Kaplan Comprehensive Cancer Center, New York University Medical School, New York, NY 10016. USA. <sup>4</sup> - These authors contributed equally to this work.

The presently accepted mechanism of action for all anti-tumor tubulin ligands involves the perturbation of microtubule dynamics during the G2/M phase of cell division and subsequent entry into apoptosis. In this article, we challenge the established dogma by describing a unique mechanism of action caused by a novel series of tubulin ligands, halogenated derivatives of acetamido benzoyl ethyl ester (HAABE). We have developed a suicide ligand for tubulin, which covalently attaches to the target and shows potent anticancer activity in tissue culture assays and in animal tumor models. These compounds target early S-phase at the G1/S transition rather than the G2/M phase and mitotic arrest. Bcl-2 phosphorylation, a marker of mitotic microtubule inhibition by other tubulin ligands was dramatically altered, phosphorylation was rapid and biphasic rather than a slow linear event. The halogenated ethyl ester series of derivatives thus constitute a unique set of tubulin ligands which induce a novel mechanism of apoptosis. This work was supported by the TL Martell Foundation and NIH Small Business Innovative Research Awards.

**#629 Inhibition mechanism and structure-activity relationships of anti-microtubule compounds, pironetin and its derivatives.** Usui, T., Kondoh, M., and Osada, H. (Antibiotics Laboratory, Riken Institute, Japan). Pironetin and its derivatives were originally isolated as plant growth regulators from the culture broth of *Streptomyces* sp. We found that these compounds inhibited the cell cycle progression of mammalian cells in M phase and showed antitumor activity against a murine tumor cell line, P388 leukemia, transplanted in mice. Pironetin induced disruption of the cellular microtubule network in normal rat fibroblast 3Y1 cells. Since the concentrations that inhibit cell cycle progression at M phase were the same as those for disruption of the microtubule network, it is suggested that the mitotic arrest induced by pironetin was the result of the loss of the mitotic spindle. Pironetin also inhibited the microtubule assembly and glutamate-induced tubulin assembly *in vitro*. Pironetin inhibited the binding of [<sup>3</sup>H]vinblastine, but not that of [<sup>3</sup>H]colchicine, to tubulin, and the *K<sub>d</sub>* values revealed that the affinity of pironetin for tubulin is stronger than that of vinblastine. These results suggest that pironetin is a novel antitumor agent which inhibits microtubule assembly. The analyses of structure-activity relationships revealed that  $\alpha,\beta$ -unsaturated  $\delta$ -lactone ring and chirality of hydroxy moiety are important for inhibitory activity of pironetins. Using biotinylated pironetin, we found that pironetin directly and covalently binds to tubulin.

**#630 Mapping the binding site of the A ring of colchicine on  $\beta$ -tubulin: the covalent reactions of 2-chloroacetyl-2-demethylthio-colchicine (2CTC) and 3-chloroacetyl-3-demethylthio-colchicine (3CTC) with cysteine residues 239 and 354.** R. Bai, J. Ewell, N. Nguyen, A. Brossl, and E. Hamel. Science Applications International Corp-Frederick and Laboratory of Drug Discovery Research and Development, NCI, Frederick MD, Facility for Biotechnology Resources, FDA and Laboratory of Structural Biology, NIDDK, Bethesda MD.

The colchicine analogs 2CTC and 3CTC are nearly equivalent to colchicine in their inhibition of tubulin assembly and are strong competitive inhibitors of the binding of radiolabeled colchicine to tubulin. Radiolabeled 2CTC and 3CTC bind to tubulin in a temperature-dependent reaction strongly inhibited by podophyllotoxin. Both radiolabeled analogs react covalently with tubulin, with about half the bound 3CTC reacting rapidly and one-fourth the bound 2CTC reacting slowly. Radiolabeled peptides were generated by formic acid, cyanogen bromide, endoproteinase Glu-C, endoproteinase Lys-C, and/or trypsin digestion. Sequential Edman degradation for sequence analysis and quantitation of radiolabel established that covalent bond formation occurred almost entirely with cys-239 and cys-354 of  $\beta$ -tubulin. About 75% of the 2CTC radiolabel was recovered in cys-239 and 25% in cys-354, while, conversely, about 25% of the 3CTC radiolabel was recovered in cys-239 and 75% in cys-354. Because of the greater reactivity of 3CTC as compared with 2CTC, this means nearly equivalent amounts of radiolabel from the two compounds were found at cys-239, but that the ratio of radiolabel from 3CTC relative to that from

2CTC was about 6:1 at cys-354. These results will be rationalized in terms of the recently described molecular model of tubulin derived from zinc-induced sheets of antiparallel protofilaments.

**#631 Steroid derivatives interacting with tubulin: from colchicine-like to paclitaxel-like effects on tubulin polymerization.** Verdier-Pinard, P., Wang, Z., Mohanakrishnan, A.K., Cushman, M., and Hamel, E. Laboratory of Drug Discovery Research and Development, NCI, Frederick, MD 21702; Dept. of Medicinal Chemistry and Molecular Pharmacology, Purdue University, West Lafayette, IN 47907.

The structural diversity of compounds interfering with tubulin polymerization and the presence of at least three different classes of binding site on tubulin (for colchicins, vinca alkaloids, and taxoids) raise the possibility that endogenous metabolites play a physiological role in the structure and function of the microtubule cytoskeleton. Circulating hormones are subject to various metabolic pathways leading to numerous byproducts. A major estrogen metabolite, 2-methoxyestradiol has modest antimetabolic activity, interacts weakly at the colchicine site on tubulin and inhibits tubulin polymerization, but it does not bind to estrogen receptors. Moreover, it has *in vivo* antitumor activity and anti-angiogenic properties. On the assumption that the antitubulin activity of 2-methoxyestradiol was critical for its properties and that the steroid A ring and the colchicine tropolonic C ring were structural homologs, we synthesized a series of analogs. We found that 2-ethoxyestradiol had enhanced activity with tubulin and a 10-fold higher cytotoxicity. The steroid 6-member B ring was our next modification site, and this study presents such derivatives with two apparently distinct modes of action on tubulin polymerization. Simple expansion to a 7-member B ring (analogous to the colchicine B ring) resulted in a compound comparable to 2-ethoxyestradiol that inhibited tubulin polymerization and colchicine binding to tubulin. Acetylation of the hydroxyl groups in this analog and 2-ethoxyestradiol yielded inactive compounds. Unexpectedly, concomitant introduction of a ketone functionality at C6 and acetylation of the hydroxyl at positions 9 and 18 or at position 18 only, produced two compounds with paclitaxel-like activity. These agents reduced the critical concentration for tubulin polymerization and enhanced tubulin polymerization into microtubules that were partially stable at 0°C.

**#632 A new 2-methoxy estrogen analog: Estrogenic activity, effects on proliferation, and alterations in tubulin dynamics.** Brueggemeier, R.W.; Bhat, A.S.; Lovely, C.J.; Coughenour, H.D.; Joomprabutra, S.; Weitzer, D.H.; Vandre, D.D.; Yusuf, F.; Burak, Jr., W.E. Colleges of Pharmacy and Medicine, OSU Comprehensive Cancer Center, The Ohio State University, Columbus, OH 43210.

An estradiol metabolite, 2-methoxyestradiol (2-MeOE<sub>2</sub>), has shown antiproliferative effects in both hormone-dependent and hormone-independent breast cancer cells. A methoxy derivative of 2-hydroxy-methyl estradiol, 2-methoxymethyl estradiol (2-MeOMeE<sub>2</sub>), was prepared for biological evaluation and comparison with 2-MeOE<sub>2</sub>. Estrogenic activity of the synthetic analogs was evaluated in two ways, one by examining affinity of the analogs for the estrogen receptor in MCF-7 cells and the other by examining the ability of the analogs to induce estrogen-responsive gene expression. 2-MeOMeE<sub>2</sub> demonstrated weak affinity for the estrogen receptor (1.7% of estradiol) and weak ability to stimulate estrogen-induced expression of the pS2 gene (0.02% of estradiol). Antitumor activity was evaluated both *in vitro* and *in vivo*. Interestingly, 2-MeOMeE<sub>2</sub> inhibited tubulin polymerization *in vitro* at concentrations of 1 and 3  $\mu$ M and was more effective than 2-MeOE<sub>2</sub>. Both 2-MeOE<sub>2</sub> and 2-MeOMeE<sub>2</sub> were equally effective in suppressing growth and inducing cytotoxicity in MCF-7 and MDA-MB-231 breast cancer cells. The cytotoxic effects of 2-MeOMeE<sub>2</sub> are associated with alterations in tubulin dynamics, with the frequent appearance of misaligned chromosomes, a significant mitotic delay, and the formation of multinucleated cells. Assessment of *in vivo* antitumor activity was performed in athymic mice containing human breast tumor xenografts. Nude mice bearing MDA-MB-435 tumor xenografts were treated i.p. with 50 mg/kg/day of 2-MeOMeE<sub>2</sub> or vehicle control for 45 days. Treatment with 2-MeOMeE<sub>2</sub> resulted in an approximate 50% reduction in mean tumor volume at treatment day 45 when compared to control animals and had no effect on animal weight. Thus, 2-MeOMeE<sub>2</sub> is a methoxy estrogen analog with minimal estrogenic properties that demonstrates antiproliferative effects both *in vitro* and in the human xenograft animal model of human breast cancer. This work was supported in part by NIH grants NCI R01 CA73698, NCI R21 CA66193, NCI P30 CA16058, and USAMRMC DAMD17-96-1-6136.

**#633 Modeling studies of COBRA, a new class of rationally designed anti-cancer drugs targeting a unique binding cavity of tubulin.** Mao, C.; Jan, S.-T.; Li, K.; Perry, D.; Vassilev, A.; Uckun, F.M. Parker Hughes Cancer Center, Drug Discovery Program, Structural Biology, Chemistry, Biochemistry, Hughes Institute, St. Paul, MN, USA.

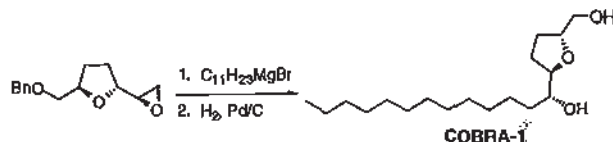
In a systematic search for novel drug binding pockets within the intermediate domain of tubulin, we discovered a previously unidentified region containing a remarkable abundance of (iso)leucine residues which could provide a highly hydrophobic binding environment for small molecule organic compounds. This unique region, located between the GDP/GTP



binding site and the taxol binding site, contains a narrow cavity with elongated dimensions which could accommodate a fully stretched aliphatic chain containing up to twelve carbon atoms. The enclosure of this putative binding cavity in  $\alpha$  tubulin (but not  $\beta$  tubulin) is provided in part by an eight amino acid insertion loop. A comprehensive structure search of the organic compound database at the Hughes Institute lead to the identification of a series of aliphatic-chain-containing compounds (namely COBRA compounds). These COBRA compounds have molecular dimensions and structural elements appropriate for hydrophobic binding interactions with the leucine-rich binding cavity of tubulin. The results of our molecular modeling and docking studies with COBRA compounds indicated that these molecules would fit much better into the  $\alpha$  tubulin binding cavity than the corresponding region on  $\beta$  tubulin. The reason for this selectivity may involve the 8-amino acid insertion loop in  $\alpha$  tubulin (not present in  $\beta$  tubulin) which serves as an enclosure to the target binding cavity. The reported compounds have a typical molecular surface area of around 350 Å<sup>2</sup>, approximately 256 Å<sup>2</sup> of which is in contact with the binding pocket on  $\alpha$  tubulin based on our calculations. The occupation of the binding pocket by COBRA-1 and others was predicted to interfere with the formation of the  $\alpha/\beta$  tubulin dimer and induce tubulin depolymerization. These predictions were experimentally confirmed in tubulin turbidity assays. All COBRA compounds studied caused partial depolymerization of tubulin and inhibited its polymerization in the presence of GTP. COBRA compounds were cytotoxic to a broad panel of human cancer cell lines at low micromolar concentrations.

**#634 Synthesis and biological activity of COBRA-1, a novel tubulin-depolymerizing anticancer agent.** Jan, S-T., Mao, C., Narla, R-K., Uckun, F.M. *Drug Discovery Program and Parker Hughes Cancer Center, Hughes Institute, St. Paul, MN 55113.*

We used a three-dimensional computer model of tubulin constructed based upon its recently resolved electron crystallographic structure for rational design of a novel class of mono-THF containing synthetic anti-cancer drugs targeting a previously unrecognized unique narrow binding cavity. This unique binding pocket has elongated dimensions and was predicted to favorably interact with the aliphatic side chains of the lead compound COBRA-1. The synthesis of the first enantiomerically pure prototype compound targeting this unique binding cavity was accomplished in an efficient two-step procedure using the THF epoxide (Li K, Vig S, Uckun FM. *Tetrahedron Letters*, 39(15), 2063-2066, 1998; US Patent 5,914,410, 1999) as a template. After the first step of epoxide opening by undecylmagnesium bromide, the debenzoylation during the second and final step resulted in the formation of COBRA-1 with an overall yield of 82%.

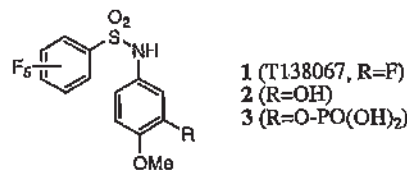


The anti-cancer activity of COBRA-1 was confirmed using MTT assays, confocal laser microscopy, and transmission electron microscopy. COBRA-1 caused destruction of microtubule organization, mitochondrial damage and apoptosis. Using two-photon confocal laser scanning microscopy, the kinetics of apoptosis in tumor cells was shown to be fast with a rapid onset at approximately 1 hr after exposure and total destruction within approximately 24 hrs. Modeling studies of COBRA-1 docked into the target binding site of tubulin revealed additional sterically available space which could be successfully exploited for the design of potentially more effective members of this novel class of anti-cancer agents. These geometric features of the binding site may provide the structural basis for the future development of more potent COBRA compounds.

**#635 Cytotoxicity and antitumor activity of the phosphate prodrug of a novel microtubule inhibitor.** Houze, Jonathan; Gergely, Joshua; Schwendner, Susan; Hoffman, Laura; Beckmann, Holger; Baichwal, Vijay; Roche, Daniel; Jaen, Juan. *Tularik Inc., Two Corporate Dr., S. San Francisco, CA 94080.*

T138067 (1) is an irreversible binder of  $\beta$ -tubulin that shows potent activity in various human tumor xenograft models and is currently undergoing phase I clinical evaluation. SAR studies around the antitumor activity of T138067 led to the identification of a promising analog, compound 2. Since the neutral form of both compounds is effectively insoluble in water, formulation of the compounds required the formation of salts of the sulfonamide moiety in the molecule. The relative instability of salts of compound 2 versus those of T138067 contributed to the choice of T138067 as the superior candidate for further development. Further investigation of compound 2 suggested that the phenol moiety might be associated with the chemical instability of its salts. A series of ester derivatives of 2 was prepared as potential prodrugs. While carboxylic esters were unsatisfactory, the phosphate ester (3) displayed the desired combination of solubility, stability and ready regeneration of phenol 2 *in vivo*. Both compounds 2

and 3 showed broad cytotoxic activity (evaluated in the NCI panel of 60 tumor cell lines) and good efficacy against MX-1 human xenografts in athymic nude mice.



**#636 A novel antitubulin agent and its phosphate prodrug effective against MX-1 human mammary tumor xenografts in athymic nude mice.** Schwendner, Susan W., Hoffman, Laura A., Thoolen, Martin J.M.C., Timmermans, Pieter B.M.W.M. *Tularik Inc., Two Corporate Drive, South San Francisco, CA 94080.*

A newly designed compound (1-methoxy-2-hydroxy-4-(pentafluorophenyl)sulfonamido)benzene, 1) prevents tubulin polymerization by covalently binding to  $\beta$ -tubulin by the same mechanism as the agent in clinical trials, T138067-sodium (2-fluoro-1-methoxy-4-(pentafluorophenyl)sulfonamido)benzene, sodium salt). The compound inhibits the growth and clonogenic potential of various tumor cell lines in culture. Its activity is not affected by the multidrug resistance (MDR) phenotype. The efficacy of this novel analog was evaluated against MX-1 human mammary tumor xenografts in athymic nude mice. A single treatment with 40 mg/kg i.v. resulted in 40% tumor regression. A dose-response relationship was seen when 1 was administered once weekly at 20, 30 or 40 mg/kg. At 30 mg/kg two mice of ten demonstrated complete tumor regression with no reappearance of the tumor with time. By comparison, vinblastine was moderately effective at inhibiting tumor growth. The phosphate prodrug of 1 was also evaluated against MX-1 mammary tumor xenografts. The dose-response relationship in tumor growth inhibition with the phosphate compound was comparable to that observed with 1. The phosphate compound was also effective at inhibiting tumor growth of 2008/C13<sup>+</sup> cisplatin-resistant human ovarian tumor xenografts in athymic nude mice.

**#637 Cytotoxicity and antitumor efficacy of T138067, a novel microtubule disrupter, against MDR-positive tumor cells.** Santha, E., Medina, J.C., Shan, B., Baichwal, V., Ladd, A., Frankmoelle, W.P., Poruchynsky, M.S., Chou, T.-C., Jaen, J.C., Timmermans, P.B.M.W.M., and Beckmann, H. *Tularik Inc., Two Corporate Drive, South San Francisco, CA 94080 (E.S., J.M., B.S., B.V., A.L., W.F., J.J., P.T., H.B.), National Cancer Institute, Bethesda, MD 20892 (M.S.P.) and Memorial Sloan-Kettering Cancer Center, 1275 York Avenue, New York, NY 10021 (T.-C.C.).*

Microtubules are linear polymers of  $\alpha$ - and  $\beta$ -tubulin heterodimers and are the major constituent of mitotic spindles, which are essential for the separation of chromosomes during mitosis. As such, a variety of plant-derived agents (e.g., vinblastine and paclitaxel) that bind reversibly to  $\beta$ -tubulin are potent inhibitors of mitotic cell growth and are useful therapeutics for the treatment of human cancer. However, tumor cells often develop resistance to these compounds. One common pathway leading to multi drug resistance (MDR) involves the enhanced expression of drug-efflux pumps (e.g., P-glycoprotein and the multidrug resistance proteins). Mounting evidence also suggests that clinical resistance to microtubule-interacting agents, in particular paclitaxel, is associated with either mutations in  $\beta$ -tubulin or changes in the expression pattern of the  $\beta$ -tubulin isotypes. We have recently described the novel microtubule-disrupting agent T138067 (2-fluoro-1-methoxy-4-pentafluoro-phenylsulfonamido)benzene) that covalently and selectively modifies the  $\beta_1$ ,  $\beta_2$ - and  $\beta_3$ -isotypes of  $\beta$ -tubulin at a conserved cysteine residue (Cys239), thereby causing cells to undergo apoptosis (Shan et al. (1999), *Proc. Natl. Acad. Sci. USA*, 96, 5686-5691). Here we show that the efficacy of T138067 in cell culture and in murine-human xenograft models is not affected by the multidrug-resistance phenotype of the tumor cells. We also present data that demonstrate that T138067 is equally efficacious in cell lines that developed resistance to paclitaxel through mutations in  $\beta$ -tubulin or via changes in the expression pattern of the various  $\beta$ -tubulin isotypes. Thus, T138067 may prove clinically useful for the treatment of multidrug-resistant human tumors or those tumors that acquire resistance to paclitaxel through alterations of  $\beta$ -tubulin expression pattern or  $\beta$ -tubulin mutations.

**#638 Synergy of T138067-sodium in combination with cisplatin against MX-1 human mammary tumor xenografts in athymic nude mice.** Schwendner, Susan W., DiMaio, Heather K., Hoffman, Laura A., Stein, Colleen K., Thoolen, Martin J.M.C., Timmermans, Pieter B.M.W.M. *Tularik Inc., Two Corporate Drive, South San Francisco, CA 94080.*

T138067-sodium (2-fluoro-1-methoxy-4-(pentafluorophenyl)sulfonamido)benzene, sodium salt) prevents tubulin polymerization by covalently binding to  $\beta$ -tubulin and inhibits the growth and clonogenic potential of various tumor cell lines in culture. Its activity is not affected by the multidrug resistance (MDR) phenotype. A dose of 30 mg/kg/hr of T138067-sodium infused i.v. for 4 hours was found to be very effective at inhibiting the growth of MX-1 human mammary tumor xenografts in athymic nude mice.

Cisplatin was also very efficacious against this tumor. The efficacy of both agents was accompanied by significant body weight loss. Administration of suboptimal doses of 3 mg/kg cisplatin i.v. bolus or 15 mg/kg/1hr T138067-sodium i.v. infusion for 4 hours was compared with the efficacy of coadministration against MX-1 tumors. The combined administration of T138067-sodium and cisplatin resulted in a significant enhancement of efficacy compared to the administration of either compound alone. This coadministration of suboptimal doses resulted in much less body weight loss and mortality than seen when these compounds are administered alone at an efficacious dose. These findings show that administration of a combination of suboptimal doses of T138067-sodium and cisplatin result in a synergistic inhibition of tumor growth with less drug toxicity.

**#639 Vinflunine and vinorelbine, novel vinca alkaloids that act by modulation of microtubule dynamic instability and treadmilling.** Ngan, V., Jordan, M.A., Wilson, L., and Hill, B.T. *Dept of Molec., Cell., & Devel. Biology, Univ. of CA., Santa Barbara, CA; USA, & Centre de Recherche Pierre Fabre, Castres, France.*

Microtubules exhibit two unusual non-equilibrium dynamic behaviors: dynamic instability, which is switching at microtubule ends between relatively slow growing and rapid shortening, and treadmilling, which is the net addition of tubulin at plus ends and loss at the minus ends. Both kinds of dynamics appear to be essential for proper mitosis. Perturbation of the dynamics by antimitotic anticancer drugs appears to be critical for their ability to block mitotic progression. We have found that vinflunine and vinorelbine exert novel effects on plus-end dynamic instability of microtubules at steady state composed of purified bovine brain tubulin. The data indicate that these drugs may inhibit cell proliferation by a mechanism that differs from vinblastine. Specifically, similar to 400 nM vinblastine, vinflunine and vinorelbine at the same concentration inhibit the rate of microtubule growth and decrease the overall dynamicity (detectable combined growth and shortening per unit time). However, in marked contrast to the action of vinblastine, vinflunine and vinorelbine do not affect the shortening rate, they reduce the fraction of time microtubules spend shortening or in an attenuated state, and they increase the duration of growth during a growing event. The distinct actions of vinflunine and vinorelbine on dynamic instability as compared with vinblastine suggest that these novel Vinca alkaloids may inhibit mitosis by a mechanism different from that of vinblastine. In related experiments with microtubules assembled from microtubule-associated proteins and tubulin, we followed  $^3\text{H}$ GTP incorporation into steady state microtubules as a means to quantitate the effects of vinflunine, vinorelbine, and vinblastine on treadmilling. We found that vinflunine and vinorelbine, like vinblastine, inhibited the treadmilling rate. However, vinflunine and vinorelbine were 7- and 1.6-times less potent than vinblastine, respectively. All three compounds appear to act by binding with high affinity to microtubule ends, and we are currently attempting to determine the number of molecules of each compound bound per microtubule and required to half-maximally suppress the treadmilling rate.

**#640 A common pharmacophore for microtubule-stabilizing agents: molecular basis for drug resistance conferred by tubulin mutations in human cancer cells.** Gussio Rick, Giannakakou Paraskevi, Nogales Eva, Downing Kenneth H., Zaharevitz Daniel, Sackett Dan, Nicolaou K.C. and Fojo Tito. *Information Technology Branch and Medicine Branch, NCI, Laboratory of Integrative and Medical Biophysics, NIDDK, NIH, Bethesda, MD, Lawrence Berkeley National Laboratory, UC Berkeley, CA, Department of Chemistry, The Scripps Research Institute, La Jolla, CA.*

The epothilones are naturally occurring antimitotic drugs that share with the taxanes a similar mechanism of action without apparent structural similarity. Here we describe two epothilone-resistant human ovarian cancer cell lines with impaired epothilone-driven tubulin polymerization, distinct  $\beta$ -tubulin mutations ( $\beta 274^{\text{Thr} \rightarrow \text{Ile}}$  and  $\beta 282^{\text{Arg} \rightarrow \text{Gln}}$ ) and cross resistance to taxanes. In the crystallographic structure of taxotere bound to  $\alpha\beta$ -tubulin, both  $\beta 274$  and  $\beta 282$  are located near the taxane ring. In addition,  $\beta 282$  is also part of the M-loop, a region involved in lateral contacts between protofilaments. We propose a common pharmacophore for the taxanes and the epothilones that is in agreement with their respective cytotoxicity in the mutant cells and with the extensive structure-activity relationship data for these compounds. Alignment of the structures for the taxanes and the epothilones allowed us to model the way in which the epothilones dock on  $\beta$ -tubulin and thus identify residues that may be crucial to drug-tubulin interaction. The model predicts two binding modes for the epothilones and shows that epothilones bind to  $\beta$ -tubulin in a similar manner to the baccatin core of taxanes. A novel epothilone analog, equipotent to epothilone B, in which the thiazole ring of the parent compound is substituted by a pyridine moiety, allowed us to identify the preferred binding mode of epothilone onto tubulin. Guided by the structure of the common pharmacophore we also identified a similar binding mode for the sarcodyctins, coral-derived tubulin stabilizing agents. In contrast to the epothilones and the taxanes, which have reduced activity in the mutant compared to parental cells, the activity of sarcodyctins A, B and their analogs was enhanced. The model presented here indicates that this enhanced activity against the  $\beta 274$  mutant cells is due to favorable interactions this particular mutation provides for sarcodyctin binding onto tubulin. The identification of a common pharmacophore for tubulin

stabilizing agents and the successful docking of epothilones and sarcodyctins onto  $\beta$ -tubulin should assist in the rational design of drugs targeting tubulin, setting the stage for further developments in cancer chemotherapy.

**#641 DNA damage-induced p21<sup>WAF1/CIP1</sup> abrogates cell death caused by microtubule-active drugs but does not affect killing of checkpoint-deficient cancer cells.** Blagosklonny M.V., Robey R., Bates S., Fojo T. *Medicine Branch, National Cancer Institute, NIH, Bethesda, MD.*

To achieve selective targeting of cancer cells with defective cell cycle checkpoints, we used microtubule-active drugs which cause cell death secondary to mitotic arrest, and took advantage of the fact that low levels of DNA damage can induce p53- and p21-dependent growth arrest without cell death. Cytostatic doses of DNA damaging drugs cause predominantly G<sub>2</sub> arrest without killing HCT116 cells which harbor wt p53. Such pretreatment for 16 hours abrogates mitotic arrest, Bcl-2 phosphorylation, p120 accumulation, and cell death caused by paclitaxel, epothilones A and B, and vinblastine. In contrast, DNA damage enhanced the cytotoxicity of FR901228 which does not affect microtubules but causes mitotic arrest. Low doses of DNA damaging drugs did not arrest p21<sup>-/-</sup> cells, p21-deficient clones of HCT116 cells, and did not protect from cytotoxicity induced by microtubule-active drugs. Introduction of p21 by adenovirus-transfer, partially protected the p21<sup>-/-</sup> cells from cytotoxicity following treatment with microtubule-active drugs. As expected, DNA damage did not induce either p53 or p21 and did not cause cell cycle arrest in E6-expressing HCT116 cells (HCT-E6). Therefore, like p21<sup>-/-</sup> cells, HCT-E6 cells were not protected from paclitaxel-induced cytotoxicity. We conclude that (i) p53-dependent p21 induction following treatment with DNA damaging drugs protects cells from cytotoxicity by microtubule-active drugs, and (ii) pretreatment with cytostatic doses of these drugs prior to microtubule-active drugs results in selective cytotoxicity to cancer cells with a defective p53/p21-dependent checkpoint. This approach may improve therapeutic indices by exploiting the disruption of checkpoint controls found in tumor cells relative to normal cells with normal checkpoint controls.

**#642 Effects on microtubules and the cell cycle of an aryl phosphate derivative of AZT.** Navara, C.S. and Uckun, F.M. *Departments of Experimental Oncology and Drug Discovery Program Hughes Institute, St. Paul, MN 55113.*

We have used confocal and timelapse microscopy to demonstrate the antimicrotubule effects of a novel aryl phosphate derivative of AZT. This compound completely breaks down both interphase and mitotic microtubules at micromolar concentrations in all cell lines tested (leukemic, breast cancer, brain cancer). At lower concentrations, normal interphase microtubule structure is disrupted and proper mitotic spindle formation is affected as evidenced by the presence of multipolar spindles. Centrosome replication is not affected by this compound because only two poles label with antibodies to the centrosomal protein  $\gamma$ -tubulin. This effect on the mitotic spindle results in a block at M-phase as evidenced by confocal microscopy and by cell cycle analysis using flow cytometry. The effects on microtubules are detected as early as 30 minutes after addition of the drug to the culture media and are complete by four hours.

**#643 Biochemical and cytotoxic comparisons of the sponge-derived natural product hemiasterlin, an antimitotic tripeptide, with other cytotoxic compounds.** Durso, N.A., Sackett, D.L., Bal, R., Gamble, W.O., Cardellina, J.H. and Hamel, E. *Laboratory of Drug Discovery Research and Development, National Cancer Institute, Frederick, MD (21702).*

Hemiasterlin, a tripeptide isolated from the sponge *Siphonochalina* sp., is a potent cytotoxic compound that inhibits both mitosis and the binding to purified tubulin of GTP, dolastatin 10, and vinblastine. These characteristics indicate that hemiasterlin binds at the vinca/peptide region of tubulin, a target for a wide variety of structurally complex natural products. Biochemical comparisons of hemiasterlin with other compounds that bind at this site present some shared, common characteristics: induction of characteristic changes in the intrinsic tryptophanyl fluorescence of tubulin; reduction in the reactivity of tubulin's sulfhydryls; inhibition of normal microtubule assembly; induction of polymeric tubulin complexes. In some cancer cell lines, hemiasterlin was compared with a variety of other cytotoxic compounds, including some with non-tubulin targets. Among these compounds, there are kinetic variations in the manifestations of cytotoxic effects. The IC<sub>50</sub> values of hemiasterlin and structurally similar natural product analogs are in the low to sub-nanomolar range, characteristic of some other antimitotic peptides. Chromatin morphologies indicate that hemiasterlin induces apoptosis more potently than paclitaxel. Because hemiasterlin's structure is relatively simple versus other antimitotic compounds that interact in the vinca region of tubulin, chemical modifications may be more readily exploited to elucidate the mechanisms of drug interaction at this important but poorly understood target domain.



**#644** p27 induction as a potential p53-independent mechanism of apoptotic response to docetaxel in non-small cell lung (NSCLC) and prostate carcinomas (CaP). Gumerlock, Paul H., Mack, Phillip C., Gustafsson, Matthew H., Togonon, Michelle G., Gandara, David R. Department of Internal Medicine, University of California, Davis, Sacramento, CA.

The taxane antimicrotubule agent docetaxel demonstrates preclinical activity in tumors with disrupted p53, unlike classic DNA damaging agents, and has shown promise in clinical trials in both NSCLC and CaP. Disrupted p53 is found at high frequencies in both NSCLC (~50%) and metastatic CaP (~70%). Loss of expression of the cyclin-dependent kinase inhibitor p27/Kip1, associated with increased ubiquitin-mediated protein degradation, has been shown in large studies of NSCLC and CaP to be a marker of poor prognosis. Ectopic expression of p27 induces apoptosis in a variety of human tumor cell lines, suggesting a second function for this tumor suppressor. We hypothesized that docetaxel-induced induction of p27 may be a p53-independent apoptotic mechanism. Human cell lines (NSCLC: wild-type [wt] p53 A549, p53-null Calu1; CaP: wt p53 LNCaP, p53-null PC3, wt and mutant p53 CWR22-R) were treated with docetaxel over a range of doses (0.1nM-10µM). Changes in protein expression were evaluated by Western blotting and Immunohistochemistry (IHC), cell cycle modulations by flow cytometric analysis of DNA content, and apoptosis by diamidine-phenylindole (DAPI) staining of condensed chromatin. In response to docetaxel, increased expression of p27 was seen at 24 hr in the NSCLC cell lines. Furthermore, p27 was posttranslationally modified in both the NSCLC and CaP cell lines, as determined by a shift in electrophoretic mobility. IHC demonstrated strong staining for p27 in the fragmenting nuclei of cells undergoing apoptosis. Flow cytometric analysis demonstrated a G2/M arrest at 24hr that was confirmed by the morphological observation of mitotic figures. **Conclusion:** The data demonstrate that p27 induction and/or modification by docetaxel is a potential p53-independent mechanism of apoptosis. Further study is needed to determine the therapeutic relevance of this p27 modulation. (Supported in part by CA62505, CA63265, RPR.)

**#645** Preclinical antitumor activity of BMS-188797, a new paclitaxel analog. Rose William C, Lee Francis Y, and Kadow John F. Bristol-Myers Squibb Co., Inc.

BMS-188797 was subjected to extensive preclinical antitumor testing using several in vivo tumor models. Its performance relative to paclitaxel, when both taxanes were compared at their respective optimal doses on the various treatment schedules evaluated, indicated a therapeutic advantage in four of six test systems. Differences of greater than one log cell kill (LCK) were obtained in favor of BMS-188797 in mice bearing L2987 and the moderately paclitaxel-resistant HCT/pk human colon carcinomas, and the murine lung carcinoma, M109. A lifespan advantage of 49% over paclitaxel was obtained for BMS-188797 in the moderately paclitaxel-resistant HOC79 human ovarian carcinoma. An insignificant therapeutic advantage (0.7 LCK) was observed for the new analog versus the A2780 human ovarian carcinoma, and both taxanes were inactive against murine M5076 sarcoma. Tissue pharmacokinetic studies in mice illustrate the longevity of tumor uptake of BMS-188797 relative to its plasma half-life, and an extensive time above the estimated minimum effective concentration of 40 nM. BMS-188797 is currently in Phase I clinical trial.

**#646** Cellular and molecular basis of collateral sensitivity to taxanes in a cisplatin-resistant ovarian carcinoma cell line. Cassinelli G., Supino R., Lanzl C., Perego P., and Zunino F. Istituto Nazionale Tumori, 20133 Milan, Italy.

The pharmacological interest of taxanes for chemotherapy of solid tumors stimulated studies to identify the cellular processes which confer sensitivity to these drugs. We recently reported that the acquisition of cisplatin-resistance in an ovarian carcinoma cell line (IGROV-1) was associated with collateral sensitivity to taxol. To investigate the cellular and molecular basis of this phenomenon, we performed a comparative study of cellular response to taxanes in the parental cell line, containing wild-type p53, and its cisplatin-resistant subline expressing a mutant p53 (IGROV-1/P11). The novel taxol analog IDN 5109 was included in this study because of its higher potency compared to taxol on both tumor systems. In each cell line the drug ability to induce apoptosis was correlated with the cytotoxic potency. However, the pattern of cellular response of the two cell lines was different. The higher susceptibility of IGROV-1 cells to IDN 5109 induced-apoptosis, as compared to taxol, was associated with a more marked p34<sup>cdc2</sup> dephosphorylation. In spite of the increased sensitivity to taxanes, the apoptotic response of IGROV-1/P11 cells was a delayed event, at least in part following the appearance of multinucleated and octaploid cells. These effects were more evident in IDN 5109-treated cells. Such a cellular response, associated with high levels of Bcl-2 and Raf-1 phosphorylation, is consistent with the expression of a mutant p53. We suggest that inactivation of p53, a component of the mitotic spindle checkpoint, could provide sensitization to taxanes as a result of a different cell death pathway involving a multinucleated status and apoptosis following DNA reduplication.

**#647** The PKC modulator bryostatin 1 enhances paclitaxel-mediated mitochondrial dysfunction in human leukemia cells (U937) ectopically expressing Bcl-x<sub>L</sub>. Wang, S., Wang, Z., Boise, L., Dent, P., and Grant, S. Departments of Medicine and Radiation Oncology, Medical College of Virginia, Richmond VA, 23298, and University of Miami, Miami, FL.

We have examined the effect of the PKC activator and down-regulator bryostatin 1 (Bry) on paclitaxel-mediated apoptosis in human leukemia cells overexpressing the anti-apoptotic protein Bcl-x<sub>L</sub>. To this end, U937 leukemia cells were stably transfected with an expression construct (pREP4) containing Bcl-x<sub>L</sub> cDNA, and clones isolated under selection pressure with hygromycin. Cells ectopically expressing Bcl-x<sub>L</sub> (U937/Bcl-x<sub>L</sub>) displayed resistance to paclitaxel (250 nM; 6-hr)-mediated apoptotic morphologic changes, DNA fragmentation, loss of mitochondrial membrane potential (MMP;  $\Delta\psi_m$ ), cytochrome c release, procaspase-3 cleavage/activation, and PARP degradation. However, subsequent, but not prior, exposure of paclitaxel-treated U937/Bcl-x<sub>L</sub> cells to bry (10 nM; 15 hr), which by itself was marginally toxic, increased the percentage of morphologically apoptotic cells, enhanced the extent of caspase-3 activation and PARP cleavage, and reduced MMP ( $\Delta\psi_m$ ) to levels approximating those observed in empty-vector controls (U937/pRep4) treated with paclitaxel alone. Enhanced apoptosis occurred primarily in the G<sub>2</sub>M population, and was accompanied by a net reduction in p34<sup>cdc2</sup> activity. Bry-mediated potentiation of paclitaxel-induced apoptosis in Bcl-x<sub>L</sub>-overexpressing cells was associated with a corresponding loss of self-renewal capacity, reflected by a reduction in clonogenicity. Lastly, the actions of bryostatin 1 were mimicked by the MEK/MAPK inhibitor PD98059 (but not by the p38 inhibitor SB203580); moreover, sequential exposure of cells to paclitaxel followed by bry or PD98059 led to a net reduction in MAPK activity. Collectively, these findings indicate that protection against paclitaxel-mediated mitochondrial damage and apoptosis conferred by Bcl-x<sub>L</sub> overexpression can be substantially overcome in a sequence-dependent manner by bry and possibly other agents that interrupt the PKC → MEK/MAPK cascade.

**#648** Potentiation of apoptosis in human cancer cell lines by the synergistic combination of Taxol and discodermolide. McDald, Hayley M., Martello, Laura A., and Horwitz, Susan B. Department of Molecular Pharmacology, Albert Einstein College of Medicine, 1300 Morris Park Avenue, Bronx, NY 10461.

The epothilones and discodermolide are recently isolated natural products that share the same mechanism of action as Taxol; that is the ability to stabilize microtubules resulting in apoptosis and mitotic arrest. This study investigated various characteristics of these drugs: (i) their cytotoxic profiles in Taxol-sensitive and -resistant cell lines; (ii) their ability to substitute for Taxol in a resistant cell line, A549-T12 that requires low concentrations of Taxol for normal cell division and (iii) their potential clinical use in combination chemotherapy with Taxol.

Cytotoxicity, immunofluorescence and flow cytometry data suggested that the epothilones, but not discodermolide, substitute for Taxol in A549-T12 cells. The cytotoxicity of discodermolide was significantly augmented in the presence of Taxol in this cell line, an observation which was not extended to the combination of Taxol with epothilone B. This led us to extensively investigate these drug combinations in four human cancer cell lines using the Combination Index (CI) method of Chou and Talalay, based on the median effect principle. This method calculates the degree of synergy, additivity or antagonism at various levels of cytotoxicity. In all cell lines tested, the concurrent combination of Taxol with discodermolide was synergistic over a 3-4-fold log concentration of either drug and exhibited no schedule dependency. In contrast, concurrent exposure of Taxol with epothilone B resulted in additivity, which again was schedule independent. Cell cycle analysis of cells concurrently exposed to nanomolar doses of Taxol and discodermolide demonstrated an increase in the proportion of hypodiploid cells, with no change in the proportion of cells at G2/M. These cells also exhibited increased levels of PARP cleavage and bcl-2 and/or bcl-x<sub>L</sub> phosphorylation suggesting that a probable mechanism for the observed synergy between Taxol and discodermolide is the potentiation of apoptosis.

**#649** Schedule-dependent cytotoxic interactions of Irinotecan (SN-38) and docetaxel in human non-small-cell lung cancer (NSCLC). Vanhoef, U., Hilger, R.A., Harstick, A., Achtenath, W., Hapke, G., and Seiber, S. West German Cancer Center, University of Essen Medical School; Rhône-Poulenc Rorer, Cologne, Germany.

The present study investigated the schedule-dependent cytotoxic interactions between SN-38 and docetaxel in human NSCLC H460 cells. Using the SRB-assay and isobologram analysis synergistic cytotoxic interactions were observed for the sequence docetaxel (2-h exposure) followed 24 hours later by an exposure to SN-38 for 2 hours. In contrast, the opposite sequence or a simultaneous 24-h exposure to both drugs resulted in additive to antagonistic interactions. Using immunoblot analysis and a histone H1 loading control, exposure of H460 cells to docetaxel did not alter TOP1 and II protein expression and had no effect on SN-38-mediated *ex vivo* inhibition of pBR322 plasmid DNA unwinding activity of H460 cells (nuclear extracts). Docetaxel significantly increased the induction of protein-linked DNA breaks (PLDBs) (PLDBs for 10 µM SN-38 with and without

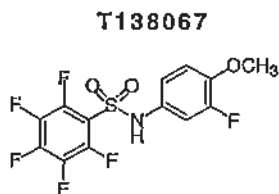
prior exposure to docetaxel (5-fold  $IC_{50}$ ):  $6.69 \pm 0.65\%$  and  $3.76 \pm 0.55\%$ , respectively [ $p < 0.001$ ]. Data on HPLC-analysis of the intracellular SN-38 pharmacokinetics showed that docetaxel decreases the cytosolic concentration of SN-38 (SN-38 concentration with and without prior exposure to docetaxel (5-fold  $IC_{50}$ ):  $3.09 \pm 0.31$  vs  $5.50 \pm 0.14$  pmol/ $5 \times 10^6$  cells [ $p < 0.001$ ]), results which are likely related to an increased nuclear DNA-binding of SN-38. **Conclusions:** The antitumor activity of the combination of docetaxel and SN-38 appears to be schedule-dependent. Synergistic cytotoxic interactions were observed for the sequence docetaxel followed by SN-38, which was associated with an increased induction of PLDBs. The data reported herein could have a major impact on further clinical trials with docetaxel and irinotecan.

**#650 A system for high through-put screening for tubulin and microtubule ligands with anti-cancer properties.** Davis, Ashley and Middleton, Kim M. Cytoskeleton, Inc. 1650 Fillmore Street, #240, Denver, CO 80206, USA.

Tubulin and microtubules are targets for a multitude of anti-tumor compounds. Tubulin polymerization can be measured by an increase in optical density over time. Previously this assay has been used on a small scale to characterize cytotoxic compounds and to screen derivatives of a parent compound. The assay has not been applicable to medium or high through-put assays before now. We present a system that is capable of screening the activity of a random library of compounds for tubulin ligands. The system is tested in 96- and 384-well format and it is suitable for screening upward of 100 000 compounds within one month. The present coefficient of variation is 16, 13 and 10% for single, duplicate and triplicate assays respectively. This research was sponsored by the NIH Small Business Innovative Research fund, GM53696-03.

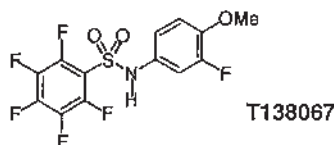
**#651 Medicinal chemistry of T138067, an antimetabolic agent that binds irreversibly and selectively to  $\beta$ -tubulin: evaluation of the pentafluorophenylsulfonamide region.** Medina, Julio C.; Clark, David L.; Houze, Jonathan; Frankmoelle, Walter P.; Rubenstein, M. Steve; Gergely, Joshua; Shan, Bei; Beckmann, Holger; Baichwal, Vijay; Rosen, Terry and Jaen, Juan C. Tularik Inc., South San Francisco, CA, USA.

We have previously described a novel series of pentafluorophenylsulfonamides, exemplified by T138067, that inhibit the growth of a broad variety of human tumor cell lines, including those that are resistant to other chemotherapeutic agents. T138067 irreversibly and selectively binds to  $\beta$ -tubulin by undergoing nucleophilic aromatic substitution (NAS) with cysteine 239. The site of NAS involves the para position of the pentafluorophenyl ring. Here we present the structure-activity relationship studies on T138067 analogs in which the pentafluorophenyl ring and the sulfonamide linker regions have been replaced by isosteres leading to the discovery of the new cytotoxic agents.



**#652 Medicinal Chemistry of T138067, an Antimetabolic Agent That Binds Irreversibly and Selectively to  $\beta$ -Tubulin: Evaluation of the Aniline Region.** Clark, David L.; Medina, Julio C.; Houze, Jonathan; Gergely, Josh; Rubenstein, Steve; Shan, Bei; Baichwal, Vijay; Jaen, Juan; Rosen, Terry. Tularik Inc., Two Corporate Drive, South San Francisco, CA 94080, U.S.A.

Tubulin is an important cellular target for anticancer agents. We have discovered a series of novel tubulin polymerization inhibitors, represented by T138067, that are potent anti-mitotic agents in cell culture and are active against cell types that express the multidrug resistance (MDR) phenotype. The structure activity studies around the aniline-derived portion of the molecule will be presented.



## SECTION 4: ANTIFOLATES AND TOPOISOMERASE INHIBITORS

**#653 Phase I and pharmacokinetic study of 10-propargyl-10-deazaaminopterin (PDX), a new antifolate.** Krug, L.M., Ng, K.K., Miller, V.A., Heelan, R.T., Tong, W., Kelly, J., Sirotnak, F.M., and Kris, M.G. Memorial Sloan-Kettering, New York, NY 10021, U.S.A.

PDX, a 10-deazaaminopterin with a propargyl substitution at carbon-10, demonstrates greatly enhanced antitumor activity over methotrexate in human non-small cell lung cancer (NSCLC) and breast cancer *in vivo* (Sirotnak et al., Cancer Chemother Pharmacol, 42:313, 1998). The improved activity appears to be due to more effective internalization by the one carbon, reduced folate transporter (rfc-1) and net accumulation in tumor cells of polyglutamylated metabolites. In this phase I trial, one patient was enrolled per dose level, expanding to 3 for toxicity. Intravenous treatment weekly for 3 weeks on a 4-week cycle resulted in dose-limiting mucositis at 30 mg/m<sup>2</sup>/week. Subsequently 27 patients with advanced NSCLC were treated every 2 weeks. Patient characteristics: women 56%, Karnofsky performance status 70% in 30%, median number of prior chemotherapy regimens 2 (range 1-4), prior radiation 56%, median age 59 (range 35-77). To date, a total of 93 4-week cycles have been administered (median 2 per patient). The dose limiting toxicity was mucositis (grade 3, 4), occurring in two patients at 170 mg/m<sup>2</sup>. Other toxicities included reversible transaminase elevation, rash, pulmonary infiltrates, conjunctivitis, and epistaxis (all grade 1 or 2). No significant hematologic toxicities were noted. At 150 mg/m<sup>2</sup>, the mean AUC was 22  $\mu\text{mol} \cdot \text{hr}$  and terminal half-life was 8 hours measured after 17 infusions in 9 patients. Urinary excretion of parent drug measured in 2 patients was 6 and 20% at 24 hours. Objective responses were documented in 2 patients (150 and 170 mg/m<sup>2</sup>) and 5 other patients with stable disease received 6, 8 (2 patients), 11, and 13 cycles of therapy. **Conclusions:** 1) The maximal tolerated dose of PDX is 170 mg/m<sup>2</sup> every 2 weeks; 2) The primary toxicity is mucositis; 3) Antitumor activity has been observed in NSCLC; 4) A phase II trial in NSCLC patients is underway at the recommended dose of 150 mg/m<sup>2</sup>.

Supported by CA-05826 and the Simon Benlevy Cancer Fund.

**#654 The multitargeted antifolate: shifting enzymatic targets during development of antifolate resistance.** Schultz, Richard M., Chen, Victor J. and Bertino, Joseph R. Lilly Research Laboratories, Eli Lilly and Co., Indianapolis, IN 46285 and Memorial Sloan-Kettering Cancer Center, New York, NY 10021.

MTA (multitargeted antifolate, LY231514) is a structurally novel antifolate that inhibits multiple folate-requiring enzymes. The pentaglutamate inhibits thymidylate synthase (TS), dihydrofolate reductase (DHFR) and glycinamide ribonucleotide formyltransferase with  $K_i$  values of 1.3 nM, 7.2 nM and 65 nM, respectively. In antifolate-naïve human carcinoma and leukemia cells, thymidine (5  $\mu\text{M}$ ) protects cells from MTA at drug concentrations near the growth inhibitory  $IC_{50}$ , but higher MTA concentrations require the combination of both hypoxanthine (100  $\mu\text{M}$ ) and thymidine to exert protective effects. We have utilized a panel of antifolate-resistant cell lines and reversal conditions to characterize mechanisms of resistance in MTA-treated cells. In TS amplified lines resulting from resistance due to either tomudex, 5-FU, or MTA exposure, the cells were >160-fold less resistant to MTA compared to the selective TS inhibitor, tomudex, and thymidine totally lacked protective activity on MTA treatment. However, these cells were protected from cytotoxicity by hypoxanthine treatment alone. In a methotrexate-resistant leukemia line due to DHFR amplification, the cells were 8-fold less resistant to MTA than the selective DHFR inhibitor, methotrexate, and MTA cytotoxicity was largely overcome by thymidine addition alone. In tumor cells with decreased drug accumulation due to defective, reduced folate carrier-mediated transport and/or polyglutamation, protection from MTA-mediated cytotoxicity required the combination of both thymidine and hypoxanthine. The results suggest that MTA is less dependent than methotrexate on DHFR as a target and less dependent than tomudex on TS as a target. The cytotoxic potency of MTA and the mechanism of action in tumor cells appear to be determined by several factors, including relative levels of target enzymes, purine/pyrimidine salvage, and intracellular concentrations of MTA and its polyglutamates.

**#655 Expression levels of thymidylate synthase as a predictive marker for tumor susceptibility to the multitargeted antifolate LY231514.** Zervas, Peter H., Roberts, Edda F., Dotzlaw, Joe E., Chen, Victor J., Schultz, Richard M., and Seitz, David E. Lilly Research Laboratories, Eli Lilly and Co., Indianapolis, IN 46285.

MTA (multitargeted antifolate, LY231514) is currently undergoing extensive clinical evaluation in a variety of tumors. From studies of cellular biochemistry, a major target of MTA is believed to be the enzyme thymidylate synthase (TS). Recent preclinical data obtained from matched pairs of tumor cell lines that are either sensitive or resistant to MTA suggest that an increased TS activity is an important resistance factor for MTA. For example, human GC3 colon carcinoma cells were developed for resistance to MTA by stepwise increases of MTA in the culture medium up to 2  $\mu\text{M}$ . Cellular resistance was stable on removal of selective pressure, and the cells showed increased TS activity (approximately 40-fold). These cells are



140-fold resistant to MTA and 23,503-fold resistant to the selective TS inhibitor, Raltitrexed. In order to assess TS expression in these cells, a real time quantitative reverse transcription-PCR assay was developed based on Lightcycler fluorescence methodology to quantify the level of TS in matched pairs of GC3 cell lines. Results of these studies indicate that TS is over expressed (approximately 20-fold) in GC3 cells that are resistant to MTA. This methodology may provide a useful technique for screening patients prior to dosing with MTA and may predict a positive outcome to treatment.

**#656 Synergistic interaction of the multitargeted antifol (MTA, LY 231514) with melphalan *in vitro* in human tumor cell lines.** Budman DR, Calabro A, Kreis W. *Don Monti Division of Oncology, North Shore University Hospital, New York University, Manhasset, New York 11030*

MTA is a prodrug antifol with potent inhibition of several key enzymes involved in folate metabolism, including thymidylate synthase, dihydrofolate reductase, glycylamide ribonucleotide formyltransferase, and aminimidazole carboxamide ribonucleotide formyltransferase. *In vitro* studies have suggested that its mechanism of action is unique from methotrexate and quinazoline antifols. MTA is currently undergoing broad Phase II/III evaluation as a single agent and in combination. We have combined a semi-automated MTT assay with median effect analysis (AntiCancer Drugs 9: 697, 1998) to search for drug combinations which may be of clinical use. Human CCRF-CEM leukemia and NCI H 460 non-small cell lung cancer cells were cultured under standard conditions, harvested at confluence, and exposed at varying periods of time to MTA and melphalan. All studies were done in triplicate. For CCRF-CEM cells, exposure to melphalan for 48, 72, or 96 hours simultaneously or sequentially with MTA resulted in marked synergism (combination index [CI] = 0.084 - 0.536) at Fa<sub>50</sub> (fraction affected by dose) depending upon sequence. For NCI H 460 cells, synergism was seen for 24 hour exposures independent of sequence (CI = 0.587 - 0.712) and additive effects were noted for 48 hour exposures. Synergism was seen for all values of Fa. These results suggest that MTA should be tested clinically in combination with an alkylating agent.

Supported by a grant from the Eli Lilly Company and the Don Monti Foundation.

**#657 Immunohistochemical detection of *in vivo* alteration of thymidylate synthase levels in a human HCT116 colon carcinoma tumor xenograft induced by the use of MTA (LY231514).** Alvarez, E., Menon, K., Bewley, JR., Spears, P., Schultz, RM., Taicher, BA., Chen, VJ and Galbreath, E. E. *Lilly Research Laboratories, Eli Lilly & Company, Indianapolis, IN, USA 46285.*

MTA (LY231514) is a multitargeted antifolate that inhibits thymidylate synthase (TS), dehydrofolate reductase and glycylamide ribonucleotide formyltransferase. The aim of this work is to determine whether MTA can alter the expression levels of TS in a tumor xenograft model. GC3 (human colon carcinoma) and an MTA resistant GC3 cell with known overexpression of TS were used to optimize the immunohistochemical conditions. A human colon carcinoma line (HCT-116) was grown as solid tumors in athymic mice. Each mouse received 4.5 Gy of whole body gamma irradiation prior to tumor cell implantation. A single cell suspension was prepared from pooled tumors in a 1:1 mixture of unsupplemented RPMI media and Matrigel®. Each animal was implanted with 5 × 10<sup>6</sup> cells subcutaneously on the lateral aspect of each thigh. When the tumors reached 300 mm<sup>3</sup> the animals were given a single intraperitoneal dose of 200 mg/kg of MTA. At 0, 1, 4, 8, 24 and 48 hours the animals were euthanized. Additionally blood samples were collected in EDTA containing tubes from each animal tested to determine circulating plasma levels of MTA. The tumors were aseptically collected and fixed in zinc buffered formalin. The tumors were paraffin embedded, sectioned and mounted. Tumor sections were deparaffinized and exposed to a mouse anti-human monoclonal antibody raised against TS (Chemicon, TS106). The proteins were visualized using an avidin-biotin complex. Overall the paraffin embedded tumors showed relatively low levels of expression of TS at all time points prior to 48 hours. At 48 hours post-treatment with MTA, the immunoreactivity levels of the anti-TS antibody are at higher levels when compared to earlier time points. This pattern suggests an *in vivo* induction of TS expression induced by MTA. This work points at the ability of MTA to induce elevated levels of TS expression when used as a single agent against the HCT-116 human colon carcinoma.

**#658 Circadian variation of thymidylate synthase (TS) mRNA and protein levels in normal tissues parallels the rhythm in TS catalytic activity and daily rhythms in DNA synthesis.** Wood, Patricia A., Bove, Kathleen, Clark, Robert N., Lincoln, David W., Maley, Frank, Hrushesky, William J.M. *Stratton VA Medical Center, Wadsworth Center, NY State Department of Health, Albany, NY 12208.*

Temporal administration of fluoropyrimidines within the circadian cycle of cancer patients and animals results in 2-8 fold differences in gut and marrow toxicities and doubling of tumor response rates. Given the known circadian coordination of tissue cytokinetics, we asked whether the S phase-regulated enzyme targeted by fluoropyrimidines and anti-folates, TS, might vary throughout the day in tissues most damaged by these drugs and at what level circadian control of TS gene expression might be regu-

lated. Bone marrow and small intestinal mucosa (SI) were obtained from normal mice at each of six equi-spaced times throughout a 24 hr cycle in several experiments and the following parameters were measured: TS catalytic activity (TSA) by tritium release assay, TS protein (TSP) by western blots using a polyclonal anti-rat TS antibody, TS mRNA levels by quantitative RT-PCR, S phase coordination by flow cytometric DNA content and histone (H) 3.2 mRNA by quantitative RT-PCR. TS activity varies 2 fold throughout the day in bone marrow and SI with unique, tissue-specific circadian patterns. The circadian rhythm in TSA parallels S phase fraction in these tissues throughout each day, demonstrating S phase coordination of TS gene expression in a physiologic, *in vivo* setting. TS mRNA levels vary 2-3 fold throughout the day coincident with TSA in marrow, while the peak in SI TS mRNA rhythm just precedes that of TSA. TSP in marrow varies 6 fold throughout the day in parallel with TSA. In conclusion, TS, the target enzyme for fluoropyrimidines and antifolates, varies throughout the day paralleling S phase coordination in normal tissues. The circadian regulation of TS gene expression occurs at both the RNA and protein levels. Circadian timing should be considered for administration of TS inhibitor drugs and measurement of TS levels.

**#659 Role of p53 in cell death following inhibition of thymidylate synthase.** Welsh Sarah J, Walton Mike I, Tiley Jenny R, Hobbs Steve M, Ahern G Wynne. *CRC Centre for Cancer Therapeutics, Institute of Cancer Research, 15 Cotswold Road, Sutton, Surrey, SM2 5NG, UK.*

Cell death following TS inhibition is incompletely defined. Commitment to cell death occurs following relatively long periods of dTTP depletion (longer than a generation time). However, under these conditions dUMP pools greatly expand and may cause elevation in dUTP pools overwhelming the pyrophosphatase dUTPase giving rise to misincorporation of uracil into DNA. A large expansion in dUTP pools is associated with low dUTPase expression and activity, mature DNA damage and an earlier commitment to cell death.

In p53 functional A549 human lung carcinoma cells, which accumulate dUTP, p53 protein was elevated within 24 h of treatment with the specific, nonpolyglutamatable TS inhibitor ZD9331. It was hypothesised that cells that accumulate dUTP, hence are able to misincorporate uracil into DNA, are committed to die earlier (by a p53 dependent mechanism) than cells in which TTP pools are depleted and no dUTP is formed. Development of a series of transfected cell lines containing modified p53 function and/or dUTPase activity should verify this hypothesis.

In the first of these experiments, A549 cells were stably transfected with HPV16 E6 (A549 E6) resulting in no detectable induction of p53 or p21 following exposure to radiation. No G1/S arrest was observed and these cells were significantly resistant to radiation. A549 E6 cells also showed resistance to ZD9331 (24 h exposure MTT) compared to parental and neo controls although a minimal difference was observed using 120 h MTT assays. This effect was also observed using Raltitrexed (Tomudex) a specific, highly polyglutamatable TS inhibitor. Clonogenic assays confirmed that there was a significant resistance to 24 h treatment with ZD9331 in cells lacking p53 (30% survival vs 85% survival in A549 E6). Several apoptosis assays (Hoescht dye staining, Annexin V-FITC binding using flow cytometry and cleavage of PARP and caspase 3) confirm that cells with wild type p53 undergo apoptosis at an earlier time point (within 24 h of treatment) than those lacking functional p53 (which die later than 24 h).

Current studies focus on defining the effect of dUTPase transfection on dUTP accumulation (ie. uracil misincorporation) and cell death following TS inhibition in these cell lines with defined p53 function. The p53 independent mechanisms through which cells die will also be investigated.

**#660 Poisoning of topoisomerase I by 1-β-D arabinofuranosylcytosine.** Pourquier Philippe, Takebayashi Yujii, Kohlhaagen Glenda, Giffre Christopher, Pommier Yves. *Laboratory of Molecular Pharmacology, Division of Basic Sciences, NCI, National Institutes of Health, Bethesda, Maryland.*

1-β-D-arabinofuranosylcytosine (ara-C) is a nucleoside analog commonly used in the treatment of leukemias. ara-C is a competitive inhibitor of DNA polymerases and can be incorporated into DNA. Its mechanism of cytotoxicity is not fully understood. Using oligonucleotides and purified human topoisomerase I (top1), we found a 4- to 6-fold enhancement of the top1 cleavage complexes when ara-C was incorporated at the +1 position relative to a unique top1 cleavage site. This enhancement was primarily due to a reversible inhibition of the top1-mediated DNA religation. Because ara-C incorporation is known to alter base stacking, and sugar puckering at the misincorporation site and at the neighboring base pairs flanking the ara-C, the observed inhibition of religation at the ara-C site suggests the importance of the alignment of the 5'-hydroxyl end to be religated with the phosphate group of the top1 phosphotyrosine bond. This study also demonstrates that ara-C treatment and DNA incorporation trap top1 cleavage complexes in human leukemia cells. These results suggest for the first time that top1 poisoning is a potential new mechanism for ara-C cytotoxicity.

**#661 Effects of the O6-methylguanine on topoisomerase I activity *in vitro* and in MNNG-treated cells.** Pourquier Philippe, Loktionova Natalia A., Pegg Anthony E., Pommier Yves. *Lab of Mol Pharmacol, DBS, NCI, NIH, Bethesda, MD & Dept. of Cell. and Mol. Physiology, Pennsylvania State University College of Medicine, Hershey, PA.*

A major part of the toxicity of methylating agents such as N-methyl-N'-nitro-N-nitrosoguanidine (MNNG) is due to the formation of O6-methylguanine (O6MG) in DNA. During replication polymerase inserts a thymine opposite to the damaged guanine which results in mutagenic G:C to A:T mutation. In human, the repair enzyme O6-alkylguanine-DNA alkyltransferase (AGT) specifically removes the methyl group of the O6MG and transfers it to a cysteine acceptor. Using oligonucleotides and purified human topoisomerase I (top1), we found a 7- to 10-fold enhancement of the top1 cleavage complexes when O6MG was incorporated opposite to a C or a T at the +1 position relative to a unique top1 cleavage site. This enhancement is due to a decrease of the top1-mediated religation as well as an increase in the enzyme cleavage step. Non covalent binding of the enzyme to the O6MG-containing DNA was not significantly affected. Using CHO cells that are constitutively lacking the AGT enzyme, we were able to detect a significant increase of covalent top1-DNA complexes after 30 minutes of treatment with 1 µg/ml of MNNG. Conversely, no increase could be detected in CHO cells transfected with the wild-type human AGT. These results demonstrate that top1 can be trapped by O6MG *in vitro* and in MNNG treated cells. They also suggest that topoisomerase I may play a role in the cytotoxicity of alkylating agents as it was suggested in former studies where yeast top1-deficient strains were more resistant to MNNG than the wild-type counterpart.

**#662 Identification of structurally and mechanistically novel topoisomerase I poisons.** Heather Dunstan, Philippe Szankasi, Cathy Ludlow, Sondra Goshie, Julian Simon, Stephen H. Friend, John R. Lamb. *Seattle Project, Clinical Division, Fred Hutchinson Cancer Research Center, Mailstop DE-551, 1100 Fairview Ave N., Seattle WA, 98109, USA.*

We have identified a series of novel double strand break inducing compounds by screening for compounds that are uniquely and selectively toxic in rad50 mutant yeast strains. The compounds were additionally selected to have no preferential toxicity in rad14 (nucleotide excision repair), or rad18 (daughter strand gap repair) strains. Of the greater than 50 compounds identified the large majority were related to known topoisomerase (Topo) I or II poisons. However there was a subset of molecules that are structurally unrelated to compounds with known functions. Using yeast strains with altered levels of the topoisomerases, we have shown that two of these compounds are Topo I but not Topo II poisons. The molecules are unrelated to each other or to the known Topo I poison camptothecin, and are not likely to be intercalators. These two novel Topo I poisons are toxic, but not differentially toxic in a matched pair of mammalian cells either with or without expression of the double strand break repair protein KU80. This behavior is similar to camptothecin and distinct from most Topo II poisons. Both compounds are active against a variety of tumor derived cells and do not appear to be subject to MDR1 mediated drug efflux. We have been able to demonstrate that at least one of the compounds is active against human topoisomerase I expressed in yeast. Additionally the compounds appear to be unaffected by mutations that render Topo I resistant to camptothecin.

It is thought that the Topo I poison camptothecin produces toxicity when a replication fork runs into cleavable camptothecin-Topo I complexes, producing a double strand break. This is supported by the observation that camptothecin toxicity is decreased by inhibition of DNA synthesis and is increased by loss of DNA damage checkpoints (for instance in *meo2* strains). We have observed that the toxicity of the novel Topo I poisons are neither inhibited by HU (inhibition of DNA synthesis), nor accentuated by loss of checkpoint function (*meo2* strains). These and other observations suggest that these novel Topo I poisons are mechanistically quite distinct from camptothecin. A model encompassing this data will be presented.

**#663 Novel non-camptothecin topoisomerase I poisons: the indenoisoquinolines.** Pommier Yves, Kohlhaagen Glenda, Strumberg Dirk, Jayaraman Muthusamy, and Mark Cushman. *Labs. Med. Chem. & Mol. Pharmacology, DBS, National Cancer Institute, NIH, Bethesda, MD, & Purdue Univ. West-Lafayette, IN.*

The activity of camptothecins in cancer chemotherapy led to the validation of topoisomerase I (top1) as a target for drug development. Limitations of camptothecins include their chemical instability (E-ring opening) and the rapid reversibility of top1 inhibition upon drug removal. Development of novel top1 poisons is also legitimized by the common knowledge that drugs from different chemical families, which share a common cellular target, generally exhibit different spectra of anticancer activity (cf. Topoisomerase II or tubulin inhibitors). We previously identified an indenoisoquinoline (NSC 314622) as a top1 inhibitor following a COMPARE analysis using camptothecin as a seed (*Mol. Pharmacol.* 1998, 54: 50-8). NSC 314622 is a non-intercalative top1 poison that produces persistent protein-linked DNA breaks. More recently, we reported the synthesis of cytotoxic indenoisoquinolines and their activity as top1 poisons (*J. Med. Chem.* 1999, 42: 446-57). We have now synthesized and tested additional indenoisoquinoline derivatives and found that some of them are very potent

top1 poisons. The indenoisoquinoline-induced top1 cleavage sites are at different genomic positions than those induced by camptothecin. One of the novel indenoisoquinoline derivatives was further studied in human cells in culture and found to be more cytotoxic than camptothecin. Protein-linked DNA breaks were also detected at nanomolar concentrations in treated cells, which is consistent with top1 poisoning by indenoisoquinolines.

**#664 Anti-tumour profile of BN80915, a novel e-ring modified topoisomerase I inhibitor.** Principe P., Marsais J., Kasprzyk, P.G., Carlson, M., Lauer J., Meshaw K., Alford T.L., Hill B., Chen S.F., Hollister B.A., Dexter, D.L. *Institut Henri Beaufour, France, Biomeasure Inc., USA, Piedmont Research Center, USA.*

BN80915 belongs to a novel family of anticancer agents, the homo-camptothecins, developed on the concept of topoisomerase-1 inhibition and reported to be characterised by the unique feature of a 7-membered β-hydroxylactone ring that, by decreasing the reactivity of the lactone ring, results in enhanced plasma stability in comparison with conventional camptothecin analogues. The pharmacological properties of this compound are being actively investigated as it undergoes clinical development. We report the results obtained from studies evaluating the schedule dependent efficacy of orally administered BN80915 in two human tumour xenograft models, A375 melanoma and MIAPaCa-2 pancreatic carcinoma, growing in nude mice. Clinical relevant benchmarks have been included at their best treatment schedule. All drugs have been tested at their MTDs calculated from prior dosing studies. Five different treatment schedules have been evaluated in each tumour model. The following criteria have been selected for *in vivo* efficacy: tumour weight, survival time, tumour growth delay and treatment response categories (complete and partial regression, stable disease and nonresponders). The results show that 1) BN80915 (0.03 mg/kg, per os, twice daily for 14 days) outperforms irinotecan (100 mg/kg, i.p., qwx3), topotecan (3 mg/kg, i.p., qdx5) and dacarbazine (200 mg/kg, i.p., qdx5) for each efficacy criteria in the A375 tumour model. Five of ten mice treated on this schedule experienced complete tumour regression; 2) similarly, for each set of efficacy criteria, BN80915 (0.03 mg/kg, per os, twice daily for 14 days) outperforms topotecan and gemcitabine (80 mg/kg, i.p., q3dx4) in the MIAPaCa-2 model. In the latter, with the same treatment schedule, BN80915 is significantly more efficient than irinotecan in terms of evolution of tumour weight. BN80915, per os, twice daily for 14 days, has also substantial activity in the colorectal HT-29 model and the androgen-insensitive DU145 and PC-3 prostate tumour models. These results strongly support BN80915 as a new valuable and promising anti-tumour agent, expected to bring substantial benefit over topoisomerase-1 inhibitors currently in cancer therapy.

**#665 Unusual potency of BN 80915, a novel E-ring modified camptothecin, towards human colon adenocarcinoma cells.** Larsen Annette K, Gilbert Cristèle, Chyzak Ginette, Pilsov Sergej Y, Nagulbneva Irina, Lesueur-Ginot Laurence, Lavergne Olivier and Bigg Dennis CH. *CNRS UMR 8532, Institut Gustave-Roussy, F-94805 Villejuif, France, Institut Henri Beaufour, F-91966 les Ulis, France.*

BN 80915 is the lead compound of a new series of E-ring modified camptothecins that has shown enhanced lactone stability and decreased binding to plasma proteins. We now show that BN 80915 induces up to 2-fold more covalent DNA-protein complexes (cleavable complexes) between purified human topoisomerase I and DNA than SN-38 and camptothecin. BN 80915 also induces DNA-topoisomerase I complexes in living HT-29 human colon carcinoma cells starting at 5 nM whereas about 20 times more SN-38 is needed to induce comparable levels of cleavable complexes under similar experimental conditions. This difference is much greater than that observed with purified enzyme, suggesting important differences between the two drugs in terms of drug stability, drug uptake or transport into the nuclear compartment. BN 80915 shows strong growth inhibitory effect on HT-29 human colon carcinoma cells with a  $LD_{50}$  of 0.3 nM after 24 hours drug exposure followed by 48 hours incubation in drug-free media. The corresponding values are 20 nM for SN-38 and 40 nM for topotecan. BN 80915 is also active against HT-29 cells growing in three dimensions as multi-cellular spheroids. Human myeloid leukemia cells overexpressing functional P-glycoprotein or MRP show no cross resistance to BN 80915 although they exhibit modest levels of cross resistance towards both topotecan and SN-38. In conclusion, the unusually potent effects of BN 80915 towards human colon carcinoma cell lines are most likely due to enhanced interaction with topoisomerase I combined with improved extra- and intracellular lactone stability.

**#666 Design and optimization of 20-O-linked camptothecin glycoconjugates.** Lerchen, H.-G., Baumgarten, J., von dem Bruch, K., Wölter, D., DiBetta, A.M., Hoffmann, M. and Fiebig, H.-H. *Bayer AG, Central Research, D-51368 Leverkusen, Oncotest Inst. for Exp. Oncology, D-79110 Freiburg, Germany.*

Irinotecan and topotecan are clinically established water soluble 2<sup>nd</sup> generation camptothecin derivatives which act by inhibiting topoisomerase I. The major disadvantages to the camptothecin class of antitumor agents are toxicity and a species-dependent *in vivo* conversion of the lactone E-ring to the biologically inactive ring-opened carboxylate form. In humans



particularly, the equilibrium is shifted to the inactive carboxylate form due to its preferential binding to human serum albumin. This may lead to an overestimation of the therapeutic efficacy of camptothecin derivatives from rodent xenograft models to man.

To improve the tumor selectivity and to stabilize the lactone ring of camptothecin, 20-O-linked glycoconjugates have been synthesized. The glycoconjugates have been designed for receptor-mediated uptake into the lysosomes of tumor cells with subsequent intracellular release of the toxophore. The optimization of the glycoconjugates according to criteria such as *in vitro* efficacy, stability in extracellular medium, water solubility and tumor selectivity will be described. Compounds with high water solubility were tested *in vitro* against the SW480, HT29 and B16F10 tumor cell lines. In parallel, compounds were examined for hydrolytic stability and camptothecin release in the cell supernatant at 24 hours by HPLC. Glycoconjugates that showed less than 5% camptothecin release compared to conjugate in the extracellular medium were deemed sufficiently stable. These glycoconjugates were then tested for toxicity against bone marrow cells and hepatocytes *in vitro*. Finally, selected compounds were tested for *in vivo* activity in the MX-1 breast tumor subcutaneous xenograft. Two glycoconjugates, BAY 38-3441 and BAY 38-3444, that contain a 3-O-modified fucose residue and a thiourea modified dipeptide spacer have been selected for further preclinical evaluations. They inhibit tumor formation in the MX-1 breast cancer model by >96%.

**#667 Anticancer activity of novel camptothecin glycoconjugates in human tumor xenograft models.** Fiebig, H.H., Steidle C., Burger, A.M., Lerchen H.G. *Oncotest Inst. for Exp. Oncology, and Tumor Biology Center, D-79110 Freiburg, Bayer AG, Central Research, D-51368 Leverkusen, Germany*

The camptothecins topotecan and irinotecan are novel registered anticancer drugs acting via an inhibition of topoisomerase I. The biologically active lactone form is converted to the inactive open ring carboxylate form by esterases. Novel 20-O-linked glycoconjugates of camptothecin have been designed for tumor targeting via carbohydrate receptors present in many tumors, furthermore for stabilisation of the lactone form during transport in blood and finally for lysosomal release of the toxophore in tumor cells.

Among a series of 60 compounds tested *in vivo* in human tumor xenografts the 2 glycoconjugates Bay 38-3444 (130) and Bay 38-3441 (134) were most active. Given intravenously (IV) daily for 3 days at their MTDs both compounds effected tumor inhibitions of more than 95% in a large cell lung cancer model LXFL 529 and the mammary cancer MX-1. Topotecan was less active in these models. Tumor inhibitions of 60 to 80% were observed in the colon models HT29 and CXF 280. Bay 38-3444 (130) was also highly active in the mammary model MAXF 401 with an inhibition of 93%. In the prostate model DU 145 Bay 38-3444 (130) was more active than topotecan (66% inhibition vs 35%, respectively). In conclusion the 2 camptothecin glycoconjugates have significant inhibitory activity in a wide range of tumor models, and are promising as new potential cytotoxic agents.

**#668 Effect of dose scheduling on the anti-tumor activity of the camptothecin glycoconjugates.** Hübner, B.L., Ebarwein, G.J., Bull, C., Fiebig, H.H., Steidle, C., Burger, A.M., Lerchen, H.G. *Bayer Corp., Oncotest Inst. For Exp. Onc. and Tumor Bio. Ctr., Bayer AG*

It is well documented that clinical anti-tumor activity with topoisomerase I inhibitors is limited by the dosing schedule and route of administration. Therefore, the anti-tumor activity of a novel 20-O-linked camptothecin glycoconjugate BAY 38-3444 was evaluated with different dosing schedules. The standard therapy schedule was intravenous (IV) administration daily for 3 days (qd x 3). In three tumor models a second cycle of 3-day IV administration was performed 10-11 days after the first cycle. In both models tested a second 3-day course led to a greater and longer lasting tumor remission. An intermittent schedule of IV administration every fourth day over a 12 day period (q4d x 3) was tested vs qd x 3 treatment in the more resistant colon model, HCT 116. BAY 38-3444 was dosed at 12 and 16 mg/kg, and topotecan was dosed on the same schedule at 1.25 mg/kg. BAY 38-3444 at 16 mg/kg showed an optimal T/C (treated compared to control value, with 0 representing a complete cure) that was the same for both schedules, 47 (q4 x 3) vs 43 (qd x 3). For topotecan the intermittent schedule did not show equivalent tumor inhibition (40 for qd x 3 vs. 79 for q4d x 3). Further scheduling flexibility was examined with oral dosing. Several studies have suggested that optimal tumor inhibition with camptothecin and related analogs may be obtained with prolonged administration due to the mechanism of action. BAY 38-3444 dosed PO daily for 30 days at 2, 4 and 6 mg/kg was curative in the MX-1 tumor model; as was topotecan dosed PO at 1.5 mg/kg for 30 days. This demonstrates that similar to other camptothecins, BAY 38-3444 is maximally effective with a prolonged dosing regimen. These studies, together with the toxicity data and *in vitro* profile, suggest that the camptothecin glycoconjugates may have considerable scheduling flexibility that can be explored clinically to maximize efficacy and minimize toxicity.

**#669 Preclinical *in vitro* and *in vivo* testing comparing toxicities of camptothecin glycoconjugates with camptothecin, topotecan and irinotecan.** Clemens GR, Wasinska-Kempka G, Hildebrand H, Sperzel M, Hartnagel RE, LeBel E, Richter A. *Bayer Corporation, Bayer AG, ClinTrials BioResearch, AnPath Services*

BAY 38-3444 and BAY 38-3441 (BAYs), glycoconjugates of camptothecin, are promising cytotoxic agents designed to be preferentially taken up by tumor cells. *In vitro* and *in vivo* toxicological comparisons of the BAYs with existing topoisomerase I inhibitors are described. Primary hepatocytes from rat, dog and man were used to assess the effect of the BAYs on AST, ALT, and LDH *in vitro*. The NOEC for human hepatocytes for both BAYs was 30 µM in contrast to 0.1 µM for topotecan. Additionally, expression of apoptosis-related genes was analyzed by TaqMan PCR in rat hepatocytes. Following incubation with topotecan or camptothecin at 10 µM for 24 hour, a strong increase in transcription was seen for p53 (600%) and bax (350%). The BAYs did not promote induction of expression of p53 or bax at a comparable concentration. In comparative studies examining colony formation of murine femoral stem cells *in vitro* there was reduced myelotoxicity of the BAYs when compared with topotecan (at the equivalent IC<sub>50</sub>). In C57BL/6 mice, treated with single i.p. doses of BAY 38-3444 daily for 3 consecutive days, myelosuppression was comparable to topotecan (dosed at the equivalent IC<sub>50</sub>); however, BAY 38-3441 produced only weak myelosuppression. An intermittent dosing schedule alleviated myelosuppression to a much greater extent with BAY 38-3444 than topotecan. In a two-cycle (5x) infusion study in dogs, BAY 38-3444 and irinotecan were dosed at their respective MTD and theoretical efficacious doses. Treatment with irinotecan promoted clinical and histopathological toxicities, whereas BAY 38-3444 was well tolerated. In conclusion, *in vitro* and *in vivo* studies with BAYs demonstrated evidence for reduced toxicities relative to existing topoisomerase I inhibitors.

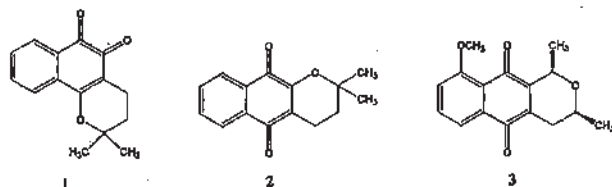
**#670 The third alpha-helix of the CAP homology domain of type II topoisomerases is critical for DNA cleavage site recognition and quinolone-action.** Strumberg Dirk, Niliss John L, Dong Jiawang, Nicklaus Marc C, Kohn Kurt W, Hedde Jonathan G, Maxwell Anthony, Pommier Yves. *Labs. of Molecular Pharmacology and Medicinal Chemistry, DBS, NCI, NIH, Bethesda, MD; Dept. of Molecular Pharmacology, St. Jude Children's Res. Hospital, Memphis, TN; Dept. of Biochemistry, University of Leicester, Leicester, UK*

We report that point mutations in the CAP homology domain of eukaryotic (yeast) type II topoisomerase (top2) (Ser<sup>740</sup>Trp, Gln<sup>743</sup>Pro, Thr<sup>744</sup>Pro and Thr<sup>744</sup>Ala) change the selection of top2-mediated DNA cleavage sites induced in presence of Ca<sup>2+</sup> or in the presence of etoposide, CP-115,953 or mitoxantrone. The homologous mutation (Ser<sup>653</sup>Trp) in E. coli gyrase also changes the pattern of DNA cleavage sites induced in the presence of Ca<sup>2+</sup> or in the presence of quinolones. We also report that the Thr<sup>744</sup>Pro mutation renders the yeast top2 enzyme sensitive to antibacterial quinolones. Thus, mutations in the α3-helix can either enhance (Thr<sup>744</sup>Pro mutation) or decrease quinolone action (Ser<sup>653</sup>Trp in E. coli gyrase & Ser<sup>740</sup>Trp in yeast topoisomerase II). This study shows that the α3-helix within the conserved CAP homology domain of type II topoisomerases is critical for selecting the sites of DNA cleavage in the G segment, and demonstrates that the α3-helix also has an important role in determining the activity and possibly the binding of drugs to the topoisomerase II-DNA complexes.

**#671 Diverse mechanisms of DNA topoisomerase II inhibition by pyranonaphthoquinone derivatives.** Krishnan Preethi and Bastow Kenneth F. *Division of Medicinal Chemistry and Natural Products, School of Pharmacy, University of North Carolina at Chapel Hill, Chapel Hill, NC 27599, U.S.A.*

Pyranonaphthoquinones like β lapachone (1) are of current interest as potential DNA topoisomerase II inhibiting anticancer agents. The present work is a detailed and systematic investigation of enzyme inhibition by 1 and two para-naphthoquinones, α lapachone (2) and eleuthine (3). For *in vitro* mechanistic studies, the inhibition and reversibility experiments used negatively supercoiled pBR322 DNA and human topoisomerase II (p170 isoform). Enzyme-DNA binding assays and topoisomerase II mediated DNA break measurements used HindIII digested pBR322 randomly labeled with <sup>32</sup>P dCTP. Compounds 1-3 are catalytic inhibitors of topoisomerase II, but the enzyme can continue to relax supercoiled DNA during extended incubation in the presence of 3. Reversibility experiments demonstrated that compounds 1 and 2 act irreversibly and confirmed that inhibition by 3 is reversible. Stepwise analysis of drug action during the topoisomerase II catalytic cycle demonstrated that 2 prevents topoisomerase II-DNA binding and induces dissociation of topoisomerase II from the DNA. In contrast, compounds 1 and 3 have minimal effect on non-covalent and pre-strand passage binding of topoisomerase II to DNA, but do cause enzyme-DNA dissociation when ATP is present. Compound 2 completely inhibits topoisomerase II mediated DNA breaks and can induce religation of DNA breaks when the equilibria are established prior to drug addition. Compounds 1 and 3 also inhibit topoisomerase II mediated DNA breaks and all compounds antagonize breaks induced by etoposide (VP-16) a prototypical enzyme poison. Interestingly, topoisomerase II-DNA binding and cleavage assay results indicated that even when etoposide stabilized cleavable complexes are established, 1 and 3 can religate breaks and also dissociate

topoisomerase II from the ternary complex. In conclusion, (i) compound 1 irreversibly inhibits topoisomerase II by religating and dissociating enzyme-DNA complexes at the post-strand passage equilibrium step of catalysis; compound 3 has the same action except it only slows the catalytic cycle and the inhibition is reversible, (ii) compound 2 inhibits topoisomerase II irreversibly by enhancing religation of cleavable complexes and dissociation of enzyme-DNA complexes.



**#672 Tirapazamine: A tumor-specific Topoisomerase II inhibitor?** Peters, Katherine B. and Brown, J. Martin. *Cancer Biology Research Laboratory, Department of Radiation Oncology, Stanford University, Stanford, CA 94305.*

Tirapazamine (TPZ), a hypoxia-selective cytotoxin, has shown activity with solid tumors in Phase II and III clinical trials in combination with radiotherapy or with cisplatin. Under hypoxic conditions, TPZ is reduced to a DNA damaging radical by cellular reductases, and we have proposed that the hypoxic cytotoxicity is the result of TPZ metabolism by a reductase or reductases associated with the nuclear matrix. As topoisomerase II $\alpha$  is highly enriched in the nuclear matrix, we investigated whether TPZ has any effect on topoisomerase II. Nuclear extracts were prepared from LFXL lung carcinoma cells that had been treated with TPZ under hypoxic or aerobic conditions. Topoisomerase II catalytic activity was examined using the kinetoplast unwinding assay. Under hypoxic but not aerobic conditions, treatment of the cells with 50–100  $\mu$ M TPZ for 1 hr abrogated the conversion of catenated DNA to the decatenated form by nuclear extracts. Importantly, there was the same loss of topoisomerase II activity for the same level of cell kill in both TPZ and etoposide treated cells, suggesting the same mechanism of cytotoxicity by both drugs. We investigated this further by measuring DNA double strand breaks caused by TPZ and etoposide with and without merbarone, a catalytic inhibitor of topoisomerase II, that prevents topoisomerase II mediated cleavage. Cells were pretreated with 200  $\mu$ M merbarone for 30 minutes before treatment with either 100  $\mu$ M TPZ or 100  $\mu$ M etoposide. Both TPZ and etoposide caused DNA double strand breaks as measured by the neutral comet assay. However, when cells were pretreated with merbarone prior to treatment with either etoposide or TPZ, the mean comet tail, a measure of DNA double strand breaks, decreased by approximately 80%. These data therefore suggest that TPZ exerts its cytotoxic effect through inhibition of topoisomerase II, probably as a result of radical damage to the enzyme. Since TPZ is only activated under the hypoxic conditions characteristic of solid tumors, this suggests that TPZ may be a tumor specific topoisomerase II inhibitor. Experiments to investigate this are currently underway.

**#673 Bisdioxopiperazine topoisomerase II catalytic inhibitors as agents to target the toxicity of topoisomerase II poisons to tumours.** Jensen, Peter B. and Sehested, Maxwell. *Finsen and Laboratory Centres, Rigshospitalet 5074, DK-2100 Copenhagen, Denmark.*

DNA topoisomerase II (topoII) is the specific cellular target of commonly used chemotherapeutic agents as etoposide and doxorubicin, which trap the enzyme at a stage its catalytic cycle when DNA is cleaved. This causes lethal DNA breaks, wherefore these drugs are termed topoII poisons. In contrast, the comparatively non-toxic bisdioxopiperazine ICRF-187 is a highly specific catalytic inhibitor of topoII, which locks the enzyme in a closed clamp form where it is inaccessible to damage by the poisons. Thus, ICRF-187 protects against etoposide cytotoxicity *in vivo* allowing a 3.6 fold increase in the LD10 of etoposide in healthy mice. Further, the blood-brain-barrier offers a pharmacological filter allowing the passage of lipophilic etoposide but not of the hydrophilic ICRF-187. We have shown in mice with intra cerebral tumours that high-dose etoposide + ICRF-187 leads to significantly longer survival than equitoxic etoposide alone (Clin. Cancer Res. 4:1367). We have therefore instigated a phase I/II trial in patients with CNS metastases from small cell lung cancer (SCLC). Encouragingly, we have already observed complete responses in three of five patients. If these results are confirmed in more patients a comparative trial against standard prophylactic cranial irradiation with its severe neurological side effects would be indicated. In order to develop catalytic inhibitors with other profiles than ICRF-187, in particular weak base antagonists for use in solid tumours (Cancer Res. 54:2959), we are developing a high-throughput system using yeast transfected with human wt or Y50F mutant topoII (Cancer Res. 58:1460) to screen libraries including our own which is based on solid phase combinatorial chemistry.

**#674 F 11782, a novel catalytic dual inhibitor of topoisomerases I and II with specific DNA repair inhibitory properties, demonstrating a broad spectrum of antitumour activities *in vitro* and *in vivo*.** Hill Bridget T, Barret Jean-Marc, Etievant Chantal, Kruczynski Anna, van Hille Benoit, Perrin Dominique and Imbert Thierry. *Institut de Recherche Pierre Fabre, 81106 Castres, France.*

F 11782, a novel fluorinated lipophilic epipodophyllid, potently inhibits both topoisomerases I and II, as judged by relaxation and decatenation assays respectively, with IC<sub>50</sub> values of 4.2 and 1.8  $\mu$ M. This interaction occurs via a unique mechanism involving the direct interaction of F 11782 with each nuclear enzyme, as shown by gel shift assays, thus influencing their subsequent DNA-binding. Thus F 11782 acts at an early step of the catalytic cycle of each of the topoisomerases. Comparable activities were not seen with conventional topoisomerase-interacting agents like etoposide, camptothecin, aclarubicin or ICRF-187. F 11782 has also been identified as a potent inhibitor of DNA repair activity *in vitro*, involving a specific inhibition of the incision step of the nucleotide excision repair pathway (IC<sub>50</sub> value = 1.1  $\mu$ M). F 11782 shows no DNA-intercalating properties and proved inactive against a range of other DNA-interacting enzymes. F 11782 is quite different from other dual topoisomerase inhibitors and most specific inhibitors of topoisomerase II, since *in vitro* it neither cleaves DNA, nor interferes with cleavable complex stabilisation.

F 11782 exhibits outstanding antitumour activity *in vivo* against a panel of experimental tumour models, with overall superiority to etoposide tested concurrently; proving curative against the P388 murine leukemia (l.v.), significantly improving survival ( $p < 0.100$ ) and inhibiting tumour growth ( $T/C < 1\%$ ) in the B16 murine melanoma (s.c.), reducing lung metastases in the B16F10 metastatic variant by 99% and significantly influencing the growth of MX-1 (ca. breast) and LX-1 (ca. lung) human tumour xenografts.

F 11782 with its unique mode of action represents an exciting new class of antitumour agent now undergoing development.

**#675 Antitumour activity of XR5944, a novel topoisomerase inhibitor.** Stewart A.J., Dangerfield W., Lancashire H., Mistry P., Okiji S., Baguley B.C., Denny W.A., Templeton D., Charlton P. *Xenova Ltd, 240 Bath Road, Slough SL1 4EF, UK; Auckland Cancer Society Research Centre, University of Auckland, NZ (MAD, BCB).*

Topoisomerases are essential enzymes in eukaryotic cells and have long been recognised as targets for intervention in the treatment of tumours. Widely used topoisomerase poisons include the camptothecin analogues and etoposide that target topoisomerase I and II, respectively. A number of compounds have been demonstrated to have activity against both topoisomerase I and II (e.g. XR5000, intoplicine, TAS-103). This approach has the advantage of avoiding drug resistance due to alterations in either of the two enzymes and may also allow the drug to act at several points in the cell cycle.

XR5944, a bis-phenazine, is a highly potent cytotoxic agent in a range of human cell lines (IC<sub>50</sub> 0.02–0.43 nM). XR5944 poisoned both topoisomerase I and II thus putting XR5944 into the class of a joint topoisomerase inhibitor. However, XR5944 may have a preference for topoisomerase I as it gave only partial inhibition of topoisomerase II-dependent decatenation of kinetoplast DNA. The action of XR5944 on both topoisomerase I and II may be due to the ability of XR5944 to intercalate DNA as shown using a DNA unwinding assay. XR5944 was found to be an exceptionally efficient DNA intercalator compared to standard agents such as doxorubicin, am-sacrine and TAS-103.

*In vivo*, in a hollow fibre model, XR5944 demonstrated significant activity against a panel of human tumour cell lines. In this model, where cells are grown in synthetic fibres implanted subcutaneously or intraperitoneally, XR5944 (5 mg/kg i.v. qdx5) gave almost complete inhibition (77–92%) of proliferation of three human tumour cell lines (H69 SCLC, HT29 colon, HCT-15 colon). TAS-103 was also tested and gave only 13–66% inhibition at its MTD using the same schedule.

This activity for XR5944 translated well to tumour-bearing animals where it has shown exceptional activity in human xenograft models. In H69 SCLC tumours, XR5944 (10 mg/kg i.v. q4dx3) induced complete regression while topotecan was only able to slow tumour growth. In the resistant HT29 colon carcinoma model XR5944 (15 mg/kg i.v. q4dx3) gave tumour stasis during the treatment period and showed longer tumour growth delay than controls (doxorubicin or TAS-103). These data demonstrate that XR5944 is a novel topoisomerase inhibitor that has exceptional antitumour activity *in vitro* and *in vivo*.

## SECTION 5: CHEMOPREVENTION: TARGETS, MODELS, BIOMARKERS, AND TRIALS

**#676 Altered gene expression in MNU-induced rat mammary tumours following long term exposure to vorozole or dehydroepiandrosterone.** Lubet, Ronald A., Hu, Lan, Wang, Yian<sup>2</sup>, Kelloff, Gary J., You, Ming. *Department of Pathology, Medical College of Ohio, Toledo, OH 43614; Chemoprevention Branch, National Cancer Institute, Bethesda, MD 20892.*



The effects of prolonged (3 months) exposure to vorozole (a competitive aromatase inhibitor) or dehydroepiandrosterone on gene expression in hormonally responsive, minimally invasive, MNU induced rat mammary tumors was determined. The genes examined for modulation were identified by a cDNA library screening procedure which makes use of competitive hybridization on duplicate plaque lift filters to identify genes with altered levels of expression when comparing the tumors with normal rat mammary gland. Following screening of ~100,000 clones in a cDNA library approximately 400 were cloned and altered expression confirmed in ~200 by dot blot analysis. These genes were then employed to examine the effects of these two classes of agents which affect the hormonal axis (aromatase inhibitors and dehydroepiandrosterone which increases levels of both androgens and estrogens) and which are effective chemopreventive agents in this model. We examined control tumors versus tumors which grew out following long term exposure to the agents. These studies show 1) that long term exposure to these agents alter gene expression; and 2) that certain of the gene changes are compound specific. Nevertheless it demonstrates that limited exposure to effective therapeutic and chemopreventive agents can cause striking and reproducible changes in a variety of genes.

**#677 Correlation of deletion RB gene with risk factors of Chinese female breast cancer.** Gu, Y., Shi, Y., Yuan, J., Zhu, K., Wu, X., Wang, X., Zhang, H. Dept. of Epidemiology, Tongji Medical University, Wuhan 430030, P.R. China.

The deletion of RB gene that as a suppressor gene have been observed frequently in breast cancer. This loss is believed to contribute to the development of breast cancer, but the significance of Rb gene and relationship of it with potential risk factors of breast cancer remain unclear.

To detect point mutation of exon 14-16 and exon 21 of Rb gene in breast cancer and analysis the influence of some related risk factors of breast cancer in it. We examined 96 female cases of primary breast cancer in Hubei province of China using the method of PCR product direct sequencing. Informations on the risk factors of breast cancer were collected by questionnaire. Mutations were detected in 19 of 96 (19.8%) at exon 14-16 and 14 cases have mutation in exon 21 (14.6%). Total mutation was 26.0% (25/96) and was found more frequently in the cases with the family history of cancer that had an affected first-degree or second-degree relative than the cases without (44.0% vs. 116.9%  $p < 0.001$ ). There are no statistically significance difference for the mutation in the age at menarche, menopause status, and number of birth, ER or PR status and smoking. Furthermore, a significant association was observed between mutation of exon 14-16 and the absence of progesterone receptor ( $p < 0.005$ ). Results of the analysis of exon 14-16 and exon 21 in comparison to the identified risk factors of breast cancer were used as basis of polychotomous logistic regression analysis (p1 and p2 are probability that exon 14-16 and exon 21 mutations, p0 is the probability of a negative test). The presence of family history of cancer was noted in particular to increase the probability of a mutation.

Our data indict Rb gene may play a role in development of Chinese female breast cancer and the women who have an affected family history of cancer have a high probability of carry a mutation of exon 14-16 or exon 21 of Rb gene according to the statistical model.

**#678 Evaluation of chemopreventive agents by *in vitro* assays.** Colacci A, Argnan A, Horn W, Sillingardi P, Vaccari M, Giungi M, Mascolo MG (IST-National Institute for Cancer Research, Biotechnology Satellite Unit, Bologna, Italy) Grilli S. (Ist. Cancerologia, Università degli Studi, Bologna, Italy).

With the aim of evaluating inhibitors or potential inhibitors of carcinogenesis process, we studied the activity of chemopreventive agents in a battery of *in vitro* model systems, representing different stages of transformation process and including cells at different level of malignancy. We profiled the *in vitro* activity of the non-steroidal antiestrogen tamoxifen (TAM) and the synthetic retinoid 4-hydroxy-phenyl-retinamide (HPR), widely used as part of therapeutic approaches to control breast cancer and presently under clinical trials as chemopreventive drugs, of some antioxidant chemicals, including N-acetyl-N-cysteine (NAC) and the more potent lipoic acid (LA) and of the protease inhibitor, antipain (AP). Some compounds were tested either as single agents or in combination. An *in vitro* modified BALB/c 3T3 transformation assay was used to assess the ability of chemopreventive single agents or combinations to inhibit cell transformation by acting as blocking and/or suppressing agents. The role of chemopreventive agents in the late steps of tumor process was assessed by examining the effect of compounds, alone or in combination, on the invasive ability and the chemotactic motility of malignant cells by using Matrigel invasion assay. The effect of the agents on components of malignant invasion, namely cellular adhesion, motility and proteolytic capability, which provide potential sites of pharmacological intervention for malignancy, was also studied by appropriate *in vitro* techniques. Thus, the efficacy of compounds on cell attachment to several substrates, including laminin (LN), collagen IV (CIV), fibronectin (FN) and vitronectin (VN) was examined. The influence of compounds on MMP2-mediated matrix prote-

olysis was also assessed by gelatin zymography. The role of chemopreventive agents in cell-cell communication, mediated by gap-junctions, was also studied in normal and transformed cells.

Experimental protocols and results, which will be illustrated in detail, give evidence for the feasibility of the proposed *in vitro* tests battery to be used for the *in vitro* screening of candidate chemopreventive agents and for qualifying these compounds for further evaluation in clinical studies.

This work was granted by Associazione Italiana per la Ricerca sul Cancro (AIRC), Milan, Ministero Sanità, Rome and Ministero Università e Ricerca Scientifica e Tecnologica (MURST), Rome, Italy.

**#679 Chemotherapeutic study of styrylpyrone derivative (SPD).** Azimahtol Hawariah, L.P. & Meenakshli, N. Program Bioscience & Biotechnology, Faculty Science & Technology, Universiti Kebangsaan Malaysia.

The combination of *in vivo* and *in vitro* model studies has led us to further investigate the efficacy of Styrylpyrone Derivative (SPD) as an anticancer agent. This study investigates the efficacy of SPD chemoprevention in the presence of a tumor promoting excipient (*Nigella sativa* oil) within the duration of treatment. SPD was generally found to display significant tumorigenicity among the premenstrual rats for all treatment weeks. However, postmenstrual rats subjected to longer periods of treatment did not respond well to SPD-probably attributed to the age factor (11-14 months old). SPD's tumorigenic effects prevail even when administered with excipients that contribute neutrally (Vitamin C) and additively (*N. sativa* oil) to tumor progression but its tumoricidal effects are modulatory to the biological nature of the additive excipient. SPD treated-regressed tumors were predominantly fibrosis, fat infiltrated and fibroadenomatous at necropsy while most of the controls were adenocarcinomatous.

**#680 Chemoprevention of colorectal cancer in mice.** Uckun, F.M., Matzke, B., Naria, R.K., Chelstrom, L., Wndorf, H., and Waurzyniak, B. Drug Discovery Program, Parker Hughes Cancer Center, Hughes Institute, St. Paul, MN 55113.

Germ-line mutations in the human adenomatous polyposis coli (APC) gene result in familial adenomatous polyposis, an autosomal dominant disorder characterized by the early onset of multiple adenomatous polyps in the large bowel with a high likelihood of developing colorectal carcinomas. Mice heterozygous for APC gene with chain-termination mutation in the 15th exon progressively develop intestinal tumors in a manner that is similar to that observed in mice which carry a multiple intestinal neoplasia (*Min*) and patients with familial adenomatous polyposis. We used this *Min*-mouse model to test the ability of a novel dimethoxyquinazoline compound to prevent development of colorectal cancer. The *Min*-mice were fed with rodent chow supplemented (0.3%) with the chemopreventive drug or vehicle in food once a week starting at 6 weeks of age and the health status was monitored. At 13 weeks of age 26% of control mice showed blood in stool or rectum whereas none of the mice fed with chemopreventive drug showed any signs of blood in rectum. Gross examination of mice sacrificed at 13 weeks of age revealed that 60% of control mice showed polyps in the intestine, whereas none of the drug-treated mice had detectable polyps. By 30 weeks of age, none of the control mice ( $n = 15$ ) were alive, 15 out of 15 mice fed with chemopreventive drug remained alive. Thus further development of this novel dimethoxyquinazoline compound may be useful in the prevention of colorectal carcinomas.

**#681 Chemoprevention of breast cancer in neu/erbB2 transgenic mice by EGF-Genistein.** Uckun, Fatih M.; Myers, Dorothea E. Drug Discovery Program and Parker Hughes Cancer Center, Hughes Institute, St. Paul, MN 55113.

EGF-Genistein is a biotherapeutic agent which inhibits the EGF-receptor tyrosine kinase and associated Src family tyrosine kinases leading to apoptosis in human breast cancer cells both *in vitro* and *in vivo* (Uckun FM, et al. *Clinical Cancer Research*, 4(5):1125-1134, 1998). Here, we examined the ability of EGF-Genistein, administered on a 1x/week schedule, to prevent the spontaneous development of breast cancer in neu/erbB2 transgenic mice overexpressing the neu protooncogene in their mammary glands. The chemoprevention program was initiated when the transgenic mice were 4 months old. EGF-Genistein was administered subcutaneously 1x/week x 10 weeks at a 5 mg/kg dose level. All 29 PBS-treated control mice developed breast cancer with a median cancer-free survival of 210 days. In contrast, only 40% of EGF-Genistein treated mice developed breast cancer and the median cancer-free survival was >300 days. EGF-Genistein treatment was not associated with any side effects. EGF-Genistein may be useful for chemoprevention of EGF-receptor expressing breast cancer and/or its recurrence.

**#682 Prognostic value of tumor-associated macrophage count in human bladder cancer.** Nakagawa, M., Hanada, T., Emoto, A., Nomura, T., Nomura, Y. Department of Urology, Oita Medical University, Oita 879-5593, Japan.

Purpose: We determined tumor-associated macrophage (TAM) count to investigate its importance in predicting clinical outcome or prognosis in patients with bladder cancer.

Materials and Methods: TAM count and microvessel count (MVC) were determined immunohistochemically in 63 patients with bladder cancer,

Including 40 superficial bladder cancers and 23 invasive bladder cancers. To examine the relationship between TAM count and clinical outcome or prognosis in bladder cancer, cystectomy rates, distant metastasis rates, vascular invasion rates and 5-year survival rates were compared between patients with low (<67) and high (≥67) TAM count.

Results: TAM count in invasive bladder cancers ( $154 \pm 12.0$ ) was significantly higher than in superficial bladder cancers ( $49 \pm 7.8$ ,  $p < 0.0001$ ). MVC in invasive bladder cancers ( $72 \pm 10.4$ ) was also significantly higher than in superficial bladder cancers ( $47 \pm 5.6$ ,  $p < 0.05$ ). There was a positive correlation between TAM count and MVC ( $r = 0.30$ ,  $p = 0.02$ ). Immunohistochemical staining using CD68/HRP mAb showed more infiltrating cells in invasive bladder cancers than superficial bladder cancers. Patients with high TAM count (≥67) showed significantly higher rates of cystectomy, distant metastasis, vascular invasion than those with lower TAM count (<67). Five-year survival rate estimated using Kaplan-Meier method was significantly lower in patients with high TAM count than those with low TAM count ( $p < 0.0001$ ).

Conclusions: Our results suggest that determination of TAM count in bladder cancer tissues is of value to predict clinical outcome or prognosis and to select appropriate treatment strategies in patients with bladder cancer.

gene amplification in 2 of 3 cases with persistent dysregulation of cyclin D1 expression. In follow-up biopsies p16 loss was seen in 7 additional cases while in 2 of the 4 cases with loss of the protein at baseline, re-expression was observed and was associated with response. Methylation of the p16 gene promoter was detected in 10 cases and 15 of the 19 biopsies examined and correlated with loss of p16 expression in 3 of these cases. In conclusion, dysregulated cyclin D1 expression appears to be an adverse prognostic factor and is associated with gene amplification in a subset of dysplastic lesions. Methylation of the p16 promoter is a frequent early event in premalignant lesions. Modulation of cyclin D1 dysregulated expression and re-expression of p16 in a subset of cases was clearly associated with response and suggests reversible mechanisms of protein expression abnormalities that could be a target for further chemoprevention approaches. Complete molecular characterization of the events underlying aberrant cell cycle regulator protein expression is ongoing and might shed more light on the mechanisms of chemoprevention.

**#685 MAP4: a p53 regulated gene that controls the sensitivity to vinca alkaloids and taxanes in breast cancer cells.** Bash-Babula, J., All, E., Zhang, C.Z., and Hait, W.N. *The Cancer Institute of New Jersey, UMDNJ-Robert Wood Johnson Medical School, New Brunswick, NJ 08901.*

p53 mutations are found in 15%–50% of breast cancers. The functional status of p53 regulates the sensitivity to anti-cancer therapies. We have previously shown that mutant p53 leads to increased sensitivity to taxanes through the derepression of Microtubule Associated Protein 4 (MAP4), which enhances microtubule polymerization. At the same time, overexpression of MAP4 renders cells resistant to vinca alkaloids. DNA-damaging drugs, doxorubicin and bleomycin, increase wild type p53 and repress MAP4 in C127 murine breast cancer cells. These changes led to microtubule depolymerization and increased sensitivity to vinca alkaloids. However, this relationship has not been shown in human cells.

We investigated whether there is a correlation between p53 status and MAP4 expression in human breast cancer which could predict responsiveness to taxane and vinca alkaloid chemotherapy. Our results indicate that whereas transcriptionally-activated targets for p53, p21/WAF1 and MDM2 are expressed at high levels in wild-type p53 containing cells, there was no significant difference in MAP4 levels between wild-type or mutant p53 containing cell lines. As in C127 cells, we found that treatment of human MCF-7 cells (wt-p53) with DNA-damaging drugs, doxorubicin and bleomycin, led to increased p53, mdm2 and p21 and decreased MAP4 protein levels. These changes predict enhanced sensitivity to vinca alkaloids and decreased sensitivity to taxanes. These findings suggest that DNA-damage of wild-type p53 containing breast cancer cells is necessary to increase steady-state p53 levels to repress MAP4. Preliminary studies show that treatment of metastatic breast cancer patients with doxorubicin leads to the induction of p53, p21 and mdm2 and a repression of MAP4 in peripheral blood mononuclear cells.

Taken together, these results suggest that through DNA-damage, the levels of MAP4 can be manipulated in breast cancers with wild-type p53 such that there is more accessible target for vinca alkaloids. This would lead to increased efficacy of combination chemotherapy where a DNA damaging drug is used with a vinca alkaloid.

**#686 Cyclooxygenase inhibitors exert anti-proliferative effects against human pancreatic adenocarcinoma cell lines that are independent of the level of COX-2 expression.** Molina, Miguel A., Sija-Arriaga, Marta, Lemolne, Michael G., Frazier, Marsha L., and Slinicropo, Frank A. *The University of Texas M. D. Anderson Cancer Center, Houston, TX.*

Cyclooxygenase (COX) enzymes regulate prostaglandin production and the inducible isoform, COX-2, appears to be involved in epithelial tumorigenesis. COX is a target of nonsteroidal anti-inflammatory drugs (NSAIDs) that prevent experimental colon cancer. We examined COX-2 expression in pancreatic carcinoma cell lines and determined whether NSAIDs could inhibit their growth. COX-2 was analyzed in pancreatic cancer cells (BxPC-3, Capan-1, MDAPanc-28, MDAPanc-3, PANC-1) and in human tumors using immunohistochemistry (anti-COX-2 monoclonal antibody, Cayman Chemical, MI), Western blot assay, and reverse transcription-PCR (RT-PCR). The effects of sulindac sulfide (Cell Pathways, PA) and NS398 (Cayman) on cell proliferation were determined using the MTS assay (Promega, WI) and cell cycle distribution and DNA content were examined in propidium iodide-stained cells by FACS analysis. Cells were incubated in the presence of drug or vehicle for 96 hr. Immunohistochemistry detected cytoplasmic COX-2 expression in 14 of 21 (67%) pancreatic cancers. Using RT-PCR, the level of COX-2 was increased relative to adjacent normal tissue and pancreas from a healthy individual. COX-2 mRNA or protein were elevated in 4 of 5 and 3 of 5 tumor cell lines, respectively. COX-2 expression correlated with the differentiation status of the tumors of origin of the cell lines. COX-2 was upregulated by treatment with epidermal growth factor in serum-deprived cells. Both a nonselective (sulindac sulfide) and a selective (NS398) COX-2 inhibitor produced a dose-dependent inhibition of cell proliferation in all five cell lines. No correlation was found between the level of COX-2 and the extent of growth inhibition. Treatment of BxPC-3 cells with sulindac sulfide and NS398 produced a significant G<sub>1</sub>

**#684 Biochemoprevention for dysplastic aerodigestive tract lesions: effects of cyclin D1 and p16 abnormalities.** Papatimitrakopoulou Vail A., Izzo Julie, Keck Jamie M., Mao Li, El-Naggar Adel K., Shin Dong M., Hittelman Walter N., Hong Waun K. *The University of Texas M. D. Anderson Cancer Center.*

To investigate the role of cell cycle regulator abnormalities in the pathogenesis of advanced premalignant lesions (APLs) (dysplastic) of the upper aerodigestive tract and the biologic effects of chemoprevention, we studied 22 participants with APLs in a prospective trial of 13-cis retinoic acid,  $\alpha$ -interferon and  $\alpha$ -tocopherol administered for 12 months with biopsies obtained at baseline, 6, 12 and 18 months. Cyclin D1 and p16 protein expression were analyzed by immunohistochemistry in a total of 79 and 77 biopsies respectively. At baseline, dysregulated cyclin D1 expression was seen in 9 (43%) of these cases and p16 loss in 4 (18%) of cases. Downregulation of cyclin D1 expression (5 cases) or maintained low-normal expression (10 cases) correlated with response in 6 of these cases, while persistently high or increased expression in 6 cases was associated with lack of response or progression in all 6 cases. This strongly suggests an association between dysregulated cyclin D1 expression and poor outcome. Interestingly, fluorescence in situ hybridization revealed *cyclin D1*



cell cycle arrest. A 1.6-fold increase in the subdiploid cell population was seen only for NS398, suggesting that this drug induced apoptosis. In conclusion, COX-2 upregulation is a frequent event in pancreatic carcinoma and cell lines. COX inhibitors had anti-proliferative effects which were related mostly to cell cycle inhibition. Growth inhibition was independent of the level of COX-2 expression. Our findings suggest that these drugs may be useful in the chemoprevention and therapy of this malignancy.

**#687 Cancer specific PCNA: a potentially powerful new biomarker for breast cancer.** Bechtel, P.E., McDermott, L.N., Schnaper, L., Hickey, R.J. and Malkas, L.H. *University of Maryland School of Medicine, Program in Oncology, Baltimore, MD; Greater Baltimore Medical Center, Towson, MD.*

Despite extensive research efforts to identify unique molecular alterations in breast cancer, to date no characteristic has emerged that correlates exclusively with malignancy. Proliferating cell nuclear antigen (PCNA) is a small nuclear protein essential for the DNA replication and repair processes within the cell. Currently, PCNA is used with limited success to analyze histological specimens as a marker for cell proliferation. We have identified a novel, cancer specific form of PCNA (csPCNA) using 2D PAGE and Western blot techniques. The csPCNA was present in malignant breast cell lines (MCF 7, Hs578T and MBA MD 468) and absent from nonmalignant breast cells (MCF 10A, MCF 10F and primary breast cells). Examination of over 30 human breast tumors and tissue has demonstrated that csPCNA was present in all malignant tissue examined and absent from all nonmalignant tissue examined. Sequence analysis of the PCNA gene cloned from MCF 7 and MCF 10A cells revealed that the gene sequences were identical, indicating that csPCNA was not the result of genetic mutation. The cancer specific protein is most likely the result of an alteration in the posttranslational modification of PCNA. Using several chromatographic techniques csPCNA has been isolated and protein characterization is currently being performed to define the structural modifications made to the protein. Currently used diagnostic tools fail to differentiate csPCNA from the PCNA endogenously present in the cell. The lack of specificity of these tools may explain the limited success of PCNA as a biomarker for cancer. The csPCNA however, has the potential to be a powerful new biomarker for breast malignancy.

**#688 Desorption Ionization Time of Flight Mass Spectrometry (SELDI-TOF-MS): A novel proteomic approach to identify bladder cancer biomarkers.** Vlahou Antonia, Mendrinos Savvas, Kondylis Filippou, Schellhammer Paul F., Lynch Donald F. and Wright Jr. George L. *Eastern Virginia Medical School, Norfolk, VA.*

Transitional cell carcinoma (TCC) of the bladder is the second most common genitourinary malignancy. At present the most reliable way of diagnosis and follow-up of TCC is histologic and cytologic analysis of biopsy specimens obtained by cystoscopy. The invasive nature of this modality presents a challenge to develop novel non-invasive diagnostic tools. The objective of this study is the identification of TCC biomarkers and development of a proteomic approach to detect TCC in voided urine. Samples from 12 patients with history of TCC, including 5 with histologically or cytologically proven TCC at the time of specimen collection, 12 patients with benign conditions of the urogenital tract and 11 normal volunteers, were analyzed by the SELDI ProteinChip™ technology (Ciphergen Biosystems, Inc). Retentate maps were compared for the identification of TCC-associated proteins. A potentially novel TCC biomarker of relative molecular mass of 3,400 was observed in 100% (5/5) of the pathologically documented TCC urines, but only in 16.7% (2/12) of the benign and 18.2% (2/11) of the normal samples. 2 of 7 urine samples from patients with a past history of TCC but with a negative diagnosis at the time of collection displayed the 3,400 Da protein. That corresponds to a sensitivity and specificity in diagnosis of 100% and 80%, respectively. These results demonstrate that SELDI technology applied to urine can be very useful in identifying novel biomarkers that could be further utilized in developing highly sensitive diagnostic tests for TCC.

**#689 Expression of cyclooxygenase-1 and cyclooxygenase-2 in N-nitrosomethyl-benzylamine-induced rat esophageal tumorigenesis.** Carlton, Peter S., Gopalakrishnan, Rajaram, Gupta, Ashok and Stoner, Gary D. *The Ohio State University College of Medicine and Public Health, Columbus, OH 43210.*

Cyclooxygenase (COX), or prostaglandin endoperoxide synthase, is the rate limiting enzyme involved in the metabolism of arachidonic acid. Known isoforms of the enzyme, COX-1 and COX-2, both catalyze the synthesis of prostaglandins and thromboxanes from a free arachidonic acid precursor. The COX-1 isoform is constitutively expressed and produces the prostanoids important for normal physiologic function. COX-2 is a mitogen-inducible isoform of cyclooxygenase and is thought to produce prostanoids at sites of inflammation. Upregulation of COX-2 has been linked to epithelial tumorigenesis in various human and animal tissues including the colon, stomach, breast, lung and esophagus. In the current investigation, normal and N-nitrosomethylbenzylamine (NMBA)-induced preneoplastic and papilloma tissues of the rat esophagus have been characterized for expression of COX-1 and COX-2. Groups of 30 F344 rats were injected subcutaneously with NMBA (0.5 mg/kg body weight) 1 time,

per week for 15 weeks or 3 times per week for 5 weeks. Half of the animals were sacrificed at 16 weeks and the remainder at 26 weeks. Results of semi-quantitative RT-PCR and Northern blot analyses indicate a correlation between the deregulation of both COX-1 and COX-2 expression and neoplastic progression in the rat esophagus. These observations were most evident in 26 week tissues dosed once per week for 15 weeks. The expression of COX-1 in preneoplastic tissues and papillomas was significantly elevated compared to normal tissues. With respect to COX-2, dosing animals once per week for 15 weeks produced significantly elevated COX-2 expression in preneoplastic tissues compared to normal tissues at 16 weeks. At 26 weeks, expression of COX-2 was significantly higher in preneoplastic tissues and papillomas compared to normal tissues. In addition, papillomas expressed significantly elevated levels of COX-2 compared to preneoplastic tissues. Semi-quantitative RT-PCR analysis is also being used to evaluate possible down-stream effectors of deregulated COX-2 expression, including apoptosis related genes Bcl-2 and Bax. Preliminary results suggest the expression of these genes is unchanged in the rat esophagus. Together, these data support the use of COX expression as a molecular target for the chemoprevention of esophageal tumorigenesis in the rat.

**#690 13-cis-retinoic acid (13CRA) causes growth suppression, cyclin D1 repression, but not RAR beta induction, in normal oral epithelial cells in an *in vitro* model of oral carcinogenesis.** Suh, Gerald D., Boyle, Jay O., Lin, Derrick, Sacks, Peter G. *Memorial Sloan-Kettering Cancer Center, Head and Neck Service, New York, NY.*

In an *in vitro* model of lung carcinogenesis retinoic acid causes growth suppression, repression of cyclin D1, and induction of RAR beta. We sought to determine the effects of 13CRA in an *in vitro* model of oral cancer. The model consists of short term cultured normal oral epithelial cells (NOE), a leukoplakia cell line (MSK Leuk1), and a head and neck squamous cell carcinoma cell line (1483). Cell growth was measured by the incorporation of tritiated thymidine after 12 hour treatments of 13CRA at concentrations of 0.5–8  $\mu$ M. FACScan was used for cell cycle analysis after treatments with similar doses of 13CRA. Cyclin D1 and RAR beta expression were measured by immunoblot analysis. 12 hour treatments of 13CRA caused 65% growth suppression at 4  $\mu$ M and 90% growth suppression at 8  $\mu$ M in NOE cells. No significant growth suppression was observed for MSK Leuk1 or 1483 cells. Cell cycle analysis revealed a 44% increase in the number of NOE cells in the G1 phase after 24 hour treatments of 2  $\mu$ M 13CRA. There was no increase in the number of MSK Leuk1 or 1483 cells in the G1 phase after 13CRA treatments up to 8  $\mu$ M. Similarly 13CRA treatments of 1–4  $\mu$ M caused a dose dependent decrease in the expression of cyclin D1 protein in NOE cells. In contrast the MSK Leuk1 and 1483 cells showed no decrease in cyclin D1 expression after 13CRA treatments up to 8  $\mu$ M. RAR beta expression was present in all three cell lines. There was no induction of RAR beta expression by 13CRA treatments up to 4  $\mu$ M in any of the cell lines. In summary, in this oral carcinogenesis model the MSK Leuk1 and 1483 cells were resistant to retinoid effects. The retinoid effect in this model was independent of RAR-beta expression. These findings demonstrate differences between retinoid effects in the oral model compared to the previously reported lung model.

**#691 Systematic evaluation of cancer chemopreventive agents: the results of Volumes 1–4 of the IARC Handbook series.** Stewart, Bernard W., *Cancer Control Program, South Eastern Sydney Public Health Unit, Locked Bag 88, Sydney 2031, Australia and International Agency for Research on Cancer, Lyon 69372, France.*

Since 1972, over 70 volumes of 'IARC Monographs on the Evaluation of Carcinogenic Risks to Humans' have been published. The evaluation process involves a Working Group convened to provide expertise relevant to the class of agent under consideration. Recently, a similar evaluation procedure has been developed to provide authoritative information on cancer prevention and, in the first instance, the efficacy of chemopreventive agents. These evaluations are published as 'IARC Handbooks of Cancer Prevention'. Establishing this evaluation process has involved a two-stage development: (1) the evaluation process itself was subject to consideration before (2) convening specific Working Groups. In common with 'IARC Monographs', the scope and type of data to be considered, and the basis upon which data are assessed, is outlined in a 'Preamble'. Each volume of the Handbook series includes this 'Preamble' which was generated by an international conference on cancer chemoprevention in 1995. The scope of data evaluated is broad. Beyond evidence of cancer chemopreventive activity in humans (observational studies and intervention trials) and animals, account is taken of adverse effects of the agent, including possible carcinogenic effects. Evaluation of cancer chemopreventive activity includes defined criteria for strength of evidence (sufficient evidence, etc). Finally, an opportunity is afforded for adoption of an overall statement which takes account of both preventive and adverse effects. The first 'IARC Handbook on Cancer Prevention' was published in 1997 and concerned non-steroidal anti-inflammatory drugs; volumes concerning carotenoids (1998), vitamin A (1998) and retinoids (in press) followed. On the basis of these evaluations, insight into the defined terms has been gained. No agent has been evaluated as having sufficient evidence of cancer

chemopreventive activity in humans. Perhaps more importantly, the available evaluations highlight the weight that should be accorded intermediate endpoints of chemopreventive activity and the role of animal models as indicators of effects in humans.

**#692 Intracellular polyamine levels, S-phase fraction and aneuploidy in patients with chronic myeloid leukemia in chronic and accelerated phase.** Tripalhi A.K., Chaturvedi R., Tekwani B.L., Ahmad R., Asim M. and Singh R.L., *Division of Haemato-Oncology, Dept. of Medicine, K.G.'s Medical College, Lucknow, U.P., India.*

Polyamines putrescine, spermidine and spermine have been implicated in the regulation of cell proliferation and differentiation. We studied intracellular polyamine levels in the peripheral blood leucocytes of patient with chronic myeloid leukaemia (CML, n = 16) and control subjects (n = 5), with the aim to correlate it with the clinical stages of disease, aneuploidy, and S-phase fraction (SPF).

Polyamines were measured using HPLC (verkolon et al), and SPF, aneuploidy were determined by flow cytometry.

Mean age of CML patients was  $35 \pm 13$  and control was  $32 \pm 12$  years. CML patients were comprised both of chronic phase (CML-CP, n = 8) and accelerated phase (CML-AP, n = 8). The values of putrescine in control, CML-CP, CML-AP were  $1.8 \pm 1.4$ ,  $26.7 \pm 18.62$ ,  $49.80 \pm 38.32$  n moles/ $10^7$  cells respectively. Spermidine values were  $3.0 \pm 0.9$ ,  $9.67 \pm 8.52$ ,  $42.95 \pm 24.23$  n moles/ $10^7$  cells respectively and spermine values were  $12.4 \pm 3.8$ ,  $11.44 \pm 9.58$ ,  $38.76 \pm 18.32$  n moles/ $10^7$  cells respectively. The aneuploidy was present in 2 patients of CML-CP (25%) and 5 patients of CML-AP (62.5%), whereas it was absent in all controls subjects. The mean values of SPF in control, CML-CP and CML-AP patients were  $0.22 \pm .21\%$ ,  $3.4 \pm 2.2\%$ ,  $13.86 \pm 3.91\%$  respectively. Spermidine/spermine ratio was 0.24, 0.85 and 1.11 respectively in control, CML-CP and CML-AP.

The levels of putrescine and spermidine were significantly high in CML-CP as compared to control ( $p < 0.01$ ). There was no significant difference in spermine levels. The putrescine, spermidine, spermine were all significantly raised in CML-AP as compared to CML-CP ( $p < 0.05$ ,  $p < 0.01$ ,  $p < 0.01$  respectively). Spermidine and spermine ratio were significantly increased in CML patients as compared to control ( $p < 0.01$ ), but there was no significant difference between CML-CP and CML-AP. S-phase fraction was significantly high in CML patients ( $p < 0.001$ ) compared to normal. It was also significantly raised CML-AP compared to CML-CP ( $p < 0.001$ ).

We conclude that intracellular polyamine putrescine, spermidine, spermine levels, aneuploidy and SPF could be important parameters for the prediction of evolution to accelerated phase in CML patients.

(The study was supported by the financial grant from UPCST, D1906/98)

**#693 Organ-specific effect of a germline p53 mutation on chemical carcinogenesis in mice: a new mouse model for cancer therapy and prevention.** Zhang, Z., Lantry, L.E., Wang, Y., Wiseman, R.W., Lubet, R.A. and You, M. *Department of Pathology, Medical College of Ohio, OH; Laboratory of Molecular Carcinogenesis, NIEHS; NC; Chemoprevention Drug Development Group, NCI, MD.*

Use of mice with a dominant negative P53 transgene ( $p53^{val135/wt}$ ) (UL53-3) in conjunction with organ specific chemical carcinogens allows one to generate *in situ* tumors containing a mutated p53. P53 mutant F1 (A/J  $\times$  UL53-3) mice bred by crossing P53 mutant mice with A/J mice were highly susceptible to lung adenoma induction by various carcinogens. Chemoprevention studies with long term exposure to glucocorticoids or green tea reduced tumor formation equally in  $p53^{val135/wt}$  vs  $p53^{wt/wt}$  mice. Treatment of microadenomas for 28 days with either taxol or Adriamycin were similarly effective (tumor number and volume) in  $p53^{val135/wt}$  vs  $p53^{wt/wt}$  mice. P53 transgenic mice were crossed with C57BL/6J mice and the resulting F1 mice (C57BL/6J  $\times$  UL53-3) were inlited with 1,2-dimethylhydrazine (DMH) or N-butyl-N-(4-hydroxybutyl)-nitrosamine (OH-BBN) which are preferential colon or bladder carcinogens respectively. While a mutant P53 increased formation of uterine sarcomas, lung adenomas, hepatomas, and colon tumors in DMH treated mice the incidence and multiplicity of OH-BBN-induced bladder lesions was similar in  $p53^{val135/wt}$  vs  $p53^{wt/wt}$  mice. In the DMH system long term chemopreventive exposure to the NSAID piroxicam, reduced the incidence of colon tumors similarly in

$p53^{val135/wt}$  vs  $p53^{wt/wt}$  mice but did not affect formation of uterine sarcomas or lung adenomas. This *in situ* model should be useful for both chemoprevention and therapeutic studies.

**#694 Vitamin E succinate induces inhibition of proliferation in prostate cancer cell lines.** Ashktorab, H., Alghazi, Y., Allen, Neapolitano, M.C., Ahmed, A., Tackey, R., Walters, C.S., and Smoot, D.T. *Cancer Center, Department of Medicine, Howard University, Washington, D.C.*

Mortality from prostate cancer is the second leading cause of cancer in men. Various studies have led to the delineation of a pathway controlling the progression of cells from quiescence, through G1, and into S phase that involves the activation of G1 cyclin-dependent kinases, and accumulation of transcription factor activity. Diets containing vitamin E are among the protective agent in varies of cancer including prostate cancer and their effects thought to be at the shifting the balance between proliferation and apoptosis. Human prostate adenocarcinoma cell line (PC3) and benign prostate Human (BPH-1) cell lines were used to determine the effect of Vitamin E succinate (VES) on proliferation (by both growth curve and measuring metabolism of soluble tetrazolium compound), cell death, and cell cycle markers. The cells were incubated with and without VES (20 $\mu$ g/ml) for 24, 48 and 72 hours. Afterwards, cells were fixed and stained with propidium iodide for flow cytometry analysis. In parallel experiments, total protein was extracted from cells and analyzed by western blot for the expression of cyclin E. Cell death was evaluated by trypan blue exclusion dye. Overexpression of cyclin E, proliferation rate, and cell death were seen in the VES treated samples in a time dependent manner in BPH-1. PC3 and BPH-1 cell death were significantly increased at 6% and 26% compare to controls respectively. At 72 hours the number of BPH-1 and PC3 cells in G0-G1 phase increased by 17% & 9% after treatment with VES respectively. The number of BPH-1 cells in S phase at 72 hr decreased by 11% after treatment with VES. At the same time points the changes in cell cycle phases in PC3 were not statistically significant. The number of BPH-1 cell death in the treated samples were increased from two fold to seven fold through 72 hr. Our data suggest that VES exposure directly induces cell arrest in BPH-1 cells possibly through a G1 cell cycle regulator cyclin E, that might play an important role in apoptosis. The effect of VES on PC3 cell cycle, cell proliferation and cell death was less than the benign prostate cell line. This differential regulation might be due to the differentiation level of the two cell lines. The role of diet specially the vitamins such as VES as a chemopreventive agent may be important in altering the cell cycle pathway and proliferation rate. More study is needed to identify the signal transduction factors responsible for the changes included by VES.

**#695 A prospective trial of continuous hyperthermic peritoneal perfusion (CHPP) with MMC in patients with advanced gastrointestinal cancers.** Qing Sanhua, Zhang Gangqin, Qi Delin. *Department of General Surgery, Nan Fang Hospital, The First Military Medical University, Guangzhou 510515, P.R. China.*

Aims to study the pharmacokinetic rationality and efficacy of CHPP preventing postoperative implanted peritoneal recurrence and metastasis of advanced gastrointestinal carcinomas. Methods NK-1 hyperthermic perfusion chemotherapy apparatus was designed, and 25 patients with advanced gastrointestinal cancers were treated by operation combined with voluminous irrigating of CHPP with MMC, compared with twenty five patients treated alone by operation as control. Results CHPP was well tolerated, no serious side effect on respiratory and cardiovascular system during CHPP. Serious hematologic, hepatic and renal complications were not observed. The pharmacokinetic study showed that concentration of MMC in peritoneal fluid was 1.7 and 4.3 times than that in portal vein and center vein respectively. The concentration in portal vein was 2.7 times than that in center vein, the concentration in center vein was the lowest. 16% patients in CHPP group ( $p < 0.05$ ) and 36% cases in control group occurred peritoneal recurrence and metastasis postoperative 3 years. 3-year survival rate was 88% in CHPP group ( $p > 0.05$ ), 76% in control group, there was no significant difference between CHPP and control groups in 3-year survival rates. Conclusion CHPP is a reasonable and effective adjuvant method for preventing postoperative peritoneal recurrence and metastasis in patients with advanced gastrointestinal cancers.



**PLENARY SESSION 3: CHEMISTRY: GENERATION OF DIVERSITY**

Combinatorial approaches to targeting tumor-specific gene sequences. Sugiyama,<sup>1</sup> H., Tao,<sup>1</sup> Z-F., Fujiwara,<sup>1</sup> T., and Saito,<sup>2</sup> I. <sup>1</sup>Tokyo Medical and Dental University, Tokyo, Japan. <sup>2</sup>Kyoto University, CREST, Kyoto, Japan.

Sequence-specific DNA alkylation has significant potential for use in molecular biology and human medicine. Minor-groove binding polyamides that contain *N*-methylimidazole (Im)-*N*-methylpyrrole (Py)-hydroxylpyrrole (Hp), which uniquely recognize each of the four Watson-Crick base pairs, are potential as novel recognition parts of sequence-specific DNA alkylating agents. Recently, we demonstrated that hybrid molecules between segment A of duocarmycin A and Py-Im diamides alkylate a predetermined sequence in the presence of distamycin A. More recently, the alkylation of predetermined 7-base pair sequences has been achieved by analogous derivatives bearing six-ring Py-Im hairpin polyamides. Double-strand alkylation at a predetermined DNA sequence is expected to have a stronger biological activity, however, our previous conjugates alkylate only one strand of the DNA helix with moderate efficiency. In this presentation, we describe a novel type of sequence-specific double-strand alkylation mediated by highly cooperative homodimer formation of a polyamide conjugate even at sub picomolar concentration of the agents. Solid-phase synthesis of this type of alkylating agents which is applicable to combinatorial approaches to targeting specific cancer cell will be presented.

**PLENARY SESSION 4: BIOLOGY AND TARGET SELECTION II**

Discovery of new targets for prostate cancer immunotherapy by EST database analysis. Pastan, I., Vasmatzis, G., Essand, M., Olsson, P., Liu, X.F., Iavarone, C., Ailey, B., Duray, P., Bera, T., and Lee, B. *Laboratory of Molecular Biology, Division of Basic Sciences, National Cancer Institute, National Institute of Health, Bethesda, MD, 20892, USA; Laboratory of Pathology, Division of Clinical Sciences, NCI, NIH, Bethesda, MD, 20892, USA.*

Antibodies targeting differentiation antigens on leukemias and lymphomas have shown great promise in the therapy of these malignancies. Also vaccines targeting differentiation antigens expressed on melanocytes and melanomas have shown clinical activity. One important feature of these antibodies and vaccines is that they do not react with antigens on essential normal tissues so that the side effects are greatly reduced. Our goal is to find differentiation antigens on non-essential normal organs (prostate, breast, ovary, uterus) that are also expressed on cancers arising in these organs, but not on essential normal organs or tissues. Most previous attempts to identify such antigens have utilized cell lines as immunogens. One difficulty with this approach is that cell lines derived from epithelial cancers usually lose expression of differentiation antigens.

In an alternative approach to the identification of such antigens, we have utilized the human EST database which currently has over 1.4 million entries. Over 50,000 of these are derived from normal prostate or prostate cancers. Our approach is to identify those ESTs that are expressed in prostate and prostate cancers and are not expressed in essential normal tissues, e.g. brain, liver, kidney, lung, etc. We do not exclude ESTs that are expressed in non-essential normal tissues: breast, ovary, placenta, testes, mature lymphocytes, etc.

After the ESTs are grouped into clusters containing identical DNA sequences, those with the desired organ specificity are identified. As expected, the cluster with the largest number of ESTs is prostate specific antigen (PSA) and human kilikrin-2, followed by prostate-specific plasma protein and semenogelin (1). These four genes are known to be highly expressed in prostate and finding them by this method validates the method. Many other prostate-specific clusters have been identified and their specificity was analyzed by experimental techniques such as multi-tissue dot blots, Northern blots and *in situ* hybridization (1).

Two new prostate specific RNA transcripts have been characterized. One is a new member of the GAGE/MAGE family termed PAGE 4 (2, 3). It is specifically expressed in normal prostate and prostate cancer, as well as in uterus and uterine cancer. The second is a truncated form of the T cell receptor gamma chain (TCR $\gamma$ ) which originates from an unrearranged TCR $\gamma$  locus, and it is initiated within the intronic sequence directly upstream of the J $\gamma$ 1.2 gene segment. The prostate-specific TCR $\gamma$  transcript consists of the J $\gamma$ 1.2 and C $\gamma$ 1 (exon I, II, III) gene segments (4). Several other prostate specific transcripts are under investigation.

Cell surface antigens discovered by this method could be targets for antibody or vaccine based therapies whereas an intracellular antigen would be used for vaccine based therapies.

**References**

- Vasmatzis, G., Essand, M., Brinkmann, U., Lee, B., and Pastan, I. Discovery of three genes specifically expressed in human prostate by expressed sequence tag database analysis. *Proc. Natl. Acad. Sci. USA.* 300-304, 1998.
- Brinkmann, U., Vasmatzis, G., Lee, B., Yerushalmi, N., Essand, M., and Pastan, I. PAGE-1, an X-linked GAGE like gene that is expressed in normal and neoplastic prostate, testis and uterus. *Proc. Natl. Acad. Sci. USA.* 95: 10757-10762, 1998.
- Brinkmann, U., Vasmatzis, G., Lee, B., and Pastan, I. Novel genes in the PAGE and GAGE family of tumor antigens found by homology walking in EST database. *Cancer Res.* 59: 1445-1448, 1999.

- Essand, M., Vasmatzis, G., Brinkmann, U., Duray, P., Lee, B., and Pastan, I. High expression of a specific T-cell receptor  $\gamma$  transcript in epithelial cells of the prostate. *Proc. Natl. Acad. Sci. USA.* 96: 9287-9292, 1999.

**PLENARY SESSION 5: PRECLINICAL DEVELOPMENT**

The use of transgenic mice in the development of farnesyltransferase inhibitors. Kohl, N.E., Anthony, N.J., Conner, M.W., Chen, H.Y., deSolms, S.J., Gibbs, J.B., Graham, S.L., Hartman, G.D., Koblan, K.S., Omer, C.A., Pollicer, A., Windle, J.J., and Oliff, A. *Departments of Cancer Research, Medicinal Chemistry, Safety Assessment and Biochemistry and Physiology, Merck Research Laboratories, West Point, PA 19486 and Rahway, NJ 07065; New York University Medical Center, N.Y., NY 10016; Cancer Therapy and Research Center, San Antonio, TX 78229.*

Since the identification of farnesyl-protein transferase (FPTase) activity in mammalian cells, there has been an intense effort to develop inhibitors of this housekeeping enzyme for use as potential, novel anti-cancer agents. The focus of the FPTase inhibitor (FTI) studies has been inhibition of the transforming activity of the Ras oncoproteins. Three *ras* genes, Ha-, N-, Ki-*ras*, encode four highly homologous, 21 kD proteins, Ha-, N-, K14A- and K14B-Ras (K14A- and K14B-Ras are encoded by splice variants of the Ki-*ras* gene)—that function in the transduction of growth promoting signals from the membrane to the nucleus. Mutated forms of the *ras* genes which encode constitutively active proteins are found in approximately 20% of all human cancers including 90% of pancreatic tumors and 50% of colon tumors.

Ras is synthesized as a biologically inactive, cytosolic protein that localizes to the inner surface of the plasma membrane where it acquires biological activity following a series of post-translational modifications (1). The first and obligatory step in this series is the transfer of a 15-carbon farnesyl isoprenoid from farnesyl diphosphate to the sulfur atom of the cysteine residue located four amino acids from the carboxyl terminus of the protein. This cysteine residue is part of the CA<sub>1</sub>A<sub>2</sub>X motif found in all FPTase protein substrates, where C is cysteine, A<sub>1</sub> and A<sub>2</sub> are usually aliphatic amino acids and X is usually serine, methionine, glutamine, alanine or cysteine. The demonstration that farnesylation is essential for the transforming ability of the Ras oncoproteins has spurred the development of inhibitors of the enzyme that catalyzes this reaction, FPTase, as anti-cancer agents.

Several methods have been used to identify small molecule inhibitors of FPTase, including random screening of defined chemicals, natural products and combinatorial libraries; and rational design based on the isoprenoid and protein substrates of the farnesylation reaction. For our *in vitro* and *in vivo* biology studies, we have used the CA<sub>1</sub>A<sub>2</sub>X peptidomimetic L-744,832. L-744,832 is the isopropyl ester prodrug of L-739,750, a potent inhibitor of FPTase activity (IC<sub>50</sub> = 1.8 nM) which shows > 1000-fold selectivity for FPTase relative to the related prenyltransferase geranylgeranyl-protein transferase (GGPTase) type I. In cell culture, L-744,832 inhibits the post-translational processing of Ha-Ras with an IC<sub>50</sub> between 0.1 and 1  $\mu$ M and blocks the anchorage independent growth of *ras*-transformed cells at a minimal inhibitory concentration of 1  $\mu$ M. Furthermore, daily subcutaneous administration of this compound to nude mice harboring Ha-*ras*-dependent tumor xenografts reproducibly inhibited tumor growth by 92% compared with vehicle-treated controls.

We have focused on *ras* transgenic mice as the preferred model for evaluation of the *in vivo* efficacy of FTIs. MMTV-*v*-Ha-*ras* oncogene harbor an activated Ha-*ras* gene under the control of the mouse mammary tumor virus promoter/enhancer and spontaneously develop mammary and salivary carcinomas. L-744,832 induced dramatic regression of these tumors in a dose-dependent manner (2). This tumor regression could be attributed entirely to increased levels of apoptosis. p53 was not required for the L-744,832-induced effects since MMTV-*v*-Ha-*ras*/p53 mice, which lack a functional p53, exhibited tumor regression and increased levels of apoptosis following treatment with L-744,832 (3). Continuous administration of L-744,832 to the MMTV-*v*-Ha-*ras* mice was required to maintain tumor regression: following cessation of treatment, tumors reappeared. However, most of these tumors regressed upon retreatment.

The MMTV-*v*-Ha-*ras* mice were interbred with MMTV-*c-myc* mice to determine whether *ras/myc* tumors, which possess high levels of spontaneous apoptosis, have the potential to regress through a further increase in apoptosis levels. The *ras/myc* tumors were found to respond nearly as efficiently to L-744,832 treatment as the MMTV-*v*-Ha-*ras* tumors, although no induction of apoptosis was observed. Rather, the tumor regression in the *ras/myc* mice was found to be mediated by a large reduction in the S-phase fraction. In contrast, treatment of transgenic mice harboring an activated MMTV-*v*-*neu* gene did not result in tumor regression.

Recent studies have established that prenylation of the different Ras proteins is more complex than originally realized. Eukaryotic cells contain a related prenyl protein transferase, GGPTase-I, which transfers the 20 carbon geranylgeranyl isoprenoid to the C-terminal cysteine of CA<sub>1</sub>A<sub>2</sub>X-containing proteins which terminate in leucine or, to a lesser extent, in phenylalanine or methionine. *In vivo*, the Ras proteins are normally farnesylated, but when FPTase activity is ablated, as upon treatment of cells with a FTI, Ki- and N-Ras, but not Ha-Ras, become geranylgeranylated. The geranylgeranylated forms of Ki- and N-Ras remain associated with the cellular membrane fraction. Furthermore, forms of oncogenic Ha-Ras and Ki-Ras engineered to be substrates for GGPTase-I by modification of the CA<sub>1</sub>A<sub>2</sub>X motif retain the ability to transform rodent fibroblasts.

In light of this biochemical "cross-prenylation" and since Ki- and N-*ras* are the most frequently mutated *ras* genes in human cancers, we evaluated the efficacy of L-744,832 in strains of transgenic mice that develop mammary tumors due to either overexpression of wild type N-Ras (4) or to expression of mutated human

Ki-Ras. While L-744,832 significantly reduced the growth rate of the mammary tumors in both of these strains of mice, the effect of the compound was less dramatic than that seen in the MMTV-v-Ha-ras mice. Notably, the anti-tumor efficacy was achieved in the absence of gross or microscopic toxicity. FPTase activity was inhibited in tumors from the treated mice as evidenced by the presence of the unprocessed form of a protein exclusively modified by FPTase. In contrast, little (N-Ras) or no (Ki-Ras) unprocessed transgene-encoded Ras protein was detected in tumors from the treated mice. These results suggest that the Ras proteins may not be the sole farnesylated proteins mediating the biological effects of the FTI in MMTV-N-ras and MMTV-Ki-ras transgenic mice.

#### References

- Zhang, F.L., and Casey, P.J. Protein prenylation: molecular mechanisms and functional consequences. *Ann. Rev. Biochem.* 65: 241-269, 1996.
- Kohl, N.E., Omer, C.A., Conner, M.W., Anthony, N.J., Davide, J.P., deSolms, S.J., Giuliani, E.A., Gomez, R.P., Graham, S.L., Hamilton, K., Handt, L.K., Hartman, G.D., Koblan, K.S., Kral, A.M., Miller, P.J., Mosser, S.D., O'Neill, T.J., Rands, E., Schaber, M.D., Gibbs, J.B., and Oliff, A. Inhibition of farnesyltransferase induces regression of mammary and salivary carcinomas in ras transgenic mice. *Nature Med.* 1: 792-797, 1995.
- Barrington, R.E., Subler, M.A., Rands, E., Omer, C.A., Miller, P.J., Hundley, J.E., Koester, S.K., Troyer, D.A., Bearss, D.J., Conner, M.W., Gibbs, J.B., Hamilton, K., Koblan, K.S., Mosser, S.D., O'Neill, T.J., Schaber, M.D., Senderak, E.T., Wandle, J.J., Oliff, A., and Kohl, N.E. A farnesyltransferase inhibitor induces tumor regression in transgenic mice harboring multiple oncogenic mutations by mediating alteration in both cell cycle control and apoptosis. *Mol. Cell. Biol.* 18: 85-92, 1998.
- Mangues, R., Corral, F., Kohl, N.E., Symmans, W.F., Lu, S., Malumbres, M., Gibbs, J.B., Oliff, A., and Pellicer, A. Antitumor effect of a farnesyl transferase inhibitor in mammary and lymphoid tumors overexpressing N-ras in transgenic mice. *Cancer Res.* 58: 1253-1259, 1998.

**Target-directed *in vitro* and *in vivo* testing procedures for the discovery of anticancer agents.** Fiebig, H.H., and Burger, A.M. *Tumor Biology Center at the University of Freiburg, Freiburg D-79106, Germany.*

The present strategy for the discovery of new anticancer agents is based on broad *in vitro* testings either against a panel of human cell lines or against isolated molecular targets in a high throughput setting. The broadest cellular screen has been developed by the US National Cancer Institute in which more than 10,000 compounds per year are being tested against a panel of 60 human cell lines in a short term assay. The cell lines include 3-8 models from a total of 8 different tumor types [1].

Testings have been carried out for 8 years. The program has identified about 12 compounds which are in clinical trial or under development now. This relatively low outcome may be due to the fact that the cell lines were cultured for many years resulting in very fast growing subpopulations which became undifferentiated or poorly differentiated as determined by their growth *in vivo* in nude mice and which are relatively resistant against standard agents except alkylating agents.

As a consequence the pharmaceutical industry is focusing today on high throughput screens against isolated molecular targets. With modern processing elements including robots complete compound libraries including several 100,000 of compounds can be screened within weeks. The drawback of this concept is that it is not clear if a new compound can cross cell and nuclear membranes, if the target has any relevance for growth inhibition and if there is any selectivity towards cancer compared to normal cells.

In order to overcome these limitations my group has pursued 2 strategies. For a primary cellular screen we use 12 slowly growing moderately and well differentiated cell lines in a monolayer assay using 4 to 6 days drug incubation time. The permanent cell lines were developed from xenografts whose characteristics are quite similar to the tumors in the clinic. For secondary screening human tumor xenografts from nude mice are being tested *in vitro* in the clonogenic assay [2]. This assay has demonstrated a high correlation of drug response compared to the clinic. For follow-up studies *in vivo* investigations in preselected models are of crucial importance to demonstrate a selectivity against tumors in comparison to the most sensitive normal tissue. In this respect, human tumor xenografts are considered as the most relevant models since the patients' tumors are growing as a solid tumor, they develop a stroma, vasculature, a central necrosis and show more or less differentiation. The response to standard agents of nude mouse grown tumors in comparison to patient tumors was very similar, 90% (19/21) in sensitive and 97% (57/59) in resistant tumors respectively. This high correct predictivity validates the xenograft system for drug development.

From over 1500 patient tumors we have established more than 350 human tumors in serial passage which are frozen in liquid nitrogen. The percentage of tumors established in serial passage was highest with 40-60% for cancers of the esophagus, cervix and corpus uteri, colon and small cell lung cancers and melanomas; 20-39% for cancers of the lung (NSCLC), soft tissue sarcomas, ovary, head and neck, pancreas, testicle, pleuramesothelias, stomach, and bladder, and low (5-19%) for cancers of the kidney, breast and prostate.

60 models were characterized in detail for the sensitivity against standard agents as well as expression of potential molecular targets such as oncogenes, growth factor receptors and resistance associated proteins.

Using these combined *in vitro* and *in vivo* testing procedures a number of novel compounds were identified as active. Agents which are in clinical trial include the

methotrexate coupled chemically to human serum albumin (MTX-HSA), NOAC a liposomal fatty acid derivative of Ara-C, flavopiridol, quinoxaline, spicamycin, ecteinascidin, rhizoxin, EO9. Compounds under development include a geldanamycin analog, and cyanocyclin A [3, 4].

The recently established primary cellular screen with a 12 slowly growing cell line panel is now being used to investigate libraries of natural products for anticancer activity. With the long drug incubation time of 4-6 days equal to 2 cell doublings, 9 out of 10 clinically established anticancer agents were identified as active. On the contrary, 35 antibiotics, 4 immunomodulators, and 8 cardiaacs were inactive. Thus, this testing strategy will allow us to identify rapidly new lead structures from natural sources.

#### References

- Grever, M.R., Schepartz, S.A., Chabner, B.A. The National Cancer Institute: Cancer drug discovery and development program. *Semin. Oncol.* 19: 622-638, 1992.
- Fiebig, H.H., Berger, D.P., Dangler, W.A., Wallbrecher, E., Winterhalter, B.R. Combined *in vitro/in vivo* test procedure with human tumor xenografts. In: Fiebig, H.H., Berger, D.P. (eds). *Immunodeficient Mice in Oncology*. Karger, Basel, Contrib. Oncol. 42: 321-351, 1992.
- Drees, M., Dengler, W., Roth, T., Labonte, H., Mayo, J., Malspeis, L., Grever, M., Sausville, E., Fiebig, H.H. Flavopiridol (L86-8275): Selective antitumor activity *in vitro* and *in vivo* for prostate carcinoma cells. *Clin. Cancer Res.* 3: 273-279, 1997.
- Burger, A.M., Fiebig, H.H., Newmann, D.J., Camalier, R.F., Sausville, E.A. Antitumor activity of 17-allylamino-geldanamycin (NSC 330507) in melanoma xenografts is associated with decline in Hsp90 protein expression. *Ann. Oncol. Suppl* 2: 132, 1998.

### PLENARY SESSION 6: IMAGING MOLECULAR TARGETS

**The role of magnetic resonance in the evaluation of cancer therapeutics.** Ross, B.D., Slegman, L.D., Chenevert, T.L., and Rechenulla, A. *University of Michigan School of Medicine, Departments of Radiology, Biological Chemistry and Radiation Oncology, Ann Arbor, MI 48109-0648, USA.*

The capabilities of magnetic resonance imaging (MRI) and spectroscopy (MRS) for the study of animal and human tumors has benefited greatly from advances in both hardware and software. These advances provide exciting opportunities to investigate anatomic, cellular and molecular events using MR methodologies. These opportunities can provide new insights into established, traditional tumor models and into new cancer models as well. Additionally, these advances can be applied to emerging therapeutic modalities such as gene therapy and can bridge the gap between gene delivery, quantitative monitoring of gene expression and correlating transgene expression with therapeutic outcomes.

An overview of the results that have been obtained using MRI/S for studying the rat 9L brain tumor model (1), which has been well characterized over the used for the past 35 years, will be given. We have shown that serial images of intracerebral tumors using MRI over time following therapeutic intervention can be used to quantitate cell kill *in vivo* (2). These studies revealed that the increases in animal survival elicited by BCNU chemotherapy are not solely attributable to the fraction of tumor cells killed but rather are a function of cell kill and altered tumor cell repopulation kinetics, both of which are proportional to treatment dose. The previous explanation for the effectiveness of BCNU chemotherapy in this orthotopic model based on the results of studies using traditional methods such as *ex vivo* colony forming assays overestimated the role of cell killing.

Methods allowing earlier and more accurate quantitation of therapeutic response in individual patients are still needed. Because diffusion MRI is sensitive to tissue structure at the cellular level, we believe that this technique has the potential to detect important quantitative information about tumor cellular changes that would occur following successful therapeutic intervention. Cellularity and the integrity of cell membranes which impede water translational mobility will affect the diffusion of water within the tumor tissue. We have used diffusion MRI to quantitate changes in the diffusion of water within tumor tissue following therapeutic intervention. These studies have revealed that cellular changes occur very early following therapeutic intervention and can be detected prior to tumor regression using diffusion-weighted MRI (3). In addition, treatment of an intracerebral 9L tumor in the rat with a single systemic dose of chemotherapy resulting in as little as 0.2 log kill can be detected by diffusion MRI. This has important ramifications considering that most patients are treated with fractionated doses of antineoplastic agents or radiation. The use of diffusion MRI may provide an important clinical opportunity for individualizing and modifying therapeutic protocols during the course of treatment.

The ability of MRS to distinguish signals from chemically distinct compounds offers the potential to measure the expression of transgenes encoding enzymes that catalyze therapeutic reactions. The use of MRI/S for quantitative noninvasive evaluation of expression of a therapeutic transgene in experimental tumors has been recently accomplished (4). Stable tumor cell lines expressing the cDNA encoding for cytosine deaminase from yeast (yCD) were grown in animals. Conversion of the nontoxic prodrug 5-fluorocytosine (5FC) to the antimetabolite 5-fluorouracil (5FU) by yCD could be observed and quantitated *in vivo* using <sup>19</sup>F MRS (4). The subsequent conversion 5FU to fluorinated nucleotides could also be observed and measured. This study demonstrated local conversion of 5FC, validating the concept of localizing chemotherapy with enzyme-prodrug gene therapy.



It also revealed kinetic information about the rate-limiting steps in the production of cytotoxic metabolites, providing new directions for optimizing yCD gene therapy.

In conclusion, the use of noninvasive imaging modalities for quantitation of therapeutic outcome, gene delivery and monitoring of cellular events is emerging as an important approach for translating findings from the lab into animal and humans. It is anticipated that advances made through interactions between scientists and machines will translate into benefits for both basic science and patient care.

#### References

- Rosenblum, M.L., Knebel, K.D., Vasquez, D.A., and Wilson, C.B. Brain-tumor therapy: quantitative analysis using a model system. *J. Neurosurg.* 46: 145-154, 1977.
- Ross, B.D., Zhao, Y.J., Neal, E.R., Stegman, L.D., Ercolani, M., Ben-Yoseph, O., and Chenevert, T.L. Contributions of cell kill and posttreatment tumor growth rates to the repopulation of intracerebral 9L tumors after chemotherapy: An MRI study. *Proc. Natl. Acad. Sci. USA.* 95: 7012-7017, 1998.
- Chenevert, T.L., McKeever, P.E., and Ross, B.D. Monitoring early response of experimental brain tumors to therapy using diffusion magnetic resonance imaging. *Clin. Cancer Res.* 3: 1457-1466, 1997.
- Stegman, L.D., Rehemtulla, A., Beattie, B., Kievit, E., Lawrence, T.S., Blasberg, R.G., Tjuvajev, J.G., and Ross, B.D. Noninvasive quantitation of cytosine deaminase transgene expression in human tumor xenografts with *in vivo* magnetic resonance spectroscopy. *Proc. Natl. Acad. Sci. USA.* 96: 9821-9826, 1999.

**Antisense Imaging.** Hnatowich, D.J. *University of Massachusetts Medical School, Worcester, MA 01655, U.S.A.*

Antisense chemotherapy may be defined as the treatment of disease with oligonucleotide drugs designed to interfere with the expression of a gene integral to the etiology of the disease. Although uncertainties concerning the mechanism of action of these drugs continue (1), efficacy is now being demonstrated in several on-going clinical trials. Last year, the US Food and Drug Administration approved for marketing the first antisense drug and the likelihood is that other antisense drugs now in clinical trials may eventually also enjoy approval. This presentation is intended to examine the question of whether antisense targeting can now be extended sensibly to antisense imaging in nuclear medicine (2).

The development of antisense chemotherapy to this point has taken several decades and, by one estimate, at least half a billion US dollars (Crooke S.T., private communication, 1999). Along the way, improvements in antisense chemotherapy have occurred which fortunately will be beneficial to the development of antisense imaging in respect to those aspects common to both. For one example, literally thousands of chemically modified oligonucleotides have been synthesized and tested in a search for second and third generation antisense drugs with improved cell membrane transport, stability to nucleases and with slower pharmacokinetics (in part to obviate the need for multiple administrations). As another example, for each mRNA target of interest, many antisense oligonucleotides of different base sequences have been tested to identify those with superior potency for chemotherapy. The requirements of antisense imaging overlap such that oligonucleotides with improved cell membrane transport and stability to nucleases should be of universal value. Likewise, base sequences with chemotherapeutic benefit may be useful for imaging as well.

The overlap between chemotherapy and imaging, however, is not perfect. For example, antisense imaging will probably benefit more from the use of oligonucleotides displaying rapid rather than slow tissue and whole body pharmacokinetics. Also, it conceivably could be preferable for imaging to select oligonucleotides with no potency for therapy. Furthermore, the mRNAs which are of interest as targets for antisense chemotherapy are not always those which are of interest for antisense imaging. While targeting the *c-myc* or *P53* mRNAs in connection with chemotherapy is obviously of interest for tumor imaging as well, not nearly so obvious is whether an imaging potential exists for the antisense oligonucleotides developed as treatments of retinitis or allergies. Conversely, it is questionable whether antisense chemotherapy against mRNAs expressed in connection with certain normal cellular functions will ever be of interest while radiopharmaceuticals capable of imaging normal cellular function could be very useful indeed.

One aspect in particular of antisense imaging contrasts with antisense chemotherapy—namely the need in the former case to radiolabel the oligonucleotide with an imagerable radionuclide. It is the fate of the radionuclide which is the primary concern of imaging in contrast to chemotherapy where the concern is the fate of the oligonucleotide. Whereas an antisense chemotherapy drug may have its specific action at the target site, the antisense imaging agent must show specific localization therein (to achieve an acceptable target/nontarget radioactivity ratio). Antisense imaging therefore requires methods of attaching radionuclides such that the label does not interfere with oligonucleotide cell membrane transport, hybridization and clearance. Methods of stably radiolabeling oligonucleotides with radionuclides are available and, in some cases, have been for years, but the influences of labeling method on transport and hybridization are only now receiving attention. Recently a new concern regarding radiolabeling has emerged which is related to the number of target mRNAs present in each target cell. In addition to a sufficiently high target/nontarget ratio, detection by imaging also requires sufficiently high radioactivity accumulation in the target. Recent reports using absolute methods of mRNA quantitation are showing only modest numbers of

target mRNAs per cell (3). If these small numbers of target mRNAs prove to be universal for most target cells, this will place a burden on the radiochemist to increase the specific radioactivity of antisense oligonucleotides radiolabeled for imaging.

At present it is not possible to predict whether antisense imaging will eventually become a useful modality in nuclear medicine. An answer should become available within several years if the interest which is now being expressed in antisense imaging persists. Should the most optimistic forecasts prove correct and it does become possible, to target virtually any diseased or normal tissue with a unique genetic component, this would truly revolutionize nuclear medicine imaging and, probably, radiotherapy as well.

#### References

- Stein, C.A. Does antisense exist? *Nature Medicine* 7: 1119-1121, 1995.
- Hnatowich, D.J. Antisense and nuclear medicine. *J. Nucl. Med.* 40: 693-703, 1999.
- Martorana, A.M., Zheng, G., Springall, F., Iland, H.J., O'Grady, R.L., Lyons, J.G. Absolute quantitation of specific mRNA in cell and tissue samples by comparative PCR. *BioTechniques*, 27: 136-144, 1999.

**Cancer Research Campaign's (CRC) program of *in vivo* pharmacokinetics and pharmacodynamics in drug development using positron emission tomography.** Aboagye, E.O. *CRC PET Research group, MRC Cyclotron Unit, Hammersmith Hospital, London, UK.*

Positron Emission Tomography (PET) is a sensitive and specific technique for studying molecular interactions non-invasively in man. A programme created in the UK between the CRC Phase III committee and the Medical Research Council (MRC) Cyclotron Unit has investigated the potential of PET in *in vivo* pharmacokinetics and pharmacodynamics imaging.

**Pharmacokinetics:** PET may be useful in providing intra-tumour and normal tissue uptake/distribution of compounds when used in a pre-phase I setting as was the case for the CRC study of [<sup>11</sup>C]-N-[2-(dimethylamino)ethyl]acridine-4-carboxamide, [<sup>11</sup>C]DACA [2, 3]. Pre-phase I studies of DACA could be performed at a dose of one-thousandth the Phase I starting dose. Total exposure (AUC) of tracer was variable in tumours and correlated with tumour blood flow measured by <sup>15</sup>H<sub>2</sub>O. Uptake of tracer was observed in brain and relatively high levels of activity were observed in heart (mainly myocardium). Of interest, cardiotoxicity was observed in phase I trials of this drug. Another tracer that has been extensively studied is 5-[<sup>18</sup>F]fluorouracil [4]. Recently, pharmacokinetic modulation of 5-fluorouracil by eniluracil, aimed at increasing systemic exposure by inhibiting the catabolic enzyme dihydropyrimidine dehydrogenase (DPD), has been studied by PET [5]. Proof of principle of mechanism of action of eniluracil was demonstrated in normal liver (organ with highest DPD levels), and tumour pharmacokinetics suggested an increased exposure of 5-fluorouracil following eniluracil treatment [5]. The tissue pharmacokinetics of [<sup>11</sup>C]temozolomide has also been studied. Of interest, the tracer showed significant uptake in high-grade gliomas compared to contralateral normal brain probably due to a compromised blood brain barrier in the tumours, and uptake of [<sup>11</sup>C]temozolomide into tumours was related to response duration.

**Pharmacodynamics:** Several radiotracers have been designed and synthesised for imaging pharmacodynamics by PET. The most widely used of these is [<sup>18</sup>F]fluorodeoxyglucose (FDG) which measures glucose transport and phosphorylation. Changes in tumour FDG after the first cycle of chemotherapy appears to provide an index of fractional cell kill. FDG-PET studies aimed at detecting sub-clinical efficacy are currently being performed alongside Phase I clinical trials. The provision of uniform guidelines by the EORTC-PET group for imaging tumour response represents an important milestone in the use of this probe [6]. Another probe of interest is 2-[<sup>11</sup>C]thymidine, which can be used to estimate the proliferation rate of tumours. Validation studies from our group have shown a strong correlation between 2-[<sup>11</sup>C]thymidine retention and MIB-1 antigen levels in gastrointestinal tumours. The same probe (different biological window) has also been used to measure thymidine salvage following thymidylate synthase inhibition by the non-classical TS inhibitor AG337. Enhancement of thymidine salvage was demonstrated as an increase in fractional retention of 2-[<sup>11</sup>C]thymidine in gastrointestinal tumours. For a large number of novel therapeutic agents, studies to confirm the proposed mechanisms of action *in vivo* in patients are of utmost importance in their development. In this regard, the pro-drug temozolomide has been labelled on two different functional groups (N-methyl and carbonyl) with carbon-11 to measure the extent of ring opening to reactive intermediates, which alkylate DNA. In addition, PET studies of tumour blood flow are being performed alongside Phase I clinical trials of the antivascular agent, combretastatin.

It is envisaged that these technological developments will enable both targeted and non-targeted therapies to be efficiently evaluated *in vivo* to ensure rapid transition of novel therapies from the laboratory to the bedside.

#### References

- Gelman, K.A., Eisenhauer, E.A., Haris, A.L., Ratain, M.J. and Workman, P. Anticancer agents targeting signaling molecules and cancer cell environment: challenges for drug development? *J. Natl. Cancer Inst.*, 91: 1281-1287, 1999.
- Osman, S., Luthra, S.K., Brady, F., Hume, S.P., Brown, G., Harle, R.J.A., Matthews, J.C., Denny, W.A., Baguley, B.C., Jones, T., and Price, P.M. Studies on the metabolism of the antitumour agent *N*-methyl-<sup>11</sup>C-N-[2-(dimethylamino)ethyl]acridine-4-carboxamide, (<sup>11</sup>C) DACA in rat and in

- man prior to phase I clinical trials. *Cancer Res.*, 57: 2172-2180, 1997.
- Harte, R.J.A., Matthews, J.C., Flavin, A., Brook, C.S., Osman, S., Luthra, S., Brown, G., Brady, F., Jones, T., Bleehan, N., and Price, P. Pre-phase I tracer kinetic studies in humans can contribute to new drug evaluation. Proc. NCI-BORTC Symposium, p50, #167, 1996.
  - Harte, R.J.A., Matthews, J.C., O'Reilly, S.M., Tilsley, Q.D.W., Osman, S., Brown, G., Luthra, S.J., Brady, F., Jones, T., and Price, P.M. Tumour, normal tissue and plasma pharmacokinetic studies of fluorouracil biomodulation with N-phosphonoacetyl-aspartate, folinic acid, and interferon alfa. *J. Clin. Oncol.*, 17: 1580-1589, 1999.
  - Saleem, A., Yap, J., Aboagye, E.O., Osman, S., Putnell, C., O'Callaghan, M., Lucas, V.S., Price, P.M., and Jones, T. Evaluation of *in vivo* tissue and tumour pharmacokinetics of 5-fluorouracil (5FU) following dihydropyrimidine dehydrogenase inactivation by cafluracil. Proc. Am. Soc. Clin. Oncol., 18: p201a, #773, 1999.
  - Young, H., Baum, R., Cremerius, U., Herholz, K., Lammertsma, A., Hoekstra, O., Prium, J., Price, P. Measurement of clinical and sub-clinical tumour response using 18F fluorodeoxyglucose and positron emission tomography: review of the technique and 1999 BORTC recommendations. *Eur. J. Cancer.* (Accepted for publication), 1999.

This work was supported by the UK Cancer Research Campaign and Medical Research Council.

### PLENARY SESSION 7: NEW OPPORTUNITIES FOR DNA AND MICROTUBULES

The use of photoaffinity labeling methods to characterize the Taxol binding site on the microtubule. Rao, S., He, L., Chakravarty, S., Ojima, I., Orr, G.A., and Horwitz, S.B. Department of Molecular Pharmacology, Albert Einstein College of Medicine, Bronx, NY 10461; and Department of Chemistry, State University of New York at Stony Brook, Stony Brook, NY 11794.

Taxol is an antitumor drug approved for the treatment of ovarian, breast and lung carcinomas. The cellular target for Taxol is the microtubule, specifically  $\beta$ -tubulin. The binding site for the drug is on the microtubule polymer and addition of Taxol to the polymer results in the stabilization of microtubules (1). The maximum effect of Taxol is observed when the drug binds to the microtubule with a stoichiometry, relative to the tubulin heterodimers, approaching one (2,3). When cells are incubated with micromolar concentrations of Taxol, there is a reorganization of the microtubule cytoskeleton with the formation of stable bundles of microtubules (4). The normal assembly/disassembly dynamics of microtubules are disrupted and cells are arrested in the G<sub>2</sub>/M phase of the cell cycle with inhibition of normal cell division.

We have used photoaffinity labeling methods to locate the sites at which Taxol interacts with the microtubule. Direct photolabeling of tubulin with [<sup>3</sup>H]-Taxol resulted in the labeling of  $\beta$ -tubulin (5). Further studies with [<sup>3</sup>H]3'-(p-azidobenzamido)Taxol (where the arylazide was incorporated into the C-13 side chain) resulted in the isolation of a photolabeled peptide containing amino acid residues 1-31 in  $\beta$ -tubulin (6). Studies with [<sup>3</sup>H]2-(m-azidobenzoyl)Taxol (where the photoreactive group is attached to the B ring of the taxoid nucleus) have shown that a peptide containing amino acid residues 217-233 of  $\beta$ -tubulin is involved in Taxol binding (7). In these photoaffinity labeling studies utilizing arylazide-containing analogues, we were never able to define the precise site of photoincorporation. Therefore, we decided to revisit the problem of defining the exact sites of photoincorporation using benzophenone-based photochemistry. [<sup>3</sup>H]7-(benzoyldihydrocinnamoyl)Taxol ([<sup>3</sup>H]7-BzDC-Taxol) was synthesized (8) and used to photolabel microtubules and map the site of photoincorporation into  $\beta$ -tubulin.

Structure-activity relationships of Taxol and its analogues with cytotoxicity and tubulin stabilization have been studied extensively. The evidence indicates that the 7-OH position is not important for Taxol activity since it may be esterified, epimerized or even removed without significant loss of activity (9). However, there are studies indicating that the size of the substituent at this position may influence activity. The presence of the bulky 7-BzDC substituent resulted in a Taxol analogue that, unlike Taxol, could not enhance the polymerization of microtubules, but could, however, stabilize GTP-induced microtubules against depolymerization by cold temperatures. One possible explanation for these results is that the 7-BzDC-Taxol may be able to bind to small oligomers, but the presence of the bulky substituent prevents tubulin dimers from adding to these stabilized nucleation centers.

The use of [<sup>3</sup>H]7-BzDC-Taxol, as a photoaffinity analogue of Taxol, is allowing us to determine the exact site of photoincorporation in the microtubule. Nogales and her collaborators have succeeded, by electron crystallography, in obtaining a model of the  $\alpha$ ,  $\beta$ -tubulin dimer fitted to a 3.7 Å density map (10). This high resolution structure of tubulin was derived from zinc-induced sheets of antiparallel tubulin protofilaments. We find excellent agreement between the binding site of Taxol in  $\beta$ -tubulin as determined by photoaffinity labeling and electron crystallography, thereby strengthening the model presented by Nogales and her co-workers.

#### References

- Schiff, P.B., Fant, J., and Horwitz, S.B. *Nature*, 277: 665-667, 1979.
- Parness, J., and Horwitz, S.B. *J. Cell. Biol.*, 91: 479-487, 1981.
- Diaz, J.F., and Andreu, J.M. *Biochemistry*, 32: 2747-2755, 1993.

- Schiff, P.B., and Horwitz, S.B. *Proc. Natl. Sci. U.S.A.*, 77: 1561-1565, 1980.
- Rao, S., Horwitz, S.B., and Ringel, I. *J. Natl. Cancer Inst.*, 84: 785-788, 1992.
- Rao, S., Krauss, N.E., Heering, J.M., Swindell, C.S., Ringel, I., Orr, G.A., and Horwitz, S.B. *J. Biol. Chem.*, 269: 3132-3134, 1994.
- Rao, S., Orr, G.A., Chaudhary, A.G., Kingston, D.G.I., and Horwitz, S.B. *J. Biol. Chem.*, 270: 20235-20238, 1995.
- Ojima, I., Bounaud, P.-Y., and Ahern, D.G. *Bioorg. Med. Chem. Lett.*, 9: 1189-1194, 1999.
- Kingston, D.G.I. in "Taxane Anticancer Agents, Basic Science and Current Status" (Edited by Georg, G.I., Chen, T.T., Ojima, I., and Vyas, D.M.) pp 203-216, ACS symposium series 583, 1995.
- Nogales, E., Wolf, S.G., and Downing, K.H. *Nature*, 391: 199-203, 1998.

Mode of action of Ecteinascidin-743 (ET-743). D'Incalci, M. Department of Oncology, Istituto di Ricerche Farmacologiche Mario Negri, Milan, 20157, Italy.

Ecteinascidin-743 (ET-743) is a marine tetrahydroisoquinoline alkaloid isolated from *Ecteinascidia Turbinata*, which has shown potent cytotoxicity against human cancer cell lines (1) and striking antitumor activity against human xenografts (2). In phase I studies performed in both Europe and US some objective responses have been seen in patients refractory to the conventional therapies and phase II studies are currently underway. ET-743 alkylates guanines at the N2 position with some degree of sequence specificity (3, 4). In order to get insight into the mechanism of action of ET-743 we have investigated the drug-induced cell cycle perturbation, the cell cycle phase specificity of ET-743 cytotoxicity, its cytotoxicity according to p53 status, the drug induced DNA damage, the alterations of transcription mechanisms and the importance of DNA repair mechanisms for the drug cytotoxicity. All of these experiments have been performed by exposing the cells for a short time (1h) to ET-743 and at drug concentrations in the range of those achieved in plasma of patients receiving the drug during the phase I trial (i.e. the nM range). The main findings can be summarized as follows:

**Cell cycle perturbations:** In the human tumor cell lines examined thus far (i.e. LoVo, SW620, Igrov-1, MOLT-4), ET-743 was found to decrease the rate of progression of S phase cells towards G<sub>2</sub> and caused a prolonged blockade in G<sub>2</sub>-M (5) as assessed by biparametric BrdUrd/DNA flow cytometry.

**Phase Specificity:** SW620 intestinal carcinoma cells synchronized in G<sub>1</sub> by elutriation showed greater sensitivity to ET-743 than S phase cells and much greater sensitivity than cells in G<sub>2</sub>-M phases cells.

**p53 status:** The greatest variation in the cytotoxic potency of ET-743 does not appear to be related to p53 status. This has been verified by comparing ET-743 cytotoxicity in p53 -/- or p53 +/- mouse embryo fibroblasts as well as in A2780 ovarian cancer cell line and p53 Ala 43 transfected subline A2780/CX3. No significant difference in the cytotoxicity of ET-743 was observed according to p53 status. However in cells expressing wild type p53 a rapid increase in the levels of this protein was observed.

**DNA damage:** ET-743 at concentrations up to 10 times higher than its effective range of IC<sub>50</sub> values, caused neither DNA breaks nor DNA-protein cross-links. In a *Saccharomyces cerevisiae* with variant deletion of topoisomerase I gene, ET-743 was as cytotoxic as in control cells expressing topoisomerase I. This suggests that topoisomerase I is not the crucial target responsible for the drug cytotoxicity. This yet does not exclude the possibility that at very high concentrations (in the  $\mu$ M range) ET-743 can poison topoisomerase I (6), but the relevance of this effect appears questionable (7).

**Transcription mechanisms:** Previous work by this laboratory showed that ET-743, at very high concentrations (in the  $\mu$ M range) could inhibit the specific binding of some transcription factors to their consensus DNA sequences (8). Since one of the most sensitive factors appeared to be NFY further experiments have been performed to ascertain if NFY-dependent transcription was impaired in tumor cells. Preliminary results indicate that this is the case using ET-743 concentrations in the nM range. Detailed studies on this point will be presented in the poster session by Mantovani et al. and are in line with results recently shown by Jin et al. (9). Whether this effect is mediated by ET-743 binding to DNA with significant structural DNA changes (10) or a direct interaction of the drug with DNA binding proteins remains to be elucidated.

ET-743 induced changes in gene expression evaluated by microarrays technology will be presented by Brogginì et al. in the poster session.

**DNA repair:** Different cell lines each with different defects in nucleotide excision repair, mismatch repair or DNA dependent protein kinase (DNA-PK) were used to evaluate the relevance of these mechanisms of repair to the cytotoxic effects of ET-743. The results obtained indicate that nucleotide excision repair deficient cells are less sensitive than the control DNA repair proficient cells, a finding that is very surprising considering that the same deficient cells are more susceptible to conventional alkylating agents. Detailed results will be presented by Dantia et al. in the poster session.

The sensitivity to ET-743 did not appear to be influenced by mismatch repair deficiency; whereas, it was increased in cells deficient in DNA-PK.

Taken together the results of these studies provide strong evidence that ET-743 has a mechanism of action different from that of other previously identified anticancer drugs.

The high sensitivity of G<sub>1</sub> cells and the relative resistance of cells exhibiting nucleotide excision repair defects make this DNA interacting drug unique as far as its mechanistic properties.



## References

- Rinchart, K.L., Holt, T.G., Fregau, N.L., Stroth, J.G., Keifer, P.A., Sun, F., Li, L.H., and Martin, D.G. Ecteinascidin 729, 743, 745, 759A, 759B, and 770: Potent antitumor agents from the Caribbean Tunicate *Ecteinascidia turbinata*. *J. Org. Chem.*, 55: 4512-4515, 1990.
- Valoti, G., Nicoletti, M.I., Pellegrino, A., Jimeno, J., Hendriks, H., D'Incalci, M., Faircloth, G., and Giavazzi, R. Ecteinascidin-743 (ET-743), a new marine natural product with potent antitumor activity on human ovarian carcinoma xenografts. *Clin. Cancer Res.*, 4: 1977-1983, 1998.
- Pommier, Y., Kohlhagen, G., Bailly, C., Waring, M., Mazumder, A., and Kohn, K.W. DNA sequence- and structure-selective alkylation of guanine N2 in the DNA minor groove by ecteinascidin 743, a potent antitumor compound from the Caribbean tunicate *Ecteinascidia turbinata*. *Biochemistry*, 35: 13303-13309, 1996.
- Moore, B.M., II, Seaman, F.C., and Hurley, L.H. NMR-based model of an ecteinascidin 743-DNA adduct. *J. Am. Chem. Soc.*, 119: 5475-5476, 1997.
- Ghielmini, M., Colli, E., Erba, E., Bergamaschi, D., Pampallona, S., Jimeno, J., Faircloth, G., and Sessa, C. In vitro schedule-dependency of myelotoxicity and cytotoxicity of Ecteinascidin 743 (ET-743). *Ann. Oncol.*, 9: 989-993, 1998.
- Takebayashi, Y., Pourquier, P., Yoshida, A., Kohlhagen, G., and Pommier, Y. Poisoning of human DNA topoisomerase I by ecteinascidin 743, an anticancer drug that selectively alkylates DNA in the minor groove. *Proc. Natl. Acad. Sci. USA*, 96: 7196-7201, 1999.
- Martinez, E.J., Owa, T., Schreiber, S.L., and Corey, B.J. Phthalascidin, a synthetic antitumor agent with potency and mode of action comparable to ecteinascidin 743. *Proc. Natl. Acad. Sci. USA*, 96: 3496-3501, 1999.
- Bonfanti, M., Caretti, G., La Valle, E., Sousa Faro, J.M.F., Faircloth, G., Mantovani, R., and D'Incalci, M. Effect of Ecteinascidin-743 (ET-743) on the interaction between DNA binding proteins and DNA. *Anti-Cancer Drug Des.*, 14: 179-186, 1999.
- Jin, S., Lin, Y., Magro, P.G., and Scotto, K.W. Repression of MDR1 gene transcription by ecteinascidin 743. *Proceedings of the American Association for Cancer Research*, 40: 314, 1999.
- Zewail-Foote, M., and Hurley, L.H. Ecteinascidin 743: a minor groove alkylator that bends DNA toward the major groove. *J. Med. Chem.*, 42: 2493-2497, 1999.

### PLENARY SESSION 9: CHANGING A CONCEPT INTO A DRUG: THE ART OF PATIENCE

**Farnesyltransferase Inhibition: Use of surrogate markers.** Adjei, A. A., Davis, J. N., Erlichman, C., Svingsen, P. A., and Kaufman, S. H. *Mayo Clinic, Rochester, MN 55905, USA.*

Farnesyltransferase (FT) is an enzyme that catalyzes the first and obligatory step in the posttranslational modification of Ras polypeptides and other G-proteins involved in cell-signaling, including Rac and Rho, as well as several proteins of diverse function such as lamins A and B. This modification enables the proteins to localize to membranes where they function.<sup>1,2</sup> Activating mutations in Ras polypeptides result in constitutive signaling, thereby stimulating cell proliferation.<sup>3</sup> Such mutations have been identified in approximately 30% of human cancers.<sup>4</sup> In addition, oncogenic Ras but not normal Ras transfected into rodent fibroblasts renders them tumorigenic. FT has, therefore, emerged as an important target for the development of anticancer agents. Several FT inhibitors (FTIs), including SCH66336, R115777, L778123 and BMS214662, have entered the clinic over the past 2 years. Because these agents represent a novel class of rationally developed anticancer agents, there is considerable interest in determining whether they interact with their putative target, *in vivo*.

While the FTIs clearly abrogate FT activity, it is unclear whether inhibition of ras farnesylation is responsible for all of the antiproliferative activities of these compounds. Geranylgeranylated forms of K-ras and N-ras, which are themselves capable of transforming cells, are detected in cells treated with FTIs.<sup>5</sup> Despite this alternative prenylation pathway, FTIs inhibit proliferation of K-ras transformed cells *in vitro* and *in vivo*. In addition, several cell types that lack Ras mutations are sensitive to FTIs *in vivo* and *in vitro*.<sup>6</sup> Collectively, these findings argue that inhibition of the farnesylation of other proteins such as rho<sup>7</sup> may also contribute to the observed antitumor properties of these agents.

In principle, any one of the farnesylated intracellular proteins could serve as an indicator for FT inhibition *in vivo*. Our initial attempts to evaluate the inhibition of Ras farnesylation in cultured cells after treatment with an FTI were unsuccessful. Subsequent studies focused on lamin A, a major structural protein of the nuclear envelope. Processing of lamin A involves farnesylation followed by further post-translational modifications.<sup>8-10</sup> When A549 lung cancer cells, HCT-116 colon cancer cells and MCF-7 breast cancer cells were treated with increasing concentrations of the FTI SCH66336 for 24 hours, a slower migrating species of lamin A corresponding to prelamin A was detected. This species was the sole antigen that reacted with antiserum raised against the lamin A prepeptide in our laboratory studies, which were based on a modification of the methods described by Sinensky et al.<sup>11</sup> In subsequent experiments, this serum was utilized to develop a histochemistry-based assay for prelamin A, which was used in clinical samples.

To determine whether FT was inhibited in patients receiving SCH66336, the presence of prelamin A was assessed in buccal mucosa cells using the histochemical assay mentioned above.

The choice of this cell type for study was based on the following: (i) presence of lamin A in these cells but not in circulating lymphocytes,<sup>12</sup> (ii) the relatively rapid turnover of this cell population, and (iii) the ready accessibility of this tissue source. Prior to treatment, none of the buccal smears contained detectable prelamin A. After treatment, however, prelamin A was readily detectable in a subset of the specimens.<sup>13</sup> This study provides the first evidence of successful inhibition of FT in the clinical setting.

## References

- Farnsworth, C. C., Wolda, S. L., Gelb, M. H., Glomset, J. A. Human lamin B contains a farnesylated cysteine residue. *J. Biol. Chem.*, 264: 20422-20429, 1989.
- Sinensky, M., Pantle, K., Trujillo, M. A., et al. The processing pathway of prelamin A. *J. Cell Sci.*, 107: 61-67, 1994.
- Lowy, D. R., Williamson, B. M. Function and regulation of Ras. *Annu. Rev. Biochem.*, 62: 851-891, 1993.
- Bos, J. L. Ras oncogenes in human cancer: A review. *Cancer Res.*, 49: 4682-4689, 1989.
- Whyte, D. B., Kirschmeier, P., Hockenberry, T. N., et al. K- and N-ras are geranylgeranylated in cells treated with farnesyl protein transferase inhibitors. *J. Biol. Chem.*, 272: 14459-14464, 1997.
- Sepp-Lorezino, L., Ma, Z., Rands, E., Kohl, N. E., Gibbs, J. B., Olf, A., Rosen, N. A peptidomimetic inhibitor of farnesyl: protein transferase blocks the anchorage-dependent and -independent growth of human tumor cell lines. *Cancer Res.*, 55: 5302-5309, 1995.
- Lebowitz, P. F., Prendergast, G. C. Non-Ras targets of farnesyltransferase inhibitors: Focus on Rho. *Oncogene*, 17: 1439-1445, 1998.
- Beck, L. A., Hosick, T. J., Sinensky, M. Isoprenylation is required for the processing of the lamin A precursor. *J. Cell Biol.*, 110: 1489-1499, 1990.
- Lutz, R. J., Trujillo, M. A., Denham, K. S., et al. Nucleoplasmic localization of prelamin A: Implications for prenylation-dependent lamin A assembly into the nuclear lamina. *Proc. Natl. Acad. Sci. USA*, 89: 3000-3004, 1992.
- Kilhic, F., Dalton, M. B., Burrell, S. K., et al. In vitro assay and characterization of the farnesylation-dependent prelamin A endoprotease. *J. Biol. Chem.*, 272: 5298-5304, 1997.
- Sinensky, M., Pantle, K., Dalton, M. An antibody which specifically recognizes prelamin A but not mature lamin A: Application to detection of blocks in farnesylation-dependent protein processing. *Cancer Res.*, 54: 3229-3232, 1994.
- Kaufmann, S. H. Additional members of the rat liver lamin polypeptide family: Structural and immunological characterization. *J. Biol. Chem.*, 264: 13946-13955, 1989.
- Adjei, A. A., Erlichman, C., Davis, J. N., Reid, J., Sloan, J., Stakkevich, P., Zhu, Y., Marks, R., Pitor, H., Goldberg, R. M., Hanson, L. H., Alberts, S., Cutler, D., Kaufmann, S. H. A Phase I and pharmacology study of the farnesyl protein transferase (FPT) inhibitor SCH 66336 in patients with locally advanced or metastatic cancer. *Proc. Am. Soc. Clin. Oncol.*, 18: 598, 1999.

**Polymer-Drug conjugates designed for intratumoral activation: Basic principles and transfer from the Laboratory to the Clinic.** Duncan, R. *Centre for Polymer Therapeutics, The School of Pharmacy, London WC1N 1AX, UK.*

Twenty five years ago Helmut Ringsdorf first proposed the use of water soluble synthetic polymers as targetable carriers for cancer chemotherapy (1). The idea was initially received with considerable scepticism. Perhaps this is understandable as at that time liposomes and immunoconjugates were at the height of fashion as the "magic bullets" that might provide improved cancer therapy. However, a dedicated and relatively small scientific community have continued to develop polymer-based antitumour pro-drugs and in recent years four compounds have progressed into Phase III clinical trial. Several compounds are currently in pre-clinical development.

Although it is still too early to know what clinical benefit polymer therapeutics can bring, recently published Phase I clinical results describing the first synthetic polymer-drug conjugate to be tested in man, N-(2-hydroxypropyl)methacrylamide (HPMA) copolymer-Gly-Phe-Leu-Gly-doxorubicin (PK1, PCB 28068) (2); have generated considerable interest. PK1 displays greatly reduced toxicity compared to free doxorubicin (MTD of 320 mg/m<sup>2</sup> doxorubicin equivalent dose) and evidence of activity in some chemotherapy refractory patients even when given at lower doses (e.g. 80, 120 mg/m<sup>2</sup>). Interest in polymer prodrugs is now growing exponentially. Polymeric drug combinations are under development (including polymer-directed enzyme prodrug therapy (PDEPT)) and also systems that may act as viral mimetics with consequent potential for use as intracytoplasmic delivery systems (discussed in 3).

The rationale for conjugate design has been reviewed at length in (4-7). It is essential that the polymer carrier is neither inherently toxic nor immunogenic and, if the polymer is non-degradable in main chain the carrier must have a molecular weight sufficiently low to allow renal elimination (i.e. less than 30-40 kDa). Careful design of a polymer-drug linker is also important. Nonbiodegradable linkers yield conjugates that have no activity unless the attached drug is membrane active. The linker between polymer and drug should preferably be stable in the circulation, but amenable to specific enzymatic or hydrolytic cleavage intratumorally (reviewed in 8). To restrict drug release to the lysosomal compartment of the cell peptidyl linkages were originally designed for cleavage by the cysteine proteases (e.g. Gly-Phe-Leu-Gly-Dox of PK1). It is now known that levels of

cysteine proteases are elevated in some tumours, a circumstance that has often been correlated with poor prognosis. Therefore polymeric prodrugs bearing peptidyl linkages cleaved by these enzymes may be also more selectively activated within particularly aggressive tumours. The drug selected must be carefully chosen. Drugs requiring liver metabolic activation, that are unstable in the lysosomal environment, or of low potency are unsuitable. The PK1 Phase I results highlight the opportunity to reduce the toxicity of highly toxic anticancer agents by polymer conjugation and compounds more potent than doxorubicin are particularly interesting candidates. The fact that attachment of hydrophobic drugs to hydrophilic polymers brings also improved water solubility (typically ~10-fold for drugs like doxorubicin and paclitaxel) is an added advantage.

From the clinical viewpoint the most interesting consequence of polymer-drug conjugation is the opportunity to capitalise on altered drug pharmacokinetics at the whole-body and cellular level (reviewed in 4-6). Unlike low molecular weight antitumour agents which penetrate cells readily, the cellular uptake of polymeric pro-drugs is restricted to the endocytic route. This limits rapid drug access to the normal sites of toxicity, and offers opportunities for passive and active tumour targeting. There is now unequivocal evidence that long circulating macromolecules and liposomes passively accumulate in solid tumour tissue due to increased vascular permeability and the lack of an effective tumour lymphatic drainage. This phenomenon was first identified using a styrene maleic anhydride-neocarzinostatin conjugate (SMANCS) by Maeda and colleagues in the mid 1980's and the term "enhanced permeability and retention (EPR) effect" was coined to describe it (9). Using a panel of mouse and xenograft tumour models it has been shown that administration of PK1 leads to substantial passive tumour targeting of doxorubicin by the EPR effect (up 20% dose/g). Similarly, HPMA copolymer-platinates produce much higher tumour levels of platinum than achievable following cisplatin administration. Although there is still much to learn about the quantitative contribution of EPR-mediated targeting in the clinical setting, both vector characteristics and the tumour-related factors governing the EPR effect are becoming better understood. Pre-clinical screening systems used routinely to select small molecule candidates are often totally inappropriate for screening novel polymeric candidates (particularly *in vitro* experiments). These complex macromolecular candidates must be selected the basis of (i) linker release kinetics, (ii) ability to demonstrate EPR-related targeting *in vivo* and ability to demonstrate improved therapeutic activity (compared to the parent drug) in appropriately defined mouse and xenograft models. Tumour models vary in their ability to demonstrate EPR-mediated targeting (% dose/g frequently declines with increasing tumour size) and tumours can display highly variable concentrations of the activating enzyme.

Most of the candidates that have so far progressed to clinical trial (PK1, HPMA copolymer-paclitaxel (PNU 166945) and HPMA copolymer-camptothecin (P&U) are designed to exhibit passive targeting by the EPR effect. It is relatively easy to additionally incorporate residues (peptides, proteins and carbohydrates) to promote receptor-mediated targeting. HPMA copolymer-doxorubicin containing additionally galactosamine (to mediate liver targeting) (PK2, FCE 28069) is undergoing Phase III evaluation. The art of patience (and perseverance) coupled with the collaborative efforts of chemistry, biology, medicine have brought the concept of polymer-drug conjugates to clinical trial. Transfer of polymer-protein conjugates to market (Oncaspar® and SMANCS) and the promising start for polymer-drug conjugates suggests an interesting future for polymer therapeutics in cancer therapy.

#### Acknowledgements

Gratitude is expressed to the Cancer Research Campaign for their vision in supporting our work at Keele Univ. (UK) and the many colleagues and collaborators involved in the design and development of PK1 and PK2; in particular, J. Kopecek and K. Ulbrich (Institute of Macromolecular Chemistry, Prague), B. Rihova (Institute of Microbiology, Prague), the skillful colleagues in Farmitalia Carlo Erba (now P & U) and the CRC Phase/II Committee.

#### References

1. Ringsdorf, H. Structure and properties of pharmacologically active polymers. *J. Polym. Sci. Polym. Symp.*, 51: 135-153, 1975.
2. Vasey, P., Twelves, C., Kaye, S., Wilson, P., Morrison, R., Duncan, R., Thomson, A., Hilditch, T., Murray, T., Burtles, S., Cassidy, J. Phase I clinical and pharmacokinetic study of PK1 (HPMA copolymer doxorubicin): first member of a new class of chemotherapeutic agents: drug-polymer conjugates. *Clin. Cancer Res.*, 5: 83-94, 1999.
3. Duncan, R. Polymer therapeutics into the 21st century. In: K. Park and R. Mersny (eds.), *Drug Delivery in the 21st Century*, in press, Washington DC: Am. Chem. Soc., 1999.
4. Duncan, R., and Kopecek, J. Soluble synthetic polymers as potential drug carriers. *Adv. Polym. Sci.*, 57: 51-101, 1984.
5. Duncan, R. Drug-polymer conjugates: potential for improved chemotherapy. *Anti-Cancer Drugs*, 3: 175-210, 1992.
6. Pulnam, D., and Kopecek, J. Polymer conjugates with anticancer activity. *Adv. Polym. Sci.*, 122: 55-123, 1995.
7. Kataoka, K. Targetable polymer drugs. In: K. Park (ed.), *Controlled Drug Delivery—Challenges and Strategies*, pp 49-71, Washington, DC: Am. Chem. Soc., 1997.
8. Brocchini, S., and Duncan, R. Pendent drugs: Release from polymers. In: E. Mathiowitz (ed) *Encyclopedia of Controlled Release*, pp 786-816, New York: Wiley, 1999.
9. Matsumura, Y., and Maeda, H. A new concept for macromolecular therapeutics in cancer chemotherapy; mechanism of tumorotropic accumulation of proteins and the antitumour agent SMANCS. *Cancer Res.*, 6: 6387-6392, 1986.

**Polymer-directed enzyme pro-drug therapy: Results of phase I studies.** Cassidy, J. *University of Aberdeen, Aberdeen, AB25 2ZD, UK.*

Polymeric drug delivery systems have the theoretical potential to be engineered to direct drug to specific organs, cells and even sub-cellular regions. They can also be designed to give pre-determined release rates at the site of action. As such this developing technology may have particular benefits as applied to cytotoxic agents which usually have a small therapeutic index. In addition, if polymers can preferentially deliver drug to the site of tumours it is possible this may circumvent clinical drug resistance.

PK1 [N-(2-Hydroxypropyl)methacrylamide copolymer doxorubicin] was developed as the result of a longstanding academic collaboration between researchers in Europe. The polymeric backbone being initially designed as a non-immunogenic plasma expander and contact lens material. Doxorubicin was chosen as the drug "payload" in view of its high level of activity across a spectrum of human solid tumors. The linker between the polymer backbone and the drug was designed to be cleaved exclusively in the lysosomal compartment after internalization of the intact copolymer by endocytosis. Pre-clinical evaluation demonstrated impressive anti-cancer activity with a reduced toxicity profile in comparison to native doxorubicin. This enhanced anti-cancer activity was shown by pharmacokinetic analyses to be due to a marked increase in tumor accumulation of drug. The mechanism of this accumulation was hypothesized to be due to EPR (enhanced penetration and retention), based on the known fenestrated nature of tumor blood vessels and the relative inefficiency of tumor lymphatic drainage. These observations were independently reproduced in several tumor models prior to clinical testing.

Clinical development of PK1 was sponsored jointly by Pharmacia Upjohn and the United Kingdom Cancer Research Campaign. A total of 36 patients (20 male/16 female) were enrolled in the phase I study with a variety of primary tumors. The mean age of patients on study was 58.3 years (range 35-72). As is usual most of these patients had received prior therapy with chemotherapy (28) and/or radiotherapy (14) for their malignancy. Eligibility criteria were those applied as standard in phase I studies. Prior exposure to anthracycline was allowed. All patients had baseline assessment of cardiac function by echocardiogram or multiple-gated angiography (MUGA). Appropriate tumor imaging was performed for disease assessment at baseline and after every 3 cycles of therapy. A total of 21 patients also consented to have imaging studies performed with radiolabelled compound in an attempt to confirm tumor localisation of the polymer.

PK1 was administered as an intravenous infusion at a concentration of 2 mg/ml (doses quoted as doxorubicin equivalents) and a rate of 4.16 ml/min. Thus patients had different infusion times for individual dosage. Detailed pharmacokinetics were performed by serial collection of blood samples and HPLC analyses for both bound drug and free doxorubicin.

100 courses of PK1 were administered. Doses ranged from 20 mg/m<sup>2</sup> to 320 mg/m<sup>2</sup>. Cohorts of three patients each were entered at non-toxic dose levels and were expanded to 6 patients in the case of significant toxicities. Nausea and vomiting were observed at all dose levels above 40 mg/m<sup>2</sup> but was easily controlled with standard anti-emetics.

Neutropenia was dose-limiting and showed a clear dose-dependency between 180 mg/m<sup>2</sup> and 320 mg/m<sup>2</sup>. The neutrophil nadir occurred at day 15 and recovery was usual by day 21. Sporadic (non-dose related) occurrences of anaemia and thrombocytopenia were observed. Minor hepatic toxicity was observed at dose levels above 120 mg/m<sup>2</sup> manifest as transient (asymptomatic) rises in transaminases. Significant oral mucositis was observed at high dose levels and contributed to the definition of maximal tolerated dose at 320 mg/m<sup>2</sup>.

Despite individual cumulative doses as high as 1680 mg/m<sup>2</sup> no congestive cardiac failure was observed. Only one of nine patients showed a significant fall in left ventricular function and disease progression probably contributed to this event, which was not attended by cardiac failure.

The pharmacokinetic behavior of PK1 was markedly different from native doxorubicin with a distribution half-life of 1.8 hours and an elimination half-life of 93 hours. This was in keeping with animal experience and supported the possibility of an EPR effect. Uptake of radiolabelled material was identifiable in 6 of 21 patients on gamma camera imaging. However the technique applied proved cumbersome and difficult to reproduce. Two documented partial responses (both in non-small cell lung cancer) and two minor responses (colorectal, breast) occurred in this phase I trial.

This phase I trial was designed as a "proof of principle" study. No untoward toxicity attributable to the polymer backbone was observed. The toxicities associated with anthracyclines were observed in an attenuated fashion with a 4-fold increase in MTD. Favorable human pharmacokinetics were confirmed and some tumor localization to support EPR was observed.

The phase II program for this compound is ongoing. The colorectal study failed to demonstrate activity in this tumor type. Activity was confirmed in non-small cell lung cancer and further studies in this tumor type are being planned. Studies in anthracycline naive and anthracycline resistant breast cancer patients are still recruiting.

PK1 was the first such systemically administered polymeric anti-cancer drug. Other drugs to follow the same development pathway are at an earlier stage, but if the promise shown by PK1 can be replicated the potential exists for a whole generation of polymers with specific targeting abilities.

Special consideration should be given to the design of future studies with agents of this nature. Imaging techniques to confirm tumor localization and correlate this with vascular parameters should be performed as early as possible. Pharmacokinetics and pharmacodynamics must be incorporated to facilitate optimal design of next generation polymers. Finally we should strive to define the optimal patient



populations that will benefit from these drugs. It is likely that important differences will emerge in the EPR effect in different tumour types and even at different stages of tumor development within one histological sub-type.

#### WORKSHOP 1: RELEVANCE OF IN VIVO MODELS FOR TARGET-DIRECTED ANTICANCER DRUG DEVELOPMENT

**Molecular characterization of human tumor xenografts for target-oriented drug discovery.** Burger, A. M., Willmann, H., Stappert, H., and Fiebig, H. H. *Tumor Biology Center at the University of Freiburg, Freiburg D-79106. Oncotest, Institute for Experimental Oncology, D-79110 Freiburg, Germany.*

The development of anticancer agents is currently being directed towards new molecular targets or aimed to exploit biological characteristics of human tumors. Thus, this approach requires disease oriented preclinical model systems which would be able to discriminate between specific and general cytotoxic antitumor activity. Engineering of target expressing human tumor cell lines or the development of transgenic and knockout animals are possible but artificial avenues. We have therefore characterized a panel of over 60 human tumors, which were established from primaries or distant metastasis as subcutaneously growing xenografts in athymic nude mice, for 27 validated or emerging molecular targets. They include oncogenes and tumor suppressor genes (k-ras, c-myc, her2, p53), enzymes (telomerase, DT-diaphorase), growth factors and their receptors (EGFR, TGF $\alpha$ , TGF $\beta$ , bFGF, ER, PR), drug resistance (mdr1, mdr3) and metastasis associated proteins (matrix metalloproteinases, uPA, nm23, CD44) or determinants of tumor angiogenesis (VEGF, angiogenin, vascular porosity and microvessel density). Target expression was determined either at the RNA (Northern blotting) or protein level (ELISA, Western blotting, immunohistochemistry).

The Freiburg human tumor xenograft panel is a collection of over 350 tumors which can all be kept in serial passage in nude mice and resemble a broad spectrum of histologic types and therapeutic responders. The 60 xenograft models selected thereof for routine drug testing procedures are capable of growing in soft agar for an *in vitro* prescreen and they show a variety of growth characteristics or chemosensitivity pattern towards standard agents very similar to the clinical situation [1, 2]. Amongst the tumor types represented are bladder (3), breast (7), cervical (2), colon (6), gastric (3), head and neck (3), lung (9), ovary (5), pancreas (2), prostate (4), renal (6), sarcomas (4), skin (4), testis (1) and uterus (1) carcinomas.

The molecular characterization of these xenografts showed that target expression can be tumor type specific or random and that this also mimics closely data reported for patient tumors.

E.g. we found that telomerase activity was present in all tumor specimens, but at various levels and that latter correlated with the ability of xenograft tissue to form colonies in soft agar, thus reflecting tumor stem cell count and aggressiveness [3].

Whilst the expression of the metastasis associated protein CD44 v6 showed inter- and intratumoral heterogeneity, matrix metalloproteinase 2 (MMP2) was expressed at high levels explicitly in melanoma and sarcoma xenografts. This would suggest that inhibitors directed against MMP2 should be assessed in these tumor types [4].

Overexpression of the epidermal growth factor receptor (EGFR) was confined to gastric cancers, adenocarcinomas of the lung and renal cell carcinomas and this was accompanied by a parallel increase in TGF $\alpha$ -expression. Screening of the immunotoxin TGF $\alpha$ -PE40 (recombinant *Pseudomonas* exotoxin A; (PE40) fused to TGF $\alpha$ ) in the human tumor xenograft panel *in vitro* showed, that this agent selectively inhibited the growth of human tumor cells co-expressing its EGFR/TGF $\alpha$  targets [5].

Angiogenic factors such as vascular endothelial growth factor (VEGF), vascular porosity (VP) and microvessel density were particular high in renal cell carcinomas [6]. Intertumoral variability of VEGF, VP and microvessel counts were seen in cancers of the breast and prostate, whilst colon carcinomas appeared to have a generally low extent of angiogenic factors. The methotrexate-albumin conjugate (MTX-HSA), a polymer prodrug designed to exploit tumortropism of polymers by the enhanced permeability and retention effect (EPR) of porous tumor vasculature [7, 8] was found particularly active *in vivo* in those renal cell tumor xenografts with the highest VP and VEGF levels. 90% tumor growth inhibition by MTX-HSA (12 mg/kg i.p. given on days 1, 8, 15) compared to untreated control tumors was seen in the RXF 944 model with a VEGF content of 20 pg/ $\mu$ g total protein and a VP of 8.6% of dose retained per gram tumor. On the contrary, the mammary tumor MAXF 449 expressing 0.3 pg/ $\mu$ g VEGF and retaining 0.7% of the polymer dose/g tumor did not respond the MTX-HSA therapy (growth inhibition <19%). Moreover, the outcome of the clinical phase I trial reported on 3 tumor responses of which 2 were renal cell carcinomas [7].

By using bioinformatics, a COMPARE algorithm is currently being developed based on expression of molecular targets and response of xenografts to experimental therapeutics *in vitro* and *in vivo*, which might accelerate target directed new drug development.

Our findings show that human tumor xenografts are extremely valuable models for target oriented drug discovery and that their molecular make up reflects the behavior of patient tumors very well. Thus, they can be used as readily available source to identify new targets and target-specific agents as well as to study tumor biology.

#### References

- Burger, D. P., Fiebig, H. H., Winterhalter, B. R. Establishment and characterization of human tumor xenograft models in nude mice. *In: Fiebig, H. H.,*

and Berger, D. P. (eds), *Immunodeficient mice in oncology. Contrib. Oncol.*, Vol. 42, pp 23-46, Basel: Karger, 1992.

- Fiebig, H. H., Berger, D. P., Dengler, W. A., Wallbrecher, E., Winterhalter, B. R. Combined *in vitro/in vivo* test procedure with human tumor xenografts. *In: Fiebig, H. H., and Berger, D. P. (eds), Immunodeficient mice in oncology. Contrib. Oncol.*, Vol. 42, pp 321-351, Basel: Karger 1992.
- Burger, A. M. Telomerase—Potential in cancer therapy. *In: Fiebig, H. H., and Burger, A. M. (eds.)* Relevance of tumor models for anticancer drug development. *Contrib. Oncol.*, Vol. 54, Basel: Karger, 1999.
- Fiebig, H. H., Klostermeyer, A., Schüler, J. B., and Burger, A. M. Characterization of matrix metalloproteinases in 47 human tumor xenografts shows high expression of MMP2 in melanomas and sarcomas. 90<sup>th</sup> Annual AACR Meeting, Philadelphia, Proc. Amer. Assoc. Cancer Res., 40: 463, 1999.
- Berger, P. D., Hebstrill, L., Hellerich, S., Schulzke, S., Dengler, W. A., Gallo, M., Pastan, R., Mertelsmann, R., and Fiebig, H. H. Cytotoxicity of TGF $\alpha$ -PE40 and correlation to expression of epidermal growth factor receptor. *Eur. J. Cancer*, 31A: 2067-2072, 1995.
- Berger P. D., Hebstrill, L., Dengler, W. A., Marme, D., Mertelsmann, R., and Fiebig, H. H. Vascular endothelial growth factor (VEGF) mRNA expression in human tumor models of different histologies. *Ann. Oncol.*, 6: 817-825, 1995.
- Hartung, G., Stehle, G., Sinn, H., Wunder, A., Schrenk, H. H., Heeger, S., Kranzle, M., Edler, L., Frei, E., Fiebig, H. H., Heene, D. L., Meier-Borst, W., and Queisser, W. Phase I trial of methotrexate-albumin in a weekly intravenous bolus regimen in cancer patients. Phase I study group of the association for medical oncology of the german cancer society. *Clin. Cancer Res.*, 5: 753-759, 1999.
- Matsunura, Y., and Maeda, H. A new concept for macromolecular therapeutics in cancer chemotherapy: mechanism of tumortropic accumulation of proteins and the antitumor agent smancs. *Cancer Res.*, 46: 6387-6392, 1986.

**Syngeneic tumor models for high-dose therapy and micrometastatic disease.** Teicher, B. A. *Lilly Research Laboratories, Indianapolis, IN 46285, USA.*

The study of high-dose therapy for cancer requires the development of laboratory models that go beyond the standard endpoints of increase in life span and delay of tumor growth. Whether combination therapies, especially chemotherapy combinations, retain increasing efficacy in the high-dose setting is the crucial question for the development of new treatment regimens (1). In models it is important to be able to determine whether there is increasing response in the primary tumor and also to detect whether there is increasing response in disease disseminated to distal organs. The primary endpoints applied in solid tumor efficacy models of tumor growth delay and tumor control require that drugs be administered at doses producing little normal tissue toxicity so that the tumor response to the treatment can be observed over a relatively long interval. It is very difficult to apply these endpoints to the high-dose setting in which normally lethal doses of anticancer agents are administered with normal tissue support, such as hematopoietic stem cell infusions. Response of tumors and metastatic disease to high-dose therapies can be assessed by use of excision assays (2). The excision assay allows the determination of cell survival after treatment of the animal by colony formation *in vitro*. The tumor excision assay allows great accuracy and fine resolution among various therapeutic regimens. Supralethal treatments can be tested. Perhaps, the greatest disadvantage of excision assays is that extended treatment regimens cannot be used because of tumor cell loss (all tumor cells present in the tumor at the time of treatment must be counted) and tumor cell proliferation over the treatment time. This assay also requires tumor models that grow well *in vivo* and have a high plating efficiency *in vitro*.

Several high-dose combination chemotherapy regimens are under clinical evaluation in the treatment of solid tumors. Drug selection for these regimens was based on knowledge of the mechanisms of action, the dose limiting toxicities and some cross-resistance data from cell culture and animals tumor studies. Knowledge of anticancer drug-drug and drug-target interactions has increased, along with appreciation of the importance of drug scheduling for individual agents and among the components in a combination regimen. Measurable drug resistance in some studies can be induced in tumor cells by a single drug exposure. Experiments in the EMT-6 murine mammary carcinoma provide an example. The EMT-6 tumor is sensitive to the cytotoxic action of many antitumor alkylating agents. Cytotoxicity in tumor cell survival assays increase logarithmically as the dose of melphalan, cyclophosphamide, thiopeta or carboplatin is increased linearly (i.e., a log-linear dose response curve). A 400 mg/kg dose of cyclophosphamide administered to tumor-bearing mice kills about 2.5 logs of EMT-6 tumor cells. Treatment of tumor-bearing mice with two doses of cyclophosphamide separated by 7 or 12 days resulted in 3 logs and 2.5 logs, respectively, of EMT-6 cell killing by the second 400 mg/kg cyclophosphamide dose. Treatment of mice with a 30 mg/kg dose of melphalan killed 2.5 logs of EMT-6 cells. However, a second melphalan dose administered 7 days later killed less than 1 log of EMT-6 tumor cells. If the second dose of melphalan was administered 12 days after the first dose 1.5 logs of EMT-6 tumor cells were killed. Thus, there was marked resistance to the second melphalan treatment (3). Because these drug doses are lethal, treated tumors must be transferred to second hosts to extend the interval between the intensification treatment. To determine whether prior chemotherapy would alter tumor growth, untreated mice were compared to those that had received prior chemotherapy. Prior treatment did not alter the growth of the tumors or tumor plating efficiency. These studies concluded that administration of melphalan induces a metabolic condition in both host and tumor, resulting in drug resistance that slowly dissipates over several weeks (4). In contrast, prior exposure to cyclophosphamide produced little or no resistance to administration of a second drug. In fact, readministration of cyclo-

phosphamide resulted in increased tumor cell killing compared to the initial treatment. This appears to be primarily an effect on the host because when an untreated or melphalan-treated host bearing a cyclophosphamide-treated tumor was given cyclophosphamide, sensitivity of the tumor to cyclophosphamide diminished.

Patients often bear micrometastases below the limits of detection at the time of treatment. EMT-6 mammary carcinoma implanted subcutaneously in the thigh in the syngeneic host was used to determine the extent of micrometastatic disease in the animals and to assess the response to therapy of disease present in various organs. Nine days after tumor implantation, EMT-6 tumor was distributed widely through the host as determined by tumor cell survival assay of specific organs (brain, liver, lungs, spleen, bone marrow, circulating blood and primary tumor) (5). There was a wide range of sensitivity of the tumor spanning 2- to 3-logs of tumor cell killing with the antitumor alkylating agents (cyclophosphamide, melphalan, cisplatin, thiotepa) depending upon the tissue in which the tumor cells were located. Tumor cells in the circulating blood were most sensitive to treatment with the primary tumor being the second most sensitive site. Tumor cells in the liver and brain were least responsive to treatment of the host with any of the four antitumor alkylating agents. Location within the host is a critically important determinant of the response of tumor to therapy.

In the absence of therapies with greater tumor selectivity, investigations have turned to the use of 'modulators', agents with little antitumor activity as single agents but which enhance the activity of cytotoxic agents (1). Several clinical trials with this type of agent in combination regimens are underway in the standard dose setting and may move to the high-dose setting. Preclinical studies from the earliest murine leukemia model systems to the present range of leukemia, solid tumor and xenograft models have suggested that tumor cure requires the eradication of nearly all tumor cells by exogenous treatment. High-dose chemotherapy regimens are based on the premise that under-treatment is the reason for failure to achieve cure in many patients. Through the use of *in vivo/in vitro* excision assays, preclinical models can be extended to high-dose chemotherapy and to the determination of the effectiveness of various drug combinations and schedules to the high-dose setting.

#### References

1. Teicher, B. A. Preclinical models for high-dose therapy. In: *High-Dose Cancer Therapy: Pharmacology, Hematopoietins, Stem Cells*, Third Edition, edited by J. O. Armitage and K. H. Antman. Lippincott Williams & Wilkins, Philadelphia, 1999, pps. 15-47.
2. Hill, R. P. Excision assays. In: *Kallman, R. F., ed., Rodent tumor models in experimental cancer therapy*. New York: Pergamon Press, 1987, pps. 67-75.
3. Teicher, B. A., Ara, G., Buxton, D. Acute *in vivo* resistance. *Clin. Cancer Res.*, 4: 483-491, 1998.
4. Holden, S. A., Teicher, B. A., Ayash, L., Frei, E., III. A preclinical model for sequential high-dose chemotherapy. *Cancer Chemotherap. Pharmacol.*, 36: 61-64, 1995.
5. Holden, S. A., Emi, Y., Kakeji, Y., Noxhey, D., Teicher, B. A. Host distribution and response to antitumor alkylating agents of EMT-6 tumor cells from subcutaneous tumor implants. *Cancer Chemotherap. Pharmacol.*, 40: 87-93, 1997.

#### WORKSHOP 3: CYTOSTATIC AGENTS: METHODOLOGY OF PHASE III TRIALS

**Early development of angiogenesis inhibitors.** Harris, A. L. *Imperial Cancer Research Fund, University of Oxford, Institute of Molecular Medicine, John Radcliffe Hospital, Oxford OX3 9DS, UK.*

Angiogenesis inhibitors, including metalloproteinases, represent a particular problem in early development unless a clear tumour regression is obtained. This is unusual and other methods are needed to assess whether a biological effect has been achieved prior to a large-scale randomized phase III/III trial. Very few studies have used pharmacodynamic endpoints as the main measure and often a maximum tolerated dose is derived. This may be greater than needed to inhibit the target and produce long term toxicity. A few studies have attempted to use other biological endpoints that may indicate that a target is being inhibited although this is difficult to measure within the tumour. One example is the whole blood cytokine assay, whereby whole blood is incubated at 37°C and stimulated with PHA to cause release of cytokines from lymphocytes and monocytes. The signalling pathways involved in the transmission of the PHA signal and cleavage of TNF $\alpha$  from the cell surface, are potential targets for several classes of drugs. It has been possible to compare the release from cell of shed TNF $\alpha$  before and after therapy in the whole blood, thus allowing protein/drug interactions and drug distribution to be maintained and fully represent the *in vivo* situation. This assay has been used to show that Marimastat was effective at inhibiting the shedase involved in TNF $\alpha$  release *in vivo*. Other methods include pharmacokinetic endpoints achieving levels of IC90 in the plasma and relating this back to xenograft models. Ideally such models should provide information to relate plasma level to inhibition of the relevant target in human tumour xenograft giving some guide therefore to clinical plasma levels desired. Novel imaging technology such as PET scanning to measure blood flow and volume may also be of value and MRI to measure vascular permeability. These are starting to be used as endpoints of studies and need to be related to pharmacokinetic and toxic endpoints. Serial biopsies are also a possibility and it has been shown that conventional chemo and endocrine therapy results in the reduc-

tion of microvessel density in breast and prostate cancer. Neo adjuvant therapy, randomised with/without chemotherapy or placebo prior to surgery would provide another method for assessing direct tumour effects of therapy.

Makris *et al.* *Cancer* 85: 1996-2000

Thavasu *et al.* *Cancer Research*, in press.

#### WORKSHOP 6: NEW CYTOKINES AND CELL-BASED THERAPY OF CANCER

**GM-CSF-secreting tumor vaccines for pancreatic cancer: From bench to clinic.** Jaffee, E. M., Cameron, J., Hruban, R., Abrams, R., Grochow, L., Donehower, R., O'Reilly, S., Weber, C., Sauter, P., Biedrzycki, B., Goehmann, M., and Yeo, C. *Departments of Oncology, Surgery, and Pathology, The Johns Hopkins School of Medicine, Baltimore, MD 21205.*

The area of vaccine development for the treatment of cancer has been one of active research for over 50 years. Of the many different vaccine approaches for the therapy of cancer, gene therapy has been one of the most promising. The introduction of cytokine and costimulatory molecule genes into tumor cells has been used in an attempt to augment the antitumor immune responses in animal models (1-2). While many of these gene transfer approaches improve the immunogenicity of the tumor (2), a study directly comparing the effects of tumor vaccines retrovirally transduced with a wide variety of cytokines identified granulocyte macrophage colony stimulating factor (GM-CSF) as the most potent cytokine for activating systemic antitumor immunity (3).

The effects of whole cell vaccines engineered to secrete GM-CSF in a paracrine fashion have been examined mechanistically (3-5). The systemic anti-tumor immunity produced with GM-CSF secreting tumor cell vaccines has been shown to be dependent on both CD4 and CD8 T cells. In addition, histological analysis of the GM-CSF secreting vaccine site has shown a marked increase in the local mononuclear cell infiltrate when compared to vaccines that do not secrete GM-CSF. It is therefore likely that the enhanced immune response is due to the unique ability of GM-CSF to promote the recruitment and differentiation of professional antigen presenting cells (APC) such as dendritic cells at the vaccine site (4-5). These professional APCs first take up and process tumor antigens and subsequently prime the T cell arm of the immune response (3, 5).

While the use of autologous cytokine secreting tumor cell vaccines have been rigorously tested in animal models, the development of autologous tumor vaccines for human testing has proved cumbersome. A completed Phase I clinical trial evaluating an autologous GM-CSF secreting tumor vaccine for the treatment of renal cell carcinoma showed promising results but uncovered a number of technical problems, particularly the routine expansion of the primary human tumor cells to the numbers required for vaccination (6). These technical limitations make the use of autologous tumor cell vaccines for the treatment of most human cancers impractical.

Two recent findings provide the immunologic rationale for an allogeneic vaccine approach. First, about half of the human melanoma antigens identified so far have been demonstrated to be shared among at least 50% of other patient's melanomas (7-8). Second, recent studies have shown that the professional APCs of the host, rather than the vaccinating tumor cells themselves, are responsible for priming CD4 and CD8 T cells, both of which are required for generating systemic antitumor immunity (5). Although the antigens recognized by the CD8 T cells were not known at the time, these studies demonstrate that tumor-specific CD8 T cells are activated via the cross-priming pathway. These findings suggest that the vaccinating tumor cells do not need to be HLA compatible with the host to generate specific antitumor immunity thereby providing rationale for a more generalized and feasible whole cell tumor vaccine approach. More recently, an allogeneic GM-CSF secreting vaccine was demonstrated to be effective in a mouse tumor model (9).

Based on these findings, a phase I trial was conducted to evaluate allogeneic irradiated, GM-CSF secreting tumor cells for safety and the induction of antitumor immunity (10). Patients were required to have an ECOG performance status of <2, prior pancreaticoduodenectomy for stage 1, 2, or 3 pancreatic adenocarcinoma, and to be seronegative for HIV. Between July, 1997 and April, 1998, 14 patients underwent pancreaticoduodenectomy and received a vaccine 8 weeks later. Three patients received  $1 \times 10^7$  vaccine cells (tier 1), 3 patients received  $5 \times 10^7$  vaccine cells (tier 2), 3 patients received  $1 \times 10^8$  vaccine cells (tier 3), and 5 patients received  $5 \times 10^8$  vaccine cells. All patients then went on to receive a 6 month course of adjuvant radiation and chemotherapy. One month after completing adjuvant treatment, all eligible patients went on to receive three additional monthly vaccinations with the same vaccine dose that they originally received. All participants experienced grade I or II local induration and erythema at the vaccine site. One patient experienced Grover's syndrome related to systemic levels of GM-CSF. No dose limiting toxicities were encountered. There was no evidence of autoimmunity including pancreatitis with a follow-up of up to 28 months post-vaccination. Delayed type hypersensitivity responses (DTH) to autologous tumor cells post-vaccination were observed in some individuals on dose tiers 3 and 4. DTH responses post vaccination appear to correlate with increased disease-free survival (as measured by no radiographic evidence of recurrence or elevated levels of CA19.9). Immunohistochemical staining of skin biopsies from patients receiving the GM-CSF vaccine demonstrated eosinophil and macrophage infiltration at the vaccine sites, and eosinophils, lymphocytes, and macrophages at the DTH sites similar to what we observed in our pre-clinical models. We conclude that allogeneic GM-CSF secreting tumor vaccines are safe in patients with pancreatic adenocarcinoma. In addition, this vaccine approach induces a dose-dependent immunity as measured by DTH responses that are also associated with a longer



disease-free survival. These findings provide strong support for accelerating the evaluation of GM-CSF vaccines in patients with what are classically considered non-immunogenic cancers such as pancreatic adenocarcinoma.

#### References

- Chen, L., Linsley, P. S., Helstrom, K. E. Costimulation of T cells for tumor immunity. *Immunol. Today*, 14: 483-486, 1993.
- Greten, T. F., Jaffee, E. M. Cancer Vaccines. *J. Clin. Oncol.*, 17(3): 1047-1060, 1999.
- Dranoff, G., Jaffee, E. M., Lazenby, A., Golumbek, P., Levitsky, H., Brose, K., Jackson, V., Hamada, H., Pardoll, D. M., Mulligan, R. C. Vaccination with irradiated tumor cells engineered to secrete murine GM-CSF stimulates potent, specific, and long-lasting anti-tumor immunity. *Proc. Natl. Acad. Sci. USA*, 90: 3539-3543, 1993.
- Steinman, R. M. Dendritic cells and immune-based therapies. *Exp. Hematol.*, 24: 859-862, 1996.
- Huang, A., Golumbek, P., Ahmadzadeh, M., Jaffee, E. M., Pardoll, D. M., and Levitsky, H. The role of bone marrow derived cells in presenting MHC class I-restricted tumor antigens. *Science*, 264: 961-965, 1994.
- Simons, L. W., Jaffee, E. M., Weber, C., Levitsky, H. J., Nelson, W. G., Cohen, L., Cliff, S., Finn, C., Hauda, K., Lazenby, A., Pardoll, D. M., Piantadosi, S., Owens, A. H., Mulligan, R. C., Marshall, F. Bioactivity of Human GM-CSF Gene Transduced Autologous Renal Vaccines. *Cancer Res.*, 57: 1537-1546, 1997.
- Rosenberg, S. A., Kawakami, Y., Robbins, P. F., and Wang, R. Identification of the genes encoding cancer antigens: Implications for cancer immunotherapy. *Adv. Cancer Res.*, 70: 145-177, 1996.
- Boon, T., Van Der Bruggen, P. Human tumor antigens recognized by T lymphocytes. *J. Exp. Med.*, 183: 725-729, 1996.
- Thomas, M. C., Greten, T., Jaffee, E. M. Vaccination with Allogeneic Tumor Cells Induces Specific Antitumor Immunity. *Human Gene Therapy*, 9: 835-843, 1998.
- Jaffee, E. M., Schutte, M., Gossett, J., Morsberger, L., Adler, A. J., Thomas, M., Greten, T. F., Hruban, R. H., Yeo, C. J., Griffin, G. A. Development and Characterization of a Cytokine Secreting Pancreatic Adenocarcinoma Vaccine from Primary Tumors for Use in Clinical Trials. *The Cancer Journal of Scientific American*, 4(3): 194-203, 1998.

#### WORKSHOP 7: PREVENTION TARGETS

**Apoptotic pathways as targets for chemopreventive agents.** Sun Shi-Yong, Suzuki Seigo, Hong Woun K., Lotan Reuben. *Department of Thoracic/Head and Neck Medical Oncology, The University of Texas M.D. Anderson Cancer Center, Houston, Texas 77030.*

The goals of chemoprevention of cancer are to inhibit the induction or suppress the progression of preneoplastic lesions to invasive cancer by using specific natural or synthetic chemical agents. Many of the agents that block or delay progression modulate cell proliferation and differentiation. Because these agents were thought to act as cytostatic agents, it has been suggested that they should be administered chronically to patients or individuals at increased risk to develop cancer. A more desirable approach is to identify agents that can eliminate aberrant clones by apoptosis rather than merely slow down their proliferation. Such agents could be administered for shorter periods of time, which may allow the use of higher doses and inclusion of agents with some reversible or moderate side effects. The increased understanding of apoptosis pathways has directed attention to components of these pathways as potential targets for not only chemotherapeutic but also for chemopreventive agents. Interestingly, an increasing number of previously identified chemopreventive agents including retinoids, vitamin D3 analogs, butyroids, phenyl acetate, monoterpenes, non steroidal anti-inflammatory agents and others) were found recently to enhance apoptosis in a variety of malignant cell types in vitro and in a few animal models in vivo. Studies by our group have highlighted the ability of the synthetic retinoids N-(4-hydroxyphenyl)-retinamide (Fenretinide, 4HPR) and 6-[3-(1-adamantyl)-4-hydroxyphenyl]-2-naphthalene carboxylic acid (CD437) to enhance apoptosis in a variety of tumor cell lines that are resistant to the natural retinoic acids. We found that 4HPR was able to target the mitochondria to increase the generation of reactive oxygen species, induce mitochondrial permeability transition, release cytochrome C to the cytoplasm and activate caspase 3 in some cell lines. Other mechanisms of 4HPR-induced apoptosis have been suggested in some tumor cell lines where 4HPR failed to increase ROS. CD437 was found to induce apoptosis in non-small cell lung cancer cells harboring wild type p53 by increasing the levels of mRNAs of the pro-apoptotic protein Bax and the death-inducing membrane receptor Killer/DR5, which contains a death domain and signals death through activation of caspase 3. Further understanding of the effects of potential chemopreventive agents on specific components of the pathways that lead to apoptosis may provide a rationale approach to use such agents alone or in combination with other agents to enhance apoptosis as a strategy for effective chemoprevention of cancer. (Supported by USPHS grants PO1 CA52051, U19 CA68437 from NCI, and P50 DE11906 from the NIDCR).

163

#### WORKSHOP 8: THE TUMOR MICROENVIRONMENT

**Hypoxia signalling as a regulator of tumor angiogenesis and therapy target.** Harris, A. L. *Imperial Cancer Research Fund, University of Oxford, Institute of Molecular Medicine, John Radcliffe Hospital, Oxford OX3 9DS, UK.*

Major recent advances in the biology of hypoxia signalling have provided new therapeutic targets. It has been found that the von Hippel Lindau syndrome protein targets a key transcription factor regulated by hypoxia, hypoxia inducible factor 1 $\alpha$ , for destruction by the proteasome in air. Under hypoxia this targeting is inhibited and hif-1 $\alpha$  is stabilised and can bind to the VEGF promoter upregulating angiogenesis. In addition, enzymes of the glycolytic pathway, endothelin-1 and several other pathways, are upregulated. It has been shown that this pathway interacts with transformation and is essential for *in vivo* tumour angiogenesis. The second transcription factor in the family, hypoxia inducible factor 2 $\alpha$  has also been found to be upregulated in renal cancer and may be responsible for the high vascularity of this tumour. The factors are rarely expressed in normal tissues and therefore inhibitors of their translocation to the nucleus or heterodimerization with the transcription partner ARNT, may be of therapeutic value. The hypoxia response element in the genes regulated by hif-1 $\alpha$  and hif-2 $\alpha$  could also be used to deliver gene therapy selectively to hypoxic areas of tumours. We have shown that this is a feasible way of delivering pro-drug activation enzymes for destruction of hypoxic cells. Using a diffusible toxin allows the surrounding normoxic tumour to be destroyed also. These pathways are also activated in the stromal cells in tumours and in particular the hif-2 $\alpha$  pathway seems to be activated in macrophages, which may be key regulators of the angiogenic response. It is already well recognised that hypoxia provides a mechanism of activation of bioreductive drugs but it also seems to be a key regulator of production of VEGF in synergy with oncogenes and therefore combined approaches to block hypoxic plus oncogene signalling may be an added synergistic benefit.

Maxwell *et al.* *Proc. Natl. Acad. Sci.*, 94: 8104-8109.

Dachs *et al.* *Nat. Med.*, 3: 515-520.

**Regulation of colon cancer angiogenesis: Implications for therapy.** Ellis, L. M., Liu, W., and Shaheen, R. M. *UT MD Anderson Cancer Center, Houston, TX, 77030 USA.*

Angiogenesis is essential for the growth and metastasis of human colon cancer. Angiogenesis is a process that is entirely dependent on the microenvironment; factors secreted by colon cancer cells must interact with endothelial cells (EC) in the microenvironment in order to induce tumor neovascularization. Furthermore, factors released by the microenvironment may initiate signals within tumor cells that ultimately lead to angiogenesis.

Initial studies from our laboratory have demonstrated that vascular endothelial growth factor (VEGF) is the angiogenic factor most closely associated with colon cancer progression and metastases (1, 2). Numerous factors increase VEGF expression in human colon cancer. A great deal of effort (and progress) has been made in developing agents that directly inhibit VEGF activity. However, an alternative strategy would be to target the upstream factors that induce VEGF expression (and potentially other angiogenic factors). It is essential to identify the factors that lead to induction VEGF in order to develop new anti-angiogenic therapeutic strategies.

Since increased VEGF expression in primary colon cancers is associated with metastases formation, we sought to determine factors that lead to VEGF induction. We examined a series of cytokines known to bind to receptors on human colon cancer cells and examined VEGF induction. IGF-I and IL-1 $\beta$  lead to a significant increase in VEGF mRNA and protein expression (3, 4). IGF binding proteins did not effect IGF-I induction of VEGF. Furthermore, induction of VEGF by IGF-I and IL-1 $\beta$  lead to an increase in transcription of VEGF without effecting mRNA stability.

IGF-I and IGF-II are both known to bind to the IGF-I receptor (IGF-IR). We therefore examined the effect of IGF-II on VEGF expression. Both IGF-I and IGF-II both lead to phosphorylation of the IGF-IR in human colon cancer cells. Similar to IGF-I, IGF-II lead to induction of VEGF. Investigations into the potential signal transduction pathways activated by phosphorylation of IGF-I receptor revealed that both Erk-1/2 and Akt were activated by IGF-I or II treatment. Inhibition of Erk-1/2 activity blocked VEGF induction by both IGF-I and II, whereas inhibition of Akt activity did not. VEGF is also induced by serum starvation and this occurs through activation of Erk-1/2 as well. Activation of Erk-1/2 is a common pathway for VEGF induction by several diverse factors.

Activation of other signal transduction molecules also leads to induction of VEGF. This has been well demonstrated for *ras* activation (5). Another signal transduction molecule associated with colon cancer progression and metastases is Src. Decreased Src activity in colon cancer cells by antisense transfection is associated with decreased tumorigenicity and growth (6). To determine if this decrease in Src activity was associated with a decrease in VEGF expression, VEGF expression in these cell lines was examined. Cells with decreased Src activity exhibited lower levels of VEGF mRNA and protein levels than the parental cell line (7). Hypoxic induction of VEGF was blocked in cells with decreased Src activity. Tumors derived from cell lines with decreased Src activity were smaller than tumors derived from the parental cell line. Vascularity was significantly decreased in tumors with decreased Src activity. These studies demonstrate that induction of VEGF is mediated through specific signal transduction pathways, and blockade of these pathways may provide a strategy for inhibition of angiogenesis.

In a model of colon cancer liver metastasis, we have used anti-VEGF receptor antibodies or VEGF receptor tyrosine kinase inhibitors to inhibit the growth and angiogenesis of liver metastases (8). These agents inhibit the growth of liver metastases and lead to a decrease in tumor vascularity and proliferation. Most importantly, we found the anti-VEGF therapy led to an increase in tumor cell apoptosis. Double staining for apoptosis and EC revealed that anti-VEGF therapy led to an increase in EC apoptosis. Further studies demonstrated that a wave of EC apoptosis preceded a wave of tumor cell apoptosis, suggesting that the mechanism for the increase in tumor cell death was secondary to vascular damage due to blockade of VEGF receptor activity. In addition to its ability to induce neovascularization, these *in vivo* studies suggest that VEGF may serve to enhance EC survival. This hypothesis is supported by *in vitro* studies done by other investigators (9).

Other factors secreted by tumor cells may play a role in protecting EC from apoptosis. EC subjected to serum starvation leads to a 5-fold increase in endothelial cell apoptosis after 6 hours. We have collected conditioned medium from various colon cancer cell lines and non-malignant human cells in an attempt to determine if factors in the conditioned medium can protect ECs from apoptosis. Colon cancer conditioned medium decreased serum-starvation induction of endothelial cell apoptosis by approximately 50%. This was in contrast to the effect of conditioned medium collected from non-malignant cells where there was no effect on EC apoptosis. Heat treatment of the colon cancer conditioned medium blocked the protective effect on ECs suggesting that a protein secreted from colon cancer cells inhibits EC apoptosis. Fractionation of the conditioned medium demonstrated that fractions <10 kd and <3 kd protected EC cells from serum-starvation induction of apoptosis. These fractions also lead to phosphorylation of EC Brk-1/2 suggesting that this pathway is involved in EC survival. Thus it is likely that, in addition to VEGF, other factors contribute to survival of tumor EC sustaining the vasculature in an otherwise adverse environment. Understanding how colon cancers prevent endothelial cell apoptosis may provide another therapeutic strategy for interfering with the nutrient supply tumors.

#### References

1. Takahashi, Y., Tucker, S. L., Kitadai, Y., Koura, A. N., Bucana, C. D., Cleary, K. R., and Ellis, L. M. Vessel counts and VEGF expression as prognostic factors in node-negative colon cancer. *Arch. Surg.*, **132**: 541-546, 1997.
2. Takahashi, Y., Kitadai, Y., Bucana, C. D., Cleary, K. R., and Ellis, L. M. Expression of vascular endothelial growth factor and its receptor, KDR, correlates with vascularity, metastasis, and proliferation of human colon cancer. *Cancer Res.*, **55**: 3964-3968, 1995.
3. Akagi, Y., Liu, W., Kie, K., Zebrowski, B., Shaheen, R. M., and Ellis, L. M. Regulation of vascular endothelial growth factor expression in human colon cancer by interleukin-1 $\beta$ . *Br. J. Cancer*, **80**: 1506-1511, 1999.
4. Akagi, Y., Liu, W., Kie, K., Zebrowski, B., and Ellis, L. M. Regulation of vascular endothelial growth factor expression in human colon cancer by insulin-like growth factor-I. *Cancer Res.*, **58**: 4008-4014, 1998.
5. Rak, J., Mitsuhashi, Y., Bayko, L., Filmus, J., Shirosawa, S., Sasazuki, T., and Kerbel, R. S. Mutant *ras* oncogenes upregulate VEGF/VPF expression: implications for induction and inhibition of tumor angiogenesis. *Cancer Res.*, **55**: 4575-4580, 1995.
6. Staley, C. A., Parikh, N. U., and Gallick, G. E. Decreased tumorigenicity of a human colon adenocarcinoma cell line by an antisense expression vector specific for *c-Src*. *Cell Growth Differentiation*, **8**: 269-274, 1997.
7. Ellis, L. M., Staley, C. A., Liu, W., Fleming, R. Y. D., Parikh, N., Bucana, C. D., and Gallick, G. E. Down-regulation of vascular endothelial growth factor in a human colon carcinoma cell line transfected with an antisense expression vector specific for *c-src*. *J. Biol. Chem.*, **273**: 1052-1057, 1998.
8. Shaheen, R. M., Liu, W., Davis, D. W., Wilson, M. R., McMahon, J., McConkey, D. J., and Ellis, L. M. A Tyrosine Kinase Inhibitor to the Vascular Endothelial Growth Factor Receptor Inhibits Angiogenesis and Growth of Colon Cancer Liver Metastases. *Surg. Forum In Press*, 1999.
9. Gerber, H. P., McMurtry, A., Kowalski, J., Yan, M., Keyt, B. A., Dixit, V., and Ferrara, N. Vascular endothelial growth factor regulates endothelial cell survival through the phosphatidylinositol 3'-kinase/Akt signal transduction pathway. Requirement for Flk-1/KDR activation. *J. Biol. Chem.*, **273**: 30336-30343, 1998.

**Combination of antiangiogenic agents with standard cytotoxic therapies in therapeutic regimens.** Teicher, B. A. *Lilly Research Laboratories, Indianapolis, IN 46285, USA.*

Cancer cure requires eradication of all malignant cells. Cancer growth, however, requires proliferation of malignant cells and normal cells. The several anticancer treatment modalities currently available, including surgery, chemotherapy, radiation therapy and immunotherapy, have been envisioned to target primarily the malignant cell. Research over the past 35 years has reinforced the hypothesis put forth by Folkman that without the proliferation of normal cells, especially endothelial cells, a tumor cannot grow beyond the size of a colony (1). The consequence of this finding is that both the normal cells and the malignant cells involved in tumor growth as well as the chemical and mechanical signaling pathways that interconnect them are valid targets for therapeutic intervention. The integration of therapeutics directed toward the vascular components, extracellular matrix components and stromal and infiltrating cells with classical cytotoxic anticancer therapies, may be regarded as a systems approach to cancer treatment (2, 3). The

combination of TNP-470 and minocycline serves as an example of the use of antiangiogenic agents along with cytotoxic therapies in treatment regimens. TNP-470, a synthetic derivative of fumagillin, is a potent inhibitor of endothelial cell migration, endothelial cell proliferation and capillary tube formation. Minocycline is a tetracycline that has matrix metalloproteinase inhibitory activity. The antiangiogenic combination of TNP-470 and minocycline administered for 2 weeks did not alter the growth of the Lewis lung carcinoma, the EMT-6 mammary carcinoma, the 9L gliosarcoma or the FsaII fibrosarcoma. However, when TNP-470 and minocycline were added to treatment with cytotoxic anticancer therapies, tumor response was markedly increased. When mice bearing the FsaII fibrosarcoma were treated with TNP-470/minocycline for 5 days prior to iv injection of the fluorescent dye Hoechst 33342, there was a shift toward greater brightness of the entire tumor cell population (4, 5). The TNP-470/minocycline treated tumors were more easily penetrated by the lipophilic dye, thus indicating that treatment with antiangiogenic agents could allow greater distribution of small molecules into tumors. When mice bearing the Lewis lung carcinoma were similarly treated with TNP-470/minocycline prior to ip injection of [ $^{14}$ C]cyclophosphamide or cisplatin, there was a 2.6-fold increase in [ $^{14}$ C] and a 5.2-fold increase in platinum in the tumors from antiangiogenic agent treated tumors compared with controls at the 6 hr time point. Increased DNA cross-linking in the tumors of antiangiogenic agent treated tumors correlated with the increases in drug levels in the tumors. [ $^{14}$ C]paclitaxel was administered to Lewis lung carcinoma-bearing mice pretreated with TNP-470/minocycline or not pretreated and tissues were collected over a 24 hr time-course (6). At early time points (1 and 15 min) after iv injection of the [ $^{14}$ C]paclitaxel, there was a 5-fold higher concentration of [ $^{14}$ C] in the tumors of pretreated animals which decreased to 2-fold by 24 hrs after [ $^{14}$ C]paclitaxel injection. In a similar study, the concentrations of platinum from carboplatin were 2- and 3-fold higher in the tumors of mice pretreated with TNP-470/minocycline at 15 and 30 min after drug administration compared with controls. By 6 and 24 hrs after carboplatin injection, the tumors of antiangiogenic agent pretreated remained 2-fold higher in platinum content than the tumors of control mice. To determine whether pretreatment with TNP-470/minocycline might alter the distribution of large molecules, [ $^{14}$ C]albumin was administered to TNP-470/minocycline pretreated and non-pretreated Lewis lung carcinoma-bearing mice. There was a 2- to 3-fold higher concentration of [ $^{14}$ C]albumin in the tumors of antiangiogenic agent treated mice over the first hour after protein injection and higher concentrations of the [ $^{14}$ C] persisted in the tumors of pretreated animals over the 24 hrs examined. The Lewis lung carcinoma is very hypoxic, having 92% of the pO $_2$  measurements <5 mmHg (7). Treating tumor-bearing mice with TNP-470/minocycline decreased hypoxia in antiangiogenic agent treated tumors to 75%. When the oxygen delivery agent, perflubron emulsion, and 95% oxygen breathing was maintained in antiangiogenic agent pretreated mice, hypoxia in the tumors was decreased to 45%. The response of antiangiogenic agent treated Lewis lung carcinoma to fractionated radiation therapy (2, 3 and 4 Gy x5) was increased 2.2-fold compared with controls. When enhanced oxygen delivery was added to antiangiogenic agent administration, the response of the tumors was increased 3.4-fold compared to controls. There was a direct relationship between decrease in tumor hypoxia and increase in response to radiation therapy.

Antiangiogenic agents represent a wide variety of chemical structures with a wide variety of biological target. The diversity in this group of molecules gives strength to the potential for this approach in therapeutic applications. The biological and biochemical pathways involved in angiogenesis are numerous and redundant; therefore, it is likely that blockade of more than one pathway related to angiogenesis and/or invasion will be necessary to have impact on the natural progress of malignant disease. The vasculature forms the first barrier to penetration of molecules into tumors. Although the antiangiogenic treatments administered in these studies did not inhibit angiogenesis in these tumors completely, the vasculature present in the treated tumors may be impaired, compared with control tumors. The incorporation of antiangiogenic agents and/or antimetastatic agents into therapeutic regimens represents an important challenge. The successful treatment of cancer requires the eradication of all malignant cells, and therefore treatment with cytotoxic therapies. The compatibility of antiangiogenic therapy and/or antiinvasion agents with cytotoxic chemotherapeutic agents is not obvious (8). Two conclusions may be drawn. First, combinations of antiangiogenic agents evoke a greater effect on tumor response to therapy than does treatment with single agents of this class. Second, treatment with antiangiogenic agents can interact in a positive way with cytotoxic therapies. The true strength of antiangiogenic therapies may be in their use in combination with traditional cytotoxic therapies, in which they will add a new dimension to the anticancer armamentarium.

#### References

1. Folkman, J. Tumor angiogenesis: therapeutic implications. *New Eng. J. Med.*, **285**: 1182-1186, 1971.
2. Teicher, B. A. Systems approach to cancer therapy (antiangiogenics + standard cytotoxic mechanism(s) of interaction). *Cancer Metastasis Rev.*, **15**: 247-272, 1996.
3. Teicher, B. A. Potentiation of cytotoxic cancer therapies by antiangiogenic agents. In: *Antiangiogenic Agents in Cancer Therapy*. B. A. Teicher, editor. Humana Press Inc., Totowa, NJ; pps. 277-316, 1998.
4. Teicher, B. A., Holden, S. A., Ara, G., Alvarez Sotomayor, B., Huang, Z. D., Chen, Y.-N., and Brem, H. Potentiation of cytotoxic cancer therapies by TNP-470 alone and with other antiangiogenic agents. *Int. J. Cancer*, **57**: 920-925, 1994.
5. Teicher, B. A., Dupuis, N. P., Robinson, M., Emi, Y., and Goff, D. Antiangiogenic treatment (TNP-470/minocycline) increases tissue levels of anticancer



- cer drugs in mice bearing Lewis lung carcinoma. *Oncol. Res.*, 7: 237-243, 1995.
6. Herbst, R. S., Takeuchi, H., and Teicher, B. A. Paclitaxel/carboplatin administration along with antiangiogenic therapy in non-small cell lung and breast carcinoma models. *Cancer Chemotherap. Pharmacol.*, 41: 497-504, 1998.
  7. Teicher, B. A., Dupuis, N., Kusumoto, T., Robinson, M. F., Liu, F., Menon, K., and Coleman, C. N. Antiangiogenic agents can increase tumor oxygenation and response to radiation therapy. *Radiat. Oncol. Invest.*, 2: 269-276, 1995.
  8. Gasparini, G., and Harris, A. L. Clinical importance of the determination of tumor angiogenesis in breast carcinoma: much more than a new prognostic tool. *J. Clin. Oncol.*, 13: 765-782, 1995.

#### WORKSHOP 12: SIGNAL TRANSDUCTION TARGETS IN CANCER DRUG DISCOVERY

Redox signaling for cancer drug discovery. Powis, G. *Arizona Cancer Center, University of Arizona, 1515 N. Campbell Av., Tucson, AZ 85724.*

Redox processes are increasingly being recognized as playing an important role in the regulation of cell growth, programmed cell death and cell transformation. Redox signaling pathways offer potential new targets for the development of anticancer drugs. A redox pathway that appears to be particularly important for the growth and death of some cancers is thioredoxin signaling. The thioredoxins are ubiquitous proteins small redox proteins containing a conserved -Trp -Cys-Gly-Pro-Cys-Lys- redox catalytic site. Mammalian thioredoxin family members include thioredoxin-1 (Trx1), mitochondrial thioredoxin-2 (Trx2) and a larger thioredoxin-like protein, p32<sup>Trx4</sup>. The active site Cys residues of thioredoxin are reduced by NADPH and thioredoxin reductase and, in turn reduce oxidized cysteine groups on proteins. When thioredoxin levels are elevated there is increased cell growth and resistance to normal mechanism of programmed cell death. An increase in thioredoxin levels seen in many human primary cancers compared to normal tissue appears to contribute to increased cancer cell growth and resistance to chemotherapy. Mechanisms by which thioredoxin increases cell growth include an increased supply of reducing equivalents for DNA synthesis, activation of transcription factors that regulate cell growth and an increase in the sensitivity of cells to other cytokines and growth factors. The mechanism for the inhibition of apoptosis by thioredoxin are just now being elucidated. Because of its role in stimulating cancer cell growth and as an inhibitor of apoptosis thioredoxin offers a target for the development of drugs to treat and prevent cancer.

Studies with a variety of human primary tumors have shown that thioredoxin-1 is over expressed in the tumor compared to levels in the corresponding normal tissue. The tumors include (with percent showing over expression) lung (50), colon (60), cervix (78), squamous cell (24) and hepatoma (85). We have recently shown by immunohistochemical studies using paraffin embedded tissue sections that thioredoxin-1 expression is increased in more than half of human primary gastric cancers. The thioredoxin-1 levels showed a highly significant positive correlation with cell proliferation measured by nuclear proliferation antigen and a highly significant negative correlation with apoptosis measured by the terminal deoxynucleotidyl transferase (Tunel) assay. Plasma and serum levels of thioredoxin, which in normal individuals are between 10 and 80 ng/ml, have been reported to be elevated almost 2-fold in patients with hepatocellular carcinoma and to decrease following surgical removal of the tumor. Serum thioredoxin is not elevated in patients with other forms of liver disease such as chronic hepatitis or liver cirrhosis.

Thioredoxin-1 acts as a growth factor and is produced by a variety of normal and cancer cells. No evidence has been found of saturable receptor binding of thioredoxin-1 to the surface cells and thioredoxin-1 appears to sensitize cells to growth factors produced by the cell itself. A redox inactive mutant thioredoxin-1 does not stimulate cell growth. Not all growth factors are enhanced by thioredoxin. Interleukin-2 (IL-2) is potentiated up to 1000-fold and basic fibroblast growth factor (bFGF) up to 100-fold by thioredoxin-1. The potentiation of these two growth factors occurs at concentrations of thioredoxin-1 of 10 to 100 nM which are the concentrations typically found in serum (see above). The mechanism for stimulation of IL-2 may include an increase in the alpha subunits of the IL-2 receptor. Thioredoxin-1 has also been shown to increase the expression by cells of a variety of cytokines, including IL-1, IL-2, IL-6, IL-8 and TNF- $\alpha$ .

One of the earliest functions ascribed to bacterial thioredoxin was as a source of reducing equivalents for ribonucleotide reductase which catalyzes the conversion of nucleotides to deoxynucleotides, the first unique step of DNA synthesis. The importance of thioredoxin for eukaryotic ribonucleotide reductase is less well understood and there may be other sources of reducing equivalent. However, irreversible inhibition of thioredoxin reductase by some anti-tumor quinones has been associated with a decrease in cellular ribonucleotide reductase activity. Thioredoxin-1 has been reported to selectively activate the DNA binding of certain transcription factors. This includes the dimeric transcription factor NF- $\kappa$ B that is involved in the cells response to oxidative stress, apoptosis and tumorigenesis, the glucocorticoid receptor and indirectly through the nuclear redox factor Ref-1, the transcription factor AP-1.

We have shown that stable transfection of mouse WEHI7.2 lymphoid cells with human thioredoxin-1 cDNA inhibits apoptosis induced by a variety of agents including dexamethasone, staurosporine, thapsigargin and etoposide. The inhibition of apoptosis caused by transfection with thioredoxin-1 is similar to the pattern of inhibition of apoptosis caused by transfection of the cells with the anti-apoptosis oncogene *bcl-2*. When inoculated into *scid* mice the thioredoxin-1 transfected cells form tumors that grow more rapidly and show less spontaneous apoptosis than vector-alone or *bcl-2* transfected cells, and are resistant to growth inhibition by dexamethasone. Thus, unlike *bcl-2* which offers only a survival advantage and requires other genetic changes to stimulate tumor growth, thioredoxin-1 offers a survival as well as a growth advantage to tumors *in vivo*. Transfection of WEHI7.2 and MCF-7 human breast cancer cells with redox inactive thioredoxin-1 potentiates apoptosis and acts in a dominant negative manner to inhibit tumor growth by the cells *in vivo*. This work provides molecular proof-of-principle that the thioredoxin redox system is a rational target for anticancer drug discovery.

Several compounds have been identified that inhibit thioredoxin signaling. They include PX-12 (1-methylhydroxypropyl 2-imidazoloyl disulfide) which was identified as an inhibitor of thioredoxin binding to the Cys<sup>73</sup> residue. The median IC<sub>50</sub> for growth inhibition of a variety of cell lines by PX-12 is 8  $\mu$ M. PX-12 has been shown to have *in vivo* anti-tumor activity against human tumor xenografts in *scid* mice and chemopreventive activity in *min* (multiple intestinal neoplasia) mice which have a germline mutation in the APC gene seen in familial adenomatous polyposis. The growth inhibition by compound PX-12 in the NCI 60 human tumor cell line panel was significantly correlated with the expression of thioredoxin mRNA. Several other inhibitors of thioredoxin have been identified by the COMPARE program from over 50,000 compounds tested by the NCI as having a pattern of cell killing activity in the 60 human tumor cell line panel similar to PX-12.

Supported by NIH Grants CA48725 and CA77204.

Numbers preceded by a "p" denote page numbers; all others denote abstract numbers.

**A**

- Aapro, M.*, 215  
*Abbensetts, K.*, 473  
*Abbruzzese, J.*, 224, 290, 341, 414  
*Abbruzzese, J. L.*, 225, 300, 336, 380, 412  
*Abdalla, M.*, 163, 473  
*Abdel-Meguid, S. S.*, 382  
*Abel, K. L.*, 510  
*Aboagye, E.*, 491, p. 3871s  
*Abo deeb, A.*, 72, 163  
*Aboody, K. S.*, 460  
*Abradelo, C.*, 620  
*Abrahamsen, N.*, 510  
*Abrahamson, J.*, 209  
*Abrams, R.*, p. 3876s  
*Achilles, E. G.*, 196, 415  
*Achterrath, W.*, 346, 649  
*Acinapura, A. J.*, 72, 163, 473  
*Adams, A.*, 619  
*Adams, J.*, 6, 184, 204, 290, 414  
*Adcock, I.*, 239  
*Adelaide, J.*, 32  
*Adema, G. J.*, 377  
*Adjei, A. A.*, p. 3873s  
*Advani, R.*, 580  
*Afar, D. E. H.*, 154, 156  
*Agarwal, V.*, 340  
*Agha-Mohammadi, S.*, 503  
*Agrawal, S.*, 584  
*Agus, D. B.*, 41  
*Aherne, G. W.*, 572, 659  
*Ahmad, R.*, 692  
*Ahmed, A.*, 694  
*Alley, B.*, p. 3869s  
*Aingorn, E.*, 49  
*Akinaga, S.*, 119, 291  
*Akiyama, S.*, 526  
*Akiyama, T.*, 119  
*Aktas, H.*, 174, 175  
*Akusjarvi, G.*, 366  
*Al-Awar, R.*, 127  
*Alback, C.*, 510  
*Albers, A.*, 150  
*Albertioni, F.*, 431  
*Alberts, D.*, 22  
*Alberts, S.*, 340  
*Albertson, H. M.*, 243  
*Alexander, W. A.*, 94  
*Alexandre, J.*, 7  
*Alford, T.L.*, 664  
*Algazy, K.*, 338, 345, 579  
*Algenstaedt, P.*, 196  
*Alghazi, Y.*, 694  
*Ali, S.*, 239  
*Ali-Osman, F.*, 555  
*Alisaukas, R.*, 454  
*Allen, D.*, 64  
*Allen, M.*, 694  
*Alli, E.*, 685  
*Allis, D. C.*, 238  
*Allred, E. N.*, 415  
*Allsbrook, W. C.*, 19  
*Almiroudis, D.*, 428  
*Alnemri, E.*, 260  
*Alonso, G.*, 165  
*Alonso, S.*, 313  
*Alrawi, S. J.*, 72, 163, 473  
*Altomonte, V.*, 24  
*Alvarez, E.*, 657  
*Alvarez-Salas, L. M.*, 587  
*Amado, R.*, 13  
*An, G. W.*, 291  
*Anasagasti, M. J.*, 65  
*Anderson, M.*, 191  
*Andlon, C.*, 165  
*Andreassi, J. L.*, 178  
*Angers, E.*, 530  
*Angevin, E.*, 7  
*Anthony, A.*, 307, 313  
*Anthony, L.*, 212, 213  
*Anthony, N. J.*, p. 3869s  
*Antolin, S.*, 165  
*Anton, L.*, 165  
*Antonian, L.*, 410  
*Aoki, K.*, 592  
*Appia, F.*, 10  
*Aracil, C.*, 474  
*Arafat, W. O.*, 419  
*Arakawa, F.*, 506  
*Arany, I.*, 386  
*Arasteh, K.*, 12  
*Ardilla-Osorio, H.*, 276  
*Arencibia, I.*, 442  
*Argnani, A.*, 678  
*Ariel, I.*, 407  
*Armand, J. P.*, 7  
*Armand, J-P.*, 348  
*Arnould, S.*, 599  
*Arrastia, C. D.*, 386  
*Arris, C. E.*, 124  
*Artemov, D.*, 397  
*Asao, T.*, 262, 563  
*Ashktorab, H.*, 694  
*Asim, M.*, 692  
*Asimakls, M.*, 115  
*Atkas, H.*, 173  
*Aubert, C.*, 578  
*Augenlicht, L.*, 211  
*Aulitzky, W. E.*, 378  
*Avallone, A.*, 218, 226, 447  
*Averbuch, S.*, 29, 99, 554  
*Avila, J.*, 314  
*Awada, A.*, 20, 513  
*Ayers, D.*, 325  
*Aylesworth, C.*, 332  
*Ayres, M.*, 538  
*Azimahtol Hawariah, L. P.*, 679  
*Azuma, I.*, 158  
*Azure, M. T.*, 199, 200  
*Azzabi, A. S. T.*, 333  
  
**B**  
*Baba, M.*, 494  
*Baccini, C.*, 384  
*Back, T. C.*, 379, 381  
*Baddeley, H.*, 14  
*Badea, I.*, 272  
*Baggs, R.*, 199, 200  
*Baguley, B. C.*, 396, 675  
*Bai, R.*, 630, 643  
*Baichwal, V.*, 635, 637, 651  
*Bailey, H. H.*, 39  
*Baker, C.*, 351  
*Baker, S.*, 1, 332  
*Baker, S. D.*, 319  
*Bakke, S.*, 553  
*Balana, C.*, 330  
*Balcerzak, S. P.*, 223, 553  
*Balestrazzi, E.*, 402  
*Banerjee, D.*, 534  
*Baohua, H.*, 464  
*Baranov, E.*, 59  
*Barazzuol, J.*, 122  
*Barbarino, M.*, 118  
*Bardelli, A.*, 36  
*Barer, F.*, 357  
*Barkhimer, D.*, 12  
*Barlow, H. C.*, 564  
*Barnadas, A.*, 214  
*Barnard, D.*, 362  
*Barret, J-M.*, 322, 674  
*Bartsevich, V. V.*, 251  
*Bar-Yehuda, S.*, 357  
*Basanez, G.*, 429  
*Basart, D.*, 539, 552  
*Basas, J.*, 478  
*Baselga, J.*, 29  
*Bash-Babula, J.*, 685  
*Basilico, C.*, 36  
*Bassano, L.*, 312  
*Basser, R.*, 10  
*Bassetto, M. A.*, 222  
*Bastow, K. F.*, 671  
*Bates, S.*, 641  
*Bates, S. E.*, 553  
*Batey, M. A.*, 543  
*Batist, G.*, 221, 530, 554  
*Baumgart, J.*, 551  
*Baumgarten, J.*, 666  
*Bavetsias, V.*, 565, 566  
*Baynes, R. D.*, 349  
*Bealieu, B. B.*, 343  
*Beauchamp, R. D.*, 21  
*Bechtel, P. E.*, 687  
*Beck, J.*, 378  
*Beckebaum, S.*, 149  
*Becker, K-F.*, 87  
*Becker, M.*, 69  
*Beckmann, H.*, 635, 637, 651  
*Bedi, A.*, 397  
*Beer, T.*, 531  
*Beerheide, W.*, 294  
*Begleiter, A.*, 259  
*Begley, M.*, 114  
*Beijnen, J. H.*, 307, 308  
*Bekesi, J. G.*, 281, 627, 628  
*Belanger, K.*, 1  
*Belcourt, M. F.*, 458, 459  
*Bell, P.*, 233  
*Bellizzi, A.*, 356  
*Bellomy, K.*, 544  
*Bender, J.*, 553  
*Bennett, R. J.*, 607  
*Ben-Porath, I.*, 371  
*Bentzen, C.*, 22  
*Bentzen, C. L.*, 62, 186  
*Benvenisty, N.*, 371  
*Ben-Yosef, T.*, 371  
*Benyumov, A.*, 270  
*Benz, C. C.*, 26, 92  
*Bera, T.*, p. 3869s  
*Berg, W.*, 465  
*Bergeron, R. J.*, 467  
*Berlin, J.*, 614  
*Bermudes, D.*, 459, 501  
*Bernard, H-U.*, 294  
*Bernardi, R. J.*, 37  
*Bernareggi, A.*, 329, 333, 613  
*Bernhard, E. J.*, 193  
*Berry, S.*, 194  
*Bertino, J. R.*, 305, 534, 654  
*Bessette, P.*, 530  
*Bevan, P.*, 512  
*Bevens, S.*, 618  
*Bewley, J. R.*, 657  
*Bhalla, K.*, 76  
*Bharaj, B.*, 481  
*Bhaskaran, V.*, 480  
*Bhat, A. S.*, 321, 632  
*Bhujwalla, Z. M.*, 397  
*Biachwal, V.*, 652  
*Bianco, A. R.*, 28, 584  
*Bianco, R.*, 28, 584  
*Bibby, M. C.*, 470  
*Biedrzycki, B.*, p. 3876s  
*Bigg, D. C. H.*, 665  
*Biglietto, M.*, 218  
*Binderup, L.*, 267  
*Bingcang, A. L.*, 560  
*Birnbaum, D.*, 32  
*Biroccio, A.*, 280  
*Bishop, C.*, 39  
*Bishop, W.*, 77  
*Bittencourt, M.*, 50  
*Black, M. H.*, 482, 484  
*Black, P. M.*, 460  
*Blackledge, G.*, 554  
*Bladou, F.*, 45  
*Blagosklonny, M.*, 134  
*Blagosklonny, M. V.*, 359, 641  
*Blair, I. A.*, 345  
*Blake, R.*, 410, 411  
*Blanke, C. D.*, 21  
*Blasi, M. A.*, 402  
*Blask, D. E.*, 146  
*Bleiberg, H.*, 20, 513  
*Blumenthal, R. D.*, 147, 390, 408, 432, 454, 456  
*Boadu, E.*, 475  
*Bodey, B.*, 74  
*Bodey, B. Jr.*, 74  
*Boeing, A.*, 21, 614  
*Boerner, S.*, 615  
*Boise, L.*, 647  
*Bol, K.*, 513  
*Bold, G.*, 256



- Bold, R. J., 290, 414  
 Bom, D., 560  
 Bombardelli, E., 626  
 Bone, R., 56, 556  
 Bonetti, A., 222  
 Bonham, L., 171  
 Bonner, J. A., 450  
 Bonzon, C., 33  
 Boo, Y. C., 275  
 Borchmann, P., 329  
 Boritzki, T., 543  
 Borner, C., 420  
 Bornmann, W. G. B., 528  
 Bortini, S., 328  
 Bos, A., 337  
 Bos, A. M. E., 328  
 Boucher, C. E., 114  
 Boudouresque, F., 44, 45  
 Boue, S. M., 558  
 Bouker, K. B., 236, 237  
 Bourcier, C., 5  
 Bourgeois, P., 513  
 Bout, A., 393  
 Boutin-Tranchant, M. E., 348  
 Bove, K., 658  
 Bower, K. A., 460  
 Bowers, G., 101  
 Bowman, A., 307  
 Boyer, C., 292  
 Boyle, F. T., 124  
 Boyle, J. O., 690  
 Bozic, C., 245  
 Brabec, R. K., 64  
 Bradbury, E. M., 121  
 Brady, B., 115  
 Brain, E., 308, 309  
 Brana, M. F., 620  
 Brank, A., 295  
 Brattihall, C., 373  
 Braunsdorfer, M., 448  
 Bray, M., 562  
 Breakefield, X. O., 460  
 Breen, J., 143  
 Breistol, K., 71  
 Brekken, J., 52  
 Brewer, G. J., 335  
 Brienza, S., 222  
 Bright, G. R., 249  
 Britten, C., 332  
 Britten, C. D., 319  
 Brodeur, G. M., 105, 106  
 Broggini, M., 303, 310  
 Brognard, J., 355  
 Broidani da Rocha, A., 360  
 Bronstein, M., 32  
 Brooks, H., 127  
 Brooks, R. C., 591  
 Brossi, A., 630  
 Brouwer, E., 518, 550  
 Brown, A., 460  
 Brown, B. A., 244  
 Brown, J. E., 445  
 Brown, J. M., 672  
 Brown, R., 601  
 Browning, R., 21  
 Brueggeheimer, R. W., 321, 632  
 Bruno, T., 280  
 Bruns, C., 290  
 Bruns, C. J., 30, 31, 414  
 Bruns, M., 11  
 Brunton, L. A., 444, 591  
 Brunsch, U., 215  
 Bruskewitz, R., 39  
 Bruzzese, F., 118  
 Bublely, G., 531  
 Buchdunger, P., 100  
 Buchsbaum, D., 419  
 Buchsbaum, D. J., 446, 450  
 Buckheit, R. Jr., 297  
 Buckheit, R. W., 250  
 Buckner, J. C., 143  
 Budillon, A., 118, 226, 447  
 Budman, D. R., 523, 656  
 Buffat, L., 245  
 Bugat, R., 599  
 Bulanahgui, C., 331  
 Bull, C., 668  
 Bullock, S. K., 238  
 Bundred, N. J., 27  
 Buolanwini, J., 555  
 Burak, W. E. Jr., 632  
 Burch, P. A., 143  
 Burchill, S. A., 43  
 Burdelya, L., 109  
 Burger, A. M., 160, 205, 279, 403, 667, 668, p. 3870s, p. 3875s  
 Burgess, M., 8  
 Burke, T. G., 560  
 Burns, M. R., 189  
 Bursten, S., 190  
 Burtles, S., 491  
 Burton, J. D., 385  
 Bush, L. R., 199, 200  
 Busson, P., 276  
 Butler, J., 179  
 Buyukkececi, F., 271  
 Buzzi, A. M., 384  
 Buzzi, G., 384  
 Buzzi, S., 384  
 Bystryn, J.-C., 153  
**C**  
 Cabot, M. C., 593  
 Cacho, M., 620  
 Cai, F., 189  
 Calabrese, C. R., 543  
 Calabro, A., 523, 656  
 Calastretti, A., 422  
 Caldas, A. P. F., 219  
 Callery, P. S., 622  
 Calvert, A. H., 124, 333, 520, 543, 564  
 Calvert, P. M., 333  
 Calvo, F., 131  
 Calvo, L., 165  
 Camboni, G., 329, 613  
 Camboni, M. G., 333  
 Camden, J., 264  
 Cameron, J., p. 3876s  
 Cameron, R., 562  
 Camoratto, A. M., 105, 106  
 Canal, P., 599  
 Cancela, A. I., 219  
 Cane, J., 72  
 Cannon, P., 485  
 Canti, G., 422  
 Cao, Z., 396  
 Capaccioli, S., 422  
 Caplan, S., 383  
 Capogrossi, M., 402  
 Caponigro, F., 118, 218, 226, 447  
 Capri, G., 613  
 Capriati, A., 328  
 Capucio, A., 428  
 Caputo, R., 28, 584  
 Cardellina, J. H., 643  
 Carducci, M. A., 405  
 Carenini, N., 616  
 Carlson, C. L., 189  
 Carlson, M., 664  
 Carlton, P. S., 689  
 Carmichael, J., 333  
 Carney, D., 114  
 Carnochan, P., 591  
 Carrascal, T., 65  
 Carroll, K., 46  
 Carroll, R. J., 228  
 Cartee, L., 123  
 Carter, J. H., 40  
 Casado, A., 214  
 Casavola, V., 356  
 Casper, J. T., 145  
 Cassidy, J., p. 3874s  
 Cassinelli, G., 646  
 Castanotto, D., 590  
 Castle, V., 140  
 Castle, V. P., 427  
 Castro, D., 507  
 Catalin, J., 578  
 Catalona, W. J., 483  
 167  
 Catane, R., 216  
 Catapano, C. V., 342, 625  
 Catlett-Falcone, R., 109, 240  
 Cavacini, L., 241  
 Cecchini, M. G., 274  
 Celis, E., 153  
 Cellarier, E., 598  
 Celli, N., 312, 313  
 Celma, C., 539, 540, 552  
 Cerniglia, G., 193  
 Cerullo, L., 63  
 Cesano, A., 148  
 Cetto, G. L., 222  
 Chabner, B. A., 304  
 Chait, B. T., 253  
 Chakraborty, C., 406  
 Chakravarti, A., 68  
 Chakravarty, S., p. 3872s  
 Challita-Eid, P. M., 90  
 Chambers, A. F., 549  
 Champagne, P., 221  
 Chan, K. C., 27  
 Chan, K. K., 546, 553  
 Chandra, J., 431  
 Chang, D., 13  
 Chang, E. H., 94, 502, 508, 535, 589  
 Chang, K.-S., 441  
 Changery, J., 140  
 Changolkar, A., 173, 174, 175  
 Chao, W., 563  
 Chao, W.-R., 568  
 Chaplin, D., 399  
 Chari, R. V. J., 461, 462  
 Charlton, P., 675  
 Charmsangavej, C., 225  
 Charpentier, D., 530  
 Chatta, G., 531  
 Chatterjee, D., 623  
 Chaturvedi, R., 692  
 Chavan, A. J., 560  
 Chelstrom, L., 680  
 Chemeris, V. V., 610  
 Chen, B. D.-M., 318  
 Chen, C., 318  
 Chen, C.-L., 145, 544, 548  
 Chen, E., 156  
 Chen, H. Y., p. 3869s  
 Chen, J. Y., 596  
 Chen, Q., 191  
 Chen, S. F., 664  
 Chen, T., 443  
 Chen, T.-Y., 47  
 Chen, V. J., 654, 655, 657  
 Chen, Y., 166  
 Chen, Y.-J., 84, 382  
 Chen, Z. S., 526  
 Chenchik, A., 247  
 Chenevert, T. L., p. 3870s  
 Cheng, J. Q., 128, 354  
 Cheresht, D., 97  
 Cherrington, J. M., 410, 411  
 Cheung, S.-T., 443  
 Chi, K. N., 586  
 Chikhale, P., 452  
 Chilikidi, K. Y., 227, 533  
 Ching, L.-M., 396  
 Chinot, O., 44, 57  
 Chipman, M., 10  
 Chishima, T., 59  
 Chiu, M. H., 546  
 Choi, L., 53  
 Choi, S., 135  
 Chollet, P., 598  
 Chong, W., 125  
 Chopra, V., 48  
 Chou, P. M., 521  
 Chou, T.-C., 637  
 Choudry, G. A., 445  
 Chouinard, E., 54  
 Chrest, F. J., 188  
 Christensen, I. J., 492  
 Christman, J. K., 295  
 Christov, K., 433, 485  
 Chrysogelos, S. A., 34  
 Chu, S. S., 125  
 Chung, L. W. K., 70, 274  
 Chung, Y.-J., 500  
 Chyzak, G., 665  
 Ciardiello, F., 28, 584  
 Cicolini, J., 578  
 Cicinmati, V. R., 149, 150  
 Clairmont, C., 501  
 Clark, A., 355  
 Clark, D. L., 651, 652  
 Clark, R. N., 658  
 Clarke, P. A., 230  
 Clarke, R., 34, 235, 236, 237, 242, 516, 567  
 Clause, B., 276  
 Cleary, K., 225  
 Clemens, G. R., 669  
 Clinchy, B., 373  
 Codegoni, A. M., 312  
 Coffey, R. J. Jr., 21  
 Coggeshall, K. M., 89  
 Cohen-Jonathan, E., 193  
 Colacci, A., 678  
 Colajori, E., 2, 3

- Cole, C., 569  
 Cole, R. B., 558  
 Coleman, R. L., 217  
 Collie-Duguid, E. S. R., 571  
 Collins, D. C., 50  
 Collyer, C. A., 619  
 Colombo, T., 626  
 Colomer, R., 214  
 Cornella, G., 218, 226, 447  
 Cornella, P., 218, 226, 447  
 Cornaglio, P. M., 36  
 Connell, C., 16  
 Conner, M. W., p. 3869s  
 Connors, J. M., 96  
 Conrad, N. K., 128  
 Constantinides, P. P., 449  
 Contessa, J., 101  
 Coombes, R. C., 239  
 Cooney, D. S., 89  
 Cooper, B., 113  
 Coppieters, S., 54  
 Coppola, D., 240, 354  
 Cordero, J. A., 552  
 Cordon-Cordo, C., 17  
 Corey, M. J., 208  
 Corney, S. J., 466  
 Cornez, N., 513  
 Cortes-Funes, H., 214, 313  
 Corvalan, J. R. F., 85  
 Cotter, F. E., 582  
 Cottu, P., 309  
 Coughenour, H. D., 632  
 Courtney, C. L., 467  
 Couzi, R., 24  
 Covey, J. M., 417, 546  
 Cozens, R., 256  
 Cracchiolo, B. M., 187  
 Crane, C. H., 225  
 Crawford, E. L., 246  
 Crepin, M., 245  
 Crespo, N. C., 354  
 Cristiano, R. J., 510  
 Croce, C. M., 260  
 Cronin, M., 212, 213  
 Cropp, G., 351  
 Crowley, J. J., 228  
 Croy, R. G., 618  
 Cui, S., 525  
 Cunningham, D., 572  
 Cunningham, J. N., 72, 473  
 Cuq, P., 578  
 Curiel, D. T., 419  
 Curran, D. P., 560  
 Curran, S., 130  
 Curtin, N. J., 124, 520, 543, 564  
 Cushman, M., 631, 663  
 Cutler, D. L., 20  
 Cvitkovic, E., 308, 309  
 Czejka, M., 448
- ## D
- Daliani, D., 6  
 Dalley, B. K., 243  
 D'Alo, F., 595  
 D'Aloisio, S., 325  
 Dalton, W., 240  
 Dalton, W. S., 23, 207, 331, 531  
 Darn, A. M., 210  
 Damia, G., 303  
 Damiano, J., 207  
 Damiano, V., 28, 584  
 Dan, M. D., 96  
 Danenberg, K., 572  
 Danenberg, P., 572  
 Dangerfield, W., 675  
 Daniell, T., 114  
 Danishefsky, S., 25  
 Danks, M. K., 509  
 Datta, S., 33  
 Dauchy, R. T., 146  
 Davidson, K., 264  
 Davidson, K. K., 497, 499  
 Davis, A., 181, 627, 628, 650  
 Davis, C. G., 85  
 Davis, D. W., 30, 31, 83  
 Davis, J. N., p. 3873s  
 Davis, N., 235  
 Davis, T., 194  
 Dawe, R., 612  
 Dawson, M. A., 115  
 D'Cruz, O. J., 285, 286, 287  
 Dean, R. T., 199, 200  
 Debinski, W., 376  
 Debiton, E., 598  
 de Boer, R., 215  
 De Bruijn, P., 577  
 Decker, R., 421  
 Deckman, I., 56, 556  
 De Jonge, M. J. A., 2, 3, 577  
 Delaloge, S., 309  
 Del Bufalo, D., 280  
 DeLeo, A., 149  
 DeLeo, A. B., 150  
 Delfino, C., 44  
 Del Grosso, A., 97  
 de Lima, C., 360  
 Delin, Q., 695  
 Dellaportas, A. M., 331  
 De Lorenzo, S., 118  
 de Luca, M., 65  
 De Lucia, L., 218  
 DeMario, M., 224  
 Dempsey, J., 127  
 de Mulder, P. H. M., 5, 377  
 Deng, J., 391  
 Denner, L., 281  
 Dennis, P., 355  
 Denmy, W. A., 619, 675  
 Dent, P., 101, 436, 647  
 DePaoli, A., 351  
 De Pas, T., 8  
 De Pascual-Teresa, B., 620  
 Depenbrock, H., 7  
 De Placido, S., 28, 584  
 Der, C. J., 231, 370  
 de Roos, W. K., 393  
 Derr, S. M., 461, 462  
 Desai, S. H., 247  
 Desiderio, A., 312  
 Desjarlais, R., 556  
 deSolms, S. J., p. 3869s  
 Desser, L., 168  
 de Valeriola, D., 513  
 De Vos, M. L., 185  
 De Vries, E., 337  
 De Vries, E. G. E., 328  
 de Vries, M. R., 392  
 de Vries, P., 451  
 De Wilde, P., 377  
 de Wilt, J. H. W., 392, 393  
 Dewsbury, P., 124  
 Dexter, D. L., 664  
 Dhar, S., 267  
 Dhawan, D., 142  
 Diab, S., 332, 374  
 Dlamandis, E. P., 481, 482, 483, 484  
 Diasio, R. B., 55, 446  
 Diatchenko, L., 247  
 Diaz, B., 362  
 Diaz, E., 621  
 DiBetta, A. M., 666  
 Dickinson, C., 427  
 Dickinson, C. D., 395  
 Dickson, G., 35  
 Diehl, V., 329  
 Di Gennaro, E., 118, 226, 447  
 Dikmen, Y., 394  
 Di Leo, A., 513  
 Di Leone, L., 219  
 Di Liberti, G., 312  
 Dillehay, L. E., 397  
 DiMaio, H. K., 638  
 Dimitroulakos, J., 277  
 D'Incalci, M., 301, 303, 310, 312, 626, p. 3872s  
 Dinh, T. V., 48  
 Dinney, C. P. N., 30, 83  
 Dionne, C. A., 105, 106  
 Dionne, J., 1  
 Di Palma, M., 309  
 DiPaola, R. S., 17, 263  
 DiPaolo, J. A., 587  
 Dittrich, C., 448  
 Dixon, S. C., 359  
 Djazouli, K., 348  
 Djulbegovic, B., 23  
 Do, C., 115  
 Doetsch, P. W., 600  
 Donald, C. D., 600  
 Donaldson, K. L., 86  
 Donate, F., 395  
 Donehower, R., p. 3876s  
 Dong, J., 670  
 Dong, Y., 285, 287, 288, 617  
 Dongling, Y., 82  
 Donnini, S., 404  
 Door, F. A., 579  
 Dorminy, C., 21, 614  
 Doroshov, J. H., 344  
 Dorr, A., 580  
 Dorr, R., 182  
 Doty, I. N., 227, 533  
 Dotzlaw, J. E., 655  
 Double, J. A., 445, 470  
 Douglas, J. J., 130  
 Douglas, K. T., 569  
 Douglas, T., 24  
 Dow, S. W., 409  
 Dowlati, A., 4, 16, 113  
 Downing, K. H., 640  
 Downs, S., 111  
 Doyle, T. D., 542  
 Drake, J. C., 233  
 Drenghier, R., 574  
 Drew, L., 137  
 Drobnjak, M., 17  
 Du, W., 352, 560  
 Ducreux, M., 216  
 Duflos, A., 322  
 Duffour, H., 57  
 Duggan, B. J., 582  
 DuHadaway, J., 136  
 DuMez, D. D., 284  
 Duncan, R., p. 3873s  
 Dunstan, H., 662  
 Dunstan, H. M., 234  
 Dupont, E., 221  
 Duray, P., p. 3869s  
 Durkacz, B. W., 520  
 Durso, N. A., 643  
 Dutta, S. K., 418  
 Duvadie, R., 125  
 DuVall, M., 417  
 Dvorakova, K., 182  
 Dwaracki, G., 149, 150  
 Dyck, J., 328
- ## E
- Eastman, A., 119  
 Eberwein, D. J., 668  
 Eck, J., 323  
 Eckhardt, G., 9  
 Eckhardt, S. G., 15, 319  
 Edelman, M., 211  
 Eden, A., 371  
 Edgington, T. S., 395  
 Eerenberg, A. J. M., 378  
 Eggermont, A. M. M., 392, 393  
 Eggert, A., 106  
 Egorin, M., 536, 537  
 Egorin, M. J., 622  
 Egyed, M., 439  
 Eilon, G. F., 299  
 Einstein, A. Jr., 531  
 Eiseman, J. L., 536, 622  
 Eisenbrand, G., 129  
 Eisenhauer, E., 325  
 Ek, O., 548  
 Elefante, L., 382  
 El Etreby, M. F., 19, 42, 434  
 Elias, I., 9, 54  
 Elisseyeff, Y., 305  
 Elkin, M., 49, 61, 407  
 Elliot, J. P., 414  
 Elliot, K., 136  
 Elliot, P., 6, 184, 204, 290  
 Ellis, L. M., p. 3877s  
 Ellman, M., 11  
 Elmstie, R. E., 409  
 El-Naggar, A. K., 684  
 Elsasser-Beile, U., 159, 161  
 Elshihabi, S., 198, 266  
 Ely, G., 192  
 Emoto, A., 682  
 Endicott, J. A., 124  
 Endres, S., 122  
 Engebraaten, O., 71  
 Engert, A., 329  
 Erba, E., 312  
 Erlichman, C., 9, 340, 615, p. 3873s



- Ernstoff, M. S., 343  
 Escobar, J., 125  
 Eshima, K., 563  
 Eskens, F., 20  
 Eskens, F. A. L. M., 53  
 Espenan, G., 212, 213  
 Essand, M., p. 3869s  
 Essigmann, J. M., 618  
 Esuvaranathan, K., 387  
 Ethier, S. P., 365  
 Etievant, C., 322, 674  
 Ette, E., 530, 531  
 Etzkorn, M., 206  
 Evans, A. E., 105, 106  
 Evans, D. B., 225  
 Evans, T. R. J., 495  
 Evans, W. K., 221  
 Evrard, A., 578  
 Ewell, J., 630  
 Ewert, D., 136
- F**
- Faber, M., 307  
 Faber, M. N., 5, 20  
 Fabregat, X., 330  
 Fahraeus, B., 373  
 Fahy, J., 322  
 Faircloth, G. T., 301, 304, 306, 310, 311, 312, 314, 315  
 Faivre, S., 329  
 Falardeau, P., 221  
 Fan, G-K., 420  
 Fan, H., 33  
 Fan, S-T., 443  
 Fang, G., 76  
 Fang, J., 416  
 Farbstain, T., 357  
 Farrugia, D., 572  
 Fazzari, M., 41  
 Fedoroff, O. Y., 606, 610  
 Feeley, R., 52  
 Feig, B., 334  
 Feld, R., 554  
 Felix, E., 300  
 Felton, S., 574  
 Feng, G., 202  
 Feng, X., 60  
 Feng, Z., 202  
 Ferdinandi, E. S., 192  
 Ferguson, J. K., 178  
 Fernandes, K., 360  
 Fernandez, A., 415  
 Ferre, R., 125  
 Ferris, C. A., 461  
 Ferry, D., 99  
 Feussner, A., 7  
 Fichtner, J., 69  
 Fiebig, H. H., 160, 205, 279, 403, 666, 667, 668, p. 3870s, p. 3875s  
 Field, T. L., 23  
 Fields, K. K., 23  
 Fields, S. Z., 342  
 Figg, W. D., 359, 553  
 Filiberti, L., 303  
 Fine, R. L., 137  
 Finger, A., 274  
 Fingert, H. J., 585  
 Finiewicz, K., 217  
 Finkelstein, D. M., 68  
 Finnegan, V., 5  
 Finney, R. E., 171, 190  
 Finniss, S., 427  
 Fiorentini, F., 2  
 Fischer, B., 206  
 Fisher, B., 325  
 Fisher, G., 580  
 Fisher, J., 343  
 Fisher, P., 436, 541  
 Fishman, P., 357  
 Flach, J., 186  
 Flessate-Harley, D., 235  
 Fletcher, T. M., 250  
 Floret, S., 22  
 Floridi, A., 280  
 Fluckiger, R., 173, 174, 175  
 Flynn, T. G., 576  
 Fodstad, O., 71  
 Fogler, W. E., 417  
 Fojo, T., 134, 553, 640, 641  
 Folkman, J., 415  
 Fondazione, M., 613  
 Fondren, G., 304  
 Foote, M. Z., 604  
 Ford, H. E. R., 572  
 Fornwald, J., 209  
 Forsyth, C., 316, 317  
 Fortier, A. H., 417  
 Fourie, J., 259  
 Fox, K., 579  
 Fox, W. D., 41  
 Fraley, K. A., 560  
 Franceschi, T., 222  
 Frankmoelle, W. P., 637, 651  
 Fraser, J. E., 549  
 Frazier, M. L., 686  
 Frederiksen, K. S., 510  
 Freedman, R. S., 152, 380  
 Freeman, J. W., 198  
 Freeman, S., 569  
 Frenster, J. H., 624  
 Freudenberg, N., 159  
 Frick, E., 205  
 Friedman-Kien, A., 12  
 Friedmann, Y., 61  
 Friend, S. H., 234, 662  
 Frisch, J., 7  
 Frischmann, K. J., 147  
 Fritz, D., 40  
 Fruehauf, J. P., 476, 517  
 Fry, D., 18  
 Fu, S., 435  
 Fuchs, E., 24  
 Fuentes, A. M., 65  
 Fujieda, S., 420  
 Fujii, H., 326  
 Fujisawa, T., 494  
 Fujiwara, T., p. 3869s  
 Fukumura, D., 196  
 Fukuoka, M., 220  
 Fukushima, K., 262  
 Fukushima, M., 547  
 Fukushima, S., 547  
 Fumoleau, P., 5, 20  
 Furet, H-P., 100  
 Furet, P., 256  
 Furth, P. A., 428  
 Furukawa, T., 526  
 Furuta, K., 132, 547
- G**
- Gabarda, A., 560  
 Gabrielsen, B., 46  
 Gadal, F., 245  
 Gagliardi, A. R. T., 50  
 Galanis, E., 341  
 Galbraith, S. M., 14, 399  
 Galbreath, E., 657  
 Gallagher, M., 338, 345, 579  
 Gallwitz, W. E., 62  
 Galons, J-P., 195  
 Gamble, W. O., 643  
 Gan, Y. H., 387  
 Gandara, D. R., 344, 644  
 Gandhi, V., 538  
 Ganesan, A., 294  
 Gangqin, Z., 695  
 Garcia, D., 22  
 Garcia, M., 330  
 Garcia, R., 453  
 Garcia-Gravalos, D., 314  
 Garde, S. V., 549  
 Gargano, J. A., 10  
 Garland, L., 331  
 Garman, E. F., 124  
 Gastineau, D. A., 143  
 Gatti, L., 616  
 Gautier, A., 245  
 Gazso, L. G., 210  
 Ge, K., 136  
 Geary, R., 580  
 Gelmon, K.A., 325  
 Geneix, J., 32  
 Geoerger, B., 148, 296  
 Georgoussi, Z., 358  
 Gergely, J., 635, 651, 652  
 Germa, J. R., 330  
 Germann, N., 348  
 Gerson, S., 4, 113  
 Gerstmayer, B., 160  
 Gessner, R., 536  
 Ghai, G., 263  
 Ghelmini, M., 3  
 Ghosh, P., 270, 284, 286  
 Ghosh, S., 79, 102, 103, 107, 110, 111, 257, 284  
 Gial, M., 481  
 Giannakakou, P., 134, 640  
 Gianni, L., 550, 613  
 Giannios, J. N., 81, 95, 138, 511, 581  
 Giantonio, B., 345  
 Giavazzi, R., 626  
 Gibbs, J., 193, p. 3869s  
 Gibo, D. M., 376  
 Gibson, A. E., 124  
 Gieselhart, L., 379  
 Gil, T., 513  
 Gilbert C., 665  
 Gilbertson, R. J., 38  
 Gill, P., 12  
 Gillette-Cloven, N., 33  
 Gillies, R., 195  
 Gillon, T., 11  
 Gilmartin, A., 209  
 Gimeno, M., 330  
 Ginopulos, P., 95, 138  
 Gioffre, C., 660  
 Giordano, S., 36  
 Giuliano, A. E., 593  
 Giungi, M., 678  
 Gizas, L. C., 147, 454  
 Gleason-Guzman, M., 22  
 Gleave, M., 583  
 Gleave, M. E., 586  
 Gmeiner, W. H., 457  
 Goan, S-R., 69  
 Goddard, P., 541  
 Goehle, S., 662  
 Goehmann, M., p. 3876s  
 Goel, R., 9, 54  
 Goger, M., 253  
 Goggins, W. B., 68  
 Going, J. J., 495  
 Goker, E., 271, 394  
 Goker, E. N. T., 394  
 Goldenberg, D. M., 91, 93, 147, 385, 390, 408, 432, 454, 456  
 Golding, B. T., 124, 543, 564  
 Golding, B. T. G., 520  
 Goldman, F., 145  
 Goldman, I. D., 471  
 Goldman, L. A., 147  
 Goldschmidt, L., 431  
 Goldstein, S. C., 23  
 Goldwasser, P., 347  
 Gomez-Navarro, J., 419  
 Goncalves, D., 360  
 Gopalakrishnan, R., 689  
 Gore, S. D., 24, 435  
 Gorin, F. A., 121  
 Goss, G., 554  
 Goss, K., 459  
 Govindan, S. V., 91  
 Gracey, S., 12, 13  
 Graham, S. L., p. 3869s  
 Granger, H., 404  
 Grant, S., 117, 123, 421, 436, 647  
 Grant, W., 306, 311, 314, 315  
 Grasberger, B., 556  
 Grasselli, G., 613  
 Gray, F., 235  
 Gray, J. W., 478  
 Gray, L. S., 261, 361  
 Graziano, M. J., 467  
 Green, A., 433  
 Green, D., 51, 56, 556  
 Green, M., 10  
 Green, M. R., 342  
 Green, S. J., 78  
 Greene, G., 567  
 Greim, G., 8  
 Grethlein S. J., 339  
 Grieshaber, C. K., 349, 350, 542  
 Griffin, R. J., 124, 520, 543, 564  
 Griffioen, A. W., 401  
 Griffiths, G. L., 91  
 Griffiths, J., 491  
 Grigg, A., 10  
 Grilli, S., 678  
 Grimm, A., 536  
 Grisoli, F., 57  
 Grivicich, I., 545  
 Grizzle, W. E., 446  
 Grochow, L., 9, p. 3876s  
 Groshen, S., 344  
 Gross-Goupil, M., 347, 348

- Grossi, P., 3  
 Grossman, S., 127  
 Groziak, M., 292  
 Grubbs, C., 433  
 Grupp, S. A., 413, 416  
 Gschwind, P., 100  
 Gu, J., 299  
 Gu, Y., 677  
 Gu, Z., 235, 242  
 Guichard, S., 599  
 Guida, C., 226  
 Guillot, M., 474  
 Guinan, P., 588  
 Gullbo, J., 267  
 Gumerlock, P. H., 644  
 Gunmarsson, P. O., 11  
 Gunzburg, W., 144  
 Guo, Y., 58  
 Gupta, A., 689  
 Gupta, V., 253  
 Gurtler, J., 73  
 Guss, J. M., 619  
 Gussio, R., 254, 255, 640  
 Gustafsson, M. H., 644  
 Gustin, A. N., 446  
 Guyon-Gellin, Y., 186  
 Guziec, F., Jr., 259  
 Guziec, L., 259  
 Guzman, A., 621  
 Guzman, C., 307, 308, 309, 313
- H**
- Haas, N. B., 11  
 Hack, C. E., 378  
 Haga, Y., 494  
 Hager, B., 405  
 Hagstrom, T., 373  
 Haimovitz-Friedman, A., 112  
 Hain, J., 144  
 Hait, W. N., 67, 176, 514, 685  
 Hajjar, G., 93  
 Hakansson, A., 373  
 Hakansson, L., 373  
 Hall, K., 388  
 Haller, D. G., 345, 579  
 Halliday, S. M., 250  
 Hallum, A., 22  
 Halperin, J. A., 173, 174, 175, 192  
 Halsey, J., 580  
 Hamann, H. J., 466  
 Hamburger, A., 536  
 Hamel, E., 630, 631, 643  
 Hamilton, A., 18  
 Hamilton, A. D., 193, 354  
 Hamilton, M., 325, 337  
 Hamilton, P. W., 582  
 Hamilton, S. A., 529  
 Hamilton, W. B., 155  
 Hamilton Stewart, P. A., 445  
 Hamman, B. H., 116  
 Hammond, L., 15, 99, 332, 574  
 Hammond, L. H., 264  
 Han, H., 607, 608  
 Han, T.-Y., 593  
 Han, W. F., 188  
 Han, X., 260  
 Han, Z., 265  
 Hanada, T., 682  
 Hanauske, A., 7  
 Hanauske, A. R., 5, 215, 328  
 Hanauske, A.-R., 187  
 Hanauske-Abel, H. M., 187  
 Hande, K. R., 21, 614  
 Handschuh, G., 87  
 Hanfelt, J., 235  
 Hannah, A., 12, 13, 351  
 Hannigan, E. V., 48, 386  
 Hansen, H. J., 91  
 Hansen-Algenstaedt, N., 196, 415  
 Hao, Z.-M., 589  
 Hapke, G., 649  
 Hara, K., 299  
 Harari, P. M., 88  
 Harbison, M. T., 31, 290, 414  
 Hardcastle, A., 572  
 Harding, M. W., 530, 531  
 Hargreaves, R. H. J., 179  
 Harmon, D., 304  
 Harms, J. F., 66  
 Harper, D., 453  
 Harper, M., 342  
 Harris, A., 53, p. 3876s, p. 3877s  
 Harris, L. C., 509  
 Harris, M., 10  
 Harstrick, A., 346, 649  
 Harter, M., 403  
 Hartley-Asp, B., 11  
 Hartman, D., 40  
 Hartman, G. D., p. 3869s  
 Hartnagel, R. E., 669  
 Hartwell, L. H., 234  
 Harwick, L. C., 151  
 Hashash, A., 537  
 Haslow, K., 51  
 Hass, G. M., 208  
 Hatfield, M., 504  
 Hauenstein, K.-H., 144  
 Haverstick, D. M., 261, 361  
 Hawkins, E., 477  
 Hawkins, L., 507  
 Hayashi, A., 158  
 Hayat, L. H. J., 468  
 Hayes, C., 490  
 Hayes-Sutter, C., 397  
 Haynes, H., 211  
 Hazlehurst, L., 207  
 He, L., p. 3872s  
 Heady, T. N., 261, 361  
 Heasley, E., 451  
 Heddle, J. G., 670  
 Heelan, R. T., 653  
 Heiden, T., 366  
 Heise, C., 504  
 Heller, R., 240  
 Hellmann, K., 524  
 Helsin, M. J., 55  
 Hembrough, W. A., 78  
 Henderson, D. R., 166  
 Hendler, A., 562  
 Hendrickson, E. A., 265  
 Hennebelle, I., 599  
 Henner, W. D., 531  
 Heo, D. S., 141  
 Herbage, I., 168  
 Herbst, R., 29  
 Herceg, Z., 515  
 Herman, T., 198  
 Hermiston, T., 504, 507  
 Hernan, R., 38  
 Herrmann, J. L., 184, 204  
 Hershberger, P. A., 37  
 Hershey, C. M., 117, 238  
 Herzyk, D., 382  
 Heun, J., 206  
 Hibner, B. L., 668  
 Hickey, R. J., 687  
 Hicklin, D. J., 30, 83  
 Hidalgo, M., 15, 332  
 Hidvegi, E. J., 210  
 Higgins, B., 41  
 High, L., 446  
 Highley, M. S., 333  
 Hilchey, S. P., 90  
 Hildebrand, H., 669  
 Hilger, R. A., 551, 649  
 Hill, B. T., 322, 639, 664, 674  
 Hill, J. E., 247  
 Hillen, H. F. P., 401 170  
 Hiller, K., 345  
 Hillman, L., 574  
 Hinds, P., 241  
 Hiroshima, K., 494  
 Hirt, W., 161  
 Hirte, H., 9, 54, 325, 554  
 Hirth, P., 410  
 Hittleman, W. N., 684  
 Hnatowich, D. J., p. 3871s  
 Ho, C.-T., 263  
 Ho, H., 100  
 Ho, M. L., 209  
 Ho, Y. S., 382  
 Hoare, S., 498  
 Hobbs, S. M., 659  
 Hochster, H., 18, 229  
 Hockenbery, D. M., 429  
 Hoekman, H., 307  
 Hoelijmakers, J. H. J., 611  
 Hoekman, K., 469  
 Hoetelmans, R. W. M., 425  
 Hoffman, J., 56, 556  
 Hoffman, L. A., 635, 636, 638  
 Hoffman, R. M., 59  
 Hoffmann, M., 666  
 Hoffmann, T., 149  
 Hoffmeyer, A., 144  
 Hofler, H., 87  
 Hofmann, F., 256  
 Hofmelster, J. K., 89  
 Hohorst, H., 559  
 Holbeck, S. L., 233  
 Holcenberg, J. S., 217  
 Holland, J. F., 627  
 Holle, A., 144  
 Hollenback, D. M., 171  
 Hollister, B. A., 664  
 Holman, P., 427  
 Holmes, S. D., 209  
 Holmlund, J., 579  
 Holmlund, J. T., 580  
 Holowachuk, E. W., 146  
 Holroyd, K., 15  
 Holt, J., 507  
 Hong, K., 26, 92  
 Hong, W. K., 684, p. 3877s  
 Hongtian, X., 82  
 Hoppel, C., 4  
 Hori, H., 201, 561  
 Horn, W., 678  
 Hornicek, F. J., 304  
 Horvath, G., 439  
 Horwitz, S. B., 648, p. 3872s  
 Hoshino, H., 494  
 Hossfeld, K. D., 346  
 Hostein, I., 230  
 Hostomsky, Z., 520, 543  
 Hou, J., 525  
 Houze, J., 635, 651, 652  
 Howell, S. B., 616  
 Howoruszko, A., 33  
 Hruban, R., p. 3876s  
 Hrushesky, W. J. M., 658  
 Hsu, C.-T., 47  
 Hsueh, C.-T., 430  
 Htun, S., 247  
 Hu, L., 676  
 Hu, Z., 302  
 Hua, S., 176  
 Huang, C. H., 472  
 Huang, C.-C., 94  
 Huang, D., 139  
 Huang, M., 297  
 Huang, S., 88, 412  
 Huang, Z., 260  
 Huber, A., 125  
 Huber, C., 378  
 Hubert, R. S., 154, 156  
 Hudes, G. R., 11  
 Hughes, A. N., 333  
 Hugo, E. R., 40  
 Hum, K., 406  
 Humphrey, R., 9, 339, 340  
 Hung, M.-C., 391  
 Hunt, K., 334  
 Hunter, C., 62  
 Hupke, M., 111  
 Hurak, S., 325  
 Hurh, J., 63  
 Hurley, C., 235  
 Hurley, L. H., 499, 603, 604, 606, 607, 608, 609, 610  
 Hurst, B., 40  
 Hurst, S., 293  
 Hurvitz, C., 145  
 Husain, S. R., 180  
 Husband, J., 490  
 Huse, W., 97  
 Hwang, J., 47  
 Hyder, K., 247  
 Hyndman, D. J., 576  
 Hyytinen, E., 70
- I**
- Iavarone, C., p. 3869s  
 Igarashi, T., 326  
 Iglesias, P., 165  
 Iizasa, T., 494  
 Iizuka, M., 353  
 Ikegaki, N., 105, 106



Ilenchuk, T. T., 549  
 Illig, C., 56, 556  
 Iltson, D., 122  
 Ilyina, E. N., 463  
 Imadalou, K., 329  
 Imano, H., 80, 424  
 Imbert, T., 674  
 Imoto, M., 75  
 Ingalls, S., 4  
 Inoue, K., 30, 83, 119, 291  
 Inoue, S., 353  
 Institoris, L., 210  
 Ionina, F., 226, 447  
 Iris, F., 245  
 Isaacs, J. T., 104, 405  
 Isaksson, A., 373  
 Ishikawa, T., 132  
 Ishmael, D. R., 529  
 Israel, R. J., 155  
 Istvan, S., 493  
 Ito, K., 239  
 Ito, Y., 253  
 Itoh, K., 326  
 Ittersohn, M., 501  
 Ivy, P., 4  
 Iyengar, B., 182  
 Izbicka, E., 169, 264, 497, 499  
 Izquierdo, M. A., 330  
 Izzo, J., 684

## J

Jacek, G., 551  
 Jackman, A., 565, 566, 572  
 Jackson, J. R., 209  
 Jacobberger, J., 113  
 Jacobs, J. W., 299  
 Jacobs, M., 12  
 Jacquesy, J.-C., 322  
 Jadeski, L., 406  
 Jaeger, R., 475  
 Jaen, J., 635, 652  
 Jaen, J. C., 637, 651  
 Jaffar, M., 557, 569  
 Jaffee, E. M., p. 3876s  
 Jain, R. K., 196  
 Jaing, J.-D., 628  
 Jakobovits, A., 154, 156  
 Jakowlew, S. B., 248  
 Jan, S.-T., 269, 633, 634  
 Janjan, N. A., 225  
 Jansen, G., 565  
 Janss, A. J., 296  
 Jaquemier, J., 32  
 Jarayaman, M., 663  
 Jarman, M., 258

Jaroszeski, M., 240  
 Jaspers, N. G. J., 611  
 Jasti, B. R., 349, 350, 542  
 Jastrow, A., 477  
 Jeffrey, A. L., 10  
 Jennissen, J. D., 108  
 Jensen, P. B., 673  
 Jhanwar, S., 305  
 Jia, W. Y., 532  
 Jia, X.-C., 85  
 Jiang, C., 546  
 Jiang, G., 140  
 Jiang, J.-D., 281, 627  
 Jiang, K., 354  
 Jimeno, J., 304, 307, 308, 310, 312, 313  
 Jimeno, J. M., 306, 309, 311, 314, 315  
 Jin, S., 302  
 Jing, X., 76  
 Jilidi, R., 276  
 Jodrell, D., 329  
 Johanson, K., 382  
 Johansson, J., 563  
 Johnson, B. E., 128  
 Johnson, C. S., 37  
 Johnson, D. H., 614  
 Johnson, D. N., 437  
 Johnson, K., 344  
 Johnson, L., 507  
 Johnson, L. N., 124  
 Johnson, M., 55  
 Johnson, M. R., 446  
 Johnson, R. K., 84, 382  
 Johnson, T., 544  
 Johnston, D., 153  
 Johnston, S. J., 571  
 Johnston, S. R., 582  
 Jolivet, J., 1  
 Jonak, Z. L., 84, 382  
 Jones, D. A., 243  
 Jones, R., 24  
 Jones, R. E., 596  
 Jong, L., 563  
 Joomprabutra, S., 321, 632  
 Jordan, M. A., 252, 639  
 Jorgensen, T. J., 594  
 Jorna, A. S., 469  
 Joshi, B. H., 375  
 Jounaidi, Y., 575  
 Jourd'han, R., 348  
 Jove, R., 109, 240  
 Judson, I., 490  
 Judy, K. D., 148  
 Juliano, R. L., 251  
 Jun, X., 102, 103  
 Jung, C. P., 112  
 Junghahn, I., 69  
 Juweid, M., 93

## K

Kabbinavar, F., 351  
 Kadow, J. F., 645  
 Kaiser, A. U., 121  
 Kaiser, H. E., 74  
 Kajimura, T., 326  
 Kakpakova, E. S., 463  
 Kamel-Reid, S., 277  
 Kamen, B. A., 217  
 Kamiya, Y., 327  
 Kang, J. O., 141  
 Kang, M. H., 553  
 Kaplan, H. A., 96  
 Karabulut, B., 271  
 Karamysheva, A., 32  
 Karashima, T., 83  
 Karpatkin, S., 60  
 Karpf, A. R., 243  
 Karsenty, G., 45  
 Kasai, S., 201  
 Kasprzyk, P. G., 664  
 Kassab, J., 350, 542  
 Katz, J., 485  
 Katz, R. L., 380  
 Kaubisch, A., 122  
 Kaufman, H., 211  
 Kaufmann, S. H., 615, p. 3873s  
 Kaur, J. A., 143  
 Kavanagh, J. J., 334, 380  
 Kawabe, T., 526  
 Kawakami, K., 374  
 Kawatani, M., 75  
 Kaye, F. J., 128  
 Kaye, S., 313, 495  
 Kazuno, H., 262  
 Keane, P. F., 582  
 Kearney, T. J., 176  
 Keck, J. M., 684  
 Kehrer, D., 337, 577  
 Keith, W. N., 493, 495, 498  
 Kelland, L., 403  
 Kelland, L. F., 126, 258, 444  
 Kelley, M. J., 128  
 Kelling, J., 252  
 Kelloff, G., 433  
 Kelloff, G. J., 676  
 Kellogg, G. E., 254  
 Kelly, J., 582, 653  
 Kelly, W. K., 17  
 Kelnner, M. J., 611, 612  
 Kelsen, D. P., 122, 430  
 Kerr, K., 296  
 Kersey, D., 63, 477  
 Kessler, D., 449  
 Keyes, K. A., 350  
 Khar, A., 167  
 Khare, P. D., 506

171

Khazaeli, M. B., 97, 450  
 Khebir, A., 276  
 Khokhar, A., 334  
 Khoo, H. E., 387  
 Killian, D., 452  
 Killian, J., 244  
 Kim, A. L., 137  
 Kim, E. E., 489  
 Kim, J., 114  
 Kim, J.-H., 567  
 Kim, K. M., 429  
 Kim, K.-M., 500  
 Kim, N. K., 141  
 Kim, W. S., 275  
 Kim, W.-Y., 253  
 Kim, Y., 35  
 Kimler, B. F., 275  
 Kimura, K., 77  
 Kinders, R. J., 208  
 Kindler, H. L., 224  
 King, A., 362  
 King, I., 458, 459, 501  
 Kinney, W. K., 191  
 Kinsella, T., 194  
 Kirkpatrick, D. L., 537  
 Kirkpatrick, J., 198  
 Kirkpatrick, R., 382  
 Kirn, D., 341, 504  
 Kirpotin, D., 26, 92  
 Kishimoto, S., 547  
 Kisker, O., 415  
 Kisselbach, K. D., 105, 106  
 Kitzes, G., 507  
 Klamut, H., 139  
 Klein, H., 216  
 Klein-Szantos, A. J. P., 472  
 Klem, R. E., 585  
 Kline, R., 485  
 Klis, D., 197  
 Knight, L., 193  
 Knighton, D., 125  
 Knox, W. F., 27  
 Ko, Y.-j., 531  
 Koblan, K. S., p. 3869s  
 Kocarek, T. A., 350  
 Kohl, N. E., p. 3869s  
 Kohlhagen, G., 623, 660, 663  
 Kohn, K. W., 670  
 Kohne, C. H., 346  
 Kohne, C.-H., 216  
 Kolesar, J., 574  
 Kondoh, M., 629  
 Kondylis, F., 688  
 Kopreski, M., 11  
 Kosoy, E., 72  
 Kotchevar, A. T., 284  
 Kothari, N., 33  
 Kothe, R., 196

Kow, Y. W., 600  
 Kratz, D., 556  
 Kraut, E. H., 223  
 Kredtke, S., 551  
 Kreis, W., 523, 656  
 Kremmer, E., 87  
 Krett, N. L., 538  
 Kreutz, W., 205, 206  
 Kris, M., 99  
 Kris, M. G., 98, 528, 653  
 Krishnan, P., 671  
 Kroes, R. A., 63, 477  
 Kroger, J., 144  
 Kruczynski, A., 322, 674  
 Krug, L. M., 653  
 Kruit, W. H. J., 378  
 Krupkin, R., 385  
 Kruszewski, M., 405  
 Kruszewski, S., 560  
 Ksenich, P., 113  
 Ktitorova, O. V., 463  
 Kubo, A., 128  
 Kudelka, A., 380  
 Kudelka, A. P., 334  
 Kuduk, S., 25  
 Kuhajda, F. P., 188  
 Kuhn, J., 574  
 Kuhn, J. G., 319  
 Kumar, A., 451  
 Kumor, K., 73  
 Kunick, C., 254  
 Kuo, J., 154, 156  
 Kuo, W.-L., 478  
 Kurachi, K., 64  
 Kuroki, M., 506, 506  
 Kurozumi, S., 547  
 Kusaba, H., 327  
 Kuwano, M., 526  
 Kuznecova, G. V., 324  
 Kuznecova, S. J., 324  
 Kuznecovs, S. J., 522  
 Kwok, T. J., 580  
 Kyle, S., 520  
 Kyprianou, N., 622

## L

Lackey, D., 292  
 Ladd, A., 637  
 Lai, P., 389  
 Laird, A. D., 410, 411  
 Lala, P. K., 406  
 Larrub, J., 293, 662  
 Lamb, J. L., 234  
 Lambert, G., 263  
 Lambert, J. M., 462  
 Lambert, K. J., 449  
 Lambert, Q., 370  
 Lancashire, H., 675

- Lane, D., 126, 541  
 Langecker, P., 12, 13, 490  
 Langer, C. J., 472  
 Langer, M., 323  
 Lantry, L. E., 693  
 Lanzi, C., 646  
 Lapets, O., 249  
 Larocca, G., 249  
 Larocca, L. M., 595  
 Larsen, A. K., 665  
 Larson, R., 217  
 Larsson, R., 267  
 Lathia, C., 9, 339, 340  
 Latreille, J., 221  
 Lattanze, J., 51  
 Laucirica, R., 428  
 Lauer, J., 664  
 Laus, R. L., 143  
 LaVallee, T. M., 78  
 Lavergne, O., 665  
 Lawrence, D. L., 185  
 Lawrence, R., 264, 499  
 Lawrie, A., 124  
 Lawson, T. A., 457  
 Laxa, B., 13  
 Lazarev, A. F., 227, 533  
 Lazarus, H., 113  
 Lazo, J., 537  
 Le, T. X., 458  
 Le, X., 412  
 Leach, M., 490, 491  
 Leach, M. O., 487  
 LeBel, E., 669  
 Le Blanc, B. W., 558  
 Lee, B., p. 3869s  
 Lee, F., 399  
 Lee, F. Y., 645  
 Lee, H., 275  
 Lee, J. E., 225  
 Lee, K., 501  
 Lee, M. H., 275  
 Lee, R. Y., 242  
 Lee, S. J., 275  
 Lee, U., 325  
 Lee, W. L., 532  
 Lee, W-C., 128  
 Leer, L. L., 190  
 Leestma, E., 63  
 Lehmann, F., 513  
 Leitzel, K. E., 519  
 Leland, P., 374  
 Lema, B., 165  
 Lemmon, M., 504  
 Lemoine, M. G., 686  
 Lentzen, H., 160, 161, 279, 323  
 Lenz, G., 360  
 Lenz, H-J., 344  
 Lenzi, R., 225, 380  
 Leonard, T. O., 66
- Leone, G., 595  
 Leone, R., 222  
 Leonessa, F., 242, 516, 567  
 Leong, K., 156  
 Leost, M., 254  
 Lerchen, H. G., 667, 668  
 Lerchen, H-G., 666  
 Lessor, T., 536  
 Lesueur-Ginot, L., 665  
 Leung, D. W., 171  
 Levi, G., 163  
 Levine, A., 145  
 Levitan, N., 16  
 Levitt, N. C., 53  
 Levitzki, A., 109  
 Lew, W., 390, 432  
 Lewandowski, F., 556  
 Lewis, B., 428  
 Lewis, C., 125  
 Lewis, I. J., 43  
 Lewis, J. E., 19  
 Lewis, L. D., 343  
 Lewis, R. A., 190  
 Lewis, R. W., 19, 42, 434  
 Lhomme, C., 348  
 Li, D., 398  
 Li, H. T., 590  
 Li, J., 88  
 Li, J. R., 590  
 Li, J-H., 139  
 Li, K., 633  
 Li, L., 82, 125  
 Li, M., 428  
 Li, Q., 292  
 Li, W., 305  
 Li, Y., 622  
 Li, Z., 458, 501, 553  
 Liang, Y., 42, 434  
 Liao, S., 506  
 Liati, P., 613  
 Liebe, S., 144  
 Liebes, L., 18, 229  
 Lieschke, G., 115  
 Lightcap, E., 6  
 Lightcap, K. D., 342  
 Lihua, F., 82  
 Lin, C-P., 47  
 Lin, D., 690  
 Lin, H-J., 140  
 Lin, H-J. L., 427  
 Lin, J., 140  
 Lin, K., 172, 250  
 Lin, S., 459  
 Lin, S. L., 458  
 Lin, S-Y., 391  
 Lincoln, D. W., 658  
 Linder, S., 366, 367, 368  
 Ling, Y-H., 627, 628
- Link, A., 254  
 Lipp, R., 346  
 Lipton, A., 519  
 Lister-James, J., 199, 200  
 Liu, A., 352  
 Liu, C., 395  
 Liu, C. N., 192  
 Liu, C-W., 489  
 Liu, D. X., 260  
 Liu, F-F., 139  
 Liu, H. Y., 532  
 Liu, J., 457, 563  
 Liu, S. C., 472  
 Liu, W., p. 3877s  
 Liu, X. F., p. 3869s  
 Liu, X-P., 103, 107, 108, 203, 289, 440, 548  
 Liu, Y-Y., 593  
 Livant, D.L., 64  
 Llorens, M. A., 330  
 Lloveras, B., 214  
 Lluch, A., 214  
 Lo, C-M., 443  
 LoBuglio, A., 97  
 Lockyer, S. D., 557  
 Loercher, A., 380  
 Logacheva, N., 438  
 Logan, T., 35  
 Logothetis, C. J., 6, 184, 204  
 Lohr, M., 144  
 Loktionova, N. A., 661  
 Loos, W., 337  
 Lopez, G., 347  
 Lopez, S., 539, 640  
 Lopez-Berenstein, G., 334  
 Lopez-Lazaro, L., 308  
 Lopez Pedrola, P., 620  
 Lorimer, I., 554  
 LoRusso, P., 29  
 LoRusso, P. M., 350, 542  
 Lotan, R., p. 3877s  
 Lou, X., 501  
 Lovely, C. J., 632  
 Lovoy, E., 46  
 Low, K. B., 501  
 Lowe, A., 341  
 Lu, H., 315  
 Lu, J., 427  
 Lu, L., 516  
 Lu, T., 609  
 Lubet, R., 433  
 Lubet, R. A., 676, 693  
 Lucktong, A., 437  
 Ludlow, C., 662  
 Lukinius, A., 267  
 Lurn, B., 580  
 Lundgren, K., 125
- Lunec, J., 38  
 Luo, L. Y., 482, 484  
 Lush, R., 531  
 Lush, R. M., 23, 331  
 Lynch, D. F., 688
- M**
- Maccio, A., 389  
 MacDonald, J. R., 198, 266, 319, 612  
 Macdonald, T. L., 261, 361  
 MacEwen, E. G., 409  
 Macey, D., 97  
 Mack, P. C., 644  
 MacKay, K., 343  
 Madan, A., 397  
 Madary, A. R., 225  
 Madden, T., 300, 336  
 Maddox, A-M., 29  
 Maddox, J., 73  
 Madelmont, J-C., 598  
 Madraswala, R., 156  
 Maegley, K., 520  
 Maffe, A., 36  
 Mages, J., 87  
 Magklara, A., 483  
 Mahajan, S., 79, 102, 107, 111, 257  
 Mahany, J. J., 331  
 Mahendran, R., 387  
 Mahoney, B., 195  
 Maier, C., 382  
 Maiese, K., 41  
 Maiti, P. K., 96  
 Majka, S., 4  
 Makower, D., 211  
 Maley, F., 658  
 Malinge, S., 245  
 Malkas, L. H., 687  
 Maloney, A., 230, 258  
 Maloney, T., 212, 213  
 Manchanda, R., 199, 200  
 Mandic, A., 367, 368  
 Mangel, L. C., 210  
 Mani, S., 224  
 Manley, P. W., 256  
 Mans, D. R. A., 219, 360, 545  
 Mansfield, P., 334  
 Mansfield, R., 10  
 Manson, L. A., 157, 162  
 Manthey, C. L., 51, 56, 556  
 Mantovani, G., 218, 389  
 Mantovani, R., 301  
 Manziona, L., 218
- Mao, C., 102, 103, 107, 269, 273, 320, 633, 634  
 Mao, H., 192  
 Mao, L., 684  
 Marasco, C., 295  
 Marchenay, C., 598  
 Marchini, S., 310  
 Marcolin, P., 226, 447  
 Marcu, M. G., 363  
 Margitich, D., 501  
 Maris, J. M., 413  
 Marko, D., 129  
 Marks, J. D., 26, 92  
 Markwart, S., 64  
 Marquis, S., 46  
 Marres, H. A. M., 377  
 Marriage, H., 541  
 Marsais, J., 664  
 Marshall, M. S., 362  
 Marsoni, S., 613  
 Martello, L. A., 648  
 Martin, J. J., 65  
 Martin, P. M., 44, 57  
 Martin, P-M., 45  
 Martinez, M., 330  
 Martini, M., 595  
 Marugan, J. J., 51  
 Marullo, M., 402  
 Marwaha, S., 148  
 Mascolo, M. G., 678  
 Massa, E., 218, 389  
 Massuti, B., 214  
 Mather, R., 53  
 Matico, R., 209  
 Matli, M. R., 418  
 Matsukawa, S., 420  
 Matsuzaki, I., 80  
 Mattem, M. R., 84  
 Matthews, S., 554  
 Matulonis, U., 530  
 Matzke, B., 680  
 Maurey, K., 46  
 Maurizis, J-C., 598  
 Maxwell, A., 670  
 Maxwell, R., 14, 491  
 Mayer, S., 346  
 Mayerson, S., 383  
 Mayo, K. H., 401  
 Mazarakou, G., 358  
 McCabe, F. L., 84, 382  
 McCabe, S., 513  
 McCaffrey, T. M., 187  
 McCarthy, K., 212, 213  
 McConkey, D. J., 30, 31, 83, 184, 204, 290, 414  
 McCormack, T., 6  
 McCormick, K., 379



- McCown, T., 488  
 McDaid, H. M., 648  
 McDermott, L. N., 687  
 McDonough, C. B., 460  
 McFadyen, M. C. E., 573  
 McFall, A. J., 370  
 McGown, A., 403  
 McGrath, C. F., 254, 255  
 McGuffie, E. M., 625  
 McIsaac, C. E., 23  
 McKay, J. A., 130  
 McKenna, W. G., 193  
 McKinney, J., 21, 614  
 McLean, M., 1  
 McLeod, H. L., 130, 571, 573  
 McLone, M., 477  
 McMahan, G., 410, 411  
 McMorris, T. C., 611, 612  
 McQuillan, A., 383  
 McSheehy, P., 491  
 Mechetner, E., 517  
 Mechetner, M., 476  
 Meck, M. M., 509  
 Medberry, P., 409  
 Medina, D. J., 67  
 Medina, J. C., 637, 651, 652  
 Meenakshii, N., 679  
 Mei, Y., 82  
 Meijer, L., 131, 254  
 Mekhaldi, S., 7  
 Melin, C., 565, 566  
 Melis, G., 389  
 Melkourian, Z. K., 437  
 Mellows, G., 512  
 Menargues, A., 552  
 Mendoza, L., 65  
 Mendrinos, S., 688  
 Mengs, U., 159, 160, 161, 279, 466  
 Menon, K., 127, 657  
 Merajver, S. D., 335  
 Merica, E. A., 531  
 Merkouris, M., 358  
 Meshaw, K., 664  
 Mesia, R., 330  
 Messinger, Y., 145, 544  
 Mestan, J., 256  
 Mett, T., 100  
 Meyers, D. E., 197  
 Miao, H-Q., 407  
 Michieli, P., 36  
 Mick, R., 193, 228  
 Mickisch, G. H., 527  
 Middleton, K. M., 181, 627, 628, 650  
 Mikovits, J. A., 172, 250  
 Miles, S., 12  
 Miller, A. R., 198, 266  
 Müller, C., 24  
 Müller, D. S., 217  
 Müller, V. A., 98, 528, 653  
 Müller, W., 383, 554  
 Millikan, R., 6  
 Milroy, R., 495  
 Minami, H., 326  
 Minoia, C., 613  
 Minuzzo, M., 301  
 Mirkin, B. L., 521  
 Mirochnik, Y., 588  
 Mishina, D., 385  
 Misset, J. L., 308, 309  
 Misset, J-L., 347  
 Mistry, P., 675  
 Mitchell, E. P., 345  
 Mitchell, F., 572  
 Mitchell, P. L. R., 10  
 Mitchell, S. C., 156  
 Miyake, H., 583, 586  
 Mkrdichian, E., 63  
 Mockel, B., 161, 279, 323  
 Modrak, D. E., 390  
 Modzelewski, R. A., 37  
 Mohamad, S. B., 561  
 Mohanakrishnan, A. K., 631  
 Mohr, T., 168  
 Molin, M., 366  
 Molina, M. A., 686  
 Molloy, C. J., 51, 56, 556  
 Molpus, K., 332  
 Momand, J., 590  
 Momiyama, H., 80  
 Monardo, C., 626  
 Moneta, D., 3  
 Monia, B. P., 591  
 Monks, A., 233  
 Monroe, P., 574  
 Montero, S., 214  
 Monti, G., 384  
 Monzo, M., 474  
 Moody, C. J., 179  
 Mookerjee, B., 24, 397  
 Moore, B. M., 604  
 Moore, M., 1, 54  
 Moore, T., 223  
 Moossa, A. R., 59  
 Moran, R. G., 177, 178  
 Morbidelli, L., 404  
 Morgan, L. R., 558  
 Morgenstern, K., 114  
 Morris, M. J., 17  
 Morrison, D., 171  
 Morrissey, D. M., 155  
 Morrow, J. D., 21  
 Moskal, J., 63  
 Moskal, J. R., 477  
 Motohashi, S., 494  
 Motoyama, S., 80, 424  
 Motwani, M. V., 112  
 Motzer, R., 465  
 Mozzillo, N., 226, 447  
 Mross, K., 550  
 Mudu, M. C., 389  
 Muggia, F., 18, 229, 344  
 Mulay, M., 13  
 Muldoon, L. L., 488  
 Muller, B., 206  
 Muller, C. Y., 217  
 Muller, H. A. G., 372  
 Muller, P., 144  
 Mundy, G., 62  
 Munger, K., 241  
 Munster, P. N., 25, 364  
 Mura, L., 389  
 Muracciole, X., 57  
 Muradore, I., 312  
 Murakata, C., 291  
 Murgu, A., 113  
 Murgoci, E., 272  
 Murray, G. I., 130, 573  
 Muschel, R. J., 193  
 Mushtaq, C. M., 342  
 Myers, D., 544  
 Myers, D. E., 145, 681  
 Myers, T. G., 233  
 Mynster, T., 492
- N**
- Naasani, J., 496  
 Nagasawa, H., 201, 561  
 Nagata, T., 253  
 Naguibneva, I., 665  
 Nagura, F., 561  
 Nakagawa, K., 128  
 Nakagawa, K., 220  
 Nakagawa, M., 682  
 Nakahara, T., 278  
 Nakajima, S., 268  
 Nakano, M., 592  
 Narla, R. K., 102, 103, 107, 197, 203, 270, 288, 289, 298, 316, 320, 369, 440, 617, 680  
 Narla, R-K., 634  
 Nash, M., 380  
 Navara, C., 79, 102  
 Navara, C. S., 270, 298, 316, 369, 486, 642  
 Neapolitano, C., 694  
 Neckers, L. M., 291, 363  
 Nelson, J., 181  
 Nelson, K., 15  
 Nelson-Taylor, T., 334  
 Nemieboka, N., 536  
 Neumann, C., 69  
 Neumann, J. M., 545  
 Neuwelt, E. A., 453, 488  
 Newell, D. R., 124, 520, 543, 564  
 Newman, A., 319  
 Newman, E. M., 344  
 Newman, R., 6  
 Newman, R. A., 300, 336  
 Ng, I. O. L., 443  
 Ng, K. K., 653  
 Ng, S., 10  
 Ngan, V., 639  
 Nguyen, N., 630  
 Nickel, P., 50  
 Nicklaus, M. C., 670  
 Nicolaou, K. C., 640  
 Nicoletti, M. I., 626  
 Nicolin, A., 422  
 Nicosta, S. V., 354  
 Niederle, N., 216  
 Nielsen, G. P., 304  
 Nielsen, H. J., 492  
 Nielsen, U. B., 92  
 Nielson, U., 26  
 Niesor, E., 22  
 Niesor, E. J., 62, 186  
 Nilsson, K., 267  
 Nishi, K., 121  
 Nitiss, J. L., 670  
 Niu, G., 240  
 Noble, M. E. M., 124  
 Noga, S., 24  
 Nogales, E., 640  
 Nomura, T., 682  
 Nomura, Y., 682  
 Nonomiya, J., 125  
 Nooter, K., 518  
 Nordle, O., 11  
 Nordquist, J. A., 529  
 Nordquist, R. E., 529  
 Norris, D., 512  
 Noyori, R., 132, 547  
 Nudelman, E., 190  
 Nundi, S., 480  
 Nunnensiek, C., 372  
 Nutley, B. P., 541  
 Nye, J., 504, 507
- O**
- Oakley, J. D., 117  
 Obach, R., 539, 540, 552  
 Obata, T., 135  
 Oberg, F., 267  
 Oberhoff, C., 551  
 Obiezu, C. O., 484  
 O'Brate, A., 474  
 Obrocea, M., 343  
 Ochakoskaya, R., 456  
 Ochs, J., 99, 554  
 O'Day, C. L., 189  
 O'Dwyer, P. J., 338, 345, 579  
 Ogawa, J-i., 80, 424  
 Ogg, C., 127  
 Ogle, T. F., 19  
 Oguma, T., 326, 327  
 Ohana, G., 357  
 Ohkura, K., 561  
 Ohnami, S., 592  
 Ohwada, H., 494  
 Ojeda, B., 214  
 Ojima, I., p. 3872s  
 Okiji, S., 675  
 Okuyama, M., 80, 424  
 Oleschuk, C., 259  
 Oliff, A., 193, p. 3869s  
 Olsen, C., 563  
 Olsson, P., p. 3869s  
 Omay, S. B., 271  
 Omer, C. A., p. 3869s  
 O'Neill, K., 145, 544  
 Onetto, N., 325  
 Ono, M., 526  
 Onozawa, Y., 326  
 Oppoliner, A., 355  
 Oratz, R., 18, 153  
 Orbo, A., 475  
 Oraadu, C., 473  
 O'Reilly, E., 122  
 O'Reilly, S., p. 3876s  
 O'Reilly, T., 100  
 Orlando, M., 76  
 Orr, G. A., p. 3872s  
 Orr, R. M., 591  
 Orremius, S., 431  
 Osada, H., 282, 423, 629  
 Osorio, L., 408, 456  
 O'Sullivan, M., 470  
 Otsuji, M., 494  
 Ottaway, J., 54  
 Ouafik, L'H., 44, 45, 57  
 Oviedo, A., 63  
 Owens, K., 155  
 Oza, A., 530  
 Ozbun, L. L., 248  
 Ozer, Z., 79

Ozsaran, A., 394

**P**

Pace, P., 239  
 Pacheco, D., 342  
 Paciotti, G. F., 417  
 Padera, T. P., 196  
 Padhani, A., 490  
 Padley, D. J., 143  
 Paganelli, G., 164  
 Pagani, O., 8  
 Page, C., 140  
 Page, M., 232  
 Pagel, M. A., 488  
 Pagliaro, L., 6  
 Paik, D. S., 238  
 Paillet, C., 7  
 Palakurthi, S. S., 173, 174, 175  
 Palmari, J., 57  
 Palmer, P., 513  
 Pande, G., 167  
 Pantazis, P., 265, 623  
 Papadimitrakopoulou, V. A., 684  
 Papahadjopoulos, D., 26, 92  
 Papandreou, C. N., 6, 184, 204  
 Papatheanassiu, A., 78  
 Paradiso, A., 356  
 Parchment, R. E., 349, 350, 542  
 Parekh, R., 232  
 Park, C., 275  
 Park, C. H., 275  
 Park, H.-J., 618  
 Park, J. S., 141  
 Park, J. W., 26, 92  
 Park, M. H., 275  
 Parmar, T. G., 176  
 Parson, M., 13  
 Partyka, J. S., 23  
 Pasini, F., 222  
 Pastan, I., 87, p. 3869s  
 Patawaran, M. B., 596  
 Patel, B., 127  
 Pathak, S., 70  
 Patnaik, A., 15, 332  
 Patt, Y., 224  
 Pattabiraman, N., 254, 255  
 Patterson, A. V., 505  
 Pautier, P., 348  
 Pavarana, M., 222  
 Pawelek, J., 501  
 Payne, G. S., 487  
 Paz-Ares, L., 313  
 Pearl, L., 258  
 Pearse, H. D., 453

Pearson, A. D. J., 38  
 Peccatori, F., 613  
 Pecker, I., 61  
 Pegg, A. E., 661  
 Pegrarn, M., 292  
 Peillard, L., 578  
 Peiyu, L., 82  
 Pelegrin, A., 578  
 Pellicer, A., p. 3869s  
 Pena, R. L. S., 596  
 Peng, L., 553  
 Penn, L. Z., 277  
 Pennacchietti, S., 36  
 Pepe, S., 118, 584  
 Peraire, C., 539, 540, 552  
 Percheson, P. B., 96  
 Perego, P., 426, 616, 646  
 Peretz, T., 216  
 Perez, R. P., 343  
 Perez-Soler, R., 334, 627  
 Perkins, C., 76  
 Perkins, J. B., 23  
 Perrey, D. A., 298, 369  
 Perrin, D., 674  
 Perrotte, P., 30  
 Perry, D., 633  
 Peshwa, M. V., 143  
 Pestell, K. E., 126  
 Peters, G. J., 545  
 Peters, K. B., 672  
 Peters, R., 563  
 Peterson, K., 465  
 Peterson, P. W., 243  
 Petrucci, R., 402  
 Petrylak, D., 485  
 Pettaway, C., 290  
 Pfaar, U., 100  
 Pfeiffer, B., 559  
 Phillips, P. C., 148, 296  
 Phillips, R. M., 445, 557  
 Pianta, T. J., 458  
 Piccart, M., 513  
 Piccart, M. J., 20  
 Pickering, E. M., 92  
 Pien, C., 6  
 Pienta, K. J., 64  
 Pierconti, F., 595  
 Pietras, R. J., 398  
 Piette, C., 405  
 Pike, J., 501  
 Pili, R., 405  
 Pillot-Brochet, C., 245  
 Pinedo, H. M., 469  
 Pinkerton, C. R., 487  
 Pinn, M. L., 188  
 Pirollo, K. F., 508, 535, 589

Pisters, P. W. T., 225  
 Pitot, H. C., 143  
 Pizer, E. S., 188  
 Platsoucas, C. D., 380  
 Plisov, S. Y., 665  
 Plumb, J. A., 601  
 Plummer, E. R., 333  
 Plunkett, W., 120  
 Podoloff, D. A., 489  
 Pohl, J., 598  
 Polizzi, D., 426  
 Pollok, B. A., 116  
 Pomatico, G., 28  
 Pommier, Y., 602, 623, 660, 663, 670  
 Poondru, S., 349  
 Popadiuk, C., 530  
 Popescu, N. C., 602  
 Portera, C., 31  
 Portielje, J. E. A., 378  
 Poruchynsky, M. S., 637  
 Posey, J., 97  
 Posner, M., 241  
 Potmesil, M., 229  
 Potten, C. S., 27  
 Potter, P. M., 509  
 Poul, M. A., 92  
 Poulsen, H. S., 510  
 Pourquier, P., 602, 623, 660, 661  
 Powis, G., 537, p. 3879s  
 Powrie, R. H., 571  
 Prager, D., 351  
 Pratesi, G., 426  
 Prendergast, G. C., 136, 352  
 Preusser, P., 216  
 Prevost, G. P., 131  
 Eribluda, V. S., 78  
 Price, P., 491  
 Price, S. M., 128  
 Principe, P., 539, 540, 552, 664  
 Priou, F., 5  
 Prise, V., 14  
 Prodromou, C., 258  
 Pronk, L., 313  
 Proulx, L., 1  
 Prunonosa, J., 539, 540  
 Pták, R. G., 250  
 Ptaszynski, M., 325, 337  
 Punt, C. J. A., 5  
 Puri, R. K., 180, 374, 375  
 Purohit, V., 349  
 Purvis, J. D., 614  
 Puskas, A., 439

**Q**

Qu, X., 525  
 Quada, J. C. Jr., 169  
 Quay, S. C., 449  
 Quintero, A., 621

**R**

Raams, A., 611  
 Rabbani, S. A., 58  
 Radinsky, R., 30, 31, 83  
 Raffo, A. J., 137  
 Rafi, M. M., 263  
 Rafique, I., 163  
 Raghunand, N., 195  
 Rago, R., 331, 531  
 Rainov, N. G., 460  
 Raisch, K. P., 450  
 Rait, A., 508, 589  
 Raitano, A. B., 154, 156  
 Raju, R., 72, 163, 473  
 Ramos, A., 620  
 Rancati, F., 422  
 Randle, T., 56, 556  
 Rangan, A., 606, 608, 609, 610  
 Ranson, M., 29, 99  
 Rao, G., 365  
 Rao, L., 167  
 Rao, N., 127  
 Rao, S., p. 3872s  
 Rashidi, H. H., 169  
 Rastegar, S., 156  
 Ratliff, A. F., 217  
 Ravi, R., 397  
 Ravic, M., 5  
 Rawlins, J. T., 243  
 Ray, J., 127  
 Raymond, E., 7, 329, 348  
 Raynaud, F. I., 541  
 Reardon, D., 101  
 Rebbaa, A., 521  
 Reddy, V. G., 142  
 Rees, P., 40  
 Rehemtulla, A., p. 3870s  
 Rehn, M., 404  
 Reich, R., 49  
 Reid, J., 340  
 Reid, T., 341  
 Reilly, R. M., 96, 562  
 Reiter, R. E., 154  
 Remers, W., 182  
 Remick, S. C., 4, 16, 113  
 Remsen, L. G., 453  
 Ren, S., 428

Rendal, E., 165  
 Reshkin, S. J., 356  
 Reyno, L., 325  
 Reynolds, K., 140  
 Reynolds, S. R., 153  
 Rey-Stolle, M. F., 620  
 Rha, S. Y., 497  
 Rheinwald, J., 241  
 Rhyu, M.-G., 500  
 Ricca, A., 280  
 Ricci, R., 595  
 Ricciardi, R. P., 172, 250  
 Riccioni, T., 402  
 Rice, W. G., 294  
 Richardson, R. L., 143  
 Richter, A., 669  
 Riedell, L., 478  
 Riofrio, M., 309  
 Riordan, N. H., 275  
 Ripple, G., 39  
 Rischin, D., 29  
 Riva, A., 626  
 Rivellini, F., 218, 226, 447  
 Roberts, E. F., 655  
 Robertson, K., 16, 113  
 Robey, R., 641  
 Robinson, A. M., 333  
 Robinson, W. A., 115  
 Rocchi, P., 45  
 Rocha Lima, C. M. S., 342  
 RoCHAT, B., 573  
 Roche, D., 635  
 Rodems, S. M., 116  
 Rodgers, A. H., 558  
 Roelvink, M., 328  
 Rogers, F. A., 622  
 Rogers-Graham, K., 370  
 Rogiers, X., 415  
 Rohlf, C., 232  
 Rolhion, C., 598  
 Romain, D., 347  
 Romain, S., 57  
 Romel, L., 341  
 Ronchi, A., 613  
 Rose, L., 345  
 Rose, M., 382  
 Rose, P., 530  
 Rose, P. E., 114  
 Rose, W. C., 645  
 Rosebrook, J., 77  
 Rossell, R., 330, 474  
 Rosen, L., 13  
 Rosen, N., 17, 25, 364  
 Rosen, P., 13, 351  
 Rosen, R. T., 263  
 Rosen, S. T., 538  
 Rasen, T., 651, 652  
 Rosenblatt, J. D., 90



- Rosenblum, M., 380  
 Rosenthal, M., 18  
 Ross, B. D., p. 3870s  
 Ross, D., 179  
 Ross, V. G., 130  
 Rossi, C., 626  
 Rossi, J., 590  
 Rostock, J. C., 216  
 Rota, R., 402  
 Rotaru, M., 272  
 Rothenberg, M. L., 21, 614  
 Rowe, N. M., 72, 473  
 Rowinsky, E., 99, 332, 574  
 Rowinsky, E. K., 15, 319, 449  
 Roy, R., 600  
 Royce, M., 334  
 Rozenblit, A., 211  
 Rozic, J., 406  
 Rubboli, D., 384  
 Rubenstein, M., 588  
 Rubenstein, M. S., 651  
 Rubenstein, S., 652  
 Rubin, A. D., 93  
 Rubin, D., 275  
 Rubin, J., 341  
 Rubinstein, L., 233  
 Rudolph, J., 56, 556  
 Ruf, W., 395  
 Ruhoff, M. S., 146  
 Ruiz, A., 417  
 Rum, G., 439  
 Runowicz, C., 229  
 Ruschel, C., 360  
 Rustin, G. J. S., 14  
 Ruther, U., 372  
 Ruther, W., 196  
 Ryan, K., 563  
 Ryan, W. F., 338, 579  
 Rybalkina, E., 438
- S**
- Sackett, D., 134, 640, 643  
 Sacks, P. G., 690  
 Sadeghi, A., 198  
 Sadura, A., 54  
 Safavy, A., 450  
 Safavy, K., 97  
 Saffran, D. C., 154, 156  
 Safgren, S., 340  
 Safrany, G., 210  
 Sager, G., 475  
 Sahani, P., 480  
 Saito, H., 420  
 Saito, I., p. 3869s  
 Saito, R., 80, 424
- Saito, S., 424  
 Saitoh, Y., 494  
 Sakamuro, D., 136  
 Sakata, I., 268  
 Salas, S. C., 386  
 Salazar, M., 610  
 Saleh, M., 97  
 Sali, A., 253  
 Saller, R., 144  
 Salmon, S., 22  
 Salmos, B., 144  
 Saltz, L., 122  
 Samant, R. S., 66  
 Sampath, D., 120  
 Sanchez, J. J., 474  
 Sanchez, J. M., 474  
 Sandler, A., 77  
 Sandor, V., 553  
 Sandu, J. S., 562  
 Sanghani, P. C., 177  
 Sanghani, S. P., 177  
 Sanihua, Q., 464, 695  
 Sanli, U. A., 271, 394  
 Santabarbara, P., 22  
 Santha, E., 637  
 Santoli, D., 148  
 Sargent, J. M., 524  
 Sartor, O., 212  
 Sarveswaran, J., 495  
 Sasaki, H., 547  
 Sasaki, Y., 326  
 Sato, B., 563  
 Sato, Y., 400  
 Satoh, T., 262  
 Sauer, L. A., 146  
 Sausville, E. A., 124, 172, 233, 250, 254, 255, 364, 403  
 Sauter, P., p. 3876s  
 Sauze, S., 44  
 Savary, C., 152  
 Sawyers, C., 351  
 Saydam, G., 271  
 Sayers, T., 379  
 Schaaf, L., 574  
 Schatzle, S., 129  
 Schellens, J., 215  
 Scheller, A., 372  
 Schellhammer, P. F., 688  
 Scher, H. I., 17, 41, 98, 528  
 Scheulen, M. E., 551  
 Schiavone, N., 422  
 Schilder, R., 472  
 Schlesinger, M., 281  
 Schlom, J., 164  
 Schmid, S. M., 62  
 Schmidt-Ullrich, R. K., 101  
 Schnaper, L., 687  
 Schnee, A., 559
- Schneider, N., 77  
 Schnier, J. B., 121  
 Schnur, G., 113  
 Schoffski, P., 215, 346  
 Scholmerich, J., 205  
 Schorr, K., 428  
 Schrijvers, D., 328  
 Schucter, L. M., 579  
 Schuldiner, O., 371  
 Schuler, M., 378  
 Schulte, T. W., 363  
 Schultz, C., 254  
 Schultz, R., 124  
 Schultz, R. M., 127, 654, 655, 657  
 Schupp, J., 194  
 Schwartzmann, G., 219, 360, 545  
 Schwartz, B., 54  
 Schwartz, G. K., 112, 122, 430  
 Schwarz, T., 159, 161  
 Schweikart, K. M., 417  
 Schwendner, S., 635  
 Schwendner, S. W., 636, 638  
 Scigalla, P., 12  
 Sciortino, D., 224  
 Scorilas, A., 481, 483  
 Scotto, K. W., 302  
 Seaman, F. C., 604  
 Seber, A., 24  
 Sebti, S., 353  
 Sebti, S. M., 193, 354  
 Sedransk, N., 4, 113  
 Seeber, S., 346, 551, 649  
 Sehested, M., 673  
 Seiden, M., 580  
 Seitz, D. E., 655  
 Seki, M., 420  
 Sekine, Y., 494  
 Selby, P. J., 43  
 Semenze, G. L., 397  
 Sentz, D., 536  
 Sepp-Lorenzino, L., 25  
 Seraj, M. J., 66  
 Sessa, C., 2, 3, 8, 613  
 Sette, A., 153  
 Seya, T., 158  
 Seymour, L., 1, 9, 54, 554  
 Seynhaeve, A. L. B., 392  
 Sezgin, C., 271  
 Sguotti, C., 218  
 Shaffer, S. A., 190  
 Shah, N., 133  
 Shahbahrani, B., 476  
 Shaheen, R. M., p. 3877s
- Shalaby, R., 26, 92  
 Shalinsky, D. R., 52  
 Shan, B., 637, 651, 652  
 Shan, S., 260  
 Shao, L., 55  
 Shao, Y., 26  
 Shapiro, R. L., 153  
 Sharkey, R. M., 93  
 Sharma, S., 570  
 Sharp, C., 56, 556  
 Sharp, S., 258  
 Sharp, S. Y., 444  
 Shawver, L. K., 410, 411  
 Shaywitz, I., 72  
 Shenoy, N., 410, 411  
 Shepard, H. M., 292  
 Shepard, R., 531  
 Sherman, C. A., 342  
 Shi, D-F., 609  
 Shi, Q., 412  
 Shi, Y., 677  
 Shibuya, K., 494  
 Shibuya, M., 400  
 Shields, J. M., 231  
 Shigeoka, Y., 326  
 Shigesada, K., 253  
 Shih, C., 127  
 Shilkaitis, A., 433  
 Shilsky, R. L., 224  
 Shimada, Y., 327  
 Shimizu, M., 119  
 Shin, D. M., 684  
 Shiotsu, Y., 291  
 Shipley, W. U., 68  
 Shirakawa, S., 547  
 Shitara, K., 400  
 Shivji, S., 460  
 Shobe, J., 395  
 Shoemaker, R. H., 172, 250  
 Shoihet, J. N., 533  
 Shoshan, M., 366, 367, 368  
 Shtil, A., 207  
 Shtil, A. A., 463  
 Shulte, T. W., 291  
 Shushmanov, S., 32  
 Shustermann, S., 413  
 Shustik, C., 383  
 Shyr, Y., 21  
 Sibley, L., 22  
 Siccardi, A., 164  
 Siddik, Z., 334  
 Siebert, P. D., 247  
 Siegall, C. B., 86  
 Siegel, S. E., 74  
 Siek, A., 13  
 Sikes, R. A., 70  
 Sikic, B. I., 580  
 Silingardi, P., 678
- Silvestri, S., 303  
 Silvy, M., 131  
 Sim, B. K. L., 417  
 Simizu, S., 75, 423  
 Simon, J., 293, 662  
 Simon, J. A., 234  
 Singer, J., 451  
 Singer, J. W., 190  
 Singh, H., 567  
 Singh, N., 142  
 Singh, R. L., 692  
 Sinicrope, F. A., 686  
 Sirotnak, F. M., 98, 528, 653  
 Sitaraman, B., 167  
 Sitja-Arnau, M., 686  
 Siu, L., 15  
 Skaar, T. C., 236, 237, 242  
 Skelton, L., 565, 566  
 Skillings, J., 331, 332, 338  
 Slagle, B., 376  
 Slamon, D., 292  
 Slaton, J. W., 30, 83  
 Slikowski, M., 519  
 Slovins, S. F., 17  
 Slowinska, B., 187  
 Sludden, J., 601  
 Smith, B., 311, 314  
 Smith, C. D., 185  
 Smith, J., 381  
 Smith, P. G., 564  
 Smith, S., 319  
 Smits, B., 143  
 Smoot, D. T., 694  
 Smyth, J., 307  
 Snyder, A. K., 162  
 Snyder, E. Y., 460  
 Soga, S., 291  
 Soignet, S., 465  
 Sola, J., 540  
 Solana, J., 621  
 Soll, R., 556  
 Son, K. K., 388  
 Sondak, V., 140  
 Song, Y. S., 532  
 Sonnichsen, D., 332  
 Soulas, F., 10  
 Sparreboom, A., 53, 337, 378, 518, 550, 577  
 Spears, P., 657  
 Sperzel, M., 669  
 Speyer, J., 229  
 Spicer, D., 344  
 Spinka, T. L., 458  
 Spiro, T., 4, 16, 113  
 Spohn, B., 391  
 Sporleder, H., 545  
 Spriggs, D., 122, 465  
 Sprinz, E., 219

- Spurlino, J., 556  
 Srethapakdi, M., 364  
 Srinivasan, S., 520  
 St. Onge, J.-M., 96  
 Stackhouse, T., 46  
 Staley, C., 225  
 Stamm, N., 127  
 Stappert, H., p. 3875s  
 Stavrovskaya, A., 32, 438  
 Steeves, R. M., 461, 462  
 Stefani, S., 219  
 Stegman, L. D., p. 3870s  
 Steidle, C., 205, 667, 668  
 Stein, C. K., 638  
 Stein, R., 91, 93  
 Steiner, J., 512  
 Stephenson, J., 332  
 Stern, J., 416  
 Stevenson, J. P., 338, 345, 579  
 Stewart, A. J., 512, 675  
 Stewart, B. W., 691  
 Stewart, D., 554  
 Stipanov, M., 21  
 Stockard, C. R., 446  
 Stoicescu, D., 272  
 Stoll, B. R., 196  
 Stoltz, M., 122  
 Stoner, G. D., 689  
 Stoter, G., 378, 518  
 Stover, D., 114  
 Strang, G., 143  
 Stratford, I. J., 505, 557, 569  
 Stratford, M., 16  
 Strathdee, G., 601  
 Stratton-Custis, M., 22  
 Strauch, S., 448  
 Stravrovskaya, A. A., 463  
 Strawn, L. M., 410, 411  
 Strobl, J. S., 437  
 Stromskaya, T., 438  
 Strumberg, D., 663, 670  
 Studer, U. E., 70, 274  
 Sturla, L. M., 43  
 Subasinghe, N., 56, 556  
 Sudbeck, E., 102, 111  
 Sudbeck, E. A., 107, 108, 257  
 Sufrin, J. R., 295  
 Sugimoto, C., 420  
 Sugiyama, H., p. 3869s  
 Sugiyama, K., 119  
 Suh, G. D., 690  
 Sukbuntherng, J., 410  
 Sullivan, D., 331  
 Sullivan, D. M., 23  
 Sullivan, K., 252  
 Sunizawa, T., 526  
 Sun, B.-F., 139  
 Sun, D., 497, 609  
 Sun, F. X., 59  
 Sun, H., 362  
 Sun, L., 410  
 Sun, S.-Y., p. 3877s  
 Sun, W., 345  
 Sunaga, H., 420  
 Sundkvist, E., 475  
 Sundqvist, K.-G., 442  
 Supino, R., 646  
 Supko, J. G., 315  
 Sutton, L. N., 148, 296  
 Suzuki, H., 80, 424  
 Suzuki, M., 132, 494, 547  
 Suzuki, S., p. 3877s  
 Svingen, P. A., p. 3873s  
 Swann, E., 179  
 Swartz, G., 78  
 Sweeley, C., 63, 477  
 Swenerton, K., 530  
 Sybert, K., 46  
 Synold, T. W., 344  
 Szabolcs, M., 485  
 Szankasi, P., 234, 662  
 Sze, D., 341
- T**  
 Taamma, A., 308, 309  
 Tackey, R., 694  
 Tada, Y., 262  
 Taher, M. M., 117, 238  
 Takada, K., 139  
 Takahashi, R., 119  
 Takamizawa, S., 77  
 Takebayashi, Y., 602, 623, 660  
 Takebe, N., 534  
 Takemura, T., 268  
 Takeuchi, Y., 547  
 Talmadge, J., 457  
 Tamagnone, L., 36  
 Tamai, K., 135  
 Tamanoi, K., 326, 327  
 Tamaoki, T., 119, 291  
 Tamura, T., 327  
 Tan, Y.-J., 294  
 Tanabe, M., 563  
 Tanaka, T., 135  
 Tang, C., 410  
 Tang, C.-B., 148, 296  
 Tang, F., 410, 411  
 Tang, N. M., 171  
 Tang, W.-H., 94, 508, 535, 589  
 Tao, Z.-F., p. 3869s  
 Taub, F., 383  
 Taya, Y., 135  
 Taylor, A. P., 408, 432  
 Taylor, C. G., 524  
 Taylor, N. J., 14  
 Taylor, S. M., 178  
 Tchilikidi, N. Y., 533  
 Tee, L., 476, 517  
 Teicher, B. A., 127, 657, p. 3875s, p. 3878s  
 Tekwani, B. L., 692  
 Templeton, D., 675  
 ten Hagen, T. L. M., 392, 393  
 Terada, M., 592  
 Termuhlen, P., 225  
 Terry, K. L., 17  
 Testa, J. R., 128  
 Telef, M., 344  
 Thalmann, G. N., 70, 274  
 Tham, D. A., 409  
 Thangaraj, K., 558  
 Theti, D., 565, 566  
 Thomas, H., 100  
 Thomas, H. D., 543  
 Thomas, J. P., 223  
 Thomas, T., 133  
 Thomas, T. J., 133  
 Thompson, J. P., 376  
 Thompson, M. J., 470  
 Thoolen, M., 465  
 Thoolen, M. J. M. C., 636, 638  
 Thupari, J., 188  
 Thurieau, C., 131  
 Thurman, A., 15  
 Tian, H., 594  
 Tibbles, H. E., 79  
 Tillman, K., 241  
 Timmermans, P., 465  
 Timmermans, P. B. M. W. M., 636, 637, 638  
 Ting, A. E., 294  
 Ting, C.-J., 47  
 Ting, C.-Y., 47  
 Titley, J. C., 126  
 Titley, J. R., 659  
 Titus, S. A., 178  
 Tobu, M., 271  
 Togonon, M. G., 644  
 Toko, T., 563  
 Tolcher, A. W., 583  
 Toledo, L., 114  
 176
- Tomaszewski, J. E., 417  
 Tombal, B., 104  
 Tommasi, S., 356  
 Tong, W., 122, 653  
 Tong, W. P., 17  
 Torres, C., 476  
 Tortora, A., 332, 338  
 Tortora, G., 28, 584  
 Townsend, C. A., 188  
 Townsend, R., 232  
 Toyoshima, K., 158  
 Tozer, G. M., 14, 399  
 Trail, P. A., 86  
 Tran, H. T., 300, 336  
 Tran, S., 35  
 Traxler, P., 100  
 Treich, I., 245  
 Treseler, P. A., 478  
 Tressler, R. J., 596  
 Tripathi, A. K., 692  
 Tromberg, B. J., 560  
 Troxell, J., 297  
 Trueman, L., 498  
 Trulli, S., 382  
 Truman, D., 343  
 Trump, D. L., 37  
 Tsan, R., 31  
 Tsuruo, T., 496  
 Tsuzuki, H., 420  
 Tucker, E., 553  
 Tucker, K., 125  
 Turner, F. B., 178  
 Tustian, A. K., 449  
 Tutting, T., 150  
 Twelves, C., 307, 313  
 Twomey, P., 46  
 Tying, S. K., 386  
 Tzung, S.-P., 429
- U**  
 Uchiuni, T., 526  
 Uckun, F. M., 79, 102, 103, 107, 108, 110, 111, 145, 197, 203, 257, 269, 270, 273, 284, 285, 286, 287, 288, 289, 298, 316, 317, 320, 369, 440, 486, 544, 548, 617, 633, 634, 642, 680, 681  
 Uges, D. R. A., 328  
 Ulick, D., 535  
 Unger, P., 531  
 Upadhyaya, A., 64  
 Urasaki, Y., 602, 623  
 Ustia, R., 271, 394  
 Ustui, T., 629  
 Uto, Y., 201, 561
- V**  
 Vaccari, M., 678  
 Vahrmeijer, A. L., 425  
 Valenti, M. R., 444, 591  
 Valerie, K., 101, 117, 238  
 Valerio, D., 393  
 Valladares-Ayerbes, M., 165  
 Vallian, S., 441  
 Vallis, K., 562  
 Valone, F. H., 143  
 Valota, O., 2  
 Van Brussel, J. P., 527  
 Van de Leemput, E., 513  
 Van den Bosch, S., 8  
 van der Gaast, A., 2, 20  
 van der Kaaden, M. E., 393  
 Van der Schaft, D. W. J., 401  
 van der Veen, A. H., 392  
 Vanderwerf, S. M., 189  
 van der Zee, A., 498  
 Van de Velde, C. J. H., 425  
 Van de Walle, B., 5  
 Van Dierendonck, J. H., 425  
 Vandre, D. D., 632  
 Van Herpen, C. M. L., 377  
 van Hille, B., 674  
 Vanhoef, U., 346, 649  
 Van Nostrand, K., 33  
 van Tiel, S. T., 392  
 Van Zuylen, L., 518, 550  
 Varma, R. K., 128  
 Vasmataz, G., p. 3869s  
 Vassil, A., 263  
 Vassil, A. D., 67, 514  
 Vassilev, A., 633  
 Vassilev, A. O., 79  
 Vaughn, D. J., 338  
 Vauthey, J. N., 225  
 Venkatachalam, T. K., 257  
 Venkataraman, R., 600  
 Verderame, M. F., 66  
 Verdi, E., 333  
 Verdier-Pinard, P., 631  
 Verdon, V., 491  
 Verheul, H. M. W., 469



- Verma, S., 530  
 Vermorken, J., 215  
 Vermorken, J. B., 328  
 Verrill, M. W., 333  
 Verschraegen, C., 380  
 Verschraegen, C. F., 334  
 Verweij, J., 2, 3, 20, 53, 337, 518, 550, 577  
 Vessella, R. L., 208  
 Vickers, S. M., 446  
 Vidal-Vanaclocha, F., 65  
 Vigano, S., 422  
 Vigushin, D. M., 239  
 Vij, U., 480  
 Viktorsson, K., 366, 367, 368  
 Vilageliu, J., 539, 540  
 Villalona-Calero, M., 574  
 Vinogradova, M. M., 463  
 Viosat, I., 131  
 Viski, A., 439  
 Visonneau, S., 148  
 Vivanco, I., 154, 156  
 Vlahou, A., 688  
 Vlodaysky, I., 49, 61, 407  
 Voelcker, G., 559  
 Vogelsang, G., 24  
 Vogt, A., 537  
 Vojnovic, B., 399  
 Vokes, E. E., 224  
 von dem Bruch, K., 666  
 Vongphrachanh, P., 465  
 Von Hoff, D. D., 15, 169, 264, 266, 319, 332, 497, 499, 574  
 Voumvourakis, K., 511, 581  
 Vuk-Pavlovic, S., 143  
 Vyas, V., 176
- ## W
- Wada, M., 526  
 Wadler, S., 18, 211, 229  
 Waggoner, D., 190  
 Wagner, G. S., 410  
 Wagner, S., 245  
 Wagner, T., 144  
 Wagstaff, J., 401  
 Wahl, A. F., 86  
 Wahl, G. M., 292  
 Wainer, I. W., 516  
 Wainman, N., 1  
 Wakelin, L. P. G., 619  
 Wallace, V. P., 560  
 Walling, J., 465  
 Walsh, D. A., 121  
 Walters, C. S., 694  
 Walton, M., 230  
 Walton, M. I., 126, 258, 659  
 Wancewicz, E., 591  
 Wanders, J., 5, 20, 215, 328  
 Wang, B., 412  
 Wang, B-L., 151  
 Wang, J., 562  
 Wang, J. M., 590  
 Wang, J-L., 260  
 Wang, K., 446  
 Wang, L. M., 532  
 Wang, L-Z., 520  
 Wang, N., 190  
 Wang, P., 85  
 Wang, Q. C., 87  
 Wang, S., 647  
 Wang, W., 198, 266  
 Wang, X., 259, 388, 677  
 Wang, X. J., 192  
 Wang, Y., 628, 676, 693  
 Wang, Z., 436, 631, 647  
 Ward, M. D., 176  
 Ward, P. A., 250  
 Ward, Y., 134  
 Warren, R. S., 418  
 Wasinska-Kempka, G., 669  
 Watabe, M., 282  
 Waters, S. J., 198, 266, 612  
 Watkins, S., 127  
 Watson, G., 571  
 Waugh, M., 343  
 Waurzyniak, B., 680  
 Waxman, D. J., 459, 575  
 Weaver, D. A., 246  
 Webb, H. K., 189  
 Weber, C., p. 3876s  
 Weber, K., 159, 160, 466  
 Weber, S., 504  
 Weeks, R. S., 189  
 Weeraratna, A. T., 104  
 Weigang, K., 8  
 Welmer, I., 8  
 Weisfeldt, M., 485  
 Weiss, G., 332  
 Weissbach, L., 304  
 Welsz, I., 628  
 Weitman, S., 264, 319, 449  
 Weitzel, D. H., 632  
 Welch, D. R., 66  
 Welch, J. N., 34  
 Welsh, S. J., 659  
 Wen, J., 76, 77  
 Wen, Y., 391  
 Weng, L-J., 435  
 Wenzel, M., 297  
 Werner, M. H., 253  
 Wesierska-Gadek, J., 515  
 Westaway, S., 590  
 Westphal, K., 8  
 Wetterwald, A., 274  
 Whang-Peng, J., 47  
 Whetstone, J. L., 321  
 Whitacre, C., 113  
 Whitacre, M., 84, 382  
 White, A. J., 520  
 White, A. W., 543  
 White, T., 190  
 Whitehead, W. E., 386  
 Whiteside, T. L., 149  
 Widdison, W. C., 461, 462  
 Wiegand, R. A., 350, 542  
 Wigginton, J. M., 379, 381  
 Wilding, G., 39  
 Wilke, H., 216, 346  
 Willey, J. C., 246  
 Williams, J., 15  
 Williams, J. I., 191, 398  
 Williams, M., 78  
 Williamson, G. J., 524  
 Williamson, K. E., 582  
 Willmann, H., p. 3875s  
 Willson, J. K. V., 4  
 Wilson, I., 14  
 Wilson, K., 56, 556  
 Wilson, L., 252, 639  
 Wiltrout, R. H., 379, 381  
 Wiltrout, T. A., 379, 381  
 Windle, J. J., p. 3869s  
 Winkler, J. D., 209  
 Winski, S. L., 179  
 Wiseman, B., 498  
 Wiseman, R. W., 693  
 Witte, O. N., 154  
 Witter, L. M., 519  
 Wittmack, E. K., 594  
 177
- ## X
- Xiang, J., 419  
 Xiang, L., 535, 589  
 Xiao, H., 235  
 Xiaodong, Z., 82  
 Xiaoping, W., 82  
 Xie, K., 412  
 Xie, Y., 525  
 Xiong, Q., 336  
 Xiyun, Y., 82  
 Xu, L., 94, 502, 508, 535, 589  
 Xu, X., 525  
 Xu, Z., 283
- ## Y
- Yafai, F., 565  
 Yamada, Y., 327, 411, 563  
 Yamaguchi, K., 119  
 Yamaji, H., 494  
 Yamamoto, H., 63, 477  
 Yamamoto, N., 327  
 Yamashita, M., 201  
 Yamori, T., 547  
 Yan, D-H., 391  
 Yan, J., 55  
 Yang, D. J., 489  
 Yang, H., 184, 204  
 Yang, J-M., 67, 514  
 Yang, M., 59  
 Yang, Q., 243  
 Yang, S., 562  
 Yang, X-D., 85  
 Yang, Y., 125, 532  
 Yano, S., 262, 563  
 Yanuka, O., 371  
 Yao, J., 395  
 Yao, K-S., 579  
 Ye, Q., 465  
 Yebra, M. T., 165  
 Yeger, H., 277  
 Yeh, T., 476  
 Yeo, C., p. 3876s  
 Yeslow, G., 11  
 Ying, Z., 456  
 Yokoyama, K., 278  
 Yonekura, K., 411  
 Yongxin, F., 82  
 Yoon, S. J., 141  
 Yoon, S-S., 275  
 Yoshida, T., 592  
 You, H. J., 600  
 You, M., 676, 693  
 Young, R. H., 68  
 Yousef, G. M., 482, 484  
 Yovine, A., 309  
 Yu, D-C., 166  
 Yu, D-F., 489  
 Yu, H., 109, 240  
 Yu, K., 435  
 Yu, N. Y., 596  
 Yu, W-C., 443  
 Yu, W-D., 37  
 Yuan, J., 677  
 Yuan, Z., 622  
 Yuen, A., 580  
 Yusuf, F., 632
- ## Z
- Zabolina, T., 438  
 Zabolina, T. N., 463  
 Zaharevitz, D., 640  
 Zaharevitz, D. W., 254, 255  
 Zahman, S., 336  
 Zahorchak, R., 246  
 Zaninelli, M., 222  
 Zarembo, S., 164  
 Zasloff, M., 191  
 Zavadova, E., 152

- Zaveri, N. T., 568  
Zehr, E. M., 68  
Zeng, Q., 397  
Zervos, P. H., 655  
Zewail-Foote, M., 603  
Zhan, C., 155  
Zhan, Q., 283  
Zhang, C. Z., 685  
Zhang, H., 263, 677  
Zhang, H. Z., 380  
Zhang, K., 543  
Zhang, K. Y. J., 429  
Zhang, M., 556  
Zhang, Q., 525  
Zhang, Y., 387  
Zhang, Z., 693  
Zhang, Z.-J., 260  
Zhao, H., 114  
Zhao, J., 493  
Zhao, R., 471  
Zhao, S.-C., 534  
Zhao, X., 278  
Zheng, F. F., 25, 364  
Zheng, H. H., 546  
Zheng, L. M., 501  
Zheng, Y., 79, 102,  
110, 111  
Zhou, L., 525  
Zhou, Y., 156  
Zhou, Z., 51, 56, 556  
Zhu, J.-W., 561  
Zhu, K., 677  
Zhu, X., 114  
Zhu, Z., 320  
Ziche, M., 404  
Zietman, A. L., 68  
Zimmer, S. G., 560  
Zimmerberg, J., 429  
Zimonjic, D. B., 602  
Zinke, H., 279, 323  
Zimm, K. R., 199  
Zou, H., 52  
Zucchetti, M., 333,  
613, 626  
Zuhowski, E., 536  
Zunino, F., 426, 616,  
646  
Zupi, G., 280  
Zurlo, M. G., 3  
Zwiebel, J., 211



Numbers preceded by a "p" denote page numbers; all others denote abstract numbers.

## A

AE-941 221  
 ABX-EGF 85  
 N-Acetyl cysteine 389  
 $\alpha_1$ -Acid glycoprotein 564  
 Acylfulvene analogs 612  
 Adeno-associated virus 488  
 Adenosine receptors 357  
 Adenovirus, 446, 488, 507  
 Adriamycin 593  
 Advanced cancer 6, 16, 21, 319, 339, 343, 384, 389  
 Aerodigestive tract lesions 684  
 AG-490 109  
 AG3340: *see* Prinomastat  
 AG3430 51  
 AIDS-related Kaposi's sarcoma 12, 219  
 Aldo-keto reductases 576  
 I-Aldophosphamide-perhydrothiazines 559  
 O<sup>6</sup>-Alkylguanine DNA alkyltransferase 598  
 Allelic losses 500  
 17-Allylamino 17-demethoxy geldanamycin 536  
 17-Allylamino 17-demethoxy geldanamycin analogues 258  
 17-Allylamino geldanamycin 230, 364  
 Alpha lipoic acid 389  
 5 $\alpha$ -reductase gene 481  
 9-Aminocamptothecin 336  
 9-Amino-[N-(2-dimethylamino)ethyl]-acridine-4-carboxamide 619  
 Aminopterin 217  
 AML1 253  
 Angiogenesis 397, 404, 405, p. 3877s  
 Angiogenesis inhibitors 416, 490, p. 3876s, p. 3878s  
 Angiogenic factors 48  
 Animal models 69, 71, 693  
 Anoikis 370  
 Antibodies 92  
 Antiestrogen resistance 237  
 Antigen 165  
 Antisense 584  
 Antisense imaging p. 3871s  
 Antisense oligodeoxynucleotides 587  
 Antisense oligonucleotides 582, 588, 589, 590  
 Antitumor agents 259  
 Aplidine 310, 311, 312, 313

APO-1: *see* Fas  
 Apolipoprotein J 597  
 Apoptosis 75, 76, 79, 80, 81, 89, 95, 104, 135, 137, 142, 249, 260, 276, 277, 278, 280, 283, 286, 367, 421, 423, 427, 428, 430, 432, 433, 434, 442, 463, 581, 628, p. 3877s  
 Aprotinin 51  
 i- $\beta$ -D  
 Arabinofuranosylcytosine 660  
 Arsenic trioxide 271, 394  
 Aryl/heterocyclic-2,4'-nitrophenylhydrazones 406, 558  
 Ascites 469  
 L-Ascorbic acid 275  
 5-Aza-2-deoxycytidine 243, 601  
 AZT 642

## B

B lymphocytes 89, 113  
 3-BAABE: *see* 3-Bromoacetylaminobenzoic acid ethyl ester  
*Bacillus Calmette-Guérin* 387  
*Bacillus Calmette-Guérin*-cell wall skeleton 158  
 Bax 419, 420, 595  
 BAY 12-9566 19, 54, 73, 339, 340  
 BBR2778 329  
 BBR3464 333, 612, 613  
 BCH-4556: *see* Troxacitabine  
 Bcl-2 280, 421, 423, 424, 425, 426, 582, 583, 584  
 Benzimidazoles 520, 543, 587  
 Benzopyrone 530  
 Benzothioapyranes 127  
 Berberine 525  
 Beta LT<sup>m</sup> 383  
 $\beta$  pep-25 401  
 B43-Genistein 145  
 Biliary tract cancer 4  
 Bin1 136  
 Biochemoprevention 684  
 Biricodar: *see* Incel<sup>m</sup>  
 Bladder carcinogenesis 159  
 Bladder carcinoma 49, 208, 387, 407, 445, 532, 682, 688  
 Bladder transitional cell carcinoma 582

Blood transfusion 492  
 Blood-brain barrier 452  
 BMS-184476 332, 338  
 BMS-188797 331, 645  
 BN80915 539, 540, 552, 664, 665  
 Bohemine 126  
 Bone marrow endothelium 274  
 Bone marrow transplantation 24, 534  
 Brain tumors 74, 210, 452, 453, 468  
 Breast cancer 34, 58, 133, 167, 214, 235, 236, 237, 239, 280, 344, 365, 391, 481, 530, 591, 677, 681, 685, 687  
 Breast tumors 92, 426, 437  
 4-*epi*-Brefeldin A 561  
 BRMS1 66  
 3-Bromoacetylaminobenzoic acid ethyl ester 281  
 (3'-Bromo-4'-hydroxyphenyl)-amino-6,7-dimethoxyquinazoline: *see* WHI-P154  
 Bronchial lesions 494  
 Bruton's tyrosine kinase 111, 257  
 Bryostatin 1 113, 318, 647  
 Bryostatin C 18  
 BTK 79  
 B<sup>9</sup>thionine sulfoximine 527

## C

C225 30  
 C-7 progesterone analogs 567  
 Cadherin 386  
 E-Cadherin 87  
 Caelyx<sup>®</sup> 348, 447, 448  
 Calanolide derivatives 257  
 Calcitriol: *see* Vitamin D  
 Calcium channel blockers 261, 361  
 Camptothecin 560, 623  
 Camptothecin glycoconjugates 666, 667, 668, 669  
 Cancer Research Campaign (CRC) p. 3871s  
 Cancer vaccines, 150, p. 3876s  
 CA4P: *see* Combretastatin A4 phosphate  
 Carbendazim: *see* FB642  
 Carboplatin 246, 338, 340, 343, 580  
 Carboxylesterase 509  
 Cationic porphyrin 608, 610  
 Cationic porphyrin analogs 609  
 CB300638 566  
 CB300907 566  
 CCI-779 7  
 CD20 89  
 CD30 197  
 CD40 241  
 CD95: *see* Fas/APO-1  
 Cell adhesion antigens 165  
 Cell adhesion-mediated drug resistance 207  
 Cell cycle arrest 120, 132  
 Cell cycle regulators 133  
 Cell death 136, 659  
 Cell differentiation 437  
 Cell growth 40, 568  
 Cell proliferation 428  
 Cell transformation 36, 231  
 Cell-mediated immunotherapy 454  
 Central nervous system tumors 148  
 CEP-701 104  
 CEP-751 104, 105, 106  
 Cervical cancer 48, 294, 386  
 CGS 27023A: *see* MMI270B  
 Chelerythrine 117  
 Chemo-immunotherapy 533  
 Chemoprevention 680, 691, p. 3877s  
 Chemopreventive agents 678  
 Chemotherapy 24, 93, 390, 453, 508, 529, 589  
 Childhood medulloblastoma 38  
 Chimeric molecules 427  
 2-Chloroacetyl-2-demethylthiocolchicine 630  
 3-Chloroacetyl-3-demethylthiocolchicine 630  
 8-Chloro-adenosine 538  
 8-Chloro-cAMP 538  
 N-4-Chlorophenyl-4-(4-pyridyl-methyl)-1-phthalazinamine: *see* PTK787/ZK22584  
 Chondrosarcoma 304  
 Chronobiology 456  
 Chronotherapy 454  
 CHS 828 267  
 CI-980 223  
 CI-1006 467  
 Cisplatin 18, 122, 218, 226, 338, 368, 398, 596, 617, 638

- c-jun* 117, 238  
 Clinical trials 491  
 Clotriazole 174  
*c-Myc* 136, 371, 472  
 COBRA 633  
 COBRA-1 634  
 Colchicine 630  
 Colon adenocarcinoma 665  
 Colon carcinoma 84, 192, 454, 464, 545, 594, 599, 657, p. 3877s  
 Colon tumors 243, 390, 470  
 Colorectal cancer 13, 130, 215, 227, 346, 425, 492, 533, 578, 680  
 Colorectal tumors 60, 457  
 Combretastatin A4 phosphate 14, 399  
 Combretastatin A4 prodrug 16  
 Complementary DNA expression array 247  
 Continuous hyperthermic peritoneal perfusion 464, 695  
 CPP32/caspase-3 81, 581  
 CPT-11: *see* Irinotecan  
 CRC: *see* Cancer Research Campaign  
 CRM197 384  
 CT-2584 190  
 2CTC: *see* 2-Chloroacetyl-2-demethylthiocolchicine  
 3CTC: *see* 3-Chloroacetyl-3-demethylthiocolchicine  
 CWR22 41  
 2-Cyanoazlridines 182  
 CYC201 541  
 CYC202 541  
 Cyclic AMP response element binding protein 358  
 Cyclic GMP 475  
 Cyclin B 255  
 Cyclin D1 130, 359, 684  
 Cyclin-dependent kinase inhibitors 115, 124, 131, 591  
 Cyclin-dependent kinase 1 129, 254, 255  
 Cyclin-dependent kinase 4 inhibitors 128  
 Cyclooxygenase inhibitors 686  
 Cyclooxygenase-1 689  
 Cyclooxygenase-2 430, 689  
 Cyclooxygenase-2 inhibitors 406  
 Cyclopentadienyl complexes 286  
 Cyclophosphamide 459, 575  
 Cyclosporin A 523  
 Cysteine chloromethyl ketone derivatives 369  
 Cytochrome P-450 1B1 573  
 Cytolysis 190  
 Cytosine-5 169  
 Cytosine deaminase 446, 504  
 Cytotoxic therapy p. 3878s  
 Cytotropic heterogeneous molecular lipid 283
- D**  
 D-19575: *see* Glufosfamide  
 Daunorubicin 532  
 DC101 225  
 Deferiprone 187  
 Dehydroepiandrosterone 676  
 Dendritic cells, 146, 147, 149, 150, 151, 152  
 (E)-2'-Deoxy-2'-(fluoromethylene)cytidine: *see* FMdC  
 2'-Deoxyinosine 578  
 Dipeptide: *see* FR901228  
 Desorption ionization time of flight mass spectrometry 688  
 Dexrazoxane 524  
 Diaminothiazoles 125  
 Dibromodulcitol 210  
 N<sup>1</sup>,N<sup>11</sup>-Diethylnorspermine: *see* CI-1006  
 13,14-Dihydro-15-deoxy-Δ<sup>7</sup>-prostaglandin A<sub>1</sub> methyl ester 547  
 Dihydrofolate reductase 534  
 Dihydropyrimidine dehydrogenase gene promoter 571  
 Dimethoxyquinazolines 289  
 5,6-Dimethylxanthenone-4-acetic acid 396  
 Discodermolide 648  
 2,5-Disubstituted-4,8-dibenzylaminopyrimido-[5,4-d]pyrimidines 564  
 DMXAA: *see* 5,6-Dimethylxanthenone-4-acetic acid  
 DNA array technology 230  
 DNA damage 641  
 DNA intercalators 620  
 DNA methyltransferase 169  
 DNA methyltransferase inhibitors 295  
 DNA topoisomerase I 660, 661  
 DNA topoisomerase I poisons 662  
 DNA topoisomerase II 670, 671  
 DNA-Interactive agents p. 3869s  
 Docetaxel 10, 218, 339, 518, 644, 649  
 Dolastatin 10 224, 300  
 Donor lymphocyte infusion 24  
 Doxorubicin 26, 330, 339, 447, 448  
 Drug delivery 195, 452, 456, 458  
 Drug design 259, 260, 273, 555, 570  
 Drug resistance 207, 355, 521, 522, 525, 573, 576, 640  
 Drug targets 181, 206  
 Drug testing p. 3870s  
 DT-diaphorase 259, 444  
 DX-8951f 326, 327  
 Dysplastic aerodigestive tract lesions 684
- E**  
 E7070 5, 94  
 Ecteinascidin 729 604  
 Ecteinascidin 736 604  
 Ecteinascidin 743 301, 302, 303, 304, 305, 306, 307, 308, 309, 310, 594, 602, 603, 604, 660, p. 3872s  
 E2F promoter 441  
 Eicosapentaenoic acid 175  
 Electrochemotherapy 138  
 Elongation factor-2 kinase 176  
 Endometrial cancer 217  
 Endostatin<sup>®</sup> 404, 409, 417  
 Endothelial cells 399  
 EO9 445  
 EO9 analogues 557  
 Epidermal growth factor 562  
 Epidermal growth factor-Gefitinib 681  
 Epidermal growth factor receptor 33, 34, 57, 88  
 Epidermal growth factor receptor tyrosine kinase inhibitors 103  
 Epithelial cancer 385  
 erbB2 214  
 erbB2 receptor 38  
 ES-285 314  
 Esophageal cancer 80  
 Esophageal tumorigenesis 689  
 EST database analysis p. 3869s  
 Estramustine phosphate IV 11  
 Estrogen 519  
 ET-743: *see* Ecteinascidin-743  
 Etoposide 219, 340, 342  
 Ewing's sarcoma 43
- F**  
 F 11782 674  
 Factor H 208  
 Farnesyltransferase 193, p. 3873s  
 Farnesyltransferase inhibitors 352, p. 3869s  
 Fas/APO-1 74, 79, 137  
 FB642 307  
 FdUMP 457  
 Fenretinide 242, 350  
 Fibroblast growth factor 35, 43  
 Flavopiridol 121, 122, 123, 421  
 fit-1 402  
 Fludarabine 120  
 Fluoroquinolones 606  
 5-Fluorouracil 13, 21, 226, 346, 457, 522, 533, 545, 578, 579  
 FMdC 596  
 Folate receptor 565, 566  
 Polyglutamate synthetase 177, 178  
 FR901228 553  
 FTI-277 353, 354  
 Fusion proteins 90, 562  
 FXR activators 186
- G**  
 G3139 17, 583, 585  
 Gall bladder carcinoma 480  
 Gastric carcinoma 216, 500  
 Gastroenteropancreatic malignancy 213  
 Gastrointestinal cancer 341, 380, 695  
 Gemcitabine 31, 83, 497  
 Gene expression analysis 244  
 Gene expression profiles 235  
 Gene therapy 89, 138, 139, 140, 409, 419, 502, 503, 504, 506, 507, 508, 510, 511, 575, 621  
 Gene-directed enzyme-prodrug therapy 505  
 Genes differentially expressed 247  
 Genistein 40, 681  
 Genotoxins 618  
 Genotyping 476  
 Germ cell tumors 372  
 GGTI-298 353  
 Gliial tumorigenesis 477  
 Glioblastoma 114, 203, 360, 511  
 Glioma 44, 57, 63, 376, 521  
 Glucosylceramide synthase antisense 593  
 Glufosfamide 598  
 Glutathione 425



Glutathione S-transferase pi (GSTP1) 532, 555  
 Glycosyltransferase 63  
 GM2-KLH/QS-21 155  
 Gonadotropin-releasing hormone 47  
 G-quadruplex DNA 606, 608  
 Granulocyte colony-stimulating factor 10, 300  
 Granulocyte-macrophage colony-stimulating factor 147, p. 3876s  
 Green fluorescence protein 59, 534  
 Green tea catechins 568  
 Growth modulation index 222

## H

Halofuginone 49, 407  
 Head and neck cancer 218, 226  
 Head and neck squamous cell carcinoma 241, 374, 377, 420  
 Heat shock protein 90 25, 363  
 Heat shock protein 90 inhibitors 293  
 HeLa cells 142  
 Hemiasterlin 643  
 Hemocyanin 155  
 Heparanase 61  
 Hepatitis B virus 443  
 Hepatitis C virus 297  
 Hepatobiliary cancer 224  
 Hepatobiliary tumors 211  
 Hepatocellular carcinoma 81, 439, 443  
 Hepatoma 146  
 HER-2/neu 26, 90, 519, 589  
 Herceptin 41, 543  
 Herpesvirus 172  
 Hexadecyl-PC 581  
 High Content Screening 249  
 High-performance liquid chromatography 349  
 HMG-CoA reductase 277  
 Hodgkin's lymphoma 197  
 Hormone-refractory cancers 499, *see also specific sites*  
 Hormonosensitivity index 45  
 4-HPR: *see* Fenretinide  
 Human herpesvirus 8 250  
 Human papillomavirus type 16 E6 gene 587  
 Human papillomavirus type 16 E6 protein inhibitors 294

HuN901-DM1 461  
 10-Hydroxy-9-dimethylaminomethyl-camptothecin: *see* Topotecan  
 4-(4'-Hydroxyphenyl)-amino-6,7-dimethoxyquinazoline: *see* WHI-P131  
 4-(4'-Hydroxyphenyl)-amino-6,7-dimethoxyquinazoline HCl 108  
 N-(4-Hydroxyphenyl)retinamide: *see* Fenretinide  
 7-Hydroxystaurosporine 119  
 1 $\alpha$ -Hydroxyvitamin D<sub>2</sub> 39  
 Hypoxia p. 3877s  
 Hypoxia-inducible factor-1 $\alpha$  397  
 Hypoxyradiotherapy 250

## I

IARC Handbook 691  
 ICRF-187 673  
 Idirubin derivatives 129  
 IDNS109 626  
 Ifosfamide 144, 487  
 I $\kappa$ B 65  
 Illudin 611  
 Imaging p. 3871s, *see also specific modalities*  
 2-Imidazolyl disulfides 537  
 Immunoglobulin 562  
 Immunoliposomes 26  
 Immunotoxins 87  
 I-motif DNA 610  
*In vitro* assays 678  
*In vivo* testing p. 3870s  
 Incel<sup>™</sup> 530, 531  
 Indenoisoquinolines 663  
 Interferon 386  
 Interferon  $\alpha$ 2b 343, 387  
 Interferon  $\gamma$  147, 385  
 Interferon regulatory factor-1 237  
 Interleukin 2 373, 379, 381  
 Interleukin 4 147, 374  
 Interleukin 4 receptor 375  
 Interleukin 12 109, 377, 378, 379, 380  
 Interleukin 13 376  
 Interleukin 13 receptor 180, 375  
 Interleukin 18 381, 382  
 Invasin 442  
 3-(Iodoacetamido)-benzoylurea 627  
 Iressa<sup>™</sup>: *see* ZD1839  
 Irinotecan 216, 227, 319, 345, 346, 509, 545, 574, 577, 614, 615, 649  
 Iron-responsive element 388

ISI641A: *see* ISIS 3521  
 ISIS 2503 591  
 ISIS 3521 580  
 ISIS 5132 579

## J

Janus kinase 3 inhibitors 107  
 JNK1 368

## K

Kahalalide F 315  
 Kallikrein 2 483  
 Kallikrein-like gene 2 (KLK-L2) 482  
 Kaposi's sarcoma-associated herpesvirus 172  
 Keyhole limpet hemocyanin 155  
 Ki-67 472, 473  
 K-ras 470  
 KT-5555: *see* CEP-701  
 KT-6587: *see* CEP-751

## L

Leflunomide derivatives 111  
 Leflunomide metabolite analogs 110  
 Leflunomide metabolite LFM-A12 102  
 Leucovorin 13, 21, 346, 579  
 Leukemia 79, 123, 217, 298, 524, 525, 647  
 Leukemia, acute 253  
 Leukemia, acute lymphoblastic 145  
 Leukemia, acute myeloid 275  
 Leukemia, chronic myelogenous 291  
 Leukemia, chronic myeloid 692  
 Levofolinic acid 226  
 Licochalcone-A 263  
 Ligand-PEG post-coating 502  
 Liposomes 330, 502  
 LNCaP cells 70  
 L-NDDP 334  
 Lonidamine 280  
 Loss of heterozygosity 479  
 Lung cancer 191, 220, 324, 353, 355  
 Lung cancer, non-small cell 138, 192, 221, 246, 472, 474, 649  
 Lung cancer, small cell 200, 223, 461, 495, 510

Lurtotecan 325, 337  
 Lutetium-177 91  
 LY 231514 654, 655, 656, 657  
 LY 355703 8  
 Lymphoma 595  
 Lysophosphatidic acid acyl transferase- $\beta$  171

## M

Magnetic resonance contrast agents 488  
 Magnetic resonance imaging 485, 490, p. 3870s  
 Magnetic resonance spectroscopy 487  
 Major histocompatibility complex 164  
 Malignancy 21  
 Malonyl-coenzyme-A 188  
 Mammary tumors 433, 636, 638, 676  
 Mannosylerythritol lipid 278, 628  
 Marimastat 220  
 Mathematical modeling 570  
 Matrix metalloproteinase 2 49  
 Matrix metalloproteinase 7 55, 592  
 Matrix metalloproteinase inhibitors 51  
 Medullary thyroid cancer 93  
 Medulloblastoma 38, 105, 296  
 MEKK1 366, 367  
 Melanoma 65, 146, 189, 240, 278, 368, 449, 598, 621, 628, *see also specific sites*  
 Melanoma-associated peptides 153  
 Melphalan 23, 656  
 MEN-10755 328  
 Merkel cell carcinoma 163  
 Met 36  
 Metastasis 59, 60, 62, 64, 65, 67, 71, 146  
 Methotrexate 471  
 2-Methoxyestradiol 78  
 1-Methoxy-2-hydroxy-4-(pentafluorophenylsulphonamido)benzene 636  
 2-Methoxymethyl estradiol 632  
 9-Methylbenz[de]imidazo[4,5-g]isoquinoline-4,6-dione 620  
 Methyl-2-benzimidazolecarbamate: *see* FB642  
 O<sup>6</sup>-Methylguanine 661  
 MGI 114 198, 266, 319

- MICROMAX® 244  
 Micrometastasis p. 3875s  
 Microtubule associated protein 4 685  
 Microtubules 273, 642, 650, p. 3872s  
 Microvasculature 82  
 Mifepristone 19, 42, 434  
 Mistletoe lectin 159, 160, 161, 279, 323, 466  
 Mitomycin-C 119, 430, 574, 695  
 Mitoxantrone 351, 531  
 MK-571 527  
 MMI270B 53  
 Molecular motors 181  
 Monoclonal antibodies 82, 94, 208  
 Morphine 358  
 MSI-1256F: *see* Squalamine lactate  
 MT-21 282  
 Mucin 1 385  
 Multidrug resistance 514, 527, 602  
 Multidrug resistance 1 567  
 Multidrug resistance 1 gene (*MDR1*) 302, 463, 532, 594  
 Multidrug resistance 1 inhibitors 251, 517  
 Multidrug resistance reversing agents 526  
 Multiple myeloma 23, 538  
 Multispecific organic anion transporter 526  
 Multitargeted antifolate: *see* LY 231514  
 Murine double minute chromosome clone number 2 590  
 Mustard 557  
 Mut L homologue 1 601  
 Myeloid malignancies 435
- N**
- NAD(P)H:quinone oxidoreductase 574  
 NAD(P)H:quinone oxidoreductase 1 179, 444  
 Nasopharyngeal carcinoma 139, 276  
 National Cancer Institute 240  
 NC381 192  
 NC384 192  
 NCO-700 299  
 Necrosis 442  
 Neomycin 577  
 neu: *see* HER-2/neu  
 Neuroblastoma 77, 105, 106, 413, 427, 509
- Nitric oxide 388  
 Nitric oxide synthase 506  
 Nitric oxide synthase 2 141  
 Nitric oxide synthase inhibitors 406  
 Non-Hodgkin's lymphoma 96  
 Novobiocin 363  
 NovoMab-G2-scFv 96  
 NQO1: *see* NAD(P)H:quinone oxidoreductase 1  
 NSC-374551: *see* Fenretinide  
 NSC-643315 403  
 NSC-655649 4  
 NSC-698215 542, 608  
 NSC-698216: *see* S(-)XK469  
 NU2058 124, 591  
 NU6027 124, 591  
 Nuclear factor- $\kappa$ B 114  
 NX211: *see* Lurtotecan  
 NX1843 173
- O**
- Oil fires 468  
 Olomoucine 541  
 Oncogene targets 624  
 Oncotopes 162  
 ONYX-015 211, 341, 504  
 Oral carcinogenesis 690  
 ORI 1202 189  
 Ornithine decarboxylase 360  
 Ovarian cancer 33, 152, 285, 380, 489, 530, 551, 646  
 Ovarian tumors 449  
 Oxaliplatin 222, 347, 599, 614, 615  
 Oxovanadium(IV) 285  
 Oxovanadium(IV) complexes 287, 288
- P**
- p16 128, 684  
 p21 359  
 p21-activated protein kinases 362  
 p21<sup>WAF1/CIP1</sup> 131, 436, 594, 641  
 p27 644  
 p53 94, 126, 134, 135, 137, 139, 141, 397, 473, 508, 535, 659, 693  
 p53 14/19 140  
 p202 391  
 Paclitaxel 17, 30, 122, 225, 342, 343, 344, 449, 451, 530, 543, 550, 580, 583  
 Paclitaxel-peptide conjugates 450
- Pancreatic adenocarcinoma 83, 412, 686  
 Pancreatic carcinoma 31, 144, 198, 266, 290, 375, 414, 497, 592, p. 3876s  
 Pancreatic tumors 199, 558  
 Paullones 254  
 PD183805 365  
 Pediatrics 38, 74  
 Peptide-MHC monomers 164  
 Peptidylglycine  $\alpha$ -amidating monooxygenase 44  
 Peripheral blood mononuclear cells 389  
 Peritoneal carcinomatosis or sarcomatosis 334  
 P-glycoprotein 67, 514, 516, 518  
 pH 206  
*Phallus impudicus* 324  
 1,10-Phenanthroline 285, 287  
 Phenylarsonic acid 440  
 Phenylbutyrate 405, 435  
 Phorboloxazole A 316, 317  
 Phosphatidylinositol 190  
 Photoaffinity labeling p. 3872s  
 Photon microscopy 486  
 PHSCN sequence 64  
 PIPER 607  
 Pironetin 629  
 PKI166 100  
 Plasminogen activator inhibitor 1 57  
 Platar: *see* L-NDDP  
 Platelet-derived endothelial cell growth factor 569  
 Platelet-derived endothelial cell growth factor inhibitors 262  
 Platinum drugs 616  
 Pleural effusion 72, 469  
 PNU-159548 2, 3  
 Pookweed antiviral protein 197, 544  
 Poly L-glutamic acid 451  
 Poly(ADP-ribose) polymerase inhibitors 520, 543, 587, 589  
 Polyamines 692  
 Polyethylene glycol post-coating 502  
 Polymerase chain reaction 69, 446  
 Polymerase chain reaction, template repeated 47  
 Polymer-directed enzyme pro-drug therapy p. 3874s  
 Polymer-drug conjugates p. 3873s  
 Poryprenol 522  
 Porphyrin 268, 499
- Positron emission tomography p. 3871s  
 Prednisone 531  
 Prinomastat 52  
 Probenecid 528  
 Pro-drugs p. 3874s  
 Progesterone receptor 480  
 Proliferating cell nuclear antigen 687  
 Promyelocytic leukemia protein 441  
 10-Propargyl-10-deazaamopterin 653  
 Prostaglandin 132  
 Prostate cancer 19, 39, 40, 42, 45, 68, 70, 76, 104, 131, 143, 184, 204, 299, 351, 359, 361, 434, 531, 543, 549, 583, 586, 623, 625, 694, p. 3869s  
 Prostate stem cell antigen 154  
 Prostate tumor inducing-1 gene 592  
 Prostate tumors 508, 588  
 Prostate-specific antigen 483  
 Prostate-specific cell surface antigen 156  
 Proteasome 184  
 Protein kinase A type 1 584  
 Protein kinase C 75, 359  
 Protein kinase inhibitors 114  
 Proteomics 232  
 PS-341 6, 184, 204, 290, 414  
 PSC 833 523  
 Pseudomonas exotoxin A 47  
 PSP-94 549  
 Psychoneuroimmunology 167  
 PTK787/ZK22584 256  
 Pyranonaphthoquinone derivatives 671
- Q**
- QS-21 155  
 Quinolinedisulfides 127  
 Quinolines 437  
 QW8184 449
- R**
- R101933 513  
 Radiation 83, 95, 139, 212  
 Radicicol derivatives 291  
 Radioimmunotherapy 93, 408  
 Radiosensitization 193, 194, 197  
 Radiosensitizers 198  
 Radiotherapy 88, 112, 138, 204, 453, 508, 589



Raf-1 362  
 Raltitrexed 572  
 RANTES 90  
 Rapamycin 296, 422  
 Ras 231, 370, p. 3869s  
 Ras inhibitors 185, 298  
 Re-188 P2045 199, 200, 558  
 Redox signaling p. 3879s  
 Reduced folate carrier 1 471  
 Renal cell carcinoma 35, 180, 373  
 Retinoblastoma gene 677  
 Retinoic acid 386  
 all-*trans*-Retinoic acid 439  
 9-*cis*-Retinoic acid 242  
 13-*cis*-Retinoic acid 405, 690  
 Retinoids 236, 242  
 RIE-1 cells 370  
 Ro-31-8220 265  
 Roscovitine 126  
 RS7 91

## S

S-1 215  
 Salicylic acid derivatives 205, 317  
*Salmonella typhimurium* 458, 459, 501  
 Sandimmune: *see* Cyclosporin A  
 Sarcoma 309  
 SB 408075 84, 462  
 SCH 66336 20  
*Schizosaccharomyces pombe* 616  
 SDZ PSC 833 344  
 SELDI-TOF-MS: *see* Desorption ionization time of flight mass spectrometry  
 Self-peptide 47  
 Sesquiterpene lactone derivatives 621  
 Signal transducer and activator of transcription 1 521  
 Signal transducer and activator of transcription 3 89, 240, 621  
 SN-38: *see* Irinotecan  
 SND47 272  
 Sodium magnetic resonance imaging 485  
 Soft tissue sarcoma 305  
 Solid tumors 2, 5, 10, 94, 97, 122, 182, 275, 300, 307, 313, 314, 325, 328, 330, 333, 336, 342, 348, 513, 528, 612, 614  
 Somatostatin receptor subtype 2 213

SomatoTher<sup>™</sup> 212, 213  
 Sphingomyelin 390  
 SPIKET-P: *see* Synthetic spiroketal pyrans  
 Squalamine 191, 398  
 Squalamine lactate 15  
 Squamous cell carcinoma 473, *see also specific sites*  
 SR-16234 563  
 SR-24023A 22  
 SR-45023A 62  
 SRD5A2 481  
 Stem cell transplantation 416  
 Steroid derivatives 631  
 SU101 351  
 SU5416 13, 411  
 SU6668 410  
 Suppression subtractive hybridization 247  
 S(-)XK469 542, 546, 608  
 Synthetic spiroketal pyrans (SPIKET-P) 269

## T

T138067 465, 635, 637, 651, 652  
 T lymphocytes 151  
 TALL-104 cells 148  
 Tamoxifen 40, 42, 58, 433, 434, 519  
 Taxanes 646  
 Taxol 76, 252, 449, 513, 648, p. 3872s  
<sup>99m</sup>Tc-EC-NIM 489  
 Tea catechins 496  
 TEI-9826: *see* 13,14-Dihydro-15-deoxy- $\Delta^7$ -prostaglandin A<sub>1</sub> methyl ester  
 Telomerase 494, 495, 496, 497  
 Telomerase inhibitors 609  
 Telomerase RNA gene promoter 493, 498  
 Testicular cancer 286, 287  
 Testosterone-repressed prostate message-2 586  
 Tetracycline 503  
 Tetrathiomolybdate 335  
 Thiourea 320  
 Thoracoscopy 72  
 THP-1 cells 318  
 L-Threitol 1,4-bis(methanesulfonate): *see* Treosulfan  
 Thrombin receptor 60  
 Thrombogen 395  
 Thymidine analogs 194  
 Thymidine phosphorylase 569

Thymidine phosphorylase inhibitors 262  
 Thymidylate synthase 292, 572, 655, 657, 658, 659  
 Thymosin  $\beta$ 15 68  
 Tirapazamine 575, 672  
 Tissue factor 395  
 TNP-470 413  
 Tomudex 226, 345  
 TOP-008 299  
 Topotecan 23, 229, 342, 347, 348  
 TRAIL: *see* Tumor necrosis factor-related apoptosis-inducing ligand  
 Transferrin receptor 94  
 Transforming growth factor  $\beta$  248  
 Transitional cell carcinoma 31, 225, 688, *see also specific sites*  
 Translation initiation 173, 174  
 Treosulfan 349, 551  
 Trichostatin A 238, 239  
 Triple helix-forming oligonucleotide 625  
 Trk B 106  
 Troxacitabine 1  
 T138067-sodium 638  
 Tubulin 273, 628, 631, 640, 650  
 $\beta$ -Tubulin 474, 630  
 Tumor growth 109  
 Tumor models p. 3875s  
 Tumor necrosis factor  $\alpha$  458  
 Tumor necrosis factor-related apoptosis-inducing ligand 76  
 Tumor necrosis factor-related apoptosis-inducing ligand receptors 77  
 Tumor xenografts p. 3875s  
 Tumor-associated macrophage count 682  
 TX-1920 201  
 TXU-pokeweed antiviral protein 544

## U

UCN-01: *see* 7-Hydroxystaurosporine  
 UIC2 shift assay 517  
 Urea 320  
 Urinary bladder: *see* Bladder  
 Urokinase plasminogen activator inhibitors 56, 556  
 Uveal melanoma 402

## V

VallGene's Gene Identification 245  
 Valspodar: *see* PSC 833  
 Vanadium(IV) 286  
 Vanadocene diacetate 270  
 Vanadocene dichloride 270  
 Vanadocenes 284, 286  
 Vascular endothelial growth factor 412, 469  
 Vascular growth factor 408  
 VGID<sup>™</sup> 245  
 Vinblastine 252  
 Vinca alkaloids 322  
 Vincristine 113  
 Vinflunine 639  
 Vinorelbine 81, 639  
 Virus-directed enzyme prodrug therapy 509  
 Vitamin D 37  
 Vitamin E 21, 40  
 Vitamin E succinate 625, 694  
 Vitaxin 97  
 VNP20009 501  
 Vorozole 676  
 VP-16 phosphate 23  
 Vunflunine 322  
 VX-710: *see* Incel<sup>™</sup>

## W

WHI-P97 103  
 WHI-P131 548  
 WHI-P154 203

## X

Xenotransplantation 69  
 XIAP 318  
 X-irradiation 210  
 XK469 542, 608  
 XRS944 675  
 XR9576 512

## Y

Yeast: *see* *Schizosaccharomyces pombe*

## Z

ZD1839 27, 28, 29, 98, 99, 118, 554